Virchows Arch (2010) 457:1–2
DOI 10.1007/s00428-010-0927-3

INVITED EDITORIAL

Introduction to the History of Pathology series

Jan G. van den Tweel · Clive R. Taylor

Received: 17 April 2010 / Accepted: 19 April 2010 / Published online: 20 May 2010
© The Author(s) 2010. This article is published with open access at Springerlink.com

"History is the essence of innumerable biographies."
Thomas Carlyle; 1795–1881

The History of Medicine is a flourishing field of interest and research, with an extensive literature and several notable books, including some in the "popular" press. Interest in the History of Pathology per se is far less evident. While admitting to bias, we are of the opinion that Pathology receives short shrift in general medical histories, an opinion that we believe is shared by many colleagues. Certainly there are many pathologists who are interested in specific historical aspects of their profession. However, there are few national or international societies concerning the history of pathology. Until recently, there was no such group in Europe, a deficiency now being remedied by the formation of a History of Pathology Working Group of the European Society of Pathology. The History of Pathology Society in America has a longer record, sponsoring a 2-h "companion meeting" at the annual United States and Canada Academy of Pathology (USCAP) meeting, but it is far from active during the remainder of the year. "Unknown Unloved" is probably the best way to describe the present situation.

J. G. van den Tweel (✉)
Department of Pathology H4.312, University Medical Center,
Heidelberglaan 100,
3584 CX Utrecht, The Netherlands
e-mail: j.vandentweel@umcutrecht.nl

C. R. Taylor
Department of Pathology, HMR 311, Keck School of Medicine
of the University of Southern California,
2011, Zonal Avenue,
Los Angeles, CA 90033, USA
e-mail: cltaylor@usc.edu

The "Companion Meeting" at the USCAP in 2008, in Denver, CO, USA, was advertised under the billing of "Famous Europeans who shaped Pathology." It drew an audience exceeding the meeting room capacity. The positive reactions of that audience stimulated subsequent initiatives to organize History of Pathology Symposia at the International Academy of Pathology Congress in Athens in 2008 and at the European Society of Pathology Congress of 2009. Both were well attended, providing food for thought and encouragement for the notion of soliciting a series of papers in this area or a small book, or as it turns out, both. Previous books have been few. Most enduring among these was the comprehensive *A History of Pathology* written by Esmond R. Long. Initially, published in 1928, a second updated Dover edition appeared in 1964. Contact with the present owners of Dover publications revealed no interest for a new edition. Fortunately *Virchows Archiv* was of a different opinion. The Editors have committed ample space over the next 2 years for a series of articles about the different aspects of our history. At the end of the series, the manuscripts will be combined into a book. We are very grateful to Professors H. Höfler, Editor-in-Chief, and F.T. Bosman, managing editor of *Virchows Archiv*, for their enthusiastic support of this project.

Although the different topics will cover the time span from antiquity to the present, the papers will not be published in chronologic order. However, because each paper is designed to stand alone, this should cause no problems. The first paper in the series appears in this issue of *Virchows Archiv* and provides an overview of the whole period, highlighting some of the key historical moments that have determined the shape of current pathology practice. Forthcoming articles will deal with particular historical periods (e.g., the Antiquities, the Roman influence,

the Arab influence), with groups of important scientists (e.g., famous anatomists—you use their names daily), or with remarkable individuals, who made special contributions, and were in many ways "early pathologists." In addition, there will be selected articles on the history of various technical and educational aspects, such as microscopy, stains and staining methods and on the founding of museums. The twentieth century will mainly be illustrated through the history of classifications of diseases. We fully realize that it is absolutely impossible adequately to cover, or even mention, everyone who has made contributions in the field, neither is it possible to cover every discovery of significance.

A coinciding relevant event is the production of an *Encyclopedia of Pathology*, to be published in 2012, also by Springer Verlag. This encyclopedia has a subsection on the History of Pathology and will carry more than 150 entries on historical persons and events. Both projects will be closely integrated.

We hope that these publications in *Virchows Archiv*, and also in the Encyclopedia, will raise the level of interest in the fascinating history of our specialty and will lead to more research and critical thought concerning what we do as pathologists and why and how we do it.

Guest Editors

Open Access This article is distributed under the terms of the Creative Commons Attribution Noncommercial License which permits any noncommercial use, distribution, and reproduction in any medium, provided the original author(s) and source are credited.

Virchows Arch (2010) 457:3–10
DOI 10.1007/s00428-010-0934-4

INVITED EDITORIAL

A brief history of pathology

Preface to a forthcoming series that highlights milestones in the evolution of pathology as a discipline

Jan G. van den Tweel · Clive R. Taylor

Received: 21 April 2010 / Accepted: 6 May 2010 / Published online: 25 May 2010
© The Author(s) 2010. This article is published with open access at Springerlink.com

"It is a poor sort of memory that only works backwards".

The Queen to Alice in 'Through the Looking Glass'. Lewis Carol. Ch 5; Wool and Water.

There is no single event, no 'Big Bang', that demarcates the beginning of pathology as a defined area of interest for early medical practitioners. In fact, the history of pathology has roots in common with all other medical specialties, arising in antiquity when men reasoned about the physical ailments that afflicted them. For obvious reasons, those gross features of disease that were directly visible, either in life, or after death in funereal preparations, came first to notice. In addition, over the last century, archaeological discoveries increasingly have been linked with palaeopathological investigations, furnishing a wealth of observations of gross external features of disease, from prehistoric peoples to the present time. As a result, museums around the world contain marble and terra cotta statues expressing processes that can now be interpreted as examples of hernias, breast tumours, varicose veins, ulcers and other diseases.

Documentation of disease really begins with Egyptian medicine, where the most important sources are the Edwin Smith Papyrus (17th century BC) and Papyrus Ebers (about 1550 BC). These records contain information on different types of bone injuries, trachoma (Nile valley), ulcerating lumps (cancer?), parasites and other diseases. However, despite the many thousands of ritualistic and painstaking embalmings during nearly 5,000 years of successive Egyptian dynasties, these surviving papyri contain only a slender body of information on pathological anatomy. Today, we know from recent investigations of mummies that bone tumours and tuberculosis of the spine occurred in Ancient Egypt, as well as atherosclerosis, gallstones and abscesses, yet there is little evidence that the Egyptians developed any systematic knowledge of these phenomena. It was not until the last three centuries BC that the Alexandrian Greeks, heavily influenced by Hippocrates, made lasting contributions to anatomy and pathology

The ideas related to Hippocrates of Cos (460–370? BC) and his school had an enormous impact on Greek and Roman medicine. With his humoural theory of the nature of disease, Hippocrates influenced medicine until the Renaissance, and beyond. Despite the flaws of this theory, Hippocratic writers left remarkably clear descriptions of many pathological features, such as wound inflammation, tumours, haemorrhoids, malaria and tuberculosis (Fig. 1). Animal dissection was practised in this time, but human dissection was not part of medical practice. Similar circumstances apply to Aristotle (384–322), who can be considered as one the founders of zoology. The first dissections of humans are attributed to the Alexandrian

J. G. van den Tweel (✉)
Department of Pathology H4.312, University Medical Center,
Heidelberglaan 100,
3584 CX Utrecht, The Netherlands
e-mail: j.vandentweel@umcutrecht.nl

C. R. Taylor (✉)
Department of Pathology, HMR 311, Keck School
of Medicine of the University of Southern California,
2011 Zonal Avenue,
Los Angeles, CA 90033, USA
e-mail: cltaylor@usc.edu

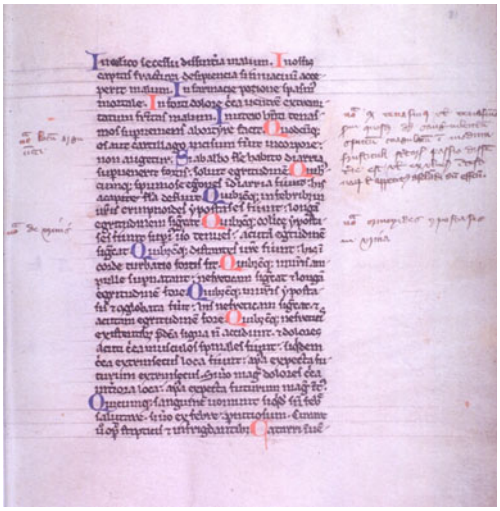

Fig. 1 Hippocrates: a page from "*Aphorismi, sive, Sententiae*" In: Hunayn ibn-Ishaq al-'Ibadi, Oxford, XIIIth century. Courtesy National Library of Medicin, Bethesda, USA

scientists Herophilos (335–280 BC) and Erasistratos (304–250). Unfortunately, their writings are all lost, and we know of their work only second hand. The Roman writers Celsus and Tertullian stated that the Alexandrians not only dissected bodies of the dead, but also performed vivisection on living criminals (as part of the punishment). Herophilos is believed to be among the first to pursue anatomy as a science, constantly trying to correlate structure with disease, while his contemporary, Erasistratos, was more a physiologist than an anatomist. Although lacking sound anatomical and physiological knowledge, they nonetheless sought to explain symptoms and complaints by reference to observed morphological changes. Both these men and their followers broke with the established Hippocratic theory. However, they were unable to introduce any new doctrine in its place, and their impact was short lived. Long before the destruction of the famous Alexandrian library in 48 BC, Hippocratic 'science' was again pre-eminent.

With the end of the Hellenistic era, many elements of Greek culture and medicine survived and were exported to newly emerging Rome. The early Roman practitioners of medicine either came from Greece or had received training in the Greek method. The most important early Roman medical writer was unquestionably Cornelius Celsus (about 30BC–38 AD). He was apparently not a physician, but an educated man with an extensive knowledge of literature. He wrote *De Re Medicina* in eight volumes. Book III contains the classic definition of inflammation: "*Notae vero inflammationis sunt quatuor, rubor et tumor, cum calore et dolore",* until now learned by every medical student.

The first century AD held few new developments. Although the humoural concept of disease was temporarily in decline, the advances of the Alexandrian School were largely neglected, in spite of the fact that Celsus had compiled the major elements in a concise form. The leading Asiatic Greek physicians were also little inclined to test their speculations openly. Human dissections ceased to performed, being unlawful in Rome, and medical practice entered the doldrums for a hundred years. Fortunately, the second century gave us a literal giant, Galen (129–201 AD). Born in Pergamus, Asia Minor, he is by many considered as the greatest medical figure of that time and maybe of all time. He followed the Greek concepts, including the Hippocratic theory of the four humours, but broadened his education and views by extensive travel, including time spent at the great school in Alexandria (Fig. 2). By (vivi)dissection of animals (pigs, monkeys), he realised the importance of such structures as the recurrent nerve and the urinary system. He described the 'crab-like' growth of cancer and introduced bloodletting. Although dispute continues, he is variously attributed to adding a 'fifth sign of inflammation', either 'loss of function', or throbbing/pulsation. Galen's views on pathology are found in his books "*Seats of Diseases*" and "*Abnormal Tumours*". His prodigious writings have been estimated as between 500 and 600 books and treatises. Although only about one third of these survived, his writings directed medicine for over a thousand years, into the Middle Ages. Unfortunately, uncritical acceptance of Galen's views over this period resulted in the same long period of unproductive medical thinking.

Pathology in the period between Galen and the late Middle Ages, was mainly influenced by Byzantine and Arab physicians, although little significant change resulted. Among the former is *Aetius* of Amida (502–575), physician to the emperor Justinian, who left excellent descriptions of

Fig. 2 Hippocrates and Galen accompanied by John Hunter in this statue at the campus of the USC Medical Center, Los Angeles Country Hospital, Los Angeles, USA. Sculptor: Salvatore Scarpitta, 1934

carcinoma of the uterus, and of haemorrhoids, condylomata, fissures and ulcers (cancers?) of the rectum. One of the greatest writers of the Arab period was Avicenna (980–1037), an illustrious physician whose major work the *"Canon Medicinae" was* based on the doctrines of Galen and Aristotle, and remained until the fifteenth century the best single work in medicine (Fig. 3). A century later he was succeeded by Avenzoar (1070–1162), who described cancer of the oesophagus and the stomach quite accurately, in addition to other lesions. However, these individual descriptions notwithstanding, the Byzantine and the Arab school did little to advance overall understanding of disease. With the decline of Arab medicine after the crusades, monasteries across Europe were the places where the tenets of Greek medicine were kept alive. Monks effectively became physicians or occupied themselves with copying and annotating ancient manuscripts, including those with medical connotations. The first indications of a revival of interest in medical knowledge coincided with the foundation of the Italian universities, having medical faculties who displayed renewed interest in anatomy and pathological anatomy. According to manuscripts from the early fourteenth century, Bologna practised human dissections as early as 1270 AD as regular part of the medical teaching for the study of anatomy, but also to study disease and legal aspects of death. Throughout the fourteenth and fifteenth centuries, dissections became increasingly common, mostly attempting to substantiate the theories of Galen. It would be another 200 years before abandonment of the humoral theory swept away cherished misconceptions and opened the way to seeing with new eyes and open minds correlations between symptoms and the underlying disease.

If there is a moment when it might be claimed that Pathology took wing as a separate specialty then it is to be found at the end of the fifteenth century, in the work of the Florentine physician, Antonio Benivieni (1443–1502), who recorded case histories and performed autopsies on some of his patients. After his death, 111 cases, among which were 20 post-mortems, were published in a little classic: *"De Abditis Nonnullis ac Mirandis Morborum et Sanationum Causis"* (About the Hidden Causes of Disease). The stage had been set and the sixteenth century then gave us several brilliant and renowned anatomists, who were increasingly aware of the pathological structures that they encountered during anatomical studies and whose names still are still used in daily pathology practise (Fig. 4). While observations of these abnormal features steadily accumulated, residual Hippocratic and Galenic influences hindered progress. Vesalius (1514–1564), who was not a keen follower of Galen, intended, according to a German contemporary, to publish his pathological observations as a separate work; however, if completed, this work has never been found.

Fig. 3 Avicenna, Canon Medicinae, 14th century. Courtesy of the National Library of Medicine, Bethesda, USA

Fig. 4 Title page of Fallopius' book: Opera Genuina Omnia. Courtesy of the National Library of Medicine, Bethesda, USA

The first to attempt formally to codify this developing new knowledge was Jean Fernel (1497–1558), who after a career in mathematics and astrology might in some ways be regarded as a full-fledged pathologist. His main work *"Medicina"* (one part called *Pathologiae Libri*), became standard throughout Europe. He classified diseases as general and special ones, and distinguished symptoms and signs, much as we do today. He diagnosed at autopsy a case of acute appendicitis, and was one of the first to suggest the syphilitic origin of some aneurysms. Important successors included the Swiss anatomist Felix Plater (1536–1614), the Dutch anatomist Volcher Coiter (1534–1576), and the German, Johann Schenk von Graftenberg (1530–1598). In retrospect it seems amazing that, in spite of the detailed work of all these anatomists, the balance of belief remained still with Galen, so deeply were these now ancient teachings embedded in the learning and practice of medicine.

The new dawn began only with William Harvey (1578–1657).The publication of "*De Motu Cordis et Sanguinis",* in 1628, revolutionised medicine and concepts of disease causation. The realisation of the circulation of blood and the function of the heart was a severe blow for the humoral theory, one that would eventually lead to its demise. Harvey also made important observations on the pathologic heart: ventricular rupture and left-sided hypertrophy in a patient with aortic valve insufficiency. In the seventeenth century, we see also the first illustrations of disease processes or pathologic changes. An early example is the drawings by the surgeon Marco Aurelio Severino (1580–1656), followed by those of Nicolaas Tulp (1593–1674). Many other physicians studied diseases at autopsy, and some collected and published their findings as 'specilegia', assemblages of autopsy reports. Of these the most important by far is Bonet's "*Sepulchretum sive Anatomica Practica"*, published in 1679. In this work Theophile Bonet (1620–1689) collected case descriptions of autopsies from the last two centuries, and then added cases of his own. The two 1,700-page volumes contain a remarkable 3,000 autopsy reports, arranged in anatomical sections "from head to toe", with comments and references. Two other important compilations of that period were the "*Spicilegium Anatomicum"* by Dutchman Theodore Kerkring (1640–1693) and the "*Anatomica Practica"* of Steven Blankaart (1650–1702). These first texts of pathological anatomy were available to the medical profession at the beginning of the eighteenth century, waiting, it seems, for somebody to put the observations that they contained into proper context. In the relative scale of time, considering that Galen's ideas endured for 1,500 years, they would not have to wait long.

Eighteenth century medicine was more sophisticated. Pathology, through an abundance of autopsies, played an increasingly important role in this development. Many pathologic observations were published in textbooks and journals. Herman Boerhaave (1668–1738) made a substantial contribution by publishing autopsy cases that related to, and clearly explained, the recent medical history of patients. Many followed; however, the one man with the vision to break with 1,500 years of Galen's influence was Giovanni Batista Morgagni (1682–1771), a medical student in Bologna, and student of the great anatomist Antonio Valsalva (1666–1723). In 1706, at the age of 24 years, Morgagni gained instant fame with his first important book, "*Adversaria Anatomica",* followed in the next years by five other volumes. His opus magnum, "*De Sedibus et Causis Morborum per Anatomen Indagatis"* (about the seats and causes of diseases through anatomical investigation), was only published in 1761 when he was 79 years old (Fig. 5). In 70 letters to an unknown friend, Morgagni described here 640 autopsies, structurally correlating the symptoms of his patients with the pathological findings at autopsy, fostering the growing belief that diseases had an anatomical substrate.

Morgagni was the highpoint of a tradition that had progressed steadily since the sixteenth century, and his work was the beginning of modern medicine and pathology. It became generally accepted that diseases were organ based. Many others (had) added to this growing body of knowledge. John Hunter (1728–1793) was not just one of them; he was an extraordinary one. Beginning about 1750, and initially working with his brother William Hunter, John Hunter was author of numerous papers to the Royal Society on exceedingly diverse topics that might be described as experimental pathology, including the use of primitive microscopes. He also was author of "*Venereal Disease"* (1786) and of *"Treatise on the Blood, Inflammation and Gunshot Wounds",* which was published by his executors in 1794. Hunter described inflammation, regarding it first as a defensive mechanism, and second as a reparative process. With him the 'doctrine of laudable pus' (Galen) died. Hunter himself died of a heart attack following a heated discussion about the admission of students at St. George's, his hospital. The Hunterian Museum at the Royal College of Surgeons in London stands as a silent witness of his enormous achievements. Remarkably, his nephew Mathew Baillie (1761–1823), who worked and trained with both John and William Hunter, extended their legacy, as well as his own, continuing the museum and expanding the teaching of morbid anatomy. Baillie is credited with not only perhaps the first systematic textbook of pathology, "*The Morbid Anatomy of Some of the Most Important Parts of the Human Body"* (1793), but also a series of beautiful copper engravings that coordinated with the text.

In the year that Morgagni died, Marie Francois Xavier Bichat was born (Fig. 6). He used his connections as army surgeon during the French Revolution to obtain permission

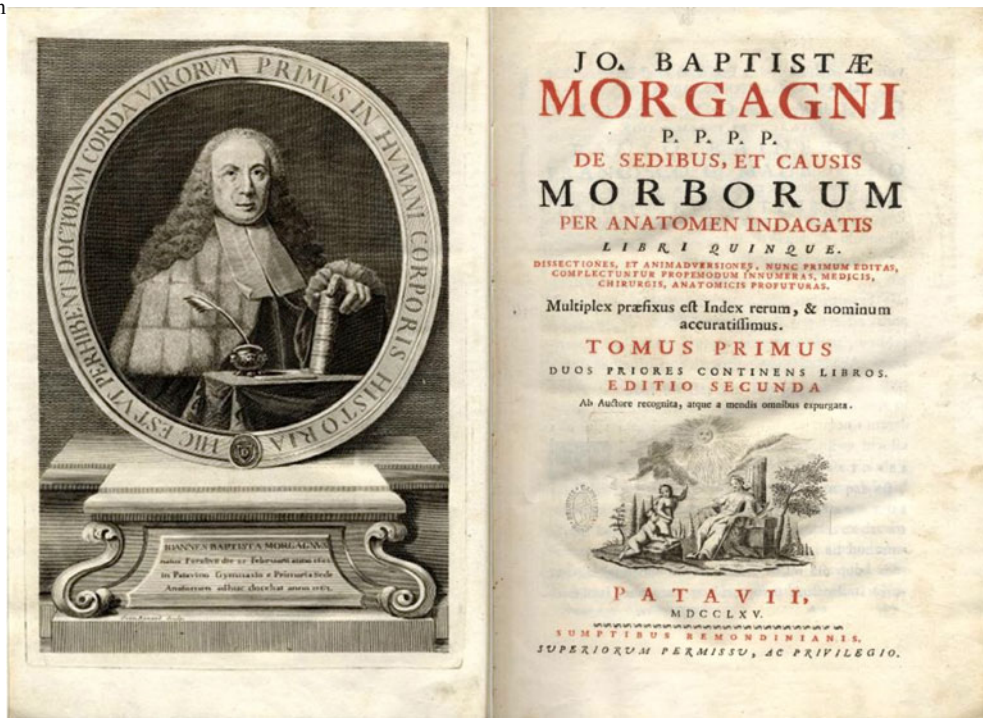

Fig. 5 A picture of Morgani in his most famous book *"De Sedibus et Causis Morborum"*. Courtesy Bilbliotheca Gambalunga, Rimini, Italy

to investigate the fresh bodies of those who were guillotined. By simple methods (e.g., cooking), without use of the microscope, he was able to identify 21 types of tissues, improving the foundation for tissue-based disease. In his autopsies, he correlated the clinical findings with "histology", a term that really gained currency 50 years later. He died at the age of 31 in 1802 of tuberculosis. His work was continued by another Frenchman, Gabriel Andral (1797–1876) who published in 1828 his "*Précis d' Anatomie Pathologique"* in two volumes, the first on general pathology and the second on special pathology.

Fig. 6 Bichat, Marie-François-Xavier. Author of "*Anatomie générale, appliquée à la physiologie et à la médecine"* (Paris, 1847). Artist Vigneron. Courtesy of the National Library of Medicine, Bethesda, USA

In Britain, Thomas Hodgkin (1798–1866), a general physician with a broad range of interests was one of the first to pursue the lead of Bichat, describing the pathological changes in tissues. In his twin papers, *On Some Morbid Appearances of the Absorbent Glands and the Spleen* (1832), he records his findings in seven autopsies, including recognisable cases of tuberculosis and also the disease that, 30 years later was, by Samuel Wilkes, given his name. Hodgkin had earlier published with Lister (father of Joseph Lister of antisepsis fame) a paper using the microscope, but notably did not employ it in his more famous 1832 publication. However, in publishing two volumes of his *"Lectures on Pathologic Anatomy"* in 1836 and 1840, Hodgkin did catch a glimpse of the new pathology: *"Lister's compound microscope might lead to useful discoveries in the future"*. British pathology was also strengthened by men as Richard Bright (1789–1858) and Thomas Addison (1793–1860). Bright is famous for his extensive studies about the relation between kidney disease and oedema and Addison for his recognition of pernicious anaemia.

From the mid-nineteenth century onwards, rather than the work of any one individual, it was 'new technology' that shaped the future of pathology. With increased availability, improved optics and reduced cost the use of the microscope grew exponentially. The time was ripe for the next giant breakthrough; pathologists were invented in a guise still more or less recognisable today.

While the microscope was the driving force, it was not the only force propelling medicine forward. The first half of the nineteenth century also witnessed a concurrent upsurge of interest in the basic sciences, particularly physiology and chemistry, leading to a more scientific approach to the study of disease. This new scrutiny gave rise to a lot of new questions. Fortuitously, at the same time, there were new scientific methods available to answer them. The role of microscopy in pathology became evident in a kind of competition between Carl von Rokitansky (1804–1878) and his one-time pupil Rudolf Virchow (1821–1902). The latter came to use the microscope routinely in his autopsy studies, whereas his mentor, Von Rokitansky did so less frequently, sometimes resulting in theoretical interpretations that were not in accord with the new evidence of the day. Von Rokitansky considered disease states to result from anomalies of the blood, inducing still more blood anomalies. He firmly believed that chemical pathologists eventually might resolve many of the unknowns in pathology. Von Rokitansky's publication of his convictions caused Rudolf Virchow to react, calling this "humoral theory" a "monstrous anachronism", despite his persisting admiration for Von Rokitansky as a great descriptive pathologist.

Virchow (Fig. 7), by many regarded as the greatest figure in the history of pathology, was a student of Johannes Müller (1801–1858) in Berlin. A case can be made that Müller was the source from which both histology and cellular pathology arose. He was one of the first to use the microscope in tissue analysis. As early as 1830, he had made extensive studies of different tissues, resulting in a book "*Ueber den feinern Bau und die Formen der krankhaften Geschwülste" (On the Finer Structure and Form of Morbid Tumors),* which appeared in 1838. In this same year, Schwann, another student of Müller, first pointed to cellular growth as the basic principle of animal life, a thesis that established for all time the cellular character of all growth. Only one step remained, the recognition of continuity of cellular life, a step that Virchow took, as expressed in his immortal aphorism "*Omnis cellula e cellula"*. Virchow's training as a student with deep interest in the basic concepts of science was followed by the same interest and devotion for his work as an (experimental) pathologist. His new insights resulted in a collection of twenty of his lectures into his most important work "*Die Cellularpathologie"* (Berlin, 1858), translated to English by Frank Chance in Cambridge in 1860. This remarkable book was a harbinger of what was to come, the next step in understanding, from organ-based disease to cell-based disease, the beginning of a 'new pathology'.

Fig. 7 Portret of Rudolph L.K. Virchow (1821–1902). Courtesy of the National Library of Medicine, Bethesda, USA, undated (approximately 1865)

With the emergence of microscopy and the ground breaking work of Morgagni, Bichat and Virchow, the specialty of pathology entered a new era in the second half of the nineteenth century. In medical schools throughout Europe, 'Inspectors of the Dead' and 'Curators of Museums' began to be replaced by Lecturers in Morbid Anatomy, then by Professors of Pathology. Many of these new professors promptly used the opportunity to claim their own department or building, setting an example that we strive to emulate even today! Although the autopsy originally was performed by many doctors, from 1850 diagnostic histopathology became more and more important, especially in the area of neoplasia, and this stimulated the development of pathology as a separate "specialty". Not all countries saw the necessity for these changes at the same time; witness the extraordinary contrast between France and Germany. In France pathology was mainly practised in laboratories in Paris, while in Germany pathology was the sum of a score of busy, productive universities. Britain was somewhere in between. There were the three generations of Monros in Edinburgh, plus the emergence of the London teaching hospitals, but it was some time before other schools appointed pathologists to chair a separate department.

The microscope totally changed concepts of disease from whole organs, to focus upon cells; it enabled the practice of histopathology and spawned numerous attendant advances in technique necessary for modern practice. Thus in the beginning slices of fresh tissue were cut by hand and examined unstained. By contrast in the last decades of the century this crude approach had given way to fixed tissues, embedding techniques, microtomes, a plethora of biological stains, and greatly improved microscopes. The man who introduced paraffin embedding in 1869 was Edwin Klebs (1834–1913). To improve the embedding process, hardening and dehydration were necessary. Chromic acid (1844), chrom-osmium-

acetic acid and Zenker's fluid entered routine use for this purpose. Formaldehyde solution was first advocated in 1893 by Isaac Blum (1833–1903) and his son Ferdinand Blum (1865–1959) and from that moment, until today, became the most used fixative. In 1865, Franz Böhmer from Würzburg published the use of alum haematoxylin as a nuclear stain. With the discovery and use of aniline dyes by Paul Ehrlich (1854–1915) the repertoire of stains available expanded rapidly, generating a new literature based upon descriptions of diseases defined by their microscopic features.

Friedrich von Recklinghausen (1833–1910) was first among a group of pathologist who dominated the last decades of the nineteenth century. Probably the most distinguished pupil of Virchow, he was both an able experimental pathologist and a practising anatomic pathologist. Although mostly remembered for his description of 'multiple neurofibromatosis', this discovery was relatively minor for he left his mark in almost every field of pathology. Von Recklinghausen was a masterly investigator of bone pathology, both the primary and the secondary bone growths. He published important studies on thrombosis, embolism, infarction, degenerations, hemochromatosis, adenomyomata of the uterus, and other many other pathologic conditions. Virchows Archiv was full of new discoveries in his period. Edwin Klebs (1843–1913), another student of Virchow, forged links between bacteriology and infectious disease. His investigations on the infectious nature of endocarditis (1878) illustrate the direction of his work. Through his discoveries, Klebs moved away from the ideas of his mentor Virchow, in that he considered aetiology as the first priority in the study of disease and relegated pathological anatomy to a secondary place. Another different view arose from the work of Julius Cohnheim (1839–1884), who broke with the traditional beliefs as to the origin of the 'pus' cell; he clearly demonstrated that they came from the blood and were not local tissue cells, as presumed by Virchow. Cohnheim's distinguished pupil, Carl Weigert (1845–1904), extended these observations to provide new understanding of the mechanisms of degeneration and necrosis.

As one enters the twentieth century, the pace of research in pathology palpably accelerated, the number of discoveries grew almost exponentially, and also the number of discoverers. At the turn of the century the Sternberg (1898)–Reed (1902) cell was born, and many basic features of histopathology were first recorded, exemplifying the primacy of the microscope in pathologic research and diagnosis. The first half of twentieth century gave us, amongst others, Ludwig Aschoff (1866–1942), who developed the concept of the reticulo-endothelial system, and Nikolai Anitschkov (1885–1964), who described the histopathology of the heart, in rheumatic fever for example, and proposed the role of cholesterol in atherosclerosis. New understanding of kidney diseases stemmed from the work of Franz Volkard and Theodor Fahr, while Paul Klemperer (1884–1964) introduced the concept of "collagen disease" (1942). The research of the pathologist Karl Landsteiner (1868–1943, he performed more than 3,600 autopsies during his training!), who provided the basis for modern blood typing (1901), had even greater implication, leading in turn to new fields of blood transfusion, and eventually tissue transplantation.

From early days of the twentieth century to the present the pace of discovery and change has accelerated still more. Ongoing advances in the fields of fixation, embedding, cutting, immunohistochemical staining, molecular methods, microscopy, and image processing have continued to yield better diagnostic tools, and new, better, more precise diagnoses. Many new journals have appeared to report these findings, including sub-specialty journals covering the broadest reaches of pathology. Numerous new entities have been described, refined, classified, re-described, and re-classified, as new techniques provided new insights. The revolutionary discoveries of fluorescein-labelled antibodies by Albert Coons (1912–1978, Fig. 8), of monoclonal antibodies by Georges Köhler (1946–1995) and César Milstein (1927–2002), and of the polymerase chain reaction by Kary Mullis (1944–) had an enormous impact leading to whole sale redefinition of many of the morphology-based disease classifications, exemplified in the successive different editions of the AFIP

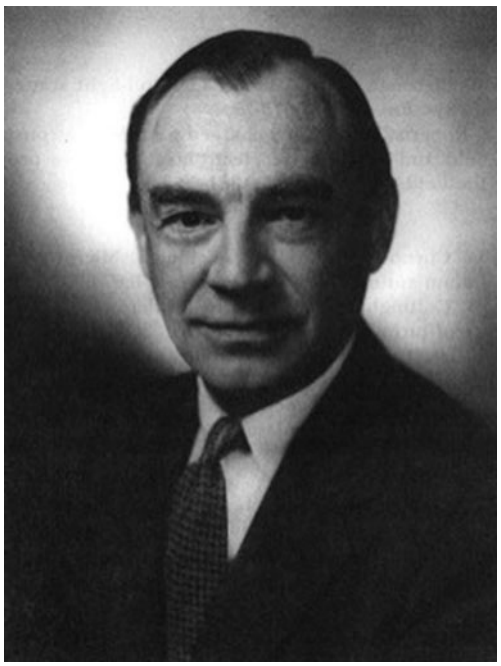

Fig. 8 Albert Coons, discoverer of immunofluorescence techniques. Courtesy of the Harvard Medical School Countway Library

tumour atlases and the WHO 'blue books'. These discoveries have shaped today's pathology practise.

Conclusion

Over a span of 4,000 years, concepts of medicine and disease have changed, driven at times by remarkable men and women, and more recently also by the relentless progress of technology. In looking for the cause of disease, the earliest physicians embraced the entire body, and often also the gods and goddesses, the stars and the heavenly bodies in their orbits. Then came the 'four humours' and other theories, holding physicians in thrall for almost 2,000 years, yielding only in the last few hundred years to the notion of organ-based disease and the rise of anatomical pathology. Next came the advent of the microscope as a scientific tool. Concepts were re-focused from organ, to tissue, to cell, ever smaller, effecting the birth of histopathology that has held sway in pathology for just a century and a half. Then, as the second millennium drew to a close, powerful new technologies began to force yet another revision of our ideas, from cell-based disease, to gene-based disease, to individual molecules and their interplay. Looking back at our history [1–10], for the interested reader, prompts us ask whether we are observing the next stage in the evolution of our discipline; whether again history is in the making. Are we attending the birth of the new pathology, the next pathology, nanopathology? From study of our past experience, we may catch a glimpse of the future; it is the best we can do. Like Alice, in these pages we have been able to look only at what has occurred; time ultimately will reveal the new face of pathology.

Open Access This article is distributed under the terms of the Creative Commons Attribution Noncommercial License which permits any noncommercial use, distribution, and reproduction in any medium, provided the original author(s) and source are credited.

References

1. Adler R (2004) Medical first. From hippocrates to the human genome. Wiley, Hoboken
2. Bynum W, Hardy A, Jacyna S, Lawrence C, Tansey E (2006) The Western medical tradition, 1800 to 2000. Cambridge University Press, Cambridge
3. Conrad L, Neve M, Nutton V, Porter R, Wear A (1995) The Western medical tradition, 800 BC to AD 1800. Cambridge University Press, Cambridge
4. Long E (1965) A history of pathology. Dover Publications, New York
5. Malkin H, Out of the mist (1993) The foundation of medicine and modern pathology during the nineteenth century. Vesalius Books, Berkley
6. Mauritz R (1987) Morbid appearences. The anatomy of pathology in the early nineteenth century. Cambridge University Press, Cambridge
7. Monti A (1900) The fundamental data of modern pathology. history, criticisms, comparisons, applications. The New Syndenham Society, London
8. Nutton V (2004) Ancient medicine. Routledge, London
9. Nuland S (2008) Doctors,the illustrated history of medical practioners. Black Dog and Leventhal Publishers, New York, 10011, illustrated edition
10. Porter R (1996) Illustrated history of medicine. Cambridge University Press, Cambridge

Virchows Arch (2010) 457:11–19
DOI 10.1007/s00428-010-0933-5

ORIGINAL ARTICLE

Stage I colorectal carcinoma: VEGF immunohistochemical expression, microvessel density, and their correlation with clinical outcome

Valeria Barresi · Carmela Di Gregorio · Luca Regiani-Bonetti · Maurizio Ponz-De Leon · Gaetano Barresi · Enrica Vitarelli

Received: 12 March 2010 / Revised: 20 April 2010 / Accepted: 6 May 2010 / Published online: 8 June 2010
© Springer-Verlag 2010

Abstract Tumor–node–metastasis (TNM) stage I colorectal cancer is commonly characterized by a good prognosis, with 5-year survival around 80–90%; nonetheless, it undergoes disease progression in a percentage of cases, although the causes of adverse clinical course still remain to be elucidated. In the present study, we analyzed and compared the immunohistochemical expression of the pro-angiogenic vascular endothelial growth factor (VEGF) as well as the microvessel density (MVD) in a series of 27 surgically resected colorectal carcinomas obtained from patients deceased because of disease progression and in a cohort of 25 colorectal cancers from patients still alive with no evidence of disease progression 5 years after the initial diagnosis. The prognostic value of VEGF expression and of MVD on the overall survival to colorectal cancer was investigated. A variable VEGF immunoexpression was demonstrated in all the analyzed cases. High VEGF expression was significantly more frequent among patients deceased of the disease. These patients also displayed significantly higher MVD counts in their cancer in comparison to the patients alive after 5 years from surgery. Moreover, both high VEGF expression and MVD appeared as significant negative prognostic markers related to a shorter overall survival to stage I colorectal carcinoma, with VEGF representing an independent variable at multivariate analysis. VEGF assessment might be used in order to select those patients with a higher progression risk and to submit them to adjuvant therapies useful to prevent adverse outcome.

Keywords VEGF · MVD · CD105 · Colorectal cancer · Prognosis · TNM stage

V. Barresi · G. Barresi · E. Vitarelli
Department of Human Pathology, University of Messina, Messina, Italy

C. Di Gregorio
Unit of Anatomic Pathology, Hospital of Carpi, Carpi, Italy

L. Regiani-Bonetti · M. Ponz-De Leon
Department of Medicine and Medical Specialities, University of Modena and Reggio-Emilia, Modena, Italy

V. Barresi (✉)
Dipartimento di Patologia Umana, Policlinico Universitario G. Martino, Pad D, Via Consolare Valeria, 98125 Messina, Italy
e-mail: vbarresi@unime.it

Introduction

Colorectal cancer represents one of the leading causes of cancer death in Western Europe and in the USA [1]. Tumor–node–metastasis (TNM) stage has been regarded as the most powerful prognostic factor for the clinical outcome of this malignancy [2, 3]. Stage I colorectal carcinoma indicates a neoplasm confined within the muscular wall of the large bowel without infiltration of local structures, in the absence of lymph nodes or distant metastasis; this category can be subdivided into two subgroups: T1, tumors spreading through the muscularis mucosae into the submucosa and T2, tumors infiltrating the muscular wall. A good prognosis, with 5-year survival around 80–90%, has been associated to stage I colorectal cancer [1, 4–6]; nonetheless, a percentage of patients with stage I carcinoma do display relapses and disease progression [5], although the reasons of adverse prognosis still remain to be elucidated. Thus, in

colorectal cancer factors predicting progression risk, in addition to the currently used clinical–pathological staging system, are needed. Indeed, although, in most cases, survival usually decreases with each higher stage group, stage group primarily reflects increasing anatomic extent of disease.

Neo-angiogenesis, the formation of new blood vessels from pre-existing ones, plays an important role in the growth and progression of tumors [7, 8]. Indeed, as long as the neoplastic mass is supplied only by the host vessels, it retains a limited volume and a low doubling time. By contrast, when the formation of new capillaries is induced by the neoplastic cells through the secretion of pro-angiogenic factors, the nutrients provided by the newly formed vessels allow a more rapid growth and the progression of the tumor [9, 10].

One key pro-angiogenic mediator is the secreted protein identified as vascular endothelial growth factor (VEGF), or vascular permeability factor, a potent angiogenic factor that promotes the migration, proliferation, and tube formation of endothelial cells [11]. VEGF pro-angiogenic activity has been demonstrated in colorectal cancer; indeed, colon cancer specimens show higher than normal overall VEGF expression, and this increase is associated with greater microvascular density and a poorer prognosis [12]. In this light, we thought that it is of interest to analyze and to compare VEGF immunohistochemical expression in a subset of surgically resected stage I colorectal carcinomas from patients deceased because of disease progression and in a cohort of stage I colorectal carcinomas from patients alive with no evidence of disease progression 5 years after the initial diagnosis. Thus, we aimed at verifying whether any difference in VEGF expression in the two groups might be at the basis of their divergent outcome. In order to evaluate the pro-angiogenic effect of VEGF in these neoplasias, we also investigated the correlations between VEGF expression and neo-angiogenesis quantified in the same cases. Finally, we tested the potential prognostic significance of VEGF immunoexpression and of neo-angiogenesis on the overall survival of patients affected by stage I colorectal cancer.

In the adenocarcinomas of the cohort, the tumor neo-angiogenesis was quantified through the assessment of microvessel density (MVD) performed using the immunohistochemical detection of CD105 (endoglin). CD105 is a 180 kDa homodimeric transmembrane glycoprotein [13], expressed on the endothelial cells of newly formed vessels in tissues undergoing active angiogenesis, such as tumors [14, 15]. In the present study, it was chosen for MVD quantification, as it has been demonstrated to be a more specific and sensitive marker for tumor neo-angiogenesis than the commonly used pan-endothelial markers, such as CD31 [16, 17].

Materials and methods

Pathologic staging of selected cases was performed on the basis of TNM system criteria [18]. The selection of the first group of patients is based on the Cancer Registry of Modena, Italy. This is a specialised, population-based colorectal cancer registry [19, 20]. Twenty-seven cases of surgically resected TNM stage I colorectal carcinomas from patients deceased of this disease were identified from a total of about 2,500 patients registered between 1984 and 2002. All these patients had shown disease progression leading to death within 5 years from the initial diagnosis.

A comparable number of TNM stage I cases (25) from patients alive 5 years after the initial diagnosis or died of independent diseases were taken from the files of the Department of Human Pathology of the University of Messina, Italy, among cases occurring during the same time period. No evidence of disease progression or relapses was recorded in this group of patients.

In none of the cases within each group, conservative local excision techniques had been used.

Finally, the cohort of the study included a total of 52 cases (30 male and 22 female patients; age range, 53–89 years; mean age, 70.3 years). None of the patients had received chemotherapy for their neoplasia. Thirty-six cases were located at the left colon (including rectum and sigma), whereby 16 were sited at the right colon (including cecum, ascendant, and transversus). Histological grade had been established according to the WHO classification system criteria; specifically, 15 cases displayed grade 1, 34 showed grade 2, whereas grade 3 was encountered in three cases. Cases were also subdivided into two groups according to the depth of infiltration within the colonic wall and, specifically, into T1 (limited to the mucosa and submucosa) and T2 (infiltrating the muscular layer).

Immunohistochemistry

All specimens had been fixed in 10% neutral formalin for 24 h at room temperature, embedded in paraffin at 55°C and cut into parallel consecutive 4-μm-thick sections for the subsequent immunohistochemical study. Briefly, the endogenous peroxidase activity was blocked with 0.1% H_2O_2 in methanol for 20 min; then, normal sheep serum was applied for 30 min to prevent unspecific adherence of serum proteins. The VEGF antigen was unmasked by microwave oven pretreatment in 10 mM, pH6.0 sodium citrate buffer for three cycles×5 min, whereas for CD105 epitope retrieval, specimens were pretreated with proteinase K (S3020, DAKO Cytomation) at room temperature for 15 min. Consecutive sections were successively incubated at 4°C overnight with the primary polyclonal antibodies against VEGF sc152 (Santa Cruz Biotechnology, Santa

Cruz, CA; w.d. 1:100) and CD105 (DAKO Corporation, Denmark, clone SN6h, w.d. 1:50). Bound primary antibodies were visualized by avidin–biotin–peroxidase detection using the Vectastain Rabbit/Mouse Elite Kit, according to the manufacturer's instructions. To reveal the immunostaining, the sections were incubated in darkness for 10 min with 3-3′ diaminobenzidine tetra hydrochloride (Sigma Chemical Co., St. Louis, MO, USA), in the amount of 100 mg in 200 ml 0.03% hydrogen peroxide in phosphate-buffered saline solution (PBS). Nuclear counterstaining was performed by Mayer's hemalum. Specificity of the binding was assessed by omitting the primary antiserum or replacing it with normal rabbit serum or PBS solution (pH 7.4). Moreover, normal renal tubules within specimens of kidney and the syncytiotrophoblast present in specimens of human term placenta were used as the positive controls for the immunoreactions [21, 22].

Quantification and statistics

The assessment of immunostained section was performed by a random principle by two independent pathologists, blinded to the clinicopathological data. For each case, the number of cancer cells with cytoplasmic VEGF expression was assessed in all optical fields, and the median value was recorded as the VEGF score of the section. Cases displaying a score 0 were considered as negative for VEGF. The median score of the cohort was utilized as the cut-off value (VEGF score, 50) to define low (VEGF score, $\leq$50) and high (VEGF score, >50) VEGF expression.

The quantification of microvessels was performed as previously described [21, 23, 24]. The assessment was done within the cancerous mass, excluding all the necrotic and the ulcerated areas, as CD105 is also expressed by the vessels of regenerating or inflamed tissues [25]. Even more, we only counted vessels with a clearly defined lumen, so as to avoid adding to the vessel count the intratumoral macrophages, which are known to express CD105 [26].

Briefly, the three most vascularized areas detected by CD105 were initially selected (so-called hot spots) under ×40 field. Then, microvessels were counted in each of these areas under a ×400 field. Only those vessels with a clearly defined lumen were counted. The mean value of three ×400 field (0.30 mm^2) counts was recorded as the MVD of the section. Then, the MVD value was converted into the mean number of microvessels/mm^2 for the statistical analyses. The vessels were counted using a Zeiss microscope by two independent observers blinded to the clinicopathological data.

Fisher's exact and chi-squared tests were performed to assess the statistical correlations between VEGF expression and the various clinicopathological parameters as well as the MVD of the analyzed cases or the status (alive or deceased of other diseases versus deceased of disease) of the patients. Mann–Whitney and Kruskall–Wallis tests were carried out in order to evaluate the statistical correlations between the MVD and the clinicopathological characteristics as well as the MVD of the tumors or the status of the patients.

Overall survival was assessed by the Kaplan–Meier method, with the date of primary surgery as the entry data. The end point was characterized as the length of survival to death for colorectal carcinoma. The Mantel–Cox log-rank test was applied to assess the strength of association between survival time and each of the parameters (age and gender of the patient, site, histological grade, T stage, VEGF immunoexpression, and MVD of the tumor) as a single variable. Successively, a multivariate analysis (Cox regression model) was utilised to determine the independent effect of each significant variable.

The MVD median value (MVD median value, 28.25) was used as the cut-off value for the MVD overall survival analysis.

A probability (P) value <0.05 was considered statistically significant. Data were analysed using the SPSS package version 6.1.3 (SPSS Inc., Chicago, IL, USA).

Results

The clinicopathological characteristic, VEGF immunoexpression and MVD of the 52 analyzed colorectal carcinomas are shown in Tables 1 and 2. VEGF immunohistochemical expression was found in the cytoplasm of the neoplastic cells in all cases (Fig. 1a) although with different percentages of stained cells. Specifically, 25 of the 52 (48%) cases displayed high (>50% of stained cells) VEGF expression. No VEGF immunoreactivity was evidenced in normal colonic epithelium. CD105 positive vessels were evidenced in all tested tumors (Fig. 1b), with MVD ranging between 1.1 to 85.5 vessels/mm^2. No immunostaining for CD105 was evidenced in the vessels within the normal mucosa distant from the tumor (Fig. 2).

Statistical analysis showed a significant association between high VEGF immunoexpression (VEGF score, >50) and high MVD (MVD, >28.25vessels/mm^2; P=0.025; Table 3) of the carcinomas. Consistently, significantly higher MVD counts were evidenced in those cases characterized by high VEGF expression (P=0.026; Table 3). With regard to the depth of infiltration, significantly higher MVD were also observed in the T1 tumors in comparison to T2 cancers (P=0.049; Table 4).

Finally, high VEGF immunoexpression and MVD counts were significantly more frequent in the patients deceased of colorectal cancer in comparison to the patients with no evidence of disease during the follow-up (P=0.003; P=0.001; Tables 3 and 4).

Table 1 Clinicopathological characteristics, VEGF immunohistochemical expression, and MVD in 52 TNM stage I colorectal carcinomas

Case	Sex	Age	Site	Grade	T	MVD (v/mm^2)	VEGF (% positive cells)	Censor	FU (months)
1	M	63	Left colon	3	2	76.6	30	NED	106
2	F	76	Right colon	2	2	22.2	25	NED	105
3	F	86	Left colon	1	1	50	50	NED	62
4	M	60	Right colon	1	2	12	25	NED	108
5	M	62	Left colon	1	2	10	50	NED	96
6	M	58	Left colon	1	2	24.4	50	NED	116
7	M	71	Right colon	1	2	1.11	10	NED	88
8	M	55	Left colon	2	2	85.5	70	NED	74
9	M	75	Right colon	2	2	1.11	20	NED	86
10	M	62	Right colon	2	2	30	2	NED	65
11	F	79	Left colon	2	2	52.2	100	NED	78
12	F	83	Right colon	2	2	1.11	70	NED	75
13	F	61	Left colon	2	2	7.77	30	DID	61
14	M	62	Left colon	2	2	1.11	60	NED	89
15	F	76	Left colon	2	2	3.33	60	NED	90
16	F	64	Left colon	2	2	1.11	10	NED	90
17	M	70	Left colon	2	2	1.11	20	NED	82
18	M	79	Left colon	2	2	1.11	50	NED	93
19	F	63	Right colon	3	2	3.33	80	NED	77
20	M	74	Right colon	2	2	60	30	NED	98
21	F	85	Left colon	2	2	10	20	NED	65
22	F	53	Right colon	2	2	3.33	25	NED	110
23	M	65	Left colon	2	2	6.66	10	NED	106
24	M	86	Right colon	2	1	60	25	NED	112
25	M	69	Left colon	2	2	1.11	25	NED	117
26	F	66	Right colon	1	2	24.4	50	DOD	68
27	F	89	Right colon	1	2	40	30	DOD	30
28	F	71	Right colon	1	2	22.2	50	DOD	32
29	F	61	Left colon	2	2	60	100	DOD	24
30	M	71	Right colon	1	2	45.5	80	DOD	48
31	M	72	Left colon	1	2	83.3	100	DOD	45
32	M	66	Left colon	1	2	31.1	100	DOD	30
33	F	60	Left colon	1	2	24.4	100	DOD	62
34	F	64	Left colon	2	2	36.6	100	DOD	120
35	F	55	Left colon	2	2	56.6	100	DOD	35
36	M	69	Right colon	3	2	40	90	DOD	19
37	M	77	Left colon	2	2	32.2	50	DOD	55
38	F	72	Left colon	2	2	53.3	100	DOD	42
39	M	73	Left colon	2	1	36.6	50	DOD	16
40	M	68	Left colon	2	2	28.8	100	DOD	117
41	M	61	Left colon	2	1	42.2	100	DOD	72
42	M	71	Left colon	1	1	30	100	DOD	36
43	M	81	Left colon	2	2	10	70	DOD	60
44	M	63	Left colon	2	2	25.5	30	DOD	123
45	F	76	Left colon	2	2	66.6	70	DOD	60
46	M	78	Left colon	1	2	50	100	DOD	61
47	M	77	Left colon	2	2	27.7	100	DOD	11
48	F	76	Left colon	1	1	47.7	40	DOD	39
49	F	79	Left colon	2	2	34.4	100	DOD	27
50	M	77	Left colon	2	2	10	10	DOD	47
51	F	75	Left colon	2	2	46.6	100	DOD	23
52	M	69	Right colon	2	2	2.22	100	DOD	14

V vessels, *FU* follow-up, *F* female, *M* male, *NED* not evidence of disease, *DID*, dead of independent disease, *DOD* dead of disease

Table 2 Clinicopathological characteristics and immunohistochemical data of the two groups of patients (alive or dead of independent disease vs dead of the disease)

Parameter	Patients	
	Alive or dead of independent disease (n=25)	Dead of disease (n=27)
Mean age	69.48±9.9	71±7.5
Sex		
M	15	15
F	10	12
Site		
Left colon	15	21
Right colon	10	6
Grade		
G1	5	10
G2	18	16
G3	2	1
T		
1	2	4
2	23	23
VEGF expression		
Low (0–50% positive cells)	19	8
High (51–100% positive cells)	6	19
MVD		
Low (<28.25 vessels/mm^2)	18	8
High (>28.25 vessels/mm^2)	7	19

M male, *F* female, *ID* intensity distribution

Univariate survival analyses revealed high VEGF immunoexpression and MVD of the tumors as well as age of the patients above 70 years as significant negative prognostic parameter for the overall survival to colorectal cancer (Table 5; Figs. 3 and 4). Multivariate analysis indicated VEGF immunoexpression as an independent prognostic parameter (P=0.025; Table 5).

Discussion

In the present study, the immunohistochemical expression of the pro-angiogenic factor VEGF and the MVD were evaluated in a series of 52 stage I colorectal carcinomas, including both cases from patients who died of the disease and from patients still alive with no evidence of disease progression after 5 years from curative surgery. We aimed at testing the hypothesis that diverse biological behavior might depend upon the difference in the quantity of neo-angiogenesis as well as in VEGF expression between these subgroups of patients.

VEGF expression was evidenced in the cytoplasm of the neoplastic cells in all cases, although with different percentages of stained cells, ranging between 2 and 100%. Specifically, 25 of the 52 (48%) cases exhibited high expression (>50% of stained cells) of this factor.

CD105 immunoreactivity, with a variable number of labeled vessels, was found in 100% of the analyzed adenocarcinomas. No immunoreaction was present in the vessels within the normal distant mucosa, thus confirming that CD105 is a more specific marker for neo-angiogenesis than the commonly used pan-endothelial markers. Statistical analysis revealed the existence of a significant correlation between VEGF expression and MVD, in line to what was previously reported by other authors [27–30]; indeed, cases characterized by higher VEGF amount displayed significantly higher MVD counts. The presence of such a

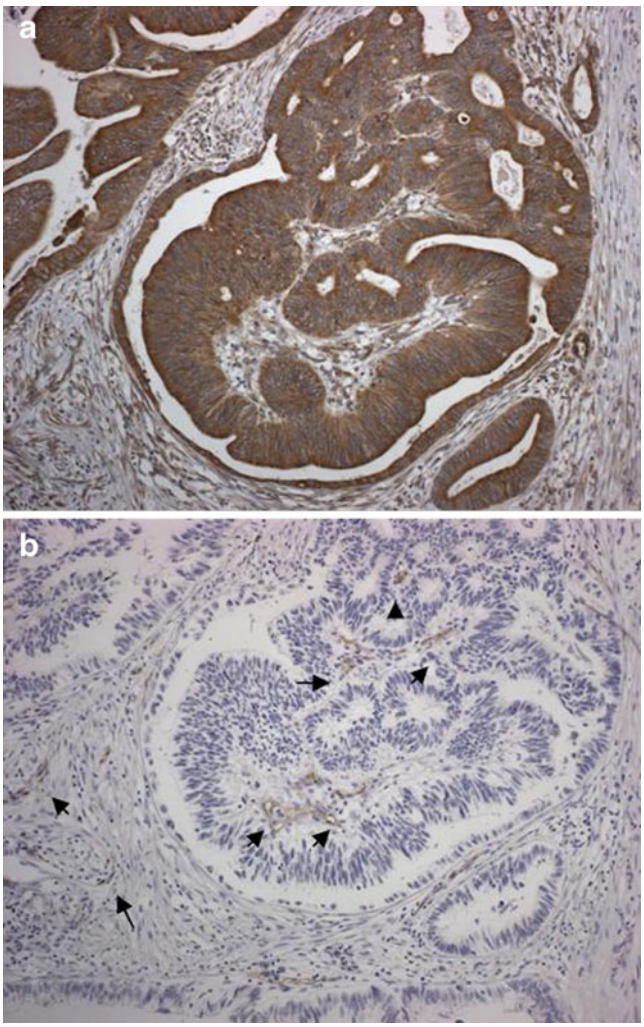

Fig. 1 **a** VEGF immunohistochemical expression was encountered in the cytoplasm of 100% of the cells of this colorectal adenocarcinoma (VEGF stain; original magnification, ×100). **b** High MVD (>28.25 vessels/mm^2) was found in the same case (CD105 stain; original magnification, ×100)

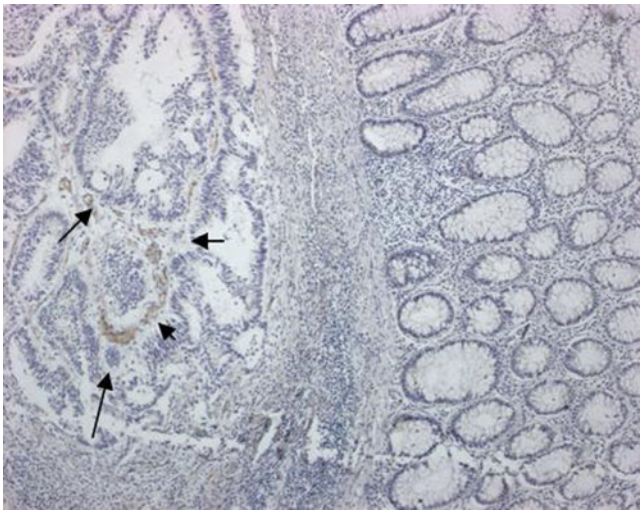

Fig. 2 CD105 positive vessels within the neoplastic tissue of a colorectal carcinoma (*left*); absence of staining in the normal mucosa of the same case (CD105 stain; original magnification, ×50)

correlation reflects the pro-angiogenic effect of VEGF in colorectal carcinoma.

Previous studies have demonstrated that high VEGF as well as high MVD behave as significant negative prognostic factors for colorectal cancer-specific survival [27, 29–31]. Herein, we evaluated for the first time the eventual prognostic role of VEGF expression and of MVD on the overall survival to stage I colorectal carcinoma.

Interestingly, a significant association emerged between high VEGF expression and high MVD and decease of the patients. In addition, the overall survival of the patients with a colorectal carcinoma characterized by high VEGF immunoexpression and high MVD was significantly shorter than that of the patients with low VEGF and MVD in their cancer. Therefore, high VEGF immunohistochemical expression as well as high MVD measured using CD105 appear as negative prognostic factors associated with poor outcome in stage I colorectal carcinoma. Moreover, multivariate analysis provided some evidence that VEGF expression is an independent prognostic parameter for stage I colorectal cancer.

Thus, in line with previous observations on colorectal carcinomas of different TNM stages [24, 27, 29–31], high MVD and VEGF expression appear to be related to higher

Table 3 Statistical correlations between MVD and the various clinicopathological parameters of the 52 analyzed colorectal carcinomas, investigated through Mann–Whitney and Kruskall–Wallis tests

Parameter	Mean rank	*P* value
Sex		
Male	25.63	0.630
Female	27.68	
Age		
≤70 years	23.43	0.177
>70 years	29.12	
Site		
Left colon	28.3	0.197
Right colon	22.43	
Grade		
1	29.03	0.540
2	24.89	
3	32.17	
T		
T1	37.91	0.049
T2	25.01	
VEGF expression		
Low (0–50% positive cells)	21.64	0.026
High (51–100% positive cells)	31	
Status		
Alive or DID	20.02	
DOD	32.5	0.003

DID dead of independent disease, *DOD* dead of disease

Table 4 Statistical correlations between VEGF immunoexpression and the various clinico-pathological parameters of the 52 analyzed colorectal carcinomas, investigated through Fisher's exact and chi-squared tests

Parameter	VEGF expression		*P* value
	Low (0–50% positive cells)	High (51–100% positive cells)	
Sex			
Male	17	13	0.575
Female	10	12	
Age			
≤70 years	13	12	1
>70 years	14	13	
Site			
Left colon	16	20	0.138
Right colon	11	5	
Grade			
1	9	6	0.651
2	17	17	
3	1	2	
T			
T1	4	2	0.669
T2	23	23	
MVD			
Low (<28.25 vessels/mm^2)	18	8	0.025
High (>28.25 vessels/mm^2)	9	17	
Status			
Alive or DID	19	6	0.001
DOD	8	19	

MVD microvessel density, *DID* dead of independent disease, *DOD* dead of disease

Table 5 Univariate and multivariate analyses for overall survival in 52 TNM stage I colorectal carcinomas

Parameter	χ^2	*df*	*P* value	β	SE	Exp (β)
Univariate analysis						
Sex	0.3605	1	0.548			
Age	3.882	1	0.046			
Site	0.5094	1	0.474			
Grade	2.4623	2	0.292			
T	1.2189	1	0.266			
MVD	9.8841	1	0.007			
VEGF	10.7356	1	0.001			
Multivariate analysis						
VEGF			0.025	1.0466	0.468	2.8479
MVD			0.073	0.8459	0.4725	2.3302
Age			0.101	0.7214	0.4408	2.0572

MVD microvessel density

progression risk in stage I colorectal carcinoma. Although tumor neo-angiogenesis alone is not sufficient for the development of metastases, the formation of new blood vessels may increase the opportunity for malignant cells to enter the blood stream and thus to give rise to metastases [32]. Even more, newly formed vessels are more permeable to tumor cells because of their fragmented membranes. As known, tumor angiogenesis is dependent on the balance between angiogenic and anti-angiogenic regulators [8]; therefore, when pro-angiogenic forces dominate, the "angiogenic switch" occurs, driving the formation of neovasculature, which may promote tumor growth and metastasis [10].

Stratification of stage I colorectal carcinomas, according to their VEGF expression, might be useful in predicting the progression risk of stage I carcinomas and in selecting those patients with a higher probability of disease progression, so that they could be submitted to adjuvant therapies. Indeed, higher VEGF expression in the neoplastic cells of colorectal cancers at higher progression risk may render them suitable candidates for anti-neoplastic therapies with drugs that target VEGF action [33, 34], neutralizing its ability to bind its receptors on the endothelial cells [35]. Besides, neutralization of VEGF has cytostatic effects on tumor biology: prevention of neovasculature formation, reduced recruitment of bone marrow-derived precursors, and "normalization," or pruning, of immature and abnormal blood vessels [33, 34, 36]. These effects lead to apoptosis of tumor endothelial cells and to a decrease in interstitial fluid pressure within the tumor, which allows greater capacity for oxygen and chemotherapeutic drugs to reach specific targeted sites [37]. In addition, the efficacy of monoclonal antibodies against CD105 in reducing tumor vascularity and metastatic risk has been recently shown in animal models [28, 38]. Nonetheless, our findings are limited by the difficulty in identifying stage I colorectal carcinomas

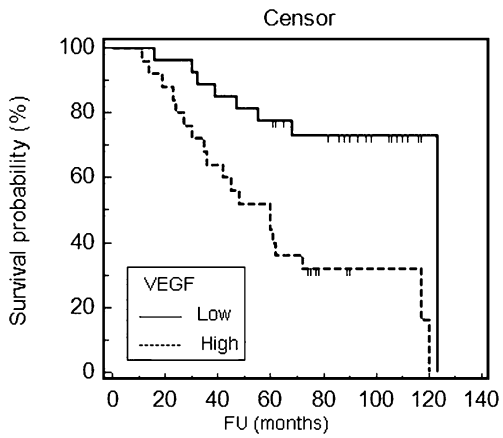

Fig. 3 Kaplan–Meier survival curves according to VEGF immunoexpression. The survival of the patients with high VEGF expression (>50% of stained cells) was significantly worse than that of the patients with low VEGF (≤50% of stained cells; *P*=0.001)

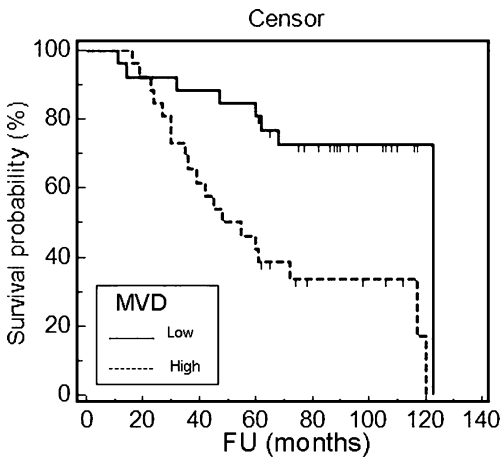

Fig. 4 Kaplan–Meier survival curves according to MVD. The survival of the patients with high MVD (>28.25 vessels/mm^2) was significantly worse than that of the patients with low MVD (<28.25 vessels/mm^2; *P*=0.001)

characterized by disease progression. As they come from a small cohort of patients, they need to be proven in larger patients' sample. Indeed, prior to clinical applications, it is mandatory to assess the VEGF prognostic value on a very large cohort of stage I colorectal carcinomas, including cases progressing or not in order to avoid overtreatment of patients.

In conclusion, the present study was carried out on a peculiar cohort of stage I colorectal carcinomas, including cases from patients deceased of the disease within 5 years from curative surgery; it has shown for the first time that high VEGF immunoexpression as well as high MVD represent negative prognostic markers associated with shorter disease specific survival in stage I colorectal cancer. New prognosticators able to predict the clinical course of this malignancy independently from the anatomic extent of the disease, reflected by the TNM staging, are needed, especially for low stage carcinomas in the aim to perform "personalized" therapies. According to our preliminary results, which warrant validation in a larger cohort of patients, VEGF assessment in colon cancer tissue might be used as a tool to discriminate those stage I tumors with a higher progression risk so that selected patients may undergo adjuvant treatments in order to prevent adverse outcome.

Conflict of interest statement We declare that we have no conflict of interest.

References

1. Landis SH, Murray T, Bolden S (1999) Cancer statistics. Cancer J Clin 49:8–31
2. Wiggers T, Arends JW, Schutter B et al (1988) A multivariate analysis of pathologic prognostic indicators in large bowel cancer. Cancer 61:386–389
3. Wu XC, Chen VW, Steele B et al (2001) Subsite-specific incidence rate and stage of disease in colorectal cancer by race, gender, and age group. Cancer 92:2547–2554
4. Di Gregorio C, Fante R, Roncucci L et al (1996) Clinical features, frequency and prognosis of Dukes' A colorectal carcinoma: a population-based investigation. Eur J Cancer 32A:1957–1962
5. Di Gregorio C, Benfatti P, Losi L et al (2005) Incidence and survival of patients with Dukes'A (stages T1 and T2) colorectal carcinoma: a 15-year population-based study. Int J Colorectal Dis 20:147–154
6. Wichmann MW, Muller C, Hornung HM (2002) The Colorectal Cancer study Group. Results of long-term follow-up after curative resection of Dukes' A colorectal cancer. World J Surg 26:732–736
7. Folkman J (1990) What is the evidence that tumour are angiogenesis dependent? J Natl Cancer Inst 82:4–6
8. Folkman J, Shing Y (1992) Angiogenesis. J Biol Chem 267:10931–10934
9. Folkman J (1995) Clinical applications of angiogenesis research. N Engl J Med 333:1757–1763
10. Hanahan D, Folkman J (1996) Patterns and emerging mechanisms of the angiogenic switch during tumourigenesis. Cell 86:353–364
11. Ferrara N, Davis-Smith T (1997) The biology of vascular endothelial growth factor. Endocr Rev 18:4–25
12. Fan F, Wey JS, McCarty MF et al (2005) Expression and function of vascular endothelial growth factor receptor-1 on human colorectal cancer cells. Oncogene 24:2647–2653
13. Cheifetz S, Bellon T, Cales C et al (1992) Endoglin is a component of the transforming growth factor-beta receptor system in human endothelial cells. J Biol Chem 267:19027–19030
14. Burrows FJ, Derbyshire EJ, Tazzari PL et al (1995) Up-regulation of endoglin on vascular endothelial cells in human solid tumours: implications for diagnosis and therapy. Clin Cancer Res 1:1623–1634
15. Miller DW, Graulich W, Karges B (1999) Elevated expression of endoglin, a component of the TGF-β receptor complex, correlates with proliferation of tumour endothelial cells. Int J Cancer 81:568–572
16. Minhajat R, Mori D, Yamasaki F (2006) Endoglin (CD105) expression in angiogenesis of colon cancer: analysis using tissue microarrays and comparison with other endothelial markers. Virchows Arch 448:127–134
17. Saad RS, Liu YL, Nathan G et al (2004) Endoglin (CD105) and vascular endothelial growth factor as prognostic markers in colorectal cancer. Mod Pathol 17:197–203
18. Sobin LH, Wittekind C (eds) (2002) TNM classification of malignant tumors. International Union Against Cancer (UICC), 6th edn. Wiley-Liss, New York
19. Ponz de Leon M, Sassatelli R, Sacchetti C (1989) Familial aggregation of tumors in the three-year experience of a population-based colorectal cancer registry. Cancer Res 49:4344–4348
20. Ponz de Leon M, Benatti P, Percesepe A (1999) Epidemiology of cancer of the large bowel—the 12-year experience of a specialized registry in northern Italy. Ital J Gastroenterol Hepatol 31:10–18
21. Barresi V, Vitarelli E, Cerasoli S (2009) Semaphorin3A immunohistochemical expression in human meningiomas: correlation with the microvessel density. Virchows Arch 454:563–571
22. Barresi V, Tuccari G (2010) Increased ratio of vascular endothelial growth factor to semaphorin3A is a negative prognostic factor in human meningiomas. Neuropathology. doi:10.1111/j.1440-1789.2010.01105.x
23. Barresi V, Cerasoli S, Vitarelli E et al (2007) Density of microvessel positive for CD105 (endoglin) is related to prognosis in meningiomas. Acta Neuropathol 114:147–156
24. Barresi V, Cerasoli S, Tuccari G (2008) Correlative evidence that tumour cell-derived caveolin-1 mediates angiogenesis in meningiomas. Neuropathology 28:472–478
25. Torsney E, Charlton R, Parums D et al (2002) Inducible expression of human endoglin during inflammation and wound healing in vivo. Inflamm Res 51:464–470
26. Fonsatti E, Del Vecchio L, Altomonte M (2001) Endoglin: an accessory component of the TGF-β-binding receptor complex with diagnostic, prognostic, and bio-immunotherapeutic potential in human malignancies. J Cell Physiol 188:1–7
27. Takahashi Y, Kitadai Y, Bucana CD et al (1995) Expression of vascular endothelial growth factor and its receptors, KDR, correlates with vascularity, metastasis and proliferation of human colon cancer. Cancer Res 55:3964–3968
28. Takahashi N, Haba A, Matsuno F et al (2001) Antiangiogenic therapy of established tumours in human skin/severe combined immunodeficiency mouse chimeras by anti-endoglin (CD105) monoclonal antibodies, and synergy between anti-endoglin antibody and cyclophosphamide. Cancer Res 61:7846–7854
29. Kang SM, Maeda K, Onoda N (1997) Combined analysis of p53 and vascular endothelial growth factor expression in colorectal carcinoma for determination of tumour vascularity and liver metastasis. Int J Cancer 74:502–507

30. Dassoulas K, Gazouli M, Theodoropoulos G (2010) Vascular endothelial growth factor and endoglin expression in colorectal cancer. J Cancer Res Clin Oncol 136:703–708
31. Ishigami SI, Arii S, Furutani M et al (1998) Predictive value of vascular endothelial growth factor (VEGF) for metastasis and prognosis of human colorectal cancer. Br J Cancer 78:1379–1384
32. Weidner N, Semple JP, Welch WR (1991) Tumour angiogenesis and metastasis—correlation in invasive breast carcinoma. N Engl J Med 324:1–8
33. Shih T, Lindley C (2006) Bevacizumab: an angiogenesis inhibitor for the treatment of solid malignancies. Clin Ther 28:1779–1802
34. Bose D, Meric-Bernstam F, Hofstetter W et al (2010) Vascular endothelial growth factor targeted therapy in the perioperative setting: implications for patient care. Lancet Oncol 11:373–382
35. WangY FD, Vanderlaan M et al (2004) Biological activity of bevacizumab, a humanized anti-VEGF antibody in vitro. Angiogenesis 7:335–345
36. Jain RK (2003) Molecular regulation of vessel maturation. Nat Med 9:685–693
37. Gerber HP, Ferrara N (2005) Pharmacology and pharmacodynamics of bevacizumab as monotherapy or in combination with cytotoxic therapy in preclinical studies. Cancer Res 65:671–680
38. Uneda S, Toi H, Tsujie T et al (2009) Anti-endoglin monoclonal antibodies are effective for suppressing metastasis and the primary tumours by targeting tumour vasculature. Int J Cancer 125:1446–1453

Virchows Arch (2010) 457:21–25
DOI 10.1007/s00428-010-0941-5

ORIGINAL ARTICLE

Indian ink vs tissue marking dye: a quantitative comparison of two widely used macroscopical staining tool

Kemal Kosemehmetoglu · Gunes Guner · Deniz Ates

Received: 6 April 2010 / Revised: 26 May 2010 / Accepted: 3 June 2010 / Published online: 18 June 2010
© Springer-Verlag 2010

Abstract The evaluation of the surgical margins is a major concern in surgical pathology, and marking of surgical margins with substances such as alcian blue, Tipp-ex, artist's pigments, colored gelatin, starch, erythrocyte layers, etc. was recommended for this purpose; Indian ink and tissue marking dyes are widely used. As there is no systematic study comparing tissue marking dyes and Indian ink as the most common substances used for the purpose, this study was conducted to compare the two. Penetration into the tissue, brightness under the microscope, the spreading area of one drop of dye on tissue paper, the intensity of colors, and unit price were compared for each of the five colors of Rotring's Indian ink and Thermo–Shandon's tissue marking dyes, applied on reduction mammoplasty specimens. Rotring's Indian ink is proved to be just as effective as Thermo–Shandon's tissue marking dye and bares the majority of the characteristics of a perfect staining substance, which are easily applied, quickly fixed, durable and cheap, contain no potential contaminants, be work safe, would not smudge/stain surrounding tissues, and look bright under the microscope without obscuring the view.

Keywords Surgical margin · Gross specimen

K. Kosemehmetoglu (✉)
Department of Pathology,
Ankara Ataturk Education and Research Hospital,
Bilkent Yolu No: 3,
06640 Ankara, Turkey
e-mail: dokemal@hotmail.com

G. Guner · D. Ates
Department of Pathology, Hacettepe University,
06100 Ankara, Turkey

Introduction

The evaluation of the surgical margins has always been a major concern in surgical pathology, and marking of surgical margins with ink or other substances is a common practice during macroscopical examination. Moreover, staining purposes can be diverse. Ink may be applied to special areas of interest other than the surgical margins, e.g., ectocervix–endocervix transition in a cone biopsy [1]. Similar-looking specimens of different individuals can be stained in different colors to reduce the risk of specimen mix-up (e.g., the value of inking breast cores, etc.). The importance of correctly staining specimens is therefore evident.

A perfect staining substance would be easily applied, quickly fixed, durable, contain no potential contaminants, be work safe, would not smudge/stain surrounding tissues, and look bright under the microscope without obscuring the view. A reasonable price and being easily available commercially would also be desirable.

Several staining techniques are proposed in the literature [2–11]. In our laboratory, India ink has been used traditionally to mark surgical resection margins and more recently with acetone or Bouin solution to aid drying. Alternative methods have been suggested in recent studies, including alcian blue solution [11] and Tipp-ex fluid [6]. These methods use one color only, and Tipp-ex is radiodense. Artists' pigments [7] have been used, but similarly, their radiodensity makes them unsuitable for the detailed mammograms of the sliced screened specimens. Another method, based on colored gelatins [2] that are painted on to the biopsy specimen before dissection, was specifically designed for impalpable breast lesions. These markers are radiolucent, quick to set, and do not smudge on or penetrate in the connective tissue. They can be applied to both fresh

and fixed tissues. Starch was also used to mark the resection margins of breast tissue simply by rolling a formalin-fixed specimen [12]. There are also commercially available marking dyes, committed to provide colorful, bright, durable, and easily applicable staining; however, generally, these are higher in cost.

Apart from several reports pioneering the different staining techniques, our searches on literature have failed to denote any studies, which compare the cost effectiveness and general efficacy of commercially available marking dye and Indian ink; therefore, we decided to compare them systematically.

Materials and methods

Inking procedure

Two surgical breast specimens (reduction mammoplasty specimen) received in the department of pathology were studied. The specimens were fixed at least overnight in 10% neutral buffered and freshly prepared formaldehyde solution, and the marking inks and pigments were applied to their external surfaces with a hair paint brush in room temperature (Fig. 1).

Indian ink (Rotring, Germany) and tissue marking dye (Thermo–Shandon marking dye) were available. We had five color options from Rotring and Thermo–Shandon (Table 1). We made sure that the tissue was blotted dry before the application of tissue stains/ink, and after staining, the external surfaces the specimens were allowed to dry for 20 s, then Bouin's solution (containing 750 ml saturated aqueous picric acid solution, 250 ml 37% formalin, and 50 ml glacial acetic acid [13]) is applied for approximately 5 s after each staining procedure.

Sections corresponding to each type and color of stains were taken and processed in the routine manner in our laboratory, sectioned, rehydrated, and thereafter cleared using ethanol and xylene, and were then examined by light microscopy after staining with Harris's hematoxylin and eosin.

Comparison of spread of stains

We used blotting paper to simulate moist tissue surface. In order to compare the spreading potential of each dye on tissue surface, we measured total surface area of spread of dye on blotting paper. We applied 30 μl of each dye using micropipette on blotting paper, and photograph was taken after 10 min of drying. Measurement of surface area was done using Spot camera and Image Analysis System (Spot Software: 4.1, Diagnostic Instruments Inc., USA) on an Olympus BX51 microscope.

Comparison of staining properties

Microphotographs of each section representing different stain/ink were taken using Spot camera and Image Analysis System (Spot Software: 4.1, Diagnostic Instruments Inc., USA) on an Olympus BX51 microscope. Dye penetrance into tissue, surface area stained, and staining densities were the three parameters that we were interested in. Surface area stained and staining densities were the two parameters reflecting how discernible the stain is. The deepest area of dye penetrance was noted, and depth of penetration was measured. For the measurement of staining densities, the same light intensity and magnification were applied to each section during microphotography. The intensity of stain was quantified by densitometry using Corel Photo-Paint Version 12.0, a com-

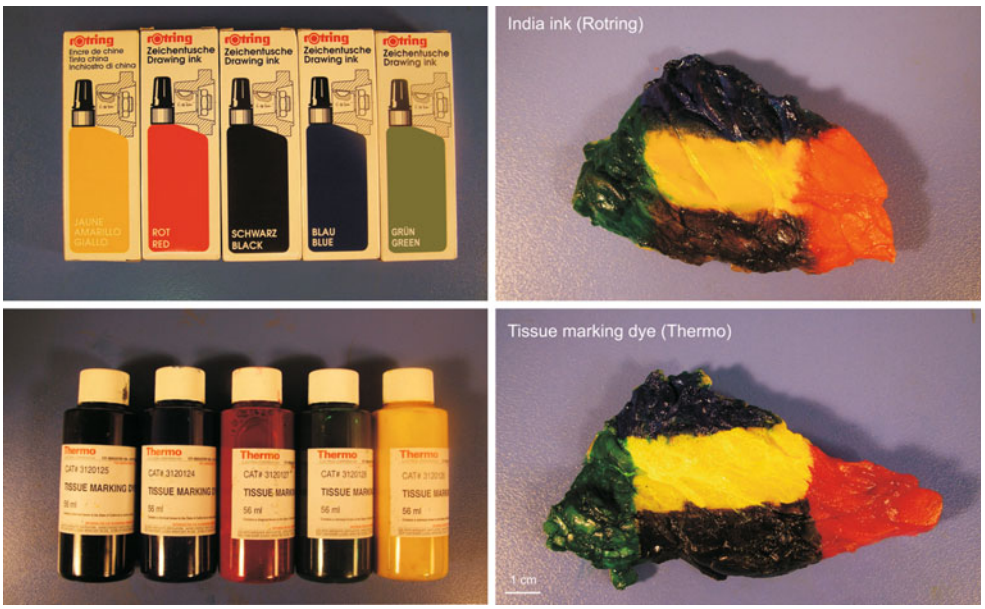

Fig. 1 Five color options of each tissue stains and application on breast specimen

Table 1 Stains/inks used in this study

Stain/Ink	Company	Color options	Cost/ml
India ink	Rotring	5 (black, blue, red, green, and yellow)	3$/23 ml
Tissue marking dye	Thermo–Shandon	5 (black, blue, red, green, and yellow)	70$/56 ml

monly used technique to compare the intensity of bands of a Western blot [14, 15]: Image is formatted in grayscale and inverted. As the high-intensity colors will have high numerical values when we measure them, the dark points (or pixels) have values near zero, and the light points have values that max out at 255. The higher the density measured, the easier the stain was seen on the microscope as a darker color. Using the "magic wand" tool, colored areas above the surface were selected and pixel area of stain was measured. We compared logarithms of density multiplied by surface area stained of each color, subsequently.

Results

A comparison of results for all properties of stains was summarized in Table 2. Both stains had approximately the same performance when spread on blotting paper is concerned; Indian ink (Rotring) seemed to be slightly less smudgy than tissue marking dye (Thermo–Shandon) on black, green, and red colors (Fig. 2).

On microscopy, Indian ink (Rotring) tended to remain on the surface and showed less tissue penetration compared with tissue marking dye (Thermo – Shandon) in respect to all colors except yellow. Blue color of Thermo–Shandon and yellow color of both Rotring and Thermo–Shandon had the deepest penetration in fatty tissues. Red color of Rotring was lost almost totally after processing; subsequently staining of a surgical margin, e.g., can be missed during routine screening. Rotring has revealed comparable results to Thermo–Shandon; even black and green colors of Rotring were more intense. On the other hand, Thermo–Shandon was better when red, blue, and yellow colors are concerned.

Discussion

Different kinds of tissue markers have been proposed in order to denote surgical margins or orientate the specimen. Acrylic, starch, alcian blue, Tipp-ex, Indian ink, gelatin (inking a specimen without the mess, etc.), and commercial products (tissue marking dyes), such as Thermo–Shandon, ScyTek, Triangle, e.g., are notable examples culled from literature, each having its own pros and cons [2–11]. Indian ink and tissue marking dye are of the most widely used tools for macroscopic purposes. According to our PubMed research results conducted in December 2009 on this topic, this study is unique on the aspect of comparing the various staining properties of commonly used Indian ink and tissue marking dyes. The inquiry sounds insignificant at first, but on further thought, the ease and comfort with which a pathologist applies tissue stains, and the quality of the tissue stain itself are hidden factors acting on the pathologist's performance.

Staining tissue margins and orientation are especially of utmost importance on breast specimens (i.e., lumpectomies), where several colors are used to locate the lesion properly, and on Moh's micrographic surgery, where the identification of the surgical margin is required. In both procedures, we deal with fatty tissues (subcutaneous fat in Moh's and breast tissue in lumpectomies), which is the logic of why we use reduction mammoplasty specimen in our study.

During inking of specimen, not only the correct staining of surgical margins but also the protection of cut surfaces and areas, which are not surgical margins, from the excess stain is important. Bouin solution, acetone, acetic acid, and alcohols are suggested to fix the stains to the wet tissue surface. Still, spreading of stains just before application of

Table 2 Macroscopical and microscopical staining properties of each color of two stains

	Spread surface area (mm^2)		Penetration depth (μm)		Surface area stained (pixels)		Mean density (0–255)			Log (surface area stained × mean density)	
	Indian	TMD	Indian	TMD	Indian	TMD	Indian	TMD	Standard	Indian	TMD
Black	260	349	31	106	132,350	84,760	171	117	255	7,355	6,996
Blue	352	336	22	231	244,009	337,412	92	101	230	7,351	7,532
Red	266	335	N/D	52	31,775	274,365	70	92	179	6,347	7,402
Green	320	369	53	92	101,632	171,274	89	47	102	6,956	6,906
Yellow	327	319	194	178	50,824	509,662	33	59	25	6,225	7,478

N/D not determined, *Indian* Indian ink, *TMD* tissue marking dye

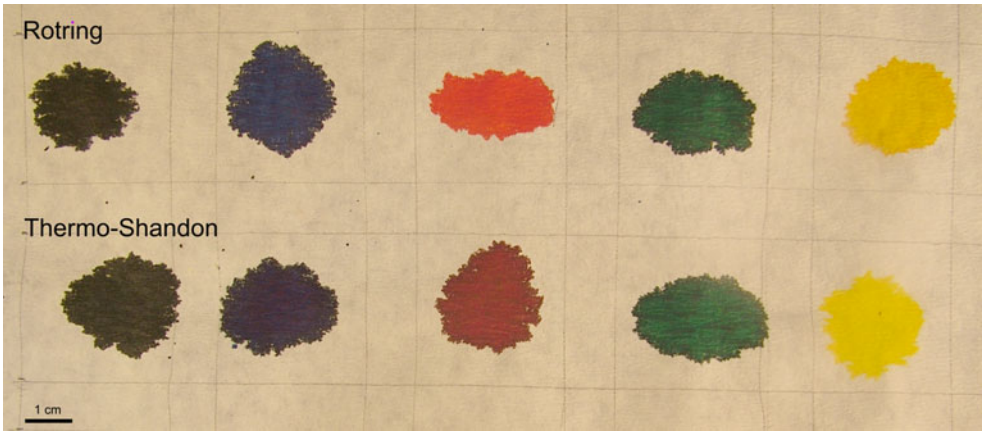

Fig. 2 Spreading of stains on blotting paper

these solutions is of concern. Rotring has been shown to be more confined than Thermo–Shandon on blotting paper.

This study established the lower tissue permeability capacity of Rotring's Indian ink compared with Thermo–Shandon's tissue marking dye. Deep tissue permeation may not be a major concern in mastectomy specimens, as a surgical margin is usually accepted as positive by surgeons if tumor is within the 1-cm distance from the margin. However, in radical prostatectomy specimens, surgical margins are regarded as negative unless a neoplastic gland is directly in contact with the dye [16]. Therefore, it is essential to use lower tissue penetrating dyes instead of deep penetrating ones especially in radical prostatectomies. Also, it must be remembered that each tissue may have different staining characteristics (e.g., penetration), and this study does not address an answer for this question.

For a comfortable visualization of a surgical margin, both stained area and density of color should be optimum. According to results of this study, it is reasonable to assume that black and blue colors of Rotring and blue, red, and yellow colors of Thermo–Shandon are the best dyes that can be easily noticed during routine microscopy. Red color of Rotring should not be used due to its disappearance after the processing of tissue. Green and yellow colors of both dyes can be used if necessary as appreciated in Fig. 3.

The choice of tissue stains depends not only on what dye is best but also on the price. Rotring is undoubtedly cheaper than Thermo–Shandon. Unfortunately, yellow and green colors of Rotring are not commercially available anymore since this company has stopped production by the time this study has been devised.

In conclusion, Rotring's Indian ink is a commercially available, easily applied, durable, reliable, and low-priced

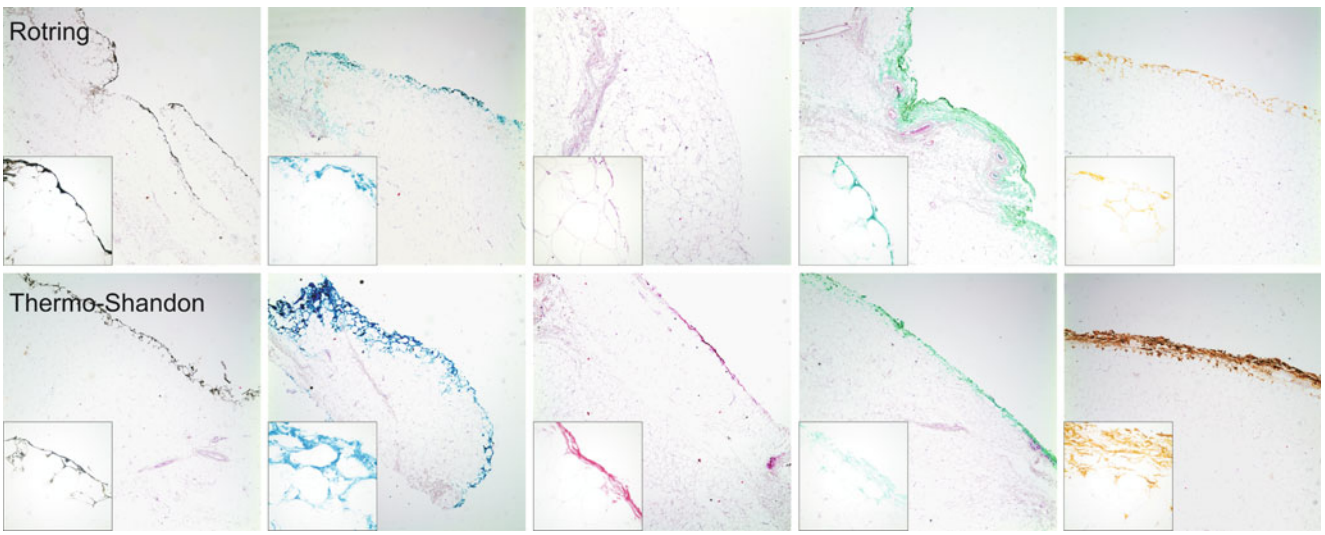

Fig. 3 Microphotographs of each color of Indian ink and tissue marking dye (×100 and ×400, H&E)

tissue marker and is proven to be as creditable as other tissue marking dyes in this study.

Conflict of interest statement We declare that we have no conflict of interest.

References

1. Dimenstein IB (2009) Grossing biopsies: an introduction to general principles and techniques. Ann Diagn Pathol 13:106–113
2. Armstrong JS, Weinzwieg IP, Davies JD (1990) Differential marking of excision planes in screened breast lesions by organically coloured gelatins. J Clin Pathol 43:604–607
3. Chan KW, Lui I, Chung WB (1989) Marking planes of surgical excision on specimens with mixture of India ink and acetone. J Clin Pathol 42:893
4. Chiam HW, Maslen PG, Hoffman GJ (2003) Marking the surgical margins of specimens: commercial acrylic pigments are reliable, rapid and safe. Pathology 35:204–206
5. Clarke TJ (1991) Differential marking of surgical excision planes. J Clin Pathol 44:87
6. Harris MD (1990) Tipp-ex fluid: convenient marker for surgical resection margins. J Clin Pathol 43:346
7. Paterson DA, Davies JD (1988) Marking planes of surgical excision on breast biopsy specimens: use of artists' pigments suspended in acetone. J Clin Pathol 41:1013–1016
8. Salerno A (1998) Fixing Indian ink on resection margins. Histopathology 33:284
9. Salerno A, Trent R, Jackson PJ, Cook MG (1995) A rapid and safe method to fix india ink on specimen resection margins. J Clin Pathol 48:689–690
10. Shinde V, Phelan C, Gater W, Thomas J (2008) Inking a specimen without the mess. J Clin Pathol 61:783
11. Wright RG, Osborne J (1991) Modification of the alcian blue method for marking breast biopsy specimens. J Clin Pathol 44:174
12. Hunter-Craig C, Lee-McDonagh B, Penman HG (1991) Marking of resection margins. J Clin Pathol 44:874–875
13. Prophet EB, Armed Forces Institute of Pathology (U.S.), American Registry of Pathology (1994) Laboratory methods in histotechnology. American Registry of Pathology, Washington
14. Corpas FJ, Chaki M, Fernandez-Ocana A, Valderrama R, Palma JM, Carreras A, Begara-Morales JC, Airaki M, del Rio LA, Barroso JB (2008) Metabolism of reactive nitrogen species in pea plants under abiotic stress conditions. Plant Cell Physiol 49:1711–1722
15. Miller L Stuff (2007) Quantifying western blots without expensive commercial quantification software. http://www.lukemiller.org/journal/2007/08/quantifying-western-blots-without.html. Accessed 10 March 2010
16. Molavi DW (2008) Prostate. In: Molavi DW (ed) The practice of surgical pathology: a beginner's guide to the diagnostic process. Springer, New York, pp 95–106

Virchows Arch (2010) 457:27–34
DOI 10.1007/s00428-010-0939-z

ORIGINAL ARTICLE

Does high-grade endometrioid carcinoma (grade 3 FIGO) belong to type I or type II endometrial cancer? A clinical–pathological and immunohistochemical study

Gian Franco Zannoni · Valerio Gaetano Vellone · Vincenzo Arena · Maria Grazia Prisco · Giovanni Scambia · Arnaldo Carbone · Daniela Gallo

Received: 6 April 2010 / Revised: 25 May 2010 / Accepted: 26 May 2010 / Published online: 15 June 2010
© Springer-Verlag 2010

Abstract This study was aimed at determining whether high-grade endometrioid carcinomas (grade 3 International Federation of Gynecology and Obstetrics) might overlap, at least partially, non-endometrioid carcinomas (type II). To this end, a panel of clinical–pathological and immunohistochemical parameters was evaluated in three different populations: low-grade endometrioid carcinomas (LGECs; n=57), high-grade endometrioid carcinomas (HGECs; n=26), and non-endometrioid carcinomas (NECs; n=30). Besides morphological appearance, HGECs appeared similar to LGECs in p53 immunostaining profile; features different from LGECs included a higher local aggressiveness, a higher invasion of lymph-vascular spaces, a lower expression of ERα and PR, and a higher proliferative index. HGECs were similar to NECs for local aggressiveness, invasion rate of lymph-vascular spaces, lymph node metastasis incidence, and proliferative index. HGECs, however, showed a lower rate of extra-nodal metastases, a lower incidence of p53 overexpression, and a higher positivity for ERα and PR. In conclusion, results from this study show that HGECs exhibit overlapping morphological and immunohistochemical features of both type I and type II endometrial carcinomas. Further research is needed to clarify the clinical value of this observation.

G. F. Zannoni (✉) · V. G. Vellone · V. Arena · A. Carbone
Department of Pathology, Faculty of Medicine "Agostino Gemelli",
Catholic University of the Sacred Heart,
Largo F. Vito 1,
00168 Rome, Italy
e-mail: gfzannoni@rm.unicatt.it

V. G. Vellone · M. G. Prisco · G. Scambia · D. Gallo
Department of Obstetrics and Gynecology,
Catholic University of the Sacred Heart,
Rome, Italy

Keywords Endometrial cancer · ER · PR · p53 · Ki67

Introduction

Endometrial cancer comprises about 4% of all cancers in women globally and develops mainly after menopause. It is the seventh most common cancer of women, with 189,000 new cases and 45,000 deaths occurring worldwide each year and with the highest incidence rates in the Western world countries [1]. On the basis of clinical behavior and etiology, endometrial cancers have long been categorized into two major classes, types I and II. Type I endometrial carcinomas are relatively indolent tumors that develop after prolonged estrogenic stimulation, this type representing the majority of sporadic endometrial carcinomas (about 70–80%). Low-grade endometrioid adenocarcinoma represents the histological prototype of type I. On the other hand, type II represents about 10–20% of endometrial carcinomas; these are more aggressive tumors and usually are not associated with endometrial hyperplasia or estrogen excess. They are typically high-grade carcinomas and include non-endometrioid differentiation, most frequently serous, less frequently clear cell [2]. This dualistic model of endometrial tumorigenesis was originally based on the Bokhman's hypothesis [3], established solely on clinical observations, and clinical–pathological correlations. However, subsequent studies have established that, apart from morphological and clinical features, type I and type II endometrial cancers also differ for genetic alterations since they have been associated with mutations from independent sets of genes. Endometrioid endometrial carcinomas involve mutations in PTEN, K-ras, and β-catenin, as well as defects in DNA mismatch repair; on the other hand, non-endometrioid

endometrial cancers frequently show aneuploidy and p53 mutations, as well as inactivation of p16 and overexpression of HER-2/neu (reviewed in [4, 5]). However, not all tumors fit into this dualistic model [6]. Indeed, high-grade endometrioid carcinomas have been classified both as type I and type II endometrial cancers [7, 8].

In the present study, we evaluated the distribution of a panel of clinical–pathological and immunohistochemical parameters in low-grade endometrioid carcinomas (LGECs), high-grade endometrioid carcinomas (HGECs), and non-endometrioid carcinomas (NECs). Evaluation included assessment of histological type and grade of tumors, extent of myometrial infiltration, occurrence of lymph-vascular space invasion, lymph node and extra-nodal metastases, staging, and expression of steroid hormone receptors, p53, and Ki67. Our aim was to determine whether high-grade endometrioid carcinomas (grade 3 International Federation of Gynecology and Obstetrics (FIGO)) might overlap, at least partially, non-endometrioid carcinomas (type II), or if they should be definitely considered as type I endometrial carcinomas.

Materials and methods

The computerized archive of the Surgical Pathology Service of the Policlinico Gemelli—Università Cattolica del Sacro Cuore, Rome, Italy was retrospectively examined for selection of endometrial carcinomas in the period January 2000–October 2008. In our institution, a written informed consent is routinely requested to patients for collection of their clinical data, as well as paraffin-embedded sections for research use. A total of 113 cases were considered suitable for the study; only cases with hysterectomy, bilateral salpingo-oophorectomy, and lymph node dissection, with more than ten lymph nodes, were included in this evaluation. To fulfill these inclusion criteria, we selected LGEC cases undergoing lymphadenectomy, due to pre-operative and/or intra-operative indications suggestive of high-stage disease. The mean number of lymph nodes collected at surgery did not significantly differ among groups, with values of 29.5±1.8, 37.2±2.8, and 31.2±2.7 (mean ± SEM), for LGECs, HGECs, and NECs, respectively. Cases with any synchronous cancer (including ovarian cancer) were excluded from the study. Histological tumor grading and staging were assessed according to the FIGO 1998 [9]. Lesions with a solid non-squamous area of less than 5% were classified as grade 1, tumors with a solid non-squamous area between 6% and 50% were classified as grade 2, and those with a solid non-squamous area greater than 50% were classified as grade 3. If marked nuclear atypia was present, the FIGO grade was elevated by one. Stages I and II were considered local disease; stages III and IV were considered metastatic disease. Pathological analysis also included tumor size, extent of myometrial infiltration (recorded in terms of absolute depth and distance to serosa), occurrence of lymph-vascular space invasion, and lymph node and extra-nodal metastases. All the specimens were routinely fixed overnight in 4% buffered formalin and embedded in paraffin. Endometrium was extensively sampled (four to ten blocks). For each specimen, two 4-μm-thick histological slides were cut at different levels and stained with hematoxylin/eosin. The study population was divided into three groups according to the histological type: LGECs, including both grade 1 and grade 2 FIGO, HGECs including grade 3 FIGO, and NECs including serous carcinoma and clear cell carcinoma [8, 10].

Immunohistochemistry

Three-micrometer-thick paraffin sections were obtained from the representative endometrial cancer blocks. The immunohistochemical staining for ERα (clone SP1), PR (clone 1E2), Ki67 (clone K-2), and p53 (clone DO-7; all from Ventana, Tucson, AZ, USA) was performed using the Ventana Benchmark XT autostainer. The analysis of all tissue sections was performed by four of the authors (GFZ, VGV, VR, and AC). In case of disagreement, sections were submitted to a rejoint evaluation by a multiheaded microscope.

Ki67 and p53

Positivity for Ki67 was expressed as the percentage of cells with positive nuclear staining in a minimum of 500 histologically identified neoplastic cells, counted under a grid at ×400 magnification (×10 ocular and ×40 objective). For p53, the percentage of cells with positive nuclear staining in a minimum of 500 histologically identified neoplastic cells was recorded, and staining patterns were subsequently calculated according to the scale previously published by Alkushi et al. [11] and Jeczen et al. [12]: 0, less than 10% of tumor cells expressed p53; 1, 10–50% of cancer cells expressed p53; and 2, more than 50% of the tumor cells expressed p53. A staining score of 2 was considered to indicate overexpression of the protein.

ERα and PR

The percentage of stained cells was categorized as follows: 1=0–25%, 2=26–75%, and 3≥76%. The staining intensity was also scored as 1 = absent or weak, 2 = strong, and 3 = very strong. The two values obtained were added to calculate a receptor score. Tumors were subsequently divided into three categories, depending on the immunohistochemical score. Category I corresponded to a score of 2, category II to a score of 3–4, and category III to a score of 5–6. Category I tumors were considered as immunonegative, whereas categories II and III tumors were considered as immunopositive.

Statistical analysis

All statistical analyses were performed using the GraphPad Prism5 Software (San Diego, CA, USA). Differences among groups in the incidence of lymph-vascular space invasion, lymph node and extra-nodal metastases, stage disease, ERα, PR, and p53-positive specimens (categorical data) were evaluated by the chi-squared test. Continuous data (i.e., tumor size, extent of myometrial infiltration, and Ki67 immunopositivity) were analyzed for homogeneity of variance using Bartelett's test. If the group variance appeared homogenous, a parametric ANOVA was used, followed by Tukey's test. If the variances were heterogeneous, log or reciprocal transformations were made in an attempt to stabilize the variances. If the variances remained heterogeneous, a non-parametric test such as the Kruskal–Wallis test, followed by Steel multiple comparison test, was used. Data are reported as mean ± SEM. $p<0.05$ was used as the critical level of significance.

Results

The study population included 57 LGECs (50.4%), 26 HGECs (23%), and 30 NECs (26.6%), these latter counting 17 cases of clear cell carcinoma and 13 cases of papillary serous carcinoma.

HGECs vs LGECs

Mean patient age in HGECs was similar to that in LGECs (58.9±1.7 vs 61.3±1.3, mean ± SEM). Mean tumor size was similar between HGECs and LGECs, although HGECs infiltrated more than LGECs, as showed by the higher extent of myometrial wall infiltration ($p<0.05$, Fig. 1). In addition,

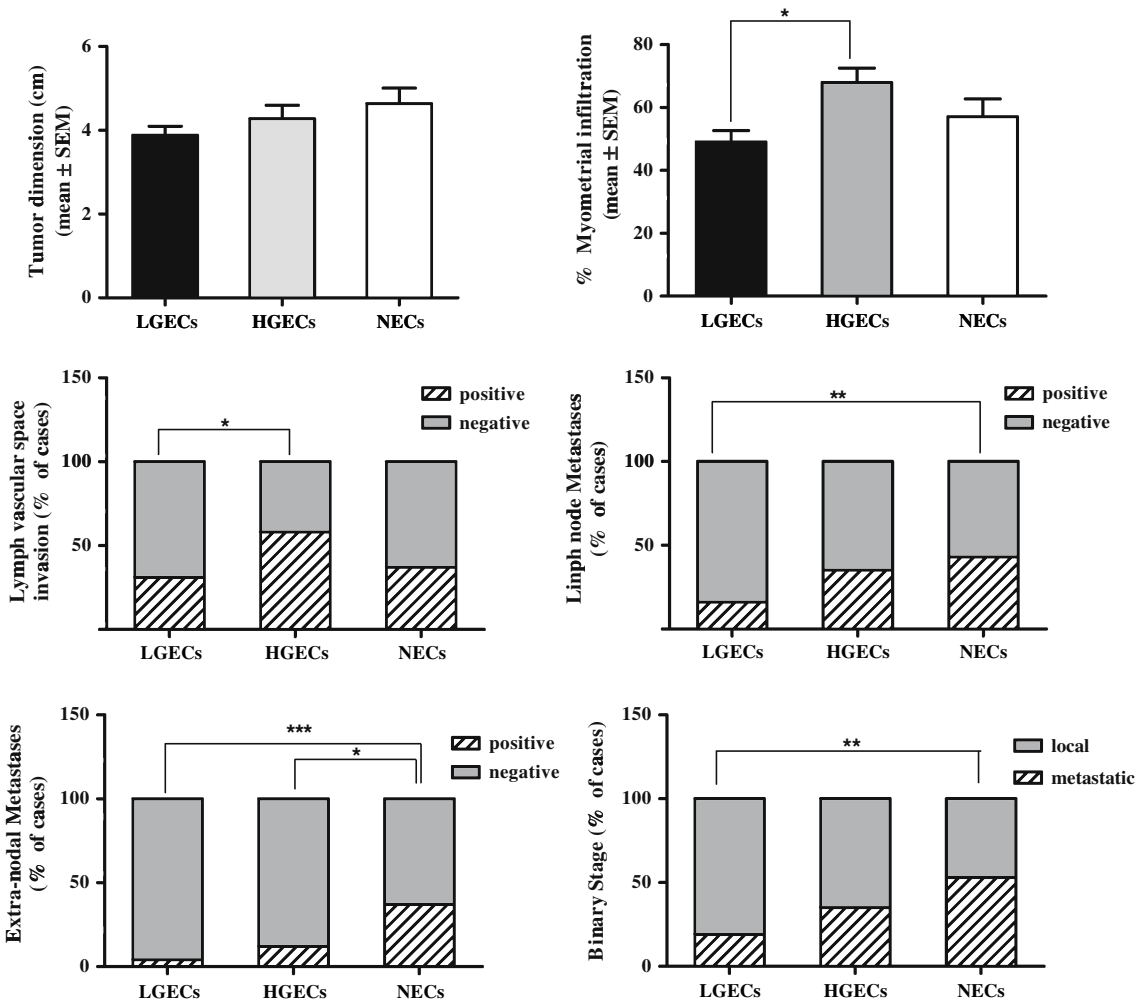

Fig. 1 Bar charts showing clinical–pathological parameters in LGECs, HGECs, and NECs. *$p<0.05$; **$p<0.01$; ***$p<0.001$. *LGECs* low-grade endometrioid carcinomas ($n=57$), *HGECs* high-grade endometrioid carcinomas ($n=26$), *NECs* non-endometrioid carcinomas ($n=30$)

lymph-vascular space invasion was more frequently detected in HGECs when compared to LGECs ($p<0.05$). On the other hand, there were no significant differences in the incidence of lymph node and extra-nodal metastases, and stage of disease between the two groups, these latter findings, however, being a likely consequence of the inclusion criteria used in the study. A lower incidence of ERα and PR immunoreactive specimens was observed in HGECs when compared with LGECs (Fig. 2a, b); these differences reached statistical significance ($p<0.01$ for both receptors). No significant differences were noticed in the incidence of p53 overexpression between LGECs and HGECs (Fig. 3a), while, as expected, HGECs showed a higher Ki67 labeling index, suggestive of a higher proliferative rate ($p<0.001$, Fig. 3b).

HGECs vs NECs

Mean patient age in HGECs was significantly lower when compared to NECs (58.9±1.7 vs 64.5±1.4, mean ± SEM, $p<0.05$), this finding being in keeping with literature data, showing that type II endometrial cancer usually affects older patients, when compared with type I [13]. Tumor size and extent of myometrial wall infiltration were similar between HGECs and NECs. No significant changes between the two groups were also observed in the incidence of

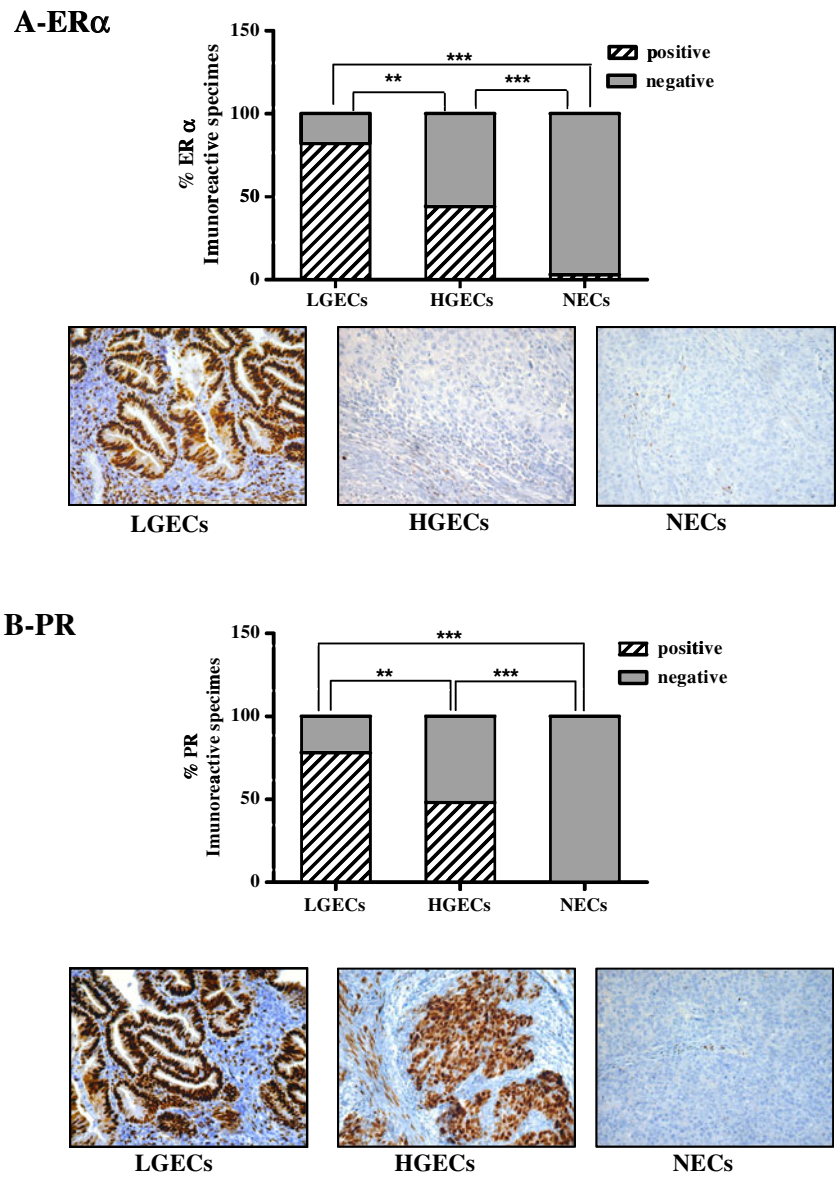

Fig. 2 **a** Bar chart showing the percentage of ERα immunoreactive specimens in LGECs, HGECs, and NECs and representative pictures of the strong nuclear protein expression observed in the majority of LGECs and of the low or absent expression seen in the majority of HGECs and NECs. Magnification ×200. **b** Bar chart showing the percentage of PR immunoreactive specimens in LGECs, HGECs, and NECs and representative pictures of the strong nuclear protein expression seen in the majority of LGECs and HGECs (although to a lesser extent) and of the absent expression in the majority of NECs. Magnification ×200. $^{**}p<0.01$; $^{***}p<0.001$. *LGECs* low-grade endometrioid carcinomas ($n=57$), *HGECs* high-grade endometrioid carcinomas ($n=26$), *NECs* non-endometrioid carcinomas ($n=30$)

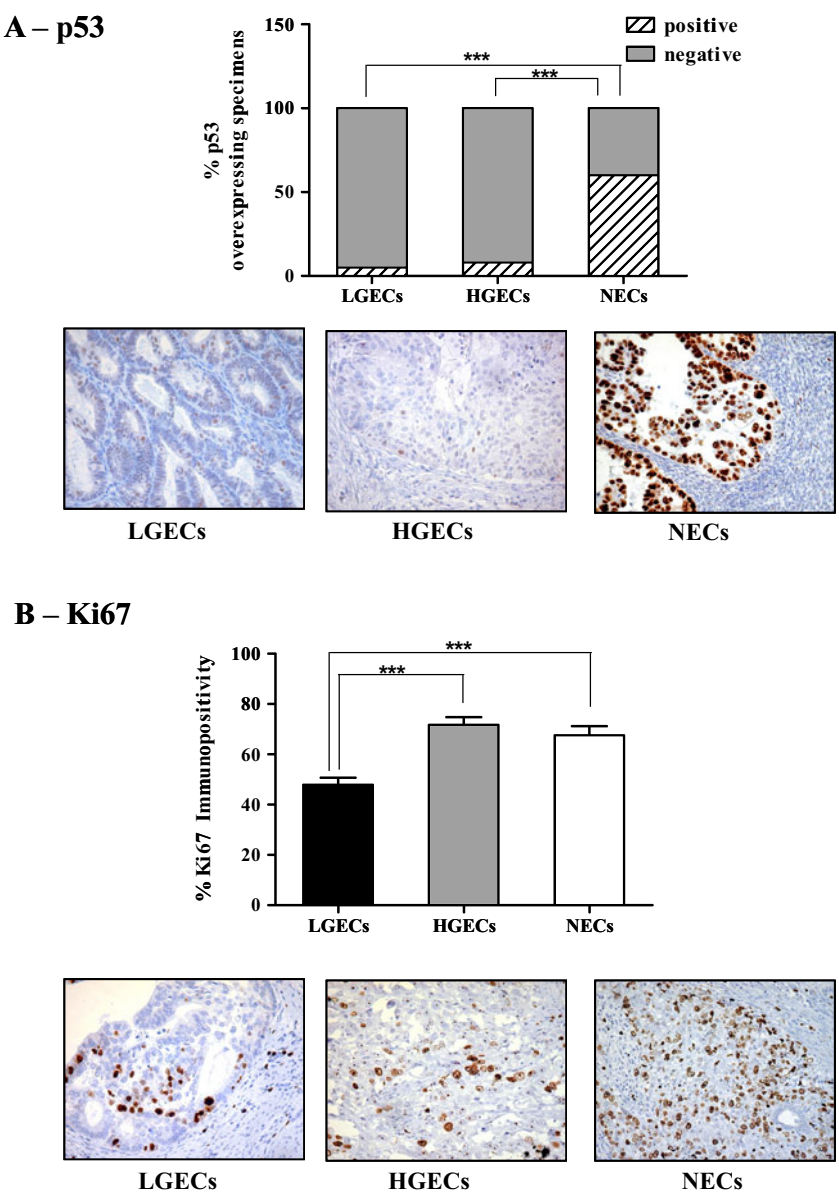

Fig. 3 **a** Bar chart showing the percentage of specimens over-expressing p53 in LGECs, HGECs, and NECs and representative pictures of the low or absent expression seen in the majority of LGECs and HGECs and of the strong nuclear protein expression observed in the majority of NECs. Magnification ×200. **b** Bar chart showing the percentage of Ki67-positive cells in LGECs, HGECs, and NECs (mean ± SEM) and representative pictures of immunostaining showing moderate expression in LGECs and strong expression in HGECs and NECs. Magnification ×200. ***$p<0.0001$. *LGECs* low-grade endometrioid carcinomas ($n=57$), *HGECs* high-grade endometrioid carcinomas ($n=26$), *NECs* non-endometrioid carcinomas ($n=30$)

lymph-vascular space invasion and lymph node metastases, while extra-nodal metastases were significantly lower in HGECs when compared to NECs ($p<0.05$, Fig. 1). A tendency toward a lower frequency of metastatic disease was observed in HGECs when compared with NECs, although this difference did not achieve statistical significance.

HGECs more frequently stained for ERα and PR when compared with NECs ($p<0.001$, Fig. 2a, b). Overexpression of p53 was significantly less frequent in HGECs compared with NECs ($p<0.001$, Fig. 3a). Finally, Ki67 labeling index was not different between the two groups (Fig. 3b).

LGECs vs NECs

Mean patient age in LGECs was lower than that in NECs (61.3±1.3 vs 64.5±1.4, mean ± SEM), although this difference did not reach statistical significance. Mean tumor size, extent of myometrium infiltration, and incidence of lymph-vascular space invasion were similar between the two groups, as a likely consequence of the inclusion criteria used for the study. Lymph node and extra-nodal metastases were significantly more common in NECs when compared to LGECs ($p<0.01$ for both parameters), and thus, NECs were more often staged as metastatic disease ($p<0.01$; Fig. 1).

Differences in immunostaining profile were often striking: LGECs showed significantly higher rates in ERα and PR positivity, when compared to NECs ($p<0.001$, for both receptors, Fig. 2a, b). The incidence of p53 overexpression in LGECs was significantly lower than that in NECs ($p<0.001$, Fig. 3a). Furthermore, LGECs showed lower Ki67 labeling index, compared to NECs ($p<0.001$, Fig. 3b).

Discussion

Two types of endometrial carcinoma are distinguished with respect to biology and clinical course. Type I carcinoma is characterized by hyperestrogenism, association with endometrial hyperplasia, frequent expression of ER and PR, and younger age; conversely, type II carcinoma is unrelated to estrogen and characterized by association with atrophic endometrium, frequent lack of ER and PR, and older age. Histologically, low-grade endometrioid carcinomas are considered type I, while type II carcinomas are typically high grade and show non-endometrioid features (mainly serous and clear cell; reviewed in [2]). The striking differences in both morphological and immunohistochemical markers observed in the present study between LGECs and NECs confirm their usual classification as prototype of type I and type II endometrial carcinoma, respectively.

Not all tumors, however, fit into this dualistic model [6] since some authors tend to classify high-grade endometrioid carcinomas (grade 3 FIGO) as type I while others consider them as type II endometrial cancers [7, 8]. The present study was aimed at determining whether HGECs should be considered definitely as type I endometrial carcinomas or if they might overlap, at least partially, type II carcinomas. Overall, as far as clinical–pathological parameters are concerned, we show here that although HGECs present a prominent myometrial infiltration and a propensity toward lymph-vascular space invasion and lymph node metastases as NECs, however, differently from NECs, they demonstrate a lower incidence of disease spread to extra-nodal sites, with a tendency toward a reduced incidence of metastatic disease. Considering the prognostic value of the above-mentioned parameters [14], HGECs may thus be set in an intermediate class between LGECs and NECs, with unique pathological and prognostic features. These differences that need to be confirmed in a larger population study might imply a different disease-based approach in the surgical and post-operative treatment of endometrial cancer [7].

p53 mutation is present in only about a third of endometrioid adenocarcinomas, while it represents the most common genetic alteration in type 2 carcinomas, with an incidence of about 70–80% in serous carcinomas [15]. Results from our study, showing the lack of significant differences in the incidence of p53 overexpression in LGECs when compared to HGECs, confirm the assumption that these sub-groups share a common pathogenetic pathway that is different from that operating in NECs, these latter showing p53 overexpression in the majority of samples [4, 16]. On the other hand, we show here that HGECs and NECs exhibit a comparable high proliferative status, significantly greater than LGECs. Notably, in addition to the traditional clinical–pathological variables, such as FIGO stage, histological type, and grade, both Ki67 and p53 protein expressions represent independent prognostic factors in endometrial cancer [17, 18]. Although we have not reported overall survival in the present study (due to the heterogeneity in the length of follow-up), we could speculate that, considering the prognostic role of p53 and Ki67, HGECs may have an intermediate behavior between LGECs and NECs, being similar to LGECs as for p53 status and to NECs as for Ki67 labeling index.

Table 1 Differences among the studied populations in the main clinical–pathological and immunohistochemical features

Studied populations	Age	TS	MI	LVSI	LM	ENM	SD	ERα	PR	p53	Ki67
HGECs vs LGECs[a]	=	(=)	↑ $p<0.05$	↑ $p<0.05$	(=)	(=)	(=)	↓ $p<0.01$	↓ $p<0.01$	=	↑ $p<0.001$
HGECs vs NECs	↓ $p<0.05$	=	=	=	=	↓ $p<0.05$	=	↑ $p<0.001$	↑ $p<0.001$	↓ $p<0.001$	=
LGEC vs NECs[b]	=	(=)	(=)	(=)	↓ $p<0.01$	↓ $p<0.001$	↓ $p<0.01$	↑ $p<0.001$	↑ $p<0.001$	↓ $p<0.001$	↓ $p<0.001$

TS tumor size, *MI* myometrial infiltration, *LVSI* lymph-vascular space invasion, *LM* lymph node metastasis, *ENM* extra-nodal metastases, *SD* stage of disease, *ERα* estrogen receptor alpha, *PR* progesterone receptor

[a] The lack of differences between HGECs and LGECs with respect to LM, ENM, and SD is a likely consequence of the inclusion criteria used in the study (see text)

[b] The lack of differences between LGECs and NECs with respect to MI, and LVSI is a likely consequence of the inclusion criteria used in the study (see text)

It is assumed that steroid hormones, especially estrogen, play a key role in the pathogenesis of endometrioid endometrial cancer, with several studies demonstrating that presence and level of steroid hormone receptors correlate with tumor grade, stage, and prognosis [19]. Indeed, low-grade tumors have been shown to be more likely ER and PR positive than high-grade neoplasms [20], while hormone receptor expression is usually negative or weakly positive in type II endometrial cancers [13]. These literature data are in keeping with our results, showing that the percentage of ERα+ and PR+ cases in HGECs were intermediate between LGECs and NECs. Notably, the differences in PR status observed among the three groups may be relevant as prognostic factors, when considering literature data showing that PR status may have greater significance for predicting survival than the ERα status in patients with histologic grade 3 [21]. Again, in term of prognosis, HGECs appear to place themselves in an intermediate position between LGECs and NECs.

An ancillary observation in the present study is that a sub-set of HGECs expresses high ERα and PR levels. It is worthy to note that, to date, hormone receptor status is not routinely assessed in endometrial cancer, and actually it does not play a key role in the selection of treatment. Indeed, there is no standard of care in the use of hormonal therapy in endometrial cancer, with this treatment being generally applied as conservative treatment in a fertility-sparing setting (early-stage disease) or as palliative in those patients too old or too sick to tolerate chemotherapy [22, 23]. Our data, on the relatively high expression of ERα and PR in a sub-set of HGECs, might indicate hormonal therapy as a valuable therapeutic tool for the management of this specific subgroup of patients. Conversely, the low/absent expression of hormone receptors in NECs gives support to the standard use of chemotherapy in advanced non-endometrioid endometrial carcinoma.

Collectively, results from the present study support the hypothesis that HGECs present mixed or overlapping clinical–pathological and immunohistochemical features of both type I and type II endometrial carcinomas (see Table 1). However, as also recently suggested by Clarke and Gilks [24], the assessment of other immunomarkers as PTEN and p16 would have been helpful to better define the immunophenotype of our studied populations, and thus, the restricted panel of markers used in the present study should be regarded as a limitation. Finally, our data support the assessment of the hormonal receptor profile as a key approach to identify a sub-set of patients eligible for hormonal therapy. In this respect, we strongly recommend hormonal receptor estimation takes place in standard clinical diagnosis of endometrial cancer, as already established in breast cancer. Further studies are needed to clarify the clinical value of these observations and to identify new molecular markers potentially helpful for the pathologist in the diagnosis of endometrial carcinomas. In turn, pathologists, taking advantage of a better characterization of tumors, may be in the unique position of being able to advise oncologists on potential treatment options.

Conflict of interest statement We declare that we have no conflict of interest.

References

1. Stewart BW, Kleihues P (eds) (2003) World cancer report. IARC, Lyon
2. Lax SF (2004) Molecular genetic pathways in various types of endometrial carcinoma: from a phenotypical to a molecular-based classification. Virchows Arch 444:213–223, Review
3. Bokhman JV (1983) Two pathogenetic types of endometrial carcinoma. Gynecol Oncol 15:10–17
4. Bansal N, Yendluri V, Wenham RM (2009) The molecular biology of endometrial cancers and the implications for pathogenesis, classification, and targeted therapies. Cancer Control 16:8–13, Review
5. Burton JL, Wells M (1998) Recent advances in the histopathology and molecular pathology of carcinoma of the endometrium. Histopathology 33:297–303, Review
6. Zorn KK, Bonome T, Gangi L et al (2005) Gene expression profiles of serous, endometrioid, and clear cell subtypes of ovarian and endometrial cancer. Clin Cancer Res 11:6422–6430
7. Bakkum-Gamez JN, Gonzalez-Bosquet J, Laack NN et al (2008) Current issues in the management of endometrial cancer. Mayo Clin Proc 83:97–112, Review
8. Amant F, Moerman P, Neven P et al (2005) Endometrial cancer. Lancet 366:491–505, Review
9. International Federation of Gynecology and Obstetrics (FIGO) (1999) Announcements. FIGO stages: 1998 revision. Gynecol Oncol 35:125–127
10. Matias-Guiu X (2009) Endometrial neoplasia. In: Nucci MR, Oliva E (eds) Gynecologic pathology. Churchill and Livingstone, London, pp 235–259
11. Alkushi A, Lim P, Coldman A, Huntsman D, Miller D, Gilks CB (2004) Interpretation of p53 immunoreactivity in endometrial carcinoma: establishing a clinically relevant cut-off level. Int J Gynecol Pathol 23:129–137
12. Jeczen R, Skomra D, Cybulski M, Schneider-Stock R, Szewczuk W, Roessner A, Rechberger T, Semczuk A (2007) P53/MDM2 overexpression in metastatic endometrial cancer: correlation with clinicopathological features and patient outcome. Clin Exp Metastasis 24:503–511
13. Mendivil A, Schuler KM, Gehrig PA (2009) Non-endometrioid adenocarcinoma of the uterine corpus: a review of selected histological subtypes. Cancer Control 16:46–52
14. Ronnet BM, Zaino RJ, Ellenson LH et al (2002) Endometrial carcinoma. In: Kurman RJ (ed) Blaustein's pathology of the female genital tract. Springer, New York, pp 501–559
15. Doll A, Abal M, Rigau M et al (2008) Novel molecular profiles of endometrial cancer-new light through old windows. J Steroid Biochem Mol Biol 108:221–229
16. Sherman ME, Bur ME, Kurman RJ (1995) p53 in endometrial cancer and its putative precursors: evidence for diverse pathways of tumorigenesis. Hum Pathol 26:1268–1274

17. Rose PG (1996) Endometrial carcinoma. N Engl J Med 335:640–649
18. Salvesen HB, Iversen OE, Akslen LA (1999) Prognostic significance of angiogenesis and Ki-67, p53, and p21 expression: a population-based endometrial carcinoma study. J Clin Oncol 17: 1382–1390
19. Carter J, Pather S (2006) An overview of uterine cancer and its management. Expert Rev Anticancer Ther 6:33–42, Review
20. Lax SF, Pizer ES, Ronnett BM, Kurman RJ (1998) Comparison of estrogen and progesterone receptor, Ki-67, and p53 immunoreactivity in uterine endometrioid carcinoma and endometrioid carcinoma with squamous, mucinous, secretory, and ciliated cell differentiation. Hum Pathol 29:924–931
21. Oreskovic S, Babic D, Kalafatic D et al (2004) A significance of immunohistochemical determination of steroid receptors, cell proliferation factor Ki-67 and protein p53 in endometrial carcinoma. Gynecol Oncol 93:34–40
22. Barrena Medel NI, Bansal S, Miller DS et al (2009) Pharmacotherapy of endometrial cancer. Expert Opin Pharmacother 10:1939–1951, Review
23. Chaudhry P, Asselin E (2009) Resistance to chemotherapy and hormone therapy in endometrial cancer. Endocr Relat Cancer 16:363–380
24. Clarke BA, Gilks CB (2010) Endometrial carcinoma: controversies in histopathological assessment of grade and tumour cell type. J Clin Pathol 63:410–415

Virchows Arch (2010) 457:35–42
DOI 10.1007/s00428-010-0936-2

ORIGINAL ARTICLE

Quantitative assessment of DNA methylation for the detection of cervical neoplasia in liquid-based cytology specimens

Jo-Heon Kim · Yoo Duk Choi · Ji Shin Lee · Jae Hyuk Lee · Jong Hee Nam · Chan Choi · Sun-Seog Kweon · Mary Jo Fackler · Saraswati Sukumar

Received: 8 February 2010 / Revised: 29 April 2010 / Accepted: 11 May 2010 / Published online: 23 May 2010
© Springer-Verlag 2010

Abstract Previously, we have shown that methylation-specific PCR (MSP) analysis of a key panel of genes may be useful as an ancillary tool for diagnosing squamous cell carcinomas (SCC) and high-grade squamous intraepithelial lesions (HSIL) in cervical scrapings. Because quantitative MSP (QMSP) is more suitable as a screening tool than conventional MSP, we investigated the diagnostic role of QMSP for the detection of SCC and HSIL in cervical scrapings. A quantitative multiplex-MSP approach was used to examine promoter methylation of five genes (APC, HIN-1, RAR-β, RASSF1A, and Twist) in biopsy-confirmed SCC (n=63), HSIL (n=45), low-grade SIL (LSIL, n=26), and negative (n=28) liquid-based cytology samples. For four genes (HIN-1, RAR-β, RASSF1A, and Twist), the methylation levels among four groups were significantly different ($p<0.001$ for each). Methylation levels of HIN-1, RAR-β, RASSF1A, and Twist were increased in HSIL and SCC samples, compared with either negative or LSIL samples. However, methylation levels were not significantly different between SCC and HSIL, with the exception of RASSF1A. Receiver-operating characteristic analysis demonstrated that HIN-1, RAR-β, RASSF1A, and Twist had the ability to distinguish HSIL/SCC from LSIL/negative samples. The two-gene combination (RASSF1A/Twist) showed the best performance in distinguishing HSIL/SCC from LSIL/negative samples. The estimated specificity of this two-gene panel for detecting HSIL/SCC was 90.7%, and its sensitivity was 74.1%. These results suggest that quantitative detection of aberrant DNA methylation in cervical scrapings may be a promising high-throughput approach for the diagnosis of HSIL/SCC.

Keywords Cervix · Squamous intraepithelial lesion · Cytology · Methylation · Quantitation · Diagnosis

J.-H. Kim
Department of Pathology, School of Medicine,
Jeju National University,
Jejusi, Republic of Korea

Y. D. Choi · J. S. Lee · J. H. Lee · J. H. Nam · C. Choi
Department of Pathology, Chonnam National University Medical School and Research Institute of Medical Sciences,
Gwangju, Republic of Korea

S.-S. Kweon
Department of Preventive Medicine,
Chonnam National University Medical School and Research Institute of Medical Sciences,
Gwangju, Republic of Korea

M. J. Fackler · S. Sukumar
Breast Cancer Program, Department of Oncology,
Johns Hopkins University School of Medicine,
Baltimore, MD, USA

J. S. Lee (✉)
Department of Pathology,
Chonnam National University Hwasun Hospital,
160, IIsim-ri, Hwasun-eup,,
Hwasun-gun, Jeollanam-do 519-809, Republic of Korea
e-mail: jshinlee@hanmail.net

Introduction

Carcinoma of the cervix is the leading gynecological malignancy worldwide and the fourth most common malignancy in Korea [1]. Since the introduction of Papanicolaou (Pap) smears in screening programs, the incidence and mortality of cervical cancer has decreased dramatically in Korea and other developed countries [2]. The goal of cervical cancer screening programs that utilize

the Pap test is to identify and treat women with invasive squamous cell carcinoma (SCC) and its precursor high-grade squamous intraepithelial lesions (HSIL). Despite the success of the Pap test as a screening test for cervical cancer, limitations in its reproducibility and sensitivity for the detection of HSIL have led to the search for more accurate molecular screening methods to aid in the diagnosis of HSIL [3, 4].

Identifying and characterizing the molecular alterations and processes that contribute to the development of the cancer phenotype is integral to determining effective biomarkers for cancer diagnosis [5]. Epigenetic silencing of a variety of genes by promoter hypermethylation is now recognized as a frequent and early event in the pathogenesis of many cancers, including cervical cancer, making such changes a potential interest as biomarkers for objective identification of cancer [6, 7]. The role of promoter hypermethylation as a diagnostic tool for cervical neoplasia screening on exfoliated cervical samples has been examined [8–16]. The power of promoter hypermethylation analysis compared with other techniques that use RNA or protein is that it is a DNA-based technique [17]. DNA is much more stable than RNA and proteins. Thus, it is more feasible to isolate and analyze DNA from archived or stored biological samples. Recently, we have noted that methylation-specific PCR (MSP) analysis of a key panel of genes may be useful as an ancillary tool for the detection of SCC and HSIL in residual, liquid-based samples of cervical scrapings [18]. These residual, liquid-based samples were stored at room temperature for several months.

In the conventional MSP method, PCR products are run on a gel, and the results are reported as methylated or unmethylated at the target DNA sequence. Consequently, this method does not allow the identification of partial levels of methylation, a feature which is extremely relevant both biologically and clinically. Thus, quantitative MSP (QMSP) has been developed in recent years to overcome this limitation of conventional MSP. QMSP is reported to be more specific and more sensitive than conventional MSP and allows for high-throughput analysis, making it more suitable as a screening tool [19–21].

At present, only a few studies have investigated the use of QMSP as a diagnostic tool for cervical neoplasia using cervical scrapings [10, 12–14, 16]. Furthermore, these studies have not included a full spectrum of cervical neoplasias. Therefore, in the current study, we examined the diagnostic role of QMSP for the detection of SCC and HSIL in cervical scrapings. A quantitative multiplex-MSP (QM-MSP) approach was used to examine promoter hypermethylation of five genes (APC, HIN-1, RAR-β, RASSF1A, and Twist) in a biopsy-confirmed, full spectrum of cervical neoplasias, including low-grade SIL (LSIL), HSIL, SCC, and negative liquid-based cytology samples.

Materials and methods

Samples

Randomly selected biopsy-confirmed SCC (n=63), HSIL (n=45), LSIL (n=26), and malignancy-negative (n=28) residual, liquid-based samples were identified from the pathology archives of the Chonnam National University Hwasun Hospital, after obtaining approval by the Institutional Review Board. Malignancy-negative cervical cytologic samples were obtained from patients who were planning to undergo a hysterectomy for benign gynecological diseases. We confirmed normal cytologic diagnoses by the histopathological examination of cervical specimens. Cervical samples were collected using the Thin Prep Cytology Collection System (CYTYC Corporation, Marlborough, MA, USA) according to the manufacturer's protocol. The sample vials were stored at ambient temperature and used within 20 months of the collection date. Mean storage time was 13 months, with a range of 9–20 months. Genomic DNA was isolated from cells spun down from 5 ml of Thin Prep Cytology Collections.

Based on Papanicolaou-stained ThinPrep slides, we determined the proportion of dysplastic cells in the liquid-based samples of HSIL and SCC. Slides were scanned at ×100 magnification to identify the areas with the highest number of epithelial cells. Two images per specimen were captured by a Digital Camera System at ×200 magnification. The number of dysplastic and non-neoplastic cells were measured by touch count in the captured image. Percentage of dysplastic cells for each specimen was calculated as $[\text{number of dysplastic cells}/(\text{number of dysplastic} + \text{non} - \text{neoplastic cells})] \times 100$. Dysplastic cells ranged from 0.9% to 55.9% (mean±standard deviation, 23.3±15.8%).

Sodium bisulfite treatment and QM-MSP analysis

The extracted DNA was treated with sodium bisulfite using the EZ DNA methylation™ kit (Zymo Research, Orange, CA, USA), converting all unmethylated cytosine to uracil. All bisulfite-modified DNA was resuspended in 10 μL of elution buffer and stored at −20°C until subsequent QM-MSP.

QM-MSP was performed in two sequential PCR steps as described by Fackler et al. [21] and Swift-Scanlan et al. [22]. In step 1, multiplex PCR was performed using external primers independent of DNA methylation status to co-amplify five genes. Five microliters of sodium

bisulfite-treated DNA was added to 45 μl of reaction buffer [1.25 μmol/L deoxynucleotide triphosphate, 16.6 mmol/L $(NH_4)_2SO_4$, 67.0 mmol/L Tris (pH 8.8), 6.7 mmol/L $MgCl_2$, 10.0 m mol/L β-mercaptoethanol, 0.1% Dimethyl sulfoxide (DMSO), and 10 units of Platinum DNA Taq polymerase (Invitrogen, Carlsbad, CA, USA)] containing 100 nmol/L each of the forward and reverse primers. Reactions were carried out using the following conditions: 95°C for 5 min; then 36 cycles at 95°C for 30 s, 56°C for 30 s, and 72°C for 45 s; and a final extension step at 72°C for 5 min. A negative control for the assay (water only) and unmethylated (U) (human sperm DNA) and methylated (M) controls (SssI-treated MDA-MB-231 cells) were included in step 1 reactions. The final PCR product was then diluted 1:5 or more in sterile distilled water, depending on the concentration of input DNA. In step 2, in the quantitative reaction, two-color real-time MSP was done on 1 μL of the diluted PCR product from step 1. The second step was carried out in a 25-μL PCR final reaction volume with 1.25 units of Platinum DNA Taq Polymerase (Invitrogen), 1× ROX (Invitrogen) passive reference dye, 1× buffer [16.6 mmol/L $(NH_4)_2SO_4$, 67.0 mmol/L Tris (pH 8.8), 6.7 mmol/L $MgCl_2$, 10.0 m mol/L β-mercaptoethanol, 0.1% DMSO], 200 μmol/L deoxynucleotide triphosphate, and 800 nmol/L of each primer set. 6-FAM/TAMRA or VIC/TAMRA-conjugated gene-specific oligonucleotide probes were used with U and M primer sets performing reactions in the same well. The real-time assay was done using a 7500 real-time PCR System (Applied Biosystems, Foster City, CA, USA). The standard curve, control, and sample DNAs were prepared essentially as described previously, with the modification that U and M gene MSP standards were cloned into plasmids. Detailed primer sequences are presented in Table 1.

Percent methylation for each gene was calculated as follows: $\%\text{methylation(M)} = [\text{number of copies of methylated } DNA / (\text{number of copies of methylated} + \text{unmethylated DNA})] \times 100$.

Statistical analysis

The Kruskal–Wallis analysis of variance (ANOVA) test was used to study differences in methylation levels among four groups (negative, LSIL, HSIL, and SCC), and the Bonferroni correction was used for paired comparisons when significant results were obtained. The methylation thresholds of individual genes for cutoff values were established by receiver-operating characteristic (ROC) analysis, where an optimal cutoff was chosen by maximizing the sensitivity and specificity. We defined the promoter hypermethylation (positive vs. negative) using the selected cutoff values. We calculated the sensitivities, specificities, and area under the curve (AUC) of five individual methylation markers. To identify gene combinations that provided the highest potential sensitivity and specificity for HSIL/SCC, we started with the single gene providing the highest AUC for HSIL/SCC and then selected additional genes providing the largest increase in sensitivity without unreasonable loss of specificity. A positive panel was defined as at least one gene in the panel exceeding the single gene decision threshold. The sensitivity, specificity, and AUC were also calculated for all panels evaluated. For all statistical analyses, the SPSS system for the personal computer (version 13.5 for Windows; SPSS INC., Chicago, IL, USA) was used, with $p<0.05$ regarded as statistically significant.

Results

Methylation levels

The methylation levels of five genes in negative, LSIL, HSIL, and SCC samples are shown in Fig. 1. For APC, no methylation and only very low levels of methylation were found among the four groups. HIN-1 and RASSF1A showed no or only very low levels of methylation in LSIL and negative samples. By contrast, RAR-β and Twist were, in part, heavily methylated in some cases of LSIL or negative samples. Statistically significant differences in methylation levels among the four groups were noted for all the target genes except APC (HIN-1, RAR-β, RASSF1A, and Twist; $p<0.0001$ for each gene; Table 2). Generally, methylation levels of HIN-1, RAR-β, RASSF1A, and Twist were higher in SCC and HSIL than in negative or LSIL cervical samples. For HIN-1 and RAR-β, the methylation levels observed in HSIL and SCC differed significantly from those of LSIL and the negative group. For RASSF1A, HSIL methylation levels differed significantly from those in negative ($p=0.000$) and LSIL ($p=0.000$) samples. For Twist, the methylation levels observed in SCC differed significantly from those of LSIL ($p=0.001$) and the negative group ($p=0.004$). Except for RASSF1A, methylation levels between negative and LSIL or between HSIL and SCC were not significantly different. RASSF1A methylation levels were significantly higher in HSIL than in SCC ($p=0.020$).

Detection of HSIL and SCC by QM-MSP

Because the goal of cervical cancer screening programs that utilize the Papanicolaou test is to identify and treat women with precancerous HSIL and SCC, we calculated the sensitivities and specificities of methylation markers alone or in sequential combinations for the diagnosis of

Table 1 Primer and probe sequences and distance from transcriptional start site

Primers and probes	Sequences	Distance to transcriptional start site
APC1 Ext F(2)	AAAACCCTATACCCCACTAC	−142 to +14 transcript variant 2
APC1 Ext R(2)	GGTTGTATTAATATAGTTATATGT	
APC1 FM	AATACGAACCAAAACGCTCCC	
APC1 FUM	TAAATACAAACCAAAACACTCCC	
APC1 RM	TATGTCGGTTACGTGCGTTTATAT	
APC1 RUM	GTTATATGTTGGTTATGTGTGTTT	
APC1 UM probe	6FAM-TTCCCATCAAAAACCCACCAATTAAC	
APC1 M probe	VIC-CCCGTCGAAAACCCGCCGATTA	
HIN1 Ext R(3)	AAACTACAAAACAAAACCAC	SCGB3A1; −206 to +80
HIN1 Ext F(2)	GTTTGTTAAGAGGAAGTTTT	
HIN1 FM	TAGGGAAGGGGGTACGGGTTT	
HIN1-FUM (2)	AAGTTTTTGAGGTTTGGGTAGGGA	
HIN1 RM	CGCTCACGACCGTACCCTAA	
HIN1 RUM (2)	ACCAACCTCACCCACACTCCTA	
HIN1 UM probe	6FAM-CAACTTCCTACTACAACCAACAAACC	
HIN1 M probe	VIC-ACTTCCTACTACGACCGACGAACC	
RAR-β Ext F	GTAGGAGGGTTTATTTTTTGTT	+34 to +269
RAR-β Ext R(2)	AATTACATTTTCCAAACTTACTC	
RAR-β FM	AGAACGCGAGCGATTCGAGTAG	
RAR-β FUM	TTGAGAATGTGAGTGATTTGAGTAG	
RAR-β RM	TACAAAAAAACCTTCCGAATACGTT	
RAR-β RUM	TTACAAAAAAACCTTCCAAATACATTC	
RAR-β UM probe	6FAM-AAATCCTACCCCAACAATACCCAAAC	
RAR-β M probe	VIC-ATCCTACCCCGACGATACCCAAAC	
RASSF1A Ext F(2)	GTTTTATAGTTTTTGTATTTAGG	−38 to +160
RASSF1A Ext R(2)	AACTCAATAAACTCAAACTCCC	
RASSF1A FM	GCGTTGAAGTCGGGGTTC	
RASSF1A FUM	GGTGTTGAAGTTGGGGTTTG	
RASSF1A RM	CCCGTACTTCGCTAACTTTAAACG	
RASSF1A RUM	CCCATACTTCACTAACTTTAAAC	
RASSF1A UM probe	6FAM-CTAACAAACACAAACCAAACAAAACCA	
RASSF1A M probe	VIC-ACAAACGCGAACCGAACGAAACCA	
TWIST Ext F(3)	GAGATGAGATATTATTTATTGTG	−415 to −162
TWIST Ext R(4)	CCTCCCAAACCATTCAAAAAC	
TWIST FM	GTTAGGGTTCGGGGGCGTTGTT	
TWIST FUM (3)	GGTTTGGGGGTGTTGTTTGTATG	
TWIST RM	CCGTCGCCTTCCTCCGACGAA	
TWIST RUM (5)	CCATCACCTTCCTCCAACAAAC	
TWIST UM probe	6FAM-AAACAATTTCCTTCCCCACCAAAACA	
TWIST M probe	VIC-AAACGATTTCCTTCCCCGCCGAAA	

HSIL/SCC. Differences in methylation levels of the investigated genes between LSIL and the negative group were not statistically significant. Therefore, the results from these two groups were combined and compared with HSIL/SCC. Based on the ROC-based threshold, we selected cutoff values and defined the promoter hypermethylation (positive vs. negative). The cutoff value was 0.1618% for APC, 0.3042% for HIN-1, 17.5339% for RAR-β, 0.4464% for RASSF1A, and 3.2976% for Twist. We calculated the sensitivities, specificities, and AUCs of methylation markers alone or in sequential combinations for the diagnosis of HSIL/SCC (Table 3).

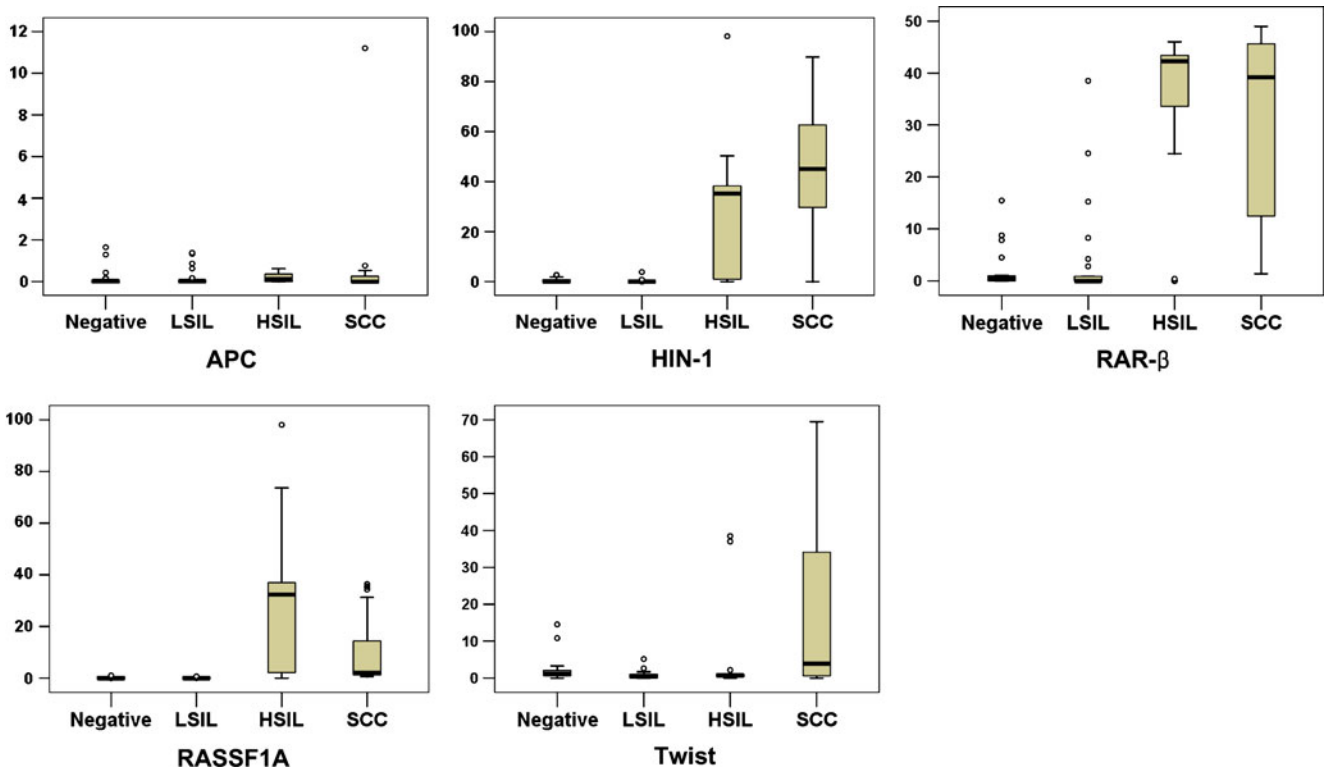

Fig. 1 Distribution of methylation levels for APC, HIN-1, RAR-β, RASSF1A, and Twist in cervical scrapings of negative, low-grade squamous intraepithelial lesion (*LSIL*), high-grade squamous intraepithelial lesion (*HSIL*), and squamous cell carcinoma (*SCC*). *Box plots* show the distribution of individual gene methylation across four subgroups. The *box* represents the middle 50% of the data. The *ends of the box* represent the 25th and 75th percentiles; the *bars* indicate the tenth and 90th percentiles, and a *horizontal line inside the box* shows the median. The *open circles outside the box* represent the extreme values

As shown in Table 3, the AUC for each individual gene except APC was significantly greater than 0.5, demonstrating that each of the four genes had the ability to distinguish HSIL/SCC from LSIL/negative samples (AUC=0.7438, 0.8080, 0.8111, and 0.6301 for HIN-1, RAR-β, RASSF1A, and Twist, respectively; $p<0.001$ for each gene). The AUC for RASSF1A was highest. RASSF1A had an HSIL/SCC detection sensitivity of 58.3%, with a specificity of 96.3%. The best two-gene combination was RASSF1A/Twist (area, 0.8560). The RASSF1A/Twist panel showed a sensitivity of 74.1% for HSIL/SCC and a specificity of 90.7%. The difference in AUC between RASSF1A and RASSF1A/Twist was statistically significant ($p=0.0341$). Addition of other genes did not improve the test performance in its ability to distinguish HSIL/SCC samples from combined LSIL/negative samples compared with RASSF1A/Twist. These data suggest that the two-gene panel (RASSF1A/Twist) was the ideal set to distinguish HSIL/SCC from LSIL/negative samples.

Discussion

Methylation analysis has shown great potential as a molecular tool for detection of cancer and its precursor lesions. In the present study, promoter hypermethylation of five genes known to be associated with cervical cancer carcinogenesis was examined in a full spectrum of cervical squamous lesions using QM-MSP. Detection of hypermethylation of at least one of two genes (RASSF1A and Twist) from exfoliated cell samples provided a sensitivity of 74.1% and a specificity of 90.7% for the detection of biopsy-confirmed HSIL/SCC.

Detection of cervical cancer at an early stage is the key to successful treatment and outcome. Although cervical cytology is the primary screening method used in the detection of SCC and its precursor lesion HSIL, the limitations of cervical cytology are well recognized [3, 4]. Therefore, reliable new markers for screening and diagnostic purposes are still needed.

Aberrant methylation of normally unmethylated CpG islands within the promoter regions of tumor-suppressor or cancer-related genes is a common epigenetic event leading to the silencing of gene expression in human cancers [23]. Numerous reports have demonstrated that tumor-suppressor genes belonging to nearly every cancer pathway or function category have silenced or diminished expression in cervical carcinoma due to abnormal promoter hypermethylation [6, 7]. In addition to the functional implications of promoter

Table 2 Methylation levels in negative, low-grade squamous intraepithelial lesion, high-grade squamous intraepithelial lesion, and squamous cell carcinoma samples

Gene	Methylation level (mean±SD)				*P* value					
	Negative (n=28)	LSIL (n=26)	HSIL (n=45)	SCC (n=63)	Overall[a]	Negative vs LSIL[b]	Negative vs HSIL[b]	Negative vs SCC[b]	LSIL vs HSIL[b]	LSIL vs SCC[b]	HSIL vs SCC[b]
APC	0.140±0.388	0.180±0.401	0.156±0.230	1.452±6.694	0.305	1.000	1.000	1.000	1.000	1.000	0.696
HIN-1	0.111±0.503	0.179±0.757	16.104±22.018	24.870±29.615	0.000	1.000	0.017	0.000	0.022	0.000	0.251
RAR-β	1.591±3.510	3.667±9.088	21.925±20.095	19.056±19.385	0.000	1.000	0.000	0.000	0.000	0.001	1.000
RASSF1A	0.053±0.196	0.044±0.144	16.938±22.680	7.945±15.669	0.000	1.000	0.000	0.157	0.000	0.180	0.020
Twist	2.075±3.170	0.797±1.109	7.561±13.246	11.835±16.239	0.000	1.000	0.410	0.004	0.171	0.001	0.479

SD standard deviation, *LSIL* low-grade squamous intraepithelial lesion, *HSIL* high-grade squamous intraepithelial lesion, *SCC* squamous cell carcinoma

[a] *P* value obtained using the nonparametric Kruskal–Wallis ANOVA test

[b] *P* value obtained using the Bonferroni correction

hypermethylation in cervical carcinogenesis, aberrant promoter methylation analysis on exfoliated cervical samples may be used as a diagnostic tool for cervical cancer screening [8–16, 18].

Liquid-based cervical cytology offers the advantage of providing a residual sample that can be used for methylation study. In our previous study, we evaluated the diagnostic efficiency of promoter hypermethylation in 12 genes in biopsy-proven SCC, HSIL, LSIL, and negative liquid-based cytology samples using a multiplex, nested MSP [18]. In ROC analysis, the three-gene combination (RAR-β, Twist, and MGMT) showed the best performance in distinguishing HSIL/SCC from LCIS/negative samples. The estimated specificity of this three-gene panel for detecting HSIL/SCC was 82.2%, and its sensitivity was 78.7%. These data suggest that aberrant DNA methylation has the potential to function as a molecular biomarker of HSIL and SCC in liquid-based cytology tests.

MSP, which has been widely used in previous studies, is limited by the fact that it provides only binary qualitative (negative or positive) results. Because of this technical limitation, MSP cannot reliably distinguish between low and high levels of methylation. As a result, QMSP has been developed in recent years to overcome this limitation of conventional MSP [19–21]. Fackler et al. developed a QM-MSP to enhance detection of low level DNA methylation for a panel of genes under conditions where the DNA concentration is limited [21]. The overall sensitivity of QM-MSP was one to ten methylated copies in 100,000 unmmethylated copies. This method allows for the setting of laboratory cutoffs of "normal" values for each gene and can more accurately segregate varied pathologic covariates based on appropriate cutoffs. In the present study, the presence of low levels of DNA methylation was observed in some negative and LSIL samples. However, based on the ROC-based cutoffs, we can reliably distinguish negative/LSIL from HSIL/SCC.

QMSP studies as a diagnostic tool for cervical neoplasia using cervical scrapings are rather sparse [10, 12–14, 16]. Furthermore, these studies have not included a full spectrum of cervical neoplasias. Wisman et al. studied promoter hypermethylation of 12 genes by QMSP in cervical scrapings obtained from cervical cancer patients (20 SCC and ten adenocarcinomas) and 19 controls with histologically normal cervices [12]. Combining four genes (CALCA, DAPK, ESR1, and APC) yielded a sensitivity of 89% (with all adenocarcinomas identified), equal to cytomorphology (89%) and high-risk human papilloma virus (HR-HPV, 90%). The four-gene QMSP proved theoretically superior to cytomorphology as well as HR-HPV in specificity (100% vs. 83% and 68%,

Table 3 Estimated sensitivity, specificity, and area under the curve of receiver-operating characteristic analysis for a panel of hypermethylated genes to distinguish HSIL/SCC samples from LSIL/negative samples

Gene panel	No. of HSIL/SCC samples with DNA hypermethylation detected/total no. of HSIL/SCC samples (%)	No. of LSIL/negative samples without DNA hypermethylation detected/total no. of LSIL/negative samples (%)	Sensitivity	Specificity	Area under the receiver-operating characteristic analysis curve (SE)	95% confidence interval
RASSF1A	63/108 (58.3)	52/54 (96.3)	58.3	96.3	0.8111 (0.0326)	0.75–0.88
RAR-β	54/108 (50.0)	52/54 (96.3)	50.0	96.3	0.8080 (0.0337)	0.74–0.87
HIN-1	58/108 (53.7)	51/54 (94.4)	53.7	94.4	0.7438 (0.0373)	0.67–0.82
Twist	38/108 (35.2)	51/54 (94.4)	35.2	94.4	0.6301 (0.0429)	0.55–0.71
APC	30/108 (27.8)	46/54 (85.2)	27.8	85.2	0.4777 (0.0469)	0.39–0.57
Two-gene combination						
RASSF1A / RAR-β	67/108 (62.0)	50/54 (92.9)	62.0	92.9	0.8386 (0.0300)	0.78–0.90
RASSF1A / HIN-1	66/108 (61.1)	49/54 (90.7)	61.1	90.7	0.7866 (0.0326)	0.73–0.85
RASSF1A / Twist	80/108 (74.1)	49/54 (90.7)	74.1	90.7	0.8560[a] (0.0286)[a]	0.80–0.91
Three-gene combination						
RASSF1A/Twist/RAR	82/108 (75.9)	47/54 (87.0)	75.9	87.0	0.8522 (0.0292)	0.80–0.91
RASSF1A/Twist/HIN	82/108 (75.9)	46/54 (85.2)	75.9	85.2	0.8515 (0.0292)	0.79–0.91
Four						
RASSF1A/Twist/RAR	83/108 (76.9)	45/54 (83.3)	76.9	83.3	0.8524 (0.0291)	0.80–0.91

LSIL low-grade squamous intraepithelial lesion, *HSIL* high-grade squamous intraepithelial lesion, *SCC* squamous cell carcinoma

[a] $P=0.0341$ for RASSF1A/Twist versus RASSF1A

respectively). Using QMSP, Kahn et al. analyzed the frequency and relative level of promoter methylation for DAPK1, IGSF4, SPARC, and TFPI2 in biopsy-confirmed 39 HSIL, 30 LSIL, and 30 negative residual liquid-based Pap tests [14]. For each gene analyzed, the frequency and relative level of methylation were increased in HSIL compared with combined negative/LSIL samples. The AUC demonstrated that methylation of each gene could distinguish HSIL from negative/LSIL samples. The combination of four genes showed improved test performance. Apostolidou et al. recently studied 28 candidate hypermethylated genes in 96 liquid-based samples using QMSP and demonstrated that the methylation status of SOX1, HOXA11, and CADM1 is able to discriminate between HSIL cases and negative controls, achieving high sensitivity and specificity [16].

In the present study, we evaluated methylation levels of five genes in a full spectrum of cervical squamous neoplasias, including 26 LSIL, 45 HSIL, 63 SCC, and 28 negative samples using QM-MSP. Methylation levels of HIN-1, RAR-β, RASSF1A, and Twist were increased in HSIL and SCC, compared with either negative or LSIL samples. In ROC analysis, four genes (HIN-1, RAR-β, RASSF1A, and Twist) had the ability to distinguish HSIL/SCC from LSIL/negative samples. The two-gene combination (RASSF1A/Twist) showed the best performance in distinguishing HSIL/SCC from LSIL/negative samples. The estimated specificity of this two-gene panel for detecting HSIL/SCC was 90.7%, and its sensitivity was 74.1%. We believe methylation analysis using QMSP could serve as the basis of a relatively sensitive and specific primary screening assay to detect cervical SCC and its immediate precursor, HSIL.

Our study is limited not only by the small number of genes but also by the relatively modest number of cases tested, which impact its statistical power. Therefore, additional studies are needed to elucidate the role of methylation markers in cervical scraping samples as a tool for detection of SCC/HSIL. Moreover, 100% sensitivity could not be reached by increasing the number of genes analyzed, pointing to the fact that the ideal combinations still need to be defined.

In conclusion, we found that QM-MSP may be useful for HSIL/SCC detection in residual liquid-based cervical cytology samples. Further studies are needed to identify additional genes that are selectively methylated in HSIL/SCC and to determine the optimal combination of genes that will provide increased clinical sensitivity while maintaining high specificity.

Acknowledgements This study was supported by a grant of the Korea Healthcare Technology R&D Project, Ministry of Health and Welfare, Republic of Korea (A080075) to Ji Shin Lee.

Conflict of interest The QM-MSP method is licensed by OncoMethylome Sciences, and the terms of this arrangement are being managed by the Johns Hopkins University in accordance with its conflict of interest policies.

References

1. Shin HR, Jung KW, Won YJ et al (2007) National cancer incidence for the year 2002 in Korea. Cancer Res Treat 39:139–149
2. Pisani P, Bray F, Parkin DM (2002) Estimates of the world-wide prevalence of cancer for 25 sites in the adult population. Int J Cancer 97:72–81
3. Nanda K, McCrory DC, Myers ER et al (2000) Accuracy of the Papanicolaou test in screening for and follow-up of cervical cytologic abnormalities: a systematic review. Ann Intern Med 132:810–819
4. Kulasingam SL, Hughes JP, Kiviat NB et al (2002) Evaluation of human papillomavirus testing in primary screening for cervical abnormalities: comparison of sensitivity, specificity, and frequency of referral. JAMA 288:1749–1757
5. Patel A, Groopman JD, Umar A (2003) DNA methylation as a cancer-specific biomarker: from molecules to populations. Ann N Y Acad Sci 983:286–297
6. Dong SM, Kim HS, Rha SH, Sidransky D (2001) Promoter hypermethylation of multiple genes in carcinoma of the uterine cervix. Clin Cancer Res 7:1982–1986
7. Virmani AK, Muller C, Rathi A, Zoechbauer-Mueller S, Mathis M, Gazdar AF (2001) Aberrant methylation during cervical carcinogenesis. Clin Cancer Res 7:584–589
8. Widschwendter A, Gattringer C, Ivarsson L et al (2004) Analysis of aberrant DNA methylation and human papillomavirus DNA in cervicovaginal specimens to detect invasive cervical cancer and its precursors. Clin Cancer Res 10:3396–3400
9. Gustafson KS, Furth EE, Heitjan DF, Fansler ZB, Clark DP (2004) DNA methylation profiling of cervical squamous intraepithelial lesions using liquid-based cytology specimens: an approach that utilizes receiver-operating characteristic analysis. Cancer 102:259–268
10. Reesink-Peters N, Wisman GB, Jéronimo C et al (2004) Detecting cervical cancer by quantitative promoter hypermethylation assay on cervical scrapings: a feasibility study. Mol Cancer Res 2:289–295
11. Feng Q, Balasubramanian A, Hawes SE et al (2005) Detection of hypermethylated genes in women with and without cervical neoplasia. J Natl Cancer Inst 97:273–282
12. Wisman GB, Nijhuis ER, Hoque MO et al (2006) Assessment of gene promoter hypermethylation for detection of cervical neoplasia. Int J Cancer 119:1908–1914
13. Shivapurkar N, Sherman ME, Stastny V et al (2007) Evaluation of candidate methylation markers to detect cervical neoplasia. Gynecol Oncol 107:549–553
14. Kahn SL, Ronnett BM, Gravitt PE, Gustafson KS (2008) Quantitative methylation-specific PCR for the detection of aberrant DNA methylation in liquid-based Pap tests. Cancer 114:57–64
15. Lai HC, Lin YW, Huang TH et al (2008) Identification of novel DNA methylation markers in cervical cancer. Int J Cancer 123:161–167
16. Apostolidou S, Hadwin R, Burnell M et al (2009) DNA methylation analysis in liquid-based cytology for cervical cancer screening. Int J Cancer 125:2995–3002
17. Widschwendter M, Jones PA (2002) The potential prognostic, predictive, and therapeutic values of DNA methylation in cancer. Commentary re: J. Kwong et al., Promoter hypermethylation of multiple genes in nasopharyngeal carcinoma. Clin. Cancer Res., 8: 131–137, 2002, and H-Z. Zou et al., Detection of aberrant p16 methylation in the serum of colorectal cancer patients. Clin. Cancer Res., 8: 188–191, 2002. Clin Cancer Res 8:17–21
18. Kim JH, Choi YD, Lee JS, Lee JH, Nam JH, Choi C (2010) Assessment of DNA methylation for the detection of cervical neoplasia in liquid-based cytology specimens. Gynecol Oncol 116:99–104
19. Jerónimo C, Usadel H, Henrique R et al (2001) Quantitation of GSTP1 methylation in non-neoplastic prostatic tissue and organ-confined prostate adenocarcinoma. J Natl Cancer Inst 93:1747–1752
20. Cottrell SE, Laird PW (2003) Sensitive detection of DNA methylation. Ann N Y Acad Sci 983:120–130
21. Fackler MJ, Malone K, Zhang Z et al (2006) Quantitative multiplex methylation-specific PCR analysis doubles detection of tumor cells in breast ductal fluid. Clin Cancer Res 12:3306–3310
22. Swift-Scanlan T, Blackford A, Argani P, Sukumar S (2006) Fackler MJ (2006) Two-color quantitative multiplex methylation-specific PCR. Biotechniques 40:210–219
23. Baylin SB (2005) DNA methylation and gene silencing in cancer. Nat Clin Pract Oncol Suppl 1:4–11

Virchows Arch (2010) 457:43–51
DOI 10.1007/s00428-010-0910-z

ORIGINAL ARTICLE

Cytological detection of papillary thyroid carcinomas by nuclear membrane decoration with emerin staining

Sofia Asioli · Francesca Maletta · Donatella Pacchioni · Rosanna Lupo · Gianni Bussolati

Received: 9 February 2010 / Revised: 26 February 2010 / Accepted: 16 March 2010 / Published online: 26 May 2010
© Springer-Verlag 2010

Abstract Decoration of the nuclear membrane by emerin staining enhances detection of nuclear irregularities typical of papillary thyroid carcinoma (PTC). Our study aims to verify whether staining with emerin is a helpful diagnostic marker in fine-needle aspiration (FNA) cytology. We first designed a prospective study on smears, Thin Prep, and cell block specimens to prove the feasibility of the procedure; subsequently, we designed a retrospective study of 78 FNA cell blocks from cases that, after surgery, turned out to be either benign (34 cases) or malignant lesions (44, of which 31 PTC). From each sample, we obtained two slides, one stained with hematoxylin and eosin (H&E) and the other with emerin. In cases classified as Thy3, HBME-1 and galectin 3 (Gal3) stains had also been performed. Two blinded observers made the judgment concerning Thy categories (as proposed by the British Thyroid Association), first on H&E, then on emerin, HBME-1, and Gal3 stained slides. On cytological preparation, emerin staining represents an effective tool for the detection of nuclear irregularities, allowing for the identification of cases of PTC. In Thy3 cases, emerin staining's sensitivity and specificity (64% and 96%) proved higher than HBME-1's (60% and 88%) and Gal3's (61% and 68%). In conclusion, the immunohistochemical definition of the nuclear membrane, as determined by emerin stain, is a useful tool in the cytological diagnosis of thyroid lesions and can help to solve inconclusive cases by highlighting nuclear irregularities typical of PTC.

Keywords Emerin · Thy3 · Cytology · Thyroid · HBME-1

Condensed abstract Emerin staining is a useful tool in the cytological diagnosis of thyroid lesions. It enhances detection of nuclear irregularities typical of papillary thyroid carcinoma, thus helping to solve inconclusive fine-needle aspiration biopsy cases.

S. Asioli (✉) · F. Maletta · D. Pacchioni · R. Lupo · G. Bussolati
Department of Biomedical Sciences and Human Oncology,
Molinette Hospital, University of Turin,
Via Santena 7,
10126 Turin, Italy
e-mail: sofia.asioli@unito.it

Introduction

The shape of the nucleus, including the presence of nuclear grooves and inclusions, coupled with changes in chromatin distribution, remains the basic microscopic criterium for the cytological diagnosis of papillary thyroid carcinoma (PTC).

Recently, we reported that tagging the nuclear membrane (NM) with antibody anti-emerin (a protein of the inner nuclear membrane) is a novel and valuable tool for the diagnosis of thyroid lesions [1]. Unlike previous immunocytochemical (ICC) studies [2–9] traditionally based on the expression of various markers such as galectin 3 (Gal3), Hector Battifora mesothelial antigen-1 (HBME-1), cytokeratin 19, and insulin-like growth factor mRNA binding protein 3 (IMP3), our approach highlights morphological details rather than aiming to detect expression of differentiation markers.

In fact, the immunohistochemical identification of molecules, such as emerin, specifically linked to fine structural components hard to detect with classical staining techniques (H&E), can allow for the detection of such components on light microscopy.

It should be noted that the traditional microscope observation of the NM irregularities typical of PTC nuclei is indirect and is based on nucleic acid staining with basic dyes, such as hematoxylin. In fact, because some parts of hetero-chromatin are strongly linked to the NM, by using

hematoxylin stain, we can indirectly obtain information on the NM itself.

As previously reported [1], staining for emerin highlights irregularities, indentations, and invaginations of the NM, thus allowing for a more definite and objective recognition of PTC diagnostic features, especially in problematic cases such as in the follicular variant of PTC (FVPTC). In emerin-stained slides, in fact, the criteria to make a diagnosis of PTC remain basically the same as in H&E slides, that is presence of NM irregularities, such as indentations, grooves, and nuclear pseudoinclusions.

In the present study, we questioned whether tagging the NM by emerin staining could improve the pre-operative cytological diagnosis of PTC. The study plan involved a prospective analysis conducted in a limited number of Thin Prep preparations, alcohol-fixed smears, and cell blocks from fine-needle aspiration biopsies (FNABs), which proved the feasibility of the procedure. Moreover, the diagnostic impact of our approach was checked retrospectively on cell blocks of cases following FNAB diagnosis. In particular, we focused our attention on cell blocks of 53 cases with a final histological diagnosis, where the pre-operative FNABs could not define the lesion as benign or malignant and, thus, were classified as Thy3 according to the guidelines of the British Thyroid Association, Royal College of Physicians, London, UK [10]. In our case study, besides, we decided to include several cases of FVPTC belonging to the Thy3 category because our intention was to test this ICC marker on one of the most problematic lesion to diagnose on FNABs and to value its ability to highlight NM irregularities, which on H&E are only focal [2].

Materials and methods

Smears and Thin Prep® (prospective study)

From ten thyroid nodules sampled with FNAB, we collected alcohol-fixed smears, preparations processed by the liquid-based thin-layer cytology Thin Prep 2000™ method (Cytyc Co., Marlborough, MA) [11], as well as cell blocks. In eight cases, a final diagnosis of a benign lesion (Thy2) was made based on H&E staining, while the remaining two cases were diagnosed as PTC (Thy5). These ten cases were used as control cases for emerin staining.

In addition, we collected five cases each of smears and Thin Preps already stained with H&E and with an established diagnosis of PTC. The slides were unmounted and processed for ICC staining. Tracing on the ICC preparations of the same area, previously recorded in H&E, allowed for the proper interpretation of the images.

For ICC staining with emerin, slides brought to phosphate-buffered saline were processed with peroxidase inhibition for 8 min. Antigen retrieval was then achieved by treatment for 30 min in citrate buffer (pH 6) at 98°C. Incubation with emerin antibody (monoclonal antibody, clone 4G5, diluted 1:50; Novocastra Laboratories, Newcastle, UK) for 1 h at 37°C was followed by incubation with secondary antibody (EnVision anti-mouse prediluted, Dako, Denmark) for 30 min and diaminobenzidine for 3 min. Finally, the slides were counterstained with light green (EA50, Merck, Darmstadt, Germany) and mounted in balsam.

Cell blocks (retrospective study)

In order to validate the impact of emerin staining on the diagnosis of PTC cases, we retrospectively collected 78 cases of cell blocks from thyroid FNABs performed at our Diagnostic Service, where thyroid FNABs are customarily processed as follows: after assessment of adequacy by quick smear of the samples, the residual material is fixed in alcohol, collected by centrifugation, then routinely processed and paraffin-embedded to obtain a cell block. Paraffin sections were stained with H&E and in cases morphologically classified as Thy3, ICC staining was also performed with antibodies anti-HBME-1 (HBME-1, 1/40 Dako, Carpinteria, CA, USA) and Gal3 (clone 9C4, prediluted, Ventana, Tucson, AZ, USA). ICC was performed according to a standard automated immunohistochemical procedure (BenchMark AutoStainer, Ventana Medical Systems, Tucson, AZ, USA). Immunoreactions were processed using a biotin-free dextran-chain detection system (Envison, dakoCytomation, Carpinteria, CA, USA) and developed with diaminobenzidine as the chromogen.

For the retrospective study, cases were selected according to the following criteria:

1. cell blocks available for immunohistochemical analysis;
2. histologically established diagnosis following operation;
3. clinical and/or radiological follow-up data available.

The original cytological diagnosis on pre-operative FNABs had been made by DP and GB and formulated according to diagnostic category reported by the guidelines of the British Thyroid Association, Royal College of Physicians, London, UK [10]. In this study, we did not include samples with insufficient materials for a cytological diagnosis (Thy1 category).

Clinical–radiological follow-up data were obtained from case record review and correspondence with referring clinicians. A final histological diagnosis followed the diagnostic criteria for definition of follicular thyroid proliferation reported in the current published studies [10, 12–16].

More specifically, follicular carcinoma (FC) was diagnosed at histology when capsular and/or vascular invasion were unequivocally present [12, 17]. PTC and its variants were diagnosed on the basis of nuclear features (i.e., nuclear clearing, grooves, and pseudoinclusions) and papillary or follicular architecture (or both) [13–15, 17, 18]. Poorly differentiated carcinoma (PDC) was diagnosed according to the "Turin proposal criteria" [16]. An encapsulated follicular neoplasm with obvious capsular invasion, but questionable nuclear features of PTC was diagnosed as "well-differentiated carcinoma, not otherwise specified" [19].

New paraffin sections from the 78 selected cases were stained with H&E and for emerin staining, as described elsewhere [1].

The H&E and emerin-stained slides, as well as previously stained preparations of the same cases, were independently and separately reviewed by two pathologists (SA and GB) blinded to both cytological and histological diagnosis; they classified each case, judging H&E-, emerin-, HBME-1-, and Gal3-stained slides separately, following the classification proposed by the British Thyroid Association. Thus, we obtained for each case, two diagnosis, for H&E- and emerin-stained preparations respectively, expressed as Thy categories. Cases described as "suspicious of malignancy" and "diagnostic of malignancy" were classified as Thy4 or Thy5 categories, respectively. "Non-neoplastic lesions" and "follicular lesions" were classified as Thy2 and Thy3 categories, respectively.

Statistical analysis

Sensitivity, specificity, and accuracy values of FNABs when using H&E and emerin tests were assessed, as reported elsewhere [20]. True negative cases were Thy2 and Thy3 lesions which were benign at final histology; true positive cases were Thy4 and Thy5 lesions which were malignant at final histology, false negative cases were Thy2, Thy3 lesions, malignant at final histology, and false positive cases were Thy4 and Thy5 lesions, benign at final histology. We calculated sensitivity and specificity of the test using H&E and emerin staining both in the 78 cases and in the subgroup of 31 cases diagnosed as PTC (follicular or classical variant). Determination of inter-observer variability was performed on 78 cases using the Cohen–Fleiss test [21, 22].

In cases where the two observers did not agree in the diagnosis, they came up with a consensus interpretation by re-classifying the preparation together.

Finally, we calculated sensitivity and specificity for HBME-1 and Gal3 stains in all Thy3 cases. Immunostaining for HBME-1 was considered positive in the presence of ≥10% immunoreactive neoplastic cells [9].

All statistical analyses were carried out using SPSS 17 software (SPSS Inc., IBM Company, Chicago, Illinois, USA).

Results

Prospective study

Emerin staining is feasible in alcohol-fixed smears and Thin Preps and emphasizes the distribution of the nuclear membrane. Smears and Thin Preps from cases with a definite cytological diagnosis of malignancy (Thy5) and with a final histological diagnosis of PTC showed strongly positive emerin staining along the nuclear membrane and nuclear irregularities with foldings, grooves, and pseudoinclusions could easily be appreciated (Fig. 1i–q).

By recording H&E cytological images, unmounting, and then restaining for emerin (see "Materials and methods"), we were able to prove the superior definition of the NM distribution as allowed by the ICC staining (Fig. 1a–h).

Retrospective study

Based on the results obtained with the above prospective study, proving the feasibility of the approach, a retrospective study was performed to validate the impact of emerin stain in order to enhance the cytological diagnosis on thyroid nodules.

The study group included 78 cases, 61 women and 17 men, with a mean age of 46 years (range 16–81). Mean size of the single or dominant nodule that was studied was 2.6 cm (range 0.5–7).

On H&E staining, the 78 FNABs were classified as Thy2 in 8 cases, as Thy3 in 53 cases, as Thy4 in 14 cases, and as Thy5 in 3 cases. Inter-observer agreement between the two pathologists (SA and GB), after the observation of slides under H&E staining in all 78 cases, was moderate (K of Cohen–Fleiss=0.4878; $p<0.005$) [21, 22].

Upon histological evaluation, the lesions were diagnosed as the following: goiter in 22 cases, of which 3 cases showed oxyphilic features and 2 cases were associated with papillary hyperplasia; adenoma in 12 cases; follicular carcinoma in 9 cases; PTC in 31 cases, of which 25 were of the follicular variant and 6 were of the classical variant; PDC in 3 cases and well-differentiated carcinoma, not otherwise specified in 1 case.

The correlation of a fine needle aspiration cytology diagnosis with both histological diagnosis and follow-up on H&E staining of all 78 thyroid nodules is summarized in Table 1. The operating characteristics yielded from pathologic evaluation are 36.36% sensitivity, 97.06% specificity, and 62.82% accuracy.

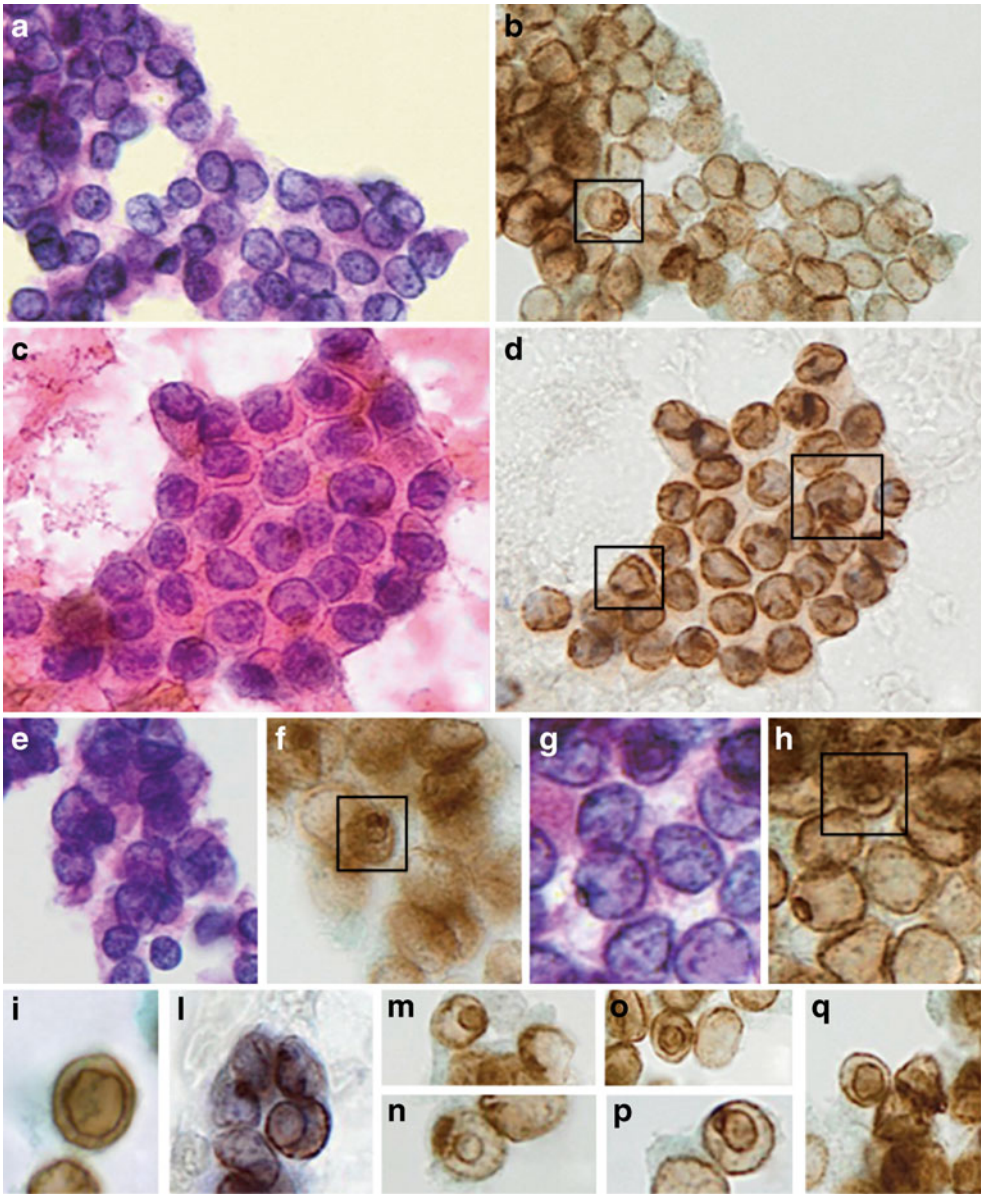

Fig. 1 Immunoperoxidase staining for emerin provides direct identification of the diagnostic features, such as typical "nuclear pseudoinclusions" (*squares*), grooves, and crescent-like figures in PTC both on Thin Prep preparations (**a**, **b**, **e**, **f**, **i**, **m**–**q**) and smears (**c**, **d**, **g**, **h**, **l**), and which are not fully appreciable on H&E slides. At high power (×40), emerin staining highlights pseudoinclusions and other nuclear irregularities (**i**–**q**)

The data obtained with emerin staining are summarized in Figs. 2 and 3. The 78 nodules were classified on the basis of emerin staining alone as Thy2 in 6 cases, as Thy3 in 36 cases, as Thy4 in 19 cases, and as Thy5 in 17 cases; in particular, emerin staining modified H&E staining classification in 2/8 cases of Thy2 as Thy3; 13/53 cases of Thy3 as Thy4, 6/53 cases of Thy3 as Thy5, and 8/14 cases of Thy4 as Thy5.

Inter-observer agreement between the two pathologists (SA and GB) concerning the classification of the Thy value after the observation of emerin staining in all 78 cases was substantial (K of Cohen–Fleiss=0.6890; $p<0.005$).

The correlation of the diagnosis by fine needle aspiration cytology with both histological diagnosis and follow-up on emerin staining of all 78 thyroid nodules is summarized in Table 1, which shows an improvement of sensitivity

Table 1 Comparison between sensitivity, specificity, and accuracy of FNABs when using H&E staining and emerin staining in the cytological diagnosis of 78 cases

	H&E stain	Emerin stain
Sensitivity	36.36% (16/44)	77.27% (34/44)
Specificity	97.06% (33/34)	94.12% (32/34)
Accuracy	62.82% (49/78)	84.61% (66/78)
Inter-observer concordance	0.4878 (moderate agreement)	0.6890 (substantial agreement)

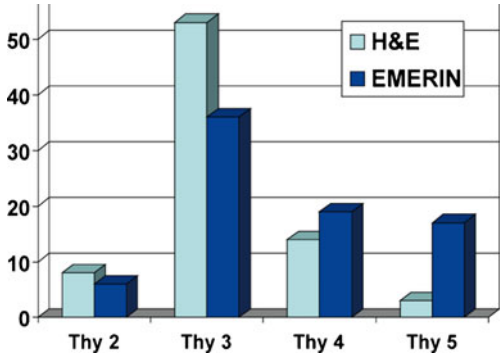

Fig. 2 Comparison between H&E and emerin samples' classification in Thy categories in all cases (78 cases)

(77.27%), specificity (94.12%), and accuracy (84.61%) of FNABs when using emerin.

Focusing specifically on 31 specific cases diagnosed as PTC at histology, 17 cases (16 FVPTC and 1 classical PTC at histology) had originally been classified as Thy3 on H&E staining, while emerin staining modified the diagnosis in 11/17 (all FVPTC, at histology) cases upgrading them to Thy4 and in 6/17 cases to Thy5 (5 FVPTC and 1 classical PTC at histology). In the 13 cases originally classified as Thy4 on H&E staining, emerin staining increased the classification to Thy5 in 8 cases (all FVPTC at histology) (Fig. 2). Thus, the measurement of the correlation of FNA cytological diagnosis of the 31 PTC cases (both classical and follicular variant) on emerin staining with histological diagnosis showed a sensitivity of 100%, since in all PTC cases, emerin staining proved able to upgrade or to confirm the lesion in the Thy4 or Thy5 categories.

Considering Thy3 cases only, sensitivity and specificity in the detection of malignancy were respectively 64.28% and 96% for FNABs when using emerin, 60.71% and 88% for HBME-1, and 60.71% and 68% for Gal3 (Table 2).

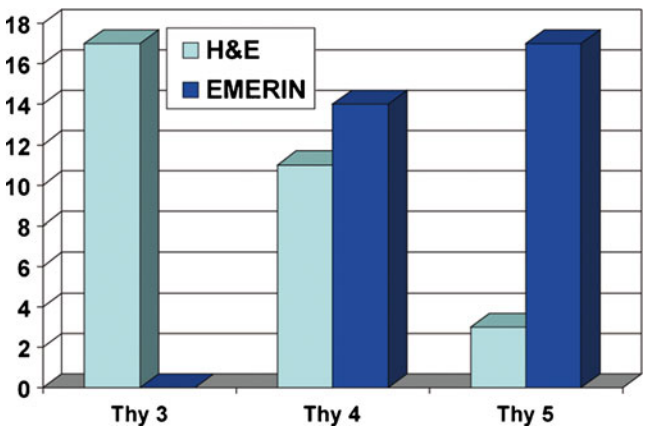

Fig. 3 Comparison between H&E and emerin samples' classification in Thy categories in papillary thyroid carcinomas cases (31 cases)

Table 2 Comparison of sensitivity and specificity of FNABs when using emerin, HBME-1, and Gal3 stains in the cytological diagnosis of 53 cases classified as Thy3 at H&E

	Emerin	HBME-1	Gal3
Sensitivity	64.28% (18/28)	60.71% (17/28)	60.71% (17/28)
Specificity	96.00% (24/25)	88.00% (22/25)	68.00% (17/25)

Discussion

Thyroid FNABs are specifically designed to screen and detect malignant nodules, and related cytological criteria for fine morphological definition have been devised. In fact, the attained specificity and sensitivity make this pre-operative test highly practical and reliable. However, a relative percentage of cases still remains undefined and is collectively grouped into the Thy3 definition [14, 18, 23]. Recently, a modified classification system of thyroid biopsy results into six categories, including unsatisfactory, has been proposed [24]. In particular, the authors separated the indeterminate category into three subroups: (1) indeterminate for neoplasia, (2) follicular neoplasm, and (3) suspicious for malignancy. They concluded that the 6-tier reporting system for thyroid FNA was effective for determining which patients needed surgery versus follow-up FNA and also guided the clinician concerning the extent of surgery.

In order to select among the undefined cases, those corresponding to malignant lesions and in need of operation, several authors have proposed a number of ancillary procedures. Immunohistochemical and molecular markers (e.g., high-molecular-weight cytokeratin, cytokeratin 19, IMP3, galectin-3, HBME-1, CD57, CITED1, fibronectin-1, CD15, CD44, platelet-derived growth factor, BRAF and *ras* mutations or RET/PTC translocation) were considered helpful in confirming a diagnosis of PTC [3–9, 25–27]. Nevertheless, the real impact of ancillary immunohistochemical markers in the pre-operative detection of malignant thyroid lesions is under debate, and various authors have found these studies not discriminatory enough to distinguish PTC from other follicular lesions [2, 28].

The present ICC approach, in contrast to previous studies, is not focused on the detection of differentiation markers, but on the morphological criteria describing the irregularity of the nuclear membrane, hence the use of light microscopical features, which already play a pivotal role in established diagnostic criteria. The present study, which extended the findings of our previous histological investigations [1], demonstrates the feasibility of emerin staining on cytological smears and Thin Preps, as well as on cell blocks. Comparison on the same nuclei of the H&E and ICC staining (Fig. 1) clearly shows the superior ability of

ICC for the definition and detection of NM irregularities and invaginations of PTC nuclei. The technique here proposed by restaining smears could thus play a role in the definition of unclear cases.

To determine if this novel ICC approach could solve, at least in part, problematic and undefined cases classified as Thy3, we undertook a retrospective study on 78 cases of FNABs, inclusive of 53 cases of Thy3 where a final definite histological diagnosis was established. We compared categorization of lesions [10] based on H&E- and emerin-stained slides and found a remarkable difference in sensitivity between these two stains (36.36% and 77.27%, respectively), thus implying that emerin staining is able to improve detection of malignant lesions; however, it is important to highlight that the low sensitivity value of FNABs reported in this study should be referred to this

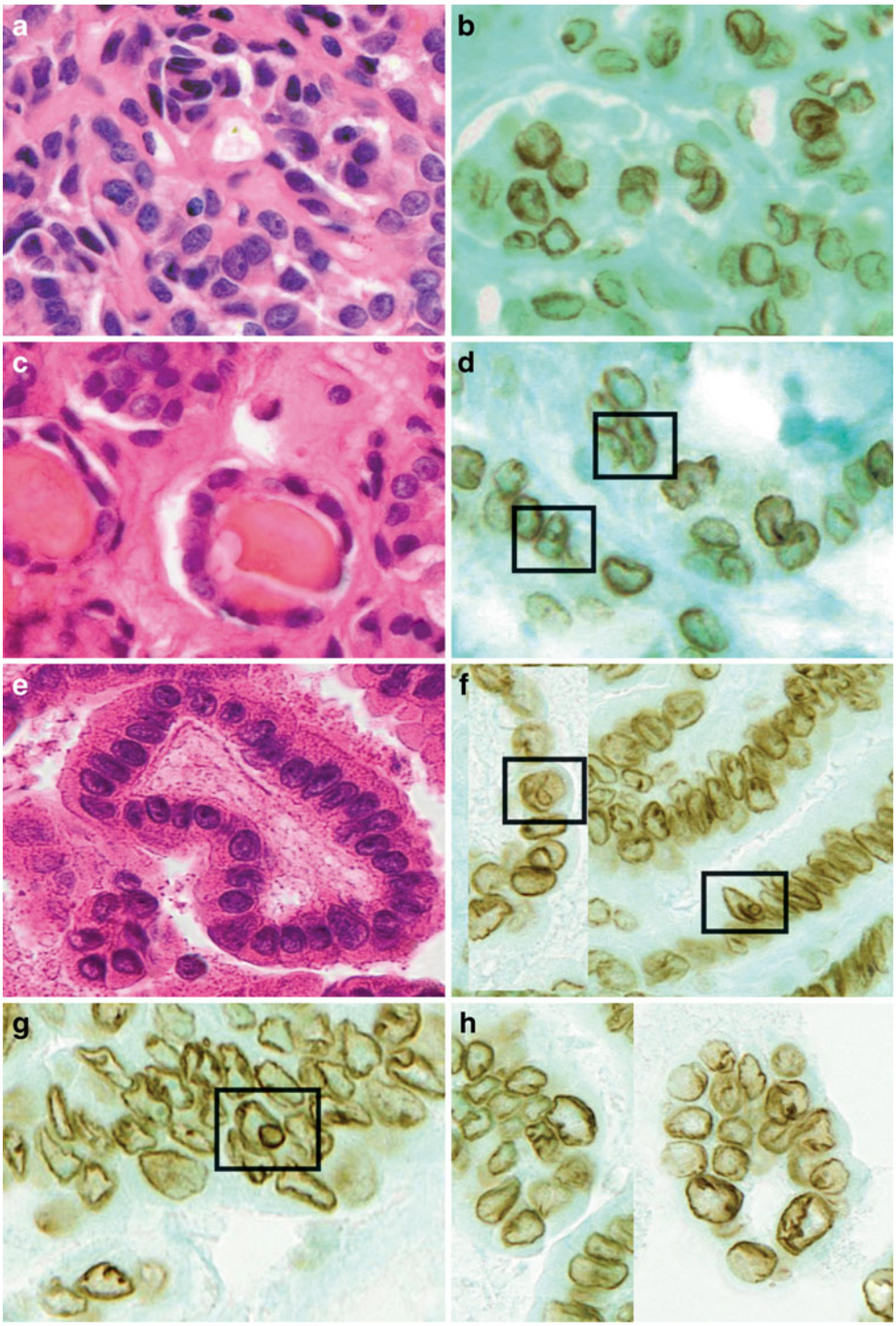

Fig. 4 Emerin staining in cell blocks: examples of PTC, follicular variant (**a**–**d**) and classical type (**e**–**h**). H&E preparations (**a**, **c**, **e**) show follicular and papillary lesions with dark nuclei and some irregularities. In emerin-stained preparations (**b**, **d**, **f**–**h**), nuclear irregularities, such as pseudoinclusions (*square*), crescent-like aspect, and grooves, are enhanced

particular case study only, which includes for a selection bias a majority of Thy3 and FVPTC cases and should not be extended to the complete spectrum of thyroid lesions, where FNABs reach very high sensitivity (92%) and accuracy levels (95%) [14, 18]. Thus, our aim is to compare sensitivity of FNABs when using H&E with FNABs when using emerin (in addition to H&E) in this subset of lesions, and the value of FNABs sensitivity here reported has no general value.

Since this innovative approach is based on morphological features rather than on the expression of markers, the subjectivity of the interpretation might be a problem: to overcome this difficulty, we assessed the inter-observer variability between two pathologists on emerin-stained slides and compared it to that observed on H&E-stained slides; we found a substantial agreement on emerin (K of Cohen–Fleiss=0.6890), superior to the one observed on H&E (K of Cohen–Fleiss=0.4878). Moreover, before analyzing all cases, the two observers established the following criteria: cases classified as Thy2 and Thy3 at H&E and presenting a majority of round or oval and regular nuclei on emerin-stained slides were confirmed in these categories; Thy2 lesions with some irregularities of NM shape like folds, grooves, or crescent-like figures were moved to the Thy3 category; all lesions presenting on emerin slides with marked nuclear irregularities in a substantial number (>30%) of cells were moved to the Thy4 category and, if pseudoinclusions were present, to the Thy5 category.

When considering our results, we found that ICC staining for emerin on paraffin sections from the related cell blocks led to a definition of two separate sets: those presenting with round or oval nuclei with smoothly linear NM and those with irregular NM folds. Linear grooves were frequent in the latter, but also occasionally appreciated in the former. Cases originally defined as Thy2 that correctly corresponded histologically to benign lesions presented with a uniformly round and regularly defined NM, as detected by emerin staining. Cases defined as Thy2 or Thy3 on H&E preparations and showing round and regular nuclei were confirmed in these categories. With regard to Thy4 and Thy5, lesions were included in these categories when marked irregularities, such as grooves and pseudoinclusions, were observed in a substantial number (>30%) of tumor cells. Nevertheless, we observed that the above criteria could not be applied in the case of oxyphilic lesions, since in at least two cases, cytological detection of extensive groovings (but no pseudoinclusions) corre-

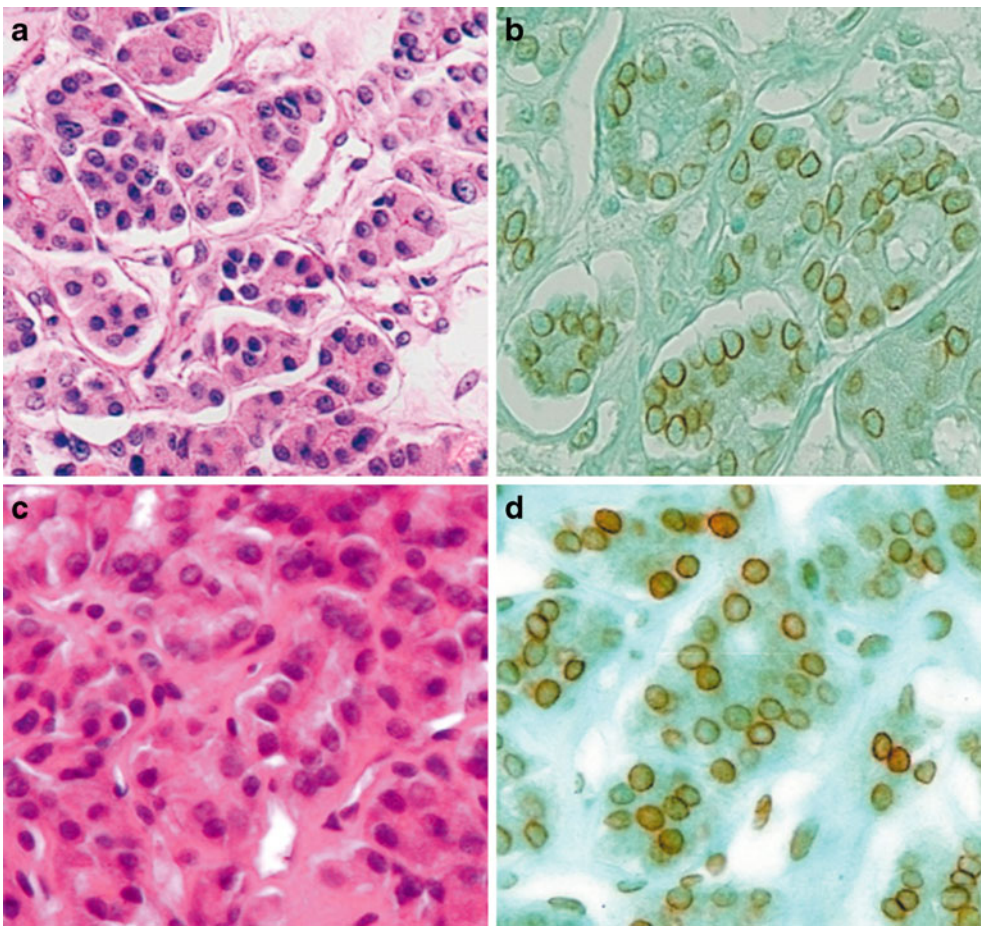

Fig. 5 Emerin staining in cell blocks: examples of goiter (**a**, **b**) and follicular adenoma (**c**, **d**). H&E preparations (**a**, **c**) show follicular lesions with dark nuclei but some irregularities. In emerin-stained preparations (**b**, **d**), nuclear irregularities are absent, with no pseudoinclusions or grooves

sponded histologically to oxyphilic areas in goiters [1, 29]. On the other hand, cases originally defined as Thy4 or Thy5, and later found to correspond to PTC (five classical type and eight follicular variant PTC) presented on emerin staining with an increased evidence of NM irregularities (Fig. 4).

Cases pre-operatively defined as Thy3 that corresponded histologically to goiters (13 cases), adenomas (12 cases), FC (9 cases), and PDC (1 case) presented with uniform, round, and regularly defined NM (Fig. 5). In 17 PTC cases (16 follicular variant and 1 classic PTC), emerin staining highlighted irregularities of the NM, namely grooves and pseudoinclusions in the nuclei. In 1 PDC case, it detected typical convoluted nuclei [16].

Moreover, in the Thy3 category, we compared the performance of emerin and HBME-1 in detecting malignancy and found superior sensitivity and specificity for FNABs when using emerin stain (64.28% and 96%, respectively) when compared to HBME-1 (60.71% and 88%, respectively). Emerin stain allowed for recognition of all PTC cases, while HBME-1 missed 7 cases of PTC. However, emerin was not able to detect any FC cases, while HBME-1 detected 5/9 FC cases. In the 2 PDC cases, HBME-1 detected both cases, while emerin identified only 1 PDC. In benign lesions, emerin overestimated the nature of the lesion in 1/25 cases (FA), while HBME-1 did so in 3/25 (2 goiters and 1 FA). The value of HBME-1 sensitivity might be due, at least in part, to the presence of 4 oxyphilic lesions (1 FVPTC and 3 FC) [30]. Gal3 stain proved less sensitive and specific than emerin and HBME-1 (Table 2).

In conclusion, emerin staining can be useful for the correct identification of PTC nuclei. Indeed, in cytological specimens, it is confirmatory in Thy2, Thy4, and Thy5 categories while it discriminates FVPTC among follicular lesions classified as Thy3. ICC for emerin staining can be performed on smears, even after H&E staining. Thus, it might be an optimal procedure in those cases currently classified as Thy3 (which in our experience reflects 10–20% of FNA exams) when the pathologist is unable to determine with confidence the nature of the lesion.

Acknowledgements The authors are grateful to *Luigi Chiusa, MD* (Department of Biomedical Sciences and Human Oncology University of Turin, Italy) for statistical support, to *Nicola Palestini, MD* (General Surgery 1, San Giovanni Battista Hospital, Turin, Italy), to *Marco Gallo, MD* (Oncological Endocrinology, San Giovanni Battista Hospital, Turin, Italy) and to *Ruth Rossetto, MD* (Endocrinology, San Giovanni Battista Hospital, Turin, Italy) for their help in providing clinical and follow-up information.

This study was supported by MIUR (ex-60%, SA); Ricerca Sanitaria Finalizzata Piedmont Region, Italy (SA); Compagnia di San Paolo "Special Project Oncology", Turin, Italy (SA, GB).

Author disclosure statement No competing financial interests exist.

References

1. Asioli S, Bussolati G (2009) Emerin immunohistochemistry reveals diagnostic features of nuclear membrane arrangement in thyroid lesions. Histopathology 54:571–579
2. Baloch ZW, LiVolsi VA (2002) The quest for a magic tumor marker: continuing saga in the diagnosis of the follicular lesions of thyroid. Am J Clin Pathol 118:165–166
3. Slosar M, Vohra P, Prasad M, Fisher A, Quinlan R, Khan A (2009) Insulin-like growth factor mRNA binding protein 3 (IMP3) is differentially expressed in benign and malignant follicular patterned thyroid tumors. Endocr Pathol 20:149–157
4. Kawachi K, Matsushita Y, Yonezawa S et al (2000) Galectin-3 expression in various thyroid neoplasms and its possible role in metastasis formation. Hum Pathol 31:428–433
5. Cheung CC, Ezzat S, Freeman JL, Rosen IB, Asa SL (2001) Immunohistochemical diagnosis of papillary thyroid carcinoma. Mod Pathol 14:338–342
6. Asa SL (2005) The role of immunohistochemical markers in the diagnosis of follicular-patterned lesions of the thyroid. Endocr Pathol 16:295–309
7. Papotti M, Rodriguez J, De Pompa R, Bartolazzi A, Rosai J (2005) Galectin-3 and HBME-1 expression in well-differentiated thyroid tumors with follicular architecture of uncertain malignant potential. Mod Pathol 18:541–46
8. Bartolazzi A, Orlandi F, Saggiorato E et al (2008) Galectin-3-expression analysis in the surgical selection of follicular thyroid nodules with indeterminate fine-needle aspiration cytology: a prospective multicentre study. Lancet 9:543–549
9. Saggiorato E, De Pompa R, Volante M et al (2005) Characterization of thyroid "follicular neoplasms" in fine-needle aspiration cytological specimens using a panel of immunohistochemical markers: a proposal for clinical application. Endocr Relat Cancer 12:305–317
10. British Thyroid Association, Royal College of Physicians (2007) Fine needle aspiration cytology. In: Perros P (ed) Guidelines for the management of thyroid cancer. Report of the Thyroid Cancer Guidelines Update Group, 2nd edn. Royal College of Physicians, London, pp 9–10
11. Fadda G, Rossi ED, Raffaelli M et al (2006) Fine-needle aspiration biopsy of thyroid lesions processed by thin-layer cytology: one-year institutional experience with histologic correlation. Thyroid 16:975–981
12. Rosai J, Carcangiu ML, DeLellis RA (1992) Tumors of the thyroid gland. Armed Forces Institute of Pathology, Washington
13. Kini SR (1996) Thyroid. In: Guides to Clinical Aspiration Biopsy, 2nd edn. Igaku-Shoin, New York, pp 521
14. Baloch ZW, Sack MJ, Yu GH, LiVolsi VA, Gupta PK (1998) Fine-needle aspiration of thyroid: an institutional experience. Thyroid 8:565–569
15. Cooper DS, Doherty GM, Haugen BR et al (2006) The American Thyroid Association Giudelines Taskforce. Management guidelines for patients with thyroid nodules and differentiated thyroid cancer. Thyroid 16:109–142
16. Volante M, Collini P, Nikiforov YE et al (2007) Poorly differentiated thyroid carcinoma: the Turin proposal for the use of uniform criteria and an algorithmic diagnostic approach. Am J Surg Pathol 31:1256–1264
17. De Lellis RA, Williams ED (2004) Tumours of the thyroid and parathyroid. In: DeLellis RA, Lloyd RV, Heitz PU, Eng C (eds) Pathology and genetics. Tumours of Endocrine Organs. IARC Press, Lyon, pp 49–77
18. Gharib H (1994) Fine-needle aspiration biopsy of thyroid nodules: advantages, limitations and effect. Mayo Clin Proc 69:44–49

19. Williams ED (2000) The Chernobyl Pathologist Group. Guest editorial: two proposals regarding the terminology of thyroid tumors. Int J Surg Pathol 8:181–183
20. Asioli S, Accinelli G, Pacchioni D, Bussolati G (2008) Diagnosis of biliary tract lesions by histological sectioning of brush bristles as alternative to cytological smearing. Am J Gastroenterol 103:1274–1281
21. Cohen J (1960) A coefficient for agreement for nominal scales. Education and Psychological Measurement 20:37–46
22. Fleiss JL (1971) Measuring nominal scale agreement among many raters. Psychol Bull 76:378–382
23. Baloch ZW, Fleisher S, LiVolsi VA, Gupta PK (2002) Diagnosis of "follicular neoplasm": a gray zone in thyroid fine-needle aspiration cytology. Diagn Cytopathol 26:41–44
24. Nayar R, Ivanovic M (2009) The indeterminate thyroid fine-needle aspiration: experience from an academic center using terminology similar to that proposed in the 2007 National Cancer Institute Thyroid Fine Needle Aspiration State of the Science Conference. Cancer Cytopathol 117:195–202
25. Fusco A, Chiappetta G, Hui P et al (2002) Assessment of RET/PTC oncogene activation and clonality in thyroid nodules with incomplete morphological evidence of papillary carcinoma: a search for the early precursors of papillary cancer. Am J Pathol 160:2157–2167
26. Al-Brahim N, Asa SL (2006) Papillary thyroid carcinoma: an overview. Arch Pathol Lab Med 130:1057–1062
27. Zhu Z, Gandhi M, Nikiforova MN, Fischer AH, Nikiforov YE (2003) Molecular profile and clinical-pathologic features of the follicular variant of papillary thyroid carcinoma: an unusually high prevalence of ras mutations. Am J Clin Pathol 120:71–77
28. Chan JK (2002) Strict criteria should be applied in the diagnosis of encapsulated follicular variant of papillary thyroid carcinoma. Am J Clin Pathol 117:16–18
29. Giorgadze T, Rossi ED, Fadda G, Gupta PK, LiVolsi VA, Baloch Z (2004) Does the fine-needle aspiration diagnosis of "Hürthle-cell neoplasm/follicular neoplasm with oncocytic features" denote increased risk of malignancy? Diagn Cytopathol 31:307–312
30. Volante M, Bozzalla-Cassione F, DePompa R et al (2004) Galectin-3 and HBME-1 expression in oncocytic cell tumors of the thyroid. Virchows Arch 445:183–188

Virchows Arch (2010) 457:53–61
DOI 10.1007/s00428-010-0938-0

ORIGINAL ARTICLE

Hypoxia and metabolic phenotypes during breast carcinogenesis: expression of HIF-1α, GLUT1, and CAIX

Chi-Long Chen · Jan-Show Chu · Wu-Chou Su · Soon-Cen Huang · Wen-Ying Lee

Received: 3 March 2010 / Revised: 13 May 2010 / Accepted: 18 May 2010 / Published online: 5 June 2010
© Springer-Verlag 2010

Abstract Hypoxia and acidosis are microenvironmental selection forces during somatic evolution in breast carcinogenesis. The effect of cobalt chloride ($CoCl_2$)-induced hypoxia on the expression of hypoxia-inducible factor (HIF)-1α, glucose transporter 1 (GLUT1), and carbonic anhydrase IX (CAIX) was assessed in breast cancer cells derived from primary sites (HCC1395 and HCC1937) and metastatic sites (MCF-7 and MDA-MB-231) by reverse transcriptase-polymerase chain reaction and immunoblotting. We analyzed these proteins' expression in tissue samples from normal breast tissue, usual ductal hyperplasia (DH), atypical ductal hyperplasia (ADH), ductal carcinoma in situ (DCIS), and invasive ductal carcinoma (IDC) using immunohistochemistry. CAIX mRNA was expressed constitutively in MDA-MB-231 cells but not in the other three cell lines. CAIX mRNA expression was increased after $CoCl_2$-induced hypoxia in all four breast cancer cell lines. The expression of HIF-1α and GLUT1 proteins was increased after $CoCl_2$-induced hypoxia in all breast cancer cell lines tested. Hypoxia significantly increased CAIX protein expression in primary cancer cells but not in metastatic ones. HIF-1α was not expressed in benign breast tissue, whereas it was significantly expressed in DH, ADH, DCIS, and IDC ($p<0.001$). GLUT1 and CAIX were expressed only in DCIS (56.8% and 25.0%) and IDC (44.1% and 30.5%), with higher expression in high grade DCIS than low/intermediate grade DCIS (79.2% vs. 30.0%, $p=0.001$ and 37.5% vs. 10.0%, $p=0.036$, respectively). High CAIX expression was significantly associated with poor histological grade of IDC ($p=0.005$). During breast carcinogenesis, the role of HIF-1α changes from response to proliferation to tumor progression. GLUT1 expression

C.-L. Chen · J.-S. Chu · W.-Y. Lee
Department of Pathology, College of Medicine,
Taipei Medical University,
Taipei, Taiwan

C.-L. Chen
Department of Pathology, Taipei Municipal WanFang Hospital,
Taipei, Taiwan

J.-S. Chu
Department of Pathology, Taipei Medical University Hospital,
Taipei, Taiwan

W.-C. Su
Department of Internal Medicine, National Cheng Kung University Hospital,
Tainan, Taiwan

W.-C. Su
Institute of Molecular Medicine, College of Medicine,
National Cheng Kung University,
Tainan, Taiwan

S.-C. Huang
Department of Obstetrics and Gynecology, College of Medicine,
Taipei Medical University,
Taipei, Taiwan

S.-C. Huang
Department of Obstetrics and Gynecology,
Chi Mei Medical Center,
Tainan, Taiwan

W.-Y. Lee (✉)
Department of Pathology, Chi Mei Medical Center,
901 Chung Hwa Road,
Tainan, Tainan County 710, Taiwan
e-mail: 7707@so-net.net.tw

W.-Y. Lee
Department of Biotechnology, Southern Taiwan University,
Tainan, Taiwan

(glycolytic phenotype) and CAIX expression (acid-resistant phenotype) may result in a powerful adaptive advantage and represent an aggressive phenotype.

Keywords Hypoxia · GLUT1 · CAIX · Breast · Carcinogenesis

Introduction

Carcinogenesis is a complex, multistep, and multipath progression of cellular populations through increasingly disordered phenotypes culminating in the emergence of an invasive cancer. This process is often described as somatic evolution; it seems formally analogous to Darwinian selection, wherein resistant phenotypes are sequentially generated after microenvironmental selection forces, ultimately leading to the emergence of a malignant population [1]. Gatenby et al. used a mathematical model to propose that microenvironmental acidosis derived from glycolysis acts as the significant selective force of somatic evolution during carcinogenesis [2]. This hypothesis was confirmed by a hybrid cellular automation model, addressing three phases of somatic evolution: hypoxia, glycolysis, and acidosis [3]. Initially, cell proliferation within ducts or on the epithelial surface remains separated from the underlying blood supply by the intact basement membrane. As cells proliferate further away from the basement membrane, the diffusion–reaction kinetics of substrate and metabolite flow to and from the blood vessels resulting in regional hypoxia and acidosis. Cellular adaptation to hypoxia includes upregulation of glycolysis and development of resistance to acid-induced toxicity. The phenotype with upregulated glycolysis and acid resistance has a powerful adaptive advantage, which promotes unconstrained proliferation, and may be a crucial selection force in the transition from a premalignant lesion to an invasive cancer. Gatenby et al. also used mathematical models, tumor spheroids, and 20 clinical specimens to propose that adaption to hypoxia and acidosis represents key events in the transition from ductal carcinoma in situ (DCIS) to invasive breast cancer [4].

The broad cellular response caused by hypoxia is mediated by the action of the transcription factor hypoxia-inducible factor 1 (HIF-1), a heterodimer composed of α and β subunits [5]. Under normoxic conditions, HIF-1α protein is degraded within minutes, whereas under hypoxic conditions, it is stabilized and upregulated. Upon stabilization, HIF-1α protein is transported into the nucleus where it heterodimerizes with HIF-1β, forming the active HIF-1 transcription complex. HIF-1 binds to the hypoxia response element in the promoters of various target genes, which mediate the increase in oxygen availability or allow metabolic adaptation to hypoxia [6].

Glucose transporter 1 (GLUT1), a membrane-bound glycoprotein, is a high-affinity glucose transporter that regulates glucose uptake [7]. GLUT1 expression increases under hypoxia, which induces greater dependence on glycolysis as an energy source. GLUT1 expression was found to be regulated by hypoxia in an HIF-1-dependent way [8].

Carbonic anhydrase IX (CAIX), a transmembrane glycoprotein, is a major downstream target of HIF-1α [9]. Its function is to regulate pH by reversible hydration of carbonic dioxide to carbonic acid ($CO_2+H_2O=HCO_3^-+H^+$). Therefore, CAIX is important to help eliminate the hypoxia-generated acid load in glycolysis. CAIX is overexpressed in a wide spectrum of human cancers, including breast cancer, but not in normal tissue [10].

Cobalt is a well-known blocker of voltage-gated calcium channels. Previous studies have demonstrated that chemical hypoxia is induced by cobalt chloride ($CoCl_2$) and physical hypoxia not only upregulating HIF-1α but also similarly affecting cellular functions, including metabolism [11–13]. Therefore, $CoCl_2$ as a hypoxia-mimetic agent provides an easily performed platform to investigate the hypoxic response.

The hypothesis proposed by mathematical, empirical, and hybrid cellular automaton models [2–4] is that evolution of glycolytic and acid-resistant phenotypes leads to invasive proliferation. To verify this, we performed in vitro and in vivo experiments to determine the role of metabolic phenotype in breast carcinogenesis. We examined the effect of $CoCl_2$-induced hypoxia on the expression of HIF-1α, GLUT1, and CAIX in breast cancer cells derived from primary sites (HCC1395 and HCC1937) and metastatic sites (MCF-7 and MDA-MB-231) by reverse transcriptase-polymerase chain reaction (RT-PCR) and immunoblotting. Using an immunohistochemistry method, we investigated these proteins expression in clinical breast tissue specimens of the spectrum of normal breast tissue, usual ductal hyperplasia (DH), atypical ductal hyperplasia (ADH), DCIS, and invasive ductal carcinoma (IDC).

Materials and methods

Cell culture and hypoxia treatment

Four human breast cancer cell lines (two cell lines from a primary ductal carcinoma, HCC1395 and HCC1937; two lines from metastatic breast adenocarcinoma in pleural effusion, MCF-7 and MDA-MB-231) were purchased from American Type Culture Collection (Manassas, VA, USA). HCC1395 and HCC1937 cells were grown in RPMI-1640 (Gibco, Invitrogen, Carlsbad, CA, USA) supplemented with 10% fetal bovine serum (FBS), 1.0 mM sodium

pyruvate, 100 units/mL penicillin, and 100 μg/mL streptomycin (HyClone, Logan, UT, USA) in a 5% CO_2 atm at 37°C. MCF-7 and MDA-MB-231 cells were cultured in Dulbecco's modified Eagle's medium (Gibco, Invitrogen, Carlsbad, CA, USA) supplemented with 10% FBS, 100 units/mL penicillin, and 100 μg/mL streptomycin (HyClone, Logan, UT, USA) in a normoxic atmosphere of 21% O_2 and 5% CO_2 at 37°C.

For hypoxia experiments, cells were treated with 150 μM $CoCl_2$ for 24 h and maintained in a 5% CO_2 atm at 37°C as our previous study [13].

Expression of HIF-1α, GLUT1, and CAIX by RT-PCR

The expression of mRNAs encoding HIF-1α, GLUT1, and CAIX was examined by RT-PCR. RNA was isolated from cells using the RNeasy Mini Kit (Qiagen, Hilden, Germany) and was reverse transcribed for cDNA synthesis using M-MLV RT (Promega Corp., Madison, WI, USA) on a GeneAmp®PCR System 9700 (Applied Biosystems, Foster, CA, USA). The amplification was performed through 30 PCR cycles. The thermal cycles were denaturation at 94°C for 30 s, annealing at 60°C for 30 s, and extension at 72°C for 1 min. β-actin was used as a housekeeping control. All amplification products were separated by electrophoresis in a 2% agarose gel containing ethidium bromide and visualized under UV light. The primer sequences were as follows: HIF-1α (452 bp), 5′-CATGGAAGGTATTGCACTGC-3′ (sense) and 5′-CACACATACAATGCACTGTGG-3′ (antisense); GLUT1 (213 bp), 5′-ACTGGGCAAGTCCTTTGAGAT-3′ (sense) and 5′-GTCCTTGTTGCCCATGATGGA-3′ (antisense); CAIX (249 bp), 5′-CAATATGAGGGGTCTCTGACTA CAC-3′ (sense) and 5′-GGAATTCAGCTGGACTGGCT CAGCA-3′ (antisense); and β-actin (208 bp), 5′-TTAAGGA GAAGCTGTGCTACG-3′ (sense) and 5′-GTTGAAGG TAGTTTCGTGGAT-3′ (antisense).

Western blot analysis

Cell lysate was extracted from the cells incubated under the normoxic or hypoxic conditions. Forty micrograms of each protein sample was loaded onto 10% sodium dodecyl sulfate-polyacrylamide gel electrophoresis, and the separated extracts were electrophoretically transferred onto Hybond-PVDF membrane (Amersham Pharmacia Biotech, Buckinghamshire, UK) in a transfer buffer. The membrane was incubated with anti-human HIF-1α mouse monoclonal antibody (Calbiochem, Germany) at a dilution of 1:500, anti-human GLUT1 rabbit polyclonal antibody (Dako, Carpinteria, CA, USA) at a dilution of 1:1,000, and anti-human CAIX rabbit polyclonal antibody (Santa Cruz Bioscience, Santa Cruz, CA, USA) at a dilution of 1:1,000 at 4°C overnight. Antibody to β-actin (Sigma-Aldrich, St. Louis, MO, USA) was a control for protein loading.

Tissue materials

A total of 168 cases of formalin-fixed, paraffin-embedded tissue from breast biopsies, partial mastectomy, and mastectomy specimens were retrieved from the surgical pathology archives of the Department of Pathology, Chi Mei Medical Center. The cases included normal breast tissue (21 cases), usual DH (22 cases), ADH (22 cases), DCIS (44 cases; 16 of low grade, 4 of intermediate grade, and 24 of high grade), and $T_{1\text{-}2}$ IDC, not otherwise specified (59 cases; 30 of node-negative and 29 of node-positive). All histologic sections were reviewed to confirm the diagnosis by an experienced pathologist (WY Lee) according to the 2003 WHO histological classification of tumors of the breast [14]. The classification of DCIS was according to the criteria outlined by Consensus Committee, based on nuclear grade, necrosis, polarization, and architectural pattern [15]. The histologic grade of IDC was based on the Nottingham histologic score as grade 1 (12 cases), grade 2 (24 cases), and grade 3 (23 cases).

Immunohistochemistry

Immunohistochemistry of HIF-1α, GLUT1, and CAIX was performed using 5-μm-thick sections of formalin-fixed, paraffin-embedded tissues placed onto positively charged glass slides, followed by routine dewaxing and rehydration. After blocking endogenous peroxidase activity, the sections were subjected to heat-induced antigen retrieval using an autoclave, and then incubated with primary antibodies at 4°C overnight. The primary antibodies used were HIF-1α (mouse monoclonal, Calbiochem, Germany, diluted 1:300), GLUT1 (rabbit polyclonal, Dako, Carpinteria, CA, USA, diluted 1:1,000), and CAIX (rabbit polyclonal, Santa Cruz Bioscience, Santa Cruz, CA, USA, diluted 1:100). Detection was done using Novolink Polymer Detection System (Novocastra Laboratories, Newcastle Upon Tyne, UK) with diaminobenzidine substrate (DAB) as the chromogen. Finally, the sections were lightly counterstained with hematoxylin. Positive and negative controls were included in all runs. Positive control was cervical squamous cell carcinoma tissue, which has previously been reported as positive for HIF-1α, GLUT1, and CAIX [16]. For the negative controls, we used non-immune serum instead of the primary antibody.

To analyze HIF-1α expression, only homogenously and darkly stained nuclei were considered, and a percentage of >1% positive nuclei was considered positive [17, 18]. The staining of GLUT1 and CAIX was scored as positive when membrane staining was seen in >1% of the cells [17, 18].

Statistical analysis

Differences of quantified protein levels between normoxic control and hypoxia-treated cells were evaluated with Student's unpaired t test. The differences and correlations of immunohistochemical results were analyzed by χ^2 test. A p value <0.05 was considered statistically significant.

Results

Effect of $CoCl_2$-induced hypoxia on mRNA expression of HIF-1α, GLUT1, and CAIX

Constitutive and hypoxia-stimulated mRNA expression of HIF-1α, GLUT1, and CAIX measured by RT-PCR is presented in Fig. 1. HIF-1α and GLUT1 mRNA expression was not altered after $CoCl_2$-induced hypoxia, whereas CAIX mRNA expression was increased after hypoxia treatment in all four breast cancer cell lines. MDA-MB-231 cells expressed notably more constitutive CAIX mRNA as compared to other cell lines.

Effect of $CoCl_2$-induced hypoxia on protein expression of HIF-1α, GLUT1, and CAIX

Western blot analysis was performed to examine the expression of HIF-1α, GLUT1, and CAIX under normoxia and $CoCl_2$-induced hypoxia. The expression of HIF-1α and GLUT1 proteins was increased after $CoCl_2$-induced hypoxia in breast cancer cell lines (Fig. 2). Constitutive and hypoxia-stimulated CAIX protein was strongly expressed in all four cell lines. CAIX protein expression was significantly increased after $CoCl_2$-induced hypoxia treatment in primary cancer cells (HCC1395 and HCC1937) but not in metastatic ones (MCF-7 and MDA-MB-231).

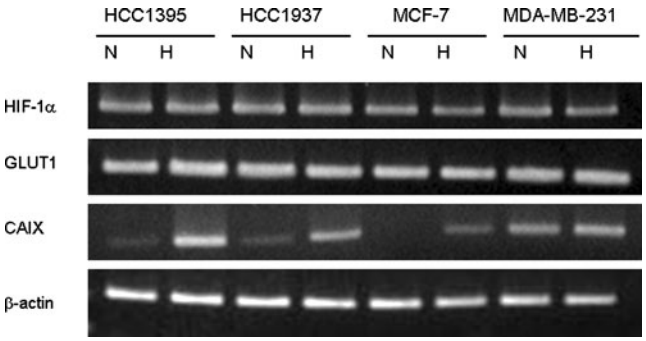

Fig. 1 mRNA expression of HIF-1α, GLUT1, and CAIX determined by RT-PCR in HCC1395, HCC1937, MCF-7, and MDA-MB-231 cells exposed to normoxia (N) or $CoCl_2$-induced hypoxia (H). CAIX mRNA expression was increased after $CoCl_2$-induced hypoxia treatment in all four breast cancer cell lines. MDA-MB-231 cells notably expressed constitutive CAIX mRNA, which was not apparent in the other three cell lines

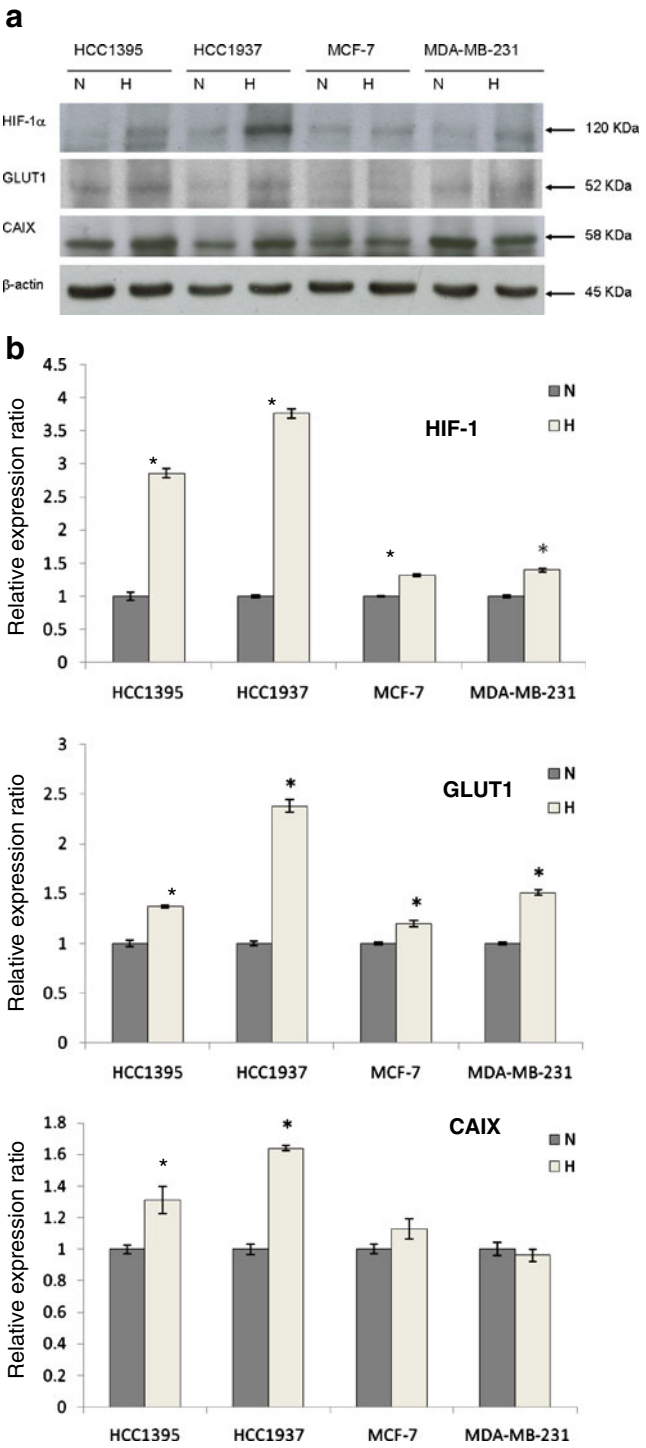

Fig. 2 Western blots from HCC1395, HCC1937, MCF-7, and MDA-MB-231 cells exposed to normoxia (N) or $CoCl_2$-induced hypoxia (H). **a** HIF-1α and GLUT1 protein expressions were increased after $CoCl_2$-induced hypoxia in all four breast cancer cell lines. Hypoxia increased CAIX protein expression in primary cancer cells but not in metastatic ones. **b** Western blots were subsequently quantified by scanning densitometry and normalized to that of β-actin. The ratio was calculated relative to that of normoxia (N), which was set to 1. The means noted with an *asterisk* were statistically different from the matched normoxic control. *N*, Normoxia, *H* CoCl2-induced hypoxia, *asterisk* $p<0.05$

Detection of HIF-1α, GLUT1, and CAIX in breast tissue specimens by immunohistochemistry

To further investigate the potential roles of hypoxia and metabolic phenotype in breast carcinogenesis, we examined the expression of HIF-1α, GLUT1, and CAIX by immunohistochemistry in a series of clinical samples of normal breast tissue, usual DH, ADH, DCIS, and IDC. The results of the immunohistochemical stains are summarized in Table 1. None of the 21 benign breast tissue samples showed expression of HIF-1α; HIF-1α was significantly expressed in DH, ADH, DCIS, and IDC ($p<0.001$). Nuclear HIF-1α expression was diffusely present in DCIS and IDC (Fig. 3). GLUT1 and CAIX were expressed only in DCIS and IDC but not in normal breast tissue, DH, or ADH ($p<0.001$). GLUT1 staining was visualized around erythrocytes as internal control. Membranous GLUT1 staining around cancer cells was seen in 56.8% of DCIS and 44.1% of IDC (Fig. 3). Membranous CAIX staining was expressed in 25.0% of DCIS and 30.5% of IDC (Fig. 3).

Correlations between hypoxia and metabolic phenotype and various pathologic features of DCIS and IDC are listed in Table 2. In DCIS, a higher HIF-1α expression was seen in low/intermediate grade DCIS than in high grade DCIS ($p=0.043$). However, GLUT1 and CAIX expression were significantly increased in high grade DCIS ($p=0.001$ and $p=0.036$, respectively). In addition, GLUT1 and CAIX positive staining were mainly present adjacent to areas of comedo necrosis in high grade DCIS (Fig. 3). In IDC, the statistical evaluation of HIF-1α expression according to histological grade or node status of IDC showed no significant correlation. Similarly, no correlation was found between GLUT1 expression and histological grade or node status of IDC. However, high CAIX expression was significantly associated with poor histological grade of IDC ($p=0.005$). There was no significant association between CAIX expression and nodal metastasis.

Table 3 shows comparisons of CAIX expression with HIF-1α and GLUT1 in IDC. CAIX expression was highly positively associated with GLUT1 ($p<0.001$) but not associated with HIF-1α.

Discussion

In the present study, $CoCl_2$-induced hypoxia caused an increase in expression of CAIX mRNA, HIF-1α protein, and GLUT1 protein in breast cancer cell lines. However, $CoCl_2$-induced hypoxia significantly increased CAIX protein expression in primary breast cancer cells but not in metastatic ones. MDA-MB-231 cells, which are highly invasive and triple-negative breast cancer cells, notably expressed constitutive CAIX mRNA and protein. High CAIX expression was significantly associated with high grade DCIS and poor histological grade of IDC. These results were in agreement with a report [19] of upregulated CAIX expression in basal-like breast cancers (so-called triple-negative phenotype), which have a particularly aggressive phenotype and are more likely to be high grade. Previous clinical studies [20–23] of CAIX in breast cancer have demonstrated the association with a poor outcome, suggesting that CAIX expression is linked to an aggressive phenotype. However, CAIX expression was not correlated with the nodal status, as previously reported [17, 20].

HIF-1α was not detected in normal breast tissue, which was consistent with a previous report [24]. Although DH and ADH are not malignant, the proliferation of cells in this type of lesions consumes more oxygen, which results in a relatively hypoxic status. Thus, HIF-1α expression in DH and ADH may occur in response to a high cell proliferation rate. In turn, HIF-1α may be adaptive for the cells in the proliferative lesion to maintain a high proliferation rate. HIF-1α expression is responsive to proliferation-induced hypoxia in the initial stage and then modulates tumor progression in later stages. Therefore, HIF-1α plays a role in the early stages of breast carcinogenesis.

GLUT1 and CAIX are HIF-1α target genes [9], but we did not observe any association between GLUT1 or CAIX and HIF-1α in the tissue samples of invasive breast cancer. The absence of an association between CAIX and HIF-1α expression is in agreement with other reports [19, 25, 26]. As our tissue sections were constructed from non-necrotic areas, our results were in agreement with previous findings, showing no association between diffusely overexpressed HIF-1α and GLUT1 or CAIX in invasive breast cancer [27]. One previous study demonstrated that CAIX expres-

Table 1 Expression of HIF-1α, GLUT1, and CAIX in normal breast tissue, usual ductal hyperplasia (DH), atypical ductal hyperplasia (ADH), ductal carcinoma in situ (DCIS), and invasive ductal carcinoma (IDC)

Lesion	*n*	HIF-1α Positive (%)	*p* value	GLUT1 Positive (%)	*p* value	CAIX Positive (%)	*p* value
Normal	21	0 (0%)	<0.001	0 (0%)	<0.001	0 (0%)	<0.001
DH	22	14 (63.6%)		0 (0%)		0 (0%)	
ADH	22	17 (77.3%)		0 (0%)		0 (0%)	
DCIS	44	36 (81.8%)		25 (56.8%)		11 (25.0%)	
IDC	59	46 (78.0%)		26 (44.1%)		18 (30.5%)	

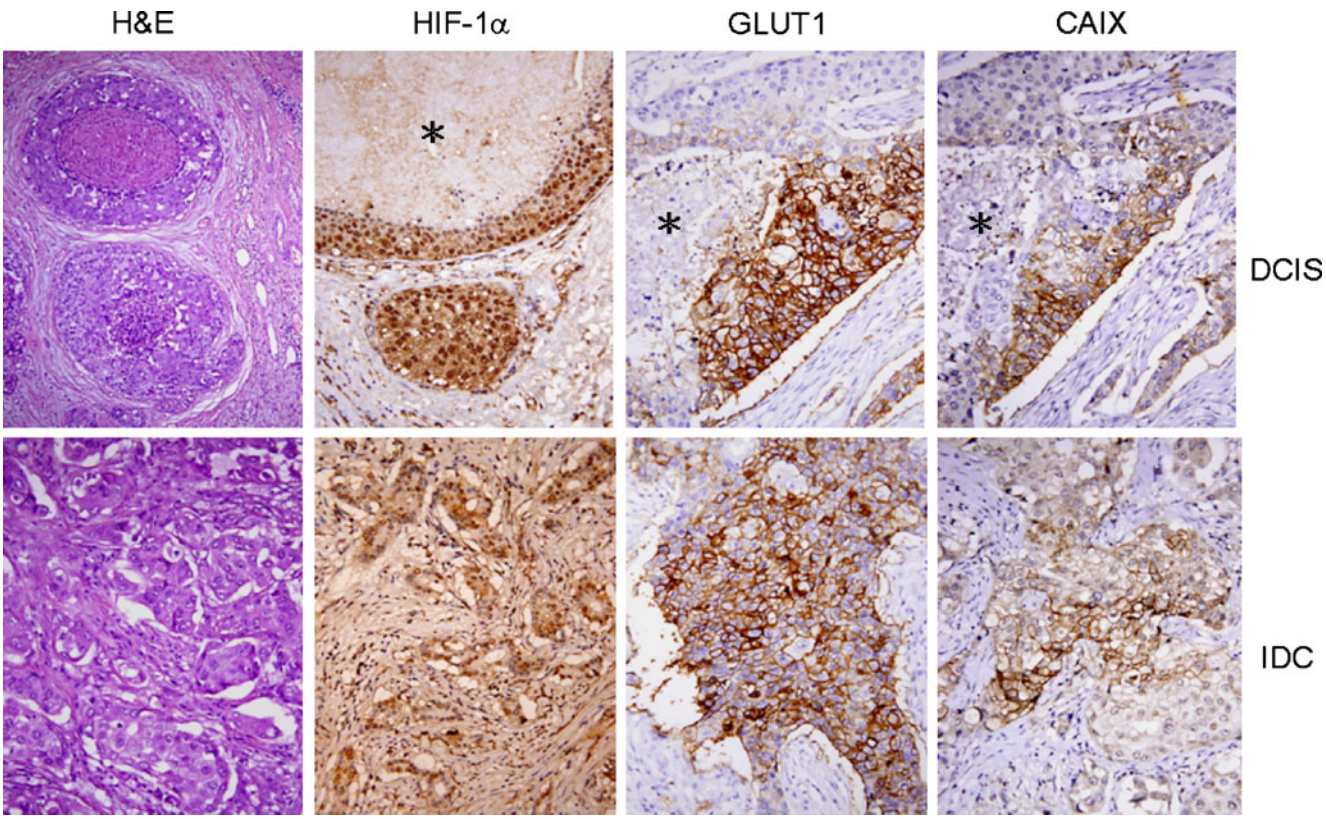

Fig. 3 H&E stain and immunohistochemical staining for HIF-1α, GLUT1, and CAIX in ductal carcinoma in situ (DCIS) and invasive ductal carcinoma (IDC). Representative staining for H&E, HIF-1α, GLUT1, and CAIX in high grade DCIS and IDC is shown. Examples of high grade DCIS, showing HIF-1α nuclear staining and membranous staining for GLUT1 and CAIX in perinecrotic region (*asterisk* comedo necrosis). Examples of IDC, showing HIF-1α nuclear staining in a grade I IDC and membranous staining for GLUT1 and CAIX in a grade III IDC

sion was significantly correlated with HIF-1α expression, whereas many HIF-1α-positive invasive breast cancers (35.4%) did not express CAIX [21]. These results indicate that HIF-1α expression alone may not be sufficient for CAIX gene activation. The previous study also showed that 41.7% of invasive breast cancers were CAIX positive but HIF-1α negative [21]. The presence of CAIX without HIF-1α expression has been demonstrated in perinecrotic regions in solid tumors [25]. This is probably due to the difference in half-lives of HIF-1α and CAIX [19, 26]. Previous findings demonstrated that HIF-1α was undetectable within minutes after re-oxygenation, whereas GLUT1 and CAIX proteins were relatively stable and persisted longer than HIF-1α [26, 28]. In addition, our results

Table 2 Expression of HIF-1α, GLUT1, and CAIX in ductal carcinoma in situ and invasive ductal carcinoma

Lesion	*n*	HIF-1α Positive (%)	*p* value	GLUT1 Positive (%)	*p* value	CAIX Positive (%)	*p* value
DCIS							
Low/intermediate grade	20	19 (95.0%)	0.043	6 (30.0%)	0.001	2 (10.0%)	0.036
High grade	24	17 (70.8%)		19 (79.2%)		9 (37.5%)	
IDC							
Grade I	12	12 (100.0%)	N.S.	4 (33.3%)	N.S.	0 (0.0%)	0.005
Grade II	24	18 (75.0%)		11 (45.8%)		6 (25.0%)	
Grade III	23	16 (69.6%)		11 (47.9%)		12 (52.2%)	
IDC							
Node-negative	30	21 (70.0%)	N.S.	12 (40.0%)	N.S.	7 (23.3%)	N.S.
Node-positive	29	25 (86.2%)		14 (48.3%)		11 (37.9%)	

N.S. no significance

Table 3 Association between CAIX expression and other hypoxia response proteins in invasive ductal carcinoma

	CAIX		*p* value
	Negative	Positive	
HIF-1α			
Negative	10	3	N.S
Positive	31	15	
GLUT1			
Negative	30	3	<0.001
Positive	11	15	

demonstrated that constitutive expression of CAIX protein in the breast cancer cell lines tested under normoxic conditions was indicative of a hypoxic-independent mechanism of CAIX expression (Fig. 2). This is consistent with previous findings showing that CAIX is induced in high-density cultures via the phosphatidylinositol-3-kinase (PI3K) pathway [29] and by the mitogen-activated protein kinase (MAPK) pathway during both normoxia and hypoxia [30]. Taken together, these observations suggest that CAIX expression is not only regulated by hypoxia but also driven by specific signaling pathways.

In clinical tissue specimens, we observed GLUT1 and CAIX expressed only in DCIS and IDC. GLUT1 and CAIX were frequently expressed in high grade DCIS. CAIX expression was significantly associated with poor histological grade of IDC. Therefore, our results suggest that the glycolytic, acid-resistant phenotype has a powerful adaptive advantage, which promotes unconstrained proliferation, and may be a crucial selection force in the transition from DCIS to an invasive cancer. GLUT1 and CAIX proteins play a role in a later stage of breast carcinogenesis.

During the course of carcinogenesis, the pre-invasive stages occur in an avascular environment because the hyperplastic cells within the ductal lumens are separated from the blood vessels by a basement membrane. In DH and ADH, cell proliferation develops hypoxia near the oxygen diffusion limit, in which HIF-1α expression is responsive to proliferation-induced hypoxia. In turn, HIF-1α may be adaptive for DH to maintain a high proliferative rate. When the proliferation persists, hypoxia-mediated GLUT1 expression, a glycolytic phenotype, allows increasing anaerobic glycolysis, in response to high levels of cellular proliferation and confers a proliferative advantage [31]. However, proliferation is again constrained by microenvironmental acidosis due to anaerobic respiration of glucose. The new environmental selection force selects for phenotypes that are resistant to acid-induced toxicity. In addition, upregulated glycolysis persists even under normoxic conditions (Warburg effect) in cancer cells [32], which gives rise to increased acid production. Acidosis induces apoptosis through p53-dependent caspase activation [33]. The transformed cells resist the acidic environment through the upregulation of H^+ transporters (e.g., CAIX), by acquiring p53 mutations or overexpression of the apoptosis-inhibitor protein Bcl-2, all of which substantially reduce acid-mediated cell death [34]. Extracellular acidity can degrade extracellular matrix and basement membranes, favoring tumor invasion [35]. Furthermore, acidosis itself can be mutagenic and clastogenic [36] and thus accelerates the progress of carcinogenesis. CAIX works to regulate pH and helps counteract the acidic condition [9]. CAIX expression, an acid-resistant phenotype, allows cells to adapt to acidosis and then contributes to tumor progression and invasive growth.

In the present study, we determined hypoxia-induced HIF-1α, GLUT1, and CAIX expression in breast cancer

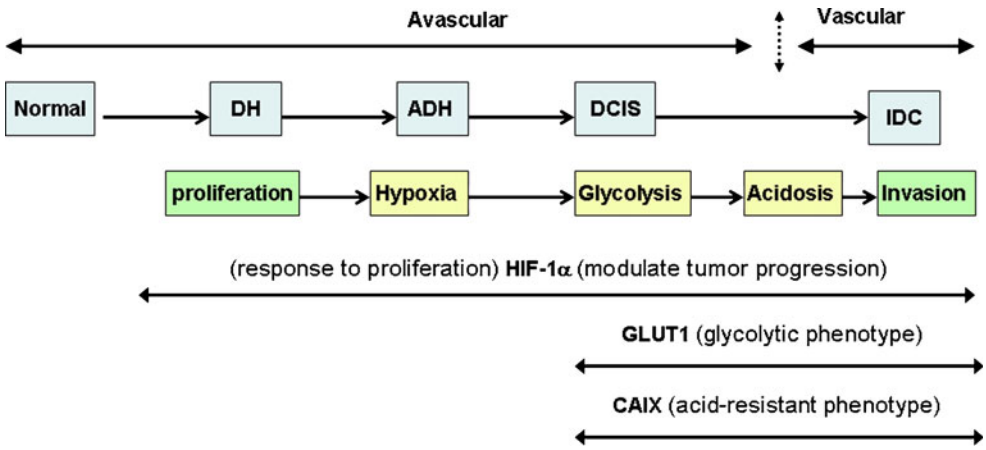

Fig. 4 A model for somatic evolution during breast carcinogenesis. Initially, ductal hyperplasia leads to a thickening of the epithelium, resulting in profound hypoxia. Hypoxia leads to upregulated glycolysis, which results in acidosis in the microenvironment. The role of HIF-1α changes from response to proliferation to tumor progression during breast carcinogenesis. GLUT1 and CAIX expression (glycolytic and acid-resistant phenotype) has a powerful adaptive advantage and may be a crucial selection force in the final stages of breast carcinogenesis

cells lines, and the hypoxia and metabolic phenotype in tissue samples of spectrum of breast lesions. We provide evidence for a model of somatic evolution adaptive to a sequence of microenvironmental changes (hypoxia–glycolysis–acidosis) during breast carcinogenesis (Fig. 4). We demonstrated that the final stages of breast carcinogenesis are driven by cellular adaptation to hypoxia and acidosis, and a glycolytic, acid-resistant phenotype is an aggressive phenotype. These results suggest that tumor prevention strategies should be aimed at interrupting the hypoxia–glycolysis–acidosis sequence. Furthermore, acknowledging the metabolic phenotype of breast cancer may lead to novel therapeutic strategies.

Acknowledgements This work was supported by grants from the National Science Council (NSC 96-2314-B-384-005-MY2) and Chi Mei Medical Center (96CM-TMU-11 and CMFHR9711), Taiwan. We thank Miss Ying-Gen Tsai for technical assistance.

References

1. Gatenby RA, Vincent TL (2003) An evolutionary model of carcinogenesis. Cancer Res 63:6212–6220
2. Gatenby RA, Gawlinski ET, Gmitro AF, Kaylor B, Gillies RJ (2006) Acid-mediated tumor invasion: a multidisciplinary study. Cancer Res 66:5216–5223
3. Smallbone K, Gatenby RA, Gillies RJ, Maini PK, Gavaghan DJ (2007) Metabolic changes during carcinogenesis: potential impact on invasiveness. J Theor Biol 244:703–713
4. Gatenby RA, Smallbone K, Maini PK, Rose F, Averill J, Nagle RB, Worrall L, Gillies RJ (2007) Cellular adaptations to hypoxia and acidosis during somatic evolution of breast cancer. Br J Cancer 97:646–653
5. Semenza GL (2000) HIF-1: mediator of physiological and pathophysiological responses to hypoxia. J Appl Physiol 88:1474–1480
6. Semenza GL (2003) Targeting HIF-1 for cancer therapy. Nat Rev Cancer 3:721–732
7. Younes M, Lechago LV, Somoano JR, Mosharaf M, Lechago J (1996) Wide expression of the human erythrocyte glucose transporter Glut1 in human cancers. Cancer Res 56:1164–1167
8. Chen C, Pore N, Behrooz A, Ismail-Beigi F, Maity A (2001) Regulation of glut1 mRNA by hypoxia-inducible factor-1. Interaction between H-ras and hypoxia. J Biol Chem 276:9519–9525
9. Potter C, Harris AL (2004) Hypoxia inducible carbonic anhydrase IX, marker of tumour hypoxia, survival pathway and therapy target. Cell Cycle 3:164–167
10. Thiry A, Dogne JM, Masereel B, Supuran CT (2006) Targeting tumor-associated carbonic anhydrase IX in cancer therapy. Trends Pharmacol Sci 27:566–573
11. Karovic O, Tonazzini I, Rebola N, Edstrom E, Lovdahl C, Fredholm BB, Dare E (2007) Toxic effects of cobalt in primary cultures of mouse astrocytes. Similarities with hypoxia and role of HIF-1alpha. Biochem Pharmacol 73:694–708
12. Fan RH, Chen PS, Zhao D, Zhang WD (2007) Hypoxia induced by CoCl2 influencing the expression and the activity of matrix metalloproteinase-2 in rat hepatic stellate cells. Zhonghua Gan Zang Bing Za Zhi 15:654–657
13. Fu OY, Hou MF, Yang SF, Huang SC, Lee WY (2009) Cobalt chloride-induced hypoxia modulates the invasive potential and matrix metalloproteinases of primary and metastatic breast cancer cells. Anticancer Res 29:3131–3138
14. DP TFA (ed) (2003) The WHO classification of tumors of the breast and female genital organs. IARC Press, Lyon, pp 10–12
15. The Consensus Conference Committee (1997) Consensus conference on the classification of ductal carcinoma in situ. Cancer 80:1798–1802
16. Lee WY, Huang SC, Hsu KF, Tzeng CC, Shen WL (2008) Roles for hypoxia-regulated genes during cervical carcinogenesis: somatic evolution during the hypoxia-glycolysis-acidosis sequence. Gynecol Oncol 108:377–384
17. Trastour C, Benizri E, Ettore F, Ramaioli A, Chamorey E, Pouyssegur J, Berra E (2007) HIF-1alpha and CA IX staining in invasive breast carcinomas: prognosis and treatment outcome. Int J Cancer 120:1451–1458
18. Koop EA, van Laar T, van Wichen DF, de Weger RA, Wall E, van Diest PJ (2009) Expression of BNIP3 in invasive breast cancer: correlations with the hypoxic response and clinicopathological features. BMC Cancer 9:175
19. Tan EY, Yan M, Campo L, Han C, Takano E, Turley H, Candiloro I, Pezzella F, Gatter KC, Millar EK, O'Toole SA, McNeil CM, Crea P, Segara D, Sutherland RL, Harris AL, Fox SB (2009) The key hypoxia regulated gene CAIX is upregulated in basal-like breast tumours and is associated with resistance to chemotherapy. Br J Cancer 100:405–411
20. Chia SK, Wykoff CC, Watson PH, Han C, Leek RD, Pastorek J, Gatter KC, Ratcliffe P, Harris AL (2001) Prognostic significance of a novel hypoxia-regulated marker, carbonic anhydrase IX, in invasive breast carcinoma. J Clin Oncol 19:3660–3668
21. Brennan DJ, Jirstrom K, Kronblad A, Millikan RC, Landberg G, Duffy MJ, Ryden L, Gallagher WM, O'Brien SL (2006) CA IX is an independent prognostic marker in premenopausal breast cancer patients with one to three positive lymph nodes and a putative marker of radiation resistance. Clin Cancer Res 12:6421–6431
22. Colpaert CG, Vermeulen PB, Fox SB, Harris AL, Dirix LY, Van Marck EA (2003) The presence of a fibrotic focus in invasive breast carcinoma correlates with the expression of carbonic anhydrase IX and is a marker of hypoxia and poor prognosis. Breast Cancer Res Treat 81:137–147
23. Hussain SA, Ganesan R, Reynolds G, Gross L, Stevens A, Pastorek J, Murray PG, Perunovic B, Anwar MS, Billingham L, James ND, Spooner D, Poole CJ, Rea DW, Palmer DH (2007) Hypoxia-regulated carbonic anhydrase IX expression is associated with poor survival in patients with invasive breast cancer. Br J Cancer 96:104–109
24. Bos R, Zhong H, Hanrahan CF, Mommers EC, Semenza GL, Pinedo HM, Abeloff MD, Simons JW, van Diest PJ, van der Wall E (2001) Levels of hypoxia-inducible factor-1 alpha during breast carcinogenesis. J Natl Cancer Inst 93:309–314
25. Sobhanifar S, Aquino-Parsons C, Stanbridge EJ, Olive P (2005) Reduced expression of hypoxia-inducible factor-1alpha in perinecrotic regions of solid tumors. Cancer Res 65:7259–7266
26. Tomes L, Emberley E, Niu Y, Troup S, Pastorek J, Strange K, Harris A, Watson PH (2003) Necrosis and hypoxia in invasive breast carcinoma. Breast Cancer Res Treat 81:61–69
27. Vleugel MM, Greijer AE, Shvarts A, van der Groep P, van Berkel M, Aarbodem Y, van Tinteren H, Harris AL, van Diest PJ, van der Wall E (2005) Differential prognostic impact of hypoxia induced and diffuse HIF-1alpha expression in invasive breast cancer. J Clin Pathol 58:172–177
28. Bruckner BA, Ammini CV, Otal MP, Raizada MK, Stacpoole PW (1999) Regulation of brain glucose transporters by glucose and oxygen deprivation. Metabolism 48:422–431
29. Kaluz S, Kaluzova M, Chrastina A, Olive PL, Pastorekova S, Pastorek J, Lerman MI, Stanbridge EJ (2002) Lowered oxygen tension induces expression of the hypoxia marker MN/carbonic

anhydrase IX in the absence of hypoxia-inducible factor 1 alpha stabilization: a role for phosphatidylinositol 3′-kinase. Cancer Res 62:4469–4477
30. Kopacek J, Barathova M, Dequiedt F, Sepelakova J, Kettmann R, Pastorek J, Pastorekova S (2005) MAPK pathway contributes to density- and hypoxia-induced expression of the tumor-associated carbonic anhydrase IX. Biochim Biophys Acta 1729:41–49
31. Brand K (1997) Aerobic glycolysis by proliferating cells: protection against oxidative stress at the expense of energy yield. J Bioenerg Biomembr 29:355–364
32. Warburg O (1956) On the origin of cancer cells. Science 123:309–314
33. Williams AC, Collard TJ, Paraskeva C (1999) An acidic environment leads to p53 dependent induction of apoptosis in human adenoma and carcinoma cell lines: implications for clonal selection during colorectal carcinogenesis. Oncogene 18:3199–3204
34. Graeber TG, Osmanian C, Jacks T, Housman DE, Koch CJ, Lowe SW, Giaccia AJ (1996) Hypoxia-mediated selection of cells with diminished apoptotic potential in solid tumours. Nature 379:88–91
35. Swietach P, Vaughan-Jones RD, Harris AL (2007) Regulation of tumor pH and the role of carbonic anhydrase 9. Cancer Metastasis Rev 26:299–310
36. Morita T, Nagaki T, Fukuda I, Okumura K (1992) Clastogenicity of low pH to various cultured mammalian cells. Mutat Res 268:297–305

Virchows Arch (2010) 457:63–67
DOI 10.1007/s00428-010-0931-7

ORIGINAL ARTICLE

High content of Langerhans cells in malignant lymphoma—incidence and significance

Daniel Benharroch · Gali Guterman · Itai Levy · Ruthy Shaco-Levy

Received: 15 March 2010 / Revised: 25 April 2010 / Accepted: 26 April 2010 / Published online: 16 May 2010
© Springer-Verlag 2010

Abstract We describe 25 patients, 14 with classical Hodgkin lymphoma and 11 with non-Hodgkin lymphoma, in all of whom an excess of Langerhans cells was evident. Except for the first three cases, in which the excess of Langerhans cells was identified on routine slides, the remaining cases were disclosed by actively investigating lymphomas with excess of CD68+ histiocytes and performing CD1a and S-100 protein immunostains. Although no clonality study was performed on the Langerhans cells, we endorse the view which states that in the above association, the Langerhans cells are polyclonal. Fourteen cases of Hodgkin lymphoma with a large number of Langerhans cells were identified in a cohort of 231 classical Hodgkin lymphomas. We compared the features of classical Hodgkin lymphoma with abundant Langerhans cells with those without Langerhans cells. Our analysis reveals that Hodgkin lymphoma with Langerhans cell excess shows greater LMP1/EBV expression (P=.007) and lower p53 expression (P=.042) in the Hodgkin–Reed–Sternberg cells but is not associated with a poorer outcome.

D. Benharroch · G. Guterman · R. Shaco-Levy
Department of Pathology,
Soroka University Medical Center and Faculty of Health Sciences,
Ben-Gurion University of the Negev,
Beer-Sheva, Israel

I. Levy
Department of Hematology,
Soroka University Medical Center and Faculty of Health Sciences,
Ben-Gurion University of the Negev,
Beer-Sheva, Israel

D. Benharroch (✉)
Department of Pathology, Soroka University Medical Center,
P.O. Box 151, Beer-Sheva 84101, Israel
e-mail: benaroch@bgu.ac.il

Keywords Langerhans cells · Classical Hodgkin lymphoma · Non-Hodgkin lymphomas

Introduction

Langerhans cells (LC), immature dendritic cells that function as antigen presenting cells, are most prevalent in the epidermis. They are also present in lymph nodes, to which they migrate after trauma to the skin [1].

Tumors featuring neoplastic proliferation of LC are collectively known as Langerhans cell histiocytosis (LCH) [2]. A minority presents as the more aggressive Langerhans cell sarcoma.

Langerhans cells histiocytosis has been described as a component in unrelated malignant tumors, mainly malignant lymphomas, including classical Hodgkin lymphoma (cHL) [3, 4]. Since the incidence of this association is very low, its biological implications and prognostic significance have not been thoroughly investigated. Isolated reports determined the clonality of LC by using the human androgen receptor gene assay. They demonstrated polyclonality of LC infiltrates in lymphomas exhibiting this association [5, 6].

In the present study, we investigated the implications of LC excess in lymphomas. We have tried to evaluate the significance of LC accumulation, predominantly in classical Hodgkin lymphoma.

Materials and methods

Three cases of lymphomas with abundant LC were identified on routine H&E sections and were the incentive for the present study. These Langerhans cells were positive for CD1a, S-100 protein, and CD68 immunostains.

Following this observation, we actively looked for LC in cHL cases and then in non-Hodgkin lymphoma (NHL) cases. We first identified 39 lymphomas in which abundant CD68-positive histiocytes were present; 27 showed excess of LC, confirmed by CD1a and S-100 protein immunoreactivity.

The immunohistochemical study was carried out with the avidin–biotin peroxidase complex method, using the Vectastain kit of Vector Laboratories (Burlingame, CA, USA). The antibodies were obtained from Dakoppats, Glostrup: CD68 (PGM1); S-100 protein (Z0311); CD15 (LeuM1); CD30 (BerH2); CD20 (L26); p53 (DO-7); LMP1 of EBV (CS1–4). Others were obtained from Immunotech, Marseille: CD1a; Santa Cruz Biotechnologies: IκB (C-21); and Biocare Medical, Walnut Creek, CA, USA: Caspase 3 (17/19 KDa). Antibodies used to study evidence of measles virus were experimental antibodies: L39/22, for nucleoprotein antigen and L77, for hemagglutinin [7].

A case was considered showing excess LC if several groups of LC were dispersed throughout the lymphoid tissue examined or rarely, if a single large collection of LC was present. This definition was determined somewhat arbitrarily, as no criterion has been established in previous studies.

Clinical features were obtained from the database of the Soroka Medical Center, as described in a previous study (Benharroch et al., Apoptosis in Hodgkin–Reed–Sternberg cells of classical Hodgkin lymphoma-revisited, APMIS, accepted for publication). A more detailed analysis was carried out for the cHL cases, since no series of NHL was available to us for comparison with the LC-rich NHL cases. For the purpose of comparison of our cHL cases with excess of LC, we used as a reference group 217 cHL patients with no evidence of LC in their tissues.

Results

Thirty patients with lymphoma and excess LC were identified. Their age range was 4–77 years. Included were 15 female and 15 male patients. Following the slides review, we excluded five cases that had no CD1a or S-100 protein immunoreactive cells. There remained 14 patients with classical HL (Fig. 1), all primary cases except for one, and 11 patients with NHL who showed LC collections. Among the NHL cases, five were T-cell/histiocyte-rich large B-cell lymphomas, four diffuse large B-cell lymphomas, one follicular lymphoma grade I, and one T-cell lymphoma (Lennert's lymphoma).

When comparing the 14 cHL patients with LC excess with the 217 cHL patients without LC of the total non-consecutive 231 cHL cases, there were slightly more male patients in the group with LC excess (8/14), but the male-to-female ratio was similar in the control group (Table 1). The majority of patients with LC excess were diagnosed at an early stage (8/10), more than in the control group, but this difference was not statistically significant. B symptoms were usually absent in patients with abundant LC. Compared to the control group, more patients with LC accumulation were alive and at the last follow-up, only a minority had a relapse (3/14); however, this difference was not statistically significant.

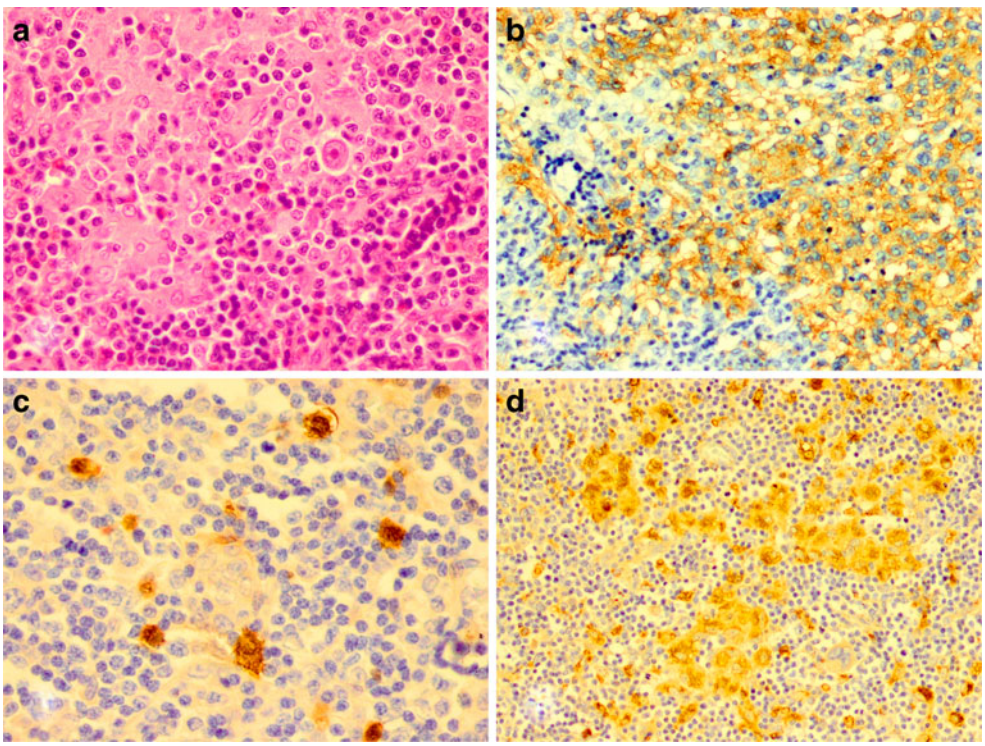

Fig. 1 Classical Hodgkin lymphoma with Langerhans cell excess: **a** Accumulation of "epithelioid histiocytes," *upper left* (H&E×340). **b** The "epithelioid histiocytes" are Langerhans cells and CD1a-positive (immunohistochemistry with diaminobenzidine substrate ×260). **C** Several LC are S-100 protein-positive (IHC with DAB×340). **d** Most LC stain also positive for CD68 (IHC with DAB ×260)

Table 1 Classical Hodgkin lymphoma with and without LC excess—clinical features

Feature		Total (*n*)	No LC n	With LC n	*P* values
Gender	Female	97	91	6	
	Male	134	126	8	0.95
Type	NS	107	99	6	
	Others	74	66	8	0.21
Stage	I–II	99	91	8	
	III–IV	82	80	2	N.S.
B symptom	Yes	84	81	3	
	No	100	95	5	0.73; 2-tailed
Outcome	NED	149	139	10	
	AWD+DOD	68	67	1	0.18; 2-tailed
Relapse	Yes	33	30	3	
	No	198	187	11	0.18; 2-tailed

LC Langerhans cells, *AWD* alive with disease, *DOD* dead of disease, *NED* no evidence of disease, *NS* nodular sclerosis Hodgkin lymphoma

When comparing the patients' age at diagnosis, cHL patients with LC had a mean age of 33.2 years, while NHL patients with LC were older, with mean age of 55.5 years ($P<.005$). The predominant histological type in the cHL with LC group was mixed cellularity while that in the reference group was nodular sclerosis ($P=.021$).

Evidence of EBV infection was more frequent in the cHL with LC group, compared with the control group ($P=.007$). Measles virus infection was also more common in the cHL patients with LC; however, this difference did not reach statistical significance.

The immunoreactivity for the typical markers of cHL (CD15, CD30, and CD20) was similar in the study and control groups.

Immunohistochemical expression of p53 was significantly greater in the control cHL group compared with the cHL with LC excess group ($P=.042$). No difference was noted between the two groups regarding the expression of IκB and caspase 3 (Table 2).

It is noteworthy that one 32-year-old patient was diagnosed with cHL, nodular sclerosis type. He was treated with six courses of ABVD (doxorubicin, bleomycin, vinblastine, and dacarbazine) and was readmitted 15 months later due to fever of several weeks' duration. CT scan demonstrated multi-cavitary lesions in both lungs. A thoracoscopic biopsy showed extensive LC infiltrate with no evidence of recurrent cHL (Fig. 2).

Discussion

In this study, we investigated the possible implications of an excess of LC in lymphoma, based on 25 patients. Analyses of lymphomas with an excess of LC are few in as

Table 2 Immunohistochemical expression of tumor markers in classical Hodgkin lymphoma with and without LC excess

Marker	Expression	Total (n)	No LC n	With LC n (%)	*P* values
LeuM1	Pos	199	187	12	
	Neg	33	31	2	N.S.
CD30	Pos	205	191	14	
	Neg	27	27	0	0.38; 2-tailed
CD20	Pos	44	39	5	
	Neg	182	173	9	0.11
LMP/EBV	Pos	84	74	10	
	Neg	156	152	4	0.007; 2-tailed
Measles v.	Pos	116	106	10	
	Neg	98	94	4	0.18; 2-tailed
p53	Pos	176	169	7	
	Neg	64	57	7	0.042
Cas 3	Pos	137	129	8	
	Neg	81	76	5	0.9
IκB	Pos	161	153	8	
	Neg	71	67	4	N.S.

LC Langerhans cells

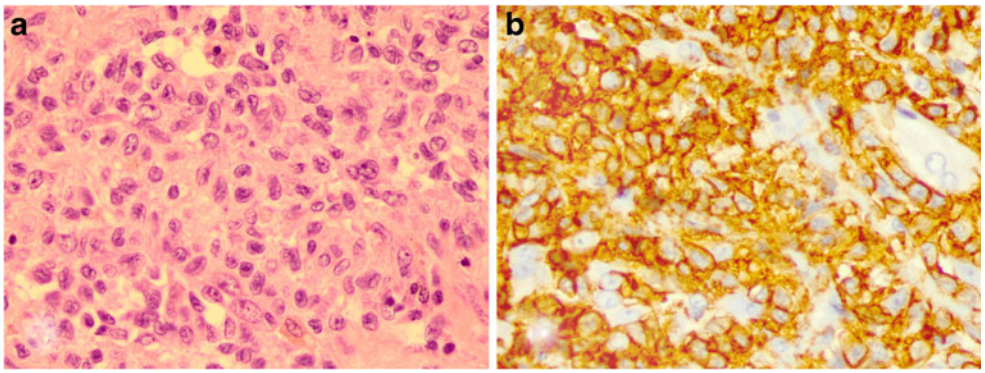

Fig. 2 Pulmonary Langerhans cell accumulation following treatment for classic Hodgkin lymphoma: **a** Pulmonary mass composed of LC (H&E×340). **b** The pulmonary LC stain positive for CD1a (IHC with DAB×340)

much as this association is rare. The literature consists mainly of case reports [8–12] with an occasional series of four or six patients and review of the literature [3, 4]. Our series, the largest to be reported, studies many clinical and pathological issues and provides analysis of the significance of this association.

We presumed that the LC collections were of polyclonal reactive nature. This is based on the concept presented in the WHO classification of tumors of the hematopoietic and lymphoid tissues [6, 13], which describes an association of Langerhans cell histiocytosis exclusively with T-lymphoblastic leukemia; excess of LC in other types of hematopoietic malignancies was regarded as polyclonal and assumed to be reactive [13–16]. Moreover, we looked actively for extensive LC infiltrates in a group of lymphoma cases with abundant CD68+ histiocytes. It is of note that CD68, though not considered a classical LC marker, is frequently positive in these cells, although sometimes only weakly.

The mean age of patients with cHL with LC was significantly younger than that of the patients with NHL and abundant LC; however, this is probably due to the usually younger age of cHL patients compared to those with NHL. Since the NHL cases in this series are heterogeneous and we did not have a control group, we focused on the cHL with LC excess for the main analysis.

The comparison between the reference group (cHL without LC) and cHL with LC group shows several differences. The histological type observed in patients with cHL and LC was predominantly mixed cellularity, while in the reference group, it was, as expected, nodular sclerosis (not statistically significant). The high EBV expression in the cHL patients with abundant LC may be related to this finding, as mixed cellularity cHL is more often linked with a high LMP1 expression. Although the histological type of cHL by itself has no impact on the prognosis, mixed cellularity cHL often presents with a higher stage and with systemic symptoms, which both carry a poor prognosis. LMP1/EBV overexpression with subsequent NF-κB activation may initiate increased cytokine production and thus explain the abundance of LC [1, 17–19].

The decreased p53 expression in the cHL with LC excess cases is difficult to interpret. The wild-type p53 product has a much shorter half life when compared with the mutated p53 product. Thus, p53 overexpression usually corresponds to expression of mutated p53. It is not excluded, then, that absence of expression signifies that the wild type p53 predominates. This in turn may support the reactive nature of the LC present in the lymphomas described above.

The assumption that high LC content in lymphomas could be a result of therapy is not supported by our findings, as all of the cHL cases in our series, except one, were primary.

Since smoking is known to be associated with pulmonary LC infiltrates [5], it could be the cause of LC excess in other lymphomas as well.

The one cHL patient who presented with pulmonary LC infiltrates after chemotherapy was a heavy smoker (45 pack/years). A short course of corticosteroids resulted in marked decrease of his pulmonary lesions. The fact that LC infiltrates occurred in a patient who smokes and decreased in response to corticosteroids is consistent with a reactive process, and not as implied by the association with "pulmonary LCH" [5, 20].

Our findings suggest that an excess of LC in cHL is not correlated with a worse outcome. We were unable to carry out a parallel analysis with accumulation of LC in NHL, in the absence of an adequate control group.

The condition described herein have to be differentiated on the one hand from dermatopathic lymphadenitis, which is a benign entity, except for the minority in which cutaneous T-cell lymphoma spreads out into the lymph node. On the other hand, it has to be distinguished from *lege artis* Langerhans cell histiocytosis which presents only rarely as an isolated lymph node involvement.

In conclusion, we described and characterized a relatively large group of primary lymphomas presenting with accumulation of LC. CHL with excess of LC is more commonly associated with evidence of EBV infection and less frequently shows p53 immunoreactivity. The mean age, male-to-female ratio, histological type, and stage at diagnosis were not significantly different in patients with cHL with and without increased LC. It seems that the accumu-

lation of LC in cHL is of a reactive nature and is not associated with a worse outcome.

Acknowledgements The study was supported in part by Kibbutz Sde Boker, Israel.

We thank Eugenia Mejirovsky for her excellent technical work.

Conflict of interest statement We declare that we have no conflict of interest.

References

1. Geissmann F, Dieu-Nosjean MC, Dezutter C, Valladeau J, Kayal S, Leborgne M, Brousse N, Saeland S, Davoust J (2002) Accumulation of immature Langerhans cells in human lymph nodes draining chronically inflamed skin. J Exp Med 196:417–430
2. Winderbank K, Nanduri V (2009) Langerhans cell histiocytosis. Arch Dis Child 94:904–908
3. Burns BF, Colby TV, Dorfman RF (1983) Langerhans' cell granulomatosis (histiocytosis X) associated with malignant lymphoma. Am J Surg Pathol 7:529–533
4. Egeler RM, Neglia JP, Puccetti DM, Brennan CA, Nesbit ME (1993) Association of Langerhans cell histiocytosis with malignant neoplasms. Cancer 71:865–873
5. Yousem SA, Colby TV, Chen YY, Chen WG, Weiss LM (2001) Pulmonary Langerhans' cell histiocytosis. Molecular analysis of clonality. Am J Surg Pathol 25:630–636
6. Christie LJ, Evans AT, Bray SE, Smith MEF, Kernohan NM, Levison DA, Goodlad JR (2006) Lesions resembling Langerhans cell histiocytosis in association with other lymphoproliferative disorders: a reactive or neoplastic phenomenon? Human Pathol 37:32–39
7. Benharroch D, Shemer-Avni Y, Myiny Y-Y, Levy A, Mejirovsky E, Suprun I, Shendler Y, Prinsloo I, Ariad S, Rager-Zisman B, Sacks M, Gopas J (2004) Measles virus: evidence of an association with Hodgkin's disease. Br J Cancer 91:572–579
8. Shin MS, Buchalter SE, Ho KJ (1994) Langerhans' cell histiocytosis associated with Hodgkin's disease. J Natl Med Assoc 86:65–69
9. Adu-Poku K, Thomas DW, Khan MK, Holgate CS, Smith MEF (2005) Langerhans cell histiocytosis in sequential discordant lymphoma. J Clin Pathol 58:104–106
10. Ibarrola de Andres C, Toscano R, Lahuerta JJ, Martinez-Gonzales MA (1999) Simultaneous occurrence of Hodgkin's disease, nodal Langerhans' cell histiocytosis and multiple myeloma IgA (κ). Virchows Arch 434:259–262
11. Almanaseer IY, Kosova L, Pellettire EV (1986) Composite lymphoma with immunoblastic features and Langerhans' cell granulomatosis (histiocytosis X). Am J Clin Pathol 85:111–114
12. Ferreri A, Fabrietti P, Vessecchia G, Laffranchi A, Lombardi L, Massimino M, Fossati-Bellani F, Giardini R (1997) Langerhans cell histiocytosis arising after Hodgkin's disease. Pediatr Hematol Oncol 14:585–588
13. Jaffe R, Weiss LM, Facchetti F (2008) Tumours derived from Langerhans cells. In: Vardiman J (ed) WHO Classification of tumours of haematopoietic and lymphoid tissue, 4th edn. International Agency for Research on Cancer, Lyon, pp 358–360
14. Raj A, Bendon R, Moriarty T, Suarez C, Bertolone S (2001) Langerhans cell histiocytosis following childhood acute lymphoblastic leukemia. Am J Hematol 68:284–286
15. Li S, Borowitz MJ (2001) CD79a (+) T-cell lymphoblastic lymphoma with coexisting Langerhans cell histiocytosis. Arch Pathol Lab Med 125:858–860
16. Feldman AL, Berthold F, Arceci RJ, Abramowsky C, Shehata BM, Mann KP, Lauer SJ, Pritchard J, Raffeld M, Jaffe ES (2005) Clonal relationship between precursor T-lymphoblastic leukemia/lymphoma and Langerhans cell histiocytosis. Lancet Oncol 6:435–437
17. Nakayama T, Hieshima K, Nagakubo D, Sato E, Nakayama M, Kawa K, Yoshie O (2004) Selective induction of Th2-attracting chemokines CCL17 and CCL22 in human B-cells by latent membrane protein 1 of Epstein-Barr virus. J Virol 78:1665–1674
18. Eliopoulos AG, Stack M, Dawson CW, Kaye KM, Hodgkin L, Sihota S, Rowe M, Young LS (1997) Epstein-Barr virus encoded LMP1 and CD40 mediate IL6 production in epithelial cells via an NF-κB pathway involving TNF receptor associated factors. Oncogene 24:2899–2916
19. Cumberbatch M, Dearman RJ, Griffiths CE, Kimber I (2000) Langerhans cell migration. Clin Exp Dermatol 25:413–418
20. Vassallo R, Ryu JH, Colby TV, Hatman T, Limper AH (2000) Pulmonary Langerhans'-cell histiocytosis. N Engl J Med 342:1969–1978

Virchows Arch (2010) 457:69–76
DOI 10.1007/s00428-010-0930-8

ORIGINAL ARTICLE

Expression of the GA733 gene family and its relationship to prognosis in pulmonary adenocarcinoma

Hiromi Kobayashi · Yuko Minami · Yoichi Anami · Yuzuru Kondou · Tatsuo Iijima · Junko Kano · Yukio Morishita · Koji Tsuta · Shinichiro Hayashi · Masayuki Noguchi

Received: 4 February 2010 / Revised: 23 April 2010 / Accepted: 26 April 2010 / Published online: 16 May 2010
© Springer-Verlag 2010

Abstract The GA733 gene family is composed of GA733-1 (TROP2) and GA733-2 (Ep-CAM), whose expression has been examined in various carcinomas and reported to be significantly associated with prognosis. The aim of this study was to investigate the expression of GA733 gene family members and to compare their prognostic significance in pulmonary adenocarcinoma. One hundred thirty paraffin-embedded specimens of small-sized pulmonary adenocarcinoma, less than 2 cm in diameter, were categorized using the classification of small-sized pulmonary adenocarcinoma devised by Noguchi et al. (Cancer 75:2844–2852, 1995) and examined immunohistochemically using a murine monoclonal antibody against Ep-CAM and a goat polyclonal antibody against TROP2. The patient survival rate was calculated using the Kaplan–Meier method. Ep-CAM and TROP2 were similarly expressed in many small-sized pulmonary adenocarcinomas. The expression of Ep-CAM was significantly related to a favorable outcome ($p=0.0185$), whereas TROP2 tended to be expressed in cases with an unfavorable outcome ($p=0.0564$), and was significantly associated with an unfavorable outcome in nonlepidic-type adenocarcinomas ($p=0.0125$). Multivariate analysis showed that TROP2 overexpression and lymph node metastasis were independent prognostic markers. Although the two GA733 proteins share structural similarity, they appear to have opposite biological significances in small-sized adenocarcinomas. As the expression of TROP2 was detected in more poorly differentiated tumors, the protein may have oncogenic activity.

Keywords GA733 family · Adenocarcinoma · Lung · Immunohistochemistry · Prognosis

H. Kobayashi · Y. Minami · Y. Anami · J. Kano · M. Noguchi (✉)
Department of Pathology, Institute of Basic Medical Sciences,
Graduate School of Comprehensive Human Sciences,
University of Tsukuba,
1-1-1 Tennodai,
Tsukuba-shi, Ibaraki 305-8575, Japan
e-mail: nmasayuk@md.tsukuba.ac.jp

Y. Kondou · Y. Morishita
Department of Pathology, Tsukuba University Hospital,
Ibaraki, Japan

T. Iijima
Division of Pathology, Ibaraki Prefectural Central Hospital,
Ibaraki, Japan

K. Tsuta
Clinical Laboratory Division, National Cancer Center Hospital,
Tokyo, Japan

H. Kobayashi · S. Hayashi
Division of Pulmonary Diseases,
Department of Internal Medicine, University of Saga,
Saga, Japan

Introduction

Lung cancer has a poor prognosis and is a major cause of death worldwide. Most lung cancer patients are initially diagnosed at an advanced stage, and few chemotherapeutic drugs elicit a satisfactory response. Therefore, there is a need to find biomarkers that are highly expressed in lung cancer from an early stage and can be used for prognostication. Lung cancer can be roughly classified into four groups: adenocarcinoma, squamous cell carcinoma, large cell carcinoma, and small cell carcinoma, among which the incidence of adenocarcinoma has been increasing recently, making it the most common histological type [1].

Previously, we established an immortalized atypical adenomatous hyperplasia cell line (PL16T) and a human

nonneoplastic bronchial epithelial cell line (PL16B) from the same patient by transfection with the gene for SV40 large T antigen [2]. We then compared the gene expression profile of PL16T with that of PL16B by suppression subtractive hybridization. Among the genes studied, GA733-1 was expressed three to 20 times higher in PL16T than in PL16B, and GA733-2 was expressed three times higher in PL16T than PL16B [2]. GA733-1 and GA733-2 belong to the GA733 gene family [3]. The GA733-1 gene is also known as TACSTD2, TROP2, M1S1, or EGP-1, whereas the GA733-2 gene is also known as TACSTD1, Ep-CAM, or KSA. Ep-CAM consists of nine exons and TROP2 is an intronless gene, formed by retroposition of Ep-CAM via an mRNA intermediate [4]. TROP2 has 49% homology with Ep-CAM, and both are type I transmembrane proteins with a single transmembrane domain [5]. Ep-CAM is a 40-kDa glycoprotein, which is reported to mediate Ca^{2+}-independent homotypic cell–cell adhesion [6]. TROP2 is a polypeptide of 35 kDa and thought to transduce an intracellular calcium signal, acting as a cell surface receptor [7]. Mutation of this gene is associated with gelatinous drop-like corneal dystrophy, an autosomal recessive disorder characterized by severe corneal amyloidosis leading to blindness [8]. Ep-CAM is expressed in many normal tissues and overexpressed in epithelial malignant tumor [9]. Ep-CAM has been highlighted as a target for immunotherapy. In addition, a correlation between Ep-CAM expression and clinical factors has been reported in squamous cell carcinoma [10], but it appears that no previous studies have analyzed the expression of Ep-CAM and TROP2 in adenocarcinoma. The aim of this study was to examine the expression of GA733 family genes in pulmonary adenocarcinomas and analyze its biological significance.

Materials and methods

Cases

We retrospectively selected 130 cases diagnosed as primary pulmonary adenocarcinoma with a maximal tumor dimension of less than 2 cm. The cause of death was related to lung cancer in all cases. The surgical resections had been performed at the National Cancer Center Hospital (Tokyo) during the period from January 1993 to December 2000. None of the patients had received chemotherapy and radiotherapy before or after surgery. Written informed consent had been obtained from all the patients (62 males and 68 females), who were aged between 38 and 82 years (median age, 60.7 years; Table 1). The patients were followed until death or up to October 12, 2007. Twenty-seven patients died during this period. In Table 1, the number of patients who died is shown in parentheses.

Tissue specimens and histological typing

All resected tumors were fixed with 10% formalin and embedded in paraffin for histologic examination. Sections were cut at a thickness of 3 μm and stained with hematoxylin and eosin and elastica van Gieson. Three pathologists (M.N. T.I. and Y.A.) examined the sections by light microscopy and classified the tumors into six histological subtypes according to the classification proposed by Noguchi et al. [11]. Briefly, they divided small-sized pulmonary adenocarcinoma into two groups: lepidic type and nonlepidic type. In addition, the lepidic type was divided into three types: type A (localized bronchioloalveolar carcinoma (LBAC)), type B (LBAC with alveolar collapse), and type C (LBAC with foci of active fibroblastic proliferation). The nonlepidic type was divided into another three types: type D (poorly differentiated adenocarcinoma), type E (acinar adenocarcinoma), and type F (true papillary adenocarcinoma). The patients with tumors classified as type A and type B showed a 100% 5-year survival rate. However, those with tumors classified as type C had a 5-year survival rate of 75%. On the other hand, the outcome of nonlepidic-type carcinomas was more unfavorable than that of lepidic-type carcinomas. Ep-CAM and TROP2 expression were determined by immunohistochemistry on paraffin-embedded tissue specimens using a mouse monoclonal antibody against Ep-CAM (ab7504, Abcam plc, Cambridge, UK, clone number Ber-EP4) and a goat polyclonal antibody against TROP2 (AF650, R&D Systems, Inc., Minneapolis, MN, USA). The antigen peptide of Ep-CAM and the protein sequence of TROP2 did not overlap. Three-micrometer-thick continuous sections were cut from paraffin-embedded tissue blocks, mounted on adhesive-coated glass slides, and then deparaffinized and rehydrated.

For staining of Ep-CAM, slides were pretreated with pronase solution (Proteinase K; Dako, Carpinteria, CA, USA) for 5 min. For staining with anti-TROP2 antibody, slides were placed in a box filled with TE buffer (pH 9.0) and autoclaved at 121°C for 10 min for antigen retrieval. After the pretreatment, the slides were removed and chilled in water.

The sections were then washed three times in wash buffer (Dako, CA, USA), followed by treatment with peroxidase-blocking solution (Dako, Glostrup, Denmark) for 5 min to quench any endogenous peroxidase. After another wash in wash buffer, the slides were incubated for 30 min at room temperature with each primary antibody (Ep-CAM; 1:10 dilution, TROP2; 1:50 dilution). After a further wash in wash buffer, the slides were incubated for 30 min at room temperature with the secondary antibody (Envision Plus dual link system peroxidase (Dako, CA, USA) for Ep-CAM and Histofine® Simple Stain MAX PO (G) (Nichirei Bioscience, Japan) for TROP2). To visualize the immunolabeled structures, the slides were reacted with

Table 1 Relationship of Ep-CAM and TROP2 overexpression and conventional clinicopathological parameters (n=130)

Characteristics	Number of patient	Ep-CAM overexpression		p value	TROP2 overexpression		p value
		No	Yes		No	Yes	
Gender							
Male	62	18	44	0.349	19	43	0.574
Female	68	25	43		24	44	
Age							
<60	60	18	42	0.49	15	45	0.07
≧60	70	25	45		28	42	
Noguchi classification							
Type A	12 (0)	4 (0)	8 (0)		5 (0)	7 (0)	
Type B	14 (0)	1 (0)	13 (0)		4 (0)	10 (0)	
Type C	63 (16)	18 (9)	45 (7)		18 (4)	45 (12)	
Type D	27 (8)	13 (4)	14 (4)		10 (0)	17 (8)	
Type E	8 (2)	3 (1)	5 (1)		4 (1)	4 (1)	
Type F	6 (1)	4 (0)	2 (1)		2 (0)	4 (1)	
Type A–C	89 (16)	23 (9)	66 (7)	0.01	27 (4)	62 (12)	0.328
Type D–F	41 (11)	20 (5)	21 (6)		16 (1)	25 (10)	
Pleural invasion							
p0	97	29	68	0.186	30	67	0.372
≧p1	33	14	19		13	20	
Vascular invasion							
v−	73	19	54	0.053	24	49	0.956
v+	57	24	33		19	38	
Nodal status							
pN0	89	24	65	0.029	29	60	0.86
≧pN1	41	19	22		14	27	
Prognosis							
Alive	103	29	74	0.02	38	65	0.071
Dead	27	14	13		5	22	

Envision Plus/HRP (DAB; Dako, CA, USA). Following incubation for 5 min, the slides were rinsed with distilled water. All sections were counterstained with hematoxylin.

Scoring of sections

Two observers (H.K. and Y.K.) scored the sections independently without any information about clinical outcome. We scored all sections in accordance with a previous report on immunohistochemistry for Ep-CAM [12]. Briefly, a total immunostaining score was calculated as the product of a proportion score and an intensity score. The proportion score represented the estimated fraction of positively stained tumor cells (0 = none; 1 = <10%; 2 = ≧10%, <50%; 3 = ≧50%, <80%; 4 = ≧80%). The intensity score represented the estimated staining intensity (0—no staining, 1—weak, 2—moderate, 3—strong). Thus, the total score ranged from 0 to 12. Ep-CAM and TROP2 overexpressions were defined as a total score exceeding 4.

Statistical analysis

Differences between the expression of Ep-CAM or TROP2 and clinical variables were estimated using the χ^2 test. Survival curves in relation to Ep-CAM expression and TROP2 expression in patients overall and for lepidic type (types A, B, and C) and nonlepidic type (types D, E, and F) were drawn using the Kaplan–Meier method and compared by the log-rank test. Additionally, the influence of each variable on survival, including gender, age, pleural invasion, vascular invasion, lymph node metastasis, Noguchi classification (lepidic/nonlepidic), Ep-CAM overexpression, and TROP2 overexpression, was assessed using the Cox proportional hazards regression model in order to find independent prognostic factors. For all analyses, a p value of less than 0.05 was considered statistically significant. All statistical analyses were carried out using the SPSS statistical software package (SPSS Inc., Chicago, IL, USA).

Results

Histological typing

The 130 pulmonary adenocarcinomas were classified into six types according to the Noguchi classification: 12 tumors were classified as type A, 14 as type B, 63 as type C, 27 as type D, eight as type E, and six as type F (Table 1). The clinicopathological characteristics of all the cases are summarized in Table 1. Pleural invasion were seen in 33 cases (25.4%), vascular invasion in 57 (43.8%), and lymph node metastasis in 41 (31.5%).

Immunohistochemical detection of Ep-CAM and TROP2

Immunohistochemistry with both the Ep-CAM and TROP2 antibodies showed a positive reaction at the cell membrane (Fig. 1a, b). However, seven cases also showed cytoplasmic positivity for TROP2 (Fig. 1c). Many lepidic-type tumors (types A, B, and C) were stained strongly for Ep-CAM (66 out of 89, 74%) and TROP2 (62 out of 89, 70.0%). Ep-CAM overexpression was seen in 87 of the 130 tumors (67%), and TROP2 overexpression was also seen in 87 tumors (67%). In type C, which includes cases with both a favorable and an unfavorable outcome, Ep-CAM expression tended to be lower in the central fibrotic area (invasive area) of the tumor, in comparison with the periphery (Fig. 2b–d). Analysis of the Kaplan–Meier curves revealed that overexpression of Ep-CAM was significantly related to a favorable outcome (p=0.0185; Fig. 3a). A similar result was seen for patients with lepidic-type tumors (types A, B, and C; p=0.0014; Fig. 3b) and also in patients with type C (p=0.0029, data not shown). However, for nonlepidic-type tumors (types D, E, and F), there was no significant difference in outcome between positive cases and negative cases (Fig. 3c).

On the other hand, overexpression of TROP2 in the tumors tended to be associated with an unfavorable

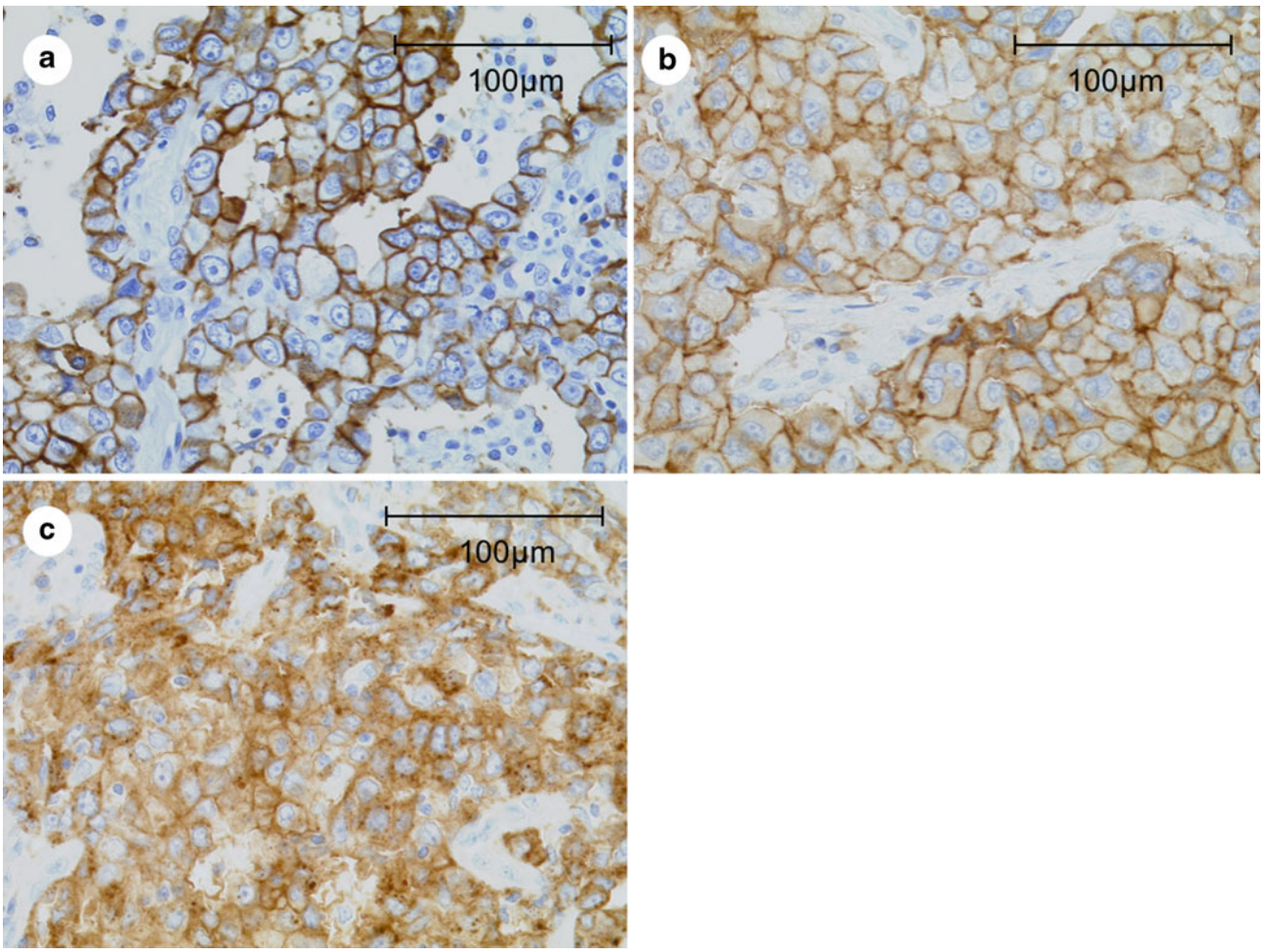

Fig. 1 Immunohistochemistry for Ep-CAM (**a**) and TROP2 (**b**, **c**). Both show a positive reaction at the cell membrane (**a**, **b**). In some cases, TROP2 also shows a positive reaction in the cytoplasm of the tumor cells (**c**). The length of the bar is 100 μm (original magnification, ×400)

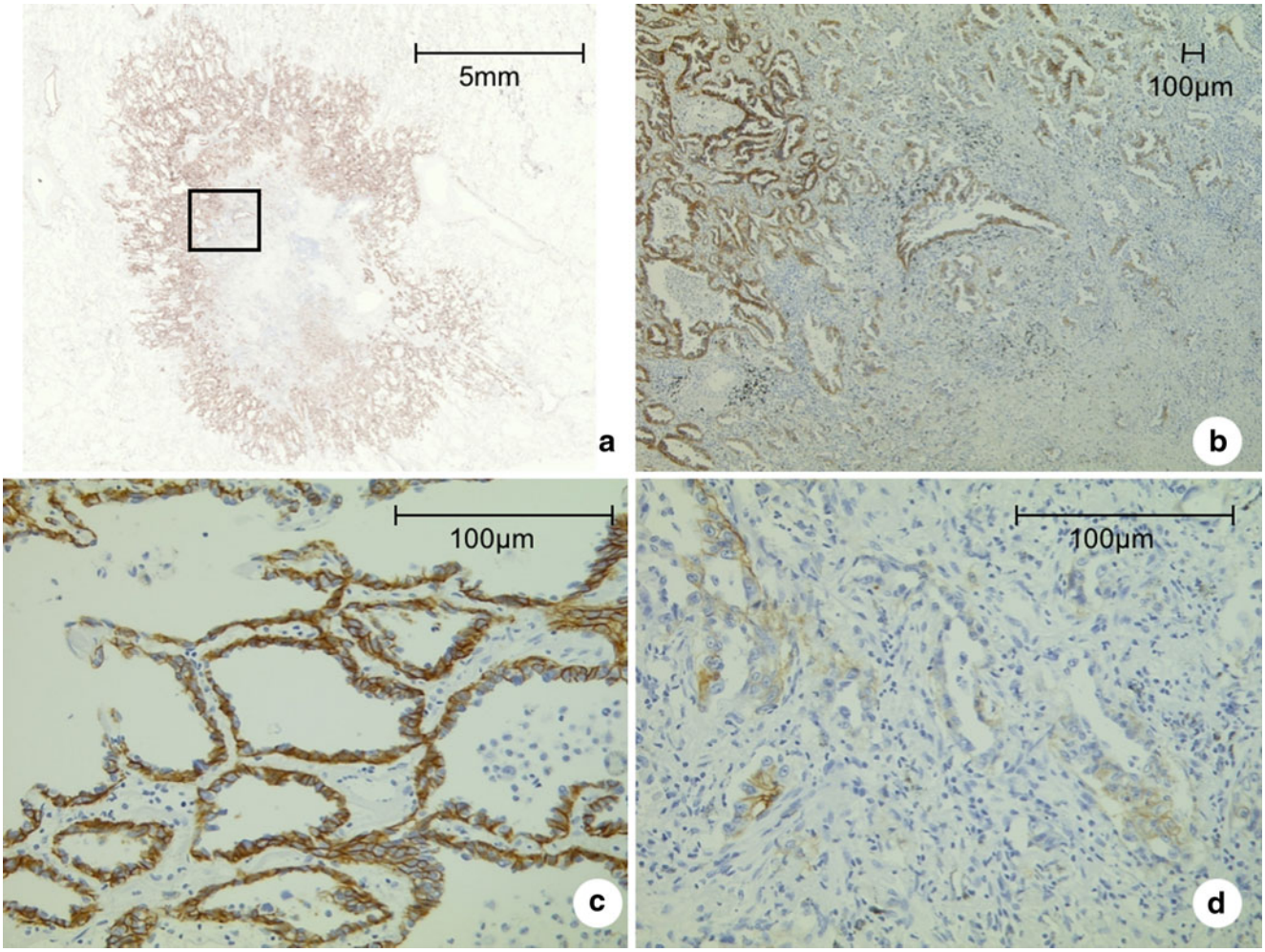

Fig. 2 Immunohistochemistry for Ep-CAM in type C adenocarcinoma. Low magnification shows a positive reaction in the marginal area (in situ lepidic growth component) of the tumor (**b**; original magnification; ×40). The expression decreased in the area showing transition from in situ lepidic growth to invasion (*boxed region*; **a**, **b**). Ep-CAM is strongly positive in the in situ lepidic growth component (**c**) but weakly positive or negative in the invasive area (**d**; original magnification; ×400)

outcome (p=0.0564; Fig. 4a). Interestingly, in nonlepidic-type tumors (types D, E, and F), TROP2 overexpression was significantly associated with an unfavorable outcome (p=0.0125; Fig. 4c). Among the seven cases positive for cytoplasmic staining, four showed a diffuse staining pattern. All of them were histologically classified as invasive lepidic-type tumor (type C), and the patients died of the disease. The other three cases showed partially positive staining for TROP2. Among them, one case was classified as invasive lepidic-type tumor (type C), and the other two cases were nonlepidic-type tumors (type D). Two of the three patients died of the disease. Therefore, in total, six of seven patients whose tumors showed cytoplasmic staining (85.7%) died of their disease.

Univariate analysis of tumor Ep-CAM and TROP2 expression in relation to clinicopathological factors revealed that Ep-CAM overexpression was correlated with the tumor growth pattern (lepidic type or nonlepidic type), lymph node metastasis, and prognosis, whereas TROP2 overexpression had no such correlation (Table 1). Multivariate analysis identified TROP2 overexpression as an independent prognostic marker (p=0.045, hazard ratio (HR) 2.884, 95% confidence interval (CI) 1.024–8.123; Table 2). Additionally, lymph node metastasis was the most independent prognostic marker (p<0.0001, HR 5.712, 95% CI 2.183–14.944).

Discussion

Many studies have addressed the relationship between Ep-CAM expression and prognosis in various cancers [10, 12–19]. For example, overexpression of Ep-CAM is reportedly correlated with an unfavorable outcome in cancers of the breast [12–15], ovary [16], gallbladder [17], and esophagus [18] and also with the presence of disseminated tumor cells

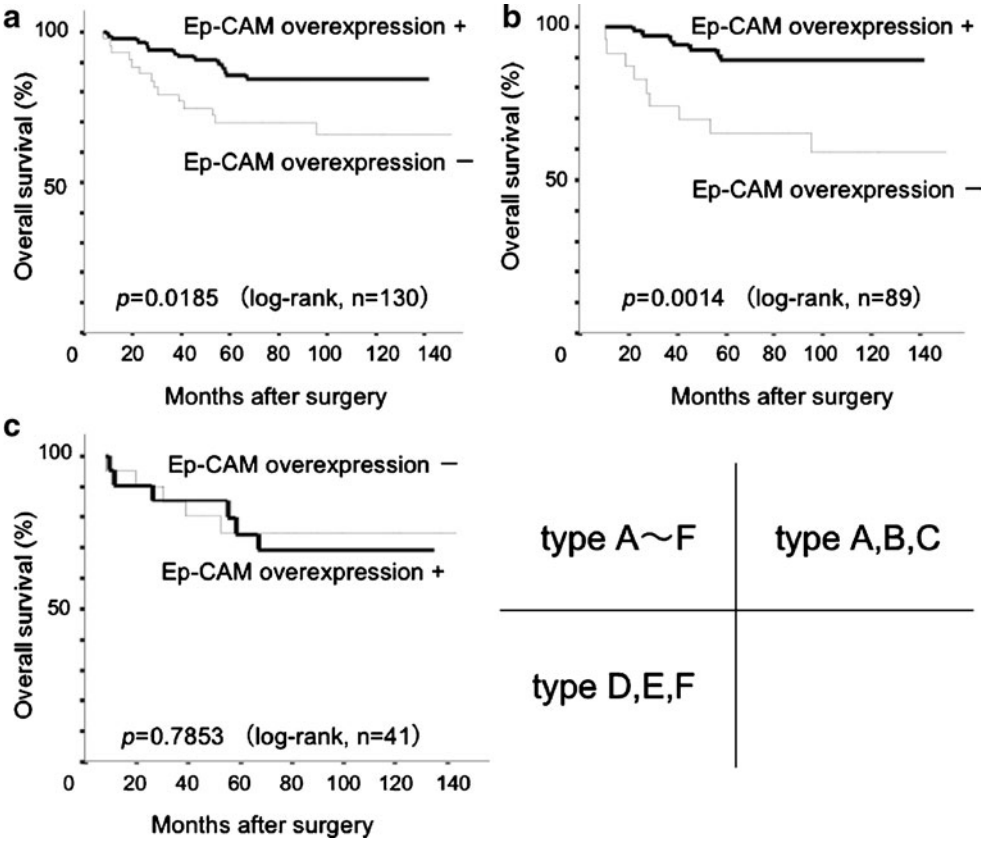

Fig. 3 Prognostic significance of Ep-CAM overexpression in 130 patients with pulmonary adenocarcinoma in relation to overall survival determined by Kaplan–Meier analysis. *Dark line*: pulmonary adenocarcinoma patients with high Ep-CAM expression. *Light line*: patients lacking, or with low Ep-CAM expression. **a** The survival curve for the total 130 patients. **b** The survival curve for patients whose tumors showed lepidic growth (types A, B, and C). **c** The survival curve for patients whose tumors showed nonlepidic growth (types D, E, and F)

in lymph nodes after complete resection of nonsmall cell lung cancer [19]. In squamous cell carcinoma of the lung, tumor expression of Ep-CAM has been reported to increase significantly with increasing involvement of regional lymph nodes and TNM stage [10]. On the other hand, it has been reported that a decrease or loss of Ep-CAM expression is correlated with an unfavorable outcome in clear cell renal carcinoma [20] and gastric cancer [21]. In the present study, Ep-CAM overexpression was correlated with a favorable outcome of pulmonary adenocarcinoma, supporting a previous study suggesting an inverse relationship between Ep-CAM overexpression and outcome of patients with squamous cell carcinoma of the lung [10].

Ep-CAM is an epithelial adhesion molecule expressed in the normal alveolar epithelium and is thought to play a role in cell–cell contact. Interestingly, Gosens et al. have shown that reduced Ep-CAM staining at the invasive margin of rectal tumor specimens was correlated significantly with tumor budding, tumor grade, and an increased risk of local recurrence [22]. They concluded that loss of membranous Ep-CAM was associated with nuclear β-catenin localization and that this contributed to reduction of cell–cell adhesions, increased migratory potential, and tumor budding. However, it is very difficult to discuss the tumor margin (budding) of lung adenocarcinoma since the direction of invasion is not easily discernible in lung cancers. Another report has indicated that adhesion induced by Ep-CAM suppresses the invasion of tumor cells in a murine model [23]. On the basis of the present findings, we hypothesize that a decrease in the expression of Ep-CAM will cause a tumor to develop an invasive nature. Suppression of Ep-CAM will lead to degradation of cell–cell attachment at the primary site and promote distant metastasis. Therefore, it is not surprising that the patients in the present series showing overexpression of Ep-CAM would have had a lower likelihood of lymph node metastasis and a more favorable outcome. The difference between our data and previous study of squamous cell carcinoma may have been due to the different histological natures of adenocarcinoma and squamous cell carcinoma. Ep-CAM was considered to be a useful prognostic marker of pulmonary adenocarcinoma and especially for identification of early invasive adenocarcinomas (type C tumors) that have an extremely favorable outcome and for which reduction surgery is warranted.

On the other hand, TROP2, like Ep-CAM, is also a member of the GA733 gene family and considered to be located on the cell membrane, but unlike Ep-CAM, its overexpression was associated with an unfavorable outcome in pulmonary adenocarcinoma. Although the number of studies is limited, overexpression of TROP2 is reportedly associated with an unfavorable outcome in colorectal

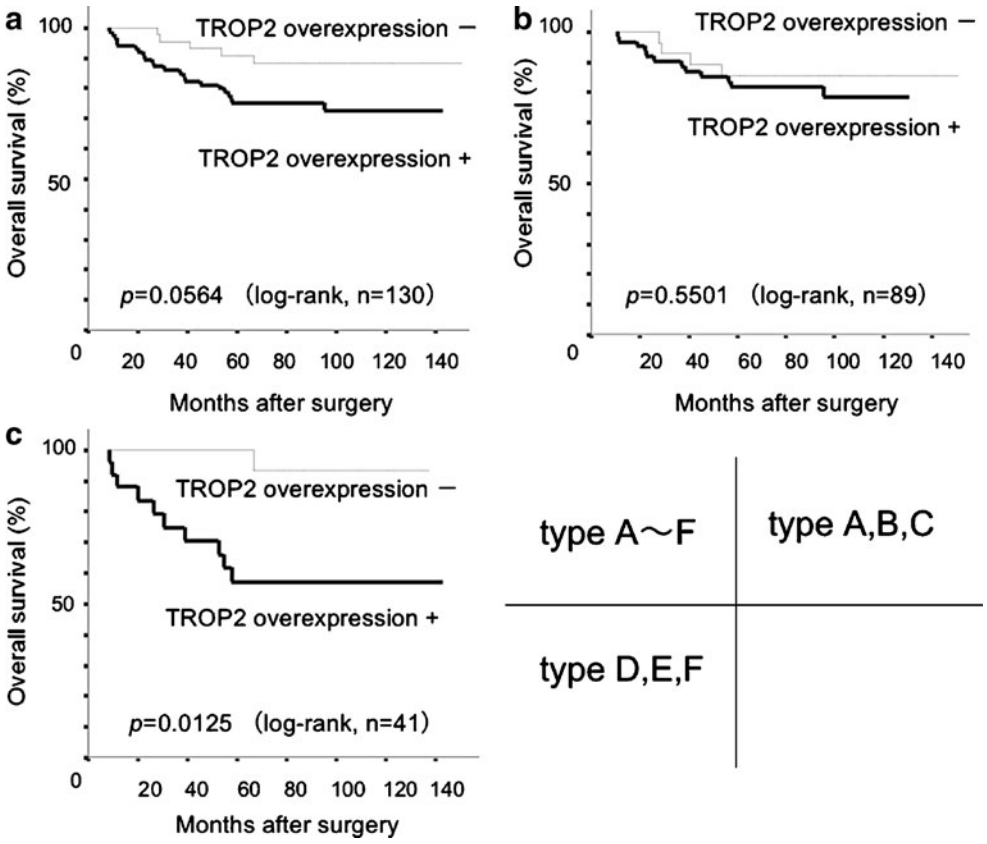

Fig. 4 Prognostic significance of TROP2 overexpression in 130 patients with pulmonary adenocarcinoma in relation to overall survival determined by Kaplan–Meier analysis. *Dark line*: pulmonary adenocarcinoma patients with high TROP2 expression. *Light line*: patients lacking, or with low TROP2 expression. **a** Survival curve for all 130 patients. **b** Survival curve for patients whose tumors showed lepidic growth (types A, B, and C). **c** Survival curve for patients whose tumors showed nonlepidic growth (types D, E, and F)

carcinoma [24], squamous cell carcinoma of the oral cavity [25], and pancreatic carcinoma [26]. Interestingly, Terrinoni et al. have indicated that *CYCLIN D1-TROP2* chimera protein in human cancer cells [27] and TROP2 may have a role in accelerating the cancer cell cycle and cell growth. As shown in Fig. 1c, expression of Ep-CAM was clearly detected at the cell membrane, whereas TROP2 was additionally expressed in the cytoplasm. Interestingly, six (85.7%) of the seven patients whose tumors showed cytoplasmic expression of TROP2 died of tumor metastasis or recurrence. Although the number of cases was limited, cytoplasmic staining of TROP2 may be associated with an unfavorable prognosis in patients with lung adenocarcinoma. The incomplete or abnormal transcription or translation of the TROP2 gene may result in cytoplasmic expression of TROP2 and correlated with its function. These findings indicate that the TROP2 gene might participate as an oncogene in pulmonary adenocarcinoma. Although Ep-CAM and TROP2 belong to the same gene family, their opposite effects in relation to the prognosis of pulmonary adenocarcinoma are intriguing. TROP2 expression was characteristically detected in nonlepidic-type advanced cancers and was correlated with tumor invasion or metastasis. Although expression of both TROP2 and Ep-CAM was shown to be associated with the outcome of lung adenocarcinoma by univariate analysis, TROP2 was the

Table 2 Multivariate analysis of survival in small adenocarcinoma

Parameter	Hazard ratio (95% CI[a])	*p* value
Gender (male vs. female)	1.488 (0.635–3.490)	0.360
Age (<60 vs. ≧60)	1.030 (0.450–2.361)	0.944
Pleural invasion (present vs. absent)	0.633 (0.257–1.556)	0.319
Vascular invasion (present vs. absent)	1.687 (0.626–4.547)	0.301
Lymph node metastasis (present vs. absent)	5.712 (2.183–14.944)	0.0001
Noguchi classification (lepidic vs. nonlepidic)	1.349 (0.549–3.312)	0.514
Ep-CAM overexpression	0.693 (0.291–1.653)	0.409
TROP2 overexpression	2.884 (1.024–8.123)	0.045

[a] Confidence interval

only independent prognostic factor indicated by multivariate analysis. It seemed that the influence of Ep-CAM expression was canceled because there was strong correlation between Ep-CAM expression and lymph node metastases. Recently, specific monoclonal antibodies against Ep-CAM (e.g., Edrecolomab) have been used for the treatment of colorectal cancer and metastatic breast cancer [28]. However, in pulmonary adenocarcinoma, it is considered that TROP2, rather than Ep-CAM, is the more powerful prognostic factor and may be a more useful therapeutic target.

Acknowledgments This work was supported in part by a Grant-in-Aid for Cancer Research (16-1) from the Ministry of Health, Labour and Welfare of Japan.

Conflict of interest statement We declare that we have no conflict of interest.

References

1. Travis WD, Brambilla E, Muller-Hermelink HK et al (2004) Pathology and genetics: tumours of the lung, pleura, thymus and heart World Health Organization classification of tumours. IARC, Lyon
2. Shimada A, Kano J, Ishiyama T et al (2005) Establishment of an immortalized cell line from a precancerous lesion of lung adenocarcinoma, and genes highly expressed in the early stages of lung adenocarcinoma development. Cancer Sci 96:668–675
3. Linnenbach AJ, Wojcierowski J, Wu S et al (1989) Sequence investigation of the major gastrointestinal tumor-associated antigen gene family, GA733. Proc Natl Acad Sci USA 86:27–31
4. Linnenbach AJ, Seng BA, Wu S et al (1993) Retroposition in a family of carcinoma-associated antigen genes. Mol Cell Biol 13:1507–1515
5. Szala S, Froehlich M, Scollon M et al (1990) Molecular cloning of cDNA for the carcinoma-associated antigen GA733-2. Proc Natl Acad Sci USA 87:3542–3546
6. Litvinov SV, Bakker HAM, Gourevitch MM et al (1994) Evidence for a role of the epithelial glycoprotein 40(Ep-CAM) in epithelial cell–cell adhesion. Cell Adhes Commun 2:417–428
7. Ripani E, Sacchetti A, Corda D et al (1998) Human Trop-2 is a tumor-associated calcium signal transducer. Int J Cancer 76:671–676
8. Tsujikawa M, Kurahashi H, Tanaka T et al (1999) Identification of the gene responsible for gelatinous drop-like corneal dystrophy. Nat Genet 21:420–423
9. Balzar M, Winter MJ, de Boer CJ et al (1999) The biology of the 17-1A antigen (Ep-CAM). J Mol Med 77:699–712
10. Piyathilake CJ, Frost AR, Weiss H et al (2000) The expression of Ep-CAM (17-1A) in squamous cell cancers of the lung. Hum Pathol 31:482–487
11. Noguchi M, Morikawa A, Kawasaki M et al (1995) Small adenocarcinoma of the lung. Histologic characteristics and prognosis. Cancer 75:2844–2852
12. Gastl G, Spizzo G, Obrist P et al (2000) Ep-CAM overexpression in breast cancer as a predictor of survival. Lancet 356:1981–1982
13. Spizzo G, Obrist P, Ensinger C et al (2002) Prognostic significance of Ep-CAM and Her-2/neu overexpression in invasive breast cancer. Int J Cancer 98:883–888
14. Spizzo G, Went P, Dirnhofer S et al (2004) High Ep-CAM expression is associated with poor prognosis in node-positive breast cancer. Breast Cancer Res Treat 86:207–213
15. Schmidt M, Hasenclever D, Schaeffer M et al (2008) Prognostic effect of epithelial cell adhesion molecule overexpression in untreated node-negative breast cancer. Clin Cancer Res 14:5849–5855
16. Spizzo G, Went P, Dirnhofer S et al (2006) Overexpression of epithelial cell adhesion molecule (Ep-CAM) is an independent prognostic marker for reduced survival of patients with epithelial ovarian cancer. Gynecol Oncol 103:483–488
17. Varga M, Obrist P, Schneeberger S et al (2004) Overexpression of epithelial cell adhesion molecule antigen in gallbladder carcinoma is an independent marker for poor survival. Clin Cancer Res 10:3131–3136
18. Stoecklein NH, Siegmund A, Scheunemann P et al (2006) Ep-CAM expression in squamous cell carcinoma of the esophagus: a potential therapeutic target and prognostic marker. BMC Cancer 6:165
19. Kubuschok B, Passlick B, Izbicki JR et al (1999) Disseminated tumor cells in lymph nodes as a determinant for survival in surgically resected non-small-cell lung cancer. J Clin Oncol 17:19–24
20. Kim HL, Seligson D, Liu X et al (2004) Using protein expressions to predict survival in clear cell renal carcinoma. Clin Cancer Res 10:5464–5471
21. Songun I, Litvinov SV, van de Velde CJ et al (2005) Loss of Ep-CAM (CO17-1A) expression predicts survival in patients with gastric cancer. Br J Cancer 92:1767–1772
22. Gosens MJ, van Kempen LC, van de Velde CJ et al (2007) Loss of membranous Ep-CAM in budding colorectal carcinoma cells. Mod Pathol 20:221–232
23. Basak S, Speicher D, Eck S et al (1998) Colorectal carcinoma invasion inhibition by CO17-1A/GA733 antigen and its murine homologue. J Natl Cancer Inst 90:691–697
24. Ohmachi T, Tanaka F, Mimori K et al (2006) Clinical significance of Trop2 expression in colorectal cancer. Clin Cancer Res 12 (10):3057–3063
25. Fong D, Spizzo G, Gostner JM et al (2008) TROP2: a novel prognostic marker in squamous cell carcinoma of the oral cavity. Mod Pathol 21:186–191
26. Fong D, Moser P, Krammel C et al (2008) High expression of TROP2 correlates with poor prognosis in pancreatic cancer. Br J Cancer 99:1290–1295
27. Terrinoni A, Dell'Arciprete R, Fornaro M et al (2001) Cyclin D1 gene contains a cryptic promoter that is functional in human cancer cells. Genes Chromosomes Cancer 31:209–220
28. Schwartzberg LS (2001) Clinical experience with edrecolomab: a monoclonal antibody therapy for colorectal carcinoma. Crit Rev Oncol Hematol 40:17–24

Virchows Arch (2010) 457:77–85
DOI 10.1007/s00428-010-0932-6

ORIGINAL ARTICLE

Proliferation analysis of the growth plate after diaphyseal midshaft fracture by 5′-bromo-2′-deoxy-uridine

Gregor Janezic · Eva-Elisa Widni · Emir Q. Haxhija · Martin Stradner · Eleonore Fröhlich · Annelie-Martina Weinberg

Received: 1 February 2010 / Revised: 27 April 2010 / Accepted: 6 May 2010 / Published online: 23 May 2010
© Springer-Verlag 2010

Abstract Both stimulative and inhibitory growth disturbances may occur after a fracture during the growth period. The exact mechanism responsible for stimulative growth disturbances in the immature skeleton is unexplained. It's possible that chondrocyte proliferation leads to overgrowth. This study investigates the effect of a fracture on the proliferation of chondrocytes at the nearby growth plate and its effect on the contra-lateral leg. Fifty-six 1-month-old Sprague–Dawley rats (weight, 100–120 g) were randomised to either an experimental or a control group. A closed mid-diaphyseal tibial fracture was produced in all animals of the experimental group using a standardised technique. On day 3, 10, 14 and 29 of the experiment, the rats were euthanised and their tibial growth plates were subjected to histological analysis. 5′-Bromo-2′-deoxy-uridine labelling was used for the quantitative analysis of chondrocyte proliferation. Safranin O staining provided the histological overview for the subsequent analysis of BrdU-labelling. Immunohistochemical analysis showed increased proliferation of chondrocytes in the growth plates of broken bones during fracture healing. This proliferation peaked on day 3 post-fracture and then reduced gradually until day 29. No increase in the rate of proliferation was observed on the contra-lateral limbs of the animals in the experimental group. Following a diaphyseal fracture of the tibia, the growth plates located next to the fracture react with increased cell proliferation. This proliferation was not observed in the contra-lateral uninjured tibia. This investigation shows that the post-traumatic length discrepancy is a local biological process at the growth plate brought about by the fracture.

Keywords Growth plate · Chondrocyte proliferation · Growth disturbance · Bone length discrepancy · 5′-Bromo-2′-deoxy-uridine

G. Janezic · E.-E. Widni (✉) · E. Q. Haxhija · A.-M. Weinberg
Department of Paediatric and Adolescent Surgery,
Medical University of Graz,
Auenbruggerplatz 34,
8036 Graz, Austria
e-mail: eva.widni@gmail.com

M. Stradner
Department of Internal Medicine, Division of Rheumatology,
Medical University of Graz,
Auenbruggerplatz 15,
8036 Graz, Austria

E. Fröhlich
Center for Medical Research, Division Core Facility Microscopy,
Medical University of Graz,
Stiftingtalstraße 24,
8010 Graz, Austria

Introduction

The phenomenon of overgrowth due to a stimulative growth disturbance following a fracture in bones with open growth plates is well documented [1–7]. [8].

The underlying pathomechanisms of this process are still not fully understood, but it is reasonable to assume that temporary local stimuli interact with the growth plate following a fracture. This may be due to an increase in the blood flow at the fracture site which may exert a direct effect. This would implicate changes in the physical and metabolic microenvironment. A temporary hypervascularity is closely associated with an increased proliferation of physeal chondrocytes [9–16]. Furthermore, the process of fracture remodelling is associated with an extensive periosteal reaction [17, 18]. Mechanical stress and strain due to fracture instability may also influence chondrocyte proliferation altering the mechanical microenvironment [19]. Finally, the

influence of the fracture on physeal processes may be initiated by an alteration of the normal gene expression brought about by locally acting growth factors [16, 20, 21].

The growth plate is a horizontal structure between the epiphysis and metaphysis, directing longitudinal growth of tubular bones through endochondral ossification. Following puberty, as the skeleton reaches maturity, the growth plate becomes thinner and ossifies, fusing the metaphysis to the epiphysis [22]. The growth plate can be divided into several zones according to the shape, size and organisation of the chodrocytes: resting/germinal zone, column/proliferative zone, hypertrophic zone, zone of provisional calcification and zone of vascular invasion [23–25]. Chondrocyte metabolism is maintained by diffusion from vessels at the epi- and metaphysis as well as the periphysis, which consists of the zone of Ranvier, responsible for longitudinal growth and the perichondral ring of LaCroix, a fibrous sheet surrounding the physis which is continuous with the periosteum and provides mechanical support for the growth plate [26].

The germinal or resting zone, adjoining the epiphysis, consists of round quiescent chondrocytes (chondrocyte progenitor cells) which regulate unidirectional bone growth [27]. Proliferating chondrocytes are flattened, line up in columns and are arranged parallel to the longitudinal axis of the bone. The chondrocytes are separated by cartilage matrix mainly consisting of type II collagen and proteoglycan aggrecans, which they synthesise. Depending on the mitotic activity of proliferating chondrocytes, each column consists of 10 to 20 cells. Therefore, this zone determines the rate of bone growth and ultimately its length. At the distal part of the column zone, chondrocytes enter the next stage of differentiation and mature into prehypertrophic and finally into fully differentiated round hypertrophic chondrocytes. This five to tenfold gain in cellular volume is achieved by the accumulation of glycogen and an increase in the number of intracellular organelles. Hypertrophic chondrocytes synthesise short-chain type X collagen, VEGF and matrix vesicles which contain high concentrations of alkaline phosphatase, initiating and regulating matrix mineralisation and vascularisation. These zones are referred to as zones of provisional calcification and vascular invasion.

Hypertrophic cells then go through programmed cell death (apoptosis). Vascularisation enables migration of osteoprogenitor cells, osteoblasts, chondroclasts and osteoclasts, which catabolise calcified cartilage tissue and cell remnants and form primary spongiosa consisting of mineralised cartilage and bony trabeculae. Finally, the bone is organised in lamellae and secondary trabeculae are gradually formed through the process of bone remodelling [23–25].

In order to estimate the increased physeal activity following a fracture, we employed an immunhistochemical method for analysing physeal proliferation during growth. The aim of this study was to analyse the rate of chondrocyte proliferation at the tibial growth plate under control conditions and following a diaphyseal fracture using 5'-bromo-2'-deoxy-uridine as the labelling reagent in a rat model. We also investigated the effect of the diaphyseal fracture on the growth plate of the contralateral uninjured tibia. Proliferating chondrocytes were analysed for their spatial and temporal progression through the growth plate in 24 h in order to determine their rate of transit through the proliferative zone.

Material and methods

Animal model and surgery

Fifty-six 1-month-old Sprague–Dawley rats weighing between 100 and 120 g were used. The animals were randomised into the experimental (n=28) or control (n=28) groups (Table 1). On day 0, the animals in the experimental group were anaesthetised by intramuscular administration of Ketanest-S® at a dose of 90 mg/kg and Rompun® at a dose of 5 mg/kg (Pfizer Corp. Austria, A-1210 Vienna). Then a simple closed transverse mid-diaphyseal fracture of their left tibia was produced according to a standardised protocol [28]. This involved dropping a 300-g weight from a height of 20 cm to drive a blunt guillotine onto the tibial diaphysis. Postoperatively, the rats were returned to their cages for nursing with free access to food and water. There was no restriction of activity. A painkiller (Rimadyl® 4–5 mg/kg) was injected subcutaneously once daily for 1 week. After the first week, Novalgin® drops were added to their drinking water for further analgesia (Pfizer Corp. Austria, A-1210 Vienna) whilst administration of Rimadyl was stopped. The control group also received analgesia in the same fashion as the experimental group.

5-Bromo-2′-deoxy-uridine labelling, euthanasia, harvesting, fixation and stabilisation of bone tissue

5-Bromo-2′-deoxy-uridine (BrdU) is incorporated into DNA in place of thymidine. Monoclonal antibodies are then directed against BrdU allowing an indirect measure of

Table 1 Study design

Groups (N=7 each)	Days of euthanasia				
Experimental group	1	3	10	14	29
Control group	1	3	10	14	29

Experimental animals were subjected to unilateral diaphyseal fracture of the left tibia at day 0

cell proliferation. As per our study protocol (Table 1), BrdU labelling (5-bromo-2′-deoxy-uridine Labelling and Detection Kit I®, Roche Diagnostics GmbH, A-1211 Vienna) was performed at specified time points (1, 3, 10, 14 and 29 days post-fracture), 1.6 ml per 100 g body weight (50 mg/kg body weight) undiluted BrdU-labelling reagent (sterile 1×10 ml BrdU stock solution 1,000× conc. in 10 mM phosphate buffered saline (PBS)) was injected intraperitoneally into the experimental and control animals. The animals were euthanised by an intracardiac injection of Pentothal® under Furane® narcosis (Abbott GmbH A-1230 Vienna) 2 h after the administration of BrdU. The left and the right tibiae were retrieved, and soft tissues removed. The samples were subsequently fixed in 4% buffered formalin (pH7.4) for 24 h. The bones were then decalcified in EDTA (pH7.0) for 2 weeks.

Embedding in paraffin and immunohistochemistry

Following fixation in formalin and decalcification, the samples were dehydrated in ascending concentrations of ethanol, 70% EtOH at 60°C for 2 h, then 96% EtOH at 60°C for 4 h and finally in acetone at 60°C for 1 h. The samples were then incubated in liquid paraffin at 60°C for 1 h and subsequently embedded with the aid of Tissue-Tek® TEC™ tissue-embedding console system.

Safranin O staining of each sample was conducted to demonstrate the histological anatomy according to standardised protocols. Coronal sections of 5 µm thickness were cut with a microtome. Sections were dried for at least 10 h at 37°C, and afterwards, for 1 h at 60°C.

Two 2 µm thick coronal sections of the growth plate were used for immunohistochemistry, one for positive

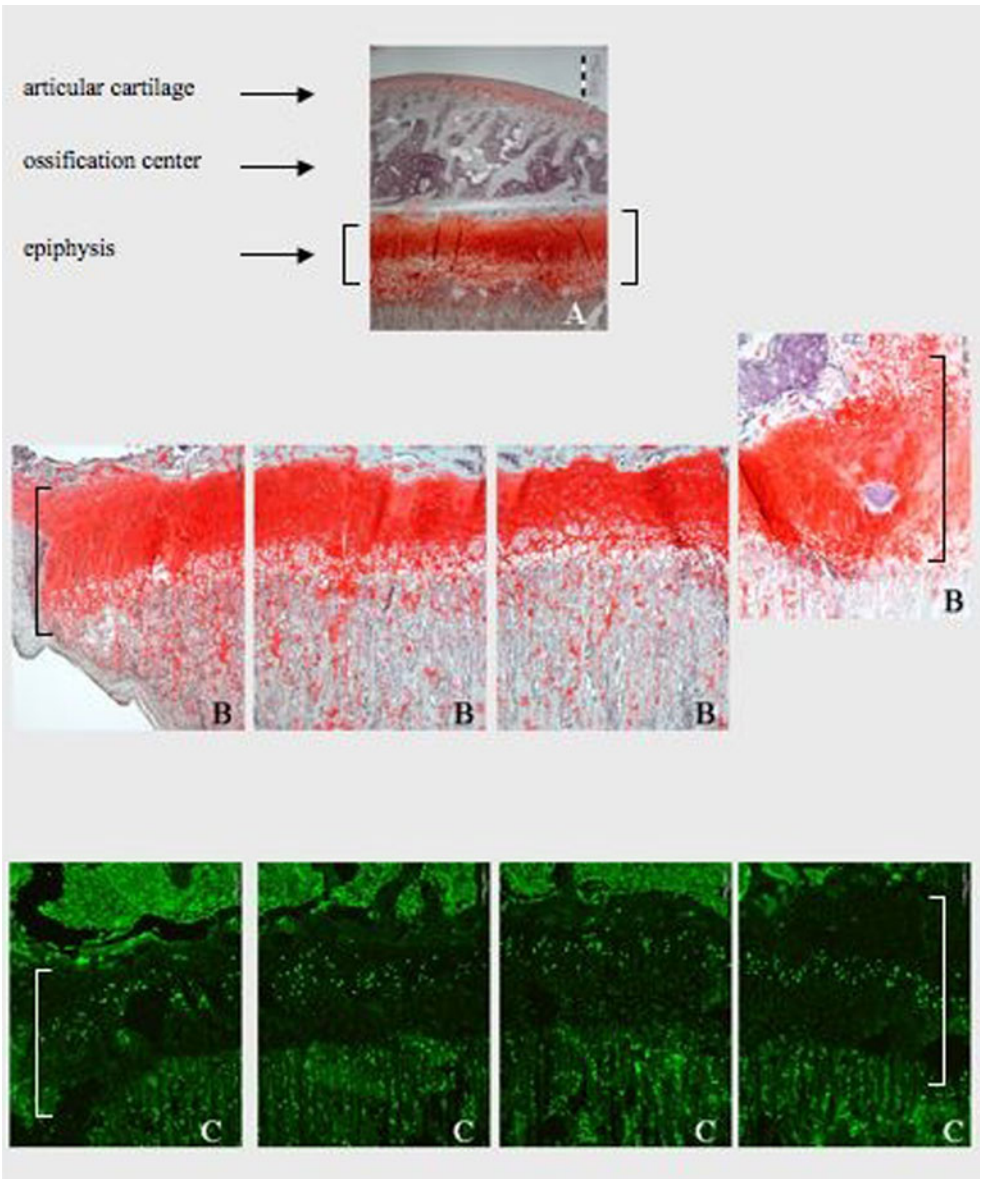

Fig. 1 Image editing. **a** Overview of the growth plate (Safranin O staining; original magnification of ×40). **b** The corresponding segments (Safranin O staining; original magnification of ×100). **c** The corresponding segments (BrdU—immunohistochemical; original magnification of ×100)

staining and the other for negative control. After drying the sections as described, they were deparaffinised in xylene initially for 5 and again for 10 min. They were then hydrated in 100%, 90%, 70% and 50% ethanol for 3 min each. Subsequently, the slides were immersed in PBS (2× 5 min) before placing them into a special container filled with Na-citrate buffer (0.01 mol; pH6.0), where they were boiled for 20 min. After cooling for 20 min, they were washed in PBS. "Positive" sections were covered with 100 µl of the diluted primary monoclonal mouse antibody (1:10 in incubation buffer containing nucleases for DNA staining). "Negative" sections were covered with 100 µl of the incubation buffer. The slides were then incubated in a humidity chamber at 37°C for 30 min and afterwards washed in PBS. Finally, 100 µl of the diluted (1:10 in distilled water) secondary antibody (anti-mouse-IG-fluorescein antibody generated in sheep) was applied to both sections. After incubation for 30 min at 37°C, slides were

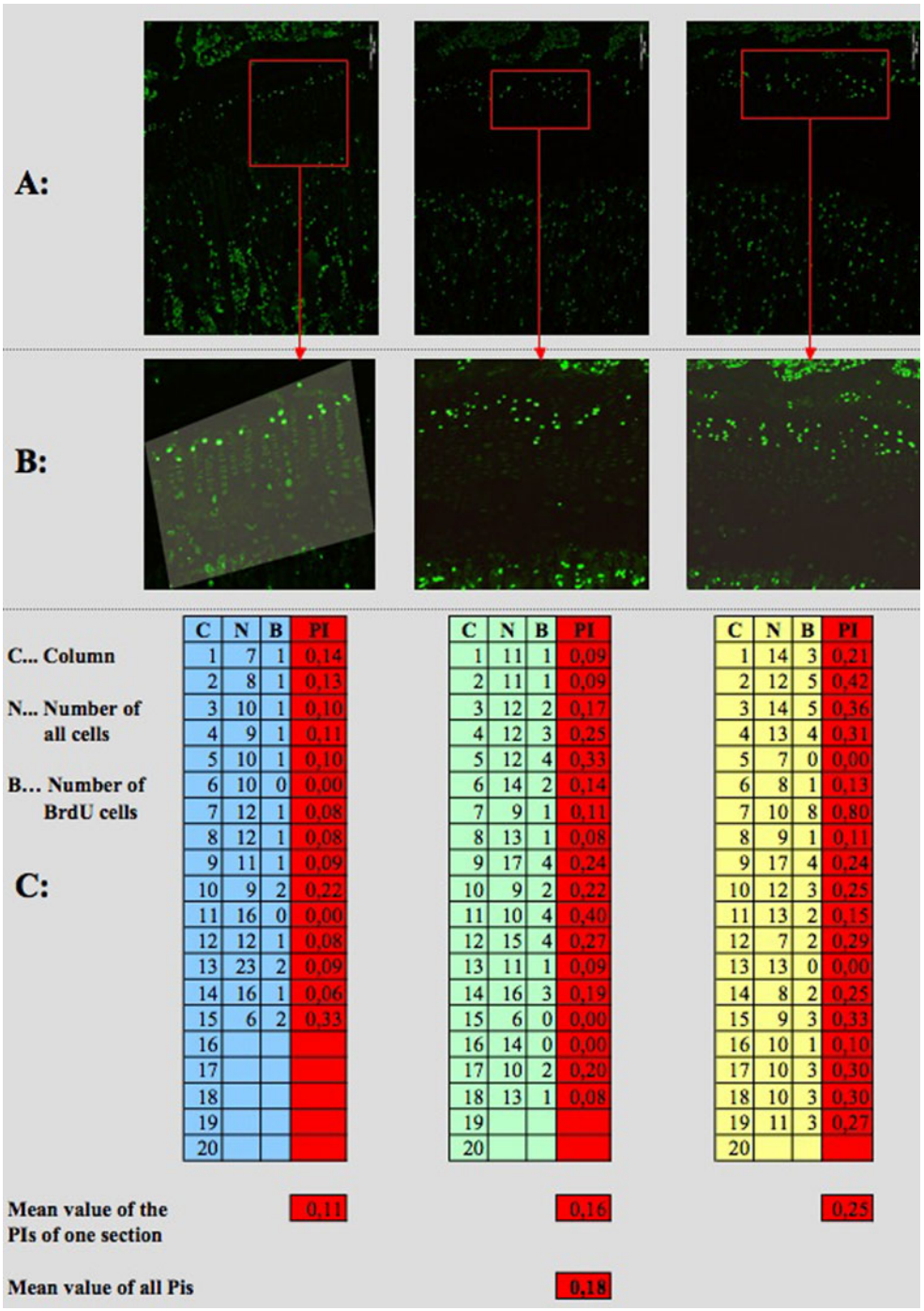

C	N	B	PI
1	7	1	0,14
2	8	1	0,13
3	10	1	0,10
4	9	1	0,11
5	10	1	0,10
6	10	0	0,00
7	12	1	0,08
8	12	1	0,08
9	11	1	0,09
10	9	2	0,22
11	16	0	0,00
12	12	1	0,08
13	23	2	0,09
14	16	1	0,06
15	6	2	0,33
16			
17			
18			
19			
20			

C	N	B	PI
1	11	1	0,09
2	11	1	0,09
3	12	2	0,17
4	12	3	0,25
5	12	4	0,33
6	14	2	0,14
7	9	1	0,11
8	13	1	0,08
9	17	4	0,24
10	9	2	0,22
11	10	4	0,40
12	15	4	0,27
13	11	1	0,09
14	16	3	0,19
15	6	0	0,00
16	14	0	0,00
17	10	2	0,20
18	13	1	0,08
19			
20			

C	N	B	PI
1	14	3	0,21
2	12	5	0,42
3	14	5	0,36
4	13	4	0,31
5	7	0	0,00
6	8	1	0,13
7	10	8	0,80
8	9	1	0,11
9	17	4	0,24
10	12	3	0,25
11	13	2	0,15
12	7	2	0,29
13	13	0	0,00
14	8	2	0,25
15	9	3	0,33
16	10	1	0,10
17	10	3	0,30
18	10	3	0,30
19	11	3	0,27
20			

Fig. 2 Method of cell counting demonstrated with this example

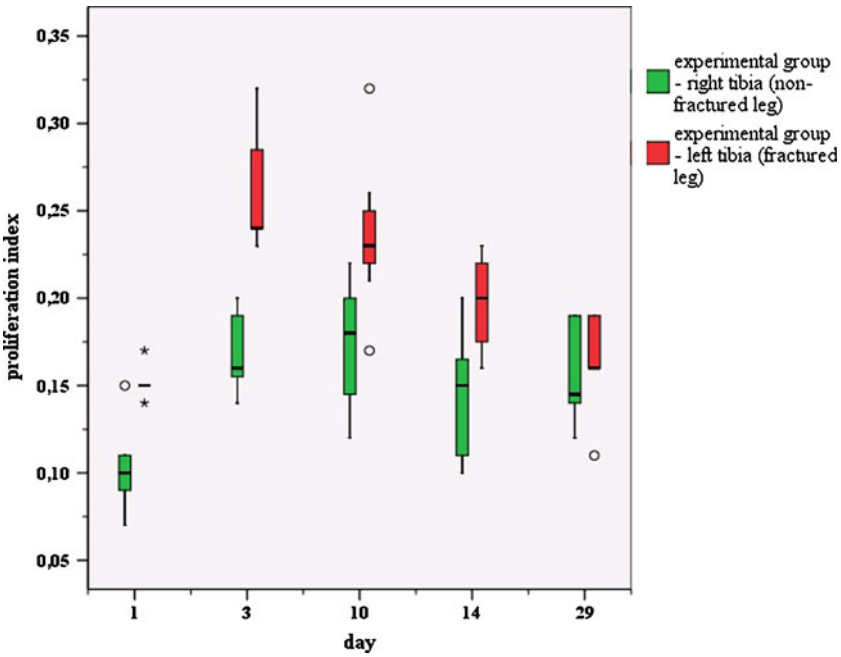

Fig. 3 Comparison of the proliferation indices of the left and the right legs of the experimental group). *X* axis represents the number of days post-fracture on which euthanasia of the rats was performed. *Y* axis specifies the proliferation index. The *lines* within the boxes indicate the median (50th percentile), the *upper* and *lower ends* of the boxes indicate the first quartile (25th percentile) and the third quartile (75th percentile), respectively. The *small circles* indicate outliers

washed in PBS and then cover slips were mounted with mounting medium (DAKO Austria GmbH A-1090 Vienna).

Image editing, cell counting, statistical evaluation

All Safranin O-stained and BrdU-immunohistochemical-stained sections were examined with a fluorescence microscope (Olympus EX51). They were photographed and digitised using Soft Imaging System (Olympus DP-Soft). The histological analysis of the Safranin O-stained samples were performed at ×40 magnification. For immunohistochemical evaluation, three regions of each growth plate were analysed at a magnification of ×100 (Fig. 1). This included two peripheral and one central region, consisting of about 15 to 20 vertical cell columns in the mid-coronal plane of the growth plate (Fig. 2a, b).

The number of cell columns and the number of cells in each column were counted, allowing for the calculation of the total number of cells in each region of interest. Then all the fluorescent BrdU-labelled cells were counted. This allowed for the calculation of a proliferation index (PI= number of fluorescent cells/total number of cells) (Fig. 2c).

The continuous data are presented as median ($p25$–$p75$ percentiles). For comparison of the broken leg versus the contra-lateral not broken leg of the same animal, the Wilcoxon test was used. Comparing the two groups (control and experimental group) continuously, variables were analysed by Mann–Whitney *U* test. A p value of less then 0.05 was regarded as significant for all kinds of analysis. Data were evaluated using SPSS for the PC (release 15.0.1, 2006, SPSS Inc. Chicago, IL, USA).

Results

Safranin O staining and BrdU labelling

Safranin O staining of the rat's growth plate revealed a similar configuration and organisation of the zones as compared to that of humans. Safranin O staining served as an orientation aid for the BrdU-labelling technique and evaluation by displaying BrdU-labelled cells as proliferating cells which line up in columns within the proliferation zone of the growth plate.

Table 2 Comparison of the proliferation indices of the left leg and the right leg of the experimental group

	Experimental group		*p* value
	Left tibia (fractured)	Right tibia (non-fractured)	
Day 1	0.15 (0.15–0.16)	0.10 (0.08–0.13)	0.043
Day 3	0.24 (0.24–0.32)	0.16 (0.15–0.20)	0.018
Day 10	0.23 (0.21–0.26)	0.18 (0.13–0.20)	0.018
Day 14	0.20 (0.17–0.22)	0.15 (0.11–0.17)	0.027
Day 29	0.16 (0.15–0.19)	0.15 (0.14–0.19)	0.194

The medians, the percentiles 25 and 75 as well as the p values are described

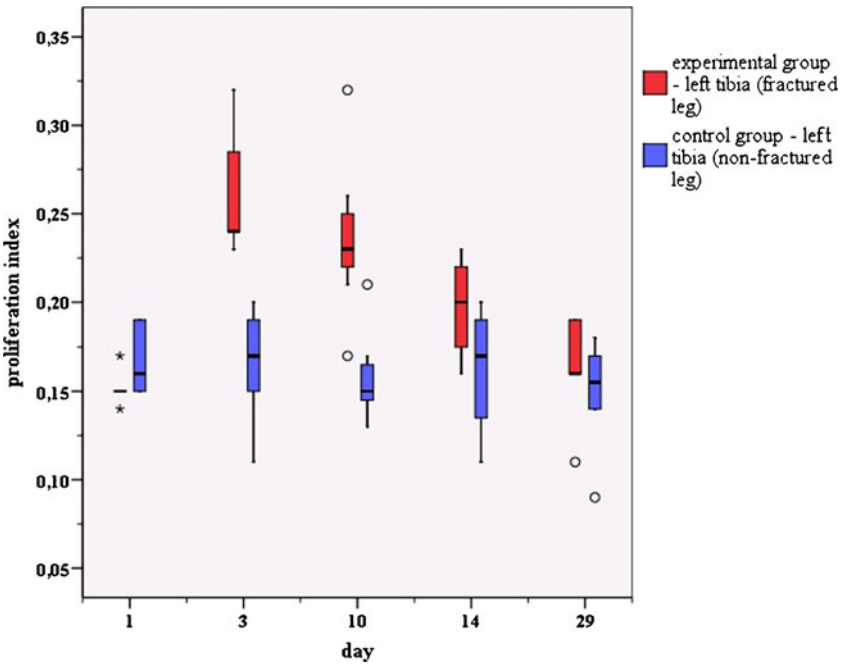

Fig. 4 Comparison of the proliferation indices of the left leg of the experimental group and the left leg of the control group. *X* axis represents the number of days post-fracture on which euthanasia of the rats was performed. *Y* axis specifies the proliferation index. The *lines* within the boxes indicate the median (50th percentile), the *upper* and *lower ends* of the boxes indicate the first quartile (25th percentile) and the third quartile (75th percentile), respectively. The *small circles* indicate outliers

Evaluation 1: cell-proliferation difference at the growth plate between left (fractured) and right (non-fractured) tibia of the experimental group on days 1, 3, 10, 14 and 29

We found significantly higher cell proliferation rate in the growth plate of the fractured bones compared to the contralateral uninjured side on days 1 (p value 0.043), 3 (p value 0.018), 10 (p value 0.018) and 14 (p value 0.027) post-fracture. On day 29, no significant difference could be detected (p value 0.194). A peak of physeal proliferation of the fractured tibia was detected on day 3. This decreased continuously until day 29 (Fig. 3; Table 2).

Evaluation 2: cell-proliferation difference at the growth plate between the fractured left tibia of the experimental group and the left tibia of the control group (non-fractured) on days 1, 3, 10, 14 and 29

Comparison of the physeal proliferation rates of the broken bones in the experimental group with the intact bones of the control showed significantly higher proliferation indices in the experimental group on days 3 (p value 0.004) and 10 (p value 0.004), but not for days 1 (p value 0.146), 14 (p value 0.083) and 29 (p value 0.369) (Fig. 4; Table 3).

Evaluation 3: cell-proliferation difference at the growth plate between right tibia of the experimental group (non-fractured) and left tibia of the control group (non-fractured) on day 1, 3, 10, 14 and 29

Comparison of the physeal proliferation rate of the contralateral intact bones in the experimental group with the intact bones of the control group did not show a significant difference on days 3 (p value 0.87), 10 (p value 0.48), 14 (p value 0.334) and 29 (p value 0.936) post-fracture. However, on day 1, physeal proliferation indices were significantly higher (p value 0.015) in the control animals (Fig. 5; Table 4**).**

Discussion

Limb length discrepancy following diaphyseal fractures of long bones are well recognised in the orthopaedic literature.

Table 3 Comparison of the proliferation indices of the left leg of the experimental group and the left leg of the control group

The medians, the percentiles 25 and 75 as well as the p values are described

	Experimental group Left tibia (fractured)	Control group Left tibia (non-fractured)	p value
Day 1	0.15 (0.15–0.16)	0.16 (0.15–0.19)	0.146
Day 3	0.24 (0.24–0.32)	0.17 (0.13–0.20)	0.004
Day 10	0.23 (0.21–0.26)	0.15 (0.14–0.17)	0.004
Day 14	0.20 (0.17–0.22)	0.17 (0.13–0.19)	0.083
Day 29	0.16 (0.15–0.19)	0.16 (0.13–0.17)	0.369

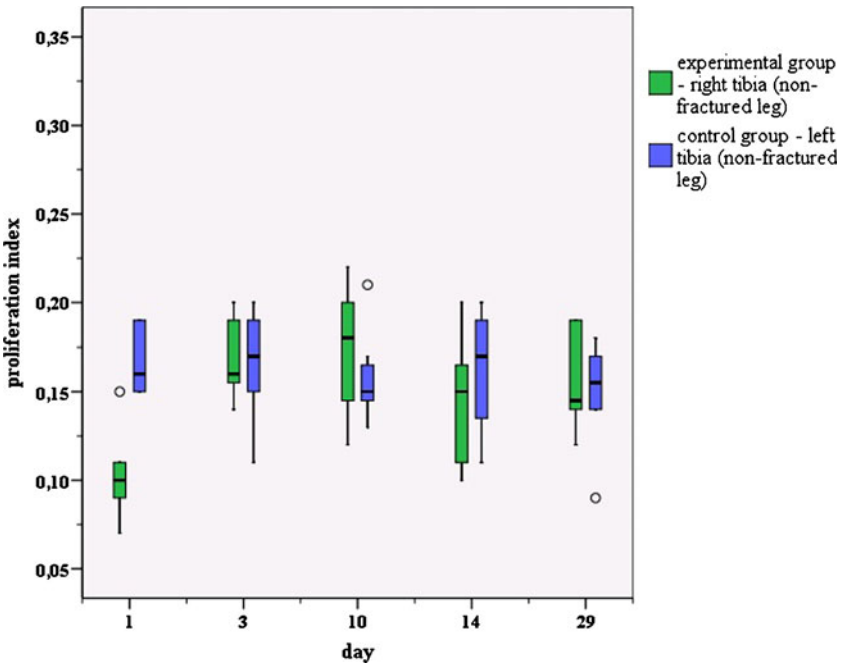

Fig. 5 Comparison of the proliferation indices of the right leg of the experimental group and the left leg of the control group. *X* axis represents the number of days post-fracture on which euthanasia of the rats was performed. *Y* axis specifies the proliferation index. The *lines* within the boxes indicate the median (50th percentile), the *upper* and *lower ends* of the boxes indicate the first quartile (25th percentile) and the third quartile (75th percentile), respectively. The *small circles* indicate outliers

Stimulation of the adjacent growth plates in the fractured bone commonly lead to overgrowth. Many theories have been proposed about the underlying pathomechanics of this phenomenon; however, the exact molecular and cellular mechanisms have yet to be fully investigated and described. The present study is the first to our knowledge to investigate chondrocyte proliferation rates at the growth plate of fractured bones.

Previous studies have demonstrated the similarities and comparability of the rat and human bony and physeal structures [29–31]. The phenomenon of overgrowth after a fracture has already been documented in rats [19, 21, 32]. This model is therefore appropriate to investigate physeal response to a diaphyseal fracture.

The use of 5-bromo-2′-deoxy-uridine has recently been reported in several studies reporting on the analysis of cell proliferation in bone and cartilage [33–35]. In 1957, Taylor and co-workers developed the first method to observe proliferating cells. Cells were labelled by radioactive thymidine which incorporated into the nuclear DNA of cells in the stage of synthesis of the cell cycle. Proliferating cells were visualised by autoradiography [36].

The recent method using 5′-bromo-2′-deoxy-uridine (BrdU) has the advantage of being less expensive, non-radioactive as well as being easier to perform [37]. The basic principle of BrdU labelling is the same as Taylor's method. BrdU is an analogue of thymidine and is incorporated into DNA instead of thymidine during the mitotic cell cycle. This study demonstrates the incorporation of BrdU into proliferating cells which were then processed and counted manually as previously reported [35, 37, 38].

This study clearly demonstrates a significantly higher chondrocyte proliferation rate in the growth plate of the fractured bone on days 1, 3, 10, and 14 compared to the contra-lateral uninjured side. The physeal cell-proliferation rate peaked on day 3 and subsequently subsided until day 29. The contra-lateral uninjured limb did not show an increase in chondrocyte proliferation (Fig. 3). Fracture repair occurs several stages in the rat which are comparable to the human. Days 1 and 3 represent the stage of inflammation at the fracture site. At day 10, early endochondral ossification is observed. This is specific for the development of cartilaginous tissue. Day 14 represents

Table 4 Comparison of the proliferation indices of the right leg of the experimental group and the left leg of the control group

The medians, the percentiles 25 and 75 as well as the *p* values are described

	Experimental group Right tibia (non-fractured)	Control group Left tibia (non-fractured)	*p* value
Day 1	0.10 (0.08–0.13)	0.16 (0.15–0.19)	0.015
Day 3	0.16 (0.15–0.20)	0.17 (0.13–0.20)	0.87
Day 10	0.18 (0.13–0.20)	0.15 (0.14–0.17)	0.48
Day 14	0.15 (0.11–0.17)	0.17 (0.13–0.19)	0.334
Day 29	0.15 (0.14–0.19)	0.16 (0.13–0.17)	0.936

the formation of woven bone, and by day 29, there is deposition of lamellar bone and the remodelling of the hard callus [20, 39–41]. The stages of fracture repair are not temporally static processes. There is overlap between the various processes and it is impossible to establish rigid limits between them. Nevertheless, our data suggests that the fracture-induced enhanced physeal chondrocyte proliferation peaks during the inflammatory and reparative phase of fracture healing process and has ceased as the bone begins remodelling.

Our data suggest the physeal proliferation associated with a diaphyseal fracture is a local phenomenon and only occurs at the growth plate adjacent to the injured bone (Fig. 4). The exact molecular pathways and signals facilitating this reaction still need to be delineated.

The physeal proliferation indices were very similar between the control group and those of the uninjured tibiae of the experimental group (Fig. 5). We therefore conclude that the phenomenon of overgrowth is a localised effect which occurs in the physes of the injured bone, and there is no evidence to support increased physeal proliferation in the contra-lateral uninjured side. This conclusion should be tempered by the fact that we have not investigated the effect of increased weight-bearing on the uninjured limb whilst the fracture heals, and we suggest that further studies are required to elucidate the effect of fracture reduction and stability on the rate of physeal proliferation.

Acknowledgments This study was supported by a grant from the AO Research Foundation, Switzerland. Furthermore, we want to thank Andrea Groselj-Strele M.Sc., Office for Biostatistics, Center for Medical Research, Medical University of Graz, for her support concerning the statistical processing.

Conflict of interest statement The authors declare that they have no conflict of interest.

References

1. Breitfuss H, Muhr G (1988) Can accelerated longitudinal growth be prevented following pediatric femur shaft fractures? Unfallchirurg 91:189–194
2. Clement DA, Colton CL (1986) Overgrowth of the femur after fracture in childhood. An increased effect in boys. J Bone Jt Surg Br 68:534–536
3. Reynolds DA (1981) Growth changes in fractured long-bones: a study of 126 children. J Bone Jt Surg Br 63-B:83–88
4. Stephens MM, Hsu LC, Leong JC (1989) Leg length discrepancy after femoral shaft fractures in children. Review after skeletal maturity. J Bone Jt Surg Br 71:615–618
5. Sulaiman AR, Joehaimy J, Iskandar MA et al (2006) Femoral overgrowth following plate fixation of the fractured femur in children. Singapore Med J 47:684–687
6. Wallace ME, Hoffman EB (1992) Remodelling of angular deformity after femoral shaft fractures in children. J Bone Joint Surg Br 74:765–769
7. Zimmermann R, Stoger A, Golser K et al (1999) Tibial growth after isolated femoral shaft fracture in the growth stage. Unfallchirurg 102:365–370
8. Laer L, Herzog B (1978) Leg length differences and rotation defects after femoral shaft fractures in childhood. Therapeutic influence and spontaneous correction. Helv Chir Acta 45:17–21
9. Aitken AP (1940) Overgrowth of the femoral shaft following fracture in children. Am J Surg 49:147–148
10. Ogden JA (2000) Skeletal injury in the child. Springer-Verlag, New York
11. Pring M, Newton P, Rang M (2005) Femoral shaft. In: Rang M, Pring ME, Wenger DR (eds) Rang's children's fractures. Lippincott Williams & Wilkins, Philadelphia, PA, pp 181–200
12. Rang M, Wenger DR (2005) Children are not just small adults. In: Rang M, Pring ME, Wenger DR (eds) Rang's children's fractures. Lippincott Williams & Wilkins, Philadelphia, PA, pp 1–10
13. Routt M Jr (1994) Fractures of the femoral shaft. In: Green N, Switontkowski M (eds) Skeletal trauma in children. WB Saunders Company, Philadelphia, pp 345–368
14. Salter R (1983) Textbook of disorders and injuries of the musculoskeletal system. Williams & Wilkins, Baltimore, MD
15. Wirth T, Syed Ali MM, Rauer C et al (2001) The influence of local vascular regeneration on growth plate activity after defined growth plate lesions. Eur J Trauma 27:58–65
16. Zionts LE, Harcke HT, Brooks KM et al (1987) Posttraumatic tibia valga: a case demonstrating asymmetric activity at the proximal growth plate on technetium bone scan. J Pediatr Orthop 7:458–462
17. Etchebehere EC, Caron M, Pereira JA et al (2001) Activation of the growth plates on three-phase bone scintigraphy: the explanation for the overgrowth of fractured femurs. Eur J Nucl Med 28:72–80
18. Lee SH, Szoke G, Simpson H (2001) Response of the physis to leg lengthening. J Pediatr Orthop B 10:339–343
19. Garces GL, Garcia-Castellano JM, Nogales J (1997) Longitudinal overgrowth of bone after osteotomy in young rats: influence of bone stability. Calcif Tissue Int 60:391–393
20. Gerstenfeld LC, Cullinane DM, Barnes GL et al (2003) Fracture healing as a post-natal developmental process: molecular, spatial, and temporal aspects of its regulation. J Cell Biochem 88:873–884
21. Kaya AE (1986) Growth plate stimulation by diaphyseal fracture. Autoradiography of DNA synthesis in rats. Acta Orthop Scand 57:135–137
22. Standring S, Ellis H, Healy JC et al (2005) Gray's anatomy: the anatomical basis of clinical practice. Elsevier Churchill Livingstone, Edinburgh
23. Ballock RT, O'Keefe RJ (2003) The biology of the growth plate. J Bone Jt Surg Am 85-A:715–726
24. Forriol F, Shapiro F (2005) Bone development: interaction of molecular components and biophysical forces. Clin Orthop Relat Res 432:14–33
25. Rauch F (2005) Bone growth in length and width: the Yin and Yang of bone stability. J Musculoskelet Neuronal Interact 5:194–201
26. Meyer U, Wiesmann HP (2006) Bone and cartilage engineering. Springer-Verlag, Berlin
27. Abad V, Meyers JL, Weise M et al (2002) The role of the resting zone in growth plate chondrogenesis. Endocrinology 143:1851–1857
28. Bonnarens F, Einhorn TA (1984) Production of a standard closed fracture in laboratory animal bone. J Orthop Res 2:97–101
29. Landry PS, Marino AA, Sadasivan KK et al (1996) Bone injury response. An animal model for testing theories of regulation. Clin Orthop Relat Res 332:260–273
30. Morini S, Continenza MA, Ricciardi G et al (2004) Development of the microcirculation of the secondary ossification center in rat humeral head. Anat Rec A Discov Mol Cell Evol Biol 278:419–427

31. Murakami S, Noda M (2000) Expression of Indian hedgehog during fracture healing in adult rat femora. Calcif Tissue Int 66:272–276
32. Ashraf N, Meyer MH, Frick S et al (2007) Evidence for overgrowth after midfemoral fracture via increased RNA for mitosis. Clin Orthop Relat Res 454:214–222
33. Okafuji N, Liu ZJ, King GJ (2006) Assessment of cell proliferation during mandibular distraction osteogenesis in the maturing rat. Am J Orthod Dentofacial Orthop 130:612–621
34. Sato C, Muramoto T, Soma K (2006) Functional lateral deviation of the mandible and its positional recovery on the rat condylar cartilage during the growth period. Angle Orthod 76:591–597
35. Sekine J, Sano K, Inokuchi T (1995) Effect of aging on the rat condylar fracture model evaluated by bromodeoxyuridine immunohistochemistry. J Oral Maxillofac Surg 53:1317–1321
36. Taylor JH, Woods PS, Hughes WL (1957) The organization and duplication of chromosomes as revealed by autoradiographic studies using tritium-labeled thymidinee. Proc Natl Acad Sci USA 43:122–128
37. Xiang Z, Markel MD (1995) Bromodeoxyuridine immunohistochemistry of epon-embedded undecalcified bone in a canine fracture healing model. J Histochem Cytochem 43:629–635
38. Haxhija EQ, Yang H, Spencer AU et al (2006) Influence of the site of small bowel resection on intestinal epithelial cell apoptosis. Pediatr Surg Int 22:37–42
39. Cho TJ, Gerstenfeld LC, Einhorn TA (2002) Differential temporal expression of members of the transforming growth factor beta superfamily during murine fracture healing. J Bone Miner Res 17:513–520
40. Einhorn TA (2005) The science of fracture healing. J Orthop Trauma 19:S4–S6
41. Gerstenfeld LC, Einhorn TA (2003) Developmental aspects of fracture healing and the use of pharmacological agents to alter healing. J Musculoskelet Neuronal Interact 3:297–303

Virchows Arch (2010) 457:87–89
DOI 10.1007/s00428-010-0940-6

LETTER TO THE EDITOR

Ezrin immunohistochemical expression in chondrosarcomas, osteosarcomas and Ewing sarcoma family of tumors

Isidro Machado · Samuel Navarro · Francisco Giner · Marco Alberghini · Franco Bertoni · Antonio Llombart-Bosch

Received: 17 March 2010 / Revised: 21 May 2010 / Accepted: 27 May 2010 / Published online: 16 June 2010
© Springer-Verlag 2010

Dear Sir,

Ezrin immunohistochemical (IHC) expression has been described in bone sarcomas, being present mainly in osteosarcomas [1–5]. Salas et al. [4] described the utility of ezrin protein expression as a tool to differentiate between conventional chondrosarcomas and chondroblastic osteosarcomas, demonstrating a specificity of 100%. In the present study, we describe ezrin IHC expression in 397 bone tumors, including 33 osteosarcomas (eight low-grade, 20 high-grade and five chondroblastic), 23 conventional chondrosarcomas (ten grade I, eight grade II and five grade III) and 341 Ewing sarcoma family of tumors (ESFT) [236 conventional, 42 primitive neuroectodermal tumor (PNET) and 63 atypical]. The sections were immunostained with ezrin antibody (clone 3C12, dilution 1:250). The cytoplasmic/membranous immunoexpression was scored as negative (<5%), poor (5–10%), moderate (10–50%) and intense (>50%). For the statistical analysis, negative and poor ezrin tumors were considered as negative, and moderate and intense ezrin tumors were considered as positive. Chi-square or Fisher's exact test was performed for statistical analysis. Ezrin immunoexpression was heterogeneous in the present series. Ezrin stained in a higher proportion of analyzed osteosarcomas cases (69%) than ESFT (40.7%) and chondrosarcomas (30%, $p=0.023$) (Figs. 1, 2, 3).

Interestingly, chondroblastic osteosarcoma tumors did not reveal ezrin expression (Fig. 2), and some cases of low-grade chondrosarcoma revealed poor ezrin immunoexpression; both results are in contrast with the study of Salas et al. [4]. However, similar to the results obtained by Salas et al. [4], the protein immunoexpression in the present series is associated with the histological grade, being higher in morphologically high-grade tumors. High-grade osteosarcomas and chondrosarcomas stained ezrin in a higher proportion (95% and 100%, respectively, $p<0.001$) than low-grade osteosarcomas and chondrosarcomas. Within the ESFT, ezrin expression was higher in atypical ESFT (58.9%, $p<0.001$) and PNET (58.6%, $p<0.001$) than in conventional ESFT (30%). The immunostaining in chondrosarcoma and osteosarcoma was mainly cytoplasmic, but several cases in ESFT also displayed a membranous pattern similar to CD99 expression. In ESFT with strong ezrin expression, apoptotic cells did not express ezrin compared with non-apoptotic cells (Fig. 3). In conclusion, based upon present experience,

I. Machado · S. Navarro · F. Giner · A. Llombart-Bosch (✉)
Pathology Department, University of Valencia,
Avda Blasco Ibañez 17,
46010 Valencia, Spain
e-mail: Antonio.llombart@uv.es

M. Alberghini · F. Bertoni
Instituto Rizzoli,
Bologna, Italy

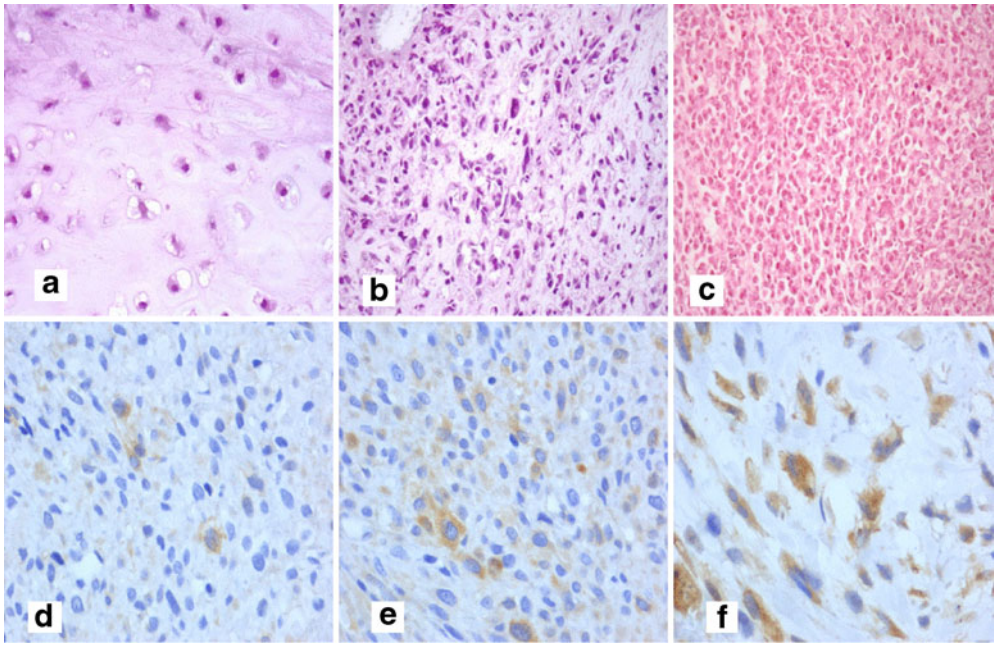

Fig. 1 **a** Chondrosarcoma grade I (H & E ×40). **b** Chondrosarcoma grade III with chondroid matrix (H & E ×40). **c** Chondrosarcoma grade III without chondroid matrix (H & E ×40). **d** Cytoplasmic ezrin expression (+) in Chondrosarcoma ×40. **e** Cytoplasmic ezrin expression (++) in Chondrosarcoma ×40. **f** Cytoplasmic ezrin expression (+++) in Chondrosarcoma ×40

ezrin IHC expression does not offer any diagnostic clues in the differential diagnosis of bone tumors since, at least, osteosarcoma, chondrosarcoma and ESFT reveal heterogeneous ezrin expression with increased expression in high-grade tumors. Ezrin cannot distinguish chondroblastic osteosarcoma from conventional chondrosarcoma as demonstrated in previous publications [4], and the histopathological study remains a crucial method for

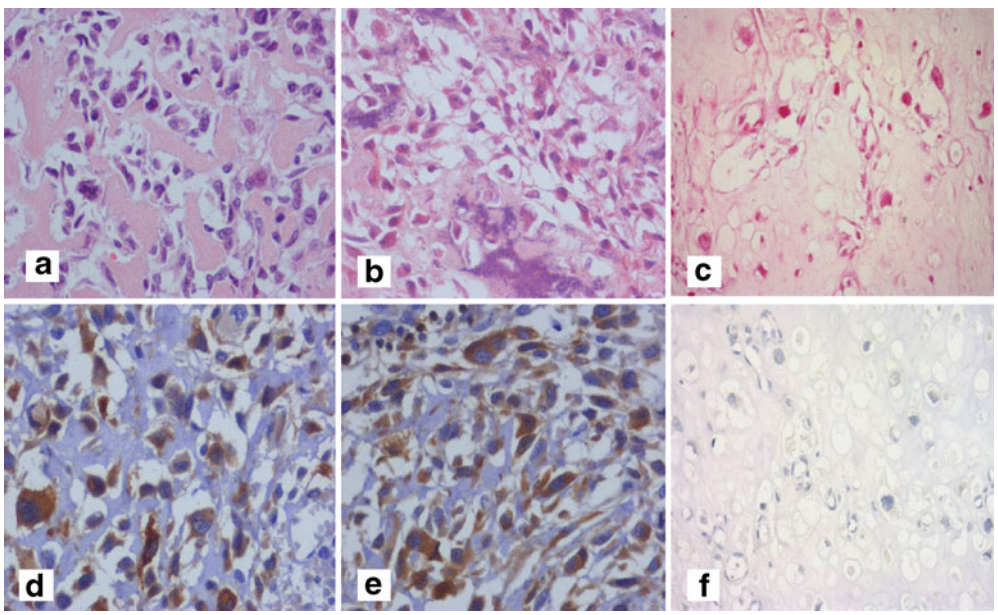

Fig. 2 **a** High-grade osteosarcoma, extensive osteoid formation (H & E ×40). **b** High-grade osteosarcoma with spindle cells (H & E ×40). **c** Chondroblastic osteosarcoma (H & E ×40). **d** Cytoplasmic and membranous ezrin expression (+++) in high-grade osteosarcoma ×40. **e** Cytoplasmic and membranous ezrin expression (+++) in high-grade osteosarcoma with spindle cells ×40. **f** Negative ezrin expression in chondroblastic osteosarcoma ×40

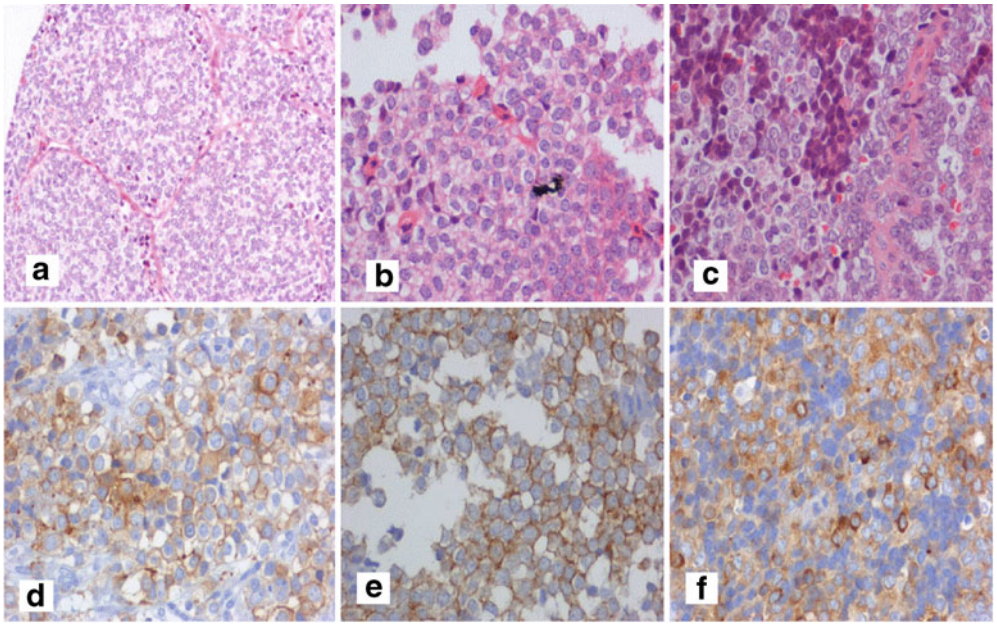

Fig. 3 **a**. ESFT/PNET variant with rossette formation (H & E ×40). **b** Atypical ESFT with clear cell (H & E ×40). **c** Atypical ESFT with several apoptotic figures (H & E ×40). **d** Membranous and cytoplasmic ezrin expression (+++) in PNET ×40. **e** Membranous ezrin expression (+++) in atypical ESFT ×40. **f** Ezrin expression (+++) in tumor cell of ESFT, absent ezrin expression in apoptotic cells ×40

differential diagnosis between the two tumors. Further studies with a large series of bone tumors are necessary to determine if ezrin IHC expression can offer additional diagnostic and prognostic information in bone tumors.

Supported This study was performed with grants from European Union (EuroBoNet project, contract no. 018814).

Acknowledgement We would like to acknowledge Elisa Alonso from the University of Valencia for the collaboration and technical assistance and Mr. David Harrison for the English language support.

Conflict of interest statement We declare that we have no conflict of interest.

References

1. Ferrari S, Zanella L, Alberghini M et al (2008) Prognostic significance of immunohistochemical expression of ezrin in non-metastatic high-grade osteosarcoma. Pediatr Blood Cancer 50:752–756
2. Ogino W, Takeshima Y, Mori T et al (2007) High level of ezrin mRNA expression in an osteosarcoma biopsy sample with lung metastasis. J Pediatr Hematol Oncol 29:435–439
3. Salas S, Bartoli C, Deville JL et al (2007) Ezrin and alpha-smooth muscle actin are immunohistochemical prognostic markers in conventional osteosarcomas. Virchows Arch 451:999–1007
4. Salas S, de Pinieux G, Gomez-Brouchet A et al (2009) Ezrin immunohistochemical expression in cartilaginous tumours: a useful tool for differential diagnosis between chondroblastic osteosarcoma and chondrosarcoma. Virchows Arch 454:81–87
5. Xu-Dong S, Zan S, Shui-er Z et al (2009) Expression of Ezrin correlates with lung metastasis in Chinese patients with osteosarcoma. Clin Invest Med 32:E180–E188

Virchows Arch (2010) 457:91–281
DOI 10.1007/s00428-010-0947-z

ABSTRACTS

Keynote Lectures

Wednesday, 1 September 2010, 11.45–12.30, Aula Duża

KL-01 New trends in breast pathology
Chairperson: T. Tot, Sweden

001
New trends in breast pathology
*M. van der Vijver**
*The Netherlands

Thursday, 2 September 2010, 11.45–12.30, Aula Duża

KL-02 Emerging mechanisms of tumor initiation and progression: lessons from the bladder cancer model
Chairperson: H. van Krieken, The Netherlands

001
Emerging mechanisms of tumor initiation and progression: lessons from the bladder cancer model
*B. Czerniak**
*The University of Texas, M D Anderson Cancer Center, Houston, USA

Bladder cancer has served as one of the most important sources of information about the events that underlie the development of human solid malignancies. Although "field effects" that alter the entire bladder mucosa appear to initiate disease, tumors develop along two distinct biological "tracks" referred to as papillary and non-papillary that present different challenges for clinical management. More recently, whole organ mapping combined with genomic platforms have identified a novel class of candidate tumor suppressors (forerunner genes) that localize near more familiar tumor suppressors but are disrupted at an earlier stage of cancer development. These studies suggested three steps for the involvement of the model tumor suppressor locus, RB1, in tumor development. In the first step, one allele of forerunner (FR) gene and RB1 is inactivated by deletions. In the second step, homozygous inactivation of the FR genes is accomplished by hypermethylation or mutations. The inactivation of FR genes is associated with the initial clonal expansion of preneoplastic urothelial cells. In the third step, the contiguous tumor suppressor, RB1, is inactivated by a mutation, which is associated with clonal evolution into carcinoma in situ progressing to invasive cancer. Furthermore, we have discovered that aggressive muscle-invasive tumors express molecular markers characteristic of a developmental process known as "epithelial-to-mesenchymal transition." Emerging evidence indicates that urothelial cancers contain subpopulations of tumor-initiating cells (cancer stem cells), but the phenotypes of these cells in different tumors may be heterogeneous, raising questions about whether or not the two major subtypes of cancer share a common precursor.

Friday, 3 September 2010, 11.45–12.30, Aula Duża

KL-03 Predictive pathology: fact or fancy?
Chairperson: F. Carneiro, Portugal

001
Predictive pathology: fact or fancy?
*F. Bosman**
*University Hospital Maastricht, Dept. of Pathology, The Netherlands

Pathology as a medical specialty has been around for about a century and a half, even though the interest in understanding disease, the focus of pathology as an academic discipline, has inspired physicians since the dawn of mankind. Understanding disease remains the primary focus of pathology. In the practice of diagnostic pathology, this knowledge, notably through its morphological expression, is applied to the diagnosis of disease through the examination of cells and tissues. Relatively new in this field is the notion of pathology as 'the science behind the cure'. This phrase, coined by the Pathological Society of Great Britain and Ireland, refers to a widening of the scope of pathology: 'Understanding disease' continues to be applied to diagnosis and classification, but now also to conceiving of new ways to treat and of new diagnostic tools assisting the physician in choosing the appropriate treatment. Targeted therapy, the target being a molecular pathway involved in the pathogenesis of the lesion, along with biomarkers that are predictive for response to treatment, are in the forefront of pathology. Targeted drugs that require 'companion' diagnostics, a combination also called 'theranostics', are reshaping the practice of pathology. It is this

paradigm shift in pathology that makes it one of the most exciting medical specialties of today. I would love to be a resident in Pathology again. The prospects for this mother of disciplines in modern medicine have never been as bright.

Is this entirely new? Certainly, the molecular revolution with 'high-throughput' technologies, array diagnostics such as 'MammaprintR' and 'deep sequencing' to name just a few technologies we have had to become familiar with, have had and will continue to have in the years to come a profound impact on the way we practice pathology. But guiding the surgeon's hand or the pen of the oncologist in prescribing drugs has been a primary responsibility for pathologists ever since examination of cells and tissues was being applied to the practice of medicine. Prognostic factors have interested pathologists long before the onset of the molecular revolution. Grading and staging of neoplastic disease based upon morphological characteristics remains the mainstay of stratification of patient groups for treatment optimization. And predictive value is not limited to molecular markers: Small cell carcinoma of the lung, to name just one example, will not be treated surgically, but chemotherapy is effective, even though as a rule not to the extent that the patient can be cured. We dispose of numerous morphological parameters that are prognostic and predictive.

That pathological parameters have predictive value is therefore nothing new. This has become more so with the discovery that steroid hormone receptor expression predicts the response to anti-hormonal treatment and that HER2/neu amplification predicts the response to HER2/neu antibodies in breast cancer. It has become clear that the type of c-Kit mutation in a GIST predicts whether or not the patient will respond to a tyrosine-kinase inhibitor (imatinib), which dose of the drug would be appropriate or which second-generation inhibitor might be used. K-RAS mutations will tell the oncologist that the patient will not respond to EGFR inhibitors in the form of small molecules (gefatinib) or monoclonal antibodies (cituximab). The latter is also a striking example of the limitations of many of the tools that we dispose of: The K-RAS mutation status will tell us who will not respond to the therapy, but not who will. Based upon detailed knowledge of the molecular characteristics of many types of cancer, pharmaceutical companies are now developing a host of new drugs and more often than not are teaming up with pathologists to develop diagnostic tests that might predict which patient groups might profit from the new drug.

This should not become a hype, the type of buzz that went around the H1N1 pandemic which in hindsight was not justified by what happened in the field. Let us remain modest. First of all, the number of diseases for which the combination of new drug and predictive molecular test exists remains limited. Secondly, the impact of this new and promising approach to final outcome should keep us modest. For colorectal cancer, new therapies have prolonged survival, but not cured more patients. Thirdly, expectations that we will be able to predict at the level of the individual patient what the best therapy would be and how the disease will respond or progress is an illusion. 'Individualized' medicine is still based upon studies on large patient groups with as outcome parameters that with a certain level of probability will indicate what might happen. A lot remains to be studied and developed. This implies also a new role for pathology. We should team up with clinical trials, using this context to conduct biomarker studies that can be implemented in daily practice. We should collaborate with drug developers to get to the desired 'companion' diagnostic tools. For pathology, exciting times indeed.

Working Group Sessions

Wednesday, 1 September 2010, 08.00–11.00, Aula Duża A

WGS-01 Diagnostic challenges in modern breast pathology

Chairpersons: I. Ellis, United Kingdom
W. Domagala, Poland

001

Novel variants of lobular intraepithelial neoplasia

*F. Tavassoli**
*USA

002

Immunophenotypic molecular subtypes of breast cancer in patients with constitutional mutations

*W. Domagala**
*Pomeranian Medical University, Dept. of Pathology, Szczecin, Poland

Objective: The following topics will be outlined: (1) Evolution of the histologic classification of breast cancer; (2) The influence of immunohistochemistry on the histologic classification of breast cancer; (3) The molecular classification of breast cancer; (4) Attempts to agree on the immunophenotypic molecular classification of breast cancer; and (5) The influence of patient's constitutional molecular background on the immunophenotypic molecular subtypes of breast cancer: prognostic significance—therapeutic implications.

Method: This lecture is to be said in Session: Diagnostic Challenges in Modern Breast Pathology, Sept 1st 08:00–11:00. The entire abstract is above in the first box. I am sending this abstract also to Dr. Rys to Krakow. Please note that the title is slightly changed as compared to the primary version.

003

Breast lesions mimicking malignancy

*Z. Varga**
*Switzerland

Cell types arising normally in the breast can occasionally exhibit peculiar overgrowth or nuclear features mimicking malignant cells and thus representing potential diagnostic pitfalls. Myoepithelial cell hyperplasia can reach an extensive mass and imitate lobular neoplasia or ductal carcinoma in situ with pagetoid spread. Ductal epithelial cells with apocrine phenotype can appear, with highly worrisome nuclear features making the distinction between a high-grade ductal carcinoma in situ and a banal apocrine change at times quite challenging. The evidence of a preserved myoepithelial layer is a commonly accepted morphological criterion for noninvasive processes in the breast. The distinction between adenosis, highly differentiated ductal carcinomas and cancerisation of the lobules through in situ ductal carcinoma can be easily done by decorating myoepithelial cells in immunohistochemical reactions. An important exception to this rule is, however, the benign microglandular adenosis, which completely lacks the outer myoepithelial layer. Intraductal epithelial proliferations can be quite florid in their extension. The question whether they represent atypical hyperplasia resp. ductal carcinoma in situ or appear simply within the scope of a florid intraductal hyperplasia occurs often in daily diagnostic service. The use of a distinct and technically reliable diagnostic panel (E-cadherin, basal cytokeratins, hormone receptors, Her2 immunohistochemistry and in situ hybridisation, collagen IV reaction, Ki-67, S-100 and myoepithelial markers) can clear the situation in most of these difficult cases and thus can lead to the correct diagnosis.

004

Immunohistochemical differentiation of intraductal breast lesions

*W. P. Olszewski**
*Center of Oncology, Dept. of Pathology, Warsaw, Poland

Objective: Immunopathological methods, particularly immunohistochemistry (IHC), are now routinely used in all invasive breast carcinoma cases as part of the evaluation of predictive factors (ER, PgR, and HER2). Other IHC-detected antigens are used for the determination of invasiveness (e.g. p63 and SMA), searching of primary (e.g. GCDFP15 and mammaglobin) or in scientific field as surrogates of genetic subtyping (ER, PgR, HER2, EGFR, LMWCK, HMWCK). Increasing breast cancer screening on one hand and advanced surgical methods of biopsy (e.g. core biopsy, vacuum-assisted core biopsy) on the other produce a growing number of pathology material in which pathologists must diagnose on the basis of scarce tissue. Most of these cases are noninvasive. However, the spectrum of possible therapies for noninvasive lesions includes observation on one side and mastectomy with radiotherapy on the other.
Method: Therefore, determination of the exact nature of intraductal breast lesions has to be precise and sure. It generates the use of IHC antibodies in intraductal breast lesions.
Results: In some cases, results of such approaches create new entities. An example of such situation is differential diagnosis between CLIS and DCIS. In a small number of cases, the interpretation of obtained stains (E-cadherin and CK34BE12) adds entities like positive hybrid lesion and negative hybrid lesion.
Conclusion: The aim of the lecture was the presentation of increasingly used IHC antibodies in intraductal breast lesions and its correlation with histological features of usual ductal hyperplasia, atypical ductal hyperplasia, lobular neoplasia, ductal carcinoma in situ, and columnar lesions (CCC, CCC+Atypia, CCH, CCH+Atypia). The other topic is IHC expression of surrogates of genetic subtyping in carcinoma in situ.

005

Low-grade and high-grade breast cancer pathways

*I. Ellis**
*United Kingdom

006

TNM7

*G. Cserni**
*Hungary

Background: The TNM, i.e. the tumour node metastasis classification of malignant tumours, is about 70 years old and was last updated in 2009. Although the oncology and pathology communities are expected to use this modified version from 2010, the Breast Working Group and the Organizing Committee has considered including a brief review of the topic in keeping with the educational aspects of the Intercongress Meetings of the European Society of Pathology.
Method: The lecture will briefly summarize the basic concepts of the TNM classification in general and will focus on the new aspects which are of interest to pathologists dealing with breast cancer specimens. Some former proposals to modify the TNM will also be discussed, including the European Institute of Oncology proposal to abolish the present categories and replace them with coded prognostic data reporting and the replacement

of the nodal categories based on the number of involved lymph nodes by categories based on the lymph node ratio (proportion of involved and examined nodes).
Results: NA.
Conclusion: The TNM has been criticized for not providing enough prognostic information to guide treatment. However, it must be kept in mind that the TNM was not devised for making treatment decisions solely on the basis of the information it provides but for reporting the anatomic extent of disease in a categorical format. TNM7 still fulfils this aim. No system is perfect, and TNM7 is not an exception to this. Should we use it, let us use it as correctly and uniformly as possible.

Wednesday, 1 September 2010, 08.00–11.00, Aula Duża B

WGS-02 Gastrointestinal stromal tumours

Chairpersons: M. Miettinen, USA
J. Lasota, USA

001
Prognostication and differential diagnosis of GIST: an update

*M. Miettinen**
*Armed Forces Inst of Pathology, Soft Tissue and Orthop Pathol., Washington, DC, USA

Objective: The precise application of modern targeted treatment of gastrointestinal stromal tumors (GISTs) requires accurate GIST diagnosis and prognostication.
Method: This review is based on existing literature on GISTs and the author's personal experience.
Results: GIST is defined as KIT or PDGFRA-driven mesenchymal tumor of the GI-tract, with a characteristic set of histologic features (spindle cell or epithelioid), and generally by immunohistochemical positivity for KIT (CD117). DOG1/Ano1 is a helpful additional marker for the positive identification of GIST. Current prognostication is based on mitotic activity, expressed as mitotic figures per 50 high-power fields in an area of 5 mm^2 and on tumor size. Different criteria are applied for gastric and intestinal GISTs because the latter, even with the same parameters, have a more malignant behavior. In the differential diagnosis of GIST, one has to consider the following facts: wide histologic variation (especially in gastric GISTs), the fact that GISTs are the most common mesenchymal tumor in the GI tract and whole abdomen, and occurrence of GISTs virtually anywhere in the abdomen and rarely in distant peripheral metastatic sites. Tumors that have to be considered in the differential diagnosis especially include true smooth muscle tumors, glomus tumor, gastrointestinal schwannoma, clear cell sarcoma, synovial sarcoma, desmoid, inflammatory fibroid polyp, inflammatory myofibroblastic tumor, and the newly described plexiform fibromyxoma and gastroblastoma.
Conclusion: Detailed histologic examination supported by immunohistochemistry and KIT/PDGFRA mutation analysis will yield optimal diagnostic accuracy.

002
Clinical significance of KIT and PDGFRA mutations in gastrointestinal stromal tumours, inflammatory fibroid polyps and mucosal malignant melanomas

*J. Lasota**
*USA

GISTs are the most common mesenchymal neoplasms of the gastrointestinal tract and represent a morphological and biological continuum from small, microscopically detected benign tumors to large sarcomas. KIT or platelet-derived growth factor receptor α (PDGFRA) oncogenic mutations are a typical molecular feature of GIST. KIT and PDGFRA genes map to chromosome 4q12 and encode highly homologous transmembrane glycoproteins. Activation of KIT regulates important cell functions, including proliferation, apoptosis, chemotaxis and adhesion. Imatinib mesylate that specifically inhibits ABL, KIT, and PDGFRA receptor tyrosine kinases has been successfully used in the treatment of clinically advanced, unresectable, and metastatic GISTs. Majority of KIT exon 11 mutants respond well to imatinib, while KIT exon 9 mutants are less sensitive to imatinib and require more aggressive treatment. Also, tumors with the PDGFRA Asp842Val substitution, which corresponds to imatinib-resistant KIT Asp816Val mutation reported in human mastocytosis, are resistant to imatinib. Although many patients benefit from imatinib treatment, resistance often develops due to secondary KIT or PDGFRA mutations or KIT locus amplification. Sunitinib mesylate, a multi-targeted inhibitor of KIT, PDGFRs, VEGFRs, FLT3, and RET receptor tyrosine kinases and other kinase inhibitors have been used for the treatment of imatinib-resistant GISTs. The type of secondary KIT mutation can indicate response to sunitinib treatment. KIT mutations were identified in mucosal MMs and PDGFRA mutations in gastric and intestinal IFPs. Although the presence of KIT mutation does not necessarily correlate with KIT expression in MM, an inhibition of KIT receptor tyrosine kinase might still be beneficial in the treatment of selected cases.

Wednesday, 1 September 2010, 08.00–11.00, Aula Średnia A

WGS-03 Novelties in inflammatory skin diseases

Chairpersons: D. Massi, Italy
W. Biernat, Poland

001

Infectious dermatites

*J. E. Calonje**
*Harrow, United Kingdom

002

Histopathology of alopecia: Getting to the root of the problem

*C. Stefanato**
*St. John's Institute for Dermatopathology, London, United Kingdom

The histopathology of primary non-scarring and scarring alopecias may be complex. The reason for this is that often, the scalp biopsy provided is inadequate, and the clinical history and pattern of the alopecia are not provided to the dermatopathologist. Increased diagnostic yield may be achieved by the combined use of transverse and vertical sections. This requires good communication between the dermatologist performing the biopsies, the dermatopathology laboratory and the dermatopathologist. Common forms of scarring alopecias include the lymphocytic, (discoid lupus erythematosus, lichen planopilaris, central centrifugal cicatricial alopecia, pseudopelade of Brocq), the neutrophilic, (folliculitis decalvans, dissecting folliculitis), and the mixed, (acne keloidalis) entities. Among the non-scarring alopecias are androgenic alopecia, telogen effluvium, alopecia areata, trichotillomania and traction alopecia. In all cases of primary alopecia, a multi-team approach involving the dermatologist for adequate tissue sampling, the laboratory for appropriate laboratory processing and the dermatopathologist, together with pertinent clinical information affords the best opportunity of arriving at the correct diagnosis.

003

Graft versus host disease: an update

*D. Massi**
*University of Florence, Dept. of Critical Care Medicine, Italy

Our current understanding of histopathological features of cutaneous graft versus host disease (GvHD) is largely based on experience gained during decades of ablative HSCT, in which day 100 was regarded as the temporal cutoff for the separation of acute vs. chronic GvHD, and traditionally, acute and chronic GvHD were considered to be distinct histopathological entities. Acute GVHD in the skin has been generally described as an interface dermatitis, with vacuolar basal alteration, dyskeratotic (apoptotic) keratinocytes in the epidermis and/or adnexal structures, scant dermal lymphoid infiltrate, and lymphocytic satellitosis. In contrast, chronic GvHD has commonly been reported as either lichenoid or sclerodermoid GVHD, characterized by homogenization of dermal collagen bundles, with little or no epidermal involvement. At variance with this dichotomic picture, histology of cutaneous GvHD following reduced intensity conditioning regimens is protean, displaying a variable constellation of histopathological alterations. These changes frequently blur the distinction between clear-cut clinical GvHD categories, as known in the classical ablative HSCT setting. Sampling errors and other technical issues may occur and may significantly affect the number of false negative cases. The utility of skin biopsies varies according to the pathologist's experience and to the prevalence of GvHD. Clinicians' overall perception is that undertreatment of GvHD is much worse than overtreatment of patients without GvHD. Therefore, early immunosuppressive therapy in patients with a skin eruption often precedes the results of the histopathological analysis. The pathogenesis and pathology of GVHD will be illustrated by elucidating the selective epithelial targets in the afferent stage and cellular response in the efferent stages.

004

Panniculitis: a practical diagnosis approach

*M. Fernandez-Figuera**
*Spain

005

Pathology of cutaneous drug eruptions with focus on the novel effects of targeted therapy for cancer

*A. Lazar**
*USA

Background: The untoward effects of pharmaceutical agents on the skin are an important source of morbiditary and can complicate the ideal selection of agents for our patients.
Method: Our practice in a large cancer center sees drug eruptions in the context of cancer treatment and must often be evaluated within a differential diagnosis with graft versus host disease on our bone marrow transplant service.

Results: With the advent of specific, targeted therapy for cancer, a new spectrum of interesting and unusual drug eruptions has emerged related to the mechanism of action of these agents.
Conclusion: This presentation will focus on the unique cutaneous effects arising in association with targeted therapy for cancer.

Wednesday, 1 September 2010, 08.00–11.00, Aula Średnia B

WGS-04 Native kidney disease: kidney and tumours
Chairpersons: M. Picken, USA
M. Wagrowska-Danilewicz, Poland

001
Nephrotic syndrome and neoplasia
M. Wagrowska-Danilewicz, M. Danilewicz*
*Medical University of Lodz, Dept. of Nephropathology, Poland

Background: The adult onset of nephrotic syndrome has been reported to be associated with underlying cancer in about 10% of cases. It is believed that the glomerular injury in many instances is due to the deposition of immune complexes in the glomerular capillaries. On the other hand, the course of illness in many cancer patients is complicated by infections, which may also be involved in the pathogenesis of glomerular injury. The malignancy is usually found simultaneously with, shortly before, or within a short time after the diagnosis of glomerulopathy. The glomerular lesion of paraneoplastic nephrotic syndrome usually presents as membranous nephropathy in patients with solid tumors, particularly adenocarcinomas of the lung and gastrointestinal tract. Minimal change disease is strongly associated with Hodgkin's lymphoma, and the most common lesions observed in patients with chronic lymphocytic leukemia are membranoproliferative glomerulopathy and membranous nephropathy. Extracapillary crescentic glomerulopathy, IgA nephropathy and focal segmental glomerulosclerosis are rarely associated with neoplasia.
Method: We present six cases of nephropathies associated with malignancies: lung, gastric and colon cancer, as well as Hodgkin's lymphoma and chronic lymphocytic leukemia. All patients were over the age of 55 and were presenting nephrotic syndrome.
Results: Membranous glomerulopathy, minimal change disease and membranoproliferative glomerulopathy were established on the basis of light microscopy, immunofluorescence and electron microscopy. The renal lesions in paraneoplastic nephropathies did not differ from idiopathic forms of glomerulopathies.
Conclusion: The search for malignancy is warranted in all patients over the age of 55 presenting with nephrotic syndrome, particularly in cases of membranous nephropathy. (This work was supported by grant of Polish Ministry of Science and Higher Education NN402 088735).

002
Plasma cell dyscrasia and renal amyloidosis: what can we learn from basic science?
*P. Westermark**
*Sweden

003
Plasma cell dyscrasia: amyloidosis, LCDD and cast nephropathy
*M. Picken**
*USA

The clinical and morphologic spectrum of plasma cell dyscrasia continues to expand. While in the most advanced stage of this disease patients are diagnosed with overt multiple myeloma, at the opposite end of the spectrum, MGUS is more typical. Not infrequently, the underlying disease is clinically silent or can be associated with renal symptoms that prompt further investigation and thus underscore the role of renal pathologists in the early detection of the underlying process. While light chain cast nephropathy affecting distal tubules and light chain amyloid or non-amyloidotic LCDD are well recognized, in recent years, attention has focussed on the pathology affecting the proximal tubules and interstitium. Proximal tubulopathy associated with an underlying plasma cell dyscrasia may be very subtle and associated with the formation of crystals or only with light chain restriction detectable in the lysomes within proximal tubules. Interstitial nephritis may be associated with a rather nonspecific morphology, and only an enhanced index of suspicion may lead to the discovery of an associated light chain restriction. Thus, renal pathologists are in an advantageous position to diagnose the underlying process at an early stage. Therefore, it is critical to perform a full investigation of the kidney biopsy, including immunofluorescence studies that employ testing for immunoglobulin light chains, as well as electron microscopy. Renal pathologists should be alerted particularly by biopsies that yield seemingly nonspecific or non-diagnostic results. Investigations with Congo red stain, careful evaluation of immunofluorescence studies, and electron microscopic analysis of organized and related deposits are necessary.

004

Non-Hodgkin lymphomas and PTLD in renal biopsies

*A. C. Feller**
*Germany

005

Cytostatic drug and radiation-associated renal lesions

*H. Regele**
*Austria

Malignant tumors might impair renal function in multiple ways. In addition to a direct impact of the tumor or its derivatives like light chains in the case of multiple myeloma, renal injury might also be a consequence of therapeutic interventions. Certain cytostatic drugs (especially platin-based compounds), but also irradiation, are long known to cause renal tissue injury. The damage might affect both the tubulointerstitial space and the vasculature. In addition, it was shown that recently introduced biological agents might lead to additional patterns of drug-induced injury. Blocking the action of VEGF in order to interfere with tumor-induced neoangiogenesis might for example cause renal thrombotic microangiopathy. In my talk, I will discuss the histological patterns of injury caused by the different treatment modalities and the underlying pathogenic mechanisms. The knowledge of these mechanisms might help prevent renal damage.

Wednesday, 1 September 2010, 08.00–11.00,
Sala Wystawowa A

WGS-05 Pitfalls in non-neoplastic lung pathology

Chairpersons: L. Carvalho, Portugal
R. Langfort, Poland

001

Pitfalls in infectious lung pathology

*K. Grunberg**
*The Netherlands

002

Pitfalls in pediatric lung pathology

*W. Timens**
*University Medical Center, Dept. of Pathology, Groningen, The Netherlands

Background: The morphological presentation of lung problems in infants and children is not always pathognomonic for a specific diagnosis. Basic patterns are not always easily recognized and may be different from the adult situation, even with the same classifying diagnosis.
Method: As lung neoplasms are seldom seen in children, this overview will focus on non-neoplastic lung disease.
Results: A main category is interstitial lung disease. The main adult patterns of interstitial disease can also be observed in children, although UIP, DIP and NSIP are rather rare and not always with similar aetiology (e.g. desquamative interstitial pneumonia, associated with smoking in adults). The distribution of the interstitial changes is in those cases similar to adults, but morphological presentation may be different because of a different lung structure. Some interstitial patterns are specific for childhood: for example, chronic pneumonitis of infancy, pulmonary interstitial glycogenosis (formerly cellular interstitial pneumonitis) and neuroendocrine cell hyperplasia of infancy, but even so, these are not always easy to discern form the other patterns. If a (wedge) lung biopsy is taken at late stage or only from the most severe abnormalities, a characteristic pattern may be obscured by nonspecific common final pathway changes like fibrosis.
Conclusion: All diffuse lung diseases in infancy can be caused by many etiologic factors. This means that although there are several hallmarks that can aid in making a proper pathological diagnosis, similar as in adults, proper clinical and radiological information is essential.

003

Pitfalls in vasculitis/vascular lung pathology

*F. Calabrese**
*Italy

004

Pitfalls in smoking-related lung diseases

*L. Carvalho**
*Faculdade de Medicina Coimbra, Dept. de Anatomia Patologica, Portugal

Objective: Tobacco and cigarettes are implicated in multisystemic carcinogenesis due to carcinogenic components that induce maintained inflammation, endocrine deregulation and genetic alterations in continuum. As ambience influence acts through a multifactorial behaviour gathering smoking, obesity and dietary mistakes, being sedentary, alcoholism, sexual promiscuity, toxic addition and general pollution, the isolated influence of smoking is reinforced. Smoking-related non-tumoral lung diseases comprise COPD, RB-ILD, DIP, ACIF/IBIP, HX (Langerhans cell histiocytosis), sarcoidosis (not consistent), eosinophilic lung, constrictive and lymphocytic bronchiolitis, emphysema together with sub-pleural and interstitial fibrosis UIP-

like or NSIP-like, as well as possible combinations of all these diseases and patterns. Smoking also increases or exacerbates infections (TP and other bacterial pneumonias, varicella pneumonia and influenza), pulmonary hemorrhage and pneumothorax and vascular walls fibrosis.

Conclusion: As smoking-related interstitial lung disease (SRILD) has been proposed to encompass clinical and radiological coordination, it means that molecular pathology achieves its role to define therapy as it is being tried in cancer. Despite observed morphology, it is possible to localize the defence response along the bronchial–bronchiolar–alveolar pathway as epithelial and mesenchymal cells develop particular ways of adaptation, either by EMT and MET. As inflammation stands through fibroblasts, cellular mTOR and macrophage activation, also epithelial hyperplasia and metaplasia, install both at bronchial and pulmonary stem cells pool. Smoking-related lung diseases are not consistent with a spectrum but rather with expertise to report delicate inflammatory changes in morphology that diverge to interstitial (and vascular) incapacities and/or to pre-neoplastic epithelial lesions and bronchial-pulmonary carcinoma.

005

Pitfalls in interstitial pneumonias

*H. Popper**
*Medical University of Graz, Institute of Pathology, Austria

Interstitial pneumonias can be classified into UIP, DIP, NSIP, OP, and DAD. Whereas DAD as an acute interstitial pneumonia is easily separated and diagnosed, due to the presence of alveolar damage and hyaline membranes, the other entities might cause problems in diagnosing. The most important distinction is between UIP and the other entities because UIP is a rapid progressive and deteriorating disease with a high mortality rate.

Usual interstitial pneumonia is histologically characterized by the presence of fibroblastic foci, cystic changes called honeycombing, areas of fibrosis and scars, and a temporal heterogeneity, which results in areas of early inflammatory changes, late changes, and also areas of uninvolved lung parenchyma. The disease usually starts from the lung periphery in a patchy distribution pattern. The lower lobes are usually more affected than the upper lobes.

The disease starts with tiny lesions where the surface epithelium is destroyed. Underneath myofibroblasts are proliferating and the stroma is changed into a myxoid stroma composed of acidic mucopolysaccharides. These lesions are called fibroblastic focus. This repair process is accompanied by a regeneration of pneumocytes, which usually undergo metaplastic changes (bronchiolization, cuboidal metaplasia, stem cell proliferation). Finally, this process results in fibrosis. Several fibrotic areas might finally confluent into a scar tissue. Fibroblastic foci are not only seen in alveolar septa but also in bronchioles and small bronchi. Scarring in these airways results in the obstruction of the airways, and the periphery of these airways undergoes a cystic dilation, accompanied by metaplasia of the epithelium; again, bronchiolization and metaplasia, even squamous metaplasia, can occur. Mucus produced by the epithelium cannot escape, and therefore, the cystic spaces increase in size, being finally visible at CT magnification. These cystic air spaces form the honeycomb lesions. In UIP, fibroblastic foci can be seen in the different stages of development: early stages with lots of myxoid matrix, immature collagen, and many proliferating myofibroblasts and old stages with lots of mature collagen and fibrocytes. Honeycomb lesions may present in a florid stage where some fibroblastic foci can be seen within the cysts, or older lesions with lots of mucus, or old lesions with secondary bacterial pneumonia overlying UIP. Also, the scars can be old, devoid of inflammatory infiltrates, or younger with scattered fibrocytes and lymphocytes. This together forms the temporal heterogeneity of UIP.

Fibroblastic foci are often used as the dominant and even sole diagnostic criterion for the diagnosis of UIP. This can result in an incorrect diagnosis since other interstitial diseases can also present with fibroblastic foci.

In the presentation, we will review several cases presenting with fibroblastic foci, which can closely mimic and might give rise to an incorrect diagnosis of UIP.

006

Pitfalls in drug-induced lung pathology

*B. Murer**
*Italy

Wednesday, 1 September 2010, 08.00–11.00,
Sala Wystawowa B

WGS-06 Molecular pathology on formalin-fixed paraffin-embedded tissues—European Network of Archive Tissue biobanking for translational research

Chairpersons: G. Stanta, Italy
F. Bosman, The Netherlands

001

Biobanking and biomolecular resources research infrastructure

*K. Zatloukal**
*Medical University of Graz, Institute of Pathology, Austria

002

The role of pathologists in translational research for patients and industry

*M. Dietel**
*Universitätsmedizin Charité, Berlin, Germany

Background: Due to continuous technical developments and new insights into the complexity of many diseases, e.g. cancer, molecular pathology is rapidly growing gaining center stage in the clinical management of tumors and pharmaceutical development of new anti-cancer drugs. Activated signaling components are the targets for the newly developed inhibitors, e.g. small molecules (gefitinib, erlotinib) and therapeutic antibodies (panitumumab, cetuximab). However, the application of the compounds in clinical trials has revealed promising results only when predictive procedures have been available for determining which patients will benefit from targeting therapy, so-called eligibility or predictive tests, e.g. Her2 in breast cancer, KRAS and EGFR mutations in colorectal cancer and non-small cell lung cancer. For the pharmaceutic industry, predictive tissue-based assays are of increasing importance in the development of new targeted drugs. FDA and EMEA stressed this issue several times during the process of approval, and pathology based analyses will become an essential factor in drug development. **Conclusion:** For pathology, the situation to become a partner in the clinical decision, which drug shall be given to the patient and which assay can be made available for a new, is a chance and a challenge in one. The issues to be solved are: (1) Morphology, in particular immunohistochemistry and in situ hybridization, must become measurable, e.g. by virtual microscopy. (2) The molecular assays must be done absolutely reliably and be reproducible. (3) Quality control, i.e. ring trials/round robin tests, must be passed by all active labs. If these challenges (and some others) are met, molecular pathology is facing an excellent development.

003

The role of biobanking and translational research for the pathologist

*F. Carneiro**
*IPATIMUP, Porto, Portugal

Among biobanking initiatives, tumour banks play a pivotal role in biomedical research. The general aim of a tumour bank is to acquire neoplastic and control non-neoplastic samples in standardized conditions for research (basic, clinical or translational). A tumour bank is a vital new resource for cancer research providing high-quality, well-characterized tissue. It is possible for pathologists to collect fresh tissue prospectively during their routine dissection procedures. In this way, the specimens can be optimally sampled and stored for both diagnosis and research purposes. Ideally, specimens are sampled immediately after surgery, prior to fixation, to ensure optimal preservation of proteins and nucleic acids. Retrospective collection of tumour tissue for study and banking purposes is feasible also because in most countries, pathology laboratories have been legally obliged to file, for at least some years, the formalin- fixed and paraffin-embedded samples that were analyzed. Over the last decade, tumour banks acquired a pivotal role in translational research in the field of oncology, providing tools for the evaluation of new predictive factors; evaluation of the value of a known target in a new entity; search for new therapeutic targets; validation of new diagnostic markers; and implementation of new diagnostic procedures, namely development of tissue-based diagnostic tests for guidance of therapy with new drugs introduced in clinical practice. In this scenario, it is a priority to emphasize the central role that pathologists play in translational research, specifically in tumor banking, by the establishment of a bridge between clinicians and basic researchers.

004

Limits and perspectives for standardization of tissue processing

*G. Bussolati**
*Italy

The paper by Pupo and colleagues is a well-conducted study on the role of the gasotransmitter hydrogen sulphide in angiogenesis. The increased effect of hydrogen sulphide in tumor-derived endothelial cells and its possible effect as a VEGF second messenger are of interest in the field of tumor angiogenesis. Criticisms: (a) It would be important to show the specificity and non-toxicity of hydrogen sulphide synthesis inhibitor on endothelial cells. (1) Experiments using the cystathionine lyase inhibitor alone on TEC proliferation and cytotoxicity are required. (2) Experiments testing the effect of cystathionine lyase on TEC motility induced by pro-angiogenic factors (i.e. FGF, HGF, nitric oxide donors, etc.) are suggested. (b) The authors should speculate on the possible reason(s) explaining the different responses of different endothelial cell types. (c) In the references, the same author (Fiorio Pla) is quoted in two different ways. (d) In "Material and Methods", the origin of a furnisher (Lonza) should be specified.

005

Standardization and controls of methods for molecular analysis in archive tissues

*G. Hoefler**
*Medical University of Graz, Institute of Pathology, Austria

Background: Formalin-fixed paraffin-embedded (FFPE) samples represent the vast majority of tissue specimens available from tissue archives, available routine diagnostics, as well as research purposes. These tissues vary among institutions with respect to pre-fixation time, formalin fixation time, concentration and buffer systems used. Therefore, it is of utmost importance to standardize the methods for molecular analyses to obtain consistent and comparable results.
Method: The first and maybe the most important step is the isolation of nucleic acids (DNA, RNA) from FFPE samples. In a recent multi-centric study performed by 13 European laboratories of the IMPACTS group, the results obtained by different laboratories varied significantly, even when the same commercial kit was used. The DNA extraction protocols used by the laboratories ranged from homemade protocols with and without purification steps to commercially available kits. The extractions were performed using the same FFPE specimens.
Results: For array applications or tests that require accurately determined DNA input, silica-based adsorption columns for DNA recovery are recommended. For RNA extractions, the best results were obtained for chromatography column-based commercial kits, with respect to quantity and quality. Quality testing resulted in the successful amplification of 200- to 250-bp PCR products from most tissues. Modifications of the protocol, especially with regard to proteinase-K digestion, led to significant improvements, also for the performance of commercial kits.
Conclusion: The results emphasize the need for standardization and control of methods for molecular analysis in archive tissues to allow the generation of valid and comparable results in both diagnostic and in research settings.

006

Approaches to the development of a European Network of Archive Tissues

*G. Stanta**
*University of Trieste, A.C.A.D.E.M., Italy

FFPE tissues taken from patients are stored, sometimes for a very long time, in the pathology archives. With this material, it is possible to do very important translational research. Any strategy is possible, such as that of large number analysis or rare entity collections. There is the necessity to transform our pathology biorepositories into a biobanking network. This can be done through a European organization that could be developed within the ESP and starting from the "IMPACTS" groups, which gained a large experience in molecular analysis validation and standardization of this kind of tissues. A European archive tissue biobank network depends on the willingness of the pathologists to participate, considering that this can significantly improve the diffusion of molecular methods, translational research and consequently acceleration of clinical application of molecular methods among pathologists. This can be done by a voluntary and collaborative participation of pathologists in specific projects, as scientific collaborators. The pathology archives will always be clinical biorepositories, and their function is going to change into a biobank function after accepting participation in a specific project, with the anonymization of the personal data of the patients. The networking system is based on low-cost activities with an easy governance and management of the biobanking system and with guarantees of protection of human material and data. Qualification, education and training will be implemented by the network organization and with the collaboration of the ESP.

Wednesday, 1 September 2010, 08.00–11.00, Aula Mała

WGS-07 Hereditary cancer

Chairpersons: J. Lubinski, Poland
R. Scott, Australia
S. Narod, Canada

001

Clinical genetics of breast/ovarian cancers

*S. Narod**
*Women's College Research, Familial Breast Cancer, Toronto, Canada

002

Chemoprevention of hereditary cancers

*J. Lubinski**
*Pomerian Medical University, Szczecin, Poland

003

Response to therapy with cisplatin in BRCA1-positive breast cancer patients

T. Byrski, J. Gronwald, T. Huzarski, E. Marczyk, P. Blecharz, J. Mitus, K. Urbanski, J. Lubinski, S. A. Narod*
*Pomeranian Medical University, Szczecin, Poland

Background: The aim was to assess the frequency of complete pathologic response after neoadjuvant treatment with cisplatin chemotherapy in women with breast cancer and a BRCA1 mutation.
Method: Forty patients with breast cancer and a BRCA1 mutation, who presented with stage I to III breast cancer between December 2006 and March 2010, were treated

with cisplatin 75 mg/m^2 every 3 weeks for four cycles, followed by mastectomy and then conventional chemotherapy. Surgery occurred 3 weeks after the final dose of cisplatin. The excised breast tissue and lymph nodes were examined for the presence of residual disease. Pathologic complete response was determined by a review of surgical specimens.

Results: Forty patients were enrolled in the study. Twenty-four patients had tumors of >2 cm and 12 patients had positive lymph nodes at diagnosis. Thirty-seven patients completed four cycles of cisplatin and three patients completed two cycles. Clinical complete response was observed in 31 patients (77%). Pathologic complete response was observed in 29 patients (72%).

Conclusion: Platinum-based chemotherapy is effective in a high proportion of patients with BRCA1-associated breast cancers. Clinical trials are warranted to determine the optimum treatment for this subgroup of breast cancer patients.

004
Clinical outcome of ovarian cancer in respect to polymorphism of low-penetrance genes

E. Grzybowska, K. Tcza, J. Pamua-Piat, S. Jdru, E. Telka, Z. Kosza, B. Zema*
*Centre of Oncology-MSC Memoria, Dept. of Molecular Biology, Gliwice, Poland

Objective: We wanted to analyze the influence of modifying genetic factors on the risk of BRCA(+) and BRCA(−) breast and ovary cancers and on clinical parameters as the age of onset and survival.

Method: The study includes three hundred forty-eight anonymous healthy women (control group), 229 persons with ovary cancer, 45 persons with breast and ovary cancer (case group). The patients under study developed breast cancer prior to ovary cancer. RFLP and ASA PCR were used to analyze mutations in BRCA genes and polymorphisms in PGR, MDR1 and TP53 genes.

Results: The presence of allele T of 660 PGR significantly decreased the risk of second malignancy (breast cancer; OR= 0.44, p=0.039). Heterozygote CT of MDR1 gene C3435T and genotypes AG and AT of G2677T/A were at lower risk of developing ovary cancer. Genotype CT of C3435T polymorphism had protective effect against developing the second malignancy, while allele TT increased the risk of breast cancer. Carriers of allele C for TP53Arg72Pro polymorphism had a significantly lower risk of developing ovarian cancer (OR=0.72, p=0.04) The best survival was found for patients carrying germline mutation in BRCA1 gene; the worst survival was observed for the group of patients with breast and ovary cancer and without germline mutation in BRCA1 gene. Alleles of TP53Arg72Pro significantly modified the survival of the group of patients who were diagnosed with breast cancer prior to ovarian carcinoma. The worst survival was connected with rare allele C.

Conclusion: Polymorphic variants of PGR, MDR1 and TP53 genes under study modified more the clinical course and the risk of second malignancy than the risk of developing ovary cancer alone.

005
DNA testing for high risk of cancers

*B. Górski**
*Poland

006
Genetics of colorectal cancers

*R. Scott**
*Discipline of Medical Genetics, School of Biomedical Sciences, Newcastle, Australia

The study of rare inherited conditions with high penetrance that predispose to colorectal cancer has significantly advanced our knowledge of the genetic basis of disease and represents a paradigm that has served to better understand the molecular mechanisms that underlie the development of disease in persons who have no apparent genetic predisposition. Inherited predispositions to colorectal cancer can be divided into essentially two groups: those that present with a premalignant phenotype (such as familial adenomatous polyposis (FAP) and the hamartomatous polyposis syndromes) and those like hereditary non-polyposis colorectal cancer, Lynch syndrome and Muir–Torre syndrome. For predispositions where the underlying genetic basis of the disease is known, much has been learned about disease penetrance and the expected spectrum of disease as increasing numbers of mutation carriers are characterized. This has lead to the reclassification of some defined syndromes as a result of the inherited predisposition being identical. Improved knowledge about disease penetrance has also resulted in a number of questions being raised with respect to what factors influence disease expression in patients known to harbour a mutation in a colorectal cancer susceptibility gene. Of particular interest are additional genetic factors (termed modifier genes) that have been correlated with disease manifestation. More recently, the focus of attention has shifted from familial aggregations of disease where there is a well-defined inherited component to population studies aimed at identifying common low-penetrance disease alleles that are associated with small affect sizes. These studies are significant not only because they are identifying genetic factors associated with colorectal cancer risk but also potential

modifier genes that are important in modulating disease expression in persons who harbour a genetic predisposition.

Wednesday, 1 September 2010, 14.30–16.30, Aula Duża B

WGS-08 Gastrointestinal tract eosinophilia

Chairpersons: K. Geboes, Belgium
G. Klöppel, Germany

001

Eosinophils in the gastrointestinal tract: function and dysfunction

G. Pineton de Chambrun, P. Desreumaux, M. Capron*
*Association de Gastroentérol., HP Huriez, Lille, France

Eosinophil functions have been associated for a long time with effector activity in adaptive immune responses during parasitic infections and inflammatory processes in allergic manifestations as well as in mucosal responses. The production by eosinophils of a vast array of cytokines as well as their expression of innate receptors and mediators confer to eosinophils a unique contribution both in inflammatory and adaptive responses but also in immunoregulation and innate immunity. Eosinophils are customary inhabitants of the gastrointestinal tract, except for the oesophagus. Beneficial function of intestinal eosinophils was their ability to defend host against helminths. However, eosinophil accumulation in the gastrointestinal tract is a common feature of numerous gastrointestinal disorders, including inflammatory bowel diseases, intestinal vasculitis, gastroesophageal reflux disease and food allergy. Primary eosinophilic gastrointestinal disorders, defined as disorders that selectively affect the gastrointestinal tract with eosinophil-rich inflammation of unknown etiology, include eosinophilic esophagitis, eosinophilic gastroenteritis and eosinophilic colitis and are occurring with increasing frequency. Decrease in the rate of parasitic infections in the developed world is associated with a rise in atopic/allergic disorders and increased hypersensitivity responses to allergens and may represent a driving factor towards the recruitment and activation of gut eosinophils in those disorders. Although the pathogenesis of those disorders is still poorly understood, new findings on gastrointestinal eosinophil proliferation and migration mechanisms involving IL-5 and eotaxins provide a rationale for specific disease therapy. The present review will summarize knowledge on the physiology of gut eosinophils and will illustrate some aspects of eosinophilic disorders of the gastrointestinal tract.

002

Eosinophilic oesophagitis

M. Genevay-Infante, L. Rubbia-Brandt, A.-L. Rougemont*
*Switzerland

Gastro-oesophageal reflux disease (GERD) and eosinophilic oesophagitis (EE) are the two main non-tumoral diseases involving the oesophagus and can develop in both children and adults. The former, the more frequent, is present in up to 20% of the Western population. It is the consequence of a massive flow of gastric contents back into the oesophagus, leading to symptoms or organ damage. Eosinophilic oesophagitis, first reported in 1978 and defined as a specific clinicopathological entity in 1993, is characterized by eosinophilic infiltration of the oesophagus. Its cause or causes are unknown despite its frequent association with an allergic setting. In 2007, a consensus meeting of the American Gastroenterological Association Institute and the North American Society for Paediatric Gastroenterology, Hepatology and Nutrition recommended diagnostic criteria for EE. Despite this increased knowledge of both pathologies, GERD and EE present considerable clinical and pathological overlap. Their distinction remains, however, crucial as their clinical outcome and treatment modalities are quite different. The pathologist has to be aware that the diagnosis cannot be based solely on pathological features. The aim of this presentation was to provide pathologist both clinical and histological diagnostic clues in order to propose the most accurate diagnosis and treatment.

003

Eosinophilic enterocolitis

*A. Driessen**
*The Netherlands

Eosinophilic gastro-enterocolitis, consisting of eosinophilic gastroenteritis (EG) and eosinophilic colitis (EC), belongs to eosinophilic gastrointestinal disorders whose diagnosis is based on gastrointestinal symptoms, an eosinophilic infiltration in the gut and the exclusion of secondary causes of eosinophilia (Collins MH 2009, Furuta GT 2008, Shifflet A 2009). EG and EC are both rare entities. EG is a predominantly benign disease occurring at any age (peak incidence, third–fifth decade). It may affect any part of the gastrointestinal tract, most commonly the stomach (25–80%) and small intestine (28–100%). EC is more uncommon, involving the colon and less frequently the rectum. Symptoms vary in function of the affected layer of the wall: mucosa (25–100%): abdominal pain, diarrhea; muscular layer (13–70%): intestinal obstruction; serosa (12–40%):

ascites. The ethiopathogenesis is not fully clear, but is sometimes related to a food allergy. Diagnosis requires a panendoscopy with biopsy. Histologic examination may, however, be hampered by the patchy distribution of the mucosal inflammation and the presence of a normal mucosa in association with muscular/serosal involvement. In this case, a full-thickness biopsy may be necessary for diagnosis. Microscopic features are the presence of numerous eosinophils in the lamina propria, extending into the epithelium (crypt abscesses) and the submucosa, associated with architectural abnormalities. In mural or serosal EG/EC, eosinophils are predominantly situated in the muscular or peritoneal layer. Differential diagnosis includes other disorders with eosinophilia, e.g. inflammatory bowel disease, celiac disease, parasitic infection, vasculitis. Several treatment modalities have been described in literature, such as restriction diets, corticosteroids or antihistamines. Surgery is restricted to the resection of stenosed segments in mural enterocolitis.

004
Systemic eosinophilic disorders and the GI tract

*A. Hoorens**
*UZ Brussel, Dept. of Pathology, Belgium

Secondary eosinophilic disorders, including infectious, inflammatory, hypersensitivity and neoplastic illnesses, always require exclusion before making the diagnosis of eosinophilic oesophagitis/gastroenteritis/colitis, particularly in case of peripheral blood eosinophilia. Parasite infections are well known to present with eosinophilia of the gastrointestinal mucosa. A drug-induced aetiology should also always be considered. Gastrointestinal eosinophils may be a feature of connective tissue disease, especially scleroderma, and can accompany vasculitis in polyarteritis nodosa and Churg–Strauss syndrome. With very pronounced peripheral eosinophilia, hypereosinophilic syndrome (HES) with gastrointestinal involvement, clonal eosinophilia and lymphocytic variant hypereosinophilia should be considered. HES is defined as eosinophilia ($\geq 1.5 \times 10^9$/L) for at least 6 months, no known cause of eosinophilia, and evidence of organ involvement. The gastrointestinal tract is affected in 25%. When only the digestive tract is involved, it may prove difficult to distinguish HES and eosinophilic gastroenteritis. Involvement of the intestinal tract in HES has been associated with limited prognosis and, in some, a fatal outcome. Eosinophilic infiltration of the GI tract in HES should be distinguished from eosinophilic infiltration of the GI tract in lymphocytic variant hypereosinophilia where eosinophilia is associated with phenotypically abnormal and/or clonal T lymphocytes. Clonal eosinophilia is characterized by neoplastic proliferation of eosinophils as part of an underlying myeloid malignancy and can accompany any one of the myeloid malignancies. Two distinct subcategories of clonal eosinophilia are recognized: chronic eosinophilic leukaemia, NOS and myeloid/lymphoid neoplasms with abnormalities involving PDGFRA/PDGFRB or FGFR1. Accurate diagnosis of all these conditions requires the correlation of endoscopic and biopsy findings together with a careful clinical examination.

005
GI eosinophilia in paediatrics

*M. Walker**
*United Kingdom

Eosinophils are powerful innate immune cells home to the gastrointestinal tract and play a major role in both host immunity to luminal pathogens and maintenance of homeostasis of intestinal epithelium in the normal gastrointestinal tract (GIT). Normal numbers at different GIT sites are defined in children. However, if in excess, eosinophils may play a key role in the pathogenesis of disease of the GIT, including primary eosinophilic gastrointestinal disease (EGIDs). Data from the World Wide Web-based registry of EGIDs show that these have a strong genetic and allergic component, 80% having coexistent atopic disease, 62% food sensitisation and 16% with a family member with similar disorders. The most studied EGID in children is eosinophilic oesophagitis; symptoms include feeding intolerance and GERD symptoms. Endoscopy shows a characteristic linear furrowing, and histological features include ≥15 eosinophils/1 HPF (peak count). There is a male preponderance and an allergic and genetic component. Around 7–8% of children are affected by food allergy, most commonly cow's milk allergy and egg and peanut allergies which may manifest as eosinophil-induced GI disorders. Eosinophilic gastroenteritis is manifest as allergic eosinophilic gastroenteritis, allergic proctocolitis and food protein-induced enterocolitis syndrome (FPIES). Eosinophilia is also seen in helminth infection, inflammatory bowel disease, coeliac disease and graft vs. host disease where eosinophil density can correlate with disease severity. Recent work has implicated duodenal eosinophilia in functional conditions, particularly paediatric dyspepsia, with success in treatment aimed at the eosinophil–mast cell axis.

006
Parasites and eosinophils in the GI tract

*G. De Hertogh**
*UZ Leuven, Dept. of Pathology, Belgium

Background: Human endoparasites belong to four groups: the protozoa and the nematodes, cestodes and trematodes. About 12 protozoan and 15 helminthic species can cause gastrointestinal (GI) pathology. Eosinophils are frequently associated with the lesions present in these conditions.
Method: PUBMED-based review of the associations between GI parasites and eosinophils.
Results: Protozoan parasites may be located on the mucosal surface or in the bowel wall in an intra- or extracellular position. Eosinophils can be increased in blood and tissues, notably with *Isospora belli*. *Dientamoeba fragilis* infection may even masquerade as allergic colitis. Invasive amoebiasis (*Entamoeba histolytica*) on the contrary has been associated with a decreased number of tissue eosinophils. Worms may be observed in the egg, larval or adult stage buried in or attached to the bowel wall. Helminthic infections are classically associated with blood and tissue eosinophilia, which can be limited to the place of attachment of the organisms. The number of eosinophils in biopsies can be very high and even suggestive of primary eosinophilic enteritis, e.g. in trichuriasis, anisakiasis and enterobiasis, and with *Ancylostoma caninum* and *Angiostrongylus* infections. Alternatively, chronic inflammation with eosinophilia may be confused with ulcerative colitis or Crohn's disease, the latter especially if granulomas are present (as with *Schistosoma mansoni* infection and more rarely in strongyloidiasis, anisakiasis and enterobiasis).
Conclusion: Eosinophils are involved in the defense against many protozoan and helminthic GI parasites. The resulting histological picture may at times be confused with other disorders such as primary eosinophilic enteritis and the idiopathic chronic inflammatory bowel diseases.

Wednesday, 1 September 2010, 14.30–16.30, Aula Średnia A

WGS-09 Emerging concepts on borderline melanocytic lesions and melanoma

Chairpersons: D. Massi, Italy
A. Zembowicz, USA

001
Emerging concepts regarding borderline melanocytic tumors

*A. Zembowicz**
*USA

002
Critical differential diagnoses in the evaluation of melanocytic lesions

*T. Brenn**
*USA

The diagnosis of invasive melanoma is straightforward in most cases. It is based on the recognition of a malignant junctional, in situ component in addition to an invasive dermal component. Classical diagnostic criteria are established mainly for superficial spreading melanoma, being the most common melanoma subtype. The morphological spectrum of melanoma is, however, wide, and distinction from both melanocytic naevi as well as non-melanocytic tumours may be challenging in individual cases. In particular, some benign melanocytic naevi may show concerning histological features overlapping with those of melanoma, resulting in significant potential for overdiagnosis. Melanocytic lesions notoriously difficult to separate from melanoma include dysplastic naevi, naevi of special sites, halo naevi, recurrent naevi, mitotically active naevi and deep penetrating as well as blue naevi. Non-melanocytic tumours may mimic melanoma by recapitulating a junctional in situ as well as a dermal invasive component showing similar cytological and architectural features, including epithelioid, spindle cell, small cell or desmoplastic differentiation, in addition to immunohistochemical expression of the so-called melanoma markers such as S100, HMB-45 and Melan A. These tumours may be of epithelial, haematolymphoid as well as mesenchymal lineage ranging from benign to outright malignant. Awareness of the critical entities in the differential diagnosis of melanoma and their differentiating features and diagnostic clues is important to avoid misdiagnosis, especially as the treatment modalities and clinical behaviours may differ significantly.

003
Molecular basis of melanocytic lesions

*A. Batistatou**
*Greece

Molecular studies of melanocytic lesions are necessary in order to identify additional prognostic and predictive biomarkers and establish the pathways of relevance for targeted therapy. The advent of biotechnology has also enabled the utilization of molecular testing as a diagnostic adjunct in the microscopic evaluation of difficult melanocytic lesions. The molecular multistep process of melano-

magenesis has been correlated to the Clark model for melanoma development. The first step of melanocytic hyperplasia and nevus formation has been linked to constitutive activation of the ERK-MAPK pathway as a result of somatic mutations of BRAF or N-RAS (or H-RAS or GNAQ). The development of cytologic atypia (dysplastic nevi) is related to alterations in cell growth, apoptosis and DNA repair; inactivation of CDKN2A; and PTEN pathways and TP53. Radial growth phase has been associated with decreased differentiation and deregulated expression of MITF, as well as deficiency in the p16INK4a-Rb pathway. Alterations in cell adhesion, such as reduction/loss of E-cadherin, increase of N-cadherin, $\alpha v\beta 3$ integrin, MMP-2 and increased expression of osteopontin are associated with the development of radial growth phase and metastatic melanoma. Alternatively, some melanomas (including acral and mucosal) arise de novo and harbor mutations/amplifications of KIT and amplifications of cyclin D1 or CDK4 genes. Other less frequent, pathogenetic pathways have also been proposed. In the near future, distinct molecular signatures of gene expression may be useful in identifying melanocytic lesions as melanomas or nevi. For melanomas, refined classification systems based on molecular analysis could provide more accurate prognostic markers and enable targeted therapy.

004

Novel targeted therapies in melanoma and the pathologists' role in therapeutic selection

*A. Lazar**
*USA

Background: When melanoma metastasizes, it is a deadly disease with unsatisfactory treatment options. It has become clear that melanoma is composed of multiple genetic subsets of disease that have different oncogene additions and thus distinct therapeutic vulnerabilities.
Method: Many clinical trials and application of targeted therapies outside of the trial setting depend on melanoma subtype and the genetic features of an individual case. Pathologists are absolutely critical in this area of testing and in therapeutic selection to enable precision medicine.
Results: Targeted therapies based on the molecular genetic features of individual melanoma cases is beginning to drive targeted therapy selection and can greatly enrich the rate of response to particular treatments.
Conclusion: This lecture will focus on the genetic features of melanoma currently most relevant to treatment and how testing drives therapeutic selection. In the very near future, such testing will be employed for treatment in virtually all cases of metastatic melanoma.

Wednesday, 1 September 2010, 14.30–16.30, Aula Średnia B

WGS-10 Native kidney disease: news and views

Chairpersons: W. Schürch, Canada
A. Halon, Poland

001

Nephron number and essential hypertension

*K. Amann**
*University Erlangen-Nürnberg, Dept. of Pathology, Germany

Nephron number as determined during nephrogenesis may be one determinant of renal disease and hypertension in later life. Various genetic and epigenetic factors, but also maternal or environmental causes, are known to influence nephron number. An involvement of the kidney in the development of hypertension has been postulated for a long time and supported by experimental studies in rats and sheep. Brenner and colleagues supposed a direct association between nephron number and blood pressure in humans. Their so-called Brenner hypothesis postulated that any reduction in nephron endowment leads to hyperfiltration of the remaining glomeruli, followed by glomerular enlargement with glomerular and then systemic hypertension, resulting in glomerulosclerosis, thereby establishing a vitious circle. In line with this theory, an association of low nephron number and development of hypertension was shown in different animal models as well as in two autopsy studies in humans. Keller et al. found in Caucasian patients with essential hypertension a significantly lower number of glomeruli per kidney than in matched controls. In parallel, mean glomerular volume was more than twice as high in hypertensive patients as in normotensive control patients, indicating compensatory glomerular enlargement. These results were confirmed in a Caucasian American population, whereas in African Americans, there was no association between glomerular number and blood pressure. The pathomechanisms linking low nephron number and hypertension are only partly understood. Among others, inappropriate activation of the renin–angiotensin system, impaired tubular salt handling leading to salt and volume retention, or post-glomerular structural changes have been discussed.

002

The new classification of lupus nephritis: a critical reappraisal

*A. Halon**
*Wroclaw Medical University, Poland

Background: Systemic lupus erythematosus (SLE) is the prototype of human autoimmune multisystemic disease and has a wide spectrum of clinical manifestations, of which renal failure is the most common and severe. About 50–80% of patient with SLE suffer from lupus nephritis (LN), and it is one of the major causes of morbidity and mortality. LN manifests as diverse patterns of immune complex-mediated renal disease involving all tissue compartments: glomerular, vascular and tubulointerstitial.
Method: The histopathological manifestations of LN are classified into several categories, originally designated by the WHO in 1982. In 2002, an international group of pathologist, nephrologists and rheumatologists formulated a new classification of LN in order to standardize definitions and improve diagnostic procedures. This review will focus on the most recent, widely practiced classification, the International Society of Nephrology/Renal Pathology Society (ISN/RPS) 2003 Classification of Lupus Nephritis, which includes various changes from predecessors.
Results: Histological prognostic factors proposed in LN including ISN/RPS 2003 Classification, Activity (AI) and Chronicity (CI) indices may not be sufficient to predict renal failure progression and response to therapy. New markers of glomerular and interstitial response to injury and renal scaring progression, such as α-SMA, PGM1 (CD68), E-cadherin, collagen IV, caspase-3, Bcl-2 and p53, can become new prognostic factors for LN.
Conclusion: The lecture will be devoted to the revision and reappraisal of a new classification of LN and the potential role and predictive ability of new markers.

003

The Oxford classification of IgA nephropathy: a review based on the Polish renal biopsy registry

A. Perkowska-Ptasinska, M. Wagrowska-Danilewicz, M. Danilewicz, A. Halon, E. Komuda, H. Karkoszka, A. Andrzejewska, K. Okon, I. Kurnatowska, M. Krasnicka, T. Hryszko, M. Kusztal*
*Poland

IgA nephropathy is a disease of a diverse course and outcome. There were several attempts to create a morphological classification that would serve as a tool efficiently defining the potential responsiveness to the immunosuppressive treatment as well as prognosis in individual cases. The last of these proposals, The Oxford classification of IgA nephropathy, was published in July 2009. The aim of our study was to compare the utility of few functioning classification systems, including Oxford and Hass classifications and Japanese histological grading, as well as our own morphological index of biopsies with IgA nephropathy. On the basis of data collected in Polish Renal Biopsy Registry, we selected 135 IgA nephropathy cases that were characterized by at least 2 years of post-biopsy follow-up, as well as satisfactory tissue material for light microscopy evaluation. Microscopical grading was performed by a group of experienced nephropathologists. The lecture will be devoted to the results and conclusions of this study.

004

The myofibroblast. From wound healing to neoplasia. With special emphasis on tissue fibrosis and fibrocontractive conditions. Twenty-five years of reflexions

*W. Schürch**
*Canada

The myofibroblast (MF) was discovered in 1971 in electron micrographs from experimental granulation tissue. This cell was shown to share features of fibroblasts and smooth muscle cells, hence its name. In due course, it was found to be the principal cell to effect wound contraction, i.e., wound healing. This unique cell was later defined at the histologic, ultrastructural, immunohistochemical, biochemical and pharmacological levels. For the surgical pathologist, the MF is best defined by its ultrastructure. Immunohistochemical studies demonstrate a heterogeneous pattern of cytokeletal phenotypes regarding actin isoforms and intermediate filaments. Five immunophenotypes were identified. Ultrastructural features that define the MF include: (a) stress fibers, i.e., bundles of microfilaments with interspersed dense bodies; (b) well-developed cell-to-stroma attachment sites, i.e. fibronexi, intercellular intermediate and gap junctions; and (d) abundant production of extracellular matrix. MFs have been observed in normal tissues, in granulation tissue and in several pathologic settings which will be discussed in detail. Numerous cells can modulate into a MF phenotype: foremost, the local resident fibroblasts, followed by pericytes, vascular smooth muscle cells, liver perisinusoidal stellate cells, kidney mesangial and tubular epithelial cells, bone marrow stromal cells and mesothelial cells. For the development of the MF phenotype, a two-stage model was proposed. Following tissue injury, complex changes in the microenvironment occur with the release of cytokines and the concerted action of a permanent feedback between intra- and extracellular tension, transforming

progenitor cells into proto-MFs and then into differentiated MFs.

Wednesday, 1 September 2010, 14.30–16.30,
Sala Wystawowa A

WGS-11 Lung tumours: mimics between benign and malignant

Chairpersons: R. Attanoos, United Kingdom
B. Papla, Poland

001
Distinguishing benign and malignant lymphoid lesions of the lung

*R. Attanoos**
*United Kingdom

002
Controversies in pulmonary epithelial proliferations: defining neoplasia from hyperplasia and metaplasia

*R. Langfort**
*National TB & Lung Disease, Research Institute, Warsaw, Poland

Three types of pulmonary preneoplastic changes (PPC) are accepted: squamous dysplasia and carcinoma in situ (SD/CIS), atypical adenomatous hyperplasia (AAH), and diffuse idiopathic pulmonary neuroendocrine cell hyperplasia (DIPNECH). SD/CIS are associated with the development of squamous cell carcinoma (SCC). AAH is a pre-invasive lesion for adenocarcinoma (ADC), and DIPNECH may progress to carcinoid. Recently, adenocarcinoma in situ (AIS, formerly bronchioloalveolar carcinoma (BAC)) was included among PPC. Pathogenesis of SCC and ADC is a multistep and multicentric process involving the transformation of the normal bronchial mucosa and alveolar lining cells through a continuous spectrum of lesions. The sequence of PPC for SCC includes: hyperplasia > metaplasia (SM) > SD > CIS > SCC; for ADC, it is hyperplasia > AAH/BAC > ADC; and for carcinoid, it is DIPNECH > tumorlet. Numerous genetic and molecular abnormalities occur in the very early stages of lung carcinogenesis, including hyperplasia and metaplasia and even in normal-appearing bronchial epithelium. It is not known which genetic changes are the most important or at what stage the process is irreversible. SM and hyperplasia can be either a repair or a reactive and reversible process of injured bronchial epithelium. It is found in purely inflammatory settings. These reactive processes usually do not progress to dysplasia and carcinoma. That is, morphology is a gold standard in the diagnosis of both reactive and PPC, and no ancillary studies can be used as a diagnostic aid. The strict histologic criteria are used to assist in the recognition and grading of mucosal lesions.

003
Handling the problematic pleural biopsy in suspected mesothelioma cases

*S. Anttila**
*HUSLAB Jorvi, Dept. of Pathology, Espoo, Finland

The most challenging diagnostic problems in pleural biopsies include distinguishing between benign mesothelial hyperplasia and epithelioid malignant mesothelioma and between reactive pleural fibrosis and sarcomatoid or desmoplastic mesothelioma. In addition, sometimes rare tumor types, such as lymphohistiocytoid malignant mesothelioma or epithelioid hemangioendothelioma, may mimic reactive processes. The first question to be considered when handling a problematic pleural biopsy is: Is the biopsy material adequate and representative as can be judged from clinical, imaging and thoracoscopic findings? If in doubt, a new biopsy should be recommended. The distinction between benign and malignant mesothelial proliferation can be made on morphological grounds only, although immunostains, e.g., for EMA and desmin, may favor either a benign or malignant lesion. The most reliable criterion of malignancy is invasion. Immunostains for broad-spectrum cytokeratins may aid in recognizing invasion both in epithelioid and spindle cell lesions. In spindle cell lesions, cytokeratins also help recognize the growth patterns of spindle cells. In reactive pleural fibrosis, a layer of cytokeratin-positive cells may be seen parallel to the pleural surface, whereas in sarcomatoid or desmoplastic mesothelioma, the pattern of spindle cells is haphazard or storiform. Negativity of immunostaining for cytokeratins in a spindle cell lesion should not automatically lead to a conclusion of a benign process as, e.g., sarcomas and about a quarter of sarcomatoid or desmoplastic mesotheliomas are cytokeratin-negative. Correlation of histological and immunochemical findings with clinical and imaging findings is of utmost importance for a correct diagnosis without unnecessary delay.

Wednesday, 1 September 2010, 14.30–16.30,
Sala Wystawowa B

WGS-12 Hematopathology (EAHP): newly defined entities in WHO classification of hematopoietic and lymphoid tissues

Chairpersons: R. Maryniak, Poland
C. Meijer, The Netherlands

001

Histiocytic and dendritic cell tumours

*S. Pileri**

*Bologna University, Dept. of Haematology and Oncology, Italy

These rare tumours stem from mononuclear phagocytes or antigen-presenting dendritic cells. The latter belong to different cell lineages (either haematopoietic or mesenchymal). Histiocytic sarcoma (HS) affects adults and is characterised by an aggressive clinical course in most instances. HS more often occurs at extranodal sides and consists of pleomorphic, atypical, large cells that are $CD68^+$, $CD163^+$, $lysozyme^+$, $CD45^+$, $CD45R0^+$, and $HLA\text{-}DR^+$. Partial expression of S-100 is recorded. Tumours derived from Langerhans cells (LC). They maintain the phenotypic profile ($S100^+$, $CD1a^+$, $Langerin^+$) and ultrastructural features ($Birbeck\ granules^+$) of LC. They include LC histiocytosis and LC sarcoma. The former represents a well-known entity, more commonly observed in children: Its behaviour varies according to the stage. The latter is a very aggressive disease of adulthood with overt cytological atypia and dismal prognosis. Interdigitating cell sarcoma (IDCS) is a very rare neoplasm of adulthood that cannot be differentiated from follicular dendritic cell sarcoma morphologically, both being composed of oval fusiform cells growing in fascicles, storiform pattern or 360° whorls. The diagnosis is based on S-100 and vimentin positivity in the absence of other lineage markers. Follicular dendritic cell sarcoma (FDCS) occurs in adults and more often presents in the lymph node, at times within the context of Castleman disease. In 90% of cases, it has an indolent behaviour. The diagnosis of FDCS relies on the expression of at least two FDC-associated markers, including CD21, CD23, CD35, CNA.42, clusterin, and CXCL13. A special variant is the so-called inflammatory pseudo-tumour-like FDCS characterised by regular EBV infection.

002

Diffuse large B cell lymphoma versus Burkitt lymphoma

*P. Kluin**

*UMCG, Dept. of Pathology, Groningen, The Netherlands

Burkitt lymphoma (BL) is a well distinct clinicopathologic entity. In children of western countries, it mainly presents at extranodal sites such as the ileocecal region. However, some diffuse large B cell lymphomas (DLBCL) share one or more pathologic, molecular and/or clinical features with BL. In the new WHO classification of 2008, it was felt that cases in which no solid diagnosis of BL or DLBCL can be made deserve more scientific attention and, therefore, should temporarily be put in a separate category. Many lymphomas in this category are the so-called double-hit (or even "triple-hit") lymphomas with a MYC/8q24 in combination with a BCL2/18q21, a BCL6/3q27 (or sometimes even a CCND1/11q13) breakpoint. By definition, a MYC/8q24 breakpoint should always be present. These double- or triple-hit lymphomas make up approximately 30–40% of all (previously diagnosed) BL in patients >60 years and represent highly aggressive tumours. Many patients fail to enter stable complete remission, even after high-intensity therapy as given for BL. Other cases that fall into this novel WHO category are DLBCL with a MYC breakpoint and other features of BL such as a very high Ki-67 proliferation index and expression of CD10 and BCL6, or cases of otherwise regular BL with an unexplained abnormal phenotype such as strong BCL2 expression. Several cases will be discussed during the session.

003

Lymphoproliferative disorders in immunodeficient patients

*H. van Krieken**

*UMC St Radboud, Dept. of Pathology, Nijmegen, The Netherlands

004

Grey zones between Hodgkin and non-Hodgkin lymphoma

*P. Kluin**

*UMCG, Dept. of Pathology, Groningen, The Netherlands

Hodgkin lymphomas (HL) consist of two main categories, classical HL (CHL) and nodular lymphocyte predominant Hodgkin lymphoma (NLPHL). The latter occasionally shows large diffuse areas. In particular in small biopsies, this generates a difficult differential diagnosis of T cell/histiocyte-rich large B cell lymphoma (THRLBCL). Immunohistochemistry with a large panel of antibodies may be of help, but cannot solve all problems, and clinical aspects should always be taken into account as well. In view of the important clinical (therapeutic and prognostic) consequences, such cases should also be evaluated by an expert hematopathologist. The second problem is the distinction between CHL and primary mediastinal large B cell lymphoma (PMBL) or diffuse large B cell lymphoma (DLBCL) NOS. There may be various situations: a mediastinal mass with a synchronous composite CHL and PMBL with divergent morphology and immunophenotype. This situation may be more frequent than thought since usually, only a small sample from the mediastinal mass is taken. Both lymphomas may also develop metachronously. The coincidence of both lymphoma types is explained by the fact that both lymphomas likely have a common (thymic) origin. Indeed, they share many genetic and molecular features as well. More difficult to

understand and diagnose are the cases that arise outside the mediastinum with mixed features of cHL and DLBCL-NOS and cases of otherwise CHL that strongly express CD20 and/or other B cell markers. In such cases, other diagnoses should be considered as well, such as EBV + DLBCL of the elderly. Several cases will be discussed during the session.

005
Peripheral T cell lymphomas: a new frontier

S. Pileri, C. Agostinelli, P. P. Piccaluga*
*Bologna University, Dept. of Haematology and Oncology, Italy

Peripheral T cell lymphomas (PTCLs) account for about 12% of lymphoid tumours worldwide. Almost half of them show such a morphologic and molecular variability as to hamper any further classification and to justify their inclusion in a wastebasket category termed "not otherwise specified (NOS)". The latter corresponds to neoplasms with aggressive presentation, poor response to therapy and dismal prognosis. Conversely to B cell lymphomas, PTCLs have so far been the object of a limited number of studies aiming to elucidate their pathobiology and identify novel pharmacologic approaches. Herewith, the authors revise the most recent contributions on the subject based on the experience they gained in the extensive application of microarray technologies. PTCLs/NOS are characterised by the erratic expression of T-cell-associated antigens, including CD4 and CD52, recently proposed as targets for ad hoc immunotherapies. They also show variable Ki-67 marking, rates >80% heralding a worse prognosis. Gene expression profiling (GEP) studies reveal that PTCLs/NOS derive from activated T lymphocytes, more often of the $CD4^+$ type, and bear a signature composed of 155 genes and related products that play a pivotal role for cell signalling transduction, proliferation, apoptosis and matrix remodelling. This observation seems to pave the way to the usage of innovative drugs, such as tyrosine kinase and histone deacetylase inhibitors whose efficacy has been proven in PTCL primary cell cultures. GEP does also allow better distinction of PTCL/NOS from angioimmunoblastic T cell lymphoma, the latter being characterised by follicular T-helper lymphocyte derivation and CXCL13, PD1 and VEGF expression.

Wednesday, 1 September 2010, 14.30–16.30, Aula Mała

WGS-13 Pathologists in favour of developing countries—presentation of ongoing projects and results of the European Meeting in Turin in April 2010

Chairpersons: D. Soldini, Switzerland
L. Viberti, Italy

001
Unity is strength: Telepathology as effective tool against the shortage of specialists

*A. M. Ferrari**
*Casa di cura "S. Pio X", Milan, Italy

The South Saharan African countries are low-resource settings where the histological diagnosis of diseases and consequently the correct managing of the patient are difficult to obtain. Telepathology allows doctors working in remote locations to obtain a definite diagnosis through the transmission of tissue specimen via remote telecommunication. In particular, the "virtual slide" system allows capturing a visual image of an entire slide of a specimen which is then forwarded to another location for diagnosis. Association Pathology Beyond Borders (APOF) in 2005, in a small rural hospital in Zambia, to supply to the lack of pathology skilled personnel, started a project to train local staff to become technicians, able to prepare histological and cytological slides and to screen conventional Pap smears. The two Zambian technicians signed out negative Pap smears, and in the presence of abnormal findings, they took pictures of significant diagnostic fields. Then the images were sent through Internet to experts in Italy who, on a rotating roster, were responsible of the final diagnosis. Since 2007, the technicians were also able to prepare histological slides from the surgical specimen: Digital images of the slides were taken through a scanner and saved in a database in a local server. Through a satellite connection and a made-to-measure archival software and web site, pathologists in Italy were able to examine the specimen, record their diagnosis and transmit it directly to Zambia. In low-income countries where no other possibilities are available, telepathology seems to be a reliable and secure diagnostic tool.

002
Leave a mark: organizational models in building and managing a pathology service in developing countries

*P. Giovenali**
*Ospedale S. Maria, della Misericordia, Perugia, Italy

The main aim of the NGO Association Pathologist Beyond Borders (Associazione Patologi Oltre Frontiera, APOF) is the improvement of activities related to anatomical pathology in developing countries to raise the health standard in those areas through the performing of histological and cytological diagnoses for therapeutic and preventive purposes, such as screening programs. An essential part of every project managed by APOF consisted in the construction and organization of new pathology services or in the implementation of already existing laboratories. While taking into

account every particular local environment, needs and available resources, APOF decided to export the same models that have proven effective in our context: The technical histological and cytological process, from the surgical sampling to the final report, was set in detail trough precise guidelines with the inclusion of procedures dedicated to process control. Similar guidelines were used to update and adjust the diagnostic parameters according to international consensuses. The allocated funds were mainly used for the purchase of equipment and consumables and for the organization of updating courses dedicated to the technical and medical staff. In places where no skilled personnel were available, longer and more in-depth classes were organized for local staff, both in the place or in Italy. The staff, once trained, passed also an examination to obtain an official and specific degree. The main purpose of this kind of management was to build a reliable system that could then be directly managed by local staff at the end of the project.

003

The great debate about screening models in developing countries: matching needs and opportunities

*S. Guzzetti**

*Ospedale Evangelico Valdese, ASL TO1, Turin, Italy

Background: Association Pathology Beyond Borders (Associazione Patologi Oltre Frontiera, APOF) started in 2005, a project with the Mtendere Mission Hospital (MMH) at Chirundu, Zambia, to build and organize a Pathology Department then to set up a screening program for cervical cancer involving women of the MMH catchment area. The aim of this study was to discuss the reliability of Pap smear in screening programs for cervical carcinoma in low-resource settings.

Method: Two local staff members were trained by some APOF members to prepare histological and cytological slides and to screen conventional Pap tests. Subsequently, resident physicians were trained by two Italian gynecologists for colposcopy. Negative smears were directly reported by the two Zambian technicians. Digital images of selected microscopic fields of suspect cases were sent over a special web site and reported by a group of experts. Finally, all slides were sent to Italy and blindly reviewed by a single expert. Positive cases were then directly managed at MMH by colposcopy, bioptic confirmation and treatment.

Results: Pap smears results are summarized in Table 1. During the first 2 years of activity, inter-observer reproducibility was analyzed using two statistic indexes: Cohen's *k* and Gwet's AC1 (the agreement between the Zambian technicians with the expert was 0.77 and 0.87 and that between the web site and the expert was 0.57 and 0.65).

Conclusion: Pap smears can be an effective screening method even in low-resource settings focusing on local human resources.

TABLE 1 – PAP SMEARS PERFORMED AT MMH IN YEARS 2006 – 2008 AND RESULTS

Diagnosis	2006	%	2007	%	2008	%
UNSATISFACTORY	50	9.2	80	8.1	133	5.7
NEGATIVE CASES	366	67.6	742	74.8	1895	81.3
OVERALL POSITIVE CASES (≥ ASC-US)	126	23.2	170	17.1	303	13.0
ASC-US	16	2.9	23	2.3	38	1.6
AGC	7	1.3	2	0.2	7	0.3
L-SIL	64	11.8	70	7.0	136	5.8
ASC-H	8	1.5	25	2.6	23	1.0
H-SIL	17	3.1	40	4.0	82	3.5
SCC	13	2.4	9	0.9	16	0.7
ADENOCARCINOMA	1	0.2	1	0.1	1	0.1
TOTAL	**542**	**100.0**	**992**	**100.0**	**2331**	**100.0**

004

Managing unusual diseases in unusual settings: Project Uganda and haemopathology

*L. Leoncini**
*University of Siena, Italy

Although in the developed world the importance of the correct diagnosis is appreciated as a critical issue, this is still an evolving concept in some of the developing countries, especially in Africa. In particular, there are striking differences in the turnaround time for histopathological diagnosis, in the accuracy of diagnosis that has a profound impact on patients' management and ultimate outcome. The current problems in practice of lymphoid/lymphoma diagnosis include—basing treatment decisions on fine needle aspiration cytology in a large proportion of cases, poor quality histology in a minority of cases where biopsies are performed, complete lack of immunohistochemistry and other supportive investigations, and lack of an update on the current criteria for the diagnosis of various lymphoid pathologies. In Africa, a majority of the laboratories still use the Working Formulation for Clinical Usage, a lymphoma classification from the early 1980s which is based on morphology alone and does not include many entities recognized in the last 20 years. Without accurate diagnosis, any research project and effective patient management cannot be instituted. Though there are no magic answers for an issue of this magnitude, on which other aspects are critically dependent, twinning between institutions in the developed countries and developing countries seems to be the most likely long-term approach. Examples of twinning approach to childhood cancer diagnosis and treatment have been Africa. These programmes have led to improvements in the diagnostic accuracy through capacity building and joint research projects with both direct and indirect technology transfer.

005

The role of APOF in low-resource settings: present and future projects for the development of surgical pathology in developing countries

*V. Stracca-Pansa**
*Italy

In the last years, the cancer issue in most African countries is more and more dramatic. The WHO AFRO and the resolution of the 58th World Health Assembly made cancer one of the health priorities in developing countries and pushed African countries to formulate National Cancer Control Programmes. Once considered a disease of the rich, the pendulum has swung dramatically, and some 70% of new cancer cases in the next decade will be in the developing world. Many poor countries are unable to cope with the accelerating burden of cancer. Furthermore, to establish any reliable oncologic treatment, it is mandatory to obtain a complete, documented histological diagnosis. Patologi Oltre Frontiera (POF, Pathologists Without Borders), a newly established Italian NGO, has the mission to strengthen or build laboratories for anatomical pathology in developing countries, train local personnel, doctors and technicians for future autonomy of the laboratory, and provide medical and technical resources for histological and cytological diagnosis in the countries where departments of pathology are completely absent or based on a very small number of pathologists. Since 2000, Patologi Oltre Frontiera, which counts on tens of volunteers (pathologists, biologists and technicians), have launched numerous projects in Tanzania, Cuba, Zambia, Kosovo, Palestine, Egypt, Uganda, Madagascar, Congo and Gibuti. Every project is tailored on the particular needs of the place, but each has to respond to some strict criteria of efficacy and sustainability, with the final goal to leave local, well-trained personnel and a modern well-equipped laboratory.

Wednesday, 1 September 2010, 17.00–18.30, Aula Duża A

WGS-14 Breast pathology business meeting

Chairpersons: T. Tot, Sweden
C. Wells, United Kingdom

001

The Breast Cancer Pathology Report in 2010

*C. Mies**
*USA

The essential purpose of the breast cancer pathology report is to communicate pathologic findings that aid in prognostication and guide the selection of appropriate local and systemic treatment for patients with breast cancer. To be clinically useful, the content of the report must change as new prognostic and predictive factors are validated and others become obsolete. In 2010, the list of useful features—those which are grounds for specific therapeutic actions—is relatively short: the anatomic extent of disease in the breast and axilla (AJCC/UICC stage), the specimen margin status, and measures of certain cancer cell proteins (hormone receptors, HER-2/neu) that predict the likelihood of response to specific adjuvant therapies. Histological subtype, carcinoma grade, the presence of lymphatic tumor emboli, the finding of Paget disease in a mastectomy specimen are also often reported, but do not inform specific treatments the way that stage, margin status and predictive markers do. In patients with node-negative, estrogen receptor-positive breast cancer, the pathologist selects a paraffin-embedded tumor sample for the Oncotype DX assay, which is used to predict the risk of

recurrence in patients treated with tamoxifen and may addend the recurrence score to the surgical pathology report. The breast cancer pathology report in 2010 is vital to appropriate breast cancer treatment, but can be expected to evolve.

002
Working on national guidelines: European guidelines
*C. Wells**
*United Kingdom

003
Working on national guidelines: British guidelines
*I. Ellis**
*United Kingdom

004
Working on national guidelines: Swedish guidelines
*D. Grabau**
*LabMedicin Skåne, Dept. of Pathology, Lund, Sweden

In order to assure the quality of pathology in all of Sweden, the Swedish Society of Pathology has instituted organ-specific quality assurance and standardization groups. These groups consist of dedicated pathologists from many subspecialty areas and are called KVAST groups. They meet regularly and their principal work is to formulate and maintain a document with guidelines which has a common framework for all the organ-specific groups. Our group prepares the guidelines for breast pathology. The mandatory sections in all the guidelines include clinical background information, instructions to clinicians as how to handle the specimens, what information is needed on the requisition form, gross description, analyses, what information must be reported by the pathologist (gross and microscopic), recommended classification system, administration and miscellaneous. Sweden has a national cancer strategy programme emphasizing a patient perspective by focusing the patient process instead of piecing the treatment process together through independent specialities, as has been done previously. In 2008, a group of breast cancer clinicians established a national quality register for breast cancer patients called INCA which also include a pathology section. In collaboration with the Swedish Breast Cancer Group and the breast KVAST group, another group called SweQA works with quality assurance programmes of the biomarkers used in routine pathology; estrogen and progesterone receptors, HER2 status, and histologic grade. The guidelines for breast pathology will require the breast pathologists to participate in the breast cancer patient process by focusing on the standardisation of requisition and pathology reports and quality assurance of biomarkers.

005
Working on national guidelines: Hungarian guidelines
*G. Cserni**
*Hungary

Background: All pathologists feel that the establishment of pathological diagnoses is somewhat subjective. Writing national guidelines is useful in order to achieve better consistency in reporting at the level of a geographic area, Hungary. As not all countries have their national guidelines on breast reporting, it was thought useful to provide some examples of how guidelines can be constructed and/or adopted.
Method: The text of the Hungarian guidelines on breast pathology reporting was written by a committee of pathologists with expertise in breast pathology. The basis of the new text was a consensus document from 10 years ago. This was rewritten, circulated, and modified several times, and the updated text, ready for wider discussion, was put on the web (Internet) along with four other texts (diagnostic radiology/imaging including nuclear medicine; surgery including reconstructive surgery; radiotherapy; and systemic therapy). The URL allowing access to the texts was widely circulated on discipline-specific web sites. A Consensus Conference was organized for live discussion, and written comments were also welcome both from the writing committee members of the other texts and from the wider medical community (the other texts were discussed similarly to allow better congruence). All relevant comments were incorporated and the pre-final text was discussed at the Consensus Conference. The writing committee finalized the text on the basis of the relevant comments discussed at the conference. The pathology Guidelines were scheduled for publication with the other texts in the national oncology journal, Magyar Onkologia (Hungarian Oncology).
Results: NA.
Conclusion: NA.

006
Working on national guidelines: Polish guidelines
*E. Chmielik**, W. P. Olszewski, J. Rys*
*Oncology Institute, Dept. of Pathology, Gliwice, Poland
Objective: The pathologists from the three major oncology centers have worked out the guidelines for breast cancer pathology reporting.
Method: The proposed report was mainly based on the European and American guidelines as well as on the seventh version of TNM classification and was prepared in cooperation with radiologists and surgeons.

Guidelines of the pathological reporting of breast cancer were accepted by the multidisciplinary board of the main national specialists representing different medical professions such as pathology, oncologic surgery, medical oncology, chemotherapy and radiotherapy, and afterwards, they were described in the supplement of the Polish Journal of Pathology (2009, vol 60, issue 3) The guidelines include the rules of interpretation of needle core biopsies and other diagnostic procedures, as well as the recommendations of gross description and processing of surgical specimens depending on the type of surgical treatment. Especially, pathology report of breast carcinoma after neoadjuvant chemotherapy was proposed. Special techniques used for diagnosis of breast lesions, their performance and interpretation are also included.
Results: Finally, the histopathological evaluation form of breast cancer has been proposed.
Conclusion: In a year after the supplement publication, it is planned to conduct a survey to find out the practical use of those guidelines. On the basis of both the answers to those questions and medicine-based evidence, Polish guidelines are going to be compiled.

Wednesday, 1 September 2010, 17.00–18.30, Sala Wystawowa B

WGS-15 Haematopathology (EAHP): indolent lymphomas

Chairpersons: P. Kluin, The Netherlands
E. Campo, Spain

001
Indolent B cell lymphomas

*E. Campo**
*Hospital Clinico, Dept. of Pathologic Anatomy, Barcelona, Spain

Indolent lymphomas are a heterogeneous group of neoplasms with different clinical and pathological features that share some common features. The tumor cells are small B and grow predominantly in the topographic sites where the corresponding normal counterpart is localized. The proliferation rate is relatively low, and the cells tend to expand towards the adjacent tissues with limited destructive capacity. Clinically, these tumours have a long indolent course and the patients may not need chemotherapy for long periods of time. However, the tumours may not be cured with the current therapies and slowly progress, increasing the tumor burden and relapsing successively during the evolution of the disease after an initial response to the therapy. In some cases, transformation to a more aggressive diffuse large cell lymphoma may occur, and then the evolution is rapid with poor response to savage therapies. Indolent lymphoid neoplasm includes chronic lymphocytic leukemia (CLL), lymphoplasmacytic lymphoma (LPL), follicular lymphoma (FL), extranodal marginal zone lymphoma of the mucosa associated lymphoid tissues (MALT), nodal marginal zone lymphomas (NMZL) and splenic marginal zone lymphomas (SMZL). CLL and SMZL present usually with a leukemic phase, whereas FL and NMZL are nodal diseases. FLs in extranodal sites such as skin and duodenum have distinctive clinical and biological characteristics that differ from the nodal counterparts. MALT lymphomas develop on a previous chronic inflammatory background that in most occasions is related to certain infections or autoimmune disorders. The morphology, phenotype, molecular alterations and genetic features of the tumours are distinctive, allowing a precise characterization.

002
Primary cutaneous lymphomas

*C. Meijer**
*The Netherlands

Wednesday, 1 September 2010, 17.00–18.30, Aula Mała

WGS-16 Constituting Meeting of the Thymus and Mediastinal Pathology Working Group

Chairpersons: W. D. Travis, USA
A. Marx, Germany

001
Problems of the 2004 WHO Thymoma Classification that need to be solved: a practicing pathologist's view

*T. Molina**
*France

002
Refinement of morphological WHO criteria for thymoma diagnosis

*W. D. Travis**
*USA

003
New diagnostic markers for improved delineation of thymoma subtypes

*P. Ströbel**
*Germany

004

Translational aspects of thymic epithelial cancers: could anti-angiogenesis be an option?

M. Marino, G. Palmieri*
*Italy

005

Has the time come for a new WHO Classification of mediastinal tumours?

*H. K. Müller-Hermelink**
*Germany

Thursday, 2 September 2010, 08.00–11.00, Aula Duża A

WGS-17 Progress in soft tissue and bone pathology

Chairpersons: P. C. W. Hogendoorn, The Netherlands
P. Dei Tos, Italy

001

Histopathological diagnostic discrepancies in soft tissue tumours

*C. Fisher**
*Royal Marsden Hospital, Dept. of Histopathology, London, United Kingdom

Background: For the management of soft tissue sarcomas, it is essential to make a correct pathological diagnosis and grade. However, these tumours are rare, with an incidence of about 25 per million population, and a general pathologist might encounter only one or two per year. Furthermore, diagnostic criteria evolve, particularly concerning ancillary investigations such as immunohistochemistry and molecular genetics.
Method: We reviewed the pathology of all patients with soft tissue tumours diagnosed elsewhere and referred for management to a specialist sarcoma unit in a 1-year period. This did not include cases sent for second opinion directly from other pathologists.
Results: In 349 specimens, we found discrepancies in referring diagnosis or grade in 27% of cases, including major discrepancies in 11% of cases and minor discrepancies in 16% of cases. Benign/malignant discordances accounted for 5% of all discrepancies. The most common discrepancies occurred in the diagnosis of gastrointestinal stromal tumours and leiomyosarcoma and in the subtyping of other spindle cell sarcomas as well in grading.
Conclusion: The findings support the guidelines by the National Institute for Health and Clinical Excellence in the United Kingdom that diagnostic review of soft tissue tumours should be performed by specialist soft tissue pathologists, i.e. those who regularly report a significant number of cases, take part in multidisciplinary team meetings and participate in an accredited external quality assessment scheme.

002

The role of fine needle aspiration cytology in the examination of soft tissue tumours

*H. Domanski**
*Labmedicin Skåne, Dept. of Pathology, Lund, Sweden

Background: Open biopsy usually provides sufficient tissue for the diagnostic workup of soft tissue tumours. Some disadvantages to open biopsy are risks of complications, high costs and occasionally delay in therapy initiation. An increasing use of minimally invasive diagnostic procedures has resulted in better acceptance of fine needle aspiration cytology (FNAC) in the diagnosis of soft tissue tumours.
Method: FNAC has been part of the diagnostic workup of patients admitted to the Sarcoma Center of Lund, Sweden since 1972. The Center has been responsible for the treatment of patients with musculoskeletal tumors in the South Sweden Health Care Region comprising 1.7 million inhabitants.
Results: The combined evaluation of clinical and radiological data and FNAC has been sufficient for making a treatment decision in most patients with sarcomas. For patients who were referred with a clinical suspicion of malignancy but in whom it was later proved to be a benign soft tissue lesion, only one visit to the Center was necessary for a therapeutic decision to be made.
Conclusion: Compared to open biopsy, FNAC is an outpatient procedure, well tolerated by patients, and with negligible risks for serious complications. Correct diagnosis of soft tissue tumours is facilitated when cytological diagnosis is based on strict cytological criteria and ancillary techniques and when FNAC is used in the context of the clinical findings. On-site, immediate evaluation of smears stained by DiffQuick is an optimal way to ensure that an adequate sample for both routine examination and for ancillary studies has been taken.

003

Lipomatous tumours that does not need MDM2 and/or CDK4 analyses

*F. Collin**
*France

004

Clinicopathological and molecular pathology of dermatofibrosarcoma

*S. Bague**
*Spain

005

Histological variants of Schwannomas

*B. Liegl-Atzwanger**
*Austria

Schwannomas are benign nerve sheath tumors (BNST) composed of cells with distinctly schwannian characteristics. The four major schwannoma subtypes are conventional, cellular, plexiform and melanotic schwannoma. However, other morphologic variants including ancient schwannoma, epithelioid schwannoma, arguably glandular schwannoma and hybrid schwannoma/perineurioma, hybrid schwannoma/neurofibroma and the microcystic/reticular schwannoma have been described. The anatomic distribution of these tumors is wide, with the majority arising in the subcutaneous tissue of the distal extremities or the head/neck region. Rarely, schwannomas occur in visceral locations. Classic schwannomas are encapsulated and are composed of two morphologically distinct components known as Antoni A and Antoni B tissue in various proportions. Verocay bodies as well as the common occurrence of thick-walled hyalinized vessels are helpful diagnostic features. Characteristically, the tumor cells express S-100 protein and the perineurial capsule can be highlighted with EMA. In contrast, schwannomas arising in visceral locations are unencapsulated, have pushing margins/focally an infiltrative growth and a characteristic morphology. It is worthy to note that there is a tendency to misdiagnose schwannomas and to overestimate their grade. Diagnostic challenges are cellular schwannomas, which may mimic a malignant peripheral nerve sheath tumor (MPNST), melanotic schwannomas, which are often mistaken as melanomas and the plexiform schwannoma, particularly in the cellular form and when occurring in the childhood simulates MPNST. The aim of the lecture will be to focus on the mentioned diagnostic challenges, the recently described microcystic/reticular schwannoma, a distinctive morphologic variant with predilection for visceral locations, as well as on BNST with hybrid features of schwannoma and soft tissue perineurioma or neurofibroma.

006

Molecular understanding of Ewing sarcomas and potential targets for treatment

*E. de Alava**
*University of Salamanca-CSIC, Spain

Bone and soft tissue sarcomas are an infrequent and heterogeneous group of mesenchymal tumors, including more than a hundred different entities. Sarcomas are quite resistant to conventional chemotherapy (anthracyclines and ifosfamide), with the exception of some subtypes such as Ewing sarcoma (ES). New drugs with proved efficacy against sarcomas include taxanes, gemcitabine, and ET-743. Preclinical studies have also identified key molecular events leading to the progression and development of ES which are good candidates to targeted therapy. Inhibitors of tyrosine kinase receptors, such as IGF-1R, c-kit, PDGFR, VEGFR, or the mTOR signaling pathway, proteasome, angiogenesis, and stress response proteins are under clinical evaluation against ES. This particular neoplasm, characterized by chromosomal translocations that originate gene fusions (EWS-FLI1, EWS-ERG), is an example of a good chemotherapy responder tumor whose survival rate shows a plateau in recent years, especially in metastatic disease. Preclinical studies have identified that new targets such as HSP90 are of relevance to ES. On the other hand, recent studies showed the role of cancer stem cells (CSCs) in sarcomas and the relevance of the identification of reliable molecular markers and possible therapeutic targets. New therapeutic approaches could be directed against CSCs. This talk describes more recent targeted therapy in sarcomas, with special emphasis on ES and the role of CSCs. We also emphasize the role of high-throughput genomics/proteomics techniques in identifying new therapeutic targets. Acknowledgements: Research at Enrique de Alava's lab is supported by the European Commission (Network of excellence on sarcomas EuroBoNet), the Ministry of Science of Spain, and the Maria Garcia-Estrada Foundation.

007

Molecular understanding of EWS translocations: implications for tumours other than Ewing sarcoma

*P. Dei Tos**
*Italy

Thursday, 2 September 2010, 08.00–11.00,
Sala Wystawowa A

WGS-18 Pathologists meet transplant physicians

Chairpersons: M. J. Mihatsch, Switzerland
A. Perkowska-Ptasinska, Poland

001

Indications for and clinical consequences of renal biopsies in kidney transplants

*H. Hopfer**
*University of Basel, Institute of Pathology, Switzerland

The transplant nephrologist decides to biopsy a given patient on the basis of clinical symptoms and laboratory data. The renal pathologist then makes a histological diagnosis which allows an evidence-based approach to specific therapy, which again will be decided on by the clinician. Renal transplant

diagnoses generally fall into one of five categories: preexisting donor-related diseases, rejection, drug toxicity, infection, recurrent or de novo renal diseases. Although many diagnoses are typically encountered during a certain phase after transplantation, clinical information alone will often not suffice to differentiate between diagnoses, which require a totally opposite treatment regimen. The timing of the biopsy is most important to achieve a successful treatment and to avoid irreversible damage to the transplant. The rule of thumb at our center is to biopsy early in delayed graft function if there is a change in serum creatinine of more than 0.5 mg/dl or there is a newly diagnosed or increased proteinuria. Sufficient biopsy material, adequate workup including C4d and SV40 immunohistochemistry, and an experienced pathologist are the other prerequisites. A close collaboration between nephrologist and pathologist with regular case discussions not only helps understand the viewpoint of the clinical/pathological partner but will also aid in patient management.

002

Pathology in zero-hour biopsies and clinical consequences: Hungarian and Polish experience

A. Perkowska-Ptasinska, E. Kemeny*
*Poland

At the University of Szeged, Hungary, we carried an original clinicopathological study to assess what type of vascular changes—if any—are associated with late graft dysfunction. We examined in 94 zero-hour biopsies the frequency and severity of nonspecific morphological lesions semiquantitatively. The wall thickness/lumen (W/L) ratio of each artery present in the biopsy was determined by morphometry. Among the arterial changes studied, only the intimal fibroelastosis (IFE) of moderate degree (frequency, 26.6%) revealed a significant correlation with serum creatinine at 48 months ($p<0.01$). In IFE, there was also a significant correlation with the frequency and severity of tubular atrophy and interstitial fibrosis ($p<0.001$). By morphometry, a significant association was found between the mean W/L ratios of arteries and the degree of IFE ($p<0.01$). According to Hungarian experience, donor kidneys with a moderate degree of IFE do indeed have a higher risk of late graft dysfunction. The analogically defined Polish retrospective study revealed that the presence of arteriolar hyalinisation in the implantation biopsy was associated with more profound reduction of GFR at 3rd, 6th and 12th months after transplantation in those patients who experienced episodes of an acute rejection ($p=0.018$) within first 12 post-transplant months. This suggests that donor-derived arteriolar hyalinisation predisposes to more severe acute rejection-associated graft damage.

003

New techniques for the identification of HLA antibodies

*G. Boehmig**
*Austria

Background: It has become evident that antibody-mediated immunity plays a critical role in acute and chronic allograft rejection. According to the Banff scheme, serological alloantibody detection represents one of the major diagnostic criteria for antibody-mediated rejection (AMR). The design of sophisticated diagnostic tests for prediction and monitoring of AMR has become a major goal in transplant medicine.
Method: An important innovation has been the establishment of solid phase HLA antibody detection using flow cytometry, ELISA or Luminex technology. In this context, Luminex-based bead array technology represents an attractive strategy for a detailed analysis of anti-HLA reactivity patterns.
Results: In recent studies, solid phase detection of preformed donor-specific antibodies (DSA) was shown to predict AMR and graft loss. Nevertheless, the actual diagnostic significance of such assays is still ill-defined and currently under intense discussion. For supersensitive bead array technology, there is a need for well-defined and standardized test thresholds. In addition, the predictive value of distinct qualitative parameters, such as DSA binding strength or antibody-triggered in vitro C4d deposition, is still to be established. In the context of allograft dysfunction post-transplant, solid phase detection of alloantibodies, with or without C4d-fixing ability, may represent a valuable diagnostic adjunct. However, the predictive value of circulating DSA in stable recipients is still under discussion.
Conclusion: The implementation of innovative serological tests can be expected to substantially improve the diagnostic repertoire in transplant medicine. Future studies are needed to clarify the actual value of such tests for allocation, targeted recipient desensitization or diagnosis of ongoing or pending rejection.

004

Diagnosis and management of polyomavirus nephropathy

*J. Kowalewska**
*Medical University Bialystok, Dept of Pathology, Poland

Objective: Polyomavirus-associated nephropathy (PVAN) is a significant clinical problem that has emerged in the last decade of renal transplantation. It affects between 1% and 10% of renal transplant recipients and is a significant cause of allograft dysfunction and failure. BK polyomavirus (BKV) is the most common cause of PVAN. The virus resides in latent form in the urinary tract in the majority of healthy individuals and is known to reactivate in immunocompromised patients.

While seen in recipients of other solid organ transplants, it affects almost exclusively renal transplant receivers. BKV primarily infects epithelial cells, causes cell lysis, gets released into urine and/or blood, and elicits virus-specific cellular and humoral immune response.

Results: Currently, the monitoring for BKV reactivation/infection includes cytologic examination of urine specimen for shedded epithelial cells infected by the virus (decoy cells) and quantitative PCR analysis of urine and serum samples for the number of vial copies. The gold standard for the diagnosis of PVAN remains allograft biopsy that can illustrate characteristic viral cytopathic effect in the nuclei of the tubular epithelial cells and the degree of associated inflammatory cell response. The infection with BKV should be confirmed by either immunohistochemical stain for SV40 or by in situ hybridization. Proposed management of BKN includes: modification of immunosuppressive regimen and/or additional regimen with cidofovir, leflunomide, IVIg, fluoroquinolones, and others.

Conclusion: In summary, PVAN is a disease of the renal allograft. Immunosuppression is the main modifiable risk factor. To ensure optimum protection, screening of all patients is essential. Monitoring, early diagnosis, and therapy need standardization.

Thursday, 2 September 2010, 08.00–11.00,
Sala Wystawowa B

WGS-19 Joint meeting of WG of breast pathology and head and neck pathology

Chairpersons: A. Skálová, Czech Republic
T. Tot, Sweden

001

Recently described breast-like tumours of the salivary glands

*A. Skálová**
*Charles University, Faculty of Medicine, Plzen, Czech Republic

Salivary and mammary glands share an identical ductuloacinar architecture, and thus, it is not surprising that lesions and tumours arising in both organs share considerable histologic similarities. Salivary-type tumours are well known in breast; in contrast, breast-like lesions are rarely described in salivary glands. One of the commonest breast conditions, benign fibrocystic disease, was not thought to have a salivary counterpart, but recently, sclerosing polycystic adenosis (SPA) was described as a distinctive neoplastic lesion of the major salivary glands. Although SPA has many histologic similarities to its mammary counterpart, it represents a true neoplastic condition characterized by clonality, focal dysplasia, and a tendency to recur. Up till now, secretory carcinoma (SC) has been considered to occur only in the breast. Recently, we published a series of 16 salivary gland tumors with histomorphological and immunohistochemical features reminiscent of SC of the breast. This is an unusual, hitherto undescribed, distinctive salivary gland tumor, with some morphological features of both salivary acinic cell carcinoma (AciCC) and mammary SC, characterized immunohistochemically by strong vimentin and S-100 protein positivity. Microscopically, the tumours exhibit a lobulated growth pattern, and they are composed of microcystic and glandular spaces with abundant eosinophilic homogenous or bubbly secretory material, which is positive for PAS, mucicarmine, MUC1, MUC4, and mammaglobin. All but one analyzable case in our study demonstrated a t(12;15)(p13;q25) ETV6-NTRK3 translocation, exactly as in breast SC. For this tumour, we propose, therefore, a designation mammary analogue secretory carcinoma (MASC) of salivary glands. No translocation was found in any conventional salivary AciCC or other salivary gland tumours with undetermined secretory features. Thus, our results support the concept that MASC and salivary AciCC are distinct entities and should be recorded separately in salivary gland tumour classifications. We believe that our study has added another example to the list of similar tumours in both organs, with MASC as the salivary gland counterpart of mammary SC. Despite the shared morphologic and immunohistochemical properties, SC of the breast and MASC of salivary glands differ in their clinical behavior. Breast SCs have a rather indolent clinical course, with a propensity to local recurrence and prolonged survival. In contrast, salivary MASCs constitute a spectrum of clinical behaviour from indolent tumours to those with a rapid clinical course characterized by metastases and cancer-related death. Supported by: Grant no. 9725 of IGA MH CR (Internal Grant Agency of Health Ministry, Czech Republic).

002

The spectrum of salivary gland-type tumours of the breast

*F. Tavassoli**
*USA

003

Update on myoepithelial lesions of salivary glands

*R. Simpson**
* Royal Devon and Exeter Hospital, Exeter, United Kingdom

Myoepithelial cells are a normal constituent of the salivary acini and smaller ducts and are found between the epithelial cells and

the basement membrane. They can be recognised with various immunohistochemical markers, although none is specific or reliable in every case. S-100, alpha smooth muscle actin (αSMA), calponin, smooth muscle myosin heavy chain (SMMHC), cytokeratins 14, and p63 are the most useful in practice. Neoplastic myoepithelial cells in both benign and malignant tumours can take several forms, including epithelioid, spindle, plasmacytoid, clear and oncocytic, and this variability largely accounts for difficulties in histopathological diagnosis. Benign salivary adenomas form a spectrum with differing proportions of luminal, basal and myoepithelial cells and stroma. Whilst clinically similar, benign myoepithelioma differs from basal cell adenoma and pleomorphic adenoma only by being composed almost exclusively of myoepithelial cells, but the very different morphology justifies the separation of the entity in diagnostic practice. Benign myoepithelioma exhibits a considerable range of microscopic features, both of architecture and cytology, but nevertheless, there are several typical appearances, all reflecting the different forms that non-neoplastic myoepithelial cells can take. Solid, myxoid and reticular growth patterns may be seen, and the component cells may be epithelioid, spindle-shaped, plasmacytoid (hyaline), clear, or oncocytic. Many tumours show more than one growth pattern or cell type, but myoepitheliomas of the minor glands tend to be composed of plasmacytoid cells and those of the parotid, epithelioid or spindle cells. The clear cell variant is relatively rare. A minor degree of nuclear pleomorphism is allowable, but mitotic figures are generally scanty. The stroma is variable in amount and is usually hyaline, fibrous or myxoid, but occasionally, it may occasionally contain chondroid material or mature fat cells. Circumscription is sometimes incomplete, particularly in tumours of the minor salivary glands, but unlike their malignant counterpart, benign myoepitheliomas do not show destructive invasion. Myoepithelial carcinoma (malignant myoepithelioma) is a rare but probably under-recognised malignancy that may arise de novo or in a preexisting benign myoepithelioma or pleomorphic adenoma. There is an equal sex incidence and a wide age distribution. Most cases arise in the parotid, but any gland may be affected. It typically has a multinodular architecture. The range of cell types reflects that seen in benign myoepitheliomas and includes pure or mixed populations of epithelioid cells (the most frequent) often arranged in trabeculae or pseudo-acinar structures with cleft-like spaces, cells with clear cytoplasm (sometimes appearing signet ring-like), vacuolated (sometimes lipoblast like), hyaline (plasmacytoid) and spindle to stellate. The nuclei of malignant myoepitheliomas may be relatively uniform small- to intermediate-sized and composed of finely distributed chromatin, lacking obvious nucleoli, or there can be marked cytological atypia, with large nucleoli. Mitotic figures may be scanty to plentiful and include atypical forms. The tumour-related matrix is generally a prominent component and is hyalinized or myxoid. Metaplastic changes are frequent and include squamous areas, often with keratinisation. Other histological features include areas of necrosis seen in both high- and low-grade tumours, as well as perineural and vascular invasion. A tumour containing more than an occasional true luminal cell should not be diagnosed as a myoepithelial carcinoma. In one series, 40% of tumours were categorized as high-grade and 60% as low-grade. Almost all myoepithelial carcinomas express S-100 protein, vimentin and broad-spectrum cytokeratin antisera, either generally or in areas. Most show at least focal staining for more specific markers such as αSMA, calponin, SMMHC, cytokeratins 5/6 or14, and p63. The MIB1 (Ki-67) index is high, and in one series, a figure >10% was suggested as diagnostic of malignancy in a myoepithelial neoplasm. Myoepithelial carcinomas are locally aggressive, and about a third of patients develop metastases and die of disease. Myoepithelial cells are also found in greater or lesser numbers in a few other carcinomas and are an integral part especially in epithelial–myoepithelial carcinoma.

004

Myoepithelial tumours of the breast

*J. Reis-Filho**
*United Kingdom

005

Update on mucoepidermoid carcinoma

*I. Fonseca**
*Portugal

Mucoepidermoid carcinoma (MEC) is one of the most common subtypes of salivary gland malignant neoplasms that can also arise as a primary neoplasm at other organ sites including the bronchopulmonary tree, the gastrointestinal tract, the skin, the breast and scattered mucous/serous glands throughout the body. MEC is characterized by the presence, in variable proportions, of three cell types: epidermoid, mucin-producing and intermediate cells that can undergo clear and oncocytic change. Tumour histology remains the major criterion to establish the prognosis of affected patients, namely grade of differentiation. MEC composed by oncocytic and/or clear cells, as well as other variant features of the neoplasm, can raise difficult diagnostic questions with both benign and malignant epithelial neoplasms. MEC has a karyotypic profile, with recurrent rearrangements of chromosomal bands 11q21 and 19p13, that usually presents as a balanced t(11;19) translocation, frequently as the sole cytogenetic alteration. This chromosomal rearrangement creates a chimerical gene product that fuses the protein coding regions of CRTC1 exon1 in-frame with exons 2-5 of the MAML2 gene. More recently, another variant fusion

gene CRTC3–MAML2 was reported. CRTC1–MAML2 fusion is present in around 70% of MEC, but not in other salivary gland benign and malignant neoplasms. It has also been found in MEC at the skin, the breast and at the uterine cervix. Evidence points to accept CRTC1–MAML2 fusion as a prognostic indicator in MEC and allowing the segregation of a group with worse prognosis, including some grade II and most grade III fusion-negative tumours.

Thursday, 2 September 2010, 08.00–11.00, Aula Mała

WGS-20 Molecular diagnosis in pathology (part I)

Chairpersons: G. Bevilacqua, Italy
P. Liberski, Poland

001

Our changing view of the genome: implications for pathology

*P. Hall**
*Pathological Society, Journal of Pathology, London, United Kingdom

The decision to undertake the sequencing of the entire human genome stemmed from many sources, in particular Rrenato Dulbecco's 1986 seminal article in Science (1986; 231:1055–1056). Extraordinary technical advances were required to facilitate this, but few could have predicted the attendant conceptual revolutions. Since the publication in 2001 of the first draft of the human genome (and the parallel reports of the sequences of many other genomes), our view of the complexity of the organisation and regulation of genomes has increased. The EnCode project (Genome Res 2007;17:669–681) further highlighted the extraordinary diversity of transcription and demonstrated that the protein coding regions are but a fraction of the transcriptome. The importance of non-coding regions in genome regulation has become manifest, and the diversity of splicing events was previously unsuspected. The previous drip of new information has become a torrent, and 'next-generation' sequencing technologies promise to increase this driving cost of sequencing entire genomes to sub-$1,000 levels. The timescale of generating data similarly collapses to a mere fraction of that required even 2 years ago. The information load will be immense and new approaches will be needed to deal with the impact of this on clinical decision making. The consequences for these developments are perhaps unfathomable at present, but we are challenged to find ways to take advantage of these developments lest pathology be bypassed by other disciplines. Central to this will be educational programmes at the undergraduate and postgraduate level to 'future proof' tomorrows clinicians, including pathologists.

002

New approaches to molecular classification of lymphomas

*L. Leoncini**, *S. Lazzi, G. De Falco, C. Bellan, A. Onnis, V. Mourmouras*
*University of Siena, Italy

Background: The era of molecular diagnostics of lymphoid malignancies started with the cloning of the immunoglobulin and T cell antigen receptor genes. Southern blot analysis was applied in clinical laboratories to establish clonality of lymphoid proliferation. This was followed by the cloning of a number of translocation breakpoints in the more common lymphomas.
Method: The advent of polymerase chain reaction provided an alternative to Southern blot analysis as it is simpler and faster. In addition, the amount of clinical material required is much smaller, and it can be performed on archival paraffin-embedded materials.
Results: Gene expression (GE) analyses by use of microarrays (MAs) have become an important part of biomedical and clinical research. The resulting data may provide important information regarding pathogenesis and may be extrapolated for the diagnosis and prognosis of non-Hodgkin lymphoma (NHL)(19). This genomic technology has revealed that existing diagnostic categories of NHL comprised multiple molecular and clinically distinct diseases. In addition, gene expression profiling studies may lead to the identification of novel targets for the development of new therapeutic agents for NHL.
Conclusion: More recently, the discovery of a novel class of small non-coding RNAs, the microRNAs, has opened a new scenario in understanding the regulation of gene expression. MiRNAs control gene expression at the posttranscriptional level, and deregulation of their physiological function has been revealed to be crucial in cancer. MiRNA expression profile can be obtained by microarray and is even more informative than GEP as a few miRNA alterations can specifically identify a tumor (histo) type.

003

EGFR mutation analyses in NSCLC—experiences of a nationwide ring trial in Germany

*M. Dietel**
*Universitätsmedizin Charité, Berlin, Germany

Background: Since non-small cell lung carcinoma (NSCLC) is being predominantly diagnosed at advanced stage, the option of a curative therapy no longer exists in most instances. Roughly speaking, the first therapeutic standard measure to treat NSCLC consists of a platinum-based chemotherapy, reaching a response rate of 30–40%. Recently, new substances have been introduced to treat

NSCLC, i.e. erlotinib (Tarceva®) and gefitinib (Iressa®). Both inhibit the epidermal growth factor receptor (EGFR1).
Results: For the EGFR-inhibitors, it is possible to predict tumor response by EGFR mutation analyses. This is the reason why the EMEA has approved Iressa treatment only after such analysis, which has to be performed pre-therapeutically. The test has to be done by pathologists who (1) should reconfirm the diagnosis on an H&E slide; (2) he then should identify and mark the tumor area, (3) followed by manual microdissection to assure that at least 40% of the material is indeed NSCLC. (4) The selected tumor tissue then should be analyzed regarding mutations in exons 19 and 21 at a minimum; preferably, exons 18 and 20 should be included.
Conclusion: These analyses should be performed only in laboratories certified by a quality control organization, e.g. QuiP (Quality in Pathology, organized by the German Soc. of Pathology and the German Ass. of Pathology). By April 2010, there are 39 Institutes of Pathology in Germany which passed the QuiP ring trials on EGFR and performed approx. 3,000 tests. If an activating mutation was detected, the anti-EGFR tyrosine kinase inhibitor Iressa was recommended as a possible treatment.

004
An update of the ESP *k-ras* quality assurance program
*H. van Krieken**
*UMC St Radboud, Dept. of Pathology, Nijmegen, The Netherlands

Thursday, 2 September 2010, 14.30–16.30, Aula Duża B

WGS-21 Promoting excellence in immunohistochemistry
Chairpersons: D. Dabbs, USA
M. Vyberg, Denmark

001
Immunohistochemistry—the new challenges
*D. Dabbs**
*Magee-Womens Hospital of UPMC, Dept. of Pathology, Pittsburgh, USA

Objective: Immunohistochemistry (IHC) became a prominent means of diagnostic investigation in the early 1980s. IHC became fairly routine in surgical pathology and rapidly supplanted electron microscopy as a way of classifying tumors.
Method: Since the 1980s, the major focus for the use of IHC has been as a diagnostic tool, chiefly for the classification of tumors as carcinoma, melanoma, lymphoma, germ cell tumor, mesothelioma, or sarcoma. The explosion of molecular diagnostics, along with clinician demands, has channeled our focus on the current state of IHC in pathology.
Results: Molecular tests and gene expression profiles that purport to predict patient outcomes and drive therapeutic decisions are currently favored by oncologists. However, IHC is the only laboratory venue that supplies molecular morphology that may be directly visualized and interpreted. In addition to diagnostic IHC, theranostic and genomic applications are also now in the menu of the pathologist.
Conclusion: Pathologists must be able to emphasize the molecular morphology of IHC and how it can supply theranostic and genomic information in addition to diagnostic applications. Our IHC challenges include standardization of the total test and the ability to quantitate results for patient care.

002
Most common laboratory pitfalls in IHC
*S. Nielsen**
*Aalborg Hospital, Dept. of Pathology, Denmark

Most common laboratory pitfalls in IHC immunohistochemistry (IHC) is a well-established technique and used daily in virtually all departments of surgical pathology as a diagnostic, predictive and prognostic tool. However, IHC is an assay influenced by multiple parameters and the final result is highly dependent on the choice and performance of these variables. In the protocol setup for IHC, both the pre-analytical, analytical and post-analytical parameters will affect IHC staining, and it is of utmost importance to be familiar with these technical aspects in order to use IHC as a diagnostic tool. In the pre-analytical phase, fixation still is the key element for a reliable result, and it is essential that fixation is standardized with respect to the choice of fixative, time to and time in fixative in order to get consistent results and to avoid false negative or false positive reactions. The implementation of new tissue processing techniques based on, e.g. modified reagents, can also affect the staining result. Regarding the analytical phase, the three key elements are: (1) appropriate epitope retrieval, (2) a sensitive and specific primary antibody, and (3) a robust detection system. In external quality programs for IHC, it has been shown that most errors in IHC are related to epitope retrieval and/or the primary antibody. To validate the performance and consistency of IHC, it is necessary to use internal and external controls. Especially the use of multi-tissue blocks containing tissues with different levels of the antigen is superior to single control blocks.

003
Most common interpretation pitfalls in IHC
*J. Klos**
*Norway

Background: The real frequency of interpretation pitfalls in immunohistochemistry is difficult to assess and may vary greatly between laboratories and pathologists. The risk of misinterpretation increases with the greater use of immunostaining as an integral part of theranostic workup, the increasing number and varying quality of available antibodies, as well as the rapidly expanding body of information regarding the complexity of IHC profiles of tumours. Growing clinical expectations for pathological evaluation are an additional challenge.
Method: The presentation will address the most important elements regarding the correct interpretation of immunostaining using AAASPIN as a simple algorithm for safer approach.
Results: A—Adequate antibody panel: Selection of antibodies is often a consequence of considered differentials, but results of immunostaining may also influence the choice of antibodies in subsequent analyses. A—Antibody clone: The spectrum of reactivity and cross-reactivity should be known. A—Aberrant antigen expression/absence may be a challenge. S—Structures: The immunoreactivity has to be present on relevant structures/cells. P—Pattern: The appropriate staining pattern has to be present. I—Intensity of staining may depend on the amount of antigen and not only technical issues. N—Number of stained cells/structures. The results of immunostaining round cutoff values in oligobiopsies should be carefully interpreted since the distribution of antigen in tumour tissue may vary. The interpretation of immunostaining must always include the proper context of both morphological and clinical data.

004
Immunoquantitation
*J. Baak**
*Norway

005
Quality assurance in immunohistochemistry
*M. Vyberg**
*Aalborg Hospital, Institute of Pathology, Denmark

Background: Optimization of immunohistochemical (IHC) staining reactions to a common standard is vital for reliable and comparable results in diagnostic pathology. Yet, staining quality varies greatly between laboratories compromising diagnostic reliability. In an external quality assessment (EQA) system, staining results from many laboratories can be compared, allowing the identification of less successful antibodies (Abs) and insufficient protocols.
Method: The Nordic Immunohistochemical Quality Control (NordiQC) scheme, established 2003, comprises a general module with three annual runs catering 15–18 IHC markers and a breast cancer module with two annual runs catering hormone receptors and HER-2. Tests for 80 markers have been carried out up to nine times. General results are published on www.nordiqc.org, recommended protocols made available, and the producers encouraged to prune poor products. Individual results are e-mailed to the laboratories, which in the case of insufficient marks are given tailored advice to improve their performance.
Results: About 270 laboratories have attended the EQA scheme and >25,000 IHC stains assessed. The overall scores have been evenly distributed between optimal (36%), good (33%) and insufficient (borderline or poor, 31%). The causes of insufficient stains could be identified in more than 90% of the cases and largely ascribed to: less successful primary Abs; improper calibration of primary Ab concentration; and insufficient, inappropriate or missing epitope retrieval. Laboratories complying with the NordiQC recommendations improve in a following test for the same marker in about 70%.
Conclusion: There is still room for improvement in laboratory proficiency. EQA may be a useful tool in promoting excellence in IHC.

Thursday, 2 September 2010, 14.30–16.30, Aula Średnia A

WGS-22 Cytology for targeted therapy
Chairpersons: F. Schmitt, Portugal
W. Olszewski, Poland

001
Lung
*W. Olszewski**
*Oncology Center Warsaw, Poland

002
Accuracy of cytology in the diagnosis of lung cancer: a cyto-histologic correlation
A. Repse Fokter, I. Kern*
*Celje General Hospital, Dept. of Pathology and Cytology, Slovenia

Objective: The examination of cytological and histological specimens plays an important role in the diagnosis, therapy and prognosis of lung tumours. The purpose of this study was to evaluate the correlation between cytology results

and corresponding histologic diagnoses in tissue biopsies obtained from bronchoscopy.
Method: We studied the cytologic diagnoses, comparing them with histology reports in 241 consecutive patients who underwent fibre-optic bronchoscopy in the period between September 1, 2008 and September 1, 2009.
Results: First we compared cytologic and histologic diagnoses according to the presence/absence of malignancy. Agreement was found in 230 out of 241 cases (95.4%), with a kappa coefficient of 0.91. There were 118 patients with negative cytology, 18 cases were suspicious, and 98 were positive for malignancy. In seven cases, the samples were unsatisfactory. Histological diagnoses were as follows: 102 negative, 7 suspicious, 112 positive and 20 unsatisfactory. We achieved excellent agreement for small cell carcinoma (22/23) and non-small cell carcinoma (69/84), while agreement in subtyping of non-small cell carcinoma was not so high.
Conclusion: Cytology is of considerable diagnostic value in pulmonary pathology, although not as specific as histology in the subtyping of carcinomas.

003
Incorporation of molecular diagnostics into clinical oncology Russian experience
*E. N. Imyanitov**
*Petrov Institute of Oncology, St. Petersburg, Russia

Application of molecular tests in routine medicine is particularly challenging due to the high costs as well as problems in communication between clinical and laboratory specialists. Our activities were aimed to incorporate the most meaningful tests into practical oncology, with all necessary adjustments to economical and health care realities in the Russian Federation: (1) A number of the most clinically relevant molecular diagnostic tests have been selected based on the literature data. (2) Cost-efficient modifications of these tests have been developed. (3) Validation of these tests has been performed in selected series of subjects. (4) Practical achievements of molecular medicine have been presented in a number of national oncological conferences and schools. (5) Translational research issues have been incorporated in the courses for medical students as well as in the advanced training of certified oncologists. (6) A series of lectures have been published in various national journals, including freely available Internet-based “practical oncology”. The panel consisting of seven non-expensive PCR tests has been developed for the diagnostics of breast–ovarian hereditary cancer syndromes. Due to a surprisingly strong founder effect in Russia, this panel was shown to have a nearly perfect sensitivity for the detection of BRCA carriers. The use of this panel allows identifying a hereditary cancer mutation in approximately 5% of non-selected breast cancer cases, 15–20% of high-risk (familial and/or early-onset and/or bilateral) breast cancer patients, and 15% of non-selected ovarian cancer cases. By now, almost 300 mutation-positive index patients have been identified, and their family members have been invited for genetic counseling and subsequent medical interventions. Another noticeable achievement includes the routine application of a simple mutation test, which allows selecting the responding patients for the treatment by EGFR tyrosine kinase inhibitors. This test does not require sequencing and is based on the combination of electrophoretic measurement of the length of amplified fragment and allele-specific PCR. This approach has already been applied to over 300 lung adenocarcinoma patients; as expected, nearly all mutation-positive subjects demonstrated an outstanding response to gefitinib. Detection of EGFR mutations has allowed optimizing the administration of expensive targeted compounds that eventually improved the accessibility of the latter to potential responders. We conclude that some of molecular tests can be introduced into clinical oncology with only limited spending of resources. Good cost/benefit ratio and activities in the dissemination of translational research knowledge are ultimate prerequisites for the acceptance of molecular diagnostics by medical oncologists.

004
Breast
*P. Vielh**
*France

005
Lymph nodes
*P. Zeppa**
*Italy

Thursday, 2 September 2010, 14.30–16.30,
Sala Wystawowa A

WGS-23 Joint meeting of Nephropathology WG and Polish Society of Transplantology
Chairpersons: M. Mengel, Canada
J. Kowalewska, Poland

001

Donor specific antibodies, C4d in renal biopsies and rejection

*H. Regele**
*Austria

According to the Banff Classification, antibody-mediated renal allograft rejection (ABMR) is defined by circulating donor-specific antibodies (DSA), C4d deposition in peritubular capillaries (PTC), and histologically detectable graft injury. These diagnostic criteria had primarily been developed and validated in biopsies from patients with early post-transplant dysfunction. Results from studies in patients without clinically detectable graft dysfunction, however, cast doubt on the universal applicability of these criteria. In my talk, I will address the following issues: (1) C4d deposits but no ABMR? Findings in protocol biopsies from patients with stable renal function indicate that C4d deposition is not necessarily always associated with renal dysfunction. The low predictive value of C4d in these patients might be due to the accommodation of grafts and highlights the fact that the diagnostic impact of C4d strongly depends on the clinical context. (2) ABMR but no C4d? Complement activation likely is not only of diagnostic importance but also part of the pathogenesis of ABMR. Results from gene expression profiling studies in human graft biopsies and from animal models, however, suggest that there also might be complement-independent mechanism of ABMR. Especially the lesions of chronic rejection might at least in part result from antibody-mediated complement-independent endothelial injury. (3) Are "atypical" staining patterns of diagnostic relevance? C4d can, in addition to the diagnostically relevant linear deposition in PTC, also be found in other locations and different staining patterns. It, however, appears that these other/additional staining patterns are of limited diagnostic value, at least for the detection of AMBR.

002

CIN toxicity: is it still a problem?

*M. J. Mihatsch**
*Universitätsspital Basel, Institute of Pathology, Switzerland

CNI toxicity (CNI-tox.) manifests itself in the tubuli as well as in the vessels, here practically exclusively in the arterioles. The epithelium of the proximal tubules mainly reveals isometric vacuolisation. Of much greater significance are the changes in the arterioles; these manifest either as TMA or much more frequently as so-called CNI arteriolopathy (CNI-Art.). CNI-Art. can be considered as a "form fruste" of TMA. The consequences of CNI-Art. can be: CNI glomerulopathy often in the form of FSGS, glomerular obsolescence, or interstitial fibrosis (striped form) with tubular atrophy. Tubular CNI-tox. is rapidly and completely reversible; CNI-Art. only early on. The severity of CNI-Art. increases with duration of therapy: mild > 270 days, moderately severe > 560 days and severe > 1,480 days. Twenty-five percent of cases of CNI-Art. are accompanied by glomerulopathy. With the increasing severity of CNI-Art. is a progressive increase in interstitial fibrosis, obsolescent glomeruli and FSGS. These changes are accompanied by a slow and irreversible rise in serum creatinine. CNI-Art./glomerulopathy was seen in 37 (5%) of biopsies between 1980 and 1989 and in 38 (7%) in 1990–1999. Between 2000 and 2004, a dramatic fall in CNI-Art./glomerulopathy cases to 19 (2%) was seen. A comparison between indication and protocol biopsies revealed CNI-Art. frequencies of 35% and 13%, respectively. In conclusion, in the last 25 years, the frequency of CNI arteriolopathy has fallen, but still occurs. A strict low-dose therapy helps avoid CNI toxicity and associated irreversible renal injury.

003

Patient selection, protocol biopsies and early steroid withdrawal

*J. Steiger**
*Universitätsspital Basel, Transplantationsimmunologie & Nephrologie, Switzerland

004

Is a protocol biopsy still helpful in patients with today's immunosuppression?

*D. Seron**
*Spain

005

Molecular transplant pathology

*M. Mengel**
*Canada

Background: Histopathology of allograft biopsies is standard for the surveillance of organ transplants. However, criteria for assessing histological lesions were empirically developed, and translating lesions into diagnosis represents arbitrary consensus. The advent of robust molecular techniques offers the opportunity for an objective measurement of the biological processes operating in the tissue.

Method: We did Affymetrix microarrays in 403 biopsies for cause, 107 six-week protocol biopsies from kidney allografts, and 105 endomyocardial allograft biopsies. The microarray results were summarized as pathogenesis-based transcript sets (PBTs). PBTs represent discrete biological events in organ transplants, e.g. infiltration by T cells. PBTs were developed in experimental models, thus representing a simple measurement of molecular changes in human tissue. The aims of our studies were to (1) define the molecular phenotype in allograft biopsies; (2) correlate the molecular phenotype with histological lesions and diagnoses; and (3) relate the molecular phenotype to clinical variables.
Results: We found a stereotyped molecular phenotype in all allograft biopsies: Increased expression of inflammation transcripts strongly correlated with the increased expression of injury transcripts and decreased expression of transcripts associated with normal parenchyma cell function. This robust molecular phenotype was associated with histological lesions of tissue inflammation, but not with current consensus for diagnosing rejection. An abnormal molecular phenotype was associated with allograft dysfunction and predictive of allograft loss.
Conclusion: The current diagnostic systems for diagnosing rejection frequently do not reflect the molecular phenotype. The assessment of the molecular phenotype in allograft biopsy can guide improvements of current diagnostics in transplant pathology.

Thursday, 2 September 2010, 14.30–16.30,
Sala Wystawowa B

WGS-24 Update in perinatal pathology

Chairpersons: P. Borralho Nunes, Portugal
E. Izycka-Swieszewska, Poland

001
Placental inflammation

*I. Scheimberg**
*Royal London Hospital, Dept. of Cellular Pathology, United Kingdom

002
Placenta and hypoxia

*J. Stanek**
*Cincinnati Children's Hospital, Dept. of Pathology, USA

There is no universally accepted system of classification of placental hypoxic lesions. Of 5,445 consecutive placentas from ≥20 weeks' pregnancies signed by the author, 2,564 placentas did not show hypoxic features (control group, GG), while 2,881 placentas showed hypoxic features (study group, SG). Five hundred seventy-four placentas showed fetal hypoxia (deep meconium penetration, erythroblasts in fetal blood), and 2,704 placentas showed placental hypoxic lesions, while 43 placentas showed both fetal and placental hypoxic lesions. Acute placental hypoxic lesions included villous infarctions (579), intravillous hemorrhage (64), and laminar membrane necrosis (736). Chronic placental hypoxic lesions included: global placental hypoxia (pre-uterine 295, uterine 238, and post-uterine 163), massive perivillous fibrin deposition (386), chorangiosis (738), microscopic chorionic pseudocysts of membranes and/or chorionic disc (516), decidual clusters of multinucleate trophoblastic giant cells (398), and excessive amount of extravillous trophoblasts (198). Three hundred ninety-seven placentas showed both acute and chronic hypoxic lesions. The SG featured more cases than the CG of preeclampsia (432 vs. 98), maternal diabetes mellitus (184 vs. 98), abnormal cardiotocography (533 vs. 343), intrauterine growth restriction (358 vs. 185), and cesarean sections (1,159 vs. 811), and less premature deliveries (1,616 vs. 1,659), congenital anomalies (178 vs. 200), and chorioamnionitis (875 vs. 1,109), respectively. In conclusion, hypoxic patterns of placental injury correlate with major types of high-risk pregnancy, fetal distress, intrauterine growth restriction, and cesarean deliveries. Non-hypoxic placentas are associated with congenital fetal anomalies and in utero infection.

003
Neuropathology of congenital infections

*C. Fallet-Bianco**
*Lagny-sur-Marne, France

During gestation, several microorganisms can infect the foetus and damage the developing nervous system, leading to severe neurodevelopmental sequelae. The acronym TORCH was introduced to refer to these organisms including toxoplasmosis, other microorganisms, rubella, cytomegalovirus and herpes simplex virus. TORCH infections share similar clinical features: The maternal infection is regularly asymptomatic, the clinical presentation of infected fetuses and neonates is quite identical, and, sometimes, a clinically silent infection in the neonatal period will be responsible for permanent neurological deficits occurring later in infancy. Extensive immunization programs, in developed countries, have led to an impressive decrease of congenital rubella syndrome, and the development of strategies of prenatal diagnosis and antimicrobial therapies has improved the management of congenital infections. Despite these significant advances, TORCH infections remain a worrying cause of vision loss, hearing loss, and

neurological disabilities in both developed and developing countries, and new syndromes have emerged such as congenital infections due to human immunodeficiency virus (HIV) and the human parvovirus B19. In addition, in the two last decades, growing evidence has supported the hypothesis of a significant association between choriamnionitis and cerebral palsy: brain lesions would result from a production of cytokines through a mechanism of toxicity. A wealth of literature has summarized current knowledge concerning epidemiology, microbiology, diagnosis and the management of congenital infections. In this presentation, we will focus on the neuropathological features of the most frequent intrauterine infections and underscore the invaluable contribution of neuropathological studies in understanding the pathogenesis of developing brain lesions.

004

Development and functions of the dura mater

*W. Squier**
*United Kingdom

The dura is more than just a fibrous covering for the brain; it has other functions, including control of venous outflow and uptake of CSF. Dural development is not complete at birth; it undergoes considerable remodelling in early life. The meninges develop from primitive mesenchyme derived from the neural crest. The dura has two leaflets, the outer periosteal and the inner meningeal which forms the falx and tentorium. Between them are the venous sinuses, which drain the entire venous outflow of the brain. Bridging veins are few and carry high blood flow. A muscular sphincter at their junction with the dura regulates blood flow when intracranial pressure increases. A venous plexus, most extensive at birth, is found in the posterior falx, tentorium and the parasagittal regions. Arachnoid granulations develop at 7 months of postnatal life. Originally thought to be responsible for drainage of CSF, they more likely monitor CSF homeostasis and pressure. Fluid channels in the dura may represent a system for the uptake of CSF. In early life, blood may reflux into these channels from the venous sinuses, causing intradural bleeding which is common in immature infants. Dural bleeding causes symptoms such as seizures and vomiting difficulties and is associated with age-related imaging changes in the underlying brain parenchyma. We do not yet understand the pathophysiology of these observations.

Thursday, 2 September 2010, 14.30–16.30, Aula Mała

WGS-25 Neuropathology

Chairpersons: B. Lach, Canada
B. Sikorska, Poland

001

Neuropathology of mitochondrial disorders

*B. Lach**
*Canada

Mitochondrial encephalomyopathies (ME) represent a heterogeneous group of diseases, secondary to respiratory chain dysfunction, impaired ATP production and energy crisis in the affected cells. ME could be associated with defective nuclear (nDNA) or mitochondrial (mDNA) genome, resulting in autosomal or maternal inheritance, respectively. Although multiple organ involvement is very common, the most affected are tissues with high oxidative metabolism such as CNS, myocardium and striated muscle. Myoclonus epilepsy with ragged red fibres (MERRF), mitochondrial encephalopathy with lactic acidosis and stroke-like episodes (MELAS), Leber's hereditary optic atrophy (LHOA), Kearns–Sayre syndrome and Leigh's disease represent the classical examples of ME. Precise phenotype/genotype correlations are very difficult due to the presence of overlap syndromes and atypical cases. The topography of lesions in the CNS determines symptomatology and varies in these conditions. Morphologically, ME are characterized by variably expressed mitochondrial abnormalities such as intra-mitochondrial crystalloid inclusions and ragged red fibres (RRF) in muscle biopsies, as well as selective neuronal loss in different CNS structures, laminar cortical necroses, microinfarctions and spongy degeneration in the grey or white matter. However, the common and diagnostically useful feature is the presence of COX-negative fibres, abnormal ultrastructure of muscle mitochondria and variably expressed vascular abnormalities. Although clinicopathological correlations are often problematic, the involvement of small caliber vessels may explain many focal CNS manifestations, while multisystem disease is very likely secondary to mitochondrial dysfunction in the neuronal component.

002

Kuru—50 years later

P. Liberski, P. P. Liberski*
*Medical University of Lodz, Dept. of Mol. Pathol. Neuropathol., Poland

Objective: Kuru, the first neurodegenerative human disease caused by infectious amyloids, was first reported to the Western medicine in 1957 by Gajdusek and Zigas.
Method: None.
Results: Kuru in the fore language means to shiver or to shake from fever and cold. Ritualistic endocannibalism

(eating of the relatives as a part of a mourning ritual, but not as an alimentary habit) was practiced not only in the kuru area but in many surrounding Eastern Highland groups which never developed kuru. The most striking neuropathologic feature of kuru was the presence of numerous amyloid plaques.

Conclusion: We may also speculate what would happen if kuru had not been discovered or did not exist. The infectious nature of Creutzfeldt–Jakob disease would probably not have been suspected until the beginning of the variant Creutzfeldt–Jakob disease (vCJD) outbreak in the UK. Creutzfeldt–Jakob disease and Gerstmann–Sträussler–Scheinker disease would have remained for decades as obscure neurodegenerations of merely academic interest. The familial forms of Creutzfeldt–Jakob disease would not have benefited from PRNP gene analysis, but only later would have been studied by linkage analysis and reverse genetics probably. The whole field would have probably remained of only arcane interest to veterinarians until the BSE epidemic began to exert its devastating effect. The discovery of vCJD would have been delayed as no surveillance would have been initiated for Creutzfeldt–Jakob disease. And, perhaps most importantly, the sea change in mentality that has led to the conception of 'protein misfolding diseases', including not only the neurodegenerative but also an increasing number of non-neurological disorders, would have been delayed by decades.

003

Cell autocannibalism in central nervous system. The role of autophagy in neurodegeneration and nervous system tumours

*B. Sikorska**
*Poland

Background: Autophagy is a process by which subcellular constituents and organelles are targeted for degradation in lysosomes. In macroautophagy, proteins and organelles are sequestrated into a double membrane-bound vacuole called autophagosome, formed by the ER membranes, under the direction of various proteins including MAP-LC3 (a microtubule-associated protein, light chain 3). In addition to maintaining cellular homeostasis, autophagy may also contribute to cell damage. Recently, autophagy was reported to be involved in many pathological processes including neurodegeneration, inflammatory processes and cancer. The role of autophagy in neurodegeneration is not only in removing protein aggregates but also in inducing the neuronal death.

Method: Autophagy in human neurodegenerative diseases and tumours of the CNS was studied using electron microscopy, immunohistochemistry and confocal laser microscopy.

Results: The presence of autophagy in prion diseases and other neurodegenerative disorders was shown. The extent of autophagy in tumours varied depending on histological type and malignancy.

Conclusion: Although the role of autophagy in neurodegenerative diseases remains unknown, at least three hypotheses must be taken into consideration: (1) removing protein aggregates, (2) one of the ways of neuron death, and (3) formation of spongiform change in prion diseases. The role of autophagy in cancer seems to be dual: On one hand, there is a growing body of evidence supporting the idea that autophagy may represent a tumor suppressor mechanism by reducing intratumoral necrosis, restricting oxidative stress and limiting chromosomal instability; on the other hand, autophagy may be an important process used by tumor cells to escape various types of stress and even therapeutic agents.

004

Advances in biology of gliomas

*W. Biernat**
*Medical University of Gdansk, Dept. of Pathology, Poland

Objective: Gliomas are the most common neoplasms of the central nervous system. The treatment of gliomas has been slowly changing for a few decades, and understanding of the glioma biology makes an important basic for the introduction of new treatment modalities.

Method: The most unfavorable prognosis concerns the group of diffuse gliomas which, due to the infiltrative growth, cannot be cured by surgery. The most common type of diffuse glioma is glioblastoma; this tumor may develop de novo (without preceding lower grade precursor lesion) or as a consequence of progression of malignancy.

Results: The molecular pathways most commonly seen in primary and secondary glioblastomas have been described, but recently, a new marker, isocitrate dehydrogenase 1 (IDH1), was defined as mutated early in the development of low-grade gliomas. The gene encoding this protein is located on chromosome 2q33. IDH1 catalyzes oxidative carboxylation of isocitrate to alpha-ketoglutarate. Nicotinamide adenine dinucleotide phosphate (NADPH) is the result of this reaction. IDH1 is somatically mutated in low-grade gliomas and glioblastomas. On the other hand, alterations of the ERK/MAPK intracellular pathway occur in circumscribed gliomas, e.g. pilocytic astrocytoma.

Conclusion: All these informations suggest that differential utility of these markersand will be presented.

005

Toward "fingerprinting" of brain tumours based on the synchrotron radiation X-ray fluorescence, Fourier transform infrared microspectroscopy (FTIRM) and discriminant analysis

D. Adamek, M. Szczerbowska-Boruchowska, M. Lankosz*
*Medical College Krakow, Dept. of Neuropathology, Poland

Objective: The neuropathologic diagnosis of brain tumours remains burdened by their well-known heterogeneity and difficulty to eliminate subjectivity in diagnosing.
Method: Synchrotron radiation-based techniques were applied to biochemical micro-imaging of brain tumours of different types and various grades of malignancy. The specimens were cryosectioned, mounted on appropriate sample supports and freeze-dried. Synchrotron radiation X-ray fluorescence was used for elemental analysis of samples. The level and distribution of P, S, Cl, K, Ca, Fe, Cu, Zn, Br and Rb was determined. The biomolecular composition of neoplastic tissues was determined by Fourier transform infrared microspectroscopy (FTIRM). The composition of the tissues was used to construct a diagnostic classifier for brain tumours using discriminant analysis (DA).
Results: It was found that Cu, S, Cl, K, and Zn are the elements of the highest importance for the discrimination of tumor grade, as well as the tumor type. Elemental analysis allowed 99% accordance with histological type and grade of tumor. The DA applied to infrared absorption spectra indicated that lipids, amide I and amide II, as well as phosphate group are of the highest importance for the discrimination of tumor type and tumor grade. The model obtained allowed differentiation between all investigated tumours and control samples as well as correct group classification in 88%.
Conclusion: It is difficult to speculate on the meaning of our findings with the biochemical perspective; however, the DA based on elemental and biomolecular composition of tissue may be a potentially valuable method assisting the recognition and maybe grading of brain tumours.

Thursday, 2 September 2010, 18.00–19.30, Aula Duża B

WGS-26 Advances in pathology of the endometrium

Chairpersons: F. Nogales, Spain
J. Kupryjanczyk, Poland

001

The endometrium in the perimenopause

*F. Nogales**
*Universidad de Granada, Dept. of Pathology, Spain

002

Endometrial iatrogenic changes

*H. Hollema**
*UMC Groningen, Dept. of Pathology, The Netherlands

003

Current controversies in endometrial carcinoma

*M. Wells**
*Univ. of Sheffield Medical School, West Riding Yorkshire, United Kingdom

Thursday, 2 September 2010, 18.00–19.30, Aula Średnia A

WGS-27 Ongoing European Project on serrated polyps. Digestive diseases WG business meeting

Chairpersons: D. Tiniakos, Greece
A. Ensari, Turkey

001

European serrated polyp project: an initiative of the ESP working group of digestive diseases

A. Ensari, B. Bilezikci, F. Carneiro, G. B. Dogusoy, A. Dursun, J. F. Flejou, K. Geboes, G. De Hertogh, C. Langner, A. Jouret-Mourin, I. Nagtegaal, J. Offerhaus, J. Orlowska, A. Ristimaki, J. Sanz, B. Savas, M. Sotiropoulou, M. Tuncyürek, V. Villanaci, N. Kursun*
*Ankara University Medical School, Dept. of Pathology, Turkey

Objective: The family of serrated polyps comprises sessile serrated adenomas/polyps (SSA/Ps), traditional serrated adenomas (TSAs), hyperplastic polyps (HPs), and mixed hyperplastic/adenomatous polyps (MPs). The lack of consensus about the definition, nomenclature, and biology of these lesions creates considerable confusion among pathologists. The aim of this study was to reach a consensus on the definition and histopathological criteria of serrated polyps on a European scale.
Method: H&E slides of 15 cases of serrated polyps were circulated among the participating pathologists across Europe in the first round. A round table discussion was made on the preliminary results in order to reach a consensus on the diagnostic criteria. In the second round, H&E slides of 55 additional cases were examined by the same group of pathologists. The participants were asked to fill in a worksheet for each case for the presence of the listed criteria together with the final diagnosis after each round. Data were evaluated for interobserver agreement using kappa statistics.

Results: Paired kappa values for the first round ranged 0.09–1.00, 0.00–0.73, 0.07–1.00 and 0.63–1.00 for HP, SSA/P, TSA, and MP, respectively. In the second round, the range of paired kappa values was 0.17–1.00, 0.04–0.96, 0.05–1.00, and 0.06–1.00 for HP, SSA/P, TSA and MP, respectively.
Conclusion: This initiative offers a better interpretation of the diagnostic criteria of serrated polyps and helps improve interobserver agreement across Europe.

Thursday, 2 September 2010, 18.00–19.30, Aula Średnia B

WGS-28 Diagnostic pathology of thyroid cancer: old and new entities

Chairpersons: M. Sobrinho-Simoes, Portugal
D. Lange, Poland

001

Cytology (FNAB) and frozen sections: when do you use them? What is their usefulness?

*G. Tallini**
*University School of Medicine, Ospedale Bellaria, Bologna, Italy

Cytology and frozen section evaluation are traditional parts of the management of thyroid lesions. Their role and usefulness are dictated by some basic facts about thyroid nodules: (1) Nodules are very common; (2) they are benign in the majority of cases; and (3) the diagnosis of malignancy is based on cytologic features (papillary carcinoma) or on the presence of invasion of the tumor capsule or of blood vessels (follicular carcinoma). The common occurrence of benign thyroid nodules mandates an effective method for preoperative screening. The diagnosis of papillary thyroid carcinoma, by far the most common thyroid malignancy, is based on the identification of specific cytologic features. Therefore, fine needle aspiration biopsy (FNAB) has easily emerged in the past 30 years as the most accurate and cost-effective tool, indeed a true cornerstone, for the preoperative management of thyroid nodules. Standardized terminology to report diagnoses is highly recommended and is being implemented worldwide. The type of genetic alterations in thyroid cancer and the very nature of FNAB samples make them ideally suited for molecular analysis. On the other end, the importance of intraoperative frozen section diagnosis has been constantly decreasing over the years as a direct consequence of the widespread application of FNAB. It is now usually performed with cases that are suspicious after FNAB and may be useful in some cases with indeterminate cytologic diagnosis.

002

How to separate follicular adenoma from follicular carcinoma and follicular variant PTC?

*M. Sobrinho-Simoes**
*Portugal

Background: The differential diagnosis between FA, FC and FVPTC is, at present, the most frequent reason for any consultancy practice on thyroid tumours. We will review this differential diagnostic problem taking into consideration that it only concerns the encapsulated type of FVPTC. The poorly circumscribed/infiltrative types of FVPTC, as well as the multinodular/diffuse type, do not create any major diagnostic doubts and are easily diagnosed, putting together the pattern of growth and the nuclear features.
Method: If one sticks to the differential diagnosis of FA, FC and encapsulated type of FVPTC, the histopathological diagnostic hints are two: invasiveness (vascular invasion rather than pure capsular invasion) and presence of PTC—nuclear features.
Results: We will discuss what to do whenever such histopathologic findings are not clear-cut enough to support a definitive diagnosis. We will review, in this context, the diagnostic value of immunohistochemical markers of differentiation and/or proliferation and that of molecular markers in a retrospective study of 240 cases of well-differentiated carcinomas of the thyroid that have given rise to metastases and/or to local, clinically aggressive recurrences.
Conclusion: The results obtained in this study will be used to determine the best diagnostic options and to support the conclusion that most, if not all, follicular tumours and well-differentiated tumours of uncertain malignant potential, as well as minimally FC without vascular invasion and noninvasive encapsulated type of FVPTC, carry a good prognosis even when treated by lobectomy alone.

003

Angioinvasive well-differentiated carcinoma, widely invasive follicular carcinoma, solid variant of papillary carcinoma and poorly differentiated carcinoma: from diagnosis to prognosis

*M. Volante**
*University of Turin, Clinic and Biol. Sciences, Orbassano, Italy

Malignant thyroid tumors are generally divided into well-differentiated and undifferentiated (anaplastic) carcinomas, the former usually having a low malignant clinical behavior and good prognosis, and the latter being almost all very

aggressive and rapidly fatal. Diagnostic criteria rely on the recognition of cytological characteristics (i.e. nuclear alterations specific for papillary carcinoma), architectural patterns (i.e. papillary, follicular, solid, trabecular, insular or diffuse), high-grade features (i.e. increased mitotic index, necrosis) and invasive properties (i.e. vascular and/or capsular invasion). All of the aforementioned features are alternatively used as diagnostic hallmarks of specific histotypes, as peculiarities of specific variants, or as markers of aggressiveness, and their recognition is therefore essential to classify and stratify prognostically each individual tumor. The presence of vascular invasion is essential to recognize the malignant nature of a follicular tumor, but its extent is the major prognostic parameter in follicular carcinoma and draws a line between minimally invasive and widely invasive forms that are characterized by distinctive clinical outcomes. Necrosis and high mitotic index usually occur in aggressive cases of papillary thyroid carcinoma, but together with the presence of solid/insular/trabecular growth patterns represent the diagnostic features of poorly differentiated carcinoma, a specific tumor entity that shows a clinical behavior intermediate between well-differentiated and undifferentiated carcinomas. At variance, the presence of a solid growth pattern in an otherwise typical papillary carcinoma depicts its solid variant, which is more often encountered in children and radiation-exposed individuals but has a clinical behavior usually similar to its conventional counterpart.

004

Medullary carcinoma and familial non-medullary thyroid carcinoma: when do you suspect the thyroid tumor is familiar?

*P. Komminoth**
*Zürich, Switzerland

Most thyroid carcinomas occur sporadically, and only a minority of cases is associated with inheritable cancer syndromes. The majority of familial thyroid cancers (FTC) occur in younger patients, are identified in both lobes and exhibit multifocality. Some of the FTC exhibit a characteristic growth pattern which we should look for, describe and make an appropriate comment in our report. Histological hints for FTC, the most important associated tumor syndromes and the involved genes (if known) are outlined below: Familial adenomatous polyposis (FAP; APC gene on 5q21): bilateral multifocal tumors with fibrosis, cribriform, solid and spindle-cell areas lacking typical nuclear features of papillary thyroid carcinomas (PTC) called cribriform-morular variant of PTC. PTEN hamartoma syndrome (PTHS/Cowden syndrome; PTEN gene on 10q23.3): multiple adenomatous nodules with a rim of fibrous tissue occasionally associated with follicular carcinomas (FTC) or PTC and C-cell hyperplasia. Carney complex (PRKAR1A gene on 17q23-24 and unknown gene on 2p16): multiple adenomatous nodules, follicular adenomas occasionally combined with FTC and PTC. Familial PTC (FPTC, unknown gene on 19p13): multicentric PTC and adenomatous nodules with or without oxyphilia. Familial PTC with renal papillary neoplasm (unknown gene on 1q21): classical PTC and renal papillary neoplasms. Familial non-medullary thyroid carcinoma type 1 (fNMTC1; unknown gene on 2q21): classical PTC without any distinguishing pathologic features. Familial multinodular goiter syndrome (FMNG; unknown gene on 14q): goiter and occasional PTC. Familial medullary thyroid carcinoma (MTC; multiple endocrine neoplasia type 2A and 2B, familial MTC; RET gene on 10q11.2): bilateral, multifocal MTC associated with diffuse and nodular C-cell hyperplasia.

Thursday, 2 September 2010, 18.00–19.30,
Sala Wystawowa A

WGS-29 Joint meeting of nephropathology WG and Polish society of transplantology—discussion of unsolved cases presented by Polish pathologists and physicians

Chairpersons: M. J. Mihatsch, Switzerland
A. Perkowska-Ptasinska, Poland

Thursday, 2 September 2010, 18.00–19.30,
Sala Wystawowa B

WGS-30 Cytopathology WG business meeting

Chairperson: M. J. Mihatsch, Switzerland

Thursday, 2 September 2010, 18.00–19.30, Aula Mała

WGS-31 Molecular diagnosis in pathology (part II)

Chairpersons: G. Bevilacqua, Italy
P. C. W. Hogendoorn, The Netherlands

001

Molecular pathology of bone and soft tissue tumours

*P. C. W. Hogendoorn**
*The Netherlands

002

Molecular cytology in thyroid cancer

*I. Marchetti**

*Pisa University Hospital, Section of Cytopathology, Italy

Background: Thirty percent of thyroid nodule fine needle aspiration (FNA) diagnoses are indeterminate or suspicious for cancer. The prevalence of malignancy in FNA samples with these diagnoses varies from 10% to 52%. The analysis on cytological samples of the status of genes involved in thyroid carcinogenesis can represent an additional tool to improve the diagnostic accuracy. Our attention was focused on BRAF gene.

Method: DNA was extracted directly from cell scraped from stained smears of 140 patients with histological diagnosis of papillary thyroid carcinoma (PTC). The cytological diagnosis was of cystic nodule in one case, microfollicular proliferations without atypia in three cases, suspicious for papillary carcinoma (SPTC) in 54 (38%) cases and PTC in 83 (60%) cases. The BRAF V600E mutational status was determined by sequencing analysis in all patients.

Results: BRAF V600E mutation was detected in 61.1% (33/54) of cases with a cytological diagnosis of SPTC and in 75.9% (63/83) of cases with a diagnosis of PTC. Combining morphological with molecular analysis, the diagnosis of PTC rose to about 80% (111/140), with an increase of 20% in the sensitivity compared to cytology alone.

Conclusion: The morpho-molecular approach to preoperative analysis of PTC surely improves the diagnostic accuracy and possibly may have important implications in the management of these patients.

003

Clinical implications of ETS–family gene fusions in prostate cancer

*S. Perner**

*Germany

004

Brain tumours

*J. Haybaeck**

*Medical University of Graz, Institute of Pathology, Austria

As indicated by the World Health Organisation (WHO), histological grading is a way of predicting the biological behaviour of neoplasms. Especially in neuropathological settings, tumour grade is often the key factor determining therapeutic decisions. Clinical, radiological, macroscopic, histological and ultrastructural factors may already be summarized in a diagnosis that very well reflects the biology of the respective tumour entity, at least to a certain degree, but usually not in a personalized manner. This is exactly the stage where molecular biology comes into play. In recent years, much effort has been made on molecular characterization of brain tumours as there is an urgent need for specific and sensitive, highly reproducible tumour markers with a prognostic as well as predictive value. State of the art in modern neuropathology therefore ranges from basic immunohistochemical profiling, evaluation of genetic susceptibility, comparative genomic hybridization (CGH) approaches, fluorescence in situ hybridization (FISH), screening for genetic hallmark mutations, evaluation of mRNA expression of specific growth factor receptors, assessment of promoter methylation status and gene expression profiling to loss of heterozygosity (LOH) analyses. The challenge now for pathologists confronted with brain tumours is to integrate knowledge derived from the latest molecular biological methods into the established panel of pure morphology-based investigations.

Friday, 3 September 2010, 08.00–11.00, Aula Średnia A

WGS-32 Electron microscopy case studies in tumour pathology

Chairpersons: J. Lloreta-Trull, Spain
M. Santucci, Italy
W. Olszewski, Poland

001

Small renal tumour with widespread metastases: the birth of a new entity

*G. Herrera**

*USA

002

Unusual hepatic neoplasm. FNA in the diagnosis of hepatic masses and the role of electron microscopy

*E. Turbat-Herrera**

*USA

003

Plasmacytoid urothelial carcinoma of the bladder

*A. Franchi**

*Italy

Background: The plasmacytoid variant of urothelial carcinoma is characterised by the presence of single malignant cells having clear or eosinophilic cytoplasm and eccentrically placed, enlarged nuclei with small

nucleoli, which are often associated with areas of conventional high-grade transitional cell carcinoma. These tumours may be mistaken for myeloma or lymphoma both at primary and metastatic sites.
Method: A case of plasmacytoid urothelial carcinoma of the bladder occurring in a 53-year-old man was studied at the histological, histochemical, immunohistochemical and ultrastructural level.
Results: Histologically, the tumour presented a superficial component of conventional invasive high-grade urothelial carcinoma, while in the deeper component, the tumour was composed of dyscohesive oval to round cells with eccentrically located nucleus and abundant eosinophilic cytoplasm. Occasionally, neoplastic cells presented one or more cytoplasmic vacuoles, which contained PAS diastase and Alcian blue-positive material. Numerous atypical mitoses were identified and there was evidence of peritumour vascular invasion. Immunohistochemically, neoplastic cells were positive for cytokeratins (7, 20, AE1/AE3, 34betaE12) and focally positive for CD138. In addition, nuclear staining for GATA-3 was present. At electron microscopic examination, neoplastic cells were embedded in collagenous matrix and showed an oval shape, with regular contour. The cytoplasm contained a moderate amount of organelles, including rough endoplasmic reticulum cysternae and mitochondria. Bundle of tonofilaments were frequently observed, while a few neoplastic elements presented intracellular lumina, lined by microvillous projections. Intercellular junctions were not observed.
Conclusion: In conclusion, electron microscopy indicates that neoplastic cells in this peculiar variant of urothelial carcinoma show aspects of squamous and glandular differentiation.

004
More than a decade of experience in pathomorphological evaluation of pituitary tumours

M. Maksymowicz, W. Olszewski*
*Poland

Background: Phenotype of pituitary tumors as determined by means of functional, radiological and surgical data, histology, immunohistochemistry and electron microscopy (EM) may be relevant for prognosis and appropriate postoperative management. In the WHO 2004 classification of pituitary adenomas, immunohistochemical evaluation represents the "gold diagnostic standard". However, immunohistochemical profiles may overlap, but ultrastructural features of these tumors are essential for subtyping adenomas with different prognosis and response to treating.
Method: Among 1,919 pituitary tumors diagnosed between 1998 and 2010 at the Department of Pathology of Cancer Center in Warsaw, there were 1,643 (85.6%) pituitary adenomas. All cases were studied by review of clinical features, histology, immunostaining (for GH, PRL, ACTH, TSH, FSH, LH, alpha subunit) and EM. The proliferative index was determined by MIB-1 labeling.
Results: Ultrastructural evaluation was useful in: GH secreting adenomas, sparsely vs. densely granulated; GH and PRL secreting adenomas; clinically nonfunctioning immunopositive (silent) adenomas; immunonegative (null cell) adenomas: nononcocytic vs. oncocytic; unusual plurihormonal: monomorphous vs. mixed cell adenomas and invasive macroadenomas with no endocrine symptoms. The proliferative index had variable, low values (0–3%).
Conclusion: Evaluation of subtype remains the most important determinant of adenoma behavior. Currently, there are no accepted means for predicting an adenoma's invasiveness and long-term aggressiveness, but morphologic separation of some subtypes of pituitary adenomas by EM provided useful knowledge for classification and management. Proliferative markers, as MIB-1, may be helpful in the diagnosis of invasive, low differentiated tumors, but we did not find a correlation between this factor and adenoma behavior.

005
EM in description of epithelioid trophoblastic tumor and beta-HCG producing

A. Marszalek, J. Bręborowicz*
*Dept. of Clinical Pathomorpholy, Bydgoszcz, Poland

006
Hyalin globules in paucicellular leiomyomas of the gastrointestinal tract are distinct from skeinoid fibers—ultrastructural evidence

J. Schroeder, P. H. Wuensch, F. Hofstaedter, A. Agaimy*
*Universitätsklinik Regensburg, Institute of Pathology, Germany

Objective: Skeinoid fibres are globular brightly eosinophilic PAS-positive extracellular collagen deposits seen commonly in gastrointestinal stromal tumours (GIST) of the small bowel. Ultrastructurally, they display similarity to "skeins of yearn", hence the name. However, hyaline globules are occasionally encountered in leiomyomatous GI neoplasms and may be mistaken for true skeinoid fibres leading, to an erroneous diagnosis of GIST.
Method: We analyzed 93 histologically and immunohistochemically well-characterized true smooth muscle neoplasms of the GI tract for the presence of hyaline globules and examined representative examples of them

from formalin-fixed and deparaffinized tissue by electron microscopy.

Results: PAS—positive intracellular and interstitial hyaline globules were detected in all benign paucicellular leiomyomas of the muscularis mucosae (n=72) and the muscularis propria (n=14) irrespective of tumour size and site, and rarely also in the adjacent muscularis propria, but in none of the leiomyosarcomas (n=7) and cellular leiomyoma (n=1). Similar to surrounding tumour cells, hyaline globules expressed desmin, alpha-SMA and h-caldesmon, but were negative for CD117 and CD34. The mostly ovoid-shaped structures displayed at ultrastructural examination variably oriented bundles of filaments with a diameter of approximately 6–8 nm. At the periphery of these inclusions, altered filamentous material was recognized in different stages of degeneration with variable condensed matrix and occasional peripheral condensation suggestive of calcification. True skeinoid fibres were not detected.

Conclusion: The above findings are consistent with a multistep degenerative phenomenon affecting individual smooth muscle cells in paucicellular GI leiomyomas. Awareness of this finding should prevent misinterpretation as GIST, particularly in small biopsies.

007
Pseudotumours of the kidney

*J. Lloreta-Trull**
*Hospital Del Mar, Dept. of Pathology, Barcelona, Spain

Several clinicopathologic entities are grouped under the concept of pseudotumour: All of them usually result in a mass effect, therefore mimicking a neoplastic process grossly and sometimes microscopically. In the kidney and the urinary tract, the diseases most often presenting as a pseudotumour are malakoplakia and xantogranulomatous pyelonephritis. In fact, both of them can be considered inflammatory pseudotumours, i.e. inflammatory processes producing a mass effect. A more restrictive use of the term inflammatory pseudotumour applies to a subset of lesions that was initially known as myofibroblastic inflammatory pseudotumour and is currently referred to as inflammatory myofibroblastic tumour. Ultrastructural examination reveals the pathogenesis of malakoplakia as a defect in the mechanisms of lysosomal extrusion from histiocytes. Thus, the profusion of secondary lysosomes constitutes an optimal milieu for the deposition of calcium salts in typical Michaelis–Gutmann bodies. On the other hand, the foamy histiocytes of xantogranulomatous pyelonephritis are characterised by a profusion of myelin bodies due to the predominant phospholipid composition of the lysosomes, resulting from chronic destruction of renal tissue and bacterial degradation. Inflammatory myofibroblastic tumour is a true neoplastic lesion with myofibroblastic differentiation and a prominent inflammatory background. This is an important differential diagnosis for both malakoplakia and xantogranulomatous pyelonephritis that may have an extensive myofibroblastic component. Similar to its crucial role in kidney tumours, electron microscopy is a useful adjunct in the diagnosis of renal pseudotumours and has been essential in the elucidation of their pathogenesis.

Friday, 3 September 2010, 08.00–11.00, Sala Wystawowa B

WGS-33 Diagnosis of infectious diseases in cytopathology: extending the diagnostic scope—Joint Meeting of the WGs of Infectious Diseases and Cytopathology

Chairpersons: G. Cathomas, Switzerland
P. Hofman, France
P. Firat, Turkey

001
Cytologic and immunocytochemical methods in diagnostic investigation of infections

*V. E. Karev**
*Russia

Objective: Infectious complications have essential value at the conditions caused by primary and secondary immunodeficiencies, including connected with a HIV or immunosuppression therapy. Laboratory diagnostics of opportunistic infections in conditions inadequate formation of antibodies is directed on revealing of antigenes of the activator.

Method: One hundred fifty samples of washing waters of bronchial tubes are investigated at diagnostic or medical bronchoscopy of patients (children and adults) with acute lymphoid (47.8%) and myeloid (16.9%) leukemia, chronic lymphoid and myeloid leukemia, Hodgkin's and non-Hodgkin's lymphomas. Patients have been surveyed in different terms after transplantation of a bone brain. Cytologic preparations were painted H&E, Ziehl–Neelsen and PAS, ICH. The cellular structure, condition epithelial cells, a degree of expressiveness and character macrophages activity epithelial and non-epithelial cells, a degree of expressiveness and character inflammations and also the presence of specific activators were estimated.

Results: Data obtained by us testify to the prevalence bacteria (26.7%) and viruses (16.9%), inflammatory processes in respiratory ways. The changes connected with specific (tumoral), mycoses (aspergillosis, zygomycosis, a candidiasis) and pneumocystosis were less often observed by defeat. In one case, it was documented as mycobacteriosis. In 32.3% of cases of pathological changes, it is not revealed; in 8.4% of

cases, the changes connected with natural return development of pathological process were observed.
Conclusion: Carrying out complex research of a biological material for the definition of character and a degree of expressiveness of pathological process and also the proof of a role of the infectious agent in the development of pathological process is expedient.

002
Diagnosis of infections in fine needle aspiration (FNA) in immunocompetent and immunocompromised patients

*B. Bode**
*Universitätsspital Zürich, Institute of Zytology, Switzerland

Fine needle aspiration (FNA) is a well-established method for the evaluation of the aetiology of superficial and deep masses. An infectious process has to be considered as a differential diagnosis in all cases, especially in the setting of immunosuppression (HIV infection, transplantation, chemotherapy, inborn defects). FNA allows a rapid distinction between neoplastic and inflammatory/infectious lesions. A wide range of pathogens including various viruses (CMV, EBV), bacteria (Gram-positive cocci, actinomyces, spirochetes, mycobacteria), fungi (*Aspergillus*, *Cryptococcus*) and parasites (toxoplasma, echinococcus) may be identified cytologically. Infectious agents may be visualised either direct in standard stainings (CMV, fungi), in special stainings (mycobacteria) or immunohistochemically (spirochetes), either on direct smears or in cell blocks. Molecular methods (in situ hybridization, PCR with sequencing) applied to FNA specimen help identify and often subtype the pathogen if required (EBV, mycobacterium tuberculosis vs. atypical mycobacteriosis). FNA is a particularly convenient method for fresh, sterile sample collection for microbiological examination with culture and drug resistance studies, playing an important role in treatment decision, e.g. in therapy of multiresistant tuberculosis. In some infectious diseases, the final diagnosis may be made by serology following indirect cytological hints in a FNA specimen (e.g. toxoplasmosis, HIV). Interestingly, infectious agents have been identified as aetiologically relevant factors in several tumor types (EBV in Burkitt lymphoma or lymphoepithelial carcinoma, HHV8 in Kaposi sarcoma, HPV in oropharyngeal carcinoma), so that the identification of the pathogens in FNAs may play an important role in the precise diagnosis of some neoplasias.

003
Usefulness of oral cytopathology in the diagnosis of infectious diseases in immunocompromised patients

*P. Hofman**
*France

Background: Cytology is an accepted and widely employed diagnostic methodology used in the early diagnosis of oral cancer. However, the diagnosis of many other specific clinical conditions of the mouth can be made from examination of smears, in particular infectious diseases.
Method: In recent years, the spectrum of infectious diseases of the mouth has changed. Firstly, oral infections observed in immunocompromised patients have dramatically increased owing to the widespread implementation of solid organ and bone marrow transplantation and in the increasing prevalence of HIV infections. Secondly, while the occurrence of many oral lesions has decreased significantly since the advent of highly active antiretroviral therapy, the incidence of oral warts has increased.
Results: In this regard, cytology can be used as a rapid, noninvasive, inexpensive and simple routine procedure in diagnosing infectious diseases of the mouth. The role of the cytopathology laboratory is diagnostic, i.e., to suggest or identify the presence of an infectious agent. However, exogenous structures that can mimic a variety of pathogens can pose a serious challenge.
Conclusion: The contaminants can be distinguished from microorganisms by their haphazard arrangement and lack of internal structure. Moreover, the absences of acute or chronic inflammation, of macrophages or multinucleated giant cells with or without granulomas, and the absence of necrosis are features that should alert the cytologist to the possibility of contamination. Finally, ancillary methods can be developed from cytological samples, which increases the specificity and the sensitivity for the diagnosis of infectious diseases in mouth.

004
The cytological peculiarities of urogenital viral infections

V. Zinserling, E. V. Lesjnak*
*Russia

005
Rapid detection of microorganisms in BAL by immunofluorescence

S. Savic, L. Bubendorf*
*Switzerland

006
Cytodiagnosis of pulmonary and extrapulmonary tuberculosis

*C. Ersoz**
*Turkey

Friday, 3 September 2010, 08.00–11.00, Aula Mała

WGS-34 Computational pathology

Chairpersons: M. Dietel, Germany
J. Szymas, Poland

001

The essentials in making a pathology diagnosis

*A. Batistatou**
*Greece

Pathology is the discipline concerned with understanding the nature of human disease. Pathologists' interpretations of tissue lesions become data, guiding decisions for patient management. Cognition, the sum of processes by which the visual input is transformed, reduced, elaborated, stored, recovered and used, is very important in pathology. Looking through the microscope at the stained tissue section (global impression and focal search) leads to perception of forms and colours. Various regions are examined under low and high magnifications. Then the pathologist puts the observed pieces of the colourful puzzle in place. An experienced pathologist proceeds promptly to pattern recognition and probably to diagnosis, while a novice takes more time, usually by not focusing on the significant areas but rather via an exhaustive search of the whole slide. Non-verbalized pattern recognition consists of short sequences which result from conversion of longer series of specific features. Alternative cognitive methods are diagnostic algorithms and the hypothetico-deductive strategy. Experienced pathologists perceive each case as a whole, constituted by parts varying in importance and relevance. And while novices prefer to use analytic reasoning strategies, which are conscious and controlled, experts often use implicit reasoning, which is unconscious and automatic and relies largely on tacit knowledge. Pathologists have faith in the analysis of morphology whose power has been appreciated even in the current molecular era. The use of virtual microscopy has a great advantage over the exchange of static images for diagnosis and training since it also allows for the initial steps to diagnosis, i.e. search, detection and perception.

002

Exploiting the O-axis of the Dutch KOPAC coding system for cervical smears

*M. E. Boon**
*Leids Cytologischen & Pathologisch Laboratorium, Leiden, The Netherlands

Background: All Dutch cervical smears (800,000 per year) are centrally archived in the Dutch national pathology database, the PALGA, in the KOPAC coding system. The KOPAC O-axis contains inflammatory events, O1 for koilocytosis, O2 for *Trichomonas vaginalis*, O3 for dysbacteriosis, O4 for Candida, O5 for *Gardnerella vaginalis*, O6 for non-inflammatory flora, O7 for *Actinomyces* (mainly in IUD users), O8 for *Chlamydia*, and O9 or nonspecific inflammatory changes (leucocytosis).
Method: The participants of this study are screenees who had a smear taken in the Dutch national screening program, on the one hand screenees born in immigrant countries (immigrants) and on the other hand screenees born in the Netherlands. The database of the SBBW, one of the responsible screening organisations, encompasses over 500,000 KOPAC cytology reports of screenees, collected between 1996 and 2005.
Results: The variation of the cytoscores was maximal for *Trichomonas* (1.9–14.0‰), whilst for *Candida*, the values were between 10.0‰ and 29.0‰. Screenees from Surinam and the Dutch Antilles had high cytoscores for *Trichomonas* and *Gardnerella*, whilst Moroccan screenees had a maximally low cytoscore for *Gardnerella* of 0.8‰. In the analysis of our data, we focussed on the odds ratio (OR). The cytoscores for the pathogens *Trichomonas* and *Candida* and for the undesirable bacterium *Gardnerella* are by-products of cancer screening. The elevated risk for colonisation of *Gardnerella* in immigrants from Surinam, Turkey, and the Dutch Antilles is truly worrisome since it is related to the acquisition of HPV.
Conclusion: This study was possible by exploiting the O-axis of the Dutch coding system for cervical smears.

003

Exploiting the Dutch network and national data base for pathology (PALGA) of over 55 million pathology reports in patient care and quality control

*M. E. Boon**
*Leids Cytologischen & Pathologisch Laboratorium, Leiden, The Netherlands

Background: The Dutch national pathology database, the PALGA, was started in 1971 by pathologists. As of 2010, all 59 Dutch pathology laboratories send their pathology reports each evening to the central database. The PALGA software can identify a patient by name, sex, and date of birth. At present, the PALGA database contains 55 million histology, cytology, and postmortem reports of 10.8 million patients, the Dutch population being 16 million.
Method: For 2009, the PALGA data traffic was analyzed.
Results: For the year of study, the data traffic comprised 2.1 million pathology reports and past pathology histories. For the Leiden Cytology and Pathology Laboratory (LCPL), exclusively serving general practitioners, 80,000 patients (out of 500,000) were added to the PALGA database, and 1,584

pathology diagnoses were asked for in the context of quality control of cervical cytology and dermatopathology.
Conclusion: In patient care, the 423 Dutch pathologists profit from the historical pathology diagnoses dating back to 1971. For quality control of the LCPL, the diagnoses of other pathology laboratories of the hospitals where the patients of the general practitioners were operated provided by the PALGA are of paramount importance. In 2010, the PALGA system will also be employed for the nationwide evaluation of the early detection of cervix, breast, and colon carcinoma.

004
Virtual microscopy in routine diagnostic procedure of pathology

*M. Dietel**
*Universitätsmedizin Charité, Berlin, Germany

Background: Virtual microscopy (VM) is now widely applied in pathology. Many studies underline the diagnostic security, the technical robustness as well as the versatility of this method. The standardization organizations DICOM, HL7 and IHE call virtual slides as whole slide images (WSI) now and integrate the technology into their standardization strategy. In contrast to the increasing application in educations, the virtual microscopy is far from routine use in surgical pathology. This goes back to several reasons concerning technical and personal requirements: costs (scanning devices and storage), scanning time (between 1 and 5 min for a biopsy and between 5 and 20 min for a surgical specimen) and speed of virtual microscopes in comparison to conventional microscopy.
Results: Caching and prefetching may speed up image loading, the bottleneck in virtual microscopy. The positive effects of different prefetching and caching technologies which depend on the user's behaviour will be discussed. Further, the process of secondary diagnostic was evaluated using the "T. Konsult Pathologie" service of the Professional Association of German Pathologists within the German breast cancer screening program.
Conclusion: In summary, it could be shown that the safety of diagnostic on WSI is comparable to the conventional diagnostic based on glass slides and a classical microscope. Discrepancies go back to problems with the difficulty of the case itself and not to technical problems with virtual microscopy.

005
Virtual microscopy in teaching pathology in Pomeranian Medical University

A. Kram, W. Domagała*
*Pomeranian Medical University, Szczecin, Poland

Objective: Microscopy is an important way of understanding the morphologic basis of diseases, and a slide seminar is part of the pathology program in medical schools worldwide. Virtual pathology which allows seeing the entire digitized microscopic slide on the computer screen has been introduced recently. Here, we share our experience in using digitized slides in teaching pathology and also discuss student's survey results. This has been the first implementation of a complete virtual pathology course for students of medicine in Poland.
Method: Two hundred twenty-four virtual slides for pathology course for medical students were produced by the use of Aperio Scanscope CS scanner and hosted in Spectrum database. Starting from the year 2006, a group of 223 Polish- and English-speaking students used glass slides and microscopes in the first year and then virtual slides in the second year. At the end of the second year, on completion of the pathology course, the students were given a questionnaire to evaluate both systems.
Results: Eighty-five percent of students preferred the screen over the microscope. Continuous and easy access to virtual slides via the Internet was indicated as one of the major advantages of virtual microscopy. Some technical problems having an adverse impact on learning efficacy were noted.
Conclusion: The move to virtual microscopy and computer-assisted pathology teaching appears to be well received by students and enhance their learning ability in the field of pathology.

006
Identity federations and image database authentication

*M. Procházka**
*Masaryk University, Institute of Computer Science, Brno, Czech Republic

007
Latest development of telemedicine platforma

*S. Vinod**
*USA

Friday, 3 September 2010, 14.30–16.30, Aula Duża B

WGS-35 Cytology and pathology of the uterine cervix—Cytopathology and Gynaecologic Pathology WGs Joint Session

Chairpersons: P. Firat, Turkey
J. Ordi, Spain

001

The current status and future of cervical cancer screening in Europe

*C. Bergeron**
*Laboratoire Cerba, Dept. of Cytology and Pathology, Cergy Pontoise, France

002

Cytological characteristics of squamous lesions and the mimickers

*L. Di Bonito**
*Italy

High-grade squamous intraepithelial lesions are characterized by moderately sized parabasal (CIN2) or basal (CIN3) dysplastic cells with marked nuclear abnormalities. Basal dysplastic cells usually display scanty cytoplasm and large hyperchromatic, coarsely granular nuclei with irregular contours. Basal dysplastic cells can be mistaken for lymphocytes, macrophages or for small benign metaplastic or endometrial cells. Regressive changes in endocervical cells can be confused with HGSIL; repair cells can be a source of confusion, but they are characterized by active nuclei with nucleoli and even distributed chromatin. High-grade dysplastic lesions involving glandular structures may exfoliate in sheets and aggregates, arising diagnostic doubts with glandular lesions. High-grade squamous intraepithelial lesions may also have some special morphologic presentations in conditions such as postmenopause because atrophy and dryness have several effects on dysplastic cells. They appear enlarged, their nuclei appear pale, and the chromatine texture is not well discernible; diagnosis can be performed by a careful comparison of abnormal cells with adjacent dry, but normal cells. Low-grade squamous intraepithelial lesions (LGSIL) are characterized by the presence of superficial and intermediate dysplastic cells. Koilocytes occur in a great number of cases, confirming the close relationship of low-grade lesions with HPV infection. Koilocytes are mature squamous cells, usually intermediate type, with abnormal, enlarged and hyperchromatic single or double nuclei surrounded by large, sharply demarcated perinuclear clear zones or halos. Koilocytes must be differentiated from inflammatory cellular changes which may be responsible for slight nuclear abnormalities and narrow perinuclear clear zones.

003

Cytological characteristics of glandular lesions and their differential diagnosis

*C. Bergeron**
*Laboratoire Cerba, Dept. of Cytology and Pathology, Cergy Pontoise, France

Objective: Since 20 years, there is an increase of incidence and mortality of adenocarcinoma as compared to epidermoid carcinoma. This increase is particularly notable for women younger than 40 years. Adenocarcinoma equals one fourth of cancers of the cervix in some countries like the UK where there is an organized screening program.
Method: The Bethesda 2001 terminology has introduced for the first time the cytological diagnosis of adenocarcinoma in situ, the glandular counterpart of high-grade squamous intraepithelial lesion (HSIL).
Results: It is a rare lesion that corresponds to 5% of abnormal Pap smears and 0.1% of all Pap smear diagnoses. Adenocarcinoma in situ is characterized by periphery radial arrangement of feather-shaped nuclei, cigar stack-shaped pseudostratified strips, rosettes images, hyperchromatic nuclei with granular structure and clean background without necrosis. On the contrary, invasive endocervical adenocarcinoma is characterized by papillary groups, lost of cellular cohesion, polymorphism of the nuclei with one or two prominent nucleoli and tumoral diathesis with dirty background, cellular debris and fragmented red blood cells. The Bethesda 2001 terminology has maintained the grey zone for glandular cells abnormalities not well defined, included in the diagnosis of atypical glandular cells of endocervical, endometrial or undetermined.
Conclusion: The efficacy of cytological screening for detecting AIS will lead to the increase of the rate of detection of AIS. This will have an impact on the incidence and mortality of invasive adenocarcinoma in the coming years. The protective effect is beginning to be seen only recently for women younger than 30 years in Australia and in England.

004

Squamous lesions of the uterine cervix

*J. Bulten**
*Radboud University, Dept. of Pathology, Nijmegen, The Netherlands

Cervical cancer is a major cause of death in women and the second most frequent cancer throughout the world, accounting for almost 15% of all malignancies in women. In this course, an overview is presented of the precursors of squamous cell carcinoma, its mimics, microinvasive carcinoma and cervical squamous cell carcinoma. The CIN terminology (cervical intraepithelial neoplasia, grades 1–3) of Richart is most widely used for cervical cancer precursors. Nowadays, it is evident that CIN is not a continuum, but reflects merely a low-grade entity (koilocytosis, flat condyloma and CIN1) and conversely a true intraepithelial neoplastic process (CIN2-3 and carcinoma in situ). In diagnosing CIN, HPV testing is not recommended. On the contrary, post-treatment HPV testing can predict

treatment failure and thus residual CIN. In grading CIN and to differentiate CIN from its mimics as atrophy, immature metaplasia or reserve cell hyperplasia immunohistochemistry (Mib1 and P16) can be applied. Due to preceding biopsies, microinvasive carcinoma is frequently overdiagnosed. Colposcopy, cytology and immunohistochemistry are not very helpful in diagnosing microinvasive growth. As the diagnosis of (micro-)invasive growth has great clinical implications, cervical excision biopsies or cones should be totally embedded and serially sampled. There are three types of invasive growth, and the invasion depth should always be measured between the last cell of the deepest invasive focus perpendicular to the (expected) site of origin. Finally, the several types of squamous cell carcinoma and its mimics are presented.

005

Glandular lesions of the uterine cervix

*G. W. McCluggage**
*United Kingdom

Friday, 3 September 2010, 14.30–16.30, Aula Średnia A

WGS-36 Neuroendocrine tumours of digestive tract

Chairpersons: A. Nasierowska-Guttmejer, Poland
R. Y. Osamura, Japan

001

Pathology of neuroendocrine tumours: diagnosis, prognosis and therapy

*R. Y. Osamura**
*Int. University of Health and Welfare, Mita Hospital, Tokyo, Japan

Background: The diagnosis of neuroendocrine tumors (NETs) is mainly established by morphology and immunohistochemistry (IHC). The NETs in digestive tract contain those of stomach, duodenum, ileum, appendix, colon and rectum. The NETs have been classified into: (1) well-differentiated neuroendocrine tumor (WDNET), (2) well-differentiated neuroendocrine carcinoma (WDNEC) and (3) poorly differentiated neuroendocrine carcinoma (PDNEC; WHO and ENTS). In addition to WHO classification, their biologic behavior is graded into G1, G2 and G3 (ENET) by Ki-67 index <2%, 3–20% and >20%, respectively, which correlates with prognosis.
Method: Our file of total 121 referred cases of GEPNETs for the IHC staining for somatostatin receptor (SSTR)2a, for somatostatin analogue therapy, indicates that the NETs of the digestive tract comprise 17.1% (21 cases) and that the majority of GEPNETs being pancreatic NETs. Among these digestive NETs, rectal NETs and duodenal NETs are prominent cases.
Results: The metastatic duodenal and rectal NEC showed a ki-67 index higher than 2%. SSTRa was positive on the cell membrane of the tumor cells of 20 cases, except for one case of rectal NET. It should be emphasized that all duodenal gastrinomas, which are well known as early metastases and sometimes as a member of MEN-1, revealed SSTR2a, which should serve as a good target molecule for the response of somatostatin analogue (SA) therapy.
Conclusion: In conclusion, it is the pathologist's role to make appropriate diagnosis (terminology), prognostication and therapeutic indication.

002

Gastric neuroendocrine tumours

*M. Malinowska**
*Oncology Institute, Dept. of Pathology, Warsaw, Poland

Objective: Neuroendocrine cells compose the diffuse endocrine system of the gastroenteropancreatic tract. Gastric endocrine tumours (GETs) are mainly composed of enterochromaffin-like cells. GETs are rare and constitute about 1% of all gastric neoplasms and about 9% of all gastrointestinal endocrine tumours. There are three types of GETs. Type 1 is the most common, well-differentiated neoplasm, polypoid, multiple usually benign, associated with chronic atrophic gastritis. Type 2 is a rare, multiple, polypoid tumor associated with the Zollinger–Ellison syndrome. Type 3 is the second most common GETs, sporadic, much larger than types 1 and 2 and have a high propensity to metastasize. Poorly differentiated tumours are rare and account for approximately 6% of GETs. Most patients have single, advanced and aggressive tumor. In 2000, the World Health Organization determined the classification for gastroenteropancreatic neuroendocrine tumours which categorizes tumours as: (1) well-differentiated neuroendocrine tumor—(a) benign and (b) uncertain malignant potential; (2) well-differentiated neuroendocrine carcinoma; and (3) poorly differentiated neuroendocrine carcinoma.
Method: In 2006, a new TNM classification system was proposed for the staging. T Primary tumor T is in situ tumor/dysplasia <0.5 mm confined to mucosa. T1 tumor invades lamina propria or submucosa or <1 cm. T2 tumor invades muscularis propria or subserosa or >1 cm. T3 tumor penetrates serosa. T4 tumor invades adjacent structures
Results: In the seventh edition TNM: T3—tumor invades subserosa, T4—tumor perforates serosa; invades adjacent structures.
Conclusion: Histopathologic grading was performed according to mitotic count and Ki67 index. Grade mitotic count (10HPF), Ki67 index (%) G1 < 2 <2; G2 2–20, 3–20; G3 > 20 > 20

003

Small intestine GEP NET

*A. Nasierowska-Guttmejer**

*Clinical Hospital MIAA, Dept. of Pathology, Warsaw, Poland

Background: Neuroendocrine tumours of the small bowel are usually sessile nodules with a diameter between 0.5 and 3 cm. These are microscopically diagnosed as well-differentiated carcinoma. Clinically, the patients show primarily the liver metastasis, bowel obstruction or sub-ileus induced by the metastatic mesenteric tumor or systemic symptoms caused by the hormonal effects of serotinin called carcinoid syndrome. Secondarily, the primary tumours are discovered during an exploration of the gut.
Method: The prognostic relevance of the WHO, the new TNM classification system, clinical staging (CS) including other prognostic factors (gender, cellular proliferation rates according to Ki-67 labeling, G differentiation of the tumour cells, etc.) were analyzed retrospectively in 98 patients (mean age 58.3 years) with histologically proven small bowel neuroendocrine tumours (NET). Overall survival (OS) and progression-free survival (PFS) data were analysed using the Kaplan–Meier method. The differences between groups were evaluated using the Cox–Mantel test.
Results: There were five patients with WHO 1, 80 with WHO 2 and the rest with WHO 3. Including pTNM and stage, there were four cases of CS I, seven cases CS II, 31 cases CS III and the rest CS IV. Significant differences between median OS were noted in patients with CS I and II vs CS III and IV and WHO 1 vs WHO 3 and WHO 2 vs WHO 3 ($P<0.05$). Additionally, there was a significant difference between OS on patients with G1 vs G3 and those with G2 vs G3. Median OS and PFS, including all patients, were 44 and 18 months.
Conclusion: Histological type (WHO) and staging are the most important prognostic factors of small bowel NETs.

004

Large intestine GEP NET

*M. Lipidski**

*CSK MSWiA, Dept. of Pathology, Warsaw, Poland

Objective: Large intestine neuroendocrine tumours should be classified (consensus 2007) into two anatomical groups: colon and rectum.
Method: When reporting neuroendocrine tumours, pathologic report should contain: tumor site, tumor size, focality, histologic type according to WHO group, mitotic count and Ki-67 index (grading), margins (proximal, distal, radial), lymphatic vessels invasion, pTNM staging, staining results. The pathologist should do at least three immunostaining procedures suspecting neuroendocrine tumor: synaptophysin, chromogranin A and MIB1 (anti-Ki-67).
Results: Colon tumours (mainly WHO groups 3 and 4) are rare, but due to the absence of early symptoms, they are discovered in stage of disseminated disease—30% of tumours have metastases at the time of diagnosis. These tumours metastasize to liver, lymph nodes, peritoneum and mesentery, with 5-year survival rate oscillating around 50%. Rectal neuroendocrine tumours (mainly WHO group 1, 2 or 3) have a better prognosis (overall distant metastases from rectal NETs occur in approximately 2.3% cases), in contradiction to their increase in number, probably due to the increase in reporting tumours removed endoscopically in polyps.
Conclusion: Thanks to prophylactic programs, there is larger opportunity to discover polypoid neuroendocrine lesions in the state of limited disease. However, it is essential to fully evaluate excision margins and to do this properly; endoscopists should carry out endoscopic submucosal dissection (ESD) as a procedure of first choice. Endoanal/rectal ultrasound is very useful in the preoperative assessment of tumor size, depth of invasion and presence of metastases in local lymph nodes. In the case of more advanced disease, other treatment options should be taken into consideration, although benefit from more aggressive surgery is unclear.

Friday, 3 September 2010, 14.30–16.30, Aula Średnia B

WGS-37 Pathologists in favour of developing countries—discussion of common projects

Chairpersons: D. Soldini, Switzerland
V. Canzonieri, Italy

Friday, 3 September 2010, 14.30–16.30, Sala Wystawowa A

WGS-38 Paediatric soft tissue and bone tumours

Chairpersons: M. Cohen, United Kingdom
J. Kobos, Poland

001

Rhabdomyosarcoma

*I. Leuschner**

*Universität zu Kiel, Institute of Paidopathology, Germany

Rhabdomyosarcoma (RMS) is the most common soft tissue sarcoma in childhood and adolescence. Currently, RMS is classified by the so-called International Classification of Rhabdomyosarcomas. This classification identifies three subgroups with different biological behaviors. Favorable prognosis include (botryoid subtype of embryonal rhabdomyosarcoma, spindle cell type of embryonal rhabdomyo-

sarcoma), intermediate prognosis ('classical' embryonal rhabdomyosarcoma), and unfavorable prognosis (alveolar rhabdomyosarcoma). Immunohistochemistry can be used to separate between embryonal and alveolar RMS. AP2 and p-cadherin are almost exclusively expressed in alveolar RMS, whereas EGF receptor and fibrillin 2 are found in embryonal RMS. In addition, the myf-4 expression of alveolar RMS is usually much stronger than in embryonal RMS. Genetic changes have been found for both embryonal and alveolar RMS. Most alveolar RMS have a balanced reciprocal translocation, t(2;13)(q35;q14). A smaller subgroup of alveolar RMS has a t(1;13) translocation. Two other translocations, a t(2;2)(q35;p23), which generates a fusion protein composed of PAX3 and NCOA1, and a t(2;X) resulting in a fusion protein PAX3/AFX, have been described in single cases. In embryonal RMS, a loss of heterozygosity (LOH) on chromosome 11p15.5 has been shown. The involved gene or genes have not yet been clearly identified, but several interesting genes are located in this area like the MyoD1 gene, the IGF-2 gene, the LDH (muscle subunit) gene, and the WT 1 gene. A possible imprinting of this gene has also been postulated.

002

Infantile fibrosarcoma and malignant fibrous tumours

*R. Alaggio**

*Anatomia Patologica, Scienze Diagnostiche e terapie, Padova, Italy

Background: Fibroblastic/myofibroblastic lesions account for 12% of pediatric soft tissue tumours and include benign neoplasms, reactive, pseudoneoplastic proliferations and, rarely, malignant tumours. The malignant lesions, registered in the Italian Protocol RMS-96, are reported to define their clinicopathologic and molecular features.

Method: Forty-eight patients with fibrosarcoma (congenital and adult) were reviewed (Table). Four cases, originally diagnosed as CIFS, with negative ETV6-NTRK3 transcript, were reclassified as composite fibromatosis (two), undifferentiated sarcoma (one) and rhabdomyofibrosarcoma (one) and excluded from this study.

Results: see Table 1 *No translocation legend: *CR* complete remission, *IICR* second complete remission, *LFU* lost at follow-up, *MTS* metastases, *DOD* died of disease

Conclusion: The identification of some recurrent chromosomal abnormalities has contributed to the redefinition of CIFS and identification of a subgroup of more aggressive fibrosarcomas lacking the typical transcript. Adult type fibrosarcomas may also occur in children. They involve more frequently the head/neck region and have a tendency to local relapse and distant metastasis.

003

Update on benign fibrous lesions

*J. Kobos**

*Medical University of Lodz, Dept.of Pathology, Poland

Some of these lesions are genuine benign neoplasms; others have a reactive nature. Nodular fasciitis is a fibroblastic/myofibroblastic proliferation mostly seen in the subcutaneous tissue, morphologically presenting a loose and culture-like growth pattern. Proliferative fasciitis (and proliferative myositis) is, likewise, nodular fasciitis, a fibroblastic/myofibroblastic proliferation with the presence of large ganglion-like cells. Myositis ossificans is a benign and reactive lesion. Fibrous hamartoma of infancy is a relatively common benign tumour of early childhood which presents three components: fibrocollagenous tissue, immature-primitive mesenchymal cells and mature fat tissue. Myofibroma/myofibromatosis is a benign tumour observed in newborns and children within the first 2 years of life, as well as in elderly patients. Fibromatosis colli is a rare benign lesion typically seen in the sternocleidomastoid muscle in infants. Microscopically, it is a proliferation of fibroblasts in between the muscle fibres forming a "scar-like" pattern. Juvenile hyaline fibromatosis is a very uncommon, non-neoplastic lesion. Fibroma of tendon sheath is a benign (possibly reactive) lesion related to tendons. Calcifying aponeurotic firbroma is the tumour more frequently seen in children. Gardner fibroma is an uncommon benign tumour mostly seen in infants, children and adolescents. Calcifying fibrous tumour is a rare benign tumor more frequently observed in children and young adults.

HISTOTYPE	SEX (m/f)	AGE RANGE (m)	SITE	Transcript ETV6-NTRK3	FOLLOW-UP (range 0-10yr)
9 Adult FS	5/4	4-16(10)	Head 5, Extremities 4	Negative	CR 5, IICR 1, LFU 2
23 CIF	14/10	0–2(0,54)	Head 1, Extremities 17, Trunk 4, Abdominal 1	12/16	CR 17, IICR 1*, LFU 5, MTS 1*
5 LGFMS	4/1	3-15(9,40)	Extremities 4, Trunk 1	Negative	CR 2, IIRC 1, MTS+LFU 1, LFU 1
4 SEF	2/2	3-9(6,5)	Head 2, Extremities 1, Trunk 1	Negative	CR 2, LFU 2
3 PMMTI	2/1	0,3-0,4(0,35)	Head 1, Extremities 2	0/3	IICR 1, MTS 1, DOD 1

004
ASPS, CCS, ES
*A. Kelsey**
*United Kingdom

005
Osteosarcoma
*P. C. W. Hogendoorn**
*The Netherlands

Friday, 3 September 2010, 14.30–16.30, Aula Mała

WGS-39 Computational pathology
Chairpersons: M. G. Rojo, Spain
Y. Yagi, USA

001
SNOMED CT in Europe
*M. G. Rojo**
*Spain

Background: A standard clinical terminology like SNOMED CT is important not only for pathology information systems but also to integrate these systems with many other hospital information systems (HIS, PACS, departmental systems, encoding, database patients) and primary care information systems.
Method: SNOMED CT includes two hierarchies (morphologic abnormality and disorder) with similar terms. A SNOMED CT implementation was designed taking into account both the difference between these hierarchies and the relationship between terms located in different hierarchies. This is especially necessary in the post-coordination of clinical expressions and the creation of subsets.
Results: The January 2010 edition of the subset of Pathology, which distributes the College of American Pathologists (CAP), contains 7,582 terms, but this subset needs to be improved to give it a clinical use. In SESCAM, 3,000 morphological concepts and 200 specimen concepts were selected to create a minimum basic set for use in pathology information systems. SNOMED CT is also used in the SESCAM telepathology portal (Project Serendipia), developed according to the IHE-Anatomic Pathology initiative and DICOM supplement-122 for medical imaging.
Conclusion: A SNOMED CT implementation strategy should not only include a list or subset of terms, but it must also consider the efficient use of relationships between terms and concept hierarchies, a mechanism for extension and update, and a plan for the coexistence or migration of legacy SNOMED II codes.

002
Latest developments in data storage devices applicable for virtual slides
*J. Görtler**
*Belgium

003
Structured reports in tumor pathology—how and why
*G. Haroske**
*Germany

Objective: Among all medical documents, pathology reports are often highly critical for patient care. In terms of information technology and knowledge engineering, presently, these reports are widely lacking adequate structure to support their usage in knowledge retrieval technologies for medical decision making, research, epidemiology, quality management and medical education.
Method: By means of literature surveys and by a questionnaire sent to vendors of pathology management systems (PMS), the degree of structure in pathology reports in PMS sold in Germany was analyzed and compared with user needs expressed by pathologists.
Results: Pathology reports are widely displayed, stored and exported as free text, identifiable by human beings, but without "observation identifiers" of a coding system not readable by a computer. A few systems allow textual information to be structured in sections partly identified by coding systems as SNOMED CT, etc. Within the sections, the information is still unstructured. At the very beginning are attempts to structure the report as a list of coded items based on templates, which are controlled for identifiers, version, and the underlying concepts and representations. This is by far the most granular structure for computer readability and knowledge engineering.
Conclusion: There are very different opinions about the aim and degree of structured reporting. Although standardization efforts have led to a series of reporting minimum requirements in tumor pathology, their implementation in structured data entry systems is still lacking. Tools for data mining in routine pathology will be decisive for all important progress in pathology informatics at all.

004
Experiences of virtual microscopy in TMA application
*G. Kayser**
*Germany

005

How to scale image information in virtual slides?

K. Kayser, S. Borkenfeld, J. Görtler, G. Kayser*
*Heidelberg, Germany

Objective: The application of virtual slides requires unequivocal definition and scaling of image information. Scaling of image information offers the evaluation of diagnosis and content-based image retrieval (CBIR).
Method: Theory in principle—image information can be extracted with or without knowledge of its content. Knowing its content (for example organ, potential diseases), we can segment biological meaningful objects (nuclei, membranes, etc.) and measure their features (size, gray values, derived parameters). The obtained results can be scaled and associated with the underlying disease. In reverse, knowing the applied algorithms and the object (and structure) features, CBIR can be applied. Without predefined knowledge, basic image information is mapped on spatial image units (pixels), called texture. They can be quantified by the application of stochastic geometry: Each biological meaningful object is composed of so-called primitives (points, fibers, rings, plateaus). Their mapping on an object can be used to detect knowledge-independent content and scalable image information.
Results: Object- and structure-based (1) and the texture-based (2) algorithms have been implemented and applied on more than 1,000 images obtained from H&E-stained glass slides of different organs (colon/rectum, lung, pleura, thyroid) in search for disease-significant areas (fields of view) and disease classification. The accuracy of the methods in field of view selection was computed to >98%, that of prospective disease classification >95%.
Conclusion: The developed algorithms permit a reliable scaling of image information that can be applied for CBIR and related tasks. References: K. Kayser et al. Diagnostic Pathology 2010, 5(Suppl 1):S12K. Kayser et al. Diagnostic Pathology 2008, 3:17.

006

Automation of image analysis in breast cancer

*J. McGee**
*United Kingdom

007

New generation of slide scanners open the way to digital pathology

*B. Molnár**
*Hungary

Background: Slide scanners with digital microscopy software solutions became available since the early 2000s. Digitalisation of the pathology laboratories and workflow process is still not achieved.
Aims: Identification, development and evaluation of digital slide scanner, laboratory, workflow, user interface and application needs including technical requirements for whole department digitalisation of the pathology laboratories.
Method: A new generation digital slide scanner was developed. It included a new dark light slide preview system for FISH scanning, then 100% safe loading mechanism, and enhanced scanning speed with frame rates of 50/second. Respective software applications (HL7 interface towards LIMS, server scanning, digital cockpit software for H/E, immunohistochemistry and FISH analysis) was developed.
Results: A middle-sized academic routine pathology department produces daily approx. 300 H/E, 200 IHC, and 35 FISH slides. Only one scanner for the H/E, for the IHC, and one for the FISH slides had to be placed without hiring any additional assistant workforce. Scanning could be performed in parallel to the sample preparation procedures due to the 10× increased scanning speed (20 s/cm^2) for any types of the slides directly to the digital slide server. The digital pathology workstation SW supported the parallel opening, viewing and evaluation of the respective slides and areas. Quantification modules became widely used for nuclear, membrane and FISH analysis.
Conclusion: The new-generation scanners make the digitalisation of the pathology laboratories financially also affordable. The software applications can contribute to the more robust, documented and comprehensive analysis of the digital cases.

Friday, 3 September 2010, 17.00–18.30, Aula Duża B

WGS-40 Mucinous tumours of the appendix

Chairperson: J. F. Flejou, France

001

Serrated and hyperplastic lesions of the appendix

*J. F. Flejou**
* Hôpital Saint-Antoine, Service Anatomie Pathologiqu, Paris, France

Hyperplastic lesions of the appendiceal mucosa are classically divided into two groups: diffuse hyperplasia and localized polyps. Localized lesions were usually diagnosed as hyperplastic polyps, but some of these lesions are now better classified as sessile serrated adenomas. Both diffuse hyperplasia and polyps are in most cases incidental findings on appendectomy specimens (performed for appendicitis or systematically sampled in a colectomy specimen). However, these lesions are significantly associated with colon adeno-

carcinoma, and therefore, their discovery in an appendectomy specimen is an indication of further examination to exclude colorectal neoplasia. Diffuse mucosal hyperplasia extends to more than one half of the circumference of the appendiceal mucosa. It exhibits elongated crypts with serrated architecture. The epithelium is composed of columnar cells alternating with large goblet cells in various proportions. The crypt bases are not serrated and are lined by regular cells with no atypia. Hyperplastic polyps are supposed to be rare in the vermiform appendix. They are localized lesions, with a histological aspect similar to the corresponding colorectal lesions. Similarly to diffuse mucosal hyperplasia, they are characterized by a serrated architecture restricted to the upper part of the crypts and by the lack of any dysplastic features. When lesions associate hyperplastic serrated features in one area and adenomatous (tubular and/or villous) features in another, they are designated as mixed adenomatous and hyperplastic polyps, as tumours of the colon and rectum. However, it is probable that at least part of these mixed lesions represent hyperplastic serrated polyps that have progressed to dysplasia. Sessile serrated adenoma (or sessile serrated polyp or serrated polyp with abnormal proliferation) is a more recently described type of colorectal polyp with a serrated architecture. They occur frequently in the right colon, and although they resemble to hyperplastic polyps, they are characterized by subtle architectural and cytological features, especially dilation and serration of the basal part of the crypts. They can be dysplastic or not. The relative frequency of sessile serrated adenomas and other serrated lesions of the appendix is not well established, but it is highly probable that many appendiceal lesions previously designated as diffuse hyperplasia or hyperplastic polyp represent cases of sessile serrated adenomas. Both types of lesions have been proven to show decreased expression of MLH1 and MGMT in a majority of cases and also BRAF mutation in a significant proportion of cases. These genetic and epigenetic alterations are similar to those observed in sessile serrated adenoma of the colon, which is now considered as a precursor lesion for a subgroup of colorectal cancer. The differential diagnosis of serrated lesions of the appendix also includes adenomas of colorectal type (more often showing villous architecture when compared to colorectal lesions) and low-grade mucinous neoplasms, often referred to as cystadenomas.

002

Adenocarcinoma, mucinous neoplasm of the appendix and pseudomyxoma peritonei

*A. Jouret-Mourin**

*Cliniques Universitaires ST LUC, Brussels, Belgium

Primary adenocarcinoma of the appendix is unusual. Some resemble typical colonic adenocarcinoma in their appearance and behaviour, but others are well-differentiated neoplasms or adenoma-like that may be associated with the pseudomyxoma peritonei syndrome without distant metastases. This pathological spectrum is confused because of terminological inconsistencies and the large variety of diagnostic criteria. Therefore, there remains a "grey area" between benign and malignant lesions. Some authors have recently proposed a new terminology based on the biological potential of the different lesions. Low-grade appendiceal mucinous neoplasm (LAMN) is defined as a subset of lesions that have low-grade cytological atypia and minimal architectural complexity. These lesions penetrate into or through the appendiceal wall often on a broad front, without overt invasion and may be associated with pseudomyxoma peritonei. Consequently, such LAMN category includes the old terms of "tumours of uncertain malignant potential, "pseudomyxoma with adenoma-like histology" and the "low-grade mucinous adenocarcinoma" which can also produce pseudomyxoma. Invasive mucinous adenocarcinoma (MACA) includes a destructive invasion of the appendiceal wall with high-grade atypia, complex proliferation (i.e. cribriform pattern), desmoplastic stroma, signet ring cells differentiation or undifferentiated tumours. Lymph node metastases occur lately, but peritoneal spreading is more frequent. Some recent publications have demonstrated that protein immunoexpression profiles offer predictive factors of adverse clinical outcomes, which should further facilitate the classification of appendiceal mucinous neoplasms. Appendiceal mucinous tumours can occur in patients who have suffered long-standing ulcerative colitis, familial polyposis and HNPCC syndrome. Most of them show microsatellite instability probably given the high frequency of serrated precursor. Pseudomyxoma peritonei syndrome is defined as the presence of abundant mucinous material on the peritoneal surface. This entity should be retained as a clinical term. Besides exceptional cases of pseudomyxoma reported in association with mucinous carcinomas at other sites, all cases of pseudomyxoma peritonei are related to appendiceal rupture with subsequent transcelomic spread of tumoral cells. Some authors have proposed that the same terminology should be used for the appendiceal primaries and the peritoneal lesions since LAMN lesions confined to the appendix have the same appearance as those that have spread to the peritoneum. In addition, any tumour capable of producing pseudomyxoma peritonei should be considered as adenocarcinoma. Therefore, the classification of pseudomyxoma perotonei includes low-grade and high-grade mucinous adenocarcinoma. The acellularity of the extra-appendicular mucin, based on extensive sampling, must be described in the pathological report because of its prognostic implications.

003

Mixed mucus-secreting and endocrine tumours of the appendix

*J.-Y. Scoazec**

*Hospices Civils de Lyon, Hôpital Edouard Herriot, France

Vermiform appendix is one of the most frequent sites of mixed endocrine–exocrine tumours in the gastrointestinal tract. One histologic type of mixed mucus-secreting and endocrine tumor is specific for the appendix: This distinctive tumour is known as goblet cell carcinoid. The others are mixed endocrine–exocrine carcinomas raising the same problems of diagnosis and management than in the other digestive locations. Goblet cell carcinoid is a highly distinctive clinical and histological entity. In contrast to the much more common pure neuroendocrine tumours of the appendix, which are usually discovered incidentally in young patients, goblet cell carcinoids present a peak of incidence in the fifth decade and are usually symptomatic. At macroscopic examination, goblet cell carcinoids present a very particular pattern of growth, resulting in the thickening of the whole appendicular wall and in a marked reduction in the calibre of the lumen, in the absence of visible tumour mass. This aspect is due to the predominant infiltration of the deepest part of the mucosa and the submucosa by tumour cells, which result in their fibrosis and thickening. At a higher magnification, tumor cells are grouped in small nests formed by large cells, with an abundant, pale, mucus-laden cytoplasm and an eccentric nucleus. These cells are strongly reactive with Alcian blue and PAS stainings. Small endocrine cells are closely intermingled with mucus-laden cells; they are usually difficult to identify by conventional stainings; they are much more easily demonstrated through the immunodetection of endocrine and neuroendocrine markers such as chromogranin A and synaptophysin. Finally, some amphicrine cells, with a combination of exocrine and endocrine markers, may be present. The number of endocrine cells admixed with mucus-laden cells is highly variable from one case to another and even from one region to another in the same tumour. There is no minimal amount of endocrine cells required for the diagnosis of goblet cell carcinoid, which is achieved by the combination of a typical macroscopic aspect, the presence of characteristic mucus-laden cells and the demonstration of even a few endocrine cells intermingled with the predominant mucus-producing population. From the molecular point of view, goblet cell carcinoids frequently harbour loss of heterozygosity in 11q, 16q and 18q. Goblet cell carcinoids carry a high risk of peritoneal dissemination, but a low risk of distant metastasis. Their prognosis is therefore much poorer than that of typical neuroendocrine tumours of the appendix: The 5-year survival is only 18% instead of 83%, all stages included; even for patients with localized disease, it is 55% instead of 94%. Importantly, the TNM classification of goblet cell carcinoid must follow the criteria used for the staging of appendicular carcinomas, not those recently proposed for appendicular "carcinoids". Mixed endocrine–exocrine carcinomas of the appendix combine an exocrine component, usually corresponding to a mucus-secreting adenocarcinoma of variable differentiation and an endocrine component, which may be well or poorly differentiated. The diagnosis of mixed tumour must be made with caution, only if the endocrine component is clearly neoplastic and represents at least 30% of the whole tumour. The prognosis and treatment are those of the most aggressive component.

Friday, 3 September 2010, 17.00–18.30, Aula Średnia A

WGS-41 Electron microscopy in neuropathology

Chairpersons: J. Lloreta-Trull, Spain
G. Cennacchi, Italy
A. Marszalek, Poland

001

Electron microscopy of muscle diseases

*C. Navarro**

*Spain

Electron microscopy has been relatively surpassed by immunohistochemistry in pathology, especially for the diagnosis of neoplastic processes. However, its use is mandatory in neurodegenerative and neuromuscular disorders of non-neoplasic origin. Ultrastructural examination has been proven to be useful in the following issues: (1) to understand the physiopathology of muscle disorders. Muscular dystrophies are produced by mutations in genes codifying proteins located at different subcellular levels. Ultrastructural alterations have been observed at the level where the defective protein is expressed, i.e. plasma membrane alterations in dysferlinopathies, caveolinopathies and sarcoglycanopathies, or nuclear envelope membrane defects in Emery Dreifuss muscular dystrophy and laminopathies. (2) To identify structures not visible with light microscopy. This is the case of intranuclear inclusions in oculo-pharyngeal muscular dystrophy, in inclusion body myositis, or tubulo-reticular inclusions seen in several autoimmune disorders and in AIDS. (3) To determine the origin of specific anomalies depicted with light microscopy. Ultrastructure of tubular aggregates, nemaline bodies, central cores or paracrystalline mitochondrial inclusions has been crucial to define the origin and organization of

such changes at the subcellular components of the muscle fiber. (4) To study in depth lysosomal storage disorders. The identification of different types of inclusions in neuronal ceroid lipofuscinosis according to the phenotype–genotype form of the disease has been especially useful, and so it was for the diagnosis of late-onset forms of glycogenosis type II, Fabry disease or others. In conclusion, electron microscopic examination is crucial to identify the subcellular structural involvement in some muscle disorders and to understand the underlying pathological mechanisms.

002

Electron microscopy of peripheral nerve

*A. Vital**
*Bordeaux University Hospital, Dept. of Pathology, France

Objective: Electron microscopic examination (EME) of a peripheral nerve biopsy (PNB) is particularly valuable to assess the type of nerve fiber lesions, endoneurial deposits and storage materials.
Method: A well-done PNB, as well as a reliable methodology for fixation and embedding of specimens, constitute a prerequisite for an informative EME.
Results: If most cases of hereditary peripheral neuropathies are now diagnosed by molecular biology, nerve lesion analysis can direct the search for mutations in specific genes. Prominent "onion bulb" formations are associated with PMP22 duplication. "Tomaculae" correspond to PMP22 deletion, but can also be observed in certain cases of P0 mutation. Other P0 mutations are mainly associated with irregularly uncompacted myelin lamellae. Discrete "onion bulb" formations in association with "pseudo-onion bulb" formations surrounding clusters of regeneration are much suggestive of connexin 32 mutation. Abnormal mitochondria point to a mitofusin 2 gene mutation. Ultrastructural evidence of macrophage-associated demyelination is very supportive in atypical cases of inflammatory demyelinating polyneuropathy. In some cases of paraproteinemic neuropathy, myelin lamellae may exhibit a regular spacing corresponding to the presence of immunoglobulin M. In others, granular immunoglobulin deposits are identified in the endoneurium. Occasionally, the endoneurial deposits have the tubular ultrastructure of a monoclonal cryoglobulin. The presence of osmiophilic lamellar inclusions in Schwann cells points to treatment intolerance. At last, EME of a PNB may help in the diagnosis of a hereditary storage disease.
Conclusion: EME can be decisive to establish the etiological diagnosis of a peripheral neuropathy and must be supported by a reliable methodology.

003

Electron microscopy of metabolic storage diseases

*I. Ferrer**
*Hospital Universitari de Bellv, Institut Neuropatologia, Spain

Metabolic diseases of the nervous system in infancy constitute a very complex group of variegated diseases with particular clinical, morphological, biochemical and genetic characteristics. Diagnosis of such disorders usually demands the collaboration of different specialists, methods, and skills. This is particularly important in order to avoid unnecessary probes and superfluous additional suffering related with inappropriate complementary examinations and visits. In recent years, molecular and genetic studies have facilitated a correct diagnosis during life, and improvements in therapy have permitted the application of new therapeutic tools in some cases. Morphological visualization of determinate lesions in skin, conjunctival, appendicular and, rarely, rectal mucosa, is extremely useful to support a clinical diagnosis. Lipidosis, mucopolysccharidosis, mucolipidosis, polyglucosan storage diseases and glycogenosis affect several cell types outside the central nervous system, including axons and Schwann cells, endothelial cells, pericytes, smooth muscle fibres, sebaceous and eccrine glands and ducts, and striate muscle. Deposits are usually too small to be visible with an optical microscope. Yet electron microscopy permits the observation of lysosomal inclusions filled with specific inclusions and deposition of abnormal material in different cells. In addition to metabolic diseases, other degenerative diseases affecting the nervous system in which the diagnosis is mainly based on key pathological markers are also subject to electron microscopy analysis during life. Nuclear neuronal inclusion body disease and infantile neuroaxonal dystrophy, among others, can be diagnosed by means of appendicular (or rectal) biopsies and by examining the nerve terminals and skin and conjunctiva, respectively.

004

Electron microscopy and neurodegenerative diseases/ prion CNS diseases

*P. Liberski**
*Medical University of Lodz, Dept. of Mol. Pathol. Neuropathology, Poland

Friday, 3 September 2010, 17.00–18.30, Aula Średnia B

WGS-42 Advances in head and neck pathology

Chairpersons: N. Gale, Slovenia
T. Helliwell, United Kingdom

001

The significance of HPV and HIV infections in sinonasal and laryngeal pathology

*L. Alos**
*Spain

002

Desmosomes in subtypes of squamous cell carcinoma of the head and neck

*N. Zidar**
*Slovenia

003

Recent advances in sinonasal inflammatory diseases

*T. Helliwell**
*United Kingdom

This presentation will cover a range of sinonasal inflammatory diseases, focussing on those where an improved understanding of pathogenesis illuminates diagnostic histopathology. The categorisation of sinonasal fungus-related diseases is important for prognosis and treatment. Fungi are common airborne allergens and can be cultured from the nasal secretions of most healthy individuals. The diagnosis of fungal sinusitis relies on the histological recognition of fungi in sinus tissue, although the morphology of fungal hyphae is of limited value in distinguishing between fungal species. Invasive fungal sinusitis is almost always encountered in patients whose immune system is compromised and is associated with necrosis and vascular invasion by fungi. Noninvasive fungal sinusitis includes sinus fungal balls and allergic fungal sinusitis, a disease characterised by so-called allergic mucin and scanty fungal hyphae. The pathogenesis of chronic rhinosinusitis involves a complex interplay between environmental factors and genetically influenced immune responses; eosinophils may be seen in both allergic rhinosinusitis and in patients with no evidence of allergy. The differential diagnosis of inflammatory polyps will be discussed. Pathologists should be aware of the many sinonasal diseases that may include a component of granulomatous inflammation including mycobacterial infection, cocaine-induced midline destructive disease and Wegener's granulomatosis, and of the value of ancillary investigations such as autoantibodies in their differential diagnosis. Autoimmunity to type II collagen is involved in relapsing polychondritis, a multisystem disorder in which destruction of the cartilages of the nose, ears and upper airway is prominent.

004

Classification and diagnosis of sinonasal adenocarcinomas

*I. Leivo**
*Haartman Institute, Dept. of Pathology, Helsinki, Finland

Salivary gland-type sinonasal adenocarcinomas can occur in the sinonasal tract, and they resemble the corresponding tumours in salivary glands. The most common types are adenoid cystic carcinoma and adenocarcinoma, not otherwise specified. Intestinal-type sinonasal adenocarcinomas mimic the histological appearances of intestinal adenomas, carcinomas, or rarely even the normal intestinal mucosa. Occurrence of the intestinal-type sinonasal adenocarcinoma has been associated with long-term exposure to hardwood (beech, oak) dusts. In the woodworking industry, these tumours can be 1,000 times more common than in the general population. The average exposure time is 40 years. Histologically, the most common appearances resemble colonic adenocarcinomas. If the resemblance is striking, the rare possibility of a metastasis from the gastrointestinal tract should be considered. Similar to colonic adenocarcinomas, intestinal-type sinonasal adenocarcinomas stain for CK20, CDX-2, and MUC2, but they also stain for CK7. Thus, the differential diagnosis between a primary intestinal-type sinonasal adenocarcinoma and a metastatic colonic adenocarcinoma cannot be based on histomorphology or immunophenotype alone. Then, the recommended approach is colonoscopy. The intestinal-type sinonasal adenocarcinoma is a high-grade malignancy. However, the prognosis of patients with hardwood dust exposure is better than in sporadic tumours. In addition, papillary growth patterns relate to a more favourable outcome. Low-grade sinonasal adenocarcinomas have not shown occupational or environmental associations. Histologically, they are papillary or glandular, with a single layer of uniform epithelial cells. Cytologically, they are bland, but malignancy is revealed by the complexity of architecture and invasive growth. Low-grade sinonasal adenocarcinomas do not express intestinal immunophenotypic markers.

Friday, 3 September 2010, 17.00–18.30, Sala Wystawowa A

WGS-43 Lymphoproliferative diseases Pediatric WG Business Meeting

Chairpersons: I. Scheimberg, United Kingdom
M. Pronicki, Poland

001

ID post transplant lymphomas: pediatric post-transplant lymphoproliferative disorders: pathology, etiology, tumor biology and epidemiology

*B. Ngan**
*Hospital for Sick Children, PediatricLabMed, Toronto, Canada

Background: Post-transplant lymphoproliferative disease (PTLD) is an important cause for morbidity and mortality in transplant recipients. Pathologically, PTLD is heterogeneous and is characterized by a spectrum of lymphoid proliferations that ranges from reactive lymphoid hyperplasia, non-clonal atypical lymphoid cells and or plasma cell proliferations to infiltrates of polymorphous, mono- or polyclonal lymphoid cells to monoclonal lymphoid cells with histopathogical features of non-Hodgkin or Hodgkin lymphoma of non-transplant patients.
Method: Pediatric PTLD biopsies in solid organ transplant recipients over a 30-year period were reviewed.
Results: There were 80 PTLD cases (12.1%) in 662 transplant recipients (217 liver, 203 heart, 197 kidney, 26 lung, 13 multivisceral and 6 small bowel). PTLD occurred in 16.5% liver, 13.8% heart, 5.1% kidney, 15.4% lung, and 23% multivisceral recipients. Thirteen PTLD had infectious mononucleosis-like and/or atypical EBV+ve lymphoid hyperplasia; five EBV-ve lymphoid hyperplasia; three EVB+ve plasmacytic hyperplasia; 14 EVB+ve polymorphous monoclonal B; 13 EVB+ve polymorphous monoclonal B, 16 EVB+ve monomorphous, monoclonal B, three were Burkitts with c-Myc translocation; five EVB-ve monomorphous, monoclonal B; 1 EVB+ve PTCL; three EVB-vePTCL; one EVB+ve Hodgkin; and one EBV-veHodgkin. Three PTLD cases had EBV+ve spindle cell tumor.
Conclusion: Histopathological diagnosis plays a central role in the identification of PTLD for the management and treatment of PTLD. It is also important in assessing the epidemiology and the understanding of the pathogenesis of PTLD. There is a high association with EBV. This study confirmed the higher prevalence of PTLD in children as compared with the published data on adults by others as well as UNOS 1995 on children.

002

Recent developments in neuroblastoma

*C. Cullinane**
*United Kingdom

Peripheral neuroblastic tumours are a group of paediatric tumours composed of cells of neural crest origin. The tumours arise in the sympathetic nervous system and range from the malignant neuroblastoma at one end of the spectrum to the benign ganglioneuroma at the other end, with an intermediate group of the tumours showing a mixed pattern. They are classified according to International Neuroblastoma Committee Classification (INPC). Their presentation and behaviour is variable, which may lead to challenges in diagnosis and management. In some patients, the disease is aggressive and lethal in spite of multimodality treatment, whereas others have an excellent outcome with minimal treatment even in the presence of disseminated disease. This talk will provide an overview of the current classification system and recent modification with regard to nodular ganglioneuroblastoma, discuss the recently introduced International Neuroblastoma Risk Group system, delineate the role of pathologist with regard to the diagnostic information required in current and future neuroblastoma trials, and present an update on favourable and unfavourable prognostic factors.

Friday, 3 September 2010, 17.00–18.30, Aula Mała

WGS-44 Computational pathology

Chairpersons: A. Batistatou, Greece
P. van Diest, The Netherlands

001

Experiences in digital pathology

P. dalla Palma, E. Bragantini*
*S. Chiara Hospital Trento, Italy

Background: Computer-assisted microscopy (CAM) offers proven solutions in immunohistochemical assessments, sharing digital slides with collaborators in different places, storing and organize pathological and clinical data and research.
Method: We initially developed an in-house system for the creation of digital slides and for remote diagnoses on frozen sections, suggesting that digital pathology would become the new standard in surgical pathology. In our institution, we adopt CAM using the Aperio Scanscope Xs for several applications:
Results: (1) Detection and semiquantitative measurement of equivocal Her2 immunoreactivity and of Ki67 in breast

cancer—our data on over 350 cases with comparison between CAM and human evaluation and with FISH analysis strongly support its feasibility and reliability in routine practice; (2) to store and analyze tissue microarrays with all associated experimental and follow-up data, permitting fast access to adjacent sections and comparing stains across multiple slides; (3) to store clinical–pathological data of patients for discussion in multidisciplinary meetings and courses.

Conclusion: In our opinion, CAM provides a unique opportunity for image visualization and analysis, archival and retrieval, which in the near future will probably replace the usual microscopy in routine practice. Bibliography 1. The virtual case. Virchows Arch. 2002, 441(2):159–164. 2. Robotic telepathology for intraoperative remote diagnosis. Am J Clin Pathol. 2001 116(5):744–752. 3. Digital Pathology: Science Fiction? Int J Surg Pathol. 2000 Oct;8 (4):261–263. 4. TMABoost: an integrated system for comprehensive management of tissue microarray data. Technol Biomed. 2006 Jan;10(1):19–27.

002

Quantification of immunohistochemistry in digital pathology

*J. Schmid**
*USA

003

Automated vision quantitative assessment of Ki-67 proliferation index in a nationwide series of patients with breast cancer

J. Konsti, M. Lundin, H. Joensuu, J. Lundin*
*University of Helsinki, Finland

Objective: An automated method for immunohistochemical assessment of Ki-67 proliferation index was developed and evaluated.

Method: Using an open source image manipulation tool, ImageJ, a macro called IhcJ was created for the assessment of immunohistochemistry stainings. The performance of the IhcJ macro was evaluated in a tissue microarray series of breast cancer specimens from 1,334 patients. The specimens were stained with an anti-Ki-67 antibody, counterstained with hematoxylin and digitized. The Ki-67 proliferation index was calculated both visually and automatically with the IhcJ macro (Fig. 1). The prognostic value of the Ki-67 proliferation index was evaluated in uni- and multivariate survival analyses.

Results: In a univariate survival analysis, the hazard ratio of distant recurrence during a median follow-up of 9.5 years for the automated Ki-67 medium area fraction was 1.77 (95% CI 1.31–2.37) and for the large area fraction 2.34 (1.76–3.10). Corresponding results for visual Ki-67 proliferation index were 1.41 (0.83–2.39) and 2.58 (1.52–4.37). In a multivariate survival analysis adjusted for known main prognostic factors, the hazard ratio for the automated Ki-67 area fraction was 1.62 (1.10–2.39) and 1.73 (1.19–2.51) for medium and large area fraction groups, respectively. The visual Ki-67 proliferation index was not a significant predictor in a multivariate survival analysis.

Conclusion: Multivariate survival analyses suggest that unlike the visual Ki-67 proliferation index, the automated Ki-67 area fraction is an independent predictor of outcome in breast cancer when other main prognostic factors are taken into account.

004

Five years of experiences with WebMicroscope for teaching basic and oral pathology in a practical course

J. Szymas, M. Lundin*
*University of Medical Sciences, Dept. of Clinical Pathology, Poznan, Poland

During the past 5 years, we have completed a transition of the basic and oral pathology practical courses from light to virtual microscopy. After a pilot feasibility study, the entire training set of glass slides was digitized and located on WebMicroscope server. Giving access to the web, computers have become perfect companions of the students. The study material consists now of over 400 fully digitized slides covering 15 entities in basic pathology and 15 entities in oral pathology. Digitized slides are linked with still macro- and microscopic images, organized with clinical information into virtual cases. We undertake a comprehensive evaluation of this new approach at the end of every academic year. In these surveys, students rate the software, the quality of the images, handling of the images, and effective use of virtual slides during the time of the practical. Satisfaction surveys demonstrate a steady improvement over the past 5 years as various student suggestions were implemented. An overwhelming majority of our students considered using digitized slides at their convenience as highly desirable. Overall, the quality of the images was rated as very good. However, due to the limitation of resolution of few primary scans, we have rescanned these slides at ×40 objective and a 3,900 × 3,090-pixel camera to alleviate these problems. Our students and faculty consider the virtual microscope as a significant improvement. The administrators of our department consider virtual microscopy as innovative and cost-effective because there is no longer the expense of the

maintenance and replacement of microscope and glass slides.

005

A web-based examination system for students using WebMicroscopy for learning oral pathology

J. Szymas, M. Lundin, J. Lundin*
*University of Medical Sciences, Dept. of Clinical Pathology, Poznan, Poland

We have developed and evaluated a user-friendly online interactive teaching and examination system for pathology courses. Already in 2006, at the end of the first course, students take a multiple-choice question exam (one correct answer per question). Every exam question is linked with a proper virtual slide and the time for the answer is unlimited. This examination system uses advanced HTML features, and the Web browser that can handle frames, JavaScript and cookies is required. Setting the screen to a resolution of 1,024 × 760 or higher and decreasing the size of the menu bars if necessary is helpful in viewing the digitized histological slide and the question at the same time. Specific instructions about answering the questions are also given at the beginning of the examination. A score is generated for questions which are correctly answered. The scores are accumulated until the student decides to quit the Web browser. In the last 5 years, an overall 92% concordance rate has been achieved on practical examination based on 50 virtual slides connected with 50 multiple-choice questions per student. The online practical examination system was evaluated by the students using a questionnaire. Students were asked to reply to a survey to evaluate the usefulness of digitized slides for practical examination. All students preferred the online examination to a traditional microscope and paper-and-pencil examination and all felt that the quality of digitized slides was superior to that of classical glass slide and allowed to make a more accurate diagnosis (rating 9.5 out of 10).

006

Use of gray level co-occurrence matrix in detecting corresponding fragments and evaluating quality of virtual slides

S. Walkowski, J. Szymas*
*Poznan University of Technology, Faculty of Computing Science, Poland

Virtual slides may be acquired using various scanners, produced by different companies. Pathologists who examine digital images captured by different scanners may subjectively assess their quality. In this work, an algorithm which may objectively compare the quality of virtual slides is proposed and implemented. In the first step, the algorithm selects some fragments of the slide captured by one scanner. Then, it finds these fragments in virtual slides acquired by scanning the same glass slide using other devices. This is done by creating overviews of the whole slides (by zooming them out) and calculating gray level co-occurrence matrices (GLCM) for each selected fragment and for the overviews of other slides using windows of adequate size. Comparing some of the Haralick features of the matrices (especially measures related to orderliness) allows estimating the positions of the fragments in other virtual slides. Detected areas, in original resolution, are used to calculate GLCM and its Haralick features again. This time, measures for evaluating the quality (like contrast) are used. Aggregation of the calculated values allows comparing the relative quality of the virtual slides. This method is tested on two sets of ten virtual slides. They were created by capturing the same set of glass slides using two different devices: robotic microscope Axioscope2 (Zeiss) equipped with AxioCam Hrc CCD camera and DeskScan (Zeiss) with standard equipment. Acquired images were stitched and converted by specialized software based on advances in aerial and satellite imaging.

007

Color/Image quality standardization in whole slide imaging

*Y. Yagi**
*USA

Free Papers Sessions

Wednesday, 1 September 2010, 14.30–16.30, Aula Duża A

FP-01 Free papers 1

001

Vacuum-assisted needle core biopsy in breast: correlation between the types of microcalcifications and the histopathology diagnosis and between the histopathology diagnosis of the biopsy and the definitive histology

M. Lacerda, P. Figueiredo, B. Duarte, F. Lopes, A. Costa, I. Gomes*
*I.P.O.Coimbra, Dept. of Surgical Pathology, Portugal

Objective: Vacuum-assisted needle core biopsy in breast (VANCB) is becoming the gold standard for non-palpable

breast lesions with microcalcifications (4). To analyze the correlations between: (1) types of microcalcifications (Le Gal classification) (1, 2) and the histological classification in B categories of the European Working Group on Breast Pathology (EWGBP) (3); (2) pre-operatory histological diagnosis of the VANCB and the definitive histological diagnosis after surgery.
Material and methods: Two hundred eight consecutive cases of VANCB of non-palpable breast lesions with microcalcifications were carried out from January 2006 to 0ctober 2009. VACORA Vacuum Biopsy System; 12–24 cores were obtained with 10-G needles. The cores and the respective paraffin blocks were X-rayed (5).
Results: (1) One hundred percent agreement of the type V Le Gal with B5 category of the EWGBP; 73.2%, 17.2%, 4.1% agreement of the type IV Le Gal with B4+B5, B2, B3 categories of the EWGBP, respectively; 42.0%, 37%, 6.9% agreement of the type III Le Gal 42.0%, 37%, 6.9% agreement with B5+B4, B2, B3 categories of the EWGBP, respectively. For type II Le Gal, 22.4%, 53.1%, and 8.2% agreement with B5+B4, B2 and B3 categories of the EWGBP, respectively. (2) One hundred percent agreement for B5 category of the EWGBP classification with the definitive histological diagnosis.
Conclusion: VANCB in breast lesions assisted the therapeutic decisions. A close interdisciplinary approach assured optimal results (6).

002

Careful initial clinical–radiologic–pathologic correlation should dictate clinical management of equivocal fibroepithelial lesions diagnosed on core biopsy

E. Resetkova, C. Albarracin, E. Arribas, N. Sneige*
*MDACC, Dept. of Pathology, Houston, USA

Objective: Equivocal fibroepithelial lesions (FEL) diagnosed on core biopsy (CB) may prove to be either fibroadenoma (FA) or phyllodes tumor (PT) at excision, due to which their management is controversial.
Method: (1) To study the outcome of 136 patients with FEL on CB over a 7-year period at our institution. Consensus on initial patient's clinical management was reached during a multidisciplinary conference based on correlation of clinical data, radiology, and pathology. (2) To examine if any clinical, radiologic or histologic parameters could predict final classification, we retrospectively reevaluated imaging findings (mammography and sonography) as well as multiple histologic criteria (e.g. pattern, stromal cellularity, stromal atypia, mitosis, etc.) on CB and correlated these with diagnosis at excision.
Results: (1) Of 57 excised lesions, 18 were classified as PTs, 10 as benign cFELs and 29 as FAs. In 79 patients with no excision, no evidence of disease progression was observed (40±21 months, mean ± SD). FELs with indeterminate or suspect imaging findings, larger size, and an equivocal comment such as "cannot rule out PT" in the pathology report were excised more frequently (P=0.05, P=0.034 and P=0.01, respectively). (2) Final diagnoses did not correlate with retrospective evaluation of any clinical data, imaging findings or histologic parameters.
Conclusion: Careful initial clinicopathologic and radiologic correlation may select majority of clinically significant lesions for proper surgical management. Follow-up may be an appropriate alternative for a subset of patients, given a good correlation. No radiologic or histologic parameters or clinical data on their own are distinctive enough to predict final classification of FELs.

003

Interpretation of topoisomerase 2a immunohistochemical stains in breast carcinoma. How to set the proper cutoff for a positive status?

W. P. Olszewski, A. Piascik, A. Wojnowska, K. Suszylo*
*Center of Oncology, Dept. of Pathology, Warsaw, Poland

Objective: Inconclusive results of the role of topoisomerase 2a (TOPA2a) in breast carcinoma biology and therapy are partially due to numerous thresholds of positivity measured by immunohistochemical (IHC) analysis. In the presented study, different criteria found in literature of the subject were compared with results of TOPA2a IHC-evaluated material (138 cases). In our study, we have the possibility to evaluate TOPA2a in breast cancer cells using two methods (immunohistochemistry (IHC) and fluorescence in situ hybridization (FISH)) in all cases. As a part of a broader study, we also were able to correlate the results of TOPA2a in in situ carcinoma, benign lesions and breast tissue without pathological changes. We have also analyzed other prognostic and predictive factors as well as clinical outcome.
Method: Using IHC and FISH methods, we compared the percentage of stained cells, strength of nuclear stain, presence of co-expressed cytoplasmatic and membranous stain, amplification of TOPA2a gene and also response to anthracyclin-containing chemotherapy from clinical data.
Results: Analyzing the obtained data, we set our own cutoff points. We assumed that the best correlation both with genomic aberrations and other data listed above, which we considered important in this study, is when both the percentage and strength of stain are taken into account. In our study, a cutoff point for positive TOPA2a status evaluated by IHC method is at least 10% of carcinoma cells with strong (3+) nuclear stain or at least 50% of carcinoma with intermediate (2+) nuclear stain.
Conclusion: The presented criteria as defined above correlate with amplification (ratio ≥1.5) and response to

anthracyclin-based neoadjuvant therapy (measured by DFS and OS).

004

PARP1 expression in breast cancer including BRCA1-associated, triple-negative and basal-like tumours: implications for anti-PARP1 therapy

P. Domagala, T. Huzarski, J. Lubinski, K. Gugala, W. Domagala*
*Pomeranian Medical University, Dept. of Pathology, Szczecin, Poland

Objective: Despite several ongoing trials of PARP inhibitors in the treatment of breast cancer (BC), PARP1 protein expression in BCs is not known. The purpose of this report is to assess the expression of PARP1 in BC including BRCA1-associated, triple-negative (TN) and basal-like (BL) tumors.
Method: Immunohistochemistry with a PARP1 antibody on tissue microarrays from 130 BRCA1-associated and 594 non-BRCA1-related BCs was used.
Results: Nuclear PARP1 expression was found in 93.1% (121/130) of BRCA1-associated and 97% (576/594) of non-BRCA1-related carcinomas. There was a significant difference between the mean nuclear PARP1 histoscore in BRCA1-associated versus non-BRCA1-associated carcinomas in all tumors ($p<0.0001$), in the BL group ($p=0.0086$), TN ($p=0.0015$) and non-BL groups ($p=0.016$), but not in the non-TN group. Among BRCA1-associated BCs, low PARP1 expression was found in 18.5% of all cases, 18.9% (17/90) of BL and 21% (22/105) of TN cancers. PARP1 negativity was determined in 6.9% of all tumors, 7.7% of basal-like and 7.6% of TN cancers. Among non-BRCA1-related tumors, low PARP1 expression was found in 8.8% of all cases, 3.1% of BL tumors, and 2.7% of TN cancers. Three percent was PARP1-negative.
Conclusion: PARP1 expression is significantly associated with BRCA1 status in BL and TN BCs. Because carcinomas with null or low PARP1 expression may show no or a partial response to PARP1 inhibitor therapy, the assessment of PARP1 expression in tumor samples by immunohistochemistry may improve the selection of BC patients for PARP inhibitor therapy.

005

A retrospective study of c-kit and PDGFRa mutations and EGFR amplification in endometrial stromal sarcomas: a report from the Spanish Sarcoma Group (GEIS-18)

R. Sardinha, T. Hernandez, S. Fraile Martín, F. Tresserra, A. Vidal, M. C. Plaza, A. Astudillo, N. Hernández, C. Balaña, E. de Alava*
*HESE, E.P.E, Serviço de Anatomia Patológica, Évora, Portugal

Objective: The expression of tyrosine kinases in endometrial stromal tumors is controversial. Several sporadic responses to imatinib have been observed in metastatic endometrial stromal sarcomas (ESS). We therefore aimed to perform a retrospective analysis of possible molecular targets in ESS: c-kit, PDGFRa and EGFR.
Method: Paraffin blocks from 67 patients with previous diagnosis of low-grade ESS and high-grade endometrial sarcomas from nine different institutions were examined and reviewed. Exons 9, 11, 13, and 17 of the c-kit gene and exons 12 and 18 of the PDGFRa gene were amplified by PCR and sequenced. The incidence and distribution of the KIT, PDGFRa, CD10 and Calponin expression were examined by immunohistochemistry, and EGFR amplification was assessed by fluorescence in situ hybridization (FISH).
Results: No mutations in c-kit and PDGFRa genes were detected. We observed several polymorphisms: I798I, exon17 (2/67); V824V, exon 18 (21/67); P567P, exon 12 (64/67); and one case with a double polymorphism V824V/G838G. Overexpressions of KIT, PDGFRa, CD10 and Calponin was detected in 2 (3%), 23 (34%), 30 (45%) and 26 (39%) cases, respectively, whereas amplification for EGFR gene by FISH was not detected.
Conclusion: Expression of KIT in cases of ESS is infrequent and always weak. PDGFRa expression was observed in 34% of the cases studied. We did not observe any mutations of c-kit and PDGFRa or amplification of the EGFR gene. So it is unlikely that patients with ESS can benefit from therapies with anti-EGFR and/or c-kit tyrosine kinase inhibitors.

006

Uterine tumors resembling ovarian sex cord tumors. A study of five cases

E. Bakula-Zalewska, A. Nasierowska-Guttmejer, A. Daska-Bidziska, M. Bidziski*
*Institute of Oncology, Dept. of Pathology, Warsaw, Poland

Objective: Uterine tumours resembling ovarian sex cord tumours (UTROSCT) cause confusion with respect to nomenclature as well as diagnostic difficulties. These tumours belong to the group of low-grade malignant neoplasms, and their clinical course likely depends on the percentage of the sex cord-like component. Morphologically, they can be divided into two groups: those with <40% sex cord-like areas (type 1) and those with more than 40% (type 2).
Method: Five patients with primary UTROSCT underwent treatment in the Cancer Center, Warsaw, between 2000 and 2010. Biopsies or excisions from all tumours were examined microscopically and immunohistochemically

(IH). Treatment and follow-up were correlated to histopathological diagnosis.
Results: Patients ranged from 24 to 69 years of age and tumour size from 3 to 24 cm. Tumours contained 25% to 70% of sex cord component (two tumours of type 1 and three of type 2). By IH examination, the sex cord-like component was keratin-positive in all five cases, while the stromal component was positive for CD10 and negative for h-caldesmon. In addition, PGR positivity was found in all cases, while SMA, CKAE1/3 and inhibin was positive in three. Four patients were treated with gestagens in addition to surgery. No recurrences were noted in any of these four patients over a 2- to 10-year period of follow-up.
Conclusion: A correct subclassification of sarcomas of UTROSCT type is of crucial importance since most patients with these rare neoplasms respond well to gestagen therapy and have a good prognosis compared to other endometrial stromal sarcomas.

007
CD 56 expression in serous invasive ovarian cancer and serous ovarian borderline tumors

W. Pokieser, S. Hauptmann*
*Wilhelminenspital Wien, Dept. of Pathology, Austria

Objective: CD56 is a cell surface glycoprotein that plays a critical role as adhesion molecule for the guidance of migration of neuronal cells during embryofetal development. It is also expressed on adult neuroendocrine cells, hematological neoplasms, as well as in various carcinomas.
Method: In this study, we retrospectively investigated the expression of CD56 in a series of 101 serous ovarian carcinomas and 37 serous borderline tumors and analyzed the significance of this marker with regard to patient outcome. Neuroendocrine cells were determined by immunohistochemical positivity of highly specific chromogranin A. Patients were treated homogenously by use of radical surgery and combined chemotherapy (carboplatin and taxol) in the case of carcinoma and of surgery alone for borderline tumors. Follow-up data were available for all patients.
Results: Sixty-seven cases (66%) of 101 invasive carcinomas, but only 1 of 37 (3%) borderline tumors, were positive for CD56 ($p>0.0001$), indicating that this phenomenon is significantly more present in invasive lesions. CD56 expression in the borderline tumor was accompanied by the presence of single scattered chromogranin A-positive neuroendocrine tumor cells, whereas in serous ovarian carcinomas, co-expression was only seen in less than a quarter of cases.
Conclusion: Our results demonstrate that CD56 positivity is much more frequently found in serous ovarian carcinomas than in serous borderline tumors; however, expression of CD56 had no prognostic effect. On the other hand, CD56 should not be used as a marker for neuroendocrine differentiation in serous neoplasm. Because of different chemotherapies in neuroendocrine ovarian carcinomas, specific neuroendocrine markers like chromogranin A or synaptophysin are recommended in these cases.

008
Are the cancer–testis (CT) antigens reliable markers of stem cells in squamous cell carcinoma of vulva?

J. Sznurkowski, A. Zabrocki*
*Medical University of GdaDsk, Dept. of Gynaecological Oncology, Poland

Objective: Vulvar cancer represents 3–5% of all gynecological malignancies. Squamous cell carcinoma is a predominating malignancy at this site as it accounts for approximately 85–90% of vulvar cancers. Analyses of humoral and cellular immune responses to autologous cancer determined cancer–testis (CT) antigens as potential targets for immunotherapy. As their expression has been identified in a variety of malignant neoplasms, they appeared as potential candidates for target therapy, i.e. T cell-mediated immunotherapy of cancer.
Method: Seventy-six patients with verified histopathological diagnosis and full clinical history were included into the study. The slides were incubated with the monoclonal antibody against MAGE-A1, MAGE-A4 and NY-ESO-1. All statistical analyses were performed with the statistical software Statistica 8.
Results: The expression of NY-ESO-1 was revealed in one case. The expression of MAGE-A4 and MAGEA-1 was identified in 66% and 12% primary tumors, 69% and 19% lymph node metastases and 54% and 33% local recurrences, respectively. Cytoplasmatic expression of these antigens was identified in suprabasal and squamoid cells of SCC (Fig. 1).
Conclusion: Vulvar SCC expresses CT antigens; however, their expression is restricted to the maturing squamoid cells of the intermediate level. This pattern of expression suggests that CT antigens are not reliable markers of tumor stem cells in vulvar SCC.

Wednesday, 1 September 2010, 17.00–18.30, Aula Duża B

FP-02 Free papers 2

002
Expression of c-kit protein does not correlate with prognosis in salivary gland carcinomas

I. Stárek, L. Kucerová, A. Skálová*
*Faculty Hospital, ENT, Olomouc, Czech Republic

Objective: The objective was to investigate the expression of c-kit protein in salivary gland carcinomas and to correlate it to prognosis.
Method: Immunohistochemistry for c-kit protein was performed in 33 carcinomas using formalin-fixed paraffin-embedded sections. For the evaluation of reactivity of tumor cells, a combination of the cytoplasmatic and/or membranous staining and the percentage of positive cells were applied. Only cases without any staining pattern were considered negative. For prognostic correlation, univariate disease-specific survival curves were calculated by the Kaplan–Meier method and distributions were compared using the log-rank test.
Results: Of all 33 cases, only six were c-kit-negative, including three low-grade mucoepidermoid carcinomas, two carcinomas ex pleomorphic adenoma and one salivary analogon of secretory mammary carcinoma. The group of 27 (82%) positive tumors was dominated by nine adenoid cystic carcinomas (all but one revealing strong reaction), followed by five acinic cell, three each mucoepidermoid and salivary duct carcinoma, two carcinomas ex pleomorphic adenoma and five other tumors, in all of which positive staining ranged from 50% to 100%, with the immunoreaction varying from weak to strong. Disease-specific survival in c-kit-negative (n=6) carcinomas did not differ from that in positive (n=27) cases (χ^2 = 0.047).
Conclusion: Of all salivary gland carcinomas, only adenoid cystic carcinoma was regularly associated with c-kit expression. Immunoreactivity in other subtypes, considering our as well as published data, greatly varies. C-kit expression harbours no significant prognostic information.
Supported by grant NS9725-4/2008, IGA, Ministry of Health, Czech Republic.

003
Oral lesions and candidiasis

S. Sarioglu, I. Karaman, C. Ecevit, U. Pabuccuoglu*
*Dokuz Eylul University, Dept. of Pathology, Izmir, Turkey

Objective: Chronic hyperplastic candidiasis (CHC) is an oral infectious lesion with a potential for progression to squamous cell carcinoma (SCC). If the histopathological features associated with candidiasis are overlooked and special techniques for fungal identification are not performed, diagnosis may be missed.
Method: During 2003–2010, all oral specimens were evaluated with periodic acid Schiff stain for structures suspicious for fungal microorganisms, serum exudation, bacterial colonization, parakeratosis, keratosis, superficial neutrophilic infiltration of mucosal or neoplastic epithelium was observed in H&E-stained sections. Forty-four histopathological materials from 30 patients with candidiasis and 28 materials from 24 patients suspicious but histochemically negative for candidiasis are included in this study. All biopsies were scored semiquantitatively for the aforementioned parameters. Candidiasis-negative and -positive cases were compared for demographical, clinical and additional histopathological features.
Results: The most frequent site for CHC or candidiasis-associated SCC was the tongue (n=25, 56.8%). Six cases (20%) were associated with SCC and one case was a SCC following long-standing CHC at the precise localization. Mild dysplasia was observed in 13 (29.5%) cases and moderate dysplasia was identified in one (2.3%) case of CHC. Among the histopathological features, the scores of parakeratosis and superficial neutrophilic infiltration was significantly higher in cases with candidiasis (Mann–Whitney U, p=0.036 and p=0.001). Only parakeratosis was more evident in cases with increased number of fungal microorganisms (Kruskal–Wallis test, p=0.033).
Conclusion: Parakeratosis and superficial neutrophilic infiltration are the most important clues for candidiasis of the oral mucosa. Association of candidiasis with pre-neoplastic and neoplastic lesions is also noteworthy.

004
Fine needle aspiration cytology of basal cell adenoma of the salivary gland. A cytohistologic correlation study of 36 cases

J. A. Jimenez Heffernan, B. Vicandi, P. López Ferrer, P. Gonzalez Peramato, J. M. Viguer*
*Hospital Puerta de Hierro, Madrid, Spain

Objective: Few cytological series describing BCA are available and diagnostic cytological criteria are not well established.
Method: This study was based on 42 cytology samples from 36 patients with BCA. Thirty-six of the aspirations procedures were performed preoperatively and six on tumor recurrence. All cases had a histopathological study.
Results: Aspirates were cellular showing groups with stroma and single cells. Groups had a variable configuration with two major forms. Some were large, three-dimensional and puzzle-like, with little ramifications. Cells were densely packed and intimately related to metachromatic stroma. Others were of medium size with prominent prolongations consisting of an inner core of hyaline stroma surrounded by tumoral cells. Ten cases showed cylindromatous stromal structures. Seven aspirations were cystic. Stroma was homogeneous with non-fibrillary morphology. Neoplastic cells showed a variable morphology from small, basaloid to larger ones with epithelioid morphology. Moderate pleomorphism was seen in five cases. There were two misdiagnosis of acinic cell carcinoma, and two cases were

considered as suspicious of malignancy. After a revision of these cases, two showed features of BCA, while in the remaining two, the suspicious of malignancy persisted because of minimal amount of stroma, predominant epithelioid cell morphology and cellular density.
Conclusion: BCA shows characteristic features that allow in many cases a precise diagnosis. It may be difficult to differentiate from epithelial-rich pleomorphic adenoma, and in these cases, a diagnosis including both possibilities seems preferable. In our series, the absence of stroma was responsible for the misdiagnosis with acinic cell carcinoma in two cases.

005

SDHB expression in paraganglioma–pheochromocytoma syndromes: advantages and limits

A. Fassina, P. Tricarico, F. Schiavi, V. Guzzardo, R. Cappellesso, M. Bombonato, G. Opocher, M. Fassan*
*University of Padova, Dept. of Pathology, Italy

Objective: Pheochromocytoma and paraganglioma are rare tumors arising from chromaffin cells. Almost 10% of them are part of typical familial syndromes: Von Hippel–Lindau disease (VHL), neurofibromatosis type 1 (NF1), multiple endocrine neoplasia type 2 (MEN2) and type 1 (MEN1), pheocromocytoma–paraganglioma syndromes (PGLs; SDHB, SDHC, and SDHD) and a newly described syndrome related to TMEM127 gene mutations. Recently, SDHB immunohistochemical analysis has been proposed as a promising molecular marker for succinate dehydrogenase mutation-related neoplasms (i.e. PGLs).
Method: All cases of reported pheochromocytomas (n=160) and paragangliomas (n=57) between 1988 and 2009 were retrieved from the archives of the Department of Pathology of Padova University. FFPE specimens were genetically characterized for familial syndromes. Syndromic cases and a control group were semiquantitatively (0, 1+, 2+) evaluated for SDHB immunohistochemical expression.
Results: Out of 217 cases, 21 cases showed SDHD (n=3), TMEM127 (n=3), RET (n=6), MEN1 (n=2), VHL (n=4), or NF1 (n=3) germline mutations. The other six sporadic cases were evaluated as control. The three SDHD-mutated cases showed either negative (n=1) or 1+ (n=2) SDHB immunostaining. Completely negative staining was also observed in a sporadic case. A strong SDHB immunoreaction was observed in 19 and a weak immunoreaction in four of the remaining cases.
Conclusion: SDHB immunohistochemical analysis, even not PGL-specific, can be used to triage genetic testing in pheochromocytoma/paraganglioma patients. Further multi-institutional studies should investigate the diagnostic power of this remarkable novel diagnostic tool.

006

Biochemical and histological effects of sitagliptin on Zucker diabetic fatty rat pancreas

C. Mega, H. Vala, E. Teixeira de Lemos, J. Oliveira, R. Fernandes, L. Ferreira, F. Teixeira, F. Reis*
*SupPolythecnic Inst. Viseu, Agrarian Sup School–DZERV, Portugal

Objective: Inhibition of dipeptidyl peptidase-4 (DPP-4) activity by sitagliptin has been shown to improve glycemic control in patients with type 2 diabetes mellitus (T2DM) by prolonging the actions of incretin hormones, but the real impact of low-dose sitagliptin treatment on pancreatic lesions is almost unknown. This study aimed to evaluate the effects of sitagliptin on the biochemical and histological (pancreatic) parameters of Zucker diabetic fatty (ZDF, fa/fa) rats, an animal model of T2DM.
Method: Diabetic (fa/fa) ZDF male rats were treated with vehicle or sitagliptin (10 mg/kg body weight per day) during 6 weeks (n=8 each). The following parameters were assessed: serum glycaemia, HbA1c, insulin and lipid profile; serum and pancreas oxidative stress (MDA) and endocrine and exocrine pancreas histology, estimating and rating inflammatory infiltrate, fibrosis, vacuolization and congestion in a semiquantitative score ranging from 0 (minimal) to 3 (severe and extensive damage).
Results: Sitagliptin in diabetic ZDF rats promoted beneficial effects on dysglycaemia, dyslipidaemia, inflammatory profile and pancreatic oxidative stress. Endocrine and exocrine pancreas presented a reduction/amelioration of fibrosis severity, inflammatory infiltrate, intra-islet vacuolation, and congestion vs the vehicle-treated diabetic rats.
Conclusion: The favourable biochemical profile promoted by sitagliptin in the diabetic rats, together with protection against endocrine and exocrine pancreatic lesions, might represent a further advantage of low doses of sitagliptin in the management of T2DM.

Thursday, 2 September 2010, 14.30–16.30, Aula Średnia B

FP-03 Free papers 3

001

Defenders of the colon: comprehensive assessment of potential prognostic immunologic biomarkers in mismatch repair-proficient colorectal cancer

A. Lugli, E. Karamitopoulou, L. Terracciano, S. Piscuoglio, G. Iezzi, G. Spagnoli, K. Baker, A. Tzankov, I. Zlobec*
*University Hospital of Basel, Institute of Pathology, Switzerland

Objective: Evidence suggests a confounding effect of mismatch repair (MMR) status on immune response in colorectal cancer. To date, the identification of cell types involved in innate and adaptive immunity which may complement the established prognostic effect of CD8 in patients with MMR-proficient colorectal cancers, representing 85% of all cases, has not been performed.
Method: MMR-proficient colorectal cancers from 1,406 patients treated at different European centres were assigned to a test group (n=839), validation group 1 (n=358) and validation group 2 (n=209) and mounted onto single- and multiple-punch tissue microarrays. Immunohistochemistry was carried out for CD3, CD4, CD45RO, CD56, CD68, CD8, CD163, FoxP3, GranzymeB, HLA-DR, iNOS, Mast cell tryptase, Mum1, PD1 and TIA-1. Independent prognostic effects were analyzed on the test group, and reevaluated using both validation cohorts.
Results: In the test group, CD3, CD8, FoxP3, Granzyme B, and TIA-1 had a significant (p<0.01) positive impact on survival while only $CD8^+$ (p=0.0021) and TIA-1+ (p= 0.0062) maintained this effect in multivariable analysis which included postoperative therapy. Among patients with $CD8^+$ tumours, TIA-1 contributed additional independent prognostic information. Patients with $CD8^+$/TIA-1 cancers experienced a 143 HR (95%CI, 109–187) increased relative risk of death compared to $CD8^+$/$TIA\text{-}1^+$ cases, a result affecting 35% of patients. Findings were confirmed in both validation cohorts.
Conclusion: The prognostic effect of combined CD8/TIA-1 phenotypes is independent of TNM stage and adjuvant therapy. The additional analysis of TIA-1 in patients with $CD8^+$ tumours translates into improved risk stratification for approximately 35% of all patients with MMR-proficient colorectal cancers.

002

Is there a proximal shift in the distribution of advanced adenomas of the colon?

M. Kiedrowski, M. Kaminski, J. Orlowska, E. Kraszewska, A. Mroz, J. Regula, W. Olszewski*
*CMKP, Gastroenterology & Hepatology, Warsaw, Poland

Objective: Several studies have suggested an increase in the incidence of right-sided colorectal carcinomas (CRC). If the CRC right shift is true, it is also likely that the incidence of right-sided advanced adenomas (RSAA) should increase in time.
Method: Two large endoscopic datasets (RETRO and PBP) have been compared. RETRO contains data from the Department of Gastroenterology between 1981 and 1994. PBP covers data from the Polish national colorectal cancer screening program (2000–2004). Only patients with advanced adenomas who underwent total colonoscopy were included into the analysis. Advanced adenoma was defined as: villous or tubulo-villous, adenoma with high-grade neoplasia or ≥1-cm lesion. Two definitions of proximality were applied. The first defined right colon is proximal to the splenic flexure and the second, additionally, the descending colon. A logistic regression analysis was used to compare the incidence of RSAA between groups, adjusted for patients' age and sex.
Results: Two hundred and 2,188 patients with advanced adenomas were found in two datasets, respectively. Both groups differed significantly according to age and sex. To adjust for possible confounders, the multivariate model was fitted.
Conclusion: There was no statistically significant increase in the proportion of patients with RSAA between both groups when adjusted for patients' age and sex.

	No of patients with RSAA	Percentage	No of patients with RSAA	Percentage
RETRO	41/200	20,5%	53/200	26,5%
PBP	550/2188	25,14%	705/2188	32,22%
	1st definition of proximality OR 1.32, 95% CI 0.82-1.89, p=0.131(adjusted for age and sex): no difference		2nd definition of proximality: OR 1.33, 95% CI 0.96-1.85, p=0.089 (adjusted for age and sex): no difference	

003

Loss of MSH2 expression in adenomas may predict a more aggressive tumor phenotype in patients with concomitant colorectal carcinoma

E. Karamitopoulou, A. Lugli, G. Peros, I. Panayiotides, E. Patsouris, I. Zlobec*
*University of Athens, 2nd Dept. of Pathology, Greece

Objective: Loss of the mismatch repair (MMR) protein MSH2 in normal colorectal mucosa has been linked to an increased risk of sporadic colorectal adenoma and with modifiable risk factors for colorectal cancer. The aim of this study was to determine whether loss of MMR proteins MLH1, MSH2, MSH6 and PMS2 in colorectal adenomas could predict a more aggressive tumor phenotype in patients with concomitant colorectal carcinoma.
Method: Two tissue microarrays (TMAs) were constructed from 49 cases of synchronous adenoma and matched colorectal cancer with full clinicopathological information and follow-up. The first included punches from carcinomas and the second from matched adenomas. TMA sections

were immunostained for MLH1, MSH2, MSH6 and PMS2 and, in negative cases, reconfirmed on corresponding whole tissue sections.

Results: Patients with MSH2-negative adenomas (n=10, 21.3%) experienced a significantly worse outcome compared to MSH2-positive (n=37, 78.7%) patients (p=0.043). Additionally, 50% of all deaths in the MSH2-negative subgroup occurred within the first 18 months after diagnosis. Evaluation of relative risks of death at 2 years of follow-up yielded a hazard ratio of 0.34 (95% CI, 0.1–0.99). Moreover, negative expression of either MLH1 or MSH2 further stratified patients by survival time with a relative risk of death of 0.3 (95%CI, 0.09–0.9; p=0.029).

Conclusion: Our preliminary results show that loss of MSH2 in adenomas from patients with synchronous colorectal cancers may predict a significantly worse outcome. If confirmed in larger prospective studies, MSH2 analysis may be useful as a screening tool to identify patients who may benefit from closer follow-up.

004

Immunological microenvironment of tumour buds in colorectal cancer stratified by mismatch repair status

I. Zlobec, P. Minoo, L. Terracciano, K. Baker, A. Lugli*
*University Hospital Basel, Institute of Pathology, Switzerland

Objective: The aims of this study were to characterize the immunological microenvironment of tumour buds and evaluate the prognostic effect of immune markers and their ratios with tumour budding stratified by mismatch repair (MMR) status.

Method: Paraffin-embedded tumour blocks from 297 patients with colorectal cancer were cut in series and double-immunostained for CK22 with anti-CD138, -CD16, -CD20, -CD21, -CD56, -CD68, -CD8, -FOXp3, -Granzyme B, -Mast cell tryptase, -CD3, and -TIA-1 and stratified into MMR-proficient and -deficient cases. Tumour buds, immune cells and the ratio of immune cells/tumour buds was obtained.

Results: MMR-deficient tumours showed significantly less tumour budding (p<0.001) and greater amounts of $CD3^+$, $CD8^+$, and Granzyme B^+ cells (p<0.001). High amounts of $CD16^+$, $CD20^+$, $CD8^+$, $CD68^+$, $FOXp3^+$, Granzyme B^+ and $CD3^+$ were linked to improved survival (p<0.001). Prognostic effects differed between proficient and deficient tumours. Marker/budding ratios showed stronger relative risks of death when compared to most markers alone. In lymph node-negative patients, high marker/budding ratios of CD16 (HR, 0.29 (0.15–0.57)), CD68 (HR, 0.33 (0.17–0.63)), CD8 (HR, 0.31 (0.16–0.59)), FOXp3 (HR, 0.34 (0.18–0.64)) and Granzyme B (HR, 0.34 (0.17–0.65)) were independently linked to improved outcome.

Conclusion: Marker/budding ratios for $CD8^+$, $CD16^+$, $FOXp3^+$, Granzyme B^+ and $CD68^+$ are stronger prognostic features than the assessment of immune markers alone. These ratios are independent prognostic factors, particularly in lymph node-negative patients. Moreover, our findings underline the considerable confounding effect of MMR status in the evaluation of immune response in colorectal cancer.

005

Human crypt stem cell dynamics in juvenile polyposis (JPS) and Peutz–Jeghers (PJS) patients

D. Langeveld, F. Morsink, V. de Boer, J. Offerhaus, W. de Leng*
*UMC Utrecht, Dept. of Pathology, The Netherlands

Objective: Pre-tumour progression is a process that precedes the adenoma–carcinoma sequence; colorectal mucosa appears normal, but cell kinetic and stem cell abnormalities suggest the existence of molecular alterations. Pre-tumour progression can be made visible by studying methylation patterns, or tags, in stem cells of the crypt. Shibata et al. (2004) showed higher crypt methylation heterogeneity in normal-appearing colonic crypts of familial adenomatous polyposis (FAP) patients compared to normal crypt mucosa of non-FAP colons. This indicates enhanced stem cell survival, which may be a predictive marker of increased neoplastic outgrowth since longer lived stem cells have the potential to gain more mutations. The objective of this study was to investigate stem cell survival in juvenile polyposis syndrome (JPS) and Peutz–Jeghers syndrome (PJS), a biomarker predictive of pre-tumour progression.

Method: DNA was isolated from laser-microdissected crypts of normal colonic JPS and PJS tissue and age-matched controls. DNA was bisulphite-converted and methylation tags were created by amplifying the CpG islands in the CSX gene. Sequence analysis of this pool of methylation tags allows characterisation of the heterogeneity among the different tags recovered from multiple stem cell pools.

Results: Preliminary results show that JPS patients with an identified germline defect harbour a greater number of unique methylation patterns when compared to normal controls. However, this appears to be germline mutation-dependent since patients with a BMPR1A germline mutation show a significantly greater number of unique methylation patterns, indicating enhanced stem cell survival, and JPS patients with a SMAD4 mutation do not. PJS patients do not show an increased number of methylation patterns.

006

LKB1 promoter amplification in sporadic Peutz–Jeghers polyps

W. de Leng, L. Brosens, F. Morsink, P. Westenend, F. Giardiello, J. Offerhaus*
*UMCU Utrecht, Dept. of Pathology, The Netherlands

Objective: Peutz–Jeghers syndrome (PJS) is a dominantly inherited disorder characterized by gastrointestinal hamartomatous polyposis, mucocutaneous melanin pigmentation and an increased risk of cancer at a relatively young age. Inactivation of tumor suppressor gene LKB1 is the underlying germline defect in PJS patients. Cases of sporadic PJ polyps have been reported. It has been stated that these polyps are extremely rare and that the fact that no molecular data were found to support the PJS diagnosis is only due to failing techniques.
Method: We aimed to identify the molecular defect in six sporadic PJ patients. These patients are characterized by the presence of a distinct PJS polyp and most importantly the presence of arborizing smooth muscle. On these six, patients we performed LKB1 germline analysis and multiplex ligation-dependent probe amplification (MLPA) to detect exon deletions and amplifications.
Results: One-point mutation and two high-level amplifications of the LKB1 promoter were identified. Interestingly, this amplification was identified in an additional four PJS patients. To study the effect of this amplification on gene and protein expression, we performed a RT-PCR and WB in two patients. A significant reduction of LKB1 expression was found when PJS polyp, and normal tissue was compared to a panel of normal colon samples.
Conclusion: These results show that polyps that were based on histology sporadic PJ polyps are indeed PJS polyps, and these patients should be monitored accordingly. Interestingly, amplification of the LKB1 promoter resulted in decreased protein expression. The exact mechanism leading to this reduction remains to be determined.

007

Epidermal growth factor receptor and insulin-like growth factor 1 receptor expression predicts poor survival in pancreatic ductal adenocarcinoma

A. Witkiewicz, C. Solomides, B. Freydin, C. Martin, S. Singh, C. Yeo, S. Peiper*
*Thomas Jefferson University, Dept. of Pathology, Philadelphia, USA

Objective: Pancreatic ductal adenocarcinoma (PDA) is characterized by poor prognosis without effective treatment strategies. Epidermal growth factor receptor (EGFR) inhibitors in combination with gemcitabine are approved for the treatment of PDA, and there is an urgent need to identify patients who are likely to respond to targeted therapies. In this study, we evaluated the expression of EGFR and insulin-like growth factor 1 receptor (IGF-1R) in PDA and correlated it with survival and clinicopathologic variables.
Method: Ninety-eight cases of PDA were included in the study. Representative sections were stained with anti-EGFR and anti IGF-1R antibodies (Ventana, Tucson, USA). Cases were scored as negative (no staining), 1+ (incomplete membranous staining), 2+ and 3+ (complete membranous staining in <30% and >30% of tumor, respectively). For statistical analysis, EGFR and IGF-1R scores were dichotomized as low (0–2) versus high (3). IGF-1R gene copy number was evaluated by automated dual chromogen in situ hybridization (ISH, Ventana, USA). For ISH, chromosome 15 (red signal) and IGF-1R (black signal) were counted in 50 cells. Association between EGFR and IGF-1R expression and pathologic variables was analyzed using Fisher's, Wilcoxon and log-rank tests.
Results: Expression of IGF-1R protein correlated with gene amplification by ISH. Significant association was observed between the presence of lymph node metastasis and high EGFR expression ($p=0.038$). Univariately significant predictors of the overall survival included EGFR, IGF-1R, lymph node status and tumor size. In multivariate model, high EGFR expression was the strongest predictor of poor survival.
Conclusion: EGFR and IGF-1R expression are important for PDA aggressiveness. The relationship between two receptors may have therapeutic implications.

008

Expression of podoplanin, vascular endothelial growth factor C and D in esophageal cancer

M. Kozlowski, L. Chyczewski, M. Garbowicz, R. Milewski, J. Niklinski, J. Laudanski*
*Medical University of Bialystok, Dept. of Thoracic Surgery, Poland

Objective: Lymph node metastasis is an important prognostic factor in esophageal cancer. Vascular endothelial growth factor C (VEGF-C) and vascular endothelial growth factor D (VEGF-D) are considered to induce both lymph node metastasis and lymphatic involvement in various cancers related to lymphangiogenesis. In many types of cancer, podoplanin (D2-40) immunostaining has recently been used to detect lymphatic vessel invasion (LVI), but invasion detected

using D2-40 immunostaining for a predictor of nodal metastasis was controversial. We examined the relationship between VEGF-C, VEGF-D and LVI and clinicopathological features in 53 patients with esophageal cancer who underwent esophagectomy.
Method: VEGF-C, VEGF-D and podoplanin expression was examined using immunohistochemical staining in surgically resected tissues. Differences in categorical data were assessed by a chi-square test or Fisher's exact test.
Results: Podoplanin expression was observed in the endothelial cells of lymphatic channels. None of podoplanin-positive vessels were blood vessels. Intratumoral lymph vessels were small and collapsed, while peritumoral lymphatic vessels with LVI were dilated and large. The expression of VEGF-C and VEGF-D protein was recognized in the cytoplasm of cancer cells, but not in the nucleus. We found that peritumoral LVI significantly correlated with lymph node metastasis (p=0.001), pathologic stage (p=0.003), tumor depth (p=0.038) and tumor size (p=0.014). The expression levels of VEGF-C and VEGF-D were associated with LVI.
Conclusion: VEGF-C, VEGF-D and peritumoral LVI may play an important role in lymphangiogenesis and the process of lymphatic metastasis of esophageal cancer.

Thursday, 2 September 2010, 18.00–19.30, Aula Duża A

FP-04 Free papers 4

001
16S rDNA heterogeneity analysis using RFLP and phylogenetics (SHARP-Screening) suggests a pathogenetic role of Alcaligenaceae species in pulmonal extranodal marginal zone lymphoma of MALT-type (BALT lymphomas)
P. Adam, U. Hentschel, C. Gernert, F. Nagl, E. Haralambieva, L. Quintanilla-Martinez, F. Fend*
*Medical University Tübingen, Institute of Pathology, Germany

Objective: For several anatomical localisations of extranodal marginal zone lymphoma of MALT type (eMZCL), an association with chronic inflammation caused by microbiological agents (e.g. *Helicobacter pylori* in the stomach) has been described. In the lung, a link between lymphomagenesis and a defined causative organism is still missing.
Method: A comprehensive diversity survey using 16S rDNA library construction followed by restriction fragment length polymorphism (RFLP) analysis, sequencing and phylogenetic tree construction was employed on nine cases each of BALT lymphoma and control lung tissues (normal fetal lung, pneumonitis, cancer). This highly sensitive method, hereafter termed "SHARP-Screening", allows for the identification of the entire bacterial population in the tissue in a cultivation-independent manner. Following the results of SHARP screening, an Alcaligenaceae-specific PCR assay was employed on 20 additional BALT lymphoma cases and 21 control lung tissues.
Results: In eight of the nine cases of BALT lymphoma, bacteria of the Alcaligenaceae family (Alcaligenes, Achromobacter, AKIW733) were detected, whereas none of the control cases showed the presence of these clades. The subsequently performed Alcaligenaceae-specific PCR assay detected bacteria of the Alcaligenaceae family in 8 of the 20 independently investigated BALT lymphoma cases and in only one of 21 control lung tissues.
Conclusion: 16S rDNA library construction in combination with RFLP screening and phylogenetic analyses (SHARP-Screening) is a novel, molecular and cultivation-independent tool for the analysis of the microbial environment in chronic inflammation processes. Betaproteobacteria of the Alcaligenaceae family may be associated with and possibly involved in the lymphomagenesis of BALT lymphomas.

002
Biological signature of activated B cell receptor signaling in diffuse large B cell lymphoma
A. Bogusz, L. Chen, T. Currie, M. A. Shipp, S. J. Rodig, J. L. Kutok*
*Brigham and Women´s Hospital, Dept. of Pathology, Boston, USA

Objective: Diffuse large B cell lymphoma (DLBCL) is the most common type of non-Hodgkin lymphoma. Recently, major advances in the molecular characterization of DLBCL have been made through gene expression profiling studies that provided more insight into the biological heterogeneity within DLBCL. One of the identified molecular subgroups has been termed the "B-cell receptor (BCR)/proliferation cluster" due to the increased expression of BCR signaling cascade components including the spleen tyrosine kinase (SYK), which has emerged as an important therapeutic target within tumors of this subgroup. In fact, a recent clinical trial with a SYK inhibitor on uncharacterized DLBCLs has shown promising results, but only in a subset of patients.
Method: We employ a novel quantitative tissue-based immunohistochemical (IHC) methodology using markers

of activated BCR signaling to assess the activity of the BCR pathway in formalin-fixed paraffin embedded primary DLBCLs.
Results: Antibodies to phosphorylated forms of Lyn, SYK, BTK, BLNK and AKT as well as FOXO1 antibody represent attractive IHC markers to evaluate the activation of BCR signaling and comprise the basis of a biological signature of activated BCR signaling in DLBCL.
Conclusion: We report on the development of a quantitative tissue-based immunohistochemical (IHC) methodology employing activation-specific antibodies against multiple components of the BCR signaling pathway that will assess the activity of the BCR pathway in formalin-fixed paraffin-embedded primary DLBCLs. This approach will identify the subset of patient tumors that are actively signaling through the BCR pathway and, therefore, will predict therapeutic responsiveness to targeted inhibition of BCR signaling.

003

Enteropathy-associated T cell lymphoma: a clinicopathologic study focussing on prognostic factors and the frequency of defective T cell receptor chains

P. Czapiewski, P. Fisch, A. Schmitt-Graeff*
*Medical University of Gdansk, Dept. of Pathology, Poland

Objective: Enteropathy-associated T cell lymphoma (EATL) is a rare highly aggressive T cell neoplasm divided into type I ($CD8^-$, $CD56^-$) and type II ($CD8^+$, $CD56^+$). We assessed clinical, histological and immunohistochemical features of EATL and their association with the outcome of patients.
Method: Twenty-one EATL patients were reevaluated for tumor type, stage, general performance, nutritional status, and survival. Immunophenotyping included CD3, CD4, CD7, CD8, CD30, CD43, CD56, CD11c, CD123, MUM1/IRF4, TCRalfa/beta, TCRgamma/delta, Ki-67, TIA-1, granzyme-B and perforin. The statistical analysis was performed using Student's *t* test and Cochrane-Cox model.
Results: A partial or complete loss of CD3 antigen was observed in 7 of 21 cases. Three lymphomas were of the alpha/beta and three of the gamma/delta TCR type, while 14 lacked TCR chains. TIA-1 was detected in 21 of 21, perforin in 16 of 21 and granzyme B in 13 of 21. MUM1/IRF4 (9/21) was significantly associated with an anaplastic or immunoblastic morphology ($p=0.023$). Dendritic cells were abundant in all specimens. A significantly prolonged overall survival (OS) was observed in patients with lower stage (I+II vs. IV, $p=0.02$) and type I EATL ($p=0.02$), with a trend for longer OS in patients in good general performance ($p=0.096$) and nutritional status ($p=0.12$).
Conclusion: Tumor stage and histological type were prognostically relevant for our EATL patients. An aberrant T cell phenotype with loss of CD 3 and TCR chains was frequent in the consistently $TIA\text{-}1^+$ tumors. MUM-1/IRF4 may be a promising therapeutical target for a subset of EATL.

004

Fatal case of Epstein–Barr virus primo-infection, haemophagocytic syndrome in a 26-year-old patient treated with azathioprine for Crohn's disease: an autopsy case

S. Smolders, S. Rotman, L. de Leval*
*Universitary Hospital Lausanne, Dept. of Pathology, Switzerland

Objective: A 26-year-old man with a history of Crohn's disease, treated with azathioprine since 2 years, presented an Epstein–Barr virus (EBV) primo-infection and exacerbation of digestive symptoms.
Method: An ileo-colectomy was performed, which showed a fatal EBV lymphoproliferation disorder along with a haemophagocytic syndrome. EBV DNA load in the peripheral blood persisted to be high loaded during hospitalisation (479,000 copies per milliliter) despite triple antiviral treatment.
Results: Autopsy revealed a systemic lymphoproliferation involving lymph nodes, gastrointestinal mucosa and solid viscera (heart, kidney, lungs, prostate, brain). This was compounded of a population of large polymorphic B cell, hypertrophic macrophages and T lymphocytes, associated to haemophagocytosis. These massive infiltrations mimicked macroscopically as ulcers in the intestinal mucosa and ranged from polymorphic with plasmocytic differentiation to monomorphic large cells. Autopsy results confirmed the absence of Crohn's disease reactivation. The EBV infection was observed in all organs within the large images of the B cell lymphoproliferations. Further postmortem investigations revealed a deficit of the azathioprine's metabolisation enzyme thiopurine methyltransferase (TPMT).
Conclusion: We report and discuss herein the observations of a complete autopsy case along with the postmortem identification of the EBV infection type and TPMT mutation in a patient treated by azathioprine for Crohn's disease. Autopsy findings and further investigations helped explain the complicate clinical evolution and the fatal issue of the patient.

005

Autophagy and its regulation in neuroblastoma

H. Sartelet, T. Inbriglio, C. Nyalendo, C. Barelli, S. Cournoyer, P. Teira, M. Duval, G. Vassal*
*CHU Sainte Justine, Dept. of Pathology, Montreal, Canada

Objective: Neuroblastoma (NB) is a frequent paediatric tumour. Despite high dose of chemotherapy, metastatic tumours have poor outcome. Autophagy is a cellular self-degradative process adapting to stress. By suppressing altered organelles by the intermediate of autophagosomes, autophagy maintains cell survival, but can play a role in programmed non-apoptotic cell death. In cancer, autophagy has an important function, but still controversial. The aim of this study was to determine if autophagy is present and could be regulated in NB.
Method: Five tissue microarrays containing 184 NBs were studied. An immunohistochemistry method was used to identify the expression of LC3, a specific autophagosome marker, and beclin 1, a positive regulator of autophagy. In addition, four NB cell lines were treated in vitro with six drugs (temozolomide, LY294002, rapamycin, vincristin, doxorubicin and cisplatin). Cell survival was measured by MTT cell proliferation assay. The autophagic vacuoles were labelled with monodansylcadaverine, and the result was measured by the intensity of fluorescence. Autophagosome formation was monitored by immunodetection of LC3 cleavage and beclin 1.
Results: Low levels of autophagy are present in a majority of NB, but the autophagy level (expression of LC3) does not represent a prognostic factor. In contrast, higher levels of beclin 1 were detected in NB with poor prognostic. In vitro, autophagy is inversely proportional to cell survival when neuroblasts are in contact with NB's classic chemotherapeutic agents and AKT path inhibitors. However, temozolomide induces autophagy without increasing cell death.
Conclusion: Autophagy is present and could be modulated by chemotherapy in NB.

Friday, 3 September 2010, 14.30–16.30, Sala Wystawowa B

FP-05 Free papers 5

001
EGFR mutation testing in non-small cell lung cancer (NSCLC)—recommendations of the IASLC-ETOP Workshop

H. Popper, K. Kerr, M. Filipits, F. Herth,*
D. Grunenwald, R. Stahel, M. Dietel, E. Smit, R. Pirker
*Medical University of Graz, Institute of Pathology, Austria

Objective: Gefitinib has received European approval for the treatment of patients with NSCLC with activating mutations of the epidermal growth factor receptor (EGFR) tyrosine kinase. In Europe, EGFR mutation testing is not well established, preventing access to new targeted therapies for NSCLC.
Method: An IASLC-ETOP European multidisciplinary workshop developed recommendations to facilitate the implementation of standardized EGFR mutation testing in routine practice.
Results: The treating physician requests EGFR mutation testing. The results should be available within seven working days. All patients with NSCLC may be tested, but exceptions can be made for carcinoids, squamous, large cell neuroendocrine, and mucinous adenocarcinomas—there is a low likelihood of mutations. No consensus agreement was achieved for prescreening algorithms, although non-mucinous adenocarcinomas most likely harbor an increased percentage of mutations. For diagnosis, the most accessible tissue is sampled; re-biopsy at recurrence or disease progression should be considered. More data on the potential heterogeneity between different biopsy sites are required. The use of cytology samples needs to be evaluated. Tumor cell enrichment of samples is often required, depending on the test used. The tumor-to-normal cell ratio is important, although the minimum tumor cell number is ill defined. No standard method exists to detect EGFR mutations. Some evaluate the known activating mutations; others detect all mutations. New mutations might be difficult to interpret since activation status of the receptor has been defined for the most common ones.
Conclusion: The pathologic report should contain tumor histology, sample size/quality, tumor cell percentage, methodology used for EGFR mutations, exons tested and mutations present/absent.

002
The presence of intra-tumoral neutrophils is an independent prognostic factor in early-stage non-small cell lung carcinomas

M. Ilie, V. Hofman, C. Butori, C. Marquette,*
N. Vénissac, J. Mouroux, P. Hofman
*CHU de Nice, LPCE, France

Objective: Cancer-related inflammation has emerged as the seventh hallmark of cancer. In the tumor microenvironment, inflammatory cells, including neutrophils, influence almost every aspect of cancer initiation and progression, including tissue invasion and metastatic potential. However, the influence of intra-tumoral neutrophils in non-small cell lung carcinoma (NSCLC) progression is currently unknown. This study was conducted in order to correlate the number of tumor-associated neutrophils (TANs) and the prognostic of stage I NSCLC.
Method: Immunostainings on 320 stage I (120 T1N0 and 200 T2N0) NSCLC included on tissue microarrays were performed with anti-myeloperoxidase and anti-CD66b anti-

bodies and quantified using the Spotbrowser V7 software. Results were then correlated with overall survival (OS), disease-specific survival (DSS) and disease-free survival (DFS) of patients.
Results: The TANs ranged from 0 to 320 cells/mm^2 tumor tissue. The presence of TANs was associated with increasing tumor size (P=0.001). Number of TANs correlated with shorter OS (P=0.05), DSS (P=0.002) and DFS (P=0.05) of patients, independently of other prognostic factors.
Conclusion: The presence of TANs is a new independent prognostic factor for short disease-free, overall and cancer-specific survival in early stage NSCLC.

003

Are neutrophils new partners for circulating tumor cells migration? A preliminary study in 180 resectable non-small cell lung carcinoma patients using both the CellSearch method and the blood neutrophil count

V. Hofman, M. Ilie, C. Butori, C. Marquette, N. Vénissac, J. Mouroux, P. Hofman*
*CHU de Nice, LPCE, France

Objective: Neutrophils within the tumor microenvironment, so-called tumor-associated neutrophils (TANs), facilitate angiogenesis, extracellular matrix breakdown and remodeling, and promote tumor cell motility. Recent studies reveal that direct communication between neutrophils and tumor cells leads to invasion and egress of tumor cells into the blood vessels. Moreover, cytokines present in blood circulation might physically link cancer cells to TANs, allowing them to travel together throughout the circulation. This study was conducted in order to correlate the presence and number of circulating tumor cells detected in resectable non-small cell lung carcinoma patients and the neutrophil blood counts evaluated at the same time.
Method: One hundred eighty consecutive patients who underwent surgery for NSCLC were included. CTCs have been detected and quantified using the CellSearch assay and the CellSearch Epithelial Cell Kit (Veridex). Results of CTC enumeration were expressed as the number of positive cells per 7.5 ml of blood. At the same time, blood neutrophils were counted and values were compared to the CTCs counts for each patient.
Results: Among NSCLC patients, 52% have CTCs preoperatively detected (range between 1 and 25 CTCs). Sixty-five of 180 patients have more than 10.000 neutrophils/mm^3. Among these patients, CTCs were found correlated with high levels of blood neutrophils in 75% of cases (p=0.05).
Conclusion: This preliminary study shows that CTCs (presence and number) are strongly associated with higher levels of blood neutrophils in NSCLC patients undergoing surgery. These results open new avenues in our understanding of CTC migration, outcome, and survival.

004

Mutations and copy number of EGFR in mixed type of pulmonary adenocarcinoma

L. Carvalho, M. Silva, P. Couceiro, A. Alarcão, M. J. Aguiar, L. Teixeira, V. Sousa*
*Faculdade de Medicina Coimbra, Dept. de Anatomia Patologica, Portugal

Objective: The EGFR genes act in the MAPK signaling pathway. Patients with non-small cell lung cancer (NSCLC) with EGFR mutations are more sensitive to treatment with tyrosine kinase inhibitors (TKIs). The different patterns recognized in adenocarcinomas were microdissected to identify mutations in EGFR and gene copy number in order to clarify their significance when selecting patients either to TKIs to be translated to small biopsies.
Method: Histological sections of 40 mixed-type adenocarcinomas from surgical specimens of the lung FFPE and were submitted to FISH by application of the probe LSI EGFR/CEP 7. Thirty-one samples were studied for EGFR exons 19 and 21 mutations by fragment analysis and by direct sequencing, respectively.
Results: FISH-positive was found in nine cases, two with amplification and one with high polysomy, by Cappuzzo's score; in one case, there were different results in the present patterns. In the 31 samples, 10 of 31 showed in-frame deletions and 4 of 20 L858R substitution in the EGFR. Only one mixed adenocarcinoma showed EGFR in-frame deletions in bronchioloalveolar pattern and Wt in acinar pattern.
Conclusion: In this set of mixed-type adenocarcinomas, the different histological patterns revealed to be inconsequent for EGFR determination of mutations and gene copy number, reinforcing the technical feasibility and reliability of small biopsies of lung cancer to determine personalized therapy.

005

Chromogranin A expression confers small cell lung cancer better prognosis

L. Carvalho, A. Alarcão, M. J. Aguiar, S. Ventura, A. Pêgo*
*Faculdade de Medicina Coimbra, Dept. de Anatomia Patologica, Portugal

Objective: Small cell lung cancer (SCLC) accounts for up to 13% of all newly diagnosed lung cancers. The prognostic value of six immunohistochemical markers (IHC) used in routine diagnosis, chromogranin A (Chromo A), cytokeratin 7 (CK7), thyroid transcription factor-1 (TTF-1), neural cell adhesion molecule/CD56, Ki-67 (MIB1) and high weight cytokeratin (LP34), was explored to enrich clinical data.

Method: A total of 100 cases (13 women, 87 men) were selected for this study to consider respective follow-up. Patients had histological diagnosis of SCLC, in accordance with the classical morphological parameters and IHC referred profile.
Results: The mean survival was 274 days (9 months) and median was 183 days (6 months). The survival mean for limited disease-SCLC was 482 days (16 months, with a 95% confidence interval of 10–22 months) and 182 days for extensive disease-SCLC (6 months, with a 95% confidence interval of 4–8 months). Significant prognostic meaning of Chromo A curves pointed to mean survival of approximately 11 months. Expression of Chromo A and CD56 had best prognosis survival mean of 726 days (24.2 months) against 234 days (7.8 months). The worst prognosis was seen with CD56 and Ki67—mean survival of 6 months against 11 months.
Conclusion: Chromo A isolated expression by neoplastic cells should be considered a prognostic factor of survival. Cases that express either Chromo A or CD56 have to be separated from cases expressing CD56 and Ki67 to delineate prognostic groups among SCLC patients, and therapy might be defined according to this profile.

006
Combined inhibition of mTOR and EGFR yields synergistic cytotoxic and biochemical effects in atypical lung carcinoid and large cell neuroendocrine lung carcinoma cells

Z. Bagó-Horváth, W. Sieghart, H. Hayden, D. Cejka, J. Werzowa, W. Berger, A. Lackner, M. Grusch, M. Filipits, K. Schmid*
*Medical University of Vienna, Clinical Institute, Austria

Objective: Epidermal growth factor receptor (EGFR) and mammalian target of rapamycin (mTOR) are crucial targets in cancer therapy that control cell survival and proliferation. Combined inhibition of both pathways yielded synergistic effects in several human cancer cell lines. However, the impact of EGFR and mTOR expression and inhibition in neuroendocrine lung tumors (excluding SCLC) is unclear.
Method: Cytotoxic effects of mTOR inhibitor everolimus and EGFR inhibitor erlotinib alone and in combination were tested using growth inhibition assays in NCI-H720 atypical lung carcinoid and SHP-77 large cell neuroendocrine lung carcinoma cells. Activation of EGFR and mTOR pathway members was analyzed by Western blotting. Cell cycle phase distribution was determined by FACS. To investigate the role of these pathways in neuroendocrine lung tumors, expression of the pathway constituents was assessed by immunohistochemistry in 110 tumor samples and correlated with survival of the patients.
Results: Combination of erlotinib and everolimus yielded highly synergistic combination effects in both cell lines. Downregulation of phosphorylated mTOR, p70-S6 kinase and Akt expression by everolimus was potentiated by the addition of erlotinib, although erlotinib alone did not affect the expression of these proteins substantially. Additionally, combined treatment showed effects on cell cycle regulation and phase distribution. Activation of both pathways could be demonstrated in all tumor entities investigated; however, no correlation with disease-free or overall survival of the patients was observed.
Conclusion: Due to these promising results, the effects of combined inhibition of mTOR by RAD001 and EGFR by erlotinib warrant further in vivo investigation in neuroendocrine lung tumors.

007
The role of epithelial–mesenchymal transition in malignant mesothelioma

A. Fassina, R. Cappellesso, A. Gazziero, V. Guzzardo, M. Fassan*
*University of Padova, Dept. of Pathology, Italy

Objective: Malignant mesothelioma (MM) is the tumor arising from the lining cells of the serosal cavities, microscopically characterized by epithelioid and/or sarcomatoid features. This supports the hypothesis that MM could be a suitable model to study in vivo the epithelial–mesenchymal transition (EMT) process by which epithelial cells acquire mesenchymal shapes and properties but also invasive and metastatic abilities during tumor progression.
Method: One hundred nine formalin-fixed paraffin-embedded MM specimens (58 epithelioid, 26 sarcomatoid, 25 biphasic) from the Pathology Department of Padova University were analyzed by immunohistochemistry (IHC; E-cadherin, N-cadherin, β-catenin, cytokeratin 5/6, vimentin, αSMA, ZEB1/2, S100A4, MMP-2 and MMP-9), by qRT-PCR analysis (E-cadherin, N-cadherin, SNAI1/2, ZEB1/2, TWIST1, miR-205), and by in situ hybridization (miR-205). Results were evaluated by Student's *t* test and Kruskal–Wallis test.
Results: IHC showed that vimentin ($p=0.007$) and αSMA ($p=0.009$) expressions were higher in sarcomatoid than in epithelioid MM, and S100A4 ($p=0.046$) was higher in biphasic than in epithelioid MM. At qRT-PCR, E-cadherin ($p=0.001$ and $p=0.014$) was expressed at lower levels, while N-cadherin ($p=0.002$ and $p=0.002$) was at higher levels in sarcomatoid than in epithelioid/biphasic MM.

SNAI2 ($p=0.001$ and $p=0.001$) was higher in both sarcomatoid and biphasic compared to epithelioid MM. TWIST1 ($p=0.044$ and $p=0.011$) expression was higher only in biphasic cases.
Conclusion: MM can be considered a suitable model to study the EMT process in vivo. Indeed, EMT is involved in MM morphological spectrum of subtypes, but also plays a fundamental role in prognosis.

008

Pulmonary arterial hypertension in end-stage Idiopathic pulmonary fibrosis: a hypothetic role for viral infections

F. Lunardi, E. Balestro, G. Cuffaro, B. Nordio, E. Rossi, M. Loy, M. Saetta, M. Valente, F. Rea, F. Calabrese*
*University of Padua, Italy

Objective: Idiopathic pulmonary fibrosis (IPF) is a destructive lung disease of unknown aetiology, characterised by progressive fibrosis and inflammation. Pulmonary hypertension represents an important complication significantly influencing patient outcome. The contribution of viral infections in the development/progression of the disease is largely debated. The aim of the study was to investigate the presence of different viral genomes in native lungs with IPF and to correlate these findings with different clinical, functional hemodynamic and morphological parameters.
Method: Tissue samples from 52 native lungs of IPF patients requiring lung transplantation and from 20 controls were analysed by polymerase chain reaction to detect different viral genomes (Epstein–Barr virus; cytomegalovirus; human herpesviruses 6, 7, 8; adenovirus; rhinovirus; influenza viruses; parainfluenza viruses; parvovirus B19; metapneumovirus and respiratory syncytial virus). Morphological parameters (fibrosis extension, muscular artery wall thickness and inflammation) were quantified using morphometry.
Results: Higher frequency of virus-positive cases was detected in IPF patients than the control group (17/52 vs 1/20, $p=0.01$), and herpesviruses were the only detected genomes. Viral IPF cases showed increased values of mean pulmonary arterial pressure, mPAP ($p=0.05$), worse performance at the 6-m walking test ($p=0.008$), and were characterized by a higher thickening of muscular arteries ($p=0.03$). No significant correlations were found with other clinical and morphological data.
Conclusion: Higher values of mPAP in viral cases may prospect a role of herpesviruses in the development of pulmonary hypertension. A more extensive vessel remodelling may be related to a well-known vessel tropism of herpesviruses.

Friday, 3 September 2010, 17.00–18.30, Aula Duża A

FP-06 Free papers 6

001

Spectrum of biopsy-proven renal diseases in adults: a 9-year review of nine regional renal databases in Poland

M. Wagrowska-Danilewicz, A. Halon, K. Okon, A. Andrzejewska, A. Marszalek, W. Salwa-Zurawska, A. Korolczuk, H. Karkoszka, A. Mroz, M. Danilewicz, A. Perkowska-Ptasinska*
*Medical University of Lodz, Dept. of Nephropathology, Poland

Objective: This is a report on the epidemiology of kidney diseases in Poland based on kidney biopsy databases from nine nephropathological centers.
Method: All adult native kidney biopsy recognitions collected in the years 2002–2009 in Warsaw, Lodz, Cracow, Wroclaw, Bialystok, Bydgoszcz, Lublin, Poznan and Katowice were retrospectively analyzed for histological type of renal disease and demographic data. Biopsies were processed for light and immunofluorescence microscopy and electron microscopy in some cases.
Results: The total number of analyzed diagnostic biopsies was 5,560. Male-to-female ratio was 2,996:2,564; the mean age was 44.2 years. The most common recognition was glomerulopathy, with the most prevalent type being focal segmental glomerulosclerosis (FSGS, 17.9%), followed by IgA nephropathy (17.3%), membranous nephropathy (11.4%), membrano-proliferative glomerulonephritis (7.3%), mesangial proliferative glomerulonephritis (7.3%), extracapillary glomerulonephritis (6.1%), and minimal change disease (5.1%). Among secondary nephropathies, the most prevalent were lupus nephritis (8%) and renal amyloidosis (4.4%) of all diagnostic biopsies, respectively. Tubulointerstitial nephritis was reported in 1.9% of all renal biopsies.
Conclusion: Collection of data relating to renal biopsies in a national registry is a useful tool for nephrologists in that it meets one of the current challenges facing the clinical research enterprise. In Poland, the most common disease recognition upon kidney biopsy in adults is chronic glomerulonephritis with a domination of FSGS. Lupus nephritis predominates among secondary types of glomerulonephritis. This report constitutes the basis for the future Polish Registry of Renal Biopsies. (This work was supported by grant of Polish Ministry of Science and Higher Education NN402 088735)

002

Renal histopathology of patients with coexisting anti-glomerular basement membrane antibodies and antineutrophil cytoplasmic antibodies

A. Vizjak, J. Lindic, V. Jurcic, D. Ferluga*
*Faculty of Medicine, Institute of Pathology, Ljubljana, Slovenia

Objective: Antibodies against glomerular basement membrane (anti-GBM) and antineutrophil cytoplasmic antibodies (ANCA) are both associated with histopathologic features of extracapillary crescentic glomerulonephritis and may coexist in some patients.
Method: Of 37 patients with anti-GBM glomerulonephritis in kidney biopsy ($n=36$) or autopsy ($n=1$), examined from 1990 to 2009 at the Institute of Pathology Faculty of Medicine Ljubljana, 11 patients (29.7%) had in addition to anti-GBM antibody-positive ANCA, specific for myeloperoxidase. Renal biopsies were examined by light and immunofluorescence microscopy techniques.
Results: The patients comprised ten women and one man (mean age 64.1±7.2 years, age range 52–78 years). Immunofluorescence microscopy showed intense linear staining for IgG and C3 along glomerular and distal tubular basement membrane in all patients. By light microscopy, irregular diffuse or focal extracapillary crescentic glomerulonephritis was found in all patients, associated with necrosis of varying extent in nine. The percentage of crescents was 33% to 100%. Extraglomerular necrotizing vasculitis of small arteries was present in six patients, and in one, elastica destruction indicative of previous vasculitis was observed. An assessment of the age of histopathologic lesions showed lesions of varying age in all biopsies. Active lesions were predominant in four and chronic in three, while active and chronic lesions of equal distribution were seen in four biopsies.
Conclusion: All our patients with coexisting anti-GBM antibodies and ANCA were older and all had renal histopathologic lesions of varying age, active and chronic. These results confirm a hypothesis that anti-GBM antibody production may start after injury to the glomerular basement membrane by ANCA.

003

Renal amyloidosis secondary to Behçet's disease: clinicopathologic features of 10 cases

K. Kosemehmetoglu, D. Baydar*
*Ankara Ataturk EAH, Dept. of Pathology, Turkey

Objective: Amyloidosis is a rare complication of Behçet's disease (BD). We describe ten patients with BD and renal amyloidosis.
Method: Kidney biopsy slides were culled from the archives and reviewed. Intensity and relative distribution of amyloid deposition in renal compartments were noted. Glomerular deposits were classified as hilar (pattern I), mesangial nodular (pattern II) and mesangiocapillary (pattern III). Chronic tubulointerstitial damage was graded from 0 to 3 (0%, 0–<25%, 25–<50% and ≥50%). Amyloid typing was performed by immunohistochemistry. Clinical information was gathered from hospital records and computer-based patient data system.
Results: All patients were male. Their age ranged from 27 to 56. Full-blown nephrotic syndrome was present in six cases. Duration of BD before diagnosis of amyloidosis differed from 24 to 192 months (mean 108), and mean follow-up period was 59.5 months. Immunohistochemical typing revealed AA amyloid in all ten. Four cases showed glomerular-dominant and two cases vascular-dominant amyloid deposition; the rest were co-dominant glomerular and vascular. The frequencies of glomerular amyloid patterns were 40% for hilar, 20% for mesangial nodular and 40% for mesangiocapillary. Hilar pattern was associated with vascular-dominant amyloid deposits. Severe proteinuria correlated with the presence of mesangiocapillary pattern. Grade III chronic tubulointerstitial injury was detected in three cases. Patients were treated with steroids and/or different immunosuppressives. Among them, two progressed to end-stage kidney failure, one showed remission, two were lost to follow-up, and rest had persistent proteinuria.
Conclusion: Renal amyloidosis in BD has a diverse pathology in terms of preferential location of amyloid deposition and its intensity. Patients follow variable clinical courses accordingly.

004

Acute and rejection and vascular remodeling on 180 post-cardiac transplant biopsies

J. Thorne, D. O´Neill, N. Mahon, F. Woods, J. Egan, M. Keoghan, A. Fabre*
*The Copse, 4 College View, Dublin, Ireland

Objective: Acute and chronic rejection is the main cause of graft dysfunction post-cardiac transplantation. Assessment of chronic rejection (cardiac allograft vasculopathy) may prove difficult on biopsies.
Method: We reviewed 180 cardiac biopsies from 23 patients who underwent cardiac transplant between 2004 and 2008 in whom donor-specific antibodies were measured (5 women, 18 men; mean age at transplant, 39.7 years (range 17–69)). Diagnosis on explanted hearts included ischaemic heart disease ($n=10$), dilated cardiomyopathy ($n=9$), hypertrophic cardiomyopathy ($n=2$), congenital

heart disease (n=1), and AMP kinase deficiency cardiomyopathy (n=1).

Results: In total, 16 levels from 180 biopsies were reviewed (n=2,880), with a majority of low grade of rejection (according to the ISHLT grading system): grade 0R, 36.1%; grade 1R, 48.8%; grade 2R, 10%; grade 3, 0.5%. Other histological features assessed were subendocardial fibrosis (n=143, 79.4%) and interstitial fibrosis (n=126, 70%). Assessment of vascular remodelling was evaluated on all biopsies and was observed in 61 (33.8%). Intimal hyperplasia/thickening of intramural vessels with wall rigidity (n=39, 62.3%) and luminal narrowing (n=23, 37.7%) was recorded. These changes were observed as early as on the first biopsy, with marked variability in the time from transplant to their first appearance (from 7 to 834 days). Eight of these developed post-transplant circulation anti-donor HLA antibodies. The rejection grade on biopsies with vascular changes was 0R–1R in 81%.

Conclusion: Detection of donor-specific HLA antibodies as well as abnormal epimural vessel on biopsies might identify cardiac allograft vasculopathy and offer an opportunity for early clinical intervention and modification of immunosuppression.

005

Expression of K^+ channel subunits in different human blood vessels

J. Markovic-Lipkovski, S. Cirovic, D. Mitrovic, S. Tatic, M. Peric, L. Gojkovic-Bukarica*

*University Medical School, Belgrade, Serbia and Montenegro

Objective: We investigate some agents (glibenclamide and resveratrol) that can prevent spasm of human blood vessels used as a graft by anti-vasoconstrictor effect of the K^+ channel opener. Therefore, it is very interesting to know the distribution and localisation of different K^+ channel subunits.

Method: In the present study, the cryostat sections of the human a. renalis, a. radialis, a. mammaria interna and v. saphena were used. Immunoperoxidase or immunofluorescent techniques were performed. For the analysis of expression of different K^+ channels, a panel of antibodies to intracellular epitopes of the C-terminal part produced in rabbits (Alomone Labs, Israel) was employed: anti-Kv1.2, anti-Kv1.3, anti-Kv1.6, anti-Kv2.1, anti-Kir6.1, anti-Kir6.2 and anti-Kca1.1. In some cases, double immunofluorescent technique with alpha-SMA antibody was applied.

Results: V. saphena expressed only Kir6.2 subunits on the smooth muscle cells of the wall. Internal a. mammaria showed expression of Kir6.1 and Kir6.2. A. radialis showed variable positivity with Kv1.2, Kv1.3, Kir6.1 and Kca1.1. Double immunofluorescent labeling with antibodies against Kv1.2 subunit and alpha-SMA revealed that Kv1.2 channel subunit is predominantly expressed in the perinuclear region of the myointimal cells and of the smooth muscle cells of the media of a. radialis. A. renalis predominantly expressed Kv1.3 channel in the endothelium. Interestingly, in few artery specimens with focal calcification or atherosclerotic plaque, we observed decreased expression of Kv1.2 channel subunit.

Conclusion: Expression of K^+ channel subunits is different in various human blood vessels.

Friday, 3 September 2010, 17.00–18.30, Sala Wystawowa B

FP-07 Free papers 7

003

Locked nucleic acid-based PCR clamping method for the detection of KRAS mutations

D. Hershkovitz, H. Elkin, Y. Peerless, O. Ben-Izhak, E. Sabo, E. Efrati*

*Rambam Health Care Campus, Dept. of Pathology, Haifa, Israel

Objective: KRAS is an oncogene that is commonly mutated in various malignancies. Mutations in KRAS are associated with lack of response to anti-EGFR treatment in colon and lung carcinomas, and patients must undergo genetic testing to be eligible for treatment. Several genetic tests for KRAS mutation analysis exist, but most are either too expensive or lack the sensitivity to identify a mutation if the percentage of tumor cells in the sample is small. The purpose of the present study was to develop a novel KRAS mutation detection method that is both cost-effective and sensitive.

Method: We designed a locked nucleic acid (LNA)-containing probe that inhibits the amplification of wild-type KRAS, thereby giving an advantage to mutated KRAS in PCR reaction (PCR clamping). The sensitivity of this method was evaluated using serial dilutions of plasmids containing wild-type and mutated KRAS fragments. The method was further evaluated on 40 archived tissue samples of colon carcinoma and compared to direct sequencing and high resolution melting (HRM) methods.

Results: LNA-based probe successfully inhibited the amplification of wild-type KRAS. The method enabled the detection of as little as 1% mutated DNA in the sample analyzed. The method was superior to direct sequencing when the percentage of malignant cells in the sample was 20% or less. There was 100% correlation between the results of PCR clamping and HRM.

Conclusion: LNA-based PCR clamping method is a cost-effective and highly sensitive method for the detection of KRAS mutations.

004

Loss of p16 protein and hypermethylation of p16 gene in bronchiolar columnar cell dysplasia

A. Sulewska, W. Pankiewicz, W. Naumnik, J. Niklinski, M. Kozlowski, J. Kowalewska, L. Chyczewski*
*Medical University Bialystok, Dept. of Clinical Molecular Biology, Poland

Objective: Bronchiolar columnar cell dysplasia (BCCD) has been proposed as a novel peripheral precancerous lesion of the lung adenocarcinoma. Hypermethylation of p16 gene occurs early during the development of squamous cell lung cancer. However, the role of gene hypermethylation during the development of adenocarcinoma remains unclear. The aim of our study was to estimate the expression of protein p16 and cellular marker for proliferation Ki-67 and to detect hypermethylation of p16 gene in BCCD.
Method: The study material consisted of specimens obtained from 145 patients surgically treated for non-small cell lung cancer in the Clinic of Thoracic Surgery, Medical University of Bialystok. BCCD was searched for in sections taken from uninvolved lung parenchyma. P16 and Ki-67 were evaluated by immunohistochemistry. Analysis of epigenetic changes was performed in 18 patients. Hypermethylation of p16 was examined by methylation-specific PCR.
Results: BCCD was identified in 27 (18.6%) patients. BCCD was observed in patients surgically treated for adenocarcinoma, squamous cell lung cancer and large cell lung cancer (23.7%, 17.6%, and 10.2%, respectively). Loss of p16 was found in 78.9% of BCCD; cytoplasmatic expression of p16 was identified in 21.1% of cases. Expression of Ki-67 indicated moderate mitotic activity of epithelium in BCCD. Hypermethylation of the p16 gene was found in 12.5% of BCCD. Methylation of p16 gene was absent in normal epithelial lung tissues.
Conclusion: Our study indicates that BCCD was seen in only 18.6% of patients with lung cancer. Loss of p16 protein and hypermethylation of p16 gene seen in BCCD points to the precancerous stage of this lesion.

005

Ewing's sarcoma cells promote osteoclast formation

R. Taylor, F. Hemingway, H. Knowles, N. Athanasou*
*Merton College, Oxford, United Kingdom

Objective: Ewing's sarcoma (ES) is a primary bone tumour associated with extensive bone destruction. To investigate the osteolysis in ES, we examined whether ES tumour cells directly resorb bone or whether they act to promote osteoclast formation and resorptive activity.
Method: Several ES cell lines + macrophage colony-stimulating factor (MCSF)-primed $CD14^+$ monocytes were cultured on coverslips and dentine with MCSF + receptor activator of nuclear factor kappa B ligand (RANKL). Cultures were examined for the osteoclast formation markers tartrate-resistant acid phosphatase (TRAP), CD51 and lacunar resorption. Release of organic matrix collagen fragments (CTX-1) was assayed by ELISA. Protein and RNA expression of osteoclastogenic factors in ES cells was investigated by Western blotting, immunohistochemistry and real-time PCR.
Results: Cultures of ES cell lines on dentine did not result in lacunar resorption or the release of CTX-1, but the formation of large $TRAP^+$ and $CD51^+$ osteoclast-like multinucleated cells capable of lacunar resorption was seen in ES monocyte co-cultures. Expression of the osteoclastogenic factors, MCSF and RANKL, was identified in ES tissue sections and ES cell lines.
Conclusion: Our results indicate that ES tumour cells do not directly resorb bone. ES cells express MCSF and RANKL, osteoclastogenic factors that are essential for osteoclast formation from mononuclear phagocytes. This RANKL-dependent mechanism is likely to contribute to the rapid, aggressive osteolysis of ES.

006

Analysis of a novel JK-1 gene expression in benign and malignant colorectal tumors

K. Kasem, A. Lam*
*Griffith Medical School, Southport–Queensland, Australia

Objective: A newly discovered gene, JK-1 (FAM134B), located in chromosome 5 p15.2 plays an important role in the molecular pathogenesis of esophageal cancer. This study aims at examining the role of this gene in colorectal tumors by analyzing the differences in gene mRNA expression in both benign and malignant colorectal tumors.
Method: The study was performed on 162 colorectal adenocarcinoma, 32 benign adenoma and 20 non-neoplastic colorectal tissues. Gene expression levels were determined using real-time PCR. The expression levels were calculated as a ratio of the Ct value for JK-1 to GAPDH and expressed as inverse ratio.
Results: The JK1 mRNA was detected in all colorectal tissues. The mean inverse ratio for JK-1 gene in adenoma samples was 0.929 ± 0.005, which was significantly higher than in non-tumor samples which was 0.901 ± 0.009 ($p = 0.005$). On the other hand, cancer samples had a mean inverse ratio of 0.875 ± 0.006, which was significantly lower than in non-tumor tissues ($p < 0.001$).

Conclusion: The under-expression of the gene in cancer suggests that loss of gene expression may promote tumor progression, that it may act as a tumor suppressor gene, or that it relates to certain genetic events in tumor pathogenesis. However, over-expression of JK-1 in adenoma samples may indicate that JK-1 has a functional role in dysplastic benign colon tumors, a function that is disrupted once the tumor progresses to a more invasive form.

Poster Sessions

Wednesday, 1 September 2010, Basement

PS-01 Poster Session Breast Pathology

0001

Subtyping estrogen receptor-positive breast carcinomas by routinely used immunohistochemical reactions

J. Kulka, A. Hajnáczky, L. Madaras, B. Székely, I. Szirtes, G. Lotz, A.-M. Tokés, M. A. Szász*
*Semmelweis University, 2nd Dept. of Pathology, Budapest, Hungary

Background: To subtype estrogen receptor (ER)-positive breast carcinomas by retrospectively analysing the results of the routinely used immunohistochemical (IH) reactions and compare the findings to the recorded conventional prognostic factors.
Method: Between 2000 and 2007, 1,415 invasive breast carcinomas were diagnosed histologically in the 2nd Department of Pathology, Semmelweis University Budapest. ER/PR, Ki67, Her2 status were recorded. Her2 score 2 cases were reevaluated by FISH. We evaluated the results in comparison with tumor type, grade, pTNM stage, vascular invasion. In 765 of 1,036 ER-positive breast cancer cases, we had complete set of data. Three groups were set: cases with $Her2^-$ and low Ki67 index (<20%) status (A, 504 samples), $Her2^-$ and high Ki67 index (≥20%) status (B, 165 samples), and $Her2^+$ status (C, 96 samples). We suggest that the latter two represent the genomic luminal B group of breast carcinomas. R 2.7.1 statistical programme was used. Value of $p \leq 0.05$ was taken as significant.
Results: Of the cases in group A, 68.7% were invasive ductal (IDC), whereas 18.8% were invasive lobular carcinomas (ILC). In groups B and C, IDC were diagnosed in 84% and 88% while ILC in 9.8% and 9.3%, respectively ($p=0.0002$). Forty-three percent of group A cases were grade 1, whereas in groups B and C, close to 40% of the tumors were grade 3; grade 1 tumors were found in 8% and 11.7%, respectively. In group A, 7.8% of tumors were grade 3 ($p<0.0001$). Vascular invasion was recorded in 28.3% of the cases in group A, while this was seen in 50.7% and 48.7% in the B and C groups, respectively ($p=0.0002$). Least pT1 tumors were present in group B (44.5%). pT1 stage was recorded in 62.3% and 63.8% of groups A and C, respectively ($p=0.0149$). pN0 was found in 61.6% of the cases in group A, while only 39.5% and 45.4% of the cases in groups B and C were pN0, respectively ($p=0.0360$).
Conclusion: According to the conventionally used prognostic factors, cases belonging to our group A of ER-positive breast carcinomas possess a favourable profile. Our groups B and C show similar prognostic features. We believe that routinely used protein profiling using a simple IH panel provides important information and may subdivide the group of ER-positive carcinomas, probably reflecting the genomic luminal subtypes (analysis of the follow-up data is in progress). Acknowledgements: ETT 29/2009 grant.

0002

Vimentin expression and immunophenotypic molecular classification of node-negative invasive ductal breast carcinomas

A. Kosierkiewicz, P. Domagala, J. Rys, J. Sir, W. Domagala*
*Pomeranian Medical University, Dept. of Pathology, Gryfice, Poland

Objective: The origin of vimentin expression in breast cancer tumor cells and its prognostic significance have been controversial. The purpose of this study was to assess the correlation between the expression of vimentin and immunophenotypic molecular classification of breast cancers.
Method: Tissue microarrays containing 305 invasive ductal breast carcinomas from axillary node-negative patients were tested by means of immunohistochemistry for the expression of vimentin, ER, PR, HER2, EGFR, CK 5/6, CK14, CK17, p 63, P-cadherin.
Results: A significant association was found between vimentin expression and immunophenotypic molecular classification ($p<0.00001$). Vimentin was expressed in 67% of basal-like, 17% of basal-like $HER2^+$, 14% of luminal B, 9% of luminal A, and 38% of unclassified carcinomas. Of 50 vimentin-positive tumors, 56% constituted basal-like, 24% luminal A, 8% basal-like $HER2^+$, 6% luminal B and 6% unclassified cancers. Sixty-four percent of triple-negative cancers expressed vimentin. Expression of vimentin was negatively associated with ER and PR ($p<0.00001$) and positively associated with CK5/6 ($p<0.001$), CK 14 and CK17 ($p<0.00001$), and nuclear p63 ($p<0.02$).

Conclusion: The results partially explain controversy in the literature concerning vimentin's prognostic significance and suggest three pathways of vimentin origin in cancer cells.

0003

Histopathologic, immunohistochemical and morphometric profiles of invasive breast carcinoma

M. Aschie, A. Mitroi, A.-A. Nicolau, I. Poinareanu, A. Chisoi, A. Iliesiu, V. Sarbu, I. Aschie*
*Institute of Pathology, Constanta, Romania

Objective: Invasive breast carcinoma represents are characterized by invasion of adjacent tissues and a marked tendency to metastasize to distant sites. In order to determine specific prognostics factors, we established histopathologic, immunohistochemical and morphometric profiles of these types of carcinoma.
Method: In our study, we investigate 120 cases diagnosed with invasive breast carcinoma in which we established microscopic characterization, immunohistochemical profiles (expression of proliferation markers, steroid receptors and Her2) and computer-assisted morphometric profiles by determining the mean values for nuclear area, cellular area and N/C ratio with Lucia Net Software. The distribution of markers and histological grade among types of carcinoma was statistically analyzed using the χ^2 test.
Results: The histological type of invasive carcinoma was: 83.5% ductal carcinoma, 9% mixed ductal and lobular carcinoma, and 7.5% lobular carcinoma. According to histological differentiation, 15% was G1, 54% was G2 and 31% was G3. Immunohistochemical expression of ER was positive in 93% and negative in 15%, for PR was positive in 85% and negative in 15% and the expression of Her2 was positive in 68% and negative in 32%. Ki67 was intensely positive in 47%, moderately positive in 43% and intensely positive in 16%. P53 was positive in 95% cases and negative in 5% of cases. Morphometric analysis revealed that mean nuclear area and N/C ratio increase are concordant with grading, but mean cytoplasmatic area has no characteristic variation.
Conclusion: The expressions of proliferation markers correlate with carcinoma grading. Poorly differentiated and triple-negative carcinoma (ER, PR and HER2) with intense expression of proliferation markers and increase mean nuclear area have negative prognosis.

0004

Profiling signalling networks in formalin-fixed and paraffin-embedded breast cancer tissues

D. Berg, C. Böllner, K. Malinowsky, A. Walch, T. Schuster, H. Bronger, K.-F. Becker*
*TU München, Dept. of Pathology, Germany

Objective: Mapping tumour cell protein networks in routinely processed clinical samples, like formalin-fixed and paraffin-embedded (FFPE) tissues, will be critical for realizing the promise of personalized molecular therapy as only a subset of patients will respond. Therefore, techniques being able to detect the entire spectrum of deregulated pathways in tumors before, during, and after treatment are required to assess success or failure of targeted therapies. The aim of our study was to monitor protein networks in FFPE breast cancer tissues with special emphasis on epidermal growth factor receptor 2 (HER2)-mediated signaling pathways to identify and validate new disease markers in order to predict response to current treatments.
Method: Using a recently developed technology for the extraction of full-length proteins from FFPE tissues, we analyzed molecules involved in HER2-related signaling by reverse phase protein microarray (RPPA) in a series of 106 FFPE breast cancer patients. To this end, we evaluated >50 commercial antibodies for specificity in lysates from FFPE breast cancer samples in Western blots and RPPA.
Results: We found HER3 (r's=0.581), the EGFR (r's=0.556) and the receptor of uPA (r's=0.585) correlating with HER2. However, we could not demonstrate any significant correlation between HER2 expression and clinicopathological parameters.
Conclusion: Our results uncover molecules linked to HER2 signaling and cancer progression. Thus, these finings provide possible new targets for cancer treatment and may assist in optimal patient selection.

0005

mTOR and S6Kp70 expression and prognostic role in human breast cancer and their relation with PI3K pathway alterations

E. Bragantini, F. Mauri, C. Eccher, M. Volante, S. Girlando, L. V. Cuorvo, C. Cantaloni, F. Buttitta, P. Dalla Palma, M. Barbareschi*
*S.Chiara Hospital Trento, U.O. Surgical Pathology, Italy

Objective: The PI3K/AKT/mTOR pathway has a fundamental role in signal transduction, and its alterations are of pathogenetic role in human cancer, including breast carcinomas (BC). Several drugs may interfere with the altered activation of this pathway, including the recently developed mTOR inhibitors. However, few data are available concerning mTOR levels in human breast cancer.
Method: The aim of the present study was to analyze the immunohistochemical expression of mTOR and p70S6K in a consecutive series of 165 BC, with long-term follow-up which had been studied for ER, PgR, Her2, p53 and MIB1 expression and for PI3K and AKT mutations.

Results: mTOR and p70S6K expression were positively associated ($p=0.002$), but were not related to other molecular markers with the exception of high p70S6K being associated with PI3K mutations ($p=0.047$). In the whole series of cases, mTOR and p70S6K are not associated with clinical outcome. However, high mTOR are associated with prolonged DFS and OS in node-positive cases, in St. Gallen high-risk group, and in patients treated with chemotherapy. High p70S6K expression was associated with prolonged DFS and OS in St. Gallen high-risk group.
Conclusion: Our data show that mTOR and p70S6K are promising biomarkers in BC whose level of expression may be of prognostic value.

0006

Proliferative activity in human breast cancer: assessment of Ki-67 automated evaluation and the influence of different Ki-67 equivalent antibodies

E. Bragantini, S. Fasanella, C. Eccher, E. Leonardi, D. Aldovini, L. Morelli, A. Ferro, L. V. Cuorvo, P. Dalla Palma, M. Barbareschi*
*S.Chiara Hospital Trento, U.O. Surgical Pathology, Italy

Objective: Ki-67 labeling index (Ki-67LI) has an important clinical relevance in breast cancer. It is extremely important to standardize its evaluation.
Method: Three hundred fifteen consecutive breast cancer immunostained for Ki-67 (223 with SP6 (Labvision) and 92 with MM1 (Novocastra) antibodies) previously examined by an experienced pathologist have been reevaluated using Aperio Scanscope Xs.
Results: Mean human Ki-67LI values were 35.91±14.35% and 28.37±18.29%, respectively, for SP6 and MM1 antibodies; mean CAM Ki-67LI values were 30.97±19.19% and 22.12±18.36%, respectively, for SP6 and MM1. Human and CAM evaluation are statistically highly correlated (Pearson, 0.859, $p<0.0001$), although human LI are systematically higher. Cases have been subdivided into three groups based on tertile distribution; cutoffs varied depending on the antibody used and on the evaluation methods: For human evaluation using SP6 and MM1, they were ≤30, 31–42, ≥43, and ≤20, 21–40, ≥41 respectively; for CAM evaluation, they were ≤19, 20–37, ≥38 and ≤12, 13–24, ≥25.
Conclusion: Our study shows that (a) CAM can be easily adopted in routine; (b) human and CAM Ki-67LI are highly correlated; and (c) Ki-67LI grouping on the basis of tertiles obtained using different evaluation methods and different antibodies shows important differences in cutoff values, underscoring that it is not correct to adopt general cutoff values to subgroup cases without taking into consideration the evaluation methods and antibody used.

0007

The antigen Ki-67: marker of the tumoral proliferation in the invasive mammary cancer and the connection with the classical prognostic factors

A. Muresan, E. Lazar, A. Dema, M. Cornianu, A. C. Faur, M. Grigoras, R. Cornea, C. Lazureanu, R. Cioroboreanu, I. Sargan*
*University of Medicine, Dept. of Pathology, Timisoara, Romania

Objective: The Ki-67 antigen is a marker of the cell cycle and of the tumoral proliferation. Due to the immunohistochemical techniques, it can be easily emphasized. The Ki-67 antigen is largely used for the estimation of the proliferation coefficient of a mammary carcinoma. The Ki-67-positive cells percent is correlated with the aggressiveness parameters or with those of tumoral progression.
Method: The studied tissue fragments from the studied carcinomas were fixed in formaldehyde 10%, included in paraffin and immunohistochemically colored using the monoclonal antibody MIB1. The positivism for Ki-67 was shown by the red coloring of the proliferating cells' nucleuses using DAB as chromogen.
Results: Out of 72 studied mammary carcinomas, 52 (72.2%) overexpressed the Ki-67 antigen. We have observed a significant connection between the Ki-67 expression and the histopathologic degree of the mammary carcinomas; we did not see any connection between the Ki-67 and the patients' age, tumor size, histological type and the clinic stage of the disease.
Conclusion: In mammary tumors, the presence of the Ki-67 antigen is considered as an unfavorable prognosis factor by rapid tumor increment, invasion and metastasis marker.

0008

VEGFR-3, LYVE-1, Prox-1, and podoplanin immunohistochemical expression in breast cancer axillary lymph nodes

L. Carvalho, A. Alarcão, C. Andrade, M. J. Aguiar, L. Teixeira, P. Couceiro*
*Faculdade de Medicina Coimbra, Dept. de Anatomia Patologica, Portugal

Objective: Lymphangiogenesis occurrence and the biomechanisms in lymph nodes are still unknown. The immunohistochemical application of the usually known lymphatic markers VEGFR-3, LYVE-1, Prox-1, and Podoplanin was explored to study lymphatic vessels in tumour metastasis and non-metastatic lymph nodes of breast cancer cases to understand the metastization pathway.

Method: Lymph nodes without and with metastases from 29 cases of invasive breast cancer were selected. Serial sections were immunostained for VEGFR-3, LYVE-1, Prox-1, and Podoplanin using immunohistochemical protocols in accordance with the respective recommendations. The microanatomical distribution of each antibody in the lymph node, different cell type expression, adjacent mesenchymal structure positivity and neoplastic cell positivity were validated and reported as negative and positive (with the cutoff +, ++, +++ for the neoplastic cells).
Results: No markedly or obvious staining was obtained for lymphatic vessels. Positive staining of metastatic neoplastic cells, lymphoid cells of germinal centres and node pericapsular fatty tissue has been observed. Immunostained neoplastic cells revealed a predominant subcapsular and perihilar location.
Conclusion: The applied primary antibodies were unsuccessfully used as lymphatic markers. The spread of neoplastic cells expressing these markers may have acquired particular characteristics to develop lymphatic dissemination until reaching lymph nodes. Lymphangiogenesis in breast cancer continues without demonstration in lymph nodes, while the fatty tissue can be implicated in epithelial mesenchymal transition (EMT). This thesis turned up by the proximity of the positive neoplastic cells to the mesenchymal components of surrounding lymph node tissue as adipocytes were immunoreactive.

0009

Finding resistance biomarkers to trastuzumab in breast cancer

M. S. Fernández García, I. Centeno Ramos, P. Menéndez Rodríguez, C. García Pravia, M. Balbín Felechosa, A. García Varona, B. Vivanco Allende, M. F. Fresno Forcelledo*
*Hospital U. Central Asturias, Oviedo, Asturias, Spain

Objective: There is a significant percentage of patients with metastatic breast cancer and HER2 receptor overexpression that do not respond to therapy directed with trastuzumab. In these patients, overall survival and disease-free time are significantly shorter. Several mechanisms that explain the resistance to therapy with trastuzumab have been reported. This paper aims to address the study of alterations in one of the signalling pathways of HER2-related trastuzumab in response to breast cancer in order to incorporate into the clinical routine of other predictive biomarkers of response to therapy.
Method: The study comprised 70 cases of metastatic breast carcinoma with HER2 overexpression (HercepTest 3+) or gene amplification (FISH). All patients were treated with trastuzumab. The assessment of PTEN and pAkt expression was based on staining intensity and percentage of stained cells.
Results: Our series showed a statistically significant association between a positive expression of PTEN and a reduced expression of pAkt ($p=0.034$). The positive expression of PTEN was associated with a better treatment response rate ($p=0.001$). It was also noted that the reduction of PTEN was associated with a shorter time of progression ($p=0.010$) and a lower overall survival ($p=0.063$). pAkt overexpression was associated with a lower overall survival ($p=0.081$).
Conclusion: Our study shows that immunohistochemical expression of PTEN and pAkt could be used as both prognostic and predictive biomarkers in breast cancer.

0010

Stromal–tumor cell interactions in breast cancer in young women

A. G. Mihaela Georgescu, M. C. Stoicea, F. Andrei, F. Vasilescu, D. Terzea, M. Mihai, D. Arsene, S. Enache, F. Cionca, G. Butur, C. Ardeleanu*
*V. Babes National Institute, Dept. of Pathology, Bucharest, Romania

Objective: Stromal components are attributed an important role in modulating tumor progression from noninvasive to invasive stages. The interrelations between stroma and tumoral cells are not elucidated and currently elicit a special interest among researchers. The aim of our study was to identify possible markers that could characterize the ways in which stromal components relate to tumor cells in breast cancer in young women (age < 35 years).
Method: Our study was performed on 30 ductal invasive breast carcinomas (age range = 23–35 years, $M=33$ years, SE=0.53) from the "Victor Babes" National Institute of Pathology. Formalin-fixed paraffin-embedded samples were analyzed immunohistochemically using an indirect bistadial technique performed with a polymer-based detection system with antibodies for MMP9, COX2, CerbB2, estrogen (ER) and progesterone (PR) receptors and for NF-kB. Statistical analysis was performed using the Student's *t* test from the Analysis Tool Pak of Microsoft-Excel 2003.
Results: We found significant statistical correlations between the immunohistochemical expressions of CerbB2, NF-kB and MMP9 in tumoral cells. CerbB2 strongly correlated with NF-kB and MMP9 in stromal cells (lymphocytes, fibroblasts), vascular structures and extracellular matrix, which varied proportionally with the histological grade. MMP9 was more expressed in stromal components, while NF-kB was more expressed in tumoral

cells. COX2 expression in tumoral cells increased with histological grade and correlated with PR and with COX2 positivity in lymphocytes and mast cells.
Conclusion: Our results indicate that MMP9, NF-kB and COX2 constitute reliable markers for stromal–tumoral cell intercommunication with possible implications in tumor progression, invasiveness and metastases.

0011

Comparing the prognostic value of proliferation markers Ki67, mitotic activity index, phosphohistone-3 and classical variables in breast cancer

E. Gudlaugsson, I. Skaaland, E. Janssen, H. Soiland, A. Malpica, J. Baak*
*Stavanger University Hospital, Dept. of Pathology, Norway

Objective: Proliferation factors have dominant prognostic value, but their independent value and reproducibility are largely unknown. The reproducibility of Ki67 was evaluated and its prognostic value compared with mitotic activity index (MAI), phosphohistone-3 (PPH3) and other variables.
Method: In 240 node-negative breast cancers, standardized immunohistochemistry was used for Ki-67 and PPH3 and a strictly formalized protocol for MAI assessment. Ki67% positive nuclei were determined by two pathologists (Ki67-1, Ki67-2), computerized interactive morphometry (CIM) and digital image analysis (DIA). Continuous variables were discretized according to established thresholds and receiver operating curve (ROC) analysis. Reproducibility, univariate and multivariate survival analysis were performed.
Results: One pathologist was well reproducible but not strongly prognostic; the other was strongly prognostic but not well reproducible. DIA-Ki67 and CIM-Ki67 both were reproducible ($r > 0.99$ and 0.94) and strongly prognostic (10-year survivals of 98% and 72%, 97% and 72%). The ROC-derived optimal thresholds differed both for the quantitative methods (6.45% for DIA, 10% for CIM) and the pathologists (4% and 13%). DIA-Ki67 with a threshold of 6.45 is the strongest multivariate prognosticator (10-year survivals of 98% and 72%), overshadowing other Ki67 thresholds and classical variables (tumor diameter, grade, ER, PR, Her2, cytokeratin 5/6). Only MAI (<3 versus ≥3) or PPH3 (<13 versus ≥13) were slightly stronger.
Conclusion: Proliferation factors MAI-3, PPH3-13 and Ki67-6.45 by digital image analysis are strong prognostic factors in node-negative breast cancer. Furthermore, Ki67 assessments by CIM or DIA are by far more reproducible than visual scoring.

0012

Study on relationship between expression of vascular endothelial growth factor (VEGF) and metastasis to axillary lymph nodes in invasive ductal carcinoma of breast

M. Halimi, E. Kord Mostafapour, Fakhrjou*
*University of Medical Tabriz, Dept. of Pathology, Iran

Objective: Vascular endothelial growth factor (VEGF) has been shown to play a major role in tumor angiogenesis in many studies. This study aimed at evaluating the relationship between VEGF expression and lymph node metastasis in patients with invasive ductal carcinoma (IDC) of the breast.
Method: In a case–control setting, we evaluated specimens of IDC in patients with and without axillary lymph node metastasis. The immunohistochemistry staining was employed for evaluating the expression of VEGF in the specimens of both groups. The rate of positive specimens was then compared between the groups. The relationship between the VEGF expression and the size and grade of tumors were assessed.
Results: Eighty women with IDC of breast, 40 cases with axillary lymph node metastasis and 40 controls without any evidence of axillary lymph node involvement, were enrolled. There were 16 (40%) and 10 (25%) cases with positive expression of VEGF in the case and control groups, respectively ($p=0.152$). The mean size of tumor was significantly higher in patients with positive expression of VEGF (4.81±2.43 cm vs 3.64±1.54 cm, $p=0.034$).
Conclusion: The current study showed that there is no significant relation between the rate of expression of VEGF in cases of IDC of the breast and the axillary lymph node metastasis; however, there may be a relation between VEGF and the size of the tumor.

0013

Abnormal membrane cytoskeletal cross-linker ezrin cellular distribution is associated with clinicopathological features in invasive breast cancer

A. Halon, P. Donizy, L. Halon, R. Matkowski*
*Wroclaw Medical University, Poland

Objective: Ezrin is member of the ERM (ezrin/radixin/moezin) protein family which acts as a membrane organizer and linker between the plasma membrane and cytoskeleton and plays a key role in the control of cell morphology, adhesion, polarity, motility and cell survival. The aim of the present study was to elucidate the clinical significance of

subcellular expression pattern of ezrin in patient with invasive breast cancer (BC).
Method: Immunohistochemistry for ezrin monoclonal antibody was performed on 311 paraffin-embedded specimens from patients with BC. Immunoreactivity was semiquantitatively scored according to Remmele immunoreactive score (IRS).
Results: Expression patterns of ezrin were divided into cytoplasmic (309, 99.36%), membranous (162, 52.1%), nuclear (44, 14.15%) and apical (16, 5.15%). Cytoplasmic pattern was the only one observed in 109 cases (35%) and mixed immunotopography in the others. There were significant positive associations between apical and membranous ezrin localization and favorable tumor characteristics and lack of lymph node metastases. Cytoplasmic ezrin staining was associated with adverse clinical outcome. Lack of apical ezrin was likely to present with bone metastases in the absence of visceral disease. Membranous ezrin localization was correlated with good prognosis both for CSOS (p=0.018) and DFS (p=0.007). A multivariate analysis demonstrated that membranous ezrin distribution is an independent prognostic factor (p=0.042).
Conclusion: The switch of ezrin localization from the apical and the membrane to the cytoplasm is correlated with dedifferentiation and adverse features in BC. Cellular ezrin distribution contributed to discriminating between patients with lymph node and distant metastases and those with better prognosis.

0014
Expression of EGFR in invasive ductal breast carcinomas

T. Ivkovic Kapicl, S. Knezevic Usaj, D. Djilas Ivanovic, Z. Nikin, B. Stojiljkovic*
*Oncology Institute of Vojvodin, Dept. of Pathology, Sremska Kamenica, Serbia and Montenegro

Objective: Epidermal growth factor receptor (EGFR) is a tyrosine kinase growth factor receptor expressed in a variety of human cancers and related with poor prognosis. Recently, the astounding development of molecule-targeting drugs such as anti-EGFR-targeting drug has attracted considerable interest of oncologists. The objective of this study was to evaluate the expression of EGFR in breast carcinomas and its possible relationship with different clinical–pathological parameters.
Method: One hundred and seventeen breast carcinomas were included in this study. Using a standard immunohistochemical technique, the expression of EGFR, HER2, and hormone receptors was investigated. In addition, haematoxylin and eosin-stained sections of these tumors were studied for several morphological parameters.
Results: EGFR-positive expression was detected in nine tumors (7.69%). Expression of EGFR was positively associated with high histological grade (p=0.023), high-grade comedo-type necrosis (p=0.000), high degree of stroma lymphocyte infiltration (p=0.027), pushing tumor margin (p=0.027), and hormone receptor-negative HER2-negative status (triple-negative phenotype, p=0.026). No significant difference of EGFR expression according to age was recognized.
Conclusion: EGFR expression is more often present in the group of triple-negative breast carcinomas, and its expression is associated with features of poor prognosis. EGFR expression might be important as a potential target for molecular therapy in breast cancer.

0016
Morphometric parameters of nucleoli and nuclei of tumor cells from primary breast cancer with positive versus negative axillary lymph nodes

K. Karpidska- Kaczmarczyk, W. Domagala, M. Kaczmarczyk, A. Kram*
*Pomaranian Medical University, Dept. of Pathology, Szczecin, Poland

Objective: The purpose of the study was to assess morphometric parameters of nuclei and nucleoli in invasive ductal breast carcinomas and to compare them with axillary lymph node status.
Method: Histologic sections from 150 tumors were stained with methyl green-pyronin Y and measurements were made using a computerized image analysis. The following seven parameters were evaluated: the nucleolar area, long-to-short nucleolar axis ratio, nucleolar shape parameter assessing the degree of nucleolar roundness, the nuclear area, long-to-short nuclear axis ratio, number of nucleoli in the nucleus and the percentage of the nuclear area occupied by nucleoli.
Results: A statistically significant association between a nuclear area, long-to-short nuclear and nucleolar axis ratio and Bloom–Richardson (B-R) histologic grade of breast tumors was found in relation to the axillary lymph node status. In B-R grade 1 tumors, the nuclear area was significantly larger in tumors with negative versus positive axillary lymph nodes (p<0.05). Long-to-short nuclear and nucleolar axis ratios were higher in B-R grade 2 tumors with negative versus positive lymph nodes (p<0.05), i.e. the shape of nuclei and nucleoli of tumor cells from node-negative cancers was more elliptic as compared to node-positive ones.
Conclusion: Morphometric parameters of nucleoli and nuclei of breast cancer cells may have prognostic value in invasive ductal breast carcinomas.

0019

Triple-negative breast cancer in the Romanian population—clinicomorphological and immunohistochemical phenotype

*M. Comanescu**

*University Emergency Hospital, Dept. of Anatomic Pathology, Craiova, Romania

Triple-negative (TN) breast tumors are described by immunohistochemical lack of expression of hormone receptors (ER and PR) and Her2/neu. This immunophenotype is associated with young age and increased biological aggressiveness, being described in the literature as an overlap with molecular basal-like subtype. The aim of our study was the illustration of the histopathological and, by the use of a wide range of biomarkers, the phenotypic features of TN tumors in our study group. Our study was multicentric, consisting of an extensive casuistry belonging to Victor Babes Institute, Bucharest, University Emergency Hospital of Bucharest, Emergency County Hospital of Craiova and spread over a period of 5 years (2005–2009). The study group consisted of 250 patients with ages ranging from 23 to 83 years (mean 52.64 years). The tumors were investigated using morphological analysis (gross and microscopic), the identification of the basal/myoepithelial phenotype, markers of cell proliferation, identification of gene abnormalities and markers of intracellular signaling pathways. The results were processed using digital image analysis, biostatistics and biomathematics. Better stratification of patients according to risk based on these markers may be useful in guiding therapy in TN breast cancers, the therapeutic decision including all the characteristics of a tumor.

0020

Quantitative protein network monitoring for uPA and PAI-1 in breast cancer

K. Malinowsky, C. Böllner, D. Berg, A. Walch, T. Schuster, M. Schmitt, K.-F. Becker*

*Technische Universität München, Institute of Pathology, Germany

Objective: The urokinase-type plasminogen activator (uPA) and its main inhibitor PAI-1 facilitate migration and invasion of cells in physiological and pathological contexts. Both factors are clinically applicable predictive markers in node-negative breast cancer patients used to stratify patients for adjuvant chemotherapy. Besides their classical functions within the plasminogen activation system, these factors are shown to play important roles in cell signaling, thus providing new possibilities to interfere with cancer progression and metastasis. Although such networks are well described in cell culture systems, their analysis in tissues was hindered because protein extraction and direct analysis was possible only from fresh or frozen material, which may be not available in routine laboratory setting.

Method: We extracted proteins from formalin-fixed paraffin-embedded tissues, being the main source of archived patient samples in pathology institutes worldwide, by a new protocol developed in our laboratory and analyzed the extracts for interactions of uPA and PAI-1 with molecules belonging to signaling cascades relevant in cancer progression in a collective of 206 breast cancer patients using protein microarrays.

Results: A substantial correlation of uPA with Erk and Stat3 expression was ascertained, while PAI-1 correlates with Akt activation and EGFR-related signaling. Statistical analysis of uPA and PAI-1 protein expression did not reveal a significant correlation of uPA or PAI-1 with staging, grading or age of the patients.

Conclusion: Network monitoring for uPA and PAI-1 in breast cancer reveals interactions with main signaling cascades, confirming the findings of cell culture experiments. Our results reveal possible mechanisms underlying cancer development, thus providing possible new targets for cancer therapy.

0021

Mammary-derived growth inhibitor (MDGI) and estrogen-induced gene 121 (EIG121): a transcriptional/posttranslational approach and potential implications for anti-EGFR therapy in invasive breast carcinomas

D. Meseure, K. Drak Al-Sibai, M. Trassard, F. Lerebours, C. Leray, S. Vacher, R. Lidereau, I. Bieche, J. M. Guinebretiere*

*Centre Rene Huguenin, Dept. of Pathology, Saint Cloud, France

Objective: EGFR is frequently overexpressed during malignant transformation and linked with resistance to cytotoxic/ hormonal drugs. Anti-EGFR therapies have shown clinical benefits in the treatment of colorectal, pulmonary, pancreatic and upper airway carcinomas. Conversely, no activating mutations have been clearly identified in invasive breast carcinomas (IBC). In an attempt to discover targeted modalities for new clinical trials, we explored EGFR mRNA levels of expression and EGFR: (1) nuclear translocation, (2) internalization with MDGI cytosolic protein and (3) lysosomal-mediated degradation by EIG121 protein.

Method: EGFR, MDGI and EIG121 mRNA expressions were investigated by quantitative RT-PCR in a series of 470 IBC. Immunohistochemistry was performed with a panel of anti-EGFR, estrogen receptor (ER), progesterone receptor

(PR), HER2, MDGI and EIG121 antibodies (Abs) in a series of 90 IBC.

Results: We observed (1) global low mRNA EGFR levels, (2) high EGFR mRNA levels (12%) in the triple-negative group (NNN), (3) EGFR protein hyperexpression (14%) in the NNN group, (4) no nuclear immunolocalization of EGFR, (5) positive correlation between EGFR mRNA and protein expression levels (0.0000049), and (6) high or normal MDGI mRNA levels (55%) and low EIG121 mRNA levels (38%).

Conclusion: Although EGFR expression is globally decreased in IBC, a targeted therapy may be justified by determining the expression levels of two EGFR pathway posttranslational regulatory proteins: MDGI (internalization) and EIG121 (degradation). Following our results, an anti-EGFR therapy seems indicated when (1) EIG121 level expression is low with normal or increased EGFR and (2) EGFR inhibitors preferred over Abs when MDGI is high.

0022

Bmi1 and Sox2—two stem cell markers identifying breast cancer patients with adverse prognosis

L. Pradel, S. Bastelberger, E. Hinterseer, J. Beil, O. Dietze, C. Hauser-Kronberger*
*University General Hospital, Dept. of Pathology, Salzburg, Austria

Objective: PolycombGroup (PcG) protein Bmi1 (B-lymphoma Mo-MLV insertion region 1) is crucial in maintaining gene silencing over cell cycles in order to control stem cell regulation and cellular identity. Sox2—the SRY (sex-determining region Y)-box 2 high-mobility group (HMG) protein—is the key trigger of pluripotency in embryonal stem cells. Deregulation of these genes is an initial step towards tumourigenesis with clinical vital difference.

Method: In this study, we applied these markers to 86 invasive breast cancer patients and five controls from breast hypertrophy prepared as formalin-fixed, paraffin-embedded (FFPE) tissue blocks. Sections were immunohistochemically (IHC) stained, evaluated and compared to histopathological data. Also, six breast cancer cell lines (MCF-7, MDA-MB231, MDA-MB453, SK-BR3, SUM-159, T47-D) provided as FFPE cytoblocks were additionally analysed.

Results: IHC identified 32.94% $Sox2^+$ and 70.13% $Bmi1^+$ patients. $BMI1^+$ expression is correlated to intermediate grade, tumours <2 cm in size and ER^+/luminal/triple positive subtypes which possess the greatest benefit to common therapies. $SOX2^+$ cases revealed patients with poor prognosis because of high grade, bigger size and increased metastasis. Also, clear correlation with basal-like and absence in normal-like phenotype were observed. 96.3% belonged to invasive ductal carcinomas, a subtype of worse prognosis in contrast to invasive lobular carcinomas, mixed forms or other subtypes.

Conclusion: SOX2 and BMI1 oncogenes, despite their pivotal role in mammogenesis and breast homeostasis, act in different ways when overexpressed, resulting in breast tumours with various prognoses. Probably, they describe different types of stem cells coexisting in adult tissue or of different origin.

0023

Podoplanin expression in cancer-associated fibroblasts predicts poor outcome of patients with invasive ductal breast carcinoma

B. Pula, A. Jethon, A. Piotrowska, C. Kobierzycki, A. Gomulkiewicz, I. Izykowska, A. Wojnar, M. Podhorska-Okolow, W. Witkiewicz, P. Dziegiel*
*University of Medicine Wroclaw, Dept. of Histology and Embryology, Poland

Objective: Podoplanin (D2-40) was recently demonstrated to be upregulated in cancer and stromal cells and was associated with increased tumor invasiveness. The role of cancer-associated fibroblasts (CAF) in tumor growth is poorly understood; therefore, we analyzed podoplanin expression in CAFs of invasive ductal carcinoma of the breast.

Method: Studies were performed on archival tissue samples of benign lesions and invasive ductal carcinoma (IDC) of the breast which were stained for D2-40. Serial sections stained for vimentin and alpha-SMA were used to identify CAFs. Expression of D2-40 in CAFs, LVD, and LVI were assessed and correlated with well-known prognostic factors.

Results: No D2-40 expression in stromal cells was shown in benign lesions and few of IDCs. The extent of D2-40 expression in CAFs correlated with grade of malignancy, LVI, and tumor size. No correlation with nodal, distant organ metastasis and LVD was observed. D2-40 expression in CAF was associated with shorter survival time.

Conclusion: Our preliminary data indicate that podoplanin may be a marker for cancer-associated fibroblasts. The results of this study demonstrate also its usefulness as a prognostic factor because of strong association with poor patient outcome.

0025

Breast cancer in young women

A. Vardouli, S. Divani, G. Kalodimos, A.-M. Fericean, E. Alexopoulou*
*General Hospital of Volos, Dept. of Cytology, Greece

Objective: Breast cancer is one of the most common human neoplasms accounting for approximately one quarter of all cancers in females. In young women, the risk is low, but because of the density of breast tissue, by the time a lump can be felt, the cancer is often advanced. Fine needle aspiration of breast lesions is routinely performed in our hospital. We reviewed our archives and found the cases of breast cancer in women under 40 years old.
Method: Between January 2003 and March 2010, 850 fine needle aspirates in breast lesions were performed in our Institution. The aspiration was done using a 21-gauge needle. Conventional and ThinPrep smears were prepared. Estrogen and progesterone receptor studies were part of the routine workup of a breast cancer as well as other markers (c-erb-B2, p53, E-cadherin, GCDFP-15).
Results: One hundred and fifty-eight of the cases were carcinomas. Ten of these patients were under 40 years old (mean age 38.2). In eight of these patients, cytology correctly diagnosed seven ductal and a tubular carcinoma. In two cases, the cytologic diagnosis was suggestive of carcinoma, and the excisional biopsy revealed a lobular and a mixed carcinoma.
Conclusion: It is mandatory in young women that a breast lesion be identified using mainly ultrasound and fine needle aspiration, which are simple and well-tolerated diagnostic tools. However, mammogram may also be recommended for younger women when a family history of breast cancer or other risk factors exist.

0026

MGMT protein expression as a potential prognostic marker in breast cancer

J. Cirullo-Neto, K. Carvalho, L. Kagohara, E. Olivieri, D. M. Carraro, I. W. Cunha, J. Vassallo, F. A. Soares, R. M. Rocha*
*Hospital do Cancer, Campinas-Sp, Brazil

Objective: MGMT repairs DNA damages via alkylation by removing a methyl group from the O6 position of guanine, acting as tumor suppressor gene in normal cells. We evaluated the MGMT protein expression in breast tumors, correlating it with others to establish its prognostic value.
Method: Sixty-four cases of invasive breast carcinomas were evaluated by immunohistochemistry (IHC) for MGMT, estrogen and progesterone receptors (ER, PR), HER-2-neu, Ki-67, p53, p63, E-cadherin, cytokeratins 5 and CK14 in order to classify the cases into luminal and basal phenotypes. Fluorescent in situ hybridization (FISH) was performed in those cases considered 2+ to assess HER-2neu gene amplification status. qRT-PCR was performed in frozen tissue to evaluate mRNA expression of MGMT.
Results: Fourteen cases were triple-negative (21.8%) and, among those, seven cases were basal-like carcinomas (10.9%). Twenty-five cases (39%) were luminal-like type A, four cases were (6.25%) luminal-like type B, and one case (1.5%) was HER-2-like type. MGMT showed significant lower expression in the basal-like tumors when compared to both luminal-like types ($p=0.007$). Tumors with basal-like phenotype presented higher positivity for p53 and Ki-67 than the luminal types ($p=0.025$ and $p=0.003$, respectively). Conversely, positive p53 and highly positive Ki-67 tumors showed a significant lower expression of MGMT ($p=0.0184$ and $p=0.0081$, respectively).
Conclusion: MGMT assessment by IHC or molecular biology techniques may represent an important prognostic factor in breast cancer. [Supported by FAPESP and CNPq]

0027

Correlations between prognostic factors in breast cancer

F. Staniceanu, E. Gramada, S. Zurac, L. Nichita, A. Ene, L. Tudorica, A. Slavnea, C. Socoliuc, C. Lazaroiu, G. Mirea, A. Dicu*
*Colentina University Hospital, Dept. of Pathology, Bucharest, Romania

Objective: It is well known that high indexes of estrogen and progesterone receptors (ER and PR) in mammary carcinoma are indicative for good prognosis and predict good response to endocrine therapy. Other important prognostic factors in mammary carcinoma are the age of the patient and histological type of tumor.
Method: We performed a retrospective study analyzing a group of 137 cases of 35- to 67-year-old female patients with mammary carcinomas reported in our department between 2007 and 2009. The histopathologic types of the tumors were established based on microscopic evaluation in HE stain, and ER (SP1 neomarkers) and PR (SP2 neomarkers) indexes were evaluated based on immunohistochemical stains.
Results: Eighty percent to 100% ER and PR positivity was by far most frequent in invasive ductal and mixed (ductal and lobular) types of mammary carcinoma (92 cases, 67.15%); intermediate levels of positivity (ER 40–50% and PR 10–20%) were reported mainly in medullary carcinoma (34 cases, 24.81%); and low levels of positivity (hormonal receptors <10%) were present mostly in perimenopausal patients.
Conclusion: Invasive ductal and mixed mammary carcinoma associates high level of positivity for hormonal receptors, especially in young patients, while medullary carcinomas of the breast (histopathologic type with better prognosis than ductal carcinoma) have lower levels of positivity for ER and PR. Age also plays an important role,

a better response for young women with positivity to hormonal receptors. Note: Staniceanu and Gramada should be regarded as first authors with equal contribution.

0028

Endosalpingiosis in axillary lymph nodes: a possible pitfall in the evaluation of sentinel lymph nodes

A. Corben, K. Garg, C. Vallejo, E. Brogi*
*MSKCC, Dept. of Pathology, New York, USA

Objective: The occurrence of benign inclusions in axillary lymph nodes (LNs) is well documented. Heterotopic mammary glands and intracapsular nevi can mimic metastatic carcinoma and are frequently encountered in the evaluation of sentinel LNs for breast cancer. Benign Mullerian inclusions (endometriosis and endosalpingiosis) are often identified in pelvic and paraaortic LNs, but only rare reports have documented the involvement of supra-diaphragmatic LNs.
Method: We report our 2003–2010 experience with three patients found to have endosalpingiosis in axillary sentinel LNs obtained for staging of breast carcinoma. All patients were postmenopausal women, with age ranging between 65 and 75 years.
Results: Endosalpingiosis involved a single lymph node in one patient and two nodes in each of the other two; it was present in the lymph node capsule in all three cases, with few glands scattered within the lymph node parenchyma in two of the patients. The glands contained ciliated and intercalated peg cells, had no periglandular endometrial-type stroma and showed no atypia or mitotic activity. The epithelium demonstrated positive nuclear immunoreactivity for WT1 and PAX8 and was devoid of myoepithelium or basement membrane. Endosalpingiosis had been misinterpreted as metastatic carcinoma at another hospital in one of the three patients, with subsequent dissection of 19 additional benign axillary LNs.
Conclusion: We conclude that endosalpingiosis can involve axillary LNs and closely simulate metastatic mammary carcinoma. Morphologic identification of ciliated cells and peg cells is most helpful to recognize this benign inclusion, and positive immunoreactivity for WT1 and/or PAX8 can be used to support the diagnosis. Correct classification of endosalpingiosis in axillary LNs is critical for accurate staging and to prevent possible overtreatment.

0030

Pathological assessment of sentinel lymph node and progression of lymph node metastasis at primary breast cancer

Y. Date, M. Takimoto, K. Matsuo, K. Suzuki, T. Sawada, M. Kushima, T. Morohoshi*
*Showa University, 1st Dept. of Pathology, Tokyo, Japan

Objective: Sentinel lymph node (SLN) biopsy has become a common procedure for breast cancer patients. Generally, if there is SLN metastasis, we do axillary lymph node (ALN) dissection. But sometimes we experience a case in which their LN metastasis is limited in SLN. So, we investigated these questions. (1) What is the factor associated to the progression of LN metastasis? (2) How is the case that we can ignore ALN dissection, even if there is SLN metastasis? (3) What is the best way to assess SLN?
Method: We retrospectively examined 94 Japanese patients who had surgical treatment for primary breast cancer between 2005 and 2009. All of them received ALN dissection after SLN biopsy. We also compared how to make sections for assessing SLN.
Results: Thirty-eight cases had no metastasis (SLN(−)Ax(−), 40.4%), 30 had only SLN metastasis (SLN(+)Ax(−), 31.9%), 21 were SLN(+)Ax(+) (22.3%), and five were SLN(−)Ax(+) (5.3%). By univariate analysis, lymphatic and/or vascular involvement was significantly correlated with the progression of LN metastasis. The cancer nest's size of metastatic SLN had more than 1 mm in all of SLN(+)Ax(+) cases. To detect SLN metastasis, making sections <2.0 mm in thickness was better than making the largest section ($p < 0.0001$). There was no correlation between how to make sections and ALN metastasis.
Conclusion: Lymphatic and/or vascular involvement was significantly correlated with the progression of LN metastasis. There was no ALN metastasis if the size of cancer nest was <1 mm in metastatic SLN. Making sections <2.0 mm in thickness was a better way to detect SLN metastasis.

0031

Audit of sentinel node handling and reporting in Kent

M. Ram, R. Liebmann*
*Harlow, United Kingdom

Objective: Sentinel lymph node biopsy (SLNB) is rapidly becoming the standard of care in staging the axilla for early-stage, clinically node-negative breast cancer. This audit reviews the laboratory handling and pathological reporting of sentinel nodes (SNs) across Kent and has been performed at the request of the Kent Cancer Network Breast Disease Oriented Group (DOG).
Method: A retrospective analysis of 20 consecutive breast SN cases from each of the five Kent hospitals was carried out. All reports and slides of positive SNs were reviewed. Detailed structured questionnaire-based enquiries to lead breast pathologists were made. Data were entered in Microsoft Excel and analysed in relation to the standards. All aspects of the pathology service were examined, including macroscopic data (number of SNs/case, dimensions, sampling and slicing details) and microscopic data

(performance of levels and immunohistochemistry, TNM staging and SNOMED coding).
Results: One site was unaware of radioactivity guidelines while another was unaware of national guidelines. Twenty-eight percent to 84% of SNs were bisected longitudinally and levels were sparingly used, except at 1 site. TNM staging and SNOMED coding in the reports were variable.
Conclusion: This audit demonstrates a substantial variation in SN handling and reporting practice across Kent. Since the quality of the pathology service in breast cancer is of paramount importance, it is imperative that a standardised approach is achieved in the handling and reporting of SNs. To achieve this, recommendations have been made and agreed upon, the success of which will be measured in a re-audit next year.

0032

Diagnostic value of automated Her2 evaluation in breast cancer: a study on 272 equivocal (score 2+) Her2 immunoreactive cases using an FDA-approved system

E. Bragantini, L. Morelli, C. Cantaloni, C. Eccher, E. Leonardi, D. Cazzolli, F. Gasperetti, D. Aldovini, P. Dalla Palma, M. Barbareschi*
*S.Chiara Hospital Trento, Dept. of U.O. Surgical Pathology, Italy

Objective: Accurate immunohistochemical (IHC) Her2 evaluation is fundamental for the therapeutic selection of breast cancer (BC) patients.
Method: We analyzed a series of 292 equivocally (score2+) Her2 immunoreactive BC; all had been stained with Dako Herceptest, evaluated by an experienced pathologist and analyzed with FISH. The automatic Aperio categorization and the percentage of immunoreactive cells as evaluated by the computer (CPV) and by the pathologist (PPV) were recorded.
Results: CAA classified seven (2.4%) cases as negative (0), 136 (46.6%) as faintly positive (1+), 134 (40.5%) as moderately positive (2+) and 15 (5.1%) as strongly positive (3+). CCA classification is associated with Her2 amplification ($p<0.0001$). The mean CPV is 18.44% SD ± 19.00 (range 0.01–76.10). CPV and PPV are significantly associated ($p<0.001$) and have similar sensitivities and specificities in identifying Her2 FISH-amplified cases. CPV has very low inter-observer variation. The difference in CPV in amplified and non-amplified subgroups is statistically significant ($p<0.001$). ROC analysis indicates that CPV is good at separating FISH not amplified from amplified cases ($p<0.001$). The optimal cutoff value maximizing both sensitivity and specificity is 17.6% (sensitivity = 73.3%, specificity = 71.6%). Reducing the cutoff value to 0.67%, it is possible to reach the sensitivity of 100% with 16.2% specificity.
Conclusion: CCA Her2 IHC evaluation is feasible and reliable; however, automated classification is not satisfactory as some amplified cases might be erroneously clustered in the score 1+ group. Compared with traditional Her2 evaluation, CAA can reduce the number of cases unnecessarily submitted to FISH.

0033

HER2 gene status assessment on cytological specimens of breast carcinoma using FISH

P. Drev, S. Frkovic Grazio*
*Institute of Oncology, Dept. of Pathology, Ljubljana, Slovenia

Objective: Assessment of HER2 status is mandatory for the treatment of patients with invasive breast cancer. According to ASCO/CAP recommendations, HER2 should be assessed on histological specimens with a validated immunohistochemical or FISH method. However, in some patients, histological material is not available and cytological specimens could be an alternative. The aim of our study was to optimise a FISH protocol for HER2 assessment on cytological samples.
Method: HER2 gene status was assessed using PathVysion HER2 probe (Abbott Molecular Inc.). FISH protocol was optimised on cytospines made from cultured cell lines with known HER2 gene status (SK-BR-3-positive, MDA-MB-453 borderline, MDA-MB-175-negative, MDA-MB-231-negative). The protocol was tested on 31 cases of primary or metastatic breast carcinoma with paired cytological and histological samples of the same tumour. FISH results obtained on paired samples were compared.
Results: In the four cell lines, the FISH protocol resulted in ratios that corresponded to the declared gene status. Analysis was successful in 27 (87.1%) cytospins and in 31 (100%) histological samples. Results were concordant in 26 of 27 (96.3%) cases (kappa 0.914). Among histological samples, 18 were negative, all also negative on cytospins, and nine were positive, of which eight were positive on cytospins. In the single discordant case (cytospin-negative/histology-positive), the analysis of the histological sample revealed intratumour heterogeneity of HER2.
Conclusion: FISH is a reliable method for the determination HER2 gene status on cytological specimens. However, FISH on cytospins is inferior to FISH on histology samples due to higher failure rate and absence of the morphologic features of the tumour.

0034

Application of image analysis in diagnostic assessment of HER2 gene status

P. Drev, S. Frkovic Grazio*
*Institute of Oncology, Dept. of Pathology, Ljubljana, Slovenia

Objective: The demand for accurate HER2 gene status testing is increasing. Application of image analysis (IA) facilitates archiving and reporting and standardises analysis of FISH reaction. The aim of the study was to evaluate the accuracy of an IA system for the determination of HER2 gene status in breast carcinoma.
Method: HER2 gene status was assessed in 203 cases with FISH using PathVysion HER2 probe (Abbott Molecular Inc.). Ratio ≥ 2 indicated amplification of the gene. Each case was analysed three times: The first result was obtained by manual analysis (MA) of the slide. Then, the slides were scanned and analysed with ARIOL-50SL IA system (Genetix inc.): The second result was the raw IA (RIA) result, and the third result was obtained by brief manual inspection and, if needed, correction of the RIA (CIA) results. The two IA results were compared with the MA results.
Results: Of the 203 cases, 43 (21.2%) were positive with MA, 65 (32.0%) with RIA and 35 (17.2%) with CIA. MA and RIA results were concordant in 161 (79.3%) cases, indicating poor agreement (kappa 0.478) and the need for inspection and correction. MA and CIA results were concordant in 191 (94.1%) cases (kappa 0.810). Among 12 discordant cases, in 11, at least one of the results was borderline (MA 3, CIA 9; median ratio discrepancy 0.54), and in a single case, the results were clear-cut discrepant.
Conclusion: IA, if adjusted to the quality of FISH reaction, is a reliable method for the analysis of HER2 gene, but inspection of RIA results is recommended in most cases and a few cases still require MA.

0035

New automated approach for FISH analysis of HER-2 amplification in invasive breast carcinomas

M. Lejeune, C. Lopez, A. Korzynska, J. Jaén, U. Neuman, T. Salvadó, L. Pons, T. Álvaro, X. Cugat, J. Baucells, R. Bosch*
*Hospital Verge de la Cinta, Tortosa, Spain

Objective: Computer-assisted digital image (DI) analysis has been used in the field of pathology to avoid human variability. This study shows a new automated method to evaluate HER-2 FISH amplification in composed DIs in a fast and easy manner.
Method: One hundred samples of invasive breast cancer were evaluated using pharmDxTMkit (DAKO). In each sample, three tumoral representative areas were selected to test the new methodology. All FISH signals are not in the same plane, so according to it, four DIs of representative areas were captured in different plains with FITC and also with Texas Red filters applying different focus settings. Definitive composite best-focus images were obtained for each filter using the "Extended Depth of field" tool of Image-Pro® Plus 5.0 software. The green channel from FITC and the red channel from Texas-Red images, captured as RGB colour images, were leveled by background subtraction using blurred large spectral low-pass-filtered images, as characteristic of non-homogeneity in light distribution. Resulting images were segmented using intensities threshold, which allows count FITC and Texas-Red signals in images. All the counted Texas Red and FITC signals were used to calculate the ratio for each sample manually and with the automated procedure, and both methodologies were compared.
Results: The k statistic was 0.935 with a $p<0.001$, showing a great agreement between the two methodologies.
Conclusion: This new automated method provides an accurate and practical alternative to the traditional manual determination of HER2- FISH amplification.

0036

New methodology to evaluate HER-2 FISH in invasive breast cancer

C. Lopez, M. Lejeune, A. Korzynska, R. Bosch, U. Neuman, T. Salvadó, N. Subirats, E. Muñoz, L. Pons, T. Álvaro, J. Jaén*
*Hospital Verge de la Cinta, Dept. of Pathology, Tortosa, Spain

Objective: In breast cancer, the efficiency of Trastuzumab (Herceptin®) therapy in unclear immunohistochemical scoring depends on the evaluation of HER-2 gene amplification using FISH. Traditional FISH evaluation is complicated and requires highly time-consuming work. This study presents a new methodology faster and easier than traditional based on the manual evaluation of HER-2 FISH using composed digital images.
Method: One hundred samples of invasive breast cancer were evaluated with FISH traditional method using pharmDxTMkit (DAKO). In each sample, three representative tumoral areas were selected to test the new methodology. An image of nuclei was captured with the DAPI filter at ×100 magnification. Without moving the section and applying different focus settings to cover the entire depth of the section, four consecutive images

were acquired with the FITC filter and then four with the Texas-Red filter. Then, using the "Extended-Depth of field" tool of Image-Pro® Plus 5.0 program, the four FITC images were superposed to obtain a new composite best-focus image with all the signals in the different plains. The same was done for the Texas-Red images. A global ratio was calculated using these composed images between all the Texas-Red and FITC signals, and it was compared with the ratio obtained with traditional evaluation.
Results: The *k* statistic was 0.968 with a $p<0.001$, showing a great agreement between the two methodologies.
Conclusion: The present work shows a new methodology to evaluate HER-2 FISH faster and easier. More evaluations should be made to show inter-laboratory agreement using this methodology.

0037
The value of the immunohistochemical panel: P53 and c-erbB2 in the prognostic appreciation of the mammary carcinomas

A. Muresan, A. M. Muresan, E. Lazar, A. Dema, A. C. Faur, M. Grigoras, R. Cornea, C. Suciu, I. Sargam*
*University of Medicine, Dept. of Pathology, Timisoara, Romania

Objective: Background: The study analyzes the positivism of the p53 protein and the oncoprotein c-erbB2 and their implication in the appreciation of prognostic invasive mammary carcinomas.
Method: In 60 invasive mammary carcinomas, we have realized the immunohistochemical determination of the p53 protein with the avidine–biotine complex method (ABC) using the DAKO p53 mouse monoclonal antibody (dilution 1:500). In 60 invasive mammary carcinomas, we have determined immunohistochemically the c-erbB2 oncoprotein with the DAKO rabbit polyclonal antibody, human anti-protein c-erbB2 (dilution 1:200). The tumoral tissues were fixed in 10% formaldehyde and included in paraffin.
Results: Out of 60 invasive mammary carcinomas, 21 (35%) have been p53-positive, and out of 60 carcinomas, 26 (43.3%) overexpressed the c-erbB2 oncoprotein. In the studied casuistic, we did not remark any connection between the p53 expression and the overexpression of c-erbB2.
Conclusion: The presently best-known mutant gene in invasive mammary cancer seems to be the p53 tumor suppressor gene. We did not remark any connection between the p53 protein expression and the tumors' sizes, patients' ages, the clinical stage of the disease and the overexpression of c-erbB2. The usage of the c-erbB2 status (HER-2/neu) in patients suffering invasive mammary carcinomas is a predictor of therapy response.

0038
Accuracy and correlative study in the diagnosis of breast lump by fine needle aspiration cytology and ultrasonography and diagnostic reliability of combined approach: a study on 222 patients

*M. Z. Rahman**
*Chittagong Medical College, Dept. of Pathology, Bangladesh

Objective: A large number of patients in Bangladesh have been suffering from breast cancer. The present study is done to see the accuracy of FNAC and USG in the diagnosis of palpable breast lesions and to see whether combination of the methods increase the diagnostic yield.
Method: Two hundred twenty-two female patients with palpable breast lump were included in this study to see the preoperative diagnostic accuracy of ultrasonography (USG) and fine needle aspiration cytology (FNAC) and to see their comparative performance. Histopathology was done in 89 cases.
Results: USG showed 88.89% sensitivity, 96.74% specificity, 84.21% PPV, 97.80% NPV and 95.45% accuracy, and FNAC showed 97.22% sensitivity, 99.46% specificity, 97.22% PPV, 99.46% NPV and 99.095% accuracy. Ultrasonography was found to be less sensitive, specific and accurate in the diagnosis of breast lump, though there is a highly significant ($P<0.001$) correlation.
Conclusion: The study has shown a much higher performance of FNAC than other previous studies. Only FNAC is enough for preoperative diagnosis of palpable breast lump. USG can enhance the diagnosis of breast lump. Combined approach is necessary when the breast lump is not well defined or not palpable.

0039
Accuracy and correlative study in the diagnosis of breast lump by FNAC, mammography, ultrasonography and diagnostic reliability of combined approach

M. Z. Rahman, S. Majumder*
*Chittagong Medical College, Dept. of Pathology, Bangladesh

Objective: A large number of patients in Bangladesh have been suffering from breast cancer. Because of existing social circumstances, female patients are hesitant to be examined by the physicians for breast lump, so report in advanced stage. The study was done to observe and compare the accuracy of FNAC, mammography and ultrasonography in the diagnosis of palpable breast lesion and to see whether combination of the methods increases the diagnostic yield.
Method: Two hundred twenty-two patients with breast lumps were included and mammography, ultrasonography,

FNAC and histopathology were done. Sensitivity, specificity and accuracy were evaluated.
Results: Thirty-six malignant cases were seen in 222 patients, mostly occurring in older age groups. Mammography and ultrasonography showed 82.76%, 88.89%, 97.22% sensitivity, 90.36%, 96.74%, 99.46% specificity and 88.39%, 95.45%, 99.095% accuracy, respectively.
Conclusion: Mammography and ultrasonography were found to be less sensitive, specific and accurate in the diagnosis of breast, lump though there is a highly significant correlation among them. However, the study has shown a much higher performance of FNAC than other previous studies.

0041
Differential diagnosis of chondroid differentiation in breast
J. Knolle, S. Hege, A. Damm, H. Zühlke*
*Klinikum Dessau, Institute of Pathology, Germany

Objective: There are only a few entities in the breast which show a chondroid differentiation. The differential diagnosis varies from the harmless choristoma to the also benign pleomorphic adenoma, to the syringioma and phylloides tumour with uncertain dignity to the high malignant metaplastic carcinoma. The differentiation between these different neoplasias is essential for the patient because of the following therapeutical procedures and the prognostic outcome. The final diagnosis in a mammary punch biopsy may be difficult or impossible because of the small specimen and the heterogeneity of the tumour.
Method: Our specimen is taken from a 66-year-old female. With mammography, new polymorph calcifications were found in the left breast. The results were classified as BIRADS 4 and surgical excision was recommended. One month after mammography, a stereotactic wire-marked diagnostic excision was performed.
Results: In histological examination, a chondroid proliferation appears with a beginning metaplastic ossification and two small foci of spindle cells and myxoid appearance. No suspicion for malignancy was found in the whole specimen. A chondroid choristoma in the left breast was diagnosed. In mammographic control 6 months later, no calcifications were detectable. So the tumour was totally removed.
Conclusion: A choristoma of the breast is very rare. In literature, it is described as choristoma (Tavassoli 1999) or as true chondroma (Rosen and Oberman 1993). The secured demarcation between the differential diagnosis is only possible at the in whole removed and nearly totally examined tumour. A chondroid differentiation in a mammary punch biopsy should be classified in the category B3. A diagnostic excision should be always performed.

0042
Inflammatory myofibroblastic tumour of the nipple: case report of a pregnant patient
A. Kovács, G. Máthé, G. Stenman, J. Mattsson, L.-G. Kindblom*
*Sahlgrenska University Hospital, Dept. of Pathology, Göteborg, Sweden

Objective: Extrapulmonary inflammatory myofibroblastic tumours (IMT) are rarely seen; only few cases have been reported in the breast. This report presents the first case of IMT in the nipple and highlights the histological features in this unusual site. The 31-year-old pregnant woman developed a palpable mass at the upper half of the left nipple, which started after lactation and increased in size during the present second pregnancy.
Method: Conservative surgical excision was performed 24 weeks of pregnancy with an uneventful postoperative course. There was spontaneous regression after incomplete removal.
Results: The pathogenesis of IMT is controversial. Initially, it was considered an aberrant reactive and/or inflammatory process, but some aggressive features suggested a neoplastic origin with chromosomal rearrangement in 2p22–24 regions.
Conclusion: IMT can be considered to be clonal proliferation of myofibroblasts, a true neoplasm with low malignant potential.

0043
Primary epithelioid angiosarcoma of the breast in an old male patient—case report and review of the literature
S. Stolnicu, C. Marian, M. Dohan, O. Preda, R. Nicolau, F. F. Nogales*
*University of Medicine, Dept. of Pathology, Targu Mures, Romania

Objective: Vascular tumors of the breast are very uncommon, consisting of variants of hemangioma and angiosarcoma. Although angiosarcoma related to chronic lymphoedema is the most frequent, it only represents 0.05% of breast tumors. Usually, primary angiosarcoma involves young pregnant females, with only six cases occurring in males reported to date. Epithelioid angiosarcoma is very unusual; their presence in males has been reported only once before in a young patient.
Method: This is the second case report of an epithelioid angiosarcoma in a male breast but the first one of poorly differentiated type. It developed in a 62-year-old patient, unrelated to hormonal dysfunction or treatment.
Results: The tumor located in the breast parenchyma had a 7-cm diameter and solid firm multinodular grey colour

areas admixed with cystic spaces with hemorrhagic content. Microscopically, the tumor was composed of mainly polygonal epithelioid tumor cells with abundant eosinophilic or pale cytoplasm and pleomorphic nuclei, arranged in solid areas and admixed with few spindle cells. Less than 25% of the tumor was composed of more differentiated areas. The tumor cells in both solid and cystic areas were positive for CD31 and vimentin but negative for CD34, ER, PR, HMB-45, and S-100 protein. Pan-Ck was positive in both epithelioid and spindle tumor cells.
Conclusion: Immunohistochemistry is very useful in order to establish a correct diagnosis; factor VIII, CD31 and CD34 can be used singly or in combination, although they may be lost in high-grade tumors. Epithelial markers may be also positive in epithelioid angiosarcoma.

Wednesday, 1 September 2010, Basement

PS-02 Poster Session Dermatopathology

0045

The semiquantitative immunohistochemical evaluation of the lymphangiogenesis density at cutaneous melanoma and its correlation with the sentinel lymph node status

*P. Buzrla**
*Faculty Hospital Ostrava, Institute of Pathology, Czech Republic

Objective: Lymphangiogenesis is a predictor of the sentinel lymph node status at cutaneous malignant melanoma. The aim of our investigation was the immunohistochemical semiquantitative evaluation of the lymphangiogenesis density and its correlation with the sentinel lymph node status. The file comprises 30 patients with cutaneous melanoma, 15 of them having the positive sentinel lymph node. The results of the investigation are partially in harmony with another study.
Method: For this investigation, the files of 30 patients with cutaneous melanoma radically excised and the sentinel lymph nodes were extirpated. The lymphangiogenesis density was immunohistochemically evaluated using CD34 and D2-40 (podoplanin). The localization of the lymphangiogenesis in cutaneous melanomas was determined and the lymphatic vessels were counted in 1 mm^2. After that, we evaluated the correlation between the lymphangiogenesis localization and the invasion depth according to Clark, following the correlation of the lymhangiogenesis density with the sentinel lymph node status.
Results: Lymphangiogenesis was dominant in the peritumorous localization of cutaneous melanomas. The lymphangiogenesis density and its localization have no influence upon the lymph node status. The correlation of the depth invasion with the lymph node status was not confirmed.
Conclusion: The results of the lymphangiogenesis localization are according to other study papers. We did not confirm the correlation between the lymphangiogenesis density and the sentinel lymph node status. It is necessary to extend the set of investigated patients with cutaneous melanoma and to use the LYVE-1 antibody. The extension of the count of patients with cutaneous melanoma and using other antibodies such as LYVE-1 are necessary in consecutive evaluations.

0046

Role of Notch signaling into cutaneous melanoma development and progression

*A.-M. Catrina Ene**, *A. Chitu Mihalcea, A. Florescu, E. Ionica, M. Sajin, O. Simionescu, M. Costache*
*University of Bucharest, Dept. of Biochemistry and Molecular, Romania

Objective: Melanoma is a malignant tumor of the neural crest-derived cells named melanocytes. It is an aggressive neoplasm due to its high rate of proliferation and invasion. Disruptions in the cellular signaling pathways promote melanoma development and progression. Aberrant Notch activation has been related to a variety of human neoplasms. We investigate the potential involvement of Notch signaling in melanoma development and progression. For this purpose, we analyzed the expression of three essential components of the Notch pathway: Notch1, ADAM10 and ADAM17/TACE.
Method: Melanoma samples from seven patients were tested and compared with normal skin samples. Immunofluorescent staining was performed on 5-μm-thick cryosections. Primary antibodies were applied and incubated overnight at 4°C. To detect the primary immune reaction, we used FITC-labeled goat anti-mouse secondary antibodies. The samples were examined using light and UV microscopy. For the Western blot technique, the Western-Breeze kit was used.
Results: Notch1 expression in normal skin was detected in the epidermis and also in hair follicles, sweat glands, sebaceous glands and blood vessels. Melanoma cells showed moderate to high levels of expression of Notch1. ADAM10 expression was detected in the epidermis and also in hair follicles. In some melanoma samples, ADAM 10 over-expression was observed. TACE/ADAM17 expression was detected only in the epidermis. Western blot analysis confirmed the presence of these proteins in cytoplasmatic and nuclear lysates.
Conclusion: We observed that the Notch signaling pathway is activated in melanoma cells. Critical members of the Notch pathway are potential therapy targets.

0047
P-53, BCL-2 and KI-67 expression in amelanotic melanomas

M. Costache, M. Sajin, M. Bura, M. Georgescu, A. M. Catrina, O. Simionescu*
*Victor Babes National Institut, Dept. of Pathology, Bucharest, Romania

Objective: Amelanotic melanoma is a subtype of cutaneous melanoma characterized by little or no pigment on visual inspection; it represents 2–8% of all melanomas. The lack of pigment makes it a great mimic of other benign and malignant lesions, a fact that can mislead the correct diagnosis.
Method: The study included a group of 34 cases of amelanotic melanomas, aged 17–83 years. Most of the tumors were thinner than 3 mm Breslow and Clark levels I to IV. The diagnostic was formulated based on special coloration for the melanic pigment (Masson–Fontana) and using immunohistochemical techniques (HMB-45, vim, S-100). The simultaneous positivity of these markers has shown the melanic aspect of the tumor. Bcl-2, ki-67 and p-53 was performed by standard immunohistochemical staining using monoclonal antibodies.
Results: bcl-2 expression was positive in 94% cases; ki-67 expression was positive in most of the cases, values between 3% and 68%; and p-53 expression was positive in most of the cases, values between 2% and 42%.
Conclusion: Our frequency detection is not related with the size of the tumor, depth, ulceration or mitotic activity. Most lesions present expression of bcl-2 in 90% of the cases and were associated with good prognosis; p-53 expression is between 3% and 62% and was associated with poor survival. Although ki-67 expression is between 6% and 71%, it is not related with the prognosis. It was suggested that p-53 and bcl-2 expression could be useful in predicting the biological behaviour. Neoplastic embolisations were identified in two cases of the study group.

0048
Amelanotic lentigo maligna

S. Dumitriu, D. Radulescu, C. Costea, S. Stolnicu, C. Ungureanu, E. Morosanu, A. Dumitriu, D. Butcovan*
*UMF Gr T Popa Iasi, Dept. of Pathology, Romania

Objective: We present the case of a 64-year-old woman who went to the dermatology department with a 3-year history of a slowly enlarging, erythematous plaque with central atrophy on the left cheek.
Method: The pathologic exam revealed an atrophic epidermis and proliferation of atypical melanocytes along the dermo-epidermal junction with formation of nests and an associated chronic inflammatory infiltrate with breach of the basement membrane, indicating a vertical growth phase.
Results: After many sections, the appearances were felt to be consistent with lentigo maligna melanoma to Clark level 2.
Conclusion: Despite wide local excision, the treatment of choice in amelanotic lentigo maligna recurrence is often seen.

0050
Difficulties in clinical and histopathologic diagnosis between the spindle cell melanoma and Kaposi sarcoma at the lower limb

L. E. Vasile, A. Condor, E. Lazăr, G. Buzete, R. Simulescu, A. Galuscan, R. Oancea*
*University of Medicine, Dept. of Cytology and Histology, Timisoara, Romania

Objective: Desmoplastic melanomas represent an extreme degree of fibroblastic or myofibroblastic metaplasia accompanied by abundant collagen synthesis. Those tumors are in general associated with high incidence of recurrence and metastasis and a poor prognosis.
Method: A patient P.C., male, 74 years old, presents at the clinical exam a right calcaneo-plantar ulcero-proliferative and multinodular lesion (2/1, 5/0, 5 cm), with a few months' course; there is local discomfort and functional impairment. Clinical diagnostic was that of Kaposi sarcoma and for the histopathology was sent a cutaneous specimen of 12/5/3 cm that contains the lesion. The specimens were examined using basic histological techniques and immunohistochemistry with antibodies anti-S100 protein, anti-CD34, anti-desmin, Melan A, HMB-45 and pan CK.
Results: Microscopically, it was identified as tumoral proliferation with spindle cells, uniform nucleus, some of them hyperchromatic, prominent nucleoli, some tumoral cells with brown melanic pigment and a rich mitotic activity. Immunohistochemical expression was intensely positive for S100 protein and Melan A and negative for HMB 45, desmin, CD34, pan CK, associated with focal lymphocytic inflammatory infiltrate. Tumoral proliferation includes adnexal structures of the skin and is ulcerated. The histopathological aspects lead to a desmoplastic melanoma. In spite of the large excision margins sidewise and in the depth, the tumor has reappeared locally after 4 months from excision and treatment, with inguinal ipsilateral metastasis.
Conclusion: The presented facts suggest a more close attention to the clinical and histopathological differential diagnosis of the tumoral cutaneous lesions in the lower limb extremities. This could influence the surgical therapeutic act.

0052

Metastatic potential of B16 melanoma in knockout (PAR-2$^{-/-}$) animals: pilot in vivo study

R. Matej, M. Zadinova, P. Pouckova, T. Olejar*
*Thomayer Teaching Hospital, Dept. of Pathology and Mol. Medicine, Prague, Czech Republic

Objective: Proteinase-activated receptor-2 (PAR-2) is a ubiquitous surface molecule. It belongs to the family of G protein-coupled receptors activated by the site-specific proteolysis of trypsin. Altered function of PAR-2 has been described in different malignant tumors. In the present study, we investigated the difference of the metastatic spread of melanoma B16 applied to knockout animals in comparison with C57Bl6 mice.
Method: Knockout mice B6.Cg-F2rl1tm1Mslb/J (PAR-2$^{-/-}$) and C57Bl6 controls were inoculated by established melanoma B16 tissue cell line subcutaneously. Fourteen days after inoculation, all primary tumors were removed and histopathologically analyzed. Onemonth after, animals of both groups started to die. After the autopsy, metastatic spread of the melanoma in different organs was evaluated in both groups.
Results: Our experiment confirmed the growth and metastatic spread in both murine groups. Removed tumors differed in volume; average weight was 0.62 g in PAR2$^{-/-}$ and 0.4 g in control animals. Metastatic spread was observed in both groups and reached 80% in PAR2$^{-/-}$ and 50% in control animals. Whether in control mice, only lung metastases were observed; local tumor recurrence and renal and lung metastases were observed in PAR2$^{-/-}$ mice.
Conclusion: The absence of functional PAR-2 could be an important factor influencing the growth and spread of melanoma in vivo probably due to the process of tumor cell migration, invasiveness and metastasis formation. However, further studies on larger animal groups need to be performed to confirm our results. Acknowledgement: Partly supported by IGA MZ NS/10423-3 and grant no. 309/09/P204 of the Grant Agency of Czech Republic.

0053

Identification of t(17;22)(q22;q13) (COL1A1/PDGFB) in dermatofibrosarcoma protuberans by fluorescence in situ hybridization in paraffin-embedded tissue microarrays. Clinical and histopathological correlation in 40 cases

A. Saez Artacho, S. Segura, R. Salgado, I. Costa, A. Toll, G. Martín-Ezquerra, M. Yébenes, F. Solé, C. Barranco, B. Espinet, R. M. Pujol*
*Udiat Centre Diagnostic, Dept. of Pathology, Barcelona, Spain

Objective: Dermatofibrosarcoma protuberans (DFSP) is genetically characterized by the translocation t(17;22)(q22;q13), resulting in PDGFB/COL1A1 fusion gene. The t(17;22) translocation leads to the activation of the PDGFB receptor that offers the possibility to use inhibitors, such as imatinib mesylate (Glivec®, Novartis), as a therapeutic alternative in locally advanced or metastatic cases. Fluorescence in situ hybridization (FISH) with specific probes allows a rapid detection of this gene. The objective of the study was to analyze the presence of the translocation t(17;22)(q22;q13) by FISH in paraffin-embedded tissue microarrays (TMA) of cases diagnosed as DFSP and dermatofibromas (DF).
Method: This is a multicentric retrospective study. Two tissue microarrays (TMA), including 40 DFSP and 20 DF, were evaluated. FISH analyses were performed using a dual-color, dual-fusion non-commercial probe. Clinical and histopathological features were systematically evaluated and association with FISH results was explored.
Results: Twenty-nine DFSP and 16 DF could be successfully evaluated. Twenty-five (86%) DFSP samples were positive for the translocation, which was not present in any DF samples. Two of the negative DFSP corresponded to more undifferentiated tumors, whereas one case exhibited overlap features with DF (this case was finally considered a deeper and more cellular variant of DF). The samples included in the study could show inter-individual variations in diagnostic criteria.
Conclusion: The COL1A1/PDGFB fusion gene is present in most of DFSP. The detection of the translocation by FISH is easier, more effective and less time-consuming than other molecular techniques and may have additional diagnostic and therapeutic interest in clinical practice.

0054

Early phase of Kaposi's sarcoma in a HIV-positive young woman

J. Ioan, G. Simona, K. Z. Iringo*
*UMF, Dept. of Pathology, Targu-Mures, Romania

Objective: AIDS-related Kaposi sarcoma is especially observed in young men with AIDS. This tumor is more rarely observed in an infected young woman and early phase is not easily diagnosed; it could be confused with inflammatory dermatosis or other skin lesions.
Method: Our paper is a case presentation.
Results: Case report: We present the case of a 20-year-old woman, diagnosed in 1998 with HIV infection, without antiretroviral treatment. Elevenyears later, she presented multiple skin erythematous plaques on the neck, trunk and lower limb. Serum level of T helper lymphocytes (CD4)

was 42/nmc. Histological exam of skin biopsies revealed in dermis a significant proliferation of irregular, small vascular channels, covered by a single layer of atypical endothelial cells. These channels were predominately arranged around preexistent mature vessels and adnexal structures. They were placed parallel to the epidermis and were marked by CD34 antibody. With this antibody, we observed that majority of these vessels were intermediary vessels whose proliferation could be suppressed by anti-angiogenic therapy. Based on clinical, histological and immunohistochemical aspects, diagnosis of Kaposi's sarcoma in early stage was made. Chemotherapy was initiated (HAART scheme) for 6 months. After this treatment, skin plaques have disappeared and serum level of CD4 increased at 146/nmc.
Conclusion: It is very important to recognize early phase of Kaposi's sarcoma and to initiate the treatment in order to improve prognosis of this lesion in HIV-infected and also immusdepressed patients.

0055

The evaluation of expression of chosen oncogenic markers in Merkell cell carcinoma with the usage of tissue microarray and immunohistochemical methods

H. Majewska, A. Zawrocki, J. Szade, P. Czapiewski, B. Pieczynska, W. Biernat*
*Gdansk Medical University, Dept. of Pathomorphology, Poland

Objective: Merkel cell carcinoma (MCC) is a rare, aggressive primary neuroendocrine neoplasm of the skin. Its molecular development is not clearly defined.
Method: We undertook an immunohistochemical analysis of a series of 19 cases of MCC by tissue microarray method. The tissue microarray from MCC were analysed with antibodies to E-cadherin, CD73, matrix metalloproteinase type 2 (MMP2), endoglin (CD105), anaplastic lymphoma kinase 1 (ALK1), nestin, nm23 (NME1), CDX2, the cell cycle regulator proteins (P21, P53, P63), oncoproteins (Bcl-2, BRAF, RAS and TWIST1). We also examined expression of the potential anticancer drug targets, i.e. topoisomerase II.
Results: Depending on the type of the analysed protein, the nuclear (p21, p53, topoisomerase type II), the cytoplasmic (Bcl2, BRAF) and membranous-cytoplasmic (TWIST, N-RAS) pattern of expression was regarded as positive. The expression of TWIST, Bcl 2, N-RAS, BRAF, p21 and topoisomerase II was irregular and showed no mutual correlations. The remaining proteins were not revealed in MCC.
Conclusion: We conclude that expression of topoisomerase II and BRAF may indicate potential benefit from targeted therapy against these markers.

0056

Expression of nuclear ubiquitous casein and cyclin-dependent kinases substrate (NUCKS) does not correlate with the expression of histone H1.0 in cells of the basal cell carcinoma

P. Ziólkowski, E. Gamian, J. Wisniewski, K. Symonowicz, K. Jurczyszyn*
*Wroclaw Medical University, Dept. of Pathology, Poland

Objective: Nuclear ubiquitous casein and cyclin-dependent kinases substrate (NUCKS) is a 27-kDa chromosomal protein of uncertain function. Its amino acid composition and the structure of its DNA binding domain resemble that of high-mobility group A proteins. Since changes in the expression of HMGA are considered as markers of tumor progression, it is possible that similar changes in the expression of NUCKS could be useful in the diagnosis of malignant tumors.
Method: We used specific antibodies against NUCKS and linker histone H1.0 for immunohistochemistry on paraffin-embedded samples in basal cell carcinoma. We also used, Ki67 marker, to compare with the above two markers.
Results: We found a high expression of NUCKS in nuclei of BCC cells which exceeded the expression of well-known proliferation marker, Ki67. The expression of NUCKS in cancer cells did not correlate with the expression of H1.0. We also assessed the expression of NUCKS and H1.0 in inflammatory cells, i.e. lymphocytes and plasma cells. This expression was entirely found in single cells and remained very low in all cases.
Conclusion: With the present study and based on our previous experience, we would like to suggest NUCKS as a novel tumor biomarker in the immunohistochemical evaluation of formalin-fixed and paraffin-embedded BCC specimen.

0057

Bowen disease of the eyelids

S. Dumitriu, C. Costea, D. Radulescu*
*UMF Gr T Popa Iasi, Dept. of Pathology, Romania

Objective: Bowen disease is a form of squamous cell carcinoma in situ. It is a distinct clinicopathologic entity of the skin and mucocutaneous junction.
Method: We present four cases of Bowen disease of the eyelids. Three patients (75%) were men and only one was a woman (25%). The mean age was 65 years. The average age at onset of the disease was 49 years.
Results: The appearance of the disease was a single or multiple erythematous, rounded to irregular, keratotic, nodular, pigmented plaques that appeared sharply demarcated from the surrounded unaffected skin. Low-power

microscopic features are hyperkeratosis, parakeratosis, a chronic inflammatory infiltrate in the upper corium and the appearance of crowding of atypical keratinocytes, with hyperchromatism. These changes are confined by an intact dermo-epidermal basement membrane
Conclusion: Surgical excision with complete removal may cure Bowen disease.

0058
Malignant chondroid syringoma of the scalp: a case report

N. Erdogan, N. Koç, D. Sahin*
*Marmara University, Saglik Hizmetleri MYO, Istanbul, Turkey

Objective: Chondroid syringoma, also known as mixed tumour of the skin, is an uncommon benign sweat gland tumour. Malignant chondroid syringoma is a very rare tumour. It may occur de novo or rarely develop in a chondroid syringoma.
Method: In contrast to the benign counterpart, which is common in the head and neck region, the malignant type occurs predominantly on the trunk and extremities.
Results: We report a case of malignant chondroid syringoma located on the scalp of a 77-year-old man.
Conclusion: The diagnosis of chondroid syringoma was made by histopathologic and immunohistochemical examination.

0059
P53 and Ki67 expression in skin epithelial tumors by immunohistochemical method

A. Fakhrjou, E. Khodaeiani, F. Taghvamanesh, S. Shadravan*
*Tabriz University, Dept. of Medical Pathology, Iran

Objective: Skin cancers are one of the most common human malignancies. Although the prognosis of these patients has improved in the last decades, there is still a need for novel treatment modalities and prevention from recurrence after the treatment of skin tumors. P53 is a tumor-inhibiting gene which is believed to be defective in many malignant situations. Ki67 is a non-histonic protein which mainly interferes with the proliferation and has many controlling effects during the cell cycle. This study aimed at evaluating P53 and Ki-67 expression in skin epithelial tumors by immunohistochemical method.
Method: In a descriptive setting, 50 biopsy samples—30 basal cell carcinomas (BCCs), ten squamous cell carcinomas (SCCs), eight keratoacanthomas (KAs) and two tricoepitheliomas (TEs)—were immunohistochemically evaluated for P53 and Ki67 expression during a 14-month period. The incidence and expression rate of these two variables were separately reported in each group of samples.
Results: The expression rate of P53 was 67.77%, 50.20% and null for BCCs, SCCs and KAs, respectively. For both TEs, it was 50%. The expression rate of Ki67 was 57.33%, 47.70%, 37.5% and zero for BCCs, SCCs, KAs and TEs, respectively.
Conclusion: This study showed that the incidence rate of P53 and Ki67-positive cells are very high in malignant epithelial tumors in the skin. The expression rate of these two variables is comparable with reports in the literature. Further studies with large sample size are recommended to be carried out for KA and TE samples.

0060
Extranodal Rosai–Dorfman disease: a case report

M.-M. Koumpanaki, P. Xirou, D. Alataki, G.-C. Balis, A. Delopoulos, F. Patakiouta*
*Theageneion Cancer Hospital, Dept. of Pathology, Thessaloniki, Greece

Objective: Rosai–Dorfman disease, or sinus histiocytosis with massive lymphadenopathy, is a rare benign, proliferative disorder that involves primarily the lymph nodes, especially in the cervical region. In almost half of the cases, synchronous extranodal sites have been reported. Isolated cutaneous extranodal Rosai–Dorfman disease can occur in <20% of the cases. We present a case of extranodal sinus histiocytosis in the subcutis of the lumbar region.
Method: We report the case of a 56-year-old female who was diagnosed with breast cancer two2 years ago and underwent mastectomy and chemotherapy. In a follow-up examination, a subcutaneous nodule was found and was surgically removed.
Results: We received a well-circumscribed, white-yellow elastic nodule measuring 1.3 cm in maximal diameter, surrounded by fatty tissue. Histologically, the nodule consisted of solid nests of large cells with abundant eosinophilic cytoplasm and large "ground glass" nuclei with prominent nucleoli. Mitoses were rare and no atypia or pleiomorphism was observed. Immunohistochemically, the cells were positive for vimentin, S-100 protein and CD68 (KP1 and PGM1). Among these cells, scattered multinucleated giant cells and inflammatory infiltrates were also found.
Conclusion: It should be pointed out that Rosai–Dorfman disease is a non-neoplastic condition; thus, it does not require additional therapy. Surgical excision is the treatment of choice. Differential diagnosis includes other histiocytic lesions, such as histiocytosis X and epithelioid mesenchy-

mal neoplasm, mainly of neurogenic origin. The case of a metastatic melanoma should always be ruled out.

Wednesday, 1 September 2010, Basement

PS-03 Poster Session Nephropathology

0062

Membranous glomerulopathy with anti-neutrophil antibodies (ANCA)-associated crescentic glomerulonephritis. An unusual case of dual glomerulopathy

M. Wagrowska-Danilewicz, D. Marian, N. Michal, K. Ilona*
*Medical University Lodz, Dept. of Nephropathology, Poland

Objective: The coexistence of anti-neutrophil crescentic glomerulonephritis with membranous glomerulopathy is very rare. Little is known about the clinical course, treatment and outcome of patients with concurrent coexistence of these nephropathies.
Method: We present the case of a 58-year-old man with rapidly progressive renal failure, anti-neutrophil perinuclear antibodies positivity, pulmonary infiltrates and vasculitis.
Results: The patient was admitted to the pulmonary department due to febrile state, weakness and weight loss. Physical examination revealed fine crackles over the left lung, leg edema, and vascular skin lesions on inferior extremities. Urinalysis showed proteinuria and hematuria with many RBC casts, and in a 24-h urine collection, the proteinuria of 2 g was observed. Serologic workup was positive for p-ANCA, negative for c-ANCA, ANA, and anti-GBM antibodies and showed normal levels of C3 and C4. HCV, HBV and HIV infection were excluded. In lab tests, the rapid increase of serum creatinine from 1.3 to 5.17 mg/dl over 2 weeks was observed. Chest CT revealed pulmonary infiltrates of left lung upper lobe. The patient underwent a kidney biopsy which showed necrotizing crescentic glomerulonephritis and membranous glomerulopathy. In light microscopy examination, glomeruli with necrotic lesions and cellular crescents were seen. Electron microscopy revealed epimembranous and intramembranous deposits. The patient was treated with steroids; cyclophosphamide and seven plasmapheresis were performed with improvement in renal function. On 1-year follow-up, his proteinuria had decreased to 300 mg/day and his creatinine had stabilized at 1.6 with eGFR of 56 ml/min.
Conclusion: In conclusion, this case illustrates membranous nephropathy superimposed with ANCA-associated crescentic and necrotizing glomerulonephritis. (Supported by grant of Polish Ministry of Science and Higher Education No. N402 088735).

Wednesday, 1 September 2010, Basement

PS-04 Poster Session Pulmonary Pathology

0066

AKT and PTEN in non-small cell lung carcinomas—acting together or apart?

C. M. Ardeleanu, F. Vasilescu, C. Iosif, D. Terzea, A. G. Mihaela Georgescu, M. C. Stoicea, M. Mihai, F. Andrei, C. Dobrea, S. Enache, M. Dumitrescu*
*V. Babes National Institute, Dept. of Pathology, Bucharest, Romania

Objective: In the last years, the study of predictive and prognostic markers of non-small cell lung carcinomas (NSCLC) has been a continuous challenge. It is well known that the imbalance between AKT and PTEN expressions plays an important role in cell proliferation, angiogenesis and tumor cell invasiveness in various solid malignancies. The aim of our study was to analyze the AKT and PTEN expressions in primitive non-small cell lung carcinomas and, also, in their metastases.
Method: We have examined AKT and PTEN immunohistochemical expressions in 64 primitive non-small cell lung carcinomas with different stages and in ten metastatic non-small cell lung carcinomas: brain, adrenal glands and lungs.
Results: AKT expression was higher in metastatic than in primitive non-small cell lung carcinomas, while PTEN was over-expressed in 98% of all tumors. There were no obvious associations between tumor stage and AKT/PTEN expression. There were no correlations between PTEN over-expression and AKT expression.
Conclusion: AKT activation may play an important role in tumor cell invasiveness in non-small cell lung carcinomas, but PTEN suppressor gene may not be involved in AKT activation.

0067

miR-21 overexpression in pulmonary adenocarcinomas and squamous cell carcinomas

L. Carvalho, M. Silva, P. Santos, C. Gomes, J. Dinis, S. Carmona, L. Cortes, M. J. Aguiar, L. Teixeira, I. Velada*
*Faculdade de Medicina Coimbra, Dept. de Anatomia Patologica, Portugal

Objective: The role of miRNAs in cancer is a rapidly emerging area of investigation. Expression profiling has

identified miRNA signatures in cancers that associate with the diagnosis, staging, progression, prognosis, and response to treatment. MiRNAs are ideal biomarkers in FFPE tissue because unlike mRNA, miRNA integrity is affected very little by formalin fixation. Previous studies have shown that miR-21 overexpression correlated with poor prognosis in NSCLC patients. In this study, we investigated the expression of mir-21 in primary carcinoma and metastasis and near non-tumor parenchyma.

Method: FFPE samples from surgical specimens and biopsies of seven pulmonary adenocarcinomas and five squamous cell carcinomas and respective metastasis together with normal lung tissue (alveolar and bronchial) from the same case; it was imperative to separate these well-characterized areas by laser-capture microdissection (LCM) prior to RNA analysis.

Results: The expression level of miR-21 by qRT-PCR was significantly higher in tumor tissues than in adjacent normal tissues ($p=0.005$). The overexpression in the metastasis samples compared to adjacent normal tissue was almost statistically significant ($p=0.051$).

Conclusion: miR-21 was overexpressed in tumor tissues relative to adjacent non-tumor tissues. We found an increase in miR-21 expression in primary carcinoma and metastasis in pulmonary adenocarcinomas when compared with miR-21 lower expression in squamous cell carcinoma. Despite the small sample studied, further investigation may indicate the therapeutic and prognostic relevance of this determination as previous studies suggest that miR-21 acts as an oncogene and has a role in tumorigenesis through the regulation of tumour suppressor genes.

0068

EGFR and KRAS mutations in mixed type of pulmonary adenocarcinoma

L. Carvalho, A. Alarcão, P. Couceiro, M. Silva, M. J. Aguiar, L. Teixeira, V. Sousa*

*Faculdade de Medicina Coimbra, Dept. de Anatomia Patologica, Portugal

Objective: The EGFR and KRAS genes act sequentially in the MAPK signaling pathway. The KRAS gene is located downstream in the transduction of signals transmitted from the transmembrane receptor EGFR to the nucleus through a series of intermediate genes. Patients with non-small cell lung cancer (NSCLC) with EGFR mutations are more sensitive to treatment with tyrosine kinase inhibitors (TKIs) without KRAS mutations. The different patterns recognized in adenocarcinomas were microdissected to identify mutations in both EGFR and KRAS in order to clarify their significance when selecting patients either to TKIs.

Method: Histological sections of 31 adenocarcinomas of the lung, FFPE, were selected to analyze EGFR exons 19 and 21 mutations and KRAS codons 12 and 13. DNA was extracted for polymerase chain reaction (PCR). Exon 19 was studied by fragment analysis; exon 21 and codons 12 and 13 were studied by direct sequencing.

Results: From the 31 samples studied, 10 of 31 showed in-frame deletions, 4 of 20 L858R substitution in the EGFR, and 5 of 31 point mutations in codon 12 of KRAS. In all cases, mutations were exclusive for EGFR and KRAS in alternative. Only one mixed adenocarcinoma showed EGFR in-frame deletions in bronchiolo-alveolar pattern and Wt in acinar pattern (KRAS Wt).

Conclusion: In this set of mixed-type adenocarcinomas, the different histological patterns revealed to be inconsequent for KRAS and EGFR determination of mutations, reinforcing the technical feasibility and reliability of small biopsies of lung cancer to determine personalized therapy.

0069

MLH1 and MSH2 methylation status in pulmonary adenocarcinomas and epidermoid carcinomas

L. Carvalho, V. Sousa, A. Gomes, A. Alarcão, P. Couceiro, M. Silva*

*Faculdade de Medicina Coimbra, Dept. de Anatomia Patologica, Portugal

Objective: Five-year survival of lung cancer is 16% and in surgical stages increases to 50% as 14–16% comprise this group. DNA methylation emerged as potential cancer-specific biomarker, and although hypomethylated, DNA can become aberrant or hypermethylated in CpG-rich areas or near promoter region of tumour suppressor genes, inhibiting apoptosis and favouring angiogenesis, metastization and DNA miss repair, resulting silencing genes of cellular homeostasis and renewal.

Method: Methylation profile and possible silencing of DNA repair genes—MLH1 and MSH2—by methylation-specific PCR and protein expression, in tumoral tissue, preneoplastic lesions when available, respiratory epithelium and parenchyma with normal histological features were searched in 40 squamous cell carcinomas (SCC) and 40 adenocarcinomas in surgical TNM staging.

Results: IHC expression of MLH1 and MSH2 in SCC and adenocarcinoma, in hyperplasia, metaplasia and in normal cylindrical respiratory epithelium appeared reduced. The frequency of promoter hypermethylation of these DNA repair genes was elevated, with a higher prevalence of methylation of MLH1 in SCC. The differences are not so obvious for MSH2 promoter region hypermethylation. No statistical correlation was defined between the status of methylation, protein expression and the clinicopathological characteristics (age, gender, TNM stage).

Conclusion: This research made in surgical specimens may have future impact on the potential characterization of gene hypermethylation in small biopsies and preneoplastic lesions in assessing the prognosis/progression of lung cancer as it was developed in FFPE tissue. It was also demonstrated that methylation status and gene IHC expression have to be enrolled in different pathways.

0070

Nuclear magnetic resonance spectroscopy applied to small samples of bronchial–pulmonary carcinomas identifies metabolic profiles

L. Carvalho, I. Duarte, C. Rocha, A. Barros, A. Gil, B. Goodfellow, A. Gomes, D. Oliveira, J. Bernardo*
*Faculdade de Medicina Coimbra, Dept. de Anatomia Patologica, Portugal

Objective: Routine diagnosis and prognostic methods may also be useful to add data to clinical information in advanced primary carcinomas if conveniently explored. The evaluation of the potential of ^{1}H NMR spectroscopy for providing biochemical information of the different histological types and for discriminating between tumour and pulmonary parenchyma as well as biochemical information about different histological types was tried as a preliminary approach.
Method: Small frozen samples of 24 pulmonary tumours were collected together with macroscopically normal parenchyma from surgical specimens before histological classification and mirror tissue was FFPE. Paired cases were directly analysed by high-resolution magic angle spinning (HRMAS) ^{1}H NMR spectroscopy (500 MHz). The spectral profiles obtained were subjected to multivariate analysis: principal component analysis (PCA) and partial least squares regression discriminant analysis (PLS-DA) with the predictive ability of the statistical models.
Results: Tumor and control tissues were clearly discriminated in the PLS-DA model with high level of sensitivity (95% of tumor samples correctly classified) and 100% specificity (no false positives). The metabolites giving rise to this separation were mainly lactate, GPC, PC, taurine, glutathione and UDP/UTP (elevated in tumors), and glucose, phosphoethanolamine (PE), acetate, lysine, methionine, glycine, myo- and scyllo-inositol (reduced in tumors compared to control tissues). Furthermore, PLS-DA allowed carcinoids to be discriminated from adenocarcinomas and epidermoid carcinomas.
Conclusion: This preliminary study raised the NMR profile between the different histological types of bronchial–pulmonary carcinomas through multivariate analysis and scaled metabolic profiles that may be delineated to improve clinical decisions in future.

0071

Correlation of the epithelial–mesenchymal transition markers with clinicopathologic features and the EGFR copy number status in non-small cell lung carcinomas

K. Kim, S.-H. Kim, J. M. Kim, K. S. Suh, E. S. Yi*
*Chungnam National University, Dept. of Pathology, Daejeon, Republic of Korea

Objective: The aim of this study was to investigate the expression of the epithelial–mesenchymal transition (EMT)-related factors (vimentin, E-cadherin, beta-catenin, twist1, slug, and snail) in non-small cell lung carcinoma (NSCLC). Association of these proteins with clinicopathologic parameters and EGFR gene amplification status was also analyzed.
Method: A total of 60 squamous cell carcinomas (SQ), 48 adenocarcinomas (AD), four sarcomatoid carcinomas, one large cell carcinoma, and one mucoepidermoid carcinoma was studied using immunohistochemistry for EMT markers and automated silver-enhanced in situ hybridization for the evaluation of the EGFR copy number.
Results: In a 114-sample NSCLC series, expression of vimentin was negatively associated with expression of E-cadherin (P=0.002) and positively correlated with expression of twist1 (P=0.022). Positivity of EGFR gene amplification was associated with a decreased expression of E-cadherin in NSCLC (P=0.037). In the 114 sample NSCLC series, 48 AD samples showed a positive correlation between vimentin and slug expression (P=0.034). On the other hand, a positive correlation between twist1 and vimentin expression was observed in 60 SQ samples from a total of 114 NSCLC samples (P=0.002). A positive correlation trend between tumor size and vimentin expression was identified for SQ (P=0.032). Expression of vimentin was significantly higher in AD than in SQ (P=0.027).
Conclusion: These results indicate that positive vimentin expression contributes to SQ tumor growth and that different expressions of the EMT phenotype in AD and SQ are implicated in different EMT pathways, resulting in new perspectives for therapeutic targeting of these tumor types.

0072

Prognostic significance of the expression of the RNA-binding protein HuR in stage I and II lung adenocarcinoma

M. Novello, L. Lauriola, G. Monego, P. Lanza, S. Serini, P. Granone, S. Ramella, F. O. Ranelletti*
*Catholic University Rome, Dept. of Pathology, Italy

Objective: The RNA binding protein HuR can stabilize and/or regulate the translation of target mRNAs affecting

cellular responses. The expression of HuR is increased in several cancers, and cytoplasmic immunoreactivity was found to be closely related to poor outcomes.
Method: We analyzed, by quantitative immunohistochemistry, the expression of HuR in 54 lung adenocarcinoma of mixed histologic type from stage I and II patients. Moreover, we evaluated the level of HuR expressed both in the nucleus and cytoplasm of tumor cells (t-HuR) and evaluated the impact of nuclear/cytoplasmic ratio (N/C) on clinical outcome.
Results: Both t-HuR and N/C were not associated with age, tumor diameter and histopathological grading, whereas high t-HuR and low N/C were associated with lymph node involvement at presentation. Cox's regression analysis, using either t-HuR or N/C as continuous covariates, showed that high t-HuR and low N/C were associated with the risk of death and metastasis. The plots of the estimates, at 5-year follow-up, of metastasis-free and overall surviving as a function of t-HuR and N/C levels, showed that the increase of t-HuR and the decrease of N/C were associated with an increase of risk. In the multivariate analysis, both t-HuR and N/C retained an independent prognostic significance relative to metastasis-free and overall survival.
Conclusion: In conclusion, these data indicate that the over-expression of HuR in lung adenocarcinoma cells is an independent prognostic marker of a poor clinical outcome. Moreover, the cytoplasmic localization of HuR expression is more relevant than the nuclear one for the tumor cell behavior.

0074

Clinical features and prognostic implications of EML4-ALK fusion gene in resected non-small cell lung cancer

H. S. Ryu, X. Xu, J.-H. Chung, H. J. Lee*
*Seoul Nat'l University Bundang Hospital, Sungnam, Republic of Korea

Objective: The EML4-ALK fusion gene has been detected in 5–7% of non-small cell lung cancers. We evaluated the incidence, prognosis and the characteristics of ALK-rearranged non-small cell lung cancers and the optimal diagnostic modality to detect ALK rearrangements in routine clinical practice.
Method: Seven hundred seventy-nine surgical specimens of non-small cell lung cancer from two institutions were analyzed. To identify ALK rearrangements, immunohistochemistry and fluorescent in situ hybridization (FISH) examination were performed and compared. The clinicopathologic characteristics of tumors with and without ALK rearrangements were analyzed. EGFR and KRAS mutations were determined by DNA sequencing.
Results: We identified 49 (6.9%) non-small cell lung cancer with ALK rearrangements within our cohort by immunohistochemistry. Forty-three (87.8%) of the 49 EML4-ALK tumors were adenocarcinomas. ALK rearrangement was associated with never smoking ($p<0.001$) and female ($p < 0001$). Patients in the EML4-ALK fusion gene in adenocarcinoma had no effect on progression-free survival and overall survival. Immunohistochemical results were correlated with FISH results.
Conclusion: The patients most likely to harbor EML4-ALK are never smokers with adenocarcinoma. But EML4-ALK was not an independent prognostic factor. Immunohistochemical staining for ALK could be used as a screening method to detect ALK gene rearrangement.

0075

Primitive malignant lung tumors at the Emergency University Hospital Bucharest

M. Sajin, I. Hulea, A. Poteca, M. Comanescu, L. Reghina, G. Simion, E. Ionescu, M. Costache*
*UMF Carol Davila, Dept. of Pathological Anatomy, Bucharest, Romania

Objective: Lung cancer is one of the most common malignant tumors worldwide, with a growing incidence. In Romania, lung cancer has a prevalence of 8% and an incidence of 17%; in terms of deaths from cancer, it ranks first place in males and fourth place in females.
Method: We analyzed the malignant lung tumors from January 2006 to February 2009 using information obtained from observation sheets of Thoracic Surgery Clinic and the database of the Pathology Department of the University Emergency Hospital Bucharest. Distribution of cases was followed depending on age, environment, gender, living and working conditions (smoking, toxic, radiation), tumor stage and histological appearance.
Results: The analysis of these data shows that most lung tumors occurred in the fifth decade of age and is more common in men. Regarding histological type and age, the most common tumors were moderately differentiated squamous carcinomas (the decade IV, V, VI and VII). Four patients were hospitalized for another disease (inguinal hernia, uterine fibroma) and were subsequently transferred to the clinic for thoracic surgery for specialist treatment.
Conclusion: Physical examination, identifying the factors contributing to lung cancer appearance and its diagnosis in early stages, as well as an adequate communication between specialists, may contribute to the decrease of mortality as well as socioeconomical costs.

0076

Impact of the excision repair cross-complementation group 1 predictive biomarker on toxicity and quality of life in advanced non-small cell lung cancer patients randomized in a large, multicenter, cisplatin-based phase III trial

E. Santoni-Rugiu, A. Vilmar, J. B. Sørensen*
*Rigshospitalet, Copenhagen, Denmark

Objective: We recently demonstrated that clinically applicable immunohistochemical evaluation of ERCC1-status by semiquantitative H-score is a promising predictive biomarker in advanced NSCLC receiving first-line, platinum-based chemotherapy (Vilmar et al. Ann Oncol, 23-03-2010, Epub ahead of print). However, current correlation of ERCC1 status with toxicity and quality of life (QOL) is unclear.
Method: To address this point, 443 patients with advanced NSCLC were enrolled in a multicenter phase III trial and randomized to triplet chemotherapy (cisplatin+paclitaxel+gemcitabine) or standard doublet regimen (cisplatin+vinorelbine). Immunohistochemistry for ERCC1 status was performed by *H* score (immunostaining intensity × % positive tumor cells) on bioptic material and then correlated with toxicity and patient-reported QOL.
Results: Two hundred sixty-four NSCLC samples were assessable/representative for ERCC1 status. Patients with ERCC1-negative tumours, especially those with adenocarcinomas, showed significantly improved outcome. However, the entire population of ERCC1-negative tumour patients displayed numerically more toxicity, reaching significance for leukopenia (P=0.015), nausea/vomiting (P=0.040) and neurotoxicity (P=0.037) in adenocarcinoma patients. Mean change in the entire population's QOL was −13.33 (ERCC1-negative, P=0.001) and −2.25 (ERCC1-positive, P=0.607) and in adenocarcinoma patients −14.86 (ERCC1-negative, P=0.006) and 0 (ERCC1-positive).
Conclusion: QOL significantly deteriorated in patients with otherwise survival-favourable ERCC1-negative NSCLC, especially adenocarcinomas, possibly due to increased toxicity. Thus, careful patient selection and prospective validation of ERCC1's predictive value to prove a true survival benefit before clinical implementation are needed.

0077

Multiple pulmonary macronodular lesions in patients with primary lung carcinoma

S. Ivanov, Y. Slavova, D. Kostadinov, A. Gocheva, M. Bogdanova, S. Angelova, D. Marinova, V. Djambazov*
*UH Pulmonary Diseases St Sofia, Bulgaria

Objective: The neoplastic multiple pulmonary macronodular lesions (MPML) predominantly result from lung metastases of primary extrapulmonary localisation of the tumor—kidney, colon, prostate, etc. Some types of lung carcinomas are with similar radiothoracic presentation in multiple cases. Goal: To evaluate patients with primary lung cancer presenting with MPML as first manifestation.
Method: Materials: 16 patients with MPML were studied for the period 2002–2009. A primary extrathoracic localisation of the tumour was searched in all cases, but such was not found. Methods: medical history, physical status, chest radiography (lesions with diameter >3 mm were evaluated as macronodular), computed tomography (CT), fiberoptic bronchoscopy (FBS) with transbronchial lung biopsy (TBLB), morphological methods: routine staining with hematoxylin–eosin, periodic acid Schiff (PAS), Alcian blue; immunohistochemical methods: thyroid transcription factor-1 (TTF-1), Ki-67, cytokeratin AE1/AE3, EMA, carcinoembryonic antigen (CEA).
Results: From the studied patients, six were males and ten were females, with age varying between 26 and 70 years. MPML were established on the chest radiography and thorax CT in all patients. In 15 of them, the morphological diagnosis was proven by FBS and TBLB and in one with thoracotomy and lung excision. From the studied 16 patients, 12 were with diffuse bronchioloalveolar carcinoma (BAC). It is interesting to note that in three cases, adenoid cystic carcinoma (ACC) was found and in one squamous cell carcinoma (SCC). The immunohistochemical studies confirmed the primary lung localisation of the tumours.
Conclusion: The primary lung carcinoma may present initially with MPML, and in this case, it is predominantly diffuse BAC or ACC and, rarely, SCC.

0078

Increased number of lymphoid follicles in emphysematous patients with α1-antitrypsin (AAT) deficiency

F. Lunardi, E. Bazzan, S. Baraldo, A. Ballarin, G. Turato, F. Rea, M. Valente, M. Saetta, F. Calabrese*
*University of Padua, Italy

Objective: Lung damage in emphysema has been traditionally attributed to an imbalanced proteases/antiproteases, especially in α1-antitrypsin deficiency (AATD). However, activation of lymphocytes with organisation in lymphoid follicles (LFs) seems to play a crucial role in disease pathogenesis. The aim of this study was to quantify the number and distribution of LFs in native lungs from patients transplanted for emphysema.

Method: We compared two groups of patients with either AATD (n=9) or normal levels (AATN, n=27). Bronchiolar, perivascular and parenchymal LFs were evaluated on sections immunostained with anti-CD20.Results were expressed as LF number per square centimeter of examined tissue and, for bronchiolar LFs, as percentage of airways with LFs.

Results: LFs, almost absent in normal lungs from donors, were frequent in subjects with severe emphysema both with and without AATD. LF total number was increased in AATD patients as compared to AATN, and this was mainly due to a higher number of parenchymal LFs (median, range: 6, 2–12 vs 2, 0–6 LFs/cm^2, p=0.0002). Perivascular and bronchiolar LFs were numerically increased in patients with AATD (5, 0–24 vs 3, 0–8 LFs/cm^2; 33, 20–100 vs 20, 0–60%), but did not reach the levels of statistical significance.

Conclusion: LF number is increased in patients with end-stage emphysema, particularly in those with AAT deficiency. These results extend our knowledge of disease pathogenesis, suggesting that lymphocyte activation is a crucial event even in AATD-related emphysema, and the excessive lung damage observed in these patients may trigger the persistence of the immune response, possibly with autoimmune mechanisms.

0079

Pulmonary lymphomatoid granulomatosis (LYG): a case report

M. Nzegwu, A. Mba, D. Olusina*
*University of Nigeria, Dept. of Morbid Anatomy, Enugu, Nigeria

Objective: (LYG) is a rare angiocentric lymphoproliferative process predominantly affecting the lung. The diagnosis of this condition is often difficult as the physical signs, history, chest X-ray, and routine laboratory investigations are usually nonspecific. Nevertheless, it is important to establish a tissue diagnosis as this lymphoproliferative disorder can be refractory to treatment and even progress to overt lymphoma.

Method: One case of pulmonary LYG in a 52-year-old Nigerian man of Ibo extraction treated in our centre in 2001 and followed up for a year is presented. The difficulty in making diagnosis is highlighted and treatment modality discussed.

Results: Our patient received two courses of cyclophosphamide and prednisolone before defaulting. There was evidence of some remission, even though incomplete, following the first course of chemotherapy (Fig. 4). However, his representation a year later with evidence of relapse was a pointer to the ongoing process of the lesion. Whether this case had progressed to lymphoma was difficult to say as he declined a readmission and further investigation.

Conclusion: A subset of angiocentric lymphoproliferative process including LYG shows clinical response to cytotoxic chemotherapy and steroid when commenced early, as is partly true here. Lymphomatoid granulomatosis should be considered in long-standing nodular pulmonary lesion and pleural effusion of uncertain aetiology.

0082

Immunohistochemical study about pathogenesis of acute respiratory distress syndrome

G. Simona, I. Jung, L. Azamfirei, D. Demian, R. Solomon, B. Grigoroiu*
*UMF, Dept. of Pathology, Targu-Mures, Romania

Objective: Despite modern treatments, the prognosis of acute respiratory distress syndrome (ARDS) remains unfavorable and its pathogenesis is not explained enough. In few recent studies, the pathogenetic and prognostic role of vascular endothelial growth factor (VEGF) and its receptors was investigated in ARDS, but the obtained results were controversial.

Method: We have compared the immunohistochemical expression of CD68, VEGF-A and its receptors (VEGFR1and VEGFR2) in normal lung (n=10) and also in early and late ARDS (within 48 h, respectively, after 4 days). Cases with ARDS were necroptic cases (n=50), and also lung biopsies (n=12). LabVision antibodies were used. Serum level of VEGF was also determined.

Results: In normal lung, all antibodies marked the endothelial and alveolar cells and also macrophages. In early ARDS, the intensity of VEGF decreased in both endothelial cells and alveolocytes, but increased in hyaline membranes (HM) after 2–3 days. VEGR1 marked the preserved alveolar cells and VEGFR2 marked alveolar macrophages. HM were negative for both receptors. In late ARDS, down-regulation was more prominent for all antibodies. Serum level of VEGF was up-regulated at the same time with decreasing VEGF intensity in lung cells, and also with HM appearance. All dyed patients presented HM, independently by phases of ARDS. CD68 marked alveolar macrophages and sometimes HM.

Conclusion: The formation of HM in ARDS showed an unfavorable prognosis. Strong intensity of VEGF and the inconstant presence of CD68 in HM proved that both destroyed alveolar cells and macrophages are responsible for VEGF production, but the increased serum level of VEGF also proved its serum extravasations in HM.

0084

Optimalization of flow cytometric assessment of TNF 945 in alveolar macrophages using multiparametric analysis

E. Stránská, P. Mandáková, M. Vašáková, R. Matej*
*University Hospital Motol, Dept. of Pathology, Praha, Czech Republic

Objective: Alveolar macrophages (AMs) contribute to the pathogenesis of different lung diseases by producing pro-inflammatory cytokines. Within the frame of the project, which is mainly concerned with cytokine expression in bronchoalveolar lavage fluid (BALF) of patients with idiopathic pulmonary fibrosis and chronic obstructive pulmonary disease, we optimized the flow cytometric (FC) examination of TNFα expression in AMs. The aim was to determine spontaneous TNFα production, the production during the culture and after stimulation with lipopolysaccharide. Furthermore, we focused on antibody selection since AMs displayed high level of autofluorescence.
Method: We examined BALF obtained from control patients. TNFα production was assessed immediately after BALF delivery, after 5-h stimulation with lipopolysaccharide (monensin, protein transport inhibitor was added after 2 h of incubation) and also after incubation with monensin only. Simultaneously, various concentrations of lipopolysaccharide were tested (0.5, 1 and 2 μg/ml). FC detection of AMs was simplified using multiparametric analysis, a combination of optical parameters along with the expression of surface markers CD14 and CD45.
Results: Concentration of 1 μg/ml of LPS was found to be optimal for AMs activation, although all tested concentrations are suitable. The high background autofluorescence of AMs can be efficiently reduced by the use of antibody conjugated with long-wave emitting fluorochrome, e.g. APC.
Conclusion: Optimalized FC protocol enables us to analyze TNFα production of AMs in BALF obtained from the patients. Supported by IGA MZ NS/10423-3 and Research Project MZO FNM 2005/6704.

Wednesday, 1 September 2010, Basement

PS-05 Poster Session Hematopathology

0087

Chronic lymphoproliferative diseases associated with chronic hepatitic viral infections

C. M. Ardeleanu, C. Dobrea, V. Arama, A. M. Vladareanu, C. Iosif, V. Molagic, H. Bumbea, D. Terzea, M. Olariu, M. Stoicea, C. Ciufu*
*V. Babes National Institute, Dept. of Pathology, Bucharest, Romania

Objective: Romania remains an area with increased incidence of hepatitic viruses (8.5 per 100,000 for HBV in 2004). Our aim was to analyze the distribution of chronic lymphoproliferative diseases (CLPD) in patients with chronic HBV, HCV, HDV infections.
Method: We studied 28 extramedullar biopsies and 29 bone marrow biopsies from 29 patients diagnosed with chronic viral hepatitis (HVC 44.8%, HBV 34.5%, HBV+HDV 17.2%, and HCV+HBV 3.5%) and suspected of CLPD.
Results: We identified 26 cases (89.6%) of B cell non-Hodgkin lymphomas (including diffuse large B cell lymphoma, marginal zone lymphoma, B cell chronic lymphocytic leukemia/small lymphocytic lymphoma, follicular lymphoma grade 1, mantle cell lymphoma), two cases (6.9%) with peripheral T cell lymphoma unspecified and one case (3.5%) of mixed cellularity Hodgkin lymphoma. If the percentage of diffuse large B cell lymphomas (34.4%) was compared to that of patients without chronic hepatitic viral infections, we noted an increased percentage of patients with marginal zone lymphoma. Diffuse large B cell lymphoma was associated with all types of chronic hepatitic viral infections, whereas marginal zone lymphoma was more frequently associated with HCV.
Conclusion: Chronic hepatitic viral infections associate more frequently with certain subtypes of CLPD, especially marginal cell lymphoma; at the same time, chronic hepatitic involvement poses serious therapeutic challenges.

0088

Significance of bone marrow fibrosis in monitoring multiple myeloma

E. Babarovic, T. Valkovic, S. Stifter, A. Duletic-Nacinovic, D. Petranovic, I. Seili-Bekafigo, K. Lucin, N. Jonjic*
*School of Medicine, Dept. of Pathology, Rijeka, Croatia

Objective: The aim of the present study was to contribute to the understanding of the importance of evaluating bone marrow biopsy (BMB) by computer-assisted digital image analysis (CIA). Moreover, the intention was to investigate the frequency of marrow fibrosis in multiple myeloma (MM) and to correlate it with plasma cell infiltration during the follow-up of patients.
Method: Bone marrow biopsy from 31 patients diagnosed with MM were analyzed at the time of diagnosis and reevaluated after the completion of the therapy. The percentage of plasma cells was estimated on immunohistochemically stained paraffin sections with anti-CD138 and Ig light chains by Alphelys Spot Browser 2 integrated system. The fibrosis was analyzed according to the European consensus on grading bone marrow fibrosis.

Results: Plasma cell percentage at the time of diagnosis ranged from 3% to 97% (median 70%) and in follow-up from 5% to 100% (median 34%). Increased fibrosis, which appeared to be restricted to areas of severe plasma cell infiltration, was seen in 26% of BMB at first diagnosis. In a follow-up study, the percentage of plasma cell infiltration decreased in 16 of 31, increased in 8 of 31 and remained nearly equal in 7 of 31 MM patients. All patients with disease progression after first-line therapy had increased fibrosis in BMB. The degree of fibrosis correlated with plasma cell percentage, clinical stage and response to therapy.
Conclusion: In all cases of MM, a BMB is essential at diagnosis as it helps identify a subset of myeloma patients with increased marrow fibrosis and response to therapy.

0090

CD 20 expression in B cell lymphomas

V. Kloboves Prevodnik, J. Lavrencak, M. Horvat, B. Jezersek Novakovic*
*Institute of Oncology, Dept. of Cytopathology, Ljubljana, Slovenia

Objective: The role of CD20 expression in the deciding for the treatment of B cell lymphoma patients with rituximab has not been well established yet. The aim of our study was to determine the CD20 antigen expression in B cell lymphomas and compare it to reactive lymphocytic proliferations.
Method: Cytological samples of 65 diffuse large B cell lymphomas (DLBCL), 56 follicular lymphomas (FL), 31 chronic lymphocytic leukaemias (CLL), 34 mantle cell lymphomas (MCL), 18 marginal zone lymphomas (MZL), 15 B cell lymphomas unclassified and 70 reactive lymphocytic proliferations (RLP) were analysed for CD20 expression by quantitative four-color flow cytometric measurements using FACSCalibur flow cytometer (BD Biosciences).
Results: The median CD20 expression in RLP was 50,657 MESF (range 14,175–251,757) and 64,936 MESF (range 2,737–679,577) in B cell lymphomas. When compared to RLP, CD20 expression was significantly higher in DLBCL ($p<0.01$) and FL ($p<0.001$), but significantly lower in CLL ($p<0.0001$). On the contrary, when CD20 expressions in DVBL, FL, MLC, MZL, KLL and B cell lymphomas unclassified were compared, it was found to be significantly lower ($p<0.001$) only in CLL and did not significantly differ from other lymphoma types ($p=$NS).
Conclusion: CD20 expression seems very similar in most histological types of mature B cell lymphomas. However, its range was very broad, varying from very low or even null to very high. Therefore, further studies should be carried out to establish at which level of CD 20 expression could rituximab be used as an effective treatment.

0091

Nodular lymphocyte-predominant Hodgkin lymphoma (NLPHL): a challenging case of histologic transformation to large B cell lymphoma

D. Meseure, C. Copie, S. Boudjemaa, B. Chetaille, C. Curtillet, P. Gaulard*
*Centre Rene Huguenin, Dept. of Pathology, Saint Cloud, France

Objective: Nodular lymphocyte-predominant Hodgkin lymphoma (NLPHL) is a rare distinct histopathologic entity with a favorable prognosis despite a tendency for recurrence. Histologic transformation (HT) to diffuse large B cell Lymphoma (DLBCL) occurs in <10% of cases.
Method: A 16-year-old boy presented with a 12-month history of left inguinal and iliac lymphadenopathies. Disease staging including CT, ultrasonography, biopsies of nasopharynx, tonsils, bone marrow and myelogram was negative. TEP-CT was positive. A surgical inguinal lymph node excision was performed.
Results: The 4.5 × 2 × 1-cm lymph node had a nodular architecture. The nodules were surrounded by thin collagen bands and composed of predominantly large tumor cells of centroblastic morphology and occasional cells with Reed Sternberg-like features within a background of small lymphocytes with admixed histiocytes, but without eosinophils or plasma cells. Tumor cells were strongly positive for CD20, CD79a, IgD and BCL6, focally positive for EMA and expressed B cell transcription factors BOB1 and OCT2. CD30 was also expressed, but CD15 and MUM1 were negative. The background was composed predominantly of small $CD3^+$ $PD1^+$ T cells. No follicular dendritic cell network or EBV was detected. This observation raised the problem of differential diagnosis between NLPHL with increased number of large cells and large B cell lymphoma. The latter was favored based on morphologic and immunophenotypic features. A chemotherapy according to LMB 2003 protocol led to the regression of lymphadenopathies with TEP-CT negativity.
Conclusion: Diagnosing HT of NLPHL may be challenging. Further studies are needed to understand the molecular pathways implicated in this transformation.

0092

Lymphoma: an overview over an eleven-year period

C. Schilling, M. Leader, N. Zainal Abidin*
*Beaumont Hospital, Dublin, Ireland

Objective: Lymphoma is the commonest haematological malignancy in the developed world. We undertook an audit of all laboratory reports from the Pathology Department of Beaumont Hospital that confirmed or suspected a diagnosis of lymphoma over an 11-year period, assessing the following: incidence of lymphoma by age at presentation and gender, site of presentation, type of lymphoma diagnosed, number of cases utilising immunohistochemistry, number of cases where bone marrow staging was performed and the results.
Method: Six hundred forty-seven cases were retrieved from the laboratory database where the histology report provided a definitive diagnosis of lymphoma or strongly suspicious for lymphoma. Seventy-seven were diagnosed as Hodgkin's lymphoma and 519 diagnosed as non-Hodgkin's lymphoma, with 51 cases strongly suspicious for lymphoma.
Results: The study showed an average age of 58.08 years at presentation, with incidence of lymphoma increasing with age and peaking at an age range of 61–70 years, reducing thereafter. The highest incidence of Hodgkin's lymphoma occurred in the age ranges 16–20 and 31–35 years. Incidence of lymphoma was similar in both genders. B cell lymphoma had the highest incidence, followed by Hodgkin's lymphoma. Three hundred thirty-one cases had a nodal site of presentation, 240 were extranodal, with the remaining from uncertain site (site labelled, for example, mediastinal mass). Brain was the most common extranodal site with 65 cases. Immunohistochemistry was performed in 92% of cases. Six percent of cases had bone marrow involvement.
Conclusion: The incidence of lymphoma for 11 years in Beaumont hospital is mostly consistent with the epidemiology established by the WHO.

0093

MMP9 immunohistochemical expression by Hodgkin–Reed–Sternberg cells as a prognostic marker in young patients with classical Hodgkin lymphoma

A. H. JFM Campos, J. Vassallo, H. Brentani, C. H. Torres, A. F. Carvalho, L. D. C Mota, F. A. Soares*
*Hospital do Cancer, Campinas-Sp, Brazil

Objective: To identify differences in gene regulation according to the status of Epstein–Barr virus (EBV) infection in classical Hodgkin lymphoma (cHL), we compared the expression profiles of three EBV-negative (L-428, L-1236, KM-H2) and one EBV-positive (L-591) Hodgkin lymphoma (HL) cell lines. We observed that 756 genes are significantly up- or downregulated in the EBV-negative cell lines as compared to the EBV-positive cell line.
Method: For four of the differentially expressed genes (caspase-1, caveolin-1, CCL20, and MMP9), immunohistochemical validation was performed in a tissue microarray (TMA) containing 148 cHL cases and the results compared to EBV infection status and patient outcome.
Results: Only CCL20 expression by Hodgkin–Reed–Sternberg (H-RS) cells was associated with EBV infection ($p<0.0001$). On the other hand, caspase-1 and MMP9 expression by H-RS cells significantly associated with lower disease-specific survival rates in patients between 15 and 45 years old, and the expression of MMP9 by neoplastic cells emerged as an independent factor of unfavourable prognosis.
Conclusion: These results suggest the ability of H-RS cells to explore different signaling pathways, regulating different genes according to EBV infection status. Of these, CCL20 protein expression was shown to be specifically associated with EBV infection in cHL cases. We also observed the expression of other proteins by H-RS cells, of which MMP9 might be promising as an independent prognostic factor for this group of patients. (Supported by FAPESP and CNPq).

0094

ERK2 and BCL2 proteins in myeloproliferative neoplasms

E. Wisniewska, E. Mizera-Nyczak, G. Dworacki, A. Marszalek*
*Collegium Medicum, Bydgoszcz, Poland

Objective: MPNs consist of polycythemia vera (PV), essential thrombocytosis (ET), and primary myelofibrosis (PMF). Though a number of clinical and diagnostic factors have been determined, the current classification in MPNs is still not satisfactory. All MPNs are characterized by JAK2 tyrosine kinase (V617F) mutation related to the deregulation of intracellular signalling pathways, e.g. RAS-ERK and PI3K-AKT, while BCL2 negatively regulates the PI3K-AKT pathway. The aim of our study was to attempt to indentify the presence and distribution of ERK2 and BCL2 expression as factors which might distinguish each MPN.
Method: Expressions of ERK2 and BCL2 were investigated (immunohistochemistry with EnVision and DAB) on trephine samples in PV, ET and PMF patients. Anti-ERK2 antibodies were directed to the epitope corresponding to a site near the C-terminal of these molecules. BCL2 antibodies bind an epitope located between amino acids 1–205 of human BCL2. Finally, sections were studied under light microscope and evaluated using a semiquantitative method.
Results: There were similarities and differences in terms of ERK2 expression among three MPN disorders. There was a widespread occurrence of anti-ERK2 in the cytoplasm as well as in the nucleus. Observed differences concern the levels of expression of this antigen in the nucleus. The

highest level was detected in PV, lower in ET and the lowest in PMF patients. Antigen binding BCL2 antibody is scarcely represented only in the cytoplasm of MPNs. A relatively high expression of BCL2 was detected only in ET.
Conclusion: Our preliminary results indicate that the expression and distribution of ERK2 and BCL2 could be suitable diagnostic discriminators of MPN.

0095

Bone marrow morphology of patients with polycythemia vera and its relation to JAK2 mutations

J. Marcinek, T. Burjanivova, T. Balhárek, P. Szepe, G. Minarik, Z. Lasabová, L. Plank*
*Jessenius Faculty of Medicine, Dept. of Pathology, Martin, Slovak Republic

Objective: Polycythemia vera (PV) is diagnosed in the presence of polyglobuly and JAK2 (JAK2V617F, resp. exon 12) mutations. Representing a "minor diagnostic criterion", bone marrow (BM) biopsy confirms PV and allows its distinction from other myeloproliferative neoplasms (MPN) and reactive conditions. In our study, we focused our attention on the impact of JAK2 mutations on BM morphology.
Method: Our series includes 64 patients with BM morphology supporting PV. JAK2 mutations were analysed by allele-specific PCR and exon 12 mutations by sequence analysis. BM morphological analysis was focused on features pivotal for MPN (cellularity, megakaryocyte / mgk/morphology and fibrosis).
Results: JAK2V617F mutation was present in 60 patients (31x heterozygous and 29x homozygous forms). Two cases showed exon 12 mutations and two were unmutated. In the majority of cases, BM showed characteristic PV morphology (hypercellularity, trilinear myeloproliferation, pleomorphic mgk morphology without dysplasias), however, often with inextensive atypical BM features (mgk dysplasias, slight reticulin fibrosis). Their presence was not related to either the heterozygous or homozygous form of JAK2V617F. In spite of the absence of some PV hallmarks (mgk morphology, trilinear myeloproliferation), the BM morphology of exon 12 cases supported the PV diagnosis.
Conclusion: Although BM morphology might be influenced by disease progression, therapy or other factors, its evaluation represents a reliable contribution to PV diagnosis. The missing identification of distinct associations of JAK2 mutation with BM morphological patterns seems to be related to insufficient data on causal MPN and/or other associated mutations. Supported by grant Vega No. 1/034/10 and Centrum of excellence at CUJFM (IMTS Code 26220120016).

0096

Consecutive intestinal biopsies for accurate therapy adjustment in patients with post-allogeneic stem cell transplantation and persistent diarrhea

L. Rodriguez Carunchio, A. Martinez, J. A. Bombi, C. Martinez, M. Rosales, X. Calvo, J. Llach, E. Carreras, M. Cuatrecasas*
*Hospital Clinic Barcelona, Dept. of Pathology, Spain

Objective: There is a wide overlap of symptoms and signs among gastrointestinal (GI) graft versus host disease (GVHD) and other GI diseases (infections, drug toxicity, etc.). The diagnosis is based upon histologic and endoscopic findings. Accurate diagnosis is important as it determines a specific treatment and contributes significantly to the morbidity and mortality of post-allogeneic stem cell transplant (SCT) patients. Persistence of GI symptoms despite initial treatment is frequent, and ulterior histologic evaluation may be helpful to address therapy.
Method: We performed a retrospective study of 29 patients with persistent diarrhea despite treatment based on the first biopsy diagnosis in order to determine the diagnostic value of serial GI biopsy evaluation in SCT patients. Simultaneous microbiologic analyses of stools and CMV antigenemia monitoring were performed.
Results: Of the 29 first rectosigmoid biopsies, 18 (62%) were diagnosed as GVHD, two (7%) as GVHD with CMV infection, four (14%) as non-CMV infection, and five (17%) as normal or unspecific. Second GI biopsies were diagnostic of active GVHD in six (17%) cases, GVHD with CMV infection in four (14%), regenerative changes post-GVHD in eight (28%), CMV infection in three (10%), and normal or unspecific in eight (28%). In 21 out of 29 (72%) patients, the histologic findings of the second biopsy were different compared to the first biopsy, leading to a therapy change in 20 (69%) patients.
Conclusion: Our results showed a reliable diagnostic value for serial GI histologic evaluation that could impact on the therapeutic decision in patients with persistent diarrhea after allo-SCT.

0097

Thymoma with subtotal loss of keratin expression: a potential diagnostic pitfall

*P. Adam**
*Medical University of Tübingen, Institute of Pathology, Germany

Objective: The differential diagnosis between thymoma and T lymphoblastic lymphoma poses major difficulties in small needle biopsies since both entities contain immature and highly proliferating T cells. One essential diagnostic

criterion favouring thymoma is the demonstration of increased numbers of cytokeratin-positive epithelial cells. We describe a series of 7 type B2/B3 thymomas with substantially reduced cytokeratin expression.
Method: Eight thymoma cases were analyzed for the expression of various cytokeratins and other epithelial markers (panCK AE1/3, CK19, CK5/6, Cam5.2, CK5/14, p63, beta-catenin, E-cadherin). As controls, 44 type B2 and B3 thymomas and 23 thymic carcinomas arranged on a multi-tissue histoarray were analyzed.
Results: With regard to cytokeratin expression, three B2 thymomas were completely negative for panCK, CK19, CK5/6 and Cam5.2. With regard to the other epithelial markers, seven of seven cases showed a strong nuclear expression of p63 and strong membranous staining for E-cadherin and beta-catenin. Analysis of control cases on a multi-tissue array showed the expression of panCK, CK19, CK5/6, Cam5.2 and CK5/14 in 100%, 88%, 80%, 60% and 91%, respectively. The other epithelial markers p63, E-cadherin and beta-catenin were found in 87%, 68% and 50%.
Conclusion: Loss of cytokeratin expression in type B2/B3 thymomas is a potential diagnostic pitfall in the differential diagnosis with T lymphoblastic lymphoma and can be expected in 10–40% of cases. Interestingly, thymomas with loss of keratin expression seem to upregulate E-cadherin and beta-catenin.

0098

An unusual uterine tumour with signet ring cell features

S. Rossella, M. Fiche, C. Achtari, N. Ketterer, L. de Laval*
*CHUV Lausanne, Dept. of Pathology, Switzerland

Objective: Lymphomas with signet ring cell features are rare, as is uterine dissemination of lymphomas. We report an exceptional case of a uterine tumor combining these two characteristics.
Method: A 61-year-old female was diagnosed in 2004 with localized nodal grade 2 follicular lymphoma (stage IA). She received local radiation therapy, experienced total remission, and did well until 2009 when a systematic CT scan evidenced a pelvic anterior–lateral mass. Total enlarged hysterectomy was performed.
Results: The anterior uterine wall contained a 4.8-cm fish flesh well-delineated mass corresponding to a mostly diffuse and focally nodular proliferation of medium to large cells with extensive signet ring cell changes. Tumor cells were CD20-, CD10-, Bcl2-, and Bcl6-positive with a low proliferation rate (<10–15%); CD21 underlined a focal follicular architecture. The vacuoles were PAS-negative and did not stain for immunoglobulin; ultrastructural analysis revealed nonspecific degenerative vacuoles. No lymph nodes were identified isolated from the surgical specimen. The tumor was considered as a secondary localization of the systemic follicular lymphoma, though no signet ring cells were evidenced in the cervical lymph node biopsy (reviewed). Follow-up showed retroperitoneal tissue infiltration (PET-CT) and normal medullar biopsy. She recently started R-CHOP chemotherapy.
Conclusion: This case illustrates both an unusual site of dissemination and challenging cytological characteristics in a follicular lymphoma. The signet ring cell changes challenged the adequate classification of this lymphoma as either a large B cell or a follicular B cell lymphoma.

Wednesday, 1 September 2010, Basement

PS-06 Poster Session Other Topics

0099

The use of genes in the study of cellular micrometastasis in experimental tumorigenesis

O. El-Hassoun, Z. Valaskova, J. Jakubovsky, I. Hulin*
*School of Medicine, Pathological Anatomy, Bratislava, Slovak Republic

Objective: Tumorigenesis is a highly complex systemic process. Until now, there is no experimental evidence concerning what happens in the whole organism and in distant sites after the application of tumor cells. Aim: We attempted to monitor what happens in the spleen when oncocells are applied to different sites.
Method: On a rat experimental model, we applied BP6 fibrosarcoma cell line with an incorporated gene for the green fluorescent protein GFP. Oncocells were applied either intraperitoneally (IP) or subcutaneously (SC). After 4 weeks, histological slides were prepared from spleen samples.
Results: Rats with IP oncocells developed multiple solid tumors in the peritoneum; those with SC oncocells developed a solid tumor. Histological sections of the spleen in both groups showed the presence of polymorphic fluorescent cells in the periarterial lymphatic sheath or the lymphatic follicles. Similar fluorescence was detected in the subcapsular area. Samples from the absolute control group showed no fluorescent activity.
Conclusion: We identified fluorescent polymorphic cells as BP6 cells even without the typical formation of a sarcoma metastasis. Our observation of a similar picture of the spleen in both IP and SC injected oncocells indicates a high level of regularity in the tumor cell behavior, disregarding the surrounding microenvironment and suggests a potential role of the spleen in actively attracting tumor cells, either to attack them or to process a form of information that will modulate further body–tumor interactions. Our model is

suitable for the study of oncocell spread from the primary site to the whole organism.

0100

Notch1 inhibition in pancreatic ductal adenocarcinoma with a receptor-specific blocking antibody diminishes anchorage-independent growth but not growth rate

N. A. Ottenhof, S. Gupta, M. Mizuma, J. Offerhaus, A. Maitra*
*UMCU, Dept. of Pathology, Utrecht, The Netherlands

Objective: Upregulation of the embryonic Notch signaling pathway has been observed in several different malignancies, among which is pancreatic ductal adenocarcinoma (PDAC). For lack of a receptor-specific blocking antibody, less specific methods were used to suppress Notch signaling in earlier research. With use of a receptor-specific monoclonal blocking antibody against the Notch1 receptor (N1-AB), we determined the exact effects of Notch1 receptor inhibition on different PDAC cell lines.
Method: After confirming active Notch1 signaling, N1-AB activity and specificity were tested with immunofluorescence and qRT-PCR. Cells were treated with N1-AB and different assays were performed to establish the effects of Notch1 receptor inhibition on growth rate and colony forming potential. In vivo experiments were performed: Mice were injected with treated or untreated cells subcutaneously and tumor growth was monitored.
Results: Treatment with N1-AB did not influence the growth rate of the cells. Colony forming potential did decline upon treatment with Notch1-AB, although this decline was only twofold. In vivo experiments did not show any differences between the untreated and treated group.
Conclusion: Although Notch1 receptor inhibition did diminish anchorage-independent growth in PDAC, this effect was much less profound than previously reported. No effect on growth rate was observed upon treatment with N1-AB, which conflicts with the general statement that Notch1 receptor inhibition results in a decline in growth rate. Notch1 should still be looked upon as a potential treatment target, but further determination of the different components of the Notch pathway and their role in tumorigenesis seems advisable.

0105

Pathomorphology of the suprarenal in the short-term lateral electrical surface stimulation of the paravertebral muscles in rabbits

J. Szarek, I. M. Kowalski, J. Wojtkiewicz, I. Babinska, W. Kiebzak, M. Gesek*
*University of Warminsko-Mazurski, Dept. of Forensic Vet. Med., Olsztyn, Poland

Objective: Due to adverse side effects, efforts are made to reduce the time of daily lateral electrical surface stimulation (LESS) therapy in the treatment of idiopathic scoliosis in children and adolescents.
Method: Studies were carried out on ten male rabbits, New Zealand purebred, aged 3.5 months, with b.m. of 2,000–2,200 g. Animals were divided into two groups ($n=5$): (1) short-term LESS was applied for 2 h daily during 3 months and (2) control group without LESS, but with other experimental parameters as in group 1. Stimulation was performed with SCOL-2 (ELMECH). Clinical, macroscopic and microscopic observations were performed.
Results: Similar growth of b.m. was observed in the rabbits from both groups during the first 2 months of the experiment. In month 3, a slightly smaller increase was observed in the animals from group 1 than in those from group 2. The mean mass of the suprarenal glands in the stimulated rabbits was 0.4253 ± 0.0033 g, while those from the group 2 were 0.2981 ± 0.0087 g. A microscopic examination revealed hypertrophy of zona fasciculata with visible overgrowth of glandular cells in rabbits from group 1.
Conclusion: The results of clinical observations as well as morphological lesions indicate the presence of adaptive stress in rabbits stimulated with short-term LESS.

0106

Is basal cell carcinoma an aggressive cancer?

C. Tamas, D. Turliuc, C. Morosanu, A. Pantazescu, L. Popa, S. Shaukat, C. Stanescu, S. Stolnicu, D. Radulescu*
*University of Medicine, Dept. of Plastic Surgery, Iasi, Romania

Objective: Basal cell carcinoma (BCC) is considered a skin cancer with long evolution and low metastatic risk.
Method: We selected for presentation three cases with BCC operated between 1995 and 2010, with a special history and evolution.
Results: The first case (42-year-old female) developed a small occipital tumour, incompletely explored and excised in another surgical department. We performed ten serial excisions (soft tissue and invaded bone) during 12 years (1996–2008) and used complex reconstructive techniques (local/muscular/free omentum flaps). The second case (65-year-old male) had a neglected frontal tumour invading the orbital region; during a period of 5 years, we performed three excisions and reconstructed the region with skin graft and temporal flap, trying to save the eye. Finally, we had to excise the invaded eyeball and we used frontal flap for reconstruction (2003). The third case (63-year-old female) had a small BCC on the left buttock, which was excised in correct limits and reconstructed with a skin graft (1995).

Five years later, a new ulcer appeared. The patient neglected the tumour during a period of 10 years. The BCC progressively invaded with a buttock, the upper third of posterior left thigh and the left gluteus maximus muscle, inducing severely altered general status and anemia. We performed a wide excision (including the muscle) and we reconstructed with a fascio-cutaneous flap and skin grafts (2010).

Conclusion: BCC can be a cancer with a high local aggressivity if the patient or the surgeon underestimates it.

0107

Basal cell carcinoma of the eyelids and periorbital region

S. Dumitriu, C. Costea, D. Radulescu, S. Stolnicu, A. Dumitriu, C. Ungureanu, E. Morosanu, D. Butcovan*
*UMF Gr T Popa Iasi, Dept. of Pathology, Romania

Objective: Eyelids represent a special location of the basal cell carcinoma (BCC) due to the proximity of the eyeball. The aim of this study was to review the clinical and histopathologic features and outcomes of eyelid basal cell carcinomas.

Method: The clinical records and histopathologic specimens of 426 patients with eyelid basal cell carcinomas were reviewed and analyzed retrospectively. The main outcome measures are clinical characteristics, lesion size, histologic subtypes, severity of peritumorous inflammation, recurrence rate and prognostic features.

Results: The most common histologic subtypes were infiltrative, nodular, and basosquamous basal cell carcinomas. Of the patients, 31.5% were previously recurrent. Recurrent basal cell carcinomas were larger, with longer duration of lesion. Basosquamous basal cell carcinomas were more likely to have prior recurrences, larger lesion size, and the highest rate of orbital invasion. Perineural invasion was most frequent in morpheaform and basosquamous subtypes. Peritumorous inflammation differed between subtypes and was highest in the superficial subtype. The recurrence rate was 6.2%.

Conclusion: The outcomes were worse than previously reported due to the delay in treatment. The prognostic factors associated with secondary orbital invasion are previous recurrences, aggressive histologic subtypes, longer duration of lesion and larger lesion size.

0108

Histological assessment of small bowel hypoperfusion lesions in the pig

A. L. Oliveira, D. Ferreira, H. Vala*
*Agrarian Superior School, Viseu, Portugal

Objective: Authors propose the use of a quantitative morphological assessment for helping in studies concerning intestinal hypoperfusion. The method was applied to small intestine mucosa stained with standard hematoxylin and eosin in pigs that underwent severe hypotension due to acute hemorrhage.

Method: Six large white pigs underwent total intravenous anesthesia with propofol and remifentanil. Arterial blood (25 ml/kg) was passively removed from the femoral artery over 20 min. Volume was replaced using Ringer lactate in group 1 and hydroxyethyl starch 130/0.4 in group 2, with a delay of 20 min after bleeding. One hour after the volume replacement, pigs were euthanized and small intestine samples were taken for histopathological examination. Parameters were classified using two specific scales (Chiu 1970; Çetin 1995; Kaplan 2007). Mucosal loss (ML) percentage and crypt/interstitium ratio were obtained (Faleiros 2001).

Results: Inflammatory infiltrate was present in all animals, varying from grade 2 to grade 3. Hydropic cellular degeneration and epithelial detachment were more pronounced in duodenum and more noticeable in group 1. In group 1, ML percentage was 2.18±0.46% in duodenum, 0.62±1.07% in jejunum and 0.45±0.77% in ileum. In group 2, ML percentage was 0.75±1.30 in duodenum and 0±0% in the other intestinal segments. In the whole small intestine was 1.08±0.78% in group 1 and 0.25±0.35% in group 2. Crypt/interstitium ratio did not present significant differences between the groups.

Conclusion: Quantitative morphological assessment may be useful in quantifying the degree of mucosal lost in small intestine stained with hematoxylin and eosin from pigs submitted to acute severe bleeding.

0110

Vasculitides associated with malignancies

M. Otani, H. Hayashi, A. Nakazawa, M. Yoshida, S. Yoshida, H. Serizawa*
*Tokyo Medical University, Dept. of Pathology, Hachioji, Japan

Objective: Vasculitis shows various kinds of physical symptoms. ANCA-related vasculitis and autoimmune disease are famous for its cause. Malignancies are also related to vasculitides. In this paper, we present two rare malignancies causing vasculitides.

Method: Case1: The patient was a 78-year-old male who had vasculitis syndrome. Computed tomography revealed aortic thrombus and narrowing of the renal arteries, suggesting polyarteritis nodosa. Case2: An 86-year-old male was diagnosed as malignant lymphoma. Acute renal failure with gross hematuria developed. MPO-ANCA was positive.

Results: Case1: The tumor in the thoracic aorta was found at autopsy. Histologically, the tumor consisted of isolated atypical cells, suggesting sarcoma. Immunohistochemically, tumor cells were positive for CD31. The same atypical cells were seen in the intrarenal arteries as emboli accompanied with vasculitides. Case2: Autopsy revealed lymphoplasmacytic lymphoma (LPL) involving kidneys. And more, amyloid deposition in the lungs and MPO-ANCA-associated crescentic glomerulonephritis, i.e. MPA, were noted.
Conclusion: Aortic angiosarcoma is an extremely rare lesion, and it is known that the tumor often causes distal emboli and presents vascilitis syndrome. The second case was diagnosed as LPL, MPA and amyloidosis. MPA is known to occur in some patients with malignancy. It has been reported that some malignancies produce vasculitides-inducing factors. In our cases, such factors produced by malignant cells might induce vasculitides.

0113

Monoclonal antibodies in the diagnostic of spinal metastases

*G. Kropczydski**
*Zabrze, Poland

The skeletal system is the third most frequent seat of metastases, and metastatic tumours are the most common bone malignancies. The diagnostic workup of spinal metastases begins with the identification of the primary neoplastic site. The aim of the study was to determine the utility of monoclonal antibodies in the diagnostic workup of spinal metastases.
Materials and methods: This is a retrospective analysis of 203 patients whose histopathologic examination confirmed the presence of neoplastic foci in the spine. Samples of metastatic tumours of 57 patients whose primary tumour sites had not been identified were subjected to an immunohistochemical analysis based on monoclonal antibodies and assays for antigens associated with tumours most often producing bony metastases.
Results: The monoclonal antibodies and assays were shown to be useful aids for the identification of the histology and location of the primary tumour in patients in whom routine histological assessments had failed to determine the histological type of tumour.
Conclusions: The length of survival of patients with malignant spinal metastases is influenced by the type of neoplasm and locally radical surgery combined with palliative radiation therapy. In many cases, effective immunohistochemical workup can contribute to halting the progression of the tumour by enabling qualification for appropriate surgical and oncological treatment.

0114

Origine and frequency of pulmonary bone fragment embolism: an autopsy study

*N. Willi**, *T. Thiesler, P. Ochsner, G. Cathomas*
*Kantonsspital Liestal, Institute of Pathology, Switzerland

Objective: Pulmonary bone fragment embolism (PBFE) is a rare event observed at autopsy. Pulmonary bone marrow embolism (BME) is more common, but both types of embolisms are considered to have little clinical relevance. The aim of this study was to analyze the frequency of PBFE and BME and correlate these events with clinical findings.
Method: In an autopsy cohort, the frequency of embolic particles of PBME and BME was evaluated by reanalyzing all pulmonary H&E- and Elastin-stained (EvG) sections.
Results: In a total of 1,002 autopsies, 5 (0.5%) PBFE and 29 (2.9%) BMEs were detected. Compared to BME, PBFE were significantly more common in patients with osteomyelitis [2 of 8 (25%) versus 0 of 29, $p<0.05$). In contrast, BME was more common in patients with costal fractures (16 of 29 versus 1 of 8, $p<0.05$), but no patient showed both types of embolism. In addition, PBEF and BME were observed in patients with bone metastasis and orthopaedic devices. The highest density (30.5 particles per square centimeter) was observed in a patient who died immediately following femoral medullary nailing, presenting with the clinical picture of pulmonary thromboembolism.
Conclusion: In the autopsy cohort analyzed, an incidence of 5‰ for PBFE was considerably higher as previously reported and PBEF showed a strong correlation with osteomyelitis, and the application of orthopaedic devices and extensive PBFE may lead to death. BME are correlated with rib fracture, but no association between PBFE and BME was observed, suggesting a different pathogenetic mechanism.

0115

Local flaps used for post-tumoral facial defects

*C. Tamas**, *S. Shaukat, L. Popa, C. Stanescu, S. Stolnicu, D. Radulescu*
*University of Medicine, Dept. of Plastic Surgery, Iasi, Romania

Objective: The reconstruction of facial soft tissue defects can be difficult because we should regain the shape and the function of the region. The facial esthetic units should be respected too, and we cannot neglect the oncological limits of excision.
Method: We are reporting 63 patients with facial tumors operated in the last 5 years (2005–2010), 71.4% (45) aged over 50 years and 66.7% (42) males. They needed excision

for basal cell carcinoma (BCC 55.6% (35), squamous cell carcinoma (SCC) 33.4% (21), and malignant melanoma (MM) 11% (7)).

Results: We performed correct oncological excision in 84% of the cases; ten patients with BCC needed re-excision. In the same surgical stage, we reconstructed the defect using local flaps for 50 patients (79.3%), local flaps and skin grafts for six patients and skin grafts only in the seven cases with MM. The main techniques used were: frontal or temporal flaps for the orbital /nasal regions, naso-genian or fan flaps for the lips and cervico-facial flaps for the cheek. When necessary, full-thickness skin grafts taken from pre- or retroauricular donor zones were performed (13 cases). After surgery, all the patients were examined by the oncologist; only 15 patients diagnosed with squamous cell carcinoma or malignant melanoma accepted the excision of the local regional lymph nodes.

Conclusion: Correct tumoural excision in the face is difficult to perform. The skin graft is the best reconstruction technique from the oncological point of view, but to respect the aesthetic and functional rules, we have to perform flaps.

0117

Indian ink vs tissue marking dye: a quantitative comparison of two widely used macroscopical staining tool

K. Kosemehmetoglu, G. Guner, D. Ates, E. Soylu*
*Ankara Ataturk EAH, Dept. of Pathology, Turkey

Objective: The evaluation of the surgical margins is a major concern in surgical pathology and marking of surgical margins with substances; Indian ink and tissue marking dyes are widely used. As there is no systematic study comparing tissue marking dyes and Indian ink, the most common substances used for the purpose, this study was conducted to compare the two.

Method: Unit price, penetration into the tissue, the spreading area of one drop of dye on tissue paper, brightness under the microscope and the intensity of colors on image analysis program were compared for each of the five colors of Rotring's Indian ink and Thermo-Shandon's tissue marking dyes applied on reduction mammoplasty specimens.

Results: Indian ink seemed to be slightly less smudgy than tissue marking dye. Indian ink tended to remain on the surface and showed less tissue penetration compared to tissue marking dye with respect to all colors, except yellow. Blue color of Thermo–Shandon and yellow color of both Rotring and Thermo–Shandon had the deepest penetration in fatty tissues. Red color of Rotring was lost nearly totally after processing. Rotring has revealed comparable results to Thermo-Shandon; even the black and green colors of Rotring were more intense. On the other hand, Thermo–Shandon was better when red, blue and yellow colors are concerned.

Conclusion: Rotring's Indian ink is proven to be just as effective as Thermo-Shandon's tissue marking dye and bares majority of the characteristics of a perfect staining substance, which are easily applied, quickly fixed, durable and cheap, contain no potential contaminants, is work-safe, would not smudge/stain surrounding tissues, and look bright under the microscope without obscuring the view.

0118

Reestablishing surgical pathology service in Kumasi, Ghana

*H. Stalsberg**
*University Hospital of North Norway, Dept. of Clinical Pathology, Tromsø, Norway

Objective: In 2005, Ghana had five active pathologists. At Komfo Anokye Teaching Hospital (KATH) in Kumasi, all histology stopped in April 2004. Reasons were a broken microtome, low budget priority, and the single pathologist overloaded with teaching and forensic autopsy commitments. The department lost accreditation to train pathologists. The head of KATH oncology department met the author during a conference and asked for help.

Method: At a planning visit to KATH, a comprehensive plan was worked out. KATH administration acquired basic new equipment. Two KATH technicians trained at the University Hospital of North Norway (UNN) for 3 months. On their return, slides were produced at KATH and sent to UNN for diagnosis. Two young doctors from KATH were trained in pathology at UNN for 4 years. Double-headed microscopes were provided from Norway. Financial support was given by both hospitals and the Norwegian Government (NORAD).

Results: Attracted by the ongoing activity, a senior histotechnician and two Ghanaian pathologists returned to KATH from Accra and Scotland. The two doctors trained at UNN returned to KATH in March 2010 as specialists in pathology. Accreditation to train pathologists at KATH is expected to be regained by mid-2010.

Conclusion: Important success factors have been: appreciation of the importance of pathology by KATH and their initiative to ask for help, personal contact and commitment, support from UNN and NORAD, a comprehensive plan for sustainable development with attention to the needs and wishes of the receiving institution, doctors for training selected by receiving hospital.

0119

The insight into the history of anatomopathological museums in Europe

E. Izycka-Swieszewska, J. Gulczynski*
*Medical University of Gdansk, Dept. of Pathomorphology, Poland

Objective: During the development of anatomy since the fifteenth century, a phenomenon of anatomical museums appeared.
Method: We present a short history of this phenomenon in Europe and give insight into the form of acquisition and exhibition of the preparations.
Results: The prototypes were "curiosities of nature" collections with one of the first founded by Aldrovandi in Bologna (sixteenth century). The next famous and focused on the human body were the collections of F. Ruysch in the Netherlands (seventeenth century). He was performing autopsies in public and after that presented preserved parts or whole bodies and osteological preparation sets as artistic dioramas in a special exhibition house. His collection, sold to Peter the Great, created the foundations for Kunstkamera in Sankt Petersburg. In the eighteenth century, teachers in surgical and anatomical schools (beginning of anatomopathology) realized the educational power of such collections. Museums like the one by H. Fragonard in Paris, France and Hunterian in Glasgow were established. The next big collection—Narrenturm in Vienna—had many exhibits obtained from Algemeine Krankenhaus. The first typical anatomopathological museum was created by R. Virchow in Berlin (nineteenth century). Virchow's motto was "no day without a preparation". In Polish universities, L. Bierkowski (Cracow) and A. Bielkiewicz (Vilnius) founded such museums. That time in all Europe, anatomopathological collections became popular, gathering preparations: osteological, wet (alcohol, formaldehyde, other preservatives), dry and mummified. The fall of phenomenon started in the second half of the twentieth century. Nowadays, we face the era of digitalisation of images but, on the other hand, collections of "plastinated bodies". The ethical and legal aspects become more important.

0120

Importance of autopsy in present medical care system

F. Staniceanu, S. Zurac, L. Tudorica, A. Slavnea, A. Bastian, E. Gramada, G. Micu, R. Andrei, C. Popp, L. Nichita, C. Socoliuc*
*Colentina University Hospital, Dept. of Pathology, Bucharest, Romania

Objective: Autopsy is an important part of pathologic activity representing the final diagnostic method both in the medical and philosophical views. Autopsy has wide educative opportunities both for trainees and specialists and represents the best internal quality control of medical care.
Method: We analyzed 367 autopsies performed in our department during 2006–2008, evaluating the concordance between clinical and postmortem diagnoses.
Results: Complete concordance was present in 50.14% of the cases, partial concordance in 41.96% and discordance in 7.90%; these proportions were established irrespective of the admission duration, except three cases of patients dead on arrival. Main problematic diagnosis was bronchopneumonia (either clinically overestimated 4.36% or underestimated 8.99%). The second in frequency as clinically unrecognized diagnosis was pulmonary vascular thrombotic occlusion, either primary or secondary (thromboembolism)—8.17%. Further discordance was due to cerebral lesions (7.08%) either as presence recognition (3.27%) or lesional type (inappropriate labeling of ischemic lesion as hemorrhage or vice versa 3.81%). Also, cancer and tuberculosis were not identified as causes of death prior autopsy (5.45% and 4.63%, respectively). Unspecific inflammation (acute pyelonephritis, endocarditis, leptomeningitis, encephalitis, sigmoid diverticulitis, phlegmonous cholecystitis, etc.) were identified postmortem (7.63%). Incidental lesions unrelated to death were identified in some cases, most often renal serous cysts and liver hamartomas, but also Peutz Jeghers polyposis, aortic aneurism and syphilitic aortitis.
Conclusion: Special attention should be given to interdisciplinary consultation in our hospital, especially for pulmonary pathology, in order to increase clinico-necroptic concordance. Postmortem surprises reemphasize the importance of autopsy as an irreplaceable link in the process of medical care optimization.

Wednesday, 1 September 2010, Basement

PS-07 Poster Session Cardiovascular Pathology

0122

Immunohistochemical heterogeneity of the non-myocytic cells in different stages of heart development

C. M. Ardeleanu, A. G. Mihaela Georgescu, M. C. Stoicea, M. Ceausu, F. M. Filipoiu, S. Enache, F. Cionca, F. Staniceanu*
*V. Babes National Institute, Dept. of Pathology, Bucharest, Romania

Objective: The heart is the earliest organ to function. Cardiac development and function depend on a complex of

factors with dynamical interactions, factors related to the cell populations and the extracellular matrix. Our purpose was to investigate the non-myocytic cell population of the human heart in different regions and stages of development.
Method: We analyzed 36 formalin-fixed paraffin-embedded cardiac tissues (22 adult, 12 fetal and 2 embryonic hearts) from our institute archives. We applied an indirect bistadial immunohistochemical (IHC) method using a Dako EnvisionTM+Dual Link System-HRP and antibodies against vimentin, desmin, smooth muscle actin (SMA), CD34.
Results: The embryonic heart morphology varies rapidly and intensely with age. In fetal myocardia, we noted a direct correlation between CD34 positivity in vessels and fibroblasts ($r=0.72$, $p=0.01$) and a direct but statistically insignificant correlation between vimentin expression in vessels and fibroblasts ($r=0.82$, $p=0.4$). In adult myocardia with post-ischemic remodelling, vimentin expression was increased compared to fetuses, in non-myocytic cells, especially fibroblasts ($p<0.001$), and in capillaries ($p=0.003$). As opposed to vimentin, desmin expression increases progressively from embryonic to adult life.
Conclusion: Embryonic and fetal non-myocytic cells show an IHC polymorphism. Fibroblasts form the numerically dominant population in adult, fetal and embryonic myocardia and, generally, express SMA. Vimentin is expressed in a variable number of elongated cells, indicating that fibroblasts are generated constantly. Myocardial vascular structures show a marked CD34 expression in all vessels, including capillaries. This study was supported by CNCSIS project I.D. 1388/2009.

0123
Aortic stenosis and aortic arch anomalies found at autopsy in newborn infants

S. Duganovska, S. Kostadinova-Kunovska, B. Dukova, M. Bogdanovska*
*Faculty of Medicine, Skopje, Macedonia, The former Yugoslav

Objective: We performed 244 autopsies of congenital heart malformations (CHM) in the period between 2001 and 2009, out of which 49 cases (30 males and 19 females) of newborn infants with stenosis of atresia of aortic ostium and aortic arch (AA) were found. The aortic stenosis varied from vaguely expressed to completely interrupted AA. In most of the cases, the infants died in the first months of their life.
Results: There were 28 infants with aortic stenosis or atresia in the region of the ostium associated with hypoplasia of the left heart; four cases were with isolated valvular stenosis, three cases with bisemilunar valvula and one with supravalvular stenosis. There were 14 cases with a narrowing of the aortic arch with coarctation of the aorta. There was tubular hypoplasia of the AA in three cases, and in other three cases, we found atresia with complete interruption of the aortic arch, four with larger number of branches on the AA and three cases with common arterial trunk. Myocardium of the left ventricle showed hypertrophy due to hypertension. Diffuse endocardial fibroelastosis was found in four cases with left heart hypoplasia. The latter was histologically detected on slides stained for elastic fibers according to Van Gieson–Orcein technique.
Conclusion: The presented aortic anomalies were associated with other heart malformations in complex cardiopathies or were combined with anomalies of other organs and systems in 15.5% of the cases.

0124
Heart transplantation: forensic contribution to the cause of death investigation

R. Henriques de Gouveia, E. Lopes, M. Clemente, N. Gaspar, F. Costa Santos, J. Costa Santos*
*Lisboa, Portugal

Objective: Cardiac-transplanted patients receive broad medical/hospital care. The authors intend to highlight the importance of legal medicine in this setting.
Method: A 21-year-old black female, heart-transplanted in 2001 due to dilated cardiopathy of valvular cause, was submitted to a medico-legal autopsy in 2007 after dying unexpectedly at home.
Results: Macroscopic examination revealed the absence of traumatic lesions and the presence of cardiomegaly, three-electrode pacemaker inserted in the right ventricle, anomalously coloured myocardium, lung oedema and congestion, chronic stasis liver and cerebral oedema. Microscopic examination showed lesions of severe cellular acute cardiac rejection (grade 3R) in a heart with graft vascular disease.
Conclusion: The medico-legal autopsy allowed the confirmation of a death of natural cause (1); the exclusion of infection and neoplasia—frequent and severe causes of morbidity in the heart-transplanted population (2); the documentation of graft vascular disease, which is related to the time span after transplantation (3); and the diagnosis and characterization of the acute rejection (4) as adequate cause of unexpected death, without prodromic signs and symptoms. Finally, it allowed the correlation of acute rejection and the suspension of immunosuppressive therapy by the patient—data obtained through the family (5). All these conclusions may provide information about death causes of the heart-transplanted population dying outside the hospital, which will complement that of transplanted inpatient deaths.

0125

Sudden adult cardiac death and Ebstein disease

R. Henriques de Gouveia, M. Shimizu, F. Costa Santos, J. Costa Santos*
*Lisboa, Portugal

Objective: Sudden death is a possible major complication of congenital cardiac malformations.
Method: The authors report the case of a 44-year-old male that unexpectedly died at work while performing a minor effort task. He was apparently healthy, apart from the occurrence of very rare "epileptic attacks". A medico-legal autopsy was performed.
Results: The autopsy—in the setting of a forensic postmortem examination—revealed heart malformations that are consistent with Ebstein's disease of the tricuspid valve, associated (as seldom may occur) to mitral valve dysplasia and patent foramen ovale.
Conclusion: The relevance of this case lies upon three facts: (1) the rarity of the pathological entity, (2) the survival of the victim until the adult age without surgical intervention and (3) the fact that the symptomatic announcing event was sudden and unexpected death.

0126

Evaluation of myocardial morphological changes and plasma cTnI concentration in rats treated with doxorubicin and tirapazamine

E. Korobowicz, J. Sliwinska, J. Dudka, A. Korga, R. Gieroba*
*Uniwersytet Medyczny w Lublini, Katedra i ZakBad Patomorfologi, Lublin, Poland

Objective: The clinical use of doxorubicin (DOX) is limited by dose-related cardiotoxicity. One-electron redox cycling of the quinone moiety has long been known to form reactive oxygen species. Tirapazamine is a relatively new cytostatic compound most efficient in areas of hypoxia, however under aerobic conditions causing significant oxidative stress. Aim: The aim of this study was to assess morphological changes in the myocardium of rats treated with doxorubicin and tirapazamine and evaluate changes in plasma level of a cardiac damage marker, cTnI.
Method: Rats were weakly treated i.p. with 1.8 mg/kg b.w. of doxorubicin and 5 or 10 mg/kg b. w. of tirapazamine for 6 weeks. Control group was given saline. Samples of myocardium and plasma were taken a week after last dose. Tissue samples were stained with hematoxylin and eosin, van Gieson method and Selye method and examined under light microscope.
Results: Myocardium of rats receiving a combination of doxorubicin and lower dose of tirapazamine exhibited similar changes as rats administered with doxorubicin solely. Animals treated with doxorubicin and higher dose of tirapazamine displayed vacuolization of sarcoplasm, wavy cardiomyocytes and fuxin-positive areas in Selye method as well as signs of minor interstitial fibrosis. All described alterations in this group were accompanied by significantly higher levels of plasma cTnI.
Conclusion: Both drugs caused cardiac changes in rats, including necrosis, mononuclear infiltrations and minor fibrosis. Combination of doxorubicin and higher dose (10 mg/kg) of tirapazamine seems to have a synergic effect on changes in myocardium.

0127

Cardiomyopathy significantly increases the amount of insoluble advanced glycation end products in cardiocytes, especially in the presence of diabetes mellitus

E. Zembala-Nozynska, D. Lange, B. Nikiel, J. Mynarczyk-Liszka, J. Noski, M. Zakliczyski, D. Konecka-Mrówka, M. Zembala*
*Institute of Oncology Gliwice, Dept. of Tumors Pathology, Poland

Objective: Disturbed glucose metabolism, particularly in diabetes, is an important factor leading to the formation of advanced glycation end products (AGE). The amount of AGE and its distribution in the cardiocytes of a diabetic myocardium and in cardiopathies is not yet well understood. Studies were performed to assess AGE deposits in cardiocytes in chronic heart failure.
Method: The diabetic groups consisted of 14 autopsy cases with diagnosed diabetes, 14 hearts explanted during transplantation with ischemic cardiopathy and diabetes, and eight hearts from dilated cardiopathy with diabetes. The two non-diabetic groups comprised hearts explanted from non-diabetic subjects: 67 with ischemic cardiopathy and 47 with dilated cardiopathy. The control group consisted of samples from 20 healthy heart donors. Immunohistochemical localization of AGE was applied, and a semiquantitative scale was used.
Results: Positive staining was present in both cardiopathic groups with diabetes (100% of cases), then gradually decreased to 71% in diabetes, nearly 50% in cardiomyopathy, and to 15% in the control group. Negative staining seemed to be characteristic of control group and non-diabetics, whereas granular and diffuse staining pattern (mixed pattern) was most frequent in diabetic groups. The semiquantitative results supported an increased AGE accumulation in cases with cardiomyopathy and in diabetes. AGE staining showed no significant correlation with patient age, BMI or diabetes duration.

Conclusion: The amount of AGE increases significantly in failing and diabetic heart cardiocytes and possesses a typical staining pattern.

0128

Deposition of advanced glycation end products (AGE) in myocardial vasculature is enhanced by both heart failure and diabetes

E. Zembala-Nozynska, D. Lange, B. Nikiel, J. Mynarczyk-Liszka, J. Noski, D. Konecka_Mrówka, M. Zakliczyski*
*Institute of Oncology Gliwice, Dept. of Tumors Pathology, Poland

Objective: Disturbed glucose metabolism, particularly in diabetes, is an important but not the sole factor leading to advanced glycation end product (AGE) formation. AGE amount and its distribution in myocardial tissues and components in cardiopathies with and without diabetes are not well documented. This study was performed to assess AGE deposits in unchanged myocardial vessels in chronic heart failure.
Method: The following groups were established: 14 hearts with ischemic cardiopathy and diabetes; eight hearts from dilated cardiopathy with diabetes; 67 with ischemic cardiopathy; 47 with dilated cardiopathy, and 14 autopsy cases with diagnosed diabetes. The control group consisted of samples from 20 heart donors. Immunohistochemical localization of AGE was applied. The semiquantitative scale served to assess reaction intensity in arteries, arterioles, capillaries, venules and veins.
Results: Both types of cardiomyopathy increased AGE accumulation in myocardial veins more than in arteries. The coexistence of diabetes increased AGE significantly in arterioles and capillaries. The type of cardiopathy did not change AGE accumulation in myocardial vessels.
Conclusion: The coexistence of both chronic heart failure and diabetes intensified AGE pathology. Both cardiomyopathy and diabetes change susceptibility on myocardial vasculature to glycation; however, chronic heart failure increases AGE deposition mostly in veins, while diabetes predisposes arterioles to AGE accumulation.

0129

Advanced glycation end products in cardiocytes are joined with lipofuscin granules

E. Zembala-Nozynska, D. Lange, J. Mynarczyk-Liszka, B. Nikiel, J. Nozyski, D. Konecka-Mrówka, M. Zakliczyski, M. Zembala*
*Institute of Oncology Gliwice, Dept. of Tumors Pathology, Poland

Objective: Disturbed glucose metabolism, particularly in diabetes, is an important factor leading to the formation of advanced glycation end products (AGE). The other intracytoplasmic garbage, lipofuscin (Lf), could theoretically also be subjected to glycation. The relation between these compounds is not yet well understood. Studies were performed for elucidating the relationship between AGE and Lf in insufficient human heart cardiocytes.
Method: The study encompassed four groups: one diabetic, two non-diabetics and one control. The diabetic group consisted of 14 autopsy cases with diagnosed diabetes; 14 hearts explanted during transplantation with ischemic cardiopathy and diabetes; and eight hearts from dilated cardiopathy with diabetes. The two non-diabetic groups comprised hearts explanted from non-diabetic subjects: 67 with ischemic cardiopathy and 47 with dilated cardiopathy. The control group consisted of samples from 20 heart donors. Immunohistochemical localization of AGE was applied. The coexistence of lipofuscin inside AGE was studied by Lf autofluorescence in AGE-positive slides.
Results: Lf granules inside AGE deposits were present in all studied groups with varying frequency, but the differences were non-significant. Lf granules joined significantly with dispersed patterns of AGE, i.e. diffuse and mixed, whereas inside granular pattern, Lf granules were found rarely.
Conclusion: We demonstrate that AGE deposits are constituted not only of glycated proteins but also partly from Lf. The frequency of this phenomenon is dependent on the grade of AGE dispersion, but not on the presence of diabetes or heart insufficiency, or both.

0130

Hereditary cardiac amyloidosis associated with transthyretin mutation

Z. Dolenc Strazar, D. Lafitić-Jasnić*
*Faculty of Medicine, Institute of Pathology, Ljubljana, Slovenia

Objective: Amyloidosis is a group of diseases characterized by amyloid deposition in various tissues. Hereditary forms of transthyretin (TTR) amyloidosis, previously regarded as rare diseases, related to the mutation in the gene encoding the serum protein TTR. The inheritance is autosomal dominant. The accumulation is seldom significant, except within the heart where the consequences of deposition are heart block, arrhythmias and sudden death.
Results: A 53-year-old man presented in 2003 with atrial fibrillation and heart failure. Echocardiography was characteristic of non-obstructive hypertrophic cardiomyopathy. In 2007, he suffered myocardial infarction. After episodes

of abdominal pains, CT was done and showed thickening of the rectum. Biopsy revealed TTR amyloid deposition. Scintigraphy showed amyloid deposition in the heart, bones, lungs, kidneys, urinary bladder and intestine. Molecular analysis confirmed amyloidosis of TTR type, with C425C-T mutation in TTR gene. In 2009, he had liver transplantation and died 2 days later. At autopsy, TTR deposition was found in almost all examined organs and was the most abundant in the heart. The heart was enlarged, weighted 1,170 g, and had very thickened walls. Left ventricle measured up to 2.6 cm and right up to 1.3 cm. Microscopically massive deposition of amyloid, positive in Thioflavin-T, Congo red and TTR staining, was confirmed.

Conclusion: Cardiac amyloidosis should be considered in elderly patients presenting with cardiac failure and/or arrhythmia, particularly if resistant to conventional treatment. More than 80 TTR mutations have been associated with amyloidosis, usually presenting with peripheral and autonomic neuropathy and/or cardiomyopathy. Early liver transplantation seems to be curative.

0133

Benign primary hemangioma of the heart: a case report

M. Orbowski, P. Kurzawa, M. Jemielity, T. Urbanowicz*
*Poznan, Poland

Objective: Hemangiomas are benign endothelial tumors commonly affecting the skin. In the heart, those tumors are extremely rare, accounting for 2% to 3% of all benign cardiac tumors. The paper describes a case of hemangioma of the heart in a 38-year-old male who suffered from tachycardia.

Method: Echocardiography and a computed tomography scan of the chest revealed a large tumor mass arising from the left atrium of the heart measuring 10×8×6 cm, attached to the right atrium, surrounding the superior vena cava and extending to the inferior vena cava. The patient underwent open heart surgery for complete resection of the tumor. Grossly, the tumor was firm and spongy. It was a reddish brown-colored mass bleeding extensively.

Results: Histologically, the tumor was composed of vascular channels of varying size. The channels were lined with endothelial cells. Immunohistochemical staining for vimentin, CD43 and CD31 was positive in most tumor cells.

Conclusion: Cardiac hemangiomas usually arise from the anterior wall of the right ventricle and the lateral wall of the left ventricle. The location and size of the presented tumor is very rare and uncommon. Although cardiac hemangiomas are often asymptomatic, the main symptoms include exertional dyspnea, arrhythmias and signs of right heart failure. In the presented case, the patient was admitted to the hospital for arrhythmia. After the surgery, the patient made an uneventful recovery and remained asymptomatic during follow-up. The prognosis of hemangioma of the heart is variable because the tumor may grow or spontaneously involute. Surgery is curative for most patients.

0134

Morphologic aspects in a case of malignant fibrous histiocytoma

*L. Parascan**
*Emergencies Institute of Cardi, Dept. of Pathology, Bucharest, Romania

Objective: They occur at any age, but mostly affect the middle-aged and the elderly. Malignant fibrous histiocytoma occurs more frequently in men. This presentation has revealed the rare occurrence of this tumor affecting a 22-year-old woman in an uncommon intracardiac, right ventricle localization.

Method: The surgical intervention consisted of tumor excision through the right atrium and tricuspid section. Post-operator evolution was favorable. The gross anatomy was a 5/4/3-cm tumor, with relatively incapsulated, hard, yellow with red and grey translucent zones. The cross-section revealed a solid aspect and white/grey/pink-colored zones. The histological slides were colored with HE, VG, Trichrome Masson, Gomori, Sudan IV and IHC.

Results: Malignant fibrous histiocytoma (MFH) is generally a high-grade pleomorphic tumor. The IHC reveals VIM diffuse positivity in the tumor; MNF 116 negativity in the tumor cells; S100 zonal low positivity in the tumor; ACT positivity in rare tumor cells dispersed; MYOGENIN negativity in tumor cells; Myo D1 negativity in tumor cells; MITF negativity in tumor cells; CALPONIN negativity in tumor cells; CD34 negativity in tumor cells, positive in vases; MDM2 negativity in tumor cells; P53 positivity 3–5% in tumor cells; and Ki67 positivity, 25% in the tumor. The IHC sustains the diagnosis of HFM of storiform-pleomorphic type (undifferentiated pleomorphic sarcoma).

Conclusion: The case described above is a very rare tumor and the only case of this type that we have met in our clinic in the last 10 years. The prognosis depends on their grade: High-grade tumors have a poor prognosis with about 20% 5-year survival rate.

Thursday, 2 September 2010, Basement

PS-08 Poster Session Soft Tissue and Bone Pathology

0137

A case report of osteolytic bone tumour

M. Sajin, L. Reghina, I. Hulea, A. Poteca, M. Comanescu, E. Ionescu, H. Orban, G. Simion, C. Carstoiu*
*UMF Carol Davila, Dept. of Pathological Anatomy, Bucharest, Romania

Objective: Adamantinoma is a primary low-grade malignant bone tumor making up <1% of all bone cancers. It predominantly arises in bone in subcutaneous location, mostly in the middle portion of the tibia (80–85%). It is a locally aggressive tumor and is extremely low-growing, with the potential to metastasize.
Method: We present the case of a 32-year-old male with a slow-growing, painful tibial tumor. Excisional biopsy was performed and the tissue has been evaluated by haematoxylin-eosin and van Gieson stains.
Results: Microscopic examination of the tissue revealed islands of epithelial cells with tubular and basaloid pattern in a fibrous stroma.
Conclusion: Adamantinoma is a rare bone tumor and can cause significant morbidity. CT and MRI are not specific in the differentiation of this tumor from other conditions; a variety of tumors and tumor-like lesions can mimic adamantinoma, but histological examination is key to its identification. It is important to recognize this rare bone tumor because adequate treatment will result in excellent prognosis.

0143

Extraskeletal myxoid chondrosarcoma—rare histopathologic variant of myxoid soft tissue tumors: case report

S. Zurac, C. Socoliuc, E. Gramada, F. Staniceanu, R. Andrei, L. Nichita, M. Olariu, T. Tebeica, I. Tudose, G. Maria, M. Niculescu*
*Colentina University Hospital, Dept. of Pathology, Bucharest, Romania

Objective: Myxoid soft tissue tumors are mesenchymal neoplasia with abundant myxoid stroma with biochemical composition of sulphated and non-sulphated glycosaminoglycans. This tumor stromal appearance is similar irrespective of tumor histopathologic type.
Method: We present the case of a 64-year-old woman with a deep-seated tumor located in the posterior region of her left calf.
Results: The tumor grew during 1 year from a relatively small size (2–3 cm) to a 10-cm mass. Magnetic resonance imaging (MRI) revealed a subfascial tumor with heterogenic signal of solid and liquid areas and perivascular growth (sarcomatous MRI characteristics). Conservative surgical excision of the lesion was decided. The tumor appeared partially well-delimitated; some difficulty occurred during profound dissection of the lesion. Macroscopic appearance revealed a 10.5/7.5/5 cm polycyclic tumor covered by whitish capsule, yellow-whitish on the cut surface. Microscopic examination showed multinodular proliferation of round/ovoid tumor cells with eosinophilic cytoplasm, forming groups, chords and strands in a myxoid stroma with rare capillary blood vessels. Hemorrhagic and necrotic areas were noted. Immunohistochemical markers revealed positivity for vimentin and S100 protein and negativity for cytokeratins, EMA, SMA, HHF35, desmin, CD34, calponin, caldesmon, GFAP. Based on the histopathologic and immunophenotypic appearance of the tumor, several entities were excluded (metastatic mucinous carcinoma, cellular myxoma, myoepithelioma, chordoma/parachordoma, myxoid liposarcoma, low-grade fibromyxoid sarcoma, and myxofibrosarcoma); our final diagnostic was grade 2 extraskeletal myxoid chondrosarcoma.
Conclusion: Extraskeletal myxoid chondrosarcoma is a rare and difficult but worthy diagnosis with a major impact on the patient's outcome. Note: Zurac and Socoliuc should be regarded as first authors with equal contribution.

0144

Primary pulmonary synovial sarcoma PNET-like type: a case report

S. Rjabceva, I. Dulinez, M. Vozmitel*
*Belarusian Medical Academy, Dept. of Pathology, Minsk, Belarus

Objective: Synovial sarcoma (SS) is probably the most common sarcoma in the lung. Histologically, SSs are subdivided into biphasic and monophasic forms. Biphasic type can be characterized by distinct epithelial (sometimes glandular) and spindle cell components in varying proportions. Monophasic type can be subdivided into monophasic fibrous type and monophasic epithelial type. The poorly differentiated cell type is a rarely histological variant of SS. The aim of this study was to describe the histopathological and immunohistochemical features of this rare cell type of SS.

Method: We studied the case of a 62-year-old woman with SS of the right lung. The tumor was removed surgically. Paraffin-embedded tissue was stained with hematoxylin–eosin. We used immunohistochemical markers such as CD99, bcl-2, CD34, SMA, vimentin, WT1 and Ber-EP4.
Results: The tumor size was 7×5×3 cm. Histologically, the tumor consisted of small, round and ovoid cells with pale nuclei; the cytoplasm was sparse. These cells were packed into dense sheets. An epithelial cell component was also present. The epithelial cells had ovoid nuclei and abundant cytoplasm. These cells formed glandular structures, sometimes with epithelial mucin. We performed immunohistochemistry for vimentin (diffusely positive), SMA (negative), CD99 (negative), CD34 (negative), WT1 (negative), bcl-2 (negative) and Ber-EP4 (positive in the epithelial cells).
Conclusion: Although the tumor cells revealed only vimentin positivity, our diagnosis of the tumor was poorly differentiated synovial sarcoma, small cell variant (PNET-like). The recognition of these cell types of SS is important to differentiate them from other malignant mesenchymal neoplasms in the lung.

0145

Unusual localization of primary synovial sarcoma: case report

K. Socha, T. Perez, C. Hopfner, J. Couturier, G. Pierron, S. Reynaud*
*Centre Hospitalier de Troyes, France

Objective: A 41-year-old male patient suffered from acute pulmonary embolism. During his hospitalisation, abdominal computed tomography revealed a renal tumor of 5 cm associated with vena cava thrombosis. This renal tumor was not fixed in PET scan, contrary to a pulmonary lesion revealed by a radiologic exam.
Method: The patient underwent a radical nephrectomy with vena cava thrombectomy. Histologically, this infiltrating, highly aggressive tumor originating from the kidney parenchyma and involving the pelvic–calyceal system and renal vessels was poorly differentiated, characterized by solid sheets or fascicles consisting of spindle atypical cells and by a little cystic epithelial component difficult to appreciate. Immunohistochemical features: $CD99^{+}$, $CD56^{+}$, $BCL2^{+}$, $pS100^{-}$, $CD34^{-}$, smooth muscle $actin^{-}$, $chromogranine^{-}$. The epithelial component was EMA^{+}, $CKae1/3^{+}$ and some scattered fusiform cells as well. The cytogenetic study and molecular biology analysis of the frozen materiel demonstrated the translocation t(X;18) and presence of SYT–SSX fusion gene transcripts.
Results: The above findings help exclude other diagnostics. The molecular genetic study demonstrated the clonality of this biphasic synovial sarcoma. SSX2 involvement is probably associated with poor prognosis and aggressive clinical behaviour of the tumor, but it requires further investigations.
Conclusion: In our case, the patient showed tumoral pulmonary embolism associated with a pulmonary tumoral lesion requiring a surgical intervention. In this presentation, we discuss some clinical and histopathologic findings useful for the differential diagnosis and medical care of patients with this tumor.

0146

Diagnostic value of SYT–SSX detected by fluorescence in situ hybridization for synovial sarcoma

L. Carvalho, M. Silva, M. J. Aguiar, L. Teixeira, A. Alarcão, P. Couceiro, V. Sousa*
*Faculdade de Medicina Coimbra, Dept. de Anatomia Patologica, Portugal

Objective: Synovial sarcoma (SS) accounts for up to 10% of soft tissue sarcomas, can occur in any part of the body, and mainly in adolescents and young adults. A specific chromosomal translocation of t(X;18)(p11.2;q11.2) can be detected in over 95% of synovial sarcomas. This study aimed to evaluate the diagnostic value of SYT–SSX detected by fluorescence in situ hybridization (FISH) for synovial sarcoma (SS) in known and potential cases.
Method: Eighteen cases were selected among small biopsies and surgical specimens diagnosed as SS or potential SS at the Hospital of the University of Coimbra between 2000 and 2009 after a review by a pathologist to select cases with variable patterns of cellularity. Interphase FISH was carried out in FFPE using a LSI SYT (18q11.2) dual-color break-apart probe.
Results: Patients with these tumors presented ages from 15 until 54, the mean age being 30 years, and the tumors occurred in 8 women and 11 men. SYT–SSX fusion was detected in 83% (15/18) of known SS; 17% (3/18) failed to show SS18 rearrangement and were classified as negative on account of only 2% of cells showing unequivocal break-apart signals. One case was not interpretable by FISH and failed to show neoplastic cells due to absent/weak fluorescent signals.
Conclusion: From an economic point of view, FISH is a method of first choice as it allows microscopic control of a true positive result. Using this approach, 80% of SS can be diagnosed by FISH only and 20% would need to be confirmed by RT-CR. (unpaired fluorescent signals in a break-apart assay).

0147

Myxofibrosarcoma with local recurrence

S. Dumitriu, D. Radulescu, C. Costea, A. Pantazescu, S. Stolnicu, C. Ungureanu, E. Morosan, L. Chelaru, A. Dumitriu, D. Butcovan*
*UMF Gr T Popa Iasi, Dept. of Pathology, Romania

Objective: Myxofibrosarcoma may occur anywhere in the body, mostly arising in the extremities and is one of the most frequent soft tissue tumours in elderly patients.
Method: We present the clinicopathologic features of 11 myxofibrosarcomas. These include five low-grade, four intermediate grade and two high grade. Six were primary tumours and five were local recurrences.
Results: Histologic examination discloses all degrees of differentiation, from slowly-growing tumour that closely resemble cellular fibromatosis to a highly cellular neoplasm dominated by architectural disarray, pleomorphism, frequent mitoses and areas of necrosis.
Conclusion: Local recurrences showed an increase in grade compared to their primary lesions. Thus, increase in grade parallels the increase in malignant potential.

0148

Malignant giant cell tumor of the tendon sheath distal phalanx: case report

N. Erdogan, N. KOÇ, D. Sahin*
*Marmara Universitesi, Saglik Hizmetleri MYO, Istanbul, Turkey

Objective: Malignant giant cell tumors of the tendon sheath are very rare. Some cases have a poor outcome. The others, despite the histologically malignant features, have a good prognosis if wide surgical excision ablates the tumor completely. The tumor exhibited histological similarities to a benign giant cell tumor of the tendon sheath.
Method: Differential diagnosis of these tumors from other soft tissue sarcomas may be difficult. Pathologic diagnosis made by histologic features; nodular pattern, presence of a combination of spindle fibroblast-like cells and histiocyte-like cells, foci of xanthomatous change, four to five atypically mitosis in one high power field.
Results: These findings were consistent with a giant cell tumor of the tendon sheath.
Conclusion: A case of malignant giant cell tumor of the tendon sheath at the right-hand fourth digits phalanx, which developed in a 58-year-old Turkish woman, is described.

0149

Paratesticular desmoplastic small round cell tumor: a challenging diagnosis

*L. Bejan**
*Emergency County Hospital, Dept. of Pathology, Târgu Mures, Romania

Objective: Desmoplastic small round cell tumor (DSRCT) is a rare malignant serosa-related tumor involving mostly the pelvic and abdominal cavities, but very uncommon in the paratesticular region. DSRCT affects young adults, mainly men, and is classically associated with a bad prognosis.
Method: We report the case of a 25-year-old man admitted to the hospital for a progressive enlargement of the right hemiscrotum with a 5-month history. A preoperative diagnosis of testicular tuberculosis was set and consecutively a right high orchiectomy was performed. At macroscopy, the testicular parenchyma showed no abnormal areas, but the tunica vaginalis was irregular and diffusely enlarged by a whitish to gray firm tumoral mass. Microscopically, the tumor consisted of nests of small, round to spindle cells, with scant cytoplasm, surrounded by a mild desmoplastic stroma. An immunohistochemical study was performed for the differential diagnosis.
Results: Immunohistochemically, the tumor cells were positive for AE1/AE3 and NSE and negative for LCA, chromogranin, synaptophysin and CD56 antibodies. Positivity and a very peculiar staining aspect were noticed with Desmin antibody: perinuclear and dot-like, suggesting a DSRCT. Fluorescence in situ hybridization (FISH) was accomplished, demonstrating EWSR1 rearrangement, which in this immunophenotypical context pleads a diagnosis of DSRCT.
Conclusion: The awareness and the knowledge of DSRCT in the paratesticular area are needed for a correct diagnosis. The differential diagnosis of this tumor with other malignancies involving this region is mandatory as it has a different clinical management.

0150

Comparison of prognosis of gastrointestinal stromal tumors depending on a primary site and a type of mutation

W. Michej, P. Rutkowski*
*Cancer Centre Instytute, Dept. of Pathology, Warsaw, Poland

Objective: Majority of primary GISTs originate from the stomach (G) or small bowel (SB). The aim of the study was

the analysis of the pathologic and molecular factors influencing the patients' prognosis after resection of primary GISTs, deriving from the stomach and intestinum, omentum (NG).
Method: In our department, a group of registered prospectively 546 primary GISTs CD117(+) comprising 303 G-GISTs (55.5%) and 243 NG-GISTs (44.5%) was analyzed; molecular examination was also made using PCR. Surgeons from our Institute compared our results, observing disease-free survival (DFS).
Results: Median size of G-GISTs as compared to NG-GISTs was significantly lower (5 vs. 8.5 cm,) and G-GISTs were characterized by lower mitotic activity (median, 3/50 vs. 5/50 HPF). In G-GIST, the most common detected mutations were exon 11 KIT (57%) and exon 18 PDGFRA, but in NG-GIST exon 11 and 9 KIT. Prognosis of G-GISTs was significantly better as compared to NG-GIST: 5-year DFS rate, 69% vs. 43%. In NG-GISTs, the following factors showed negative impact on DFS based on analysis: mitotic index >5/50 HPF, primary tumor size >5 cm, pathological subtype: spindle. The high prognostic significance of AJCC staging system classification in G- and NG-GISTs was confirmed also in multivariate analysis.
Conclusion: Reliability of AJCC risk classification after resection of primary GIST was confirmed. Patients with primary GIST, originating from the stomach, have better prognosis as compared with GISTs located in other places. In both groups, primary tumor size and mitotic activity are still the most important prognostic factors.

0151
Malignant peripheral nerve sheath tumor: report of three cases with EGFR overexpression

U. S. Tetikkurt, E. Kusku, F. Demir, A. Dengizmen, I. S. Ergun, N. Erdogan*
*Taksim Training Hospital, Dept. of Pathology, Istanbul, Turkey

Objective: Malignant peripheral nerve sheath tumors (MPNST) are highly aggressive sarcomas which may be encountered either sporadically or in the context of the inherited tumor syndrome, neurofibromatosis type 1 (NF1). Epidermal growth factor receptor (EGFR) overexpression has been reported in MPNST, which has been implicated in their pathogenesis. We present three cases that have different pathogenetic origins.
Method: The first patient was a 67-year-old woman who received radiotherapy to the axillary region following radical mastectomy for breast cancer 20 years ago. She presented with a mass in the axillary region that has been growing during the last 1.5 years. Second case was a 25-year-old man who was admitted with a 6.5-cm mass in the right anterior femoral region. The tumor was low-grade and consisted of cartilaginous heterologous component. Third case was a 39-year-old man with congenital café-au-lait spots and soft tissue swellings all over his body. He was admitted for soft tissue swellings in the left axilla and in the neck region 4 and 3 years ago, respectively. Both of the lesions were diagnosed as plexiform neurofibroma. Currently, the patient attended with 10-cm mass in the gluteal region. Pathologic diagnosis was consistent with MPNST.
Results: The first and the third cases showed a higher EGFR expression than the second case.
Conclusion: We aimed to describe the morphological features and discuss the clinical background and different pathogenetic origins of these three cases with MPNST. The role of EGFR overexpression was also evaluated in this case series.

0154
Sclerosing variant of retroperitoneal PEComa

R. Santi, A. Franchi, D. Villari, G. Nicita, G. Nesi*
*University of Florence, Italy

Objective: PEComas are a heterogeneous group of mesenchymal neoplasms characterised by the presence of epithelioid cells in a perivascular distribution (perivascular epithelioid cells, PEComas) and exhibiting the expression of both muscle and melanocytic markers. PEComas generally show a benign course, but cases with an unfavourable outcome have been reported. There are currently no established pathological criteria for malignancy.
Method: We report the case of a 66-year-old woman presenting with an 8-cm retroperitoneal mass contiguous to the left kidney. Light and electron microscopic analyses, along with immunohistochemical studies, were performed.
Results: Histologically, the tumour consisted of small clusters and trabeculae of monomorphous epithelioid cells within an abundant sclerotic and hyalinised stroma. A radial arrangement of the neoplastic cells around small/medium-sized vascular channels was occasionally observed. Mitoses were absent and the proliferation index was <1%. Neoplastic cells showed immunoreactivity for smooth muscle actin and HMB-45. On electron microscopy, neoplastic cells contained a variable number of dense granules, whereas bundles of microfilaments were occasionally identified in the peripheral cytoplasm. A diagnosis of sclerosing PEComa was established.
Conclusion: A sclerosing variant of PEComa has recently been described. Although rarely encountered, the incidence of this tumour should not be underestimated, particularly when the retroperitoneum is affected and the patient is a

middle-aged woman. Further studies are needed to better clarify the histogenesis and biological behaviour of this uncommon entity.

0155

Osteoclast-like giant cells in pelvic leiomyosarcoma: characteristic immunophenotype and possible histogenetic origin

A. Batistatou, V. Siozopoulou, S. Kamina, E. Balassi, V. Malamou-Mitsi*
*Greece

Objective: Leiomyosarcoma of soft tissues with osteoclast-like giant cells (OLGCs) is a rare neoplasm. The nature of OLGCs is controversial since some investigators hypothesize that they derive from the neoplastic smooth muscle cells, while others believe that they derive from tissue-associated macrophages (TAMs). The aim of the present study was to determine the immunophenotype of OLGCs and to compare it with that of the malignant smooth muscle cells in a case of pelvic leiomyosarcoma.
Method: In the Pathology Department, we received a neoplastic mass arising at the broad ligament, measuring 6.5 × 6.5 × 5.3 cm, from a 61-year-old woman. The neoplasm was fixed in neutral-buffered formalin and representative sections were taken. Immunohistochemical staining for vimentin, desmin, SMA, HHF-35, myoglobulin, MyoD1, CD68, KP1, PGM1, CD14 and CD45RO was performed.
Results: Microscopic examination revealed the presence of a highly cellular neoplasm, with areas of necrosis. The neoplastic cells were spindle, with pleomorphic nuclei and abundant atypical mitoses. Many OLGCs were also noted. Immunohistochemistry showed that the malignant smooth muscle cells expressed vimentin, desmin, SMA, myoglobulin, MyoD1 and HHF-35, while they were negative for CD68, KP1, PGM1, CD14 and CD45RO. The OLGCs reacted strongly to CD68, KP1, PGM1 and CD45RO and were negative for all other markers. The diagnosis was giant cell-rich leiomyosarcoma.
Conclusion: The immunophenotype of OLGCs is similar to that of cells of the mononuclear phagocyte series and differs from that of malignant smooth muscle cells. Our findings indicate that the OLGCs derive from TAMs, possibly as a host reaction to neoplastic cells.

0156

An audit of the rate of soft tissue sarcoma presentation in Beaumont Hospital, Dublin, over a ten-year period

C. Beggan, F. Giwa-Amu, M. Leader*
*Carrickmacross, Ireland

Objective: We examined the incidence of soft tissue sarcoma diagnosis over a 10-year period. The incidence of soft tissue sarcomas in Ireland is unknown, and we set out to compare our rates to internationally published figures and examine the epidemiology of these cases. Data recorded: gender, age, site, grade, size and type, primary v recurring, margins, immunohistochemistry and consultant care.
Method: All cases reported as 'sarcoma' from 1999 to 2009 were compiled. Cases without a definite diagnosis of sarcoma were excluded.
Results: The cases reviewed belonged to 28 different subtypes of sarcoma, with leiomyosarcoma of greatest incidence (16%). The most affected age at presentation was 15–64. Gender distribution was almost equal (M/F 53:47). The majority (51%) of cases were located in the trunk. Ten commonly used immunohistochemical markers were identified, with vimentin being the most common (34%). Over 50 surgeons were responsible for the care of these sarcomas. Less than half the cases were graded at diagnosis. Of those graded, 61% were high grade, 13% intermediate grade and 25% low grade. The size at presentation ranged from 1 to 32 cm (mean 5.6 cm).
Conclusion: Soft tissue sarcomas are a widely diverse group of uncommon tumours. We confirmed that our incidence rates are comparable with those published in the USA, with leiomyosarcoma being the most common subtype. Of note is that over 50 surgeons were involved in the management of these cases over 10 years. This would suggest a need for a nationalized specialist centre with surgeons experienced in the treatment of these rare tumours.

0157

Composite ganglioneuroblastoma in adult

G. Benkhedda, N. Khelifi, A. Lamouti*
*Pathology, Blida, Algeria

Objective: Ganglioneuroblastoma (GNB) is a tumour arising from nerve tissue which is intermediate between benign ganglioneuroma and malignant neuroblastoma. It is thought that this tumour arises from a single cellular clone and that the morphologically distinct components of ganglioneuroblastoma represent cells in different stages of differentiation. It is an extremely rare neoplasm of adults. It usually occurs in young children with equal frequency in either sex.
Method: We present the case of a retroperitoneal ganglioneuroblastoma in a 47-year-old man.
Results: Macroscopy: well-encapsuled tumoral mass measuring 16 cm in its large axis. It was yellow in color and has areas of hemorrhage, necrosis and cystic degeneration. Microscopy: The tumor was composed of two distinct

components. In the dominant component, there were neural cells with spindle-shaped nuclei and ganglion cells with large acidophilic cytoplasms in between them. In the second component, tumoral cells were small and have narrow cytoplasms and round, dark staining nuclei. Immunohistochemical analysis showed that tumor cells were strongly positive of NSE and focal positive staining of chromogranin A and synaptophysin. Protein 100 is positive on the level of the intricate spindle-shaped cells to the proliferation.
Conclusion: Ganglioneuroblastoma is a rare childhood tumor and rarely appears in adults. In adults, this tumour is generally discovered by accident or by compression. Ganglioneuroblastoma can look like a neuroblastoma in a partial ganglioneuroma stroma. In adults, prognosis depends on surgical margin resection.

0158

Calcifying aponeurotic fibroma: a case report

*A. S. Demiroz**
*S. Urfa Egit. Ve AR Hastanesi, Dept. of Pathology, Sanliurfa, Turkey

Objective: Calcifying aponeurotic fibroma is a rare soft tissue tumor of children and adolescents. These lesions are presented as slow-growing painless masses that usually affect the distal part of the extremities. They are locally aggressive tumors that infiltrate the surrounding muscle and fascia. Recurrence rate is over 50%, but malign transformation is very rare. We report a 14-year-old boy with calcifying aponeurotic fibroma.
Method: We present a 14-year-old boy with non-movable firm mass on his leg. It was represented as a 2 × 1.5-cm diameter mass which surrounded the peroneal tendon with an infiltrating contour on X-ray and MRI. Fibroblastic proliferation areas, dense collagenous stroma, calcification and osteoid matrix were observed histopathologically. The tumor infiltrated peripheral muscle tissues and surrounding vessels and nerves. There were no mitotic figures and evidence of atypia. Overall, histopathologic and radiologic features exhibited the same characteristics of calcifying aponeurotic fibroma.
Conclusion: Calcifying aponeurotic fibroma is a locally aggressive tumor with a high rate of recurrence. Especially in young patients, those under 5 years of age had higher risk of recurrences. Very few cases of malignant transformation have been reported. Surgical total excision is suggested if ever possible and is the mainstay of the treatment approach. However, it is not possible in most of the cases because of its locally infiltrative behaviour. Differential diagnoses include aggressive fibromatosis, nodular fasciit, fibrosarcomas, monophasic synovial sarcoma and some other malignant spindle cell tumors. Surgical management should be conservative; excision and re-excision, if necessary, are preferable to radical or mutilating surgical procedures to maintain the function of the extremity.

0159

Elastofibroma dorsi: case report. Clinicopathological findings

*S. Papaemmanouil**
*G. Papanikolaou General Hosp., Dept. of Pathology, Thessaloniki, Greece

Objective: Elastofibroma is a tumor-like lesion of soft tissue characterized by a large number of coarse, enlarged elastic fibers and fatty tissue. Its usual location, in the scapular area, deep in the latissimus dorsi and rhomboid muscles, led to the name "elastofibroma dorsi". Most of the elastofibromas are usually asymptomatic, unilateral and occur mainly in middle-aged and elderly women. Clinically, these lesions may simulate an aggressive soft tissue tumor.
Method: Design: A 56-year-old woman presented with a slow-growing subcutaneous mass in the right lateral chest wall. CT scan revealed an ill-defined solid mass, lying deep within the latissimus dorsi. The diagnosis of elastofibroma was suspected and the patient underwent a simple excision of the mass. The surgical specimen consisted of a poorly circumscribed mass, measuring 6×4×3 cm, with gray-white cut surface and elastic consistence. The sections were examined with H+E and elastic stains and followed by immunohistochemical study for a-SMA, CD34, and H-Caldesmon.
Results: The lesion was composed of a mixture of collagenous stroma, few spindle cells, mature adipose cells and large coarse eosinophilic elastic fibers, which stain with Verhoeff-elastica and Masson-Trichrome. The spindle cells were positive for CD34 and negative for a-SMA and H-Caldesmon. The microscope findings confirmed the preoperative diagnosis.
Conclusion: Elastofibroma is an unusual benign lesion cured by simple excision. The irregular elastic fibers may be the result of abnormal elastogenesis. The familial occurrence supports a genetic predisposition to this lesion. The most important differential diagnosis consideration is desmoid fibromatosis.

0160

Evaluation of the prognostic value of TOP2a and survivine protein expression in sarcomas

I. W. Cunha, L. de Brot, K. Carvalho, R. M. Rocha, R. Falzoni, L. F. Lima-Reis, F. A. Soares, J. Vassallo*
*Hospital do Cancer, Campinas-Sp, Brazil

Objective: Soft part sarcoma (SPS) represents a difficult working area, either for the pathologist and the oncologist. Prognostic factors are limited in these tumors, and the search for clinically relevant molecular markers is relatively incipient. We have proposed the present study based on previous results by our group on differential gene expression of soft tissue tumors, which showed significant overexpression of the TOP2a gene in sarcomas. As TOP2a is coded by a gene sited in chromosome 17, we have also included HER-2-neu. Survivine was also included as previous studies have shown a significant correlation with survival in SPS. Our aim was to evaluate immunohistochemical protein expression of the three genes and also assess the gene copy numbers of TOP2a and HER-2-neu by FISH analysis in SPS in order to verify the existence of prognostic value on these parameters.
Method: Paraffin-embedded tissues from 274patients with SPS were included in the study.
Results: Analysis of multiple parameters showed that combined immunohistochemical expression of TOP2a and survivine were significantly associated with overall survival among sarcomas. This association was also valid when only high-grade sarcomas were analysed. There was no correlation between gene amplification and protein expression of TOP2a, or with HER-2-neu.
Conclusion: The present results indicate that combined immunohistochemical study of TOP2a and survivine may emerge as a relevant prognostic factor for clinical usage. (Supported by FAPESP and CNPq).

0162
Disease amelioration of K/BxN mouse model of spontaneous chronic polyarthritis by monoclonal anti-CD8 therapy

L. Carvalho, A. Alarcão, M. J. Aguiar, L. Teixeira, M. Silva, B. Raposo, H. Carvalheiro, J. Silva, L. Graça, M. Souto-Carneiro*
*Faculdade de Medicina Coimbra, Dept. de Anatomia Patologica, Portugal

Objective: The inflammatory amelioration of affected joints was characterized by AA-PAS and Herovici methods in a K/BxN mouse model of spontaneous chronic arthritis that shares many similarities with rheumatoid arthritis (RA) and was used to study the potential of $CD8^+$ T cell depletion with monoclonal antibodies (mAb) to stop and reverse experimental arthritis progression.
Method: Five groups of mice (including control) were treated with specific anti-CD8 mAb (YTS105 and YTS169.4) with and without thymectomy. $CD8^+$ T cells from the blood and articular infiltrate of K/BxN mice were characterized for cell surface phenotypic markers and for cytokine production. Affected joints were submitted to routine decalcification and paraffin inclusion.
Results: Mice receiving anti-CD8 mAb improved the arthritis score 5 days after treatment. Recovery of the $CD8^+$ T cells was associated with a new increase of the arthritis score after 20 days. Thymectomized and antiCD8 mAb-treated mice improved arthritis score permanently. Anti-CD8 mAb-treated animals normalized the serological levels of TNF-a, IFN-, IL-6 and IL-5, and histological analysis showed an absence of inflammatory infiltrate.
Conclusion: To the best of our knowledge, it was shown for the first time that K/BxN mice activated and effector memory $CD8^+$ T cells are present in the peripheral blood and joints and that they play an important role in arthritis maintenance since treatment with specific anti-CD8 mAbs significantly improved disease signs, supported by histological observations. These results document that $CD8^+$ T cells should be regarded as major players in the K/BxN model of experimental arthritis alongside $CD4^+$ T cells and B cells.

Thursday, 2 September 2010, Basement

PS-09 Poster Session Gynaecological Pathology

0169
Prognostic factors in carcinoma of the vulva

S. Dumitriu, D. Radulescu, C. Costea, A. Dumitriu, C. Ungureanu, S. Stolnicu, E. Morosanu, D. Butcovan*
*UMF Gr T Popa Iasi, Dept. of Pathology, Romania

Objective: Early invasive squamous cell carcinoma of the vulva has emerged as a controversial issue in recent literature. Reports illustrating metastatic disease in the inguinal lymph nodes have conflicted with other reports suggesting local treatment only.
Method: The clinical and pathologic characteristics of squamous cell carcinoma of the vulva in 14 women treated by vulvectomy were evaluated in relation to inguinal node status and survival. Tumor diameter, depth of invasion, clinical node status, vascular invasion and pattern of invasion were all individually correlated with the pathologic status of the inguinal nodes.
Conclusion: When evaluated in combination, the clinical diameter of the lesion was the most important predictor of survival; depth of invasion and vascular invasion contributed additional information.

PS-09.1-0170

The prognostic factors of granulosa cell tumour of the ovary

S. Dumitriu, D. Radulescu, C. Costea, A. Pantazescu, S. Stolnicu, C. Ungureanu, E. Morosanu, D. Butcovan*
*UMF Gr T Popa Iasi, Dept. of Pathology, Romania

Objective: Granulosa cell tumours of the ovary are rare malignancies with a relatively favorable prognosis. These tumours have preponderance for local spread and extremely late recurrence. The aim of this study was to investigate the pathologic features related to disease recurrence in adult-type ovarian granulosa cell tumors.
Method: Four patients with granulosa cell tumours were retrospectively reviewed, and we analysed clinical and pathological characteristics.
Results: The most common presenting symptom was abnormal uterine bleeding (74.5%). Mean age was 49.7 years. The median follow-up was 87 months. According to univariate analysis, there were only two significant factors for overall survival: stage and presence of residual disease. The 5-year survival rate was 61% and median survival after recurrence was 18 months.
Conclusion: Despite the small number of patients, the study showed that stage and macroscopic residual disease are significant prognostic factors.

0171

PECOMA (perivascular epithelioid cell tumor)-like epithelioid endometrial stromal sarcoma in uterus: case report

E. Kimiloglu Sahan, S. Tuzlali, A. Akyildizi Igdem, N. Erdogan, Y. T. Ayanoglu*
*Taksim Training Hospital, Dept. of Pathology, Istanbul, Turkey

Objective: The World Health Organization recently recognized a family of neoplasms showing at least partial morphological or immunohistochemical evidences of a putative perivascular epithelioid cell (PEC) differentiation. It is characterized by an epithelioid morphology, clear to eosinophilic granular cytoplasm, perivascular location and co-expression of smooth muscle and melanocytic markers. Malignant perivascular epithelioid cell tumour (PECOMA) is an extremely rare mesenchymal neoplasm, although only 14 cases of uterine PECOMA have been described.
Method: A 71-year-old woman presented with postmenopausal bleeding. The diagnosis was mixed Mullerian tumoral proliferation in the probe cüretage material. Later on, total abdominal hysterectomy and bilateral salpingo-oopherectomy was performed. Macroscopically, the specimen had a 6.5 × 3 × 1-cm polypoid mass in the uterine cavity. Microscopically, there was a tumoral proliferation of swollen epithelioid cells that formed sex cord-like tubular formations and showed trabecular and insular patterns. One-layered columnar cells laid the endometrial glands peripherally of this proliferation. The neoplastic cells had mild hyperchromatism and pleomorphism and mitosis. There was no necrosis. Ki-67 proliferation index was 2–3%; the neoplastic cells were positive for vimentin, estrogen receptor, progesterone receptor, smooth muscle actin and Bcl-2, but negative for pancytokeratin, CD34, HMB-45 and alpha-inhibin immunohistochemically.
Results: By the help of these findings, we reported the case as 'PECOMA-like epithelioid-type endometrial stromal sarcoma', though HMB-45 was negative, but the morphological findings were similar.
Conclusion: We present the case here because of its rareness and to discuss it with the description of additional cases; more insight into their behavior and predictive morphological parameters may be achieved.

0172

Intestinal-type adenocarcinoma in a background of mature cystic teratoma of the ovary: case report

E. Kimiloglu Sahan, S. Tettkurt, N. Erdogan, Y. T. Ayanglu, U. Kafrinoglu*
*Taksim Training Hospital, Dept. of Pathology, Istanbul, Turkey

Objective: Mature cystic teratoma of the ovary, frequently called a dermoid cyst, is the most common of all ovarian neoplasms and represents the majority of benign ovarian neoplasms in women <30 years of age. Malignant transformation of mature cystic teratoma of the ovary occurs in approximately 2% of all cases. Patients found to have malignant transformation in a mature cystic teratoma are likely to be postmenopausal. Adenocarcinoma has been reported to occur in 6.8% of cases of mature cystic teratoma.
Method: The operation of total abdominal hysterectomy and bilateral salpingo-oophorectomy was performed on a postmenopausal woman of 55 years. In the macroscopical sections of the ovary, there were multiple cysts which had 3.5 cm of greatest diameter. There were sebum-like material and hair in some of these cysts. Microscopically, there was a malignant proliferation of epithelial type that formed tubular, cribriform and polyadenoid formations. The cells of this proliferation were large and pleomorphic and had a high mitotic index. There was necrosis widely. Columnar epithelium was lying in the cystic spaces. There were lipid-

laden macrophages and histiocytic multinuclear cells, lymphoplasmositer inflamatuar cell infiltration around them. There were hair follicles focally. Immunohistochemically, tumor cells were positive for cytokeratin 7 and CDX-2 diffusely and negative for cytokeratin 20.
Results: The diagnosis was intestinal-type adenocarcinoma in a background of cystic teratoma. Endoscopically and colonoscopically, there was no tumor in intestines.
Conclusion: Although gastrointestinal epithelium is found in mature cystic teratoma, intestinal adenocarcinoma is uncommon in the ovary. Because of its rareness, we present the case here.

0176

Expression of lymphangiogenesis-associated markers VEGF-D, D2-40 and Prox-1 in human cervical squamous cell carcinoma

V. Bravou, N. Sotiropoulou, S. Kouneli, V. Damaskou, E. Papaspirou, H. Papadaki*
*University of Patras, Dept. of Anatomy-Histology-Embryology, Greece

Objective: Cervical carcinoma metastasises mainly via the lymphatics. Attempts to correlate the expression of various lymphatic markers with lymph node metastasis have provided contradictory results. We investigated the expression of lymphangiogenesis-associated molecules in human cervical squamous cell carcinoma (SCC).
Method: The expression of VEGF-D, Prox-1 and D2-40 were evaluated by immunohistochemistry in paraffin-embedded tissue samples from 72 cases of invasive cervical SCC. Correlations with tumour grade, FIGO stage, lymph node metastases, lymphatic emboli and inflammation were also examined.
Results: Cytoplasmic and/or nuclear VEGF-D expression in the tumor cells was found in 63 of 72 (87%) cases and correlated significantly with LN metastasis ($p=0.003$), lymphatic emboli ($p=0.017$) and FIGO stage ($p=0.023$). D2-40 and Prox-1 were expressed in the lymphatic endothelium, while in 35 of 72 (%) cases, nuclear staining for Prox-1 in the tumor cells was also observed. There was a significant correlation between D2-40 peritumoral lymph vessel density (LVD) and the presence of lymphatic emboli ($p=0.009$) as well as between both intratumoral and peritumoral Prox-1 LVD and the degree of inflammation ($p<0.001$). A significant correlation of VEGF-D expression with peritumoral D2-40 and Prox-1 LVD ($r=0.281$, $p=0.017$ and $r=0.258$, $p=0.03$, respectively) was also noticed.
Conclusion: Our results indicate that VEGF-D seems to be implicated in lymphangiogenesis and in the progression of cervical SCC, and D2-40 may be a useful diagnostic tool in the assessment of lymphatic emboli. Inflammation also probably plays a critical role in promoting lymphangiogenesis.

0177

Immunohistochemical expression of Mena, E-cadherin, Ki67 and p16 antibodies in cervical intraepithelial neoplasia and carcinomas

J. Ioan, G. Simona, E. Istvan*
*UMF, Dept. of Pathology, Targu-Mures, Romania

Objective: Some studies revealed that E-cadherin, which plays an important role in the intercellular adhesion of epithelial cells, presented alterations in cervical lesions, but clinical significance has not yet been understood. On the other hand, Mena (mammalian Ena) expression, one of the actin-binding proteins which belong to the Ena/VASP family (enabled/vasodilator stimulated phosphoprtotein), was not studied yet in cervical intraepithelial neoplasia (CIN) or cervical carcinomas (CC).
Method: We have analyzed in biopsic cervix specimens the immunohistochemical expression of Mena, E-cadherin, Ki67 and p16 antibodies in 30 cases with CIN (1, 2 and 3) and ten cervical carcinomas. All antibodies were provided by LabVision.
Results: We observed that E-cadherin intensity decreased from CIN to CC, but did not present statistical differences between different grades of CIN. Mena was not expressed in normal cervical epithelium, but its expression was increased at the same time with increasing grade of CIN, and significant up-regulation upon transition to invasive carcinoma was observed. In cases with CIN1/CIN2 and immunophenotype $Ki67^{-}/p16^{-}$, Mena was not expressed and E-cadherin intensity had higher intensity than in cases $Ki67^{+}/p16^{+}$.
Conclusion: Correlation between Mena, E-cadherin and also Ki67 and p16 immunoexpression could be an important prognostic factor in cervical lesions and could help the pathologist define more accurately the grade of CIN and to determine the risk for malignant transformation.

0178

Distribution of human papillomavirus genotype and significance of expression of p16 and bcl-2 in patients with cervical squamous intraepithelial neoplasia from Korean women

M. Kim, S. Lee*
*Yeungnam University, Dept. of Pathology, Daegu, Republic of Korea

Objective: Human papillomavirus (HPV) is considered to be most important agent in cervical carcinogenesis and is also associated with precancerous lesion. Prevalence and distribution of HPV genotype varies geographically. Early detection of cervical intraepithelial neoplasia (CIN) results in the prevention of progression to cancer. This study investigates the distribution pattern of HPV and the expression of p16 and bcl-2 in CIN among Korean women.
Method: We selected 177 samples of CIN (CINI 25, CINII 14, CINIII 98) and 40 squamous cell carcinoma obtained by punch biopsy or conization. All of them had HPV genotyping in routine Pap smear using DNA chip. The tissue specimens were immunohistochemically stained for p16 and bcl-2.
Results: HPV DNA was detected in 92% of the specimens. The most prevalent HPV type was HPV 53, including multiple infection in CIN I, while HPV 16 was the most common type in CIN II and III. HPV 58 was the second most common type in CIN III. Multiple infection was detected in 26.3% of the sample. P16 expression was observed in all of CIN lesions and was significantly correlated with HPV infection. There was a positive correlation between the expression of bcl-2 and HPV 16 observed in CIN III.
Conclusion: The distribution of HPV genotype in Korean women disclosed a somewhat different pattern from that of western countries by showing a higher prevalence of HPV 58, 56 and 52. Immunoexpression of p16 was intimately associated with HPV infection and was a highly sensitive marker for CIN. Bcl-2 had correlation with HPV 16-associated CIN III.

0179

P 16 as a diagnostic marker of cervical intraepithelial neoplasia in cervical biopsies

S. Sramek Zatler, A. Repše Fokter*
*General Hospital Celje, Dept. of Pathology, Slovenia

Objective: The protein p16(Ink4a) is overexpressed in cervical lesions associated with high-risk human papillomavirus (HPV) subtypes 16 and 18, but not in low-risk HPV subtypes 6 and 11 or non-HPV-associated cervical lesions. Distinction between low- and high-grade cervical lesions is very important for the management of patients with cervical intraepithelial neoplasia. In this study, we wanted to determine the usefulness of p16(Ink4a) expression in biopsy specimens with indistinct initial histologic diagnosis (CIN 1-2).
Method: We applied immunostaining for p16(Ink4a) in 47 consecutive cervical biopsy specimens with equivocal initial histologic diagnosis (CIN 1-2) during the period between January 1, 2009 and December 31, 2009.
Results: Diffuse positive expression in the lower third of epithelium was found in 21% (10/47) of cervical biopsies; in 47% (22/47), the positive expression extended to two thirds of the epithelium, suggesting the diagnosis of CIN 2. Fifteen biopsy specimens (32%) were negative or only focally positive for p16(Ink4a), indicating the diagnosis of immature squamous metaplasia.
Conclusion: The data support the routine use of p16(Ink4a) immunohistochemical evaluation of cervical biopsy specimens for better discrimination of negative, low-grade and high-grade cervical lesions.

0180

Cervical adenocarcinomas concomitant with CIN or squamous cell carcinoma lack gastric phenotype

Y. Wani, K. Notohara*
*Kurashiki Central Hospital, Dept. of Pathology, Japan

Objective: Uterine cervical adenocarcinoma with gastric phenotype was recently proposed and shows an aggressive clinical course. The aim of the study was to examine whether the gastric phenotype is present in cervical adenocarcinoma in situ (AIS) or invasive adenocarcinoma (AC) concomitant with cervical intraepithelial neoplasia (CIN) or invasive squamous cell carcinoma (SC).
Method: Fifteen cases of cervical glandular neoplasms concomitant with CIN or SC were retrieved from KCH files and subclassified by AIS+CIN3 (n=8), AC+CIN1-2 (n=2), AC+CIN3 (n=3), AC+SC (n=2). Of those, AC and SC were independently present and the so-called adenosquamous carcinoma was excluded. In addition, no cases of minimal deviation adenocarcinoma were observed. We evaluated the presence of gastric morphology based on the criteria previously described by Kojima et al. (AJSP 2007). In immunohistochemistry, the staining of MUC6 and HIK1083 was performed and scored as negative; <10%, focal; 10% to <30%, diffuse; 30% or more.
Results: All 15 cases lack gastric morphology. MUC6 was positive in four cases (diffuse, n=1; focal, n=3), whereas all cases were negative for HIK1083.
Conclusion: Cervical AIS or AC concomitant with CIN or SC seems to be unrelated with adenocarcinoma with gastric phenotype.

0182

A premenopausal extramammary (vulvar) Paget's disease: case presentation

C. Lazureanu, E. Lazar, A. Dema, S. Taban, M. Cornianu, A. Muresan, A. Faur, R. Cornea*
*University of Medicine, Dept. of Pathology, Timisoara, Romania

Objective: Paget's disease of the vulva is an unusual kind of skin cancer that arises from glandular cells, and its incidence is almost exclusively encountered in postmenopausal women (65–70 years old).
Method: Vulvar skin fragments from a 46-year-old woman were submitted for definite pathological diagnosis due to a prolonged intercourse pain and itching in the genital area, thought to be linked with lichen sclerosus et atrophicus. The tissue fragments were routinely processed (buffered 4% formalin fixation, paraffin-embedded, 5-μm-thick section), stained with H&E, AB-PAS and supplementary immunohistochemical reactions with CEA, EMA, HER2/neu, pan-CK and HMB45.
Results: Intraepidermal presence of large tumor cells with vesicular, pleomorphic nuclei and well-represented, foamy cytoplasm, positive for AB-PAS, arranged in small nests with central lumen near the rete ridges or dispersed singly throughout the whole thickness of squamous epithelium raises the suspicion of Paget's disease. This opinion was confirmed by the positive immune reaction of the mucin-secreting intraepidermal tumor cells for CEA, EMA, panCK and HER2/neu. The tumor cells were negative for HMB45 and presented a high mitotic rate: 33% of tumor cell nuclei were stained with Ki67 antigen. The final diagnosis was extrammamary (vulvar) Paget's disease, Wilkinson 1a (primary intraepithelial).
Conclusion: Seldom among vulvar neoplasia, Paget's disease must be taken into count even in premenopausal women; its prompt diagnosis enables the surgeon to perform the radical cure for selected cases (those with only intraepidermal/intraepithelial spread).

0183

Characteristics of transmembranous glycoprotein CD44, PTEN protein and Ki 67 in endometrial hyperplasia and carcinoma

O. Mahmajeva, R. Kleina, M. Sperga, V. Groma, A. Dabuzinskiene*
*Riga Stradins University, Dept. of Pathology, Latvia

Objective: The objective was to evaluate the expression of CD44 and PTEN protein in atrophy, various hyperplasias (EH), carcinoma of endometrium (EC) and its correlations with proliferation rates
Method: From 49 analyzed EC (also treated with tamoxifen) for immunohistochemical examination, we have chosen 17 and compared them with 15 hyperplasia with atypia, 17 without it and eight glandulostromal atrophy cases. Immunohistochemical evaluation was done with CD44, PTEN, Ki 67 (DAKO) antibodies. Expression of markers was stated into 3 degrees. PTEN presence and proliferation index was evaluated in percent. The results were compared with χ^2 and Fisher test ($p<0.05$).
Results: CD 44 was negative in endometrial atrophy and hyperplasia. PTEN protein expression in EH was around 100%. Expressed CD 44 marker was in atypical hyperplasia and EC. Comparison of these two groups showed that χ^2 is 4.44 ($p=0.217$), Fisher test $p=0.636$. Essential distinction was found between hyperplasia with atypia and without it: $\chi^2=9.700$, $p=0.021$, Fisher test $p=0.015$. In atypical EH, PTEN protein expression decreases in epithelium till 67.5%, but is still high in stroma. In EC, immunoreactivity of PTEN was 20.7–50.4%. Sometimes, PTEN loss goes parallel with the reduced proliferative activity in cystic atrophic glands in G0 stage of mitosis.
Conclusion: (1) CD44 expression is increasing in hyperplastic processes and EC, but there are no differences of CD44 in atypical hyperplasia and endometrial carcinoma. (2) PTEN protein expression in EH and EC was variable, but with tendency towards its diminution in cystic glands, atypical hyperplasia and EC.

0184

The association between neoplasia of the endometrium and others benign genital lesions: independent or similar mechanism?

M. Sajin, A. Ionescu, M. Comanescu, I. Hulea, L. Reghina, A. M. Lazaroiu, I. Caruntu, M. Costache, G. Simion, M. Carstoiu, D. Secara*
*UMF Carol Davila, Dept. of Pathological Anatomy, Bucharest, Romania

Objective: It is generally believed that hyperoestrogenic status is one of the most important etiopathogenic factors of premalignant and malignant lesions of endometrium. This study characterises the association between the presence of premalignant and malignant lesions and other benign clinicopathological manifestations of hyperoestrogenism in the genital area.
Method: The study comprised 83 resection specimens that were formalin-fixed and paraffin-embedded. The sections were marked with standard and special stainings (ER, PGR, Ki-67, PTEN).
Results: The study group included women with ages between 39 and 67 years. From a total of 83 hysterectomies, 25 presented both histological evidence of premalignant or malignant endometrial lesions and other associated lesions: endometrial (4), endocervical (2) polyps, leiomyoma (16), adenomyosis (4), ovarian cysts (10).
Conclusion: In conclusion, the altered expression of oestrogenic status reflects the pathogenic mechanisms of endometrial neoplasia. Assessment of these histopathological patterns may be a useful clinical and prognostic tool for

the follow-up of women with predisposition for neoplastic lesions of the endometrium.

0185

Uterine (subendometrial) schwannoma

M. Scarpatetti, K. Bodo, F. Moinfar*
*Medical University Graz, Austria

Objective: Schwannoma of the uterus is a benign but very rare neoplasia. We report a case of uterine schwannoma occurring in a 51-year-old woman with a recent history of abnormal uterine bleeding.
Method: The curettage material was routinely processed and stained with H&E. In addition, immunohistochemistry was performed with antibodies against S100-protein, SMA, CD 117, Caldesmon, Melan A, HMB 45, CD 10 and MIB-1.
Results: In histological investigation, very few preexisting non-neoplastic glands and a tumor with dense fibrillary matrix was seen. The nuclei were oval to bipolar and cells showed no borders. Few psammoma bodies were seen in the tumor, also incipient Verocay bodies. The tumor cells were intensely positive for S-100 protein; no reaction with all other antibodies was seen. Less than 1% of tumor cells were positive for MIB-1.
Conclusion: The histopathology and the immunohistochemistry in this case revealed an exceedingly rare example of a uterine (subendometrial) schwannoma.

0187

Expression of PTEN, ß-catenin and estrogen receptor in endometrial hyperplasia: an immunohistochemical study

S. Wojtylak, B. Pieczynska, K. Klonowska, A. Zawrocki, W. Biernat*
*Medical University of Gdansk, Dept. of Pathology, Poland

Objective: Type I endometrial carcinomas with endometrioid and mucinous morphology develop in the patients with chronic hyperestrogenism. These tumors show frequent PTEN (30-50% of cases) and β-catenin mutations (15-20% of cases).
Method: The study group consisted of 79 cases of endometrial hyperplasia (EH) and 19 cases of endometrial atypical hyperplasia (EAH). As a control group, 43 cases of anovulatory cycle endometria (ACE) were selected. The immunohistochemical analysis was performed on the endometrial curettings by means of tissue microarray. For the objective evaluation of analysed proteins, expression *H* scores (percentage of positive cells) have been used.
Results: The mean *H* score of PTEN expression was 177.16 in ACE, 111.5 in EH and 102.92 in EAH ($p<0.05$ ACE vs. EH and EAH). Mean *H* score of ER was 148.88, 173.1 and 212.12, respectively ($p<0.05$ between all groups). Mean *H* score of membrane β-catenin expression was 95.47, 89.47 and 74.92, respectively ($p<0.05$ between all groups). Percentage of cases with positive nuclear β-catenin expression was 10.8%, 12.3% and 38.5%, respectively ($p<0.05$ EAH vs. ACE and EH).
Conclusion: Expression of analysed proteins significantly distinguishes endometrial hyperplasia from disordered endometrial proliferation. The most extreme level of abnormal expression of the studied proteins was seen in atypical hyperplasia, confirming its close relationship to endometrial carcinoma. Analysis of PTEN and β-catenin expression may be a useful adjunct in small endometrial biopsies from patients with suspected precursor states for endometrial carcinoma.

0188

Immunohistochemical profile of cotyledonoid dissecting leiomyoma of the uterus

E. Zielinska-Pajak, L. Liszka, J. Pajak, D. Golka*
*Medical University of Silesia, Dept. of Histopathology, Katowice, Poland

Objective: Cotyledonoid-dissecting leiomyoma of the uterus (CDLU, also known as Sternberg tumor) is an extremely rare variant of smooth muscle neoplasm. Less than 30 cases of CDLU have been reported so far. CDLU is characterized by alarming distinctive gross appearance suggestive of a malignant neoplasm, but paradoxically universally benign clinical behavior. Although the histopathological picture of CDLU was well described, there are few if any data which may explain extrauterine overgrowth of the tumor.
Method: Four previously not described cases of CDLU were submitted to histopathologic examination and selected immunohistochemical assays (p16, Ki67, bcl-2, WT-1, p53). Results of immunohistochemical stainings were compared to those previously reported in benign and malignant uterine smooth muscle neoplasms.
Results: The age of patients with CDLU ranged from 33 to 52 years (median 50 years). Grossly, all the tumors were exophytic and composed of irregular nodular protrusions. Median diameter of tumors was 8 cm (range 3–11 cm). Microscopically, the cases were composed of smooth muscle fascicles dissecting the extratumoral myometrium and forming swirled nodules, similarly to previous CDLU reports. Nuclear p16 expression was seen in <1% of tumor cells. Ki-67 proliferative index in all

CDLU cases was below 1%. Bcl-2 was expressed focally in a single case and diffusely in three other cases. WT-1 diffuse nuclear expression was seen in all cases. All cases were p53-negative.
Conclusion: p16/Ki-67/bcl2-/WT-1/p53 immunohistochemical expression patterns in CDLU resembled those previously reported in uterine usual type leiomyomas and did not explain the distinctive gross appearance of these tumors.

0190

A panel of antibodies to distinguish the different histological subtypes of the epithelial ovarian carcinoma

E. Gradhand, S. Gründig, O. Kuss, S. Hauptmann*
*Medizin. Universität Halle, Institute of Pathology, Germany

Objective: Epithelial ovarian carcinoma (EOC) is subdivided into five histological subtypes: serous, mucinous, endometrioid, clear cell, and transitional. The differential diagnosis between these subtypes is mostly unproblematic, but is getting difficult in poorly differentiated tumors. The aim of the present study was to establish an immunohistochemical marker panel in a series of unequivocal highly differentiated EOCs that simplify the differentiation in difficult EOCs.
Method: We performed an immunostaining study in a small series of highly differentiated EOCs (47 cases). After examining the cases with 23 markers, we identified 13 antibodies as useful markers (CA19-9, CD15, CA125 CD99, CD44v6, CD44H, Claudin1, EGFR, FAK, OPN, p63, p53, and PR). The percentage of the antibody-marked tumor cells per tumor was observed counted. The *F* test was used to determine differences between the means of percent expressions of the antibodies. For predicting the histological subtype from the antibodies data, a multinominal logistic regression model was performed. We additionally accomplished a leave-one-out method cross-validation experiment to mimic real-life situation of predicting an unknown histological type.
Results: In 89% of the cases, the initial multinomial regression model (using all observations) was able to predict the correct subtype. However, this number reduced to 43% in the leave-one-out experiment.
Conclusion: The match of 89% correct predictions in the full data set is in agreement with another publication (84%) using a similar panel. However, the low number of correct predictions in the leave-one-out experiment affirms that this is no valid panel to distinguish the histological types of EOCs by immunohistochemistry.

0191

Immunohistochemical aspects of differential diagnosis in ovarian and testicular malignant tumors

I. Poinareanu, M. Aschie, A. A. Nicolau, A. F. Mitroi, A. Chisoi, A. Iliesiu, A. M. Cretu, J. Stanisici, G. Resul, M. Enciu*
*University Ovidius Constanta, Faculty of Medicine, Romania

Objective: Teratomas usually manifest as masses in descended or undescended testes, in extratesticular tissues where germ cells tumors occur and in ovary in females. Teratomas are germ cell tumors composed of an array of tissues derived from two or three embryonic layers in any combination.
Method: Our report presents two cases of immature teratomas. The first patient is a 34-year-old man admitted in Surgical Department of County Hospital of Constanta for increased size in the left testicle in last 6 months, and the second case is a 15-year-old girl hospitalized in the same department for retroperitoneal tumoral mass. CT scan shows in both cases testicular and ovarian mass with non-homogeneous structure, surrounded by liquidian areas.
Results: Histological exam revealed in both situations immature teratoma with mesenchymal, epithelial adenocarcinoma and neuroepithelial features and mature zones with condroid tissues. There are no specific immunohistochemical markers for teratoma, but individual antibodies can be used to identify particular tissues. In both cases, chromogranin, synaptophysin and AFP were positive. There was no correlation found for the rest of IHC markers used for these cases, markers that were positive or negative (PLAP, beta-HCG, CD 117, S 100). Prognosis was favorable after surgery on the young man, but the young woman was given chemotherapeutical support.
Conclusion: Immature teratomas are rare germ cell tumors. The incidence in children is 2% to 3% of ovarian and testicular tumors. In both cases, the IHC confirms immature teratoma diagnosis. Immature intestinal type of glands were positive for AFP, and neuroepithelial structures were positive for chromogranin and synaptophysin that sustain immature teratoma.

0192

Giant ovarian lymphangiomas

S. Stolnicu, M. D. Chifu, K. Szabo, J. Augustine, S. Thomas, O. Preda, L. Puscasiu, A. Nicolae, F. F. Nogales*
*University of Medicine, Dept. of Pathology, Targu Mures, Romania

Objective: Vascular tumors of the ovary are rare, with only 18 lymphangiomas published in the literature so far. They

are usually asymptomatic and represent an incidental finding. Histologically, most lymphangiomas are of cavernous type and do not exceed 4–5 cm in diameter. We report two unusually large lymphangiomas measuring 7 and 9 cm in diameter, respectively, both of them presenting with ultrasonographical images of malignancy due to the large size and multicystic appearance.
Method: Patients were 50 and 51 years old, respectively, the latter with a clinical history of 20 pregnancies and associated leiomyoma and endometrial polyp. The former was operated for a large pelvic cystic mass which was on microscopic examination diagnosed as a borderline serous tumor of the left ovary.
Results: Macroscopically, they were poorly defined multicystic tumors that on cut section were dramatically reduced in size (deflated), oozing a clear, thin fluid. Microscopically, there was an anastomosing network of empty-appearing cystic spaces that were lined by flattened cuboidal cells without atypia. Immunohistochemically, their vascular nature was demonstrated as the cells lining the cystic network were positive for CD31, CD34 and D2-40 (podoplanin) and negative for epithelial markers.
Conclusion: Lymphangiomas are benign masses and their histogenesis is uncertain. They may represent a reactive process occurring after impaired or blocked regional lymphatic drainage related to conditions such as chronic follicular salpingitis, radiation therapy or various neoplastic processes. One of our cases lacked any association and the other one was associated with a surface, noninvasive tumour. We thus conclude that our cases are likely to be true neoplasms.

0194

Placental mesenchymal dysplasia (PMD) with mosaic triploidy and chorangiomas presenting as a partial hydatidiform mole (PHM)

J. Stanek, M. Khalequzzaman*
*Cincinnati Children's Hospital, Dept. of Pathology, USA

Objective: PHM may show radiologic, gross, and histological features overlapping with PMD. PMD with aneuplodies has been reported, but not with a mosaic triploidy.
Method: A 2,500-g male fetus without hemihypertrophy or congenital malformations was born at 34 weeks gestation. The 900-g dysmature and focally hydropic placenta showed varicose dilatation of focally thrombosed chorionic vessels, and two translucent thin-walled septal cysts grossly suggestive of PHM. The stem villi showed myxoid stromal change. There was no trophoblastic hyperplasia or pseudoinclusions. The chorionic and stem vessels were dysplastic. Two 2.5- and 2.2-cm glut-1 positive capillary chorangiomas were found.
Results: 69,XXY/46,XY karyotype was revealed by FISH. Amplification of three microsatellite loci on chromosome 11p15.5 showed that the predominant cell line was 46,XY. There was no evidence of paternal isodisomy of Beckwith–Wiedemann syndrome.
Conclusion: This unique PMD case with mosaic diandric triploidy and chorangiomas was grossly suspicious for PHM because of the presence of thin-walled translucent "hydatid" vesicles admixed with placental tissue. However, a large for gestational age and dysmature fetus without anomalies and characteristic gross and microscopic placental findings were diagnostic of PMD. The distinction between PHM and PMD is clinically valid as PHM can be complicated by persistent gestational trophoblastic disease or trophoblastic tumors. The presence of diandric triploidy is not automatically equivalent to PHM.

0197

Expression of p53 protein phosphorylated at serine 20, serine 392 and apoptosis-related proteins in ovarian carcinomas

J. Bar, I. Slomska, L. Noga, J. Rabczynski, M. Grybos, M. Jelen*
*Medical University Wroclaw, Dept. of Pathomorphology, Poland

Objective: The biological role of phosphorylation of the p53 protein in tumour cells is still investigated. The study evaluated p53 protein overexpression, p53 phosphorylated at serine 20 (Ser20), serine 392 (Ser392), and expression of Bax, CAS proteins in ovarian neoplasms and their association with clinicopathological parameters.
Method: The expression of analyzed proteins was examined on 145 malignant and 50 benign ovarian neoplasms using immunohistochemistry.
Results: Differences between the expression of studied proteins in benign and malignant ovarian neoplasms were significant ($P<0.001$). p53-Ser20 phosphorylation was associated with advanced stage ($P=0.03$). p53 protein overexpression was associated with poor differentiated tumour ($P=0.001$), while the differences between CAS expression were observed in moderate and poor tumour grade ($P=0.03$). The correlations between Bax/p53-Ser392, CAS/p53-Ser20 and p53-Ser392 expression were found in ovarian carcinomas ($P<0.01$). p53/CAS-positive cancers were associated with poor differentiated ($P=0.005$) and advanced tumours ($P=0.001$). p53/Bax-positive cases were

found in poorly differentiated cancers (P=0.001). These immunophenotypes revealed phosphorylation of p53 at Ser20 and 392 in 60.0% of cases.
Conclusion: Our results suggest that the expression of p53 protein phosphorylated at Ser20 might depend on the morphological maturity of tumour cells. The revealed associations between Bax, CAS and p53 protein phosphorylated at serine 20 and 392 expression indicate that phosphorylation of p53 protein at Ser20 and 392 might play a role in the regulation of apoptosis-related protein expression in ovarian carcinomas.

0199
Experimental model of female hormonal sterility received by influence on a bitch rat of long constant illumination
S. Abuzaid, I. Kuzmina, G. Gubina-Vakulik, N. Kolousova*
*National Medical University, Kharkov, Ukraine

Objective: Female hormonal sterility is successfully treated. The experimental model of this morbid condition of ovaries is necessary for the approbation of various methods of treatment of female hormonal sterility. In this connection, we have estimated histologically the structural changes of ovaries of a rat after the long maintenance in the conditions of constant illumination.
Method: Two groups of females Vistar rats at the age of 3 months are generated: control group (Cgr), six individuals, and basic group (Bgr), six individuals. Rats of Bgr within 7 months were contained in the conditions of constant illumination and rat Cgr in other premise, in conditions of usual change of day and night. Ovaries are studied histologically.
Results: The ovary of rats Bgr has reduced dimensions. Absence of normal follicles of any degree of maturing and yellow bodies, presence of cystically variated follicles, a considerable quantity of atretic follicles, and presence of white bodies are microscopically observed. It is possible to assume that constant illumination of animals causes stimulation of the production of serotonin and inhibition of the production of a melatonin by a cone-shaped gland. In the beginning, there is a stimulation of a hypothalamus–hypophysial–ovarian axis and then exhaustion of compensatory mechanisms and development of hormonal sterility.
Conclusion: The maintenance of bitch rats in the conditions of constant illumination leads to development in ovaries of pathological changes, characteristic of hormonal sterility. Necessary level of ovarian insufficiency can be dosed by change of duration of the period of constant illumination of animals.

Thursday, 2 September 2010, Basement

PS-10 Poster Session Cytopathology

0200
Overexpression of P16INK4A can correct an underdiagnosed HGSIL?
S. Divani, A. Vardouli, G. Kalodimos, A. Fericean, E. Alexopoulou*
*Volos General Hospital, Clinical Cytology, Greece

Objective: The expression of P16 protein is associated with a high risk of HPV infection. The purpose of this study was to evaluate if overexpression of P16INK4A protein can be a useful biomarker to detect dysplastic cells in cervical smears of women with normal colposcopic findings but HGSIL cytology.
Method: Cases were retrospectively searched in cytology data of the past 5 years. One hundred thirty-nine cervical smears from patients with HGSIL were reviewed by two cytologists. The colposcopic results concerning those cases were also obtained from the records. Forty-three of 139 (30.9%) women had no pathologic colposcopic findings. Immunocytochemistry for P16 was performed on all cases with normal colposcopy and HGSIL cytology. The immunocytochemical staining results were estimated and classified into four grades: 0, 1 (1–5% positive cells), 2 (5–25% and patchy), 3 (>25% and diffuse).
Results: The P16 protein expression was not observed in two cases (4.6%), whereas it was strong and diffuse in nine patients (20.9%). Strong and patsy P16 expression was detected in 13 patients with HGSIL cytology and normal colposcopy (30.2%). Rare positive cells (1–3% cells with nucleus stained with anti-P16 antibody) were present in 19 cervical smears (44.2%).
Conclusion: Colposcopy with guided biopsy detects approximately two thirds of CIN 3 cases (Gage et al., National Cancer Institute, USA, 2006). Increased expression of P16INK4A reflects the increasing expression of viral oncogenes in dysplastic cervical cells. P16INK4A is a specific biomarker to identify HGSILs, so it could be a useful adjunct for the reevaluation women with HGSIL cytology and normal colposcopy in order to correct the underdiagnosed HGSILs and prevent delay in therapeutic managements.

0202

A ring validation study prior to introduction of computer-assisted screening in the Dutch cervical screening programme

F. van Kemenade, B. Ooms, H. Beerman, E. Boers, H. Bulten, H. van der Linden*
*VU Medisch Center, Dept. of Pathology, Amsterdam, The Netherlands

Objective: Prior to the introduction of computer-assisted screening in the Netherlands, it was agreed upon to first validate this method with an a priori agreed upon uniform protocol for validation. Aim was a kappa value of 0.6 or higher.
Method: A validation sample set was made of 280 anonymized routine screen samples, enriched for abnormalities (to 15%). Two screeners from one laboratory scored these with either computer-assisted screening or conventional thin-layer cytology. Slides were scored dichotomously independently for either mode of screening as either within normal limits or outside normal limits. The procedure was supervised by an external quality pathologist. After a pilot (n=2), the 'set' was transported to other laboratories for the application of a similar protocol. All scores were computed from six different laboratories (n=3,305).
Results: This nationwide validation study required on average 4 weeks in the participating laboratories. First two kappa scores were 0.86 (95% CI 0.83–0.89) and 0.72 (95% CI 0.683–0.77) for the two techniques. After 6 months, four additional laboratories had accomplished the validation procedure. Cumulative kappa score for six laboratories was 0.77 (95% CI 0.75–0.78, n=3,305) All average scores were above the preset norm of 0.6.
Conclusion: A nationwide validation protocol could be accomplished without complications. The results showed good agreement between computer-assisted screening and conventional screening on thin-layer technique. The validation protocol allows for the implementation of computer-assisted screening in programme-based screening in the Netherlands since detection rates will not alter in a significant manner.

0204

Diagnosis of malignant mesothelioma by fine needle aspiration cytology

M. Almeida, P. Campos*
*Hospital Santa Maria, Patologia Morfologica, Lisbon, Portugal

Objective: Cytopathologic descriptions of mesotheliomas are limited. This study shows the results of fine needle aspiration (FNA) cytology in ten cases of malignant mesothelioma.
Method: Material was obtained by CT-guided fine needle aspiration (FNA). Smears were stained with Giemsa and Papanicolaou stain, and cell block sections, when done, were stained with hematoxylin and eosin. Immunocytochemical (ICC) studies were done in smears/cell block using adenocarcinoma markers (CEA, EMA, CD15, CK7 and TTF1) and mesothelial markers (calretinin, WT1, CK5/6).
Results: All mesotheliomas except three of peritoneal origin were from the pleura. There were nine epithelial malignant mesotheliomas (EMM) and one sarcomatous mesothelioma (SMM). All mesotheliomas except three of peritoneal origin were from the pleura. There were nine epithelial malignant mesotheliomas (EMM) and one sarcomatous mesothelioma (SMM). In FNA, all EMMs were highly cellular, with a large number of small sheets, and tridimensional clusters with smooth or lobulated contours as well as single cells. The cells were round to polygonal with abundant cytoplasm and well-defined cell borders and the nuclei were predominantly centrally located, round to oval, medium to large with fine chromatin and small but prominent nucleoli; occasional binucleation was noted. The SMM showed malignant spindle-shaped cells with scant, ill-defined cytoplasm singly and in loose clusters, in a bloody background. Immunocytochemical staining on the smears/cell block were positive for calretinin, CK5/6,CK7 and WT1 and negative for CD15,CEA and TTF1.
Conclusion: Cytologic findings coupled with immunocytochemical studies and in combination with radiologic information and clinical history are highly accurate in the diagnosis of malignant mesothelioma.

0205

Solid pseudopapillary tumor of the pancreas diagnosed on endoscopic ultrasound-guided fine needle aspiration material

A. Demir, R. Sadik, P. Saksena*
*Sahlgrenska University Hospital, Dept. of Clin. Pathology and Cytology, Gothenburg, Sweden

Objective: Solid pseudopapillary tumor (SPPT) of the pancreas is a rare, low-grade, epithelial neoplasm that is usually discovered incidentally in young women.
Method: We present a 42-year-old woman with 5 × 4-cm round tumor in the caput pancreatis. Endoscopic ultrasound-guided fine needle aspiration (EUS-guided FNA) was performed. Smears were stained with Giemsa and Mc Manus. Cell block was used for eosin, Mc Manus and immunohistochemical stainings.
Results: Cell-rich smears showed single cells and aggregates of uniform cells forming branching papillary clusters with delicate myxoid fibrovascular cores. The nuclei of the

cells were round or oval; nucleoli were small or inconspicuous. Cytoplasms were usually vacuolated. Intra- and extracytoplasmic myxoid globules were noticed. Tumor cells showed diffuse positivity for CD10, progesterone receptor and CD56 and focal positivity for synaptophysin and AE1/AE3. Chromogranin A, CK8/18, CK7, Tag72 were negative. Ki67 showed low (<1%) positivity. The case was diagnosed as SPPT based on morphological and immunohistochemical features, which was confirmed on the surgical material.
Conclusion: Distinguishing SPPT from other pancreatic tumors, especially pancreatic endocrine tumors, can be challenging. Clinical setting, cytomorphologic features, and immunostains of the cell block help distinguish SPPT from pancreatic endocrine tumors, acinar cell carcinoma, and papillary mucinous carcinoma.

0206
The role of breast FNAC in diagnosis: a survey of current practice in an anticancer institute

T. Gavressea, M. Sevastiadou, H. Ntoula, A. Alexiadou, P. Manikhs, H. Trihia*
*Cancer Hospital Metaxas, Dept. of Cytopathology, Nea Smirni, Greece

Objective: Most countries, including Greece, have adopted the triple assessment approach to breast diagnosis, with FNAC as the first-line pathological investigation with the exception of microcalcifications. The majority of European countries use similar reporting systems for breast FNAC (C1–C5), in keeping with the European Guidelines for Quality Assurance in Breast Cancer Screening and Diagnosis.
Method: In order to explore current practice in our hospital, we reviewed 390 breast FNAs within a 1-year period, collected and interpreted by both the cytopathologists and less by the surgeons, where no clinical data were available.
Results: There were a total of 156 cancers (40%), of which 150 were diagnosed by FNA (128 as C5 and 22 as C4). Overall, 142 were diagnosed as C5 (36.4%), 40 as C4 (10.2%), 47 as C1 (12.1%) and 161 as C2 (41.3%). Of the 142 C5, 128 were confirmed histologically (mastectomy specimens), whereas in 13 patients, there was no feedback information. There was one false positive case concerning two separate fibroadenomas, one of which in the mammary tail, sent to the lab as axillary lymph node. In the C4 category, there were 22 carcinomas, two fibroadenomas, one fibrocystic disease, and 15 had no confirmatory biopsy. In the C1 category, there were six carcinomas (four ductal, one lobular, one metaplastic), two columnar cell change and one fat necrosis.
Conclusion: Our results confirm the accuracy of FNA in the diagnosis of malignancy and show the major importance of a multidisciplinary approach and knowledge of the clinical and radiologic data by the interpreters of the FNAs.

0207
Benign renal tumors mimicking malignancy in fine needle aspiration biopsy samples: report of three cases

H. Gutnik, M. Strojan Fležar, Z. Ovcak, J. Pižem*
*Medical Faculty Ljubljana, Institute of Pathology, Slovenia

Objective: Fine needle aspiration biopsy (FNAB) is a well-established method to diagnose renal tumors. However, it is challenging to diagnose rare benign renal tumors with unusual cytomorphology mimicking malignant tumors. We report three such cases.
Method: All three kidney tumors were discovered by ultrasound examination, and ultrasound-guided FNAB was performed. The first case was a multicystic renal tumor in the right kidney of a 64-year-old woman. The second case was an atypical cyst in the left kidney of a 45-year-old man. The third case was a solid tumor in the left kidney of a 24-year-old woman.
Results: Case 1: Papillary-like structures and macrophages, supplemented by immunocytochemistry, rendered a diagnosis of renal carcinoma, papillary type, while disregarding stromal fragments. Histological diagnosis was a mixed epithelial and stromal tumor (MEST). Case 2: Similar morphology led to the same cytological diagnosis as in the first case with subsequent histological diagnosis of a cystic nephroma. Case 3: Small groups of severely atypical cells were suspicious of a malignant tumor, possibly a metastatic one. The histological diagnosis was juxtaglomerular tumor, confirmed immunohistochemically and by electron microscopic examination only after additional clinical data about unexplained arterial hypertension from the age of 15 were obtained.
Conclusion: Cytologic samples of cystic renal tumors should be evaluated cautiously, including the possibility of MEST/cystic nephroma group of tumours. The case of juxtaglomerular tumour shows the utmost importance of reporting the relevant clinical data to the pathologist.

0208
Cytological features of embolized meningiomas

J. A. Jimenez Heffernan, C. Corbacho, E. Tejerina, J. M. Cañizal, C. Salas, E. Sanz Ortega*
*Hospital Puerta de Hierro, Madrid, Spain

Objective: In some meningiomas, primarily with a large vascular supply, preoperative embolization is performed a

few days before surgery in order to soften the tumor and minimize intraoperative bleeding. Post-embolization histological changes consist mainly of necrosis, ischemic cellular changes, vascular fibrinoid necrosis and increased proliferative index. These changes may result in overgrading. We have found no description of such changes in the cytological literature.

Method: We reviewed 22 cases of meningiomas with prior embolization. In 13 of them, relevant cytological changes induced by embolization were present. Cytological material was obtained during intraoperative consultation, either by scrapping or squashing of tissue samples. On histology, all of them were grade I meningiomas and showed intravascular embolic material.

Results: Cytology revealed relevant cellular dissociation with frequent single cells. Ischemic cellular changes were a common finding and consisted of cell shrinkage, nuclear piknosis and ill-defined cytoplasmic limits. Ischemic changes were better appreciated in single cells. Eight cases showed histiocytes and neutrophils. Confluent areas of necrosis were seen in one case. None of the cases showed cellular atypia or significant mitotic activity. Embolic material was seen cytologically in four cases. Of the 22 embolized meningiomas, nine of them showed no significant cytological abnormalities.

Conclusion: Embolization of meningiomas induces cytolomorphological changes that may be relevant in some cases. Greater cellular dissociation and ischemic changes, as well as inflammation, may result in a worrisome cytological image. When faced with such changes, the pathologist should always consider the possibility of embolization, avoiding overgrading or misdiagnosis.

0210

Cytological and clinical statistic correlations in the evaluation of periodontal disease at the diabetic patients with infectious gastritis

L. E. Vasile, A. Galuscan, R. Oancea, E. Lazar, C. Marchese, R. Simulescu, H. Sarandan, O. Rada*
*University of Medicine, Cytology and Histology, Timisoara, Romania

Objective: The cytodiagnostical marks for periodontal disease stood at the basis of the lesion framing at the diabetic patients with infectious gastritis.

Method: Cytological smears have been gathered in a period of 6 years (2004–2009) from 77 diabetic patients, *Helicobacter pylori*-positive, with a diagnostic of chronic periodontal disease. The diagnosis was made with radiological exam and clinical analysis. The samples were air-dried or alcohol-fixed before staining with cytological methods (Papanicolaou, Blue-Polichrom-Tanin-Dragan). The statistical comparison of different parameters was made using Mann–Whitney *U* test and Spearman rank order correlation, with the aim of establishing statistically relevant differences and Spearman correlation coefficients (r) between glucose in blood and periodontal disease, age- and sex-related, the length of the diabetes disease, the cytological periodontal stage and the length of the periodontal disease, age-related.

Results: The statistical calculation has revealed important differences of the blood glucose between the cytological periodontal stages 1 and 2 ($p<0.05$), 1 and 3 ($p<0.01$), and 1 and 4 ($p>0.00000$). In a similar way, there were also differences between stages 2 and 3 ($p<0.01$), 2 and 4 ($p>0.00000$), and 3 and 4 ($p<0.01$).

Conclusion: The neutrophils that have been drawn by the presence of bacteria or by the erosion areas of the oral and gastric mucosa can promote an increased gravity of the epithelial lesions, suggesting a particularity of the microbial infection at the diabetic patient who has hyperglucidic stress with the modification of the cellular and humoral immunity in the background.

0212

Peritoneal effusions analysis in malignant diseases: comparison of various biochemical tests with ascitic cirrotics

A. M. Cretu, M. Aschie, G. Preda, N. Rosoiu*
*Clinical Emergency Hospital, Phatological Anatomy Laborator, Constanta, Romania

Objective: Treatment of malignant peritoneal effusions is generally palliative; therefore, quality of life issues, as well as the risks and benefits of the therapeutic options, become more critical. Cytomorphologic examination alone provides only limited sensitivity for the detection of metastatic carcinoma cells in many cases of serous effusions. Early diagnosis and management of peritoneal metastases from cancer patients represent new directions of researches.

Method: The current study was aimed at differentiating peritoneal liquids encountered in 81 available cases, chosen to show both biochemical patterns (benign and malignant) and in this way to achieve a diagnostic value of the biochemical method. A panel of 17 biochemical markers (TP, ALB, LDH, TC, GL, TL, TG, AA, ALP, U, TB, DB, AST, ALT, Mg, Fe, K) were determined from the resulted supernatant after centrifugation in blood and peritoneal fluid using automatic and semi-automatic biochemistry analyzer.

Results: Thus, of all measured parameters, the highest accuracy in the differential diagnosis between malignant and the benign cases (cirrhosis) was obtained by measuring

peritoneal effusions TC (90%), peritoneal fluid LDH (85.36%) and SAAG (85%).
Conclusion: It is concluded that a suitably chosen panel, consisting of the best specific markers found, can be of great value for the initial differentiation and subsequent guidance in the diagnosis. Abbreviations: *TP* total proteins, *ALB* albumin, *LDH* lactate dehydrogenase, *TC* total cholesterol, *GL* glucose, *TL* total lipids, *TG* trglycerides, *AA* alpha amylase, *ALP* alkaline phosphatase, *U* urea, *TB* total bilirubin, *DB* direct bilirubin, *AST* aspartate aminotransferase, *ALT* alanine aminotransferase, *Mg* magnesium, *Fe* iron, *K* potassium, *PE/S* effusions/serum ratio, *SAAG* serum-ascitic albumin gradient, *SAG* serum-effusion gradient.

Thursday, 2 September 2010, Basement

PS-11 Poster Session Endocrine Pathology

0213
Hyalinizing trabecular tumor of the thyroid mimicking papillary thyroid carcinoma
A. Borda, A. Loghin, A. Boila, K. Branzaniuc, T. Mezei, N. Berger*
*University of Medicine, Dept. of Histology, Tirgu Mures, Romania

Objective: Hyalinizing trabecular tumor (HTT) is an unusual type of thyroid follicular neoplasm that may represent a major diagnostic problem in routine thyroid practice.
Method: We present the case of a 31-year-old woman in which a fine needle aspiration (FNA) was performed for a 2.2-cm unique nodule, incidentally discovered in the left thyroid lobe. A hemi-thyroidectomy was performed as the aspiration specimen was reported suspicious for papillary thyroid carcinoma (PTC). Macroscopically, the nodule was light tan and well circumscribed. In microscopy, it had prominent trabecular architecture and cytological features strongly suggesting a PTC: nuclear enlargement with particularly abundant nuclear grooves and cytoplasmic invaginations. An intratrabecular abundant, homogenous and eosinophilic hyaline material was also noticed. Immunohistochemistry, including anti-thyroglobulin, anti-TTF1, anti-HBEM1, anti-CK19 and anti-MIB1 antibodies, was performed.
Results: The tumor cells were strongly positive for thyroglobulin and TTF1 and were negative for HBEM1, CK-19 and chromogranin. A characteristic membranous and peripheral cytoplasmic staining was noticed with MIB1 antibody.
Conclusion: Despite the cytological aspect, a diagnosis of HTT was made based on the well-circumscribed character of the tumor and the negativity for HBEM1 and CK-19. Moreover, the unique reactive pattern of MIB1 was an important clue to the diagnosis. Careful evaluation is needed in such cases in which cytological criteria are too obviously suggesting a PTC. The differential diagnosis is essential because unlike PTC, HTT is considered a benign tumor and has a different behavior and therapeutic approach.

0214
Fine needle aspiration is a reliable method in the preoperative evaluation of thyroid nodules
A. Borda, A. Loghin, T. Mezei, K. Branzaniuc, R. Catana, C. Moldovan, N. Berger*
*University of Medicine, Dept. of Histology, Tirgu Mures, Romania

Objective: Thyroid nodules are a common clinical problem and the fine needle aspiration (FNA) has become a standard procedure for their clinical triage. Its widespread use allows a better selection of patients in need of surgical treatment.
Method: Four thousand three hundred fifty-nine FNA were performed between 1998 and 2008, always by the same pathologist using a 27-gauge needle and a Cameco suction device. At least three aspirations were carried out, and three to five slides were obtained for each nodule. They were immediately fixed in alcohol and stained with hematoxylin–eosin or with Papanicolaou. The cytological diagnosis was classified in four categories: inadequate, benign, suspicious and malignant. Six hundred thirty-eight cases had a histological follow-up. The benefits of the cytologic diagnosis were estimated by statistical analysis (EpiInfo software version 3.4.3).
Results: The sensitivity of FNA was 79.22% and the specificity 91.54%. There were 3.46% false negative and 17.71% false positive findings. The P value was <0.0001, considered extremely significant. The main causes of diagnostic errors were sampling errors, similar cytological features for different entities, failure to recognize the follicular variant of papillary carcinoma, and coexistence of non-neoplastic and neoplastic processes in the same gland.
Conclusion: Although the sensitivity and the sensibility does not attain 100%, FNA proves to be the most reliable and cost-effective method for distinguishing benign from suspicious or malignant thyroid lesions. Limitations of the method included false negative, non-diagnostic and indeterminate or "suspicious" results. Nevertheless, the routine use of FNA reduces the rate of unnecessary surgery for thyroid nodules.

0215

Mixed medullary and papillary carcinoma of the thyroid gland. Case report

D. G. Ciobanu Apostol, M. Danciu, D. Ferariu, C. Preda, C. Vulpoi, C. Cristea, R. Danila, A. Grigorovici, M. S. Mihailovici, V. Mogos*
*UMF Gr T Popa Iasi, Dept. of Pathology, Romania

Objective: Medullary (MTC) and papillary thyroid carcinoma (PTC) have always been considered different from each other, in their cell origin, histopathological features and incidence. We describe one rare case with simultaneous multicentric PTC, classic or oncocytic type, in one lobe and "composite thyroid carcinoma" with mixed features of MTC and PTC in the other one. These tumors were associated with Graves' disease.
Method: Surgical specimens were routinely processed, paraffin-embedded, and HE-, van Gieson- and Grimelius-stained. Immunohistochemical study included antibodies anti-cytokeratin 7 (CK7), chromograninA (CgA), thyroglobulin (TG), calcitonin (CT), and HBME1.
Results: In the right lobe, there were two, tan brown, nodular lesions measuring 1.5 and 0.7 cm, respectively, consisting of PTC oncocytic type with follicular and focal papillary pattern and a classic variant of PTC. In the lower pole of the left lobe, a grayish nodule of 0.6 cm, with trabecular, follicular and focal papillar architecture was detected, presenting small tumor cells, pleomorphic nuclei and occasional cytoplasmic pseudoinclusions. Tumor cells showed intense positive expression for TG, CK7 and moderate reactivity for CgA and CT. HBME1 was focally positive with membrane staining along lateral and abluminal surfaces.
Conclusion: Our case report emphasizes the role of detailed histopathological analysis, especially when thyroid nodules harbor various aspects, and the use of immunohistochemistry in the identification of rare types of thyroidian neoplasm. This case might be explained by the possibility of activating a common tumorigenic pathway for both follicular and parafollicular thyroid cells or a common stem cell.

0216

Thyroid metastasis of clear cell renal cell carcinoma: a series of three cases

*L. Bejan**
*Emergency County Hospital, Dept. of Pathology, Târgu Mures, Romania

Objective: Thyroid metastases are extremely rare, the kidney being the most frequent primary tumor site.
Method: We report three cases of thyroid metastasis of clear cell renal cell carcinoma (CC-RCC), one of them being the primary manifestation of a renal tumor and the other two with a previous 9- and 10-year, respectively, history of renal neoplasm. The first case, a 64-year-old man, was admitted to the hospital with an initial diagnosis of bilateral goiter, while for the other two, a 72-year-old man and an 80-year-old woman, the discovery was incidental.
Results: On gross examination, white grayish ill-circumscribed solid nodules were described in the right lobe (one nodule, first case), in the left lobe (two nodules, second case) and in both lobes (multiple nodules, third case). All three cases presented similar microscopic tumoral aspects: a solid architecture, polygonal cells with abundant clear or eosinophilic cytoplasm, distinct cell borders and moderately enlarged nuclei with proeminent nucleoli. Since the microscopic aspect did not correspond to any primary tumor of the thyroid, immunohistochemistry was performed. In all cases, the tumor cells stained positive for CD10 and negative for thyroglobulin, supporting the diagnosis of a thyroid metastasis of CC-RCC.
Conclusion: Thyroid metastases of CC-RCC are uncommon and may represent the first sign of a yet undiagnosed asymptomatic renal tumor or a metastasis from a tumor surgically removed years before (up to 10 years). In setting a correct diagnosis, immunohistochemical studies together with the medical history are extremely important.

0221

Primary angiosarcoma of the thyroid gland. A case report

*K. Bednarek-Rajewska**
*Poznan, Poland

Objective: Primary angiosarcoma of the thyroid is a rare and controversial entity most commonly seen in patients from the Alpine regions with a long-standing history of colloid goiter. Purpose: We describe a case of primary, poorly differentiated angiosarcoma in a 57-year-old male who presented with a rapidly enlarging thyroid mass and mild dysphagia during the preceding month.
Method: A CT scan of the neck revealed a large tumor mass in the upper pole of the left lobe of the thyroid measuring 6.5×5.5×7 cm extending into the surrounding adipose tissue and infiltrating the left internal jugular vein. Lymphadenopathy was identified in the left submandibular region and lower neck. Cytomorphologically, the aspirate was cellular, with variably cohesive clusters of atypical spindle cells and necrotic masses. Thyreoidectomy procedure was performed. Histologically, the tumor was composed of spindle, polygonal and epithelioid cells with vesicular nuclei and prominent nucleoli growing in solid sheets and occasionally forming cleft-like vascular spaces

filled with erythrocytes. Extensive necrosis was present. Mitotic activity was 28 mitoses/10 HPF. Immunohistochemical stains showed tumor positivity for CD31, vimentin, factor VIII, WT-1, M-ACT and CD99.
Conclusion: The prognosis in primary angiosarcoma of thyroid is generally poor especially if the tumor penetrates the capsule of the thyroid or if there are metastases present. The patient developed further metastases in the cervical lymph nodes within few weeks after thyroidectomy despite radio- and chemotherapy. Due to the rapid progression of the disease, the patient was scheduled for palliative radiotherapy. The patient succumbed to the disease 14 months after diagnosis.

0223

A histological and immunohistochemical analysis of 39 cases of adrenal pheochromocytoma

M.-S. Mihailovici, L. D. Ivan, M. Danciu, L. Marin, D. G. Ciobanu Apostol, C. Ungureanu, E. Morosan*
*Gr T Popa UMF Iasi, Dept. of Pathology, Romania

Objective: Pheochromocytoma can be defined as a paraganglioma of the adrenal medulla and has been called the "10% tumor" because approximately 10% are bilateral, 10% are extra-adrenal, 10% occur in children, and 10% are malignant. Aim: In this report, we described the histopathological aspects of pheochromocytoma in correlation with immunohistochemical reaction.
Method: The study group included 39 cases of pheocromocytoma diagnosed by the chromaffin reaction, HE and van Gieson's reaction. Immunohistochemistry included monoclonal antibodies: chromogranin A, neuron-specific enolase and S100 protein.
Results: The 39 patients have encapsulated, usually soft, and, on section, yellowish-white to reddish-brown tumors. The larger tumors had areas of necrosis, hemorrhage and cyst formation. Histopathologically, the tumor cells are characteristically arranged in well-defined nests (zellballen) bound by a delicate fibrovascular stroma, which may contain amyloid. The cells vary considerably in size and have a finely granular basophilic or amphiphilic cytoplasm. The nuclei, usually round or oval with prominent nucleoli, may contain inclusion-like structures. Lipid accumulation may develop in the cytoplasm and lead to confusion with adrenal cortical tumors. Giant, hyperchromatic nuclei are common and are not an expression of malignancy. Chromogranin A and NSE were positive. Sustentacular cells form a peripheral coat around the "zellballen" and were strongly reactive for S100 protein.
Conclusion: All our cases were benign, although 10% of pheochromocytomas are malignant and have a marked tendency to metastasize to skeletal system, particularly the ribs and spine. The sustentacular cells are more numerous in pheochromocytomas associated with MEN than in sporadic cases.

0225

Primary carcinoid tumor of gallbladder

C. Comingle, Ü. Sekmen, G. Altaca, B. Bilezikçi*
*Baskent University, Faculty of Medicine, Istanbul, Turkey

Objective: Primary carcinoid tumor of gallbladder is a rare neoplasm. They usually present as a polypoid lesion.
Method: We report an incidentally found carcinoid tumor of gallbladder located in the cystic duct occurring in a 79-year-old male patient detected in cholecystectomy material.
Results: Histopathologically, in cystic duct, an incidental neoplasm measuring 2 mms in maximum diameter was detected, which was grossly unremarkable. The tumor constituted glandular structures. It was not invading muscular layer. Immunohistochemically tumor was positive for synaptophysin. Patient is alive and well after 8 months.
Conclusion: Definite diagnosis of carcinoid tumor of gallbladder is usually made on histopathological examination after surgery. Our case is unique in that it was found incidentally, which was grossly unremarkable. It seems so that surgery alone is a reliable definite management for these small carcinoid tumors.

Thursday, 2 September 2010, Basement

PS-12 Poster Session Molecular Pathology

0226

KRAS genotyping on formalin-fixed, paraffin-embedded (FFEP) colorectal cancer tissue in diagnostic routine: comparison of methods

M. L. Caruso, A. Cavallini, A. M. Valentini, D. Campanella, R. Armentano, M. Pirrelli*
*IRCCS, Pathologic Anatomy, Castellana Grotte, Italy

Objective: Accurate identification of KRAS mutations has great importance for target therapy. Reproducibility and cheapness of different methods are crucial to be safely applied in colorectal routine diagnostic setting.
Method: One hundred twelve FFEP specimens, previously studied by ARMS/Scorpions real-time PCR (Therascreen, Roche, Italy) designed as reference method, were in parallel analysed by other two methods: restriction fragment length polymorphism-PCR (Ampli-set-K-Ras, Bird, Italy) and PCR/reverse hybridization tests (K-Ras

StripAssay, ViennaLab, Austria), respectively, called methods A and B. The methods were compared considering the results, costs, and working times. Regarding KRAS genotype, 112 selected samples were: 40 wild type (wt), 40 mutated in codon 12, and 32 in codon 13.
Results: Six of 40 wt samples showed mutation on codon 12: Three were false positives of method A and three of method B. Two of 40 samples mutated in codon 12 resulted also positive on codon 13 by method B. Since method A is based on cleavage action of the restriction enzyme, we have increased both restriction enzyme concentration and digestion time, abolishing the false positives. On the contrary, there was no way of acting on method B.
Conclusion: Although method A does not define the codon 12 mutation type and is time-consuming, it leads to the same results of the reference method operating our slight methodological modifications. Method A resulted cheap (45% of the reference kit price), useful and reproducible for routinely KRAS testing in colorectal target therapy. Work was supported by Fondazione Cassa di Risparmio di Puglia, Italy.

0227

Mismatch repair proteins expression and BRAF V600E mutation analysis in a subset of CCR patients under 50 years

J. P. Flores Gutierrez, A. Luevano Gonzalez, A. Quintanilla Guzman, N. Vilches Cisneros, O. Barboza Quintana, R. Garza Guajardo, R. Ortiz Lopez, J. Ancer Rodriguez*
*Hospital Universitario UANL, Dept. of Anatomic Pathology, Monterrey, Mexico

Objective: Colorectal carcinoma (CRC) is a worldwide common malignancy; young patients represent a third of all cases, with a rise over the last years. Fifteen percent of CRC have microsatellite instability (MSI) due to alterations in mismatch repair (MMR) genes. Familiar MSI cases (5%) have germline mutations. Sporadic MSI CRC (15%) have hypermetilated MLH-1 promoter. BRAF V600E mutation exclusively occurs in sporadic MSI CRC. Immunohistochemistry detects MSI cases with high concordance with microsatellite analysis. The objective was to compare histopathology and patterns of expression of MMR proteins and BRAF V600E mutation in patients below and over 50 years old and determine if age is a risk factor for defective MMR protein expression and BRAF mutations.
Method: One hundred six patients <50 years were retrieved. Age, sex, location, histologic type, TNM, infiltration and metastatic lymph nodes data were collected. MLH1 and MSH2 immunohistochemistry and BRAF RT-PCR mutation was performed in 48 <50 years and 48 patients >50 years as control group. Student's t, χ^2 and logistic regression analysis were carried out.
Results: Medullary and mucinous types were more frequent among young patients and intestinal type in older patients ($p=0.0008$). No differences were noticed regarding clinicopathological stages between groups. MMRP expression was absent more frequently in <50 and MSH2 was negative in 13.8% of these patients. No BRAF mutations were detected in any group.
Conclusion: We found an association between young age and defective MMR expression (OR 4.28). MSH2 lack of expression is more frequently due to a germline mutation. The fact that none of our patients had BRAF mutation could be partly due to the small sample size or alternate V600E or K-ras mutations.

0228

VEGFA amplification correlates with adverse outcome in colorectal cancer

T. Vlajnic, I. Zlobec, E. Karamitopoulou, M. Bihl, L. Tornillo, S. Schneider, A. Lugli, L. Terracciano*
*Basel, Switzerland

Objective: Angiogenesis plays an important role in the progression of colorectal cancer (CRC). Evidence from preclinical and clinical studies indicates that vascular endothelial growth factor (VEGFA) is the predominant angiogenic factor in CRC. VEGFA is expressed in approximately 50% of CRCs, with minimal to no expression in normal colonic mucosa. Therefore, the aim of this study was to analyze the prognostic impact of VEGFA amplification in CRC.
Method: VEGFA gene amplification was evaluated in a large series of sporadic CRC resections ($n=1,280$) by FISH analysis using the tissue microarray technique. Spectrum Green-labeled probes originated from the FISH Clone RP1-261G23 were used together with Spectrum Orange-labeled probes for the respective centromere 6 as a reference. The VEGFA amplification status was compared to relevant clinicopathological features.
Results: VEGFA amplification was detected in 39 patients (3%) and was significantly associated with higher T stage and higher tumor grade, presence of vascular invasion, right-sided location ($p<0.001$) and B-RAF mutation ($p=0.015$). Additionally, VEGF amplification was associated with worse survival in univariate ($p<0.001$) and multivariable analysis ($p<0.001$; HR (95% CI), 2.06 (1.4–3.0)).
Conclusion: VEGFA amplification seems to highlight a small subset of CRCs with aggressive phenotype. Therefore, FISH analysis of VEGFA could represent an alternative evaluation system for identifying patients with poorer

clinical outcome who could be candidates for anti-VEGFA therapies.

0229

K-RAS and B-RAF mutation detection in routine diagnostic analysis of colorectal cancer in the Greek population

A. Saetta, A. Stamatelli, E. Palliou, A. Tserga, P. Tsiorva, G. Levidou, S. Stratigoula, K. Penelope, N. Kavantzas, N. V. Michalopoulos, E. Patsouris*
*University of Athens, 1st Dept. of Pathology, Greece

Objective: K-Ras oncogene is frequently mutated in colorectal cancer and is currently established as a predictive biomarker for anti-EGFR targeted therapy. B-Raf is a serine/threonine kinase of the RAS/RAF/MEK /ERK signal transduction pathway which is mutated in a subset of K-Ras wild-type patients with colorectal cancer. The aim of this study was to examine the mutational status of K-Ras and B-Raf genes in correlation with tumor clinicopathological characteristics.
Method: DNA was extracted from microdissected formalin-fixed paraffin-embedded tissues. Three hundred forty-four cases were screened for K-Ras and B-Raf mutations at codons 12 and 13 and exon 15 respectively using high-resolution melting analysis, sequencing and/or pyrosequencing. Statistical analysis was performed using STATA for Windows.
Results: K-Ras mutations in codons 12 and 13 were present in 133 out of 344 cases. The most frequent types of mutation were pG12D and pG12V at codon 12 and pG13D at codon 13. B-Raf mutations in exon 15 (pV600E) were present in 4.6% of analyzed samples. B-Raf mutations were observed in a marginally higher frequency in women, whereas K-Ras mutations were positively correlated with patients' age. Moreover, there was a higher prevalence of B-Raf mutations in low-grade carcinomas ($p=0.005$).
Conclusion: The detected mutation frequency as well as the prevalence of specific mutation types is in accordance with previous studies. The observed correlation of B-Raf mutation with tumor grade implies its importance as a marker of tumor aggressiveness. The applied methods (HRM and pyrosequencing) were proven to be sensitive, fast and accurate for mutation detection in a clinical setting.

0230

Mutational analysis of PIK3CA and AKT1 genes in Greek patients with urothelial bladder carcinoma

A. Saetta, N. Prekete, M. Karlou, G. Levidou, P. Korkolopoulou, P. Pavlopoulos, M. Nikolaos, P. Efstratios*
*University of Athens, 1st Dept. of Pathology, Greece

Objective: Aberrant activation of the phosphatidylinositol-3-kinase (PI3 kinase)-AKT pathway is frequently observed in a wide range of cancers such as breast, colorectal, ovarian and lung. Several components of this pathway such as PI3K and AKT can constitute potential therapeutic targets, and many small molecule inhibitors are in development on early clinical trials. The aim of this study was to examine the possible significance of somatic point mutations in PIK3CA and AKT1 genes as biological markers or therapeutic targets in primary urothelial bladder carcinoma.
Method: One hundred twenty-two urinary bladder cancer specimens were screened for activating mutations in exons 9, 20 of the PIK3CA gene as well as in exon 4 of AKT1 gene by PCR-SSCP and high-resolution melting analysis. Mutations were identified for PIK3CA gene with sequencing and for AKT1 gene with pyrosequencing and statistical analysis was performed.
Results: Four different mutations were detected in exon 20 of PIK3CA gene (3.3%). The mutations were identified as p.A1035T, p.A1046V, p.H1047R and p.G1049R. One out of 120 cases was mutant in exon 9 of PIK3CA gene (0.8%, p.E542K). The AKT1 p.E17K mutation was identified in 2 out of 105 bladder tumours (1.9%). Statistical analysis did not reveal any correlation with clinicopathological parameters ($p>0.10$).
Conclusion: Mutations in PIK3CA gene are quite frequently observed in bladder cancer, implying their importance as potential targets for anticancer treatment. On the other hand, mutations in AKT1 gene are not a common event in this type of cancer.

0231

Analysis of DNA integrity, morphology, antigenicity with different preservation methods in brain tissue

A. Saetta, G. Agrogiannis, P. Korkolopoulou, A. Gavriil, N. Kavantzas, E. Patsouris, E. Michalitsi, A. Stamatelli, N. Prekete, E. Palliou*
*University of Athens, 1st Dept. of Pathology, Greece

Objective: Due to the potential carcinogenicity of formaldehyde, its replacement by substitute fixatives is recommended and could increase the possibility for application of molecular biology approaches. The aim of this study was to examine DNA preservation, morphology and antigenicity of brain tissues after fixation with a formalin-free fixative in comparison with formalin-fixed tissues as well as frozen ones.
Method: Calibrated specimens from six different areas (frontal, parietal, occipital lobes, hippocampus, cerebellum and basal ganglia) of 20 brains from elderly individuals (age > 70) were fixed for 24 h in two different fixatives (formalin, formalin-free fixative-RCL2) at room tempera-

ture. Tissues were stained with hematoxylin–eosin for histological examination and their antigenicity was determined by immunohistochemistry. The integrity of DNA extracted from the samples with formalin fixation or formalin-free fixation was compared with that of cryosections with gel electrophoresis and the Bioanalyzer. Furthermore, PCR-PFLPs and real-time PCR (high-resolution melting analysis) were performed in order to assess the suitability of the extracted DNA for downstream molecular pathological applications.

Results: Immunohistochemistry with antibodies against b-amyloid and tau did not reveal any significant differences in reactivity for both fixatives. On the other hand, DNA extracted from frozen samples was of comparable integrity with that from formalin-free fixation. Amplification efficiency for short DNA fragments (140–240 bp) was similar between all preservation methods; however, long fragments (854 bp) could not be amplified from formalin-fixed tissues.

Conclusion: The formalin substitute fixative used in this study provided good histopathological quality, and also the extracted DNA performed better at the subsequent molecular biological procedures.

0232

Mutational analysis of K-ras, B-raf, EGFR, PIK3CA, AKT-1 gene and pERK expression in carcinogenesis of esophagus

A. Saetta, K. Tasioudi, S. Sakellariou, G. Levidou, N. Michalopoulos, T. Dimitrios, N. Prekete, I. Thymara, P. Korkolopoulou, E. Patsouris*
*University of Athens, 1st Dept. of Pathology, Greece

Objective: The molecular mechanisms underlying the development of esophageal cancer remain elusive. The aim of this study was to examine the simultaneous presence of alterations in two main signal transduction pathways, Ras/Raf/MEK/ERK and PI3K/AKT, which are implicated in carcinogenesis. The prognostic significance of pERK expression was also investigated.

Method: Genomic DNA was extracted from 32 paraffin-embedded tissue blocks (9 squamous-cell, 2 adenosquamous cell and 21 adenocarcinomas). Additionally, in 15 cases, tumor cells were collected using laser microdissection in order to minimize contamination with stromal and normal cells. We searched for somatic mutations in K-ras, B-raf, EGFR, AKT-1 and PIK3CA genes by performing high-resolution analysis and pyrosequencing. The expression of activated ERK protein was assessed by immunohistochemistry.

Results: K-ras mutation at codon 12 was detected in one laser-microdissected adenocarcinoma out of 32 specimens (3%), whereas no mutations were found in exon 15 of B-raf gene, in exons 19 and 21 of EGFR gene, in exon 4 of AKT-1 gene and in exon 20 of PIK3CA gene. pERK nuclear expression was positively correlated with disease grade and stage and nuclear staining intensity with grade. Furthermore, pERK cytoplasmic immunopositivity was correlated with tumor grade.

Conclusion: Mutations in K-ras gene are not frequently detected in esophageal cancer, but do exist. The lack of mutations in B-raf, EGFR, AKT-1 genes implies that these may not play an important role in the pathogenesis of esophageal cancer. The correlation of pERK nuclear expression with stage and grade implicates pERK as a marker of local tumor aggressiveness.

0233

Comparison of three methods for "KRAS" mutation testing in patients with metastatic colorectal cancer

A. Vasikova, D. Dvorakova, L. Ostrizkova, D. Brancikova, Z. Pavlovsky, J. Kyclova, J. Mayer*
*AMIS Travel Agency, Prague, Czech Republic

Objective: Mutation analysis in RAS/RAF signaling pathway plays a key role in treatment decision in patients with metastatic colorectal cancer (mCRC). At this time, several methods are available for *KRAS* mutation detection; there are also commercially available kits, but validated methods and standardized testing procedures are still lacking.

Method: Genomic DNA was extracted from formalin-fixed paraffin-embedded (FFPE) tumor tissues after the evaluation of material by pathologists. For mutation analysis of *KRAS* gene, we used three methods: direct sequencing, allelic discrimination and high-resolution melting (HRM).

Results: We tested 21 tumor samples (primary tumors and metastasis) from 15 patients with mCRC. We identified *KRAS* mutation in 5 of 15 (33%) patients using allelic discrimination, while HRM detected mutations in 6 of 15 (40%) patients. Due to low burden of tumor cells in two cases and limited sensitivity of sequencing, only 13 patients were evaluated by this method. Out of them, four (31%) patients showed positivity. We performed sensitivity testing: allelic discrimination (5% of mutant DNA), HRM (10%) and sequencing (25%).

Conclusion: Allelic discrimination is a convenient, fast and sensitive method designed for the detection of specific mutations. Test costs are proportional to the number of tested mutations since a specific assay has to be used for each mutation. Sequencing has a limited application due to low sensitivity, while HRM represents a sensitive, rapid and cost-limited methodology, but displays higher rate of false positive results if DNA is in poor quality. This technique is suitable for routine screening; however, precise identification of mutations is not possible. Therefore, a combination of at least two methods is highly recommended.

0234

O6-methyguanine-DNA methyltransferase evaluated by immunohistochemistry: best practice for clinical and research assessment

J. Cirullo-Neto, K. Carvalho, L. Kagohara, E. Olivieri, D. M. Carraro, I. W. Cunha, J. Vassallo, F. A. Soares, R. M. Rocha*
*Hospital do Cancer, Campinas-Sp, Brazil

Objective: MGMT repairs DNA damages and act as a tumor suppressor gene in normal cells, preventing DNA mutation. Several different approaches for MGMT immunohistochemical (IHC) testing have been used, resulting in a not universally accepted standard. We evaluated the IHC expression of MGMT using five different primary antibodies in 59 invasive breast carcinomas in order to establish the most reliable marker for this protein. The results of immunostaining were compared to qRT-PCR, used as a parameter of reliability of gene expression.
Method: Cases were randomly selected to build a tissue microarray. The five primary antibodies to MGMT were provided by: MT3.1 (NeoMarkers, GeneTex and Santa Cruz), SPM287 (Santa Cruz) and MT23.2 (Zymed). Heat-induced antigen retrieval in citrate and the Advance™ (Dako) detection system were used. IHC was visually analyzed by microscope and automated analyzed by software applied to digital slides. qRT-PCR was performed in all tumors for transcript expression quantification.
Results: Antibody SPM287 (Santa Cruz) showed the highest sensitivity ($p<0.001$), and antibody MT3.1 (Santa Cruz) showed the least sensitivity ($p<0.001$). Antibody MT23.2 (Zymed) showed higher levels of cytoplasm staining, which was not observed in the other antibodies tested ($p<0.001$). qRT-PCR results showed that 94.9% of the samples showed hypoexpression of MGMT when compared to normal breast ($p<0.001$). SPM287 (Santa Cruz) was the only antibody which showed a positive and significant correlation with the results obtained by qRT-PCR ($p=0.027$).
Conclusion: This antibody seems to be reliable and effective for research and clinical practice in breast cancer. (Supported by FAPESP and CNPq).

0235

O6-methyguanine-DNA methyltransferase evaluated by immunohistochemistry: best practice for clinical and research assessment

J. Cirullo-Neto, K. Carvalho, E. Olivieri, D. Carraro, L. Kagohara, I. Cunha, J. Vassallo, F. Soares, R. Rocha*
*Cancer Hospital A C Camargo, São Paulo, Brazil

Objective: MGMT repairs DNA damages and act as a tumor suppressor gene in normal cells, preventing DNA mutation. Several different methods for MGMT immunohistochemical (IHC) testing have been used, resulting in no universally accepted standard. We evaluated the IHC expression of MGMT of five different primary antibodies in invasive breast carcinomas.
Method: Fifty-nine breast carcinomas were randomly selected for a TMA construction. Five different primary antibodies against MGMT were used for the IHC study: clone MT3.1 (NeoMarkers, GeneTex and Santa Cruz), SPM287 (Santa Cruz) and MT23.2 (Zymed). Heat-induced antigen retrieval in citrate and Advance™ IHC detection system were used. IHC was visually analyzed by microscope and automated analyzed by software applied to digital slides. qRT-PCR was performed in all tumors for transcript expression quantification.
Results: Antibody SPM287 (Santa Cruz) showed the highest sensitivity ($p<0.001$), and antibody MT3.1 (Santa Cruz) showed the least sensitivity ($p<0.001$). Antibody MT23.2 (Zymed) showed higher levels of cytoplasm staining, which was not observed in the other antibodies tested ($p<0.001$). Fifty-nine samples (94.9%) showed hypoexpression of MGMT when compared to normal breast evaluated by qRT-PCR ($p<0.001$). SPM287 (Santa Cruz) was the only antibody which showed a positive and significant correlation with the results obtained from qRT-PCR ($p=0.027$).
Conclusion: Antibody SPM 287 (Santa Cruz) presented to be the most sensitive and specific antibody for the IHC evaluation of MGMT. This antibody seems to be of reliable and effective use for research and clinical practice in breast cancer.

0239

MGMT as a potential prognostic marker in breast cancer

J. Cirullo-Neto, K. Carvalho, L. Kagohara, E. Olivieri, D. Carraro, I. Cunha, J. Vassallo, F. Soares, R. Rocha*
*Cancer Hospital A C Camargo, São Paulo, Brazil

Objective: MGMT repairs DNA damages, via alkylation, by removing a methyl group from the O6 position of guanine. It acts as tumor suppressor gene in normal cells and prevents DNA mutation. We evaluated MGMT expression in breast tumors, correlating it with other prognostic factors.
Method: Sixty-four cases of invasive breast carcinomas were randomly selected for a TMA construction. Immunohistochemistry (IHC) was performed for MGMT and also for ER, PR, HER2, Ki67, p53, p63, E-cadherin, CK5 and CK14 for luminal and basal phenotype classification. IHC was evaluated following the guidelines for each marker most recommended in the literature. Fluorescent in situ

hybridization (FISH) was performed in those cases considered 2+ in order to assess HER2 gene amplification status. qRT-PCR was performed in frozen tissue from our tumor bank for all cases in order to evaluate mRNA expression of MGMT.
Results: Fourteen cases were triple-negative (21.8%), and among those, seven cases were basal-like carcinomas (10.9%). Twenty-five cases (39%) were luminal-like type A, four cases were (6.25%) luminal-like type B, and one case (1.5%) was HER2-like type. MGMT showed significant lower expression in the basal-like tumors when compared to the luminal-like ones (p=0.007). Basal-like phenotype tumors presented higher positivity for p53 and Ki67 than the luminal types (p=0.025 and p=0.003, respectively). Positive p53 and high Ki67 tumors showed significant lower expression of MGMT (p=0.0184 and p=0.0081, respectively).
Conclusion: MGMT assessment by IHC or molecular biology techniques may represent an important prognostic factor in breast cancer.

0240

Anticol11a1 a marker of infiltration in bronchioloalveolar lung carcinoma

N. Fuentes, C. G. Pravia, P. M. Rodriguez, J. R. De los Toyos, M. G. Ocaña, J. Del Amo, L. Simón, L. Barneo, M. Fresno*
*Hospital Universitario Oviedo, Spain

Objective: The col11A1 gene codifies a protein expressed during cartilage and osteomorphogenesis which is present in the setting of several types of infiltrating malignant desmoplasia. Our team generated a monoclonal antibody against procol1A1 which was tested for infiltrating ductal pancreatic carcinoma versus chronic pancreatitis differential diagnosis and infiltrating ductal carcinoma of breast versus sclerosing adenosis differential diagnosis.
Method: To investigate its usefulness in order to assess the presence of invasion in bronchioloalveolar lung carcinomas (BAC), we carried out immunostaining with the monoclonal antibody antiCol11A1 in a series of nine BAC and six lung adenocarcinomas with bronchioloalveolar pattern.
Results: The results show lack of staining in seven of nine BAC, whereas all six adenocarcinomas with bronchioloalveolar pattern did stain (significance, p=0.0034).
Conclusion: Our conclusion is that the monoclonal antibody AntiCol11A1 could be a useful marker of invasion in BAC when invasion is doubtful.

0241

PARP-1 Val762Ala polymorphism is associated with reduced risk of non-Hodgkin lymphoma in Korean males

C. Choi, X.-M. Jin, H.-N. Kim, I.-K. Lee, K.-S. Park, H.-J. Kim, J.-S. Choi, S.-W. Juhng*
*Chonnam National University, Dept. of Pathology, Hwasun, Republic of Korea

Objective: Poly(ADP-ribose) polymerase-1 (PARP-1) is a nuclear enzyme that plays a role in DNA repair, differentiation, proliferation, and cell death. The polymorphisms of PARP-1 have been associated with the risk of various carcinomas, including breast, lung, and prostate. We investigated whether PARP-1 polymorphisms are associated with the risk of non-Hodgkin lymphoma (NHL).
Method: Subjects from a Korean population consisting of 573 NHL patients and 721 controls were genotyped for five PARP-1 polymorphisms (Asp81Asp, Ala284Ala, Lys352Lys, IVS13+118A>G, and Val762Ala) using high-resolution melting polymerase chain reaction (PCR) and an automatic sequencer.
Results: None of the five polymorphisms were associated with overall risk for NHL. However, the Val762Ala polymorphism was associated with reduced risk for NHL in males [odds ratio (OR), 0.62; 95% confidence interval (CI), 0.41–0.93 for CC genotype and OR, 0.84; 95% CI, 0.60–1.16 for TC genotype], with a trend toward a gene dose effect (p for trend, 0.02). Asp81Asp (p for trend, 0.04) and Lys352Lys (p for trend, 0.03) polymorphisms revealed the same trend. In an association study of PARP-1 haplotypes, haplotype ACAAC was associated with decreased risk of NHL in males (OR, 0.75; 95% CI, 0.59–0.94).
Conclusion: The present data suggest that Val762Ala, Asp81Asp, and Lys352Lys polymorphisms and the haplotype-ACAAC in PARP-1 are associated with reduced risk of NHL in Korean males.

0242

H2AFX polymorphisms are associated with decreased risk of diffuse large B cell lymphoma in Korean

C. Choi, X. M. Jin, H.-J. Kim, J.-S. Choi, S. W. Juhng*
*Chonnam National University, Dept. of Pathology, Hwasun, Republic of Korea

Objective: H2AFX is a core histone involved in the cellular response to DNA double-strand breaks and nucleosomal organization of chromatin. Its polymorphisms have been associated with the decreased risk of non-Hodgkin

lymphoma (NHL, -417AA) and increased risk of breast cancer (−1654AG/GG and −1420GA/AA).
Method: To investigate the effect of H2AFX polymorphisms on NHL risk in Koreans, six polymorphisms were tested for association in 573 NHL patients and 721 cancer-free controls. The five polymorphisms were located in the promoter region, −1654A/G (rs643788), −1420G/A (rs8551), and −1187T/C (rs7759), −676T/G (rs2509851), and −417G/A (rs2509049). Another one, 1057C/T (rs7350), was in the 3′UTR.
Results: The −1420AA genotype was associated with decreased DLBCL risk (OR, 0.65; 95% CI, 0.43–0.97), and there was a trend for allele dose effect (p trend=0.026). The A allele showed decreased risk when compared with the G allele (OR, 0.81; 95% CI, 0.67–0.98). The −1187CC genotype demonstrated a decreased DLBCL risk with borderline significance (OR, 0.70; 95% CI, 0.48–1.02). And there was a trend for an allele dose effect with borderline significance (p trend=0.06). The T allele revealed an increased risk (OR, 0.84; 95% CI, 0.70–1.00) than the C allele. However, there were no associations between the polymorphisms and the risk of overall NHL, all B cell lymphoma, or all T cell lymphoma, respectively.
Conclusion: The results suggest that H2AFX −1420AA, and −1187CC genotype might be associated with the decreased DLBCL risk in Korean people.

0243
p14ARF–MDM2–p53 immunohistochemical surveillance in retinoblastoma

L. Carvalho, A. Alarcão, C. Fonseca, L. Teixeira, M. J. Aguiar, R. Proença*
*Faculdade de Medicina Coimbra, Dept. de Anatomia Patologica, Portugal

Objective: Retinoblastoma presents between 3 and 18 months in heritable cases and 18 to 24 months in sporadic cases. The heterozygotic Rb^{+}/Rb^{-} requires a single silencing mutation of the heritable functioning Rb allele to subsequent tumor development as pRb capacity to arrest cell cycle in G1 is lost by E2F transcription factor liberty. The immunohistochemical (IHC) expression of p53 and p14ARF together with MDM2 may be a useful way to proximate the potential disruption of p53 suppressor pathway together with the known Rb function as an easy way to explore in routine diagnosis.
Method: Material: A set of 24 FFEPE tumours was collected from HUC, Ophthalmic Pathology Laboratory, Coimbra, as clinical records of age, gender, heritable pattern, Reese–Ellsworth stage and prognosis. Methods: Antibodies against p53, p14 ARF and MDM2 were applied on a representative section of each case and a uniform semiquantitative score was registered (−%, + <25%, ++ 25–70%, +++ >70% cells).
Results: There was general positivity for all antibodies: p53 (21/21), p14ARF (21/24), MDM2 (23/24). All p14ARF-positive cases also expressed p53 and MDM2.
Conclusion: The generalized IHC expression of p53, p14ARF, and MDM2, together with the accelerated malignant evolution of retinoblastoma, stresses the function of p14ARF and MDM2 as genes interfering in the p53 suppressor pathway with aggressive behaviour in the Rb pathway loss and corroborated by p53 wild-type expression as an inefficient control. This study ought to be enlarged in order to understand the real role of the aforementioned genes through their variable crossed pathways.

0244
Cytokine effects on the cell cycle and death of lung and prostate carcinoma cells

V. Galani, M. Kastamoulas, G. Chondrogiannis, G. Vartholomatos, E. Vlachopoulou, D. Arvanitis, T. Liloglou, E. Kolettas, D. Baltogiannis, N. Sofikitis, P. Kanavaros*
*Medical School of Ioannina, Laboratory of Anatomy-Histol., Greece

Objective: Since cytokines are involved in cell cycle/death regulation, we investigated the effects of TNFa, IL1β, IL13, IFNγ, IGF1 and Fas/CD95 on cell cycle/death of A549 lung and LNCAP (androgen-dependent) and PC3 (androgen-independent) prostate carcinoma cell lines.
Method: Flow cytometry (PI and PI/annexin) and Western blot were used for the analysis of cell cycle/death (apoptotic and total cell death) and protein expression, respectively. Cell death was also analyzed by Hoechst and Crystal violet staining.
Results: Flow cytometry showed that (a) the TNFa or IL1β or IL13 anti-cell death effects on Fas induced A549 cell death were attenuated by inhibitors of NFkB (BAY 117082), PI3K (LY 294002), JNK (SP600125), P38 (SB203580) and ERK (UO126) pathways; (b) TNFa or IL1β did not alter Fas-induced cell death in A549 cells with suppression of the canonical (IKKβ) or the non-canonical (IKKα) NFκB pathway; (c) Fas or TNFa increased LNCAP cell death in comparison to control; and (d) TNFa increased Fas-induced LNCAP and PC3 cell death. Western blot showed (a) cleaved PARP1 protein in Fas-treated cells, (b) TRAF1 protein and decreased IkBα protein expression in TNFa treated cells and (c) no alterations of Fas, bcl2, bclxl, bax, bak and bad protein expression.

Conclusion: TNFa, IL1β and IL13 decreased Fas-induced A549 cell death, whereas TNFa increased Fas-induced LNCAP and PC3 cell death. The anti-cell death effects of TNFa, IL1β and IL13 on Fas-induced A549 cell death were mediated, at least partially, by the NFkB, PI3K and MAP kinase pathways.

0245

LGR5 protein expression in human normal and malignant tissue

E. Hinterseer, S. Bastelberger, L. Pradel, J. Beil, B. Alinger, M. Kasper, F. Aberger, M. Eberl, W. Gruber, O. Dietze, C. Kronberger*
*General Hospital and PMU, Salzburg, Austria

Objective: The orphan leucine-rich repeat containing G-protein-coupled receptor LGR5 (GPR49/HG38/FEX) is a novel marker for adult stem cells in small intestine, colon and hair follicles. It is suspected to have a pivotal role in cell proliferation and tumor formation and seems to be a potential therapeutic target. LGR5 expression is poorly investigated and neither its function in stem cells nor during tumor formation is known.
Method: Our aim was to identify a LGR5 antibody with a high specificity among different providers (Epitomics®, MBL®, Sigma®, Biosite®, Abgent®) for screening selected human formalin-fixed and paraffin-embedded (FFPE) tissue samples by automated immunohistochemical staining. For proving antibody specificity, in situ hybridization with a cRNA probe of LGR5 is carried out on the same tissue samples used for immunohistochemistry. As positive control, we generate a LGR5 expressing human keratinocyte cell line (HaCaT) by retroviral transduction.
Results: The LGR5 antibody from Epitomics® stains the outer root sheath of human hair follicle in anagen, whereas Sigma-Aldrich®'s anti-LGR5 antibody recognizes LGR5 in the inner root sheath. Nerve tissue is completely negative using the Epitomics® antibody, but contrarily, the anti-LGR5 antibody from MBL® shows strong staining of Purkinje cells as well as of other nerve cells in the cortex and spinal cord. The Sigma-Aldrich® antibody also shows slight nerval staining, but nuclear. Anti-LGR5 antibodies from Biosite® and Abgent® are all-around negative under the tested conditions.
Conclusion: All antibodies were optimized but the IHC results are quite incoherent; therefore, further investigations need to be done.

0246

The mutational analysis of EGFR, PIK3CA and PTEN genes in neuroblastic tumors

E. Izycka-Swieszewska, M. Brzeskwiniewicz, A. Wozniak, E. Drozynska, W. Grajkowska, T. Klepacka, J. Limon*
*Medical University of Gdansk, Dept. of Pathomorphology, Poland

Objective: Neuroblastoma is one of the most common pediatric solid tumors. Although the signal transduction pathway PIK3/AKT/mTOR is often activated in human cancer, its role and ways of activation in neuroblastoma are not well established.
Method: The aim of the study was to analyse the mutational status of EGFR (exons 18–21), PIK3CA (exons 5, 6, 10 and 21), and PTEN, as well as to assess EGFR copy number. The study was performed on paraffin-embedded tissue sections from 106 cases of neuroblastoma. For mutational analysis, polymerase chain reaction (PCR) was used and then amplified fragments were sequenced directly. Fluorescence in situ (FISH) was used for EGFR copy number evaluation.
Results: In two tumors (2.7%), c.931 A>G (p.I311V) mutation of PIK3CA (exon 5) was found. In addition to this, six polymorphisms in EGFR c.2184+19 G>A, c.2361 G>A and c.2508 C>T, in PIK3CA c.1060-17 C>A and c.1145+54 A>G and in PTEN c.285 A>T were detected. The latter one was not described previously. The most frequent polymorphisms were EGFR c.2631 G>A (73.2%), PI3KCA c.1060-17 C>A (65.6%), and PI3KCA c.1145+54 A>G (59%); however, the incidence is comparable with population frequency in Caucasians. FISH analysis showed no EGFR gene amplification, though polysomy in many cases was observed.
Conclusion: Our results show the low frequency of mutations in genes which are involved in PIK3/AKT/mTOR pathway in neuroblastoma. Study supported by grant from Polish Ministry of Science and Higher Education (N401 176 31/3867).

0248

Metabolic phenotyping of high-grade glioma biopsies

D. Monleon, J. M. Morales, A. Gonzalez Segura, J. Gonzalez Darder, M. Cerda Nicolas, C. Lopez Gines, R. Gil Benso*
*Hospital Clinico Valencia, Fundacion Investigacion, Spain

Objective: Glioblastoma multiforme (GBM) and anaplasic astrocytoma (AA) are astrocytic neoplastic entities of the

central nervous system that appear in adults, with high biological and clinical aggressiveness. Despite the definition of new neoplasm genetic subgroups, the most relevant information in the prognostic of the patient still comes from factors as patient age, localization and size of the tumour, oedema and mass shifting. Metabolic phenotyping may provide new information for a better management of this disease.

Method: We collected molecular profiles based on HRMAS spectra for 31 high-grade glioma biopsies (25 GBM and 6 AAs). The amount of human tumor tissue analyzed for each subject ranged from 20 to 40 mg. All samples were analyzed by post-HRMAS histopathology to assess the tissue integrity and double validate histological diagnosis.

Results: Two major metabolic groups were detected, which included 16 and 11 samples, respectively. Most AAs were located in the same group. The phospholipid patterns and the glutamine/glutamate metabolic relatives seem to be the most relevant contribution to this grouping pattern.

Conclusion: HRMAS provides high-resolution glioma molecular profiles. One of the groups detected, which include most AA samples, seems to reflect a less aggressive type of tumor. Metabolic discrimination between these subgroups includes the levels of some metabolites which can be seen by MRS 'in vivo'.

0249

Mutations in the cystic fibrosis transmembrane regulator gene and relation with IVS8-poliT and Y chromosomal microdeletions

M. Rongioletti, F. Papa, M. B. Majolini, C. Vaccarella, M. Cortesi, G. Bruno, A. Falconio, L. Bonito, V. Panetta, G. M. Liumbruno*

*San Giovanni Calibita Hospital, Rome, Italy

Objective: An association between cystic fibrosis transmembrane regulator (CFTR) gene mutations and infertility has been hypothesized. This study investigated the frequency of the CFTR gene mutation in a group of consecutive candidates for assisted reproductive techniques and the relation between CFTR mutation, IVS8-poliT and Y chromosomal microdeletions.

Method: Four thousand eight hundred forty-nine patients (2,817 females and 2,032 males) were screened for 53 CFTR gene mutations and IVS8-poliT polymorphism by multiplex PCR; 117/2,032 (5.8%) were azoospermic patients (APs) investigated for Y chromosomal deletion by multiplex PCR. Frequencies of mutation were separately calculated and the chi-square test was used for comparisons.

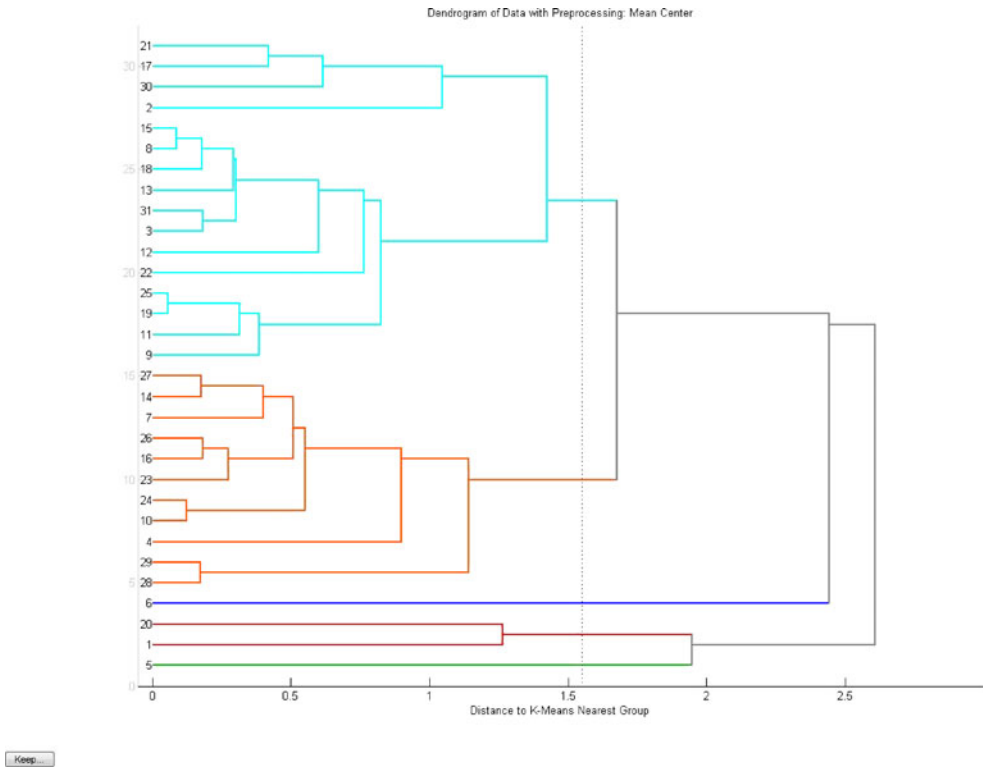

Results: CFTR mutations were detected in 4.2% of the subjects, a percentage similar to that reported in the general population. The most common mutation was ΔF508/N (1.51% of patients); only mutation N1303k/N (0.29%) showed a different gender distribution (0.54% in males and 0.11% in females, $p=0.005$). The IVS8-poly-T showed a frequency of 71.2% for 7T/7T alleles, 19.6% for 7T/9T alleles, and only 0.27% for 5T/5T alleles. One in 117 APs showed a Y chromosomal microdeletion and was negative for CFTR mutation; 4 in 117 APs had CFTR mutation. The following distribution of IVS8-poly-T polymorphism in APs was detected: 5T/5T=0.86%, 9T/9T=0.86%.
Conclusion: Our data show no evidence of associations between azoospermia, CFTR mutation, IVS8-poly-T and Y-chromosomal microdeletions.

0250

From human papillomaviruses and cervical carcinoma to HPV detection

M. Uvirova, J. Dvorackova, D. Konvalinka*
*CGB Laboratory a.s., Dept. of Pathology, Ostrava Vítkovice, Czech Republic

Objective: Human papillomaviruses (HPV) DNA was found in most of cervical carcinomas (85–99.7%) and cervical lesions. HPV are double-stranded DNA viruses, invading mucosal or cutaneous epithelium. More than 100 different types of HPV are already known. Chance for elimination of HPV infection decreases with age: HPV-positive women over 35 years are at higher risk of developing cervical carcinoma. For carcinoma development, the most important is the interaction of E6 and E7 proteins with human p53and pRb proteins, respectively.
Method: High-risk (HR) HPV test was performed by Hybrid Capture® 2 technology (Qiagen). Genotyping of HPV types was done via polymerase chain reaction and reverse hybridization with use of Inno-LiPA technology (Innogenetics). Women with positive diagnosis of gynaecological cytology—ASCUS, LSIL, HSIL—and before vaccination against HPV were tested.
Results: From March 2006 to March 2010, a total of 1,164 patients were tested. Only 291 (25%) were HR HPV DNA-positive, of whom 85 (29.2%) were over 35 years. Case report presents an interesting case of positive Hybrid Capture® 2 test with proven cross-hybridization. Result was confirmed by HPV genotyping with use of Inno-LiPA technology.
Conclusion: The use of the HPV DNA test allows the detection of HPV infection with high sensitivity and specificity. Such result can more efficiently specify unclear outcomes of other screening methods, such as cytology. HPV DNA test has been already incorporated into routine screening within several countries.

0251

HPV prevalence in chronic gastritis

N. Yigit, Z. Kucukodaci, A. Haholu, H. Baloglu*
*GATA Training Hospital, Dept. of Pathology, Istanbul, Turkey

Objective: HPV is one of the best-known etiologic agents for squamous epithelia-related neoplastic lesions including the cervix, larynx and skin. In recent years, some of non-squamous epithelia-driven tumors like stomach, colon and lung adenocarcinomas were reported to be containing HPV. The prevalence of HPV in gastric adenocarcinomas, which is reasonably related to chronic gastritis and gastric intestinal metaplasia, is varied between 15% and 45% in large-scale studies. Regardless of being 'passenger' or 'driver', to show HPV prevalence in chronic gastritis with metaplasia, the well-known two predisposing lesions of gastric cancers was our aim in the present study.
Method: DNA extracted from formalin-fixed paraffin-embedded gastric biopsies of 50 cases was tested for HPV-DNA by PCR assay. Consensus primers were used. The presence of a 140-bp fragment was accepted as HPV positivity.
Results: Eight out of 50 biopsies were found HPV-DNA-positive (16%).
Conclusion: HPV may accompany gastritis and metaplasia. HPV deserves more studies for pre-neoplastic and neoplastic gastric lesions to enlighten the 'passenger–driver' dilemma.

0252

Is p. Asn680Ser polymorphism of follicle stimulating hormone receptor (FSHR) associated with regulation of FSHR gene expression?

G. Zalewski, A. Sulewska, S. Wołczyński, L. Chyczewski*
*Medical University, Bialystok, Poland

Objective: FSHR genetic variability in position 2039 A>G (rs6166, p.Asn680Ser) was shown clinically to correlate with response to controlled ovarian hyperstimulation with gonadotropins. The aim of the study was to correlate rs6166 with the expression of FSHR-dependent genes such as FSHR itself and LHR.
Method: Fourteen consecutive patients undergoing IVF treatment due to idiopathic or male factor-related infertility were recruited. Genotype was determined by AS-PCR. The cells were obtained by ovary puncture and cultured for 7 days to regain responsiveness to FSH in gonadotropin-free medium. Stimulation was carried out in serum-depleted

environment using 0.5 UI/ml rFSH. Total RNA was isolated after 24 h of incubation. Gene expression was accessed by real-time PCR. All analyses were performed in at least two biological replicates.
Results: Distribution of Asn680Ser genotypes was as follows: six homozygotes Asn/Asn, seven heterozygotes Asn/Ser and one homozygote Ser/Ser. Expression of FSHR in all stimulated samples was increased by a mean factor of 2.61 (CI, 0.57–12.88, $p<0.001$). Homozygotes Asn/Asn presented significantly higher ($p=0.03$) rFSH-induced expression of FSHR as compared to carriers of Ser allele with mean fold change of 3.56 (CI, 0.84–16.2) vs 2.22 (CI, 0.67–5.9), respectively. Induced expression of LHR, although significantly upregulated, showed no difference with respect to FSHR genotype.
Conclusion: This is a preliminary report of correlation of FSHR genotypes of rs6166 polymorphism with FSHR mRNA expression. Altered FSH-induced FSHR transcript level is likely to explain different clinical behavior of patients with FSHR gene variants.

0254

The role of adamantinoma of long bones and osteofibrous dysplasia stromal cells in tumour osteolysis

R. Taylor, F. Hemingway, H. Knowles, N. Athanasou*
*Merton College, Oxford, United Kingdom

Objective: Adamantinoma of long bones (ALB) and osteofibrous dysplasia (OFD) are rare, osteolytic primary bone tumours of uncertain origin. To investigate the nature of the proliferating fibroblastic stromal cells in ALB and OFD and to determine cellular mechanisms of osteolysis in these tumours, we carried out cell culture and molecular studies on two cases of ALB and two cases of OFD.
Method: ALB and OFD cells were cultured on coverslips and dentine in the presence and absence of macrophage colony-stimulating factor (MCSF)-primed $CD14^+$ monocytes + MCSF + receptor activator of nuclear factor kappa B ligand (RANKL). Cultures were examined for the osteoclast formation markers tartrate-resistant acid phosphatase (TRAP), CD51 and lacunar resorption. ALB and OFD cells were examined for osteoblast markers (mineralisation nodule formation, alkaline phosphatase).
Results: Few cultured ALB and OFD stromal cells expressed epithelial markers (epithelial membrane antigen [EMA] and cytokeratin). OFD cells expressed osteoblast markers. Cultured ALB and OFD stromal cells showed no ultrastructural evidence of epithelial differentiation. ALB and OFD cells were not capable of lacunar resorption, but co-cultures of ALB or OFD stromal cells and monocytes resulted in the formation of multinucleated $TRAP^+$ and $CD51^+$ cells capable of lacunar resorption.
Conclusion: Our findings indicate that OFD and ALB stromal cells express epithelial and osteoblast markers. These cells support osteoclast formation from mononuclear phagocytes via a RANKL-dependent mechanism, which may contribute towards the aggressive bone destruction associated with this tumour.

Thursday, 2 September 2010, Basement

PS-13 Poster Session Neuropathology

0255

Radiotherapy induced sPNET in a 40-year-old female 11 years after subtotal excision and radiotherapy of oligoastrocytoma: report of a case

P. Czapiewski, J. Dzierzanowski, T. Szmuda, P. Sloniewski, E. Izycka-Swieszewska, W. Biernat*
*Medical University of Gdansk, Dept. of Pathology, Poland

Objective: Supratentorial primitive neuroectodermal tumor (sPNET) is an embryonal tumor usually developing supratentorially in children or young adults and composed of undifferentiated or poorly differentiated neuroepithelial cells. It is a relatively rare tumor in middle-aged people and extremely rarely develops after radiotherapy. We report an extraordinary case of sPNET in a 40-year-old female that developed 11 years after radiotherapy of oligoastrocytoma.
Results: A 40-year-old female was regularly followed after treatment of oligoastrocytoma of the left frontal lobe. The tumor was subtotally resected and treated with radiotherapy 11 years ago. The patient has persistent mild aphasia and mild right hemiparesis. CT performed due to increased incidence of headaches revealed a cystic lesion of the left frontal lobe, 4 cm in diameter, located below the previous tumor. The recurrence of oligoastrocytoma was suspected; however, the diagnosis of sPNET was rendered.
Conclusion: Long survival in patients successfully treated for primary brain tumors may yield in independent treatment-induced primary malignancies of the central nervous system.

0256

Relation between MMP-2, MMP-9 and Ki-67, CD44v6 in human malignant brain tumors. Preliminary study

J. Bar, A. Markowska-Woyciechowska, L. Noga, R. Kwiatek, M. Banas, B. Paradowski, W. Zub*
*Med. Uniwersity Wroclaw, Dept. of Pathomorphology, Wrocbaw, Poland

Objective: The interaction between different proteins plays an important role in the metastatic ability of brain tumor cells. The purpose of this study was to evaluate the expression of MMP-2, MMP-9, CD44v6, and Ki-67 in gliomas of different grades of malignancy and correlate the expression between the studied proteins in tumors.
Method: Expression of MMP-2, MMP-9, CD44v6, Ki-67 was evaluated on 48 formalin-fixed paraffin-embedded tissue blocks divided into: glioblastomas multiforme (n=28), anaplastic astrocytomas (n=11), anaplastic oligodendrogliomas (n=2) and normal brain tissue (n=7) using immunohistochemistry.
Results: MMP-2, MMP-9, CD44v6 and Ki-67 expression was found in 40.6%, 46.8%, 59.3%, 34.3% of gliomas, respectively.MMP-2 immunopositivity was significantly higher in glioblastoma multiforme than anaplastic astrocytomas (P=0.03). No immunoreaction for all proteins was found in normal brain tissues. MMP-2, MMP-9, CD44v6, Ki-67 immunoreactivity was significantly higher in glioblastomas when compared with anaplastic gliomas (P=0.05). In gliomas, the percentage of positive cells and the intensity of the immunostaining were proportional to the degree of malignancy. Positive correlations between Ki-67 and MMP-9 (P=0.002), MMP-2 and MMP-9 (P=0.02), MMP-9 and CD44v6 (P=0.01) were found in malignant brain tumors.
Conclusion: These results suggest that relationship between MMP-2, MMP-9, and MMP-9 and Ki-67 and CD44v6 indicate that expression of both matalloproteinases may facilitate the migration of tumor cells and increase their proliferative activity.

0257

Methylation status of MGMT (O6-methylguanine DNA methyltransferase) promoter in high-grade gliomas

G.-Y. Choe, S.-Y. Moon*
*Seoul National University, Bundang Hospital, Seongnam, Republic of Korea

Objective: Gliomas are most common among primary brain tumors, and glioblastomas (GBL) are most fatal among gliomas. Surgical operation concomitant with chemoradiotherapy is adopted to treat gliomas. Temozolomide (TMZ) is a new oral cytotoxic agent with less myelosuppression. Epigenetic silencing of O6-methylguanine-DNA-methyltransferase (MGMT) by promoter methylation is associated with improved survival in GBL treated with TMZ. In this study, we investigated MGMT promoter methylation in gliomas treated with concomitant chemoradiotherapy (CCRT) following operation.
Method: In 40 cases of gliomas including 31 GBL, six anaplastic astrocytomas (AA) and three anaplastic oligodendrogliomas (AO), formalin-fixed, paraffin-embedded archival samples were used to evaluate the methylation status of MGMT promoter via methylation-specific PCR.
Results: MGMT promoter methylation was detected in 15 cases (37.5%) of gliomas. MGMT promoter methylation was detected in 41.5% of GBL, in 16.7% of AA, and in 33.3% of AO. GBL with methylation had significantly more prolonged overall survival (mean 32.46 months) compared with unmethylated GBL (mean 12.95 months, p=0.012). Methylated GBL also had more prolonged progression-free survival (mean 21.74 months) compared with unmethylated GBL (mean 7.41 months, p=0.068).
Conclusion: The frequency of MGMT promoter methylation in Korean glioma patients was similar to those in Western countries. These data indicate that MGMT promoter methylation is prognostically significant in GBL given CCRT. MGMT promoter methylation status is considered to be a valuable predictive factor in the routine clinic for GBL.

258

Spinal cord glioneuronal tumor with rosetted neurophil islands: case report

N. Comingle, F. Ozkan, A. I. Dogan Ekici, O. Aydin, O. Buge, O. Kilickesmez, U. Ture*
*Yeditepe University, Faculty of Medicine, Istanbul, Turkey

Objective: Three new entities have been recently added to the group of glioneuronal tumors: papillary glioneuronal tumor (PGT), rosetted glioneuronal tumor with neurophil-like islands, and rosette-forming glioneuronal tumor (RGNT) of fourth ventricle. In particular, rosetted glioneuronal tumor with neurophil like islands needs to be distinguished from RGNT and PGT. The lesion currently is considered a variant of astrocytoma, WHO grade II or III.
Method: We present a 14-year-old female patient having been under observation because of scoliosis and urinary incontinence. Radiologically, on MRI, a mass lesion was detected located intramedullary at C5 and T5 and an expansion in spinal canal. Solid component of the mass extends between C7-T3 vertebrae and measures 51×18×22 mm. This solid component of the tumor was heterogeneously hypointense on T1 and heterogeneously hyperintense on T2 images. Surgically, C5, 6, 7 and T1 hemilaminotomy and intradural intramedullary tumor excision were performed. Histopathological examination showed a mixed glioneuronal tumor composed of oligodendrocyte-like cells constituting neurophil-like islands, astrocytic cells and neurons scattered in glial tissue. Immunohistochemically, glial tissue was GFAP-positive and neurophil-like areas and big neurons were synaptophysin-positive. In astrocytic component Ki-67, the proliferation index was below 1%. P53 was negative.

Results: Consequently, the final diagnosis was spinal cord glioneuronal tumor with rosetted neurophil-like islands—WHO grade 2. These cases can be confused with oligodendrogliomas, astrocytomas and ependymomas. Oligodendrogliomas are distinct with their molecular genetic features.
Conclusion: Our case is unique in that it is the youngest reported patient having this tumor located in the spinal cord.

0260

Proliferative activity in all subtypes of the glioblastoma

B. Jarosz, M. Jarosz, R. Rola, T. Trojanowski*
*Lublin, Poland

Objective: Glioblastoma is the most malignant and the most frequent primary brain tumour in adults. It accounts for 60–75% of astrocytic tumours. The tumour has two variants: giant cell glioblastoma and gliosarcoma. The purpose of the study was to show the differences between values of the MIB-1 proliferative indexes of glioblastoma, giant cell glioblastoma and gliosarcoma.
Method: Surgical specimens from 60 patients were formalin-fixed, paraffin-embedded immunostained using MIB-1 antibody. Next, proliferative index (PI) was calculated. Analysis of variance (ANOVA) was used to test the hypothesis that mean values of MIB-1 PI were equal for each diagnosis group.
Results: The mean values of MIB-1 PI were as follows: glioblastoma, 25.7% (14.7–43,7%); giant cell glioblastoma, 21.7% (4.9–39.7%) and gliosarcoma, 27.2% (12.5–46.9%), but there were no statistically significant difference in the MIB-1 PI mean value between diagnostic groups.
Conclusion: We observed that proliferative activity shows regional variation and was the most prominent in glioblastoma with small cells. In giant cell glioblastoma, it was much lower. Because of the absence of significant differences of MIB-1 PIs in our study, in the future, the study will be repeated on 40 cases in each group of that tumour.

0264

The extracellular matrix and diffusion barriers in the focal cortical dysplasias of brain—an immunohistochemical study

J. Zamecnik, L. Vargova, A. Homola, P. Marusic, P. Krsek, K. Kuncova, E. Sykova*
*Charles University, Dept. of Pathology and Mol. M, Prague, Czech Republic

Objective: Changes in the geometry and composition of the extracellular space (ECS) may influence the epileptogenesis in focal cortical dysplasias (FCD) of the brain.
Method: Tissue ECS volume and geometry (the geometrical factor "tortuosity", reflecting various ECS diffusion barriers) were studied in cortical samples of 21 patients surgically treated for epilepsy, including nine patients with FCD type I and of six patients with FCD type II, by real-time iontophoretic method. Consequently, the samples were subjected to immunohistochemical analysis of the composition of the extracellular matrix (ECM) and morphology of the $GFAP^+$ glial cell processes.
Results: In both FCD type I and FCD type II, the tortuosity of the ECS was significantly increased: 1.61±0.01 and 1.69±0.02, respectively; control = 1.46±0.01 (mean ± SEM). The ECS volume fraction was not significantly changed. When compared to controls, no significant changes in ECM composition were noted in FCD type I. However, we observed an increase in $GFAP^+$ glial processes in both types of FCD and pathological accumulation and distribution of some ECM molecules (tenascins C and R, hyaluronate, chondroitin sulphate, reelin) in the ECS of FCD type II.
Conclusion: The ECS of FCD has increased tortuosity, reflecting the increase of diffusion barriers in the ECS due to gliosis and pathologic accumulation of some ECM molecules. We propose that disturbed extrasynaptic transmission, mediated by the diffusion of neuroactive substances through the ECS of such cortex, represents another factor of epileptogenicity in FCD. Support: IGA MZCR NS9915-4 and MZOFNM2005.

0265

Hemangiopericytoma of the pineal body: case report

S. Uyar Bozkurt, N. Comingle, B. Oz*
*Marmara University, Istanbul, Turkey

Objective: Hemangiopericytomas are rare mesenchymal neoplasms that presumably derived from pericytes. Although HPC mas generally attached to the cranial and spinal dura, intraparenchymal and intraventricular rare tumors have been reported.
Method: A 27-year-old male patient presented with headache, nausea and blurred vision 2 months ago. Cranial MRI revealed contrast-enhanced lesion 3 × 3 cm in diameter in pineal gland location. Given the findings of the preoperative imaging studies, the lesion was consistent with parenchymal tumors of the pineal gland. A right occipital craniotomy and resection of the lesion was performed. Histologically, the tumor was composed of clusters of monotonous, closely packed, small neoplastic cells. Nuclei are oval to round with granular chromatin and inconspicuous nucleoli. Mitosis was rare and necrosis was not found. Stroma contained dilated, slit-like vascular channels lined by flattened endothelial cells. Reticulin stain

showed increased reticulin network of investing group of neoplastic cells. Neoplastic cells were diffusely immunoreactive with BCL-2, but were negative with epithelial membrane antigen, chromogranin, synaptophysin, PGP 9.5, S-100 protein, and CD 34. A MIB-1 labeling index was 5%.
Results: A diagnosis of hemangiopericytoma was made based on light microscopy and conventional histochemical and immunohistochemical studies. Differential diagnosis included pineal parenchymal tumors and meningiomas.
Conclusion: The present case provides one unique example of a rare entity to the diverse spectrum of the pineal region neoplasms encountered in neuropathology.

0267

Cancer metastasis to intracranial meningioma

E. Izycka-Swieszewska, P. Czapiewski, E. Szurowska, D. Borof, O. Pierzak, W. Kloc*
*Medical University of Gdansk, Dept. of Pathomorphology, Poland

Objective: Tumor-to-tumor metastases are very rare. The most common intracranial tumor recipient is meningioma.
Method: Case study.
Results: (1) A 70-year-old man was admitted in 2009 due to a rapid onset of the right hemiparesis. His history revealed: 2003—nephrectomy due to renal clear cell carcinoma (RCC) T1N0M0, 2003—detection of parieto-temporal meningioma 2.5/2.2 cm; he denied the operation; 2005—diagnosis and hormonotherapy of prostatic cancer; 2003–2008 radiological follow-up of meningioma. In CT at admission, the tumor was 6.2/3.2 cm and contained intensively contrast-enhanced 1.5-cm area with surrounding edema. The tumor was removed but complicated with a hematoma. Histologically, it consisted of whorled clusters of spindle cells with focal necrosis and mitotic index of 5/10 HPF. The separating, well-vascularized area was composed of clear cells. Meningioma immunophenotypes were S-100^{+}, vimentine^{+}, progesterone receptor^{+}, and CD10^{-}, while focus were S-100^{-}, vimentine^{-}, progesterone receptor^{-}, and CD10^{+}. The diagnosis was atypical meningioma (G2) with RCC metastasis. (2) A 57-year-old man with a 2 year's history of a colorectal cancer (T3N1M1) was admitted in 2009 due to severe headaches. CT revealed an enhancing temporal lobe tumor 2.5/3.2 cm surrounded by edema. The neurosurgeon resected brain metastasis and the radiologically undescribed meningeal tumor 0.9/0.4 cm. Histologically, meningeal tumor was a meningothelial meningioma (G1) with a 0.3-cm focus of metastatic adenocarcinoma (CK^{+}, CDX2^{+}).
Conclusion: Cancer metastasis to meningioma can be the first manifestation of the metastatic stage of disease. Metastasis to meningioma should be included into differential histopathological diagnosis in patients with systemic malignancies.

0268

A solitary laryngeal plexiform neurofibroma in a pediatric patient

M. Sajin, G. Bruma, C. Chirita, A. Enculescu, G. Simion, R. Guran, M. Stanculescu*
*UMF Carol Davila, Dept. of Pathological Anatomy, Bucharest, Romania

Objective: Neurofibroma is the most frequent neurogenic tumor in the first year of life. It is a benign proliferation of Schwann cells, perineurial cells, and fibroblasts, which may occur in association with neurofibromatosis type 1 or sporadically. The most common sites of laryngeal involvement are the aryepiglottic folds and the arytenoids, areas of the larynx rich in terminal nerve plexuses. Clinical findings: A 1-year-old girl presented with airway obstruction and stridor with a progressive nature since birth. Direct laryngoscopy: laryngeal tumoral mass, located in the supraglotic area. Complete surgical excision was performed.
Method: All anatomical pieces were fixed in 10% formaldehyde solution, paraffin-embedded, cut and stained (hematoxylin–eosin and Van-Gieson).
Results: Macroscopically: 1-cm whitish multinodular mass, firm consistency, myxoid cut surface Microscopically: The submucosal nerve fibers were expanded in a plexiform pattern, infiltrating between the submucosal glands due to a proliferation of small, delicate, wavy, spindle cells with markedly elongated, wavy nuclei with pointed ends and coarse collagen fibres, embedded in a myxoid matrix. Immunohistochemistry: positivity of the nervous fibers for CD34 and S100 protein. ACT was negative in the nervous fibers and positive in the blood vessels. Ki67 was negative. Histopathology diagnosis: plexiform neurofibroma of the larynx.
Conclusion: Neurofibroma of the larynx is a rare condition that should be considered in the differential diagnosis of children presenting with a submucosal laryngeal mass even without the other clinical signs of NF1 or NF2. It has a high rate of recurrence or residual disease due to the possibility of malignant transformation.

0271

Magnetic resonance microscopy of brain biopsies for detecting microstructural patterns

D. Monleon, A. Gonzalez Segura, J. M. Morales, J. Gonzalez Darder, M. Cerda Nicolas, C. Lopez Gines, R. Gil Benso*
*Hospital Clinico Valencia, Fundacion Investigacion, Spain

Objective: Brain lesions are highly heterogeneous both clinically and morphologically. The morphological study of these lesions is based in their cellular characteristics, different tissue organization patterns, vascular network, collagen distribution, presence of calcium, etc. MR imaging of excised tissue samples may provide valuable information about lesion structure and microarchitecture, increase the diagnosis specificity and help for better tissue characterization.
Method: Fifteen brain lesions biopsies from the Hospital Clinico Universitario de Valencia were fixed with formalin and embedded in a gel matrix for minimizing motion artifacts. MR microscopy images and optical microscopy images were obtained for all of them. MR microscopy images included T1, T2, T2* and DWI. Images were subsequently analyzed by hierarchical clustering.
Results: MR microscopy of brain biopsies shows high resolution and quality. Major histological findings (for example, healthy, vascular, proliferative or necrotic tissue) exhibit differential MR parameters values (T1, T2 and diffusion coefficient among others). Hierarchical cluster analysis of these parameters revealed different MR patterns correlating with relevant histopathological and immunohistochemical features.
Conclusion: MR microscopy provides functional, microstructural and biophysical information complementary to that obtained by conventional histopathology. Our approach and findings may help in multidisciplinary groups for better integration of histopathology and MRI in brain lesion diagnosis.

0272
Interaction of vesicular monoamine transporter 2 (VMAT2) and neuromelanin pigment among the midbrain dopaminergic neurons in man

P. Pasbakhsh, D. German*
*Tehran University of, Medical Science, Iran

Objective: Neuromelanin (NM) pigment accumulate with age catecholaminergic neurons in man, and ventral substantia nigra dopaminergic neurons that are most vulnerable to degeneration in Parkinson's disease (PD) contain the greatest amount of this pigment. In vitro data indicate that NM pigment is formed from the excess cytosolic catecholamine that is not accumulated into synaptic vesicles via the vesicular monoamine transporter2 (VMAT2).
Method: Using semiquantitative immunohistochemical methods in human postmortem brain, we sought to examine the relationship between the contents of VMAT2 and NM pigment. The immunostaining intensity (ISI) was measured for VMAT2 in two regions of the midbrain dopaminergic cell complex. The ISI of the cells was related to the density of NM pigment within the cells. We also measured the ISI for tyrosine hydoxylase (TH) and examined the noradrenergic neurons in the locus coeruleus (LC) in brain 22–-65 years of age.
Results: (1) Ventral substantia nigra neurons had the lowest VMAT2 ISI of all neurons in the midbrain cell complex, whereas over twofold higher levels are found in most ventral tegment area neurons. (2) There was an inverse relationship between VMAT2 ISI and neuromelanin pigment in midbrain dopaminergic neurons. (3) Neurons with the highest VMAT2 ISI resided in the LC. (4) Neurons with high VMAT2 ISI also had high TH ISI.
Conclusion: These data support the hypothesis that among the midbrain dopaminergic neurons, the ventral substantia nigra dopamine neurons accumulate the highest levels of NM pigment because they have the lowest levels of VMAT2, which thereby renders them especially vulnerable to degeneration in PD.

0273
Histopathological aspects and protein aggregation in mitochondrial myopathies

S. Zurac, A. Bastian, G. Micu, E. Gramada, C. Socoliuc, C. Popp, R. Andrei, T. Tebeica, C. Lazaroiu, F. Staniceanu, H. Goebel*
*Colentina Universitary Hosp., Dept. of Pathology, Bucharest, Romania

Objective: Human mitochondrial diseases have a relatively high incidence, multiple genetic causes and quite diverse clinical, biochemical and morphological phenotypes requiring a multidisciplinary approach for diagnosis. The study of protein aggregation in muscle fibres in these disorders may offer new insights on their complex pathogeny.
Method: We studied morphological aspects of the "ragged red" fibres—targeting our interest on the types and location of different protein aggregates. We selected diagnostic muscle biopsies from seven unrelated patients and used histological, histochemical, enzyme histochemical, ultrastructural and immunohistochemical techniques.
Results: The expression of cytoskeletal, transsarcolemmal, sarcomeric, chaperone type and nuclear proteins revealed that "ragged red" fibres and "ragged red" regions of the fibres accumulate diverse proteins, of which desmin, alpha B crystallin, as well as N-CAM, dysferlin and heat shock protein appear to be regular ones. None of our cases had any accretion of plectin, actinin, beta and gamma dystroglycan. Other proteins showed variable expression.
Conclusion: As the list of members in the "protein aggregate myopathies" family is constantly enlarging, the study of protein accumulation in mitochondrial myopathies is of clear interest for the future. Note: Zurac

and Bastian should be regarded as first authors with equal contribution.

Friday, 3 September 2010, Basement

PS-14 Poster Session Uropathology

0275

Audit of prostate core biopsies 2005–2009

S. Prendeville, S. S. Harrun, L. H. Kamaruddin, M. Leader*
*Co. Kerry, Ireland

Objective: Prostate biopsy is performed to detect carcinoma in those at high risk on the basis of elevated PSA and abnormal digital rectal examination. Re-biopsy is often performed following an initial atypical diagnosis or rising PSA.
Method: All histopathological reports of prostate biopsies at Beaumont Hospital, Dublin, during the time period 1 January 2005 to 1 January 2009 were analysed. A total of 1,483 reports were retrieved and the data were recorded and analysed.
Results: All prostate biopsies were grouped into initial biopsy (no previous biopsy recorded) and repeat biopsy (at least one previous biopsy recorded). Multiple report parameters were recorded for each biopsy including diagnosis, number of cores taken, number of positive cores and Gleason grade, and these were compared for the two groups. In the original biopsy group, all biopsies reported as atypical (but not meeting criteria for carcinoma) were further analysed for changes on follow-up biopsy. In the repeat biopsy group, repeat biopsies performed for increased PSA and for previous atypical diagnosis were analysed separately and compared.
Conclusion: Repeat prostate biopsy is often performed for persistently elevated or rising PSA and previous diagnosis of atypical changes. Our study assessed the likelihood of finding carcinoma in a follow-up biopsy performed for these two reasons. Our study also compared the biopsy adequacy and extent and grade of carcinoma found in both initial and repeat biopsies. The findings are significant in determining the likely clinical course and appropriate management of patients with atypical diagnoses and elevated PSA.

0276

Cytological features, loss of basal cells and AMACR expression in some hyperplasic and precancerous lesion of the prostate

V. Zakharava, T. Liatkouskaya, E. Cherstvoy*
*Belarusian State, Medical University, Minsk, Belarus

Objective: Since atypical adenomatous hyperplasia (AAH), post-atrophic hyperplasia (PAH) and proliferative inflammatory atrophy (PIA) of the prostate demonstrate both overlapping histological features and generality of biological properties with prostatic intraepithelial neoplasia (PIN) and atypical small acinar proliferation (ASAP), these processes were proposed in probable precancerous lesions of the prostate.
Method: We studied the cytological features with the use of morphometry. The expression of AMACR and cocktail HWC+p63 was estimated with the use of immunostaining. For the image analysis, the software WSIF ImageJ and ImageScope was used.
Results: BC layer was fragmented in most of cases PAH, PIA, AAH. The BC loss in PAH–PIA was 6% and 20% accordingly and was below that in PIN—42%, AAH—83%, and ASAP—84%. Analysis of cytological features and nucleolus frequency showed that PAH–PIA was similar to PIN–ASAP and above that in AAH. Prominent nucleolus was identified in atrophy, precancerous lesions and PCa. Frequency of prominent nucleolus in PAH (63% cases, 4% in cases) and PIA (44% and 13% accordingly) was below that in PIN (58% and 11%), ASAP (59% and 27%) and PCa (78% and 55%). AMACR expression was moderately strongly positive in precancerous lesions and PCa and weakly positive in other groups. Area of AMACR expression in PIN and ASAP was above that in AAH, PAH, PIA and below that in cases PCa.
Conclusion: We identified that PAH and PIA showed more aggressive cytological properties than AAH and was indistinguishable from PIN-ASAP according to cytological features. Meanwhile, PAH and PIA take intermediate position between BPH and PIN-ASAP according to BC loss, frequency of prominent nucleolus and AMACR expression.

0277

Rare tumors of the prostate diagnosed by a core needle biopsy

K. Socha, C. Hopfner, S. Mehaut, P. Brun, J.-M. Schouler*
*Centre Hospitalier de Troyes, France

Objective: Presentation of 2 rare lesions of the prostate.
Method: A 69-year-old man, with PSA 16,04 underwent a needle biopsy of the prostate. A histological examination of 11 biopsique carrots showed an infiltrating tiny lesion within adipose periprostatic tissue at the level of one biopsy of the left lobe nodule. The lesion consisted of little irregular glands and solid nests of atypical cells PSA^{-} and $CK7^{+}$, and $CK20^{+}$. We proposed a diagnostic of a metastasis/infiltration of unknown primary origin, likely from the urinary tract. This was confirmed by a cystoscopy revealing a tumor which had a histologic appearance of a choriocarci-

noma, finally classed as a poorly differentiated urothelial carcinoma with a choriocarcinoma differentiation.
Results: The second case concerns a 35-year-old patient with decompensated cirrhosis admitted to the hospital for a gastroenterology bilan. Rectal examination revealed an enlarged prostate. The hemostase was necessary after a core needle biopsy of the prostate. The histological examination demonstrated a highly vascular tumor composed of chief and sustentacular cells arranged in an alveolar pattern. Immunohistochemical study confirmed a paraganglioma. There were no signs of malignancy; however, we did not observe any prostatic parenchyma at the tumoral level.
Conclusion: Many significant non-epithelial tumors may arise in the prostate gland; although they are rare, their recognition by the pathologist is essential as their treatment and prognosis are quite variable. The core needle biopsy allows for a diagnostic of a variety of tumors, and one should not ignore, in spite of the absence of clinical symptoms and complementary information, the risk of metastatic lesion in the prostate.

0278
Latent prostate cancer in association with benign prostatic hyperplasia after the Chernobyl accident in Ukraine

A. Romanenko, A. Chekalova, P. Harkonen, A. Vozianov*
*Institute of Urology, Kiev, Ukraine

Objective: During the 24-year period subsequent to the Chernobyl accident, the morbidity of prostate cancer in Ukraine has increased from 12.0 to 28.6 per 100,000 male population. The prevalence and immunohistochemical (IHC) study of latent, incidentally found prostate cancer (LPC) in patients who underwent surgery for benign prostatic hyperplasia (BPH) were studied.
Method: BPH samples were obtained by prostatectomy from 120 Ukrainian patients operated between 2007 and 2009 consisting of 30 patients from the so-called clean (without radio-contamination) areas (control group 1) and of 90 patients living in Cesium 137 (^{137}Cs)-contaminated areas of Ukraine (group 2). Ki-67, p53, p27Kip-1, p63 and Bcl-2 proteins were IHC-investigated in BPH from all patients.
Results: The incidences of LPC (Gleason score 4), chronic prostatitis, proliferative inflammatory atrophy (PIA) and prostatic intraepithelial neoplasia (PIN) were 16.67%, 53.34%, 20%, and 26.67% in group 1 and 12.23%, 64.45%, 43.45%, and 36.67% in group 2, respectively. Greatly elevated levels of p53, Ki-67, and Bcl-2 associated with decreased levels of p27Kip-1 and p63 in areas of PIA and less LPC and PIN in group 2 compared with group 1 patients were obtained with statistically significant differences.
Conclusion: Our study suggests that chronic long-term low-dose radiation exposure might result in the increase of chronic inflammation, and it is now found to be associated with increased incidences of PIA and PIN in BPH accompanied by p53, p27KIP-1, and Bcl-2 alteration, which in turn could lead to prostate carcinogenesis.

0280
Mixed peripheral ductal prostatic adenocarcinoma in radical prostatectomies: a five-year experience in a small Spanish Community Hospital

C. L. Menendez, P. Benito, E. Fuente, P. Gozalvo, B. Corrales, C. Murias, V. Venta, N. Beridze, F. Dominguez*
*Gijon, Spain

Objective: Ductal prostate cancer (DPC) is a rare morphologic variant of prostatic cancer. They can arise centrally or peripherally. They have characteristic growth patterns and morphology. They usually appear combined with common acinar adenocarcinoma.
Method: We reviewed 71 consecutive radical prostatectomies from 2005 until the end of 2009. Immunohistochemical analysis were performed with P504S, p63, 34BE12, p63, PSA, Bcl2, chromogranin A, synaptophysin, p53, Ki-67, CK7, CK20, CEA and CD56 using the L-SAB method.
Results: Four mixed DPCs were found (5.6% of the total) with no previous treatment. Two cases had a minor DPC component: case 3: age 66, RP with 5% of cancer (bilateral), 25% of DAP, GS 4-3, focal EPE and seminal vesicle (SV) invasion and positive margin; case 4: age 53, 20% of cancer(bilateral), 20% of DPC, GS 4-3, no EPE or SV invasion, lymph node (LN) negative. Two cases had a major ductal component: case 1: age 63, 25% of adenocarcinoma (bilateral), 40% of DPC, GS 3-4, multifocal EPE, SV and LN negative; case 2: age 60, 40% of carcinoma, 70% DPC; occasional EPE, no SV invasion, LN negative. It showed prominent sclerotic stroma. Focally, it had a peculiar pattern: central solid bland spindle/basaloid areas (HMWK, neuroendocrine markers, Bcl-2, PSA and CEA^{+}).
Conclusion: That low incidence correlates with that described in the literature. They all shared typical ductal features and conventional acinar carcinoma at least focally. Case 2: predominantly ductal, had an additional morphology: basaloid–neuroendocrine differentiation.

0281
Preoperative data predictive for final tumor volume in radical prostatectomy specimens

A. Loghin, A. L. Carmen Dema, V. Bacarea, C. Moldovan, M. Decaussin-Petrucci, A. Borda*
*University of Medicine, Dept. of Histology, Tirgu Mures, Romania

Objective: Tumor volume is a powerful predictor of patient outcome in prostatic adenocarcinoma. Preoperative assessment of prostate cancer tumor volume is still a big challenge. The present study attempted to identify the most predictive biopsy variables for final tumor volume in radical prostatectomy specimens.
Method: We reviewed 128 prostate needle biopsies in patients who subsequently underwent radical prostatectomy. The preoperative data collected were: PSA, preoperative ultrasound, total prostate volume, number of positive biopsies, total percentage of cancer in the biopsy and Gleason score. Prostatectomy specimens were entirely embedded and mounted whole. Tumor volume was measured using the grid method. Preoperative data were compared with final tumor volume in radical prostatectomy specimens by univariate and multivariate analysis.
Results: The number of positive biopsies ($p<0.001$), total percentage of cancer in the biopsy ($p<0.001$) and Gleason score ($p<0.001$) were significant predictors of tumor volume on linear regression analysis. PSA value ($p=0.102$) and preoperative ultrasound total prostate volume ($p=0.07$) were not significant predictors of tumor volume. On multivariate logistic regression analysis, we designed a model to predict final tumor volume. This model contains all the predictors mentioned above and significantly correlates with final tumor volume ($p<0.001$).
Conclusion: Preoperative data (Gleason score, number of positive biopsies and total percentage of cancer in the biopsy) can be used to predict the volume of prostate cancer with acceptable accuracy. These variables must be mentioned to the clinician in order to help in the therapeutic decision.

0282

"Negative" histopathology (stage pT0) in a radical prostatectomy specimen after a preoperative diagnosis of prostatic adenocarcinoma

M. Ligaj, K. Sikora, R. Sosnowski*
*Warsaw Cancer Center, Dept. of Pathology, Poland

Objective: In rare cases, histologic assessment of the entire radical prostatectomy specimen (RPS) after a positive biopsy does not reveal residual tumour. We analyze the incidence of "vanishing prostatic carcinoma" in our institution and present algorithm of pathologic workup of "negative" RPSs.
Method: Among 589 RPSs from patients treated for prostatic adenocarcinoma (January 1997–December 2009), ten cases (1.70%) showed no residual carcinoma despite complete sampling. A five-step protocol of additional pathologic workup included: (1) preoperative biopsy review; (2) "second look" review of the RPS; (3) immunohistochemistry (34betaE12, p63) performed on suspicious foci; (4) deeper levels of each block with PIN high grade and/or of blocks with areas where cancer was seen in the biopsy; and (5) block-flipping of regions specified above with deeper levels.
Results: Cancer diagnosis had been made in transurethral resection (TURP) specimen (two patients) and core biopsy (eight patients). The TURP cases were excluded on the assumption of complete pre-prostatectomy carcinoma resection. Biopsy review (protocol step 1) confirmed prostatic carcinoma in seven core biopsy specimens (1.18%). In one case, diagnosis of adenocarcinoma made in another institution was not confirmed. Steps 2–5 revealed residual carcinoma in a further four RPs. Despite full workup, no residual tumour was seen in three RP specimens (0.51%). All three "negative" cases had undergone MAB prior to RP and showed no clear evidence of residual carcinoma.
Conclusion: "Vanishing prostate carcinoma" is a rare phenomenon, with higher incidence after neoadjuvant hormone therapy. Extensive histologic workup of RP specimen reduced the rate of pT0 RP after a positive core biopsy from 1.18% to 0.51%.

0284

CD10 expression in prostate cancer—preliminary results

D. Anderco, E. Lazar, S. Taban, D. Herman, C. Lazureanu, M. Cornianu, A. Muresan, V. Bucuras, R. Bardan, A. Dema*
*Timisoara, Romania

Objective: CD10 is a transmembrane neutral endopeptidase strongly expressed by normal prostatic epithelium. Loss of CD10 expression is an early event during prostatic carcinogenesis. The aim of this study was to evaluate CD10 expression in different stages of prostate tumors and its correlation with classical prognostic factors.
Method: Twenty cases of prostatic cancer with different pathological stages (four cases—organ-confined disease, four cases—locally advanced disease, six cases—metastatic disease and six cases—hormone-resistant disease) were selected and further CD10 immunostained. The malignant foci were evaluated for the presence, pattern and intensity of reaction. We also assessed the classical prognostic factors like tumor grade, pathological stage and resection margin status.
Results: Our study showed a marked heterogeneity of CD10 expression. We noticed a membranous and/or cytoplasmic pattern of reaction. CD10 stained positively predominant at the apical membrane of the malignant glands ($n=14$). Gleason pattern 2 carcinomas showed a focal membranous apical reaction, while some of Gleason pattern 3 tumors expressed CD10 in both membranous and

cytoplasmic compartments. Cytoplasmic CD10 expression was almost exclusively noticed in Gleason pattern 4 and 5 tumors and in metastatic and hormone-resistant cases (n=6).
Conclusion: Our study suggests some prognostic value for membranous and cytoplasmic pattern of CD10 expression in prostate tumors. To eliminate discrepancies on this issue, further standardization of both immunostaining procedure and interpretation is mandatory. Larger prospective studies are also required to confirm predictive CD10 significance in prostate cancer progression.

0285

High CD10 expression in lymph node metastases from surgically treated prostate cancer independently predicts early death

C. Rocha, N. Saxer-Sekulik, I. Zlobec, G. Sauter, G. N. Thalmann, A. Fleischmann*
*Universität Bern, Institute of Pathology, Switzerland

Objective: Patients with nodal positive prostate cancers are an important cohort with poorly defined risk factors. CD10 is a cell surface metallopeptidase that plays a role in the progression of various cancers and has been shown to be associated with early biochemical failure in surgically treated prostate cancer.
Method: CD10 expression was evaluated in 119 nodal positive, hormone treatment-naïve prostate cancer patients using tissue microarrays constructed from primary tumors and lymph node metastases. All patients underwent radical prostatectomy and standardized extended lymphadenectomy.
Results: In the primary tumor, high CD10 expression was significantly associated with earlier death of disease (5-year survival: 73.7% vs. 91.8%, p=0.043) when compared with low CD10 expression. In the metastases, high CD10 expression was significantly associated with larger total size of metastases (p=0.015), earlier death of disease (5-year survival: 87.3% vs. 71.5%, p=0.037) and death of any cause (5-year survival: 87.2% vs. 70.0%, p=0.009) when compared with low CD10 expression.
Conclusion: CD10 expression in metastases added independent prognostic information for overall survival (p= 0.018) that might help schedule adjuvant therapies.

0286

Cytoplasmic cyclin D1 in lymph node metastases independently predicts survival in surgically treated nodal positive prostate cancer patients

C. Rocha, N. Saxer-Sekulik, I. Zlobec, G. Sauter, G. N. Thalmann, A. Fleischmann*
*Universität Bern, Institute of Pathology, Switzerland

Objective: Prognostic factors in nodal positive prostate cancer are poorly defined. Cyclin D1 is expressed in prostate cancer cells and might be prognostically relevant.
Method: Nuclear and cytoplasmic cyclin D1 expression was evaluated in 119 nodal-positive prostate cancer patients undergoing radical prostatectomy and extended lymphadenectomy. Cyclin D1 was correlated with various tumor features and biochemical recurrence-free (bRFS), disease-specific (DSS) and overall (OS) survival.
Results: In primary tumors, high nuclear cyclin D1 expression was significantly correlated with poor tumor differentiation and large nodal tumor burden. In metastases, high cytoplasmic cyclin D1 expression was significantly correlated with low nodal tumor burden and predicted independently unfavourable outcome compared to patients with low expression (5-year bRFS: 26.4% vs. 12.5%, p= 0.008; 5-year DSS: 80.7% vs. 56.3%, p=0.023; 5-year OS: 78.7% vs. 56.3%, p=0.011). These patients had a 2.5-fold elevated risk of dying from cancer compared to patients with low cytoplasmic cyclin D1 expression (p=0.018).
Conclusion: The subcellular location of cyclin D1 expression in prostate cancer might impact on important biological properties. Survival stratification according to biomarker expression in metastases indicates an important role for tumor sampling from these tissues. Cyclin D1 in metastasizing prostate cancer might serve for targeted therapies.

0287

Immunohistochemical assessment of lymph vessel architecture and lymphangiogenetic marker vascular endothelial growth factor-C (VEGF-C) in prostate carcinoma. Correlation with tumor grade and lymph node status

K. Gyftopoulos, I. Lilis, H. Kourea, H. Papadaki*
*University of Patras, Dept. of Anatomy, Rion, Greece

Objective: Lymphangiogenesis is considered an essential procedure that facilitates lymphatic invasion in many tumors. It is not clear, however, whether lymph node metastasis depends on preexisting or newly formatted lymph vessels. We immunohistochemically evaluated the lymph vessel architecture and the expression of VEGF-C in prostate carcinoma cases and examined the correlations with tumor grade and lymph node status.
Method: Mean lymph vessel density (LVD) was assessed by lymph vessel markers D2-40 and LYVE-1 in 87 cases (64 with positive L+ and 23 with negative L− node status) of prostate carcinoma. Correlations of lymph vessel density with VEGF-C expression, tumor grade and lymph node status were evaluated.
Results: Lymph node status was marginally correlated with Gleason grade (chi-square, p=0.052). Mean LVD assessed

by D2-40 and LYVE-1 showed no differences between L+ and L− cases (*t* test, $p>0.05$ in both cases). When LVD was correlated to tumor grade, no statistically significant differences were present. On the other hand, VEGF-C expression was increased in L+ cases and correlated well with lymph node status (chi-square, $p=0.041$). Interestingly, VEGF-C correlated well with D2-40-assessed LVD (but not LYVE-1) in both intratumoral and peritumoral lymph vessels (ANOVA, $p<0.0001$).

Conclusion: Our results indicate that VEGF-C is essential for tumor lymphangiogenesis in prostate carcinoma. Both D2-40 and LYVE-1 may reveal lymph vasculature, the latter, however, showing lower expression, probably limited to a specific lymph vessel subpopulation. It is possible that lymph node metastasis is independent of newly formed lymph vessels.

0288

Bmi1 is repressed in primary prostate cancer but re-expressed in bone metastatic disease

E. Karamitopoulou, C. Rentsch, A. Wetterwald, M. Germann, N. Guzman, R. Markwalder, M. Cecchini, G. Thalmann*

*University of Athens, 2nd Dept. of Pathology, Greece

Objective: Polycomb group genes (PcGs) actively control epigenetic regulation of gene expression in human progenitor cells. Expression of the PcG Bmi-1 has been associated with cancer stem cell activation. High Bmi-1 mRNA expression in primary prostate cancer (CaP) has been shown to be a sign of poor prognosis, and activation of the PcG pathway has been associated with metastatic CaP cells in vitro and in vivo. Therefore, Bmi1 expression in the primary tumor may be a predictor of potentially lethal disease in CaP.

Method: A tissue microarray (TMA) consisting of control samples and primary tumor tissue samples of 284 CaP patients and tissue samples of 71 patients with CaP bone metastases was generated, stained and evaluated for Bmi1 expression. Median follow-up of the patients was 7.7 years. Bmi1 expression was correlated with clinical parameters.

Results: Non-malignant prostate tissue generally showed high Bmi-1 expression. In contrast, only 12% of the localized prostatic carcinomas demonstrated Bmi1 expression. Along with a significant enrichment of Bmi1-positive cancer cells in bone metastases, a significantly higher fraction of Bmi1-positive samples was found in bone metastases as compared to primary tumors (41% vs 12%, $p<0.01$). No correlation was found for Bmi1 expression and clinical parameters in CaP.

Conclusion: Bmi1 expression in the primary CaP is not a predictor of worse outcome or bone metastatic disease, although bone metastases are associated with Bmi1 re-expression. This finding suggests a potential role of PcG Bmi1 in prostate cancer progression and metastasis.

0289

Large cell neuroendocrine carcinoma in urinary bladder

S. Arslankoz, O. Tanas, D. Baydar*

*Hacettepe University, Dept. of Pathology, Ankara, Turkey

Objective: Large cell neuroendocrine carcinoma (LCNEC) of the urinary bladder is a rare tumor with only a few cases reported. The diagnosis is based on the criteria established in lung tumors. We report the clinical and histological data of six patients with LCNEC in urinary bladder.

Method: The clinical charts and histological slides of six patients with the LCNEC diagnosis in urinary bladder from a single institute were reviewed. The diagnosis was confirmed by the use of immunohistochemistry with at least two positive neuroendocrine markers (synaptophysin, chromogranin and/or CD56).

Results: All patients were male. Their age ranged from 38 to 74. The most frequent clinical presentation was gross hematuria. Their histology had overlapping features with urothelial carcinoma and was difficult to differentiate without immunohistochemistry. The most useful features were extreme hypercellularity (6/6), lack of exophytic papillary component (5/6), nuclear molding (4/6), finely stipled chromatin (4/6) and exuberant mitotic rate (most >10/hpf) with innumerable apoptotic figures. In three cases, there were foci of admixed invasive or in situ urothelial carcinoma, in one case admixed adenocarcinoma. All tumors were infiltrative to muscularis propria at the time of diagnosis, except the most recent one which did not have muscle sampled in resection. Distant metastases were found in liver, spleen and bones of one patient. Three patients underwent radical cystoprostatectomy; all patients received adjuvant or neoadjuvant chemotherapy, and one was given additional radiotherapy.

Conclusion: Distinction between LCNEC and urothelial cancer is important because of likely different therapeutic options. LCNECs are highly aggressive tumors with at least pT2 disease at diagnosis.

0290

Myofibroblastic stromal reaction in pTa and pT1 papillary urothelial carcinoma of the urinary bladder

*Z. Marusic**

*Sestre Milosrdnice Hospital, Dept. of Pathology, Zagreb, Croatia

Objective: The most important element in pathologic evaluation of urothelial cancer is recognition of the

presence and extent of invasion. Our research objective was to analyze myofibroblastic stromal reaction in papillary urothelial carcinoma of the urinary bladder with lamina propria invasion and compare it with lamina propria of noninvasive carcinoma.
Method: Immunohistochemical analyses of vimentin, smooth muscle actin (SMA) and desmin reactivity were performed in 50 pTa and 50 pT1 papillary urothelial carcinomas of the urinary bladder obtained by transurethral resection. The reaction was graded as 0—no reaction, 1—positive reaction in <33% of lamina propria cells, 2—positive reaction in 33–66% of lamina propria cells and 3—positive reaction in >66% of lamina propria cells. Distribution patterns of vimentin- and SMA-positive cells were graded as fascicular (organized) and reticular (disorganized), respectively.
Results: Reactive stroma in pT1 carcinoma showed increased vimentin and SMA expression ($p<0.001$, chi-square test) compared to lamina propria of pTa carcinoma. There was no significant difference in desmin expression. The distribution pattern of both vimentin- and SMA-positive cells was reticular in invasive and fascicular in noninvasive carcinoma ($p<0.001$, chi-square test).
Conclusion: Our study indicates that an increased number of cells with myofibroblast immunophenotype as well as an altered, disorganized pattern of myofibroblast distribution can be demonstrated in invasive (pT1) papillary urothelial carcinoma of the urinary bladder when compared to pTa carcinoma. These findings, especially the latter, may be used as a helpful additional diagnostic tool in cases suspicious of lamina propria invasion.

0291
Gemcitabine vs sirolimus in chemically induced bladder tumours: preliminary results

C. Nóbrega, A. Colaço, L. Santos, H. Vala, L. F. Palomino, C. Lopes, P. A. Oliveira*
*Instituto Politécnico de Viseu, Escola Superior Agrária, Portugal

Objective: Bladder cancer's incidence is increasing worldwide. To improve the results of current bladder cancer treatments, new drugs are being tested in single use or in associations. Gemcitabine is metabolized to the active diphosphate and triphosphate, which is integrated into the DNA and causes cessation of DNA polymerization. Sirolimus inhibits mTOR protein kinase. Our aim was to study and compare the effect of gemcitabine and sirolimus in bladder cancer chemically induced in mice.
Method: *N*-butyl-*N*-(4-hydroxybutyl) nitrosamine was administered to ICR male mice in drinking water for 12 weeks. One group was treated with gemcitabine (0.05 mg/kg, i.p.) and the other with sirolimus (1.5 mg/kg, i.p.). All animals were killed at the end of the experiment.
Results: Animals not treated showed a higher incidence of neoplastic and pre-neoplastic lesions than animals treated (77% simple hyperplasia, 69% nodular hyperplasia, dysplasia 100%, CIS 15% and invasive carcinoma 54%). Gemcitabine group showed simple hyperplasia 66.7%, nodular hyperplasia 46.67%, dysplasia 100%, squamous carcinoma 40%, low level papillary carcinoma 6.67%, high-grade papillary carcinoma 6.67%, and invasive carcinoma 20%. Sirolimus showed 71.4% simple hyperplasia, nodular hyperplasia 28.6%, dysplasia 85.7%, squamous carcinoma 35.7%, and invasive carcinoma 7.1%. Cis was not observed in either sirolimus or gemcitabine groups.
Conclusion: Histopathological studies showed that both drugs reduce tumour incidence. Despite that the differences were not statistically significant, sirolimus was more effective than gemcitabine. Given their different mechanisms of action and the synergistic effect observed with these two drugs in vitro in other types of tumours, further trials with their combination should be considered.

0293
The most appropriate immunohistochemical panel for discriminating poorly differentiated invasive tumors in transurethral resection specimens

A. Dema, D. Dobre, S. Taban, C. Lazureanu, E. Lazar, D. Herman, M. Cornianu, A. Muresan, R. Cornea, A. Faur, V. Bucuras*
*University of Medicine, Dept. of Pathology, Timisoara, Romania

Objective: The accurate diagnosis of poorly differentiated invasive carcinomas in transurethral resection (TUR) specimens using only H&E-stained sections continues to be a challenge for the pathologist. The aim of this study was to evaluate and select an optimal immunohistochemical (IHC) panel of antibodies to establish the urothelial or prostatic origin of poorly differentiated tumors in TUR specimens.
Method: IHC was performed to detect cytokeratin (CK) 7, CK20, high-molecular-weight CK (HMWCK), p63, prostate-specific antigen (PSA) and P504S/AMACR in 24 cases of poorly differentiated invasive tumors: 12 poorly differentiated prostatic adenocarcinomas (Gleason score ≥ 8) and 12 high-grade urothelial carcinomas. The youngest patient was 56 while the oldest was 84 years of age.
Results: The sensitivities for labeling prostate cancers were: PSA (92%), AMACR (92%), CK20 (17%), CK7 (8%), p63 (0%), and HMWCK (0%), while urothelial high-grade carcinomas demonstrated the following rates of positivity: HMWCK (92%), CK7 (92%), p63 (83%), CK20 (67%), AMACR (33%), and PSA (0%). Co-

expression of CK7/20 was noticed in 67% of the urothelial carcinoma cases, but it lacked in prostate carcinomas.
Conclusion: Our results indicate that a panel of four markers, PSA, HMWCK, CK7 and p63, can determine, in the majority of the cases, the definite primary site of origin of a poorly differentiated invasive tumor diagnosed in TUR specimens. In spite of the high rate of positivity in prostate carcinomas (92%), AMACR is less useful for this purpose since 33% of high-grade urothelial invasive carcinomas expressed this marker too.

0294
Histological and ultrastructural analysis of seminiferous tubules wall layers in ageing testis

I. E. Plesea, M. Gherghiceanu, S. D. Enache, E. Mandache, M. Hortopan, O. T. Pop*
*University of Medicine, Craiova, Romania

Objective: The authors evaluated possible morphological changes of basement membrane (BM) and lamina propria (LP) of seminiferous tubule wall (ST) related to ageing.
Method: Surgical samples of testicular tissue from 28 cases with orchiectomy for prostate adenocarcinoma were processed for light microscopy and transmission electron microscopy (TEM) examination. Seven age groups (AgGr) between 50 and 80 years were designed. Tissue samples were immunomarked for collagen IV and smooth muscle actin. Images were acquired and measured with a specialized software. Thirty STs were randomly selected, with ×40 objective, for each case. Five random determinations for each ST and each parameter were performed. Mean values/tubule, case and AgGr were calculated for each parameter. Regression line (RL), slope and significance test for slope were determined for each parameter correlation with ageing.
Results: BM mean value was around 0.5 μm, with narrow limits of ranging in AgGr but more extended individual limits. RL showed discrete decreasing trend with ageing, but without an obvious statistical correlation. LP mean value was around 6 μm, also with narrow limits of ranging in AgGr and more extended individual limits. RL decreased discretely with ageing, but without an obvious statistical correlation. TEM showed more prominent BM material and more collagen fibers and less fibroblasts in LP of older AgGr and higher fibroblasts density in LP of younger AgGr.
Conclusion: Our results showed that BM thickness is apparently decreasing with ageing, whereas LP presents extremely variable degenerative changes, with a "mosaic", focal distribution and no tendency to advance with ageing.
Acknowledgement: Work supported from the Research Project 41-015/2007 finaced by Romanian Ministry of Education and Research through CNMP.

0295
Age-related changes of testicular intralobular interstitial tissue

I. E. Plesea, A. Borda, S. D. Enache, A. Loghin, C. G. Cotoi, O. T. Pop*
*University of Medicine, Craiova, Romania

Objective: The authors evaluated the possible influences of ageing on the morphology of testicular intralobular interstitial tissue (TIIT).
Method: The studied material consisted of surgical samples of testicular tissue from 192 cases with orchiectomy for prostate adenocarcinoma. Tissue samples were fixed in neutral buffered formalin embedded in paraffin, stained with hematoxylin–eosin and Goldner trichrome and immunomarked for CD34. Images were acquired and measurements were performed with a specialized image analysis software after previous calibration. The assessed parameters were TIIT amount (P-TIIT) and intralobular vascular network (IVN). Ten fields were randomly selected for each case, with ×20 objective. Mean P-TIIT (mP-TIIT)/field, mP-TIIT/case and mP-TIIT/age group were determined. Regression line (RL), slope (m) and significance test for slope (p) were determined in order to assess the correlation of TIIT amount changes with ageing.
Results: Intralobular septae showed variable amount of collagen fibers, from simple linear fibrillary assemblies to marked thickening with obvious septal enlargement. The latter were seen mostly in the outer region of the lobules, but without any significant spread. TIIT amount had a mean value of 25% of intralobular parenchyma. RL showed a discrete decreasing trend with ageing ($m=-0.01$) confirmed by "p" value ($p=0.018$). Arteriolar wall presented degenerative changes with limited extension and variable intensity. Peritubular and intramural capillaries were present in all age groups. Endothelial cells revealed no significant changes.
Conclusion: Our results showed that intralobular fibrosis had no obvious increasing trend with ageing and IVN revealed only focal changes, not related with ageing.
Acknowledgement: Work supported from the Research Project 41-015/2007 financed by Romanian Ministry of Education and Research through CNMP.

0297
Bilateral malignant Leydig cell tumor with unilateral undescended testis and multiple metastases

C. Comingle, A. Yüksel, E. Demiralay, Y. Akman, H. Özdemir*
*Baskent University, Faculty of Medicine, Istanbul, Turkey

Objective: Leydig cell tumors (LCTs) are usually benign tumors, but approximately 10% of them are malignant. It has been reported that approximately 3% of the LCTs are bilateral. Data regarding a relationship between sex cord stromal tumors and cryptorchidism are scarce.
Method: We present an unusual case of bilateral testicular malignant LCT with left-sided undescended testis, metastatic to subcutaneous tissue, lymph nodes, bones and brain.
Results: Clinical course was aggressive, resulting in the death of the patient in 30 days after the diagnosis was given.
Conclusion: We still need for further studies about optimum management of malignant LCTs.

0298

Primary testicular carcinoid

A. Loghin, E. Fulop, K. Branzaniuc, C. Moldovan, O. Preda, A. Borda*
*University of Medicine, Dept. of Histology, Tirgu Mures, Romania

Objective: Primary carcinoid of the testis is a rare neoplasm, making up for <1% of testicular neoplasms. Only a few studies were published on this subject presenting the clinicopathological characteristics, immunohistochemical features and the controversial histogenesis of primary testicular carcinoid tumor and its differential diagnosis.
Method: We present the case of a 52-year-old man who sought care for a painful testicular tumefaction which had been discovered 3 months prior and developed rapidly. The patient underwent radical right orchiectomy. Standard and immunohistochemical stains were performed.
Results: Gross examination revealed a 2-cm intraparenchymatous, well-circumscribed, pale yellow, solid and homogeneous tumor. Microscopic examination showed a nested or trabecular architecture associated with tubular and papillary structures within a scarce stroma without necrosis. Tumor cells had an abundant cytoplasm, with regular, round or oval nuclei, moderate anisokaryosis and rare mitoses. Surrounding parenchyma was only slightly modified. Immunohistochemistry showed positivity for cytokeratin (AE1\\AE3), chromogranin, synaptophysin and serotonin and negativity for inhibin, calretinin, PLAP and alpha-fetoprotein. Proliferation index (MIB1) was under 2% and p53 staining was negative.
Conclusion: Primary testicular carcinoid is an extremely rare neoplasm whose histogenesis remains disputed. For a correct diagnosis, a metastatic carcinoid tumor from other site should be excluded in the first place.

0300

Evaluation of the prognostic value of peritumoral inflammatory response in patients with penile carcinoma

A. F. Freitas-Rodrigues, I. W. Cunha, G. C. Guimaraes, S. C. Zequi, A. Lopes, R. M. Rocha, F. A. Soares, J. Vassallo*
*Hospital do Cancer, Campinas-Sp, Brazil

Objective: In spite of the low incidence in industrialized countries, penile carcinoma (PC) represents 2.1% of all malignancies among Brazilian men. Peritumoral immune response has been described to have influence in prognosis in some tumor types, but its role in PC has not yet been addressed. The purpose of the present study was to evaluate inflammatory infiltrate cell components and to evaluate its relationship with clinicopathological features in order to establish the prognostic value of immune response in patients with PC.
Method: One hundred fifty-five patients diagnosed at our hospital, with a minimum 5-year follow-up were included in the study. Representative paraffin-embedded tissue was submitted to immunohistochemical evaluation using antibodies to CD1a, CD3, CD4, CD8, CD20, CD56, CD68, CD138, granzyme B, S100 protein, HLA-DR and FOX-P3.
Results: Elevated plasma cell infiltrate detected by conventional morphology and CD138 correlated with more favorable event-free survival ($p=0.04$), indicating a protective mechanism of elevated plasma cell counts. However, when the presence of lymph node neoplastic infiltration was evaluated in a multivariate analysis, only this parameter remained as having prognostic value.
Conclusion: It is concluded that the role of inflammatory response on prognosis is relevant, especially for CD138, but this importance does not prevail over the value of lymph node status. (Supported by FAPESP and CNPq).

0301

Unusual morphologies in adult epithelial kidney tumors

C. M. Ardeleanu, M. Mihai, B. Serbanescu, A. Iordache, R. Stoica, M. Lesaru, A. G. Mihaela Georgescu, S. Enache, V. Enache, F. Cionca, I. Sinescu*
*V. Babes National Institute, Dept. of Pathology, Bucharest, Romania

Objective: Light microscopic diagnosis of renal tumors using the World Health Organization (WHO) is often

difficult due to variable histology. Six separate epithelial renal tumors with distinct morphologies are described in the present study.
Method: Formalin-fixed paraffin-embedded tissue specimens from patients diagnosed with renal tumors described on computed tomography and surgically treated in Fundeni Clinical Institute in the last 2 years were sectioned at 4 μm. The slides were stained with the usual hematoxylin&eosin staining for histological diagnosis. We selected cases with unusual morphologies for conventional epithelial parenchymal renal tumors on light microscopy; clear cell renal cell carcinomas with variable nuclear grading and pure non-epithelial kidney tumors were excluded. Immunohistochemical studies were performed in the Department of Pathology and Immunohistochemistry at "Victor Babes" National Institute. This work was supported by the Grant PNII no. 62089/2008.
Results: The selected cases were classified as renal oncocytosis, collision renal tumor, metastatic undifferentiated carcinoma in clear cell renal carcinoma, clear cell carcinoma with partly sarcomatoid morphology and two unclassified renal cell carcinoma.
Conclusion: The importance of recognizing renal tumors with unusual morphologic features lies in the potential diagnostic, prognostic or therapeutic implications that accompany these particular types of renal tumors. Clinical and imaging data, tumor sampling and ancillary studies can be helpful in rendering the correct diagnosis.

0302

Mixed epithelial and stromal tumor of the kidney

C. Comingle, E. Demiralay, A. Yüksel, Y. Akman, H. Özdemir*
*Baskent University, Faculty of Medicine, Istanbul, Turkey

Objective: Mixed epithelial and stromal tumor of the kidney (MESTK) is a recently described rare neoplasm. Malignant transformation, recurrence and metastasis are rare; therefore, histopathological distinction from other renal neoplasms, especially from renal cell carcinoma, is important. Histologically, the tumor is composed of biphasic components, including cysts and tubules embedded in the spindle cell stroma.
Method: We report a case of a MESTK in a 60-year-old woman who presented with an incidental renal mass but without any urinary complaints.
Results: Clinical course is uneventful after 5 months.
Conclusion: This is a unique case resulting in differential diagnosis which should be distinguished from malignant tumors of kidney.

0303

Primitive neuroectodermal tumor—a very unusual and highly aggressive tumor of the kidney

A. Dema, S. Taban, C. Lazureanu, E. Lazar, A. Muresan, M. Cornianu, V. Bucuras, R. Bardan, R. Herbeck, A. Vaduva*
*University of Medicine, Dept. of Pathology, Timisoara, Romania

Objective: Primitive neuroectodermal tumors (PNET) occur predominantly in childhood in the central nervous system and soft tissue. PNET of the kidney are rare and highly aggressive tumors that can be mistaken for a variety of other small blue cells tumors. We present a rare case of kidney PNET in an adult with rapidly fatal outcome.
Method: This case was of a 55-year-old patient who was hospitalized for a left renal tumor discovered during an ultrasound examination. On CT scan, a solid non-homogeneous tumor with 15-cm maximum diameter was detected in the left kidney; there were also visualized enlarged hilar and paracaval lymph node masses which included the left renal vein. A left perifascial nephrectomy with adrenalectomy was performed.
Results: On gross examination, the tumor presented as a large, lobulated, friable, grey-white mass with hemorrhagic foci which replaced most of the kidney. The tumor exhibited primitive undifferentiated round cell morphology on H&E-stained slides. Immunohistochemical study revealed positive reaction for vimentin, NSE and CD99, while CK (MNF116), EMA, LCA, CD20, CgA, CD34, desmin, actin were negative. Soon after surgery, bilateral pleurisy with secondary lung involvement images precipitates the fatal outcome of the patient.
Conclusion: The occurrence of PNET in the kidney of an adult is very unusual, this case being the first diagnosed in our department in a period of 10 years. It confirms the advanced stage at presentation and the aggressive behavior of the renal PNET. For an accurate diagnosis, immunohistochemical reactions play an extremely important role.

0304

Synchronous appearance of carcinoma, adenoma and leiomyoma in kidney: a case report

M.-M. Koumpanaki, A. Baliaka, G.-C. Balis, A. Dimasis, F. Patakiouta*
*Theageneion Cancer Hospital, Dept. of Pathology, Thessaloniki, Greece

Objective: Papillary carcinomas comprise 10% of the renal cell carcinomas. The patients are usually middle-aged men. Papillary adenomas are often found in patients undergoing haemodialysis. Leiomyomas are benign

mesenchymal neoplasms that are considered to arise from the renal capsule.
Method: Six months ago the patient, a 71-year-old woman, suffered from pneumonia and was hospitalised. After a few months, in a follow-up CT scan, a tumour was found on her right kidney and a nephrectomy was scheduled.
Results: On cut sections, we found a well-circumscribed yellowish tumour, 4.5 cm in maximal diameter, a capsular, whitish, elastic nodule sized 0.5 cm, as well as a small, cystic-like formation. Microscopically, they corresponded with a papillary carcinoma type 1 with numerous foamy macrophages and calcifications, a papillary adenoma and a benign mesenchymal neoplasm, immunohistochemically identified as a leiomyoma.
Conclusion: Papillary carcinomas can be bilateral or multifocal, usually in hereditary cases. Predictive factors are identical to the ones of clear cell carcinomas. Type 1 tumours with extensive necrosis, abundant macrophages and absence of a sarcomatoid dedifferentiation are associated with a better prognosis. The presence of adenomas or leiomyomas does not to seem to have an affect on the outcome. A year after the nephrectomy, the patient is alive and well.

0305

Renal angiomyolipoma associated with endometriosis

A. Wittersheim, S. Casnedi, S. Croce, C. Renard, L. Obringer, A. Neuville*
*University Hospital, Strasbourg Cedex, France

Objective: Angiomyolipoma is a rare neoplasm composed of varying admixtures of blood vessels, smooth muscle cells and adipose tissue. There is a strong association with tuberous sclerosis. We describe the first case report of multifocal renal angiomyolipoma developed on tuberous sclerosis and associated with endometriosis.
Method: Imaging studies in an asymptomatic 37-year-old woman, affected by tuberous sclerosis with TSC1 gene mutation, revealed a partially solid and cystic mass measuring 7 cm involving the left kidney and a solid mass measuring 0.6 cm in the right kidney.
Results: The surgical specimen consisted of two left nephron-sparing procedures and one at the right side with firm, pale nodules measuring 6.5, 1.5 and 0.6 cm. The tumors were composed of spindle and epithelioid cells with an abundant pale eosinophilic or clear cytoplasm with round nuclei, mild atypia and low mitotic activity. Rare islands of adipose tissue were observed. In the two left tumors, the predominant smooth muscle cells were associated with some foci of endometriosis. The spindle and epithelioid cells were immunoreactive with HMB45 and smooth muscle actin. The estrogen and progesterone receptors were positive in stromal and epithelial cells of endometriosis. The spindle cells of angiomyolipoma were positive with progesterone receptors.
Conclusion: Multifocal PEComa of the female genital tract associated with diffuse endometriosis was described by Froio et al in 2008, but to our knowledge, this is the first case report of renal angiomyolipoma associated with endometriosis. This association represents a supplementary proof of potential role for hormones in the pathogenesis of angiomyolipoma.

0306

Translocation-associated renal cell carcinoma (RCC) in young woman: case report

K. Socha, C. Hopfner, A. Vieillefond, O. Brunschvicg*
*Centre Hospitalier de Troyes, France

Objective: A renal masse was found incidentally on imaging in a 30-year-old woman. It was classed as a Bosniak type III cyst.
Method: Gross findings showed a 3.5 partially cystic, well-circumscribed and tan-yellow renal tumor. Histologically, it contained cells having voluminous cytoplasm (ranging from eosinophilic granular to clear) arranged in sheets, nests, trabeculae, pseudoalveolar structures and papillae. There were no psammoma bodies. Diagnostic hypothesis: variant of multilocular RCC, papillary or chromophobe carcinoma?
Results: Immunohistochemistry: $CK7^{-}$, VIM^{-}, $p504S^{+}$, HMB45/ MelanA $focally^{+}$, CD10 $focally^{+}$. Complementary study: TFB^{+}. Our final diagnostic was: RCC with translocation, known as tumor associated with MiTF/ TFE family translocations, found mainly in young patients and children. In contrast to TFE3 (Xpll.2) translocation tumors, TFB-RCCs are extremely rare (12 cases published). They are characterized by a translocation between the α gene at 11q12 and the first intron of the TFEB gene at 6p21. Translocation-associated RCCs are likely to be present at higher TNM stage. Our patient (pT1N0) presented no evidence of disease 1 year after resection.
Conclusion: Literature analysis confirmed an increase in advanced stage presentation and a worse outcome in pediatric translocation ($TFE3^{+}$) RCC compared with classic ($TFE3^{-}$) RCC. Little is known about TFB RCC's behaviour. Taking into consideration a morphologic heterogeneity of these tumors and their supposed worse prognosis, a screening for translocations with consistent use of antibodies against TFE3 and TFB in all unusual cases of RCCs, regardless of patient age, however, especially in young patients, seems necessary to determine the true incidence of these tumors.

Friday, 3 September 2010, Basement

PS-15 Poster Session Digestive Disease Pathology

0307

Acute onset alendronate-induced esophageal ulcers: a case report

C. Comingle, H. Ü. Ünal, E. Demiralay, G. Tükenmez Demirci*
*Baskent University, Faculty of Medicine, Istanbul, Turkey

Objective: Alendronate sodium is used primarily in the treatment of osteoporosis. Severe esophageal injury has been reported as a rare adverse effect of alendronate.
Method: We present a case of widespread longitudinal esophageal ulcers between 26 and 34 cms appearing within 8 h of oral alendronate treatment. A 46-year-old woman who had hypothyroidism began alendronate treatment for osteoporosis prevention. She presented with severe dysphagia and abdominal pain 8 h after taking the first pill. Upper endoscopy has been performed and biopsy samples from the esophageal ulcers have been taken. Histologically, epithelial infiltration of neutrophils and eosinophils was seen and within leukocytic exudate fragments neutrophils and eosinophils were detected, suggesting a hypersensitivity reaction. No sign of organisms or a neoplasm was present.
Results: Alendronate treatment was discontinued. After 2 weeks, repeat endoscopy showed marked improvement of esophageal ulcers.
Conclusion: This is a unique case reporting acute onset alendronate-induced esophageal ulcers.

0309

CagA, CagA EPIYA motifs and histopathological features in gastric *Helicobacter pylori* infection

S. Sarioglu, M. Guvenir, O. Yilmaz, A. Olivares, C. Gönen, M. Soyturk, H. Ellidokuz, G. I. Perez Perez*
*Dokuz Eylul University, Dept. of Pathology, Izmir, Turkey

Objective: The aim of the study was to identify carboxyl terminal regions of the CagA (EPIYA motifs) in Turkish *Helicobacter pylori* strains and compare cagA positivity and EPIYA motifs with demographic characteristics and histopathological findings in patients with dyspepsia.
Method: Antrum and corpus biopsies from 124 patients with dyspepsia were evaluated by histopathology, rapid urease test (RUT) and culture. *H. pylori* cagA polymerase chain reaction (PCR) products ranging from 370 to 570 bp were amplified and products purified by QIAquick PCR kit (Qiagen) and sent to Macrogen for sequencing.
Results: Eighty-nine (71.8%) patients were *H. pylori* positive by at least two of the tests, including RUT, histopathology and culture. Thirty (48.4%) patients were colonized with cagA-positive strains from the 62 *H. pylori* culture-positive patients. We found significantly higher scores of inflammation of pits in antrum and corpus and atrophy in corpus in CagA-positive patients; there were no differences in relation with intestinal metaplasia and with inflammation of the lamina propria. Of the 30 CagA *H. pylori* strains, 21 (70%) had three EPIYA motifs (EPIYA-ABC) and seven (23.3%) had more than three EPIYA motifs (EPIYA-ABCC). However, no association was found between inflammation scores, intestinal metaplasia or atrophy with differences in the EPIYA motifs. We found two patients (6.7%) colonized with more than one strain (EPIYA ABC and ABCC) based on phylogenetic analysis and variation in cagA genotype.
Conclusion: CagA positivity strongly correlated with gastric histopathological inflammation patterns, but there was no association with the number or type of EPIYA motifs.

0310

Do gastric lymphoid infiltrates remain a challenge for pathologists?

I. Theate, C. Sempoux, H. Antoine-Poirel, A. Jouret-Mourin*
*UCL St-Luc, Dept. of Pathology, Brussels, Belgium

Objective: Gastric MALT (mucosa-associated lymphoid tissue) lymphoma is closely related with *Helicobacter pylori* (Hp) colonization and represents a multistage process from gastritis to lymphoma. For the differential diagnosis of MALT lymphoma and reactive inflammation, Wotherspoon proposed a histomorphological scoring with two intermediate categories, grades 3 and 4. Genetic studies (Ig clonality and/or translocations and chromosomal aberrations) have not brought so far definite arguments to confirm or discard lymphoma in these problematic scores.
Method: We reviewed 14,071 HE biopsies containing "gastric lymphoid infiltrates", retrieved from our files from January 2004 to December 2008 in order to evaluate the relevance of ambiguous Wotherspoon score on the follow-up.
Results: From these biopsies, 124 samples (0.9%) from 77 patients were ambiguous or lymphomatous. Thirty-four patients (44%) suffered from lymphoma with a predominance of MALT lymphoma (50%), as well as diffuse large B cell lymphoma (29%), mantle cell lymphoma (15%), Burkitt-like lymphoma (3%) and follicular lymphoma (3%). The remaining 43 patients were affected by Wotherspoon grade 2 to 4 gastritis, with a complete follow-up available for 17 (40%). Lymphoma was present in further biopsies in

six cases (35%), initially coming from either grade 4 (5/6) or grade 3 (1/6). Hp was only observed in two of six lymphoma cases in the first biopsy.
Conclusion: Wotherspoon grades 3 and 4 remain a challenge for pathologists. Clinical follow-up combined with histology and immunohistochemistry should be still considered as the gold standard for the diagnosis. Moreover, pathologists must keep in mind that aggressive lymphomas can also involve the stomach.

0311
Correa's model—comprehensive or partial explanation for carcinogenic process triggered by the *Helicobacter pylori* infection?

S. Zurac, G. Micu, F. Staniceanu, A. Bastian, E. Gramada, C. Popp, L. Nichita, D. Simeanu, M. Olariu, R. Mateescu, R. Voiosu*
*Colentina Universitary Hosp., Dept. of Pathology, Bucharest, Romania

Objective: As a group 1 carcinogen for gastric cancer, *Helicobacter pylori* (HP) was involved in many studies and researches focused on physiopathology and morphopathologic changes induced by this bacterium. We proposed to study the precancerous epithelial alteration in patients with HP chronic gastritis, their regression or progression after anti-infectious treatment.
Method: The study included 3,069 gastric endoscopy biopsies performed between 2005 and 2009 in our hospital. Histopathologic diagnosis of these biopsies was made using Sydney criteria. The patients were divided into two groups based on the presence or absence of HP: Group A included 1,414 HP-positive patients and group B included 1,653 HP-negative patients. We evaluated several histopathological parameters, correlating the degree of inflammation, atrophy, metaplasia, regenerative hyperplasia and dysplasia with the presence of HP.
Results: Our study identifies an overall tendency towards regression of premalignant lesions of gastric epithelium after HP eradication, as well as an increasing number of patients diagnosed with early gastric cancer, thus consolidating the results of studies who foretell the significant decrease of gastric cancer mortality. These lesions are present years before becoming clinically manifest and consequently treatable.
Conclusion: In respect to carcinogenic mechanisms, some of our results confirm the carcinogenic cascade triggered by the HP infection, as was proposed by Correa et al. in 1975. However, we obtained data leading to the idea that the "precursor lesions" could appear (and histopathologically evaluated) independent from one to the other, which seemed to be through other possible steps. Note: Zurac and Micu should be regarded as first authors with equal contribution.

0312
Intestinal metaplasia and cytokeratin 7/20 pattern of cardiac mucosa in patients with *Helicobacter pylori* infection

M. Micev, M. Cosic Micev, V. Todorovic, N. Drndarevic, I. Jovanovic, S. Djuranovic*
*Clinical Centre of Serbia, Dept. of Histopathology, Belgrade, Serbia and Montenegro

Objective: Specialized Barrett-type intestinal metaplasia (SIM) seems to be a stronger risk factor for malignancy than non-Barrett cardiac intestinal metaplasia (CIM). The pathogenesis of SIM and that of CIM are thought to be associated with gastro-oesophageal reflux disease and *H. pylori* infection, respectively, but are still controversial. Recent studies regarding the expression of cytokeratin CK7 and CK20 in intestinal metaplasia (IM) found at the gastroesophageal junction are conflicting, especially in regard to associated *H. pylori* infection.
Method: We studied the expression of CK7 and CK20 on 45 biopsy specimens of gastric cardia from patients with *H. pylori* infection and histological evidence of IM (group 1) and 36 biopsy specimens from patients with *H. pylori* infection but without evidence of IM (group 2). The distinction between SIM (18/45 cases) and CIM (27/45 cases) was defined morphologically rather than by biopsy site.
Results: On the intestinalized cardiac mucosa, most often we observed the so-called Barrett-type CK7/20 staining pattern consisting of band-like CK20 staining of the surface epithelium and superficial glands and moderate to strong CK7 staining of both superficial and deep glands, i.e. it was found in 12 of 18 cases of SIM, in 19 of 27 cases of CIM and in 23 of 36 cases of non-intestinalized cardiac mucosa or in 14.8%, 23.5% and 28.4% of patients, respectively.
Conclusion: We have found no statistically significant differences in Barrett-type CK7/20 staining pattern between SIM and CIM as well as between intestinalized and non-intestinalized cardiac mucosa in patients with *H. pylori* infection.

0314
Expression of Her2/neu in gastric adenocarcinomas

A. Batistatou, E. Lampri, S. Kamina, V. Malamou-Mitsi*
*Greece

Objective: In gastric adenocarcinoma, overexpression of HER2 has been correlated to tumour location and histologic

type and varies considerably in the few published studies, probably due, at least in part, to the racial heterogeneity of patients included. The aim of the present study was to investigate the immunohistochemical expression of HER2 protein in gastric adenocarcinomas of Greek patients who live in the area of Epirus.

Method: A total of 90 primary gastric adenocarcinomas were retrieved from the archives of the Department of Pathology (63 men and 27 women). They were all located in the stomach, away from the oesophageal–gastric junction. Forty-eight were intestinal type, 37 diffuse type and 5 mixed (Lauren classification). Immunohistochemical analysis of samples was performed using the polyclonal rabbit anti-human c-erb-2 Oncoprotein (DAKO) antibody on paraffin sections. HER2 scoring was performed according to published consensus panel recommendations.

Results: Overexpression of HER2 ($IHC3^+$ and 2+) was detected in eight adenocarcinomas (8.9%). Specifically, score 3+ was assigned to five cases (5.6%, four intestinal type, one diffuse type) and 2+ to three cases (3.3%, two intestinal type, one diffuse type). Score 1+ was detected in ten cases (11.1%, eight intestinal type, one diffuse type and one mixed), and 0 in 72 cases (80%). In two cases with score 3+, adjacent dysplastic epithelium was noted, which was also 3+.

Conclusion: The results of the current study are comparable with those of the literature, indicating that assessment of immunohistochemical expression of HER2 in gastric adenocarcinomas could lead to the stratification of patients, the goal being the optimal personalized treatment.

0316

The prognostic value of Her-2/neu expression in gastric cancer patients from lower Silesia in Poland

A. Halon, P. Donizy, L. Halon, R. Matkowski, J. Rudno-Rudzinska, W. Kielan, J. Rabczynski*
*Wroclaw Medical University, Poland

Objective: Overexpression of HER-2/neu was most widely explored in breast cancer. HER-2 positivity is reported as 6–35% in gastric cancer (GC). The aim of the study was to assess the prognostic significance of HER-2 in GC patients from Lower Silesia, the southwestern region of Poland.

Method: Immunohistochemistry (IHC) for HER-2 monoclonal antibody was performed on 82 paraffin-embedded specimens. IHC expression of HER-2 was evaluated using the Remmele scale (IRS) and standardised HercepTest modified for GC.

Results: The status of HER-2 protein expression was observed as the following: (1) IHC 0, IRS 0—37 cases (45.1%); (2) IHC 1+ (22, 26.8%), IRS 1/2/3 (21, 25.6%); (3) IHC 2+ (17, 20.7%), IRS 4/6/8 (20, 24.4%); and (4) IHC 3+ (6, 7.3%), IRS 9/12 (4, 4.9%). HER-2 overexpression was detected in 23 (28%) tumors in HercepTest (IHC 2+/3+) and in 24 (29.3%) in IRS scale (IRS 4-12). No correlations were found between HER-2-postive GC and tumor size, local and distant metastases. Tumor stage at diagnosis and age were the only covariate with negative prognostic significance in patient survival ($p=0.028$ and $p=0.0048$). There was no significant difference in survival between HER-2-positive and -negative tumors ($p=0.454$).

Conclusion: HER-2 positivity rate observed in GC in patients from Lower Silesia is as high as in breast cancer. Immunohistochemical detection of HER-2 expression is neither a predictor of survival of patients with GC nor does it identify subgroups of patients at higher risk for recurrence of disease.

0317

MMP-2, MMP-9/TIMP-1, TIMP-2 immunophenotype identifies clinical outcome in gastric cancer patients

A. Halon, P. Donizy, L. Halon, J. Rudno-Rudzinska, W. Kielan, J. Rabczynski*
*Wroclaw Medical University, Poland

Objective: Breakage or degradation of extracellular matrix (ECM) and basement membrane (BM) is a critical step in tumor progression. Matrix metalloproteinases (MMPs) and their tissue inhibitors (TIMPs) take important roles in these processes acting in a coordinated manner to form an integrated system. The aim of the study was the evaluation of MMP-2, MMP-9, TIMP-1 and TIMP-2 expression and the correlation with clinicopathological parameters and survival in GC.

Method: Formalin-fixed paraffin-embedded tissue sections from 82 gastric cancers were studied for the expression of MMP-2, MMP-9, TIMP-1 and TIMP-2 protein by immunohistochemistry. Immunoreactivity of neoplastic/epithelial tissue and tumor stroma was scored according to Remmele IRS. Results were correlated with tumor grade, Lauren classification, stage, lymph nodes status, distant metastases and overall cancer specific survival (OS).

Results: MMP-2 and MMP-9 expression was positive in 78 of 82 cases (95.1%). Seventy-two of 82 (87.8%) and 40 of 82 (48.8%) GC expressed TIMP-1 and TIMP-2, respectively. High expression of MMP-2 ($p=0.047$) and TIMP-2 ($p=0.011$) was associated with Lauren intestinal tumor type. High epithelial TIMP-2 expression was associated with distant metastases ($p=0.036$). High epithelial TIMP-2 expression was associated with shorter OS ($p=0.025$) and high epithelial MMP-2 with better survival ($p=0.017$).

Conclusion: High epithelial TIMP-2 immunoreactivity is significantly associated with shorter survival and distant metastases. Epithelial MMP-2 overexpression identifies GC

patients with better clinical outcome. Increased TIMP-2 expression reflects its crucial role in predicting the aggressive GC behavior.

0318

Expression of chemokine SDF-1a and its receptor CXCR4 is a marker for an unfavorable prognosis in gastric cancer

J.-M. Kim, D. Y. Jo, H. J. Lee*
*Chungnam National University, Dept. of Pathology, Daejeon, Republic of Korea

Objective: To investigate the effects of the expression of the chemokine stromal cell-derived factor (SDF)-1α and its receptor CXCR4 on the prognosis of human gastric cancer, the clinicopathological features and the clinical outcomes were analyzed.
Method: The expression of SDF-1α and CXCR4 proteins were studied by immunohistochemistry in 221 specimens of primary gastric cancer.
Results: The patients were categorized into three groups according to the expression of CXCR4 and SDF-1α; high CXCR4/high SDF-1α, low CXCR4/low SDF-1α, and high CXCR4/low SDF-1α–low CXCR4/high SDF-1α. There were no significant differences in age, gender, histology, tumor location, lymphovascular invasion, or proportion of tumor size >5 cm between three groups. However, high CXCR4/high SDF-1α tumors were significantly associated with invasion depth of the tumor (T status, P=0.001), lymph node involvement (N status, P=0.029), and higher stage III/IV (P=0.001) compared with low CXCR4/low SDF-1α tumors and high CXCR4/low SDF-1α–low CXCR4/high SDF-1α tumors. Furthermore, the patients with high CXCR4/high SDF-1α expressions had worst prognosis (5-year survival rate, 26.7%; median, 2.2 years; range, 0.8–3.6 years), whereas patients who had low CXCR4/low SDF-1α expressions showed the most favorable prognosis (5-year survival rate, 57%; median, not reached; log-rank test, P = 0.01).
Conclusion: Thus, CXCR4 and SDF-1α are considered to be useful prognostic factors in gastric cancer, and the combination of high CXCR4 protein expression with high SDF-1α expression indicates a dismal prognosis.

0321

HER2 amplification and overexpression in gastric cancer: analysis of subtype specificity and optimal detection methods

C. Moelans, A. N. Milne, F. H. Morsink, R. Sitarz, W. P. Polkowski, R. Maciejewski, P. J. van Diest, G. J. Offerhaus*
*UMC Utrecht, Dept. of Pathology, The Netherlands

Objective: The recent ToGA trial indicates that Herceptin is a new, effective, and well-tolerated treatment for HER2-positive gastric cancer (GC). Current diagnostic methods to detect HER2 amplification and overexpression should be carefully evaluated. Furthermore, potential subpopulations of GC (intestinal vs diffuse, cardia vs distal, early-onset GC) should be evaluated for their frequency of amplification and overexpression.
Method: Tissue microarray (TMA) blocks of 108 early-onset GCs and 91 conventional GCs were stained with immunohistochemistry (IHC, Hercep test, DAKO) and chromogenic in situ hybridization (CISH, SPoT-Light, Invitrogen).
Results: Overall, there was 3% HER2 overexpression (5/199) and 5% (9/199) amplification. Furthermore, 1.5% of the patients showed a 2+ IHC score and 3.5% showed a low level CISH amplification. Early-onset GC showed a lower frequency of amplification/overexpression than conventional GC: no overexpression and 2% amplification versus 6% overexpression and 8% amplification. IHC and CISH showed 94% concordance. In 5 of 199 cases (2.5%), IHC showed clinically relevant heterogeneity not seen by CISH. Cardia tumors had more amplification and overexpression than distal tumors: 9% versus 3% and 7% versus 2%, respectively (NS). HER2 CISH showed more amplification in the intestinal type (7%) compared to the mixed (5%) and diffuse type (3%) GCs (p=0.03). A similar trend was seen for HER2 IHC and histology type (p=0.067).
Conclusion: This study reports lower amplification and overexpression frequencies than previously described but confirms previous studies showing different frequencies depending on the type and localisation of the GC. There was a lower amplification and overexpression frequency in early-onset GC and a lower heterogeneity rate by CISH compared to IHC.

0322

Alfa-metyl-acyl-CoA racemase (AMACR) expression in gastric cancer—prognostic factor or a dead end?

A. Mroz, Z. Lewandowski, M. Kiedrowski, J. Regula, K. Ptaszynski, W. Olszewski*
*CMKP, Gastroenterology & Hepathology, Warsaw, Poland

Objective: AMACR plays role in beta oxidation of branched fatty acids. It is expressed in several neoplasms like prostatic, hepatic and thyroid cancers. It is also believed to be expressed in gastric carcinoma (GC), particularly in better differentiated and less advanced lesions. The aim of the study was to assess AMACR expression in GC and its correlation with clinical and histological prognostic factors.

Method: Eighty-two consecutive GC cases (M/F 52:30, mean age 64.3 (30–81) were analyzed after a detailed histological and clinical reevaluation. Immunohistochemical staining was performed and the expression of AMACR was assessed semiquantitatively (0—no expression, 3—intensive, diffused expression). For statistical analysis, Fisher's exact test was used.
Results: There were 33:39:10 cases with glandular, diffused and mixed histology, respectively, according to Lauren classification. Thirty-three localized in antral part and 49 in corpus or fundus. AMACR expression was present in 49 GC (59%). No statistically significant correlation between AMACR expression and age, sex (p=0.63), localization (p=0.81), tumor histology (p=0.375) and differentiation, Lauren groups (p=0.27) or tumor staging (p=0.48) was revealed.
Conclusion: According to our results, the correlation of AMACR expression with the aforementioned parameters cannot be confirmed. Negative results might have been caused by low statistical power due to the limited number of patients. Therefore, its utility as prognostic factor needs further validation.

0326

Concordance of HER2 dual-color, dual-hapten in situ hybridization (DDISH) with fluorescence in situ hybridization on gastric carcinoma

I. Loftin, R. Miller, A. McElhinny, P. Roche, M. Padilla, J. Ranger-Moore, P. Wu*
*Ventana Medial Systems, Molecular Probes, Tucson, AZ, USA

Objective: It is well established that the HER2 gene, located on chromosome 17, is amplified in ~30% of breast cancer patients. Determination of HER2 gene amplification and/or protein overexpression dictates the eligibility of patients for Herceptin® (trastuzumab) therapy, a monoclonal antibody that targets HER2 and can significantly improve prognosis. Recent studies indicate that HER2 is overexpressed in a percentage of gastric cancers, and Herceptin also is a promising therapy for these patients. Thus, accurate diagnosis of HER2 status is required for breast and gastric patients. Here, a new fully automated, HER2/CHR17 dual-color, dual-hapten brightfield in situ hybridization method (DDISH) was compared with Dako HER2 FISH PharmDx Kit on gastric samples.
Method: Two hundred five invasive gastric carcinoma cases were evaluated with DDISH and FISH. A HER2 repeat-depleted, dinitrophenyl (DNP)-labeled probe targeted the gene and was detected with silver in situ hybridization. A digoxigenin (DIG)-labeled chromosome 17 probe was detected by an alkaline phosphatase-driven Red ISH detection. All assay steps, from deparaffinization through counterstaining, were fully automated and required ~12 h. HER2 SISH and CHR17 Red signals were enumerated using conventional light microscopy, the HER2/CHR17 ratio calculated, and the gene status compared to FISH.
Results: Overall concordance between the HER2/chromosome 17 DDISH assay and FISH was 94.5%.
Conclusion: The automated HER2 (DDISH) assay yielded excellent correlation with FISH. These data indicate that DDISH is a valuable diagnostic test for the determination of HER2 gene status in gastric carcinoma.

0328

A rare case of pyloric obstruction due to Brunner's gland hyperplasia

A.-M. Feritsean, G. Kalodimos, K. Koti, S. Divani, D. Koutarelos, E. Alexopoulou*
*General Hospital of Volos, Greece

Objective: Brunner's gland hyperplasia is a rare lesion, with fewer than 240 cases having been reported in the literature. It is considered to be a hamartoma, developing from the submucosal glands, usually in the first or second part of the duodenum. Most of the lesions described were polypoid and <2 cm in greatest diameter. Often, there is an association with peptic ulcer disease.
Method: We report the case of a 31-year-old man who presented with abdominal pain, vomiting and upper gastrointestinal bleeding. The anamnestic data showed chronic ulcer disease. He also was anaemic, with a slight raise in blood eosinophilia.
Results: The radiological examination of the upper gastrointestinal tract revealed pyloric stenosis due to a polypoid mass measuring 1 cm. Preoperative diagnosis of the mass could not be established. The mass was excised and at the same time a vagotomy with pyloroplasty (Finney) was performed. Brushing cytology of the surgical specimen revealed a great number of aggregated Brunner's glands without any atypia, as well as many lymphocytes. A frozen section was negative for malignancy. The histologic diagnosis was that of diffuse nodular Brunner's gland hyperplasia (hamartoma) accompanied by lymphocytic infiltration. The rate of cellular proliferation was low. During the postoperative period, there were no complications. A subsequent gastroscopy showed no pathologic findings, and the patient is well at present.
Conclusion: Our case is reported because of its rarity and the difficulties in preoperative diagnosis. The literature is also reviewed.

0329

East European picture of coeliac disease

M. Danciu, M.-S. Mihailovici, A. Plesa, D. G. Ciobanu Apostol, E. Morosan, C. Ungureanu, K. Rostami*
*UMF Gr T Popa Iasi, Dept. of Pathology, Romania

Objective: Although the autoimmune process targets mainly the intestinal mucosa, coeliac disease (CD) present with a variety signs and symptoms affecting any organ or tissue. Aim: The aim was to assess the clinical behavior of coeliac disease in a secondary care setting in Iasi Romania.
Method: From April 2002 to December 2009, 175 adults were screened for CD. Patients were referred because of malabsorption and classical gastrointestinal symptoms (chronic diarrhoea, abdominal pain, weight loss and iron deficiency anemia). The diagnosis was based on clinical presentation, serology including IgA EMA or IgA-tTGA and duodenal biopsy. Results of intestinal biopsy were classified according to the revised Marsh criteria 1999.
Results: Of the 175 subjects suspected cases, 91 underwent small bowel biopsy and 55 of 91 serology. The most common clinical presentation was weight loss in 60 of 91 and chronic diarrhoea and anemia in 78 of 91. Histology revealed microscopic enteritis (Marsh 0–II) in 43 of 91 and macroscopic lesions (Marsh IIIa–IIIc) in 48 of 91, respectively.
Conclusion: There are not many studies on the epidemiology, investigation or clinical behavior of CD in East European countries. Most of the cases in this study were diagnosed from 2005 onward, indicating increasing awareness on CD. Classical presentations were predominant and more prevalent compared to atypical forms of disease. This still may indicate a high threshold for performing serology and small bowel biopsies in cases with atypical presentations.

0330

Synchronous small intestinal inflammatory fibroid polyp and GIST

M. L. Caruso, A. M. Valentini, R. Armentano, M. Pirrelli*
*IRCCS, Pathologic Anatomy, Castellana Grotte, Italy

Objective: In the differential diagnosis of GIST, associated mesenchymal lesion represents an additional challenge.
Method: A 51-year-old woman with intestinal occlusion at surgery showed an ileal invagination on polypoid mass of 4 cm and an ileal suberosal nodule of 1 cm.
Results: The polypoid lesion, ulcerating the mucosa and growing in the muscular wall with subserosal hourglass-like expansion, showed a monotonous hypocellular mesenchymal proliferation ($CD34^+$, $CD117^-$) with prominent vascular network in myxoid inflammatory stroma. Considering the peculiar degenerative, inflammatory pattern of the polyp due to ischemia and the existence of a subset of GIST c-Kit negative, differential diagnosis was GIST ($c\text{-}Kit^-$) or inflammatory fibroid polyp ($CD34^+$). After a careful review of the clinical and immunohistochemical and pathological findings, final diagnosis was inflammatory fibroid polyp (IFP). The minor nodule showing a spindle cell proliferation ($CD117^+$) was diagnosed as GIST. To our knowledge, no other studies report IFP and GIST occurring synchronous in the ileum.
Conclusion: The correct definition of these lesions is crucial: Defining both tumors as GISTs, prognostic and therapeutic assessment becomes poor (multiple familial or advanced metastatic GIST). The recent discovery of PDGFR mutation (the mutually exclusive mutation of wild-type cKIT GISTs) in the IFP questions his reactive nature and raises the possibility of a neoplastic process. Then, the questions arising are whether the two tumors represent a fortuitous coexistence or involve the same carcinogenic agents on the same gene (located in the chromosome 4q) and if the proliferation can be inhibited by STI571.

0332

Colonic mantle cell lymphoma in situ: a report of a unique case

A. Galvao Neto, N. Shafi, P. Protiva, G. Oroszi, A. Sahakian*
*VA Healthcare System, West Haven, USA

Objective: Colonic mantle cell lymphoma (MCL) represents 1–4% of malignant tumors of the GI tract. They are extremely difficult to diagnose due to the small sampling size, immune hyperplastic responses which may mimic lymphoma, and very early phase of neoplasia.
Method: H&E-stained slides from 2007 were reevaluated. Immunohistochemical (IHC) stain for BCL1 (cyclin D1) was performed. H&E-stained slides and IHC stain for CD20, BCL1, CD5, kappa, lambda, CD19, CD20, CD5, CD10, and CD23 were evaluated. Flow cytometry was done on bone marrow and lymph node biopsy. FISH study for t(11;14) (q13,q32) was done.
Results: A 45-year-old man was admitted to the hospital in 2007 for a bright red blood per rectum (BRBPR). Colonoscopy showed rectal erythema thought to be prep-related. Random biopsies taken were signed out as colonic mucosal lymphoid aggregates and revised to MCL in situ upon reevaluation. In 2009, he was readmitted for BRBPR

and a 10-lb weight loss, lower abdominal discomfort, fatigue and soaking night sweats. Colonoscopy displayed mucosal edema in cobblestone pattern with erythema, ulcerations and a mass-like appearance of folds which were biopsied and signed out as MCL.
Conclusion: In situ MCL lymphoma is not a so well-recognized entity, much less in the GI tract where it has never been described before. We emphasize the need to be aware of GI lymphomas in general, specifically a rare entity such as in situ MCL, knowing that this may represent a disease in progress.

0333
Undifferentiated carcinoma versus acromic melanoma of rectum—case report

A.-A. Nicolau, M. Aschie, I. Poinareanu, A.-F. Mitroi, A. Chisoi, A. Iliesiu, G. Resul, J. Stanisici, M. Enciu, I. Aschie, A.-M. Cretu*
*Constanta, Romania

Objective: Gastrointestinal (GI) involvement by malignant melanoma is predominantly metastatic. The concept of primary malignant melanoma of the GI tract has been validated for lesions involving the esophagus, stomach, small bowel, and anorectum, (the most common site). The existence of primary melanoma of the large bowel is a controversial topic. Six cases of apparent primary colonic melanoma have been reported to date, two of which in the rectum.
Method: A 65-year-old Caucasian man presented in emergency following a massive rectal bleeding. Rectal examination revealed an anterior fleshy mass situated 4 cm from the anal verge. The patient said he had been bleeding intermittently for 4 months but without any pain or change in bowel habit. Rigid sigmoidoscopy demonstrated a polypoid lesion at the anorectal angle. The surgical specimen was analyzed macroscopically and microscopically using routine and immunohistochemical staining. Dermatological and ophthalmological examinations revealed no evidence of a cutaneous or an ocular primary lesion.
Results: Histopathologic examination on routine staining demonstrated undifferentiated malignant cells with pleomorphic nuclei and atypical mitosis, suggesting the possibility of an acromic melanoma or undifferentiated carcinoma. Immunostains for pancytokeratin, CEA and EMA were positive and showed negative reaction for HMB 45, S-100 and Melan-A, establishing the diagnosis of undifferentiated carcinoma.
Conclusion: Malignant melanoma of the anorectum is an uncommon condition. An expeditious diagnosis and care within a multidisciplinary team can have an important bearing on prognosis. Morphologically, the differential diagnosis of melanoma includes undifferentiated carcinoma, GIST, clear cell sarcoma, and epithelioid malignant peripheral nerve sheath tumor.

0334
Primary anorectal melanoma—immunohistochemical and genetic analysis

D. Ziak, J. Dvorackova*
*CGB Laboratory S.A., Ostrava, Czech Republic

Objective: Melanoma is a rare tumor of the anorectal area and accounts 0.1% to 1.7% of all anal tumours and approximately 1% of all primary melanomas. Besides the positivity with conventional melanocytary immunohistochemical markers S100, HMB45, Melan A are primary anorectal melanomas positive also with marker CD117 and negative with monoclonal antibody CEA. The primary anorectal melanoma is a typical BRAF mutation (exon 15+11) and the allelic loss NF1 associated with neurofibromatosis.
Method: The melanocytary lesion of a 79-year-old woman in the anorectal canal was examined with immunohistochemical antibodies: S100, HMB45, CK AE1/AE3, CD117 and monoclonal CEA (DAKO), and FISH method with the use of combined sound Vysis PREB1/LSI MYB/LSI CCND1/CEP 6 (Abbot, USA).
Results: Our examination stated positivity with S100, HMB45, Melan A and sporadic positivity with CD117 and negativity with monoclonal antibody CEA. Further, amplification of the gene RREB1 (locus 6p25) and CCND1 (locus 11q13) was found.
Conclusion: The results of our analysis confirm genetic abnormalities associated with melanoma, and our immunohistochemical analysis prefers primary melanoma before metastatic melanoma of the anorectal canal.

0336
Human crypt stem cell dynamics in familial adenomatous polyposis

D. de Boer, D. Langeveld, F. Morsink, J. Offerhaus, W. de Leng*
*UMCU, Dept. of Pathology, Utrecht, The Netherlands

Objective: Stem cells in the intestinal crypt are believed to be the target cells for the initiation of tumourigenesis and adenoma development. Macroscopic and histological normal-appearing colorectal mucosa of patients with symptomatic familial adenomatous polyposis (FAP) harbour cell kinetic and stem cell abnormalities, suggesting the exis-

tence of pre-tumour progression. Pre-tumour progression can be made visible by studying methylation patterns, or tags, in stem cells of the crypt where heterogeneity among these tags is a representation of a genetic drift and stem cell survival. Increased stem cell survival may be a predictive marker of an increased risk of neoplastic outgrowth. The objective of this study was to investigate potential biomarkers predictive of adenoma development; the focus lies on alterations in stem cell survival.

Method: DNA was isolated from laser-microdissected crypts of normal colonic FAP tissue and age-matched controls. DNA was bisulphite converted and methylation tags were created by amplifying the CpG islands in the CSX gene. Sequence analysis of this pool of methylation tags allows characterisation of the heterogeneity among the different tags recovered from multiple stem cell pools.

Results: The bisulphite treatment, with subsequent sequencing, showed a significantly ($p=0.030$) greater number of unique methylation tags for FAP patients (2.8 unique methylation tags) compared to control patients (2.1 unique methylation tags), which indicates enhanced stem cell survival.

Conclusion: This increased stem cell survival supports the idea of pre-tumour progression since longer lived stem cells have the potential to gain more mutations with higher risk to develop into a carcinoma.

0337

Colonic carcinogenesis induced by 1NC and PCNA and p53 expression

L. Carvalho, A. Alarcão, L. Teixeira, P. Sá, N. Coelho, P. Barreto, K. Cavalcanti, A. Cabrita*

*Faculdade de Medicina Coimbra, Dept. de Anatomia Patologica, Portugal

Objective: 1-Naphtyl *N*-methylcarbamate (1NC) is considered of low toxicity when applied according with the good practice rules. The evaluation of morphology and proliferation rates of experimentally induced adenocarcinomas by 1NC and DMH was tempted.

Method: Thirty Wistar 8-week male rats were distributed into three groups (ten rats each) submitted to dimethylhydrazine (DMH) 15 mg/week during 8 weeks (group II), 1NC 60 mg/l in drinking water for 8 weeks (group III), and without manipulation (group I). Killed at the end of the 28ª week, lesions were collected and FFPE, PCNA and p53 antibodies were applied to sections of all tumours by the streptavidin–biotin/HRP method.

Results: In groups II and III, lesions were exophytic (2–4 cm), well-differentiated adenocarcinomas, except for one case 1NC-induced a moderately differentiated adenocarcinoma. Proliferation rate—PCNA was higher in group III (1NC-induced): six negative cases in group II against three negative cases in group III; the cutoff: + (<25% positive nuclei), ++ (25–75%) and +++ (>75%), demonstrating five cases ++ and +++ in group III and one case +++ in group II (as the other three cases were +). For p53 nuclear immunostaining, six were positive in 1NC-induced cases against four by DMH.

Conclusion: Despite the small sample of this preliminary study, 1NC revealed to induce more aggressive adenocarcinomas with a higher proliferation rate when compared with the DMH, probably by apoptosis blockage. In general, macroscopic tumors were pediculated and developed from deep crypts where the functional stem cells pool is supposed to be.

0341

Tumor budding added to K-RAS analysis improves the individualized prediction of response to anti-EGFR therapies for metastatic colorectal cancer patients

I. Zlobec, F. Molinari, V. Martin, L. Mazzucchelli, P. Saletti, R. Trezzi, S. De Dosso, T. Vlajnic, M. Frattini, A. Lugli*

*University Hospital Basel, Institute of Pathology, Switzerland

Objective: Tumor budding or dedifferentiated single cells/small clusters at the invasive front of colorectal cancer is a histological feature highly predictive of lymph node and distant metastasis and an independent prognostic factor. We hypothesized that the evaluation of tumor budding could complement K-RAS analysis to improve the individualized prediction of response to anti-EGFR-based therapies in metastatic colorectal cancer (mCRC) patients.

Method: Forty-three patients with mCRC treated with cetuximab or panitumumab were entered into this study. According to the RECIST criteria, 30 patients had stable or progressive disease (non-responsive, NR), while 13 patients had a partial response (PR). Tumor buds were evaluated from whole tissue sections stained for pan-cytokeratin, evaluated in the densest region using a ×40 objective, and "high-grade" tumor budding was defined as 15 buds/high-power field.

Results: Tumor buds and K-RAS mutation both correctly classified 68% of patients. All patients with K-RAS mutation ($n=7$) or high-grade tumor budding ($n=11$) were NR, of which four patients had both features. All 13 PR were K-RAS wild type with low-grade tumor budding. Combined, the predictive value of K-RAS and tumor budding was 80%. Additionally, high-grade tumor budding was significantly related to worse

progression-free survival (HR (95%CI), 2.8 (1.3–6.0, p=0.008)).
Conclusion: The combined analysis of tumor budding and K-RAS mutational status accurately predicted response in 80% of patients. If confirmed on larger cohorts, the addition of tumor budding to K-RAS analysis may represent an effective approach for individualized patient management in the metastatic setting.

0342
Consensual proposal for centralized KRAS testing of patients with colorectal carcinoma in Slovakia
M. Kalman, L. Plank, Z. Lasabová, T. Burjanivová, G. Minarik, M. Konecný, Z. Bartošová, D. Ilencíková*
*Faculty Hospital Martin, Dept. of Pathology, Slovak Republic

Objective: Identification of gene KRAS somatic mutations (in codons 12, 13) represents accepted biomarker predicting resistance to EGFR inhibitors therapy in patients with colorectal carcinoma (CRC). It is expected that approx. 40% of patients with CRC show one of KRAS mutations. The objective was to develop a centralized programme of KRAS testing in bioptically examined both frozen and/or formalin-fixed paraffin-embedded CRC tissues.
Method: Inter-institutional and interdisciplinary cooperation (of pathologists, geneticians, molecular biologists and oncologists of all three centers) during the last 15 months based on mutual exchange of ideas, materials and laboratory protocols and common meetings and seminars. In the centres, the following three methodical options were tested—sequencing, RT-PCR (TheraScreen®) and SNaPshot multiplex analysis—and the results of the examinations were retested using another method to verify specificity and sensitivity of the testing.
Results: Numbers of tested cases/percentage of KRAS unmutated cases were the following: Center 1: n=290/59.3% unmutated cases, center 2: n=679/61% and center 3: n=841/65.4% of unmutated cases. Altogether, from 1,810 analyzed patients, 62.9% showed CRC with unmutated and 37.1% with mutated KRAS gene. The advantages and disadvantages of all methods tested were evaluated.
Conclusion: On the basis of the described programme, we have developed national guidelines for centralized KRAS testing of CRC in Slovakia, accepted by the authorities of the Ministry of Health and insurance companies. The main outcome of the programme is represented by a possibility offered to every patient with CRC to have the tumor tissue tested for KRAS mutations.

0343
Possible correlations of the K-ras gene mutational status in colorectal carcinoma
C. M. Ardeleanu, F. L. Cionca, G. Cardos, M. Mihai, A. G. Mihaela Georgescu, M. Stoicea, S. Enache, V. Enache, G. Butur*
*V. Babes National Institute, Dept. of Pathology, Bucharest, Romania

Objective: Gain-of-function K-ras point mutations, present in 20–40% of the colorectal carcinomas, maintain the active form of the ras p21 protein and lead to epidermal growth factor receptor (EGFR)-independent activation of intracellular signaling pathways, making the anti-EGFR tumor therapy ineffective. The aim of the present study was to identify possible correlations between the mutational status of the K-ras gene and the histopathological findings in patients with colorectal adenocarcinoma.
Method: We studied 34 patients with colorectal adenocarcinoma (30) or liver metastases of colorectal adenocarcinoma (4; male/female, 19:15; age range, 34–87; average age 61). The formalin-fixed paraffin-embedded tissue samples were analyzed using an indirect bistadial immunohistochemical (IHC) technique, performed with a Dako EnVision+ Dual Link System-HRP, with antibodies for the EGFR and the ras protein. Mutations in exon 2 and codon 12 of the K-ras gene were detected by PCR–restriction fragment length polymorphism analysis, with *Mva*I restriction enzyme.
Results: K-ras mutations were present in 23.52% of the cases, seven adenocarcinomas and one liver metastasis. EGFR was positive in ten cases in tumor cells and in seven cases in the vessels. Immunohistochemical overexpression of ras protein was detected in 15 samples. The relationship between the positivity of the K-ras mutation and the positive immunohistochemical reaction for EGFR and the ras protein did not reach statistical significance.
Conclusion: There were no significant correlations between the mutational status of the K-ras gene and the IHC reaction for EGFR and ras p21 protein, proving once more the major role of molecular analyses in colorectal carcinoma anti-EGFR therapy.

0344
Abnormal expression of MUC2 associated with p53 overexpression in colorectal carcinomas
M. Bamba, S. Takemura, R. Kushima, K.-i. Fukuda, M. Masuyama, T. Shigematsu, T. K. Kobayashi, H. Sugihara*
*Saiseikai Shiga Hospital, Dept. of Pathology, Ritto, Japan

Objective: We reported a case of the colonic choriocarcinoma, of which the accompanying intramucosal adenocarcinomatous area consisted of two components: One revealed normal supranuclear expression of MUC2, and the other revealed abnormal cytoplasmic expression of MUC2 and overexpression of p53 due to a point mutation in exon 5 of TP53. It is thus possible that overexpression of p53 is related to abnormal expression of MUC2 during progression of colonic choriocarcinoma. To investigate whether this relation is seen generally, we examined expressions of p53 and MUC2 in colorectal adenocarcinomas.
Method: This study was based on the analysis of 31 surgically and endoscopically resected colorectal carcinomas. H&E and immunohistochemical stainings with the monoclonal antibodies p53, MUC2 and CDX2 were carried out.
Results: All areas of 12 lesions and a part of two lesions revealed overexpression of p53 (45.2%). For CDX2, the nuclei of cancer cells were positive diffusely in 29 lesions and partially in one lesion. The remaining one lesion showed an abnormal, dot-like cytoplasmic staining pattern. For MUC2, cancer cells were negative or weakly positive in 28 lesions and abnormally positive in five lesions (16.1%). Three out of 31 lesions revealed not only overexpression of p53 but also abnormal expression of MUC2 (9.7%).
Conclusion: In this study, colorectal adenocarcinomas with overexpression of p53 and abnormal expression of MUC2 were relatively rare. Therefore, such a pattern of p53 and MUC2 expressions may be specific to colonic choriocarcinoma, possibly related to the occurrence of a choriocarcinomatous component from the background adenocarcinoma.

0345

Mismatch repair proteins expression and BRAF V600E mutation analysis in a subset of CCR patients under 50 years

*A. Luevano**
*Hospital Universitario, Dept. of Anatomic Pathology, Monterrey, Mexico

Colorectal carcinoma (CRC) is a worldwide common malignancy, with a rise over the last years. Fifteen percent of all CRC have microsatellite instability (MSI) due to alterations in mismatch repair (MMR) genes. Germline mutations occur in 5%. Sporadic MSI CRC (15%) have hypermethylated MLH-1 promoter. BRAF V600E mutation exclusively occurs in sporadic MSI CRC. Immunohistochemistry detects MSI cases with high concordance with microsatellite analysis.

Objectives: The objective was to compare histopathology and patterns of expression of MMR proteins and BRAF V600E mutation in patients below and over 50 years old and determine if age is a risk factor for defective MMR protein expression and BRAF mutations.
Methods: One hundred six patients <50 years were retrieved. Clinocopathological data were collected. MLH1 and MSH2 immunohistochemistry and BRAF RT-PCR mutation were performed in 48 <50 years and 48 patients >50 years as control group. Student's t test, χ^2 and logistic regression analysis were carried out
Results: Medullary and mucinous types were more frequent among young patients, intestinal type in older patients. No differences were noticed regarding clinicopathological stages between groups. MMRP expression was absent more frequently in <50 and MSH2 was negative in 13.8% of these patients. No BRAF mutations were detected on any group.
Discussion: We found an association between young age and defective MMR expression (OR 4.28). MSH2 lack of expression is more frequently due to a germline mutation. The fact that none of our patients had BRAF mutation could be partly due to the small sample size or alternate V600E or K-ras mutations.

0347

Expression of E-cadherin and beta-catenin in primary and metastatic foci of colorectal carcinoma. Correlation with selected clinical and morphological parameters and the assessment of its prognostic value

R. Peksa, R. Rzepko, A. Nalecz, A. Zawrocki, W. Biernat*
*Medical University of Gdansk, Dept. of Patomorphology, Poland

Objective: Colorectal carcinoma is the second most often diagnosed malignant neoplasm in Poland, being the second most common malignancy causing death among men and the third among women. Staging is one of the most important prognostic factors. Patients with tumor invading the whole thickness of bowel wall without lymph node metastases have 5-year survival rates between 70% and 80%. With additional lymph node metastases, the 5-year survival rate is much shorter, between 25% and 50%. Currently, the new prognostic factors such as adhesion molecule expression are extensively studied, which potentially may influence further treatment. Aims: (1) Comparative assessment of E-cadherin and beta-catenin expression in primary and metastatic foci of colorectal carcinoma and (2) correlation with selected clinical and morphological parameters, study of survival time and the assessment of its prognostic value.

Method: One hundred twenty-nine patients after surgery with stage III (106) and IV (23) colorectal carcinoma were qualified to this investigation. The expression of the E-cadherin and beta-catenin was studied by immunohistochemistry in primary and metastatic foci.
Results: E-cadherin was expressed in 60.5% while membranous staining of beta-catenin was reduced in 38.7% of primary tumors. In lymph nodes, 72.8% and 70.5% of metastatic tumors were positive for E-cadherin and membranous beta-catenin staining, respectively.
Conclusion: E-cadherin expression was correlated with membranous beta-catenin expression in the primary tumor and in the lymph node metastases. Expression of E-cadherin correlates with the larger amount of neoplastic stroma. No correlation was found between survival time and the expression of E-cadherin and beta-catenin in primary and metastatic foci of colorectal carcinoma.

0348

Comparison of transforming growth factor Beta 1 with GLUT-1 and bak in human colorectal cancers

A. Wincewicz, S. Sulkowski, M. Koda, M. Baltaziak, L. Kanczuga-Koda*
*Medical University Bialystok, Dept. of Pathology, Poland

Objective: Transforming growth factor beta1 (TGF-beta1) is a crucial agent in colorectal carcinogenesis which interferes in growth signaling pathways of intestinal cells and adjacent immune cells. We aimed to evaluate relations among TGF-beta1, a cytoprotective and hypoxia-induced protein–glucose transporter 1 (GLUT-1) and proapoptotic protein Bak in human colorectal cancer.
Method: Expressions of TGF-beta1, GLUT-1 and Bak were detected by immunohistochemistry in 108 primary tumors of colorectal cancers.
Results: Immunoexpression of TGF-beta1 was observed both in the cytoplasm of cancer cells and adjacent inflammatory cells. GLUT-1 was visualized in membranous fashion and Bak was detected in the cytoplasm of malignant cells. Cancer immunoreactivities to TGF-beta1 correlated with GLUT-1 ($p>0.001$, $r=0.355$) and Bak ($p=0.001$, $r=0.320$) in all patients and subgroups of different clinical and pathological traits. TGF-beta1 of immune cells failed to associate significantly with GLUT-1 and Bak expressions in cancer cells.
Conclusion: The accumulation of TGF-beta1 cancer expression is associated with augmentation of apoptosis highlighted by Bak immunostaining and with increase of glucose uptake marked by higher index of GLUT-1-positive cancer cells. Diversity of Bak and GLUT-1 association with TGF-beta1 depends on the origin of TGF-beta1 expression and probably reflects different impacts of TGF-beta1 on malignant cells and immune cells.

0349

Expression of E2F1 and prognosis of patients with Astler–Coller stage B2 and C colorectal cancer treated with 5-FU-based adjuvant chemotherapy

V. Sulzyc-Bielicka, P. Domagala, D. Bielicki, K. Safranow, W. Domagala*
*Pomeranian Medical University, Szczecin, Poland

Objective: E2F1 affects the genes coding thymidylate synthase, which is the main molecular target for 5-fluorouracil. The aim of the study was to assess the association of E2F1 expression in Astler–Coller stage B2 and C colorectal cancer (CRC) cells with survival.
Method: Nuclear E2F1 was detected by immunohistochemistry on tissue microarrays from 259 CRCs. One hundred ninety-two patients received adjuvant chemotherapy.
Results: High expression of E2F1 was found in 37.5% of CRCs. It was more commonly found in B2 group as compared with group C ($p=0.01$). High expression of E2F1 was associated with worse overall survival (OS, $p=0.028$) in stage B2+C group of patients. Low expression of E2F1 was associated with better OS in the whole B2 group ($p=0.039$) and in B2 subgroup not treated with chemotherapy ($p=0.035$).
Conclusion: The expression of E2F1 may have prognostic significance in stage B2 group of patients, but not in the group of patients treated with chemotherapy. This work was supported by grant KBN 2P05B 174 28.

0350

Liver regeneration and its clinicopathological impact

J. G. Tralhão, A. Abrantes, B. Oliveiros, D. Cardoso, M. F. Botelho, F. Castro-Sousa*
*Coimbra Faculty of Medicine, Dept. of Surgery, Portugal

Objective: To our knowledge, this study is the first concerning human liver regeneration (HLR) evaluated by the hepatic extraction fraction (HEF) calculation using radioisotopic methods. We studied the HEF as an indicator of HLR of patients who underwent hepatectomy (HR).
Method: Ninety-five patients with colorectal metastases ($n=69$), hepatocellular carcinoma ($n=16$) and other tumors ($n=10$) were included. Thirty-five underwent major hepatectomy (MAHR) and 63% minor hepatectomy (miHR). HLR was assessed after intravenous bolus injection of ^{99m}Tc-Mebrofenin. In this study, we evaluated the preoperative HEF (T0) and in the fifth day (T5) and

1 month after HR (T30). HEF values of 98.8±0.4% were normal.
Results: In the overall patient population, the mean HEF values in our series were 97.3±9.6% for T0, 97.5±8.3% for T5 and 98.7±4.1% for T30 (ns). Related to the subgroup of 35 patients treated by MAHR, the HEF values were 97.2±5.3% (T0), 95.6±12.6% (T5) and 98.9±1.8% (T30) (ns). For the 60 patients who underwent miHR, the HEF values were 97.4±11% (T0), 98.8±2.4% (T5) and 98.6±4.7% (T30) (ns).
Conclusion: Our results strongly support the concept that the HLR is early enough to normalize the HEF at day 5 after HR. We have demonstrated that HLR is early, fast, non-anatomical and functionally complete 5 days after liver resection. This fast functional liver recovery has high clinical importance because considering this quick functional recovery, adjuvant chemotherapy can begin much earlier after surgical resection than the 3 week's dogma.

0351
Clinical and histopathological study of nonalcoholic steatohepatitis

M. Comanescu, V. Comanescu, C. Popescu, M. Popescu*
*University Emergency Hospital, Dept. of Anatomic Pathology, Craiova, Romania

Objective: Non-alcoholic steatohepatitis (NASH) is a liver injury characterized by a spectrum of histological alterations which closely resemble alcoholic hepatitis steatosis, but occur with no significant alcohol consumption. The aim of the study was to examine the relationships between the degree of hepatic steatosis and various histological features of the accompanying hepatitis.
Method: In our study, we included 75 liver biopsies of patients aged between 38 and 64 years. Because clinicopathological correlation is essential in the diagnosis of NASH, we included in our study only patients with a complete report: clinical data (gender, age, BMI and associated diseases) and results of laboratory tests.
Results: Out of 463 consecutive liver biopsies, 75 showed steatosis, hepatocyte injury (ballooning degeneration, necrosis), lobular inflammation, with or without pericellular fibrosis and Mallory bodies, all consisting with the diagnosis of NASH. Mild, moderate and severe steatosis was present in 21, 46 and 8 cases, respectively. Cirrhosis was present in five cases, and 11 cases showed severe necro-inflammatory activity. The cases with moderate and severe steatosis were more often associated with higher degrees of necroinflammatory activity and fibrosis. Lesions were zone 3 predominant (centrilobular region). A Perls' Prussian blue stain for iron was positive in six cases. We performed multifactorial analysis of the cases establishing correlations between histological (activity, fibrosis and steatosis) and clinical data.
Conclusion: The increasing prevalence of NASH and the lack of standardized diagnostic criteria confirm the need of more studies to define a strategy of approach of this important liver disease.

0353
GFAP, SMA and CK7 expression in liver biopsies with chronic B and C viral hepatitis

E.-Z. Emeric, I. Egyed-Zsigmond, I. Jung, G. Lorincz-Marton, D. Georgescu, S. Gurzu, T. Mezei*
*UMF, Dept. of Pathology, Targu-Mures, Romania

Objective: Hyperplasia of quiescent or activated stellate cells and also oval cells reflects the reactive changes leading to fibrosis in liver tissue.
Method: A retrospective comparative study between chronic B and C viral hepatitis using GFAP, SMA and CK7 antibodies was performed. We have analyzed portal and/or lobular localization and quantified the intensity of those cells which were marked by these antibodies.
Results: Our study included 100 cases, 50 with chronic B and 50 with chronic C viral hepatitis. In chronic B viral hepatitis, we observed a high lobular and portal reactivity which was marked only by SMA. In chronic C viral hepatitis, high expression of CK7, GFAP and SMA was revealed by portal areas.
Conclusion: The reactive changes observed in biopsy specimens provided by patients selected for biopsy examination seem to have greater importance in C than B viral chronic hepatitis regarding a successful antifibrotic treatment.

0355
Impact of hepatic artery selective clamping in hepatocellular function

J. G. Tralhão, A. Abrantes, C. Gonçalves, B. Oliveiros, D. Cardoso, A. B. Sarmento, M. F. Botelho, F. Castro-Sousa*
*Coimbra Faculty of Medicine, Dept. of Surgery, Portugal

Objective: Hepatic pedicle triad occlusion is often used to prevent bleeding during hepatectomy despite the ischemia and reperfusion liver injury iatrogenically induced. This study aimed to estimate the impact of selective clamping of the hepatic artery (SCHA) in hepatocellular function.
Method: (1) Forty Wistar rats were divided into four groups: three groups were subjected to a SCHA ischemia period for 60 min: (A (n=13) submitted to a continuous SCHA; B (n=13) underwent an intermittent SCHA for

30 min with 5 min of reperfusion; C (n=6) underwent an intermittent SCHA for 15 min with 5 min of reperfusion)) and group D (n=8) without SCHA. (2) Determination of liver blood markers and hepatic extraction function (HEF) using ^{99m}Tc-mebrofenin 3 days before and after surgery. (3) Isolation of hepatocytes from the biopsy performed after surgery to evaluate oxidative stress (DCFH2-DA), characterization of cell death (annexin-V/propidium Iodide) and assessment of mitochondrial membrane potential (JC-1 probe) by flow cytometry.
Results: (1) There was significant increase of blood markers before and after SCHA, but without differences between groups (ns). (2) HEF maintained normal values without differences between groups (ns). (3) There were no significant differences in viability and in the type of cell death, as well as in the production of reactive oxygen species between groups (ns).
Conclusion: The SCHA compared to previous studies performed by us where total hepatic pedicle triad was clamped shows an increase of cell viability with a decrease of hepatocyte necrosis and/or apoptosis. SCHA is a potential alternative to decrease preoperative bleeding, maintaining hepatocellular function.

0356

Impact of selective portal vein clamping in hepatocellular function in the murine model

J. G. Tralhão, A. Abrantes, C. Gonçalves, C. Carvalho, B. Oliveiros, D. Cardoso, A. B. Sarmento, M. F. Botelho, F. Castro-Sousa*
*Coimbra Faculty of Medicine, Dept. of Surgery, Portugal

Objective: The selective portal vein clamping (SCPV) is a potential alternative to decrease preoperative bleeding, maintaining hepatocellular function. This study aimed to evaluate the effect of SCPV in hepatocellular function.
Method: (1) Fifty-two Wistar rats were divided into four groups: Three groups of animals were submitted to a SCPV ischemia period for 60 min (A (n=21) was submitted to a continuous SCPV, B (n=12) underwent an intermittent SCPV for 30 min with 5 min of reperfusion, C (n=10) underwent SCPV for 15 min with 5 min of reperfusion)) and group D without SCPV (n=9). (2) Determination of liver blood markers and hepatic extraction function (HEF) using ^{99m}Tc-mebrofenin 3 days before and after surgery. (3) Isolation of hepatocytes from the biopsy performed after surgery to evaluate oxidative stress (DCFH2-DA), characterization of cell death (annexin-V/propidium Iodide) and assessment of mitochondrial membrane potential (JC-1 probe) by flow cytometry.
Results: (1) Mortality: A—62%, B—17%, C—30% and D—0% (p<0.03). (2) There was a statistically significant increase of the AST values (p<0.025) and LDH (p<0.002), but without differences between groups (ns). (3) HEF significantly decreased (p<0.0001), but without differences between groups (ns). (4) There were no significant differences in viability and in the type of cell death or in the production of reactive oxygen species between groups (ns).
Conclusion: The SCPV compared to previous studies performed by us where total hepatic pedicle triad was clamped shows an increase of cell viability with a decrease of hepatocyte necrosis and/or apoptosis. However, SCPV above 30' should be avoided given the high mortality observed.

0357

Oxidative stress and liver morphology of rats received doxorubicin and tirapazamine

E. Korobowicz, I. Syroka, J. Dudka, A. Korga, R. Gieroba*
*Uniwersytet Medyczny w Lublini, Katedra i ZakBad Patomorfologi, Poland

Objective: Tirapazamine (TPZ) selectively kills hypoxic tumor cells. Doxorubicin (DOX) is one of the most effective drugs against a wide variety of cancers. It is widely accepted that oxidative stress is involved in DOX organ toxicity. TPZ, similarly to DOX, is activated to TPZ free radical by the action of several NADPH-dependent reductases and generate reactive oxygen species. NADPH is also an essential cofactor for glutathione-dependent enzymes that constitute major cellular defenses against oxidative damage. Aim: The aim of the study was to evaluate oxidative stress and liver morphology changes in rat that received TPZ in addition to DOX administration.
Method: Male Wistar rats were treated i.p. with DOX (1.8 mg/kg b.w.) and TPZ (5 or 10 mg/kg b.w.) weekly for 6 weeks. Seven days after the last treatment, animals were killed and liver samples were analyzed for NADPH, MDA, GSH levels and histopathological changes. Blood samples were analyzed for ALT, AST activities and bilirubin concentration.
Results: ANOVA test revealed significant higher levels of NADPH and MDA in liver in group receiving a higher dose of TPZ with DOX vs. DOX group. There were no differences between group TPZ+DOX vs. DOX of liver GSH concentration and plasma ALT activity, but levels of GSH and ALT in all these groups were significantly higher compared to control. Microscopically, hydropic degeneration, necrosis, inflammatory cell infiltration and vascular lesion were observed in TPZ+DOX group.
Conclusion: Tirapazamine causes oxidative stress in liver of rats receiving DOX. This study suggests enhanced toxicity by TPZ in rat livers which received DOX.

0358

The influence of tetraiodothyronine-supplemented diet on selected redox equilibrium markers and liver morphology in rats treated with doxorubicin

E. Korobowicz, A. Korga, J. Dudka*
*Uniwersytet Medyczny w Lublini, Katedra i ZakBad Patomorfologi, Poland

Objective: The toxicity of doxorubicin results from reactive oxygen species generation. ROS production depends on tissue-specific enzymatic performance. Liver is an organ that is characterized by very intensive activity of these enzymes. As a result, redox equilibrium disorders may appear. Moreover, changes in thyroid hormone concentrations are accompanied by ROS production. Thus, disorders in iodothyronine hormones status may result in the intensification of doxorubicin-induced oxidative stress. Aim: The aim of this study was to evaluate the influence of DOX and T4-associated treatment on selected redox equilibrium markers and histopathological evaluation of the liver.
Method: Rats were treated with DOX (.5 mg/kg, i.p.) once a week for 10 weeks. Apart from DOX, thyroxin was simultaneously given in drinking water 0.2 and 2.0 mg/l, respectively. The concentration of lipid peroxidation products—malondialdehyde (MDA) and total glutathione—were measured in liver homogenates. Liver morphology was evaluated in H+E and PAS diastase staining.
Results: Higher levels of MDA in liver of all tested groups and at the same time in rats treated with DOX plus T4 lower concentrations of total glutathione compared to control were observed. Morphological evaluation of liver did not show any symptoms of necrosis and steatosis, but a decrease in glycogen content in DOX+T4 group compared to DOX treatment was noticed.
Conclusion: Thyroxin supplementation causes redox equilibrium disorders and oxidative stress in liver of rats receiving DOX. The study revealed the normalizing influence of thyroxin on glycogen deposits that were observed after doxorubicin treatment.

0359

Dysadherin expression in human hepatocellular carcinoma: preliminary results

E. Papageorgopoulou, M. Paleologou, V. Fatourou, E. Felekouras, E. Antoniou, Y. Ino, S. Hirohashi, C. Kittas, I. Delladetsima, D. Tiniakos*
*Medical School,University of Athens, Greece

Objective: Dysadherin is a cancer-associated cell membrane glycoprotein that inhibits cell–cell adhesion. In many types of cancer, dysadherin is related to decreased E-cadherin expression, promotes metastasis and is an independent predictor of poor patient survival. Dysadherin expression in human hepatocellular carcinoma (HCC) has not been studied to date.
Method: We studied by immunohistochemistry 70 HCC (grade I, 11; II, 28; III, 24; and IV, 7) from 70 patients (M/F 3.5, mean age 65.7 range 45–85 years) with monoclonal antibodies specific for dysadherin (clone NCC-M53) and E-cadherin (clone 36/E-cadherin). Immunostaining of inflammatory and endothelial cells was used as internal positive control for dysadherin (DYS) expression.
Results: Non-neoplastic hepatocytes and cholangiocytes were DYS-negative. In neoplastic cells (NC), DYS-specific immunostaining was mainly membranous, while some cases showed additional NC cytoplasmic positivity. The majority of HCC (43/70, 71.4%) had 0–9.9% DYS (+) NC, 18.6% (13/70) showed 10–50% (+) NC, while 10% (7/70) had >50% (+) NC. DYS expression was negatively correlated with E-cadherin expression ($p<0.05$), while a positive statistically significant correlation was observed between strong DYS immunostaining (>50%+NC) and tumour grade ($p<0.05$). There was no correlation with tumour size, vascular invasion or other clinicopathological parameters examined.
Conclusion: Normal hepatocytes and cholangiocytes do not express dysadherin. In HCC, increased dysadherin expression is observed in approximately one third of the cases; it is more extensive in high-grade tumours and is related to decreased E-cadherin expression.

0363

Klippel–Trenaunay syndrome with clinical presentation as metastatic liver disease: a case report

S. Stadlmann, D. Lenggenhager, R. A. Kubik-Huch, J. H. Beer, G. Singer*
*Kantonsspital Baden, Institute of Pathology, Switzerland

Objective: Klippel–Trenaunay Weber syndrome (KTWS) is a rare congenital malformation characterized by hemangiomata, varicose veins and bone and soft tissue hemihypertrophy. KTWS can include additional vascular and lymphatic system abnormalities in various organs, but involvement of the liver is rare. We report a case of KTWS simulating metastastic liver disease.
Method: A 39-year-old male with KTWS presented with a tumor mass in the right abdomen. Ultrasonography revealed a 15-cm cystic abdominal tumor and additional hypodense lesions in liver segments I, II, and VIII. A CT scan additionally showed multiple hypodense lesions in the spleen, peritoneum, lung, right scrotum, soft tissue and enlarged abdominal lymph nodes, highly suspicious for metastatic disease.

Results: Laboratory data values were: gammaGT 90 U/l (normal 10–71), LDH 765 U/l (normal 240–480), albumin 29 g/l (normal 34–48), and alpha feto-protein 121.6 μg/l (normal <7). Histopathology of the cystic abdominal tumor mass showed a complex vascular malformation of lymphangioma–hemangioma type. Evaluation from two different tumorous liver lesions revealed nodular hepatic tissue separated by fibrous septa with reactive ductules and atypical vessels, consistent with multiple focal nodular hyperplasia (FNH) in the setting of KTWS.
Conclusion: The spectrum of KTWS can include arterial and lymphatic system abnormalities beyond the classical manifestation. Our findings support the concept that multiple FNH characteristically occurs in a syndromic form and is induced by an irregular blood supply in the liver, with localized hyperperfusion leading to reactive nodular proliferation of liver tissue.

0364

Microscopic evaluation of metaplastic and dysplastic changes in the mucous of the gallbladder

D. Lacka, A. Nasierowska-Guttmejer*
*CSK MSWiA, Zaklad Patomorfologii, Warsaw, Poland

Objective: In the intra- and extrahepatic biliary ducts, precancerous changes such as hyperplasia, metaplasia and dysplasia are diagnosed. In the gallbladder, cholecystitis chronica is diagnosed often with a disregard of the features of hyperplasia and metaplasia. Generally accepted markers of precancerous changes of the gallbladder and biliary ducts are still to be found. Aim: The aim was to define the accumulation of TP53 protein and MIB1 activity in hyperplasia, metaplasia and dysplasia of the mucous membrane of the gallbladder.
Method: The material comprises 325 gallbladders operated by laparoscopy and fixed in formalin. Specimens were embedded in paraffin. In the microscopic sections with hyperplasia, metaplasia and dysplasia immunohistochemical stainings for TP53 and MIB1 were done along with mucycarmin and PAS with Alcian blue stainings (mucous presence).
Results: The histopathologic diagnosis revealed 295 cases (91%) of chronic calculous cholecystitis, 23 cases of acute inflammation and secen cases of cancer. Hyperplasia, metaplasia or dysplasia were found in 44 cases (13.5%) with chronic inflammation and accounted for hyperplasia without metaplasia—26 cases, pseudopyloric or intestinal metaplasia—16 cases, dysplasia—2 cases. Mucous stainings confirmed the presence of pseudopyloric and intestinal metaplasia, which helped distinguish them from adenomyosis focuses. IHC confirmed the accumulation of TP 53 protein and proliferative activity in metaplasia and dysplasia of the mucous membrane.
Conclusion: Mucous stainings and positive TP53 and MIB1 reactions suggest that metaplasia and dysplasia of the mucous membrane of the gallbladder can be classified as intraepithelial neoplasia changes. More research should be done.

0365

Correlation of clinical and histopathologic features of hepatocellular carcinomas diagnosed in hepatectomy specimens

G. Bulbul Dogusoy, N. Bassullu, I. Turkmen, Y. Tokat, O. Yaprak, Y. Yuzer, M. Dayangac*
*Istanbul Bilim University, Dept. of Pathology, Turkey

Objective: We aimed to investigate the relationship between the findings in total or partial hepatectomy specimens.
Method: One hundred six cases were collected who had total transplantation or partial hepatectomies because of liver cirrhosis (LC), HCC or other hepatic disorders from the archives. Then, clinical, histopathologic features and serologic findings of the cases were reviewed. The relationship between the histopathologic features and endoscopic, clinical and serologic results were investigated statistically using comparison tests.
Results: For the last 2-year period, data from 106 patients who underwent transplantation or hepatectomy were collected. Ninety-five had total, ten had partial hepatectomies, and one had metastasectomy. After the gross and microscopic examination, 86 cases were diagnosed as LC, 32 had HCC, three had parasitic cystic disease and ten had other unusual diseases. Among LC cases, 34 had hepatitis B virus (HBV), seven had hepatitis C virus (HCV), three had mixed virus etiology, six were alcoholic and 14 were due to other causes. Among LC patients, 32 had HCC. Fourteen cases were found to have one, seven had two and 11 had more than two tumors. Twenty-two of the HCCs were located in the right, while nine had tumors in the left and right; one case had tumors in the right, left and caudate lobe.
Conclusion: The results demonstrated that the most common hepatic disorder was cirrhosis due to HBV in the hepatectomy specimens and HCC seen in one third of them. Studies with follow-up and response to therapy will form the basis of our future projects.

0366

Metastatic solid pseudopapillary tumor of the pancreas. Experience at Hospital Clinic, Barcelona, Spain

M. Cuatrecasas, S. Hakim, M. Cubel, J. A. Bombi, M. A. Lopez Boado, J. R. Ayuso, J. Ferrer, L. Fernandez Cruz, J. Maurel*

*Hospital Clinic Barcelona, Dept. of Pathology, Spain

Objective: Solid pseudopapillary tumor of the pancreas (SPTP) represents 1–2% of pancreatic tumors, it affects young women, and surgery is the treatment of choice. Histologic features include loosely cohesive, relatively uniform polygonal cells surrounding delicate capillary-sized blood vessels. Most tumors are positive for beta-catenin, CD10, progesterone receptors and neuroendocrine markers. Mutations in the beta-catenin gene are frequent. Although considered benign, they are currently classified as low-grade malignant epithelial neoplasms.
Method: A 31-year-old woman presented with abdominal pain. A tumor in the pancreatic head with liver metastasis is diagnosed by TC. Fine needle aspiration cytology is diagnostic of SPTP. We reviewed four more cases of SPTP.
Results: All five tumors occurred in women <50 years old that presented with abdominal pain or asymptomatic. Tumors ranged from 1.4 to 18 cm. Four were located in the tail and one in the pancreatic head. All patients underwent surgery with negative margins. One patient had hepatic and nodal metastases as well as lymphatic and perineural invasion. All tumors were positive for CD56 and CD10, three for progesterone receptors. None of the patients presented tumor recurrence (2 months to 14 years).
Conclusion: Solid pseudopapillary tumor of the pancreas should be included in the differential diagnosis of pancreatic masses. Surgery is usually curative and should also be attempted in rare cases with an aggressive behaviour. Despite the characterization of the morphologic and molecular features of this enigmatic neoplasm, more work is needed to uncover its cell of origin and true histogenesis.

0368

Serous cystic neoplasms of the pancreas. Histopathologic study of 31 cases

J. Pajak, L. Liszka, E. Zielinska-Pajak, S. Mrowiec, D. Golka*

*Medical University of Silesia, Dept. of Histopathology, Katowice, Poland

Objective: Serous cystic neoplasms (SCN) are rare pancreatic tumors. The aim of the study was to describe histopathological characteristics of 31 SCN diagnosed in a single center during a 20-year-long period.
Method: Pathological reports including macro- and microscopic descriptions of SCN cases as well as routine slides were retrieved from institutional databases (1989–2010) and retrospectively reevaluated. Only cases with available original slides were included in the study.
Results: Several clinicopathologic SCN subtypes were distinguished: 25 serous microcystic adenomas (80.6%), five serous oligocystic and ill-demarcated adenomas (16.1%) and a single case of microcystic adenoma coexisting with multiple serous cysts in von Hippel–Lindau patient (3.2%). There were 25 females (80.6%) and six males (19.4%). Median patients' age was 63 years (range 31–93 years). Fifteen cases (48.4%) were localized in the head of the pancreas, 11 (35.5%) in the pancreatic body, and five (16.1%) in the tail. Median tumor diameter was 4.0 cm (range 1–12 cm, the diameter of three tumors was not known). Eleven cases (35.5%) were diagnosed in pancreaticoduodenectomy specimens, six (19.4%) in middle segment pancreatectomy specimens, and four (12.9%) in distal pancreatectomy specimens. Six cases (19.4%) were enucleated, two cases (6.4%) were diagnosed in open biopsy and two (6.4%) cases were found during autopsy.
Conclusion: SCN is found in middle-aged or older patients, mainly women. SCN may be localized in each pancreatic segment and grow to large masses. The reasons for preferential existence of SCN in females remain unknown.

0369

P53, Ki-67, CD 117 expressions in gastrointestinal and pancreatic neuroendocrine tumors and the evaluation of these tumors with clinicopathological and prognostic parameters

E. Kimiloglu Sahan, N. Erdogan, S. Ceylan, I. Ulusoy*

*Taksim Training Hospital, Dept. of Pathology, Istanbul, Turkey

Objective: Gastrointestinal and pancreatic neuroendocrine tumors (GEPNETs) originate from the cells of the diffuse endocrine system. Their molecular genetic mechanism of development and progression is complex and remains largely unknown. The purpose of this study was to review the gastrointestinal and pancreatic neuroendocrine tumors and to investigate these tumours with an emphasis on their clinicopathological characteristics.

Method: Twenty-one patients were reviewed and classified as well-differentiated neuroendocrine tumor, well-differentiated endocrine carcinoma and poorly differentiated endocrine tumor. We performed immunohistochemistry to characterise the expression of the immunoreactivity for synaptophysin, chromogranin, p53, Ki67 and CD 117.
Results: Mean age of the 21 patients was 43.86 ± 3.78. Thirteen (61.9%) of the patients were males and eight (38.1%) of the patients were females. The method of statistics we used was SPSS 11.0. According to Spearman's correlation test, there was a good correlation between Ki-67 expression and tumor type ($p<0.005$, $r = 0.597$). Also, there was a good correlation between p53 expression and tumor type ($p<0.05$, $r = 0.521$). But there was no correlation between CD 117 expression and tumor type ($p>0.05$, $r = 0.471$). Of the tumors, 38.1% were located in stomach, 38.1% located in appendix, 4.8% located in duodenum, 4.8% located in ileum, 9.5% located in colon and 4.8% located in pancreas, respectively.
Conclusion: The depth of invasion, tumor size, the presence of solid pattern, large tumor cells and local distant metastases correlated with the degree of malignancy ($r = 0.699, 0.833, 0.671, 0.705, 0.882$, respectively, $p<0.001$).

0370
CK19 and Ki-67 immunohistochemical staining in gastroenteropancreatic neuroendocrine tumours (GEP-NETs)

C. Rowsell, S. Singh, C. Law, N. Ingber, E. Hsieh*
*Sunnybrook HSC, Dept. of Anatomic Pathology, Toronto, Canada

Objective: Ki-67 is used in GEP-NETs as a marker of biologic behavior. CK19 is a marker of poor prognosis in pancreatic neuroendocrine tumours, but its importance in gastrointestinal neuroendocrine tumours is less clear.
Method: Blocks from GEP-NETS were stained with Ki-67 and CK19 antibodies. Ki-67 was used to group tumours according to the ENETs grading system. CK19 was evaluated for intensity and percentage of cell staining.
Results: Sixteen of 18 (89%) pancreatic tumours and 26 of 29 (90%) GI tumours expressed CK19. With respect to Ki-67 in pancreatic tumours, 9 of 18 (50%) were G1, 3 of 18 (17%) were G2, and 6 of 18 (33%) were G3. In GI tumours, 18 of 29 (62%) were G1, 10 of 29 (34%) were G2, and 1 of 29 (3%) G3. Four pancreatic tumours and six GI tumours had distant metastases. Of the four pancreatic tumours, two were G1, one was G2, and one was G3; two stained diffusely with CK19, while the remaining two showed weaker staining. Three metastatic GI tumours were G1 and three were G2; Allred score for CK19 was 4–5 in five of six (83%). There was no significant difference between tumours with and without metastases with respect to Ki-67, but in GI tumours, CK19 had a higher mean Allred score in tumours with metastases (4.3 versus 3.3) which approached statistical significance ($p=0.07$).
Conclusion: CK19 staining is common in GEP-NETs. This near-ubiquitous positivity may limit its potential as a prognostic marker. Further study is needed regarding the prognostic value of Ki-67 since half of the tumours with metastases had low proliferation rates.

0372
Adenocarcinomas of the pancreas in patients in the age of 45 or younger. Clinicopathologic study of 33 patients

L. Liszka, J. Pajak, E. Zielinska-Pajak, S. Mrowiec, D. Golka*
*Medical University of Silesia, Dept. of Histopathology, Katowice, Poland

Objective: Pancreatic adenocarcinoma (PA) is a very rare lesion in young patients. Patients in the age of 45 or younger reported previously constituted <5% of all patients with PA. The clinical and histopathological data concerning these patients are therefore scanty. The aim of the study was to describe characteristics of 33 young patients with PA treated and diagnosed in a single center during a 20-year-long period (1989–2010).
Method: The original gross descriptions, routine hematoxylin–eosin slides as well as available clinical data of 33 PA cases were reevaluated. Only cases with available original slides were included in the study.
Results: There were 30 (90.9%) cases of pancreatic ductal adenocarcinomas (not otherwise specified), two (6.1%) cases of adenocarcinoma associated with intraductal papillary mucinous neoplasm and a single (3%) case of adenosquamous carcinoma. Twenty (60.6%) patients were males and 13 (39.4%) were females. Median age of patients was 42.0 years (range 23–45). Twenty-one (63.6%) patients were treated with pancreaticoduodenectomy, three (9.1%) with distal pancreatectomy, and two (6.1%) with total pancreatectomy. In seven (21.2%) patients, PA was diagnosed in open surgical biopsy specimen (the majority of these patients were treated with palliative surgery). Follow-up data were available for 23 patients—among these patients, 21 died of the disease. A single patient died in

postoperative period. Another patient survived for 11 years and died of unrelated cause.
Conclusion: PA occurs infrequently in young patients. Although some cases are diagnosed early and may be treated with potentially curable surgery, long-term survivals are rather exceptional.

0373
Granulomatous pancreatitis in a patient with LADA type diabetes mellitus

V. Mandys, M. Kheck, M. Andel*
*3rd Faculty of Medicine, Dept. of Pathology, Prague, Czech Republic

Objective: The aim of this presentation was to demonstrate an unusual case of granulomatous pancreatitis discovered in a patient suffering from the LADA type diabetes mellitus.
Method: Samples of pancreatic tissue obtained during the postmortem examination were processed by a routine histological technique. The slides were stained with H&E, trichrome and van Gieson method. Immunohistological methods were used to detect markers of endocrine cells of islets of Langerhans and of macrophages.
Results: A 71-year-old female patient suffering from diabetes mellitus LADA type, generalized atherosclerosis and hypertension died due to pulmonary embolism. Lipomatosis of pancreatic tissue was observed during the postmortem examination. Histologic examination of pancreatic tissue discovered multiple small non-caseating epithelioid cell and giant cell granulomas replacing the islets of Langerhans.
Conclusion: To our knowledge, our case represents the first description of non-infectious granulomatous pancreatitis associated with diabetes mellitus of LADA type.

0374
Assessment of Crohn's disease inflammatory and fibrostenotic lesions. Histologic correlation with magnetic resonance

M. Cuatrecasas, J. Rimola, M. L. Cabañas, O. Garcia-Bosch, S. Rodriguez, M. Pellise, E. Ricart, J. Panes*
*Hospital Clinic Barcelona, Dept. of Pathology, Spain

Objective: Evaluation of Crohn's disease (CD) activity is crucial to optimize therapeutic strategies. Differentiation between inflammatory and fibrostenotic lesions is decisive since the former are treated with drugs, while the latter require surgery. CD activity is based on a combination of clinical, biochemical, endoscopic and radiologic findings, which cannot reliably distinguish between both entities. In patients with refractory symptoms, therapy decisions rely heavily on histologic diagnosis.
Method: Preoperative MR imaging was performed in 27 CD patients undergoing elective bowel resection. MR evaluated wall thickness, pre- and post-contrast wall signal intensity, relative contrast enhancement, presence of edema, and luminal stenosis. Matched histological sections of the MR images were stained with hematoxylin and eosin (HE). Evaluation of wall and submucosa thickness, percentage of inflammatory and fibrous components in the mucosa and submucosa (Masson's trichromic and reticulin stains), submucosal edema, and vascularity (CD31 stains).
Results: Cases assessed as inflammatory by HE had higher early post-contrast signal intensity by RM than fibrostenotic cases ($p=0.009$). Submucosal thickness correlated with early fibrosis (reticulin, $p=0.007$), but only a trend with high vascularity (CD31). Fibrostenotic cases had submucosal thickness inversely correlated with early signal capture and with relative contrast enhancement. Mucosal inflammation was inversely correlated with submucosal fibrosis and thickness ($p=0.007$). Established fibrosis (trichromic) had no delayed signal capture ($p=0.038$).
Conclusion: There is a good correlation between histologic and MR findings. MR may reliably differentiate between inflammatory and fibrostenotic lesions, and it may have an important role as a new pre-surgical biomarker in the management of CD.

0376
The role of standard endoscopic biopsy in diagnosis of gastric gastrointestinal stromal tumors managed in The Holycross Cancer Centre, Kielce, Poland, in years 2000–2010

*W. Rezner**
*Holycross Cancer Centre, Dept. of Neoplasm Pathology, Kielce, Poland

Objective: Intramural character of growth makes gastrointestinal stromal tumor (GIST) difficult or impossible to access by endoscopic biopsy forceps, and therefore, the diagnostic yield of the biopsy does not exceed 40%, even with the use of special techniques. The aim of the study was to evaluate the role of standard endoscopic biopsy in preoperative assessment of gastric GISTs.

Method: From among 24 cases of all gastric GISTs managed in our institution in the years 2000–2010, we selected 17 cases where standard forceps biopsy from subepithelial mass was obtained. We excluded five cases with no subepithelial mass visible endoscopically and two cases of small incidental GISTs in patients operated for other neoplasms. Biopsies diagnosed as negative for GIST were analysed retrospectively with serial sectioning and immunostains including, where appropriate, CD-117, CD-34, SMA, S-100 and calponin in search for neoplastic tissue which could have not been apparent in original HE-stained slides.
Results: None of the biopsy samples analysed retrospectively contained neoplastic tissue. Material which enabled histopathological and immunohistochemical diagnosis of GIST was obtained in 5 out of 17 cases. Mucosal ulceration was present in all cases of diagnostic biopsies and in 4 out of 12 non-diagnostic biopsies.
Conclusion: No GIST tissue was originally missed in biopsy material, so the diagnostic yield of standard endoscopic biopsy in diagnosis of gastric GISTs approached one third of the cases.

0377

Immunohistochemical markers utilized in differential diagnosis between primary ovarian carcinoma from metastatic colorectal carcinoma

A. Iliesiu, M. Aschie, M. Anca, N. Anca, I. Poinareanu, A. Chisoi, P. Corici, V. Sarbu, I. Aschie*
*Clinical Emergency Hospital, Dept. of Pathology, Constanta, Romania

Objective: Colorectal adenocarcinoma is the most common tumor that metastasizes to the ovary and is often difficult to distinguish from primary ovarian mucinous carcinoma. An immunohistochemical marker CDX-2 was found to have a diagnostic value in establishing the gastrointestinal origin of metastatic tumors. Obtaining the correct diagnosis is difficult but crucial to treatment and prognosis.
Method: In our study realized in Clinical County Emergency Hospital Constanta, we evaluated the immunohistochemical expression of CDX2 and also the expression of cytokeratin 7, cytokeratin 20, CEA, MUC2 in 86 cases representing 45 ovarian adenocarcinoma and 41 metastatic colorectal adenocarcinomas involving ovaries.
Results: Searching the tumor registry and pathology database of our hospital, we found that the median age of the study group was 50 years (range, 24–78). Metastatic colorectal adenocarcinoma were almost always negative for MUC5 (98.6%), often negative for CK7 (89.9%), focal or diffuse positive for CDX2 (98.2%), diffuse positive for CK20 (56.9%), focal or diffuse positive for MUC2 (51.2%), and diffuse positive for CEA (43.4%). Almost all of the primary ovarian carcinomas lacked immunoreactivity for CDX-2. In contrast, metastases to the ovary from colorectal primaries showed CDX-2 immunoexpression.
Conclusion: CDX-2 is a useful marker for differentiating primary ovarian carcinoma from carcinomas metastatic to the ovary. CK7, CK20, CDX2 and MUC2 IHC staining is a useful adjunctive diagnostic tool to differentiate metastatic colonic tumours from primary ovarian tumours, in addition to clinical history and gross and microscopic findings.

0378

Multicystic mesothelioma—a case report

*J. Jeruc**
*Faculty of Medicine, Institute of Pathology, Ljubljana, Slovenia

Objective: Multicystic mesothelioma or multilocular peritoneal inclusion cyst is a rare tumor with a predilection for pelvic surfaces of the peritoneum. Most frequently, it occurs in women of reproductive age who have a history of previous pelvic surgery or infection.
Results: A 20-year-old man with no significant past medical history presented with abdominal pain lasting 5 days in the ileocecal region. Despite normal white cell count, acute appendicitis was suspected and the patient underwent surgery, during which a multicystic mass measuring 6.5 cm in the longest diameter was found. Cysts were thin-walled, translucent, with a smooth outer surface, and mostly filled with clear and some with hemorrhagic fluid. Histologically, they were lined by a single layer of cuboidal polygonal and focally hobnail-shaped cells with small uniform nuclei without mitotic activity. Cells stained positive for cytokeratin, calretinin and WT-1, but were negative for endothelial markers, CEA and estrogen and progesterone receptors. The loose connective tissue between cysts was infiltrated by lymphocytes and granulocytes. The diagnosis of multicystic mesothelioma was made. Three months after surgery, the patient is doing well.
Conclusion: The majority of investigators considers this entity to be an unusual type of mesothelial neoplasm that has a tendency to recur locally and may rarely transform into a conventional mesothelioma. Some, however, consider the lesion to be a non-neoplastic reactive mesothelial proliferation. Multicystic mesothelioma has an indolent course, but approximately one half of cases recur. The differential diagnosis includes malignant mesothelioma, cystic lymphangioma, pseudomyxoma peritonei and mesenteric and omental cysts.

0380

Significance of histopathological tumor regression after neoadjuvant chemotherapy in adenocarcinomas of the upper gastrointestinal tract: what we can learn from 589 cases

R. Langer, D. Reim, A. Novotny, K. Ott, M. Feith, C. M. zum Büschenfelde, J. Engel, H. Friess, H. Höfler, K. Becker*
*Technische Universität München, Institute of Pathology, Germany

Objective: We analysed a series of 589 upper gastrointestinal (GI) adenocarcinomas treated by neoadjuvant chemotherapy (CTX) between 1989 and 2009, which all were consistently worked up and evaluated by a standardized tumor regression grading system (TRG) in our institution.
Method: One hundred eight esophageal adenocarcinomas (EA), 175 adenocarcinomas of the esophagogastric junction (AEJ) and 306 gastric carcinomas (GC) treated by a cisplatin/5-FU-based CTX were included. TRG was determined using a four-tiered system based on the estimation of the percentage of residual tumor in relation to the previous tumor bed.
Results: In total, 25 patients (4%) had a complete tumor regression (TRG1a) and 111 patients (19%) had a subtotal regression (TRG1b, 1–10% residual tumor). Partial tumor regression (TRG2, 11–50%) was observed in 151 cases (26%); 302 patients (51%) had minimal or no regression (TRG3, >50%). Tumor regression was significantly associated with post-treatment ypT, ypN, ypL category, R status and survival ($p<0.001$) and was shown to be an independent prognostic factor for survival ($p=0.02$). Some characteristics relating to the tumor site were, in particular, the higher frequency of total or subtotal tumor regression in EA and AEG ($p<0.001$) and the association of pretherapeutic tumor grading and Lauren's classification with tumor regression ($p=0.001$) in GC.
Conclusion: We present our 20 year's experience of a highly standardized evaluation of upper GI adenocarcinomas after neoadjuvant CTX demonstrating highly objective and prognostic relevant information from a very large collective. We recommend the implementation of a standardised TRG system in every pathological report of these tumours.

0381

Fibroelastotic changes of the gastrointestinal tract as polyp-causing lesions

B. Märkl, C. Cacchi, H. Arnholdt*
*Klinikum Augsburg, Dept. of Pathology, Germany

Objective: Fibroelastotic changes (FEC) of the gastrointestinal tract (GIT) are rare lesions. Only 35 cases have been reported in the literature. Their role as an own entity is unclear and is not generally accepted.
Method: After initial recognition of an elastotic lesion in a hemicolectomy specimen, special attention was paid to amorphic accumulations in H&E-stained slides of GIT specimens. Elastica-van-Giesson staining was performed to verify the elastotic origin.
Results: Within 3 years, a total number of 21 polypoid lesions were collected. One lesion was found in the ileum and six lesions occurred in the stomach. The 14 remaining cases were colon specimens. In five cases, FEC were associated with neoplastic lesions. In 16 cases, however, the accumulation of elastotic fibres was the only histomorphological finding. One patient received intensive short intervals surveillance because of a highly suspicious endoscopic finding in the stomach. In two cases, a clinical relevant stenosis was caused by a submucosal thickening of the bowl wall with massive accumulation of elastotic fibres. Right hemicolectomy was performed in both cases.
Conclusion: Fibroelastotic changes are not as exceedingly rare as thought before. They are the only histological finding in a certain number of polypoid lesions in the GIT.

0382

Expression of p53, VEGF and collagen IV in gastrointestinal stromal tumors and its relationship with clinicopathological parameters

S. Rjabceva, Y. Rogov, I. Dulinez, M. Vozmitel, A. Krilov*
*Belarusian Medical Academy, Dept. of Pathology, Minsk, Belarus

Objective: Gastrointestinal stromal tumors (GISTs) have a spectrum from minimal indolent tumors to sarcomas. The aim of this study was to assess the expression of p53, VEGF and collagen IV in GISTs and to establish immunohistochemical correlations with clinicopathological parameters.
Method: Twenty-four cases diagnosed as GIST were examined by both light microscopy and immunohistochemistry (IHC). We used IHC markers such as p53, VEGF and collagen IV. All tumors were classified by the risk grade system by Miettinen et al.
Results: Of the tumors, 8/33.3% were classified into low risk grade (LR), 6/25% in the intermediate risk (IR) and 10/41.7% in the high risk group (HR). Focal necroses (50%, 50% and 50%, respectively) and microhemorrhages (37.5%, 50% and 90%, respectively) were present in GISTs of all groups. A p53 expression was correlated with a high risk grade ($r=0.48$, $p=0.0335$). GISTs of all groups showed VEGF expression (62.5%, 66.7% and 60%, respectively).

Collagen IV expression, as staining of the continuous basement membranes of vessels, varied from 25% in LR GISTs to 16% to 10% in IR and HR tumors, respectively. Gamma's correlation test revealed correlation between microhemorrhages and grade (r=0.70, p=0.0019), tumor necroses and p53 (r=0.55, p=0.0245), tumor necroses and collagen IV (r=−0.55, p=0.0107) and VEGF and collagen IV (r=−0.49, p=0.0213).

Conclusion: This study showed that both high p53 expression and the presence of tumor microhemorrhages are possibly related with unfavorable prognosis. In addition, we found that a tumor necrosis was correlated with a p53 and collagen IV.

0383

Smooth muscle tumors with CD117/CD34 positivity cells

*S. Rjabceva**

*Belarusian Medical Academy, Dept. of Pathology, Minsk, Belarus

Objective: Immunohistochemically, smooth muscle cells are characterized expression of SMA and desmin. The aim of this study was to describe the clinicopathological and immunohistochemical features of smooth muscle tumors (SMT) with CD117/CD34 positivity cells.

Method: Eleven cases diagnosed as SMT were examined by both light microscopy and immunohistochemistry (IHC). I used IHC markers such as CD117, CD34, smooth muscle actin, desmin, vimentin, NSE and S100.

Results: The patients (M/F=4:7), with age ranging between 18 and 70 years (mean = 48.3), had SMT. A tumor size varied from 1.5 to 17 cm (mean = 8.9 cm). Tumors were localized in the esophagus (5/45.5%), stomach (1/9.1%), colon (1/9.1%), retroperitoneum (1/9.1%) and in the pelvis (3/27.3%). Histologically, tumors are composed of elongated or ovoid cells with pale nuclei and eosinophilic cytoplasm which is distinctly fibrillar. Immunohistochemically, cells of SMT were positive for SMA (100%), desmin (100%), vimentin (100%) and NSE (72.7%), but they were negative for CD117, CD34 and S100. I found that the scattered cells of the tumors were characterized by the expression of CD117 (11/100%), CD34 (7/63.6%) and S100 (5/45.5%). These cells were located diffusely or focally in the SMT. The immunophenotype of these cells was similar to immunohistochemical features of the interstitial cells of Cajal or the gastrointestinal stromal tumor (GIST).

Conclusion: Although the scattered tumor cells revealed CD117 positivity, the histological finding was similar to SMT and was different from GIST. SMT colonized by CD117/CD34-positive cells should not be confused with GISTs.

0385

Updates of TNM classification: for the better or worse?

B. Karabulut, A. M. Sonmez, D. Turan, N. Kursun, A. Ensari*

*Ankara University Med School, Turkey

Objective: For the prognostic evaluation of tumours, the TNM classification is updated periodically. The use of this classification for colorectal cancer (CRC) has caused some problems in the assessment of metastatic lymph nodes. In this study, we have investigated the effect of the updates on metastatic lymph node interpretation and, hence, staging.

Method: H&E slides of 83 cases of CRC were reevaluated microscopically to assess the number of metastatic lymph nodes according to the criteria of TNM5, TNM6 and TNM7. Clinical parameters such as gender and age of the patients, tumour location, grade, and stage were retrieved from the patients' files. Mann–Whitney, Kruskal–Wallis, Wilcoxon signed ranks and multiple comparison tests were used for statistical analysis.

Results: There were 48 men (57.8%) and 35 women (42.2%) with a mean age of 63.14 years (ranging from 31 to 87). The tumour was located in the right colon in 11 cases (13.3%) and 72 cases in the left colon (86.7%). There were three grade 1 (3.6%), 58 grade 2 (69.9%), and 22 grade 3 tumours (26.5%). The number of metastatic lymph nodes was significantly higher in grade 3 tumours compared to grade 2 tumours in TNM5, TNM6 and TNM7. According to TNM5, significantly more metastatic lymph nodes were determined than TNM6 and TNM7 (p<0.05 and p<0.001, respectively), whereas TNM6 revealed significantly more metastatic lymph nodes in comparison to TNM7 (p<0.001).

Conclusion: Our results show that there is significant variation between updates of TNM in terms of metastatic lymph node yield which will inevitably cause variation in the TNM classification.

0386

Metastatic ileal gastrointestinal stromal tumor of the mandible

O. Yapicier, A. Cildir, O. Karadeniz, S. Sezgin Ramadan, Y. Kapran*

*Anadolu Medical Center, Kocaeli, Turkey

Objective: Metastatic lesions to the mandible are rare, comprising <1% of all malignancies. An 82-year-old woman presented with a painful swelling in the right mandible growing progressively for 3 months.

Method: Computed tomography (CT) showed intraosseous expansile and destructive lesion in the corpus of the right

mandible 23 × 21 mm in size expanding to the soft tissue laterally. After administration of contrast material, moderate enhancement was seen throughout the mass. The biopsy showed stromal tumor immunopositivity for CD117. The patient had a medical history of ileal tumor resection 5 years ago at another institute which was diagnosed as gastrointestinal stromal tumor (GIST) and classified as intermediate risk group for potential of malignancy.
Results: The mandibular tumor was considered as a metastatic gastrointestinal stromal tumor. No tumor was seen on positron emission tomography (PET)/CT other than the mass in the right mandible. The histopathology of the ileal tumor was seen and the diagnosis was confirmed. Imatinib treatment was started at a dose of 400 mg daily. Resection of the mandibular mass was planned by plastic and reconstructive surgeons.
Conclusion: Liver and peritoneum are usual metastatic sites for gastrointestinal stromal tumors. To the best of our knowledge, metastasis of ileal gastrointestinal stromal tumor to the mandible has not been previously reported in the English literature.

Friday, 3 September 2010, Basement

PS-16 Poster Session Head and Neck Pathology

0387
Mycobacterium tuberculosis infection within Warthin's tumor of the parotid gland

A. C. Faur, E. Lazar, A. Dema, M. Cornianu, S. Taban, M. Grigoras, A.-M. Vesa, D. G. Stef, L. S. Gotia*
*University of Medicine, 'V Babes' Timisoara, Romania

Objective: Warthin's tumor is the second most common neoplasm of the parotid gland accounting for 6–30% of parotid neoplasms. However, parotid gland is an extremely rare site for extrapulmonary tuberculosis.
Method: Between 2003 and 2010, 30 cases of Warthin's tumor were diagnosed at the Pathology Department of City Hospital Timisoara, but only one case of *Mycobacterium tuberculosis* infection within Warthin tumor was analysed. A 47-year-old man with a history of pulmonary tuberculosis was admitted at the Maxillofacial Department with a slow-growing right parotid mass. A 2.2/1.5-cm diameter mass was excised and formalin-fixed paraffin-embedded tissue samples were cut at 4 μm and stained using hematoxilin and eosin (HE).
Results: On the HE stain, pathological examination revealed cystic spaces lined by proliferative oncocytic basal and luminal columnar epithelium and markedly lymphocytic infiltration. A very large part of the section was occupied by chronic granulomatous inflammation with caseous necrosis, epithelioid granulomas and multinucleated giant cells; some were of the Langerhans' giant cell type.
Conclusion: Tuberculosis of the parotid gland is extremely unusual and constitutes about 2.5% to 10% of the parotid lesions. To our knowledge, only six cases of tuberculosis within Warthin's tumor have been reported in the English language literature. In this report, we present a new patient with parotid gland tuberculosis within Warthin tumor.

0389
Androgen receptor status in salivary gland cancers

D. Sygut, R. Kordek, J. Piekarski, S. Okla, M. Ziólkowska, S. Sporny*
*Medical University Lodz, Dept. of Pathology, Poland

Objective: The purpose of this study was to assess the immunohistochemical (IHC) status of androgen receptor (AR) in various salivary gland cancers.
Method: The study group consisted of 61 cases of primary salivary gland cancers from 61 patients (F/M=32:29, age 12–78 years). These were 15 adenoid cystic carcinomas (AdCC), 12 adenocarcinomas NOS (AdC), 12 mucoepidermoid carcinomas (MEC), 10 acinic cell carcinomas (ACC), 5 carcinomas ex pleomorphic adenomas (CaexPA), 5 salivary duct carcinomas (SDC), 1 basal cell adenocarcinoma (BCAC) and 1 large cell neuroendocrine carcinoma (LCNEC). IHC reactions with monoclonal mouse anti-human androgen receptor antibody (Dako, clone AR441) were done on 4-μm-thick sections cut from representative archival paraffin block. In each positive case, the revealed strength of AR expression was assessed as total score (TS) according to Allred score.
Results: The AR expression was found in five AdC NOS, four CaexPA, four SDC, four ACC, three MEC, and one AdCC and BCAC, and calculated TS ranged from three to eight points. TS had eight points in six cases, seven in three cases, six in one case, five in three cases, four in two cases and three in four cases.
Conclusion: AR expression was found in 22 of 61 (36%) primary salivary gland cancers. The strength of AR expression differed in various salivary gland cancers, and it was most frequent in CaexPA (4/5) and SDC (4/5) and less frequent in AdC (5/12) and ACC (4/10), whereas only found incidentally in others.

0390
Mena expression in normal and neoplastic salivary glands

*G. Simona**
*UMF, Dept. of Pathology, Targu-Mures, Romania

Objective: Recently, studies revealed that human orthologue of murine Mena (mammalian Ena), an actin regulatory protein involved in the control of cell motility and adhesion, is modulated during breast, colon and pancreatic carcinogenesis. In our previous studies, we observed that Mena was modulated during colon and cervix carcinogenesis. In this study, we analysed Mena expression in lesions of salivary glands (SG). Previous studies regarded only Maspin expression in these lesions, a protease inhibitor which is increased in benign tumors but decreased in SG carcinomas.
Method: We have analyzed Mena expression in normal SG (n=10) and also benign (n=20) and malignant (n=30) lesions of SG. For the immunohistochemical staining, we used the murine Mena antibody, provided by BD Biosciences. Mena expression was quantified in cytoplasma of tumor cells.
Results: All normal SG and their benign lesions were Mena-negative. It included ten pleomorphic adenomas and ten Warthin's tumors. Ductal adenocarcinomas (n=10), independently by their histological grade and also carcinomas with acinary cells (n=5) and squamous carcinomas (n=10), were positive. No difference of Mena intensity in positive cases was observed. All lymphomas (n=5) were Mena-negative.
Conclusion: This is the first study in literature about Mena expression in SG tumors. Our results prove that Mena plays a role in carcinogenesis of different organs, including SG, but the exact mechanism is not yet known. In accordance with different previous studies about Maspin expression in SG lesions, it seems that these two antibodies are reversely correlated. Future studies are necessary in order to elucidate their role in SG tumors.

0391
Secondary tumors of the salivary glands

*A. C. Faur**
*University of Medicine, 'V Babes' Timisoara, Romania

Objective: Secondary tumors of salivary glands are rare and constitute about 5% of all malignant salivary neoplasm.
Method: A study has been carried out for 7 years on 184 cases of salivary gland tumors, and only one case of salivary metastatic lesion was diagnosed. A 79-year-old female with a history of a right temporal malignant melanoma was admitted at the Plastic Surgery Department of County Hospital of Timisoara. Six months after the surgery, the patient returned to this clinic with a rapidly growing mass in the right temporal region and right preauricular region. A 2 × 2-cm diameter tumor was excised with adjacent lymph nodes. A superficial parotidectomy was performed also, preserving the facial nerve and its branches. Formalin-fixed paraffin-embedded tissue samples were cut at 4 μm and stained using hematoxylin and eosin (HE).
Results: On HE stain, the periparotid and temporal region lymph nodes were infiltrated by malignant melanoma cells. The parotid tissue also had metastatic lesions. The metastatic malignant melanoma lesion consisted of epithelioid neoplastic cells with cytologic and nuclear atypia, large nucleoli, atypic mitotic figures and abundant melanin pigmentation. Necrosis and hemorrhage were also seen.
Conclusion: The parotid gland and its lymph nodes are possible sites of metastasis from head and neck tumors, especially squamous cell carcinoma or melanoma. The rarity of salivary secondary tumors prompted us to report this case.

0392
Mucoepidermoid carcinoma of the maxilla. Report of a rare case

A.-M. Feritsean, G. Kalodimos, I. Zourou, A. Vardouli, K. Chatzis, E. Alexopoulou*
*General Hospital Of Volos, Greece

Objective: Primary intraosseous mucoepidermoid carcinoma of the jaws is a rare lesion accounting for <5% of all mucoepidermoid carcinomas reported in the literature. It is a neoplasm of adult life and affects females twice more frequently than males. Histologically, it is a low-grade carcinoma usually affecting the mandible. The radiologic presentation is that of uni- or multilocular lesions. Their origin still remains controversial.
Method: We report the case of a 66-year-old female who presented with a painful swelling in the left maxilla of 2 month's duration. There was no history of previous surgical intervention. Clinical examination revealed an ulcerated swelling. Cervical lymphadenopathy was absent.
Results: The radiological examination showed a unilocular compact lesion in the maxilla, not unequivocally diagnostic of malignancy. Surgical excision of the lesion together with a small part of the maxilla was performed. Grossly, it was a solid mass of relatively soft and only focally bony consistence measuring 1.5 cm. On brushing cytology of the surgical specimen, groups of mucous cells without any significant atypia intermingled with aggregates of squamous cells. The histologic diagnosis, confirmed by histochemical and immunohistochemical methods, was that of low-grade mucoepidermoid carcinoma of the maxilla. The postoperative period was

uneventful. The patient is on regular follow-up and is disease-free after 4 years.
Conclusion: Our case is reported because of its rarity, and at the same time, the literature is reviewed and speculations about the pathogenesis of mucoepidermoid carcinomas are attempted.

0393

Odontogenic myxoma (OM) in the maxilla: a case report and review of the literature

S. Papaemmanouil, N. Pastelli*
*G. Papanikolaou General Hosp., Dept. of Pathology, Thessaloniki, Greece

Objective: Odontogenic myxoma is an intraosseous tumor of the jaws, relatively benign with locally aggressive behaviour. Most of the OMs are slowly growing with no symptoms. Large tumors cause painless expansion. It occurs in patients over the age of 10 and is mostly located in the mandible.
Method: A 45-year-old man was presented with a progressively enlarging mass in the maxillary area. The imaging findings revealed a large, rather well-circumscribed tumor mass in the body of the maxillary bone. The mass was excised by peripheral ostectomy.
Results: The gross examination revealed a grey-white mass with translucent mucinous appearance measuring 7×4.5×4 cm. The sections were examined with H+E and mucin stains and followed by IHC study for MIB-1 (ki-67). The morphologic, histochemical and IHC data were consistent with an odontogenic myxoma.
Conclusion: Our study comments on the imaging findings of macroscopic and microscopic features and the differential diagnosis of this tumor. The current literature is reviewed.

0397

Comparison of MMP-2, MMP-9, KAI1 expression in oral squamous cell carcinomas and in adjacent marginal tissue

J. Bar, M. Kos, M. Jelen, L. Noga, W. Engelke, U. Kellner*
*Medical University Wroclaw, Dept. of Pathomorphology, Poland

Objective: The role of interactions between MMP-2, MMP-9 and KAI1 protein expression as markers involved in aggressive behaviour of tumours is still under investigation. The study aimed to evaluate and compare MMP-2, MMP-9 and KAI1 expression in primary oral squamous cell carcinomas (OSCC) and adjacent marginal normal squamous cell epithelium and to estimate their association with each other in relation to clinical variables.
Method: MMP-2, MMP-9, and KAI1 expression was evaluated on primary OSCC (n=54) and adjacent marginal normal tissues (n=32) using immunohistochemistry.
Results: Significant differences between MMP-9 and KAI1 expression was found in OSCC and marginal normal tissue (P=0.01, P=0.001, respectively). In normal tissue, MMP-2, MMP-9 expression was found in basal cell layers and also frequently was observed in stromal tissues with inflammatory component. KAI1 protein was not observed in stromal tissues. No significant differences were observed between MMP-2, MMP-9, KAI1 expression and tumour grade and stage. Inverse correlation between MMP-2 and KAI1 expression was found in OSCC (P=0.006). KAI1-negatve/MMP-2-positive cases were observed mainly in high tumour grade and in advanced stage of tumours.
Conclusion: Inverse correlation revealed between KAI1 protein and MMP-2 expression in OSCC could affect the function of KAI1 suppressor protein and influence the metastatic potential of the tumour cells. Our results suggest that accumulation of MMP-2 and MMP-9 in the surrounding tissue may enhance local invasion in OSCC.

0398

Expression of MMP-2 and PTEN in laryngeal squamous cell carcinoma—biological predictors?

M. Bodnar, P. Burduk, W. Kazmierczak, A. Marszalek*
*Collegium Medicum, Bydgoszcz, Poland

Objective: Reliable predictors of laryngeal squamous cell carcinoma (LSCC) biology are still missing. The aim of this study was to investigate two newly discovered factors (MMP-2 and PTEN) in LSCC patients with correlation to the stage of the disease.
Method: We used 41 specimens from surgical resections selected from 25 patients and divided into controls (12 samples) and LSCC (29 samples). We used standard immunohistochemistry for MMP-2 and PTEN expression studies with EnVision system and DAB as a chromogen. Antigen expression was classified as followed: 0—no positive cells, 1—<10%, 2—10–50%, 3—above 80% positive cells. All results were statistically evaluated using Mann–Whitney U test and ANOVA, with statistical significance at $p<0.05$.
Results: In patients with LSCC, the expression PTEN was detected in the cytoplasm of 20% tumor cells and 30% stromal area ($p<0.05$) while in controls only in 5% of

stromal area ($p<0.05$ vs LSCC). PTEN expression was decreased in tumor cells in N+ vs N0 cases (10% vs 30%). In LSCC, MMP-2 was found in 3.5% of the tumor cells, but in 45% of stromal area ($p<0.05$). There was no MMP-2 expression in controls, while expression level (0–3 scale) was higher in tumor cells versus stromal compartment. MMP-2 stromal expression in N0 and N+ cases was 50% versus 38% of the area, respectively.
Conclusion: We might conclude that decreased PTEN expression in tumor cells predicts lymph node involvement, which then is accompanied by decreased expression of MMP-2 in stromal area in the main lesion.

0401
Mucosal large cell neuroendocrine carcinoma (mLCNEC) of the head and neck regions: a new clinicopathologic entity

K. Kusafuka, M. Abe, Y. Iida, T. Onitsuka, T. Nakajima*
*Shiuzoka Cancer Center, Pathology Division, Nagaizumi, Japan

Objective: Large cell neuroendocrine carcinoma (LCNEC) is well known as a subtype of lung cancer, but it is extremely rare in the head and neck regions. Our objective was to establish mucosal LCNEC (mLCNEC) as a new entity in the head and neck regions.
Method: We reestimated 814 surgically resected specimens of the primary mucosal carcinoma in the head and neck regions, including 24 basaloid squamous cell carcinoma, during 2002–2009. The immunostainings for neuroendocrine (NE) markers such as CD56, chromogranin-A and synaptophysin were performed. In the cases which were positive for two or three NE markers, we re-diagnosed as "mLCNEC".
Results: Only eight cases (0.98%) were re-diagnosed as mLCNEC. All cases were male and their mean age was 64.6 years. Three cases occurred in the tongue base, four cases in the larynx and one case in hypopharynx. Although seven cases showed numerous regional lymph node metastases, only one case showed death of disease. Histologically, mLCNEC showed the sheet-like, trabecular, organoid pattern growth of relatively large basaloid cells in which the central necrosis, rosette formation, peripheral palisading, and high mitotic figures were sometimes seen. Immunohistochemically, mLCNEC indicated to be positive for two or three NE markers. Only three cases of mLCNEC were immunopositive for TTF-1, whereas all cases except one case were only focally immunopositive for p63. All cases showed high proliferating activity.
Conclusion: We propose that mLCNEC can occur in the head and neck regions and is a new clinicopathological entity. The prognosis of mLCNEC remains unclear.

Friday, 3 September 2010, Basement

PS-17 Poster Session Paediatric Pathology

0402
Massive ovarian edema et fibromatosis

M. Tolovska, M. Ristovski*
*Institute of Pathology, Skopje, Macedonia, The former Yugoslav

Objective: Massive ovarian edema is an unusual cause of ovarian enlargement in young women. It is due to the accumulation of edema fluid and in some cases is associated with mature cystic teratoma. The patients are young (average 21 age), with present abdominal pain, menstrual abnormalities or evidence of hypergonadism. The ovarian enlargement is unilateral in 90% of cases.
Method: We report a case of a 12-year-old girl with tumor of the left ovary. Grossly, the enlarged ovary's greatest dimension was 18 × 20 cm (1,900 g), composed of solid mass with large gelatinous and hemorrhagic foci. Paraffin sections from 20 samples were stained with HeEo and immunostained for vimentin, S100 protein, SMA, desmin and CD34.
Results: Histological findings were identical in all slides. Ovarian stroma cells were scattered within abundant edematous fluid, and in some foci, hypocellular stroma surrounded follicles. In the cortex, follicles were dilated in fibromatous stroma with rare luteinized cells. CD34 confirmed the presence of many vessels with thrombi composed of fibrin-causing hemorrhagic necrosis. In some areas of necrosis, we found foci of dystrophic calcification suggesting an older process.
Conclusion: Massive ovarian edema is a lesion which can be misdiagnosed as a neoplasm. The cause is unclear. It has been attributed to intermittent torsion of the ovarian pedicle and interference with its lymphatic drainage. The fibromatosis and massive edema represent two ends of the same disorder.

0403
Post-neonatal cardiac death associated with intimal fibroplasia of coronary and of major systemic arteries

M. Bergmann, J. Chnayna, M.-C. Osterheld*
*University Hospital Lausanne, Dept. of Pathology, Switzerland

Objective: Intimal fibroplasia is a variant of fibromuscular dysplasia (FMD), a non-inflammatory and non-atherosclerotic arterial segmental disease, resulting in narrowing of the lumen. FMD of coronary arteries is a

rare pathology associated with cardiac and sudden death occurring during infancy, childhood and young adulthood.
Method: We describe the case of a female infant born prematurely (gestational age 33+4/7) presenting a mild supravalvular aortic stenosis associated with an atrial septal defect and cardiac valvular dysplasia. During the first weeks of life, she developed a progressive obstructive cardiomegaly and she died at day 55 of a cardiogenic shock.
Results: The autopsy confirmed a marked cardiac hypertrophy and the aforementioned congenital cardiac anomalies. Histologically, we observed a myxomatous thickening of the aortic, pulmonary and mitral valves and a significant segmental intimal fibroplasia of all coronary arteries, producing subtotal obstruction of the right coronary artery. The myocardium presented multiple areas of infarction of various ages and foci of interstitial fibrosis with calcifications. Sampling of the aorta and its major branches showed mild to moderate intimal fibroplasia of the aorta, celiac trunk, superior mesenteric and left renal arteries.
Conclusion: The pathogenesis of FMD is unclear: Mural ischemia, hormonal, genetic and mechanical factors have been suggested. This case supports the theory of a congenital origin and emphasizes the importance of an extensive examination of coronary arteries when performing autopsy in paediatric patients as FMD is a segmental disease, and it must be considered in the etiologic differential diagnosis of cardiac and sudden death in paediatric age.

0404
Increased amount of chorionic disc extravillous trophoblasts (EVT) in placental hypoxia

*J. Stanek**
*Cincinnati Children's Hospital, Dept. of Pathology, USA

Objective: Increased amount of EVT in the maternal floor was found in preeclamptic placentas. This analysis intends to retrospectively prove that the EVT is increased in the whole chorionic disc also in other than preeclampsia clinical conditions at risk for fetal and placental hypoxia.
Method: Frequencies of clinical and placental parameters of 189 consecutive cases with more than five cell islands per full-thickness paracentral section of grossly unremarkable placenta (study group, SG) were compared to all remaining 1,006 placentas (control group, CG).
Results: The numbers of placental septa/cell islands were statistically significantly ($p<0.05$) higher in the SG than in the CG in association with preeclampsia, chronic hypertension, diabetes mellitus, oligohydramnios, intrauterine growth restriction, induction of labor, cesarean sections, low 5-min Apgar score, small placentas, placental infarction, massive perivillous fibrin deposition, decidual arteriolopathy, diffuse placental hypoxia, microscopic chorionic pseudocysts, and maternal floor clusters of multinucleate trophoblastic giant cells. The reverse was seen in the premature rupture of membranes, perinatal mortality, abnormal umbilical cord, acute chorioamnionitis, chronic villitis of unknown etiology, and histological placental meconium staining.
Conclusion: The amount of chorionic disc EVT is increased in association with clinical conditions and placental lesions known to be associated with hypoxia, but is decreased in "non-hypoxic" clinical conditions and placental lesions. Counting the placental septa and cells islands can serve as a surrogate test of placental hypoxia, not only in preeclampsia.

0405
Pseudo-TORCH and the cerebro-costo-mandibular syndrome

J. Stanek, A. Oestreich*
*Cincinnati Children's Hospital, Dept. of Pathology, USA

Objective: While the posterior rib gaps and Pierre Robin sequence are well documented, components of the cerebro-costo-mandibular syndrome (ccms), the "cerebral" part thereof is more variable, including mental retardation in survivors, hydrocephalus, severe hypoplasia of frontal and occipital lobes, abnormal olfactory bulbs, cerebral heterotopias, or gliosis.
Method: This is a case report of unusual brain findings in ccms, to our knowledge found for the first time at postmortem examination.
Results: Because of fetal hydrops and congenital anomalies found on prenatal ultrasound, a 23-week pregnancy was terminated to reveal a fetus with multiple rib gaps, dysmorphic facial features, prominent micrognathia, high-arched palate, club feet, dysplastic organ of Corti, incomplete visceral rotation, pseudoglandular transformation of the pituitary gland, mucosal eosinophilia of the stomach and intestines, microcalcifications of liver, and extensive, diffuse, predominantly perivascular and not only periventricular brain calcifications. There was no laboratory evidence of intrauterine infection either clinically or by in situ hybridization.
Conclusion: This case illustrates a not yet described pseudo-TORCH, congenital infection-like, presentation of the ccms with extensive brain calcifications and mucosal eosinophilia of the gastrointestinal tract. Extensive brain calcifications were described in other genetic syndromes such as Baraitser–Reardon syndrome, Aicardi–Goutieres syndrome, and mitochondrial encephalopathies, but not the

ccmc. Calcium metabolism can have genetic background in the ccms and explain cerebral dysfunction in at least a subset of the syndrome.

0406

Alveolar capillary dysplasia/misalignment of pulmonary veins: report of four cases

S. Boudjemaa, V. Belle Mbou, M. Larroquet, H. Ducou Le Pointe, A. Coulomb*
*Hospital Armand Trousseau, Dept. of Pathology, Paris, France

Objective: Alveolar capillary dysplasia (ACD) with or without misalignment of pulmonary veins (MPV) is an uncommon congenital cause of persistent pulmonary hypertension of the newborn characterized by a lack of alveolar and vascular development. Most are sporadic, but familial ACD/MPV has been reported, linked to the gene FOXF1 on chromosome 16 q24.1-q24.2. It is universally fatal and diagnosis is entirely dependent on the pathological examination of surgical lung biopsy specimen. Four cases of ACD, three with MPV, are reported.
Method: The four neonates were full term, without associated congenital anomalies. They were admitted to the paediatric intensive care unit for hypoxia and severe pulmonary hypertension unresponsive to maximal cardiorespiratory support, including high-frequency ventilation, inhaled nitric oxide and extracorporeal membrane oxygenation.
Results: Surgical lung biopsies performed in three cases and postmortem lung examination in one case showed pathological findings of ACD, characterized by poor capillary apposition and density and medial arterial hypertrophy. These lesions were associated with misalignment of pulmonary veins in three cases. The four infants died of refractory hypoxemia during the first 2 months of life.
Conclusion: These observations emphasize the importance of considering ACD with or without MPV in all newborn infants who present a persisting severe pulmonary hypertension without anatomical cause. Histological diagnosis based on early surgical lung biopsy may prevent from using costly, invasive and ineffective treatments and procedures such as extracorporeal membrane oxygenation.

0407

A case of complete trisomy 9: autoptic, cytogenetic and radiologic findings

E. Gradhand, S. Becker, C. Richter, D. Wand, C. Kunze, S. Hauptmann*
*Medizin. Universität Halle, Institute of Pathology, Germany

Objective: An autopsy of a female fetus of the 22+2nd gestational weeks was performed after an induced abortion due to multiple intrauterine malformations suspecting a chromosomal disorder.
Method: Prior to the autopsy, the 220-g female fetus was extensively X-rayed. We performed an autopsy including histological examination of all organs. Cytogenetic analysis was performed using both chorionic trophoblast and tendon fibroblasts.
Results: The fetus was characterized by pronounced global hydrops, craniofacial dysmorphy and malformations of both hands and feet. We found a complex cardiac malformation, unilobular lungs, dysmorphic liver and spleen, malrotated and doubled right kidneys, and an aplasia of the left kidney. The parenchymatous organs showed inconspicuous histomorphological architecture. In the cerebrum, no corpus callosum was found and immature neuronal rosettes in both optical nerves were detected. X-ray showed vertebral clefts, a slight hypertelorism, skeletal dysplasias of both hands, and confluent frontal and occipital fontanelles. Cytogenetics turned out a complete trisomy 9 (GTG-Banding).
Conclusion: We present radiological, autoptic and cytogentic findings in a case of a very rare chromosomal aberration which mostly occurs as a mosaic or partial trisomy 9. This chromosomal abnormality usually induces early abortion. Therefore, a fetus with trisomy 9 and a gestational age of 22+2 weeks is very uncommon. We found multiple malformations of the skeleton and organs, mostly located in the midline.

0409

Holoprosencephaly with cyclopia: presentation of two fetuses with multiple congenital malformations and investigation of sonic hedgehog (Shh) expression

P. Papanastasopoulos, J. Coulouras, P. Aroukatos, M. Repanti, E. Farri-Kostopoulos, H. Papadaki*
*General Hospital Agios Andrea, Dept. of Pathology, Patras, Greece

Objective: Holoprosencephaly is the commonest forebrain developmental anomaly occurring in 1 of 16,000 live borns. Sonic hedgehog is the major gene implicated in holoprosencephaly.
Method: Two fetuses of 27-week and 32-week pregnancies, terminated due to multiple congenital malformations, were autopsied, and paraffin-embedded tissue sections were examined microscopically. Shh expression was investigated immunohistochemically in orbital and CNS sections.

Results: Twenty-seven-week fetus: karyotype 46XX; alobar holoprosencephaly, true cyclopia, proboscis formation, pituitary gland anterior lobe agenesis, atretic anus and vagina, hypertrophic clitoris, female internal genitalia, right hand oligosyndactyly, left-sided overriding fourth and fifth toes, ventricular septal defect, hypoplastic left heart complex, truncus arteriosus, asplenia, irregular liver lobation, left kidney agenesis, right kidney cystic dysplasia, hypoplastic right ear auricle, external auditory meatus atresia. Thirty-two-week fetus: karyotype 46XY; alobar holoprosencephaly, synophthalmia, proboscis formation, hypoplastic right heart complex, patent foramen ovale, ostium secundum defect, tricuspid valve and pulmonary artery atresia, pulmonary arteries analogous branching from the aorta. No teratogenetic factors and consanguinity were reported. Histological examination revealed scattered rosette-like structures in areas of dysplastic retina in both cases. Immunohistochemical expression of Shh was negative.
Conclusion: The absence of Shh immunostaining suggests a potential causative role in the pathogenesis of the above phenotypes. Even though both karyotypes were normal, the authors could not exclude the possibility of the existence of chromosomal alterations not detectable by routine karyotypic analysis. Finally, to our best knowledge, the above phenotypes do not seem to match any known clinical syndromes, and we therefore consider their origin unknown at present.

0412

The impact of nutritional colourant tartrazine (E102) on morphological state of thymus of rat descendants

I. Goryanikova, I. Sorokina*
*Lugansk State Medical University, Dept. of Pathomorphology, Ukraine

Objective: Synthetical colourant of yellow colour tartrazine (E102) whose application is prohibited in some countries of EU got widespread use. The aim of the work was the assessment of influence tartrazine to thymus of infant rat descendants 1 month from birth from mothers who had been taking tartrazine during gestation and feeding.
Method: It was histologically discovered that density of cortical and medullar thymocytes was much higher than in the control group. Mitosis is often diagnosed in the subcapsular zone. The most part of thymocytes of this zone is apoptosis amenable, cells with low concentration of DNA in the nucleus, with the sings of dystrophy and necrosis often met. Thymus medullary substance generally consists of fine lymphocytes. The small bodies of thymus, which are situated in medullary substance, are few in number and fine.
Results: Immunohistochemical investigation with MCA defined the signs of thymocyte-interrupted maturation of depletion of CD4 and CD8 population and macrophage ED1 and B lymphocytes CD45RA amount rising.
Conclusion: Thymus morphological specification of infant rats with tartrazine intoxication (during 1 month) indicates frank hyperplasia of thymus lymphoid with underlying maturation retention, and component lymphocyte immunological differentiation points to antigenic activation, which influenced the test animals.

0413

Pleuropulmonary blastoma: a challenging congenital tumor of fetal lung

S. Boudjemaa, M. Larroquet, V. Belle Mbou, J. van den Akker, L. Boccon-Gibod, A. Coulomb*
*Hospital Armand Trousseau, Dept. of Pathology, Paris, France

Objective: Pleuropulmonary blastoma (PPB), a rare tumor arising during fetal lung development, can be part of an inherited cancer syndrome. About 20% of children with PPB have a family history of cystic nephroma and rhabdomyosarcoma. It is related to DICER 1 mutations on 14q32 and consists in malignant mesenchymal cells and cysts lined by benign epithelium.
Method: We report our experience in a paediatric pathology center. Two girls of 1 and 39 months presented pulmonary lesions, the first purely cystic and the second purely solid, corresponding histologically to early type I and type III PPBs.
Results: The first patient underwent an upper lobectomy with an unremarkable postoperative outcome. The second patient presented a thoracic relapse 3 years after initial treatment consisting in upper lobectomy, pre- and postoperative chemotherapy. Tumoral karyotype revealed complex clonal chromosomal aberrations, dominated by interstitial 14q32, 7q22 deletion and trisomy 8. No familial history of neoplasia. She is disease-free 14 years after presentation.
Conclusion: PPB must be taken into account in the evaluation of cystic and even solid pulmonary lesions in children under 6 years. A correct histologic diagnosis is needed to identify early PPB, which may be difficult to differentiate from congenital pulmonary airway malformation (CPAM), to appropriately manage patients and to identify an inherited predisposition to PPB. Recent data showed that DICER1 on 14q32, a gene implicated in miRNA synthesis, plays a crucial role in lung development.

Loss of DICER1 alters miRNA-dependent regulation of diffusible growth factors that induce mesenchymal cell proliferation.

0415
Proliferation index measured with Ki-67 and/or topoisomerase II alpha expression is a useful prognostic factor in neuroblastoma

E. Izycka-Swieszewska, B. Lipska, E. Drozynska, W. Grajkowska, D. Perek, A. Wozniak, T. Klepacka, G. Kobierska-Gulida, J. Limon*
*Medical University of Gdansk, Dept. of Pathomorphology, Poland

Objective: Proliferation index assessed immunohistochemically with Ki-67 (PI Ki67) is the accepted prognostic factor in some types of cancer. Topoisomerase II alpha (TOPO2a) expression is another marker of cellular proliferation. The significance of both markers in neuroblastoma (NB) is not well established. The study objective was to evaluate their prognostic impact and pathoclinical relations in a series of NB tumors.
Method: Examined group consisted of 103 patients. Analyzed data included: patients' age, tumor histology, location, stage, MYCN status and overall survival. Ki67 and TOPO2a PI values were established on slides as percent of immunopositive nuclei for 100–1,000 neoplastic cells.
Results: PI Ki67 ranging 0–72% (median 18%) and TOPO2a ranging 0–58% (median 20%) were lower in children older than 18 months (>18 m, $p=0.0002$ and $p=0.01$, respectively). The two markers were strongly interrelated ($r=0.83$). Higher Ki-67 and TOPO2a correlated with higher MKI and adrenal location and inversely with increasing tumor differentiation. The cutoff values of PI Ki67 ≥ 30% and TOPO2a ≥ 25% correlated with fatal outcome of the disease. In the subgroup of patients, >18 m significant correlations between higher values of both PI markers and metastatic stage, unfavorable histology, high MKI, MYCN amplification, and adrenal localization were observed. At cutoffs Ki67 ≥ 10% and TOPO2a ≥ 25%, the markers predicted long-term unfavorable outcome by Kaplan–Meyer analysis. Cox regression analysis indentified PI (assessed jointly as Ki67 ≥ 10% + TOPO2a ≥ 25%) as the independent prognostic factor.
Conclusion: Ki67 and TOPO2a PI markers have prognostic significance and clinicopathological correlations in NB. We propose to include PI to the standard histological assessment protocol of NB tumors.

Friday, 3 September 2010, Basement

PS-18 Poster Session Infectious Disease Pathology

0417
Risk factors for fatal outcome in AH1N1 influenza patients

F. Staniceanu, A. Streinu-Cercel, S. Zurac, L. Nichita, C. Popp, G. Micu, E. Gramada, A. Bastian, R. Andrei, C. Socoliuc, M. Olariu*
*Colentina University Hospital, Dept. of Pathology, Bucharest, Romania

Objective: There are few clinical studies of the systemic human pathology of the novel AH1N1 influenza infection. We decided to test the hypothesis that fatal cases of influenza occur mainly in association with important comorbidities as was stated based in previous studies.
Method: We included in our study 97 patients with fatal AH1N1 influenza. During autopsy, we largely sampled vital organs—brain, lungs, heart, liver, kidney, lymphoid organs—lymph nodes and spleen and any other diseased organ.
Results: In our group, sex ratio was male/female = 1.7:1; patients were 5 and 76 years old (mean age 42.01). Nine women were pregnant/parturient (9.28%). Other patients presented obesity, malignant neoplasia, diabetes mellitus, cardiac diseases and tuberculosis. We analyzed the prevalence of these comorbidities in the general population (see Table). However, 48 patients did not have any comorbidities or any known cause of immunosuppression.
Conclusion: Our study group was heterogeneous with a large age distribution and different associated diseases. We identified new risk factors for fatal outcome in AH1N1 patients (obesity and/or pregnancy) and exclude other diseases as risk factor for severe evolution (diabetes mellitus). We have to emphasise that in half of the cases, there were no comorbidities or special status to actuate the severity of the disease. These findings are reinforcing the statement that the novel influenza has a different behavior than common influenza.

0418
Pathologic aspects in AH1N1 virus-related deaths in Romania

F. Staniceanu, S. Zurac, A. Streinu-Cercel, C. Popp, L. Nichita, E. Gramada, A. Bastian, G. Micu, R. Andrei, M. Olariu, M. Petre*
*Colentina University Hospital, Dept. of Pathology, Bucharest, Romania

Objective: Novel influenza is an acute viral infection of the respiratory tract caused by type A influenza virus, affecting by now the entire world. Although the illness is mild and self-limited in a great majority of cases, few patients may have a severe clinical course eventually leading to death.
Method: We studied necroptic tissue samples from 97 patients submitted over a 4-month period from a total of 7,008 positive cases identified in Romania since the outbreak of this type of influenza. Data collected included demographic and clinical information.
Results: Most of the patients (65.97%) were adults between 21 and 50 years (median age, 42.01 years), male/female ration 1.7:1. The vast majority of the cases revealed diffuse alveolar damage, interstitial pneumonia and bronchopneumonia, all of them associating severe cytopathic effect in the bronchial and alveolar epithelial cells; 17 cases presented pulmonary ischemic lesions. More than half of the cases (59.79%) presented myocardial interstitial inflammatory infiltrate with full-blown picture of myocarditis in 11 patients. Of the patients, 80.41% had lymphocytic depletion in lymphoid organs. Lymphocytic meningitis, meningothelial hyperplasia, acute tubular necrosis, and liver steatosis were identified in some cases.
Conclusion: The respiratory tract is the major target of influenza A H1N1 virus. Pulmonary lesions are the main cause of death in all patients with new influenza virus infection, but most of them had significant extrapulmonary comorbidities.

0419

Role of HPV-mRNA detection in HPV infections

M. Rongioletti, F. Papa, M. B. Majolini, V. Panetta, C. Vaccarella, A. Falconio, G. Bruno, L. Bonito, M. Cortesi, R. Mari, G. M. Liumbruno*
*San Giovanni Calibita Hospital, Rome, Italy

Objective: HPV DNA has been identified in almost all cervical cancers, and women with active HPV infection (HPVI) express E6/E7 oncogenes. As only a small proportion of infections progress towards cancer, it is important to distinguish transient HPVIs from persistent or progressive ones.
Method: One hundred ninety-six samples were tested by conventional Pap smear, HPV-DNA test and typing, E6/E7-mRNA expression from HPV types 16, 18, 31, 33, 45. *K*-statistic value was used in order to identify possible significant associations.
Results: Pap-smear: negative (NEG), 248 (68.5%); atypical cells of undetermined significance (ASCUS), 50 (12.4%); low-grade squamous intraepithelial lesion (LSIL), 36 (9.9%); high-grade squamous intraepithelial lesion (HSIL), 28 (7.7%). One hundred ninety-two of 362 samples (53.04%) were positive to the HPV-DNA test and 80 of 362 (22.10%) to the HPV-mRNA test. The HPV-DNA test was positive in 110 of 248 (44.4%) of NEG, 37 of 50 (74.0%) of ASCUS, 22 of 36 (61.1%) of LSIL and 23 of 28 (82.1%) of HSIL; the E6/E7-mRNA test was positive in 25 of 248 (10.1%) of NEG, 17 of 50 (34.0%) of ASCUS, 15 of 36 (41.7%) of LSIL and 23 of 28 (82.1%) of HSIL.
Conclusion: The detection of HPV-mRNA shows a greater association with the degree of development of atypical or malignant lesions in comparison to the presence of HPV-DNA. The mRNA test might be a second level tool for the appropriate follow-up of ASCUS and LSIL patients with persistent or progressive HPVIs.

0420

Combination of multiple sclerosis with chronic herpetic meningoencephalitis

M. Nedzvedz, G. Nedzvedz, A. Nedzvedz, A. Buniak, G. Petrovitch*
*Medical University, Dept. of Pathologoanatomic, Minsk, Belarus

Objective: Etiology of multiple sclerosis (MS) includes the virus infection which plays probably an important cofactor role in the pathogenesis of disease. Clinical and morphological analysis of the cases of chronic herpetic meningoencephalitis (CHME) and MS permitted to discover two cases of a combination of diseases: man, age 58 years (onset of MS since 18 years), and woman, age 65 years (onset of MS since 27 years).
Results: Autopsy revealed the small plaques in white matter of brain and cord and some foyers of necrosis in frontal lobe and brain stem. The histological signs of chronic inflammation were established in both cases. Leptomeninges and brain were infiltrated by lymphocytes and macrophages (perivascular cuffs). The progressive lesions of cortical neurons and proliferation of macroglial cells were constant histological findings. Etiological diagnosis of CHME was established on the base of typical intranuclear viral inclusion types I and II in the cells of brain as well as on the revealing of HSV antigens in histological slice. Laminar nonischemic necrosis was found in the cortex of frontal and parietal lobes. In the brain stem, necrosis appeared as the small foci of destruction of nervous tissue. In one case, laminar necrosis were detected in white matter of hippocampe.
Conclusion: Thus, the morphological investigation on the light microscopic level permits correctly to recognize the combination of MS and CHME.

0422

Whipple's disease associated whit Crohn's disease

M. L. Caruso, M. Pirrelli, M. Mastronardi, A. M. Valentini*
*IRCCS, Pathologic Anatomy, Castellana Grotte, Italy

Objective: We present the first case reporting the exceptional association of Whipple's and Crohn's disease.
Method: A 59-year-old man developed since 2005 diarrhea, abdominal pain, weight loss, and polyarthralgia. Endoscopy showed aphthous ulcers in terminal ileum and colon. Histology revealed a rich collection of epithelioid granulomas in the lamina propria with chronic inflammation. A diagnosis of Crohn's disease (CD) was given and steroid therapy was administered. Diarrhea and abdominal pain quickly subsided. Perduring a severe weight loss, a gastroduodenal endoscopy was performed. Oedema with whitish spots in the duodenum was observed. Histology demonstrated lymphangiectasia and an infiltration of PAS positive foamy histiocytes in the lamina propria. Immunohistochemistry for *Tropheryma whipplei* was positive.
Results: Whipple's disease (WD) diagnosis was made and an antibiotic therapy was given. In respect to symptomatic improvement, persistence of the bacterium was demonstrated in the following performed gastric and duodenal biopsies. Immunohistochemistry in previous ileal and bowel specimens was positive in the ileum.
Conclusion: In WD, the macrophages seem to be of central importance in the development of the disease. This infection shares with CD the pathogenetic hypothesis that a defect in cellular immune response contributes to the development of the disorder. Evidences also suggest that bacteria play a role in the onset and perpetuation of CD. This case strengthens the immunological hypothesis in the pathogenesis of the disorders. The functional defect of the macrophages caused by WD can explain the amazing number of granulomas in Crohn's-affected specimens. The double immunological defect due to CD and CD may contribute to the lack of eradication of the bacteria.

Friday, 3 September 2010, Basement

PS-19 Poster Session IT

0423

The use of digital microscopy and Internet in the pathological diagnosis—own experience

E. Kaznowska, J. Pankowski*
*SZGiChP, Dept. of Pathology, Rzeszow, Poland

Objective: The aim of the study was to analyze the experience obtained during pathological diagnosis using digital microscopy and telepathology.
Method: There were 594 microscopic examinations performed over the Internet using a dynamic digital microscope NICON-COOLSCOPE, scanners APERIO-SCANSCOPE and OLYMPUS dotSlide, between January 2007 and March 2010. The study included 213 intraoperative studies, 317 cytology specimens and 62 oligobiopsies. The specimens were prepared and sent electronically by four cytotechnicians and assessed by five pathologists. All diagnoses were verified through routine, light microscopy assessments.
Results: In cases of intraoperative, frozen sections studies as well as oncologically positive cytological diagnoses, above 98% agreement was noted between the diagnoses made due to evaluation over the Internet and the routine assessment. The agreement of 100% was achieved in cases of benign lesions and the assessment of bronchial surgical margins.
Conclusion: (1) The efficiency of histological slide examination by sending digital images via the Internet in cases of intraoperative frozen sections during thoracic surgery or to confirm "positive" results is comparable to the traditional assessment in a light microscope. (2) Application of this method enables surgeons at the hospitals which do not have a readily available pathologist to perform the surgical procedures.

Friday, 3 September 2010, Basement

PS-20 Poster Session Electron Microscopy

0424

The role of electron microscopy in the diagnosis of childhood glomerulopathies

M. Mehrazma, I. Jahanzad, N. Hooman, A. Ostadali Makhmalbaf*
*Ali-Asghar Children Hospital, Dept. of Pathology, Tehran, Iran

Objective: Optimum diagnosis of glomerulopathies requires light microscopy, immunofluorescence and electron microcopy. In fact, electron microscopy has a confirmatory role in glomerular diseases. In this study, the value of electron microscopy in the diagnosis of glomerulopathies in children was investigated.
Method: The contribution of electron microscopy to the final diagnosis was graded as necessary—diagnosis could not be reached without it; supportive—it increased the level of confidence in the final diagnosis; and noncontributory—the diagnosis does not need electron microscopy for confirmation.

Results: One hundred thirty-four cases of renal biopsy with some clinical data are reviewed. The contribution of electron microscopy to the final diagnosis was necessary in 51 cases (38%), supportive in 40 cases (30%) and noncontributory in 43 cases (32%).

Conclusion: It is concluded that ultrastructural study was an essential tool in the study of renal biopsy in childhood glomerulopathies, suggesting that electron microscopy still remains a useful tool in the diagnosis of glomerular disease.

Virchows Arch (2010) 457:283–290
DOI 10.1007/s00428-010-0953-1

INVITED EDITORIAL

The birth of endocrine pathology

How Erdheim misunderstood parathyroids

Anton H. M. Vermeulen

Received: 25 May 2010 / Revised: 9 July 2010 / Accepted: 18 July 2010 / Published online: 3 August 2010
© The Author(s) 2010. This article is published with open access at Springerlink.com

The structure that would later be called the parathyroid gland was first observed around 1850, the second half of the nineteenth century in which so many new discoveries in anatomy and histology were made [1]. The first description of "a small compact yellow glandular body" [3] was followed 30 years later by the notion that removal of this structure might be responsible for acute tetany occurring after thyroidectomy. This was the period during which detailed anatomical and histological observations led to increased understanding of bodily functions in health and disease, including that of the parathyroids [2]. The pathologist Jacob Erdheim (1874–1937) built on these new discoveries in elucidating through clinical observations as well as experimental studies how parathyroids play a role in calcium metabolism and how their dysfunction leads to serious bone pathology. The story illustrates that scientific discovery is not a linear process: Erdheims understanding of parathyroid function was hampered through his misinterpretation of some of his observations.

The first observation and discovery of the parathyroid glands

The first written observation of a parathyroid gland was made by Richard Owen (1804–1892) in an Indian Rhinoceros with a weight of approximately 5,000 lbs avoirdupois (±2,267 kg). Owen described *"a small compact yellow glandular body was attached to the thyroid at the point where the veins emerge"* [3]. The dissection took place during the winter months of 1849–1850, and Owen presented his findings at a meeting of the Zoological Society on February the 12th, 1850. The lecture was published in 1862 in the "Transactions of the Zoological Society" [4].

The definitive discovery of the parathyroid glands was made in 1877 by Ivar Sandström (1852–1889, Fig. 1) then a medical student. As a prosector at the department of anatomy in Uppsala he published his findings in the "Upsala Läkareförenings Förhandlingar for 1879–1880", (Fig. 2) a Swedish journal [5, 6]. Sandstrom wrote: "*About three years ago (1877) I found on the thyroid gland of a dog a small organ, hardly as big as a hemp seed, which was enclosed in the same connective tissue capsule as the thyroid, but could be distinguished therefrom by a lighter color. A superficial examination revealed an organ of a totally different structure from that of the thyroid, and with a very rich vascularity ....*" [6]. Hampered by lack of time and shortage of material Sandström could only continue his studies in the winter of 1880 after a delay of 2 years. While his investigations embraced several species, including man, dog, cat, rabbit, ox, and horse, his main interest was the anatomy and the microscopic features of these glands in humans. In 43 completely performed autopsies Sandström was able to demonstrate two parathyroid glands on each side of the thyroid; in seven cases of in situ dissections he found a smaller number of these tiny glands. Sandström gave a meticulous description of these glands, concerning their anatomic localization, size, shape, and color. In his microscopic examination he described the parathyroids as "vascular glands", richly vascular structures made up of solid fields, trabeculae, and glandular cells, sometimes arranged in follicles with focal presence of colloid, but without ducts (Fig. 3).

A. H. M. Vermeulen (✉)
Department of Pathology, Maastricht University Medical Center,
P. Debyelaan 25,
6229 HX Maastricht, The Netherlands
e-mail: ahmverm@gmail.com

Fig. 1 Ivar Sandström (1852–1889) [6]

Referring to the embryological studies of the thyroid by Robert Remak [7] two decades earlier, and the contemporary studies of Kölliker [8], Sandström considered his "structures" to be embryonic thyroid glands arrested in

UPSALA LÄKAREFÖRENINGS
FÖRHANDLINGAR

Band. XV. 1879—1880. N:r 7 & 8.

Fredagen den 5 Mars.

SANDSTRÖM, Glandulæ parathyreoideæ. — BLIX, Myograf. — SANDSTRÖM, Prostatapreparat. — WIDE, Lefverpreparat. — HOLMGREN, Retinaströmmen. — Svar till *H. Cohn* om färgblindheten. — Föreningens yttrande mot *K. Wickselis* föredrag om dryckenskap.

1. Om en ny körtel hos menniskan och åtskilliga däggdjur

af

IVAR SANDSTRÖM.

För snart tre år sedan påträffade jag å sköldkörteln af en hund en liten, knappt hampfröstor bildning, som låg innesluten

Fig. 2 Announcement of Sandström´s discovery of the parathyroid glands [5]. Courtesy of the library University of Amsterdam (UvA, UBM: V.V. 1241)

various stages of development and named them "glandulae parathyreoideae". Sandström had no notion of the physiological significance of the parathyroids, but he assigned them an important role in the pathological growth process particularly given their embryonic nature. With due respect he pointed to previous descriptions of these glands by Remak, who described them in kittens [7] and by Virchow in man [9]. His excellent presentation of the subject was translated into German and sent to a German Journal. Remarkably, the article was refused because of excessive length, a reason open to serious debate given the enormous size of many scientific articles in German Journals those days! As an abstract the paper was finally published in 1880 in a few German Journals [10].

The rise of thyroid surgery and its complications

Cachexia strumipriva and tetany

Sandström's discovery remained unnoticed for more than 10 years, coincidentally a period when thyroid surgery not only achieved its first successes but also experienced significant and severe complications, particularly in some parts of Switzerland, those days known for many cases of endemic goiter [11]. Theodor Kocher (1841–1917) from Bern, considered by many as the father of thyroid surgery, popularized the idea that removal of the thyroid gland did not induce adverse effects in man. Jacques-Louis Reverdin (1842–1929) from Geneva held similar views. Kocher, however, was alerted by disturbing information reported by Reverdin, who described a number of strumectomized patients who showed alarming symptoms of increasing anemia, physical and mental inertia. Kocher succeeded tracing 34 patients, 20 of them showed various stages of myxedema and cretinism. Shortly afterwards in 1883 during a spring meeting for German surgeons in Berlin, Kocher warned his colleagues to abandon total strumectomy [12]. The same year Kocher published his article on the effects of total strumectomy and introduced the term "Cachexia strumipriva" (myxedema after total thyroidectomy) [13].

In addition to these long-term complications, surgeons were becoming increasingly alarmed by one of the acute complications after (sub-)total strumectomy, namely the unpredictable occurrence of tetany that could result in a fatal outcome. In 1881, Nathan Weiss (1851–1883) published a thorough clinical and neurophysiological study on tetany in which he presented three of Billroth's patients who suffered from postoperative attacks of tetany [14]. In one case the attack proved fatal. Weiss believed that there was a causal link between the occurrence of tetany and surgery, hereby departing from the traditional view that tetany and cachexia strumipriva were simply successive

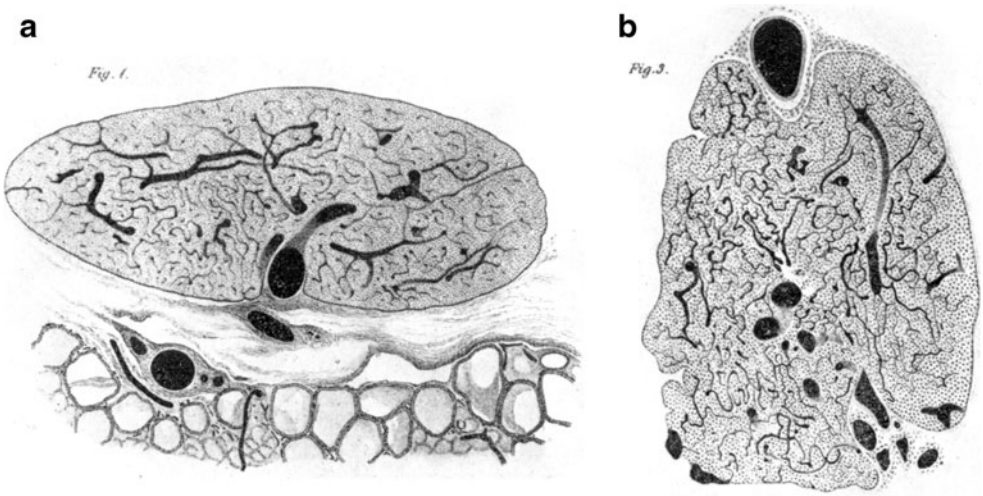

Fig. 3 **a** Transection through the parathyroid and part of the thyroid gland in dog. Acid potassium bichromate 2% solution, eugenol, Canada Balsam. Vessels injected. Drawn at Hartnack object 4, ocular 3, tube not drawn out; **b** section of the parathyroid from man. Blood vessels injected. Acid potassium bichromate 2% solution, carmine, eugenol, Canada Balsam. Drawn at Hartnack object 4, ocular 3, tube not drawn out [6]

stages of a single disorder caused by strumectomy [15]. By animal studies Gley made an attempt to unravel the causes of these two complications and was the first investigator to draw attention to Sandström's parathyroid glands.

The first animal experiments

Eugéne Gley (1857–1930), professor of physiology at the School of Medicine in Paris, provides a stellar example in history of pathology and medicine, not only of the use of planned animal experiments for the investigation of clinical problems, but also the importance of a thorough study of the literature as an intrinsic part of the experimental design. In the 1880 edition of Schmidt's Jahrbücher [16], Gley became acquainted with Sandström's abstract, describing the parathyroids. The "Jahrbücher" was notable for publishing lectures and investigations from every discipline in medicine inside and outside Germany in a concise but comprehensive survey [17]. So, after a lapse of more than 10 years, Gley rediscovered the external parathyroid glands and named them "glandules thyroidiennes" [18, 19] because he, like Sandström, regarded the parathyroids as embryonic thyroid tissue. In his animal experiments Gley showed that simultaneous removal of the thyroid and two external glandules thyroidiennes (as he named "thyreoidectomie complète") led to a lethal tetany in 90% of his cases. Notably, removal of both external parathyroids leaving the thyroid gland unaffected did not provoke any symptom of tetany. Unfamiliar with the actual total number of parathyroids in rabbits, coupled with incomplete microscopic observations, Gley drew the erroneous conclusion that: "*a true functional association may possibly exist between the thyroid and the parathyroid glands*" and was unable more clearly to define their function [20]. Nonetheless, Gley was the first investigator to assign a vital role of the parathyroid glands, albeit that the role still lacked clear definition.

Alfred Kohn, Giulio Vassale, and Francesco Generali

Alfred Kohn (1867–1959) dedicated his whole life to the study of endocrine organs, utilizing the rich resources of the department of histology of Prague that provided a reliable anatomical basis for his experimental investigations. By means of preparing numerous serial sections through the thyroid gland and adjacent organs of the neck in humans and several mammals, Kohn demonstrated the presence of four parathyroids in cat [21] and rabbit [22]: two external parathyroids and two parathyroids within the thyroid gland, one within each lobe; these 'internal' parathyroids were unknown to Gley providing the source of some confusion in his experiments in rabbits. Unlike both Sandström and Gley, Kohn was convinced of the separate identity of the parathyroid glands. Because Kohn questioned from the beginning the identical nature of thyroid and parathyroid glands he gave the latter the non-committal term "Epithelkörperchen" (epithelial bodies), taken from Maurer's article about amphibians [cited in 21], a nomenclature still common in recent German literature. Applying Kohn's results, the Italian investigators, Giulio Vassale (1862–1912), a pathologist from Modena and Francesco Generali, demonstrated in their first animal experiments that removal of all parathyroid glands in cat and dog, leaving the thyroid gland intact, ended in fatal tetany in both species [23]. From these experiments the investigators concluded that the parathyroids play a unique and separate role and should not be considered as embryonic thyroid remnants. Further they were unable to show any compensatory function of the parathyroid glands after removal of the thyroid. In a second set of experiments Vassale and Generali carried out a series of parathyroidectomies, ranging from removal of only one to a total removal of the parathyroids, with and without thyroidectomy. Once again they came to the same conclusion; the parathyroids were separate organs, distinct from the thyroid. [24].

Osteitis fibrosa in "Virchow's Festschrift"

Virchow's (1821–1902) 70th birthday in 1891 was a notable occasion that merited special celebration. To mark the event 13, of his residents, men like Friedrich Daniel von Recklinghausen (1833–1910, Fig. 4), Edwin Klebs (1834–1913), and Paul Grawitz (1850–1932), compiled and published a festschrift entitled: "Festschrift Rudolf Virchow zu seinem 71. Geburtstage" [25]. The festschrift (Fig. 5), illustrated with (chromo-) lithographic figures and tables contained contributions on pathology, physiology, and chemistry was a remarkable testament of the times in pathology. It included an extensive 89-page contribution by Von Recklinghausen entitled: "Die fibröse oder deformirende Ostitis, die Osteomalacie und die osteoplastische Carcinose in ihren gegenseitigen Beziehungen (…..in their mutual relations)" [26], in which he presented 16 cases of various bone disorders, categorized into three groups as indicated in the title. Under the heading of 'fibrous osteitis', Von Recklinghausen described a number of cases of Paget´s disease and two cases of osteitis fibrosa-like bone disorders. Fifty years later these latter two cases were revisited and revised by the endocrinologist Fuller Albright (1900–1969) as polyostotic fibrous dysplasia [1]. Besides four patients with osteoplastic bone metastases Von Recklinghausen also discussed (under the heading: "extensive bone malacia") five (!) subcategories of osteomalacia, and one condition, being his immortal case of osteitis fibrosa.

This famous case starts with the touching clinical history of Herr Bleich, translated by Albright: "Herr Bleich was a 40 year old married mason who years before had undergone a mercury cure for syphilis. In April 1888, he fell from a 3-m high ladder onto his left side; eight days later he was admitted to the Surgical Clinic because of severe pain in his hip joint. It was not clear whether a fracture of the neck of the femur or a coxitis was present. He was treated with extension until August, when improvement was so far advanced that he began to walk with a stick. In October the patient slipped, fell against a bench, and fractured his clavicle. He was readmitted to the Surgical Clinic. There he underwent a transverse fracture of the diaphysis of the right femur while lying in bed, the bedpan was clumsily maneuvered! Continued pain and unsatisfactory union made it necessary to transfer him to a nonclinical division of the City Hospital. When he was again examined in the Clinic in the course of the summer of 1889, he not only showed the most extensive bending of several long bones, but complained of excruciating pain in many bones and appeared very emaciated. Although the fracture seemed to heal, the patient was unable to raise the leg; marasmus increased and he died on October 4, 1889" [1]. Urine was never tested [26].

Fig. 4 Von Recklinghausen as Professor of Pathology at the University of Strassbourg in the period 1872–1906. Courtesy of Verlag Degener & Co, Inh Manfred Dreiss [38]

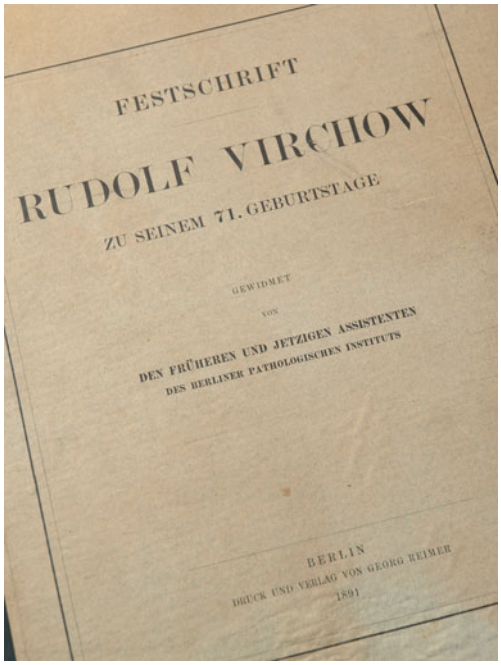

Fig. 5 Festschrift dedicated to Rudolf Virchow's 71st birthday by his former and present residents. The book was printed and published in 1891, the year Virchow celebrated his 70th (!) birthday (October 13, 1891) [25]

The clinical picture is followed by a detailed anatomical and microscopic examination of the skeleton revealing all the characteristics of severe hyperparathyroidism: many skeletal deformities, fractures, fibrosis, hematogenous pigment, cysts (Fig. 6), and conglomerates of giant cells. This case reported by Von Recklinghausen and diagnosed as " Fibröse Ostitis. Multiple Osteosarkome", was classified as " metaplastic malacia", in which metaplasia indicates replacement of pre-existing compact bone by newly formed fibrous osteoid. By use of the designation "Osteosarkome", Von Recklinghausen referred to the brown tumors termed "Myeloidtumoren" or "Riesenzellensarkomen", a nomenclature that still was employed in 1910 in his posthumously published monograph "Untersuchungen über Rachitis und Osteomalacia" [27].

On the basis of his microscopic findings von Recklinghausen concluded that the cause of many forms of chronic fibrotic osteitis, including the Bleich case, was to be found in pathologic changes within the vascular system. In his mono-

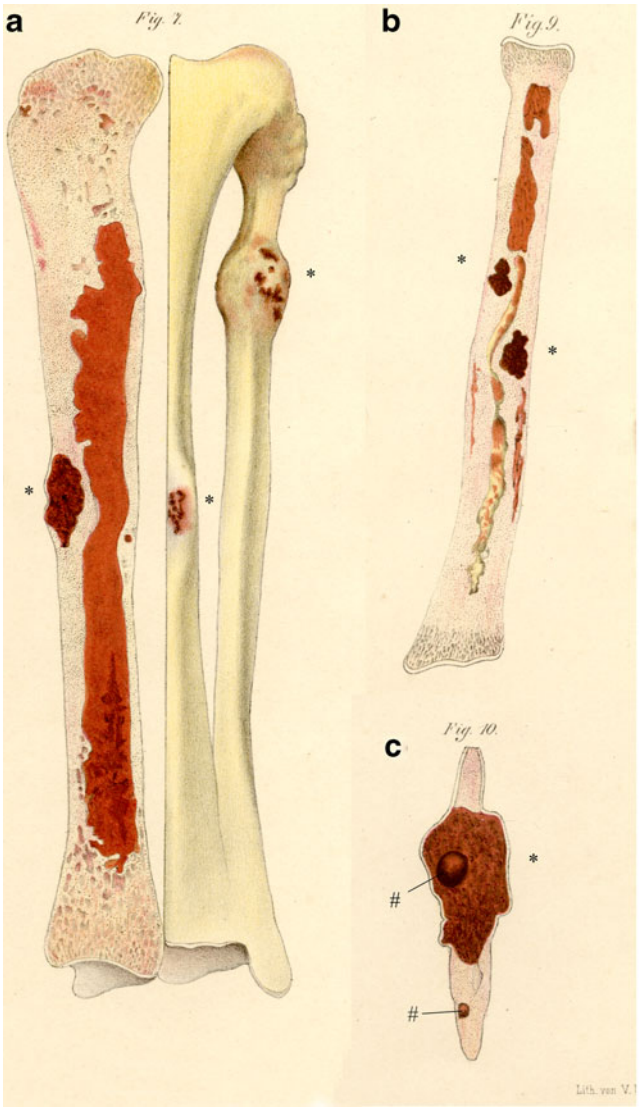

Fig. 6 **a** Left tibia and fibula, sagittal section through tibia; cortical new bone formation in the diaphysis with localization of brown tumor (*asterisk*). Expanding brown tumor (*asterisk*) in the proximal part of the fibula; **b** left radius, new bone formation in the diaphyseal cortex with two brown tumors (*asterisk*); **c** longitudinal section of a rib segment; expansive brown tumor (*asterisk*) with a smooth-walled cyst (*number sign*); intra-osseous cyst in porous section (*number sign*). Chromolithographic table [26]

graph he referred to the dissertation of Gerhard Engel from1864 [28] where an almost identical case was presented; a finding recognized in the German literature where osteitis fibrosa is also known as an "Engel-Recklinghausen" disease.

The relationship between osteitis fibrosa and tumor of the parathyreoids: the first evidence

In his hand-written autopsy report of Mr. Bleich, Von Recklinghausen described a structure suggestive of an enlarged parathyroid gland, but nevertheless failed to establish a causal relationship between osteitis fibrosa and pathological changes in the parathyroids. Years later, in 1933, Adolphe Jung, a surgeon from Strasbourg re-examined two autopsy reports of osteitis fibrosa; both autopsies were carried out by von Recklinghausen, one case dated 1901 and the Bleich report that contained the remark: "*Below the thyroid, on the left side, a lymph node, brownish-red… normal thyroid volume, size of the thyroid …*". Possibly this " lymph node" was a parathyroid adenoma [29].

In 1904, Max Askanazy (1865–1940) from Bern published a classic case of osteitis fibrosa [30] in a 51-year-old female patient who died from her illness. At autopsy Askanazy found goiter of the right thyroid lobe and a soft red-white tumor of 4.5×2×2 cm fixed to the left lobe. He considered the diagnosis of a tumor of a parathyroid gland. In discussing a possible cause of the skeletal abnormalities, Askanazy recommended paying special attention to the thyroid and other "vascular glands", without specifically referring to the fact that the patient had a parathyroid tumor.

Breakthrough in the animal experiment: Jacob Erdheim

Many surgeons continued to harbor the possibility, if not the firm belief, that thyroidectomy played a role in the occurrence of tetany and remained skeptical about the findings of Vassale and Generali. Moreover, many questioned the validity of applying conclusions drawn from animal experiments to human beings. All of this was to change around the turn of the century with the meticulous work of Jacob Erdheim (1874–1937), a pathologist from Vienna (Fig. 7). Erdheim developed a special interest in bone pathology and pathology of endocrine organs publishing several articles on these topics, in the course of which he made major contributions to clarifying the nature and role of the parathyroid glands [33].

In an ambitious animal experiment with rats Erdheim furnished convincing evidence that total parathyroidectomy leads to tetany. In the context of these animal studies he also examined three autopsy cases of patients who died of tetany after subtotal thyroidectomy. In none of these cases could there be found any remnant of functioning parathyroids. To achieve optimal results Erdheim proceeded with a remarkable degree of thoroughness assembling an astonishing number of histological slides; more than 10,000 sections of 30 μ were prepared! In his animal experiment Erdheim made use of the rat because this animal has only two parathyroid glands, and these are easily accessible. Selective destruction of both glands and all their parts was

carefully controlled and demonstrated by Erdheim, again by preparing serial histological sections of the neck organs.

A number of Erdheim's laboratory animals survived the attacks of tetany. Here again he displayed characteristic tenacity and indefatigability, continuing to follow these animals, as a result of which he made an additional surprising observation. On the 10th day after total parathyroidectomy, Erdheim observed developing abnormalities in enamel and dentin of the continuously growing incisors in a number of the rodents, their molars remained unchanged. In almost all surviving rats, three months after surgery, abnormal opacities were apparent in the tooth enamel and deficient calcium deposits in the dentin of the incisors could be histologically confirmed. The outcome of this disorder was severe, leading to deformity, fracture, and failure of the incisors (Fig. 8), followed by infection, ulceration, and abscess formation. The results of these experiments identify Erdheim as the first investigator to establish a role of the parathyroid glands in calcium metabolism. Erdheim presented his investigations, combined with many interesting historical, clinical, and pathological notes from the literature in the form of an impressive review article, entitled: "Tetania parathyreopriva" [15].

Fig. 7 Jacob Erdheim (1874–1934). After his education in the Department of pathology under professor Weichselbaum, Erdheim worked in a children's hospital for many years. Shortly after his appointment as pathologist in the Vienna Municipal Hospital, he was appointed as full professor of pathology. Courtesy Bildarchiv der Medizinischen Universität Wien

Erdheim's theory

Erdheim's experiments and his conclusions with respect to a role for the parathyroid glands in calcium metabolism caused general surprise and almost immediately raised questions concerning the function of the parathyroid glands in pathologic conditions such as osteomalacia, a disease that already was considered to be an "anomaly" in calcium metabolism.

Erdheim examined six autopsy cases of osteomalacia thoroughly. In four patients he found hyperplasia or microscopically observable foci of epithelial proliferation in one or more parathyroids; in one case a tumor of a single parathyroid gland was found [31].

In a subsequent experiment Erdheim demonstrated increased parathyroid volumes in rachitic rats [32]. Based on the sum of his observations, Erdheim came to consider the parathyroid glands as an important link in the pathogenesis of rickets and osteomalacia.

His hypothesis was stated as follows: "*The parathyroid glands normally produce a fluid that enables osteoid to calcify. In cases of rickets and osteomalacia, this secretion is consumed or disintegrated in an unknown aberrant way, hampering osteoid to calcify which causes the characteristic changes of both disorders. The increased amount of osteoid induces stimulation of the parathyreoid glands resulting in hypertrophy or hyperplasia.*" [32].

Doubts on Erdheim's theory in literature

Erdheim's theory that increased parathyroid size is the result of, not the cause of, osteomalacia and rickets was generally accepted and further was also applied to osteitis fibrosa by several authors, who considered the latter disorder to be a variant of osteomalacia. Erdheim neither confirmed nor contested this view. Friedrich Schlagenhaufer (1866–1930), coincidentally also a pathologist from Vienna, was the first to question the applicability of Erdheim's theory to cases of osteitis fibrosa [34]. At a meeting of the "k.k. Gesellschaft der Ärzte in Wien" in 1915, Schlagenhaufer presented two cases of parathyroid tumor diagnosed at autopsy. Both patients suffered from osteomalacia, one of them with signs of osteitis fibrosa of the skull base. In the ensuing discussion Schlagenhaufer advocated removal of the parathyroid tumor in similar cases as a mode of therapy, an opinion supported by Maresch, one of his pathology colleagues. This interesting and practical suggestion gave rise to a rapidly expanding literature on the subject in the ensuing years. In one study of the literature, Siegfried Hoffheinz (1892–1953?) collected and described in 1925 seventeen autopsy cases of osteitis fibrosa [35]. In 12 cases, only one enlarged parathyroid gland was identified; in the

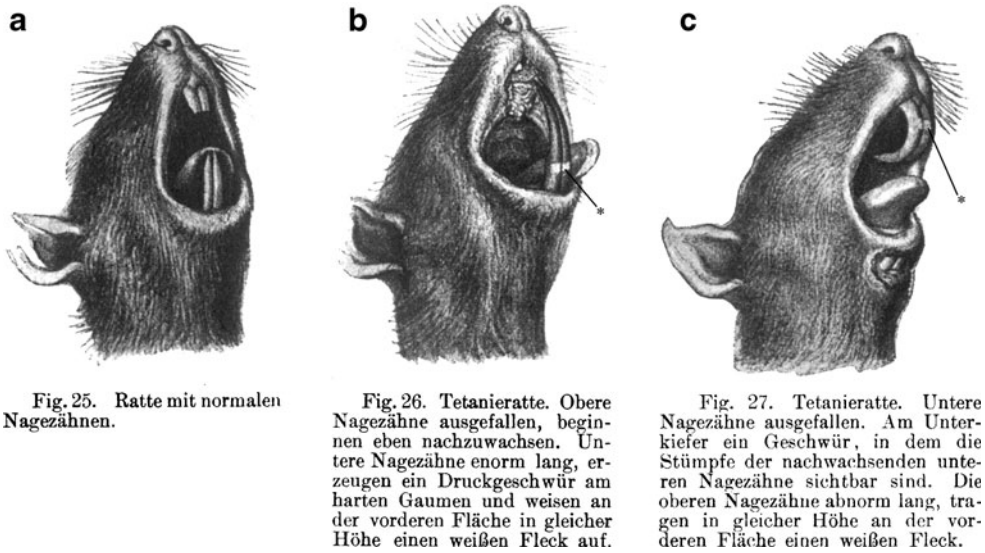

Fig. 25. Ratte mit normalen Nagezähnen.

Fig. 26. Tetanieratte. Obere Nagezähne ausgefallen, beginnen eben nachzuwachsen. Untere Nagezähne enorm lang, erzeugen ein Druckgeschwür am harten Gaumen und weisen an der vorderen Fläche in gleicher Höhe einen weißen Fleck auf.

Fig. 27. Tetanieratte. Untere Nagezähne ausgefallen. Am Unterkiefer ein Geschwür, in dem die Stümpfe der nachwachsenden unteren Nagezähne sichtbar sind. Die oberen Nagezähne abnorm lang, tragen in gleicher Höhe an der vorderen Fläche einen weißen Fleck.

Fig. 8 **a** Rat with normal incisors; **b** loss of both upper incisors and new growth. Enormous elongation of the lower incisors and pressure ulcer of the hard palate. Witte spot (*asterisk*) on the front side of both lower incisors. **c** Loss of both lower incisors. Ulcer of the mandible with visible new growth of lower incisors. Abnormal extension of both upper incisors and white spot (*asterisk*) on the front side of both incisors [15]. Courtesy of the library University of Nijmegen

remaining cases two to four glands were enlarged. Whether the glands were hyperplastic or adenomatous was not established. Hoffheinz concluded somewhat tentatively, that Erdheim's "compensatory theory" probably did not apply to cases of osteitis fibrosa. One of the authors cited in the Hoffheinz paper even went so far as proposing the existence of a true parathyroid tumor in his autopsy case of osteitis fibrosa.

Medical practice: Mandl's biological experiment by surgical intervention

A practical proof that Erdheim's theory was not applicable in cases of osteitis fibrosa was provided by Felix Mandl (1892–1957), then resident of the university surgical clinics in Vienna [36]. In December 1925, Mandl examined and admitted to hospital a 38-year-old patient who suffered severe generalized osteitis fibrosa for 5 years. Major deformities were detected radiographically in both femora and in the pelvis; the skeleton was intensively decalcified and the excretion of calcium in urine was strongly increased. Initially, in concurrence with the generally held belief that Erdheim's theory applied to osteitis fibrosa, the patient was treated with tablets of 'parathyreoidin' (a parathyroid extract) and subsequently discharged. However, after a subsequent spontaneous fracture of the femur, the patient's general condition deteriorated, leading to readmission 4 months later. Again, consistent with Erdheim's compensatory theory, Mandl implanted four parathyroid glands from an accident victim, without any result. At this point, having achieved no clinical benefit, and having no further therapeutic options at his disposal Mandl began to question the validity of Erdheim´s theory: was this theory really suitable in cases of osteitis fibrosa?

Influenced by Schlagenhaufer's proposal previously for removal of a parathyroid tumor in osteitis fibrosa, and perhaps encouraged by Hoffheinz's review of the literature offering tentative support, Mandl decided to intervene surgically, although clinical examination did not reveal enlarged glands in the neck area. However, during surgical exploration a definitive parathyroid tumor, measuring 25× 15×12 mm, was found and removed. The resected specimen was examined by Erdheim and Maresch and identified as parathyroid tissue; however, no precise diagnosis was made (hypertrophy or tumor) [36, 37]. Post-operatively the patient reported subjective improvements in symptoms, the pain disappeared and the patient was able to walk again using crutches. Furthermore, X-ray examination showed an increased density of the skeleton, and urine calcium excretion was significantly decreased.

This planned surgical intervention, which Mandl subsequently considered as a biological experiment, was a critical first step in proving a causal relationship between a parathyroid tumor and osteitis fibrosa; the parathyroid tumor was the cause, the osteitis fibrosa the result. This conclusion was, of course, directly opposed to Erdheim´s compensatory theory. Mandl, perhaps in an exercise of diplomacy and respect, used the term "dysfunction" to indicate that in this special circumstance the enlarged parathyroid gland was the direct cause of the skeletal abnormalities. His conclusion that carried the benefit of offering a logical therapeutic response, namely resection of the tumor, in accordance with the inspired proposal by Schlagenhaufer was based on a single observation a decade earlier. This whole history of pathology and pathogenesis, complex and at times controversial, occurred in a period of 50 years, from the discovery of the existence of the parathyroid glands in man, to their linkage with osteitis fibrosa, and ultimately to successful surgical intervention

for relief of the disease, a remarkably short time, as histories go, just two generations of physicians, surgeons, and pathologists.

Acknowledgments The author wishes to thank Erik Vermeulen for his critical remarks and Rob Reinders for his assistance in preparing the photographs. He is also grateful to Mr. Dreiss of Verlag Degener & CO for providing figure 4.

Conflict of Interest statement The author declares that he has no conflict of interest.

Open Access This article is distributed under the terms of the Creative Commons Attribution Noncommercial License which permits any noncommercial use, distribution, and reproduction in any medium, provided the original author(s) and source are credited.

References

1. Albright F (1948) A page out of the history of hyperparathyroidism. J Clin Endocrinol 8:637–657
2. Boothby W (1921) The parathyroid glands: a review of the literature. Endocrinology 5:403–440
3. Owen R (1862) On the anatomy of the Indian Rhinoceros (Rh. unicornus, L.). Trans Zool Soc Lond 4:31–58
4. Cave AJE (1975) Richard Owen and the discovery of the parathyroid glands. In: Underwood EA (ed) Science medicine and history, vol 2. Arno Press, New York, pp 217–222
5. Sandström I (1880) Om en ny körtel hos menniskan och atskilliga däggdjur. Ups Läkareförens Förh 15:441–471
6. Seipel CM (1938) On a new gland in man and several mammals (glandulae parathyreoideae) by Ivar Sandström. In: Peters CH, Fulton JF (eds) On a new gland in man and several mammals (glandulae parathyreoideae). The Johns Hopkins Press, Baltimore, pp 14–44
7. Remak R (1855) Untersuchungen über die Entwickelung der Wirbelthiere. G. Reimer Berlin
8. Koelliker A (1879) Entwicklungsgeschichte des Menschen und der höheren Thiere. Verlag von Wilhelm Engelmann, Leipzig
9. Virchow R (1864-1865)Die krankhaften Geschwülste. Dreissig Vorlesungen gehalten während des Wintersemesters 1862-1863 an der Universität zu Berlin. Springer Verlag Berlin-Heidelberg-New York. 1978 ed. Vol. Band 3/I. Erste Hälfte. Verlag von August Hirschwald, Berlin p 13
10. Seipel CM (1938) Ivar Sandström 1852-1890 by A.Hammar (English translation). In: Peters CH, Fulton JF (eds) On a new gland in man and several mammals (glandulae parathyreoideae). The Johns Hopkins Press, Baltimore, pp 3–13
11. Hæger K (1988) The illustrated history of surgery. Bell publishing company, New York, pp 241–243
12. Thorwald J (1957) Kocher oder Berner Tragödien. In: Das Weltreich der Chirurgen. Deutscher Bücherbund, Stuttgart-Hamburg, pp 55–112
13. Morton LT, Normann JM (ed) (1991) Morton's medical Bibliography. 5th edn. Scolar Press, Aldershot, p 599
14. Weiss N (1881) Ueber Tetanie. Samml Klin Vortr Inn Med 63:1675–1704
15. Erdheim J (1906) Tetania parathyreopriva. Mitt a d Grenzgeb d Med u Chir 16:632–744
16. Berger W (1880) Ueber eine neue Drüse beim Menschen und bei verschiedenen Säugethieren; von Dr. Ivar Sandström. Schmidt's Jahrbücher der in-und ausländischen gesamten. Medicin 187:114–118
17. von Brunn W (1963) Medizinische Zeitschriften im neunzehnten Jahrhundert. Beiträge zur Geschichte der allgemein-medizinischen Fachpresse. Georg Thieme Verlag, Stuttgart
18. Gley ME (1891) Sur les fonctions du corps thyroïde. Compt rend hebd Soc de biol 43:841–847
19. Gley ME (1892) Effets de la Thyroidectomie chez le lapin. Arch de Physiol 4:135–147
20. Gley ME (1901) The Pathogeny of exophtalmic Goitre. BMJ 2256:771–773
21. Kohn A (1895) Studien über die Schilddrüse. Arch f mikr Anat 44:366–422
22. Kohn A (1896) Studien über die Schilddrüse II. Arch f mikr Anat 48:398–429
23. Vassale G, Generali F (1896) Sur les effets de l'extirpation des glandes parathyréoïdes. Arch Ital Biol 25:459–464
24. Vassale G, Generali F (1896) Sur les effets de l'extirpation des glandes parathyréoïdiennes. Arch Ital Biol 26:61–65
25. Festschrift Rudolf Virchow zu seinem 71. Geburtstage gewidmet von den früheren und jetziger Assistenten des Berliner pathologischen Instituts. (1891) G. Reimer, Berlin
26. Recklinghausen v F (1891) Die fibröse oder deformierende Ostitis, die Osteomalacie und die osteoplastische Carcinose in Ihren gegenseitigen Beziehungen. In: Festschrift R. Virchow zu seinem 71. Geburtstage. G. Reimer, Berlin
27. Recklinghausen v F (1910) Untersuchungen über Rachitis und Osteomalacie. Gustav Fischer, Jena
28. Engel G (1864) Ueber einen Fall von cystoider Entartung des gesammten Skelets. Inaugural-Dissertation. Thesis, Giessen
29. Jung AM (1933) Étude clinique de l'hyperparathyoïdisme. Cong fr Chir 42:199–268
30. Askanazy M (1904) Über Ostitis deformans ohne osteoides Gewebe. Arb a d Geb d path Anat Inst zu Tübingen 4:398–422
31. Erdheim J (1907) Über Epithelkörperbefunde bei Osteomalacie. Sitzungsber d kais Akad d Wissensch in Wien, math naturw. Klasse Abt III 116:311–370
32. Erdheim J (1914) Rachitis und Epithelkörperchen. Alfred Hölder. In Kommission bei Alfred Hölder KuK. Hof-und Staatsdruckerei, Wien
33. Rabson AM (1959) Masters of modern Pathology: Jakob Erdheim. Arch Pathol 68:357–366
34. Schlagenhaufer F (1915) Zwei Fälle von Parathyreoideatumoren. Offizielles Protokoll der k.k. Gesellschaft der Aerzte in Wien Sitzung von 3 Dezember 1915. Wien Klin Wchenschr 28 (2):1362
35. Hoffheinz S (1925) Über Vergrößerungen der Epithelkörperchen bei Ostitis fibrosa und verwandten Krankheitsbildern. Virch Arch f pathol Anat 256:705–735
36. Mandl F (1925) Therapeutischer Versuch bei Ostitis fibrosa generalisata mittels extirpation eines Epithelkörperchentumors. Wien Klin Wchenschr 38:1343–1344
37. Mandl F (1926) Klinisches und Experimentelles zur Frage der lokalisierten und generalisierten Ostitis fibrosa. Arch f klin Chir 143:245–284
38. Altmann HW (1982) Pathologie und Pathologen in Würzburg. In: Baumgart P (ed) Vierhundert Jahre Universität Würzburg. Verlag Degener & Co, Inhaber Gerhard Gessner, Neustadt an der Aisch, pp 1011–1025

Virchows Arch (2010) 457:291–297
DOI 10.1007/s00428-010-0945-1

REVIEW AND PERSPECTIVE

Serrated polyps of the colon and rectum (hyperplastic polyps, sessile serrated adenomas, traditional serrated adenomas, and mixed polyps)—proposal for diagnostic criteria

Daniela E. Aust · Gustavo B. Baretton · Members of the Working Group GI-Pathology of the German Society of Pathology

Received: 6 January 2010 / Revised: 20 June 2010 / Accepted: 20 June 2010 / Published online: 9 July 2010
© Springer-Verlag 2010

Abstract Until recently, two major types of colorectal epithelial polyps were distinguished: the adenoma and the hyperplastic polyp. While adenomas—because of their cytological atypia—were recognized as the precursor lesions for colorectal carcinoma, hyperplastic polyps were perceived as harmless lesions without any potential for malignant progression mainly because hyperplastic polyps are missing cytological atypia. Meanwhile, it is recognized that the lesions, formerly classified as hyperplastic, represent a heterogeneous group of polyps with characteristic serrated morphology some of which exhibit a significant risk of neoplastic progression. These serrated lesions show characteristic epigenetic alterations not commonly seen in colorectal adenomas and progress to colorectal carcinoma via the so-called serrated pathway (CpG-island-methylation-phenotype pathway). This group of polyps is comprised not only of hyperplastic polyps, but also of sessile serrated adenomas, traditional serrated adenomas and mixed polyps, showing serrated and "classical" adenomatous features. Diagnostic criteria and nomenclature for these lesions are not uniform and, therefore, somewhat confusing. In a consensus conference of the Working Group of Gastroenterological Pathology of the German Society of Pathology, standardization of nomenclature and diagnostic criteria as well as recommendations for clinical management of these serrated polyps were formulated and are presented herein.

Keywords Hyperplastic polyp · Sessile serrated adenoma · Traditional serrated adenoma · Serrated pathway · Precancerous lesion · Colorectum

Members of the consensus conference: F. Autschbach (Heilbronn), S. Baldus (Düsseldorf), Hendrik Bläker (Heidelberg), H. Koch (Bayreuth), C. Langner (Graz), J. Lüttges (Saarbrücken), M. Neid (Bochum), P. Schirrmacher (Heidelberg), A. Tannapfel (Bochum), M. Vieth (Bayreuth).

D. E. Aust (✉) · G. B. Baretton
Institute for Pathology, University Hospital Carl Gustav Carus, TU Dresden,
Fetscherstrasse 74,
01307 Dresden, Germany
e-mail: Daniela.Aust@uniklinikum-dresden.de

Members of the Working Group GI-Pathology of the German Society for Pathology
German Society for Pathology, Working Group GI-Pathology, Invalidenstr. 90, D-10115 Berlin, Germany

Introduction

Until recently, epithelial polyps of the colon and rectum have been classified as non-neoplastic lesions, e.g., hyperplastic or metaplastic polyps, and neoplastic adenomas (tubular, tubulovillous, villous) [1]. The distinctive feature was the presence of cytologic dysplasia or intraepithelial neoplasia (IEN), which was considered to be a *conditio sine qua non* for the diagnosis of an adenoma.

Over the last few years, however, it has been demonstrated that hyperplastic polyps/serrated lesions without the presence of IEN are, in fact, clonal epithelial proliferations with underlying genetic alterations mainly in KRAS [2, 3] and BRAF [4–6]. In addition, it has been shown that the normal shedding of epithelium, which is induced by a special form of apoptosis (anoikis), is blocked in hyperplastic polyps (and serrated adenomas). Presumably, this inhibition is mediated by activated/mutated RAS or RAF [7, 8]. The characteristic serrated morphology of the crypts can be explained by a high number of retained cells with

defective anoikis [9]. As early as 1999, Iino and Jass found hyperplastic/serrated polyps preceding microsatellite instability (MSI) colorectal carcinomas indicating that serrated polyps are involved in the carcinogenesis of a subgroup of colorectal carcinomas [10, 11]. On the other hand, Jass et al. demonstrated that "classical" adenomas are most likely *not* the precursor lesions of sporadic colorectal carcinomas with high (type 1, according to Jass et al.) and low (type 2, according to Jass et al.) microsatellite instability (MSI-H and MSI-L) since BRAF-mutations and CpG-island methylation, which are frequently detected in these carcinomas, were only very infrequently observed in adenomas [12].

CpG-island-methylation-phenotype (CIMP) describes an epigenetic methylation of CpG islands in promoter regions of the genome, which silences the transcription of genes [13]. Depending on the number of methylated genes, a phenotype with high (CIMP-H) and low methylation (CIMP-L) can be distinguished. Mismatch repair genes (e.g., MLH1, MGMT) are often silenced which leads to microsatellite instability. These molecular changes can be detected in subgroups of serrated polyps: the (traditional) serrated adenoma (TSA) and the sessile serrated adenoma (SSA, which in recent studies is referred to as a "sessile serrated lesion", see paragraph "sessile serrated adenoma") [14], indicating that SSAs and TSAs could be the precursor lesions of these cancers. In addition, an aberrant DNA-methylation occurs very early in the development of these lesions [15]. This so-called CIMP-pathway is viewed as a new pathway of sporadic colorectal carcinogenesis. Some authors postulate that this novel pathway accounts for 30% of all sporadic colorectal carcinomas [4, 12].

There is some evidence that the neoplastic progression within this pathway is faster than within the classical adenoma–carcinoma sequence [16, 17]. Recent case reports suggest that the progression of an SSA to a carcinoma may take as little as 8 months [18]. In a larger cohort, a significant association between large serrated polyps and synchronous advanced adenocarcinomas could also be detected [19]. These novel findings have an enormous impact on the clinical management of different serrated polyps [20, 21].

Still, there is a scientific debate about the morphological criteria for the diagnosis of the different serrated polyps. Accordingly, the nomenclature is inconsistent and partly confusing because different terms are used synonymously (e.g., sessile serrated adenoma/sessile serrated lesion/sessile serrated polyp). It is, therefore, not surprising that serrated precursor lesions are still misdiagnosed and categorized wrongly. Misdiagnosis might lead to an inappropriate therapy and follow-up care. The potential for malignant progression of these lesions is still not clear and has to be studied in prospective clinical trials with standardized morphological criteria for diagnosis.

A standardized diagnostic nomenclature for the German speaking countries was formulated using 19 selected cases encompassing the whole spectrum of serrated lesions during a consensus meeting of the working group, Gastroenterological Pathology of the German Society for Pathology, on 29 April 2008 in Düsseldorf, Germany. This included an elaborate discussion of the diagnostic criteria.

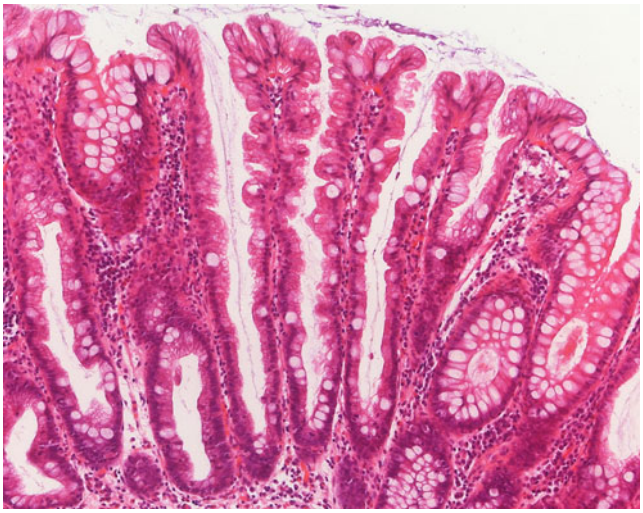

Fig. 1 Hyperplastic polyp with elongated crypts, serrated architecture in the upper half of the crypts, small, basally placed nuclei without atypia in cytology and architecture (×10)

Diagnostic criteria

Hyperplastic polyp (HP)

HPs are by far the most common serrated polyps (80–90%). They occur most often in the distal part of the colon and rectum. Grossly, these are slightly elevated lesions with a diameter of usually less than 5 mm.

Microscopically, hyperplastic polyps are characterized by elongated crypts with serrated architecture in the upper half of the crypts. Occasionally, these changes can be detected only in the upper third and on the surface of the crypts. This leads to an irregular distension with serration in the upper half of the crypt (Fig. 1; Table 1).

The proliferation in the basal half (non-serrated) of the crypt is regular. The nuclei are small, uniform, and basally

Table 1 Features of hyperplastic polyps

- Localization: left colon and rectum
- Slightly elevated
- Diameter usually <5 mm

Microscopy:

- Elongated crypts
- Serration in the top half or top third of the crypts
- Small, uniform, basally placed nuclei
- No cytological atypia or architectural dysplasia

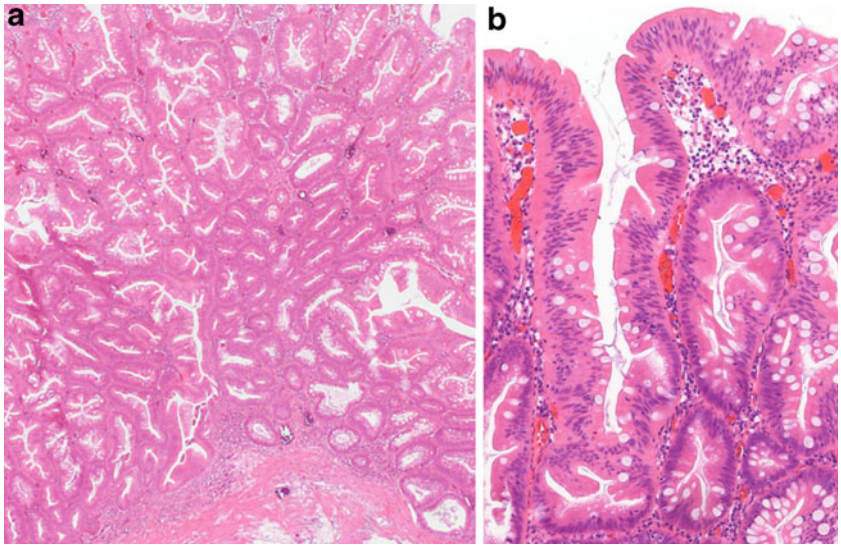

Fig. 2 Traditional serrated adenoma **a** polypoid neoplasia with a serrated pattern, eosinophilic cytoplasm and cytological atypia/low grade IEN (×2.5); **b** eosinophilic cytoplasm, vesicular and stratified nuclei (×10)

placed. There is no crowding of the nuclei in the upper half of the crypt. There is no cytological atypia or intraepithelial neoplasia. In contrast to the sessile serrated adenomas, HPs show no structural or architectural changes. In the literature, three HP subtypes are distinguished according to their cytoplasmic differentiation [22]:

1. microvesicular type (most common)
2. goblet cell type
3. mucin poor type (rarest subtype).

Because it is difficult to distinguish the different subtypes in practice [14] and the clinical relevance of reporting these subtypes is questionable [23], it is not recommended by the working group to subclassify the HPs in routine diagnostics.

The risk of malignant progression for most of the small distally located HPs in the colon and the rectum is very low. In contrast, an HP with a diameter of more than 10 mm and a localization in the proximal colon should be completely removed because some case studies and studies with small cohorts (investigating adenocarcinomas in association with large or giant hyperplastic polyps) suggest that at least some HPs have malignant potential [24, 25]. The occurrence of multiple hyperplastic polyps within the hyperplastic polyposis syndrome is associated with colorectal carcinomas [26–28].

Table 2 Features of TSA

• Localization : more frequent in the left colon and rectum
• Polypoid
Microscopy:
• Dysplasia/IEN
• Diffuse eosinophilic cytoplasm
• ECF
• Prominent serration

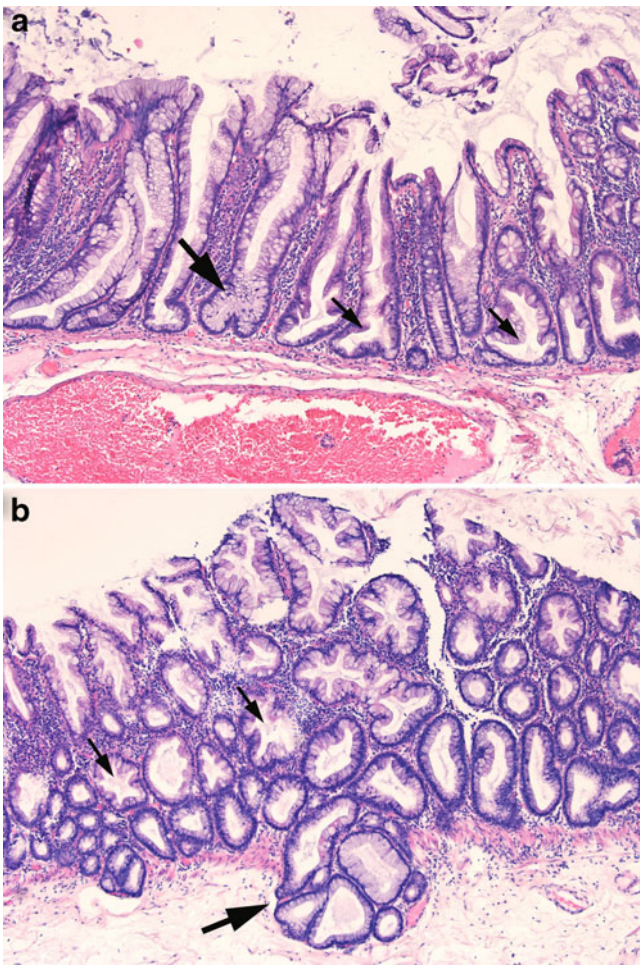

Fig. 3 Sessile serrated adenoma. **a** Branched crypts (*bold arrow*), T- and L-shaped bases of the crypts (*thin arrows*) and columnar dilatation of the crypts (×2.5); **b** serration reaching to the lower third of the crypts (*thin arrows*), inverted crypts below the muscularis mucosae (*bold arrow*) (×2.5) (with permission from PD. Dr. M. Vieth)

Table 3 Features of SSA (decisive diagnostic criteria are printed in Italic)

- Localization: right colon
- Sessile
- Diameter >5 mm

Microscopic:

- Hyperserration, serration in the lower third of the crypts with and without branching of the crypts
- T- and L-shaped crypts above the muscularis mucosae
- Inverted crypts (pseudoinvasion) below the muscularis mucosae
- Columnar dilatation in the lower third of the crypts (with and without the presence of mucus)

Furthermore:

- Shifting of the proliferation zone to the middle third of the crypts
- Vesicular nuclei with nucleoli
- Mature goblet cells at the base of the crypts

The definition of hyperplastic polyposis is as follows [29]:

1. at least five microscopically confirmed hyperplastic (serrated) polyps proximal to the sigmoid colon, two of which are >1 cm in diameter or
2. every number of hyperplastic (serrated) polyps proximal to the sigmoid colon in patients with a first degree relative diagnosed with hyperplastic polyposis, or
3. more than 30 hyperplastic (serrated) polyps regardless of their size and location.

When one of these criteria is met, the diagnosis, hyperplastic polyposis, should be communicated to the clinician. Recent evidence suggests that there is not only a recessive inherited syndrome but also an autosomal dominant inherited syndrome (serrated pathway syndrome) of hyperplastic polyposis [30].

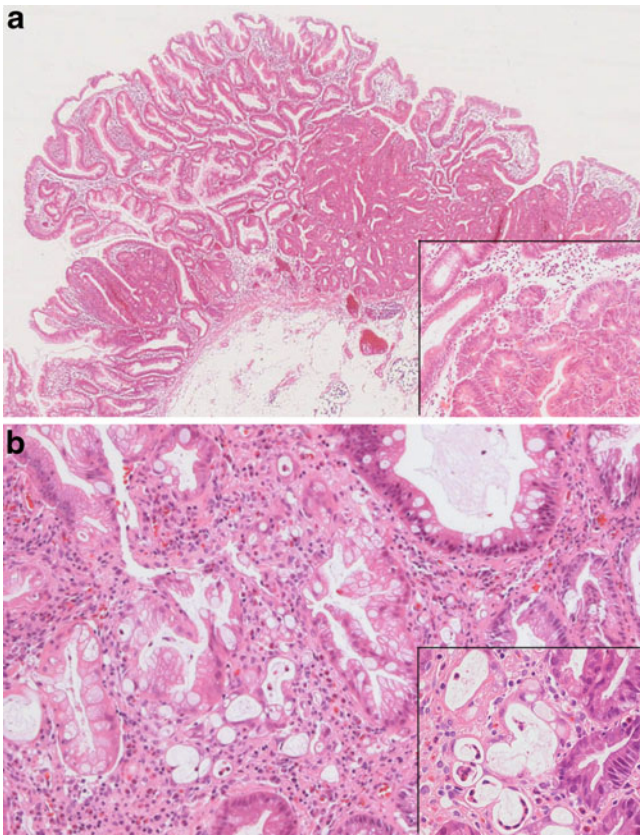

Fig. 4 SSA with serrated IEN. **a** High-grade IEN with gland-in-gland formation and "bottom-up" morphology (×1.25, *Insert* ×10), **b** high-grade IEN with partly mucinous and partly signet ring cell differentiation (×10, *Insert* 40×)

Traditional serrated adenoma

The traditional serrated adenoma (TSA) is the rarest variant of serrated lesions (1–6%). It has been known since 1990 by the term "serrated adenoma" as a rare variant of adenomas (1%) [31]. Grossly, TSAs are pedunculated or villous polyps, which are more common in the left side (60%) than in the right side of the colon in mostly elderly patients. By definition, the TSA microscopically shows IEN (90% LG-IEN and 10% HG-IEN). Prominent serration

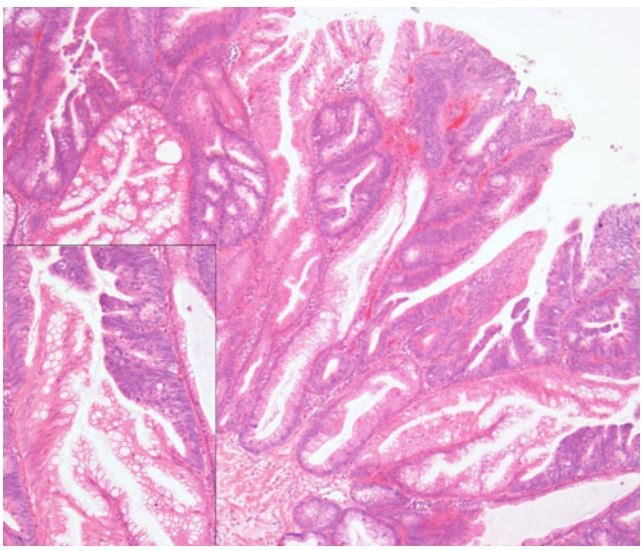

Fig. 5 Tubular adenoma with high-grade IEN and SSA (mixed polyp) (×4, *Insert* ×20)

Table 4 Serrated polyps—recommended follow-up according to the German S3 guideline "Colorectal Cancer" [20]

Diagnosis	Risk for carcinoma	Interval for control
HP	None	No indication for follow-up
SSA	Present, degree of risk not known	3 years
TSA	Present, as high as classical adenomas, possibly higher	3 years
Mixed polyp	Present	3 years

The stated intervals for control apply to completely removed lesions. In case of an incomplete or in case of a resection in piecemeal technique a control examination with endoscopy and biopsy should take place after 2 to 6 months

and diffuse cytoplasmic eosinophilia with occurrence of so called ectopic crypt formation (ECF) is also detectable in the TSAs. ECF consists of small budding aberrant crypts which lost their orientation towards the lamina muscularis mucosae (Fig. 2; Table 2) [32].

Filiform serrated adenomas with finger-like projections and prominent serrations are an unusual variant of TSA with comparable staining patterns for MGMT, mismatch repair proteins, β-catenin, Ki-67, and p53. They show a predilection for the rectum [33].

Sessile serrated adenoma (SSA)

With a frequency of 15–20%, the SSA is the second most common form of serrated polyps. Grossly, SSAs are flat or slightly elevated lesions typically >5 mm in diameter and localized in the right part of the colon. The microscopic characteristic of the SSA is hyperserration and dilatation of the crypts (with reduced stroma and back-to-back positioning of the dilated crypts) with T- and L-shaped branching at the crypt base. The muscularis mucosae appears thinner than normal and inverted crypts can be found below the muscularis mucosae (so called pseudoinvasion). Other features of the SSA are the presence of mature goblet cells at the base of the crypts, the presence of proliferation in the middle third of the crypt and the detection of slightly enlarged vesicular nuclei with nucleoli [12, 14] (Fig. 3; Table 3).

According to the consensus, the four most important diagnostic features for SSA are:

- hyperserration/serration in the lower third of the crypts (with and without branching)
- T- and L-shaped crypts above the muscularis mucosae
- inverted crypts (pseudoinvasion) below the muscularis mucosae
- columnar dilatation in the lower third of the crypts (with or without mucus)[1]

[1] Comment: In a multivariate analysis of 212 serrated lesions the presence of goblet cells at the base of the crypts proved to be an important feature in the discrimination between HP and SSA [34]

To date, there are no quantitative criteria for the diagnosis of SSA because SSAs have a complex architecture guiding the diagnosis. For pragmatic reasons, the consensus group suggests that the presence of two of the four most important diagnostic features should be present in at least two different crypts to warrant the diagnosis, SSA. The crypts do not have to be next to each other. These diagnostic criteria should also be used for the appendix. This pragmatic approach to the diagnosis of SSAs has been used by the members of the consensus working group with good interobserver concordance, but of course has to be validated in future prospective studies.

There is some controversy about the use of MUC6 staining, which was shown to distinguish HP (MUC6 negative) and SSA (MUC6 positive) in some studies [35]. More recent analyses revealed a relatively high specificity (82%), but relatively low sensitivity for MUC6-expression in SSAs [36]. The consensus group does, therefore, not advise MUC6 as a diagnostic tool for the differentiation of HP and SSA.

It is essential for the diagnosis of SSA that basal mucosa can be evaluated, therefore, when basal parts of the lesion are missing, it is recommended to use the term sessile serrated polyp (SSP). The pathological report should discuss the differential diagnosis and explain why a definite diagnosis could not be determined. The term sessile serrated polyp, however, should be limited to the cases in which basal mucosa is not included in the specimen and should not be used as a "wastebasket diagnosis".

As already mentioned, SSAs are also referred to as sessile serrated lesions in recent reviews. This new term has been explained by the authors with the fact, that intraepithelial neoplasia is missing in SSA and therefore the term adenoma is not adequate for this entity [14]. The term "lesion" was generated primarily as a term for the gross appearance and may be useful for endoscopy, but we would like to raise some doubt about the appropriateness of the term "sessile serrated lesion" for microscopic diagnosis since it leaves a lot of room for interpretation. The question which of the two terms—sessile serrated adenoma or sessile

serrated lesion—will prevail nationally and internationally is still open. The consensus conference recommends the use of the term SSA, which has been included in the most recent German S3 guidelines for the diagnosis and treatment of colorectal cancer [20].

Another controversial issue in diagnosis and nomenclature are those SSAs with intraepithelial neoplasia (Fig. 4). Recently, an adenoma-like IEN (usually top–down) was distinguished from serrated dysplasia (serrated type), which occurs irregularly (in most cases bottom–up) in SSAs (Fig. 4). The international literature uses the term "mixed polyp" for *all* SSAs *with* IEN. In the opinion of the consensus group this could lead to a misleading mixture of terms which disregards the malignant potential of SSA with "serrated dysplasia". Accordingly, it is recommended to temporarily classify this group as "SSA with dysplasia/IEN" (either LG-IEN or HG-IEN). This term allows a clear distinction from mixed polyps with adenoma-like IEN, which might be important because of the different biological behavior of these two lesions.

Mixed polyp

According to the World Health Organization mixed polyps are combinations of conventional (tubular, tubulovillous, and villous) adenomas with different grades of IEN (most commonly top–down morphology) and serrated lesions. These lesions were interpreted as collision tumors in the past (Fig. 5).

The term mixed polyp completely lacks the reference to the inherent IEN and therefore is regarded as potentially misleading by the consensus group because it does not reveal the preinvasive character of the lesions in an adequate manner. Nevertheless, "mixed polyp" is an internationally used and defined term and should be used in the pathological reports for these lesions. It is recommended, however, to first describe the components of the "mixed polyp" and then include the term "mixed polyp" in parentheses (e.g., sessile serrated and tubulovillous adenoma (mixed polyp) with low grade IEN).

There are different forms of mixed polyps according to their components:

- SSA and TSA
- SSA and conventional adenoma
- TSA and conventional adenoma,
- and as a rare combination: HP and conventional adenoma.

Each of them should be diagnosed with a specification of the grade of IEN: (mixed polyp) with LG-IEN or HG-IEN.

The following terms, however, should not be used: "serrated polyp with abnormal proliferation", "sawtooth polyp" and "SSA and HP (mixed polyp)".

Clinical course and relevance

SSA, TSA, and mixed polyps should be removed completely.

When describing mucosectomies, which are performed to remove SSA, TSA or hyperplastic polyps, the microscopic diagnosis should include the status of resection. In case of an incomplete resection or an impossible assessment of the resection status for the pathologist (due to a resection in the piecemeal technique) the pathologist should recommend a control endoscopy to ensure complete removal. Endoscopic follow-up should be performed as stated in the recent S3 guideline "Colorectal Carcinoma" (Table 4). The common hyperplastic polyps of the rectum are not associated with a risk of progression to cancer. Here, the R-status does not need to be described in detail and endoscopic follow-up is not necessary.

Keeping in mind the limited knowledge about the biologic behavior of the serrated lesions, we should increase our efforts to detect and collect cases with proper clinical follow-up, which could be subjected to studies evaluating the malignant potential of these lesions.

Acknowledgment We would like to thank M. Muders for his help in the preparation of this manuscript.

Conflict of interest statement We declare that we have no conflict of interest.

References

1. Morson BC (1962) Precancerous lesions of the colon and rectum. Classification and controversial issues. Jama 179:316–321
2. Otori K, Oda Y, Sugiyama K et al (1997) High frequency of K-ras mutations in human colorectal hyperplastic polyps. Gut 40:660–663
3. Ajioka Y, Watanabe H, Jass JR et al (1998) Infrequent K-ras codon 12 mutation in serrated adenomas of human colorectum. Gut 42:680–684
4. Chan TL, Zhao W, Leung SY et al (2003) BRAF and KRAS mutations in colorectal hyperplastic polyps and serrated adenomas. Cancer Res 63:4878–4881
5. Preto A, Figueiredo J, Velho S et al (2008) BRAF provides proliferation and survival signals in MSI colorectal carcinoma cells displaying BRAF(V600E) but not KRAS mutations. J Pathol 214:320–327
6. Velho S, Moutinho C, Cirnes L et al (2008) BRAF, KRAS and PIK3CA mutations in colorectal serrated polyps and cancer: primary or secondary genetic events in colorectal carcinogenesis? BMC Cancer 8:255
7. Jass JR, Whitehall VL, Young J et al (2002) Emerging concepts in colorectal neoplasia. Gastroenterology 123:862–876
8. Kambara T, Simms LA, Whitehall VL et al (2004) BRAF mutation is associated with DNA methylation in serrated polyps and cancers of the colorectum. Gut 53:1137–1144
9. Tateyama H, Li W, Takahashi E et al (2002) Apoptosis index and apoptosis-related antigen expression in serrated adenoma of the

colorectum: the saw-toothed structure may be related to inhibition of apoptosis. Am J Surg Pathol 26:249–256
10. Iino H, Jass JR, Simms LA et al (1999) DNA microsatellite instability in hyperplastic polyps, serrated adenomas, and mixed polyps: a mild mutator pathway for colorectal cancer? J Clin Pathol 52:5–9
11. Jass JR, Biden KG, Cummings MC et al (1999) Characterisation of a subtype of colorectal cancer combining features of the suppressor and mild mutator pathways. J Clin Pathol 52:455–460
12. Jass JR (2007) Classification of colorectal cancer based on correlation of clinical, morphological and molecular features. Histopathology 50:113–130
13. Toyota M, Ahuja N, Ohe-Toyota M et al (1999) CpG island methylator phenotype in colorectal cancer. Proc Natl Acad Sci USA 96:8681–8686
14. Kudo S, Lambert R, Allen JI et al (2008) Nonpolypoid neoplastic lesions of the colorectal mucosa. Gastrointest Endosc 68:S3–47
15. Dong SM, Lee EJ, Jeon ES et al (2005) Progressive methylation during the serrated neoplasia pathway of the colorectum. Mod Pathol 18:170–178
16. Goldstein NS (2006) Small colonic microsatellite unstable adenocarcinomas and high-grade epithelial dysplasias in sessile serrated adenoma polypectomy specimens: a study of eight cases. Am J Clin Pathol 125:132–145
17. Lazarus R, Junttila OE, Karttunen TJ et al (2005) The risk of metachronous neoplasia in patients with serrated adenoma. Am J Clin Pathol 123:349–359
18. Oono Y, Fu K, Nakamura H et al (2009) Progression of a sessile serrated adenoma to an early invasive cancer within 8 months. Dig Dis Sci 54:906–909
19. Li D, Jin C, McCulloch C et al (2009) Association of large serrated polyps with synchronous advanced colorectal neoplasia. Am J Gastroenterol 104:695–702
20. Schmiegel W, Reinacher-Schick A, Arnold D et al (2008) Update S3-guideline "colorectal cancer" 2008. Z Gastroenterol 46:799–840
21. Freeman HJ (2008) Heterogeneity of colorectal adenomas, the serrated adenoma, and implications for screening and surveillance. World J Gastroenterol 14:3461–3463
22. Torlakovic E, Skovlund E, Snover DC et al (2003) Morphologic reappraisal of serrated colorectal polyps. Am J Surg Pathol 27:65–81
23. Noffsinger AE (2009) Serrated polyps and colorectal cancer: new pathway to malignancy. Annu Rev Pathol 4:343–364
24. Azimuddin K, Stasik JJ, Khubchandani IT et al (2000) Hyperplastic polyps: "more than meets the eye"? Report of sixteen cases. Dis Colon Rectum 43:1309–1313
25. Warner AS, Glick ME, Fogt F (1994) Multiple large hyperplastic polyps of the colon coincident with adenocarcinoma. Am J Gastroenterol 89:123–125
26. Jeevaratnam P, Cottier DS, Browett PJ et al (1996) Familial giant hyperplastic polyposis predisposing to colorectal cancer: a new hereditary bowel cancer syndrome. J Pathol 179:20–25
27. Renaut AJ, Douglas PR, Newstead GL (2002) Hyperplastic polyposis of the colon and rectum. Colorectal Dis 4:213–215
28. Torlakovic E, Snover DC (1996) Serrated adenomatous polyposis in humans. Gastroenterology 110:748–755
29. Hamilton S, Vogelstein B, Kudo S et al (2000) Carcinoma of the colon and rectum. In: Hamilton S, Aaltonen L (eds) Pathology and genetics tumors of the digestive system. IARC Press, Lyon, pp 105–143
30. Jass JR, Baker K, Zlobec I et al (2006) Advanced colorectal polyps with the molecular and morphological features of serrated polyps and adenomas: concept of a 'fusion' pathway to colorectal cancer. Histopathology 49:121–131
31. Longacre TA, Fenoglio-Preiser CM (1990) Mixed hyperplastic adenomatous polyps/serrated adenomas. A distinct form of colorectal neoplasia. Am J Surg Pathol 14:524–537
32. Torlakovic EE, Gomez JD, Driman DK et al (2008) Sessile serrated adenoma (SSA) vs. traditional serrated adenoma (TSA). Am J Surg Pathol 32:21–29
33. Yantiss RK, Oh KY, Chen YT et al (2007) Filiform serrated adenomas: a clinicopathologic and immunophenotypic study of 18 cases. Am J Surg Pathol 31:1238–1245
34. Wieczorek K, Stolte M, Baretton G et al. (2009) Serrated lesions of the colorectum: morphologic characterisation of a large collective. Der Pathologe Suppl 1:7
35. Owens SR, Chiosea SI, Kuan SF (2008) Selective expression of gastric mucin MUC6 in colonic sessile serrated adenoma but not in hyperplastic polyp aids in morphological diagnosis of serrated polyps. Mod Pathol 21:660–669
36. Bartley AN, Thompson PA, Buckmeier JA, Kepler CY, Hsu CH, Snyder MS, Lance P, Bhattacharrya A, Hamilton HR (2010) Expression of gastric pyloric mucin, MUC6, in colorectal serrated polyps. Mod Pathol 23:169–176

Virchows Arch (2010) 457:299–307
DOI 10.1007/s00428-010-0952-2

ORIGINAL ARTICLE

HER2 diagnostics in gastric cancer—guideline validation and development of standardized immunohistochemical testing

Josef Rüschoff · Manfred Dietel · Gustavo Baretton · Susanne Arbogast · Axel Walch · Geneviéve Monges · Marie-Pierre Chenard · Frédérique Penault-Llorca · Iris Nagelmeier · Werner Schlake · H. Höfler · H. H. Kreipe

Received: 10 November 2009 / Revised: 2 July 2010 / Accepted: 13 July 2010 / Published online: 28 July 2010
© The Author(s) 2010. This article is published with open access at Springerlink.com

Abstract Trastuzumab-based therapy has been shown to confer overall survival benefit in HER2-positive patients with advanced gastric cancer in a large multicentric trial (ToGA study). Subgroup analysis identified adenocarcinomas of the stomach and gastroesophageal (GE) junction with overexpression of HER2 according to immunohistochemistry (IHC) as potential responders. Due to recent approval of trastuzumab for HER2 positive metastatic gastric and GE-junction cancer in Europe (EMEA) HER2 diagnostics is now mandatory with IHC being the primary test followed by fluorescence in situ hybridization (FISH) in IHC2+ cases. However, in order to not miss patients potentially responding to targeted therapy determination of a HER2-positive status for gastric cancer required modification of scoring as had been proposed in a pre-ToGA study. To validate this new HER2 status testing procedure in terms of inter-laboratory and inter-observer consensus for IHC scoring a series of 547 gastric cancer tissue samples on a tissue microarray (TMA) was used. In the first step, 30 representative cores were used to identify specific IHC HER2 scoring issues among eight French and German laboratories, while in the second step the full set of 547 cores was used to determine IHC HER2 intensity and area score concordance between six German pathologists. Specific issues relating to discordance were identified and recommendations formulated which proved to be effective

J. Rüschoff (✉) · I. Nagelmeier
Targos Molecular Pathology GmbH und Pathologie Nordhessen,
Germaniastr 7,
34119 Kassel, Germany
e-mail: rueschoff@patho-nordhessen.de

M. Dietel
Department of Pathology, Humboldt University, Campus Charité,
Berlin, Germany

G. Baretton
Institute of Pathology,
University Hospital Carl Gustav Carus Dresden,
Dresden, Germany

S. Arbogast
Department of Pathology & Tissue Biomarkers, MML,
Pharma Development, Roche Diagnostics GmbH,
Penzberg, Germany

A. Walch
Institute of Pathology, Helmholtz Zentrum München—German
Research Center for Environmental Health (GmbH),
Neuherberg, Germany

G. Monges
Département de Biopathologie, Institut Paoli Calmettes,
Marseille, France

M.-P. Chenard
Département de Pathologie, Hôpital de Hautepierre,
Strasbourg, France

F. Penault-Llorca
Service d'Anatomo-Pathologie, Centre Jean Perrin,
Clermont-Ferrand, France

W. Schlake
Pathologisches und Gewerbepathologisches Institut,
Gelsenkirchen, Germany

H. Höfler
Pathological Institute, University of Munich,
Munich, Germany

H. H. Kreipe
Institute of Pathology, Medizinische Hochschule Hannover,
Hannover, Germany

to reliably determine HER2 status in a prospective test series of 447 diagnostic gastric cancer specimens.

Keywords HER2 · Immunohistochemistry (IHC) Gastric carcinoma · Diagnostic test

Introduction

The human epidermal growth receptor 2 gene (*HER2*, also known as *ERBB2* and *HER2/neu*) is now well recognized as a key in the development of certain solid human tumors, most notably in breast cancer. In breast cancer, *HER2* gene amplification almost invariably induces and occurs before HER2 protein overexpression on the tumor cell surface [1, 2]. Monitoring of the tumor HER2 status (gene amplification and/or protein overexpression) in breast cancer has become routine as the positive HER2 status detected in around 25% of these cancers is associated with poorer prognosis, more aggressive disease, and an increased risk of disease recurrence [3–5]. Furthermore, in breast cancer the determination of HER2 status is necessary for optimal application of HER2-directed therapies such as trastuzumab (Herceptin®, Roche), which increases overall survival in both the metastatic [6, 7] and adjuvant settings [8–10], and predicts response in the neo-adjuvant setting [9, 10].

Data reported in the literature for HER2 positivity rates in gastric cancer vary from about 7–43% (for review see, [11]) with most studies demonstrating values of about 15–25% [11–14]. Furthermore, a HER2-positive status in gastric cancer also appears to be associated with poorer prognosis, more aggressive disease, and shorter survival [12, 14–19]. Preclinical studies have indicated that trastuzumab exerts antitumor activity in HER2-overexpressing human gastric cell lines and xenograft models [19–21]. As a consequence, the addition of trastuzumab to fluoropyrimidine/platinum-based therapy has been investigated in a large-scale (n=584) randomized study in patients with HER2-positive advanced gastric cancer, the ToGA trial, the primary results of which have been presented and showed that trastuzumab significantly improved the primary endpoint, median overall survival, by nearly 3 months (11.1 to 13.8 months, p=0.0046) with no impact on overall treatment safety. Moreover, an increased benefit from trastuzumab treatment was seen for patients who had higher levels of HER2 protein expression, including subgroups for IHC2+/FISH+ and IHC3+ (median survival increased from 11.8 months for the chemotherapy treatment arm to 16.0 months for the chemotherapy with trastuzumab arm) [22, 23]. Thus, very recently the European board, EMEA, approved trastuzumab for the treatment of metastasized adenocarcinomas of the stomach and the esophageal junction [24]. Thereby immunohistochemical testing is the primary method of choice to determine HER2 status in gastric cancer. FISH is restricted to those cases that have equivocal (IHC2+) HER2 expression.

The method of HER2 scoring within the phase III ToGA trial was essentially based on a separate (so-called pre-ToGA) validation study where immunohistochemistry (IHC) protein expression and fluorescence in situ hybridization (FISH) gene amplification was correlated in a series of 168 gastric cancer resection specimens [11]. An international consensus was reached to modify the breast scoring system for IHC by accepting strong incomplete (basolateral) membranous staining as positive (3+) and by abolishing the 10% area cut-off for this group in biopsies. A patient was considered to have HER2-positive gastric cancer with a score of IHC3+ (HercepTest) and/or FISH-positive result. Screening of nearly 4,000 patients in 24 countries for entry to the ToGA trial revealed a 22.1% HER2-positivity rate [25]. Furthermore, HER2-positivity rates were higher in gastroesophageal junction than gastric cancer (33% vs. 21%, p<0.001) and in intestinal than diffuse or mixed cancer (32.2% vs. 6.1% vs. 20.4%, p<0.001). Concordance between IHC and FISH was 87.5%: while in breast cancer, most IHC0/1+ results are FISH negative, the frequency of IHC0/1+ samples testing as FISH-positive was similar as IHC2+/FISH-positive samples (23% vs. 26%) [25].

The aim of our current study was to validate this HER2 testing procedure by determining whether pathologists from different sites are able to reproduce the method of gastric cancer HER2 status evaluation as it was used by the study pathologist (JR) within the ToGA study.

In a first step, inter-laboratory variation was assessed using 30 gastric cancer core biopsy tissue microassay samples (TMAs) using different HER2 IHC methods. In a second step, inter-observer variation of HER2 IHC scoring was tested in a series of already stained gastric cancer TMAs (n=547). A consensus practical guideline for accurate HER2 analysis in gastric cancer was then developed on the basis of these data. Finally, for validation of these guidelines a series of 447 prospective diagnostic gastric cancer specimens were tested at five participating sites throughout Germany.

Materials and methods

All study TMAs were based on a series of 547 gastric cancer core biopsy specimens assembled and provided by Prof. Kreipe (Hannover). All individual patients gave written informed consent for biological studies at their initial presentation. All samples were obtained from surgery performed for diagnostic and/or therapeutic purposes and were used according to German ethical regulations. The study followed the guidelines of the Declaration of Helsinki and

patient identity of the pathological specimens remained anonymous in the context of this study.

In a first step, a 30-core TMA set was pre-selected that provided a representative of all tumor types (intestinal, mixed, and diffuse) according to Lauren classification as well as different HER2 expression and amplification levels. Core size was 0.4 cm and each represented a different tumor sample. HER2 assessment was performed using different commercial assays according to the manufacturers' instructions at the different participating sites (n=8). IHC immunostaining was conducted using HercepTest™ (Dako Denmark A/S, Glostrup, Denmark) and/or the PATHWAY® HER2/neu (4B5) antibody (Ventana Medical Systems SA, Illkirch, France). *HER2* amplification was determined by FISH assays, using either *HER2* FISH pharmDX™ (Dako Denmark A/S) or PathVysion® (Abbott Laboratories, Des Plaines, IL, USA). Automated bright-field dual-color silver in situ hybridization (SISH) assay (BDISH; Inform™, Ventana Medical Systems SA) was used to determine gene amplification at three of the participating sites [26]. Evaluation was performed according to the modified gastric cancer testing protocol [11] taking incomplete basolateral or only lateral staining into account. As TMA cores were tested analogous to biopsies the 10% cut-off was recorded but not regarded for the final scoring (i.e., 1+, 2+, and 3+). FISH and BDISH were performed according to the manufacturers' recommendations with ratios above 2.0 being considered amplified.

In a second step, the complete TMA sample series of 547 tumor cores was used to determine inter-observer variation of HER2 expression (staining intensity and area stained) scoring independent of inter-laboratory staining variation. Thus, TMAs used for evaluation were already IHC stained using the 4B5 antibody (Ventana Medical Systems SA) at the Hannover laboratory that supplied samples.

Data for the first 30-core TMA set were presented and discussed at a 2-day consensus meeting conducted at the Institute of Pathology, Charite, Berlin (27/28 March 2009). After a consensus was reached about specific issues concerning HER2 scoring by IHC in gastric cancer, the second full set of 547 cores were evaluated independently by six German pathologists (GB, MD, HH, JR, SA, AW). The complete 547 TMA set was scanned (Provito GmbH, Berlin, Germany) and provided as virtual slides to the panelists. By use of this data set, all cases that resulted in discordant IHC scores between observers were then individually discussed at a separate meeting in Düsseldorf (10 June 2009) to determine the most reproducible practical guideline for HER2 testing in gastric cancer. Statistical analyses were performed using the statistical program R version 1.9.1 and Microsoft® Excel®. Kappa statistics was calculated according to the method of Conger (1980) by package "irr" of program R [33]. In order validate these guidelines in routine practice a series of n=447 prospective diagnostic gastric cancer samples have been tested at five different participating sites throughout Germany which comprised either a biopsy tissue block or one representative tissue block of resection specimen. Thereby, four sites followed the algorithm as proposed by EMEA with IHC (4B5, Ventana) being used first and one center applied both IHC and ISH (BDISH, Ventana) to all n=152 specimens at their site.

Results

Inter-laboratory reproducibility of *HER2* scoring in gastric cancer

In total, 29 of 30 cores of the first TMA set showed evaluable tumor tissue when evaluated by HercepTest and 4B5 antibody at 7 and 8 sites, respectively. The core with non-evaluable tumor tissue was excluded. A HER2 score deviation ≤1 was found in 14/29 cores (48.3%) when HercepTest was used as compared to 22/29 cores (75.9%, p=0.002) when 4B5 was used, despite one more site being included for the latter. Consensus HER2 scores was reached for all but 1 site for 11 (37.9%) tumors with HercepTest and by 13 (44.8%) tumors with 4B5. Consensus HER2 scores between sites with each IHC test increased as a function of fewer sites being in agreement.

In total, 27 tumor cores were evaluable for *HER2* gene amplification by hybridization assays. Comparison with *HER2* amplification according to FISH/BDISH results with HER2 IHC scores unanimously agreed by all sites as negative (0/1+) or positive (2+/3+) revealed a tendency towards higher sensitivity for 4B5 detecting positive *HER2* amplification (Table 1). In particular, five out of eight ISH-positive tumor cores were scored as 2+/3+ by 4B5 whereas this was the case in only two cores with HercepTest; IHC scoring was equivocal with some positive and some negative classifications in three cases by 4B5 and six cases by HercepTest, respectively. There was no difference between both test platforms with respect to the ISH-negative cases with the one equivocal case testing negative at some sites and as positive at others.

Pitfalls and rules of *HER2 IHC* scoring

Reviewing of the 30 core TMA slides disclosed several pitfalls that were mainly related to interpretation of staining rather than staining variation at different lab sites. After panel discussion the following pitfalls turned out to be the major reasons for inter-oberserver variation. Figure 1 shows examples of potential pitfalls and of different scores that can be obtained by HER2 receptor staining. HER2

Table 1 Inter-laboratory comparison: comparison of *HER2* amplification status according to FISH/BDISH results with HER2 IHC scores

FISH/BDISH result (n=27)	IHC score					
	4B5			HercepTest		
	Negative (0/1+)	Equivocal (0/1+ vs. 2+/3+	Postive (2+/3+)	Negative (0/1+)	Equivocal (0/1+ vs. 2+/3+	Positive (2+/3+)
Negative (n=18)	12	5	1	11	7	0
Equivocal (n=1)	0	1	0	0	1	0
Positive (n=8)	0	3	5	0	6	2

expression may occur in areas of gastric mucosal metaplasia and towards reactive epithelial cells bordering ulcers (Fig. 1a). Discordant results can also occur where <10% of tumor cells are stained. This holds particularly true if only a few (<5) cells were evaluated. Such small cell groups tend to show unspecific rather pericellular and granular instead of distinct intercellular staining particularly at the edges of the TMA cores (Fig. 1b). Another source of false positive scoring is diffuse cytoplasmic reaction with or without nuclear staining (Fig. 1c). For evaluation of membranous staining specific for scoring it turned out that consideration of microscope magnification is of importance to reach high inter-observer agreement. Accordingly, strong HER2-positive (3+) staining may be visible to the naked eye and displays unequivocal membranous staining already at low magnification (×2.5/×5) as shown in Fig. 2d,e. An example of heterogeneous staining is given in Fig. 1f. Areas of 3+ HER2-positive cells (visible at low magnification ×2.5) in less than 10% of tumor cells are admixed with those where unequivocal membraneous staining can only be disclosed at medium magnification (first at ×10 corresponding to 2+ intensity) and with some areas showing barely visible expression (membranous staining confirmed only at ×40, corresponding to 1+). Fig. 1g shows focal staining (<10% of the tumor) where unequivocal membranous staining could first be recognized at medium magnification (×10, Fig. 1h). In contrast demonstration of IHC 1+ score needs high magnification (×40) to confirm an unequivocally intercellular membranous HER2 expression (Fig 1i).

Figure 2 summarizes the recommended stepwise process of standardized IHC scoring in gastric cancer. At first tumor and tissue quality issues have critically to be checked. Most of all, unspecific staining within non-neoplastic lesions such as intestinal metaplasia have to be excluded from scoring and also edge and crushing artifacts affecting tumor cells. In a second step, only distinct membranous staining either complete (chicken-wire type), basolateral or only lateral between cell–cell contacts in a cluster of at least five cells are considered if biopsies are scored. This excludes any equivocal staining, e.g., rather thickened or granular at basal cell basement membrane or at a single isolated cell surrounded by a shrinkage rim. Any staining at the luminal site of a tumor gland is suspicious of artifactual staining not specific for scoring particularly if it is not associated with distinct intercellular staining and should therefore be excluded. In the third step the final scoring should be done taking the microscope magnification into account at which unequivocal membrane staining can readily be confirmed.

Inter-observer reproducibility of *HER2* scoring in gastric cancer

After discussion and definition of the above-mentioned pitfalls and rules for reliable IHC scoring the full TMA set (547 cores) stained by 4B5 was graded with respect to both intensity and area scores by six pathologists. A HER2 score deviation ≤1 between pathologists was now found for 95.6% and 91.8% of TMAs for intensity and area scores, respectively. Consensus agreement for HER2 staining intensity scores between all except 1 or 2 of the 6 pathologists was found for 512/547 (93.6%) and 470/547 (85.9%) tumors, respectively, while corresponding consensus agreement for area stained scores rates were 505/547 (92.3%) and 465/547 (85.0%) tumors, respectively.

Calculation of interrater kappa values showed moderate agreement (k=0.61) if all intensity scores (IHC 0–3+) were considered. However, if negative (IHC 0/1+) was calculated against positive (IHC2+/3+) kappa value rose to 0.805 indicating an “almost perfect agreement”. In fact, this implies that 92.5% of the six pathologists were in complete agreement in all 547 cores. In five cases, there was marked discordance with half scoring a case IHC 0/1+ and half IHC2+/3+. Reevaluation of these cases (Düsseldorf meeting) disclosed that in all of these cases the number of evaluable tumor cells was below five cells.

Validation of guidelines by application to diagnostic specimens

In order to demonstrate the value of the defined IHC scoring rules with respect to routine practice and gene amplification status a total of 447 diagnostic gastric cancer

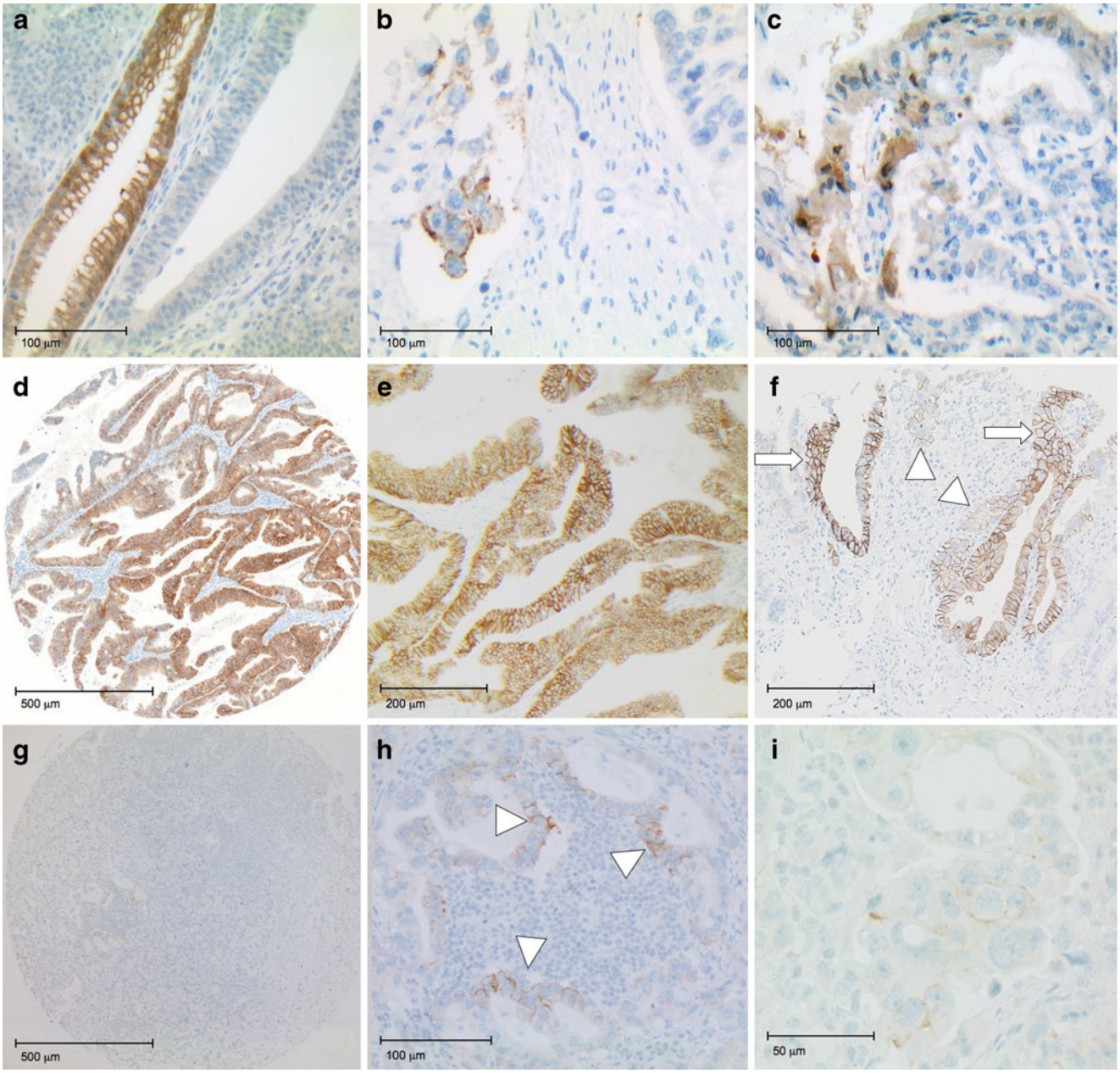

Fig. 1 Photomicrographs of TMA examples. **a**–**c** Artifacts leading to potential mis-scoring on IHC: **a** intestinal metaplasia, **b** edge artifact at TMA border with granular (not linear) pseudo-membranous staining, and **c** cytoplasmic as well as nuclear staining. **d**–**h** Intensity scoring: **d** Score 3+ visible by naked eye with membranous staining clearly visible at low magnification (obj. ×5) being either complete, baso-lateral or lateral (**e**, ×10). **f** Photomicrograph of TMA sample showing distinction between 2+ and 3+ IHC using 4B5 antibody. *Arrows* indicate areas with clearly visible membrane staining at low magnification (i.e., 3+), focally in <10% of tumor); *arrowheads* indicate areas where membrane staining is only visible at ×10 magnification (i.e., 2+). **g** TMA core suspicious of some focal staining at ×5 which turned out to be a focally specific membranous staining in groups of at least five cells at medium magnification (**h**, ×20; see *arrowheads*). **i** Very weak staining where membranous staining is barely visible and could only be demonstrated using high magnification (**i**, ×40)

specimens were prospectively tested at five participating sites (Berlin, Dresden, Hannover, Kassel, Munich). The mean positivity rate was 22.8% (102/447). In one site, both IHC and ISH test were applied in parallel to a total of 152 gastric carcinomas. Accordingly, the consented testing guidelines resulted in a high concordance between IHC and ISH. All IHC3+ tumors (n=24) showed *HER2* gene amplification (100% concordance), which was the case in 32% of the IHC2+ (n=47) and in 5% of the IHC 1+ (n=41) cases. Interestingly, most of IHC2+ and IHC1+ (76.5%) showed low level amplification (ratio 2–3) which was only the case in 16% of IHC3+ tumors.

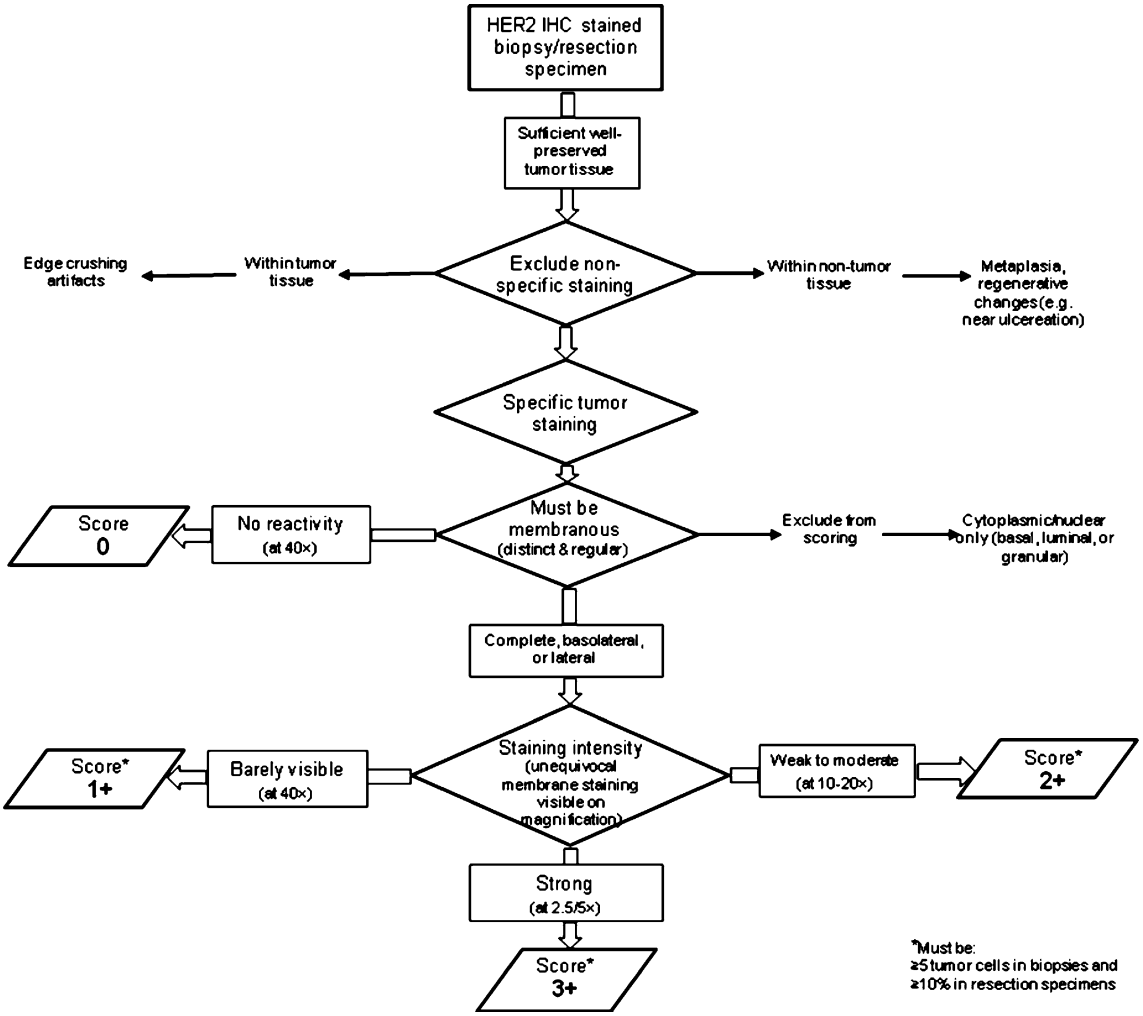

Fig. 2 Stepwise approach to IHC scoring in gastric cancer: tissue and quality issues (mod. acc. to [31])

Discussion

The modified HER2 immunoscoring method that has been shown to be predictive of response to trastuzumab-based therapy in patients with advanced gastric cancer in the ToGA study [22] was shown to be reproducible between different pathologists in our study as long as special precautions were adopted. Furthermore, our study indicates that HER2 status determination in gastric cancer needs special and specific training and guidelines for pathologists in a similar manner to that already adopted for pathologists for breast cancer testing. However, the specific guidelines for breast cancer are not applicable to gastric cancer in several aspects, as there are important and significant differences in HER2 status determination between breast and gastric cancer (Table 2).

Thus determination of HER2 status by just transferring the breast cancer IHC scoring roles to gastric cancer may lead to a significant loss of patients. In a recent paper by Barros-Silva et al. [27], resection specimens of 463 gastric adenocarcinomas were tested using the breast cancer scoring rules. Accordingly, these authors classified 3.9% as IHC2+ and 5.4% as IHC3+. The corresponding values in the TOGA trial with 12% IHC2+ and 11% IHC3+ were about twice as high [23]. The same holds true if one compares TMA data which were classified as IHC2+ (1.6%) or IHC3+ (3.2%) if breast cancer scoring was applied [28]. As the same group also tested gastric cancer TMAs using our proposed gastric cancer specific scoring [11] the corresponding rates were 4% IHC2+ and 13% for IHC3+, demonstrating an about fourfold increase of HER2 positivity rate [29]. Therefore, it is supposed that application of breast cancer scoring to gastric cancer may produce an up to 50% false-negative rate if IHC is used as the primary test platform as favored by EMEA.

On the other hand, if FISH is used as first screening step only few IHC3+ positive cases may be missed but one may be faced with a quite high percentage of non-responders according to ToGA data [22, 23].

Therefore, based on the presented consensus study a number of specific recommendations can be made for reliable

Table 2 HER2 diagnostics in gastric cancer—differencies to breast cancer (acc. to [32])

		Gastric cancer	Breast cancer
IHC scoring	Extent (Area Cut-off)	Biopsy specimens≥5 Cells Resection specimens: ≥10%	≥10% (≥30%)[a]
	Circularity	Mostly missing (often only lateral in IHC2+/3+)	A must in IHC2+/3+
(F)ISH analysis	Cell number	20 cohesive tumor cells showing highest gene count (add 20 new if ratio 1.8–2.2)	20 cohesive tumor cells showing highest gene count (add 20 new if ratio 1.8–2.2)
	Amplification	Ratio≥2.0	Ratio≥2.0 (≥2.2)[a]
HER2 positivity	Tumor type	About 30% of intestinal-type GC about 15% of mixed-type about 5% of diffuse type (signet ring type typically negative)	15–25% of ductal type (G2/G3); almost never in subtypes such as lobular, medullar and ductal G1
	Tumor location	About 30% at cardiac/GE-junction about 15% of gastric cancer	No correlation
Patient selection	FISH vs. IHC	IHC more predictive than FISH: IHC primary test[b] FISH only if IHC2+	FISH/IHC equally predictive:

[a] Acc. to ASCO/CAP [31]

[b] Acc. to approval by EMEA

HER2 status determination in gastric cancer. Since HER2 expression is mainly restricted to intestinal-type, gland-forming gastric cancer cells incomplete, often basolateral or only lateral, membranous IHC staining is the rule rather than an exception for HER2-positive gastric cancer [11]. Thus, unlike for breast cancer, circularity of IHC staining is no longer a criterion for HER2 IHC scoring in gastric cancer.

A key issue for the classification of positive HER2 expression is a membranous staining that can be unequivocally assessed as linear staining at cell–cell contact sites. Strong tumor HER2 IHC staining is usually already directly visible, particularly if most of the tumor is stained. In these cases, only low magnification (×2.5–5) is needed to confirm strong staining intensity. In any case where high magnification (×40) is required for unequivocal demonstration of membranous staining, the tumor is scored IHC 1+ (Fig. 1i). It should, however, be mentioned that quality of lenses and brightness of the microscopic light might be of influence as well. Nevertheless the inter-observer variation results within this ring-study prior and after application of the magnification rule clearly are in favor of such an approach over non-standardized wording, e.g., of "barely visible" for IHC1+.

Recommendation 1

For reproducible intensity scoring, the degree of microscopic magnification (*x*-fold) at which membranous (linear intercellular) staining is clearly visible should be considered.

According to the pre-ToGA HER2 validation study [11], IHC HER2 expression is often focal in gastric cancer which could largely be confirmed by the ToGA study [25]. An assessment area cut-off of at least 10% stained tumor cells, as originally proposed for HER2 scoring in breast cancer, was omitted in gastric cancer biopsies. A rather focal HER2 staining was also frequently observed in our current series of TMAs. Inter-observer agreement was especially low if less than five cells were stained. The minimum number of cells that could reliably be assessed was five. Thus, in biopsies a focus ("clone") that is allowed to be scored should have at least five stained evaluable cells.

Recommendation 2

Since focal HER2 expression is an issue in gastric cancer, biopsies should only be it evaluated if at least five cohesive, unequivocal tumor cells are stained. In resection specimens, the 10% cut-off should be kept. Thus scoring procedure is different for biopsies and resection specimen [23].

Thereby, only unequivocal intercellular staining is accepted; even ring-shaped staining of a single tumor cell is not accepted either due to the cell number criterion (see above) or difficulties in exclusion of edge artifacts. The pre-ToGA HER2 scoring validation study used HercepTest as the only IHC assay [11]. The different laboratory sites generally used two different IHC assays (HercepTest and 4B5) concurrently. Both assays resulted in a somewhat degree high inter-laboratory discordance, which appeared to be higher when HercepTest was used. These observations could essentially be confirmed by the validation set where 4B5 was used in 447 prospective stomach cancers and in parallel with BDISH in 152 of these cases. Interestingly, all IHC3+ tumors showed *HER2* gene amplification.

Recommendation 3

Use of FDA approved antibodies is recommended for selection of *HER2*-positive patients in gastric cancer. Besides HercepTest which was applied in the ToGA study another antibody approved by the FDA for breast cancer testing (4B5) appeared to be at least as sensitive, possibly showing even higher inter-laboratory concordance for *HER2 IHC* scoring and a closer relationship between *IHC3+* and *HER2* gene amplification.

Given the evolving and provisional status of HER2 status determination for gastric cancer, we make a final recommendation as follows.

Recommendation 4

Participation in proficiency testing tools such as QUIP (Qualitätssicherungs-Initiative der Deutschen Gesellschaft für Pathologie und des Berufsverbandes Deutscher Pathologen zur diagnostischen Immunhistochemie und Molekularpathologie) at the Dresden Laboratory is strongly recommended since *HER2* testing is quite different in gastric cancer as compared to breast cancer (www.ringversuch.de).

We could show that application of the consented guidelines to a total of 447 diagnostic gastric cancer specimens resulted in a positivity rate of 22.8% which is quite in the range of the ToGA study with 22.1% [25]. Within a subset of 153 tumors, all cases were tested in parallel by IHC and ISH. A complete concordance between both methods could be demonstrated within the IHC3+ group being all amplified by BDISH. Even so, according to ToGA trial data amplification was not sufficient enough to reliably detect the patients that had a significant benefit from trastuzumab therapy [22]. Although most of amplified IHC0 and IHC1+ cases had low level amplification (ratio 2–3) both in ToGA and in our own validation series up to now it is not quite clear whether there is a predictive correlation between therapy response and amplification level in gastric cancer which is obviously not the case in breast cancer [30].

Finally, it turned out that due to heterogeneity of at least some advanced GC both in the mixed-type and in the intestinal-type precise scanning of tumors is of importance particularly if FISH techniques at high magnification (×100) are used. This might be in favor for light-microscopically based ISH techniques where even small amplified tumor cell foci can readily be recognized (data not shown).

Acknowledgments This validation study was funded by F. Hoffmann-La Roche Ltd (Roche), Basel, Switzerland. The authors thank L. Miller for medical writing support.

Conflict of interest J.R, M.D., G.B., A.W., G.M., M.P.C., F.PL, W. S., H.H.K. were reimbursed for their attendance of the consensus meeting and for consumables used for testing of the validation set of diagnostic gastric cancer specimens by F. Hoffmann-La Roche Ltd (Roche), Basel, Switzerland.

Open Access This article is distributed under the terms of the Creative Commons Attribution Noncommercial License which permits any noncommercial use, distribution, and reproduction in any medium, provided the original author(s) and source are credited.

References

1. Simon R, Nocito A, Hübscher T, Bucher C, Torhorst J, Schraml P, Bubendorf L, Mihatsch MM, Moch H, Wilber K, Schötzau A, Kononen J, Sauter G (2001) Patterns of her-2/neu amplification and overexpression in primary and metastatic breast cancer. J Natl Cancer Inst 93:1141–1146
2. Vincent-Salomon A, Pierga JY, Couturier J, d'Enghien CD, Nos C, Sigal-Zafrani B, Lae M, Fréneaux P, Diéras V, Thiéry JP, Sastre-Garau X (2007) HER2 status of bone marrow micrometastasis and their corresponding primary tumours in a pilot study of 27 cases: a possible tool for anti-HER2 therapy management? Br J Cancer 96:654–659
3. Slamon DJ, Clark GM, Wong SG, Levin WJ, Ullrich A, McGuire WL (1987) Human breast cancer: correlation of relapse and survival with amplification of the HER-2/neu oncogene. Science 235:177–182
4. Slamon DJ, Godolphin W, Jones LA, Holt JA, Wong SG, Keith DE, Levin WJ, Stuart SG, Udove J, Ullrich A et al (1989) Studies of the HER-2/neu proto-oncogene in human breast and ovarian cancer. Science 244:707–712
5. Ross JS, Fletcher JA (1998) The HER-2/neu oncogene in breast cancer: prognostic factor, predictive factor, and target for therapy. Oncologist 3:237–252
6. Slamon DJ, Leyland-Jones B, Shak S, Fuchs H, Paton V, Bajamonde A, Fleming T, Eiermann W, Wolter J, Pegram M, Baselga J, Norton L (2001) Use of chemotherapy plus a monoclonal antibody against HER2 for metastatic breast cancer that overexpresses HER2. N Engl J Med 344:783–792
7. Marty M, Cognetti F, Maraninchi D, Snyder R, Mauriac L, Tubiana-Hulin M, Chan S, Grimes D, Antón A, Lluch A, Kennedy J, O'Byrne K, Conte P, Green M, Ward C, Mayne K, Extra JM (2005) Randomized phase II trial of the efficacy and safety of trastuzumab combined with docetaxel in patients with human epidermal growth factor receptor 2-positive metastatic breast cancer administered as first-line treatment: The M77001 study group. J Clin Oncol 23:4265–4274
8. Romond EH, Perez EA, Bryant J, Suman VJ, Geyer CE Jr, Davidson NE, Tan-Chiu E, Martino S, Paik S, Kaufman PA, Swain SM, Pisansky TM, Fehrenbacher L, Kutteh LA, Vogel VG, Visscher DW, Yothers G, Jenkins RB, Brown AM, Dakhil SR, Mamounas EP, Lingle WL, Klein PM, Ingle JN, Wolmark N (2005) Trastuzumab plus adjuvant chemotherapy for operable HER2-positive breast cancer. N Engl J Med 353:1673–1684
9. Smith I, Procter M, Gelber RD, Guillaume S, Feyereislova A, Dowsett M, Goldhirsch A, Untch M, Mariani G, Baselga J, Kaufmann M, Cameron D, Bell R, Bergh J, Coleman R, Wardley A, Harbeck N, Lopez RI, Mallmann P, Gelmon K, Wilcken N, Wist E, Sánchez Rovira P, Piccart-Gebhart MJ; HERA study team (2007) 2-year follow-up of trastuzumab after adjuvant chemotherapy in HER2-positive breast cancer: a randomised controlled trial. Lancet 369:29–36

10. Arnould L, Arveux P, Couturier J, Gelly-Marty M, Loustalot C, Ettore F, Sagan C, Antoine M, Penault-Llorca F, Vasseur B, Fumoleau P, Coudert BP (2007) Pathological complete response to trastuzumab-based neoadjuvant therapy is related to the level of HER-2 amplification. Clin Cancer Res 13:6404–6409
11. Hofmann M, Stoss O, Shi D, Büttner R, van de Vijver M, Kim W, Ochiai A, Rüschoff J, Henkel T (2008) Assessment of a HER2 scoring system for gastric cancer: results from a validation study. Histopathology 52:797–805
12. Park DI, Yun JW, Park JH, Oh SJ, Kim HJ, Cho YK, Sohn CI, Jeon WK, Kim BI, Yoo CH, Son BH, Cho EY, Chae SW, Kim EJ, Sohn JH, Ryu SH, Sepulveda AR (2006) HER-2/neu amplification is an independent prognostic factor in gastric cancer. Dig Dis Sci 51:1371–1379
13. Yano T, Doi T, Ohtsu A, Boku N, Hashizume K, Nakanishi M, Ochiai A (2006) Comparison of HER2 gene amplification assessed by fluorescence in situ hybridization and HER2 protein expression assessed by immunohistochemistry in gastric cancer. Oncol Rep 15:65–71
14. Zhang XL, Yang YS, Xu DP, Qu JH, Guo MZ, Gong Y, Huang J (2009) Comparative study on overexpression of her2/neu and her3 in gastric cancer. World J Surg 33:2112–2118
15. Uchino S, Tsuda H, Maruyama K, Kinoshita T, Sasako M, Saito T, Kobayashi M, Hirohashi S (1993) Overexpression of c-erbB-2 protein in gastric cancer. Its correlation with long-term survival of patients. Cancer 72:3179–3184
16. Nakajima M, Sawada H, Yamada Y, Watanabe A, Tatsumi M, Yamashita J, Matsuda M, Sakaguchi T, Hirao T, Nakano H (1999) The prognostic significance of amplification and overexpression of c-met and c-erb B-2 in human gastric carcinomas. Cancer 85:1894–1902
17. Allgayer H, Babic R, Gruetzner KU, Tarabichi A, Schildberg FW, Heiss MM (2000) c-erbB-2 is of independent prognostic relevance in gastric cancer and is associated with the expression of tumor-associated protease systems. J Clin Oncol 18:2201–2209
18. García I, Vizoso F, Martín A, Sanz L, Abdel-Lah O, Raigoso P, García-Muñiz JL (2003) Clinical significance of the epidermal growth factor receptor and HER2 receptor in resectable gastric cancer. Ann Surg Oncol 10:234–241
19. Tanner M, Hollmén M, Junttila TT, Kapanen AI, Tommola S, Soini Y, García-Muñiz JL (2005) Amplification of HER-2 in gastric carcinoma: association with topoisomerase IIalpha gene amplification, intestinal type, poor prognosis and sensitivity to trastuzumab. Ann Oncol 16:273–278
20. Matsui Y, Inomata M, Tojigamori M, Sonoda K, Shiraishi N, Kitano S (2005) Suppression of tumor growth in human gastric cancer with HER2 overexpression by an anti-HER2 antibody in a murine model. Int J Oncol 27:681–685
21. Fujimoto-Ouchi K, Sekiguchi F, Yasuno H, Moriya Y, Mori K, Tanaka Y (2007) Antitumor activity of trastuzumab in combination with chemotherapy in human gastric cancer xenograft models. Cancer Chemother Pharmacol 59:795–805
22. Van Cutsem E, Kang Y, Chung H, Sawaki A, Lordick F, Hill J, Lehle M, Feyereislova A, Bang Y (2009) Efficacy results from the ToGA trial: A phase III study of trastuzumab added to standard chemotherapy (CT) in first-line human epidermal growth factor receptor 2 (HER2)-positive advanced gastric cancer (GC). J Clin Oncol 27:18 s (suppl; abstr LBA4509)
23. Bang Y, Van Cutsem C, Feyereislova A, Chung H, Shen L, Sawaki S, Lordick F, Ohtsu A, Omuro Y, Satoh T, Aprile G, Kulikov E, Hill J, Lehle M, Rüschoff J, Kang Y-K (2010) Phase III, randomised clinical trial to compare trastuzumab in combination with chemotherapy versus chemotherapy alone for the treatment of HER2-positive advanced gastric or gastro-oesophageal junction cancer. Lancet, submitted
24. EMEA, European Medicines Agency (2009): Opinion www.emea.europa.eu/pdfs/human/opinion/Herceptin_82246709en.pdf
25. Bang Y, H. Chung H, Xu J, Lordick F, Sawaki A, Al-Sakaff N, Lipatov O, See C, Rueschoff J, Van Cutsem E (2009) Pathological features of advanced gastric cancer (GC): relationship to human epidermal growth factor receptor 2 (HER2) positivity in the global screening programme of the ToGA trial. J Clin Oncol 27:15s (suppl; abstr 4556)
26. Dietel M, Ellis IO, Höfler H, Kreipe H, Moch H, Dankof A, Kölble K, Kristiansen G (2007) Comparison of automated silver enhanced in situ hybridisation (SISH) and fluorescence ISH (FISH) for the validation of HER2 gene status in breast carcinoma according to the guidelines of the American Society of Clinical Oncology and the College of American Pathologists. Virchows Arch 451:19–25
27. Barros-Silva JD, Leitão D, Afonso L, Vieira J, Dinis-Ribeiro M, Fragoso M, Bento MJ, Santos L, Ferreira P, Rêgo S, Brandão C, Carneiro F, Lopes C, Schmitt F, Teixeira MR (2009) Association of ERBB2 gene status with histopathological parameters and disease-specific survival in gastric carcinoma patients. Br J Cancer 100:487–493
28. Tapia C, Glatz K, Novotny H, Lugli A, Horcic M, Seemayer CA, Tornillo L, Terracciano L, Spichtin H, Mirlacher M, Simon R, Sauter G (2007) Close association between HER-2 amplification and overexpression in human tumors of non-breast origin. Mod Pathol 20:192–198
29. Marx AH, Tharun L, Muth J, Dancau AM, Simon R, Yekebas E, Kaifi JT, Mirlacher M, Brümmendorf TH, Bokemeyer C, Izbicki JR, Sauter G (2009) HER-2 amplification is highly homogenous in gastric cancer. Hum Pathol 40:769–777
30. Dowsett M, Procter M, McCaskill-Stevens W, de Azambuja E, Dafni U, Rueschoff J, Jordan B, Dolci S, Abramovitz M, Stoss O, Viale G, Gelber RD, Piccart-Gebhart M, Leyland-Jones B (2009) Disease-free survival according to degree of HER2 amplification for patients treated with adjuvant chemotherapy with or without 1 year of trastuzumab: the HERA trial. J Clin Oncol 27:2962–2969
31. Wolff AC, Hammond ME, Schwartz JN, Hagerty KL, Allred DC, Cote RJ, Dowsett M, Fitzgibbons PL, Hanna WM, Langer A, McShane LM, Paik S, Pegram MD, Perez EA, Press MF, Rhodes A, Sturgeon C, Taube SE, Tubbs R, Vance GH, van de Vijver M, Wheeler TM, Hayes DF (2007) American Society of Clinical Oncology/College of American Pathologists guideline recommendations for human epidermal growth factor receptor 2 testing in breast cancer. J Clin Oncol 25:118–145
32. Rüschoff J, Nagelmeier I, Baretton G, Dietel M, Höfler H, Schildhaus HU, Büttner R, Schlake W, Stoss O, Kreipe HH (2010) HER2 testing in gastric cancer. What is different in comparison to breast cancer? Pathologe 31:208–217 [German]
33. Conger AJ (1980) Integration and generalization of Kappa for multiple raters. Psychol Bull 88:322–328

Virchows Arch (2010) 457:309–317
DOI 10.1007/s00428-010-0917-5

ORIGINAL ARTICLE

Multicentre validation study of nucleic acids extraction from FFPE tissues

Serena Bonin · Falk Hlubek · Jean Benhattar · Carsten Denkert · Manfred Dietel · Pedro L. Fernandez · Gerald Höfler · Hannelore Kothmaier · Bozo Kruslin · Chiara Maria Mazzanti · Aurel Perren · Helmuth Popper · Aldo Scarpa · Paula Soares · Giorgio Stanta · Patricia J. T. A. Groenen

Received: 8 September 2009 / Revised: 12 February 2010 / Accepted: 31 March 2010 / Published online: 28 July 2010
© The Author(s) 2010. This article is published with open access at Springerlink.com

Abstract In most pathology laboratories worldwide, formalin-fixed paraffin embedded (FFPE) samples are the only tissue specimens available for routine diagnostics. Although commercial kits for diagnostic molecular pathology testing are becoming available, most of the current diagnostic tests are laboratory-based assays. Thus, there is a need for standardized procedures in molecular pathology, starting from the extraction of nucleic acids. To evaluate the current methods for extracting nucleic acids from FFPE tissues, 13 European laboratories, participating to the

Serena Bonin, Falk Hlubek and Patricia J. T. A. Groenen contributed equally to the realization of this paper.

Electronic supplementary material The online version of this article (doi:10.1007/s00428-010-0917-5) contains supplementary material, which is available to authorized users.

S. Bonin · G. Stanta (✉)
ACADEM Department-University of Trieste and ICGEB,
University of Trieste, Cattinara Hospital- Pathology Bldg,
Strada di Fiume 447, 34149 Trieste, Italy
e-mail: stanta@icgeb.org

F. Hlubek
Institute of Pathology,
Ludwig-Maximilians-University of München,
Thalkirchner Straße 36, 80337 München, Germany

J. Benhattar
Institute of Pathology-CHUV and University of Lausanne,
Bugnon 25, 1011 Lausanne, Switzerland

C. Denkert · M. Dietel
Institute of Pathology, Charité-University Medicine,
Charitéplatz 1, 10117 Berlin, Germany

P. L. Fernandez
Department of Pathology, Hospital Clínic-IDIBAPS,
University of Barcelona,
Barcelona, Spain

G. Höfler
Institute of Pathology, Labor für molekularpathologische
Diagnostik, University of Graz Medical School,
Auenbruggerplatz 25, 8036 Graz, Austria

H. Kothmaier · H. Popper
Institute of Pathology, Molekulare Lungen-und Pleurapathologie,
University of Graz,
Auenbruggerplatz 25, 8036 Graz, Austria

B. Kruslin
University of Zagreb-School of Medicine,
Ljudevit Jurak Department of Pathology,
Sestre milosrdnice University Hospital,
Vinogradska 29, 10000 Zagreb, Croatia

C. M. Mazzanti
Division of Surgical, Molecular and Ultrastructural Pathology,
University of Pisa and Pisa University Hospital,
Pisa, Italy

A. Perren
Institute of Pathology, Technische Universität München,
München, Germany

A. Scarpa
Department of Pathology and ARC-Net Research Center,
University of Verona,
Policlinico GB Rossi, Verona, Italy

European FP6 program IMPACTS (www.impactsnetwork.eu), isolated nucleic acids from four diagnostic FFPE tissues using their routine methods, followed by quality assessment. The DNA-extraction protocols ranged from homemade protocols to commercial kits. Except for one homemade protocol, the majority gave comparable results in terms of the quality of the extracted DNA measured by the ability to amplify differently sized control gene fragments by PCR. For array-applications or tests that require an accurately determined DNA-input, we recommend using silica based adsorption columns for DNA recovery. For RNA extractions, the best results were obtained using chromatography column based commercial kits, which resulted in the highest quantity and best assayable RNA. Quality testing using RT-PCR gave successful amplification of 200 bp–250 bp PCR products from most tested tissues. Modifications of the proteinase-K digestion time led to better results, even when commercial kits were applied. The results of the study emphasize the need for quality control of the nucleic acid extracts with standardised methods to prevent false negative results and to allow data comparison among different diagnostic laboratories.

Keywords FFPE · Multicentre study · Molecular analyses standardisation · PCR · DNA · RNA · Isolation

Introduction

One of the major challenges in oncology is a correct prediction of individual recurrence risk and the prediction of efficacy and safety of therapy. Histopathology is only partly able to mirror and predict the clinical behaviour of individual tumours. Through the application of molecular tools, otherwise indistinguishable tumour subgroups have been identified and the definition of a precise gene mutation pattern has highlighted classes of tumours with clinical prognostic implications [1]. Moreover the application of molecular tests such as real time PCR based assays has become feasible thanks to the use of formalin-fixed paraffin embedded samples [2], which represent the most valuable source of diagnostic materials. As a consequence, in the near future molecular approaches in formalin fixed and paraffin embedded (FFPE) material will become part of the routine process of cancer diagnostics. At the present time most of the methods applied in molecular pathology are laboratory-based assays and commercial kits not directly intended for diagnostic purposes. Therefore there is a need to establish guidelines with standardised procedures for molecular methods, starting from an analysis of the currently used methods of nucleic acids extraction.

This collaborative study includes 13 European laboratories of the IMPACTS group (www.impactsnetwork.eu) and was conducted to evaluate the performance of nucleic acids extractions using the same formalin-fixed paraffin-embedded specimens. The aim of the study is to assess if the different methodologies used for nucleic acids extraction in different laboratories might affect the results.

Materials and methods

Four cases of formalin-fixed paraffin-embedded tissues were distributed to the participants in the study in two rounds. In detail, the Trieste group delivered one colorectal cancer specimen during the first control round. The Berlin group delivered an ovary cancer sample and the Graz group delivered two lung cancer cases in the second control round. Surgical specimens with a large amount of tissue were used to ensure to have sufficient material for the multicentre analysis. Comparable tissue areas distributed in 2 to 4 sections of 5 μm in thickness were used per test and distinct tissue blocks of the same cases were selected for RNA and DNA extractions. The sections were collected sequentially: each following section was given to a different participant in order to obtain the most homogeneous representative tissues in all the different laboratory tests. Tissue slides were sent under vacuum at room temperature. The colon cancer samples were dated 2002, while the lung and ovarian cancer specimens were dated 2008. Each laboratory used the protocol that was routinely used for standard DNA and/or RNA extractions as reported in Supplemental 1, 2 and 3. Although interesting, it was technically not feasible to test the different extraction methods by the diagnostic laboratories. The homemade protocols for the extractions are referred to detailed references, while the commercial kits are referred to the manufacturer's manuals. Each nucleic acid extract was quantified by means of Nanodrop (ThermoScientific). The total amount of nucleic acids and A_{260}/A_{280} results were recorded for each extract. The quality assessment for DNA extracts was performed by the use of the BIOMED-2 control gene PCR method as previously described [3]. This method is based on a multiplex PCR resulting in a ladder of fragments (100, 200, 300, and 400 bp) to check the quality and amplifiability of DNA from FFPE materials.

P. Soares
Institute of Pathology and Molecular Immunology, (IPATIMUP),
University of Porto,
4200-465 Porto, Portugal

P. J. T. A. Groenen
Department of Pathology,
Radboud University Nijmegen Medical Centre,
Nijmegen, The Netherlands

In detail, the undiluted DNA sample and 100 ng of the sample were amplified. In case no amplified band was detected (like the colon and lung specimens from participant 1), multiple DNA concentrations (10, 50, 200 ng) were amplified as well. The BIOMED-2 control gene PCR was run for all samples in one laboratory (Molecular Pathology, RUNMC, Nijmegen) and analyzed by electrophoresis on agarose gel.

For the first control round, RNA (colon cancer specimen) quality assessment by RT-PCR was performed in each laboratory using their routinely method with their usual fragment length amplification. All the protocols were based on DNA digestion and cDNA synthesis by the use of the random priming approach. In the second control round, for RNA extracts, DNase treatments and cDNA synthesis were all performed in one lab (Trieste), as previously reported [4], after re-quantification of RNA. Complementary DNAs were then submitted in dry ice to Munich (LMU) for PCR analysis as described hereafter. Quality test for RNA was performed by amplifying different fragments of PBGD (Porphobilinogen deaminase) (150 and 250 bases), B2M (Beta-2-microglobulin) (200 bases) and β-actin (103 bases) housekeeping genes. As negative control, pure DNAse treated RNAs of a representative number of samples were used in the PCR reactions for specificity testing. Because the ovarian cancer samples yielded by far the lowest amount of RNA and neither PBGD nor B2M was detectable by PCR subsequent to standard reverse transcription procedure using random primer, these RNA samples were reverse transcribed using a PCR-target specific primer (β-actin forward, see below). The β-actin specific cDNA was amplified by PCR resulting in an amplification product of 103 bases. PCR products were analysed by agarose gel electrophoresis (3% w/v). For all PCR reactions, 200 ng cDNA (50 ng control cDNA, cell line) and the AmpliTaq Gold DNA polymerase (Applied Biosystems, Darmstadt, Germany) were used with 40 amplification cycles (10 min. 94°C; 40 cycles of 30 sec. 94°C, 30 sec. 60°C, 1 min. 72°C and one cycle 10 min. 72°C). For the β-actin and PBGD (250 bp amplicon) specific PCR, 1.5 mM $MgCl_2$ and 0.2 mM dNTP-mix were used. The 150 bp amplicon PBGD-PCR employed 2.0 mM $MgCl_2$ and the B2M specific PCR (200 bp) 2.5 mM $MgCl_2$. The primer sequences were as follows:

PBGD (250 bp): forward: 5′-CTGGTAACGGCAAT GCGGCT-3′, reverse: 5′-TTCTTCTCCAGGG CATGTTC-3′; PBGD (150 bp): forward: 5′-TGCCAGAGAAGAGTGT GGTG-3′, reverse: 5′-AT GATGGCACTGAACTCCTG-3′; B2M (200 bp): forward: 5′-GTTGACTTACTGAAGAATGG AG-3′, reverse: 5′-GATGCTGCTTACATGTCTCG-3′; β-actin (103 bp): forward: 5′-TTGCGGAT GTCCACGTCA-3′, reverse: 5′-GCCCTGAGGCACTCTTCCA-3′

Results

DNA

Thirteen European participants were involved in the validation testing of DNA. The laboratories originating in Austria, Croatia, Germany, Italy, Portugal, Spain, Switzerland and The Netherlands were kept anonymous and were ranked according to the protocol type. The methods used by each participant were divided into 3 major groups, since the protocols within each group were similar.

1. DNA extraction with precipitation of the DNA either by NaAc/EtOH (Participants 1, 2, 5) or by isopropanol (Participants 3, 4). Participant 4 took part only in the second round of DNA validation (lung and ovary cancer specimens).
2. DNA extraction without further precipitation or purification (Participants: 6, 7 and 8, the latter only for the colon cancer sample)
3. DNA extraction using silica based adsorption columns for purifying DNA (Participants: 9, 10, 11, 12 and 13).

Details on the used protocols are provided in Supplemental Tables 1 and 2. The criteria used for evaluation of the DNA extracts were: 1) the DNA yield obtained by the extraction and 2) the DNA quality assessed by the purity measured by spectral-photometry (A_{260}/A_{280}) and by BIOMED-2 gene control PCR to test PCR-amplifiability. The median amounts of extracted DNA for each sample are reported in detail in Table 1 and Fig. 1, and show that the total amount of DNA extracted was highly dependent on the method used. The highest DNA-yields were obtained by the use of homemade methods that do not employ further purification of the DNA (Table 1, protocol type 2). Note that in these DNA extracts, the measured concentration does not reflect the actual DNA quantity because of the co-presence of RNA and proteins debris, as it is apparent from the A_{260}/A_{280} ratio (Supplemental Table 1). Thus, the DNA yield and concentration of these specimens are only indicative. A lower DNA yield was obtained when using column based methods or homemade methods including a DNA precipitation step. This trend was shown for all the analyzed specimens.

Differences in the purity of the DNA extracts hardly affect the PCR-amplifiability (Table 2 and Fig. 2). The quality of the DNA extracted from the lung specimens allowed amplification of the 300 bp band of the control gene PCR for all protocols. Some protocols allowed amplification of the 400 bp fragment, although this band was only faintly detected. For the colon sample, many protocols allowed DNA-amplification of the 200 bp band as the maximal amplifiable length, while two homemade protocols only successfully amplified the smallest sized

Table 1 Results on the nucleic acids extraction quantities

	DNA yield by protocol type			RNA yield by protocol type		
Sample	Protocols type 1	Protocols type 2	Protocols type 3	Protocols type 4	Protocol type 5	Protocols type 6
Colon ca.	72.8 μg (70-80)	237 μg (145-274)	46.5 μg (39-76)	19.5 μg (17-22)	38.4 μg (30-47)	48.4 μg (12-70)
Ovarian ca.	17.4 μg (11-26)	85.8 μg (70-101)	8.1 μg (4-9)	1.8 μg (1.5-4.9)	2.6 μg (1.6-3.6)	5.7 μg (2.5-6.8)
Lung ca 1	35.1 μg (27-51)	144 μg (125-163)	15.6 μg (16-19)	9.2 μg (5-22)	41.0 μg (37-45)	32.3 μg (8-41)
Lung ca. 2	25.9 μg (16-37)	160 μg (134-186)	16.9 μg (15-19)	8.9 μg (6-9)	20.8 μg (19-23)	22.9 μg (7-40)

For each sample the median amount of extracted nucleic acid and the 25th and 75th centiles (in brackets) with respect of the protocol type are reported.

control amplicon of 100 bp. From one participant using a homemade protocol, DNA extracts from colon and lung specimens did not allow amplification of the control genes. Regarding the DNA extraction procedures characterised by purification steps, it seems there is no clear correlation among quantities of detected DNA and PCR performance; even for low amounts of extracted DNA the PCR performance was good.

RNA

The validation of RNA isolation methods was performed by 10 participants from 8 European countries (Austria, Germany, Croatia, Italy, Portugal, Spain, Switzerland and The Netherlands). The participants were kept anonymous using the numbering of the DNA validation tests. The extraction protocols can be divided into 3 major groups as follows (numbered sequentially according to DNA protocols):

4. RNA extraction using phenol extraction and isopropanol precipitation- homemade protocols (Participants 2, 4, 5)
5. RNA extraction using phenol extraction and isopropanol precipitation- commercial mono-phase solutions (Participants 8, 11)
6. RNA extraction using silica based columns for purification (Participants: 3, 4 only for Colon Cancer sample, 6, 7, 9, 12)

The criteria for assessing the quality of the RNA isolation method were: 1) the RNA yield and 2) the RNA quality determined by purity detection using spectral-photometry (A_{260}/A_{280}) and by amplification methods. The RNA was isolated from a single case of colorectal cancer, two lung cancer cases and one ovary

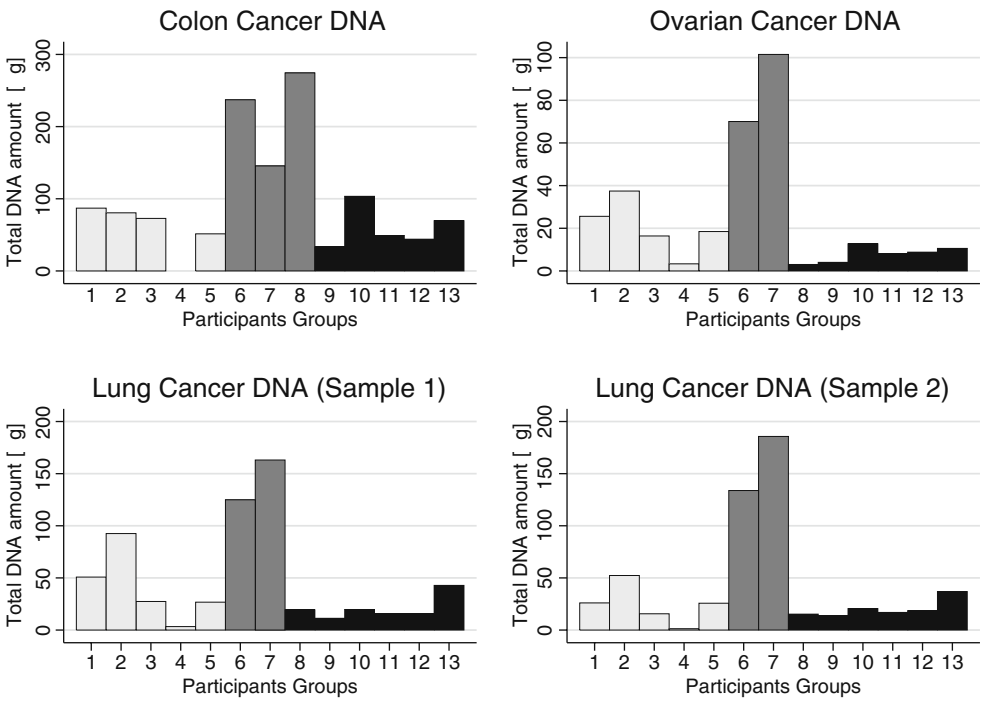

Fig. 1 Bar graph representing the total amount of extracted DNA from colon cancer, ovarian cancer and lung cancer (2) specimens by the use of different protocol types. Light grey bars are referred to protocol type 1 (DNA extraction with precipitation step); medium grey bars are referred to protocol type 2 (DNA extraction without purifications steps) and dark grey bars are referred to protocol type 3 (DNA extraction with commercial kits based on the use of silica based columns)

Table 2 Performance of the extracted DNAs in the BIOMED-2 gene control PCR

Protocol Type	Participant	Colon Ca.	Ovarian Ca.	Lung Ca. 1	Lung Ca. 2
1	1	0	200	0	0
1	2	200	100	400	300
1	3	100	100	300	300
1	4	nd	100	300	300
1	5	200	100	400	400
2	6	200	100	400	300
2	7	200	100	400	400
3	8[a]	100	100	400	300
3	9	200	100	400	300
3	10	200	100	300	400
3	11	200	100	300	300
3	12	nd	100	300	300
3	13	nd	100	400	300

The performance is expressed in base pairs referred to the longest PCR fragment that was amplified. The 400 bp band, when detected, was only weakly present.

nd= not determined, these participants (4, 12 and 13) did not send their DNA samples for general quality control testing.

[a] This participant used protocol type 2 for the colon cancer sample, as underlined.

cancer tissue. The median amount of extracted RNA is reported in Table 1 and Fig. 3. Regarding the protocol type, the RNA yield was higher with the use of commercial kits based on silica column purification (protocol type 6), followed by the use of commercial solutions and the homemade protocols. The Qiagen RNeasy FFPE kit using an extended proteinase-K digestion time revealed the best performance regarding the yield (Supplemental Table 4). However, when the Qiagen RNeasy FFPE kit was used by different participants, remarkable differences in RNA yield were observed (Supplemental Tables 3 and 4, Fig. 3 participant 12 vs. 7).

The RNA quality was measured by RNA purity detection using spectral-photometry (A_{260}/A_{280}). The highest purity was obtained by silica based column purification procedures (protocol type 6) (Qiagen RNeasy FFPE kit and Roche High Pure RNA Paraffin kit) with the exception of the Gentra kit and was followed by the homemade protocol (protocol type 4) based on phenol extraction and isopropanol precipitation. The commercial solution method (protocol type 5) gained the least pure RNA measured by the A_{260}/A_{280} absorption ratio. To further validate the RNA quality a standardized PCR procedure was used with four different amplicon lengths (103 bp, 150 bp, 200 bp, 250 bp) after standard reverse transcription. The original RNA of the samples was used as negative control resulting in no PCR product. Taken together, the column based commercial kits (protocol type 6 - Qiagen RNeasy FFPE kit and Roche High Pure RNA Paraffin kit) yielded the best assayable RNA quality (Table 3, Fig. 4). Interestingly the performance of the RNA in the RT-PCR reaction did not always correlate with RNA purity data, as RNA obtained by commercial solutions with the least pure RNA (protocol type 5) performed better than RNA extracted by homemade protocols (protocol type 4; see Table 3).

Discussion

Diagnostic methodologies need per definition a basic level of standardization in order to obtain concordance in the responses among hospitals. Immunohistochemistry (IHC) is the most widely used method to detect proteins in FFPE tissues for diagnostic purposes. Despite the standardization of immunohistochemical staining protocols, some factors could still vary among samples and laboratories, such as tissue fixation (duration), choice of antibodies, and the threshold for interpretation of positive immunostaining, which may dramatically

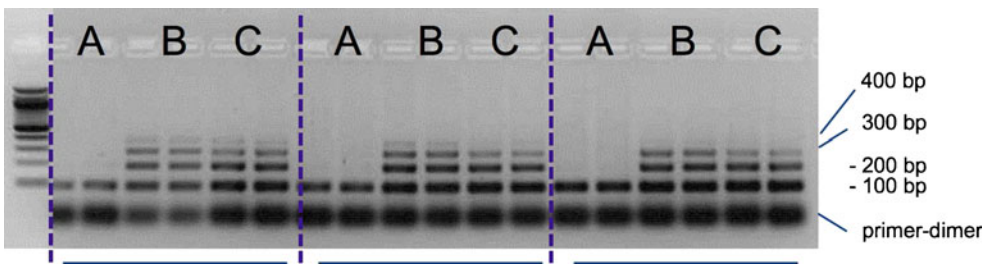

Fig. 2 BIOMED-2 control gene PCR results of the extracted DNAs in duplicate of group 9, 6 and 2 (protocol type 3, 2 and 1 respectively). DNA was extracted from ovary (**a**), lung 1 (**b**) and lung 2 (**c**). The size of the amplified products is indicated. The lowest thick band represents primer-dimer products

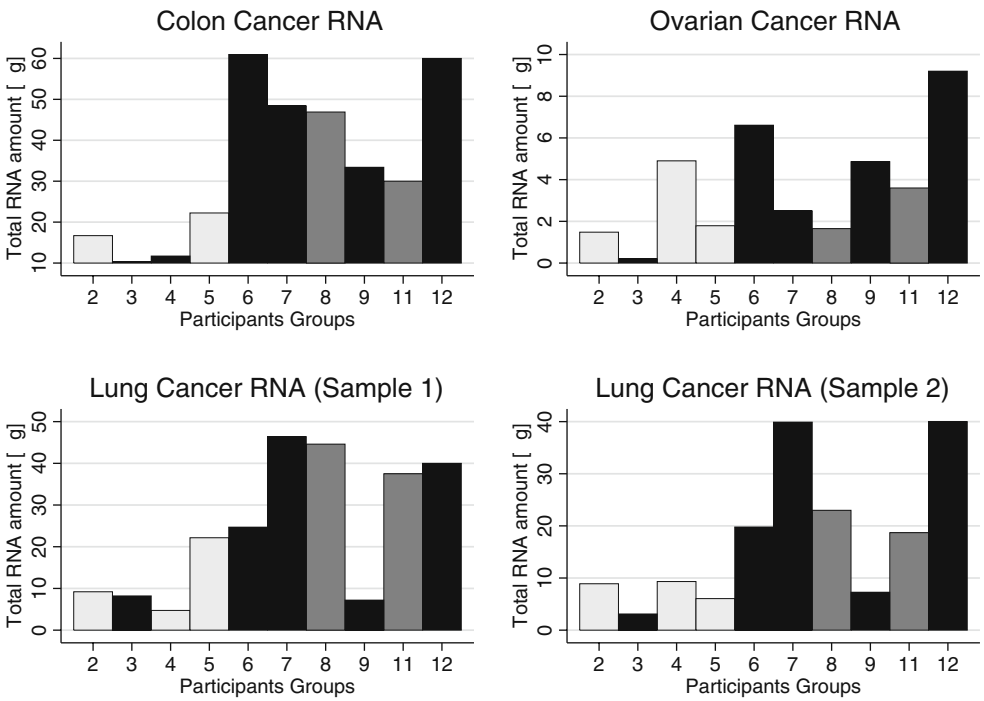

Fig. 3 Bar graph representing the total amount of extracted RNA from colon cancer, ovarian cancer and lung cancer (2) specimens by the use of different protocol types. Light grey bars are referred to protocol type 4 (RNA extraction with homemade protocols); medium grey bars are referred to protocol type 5 (RNA extraction with monophasic commercial solutions) and dark grey bars are referred to protocol type 6 (RNA extraction with commercial kits based on the use of silica based columns)

affect test accuracy and reproducibility. In any case IHC is considered an accurate diagnostic method because there are guidelines and inter-laboratory quality controls through the cross-testing of cases that guarantee the reliability of the assays. Nowadays, there is great interest and need for molecular pathology tests in order to better characterize pathologies and better define the individual patient profile for tailored therapy. In the present study, we have systematically compared the results of different homemade and commercial protocols for DNA and RNA extraction on the same set of FFPE tissue specimens used in several laboratories in order to define reliable criteria on nucleic acid extraction from FFPE tissues.

The design of this multicentre study allows determining the specific effects of the different extraction protocols, since the quality control experiments and interpretation of the multicentric results were performed in a single laboratory. Nonetheless, we cannot entirely exclude the possible effects of additional parameters, such as different technicians and laboratory equipments, which may influence the results. However, as the extractions were performed by experienced technicians in molecular diagnostic laboratories, we anticipate a minimal effect of these parameters.

The FFPE tissues used in this study originate from routine diagnostics of three different pathology departments. Hence it may well be possible that fixation time and the size of the tissue pieces used, which is important for the fixation rate, varies. Formalin not only cross-links proteins and nucleic acids, it also modifies RNA by adding monomethylol groups to all the four bases blocking reverse transcription [5]. However it has been shown that the efficiency of extracting amplifiable RNA and DNA from FFPE tissue is inversely proportional to the fixation time [6, 7] and thus standardized fixation conditions are important. This was not specifically addressed in the current study since all laboratories used serial sections of the same tissue block of each cancer tissue.

DNA

DNA extraction protocols that used purification of the extracted DNA, either by precipitation (protocol type 1) or by using silica-based columns (protocol type 3) gave comparable results in terms of yield and purity of the DNA. The apparent yield of DNA by the use of these protocols is less comparable to protocols that do not employ any purification (protocol type 2), which is not surprising, since the measured DNA-concentration in the unpurified samples reflects the presence of RNA and DNA. Yield and concentration from protocols that do not employ purification steps is thus not accurate since degraded RNAs as well as protein debris are also quantified, overestimating thereby the real DNA amount.

The PCR-amplifiability of the DNA samples was not drastically affected by the use of different DNA-extraction protocols. Our study showed that the measurement of amplifyability of the DNA by performance of the BIOMED-2 control gene PCR is the preferred parameter, superior to spectrophotometrical determination of the A_{260}/A_{280} ratio, to measure DNA-quality for diagnostic molecular testing. In general, DNA obtained from FFPE samples that allows amplification of 300 bp is considered as good DNA-quality and can be

Table 3 Results on RNA quality assessment by PCR

Protocol Type	Participant	Colon Ca[a]	Ovarian Ca	Lung Ca. 1	Lung Ca. 2
4	2	150	103	200	200
4	4[b]	200	103	200	200
4	5	160	103	200	200
5	8	127	103	-	250
5	11	250	103	250	200
6	3	160	103	150	-
6	6	185	103	250	250
6	7	200	103	250	250
6	9	110	103	-	-
6	12	293	103	250	250

Results are expressed in base pairs referred to the longest amplifiable PCR product.

The larger the PCR product, the better the RNA quality was considered.

[a] no PCR for longer amplicon was performed in the first round of testing; the analysed housekeeping genes were: ACTB (Beta-Actin), PBGD (Porphobilinogen deaminase), PDHB (Pyruvate dehydrogenase, beta), GUSB (Glucuronidase, beta), FGFR3 (Fibroblast growth factor receptor 3).

[b] This participant used for colon cancer specimen the protocol type 6, as underlined.

(-) no PCR product was obtained (150 bp or larger amplicons).

used for many molecular tests, including clonality testing using the BIOMED-2 primers and protocols [8]. Array comparative genomic hybridization (aCGH) was successful using DNA samples from FFPE tissues, which allowed amplifying 200 bp in the BIOMED-2 control gene PCR [9]. Based on evaluation of the DNA-amplifyability, there is not a single DNA-extraction protocol that is highly superior to others. The majority of the DNA-extraction protocols, except for the DNA-extraction protocol by participant 1, give similar and comparable results. There was only a minor difference in outcome, showing less performance of the DNA-extraction protocol used by participants 3 and 8a. However, as this was seen only in one of the four tested samples, there is no solid reason to avoid the use of these protocols.

Upon selection of the protocol to use in a diagnostic laboratory, also the requirements for the specific molecular test should be taken into consideration. It should be realised that molecular tests that require a standardized input of DNA, should use purified DNA-samples, allowing the most accurate DNA-quantification. For complex multiplexed PCRs or tests that require a specific accurate input of DNA per PCR test, like B- /T-cell clonality assessment, [8], as well as for application of array-CGH [6], MLPA-based tests [7], we strongly recommend using type 3 protocols that use silica based adsorption columns for purifying DNA.

For other molecular tests like PCR followed by direct sequencing, however, purification may not be essential. The use of protocols without further purification (protocol type 2) has an additional advantage, it is more rapid and less expensive compared to DNA-protocols that employ purification steps. We therefore recommend the use of a simple DNA-protocol, such as the type 2 protocols (DNA extractions without further purification or precipitation), for general molecular tests as mutation and translocation detection. Whichever the method used, it is highly recommended to employ only optimized and controlled reagents. This can be an important source of result variability.

RNA

The RNA isolation methods affected the yield of the extracted RNA, even when extraction conditions (proteinase K incubation time and temperature) were comparable (Supplemental Table 3). Proteinase K digestion is an important step affecting the RNA yield. In fact, we observed that an extended digestion time resulted in a more efficient extraction, especially from colon and ovarian tumour tissue using the Qiagen RNeasy FFPE kit. This is consistent with previous reports demonstrating that increas-

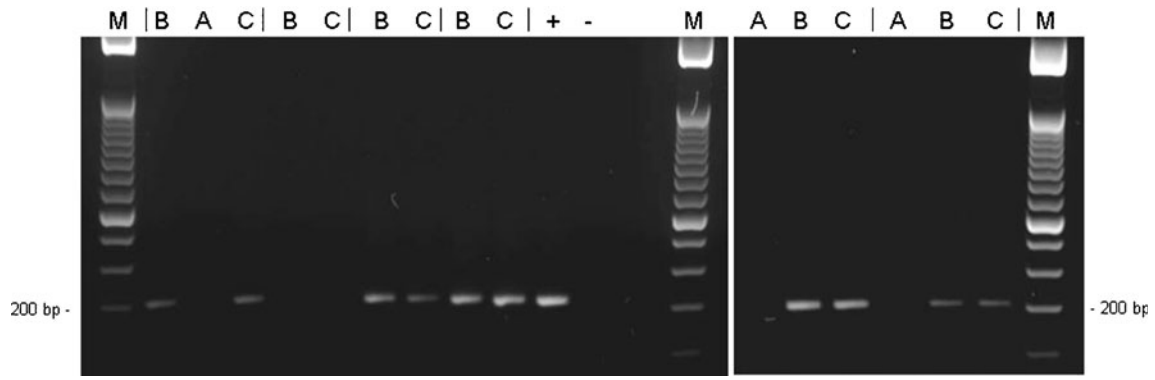

Fig. 4 B2M housekeeping gene specific RT-PCR results of the extracted RNAs of the group 2, 11, 6, 3, 7 and 12 (protocol type 4, 5 and four times 6, respectively). RNA was extracted from ovary (**a**), lung 1 (**b**) and lung 2 (**c**). The PCR products were separated in 3 % (w/v) agarose gels. The size of the amplification products is indicated (200 bp). M: size marker (50 bp DNA Ladder, Invitrogen, Karlsruhe, Germany)

ing proteinase K digestion time improved the RNA yield [6, 10, 11]. Formalin fixation preserves cellular structures by crosslinking biomolecules and thus traps nucleic acids and prevents the extraction of amplifiable RNA and DNA. By extending the digestion time to at least 16 hours, proteinase K is thought to release protein cross-linked nucleic acids more efficiently to permit subsequent RNA/DNA isolation, e.g. by column based methods [6]. Surprisingly, extended proteinase K incubation had no effect on the RNA quality evaluated by RT-PCR.

The RNA quality assessment by spectral photometry did not correlate with the maximum amplifiable length (Tables 1 and 3). The ratio $A_{260/280}$ is an indicator of possible contaminants [12] and the presence of inhibitors for subsequent reactions, however, this measurement is highly variable [13] and does not assess the length of the RNA extracted. Similarly, the widely used quality assessment by capillary electrophoresis (Bioanalyzer or Experion) is not predictive of the utility of RNA samples isolated from FFPE tissue in molecular analyses, since the most limiting factor for RT-PCR and presumably other enzymatic procedures, is the chemical modification of RNA by formaldehyde, which is not resolved by electrophoretic assays [10, 14].

Regarding the high degree of degradation of RNA in FFPE tissues, the ability of amplifying 250 bp PCR-fragments indicates RNA of very good quality. Nevertheless, the successful amplification of target mRNA fragments ≥200 bp in length was considered good RNA quality [11, 15]. All isolation methods resulted in RNA of useful quality for expression analyses in archival and diagnostic tissues, since shorter amplicons are sufficient for quantitative PCR [15–17]. This study reveals that column based methods (protocol type 6) provided best RNA quality assessed by RT-PCR from most of the tissues. Moreover these methods, in comparison to homemade protocols and commercial monophasic solutions, are less time-consuming by omitting the precipitation step to isolate the RNA. Small adjustments of the manufacturer's instruction (e.g. proteinase K digestion) may have caused inter-laboratory variability both in RNA quantity and quality, which is consistent with earlier reports demonstrating that different results were obtained by different groups using the same commercial kits [10, 15].

Although homemade RNA extraction methods (protocol type 4) or commercial solutions (protocol type 5) may be suitable for certain applications in research and diagnostics using short amplicons (below 160 bp), our results demonstrate that among the analyzed methods , particularly the Qiagen RNeasy FFPE kit including an extended proteinase-K digestion period is recommended. Due to the observed inter-laboratory variability, further standardization of the techniques, including commercial kits, is recommended for research and diagnostic applications in molecular pathology.

Acknowledgements We are grateful to the teams of the IMPACTS group and their technicians for their support to make this European collaboration successful. We particularly acknowledge:

Dr. Andreas Jung, Beate Luthardt and Sabine Pfeiffer (LMU, Munich), Birgit Geist (Technische Universität, Munich), Annemiek W. M. van Raaij and Paul D.M. Rombout (RUNMC, Nijmegen), Giorgio Basili and Marisa Donada (Trieste), Marina Montresor, Maria Scardoni and Anna Bertolaso (Verona), Martina Susa (Zagreb), Dr. Dolores Colomer and Xarxa de Bancs de Tumors de Catalunya for technical assistance (Barcelona), Hugo Seca (Porto), Andrea Hofmann, Elisabeth Lackinger and Martina Wild (Graz, Labor für molekularpathologische Diagnostik), Iris Halbwedl (Graz, Research Unit for Molecular Lung- and Pleurapathology). We also thank Dr. Valentina Melita for the English revision of the manuscript.

Conflict of interests The authors declare no conflicts of interests, but F.H. received funding from Roche Diagnostics GmbH, Penzberg, Germany.

Open Access This article is distributed under the terms of the Creative Commons Attribution Noncommercial License which permits any noncommercial use, distribution, and reproduction in any medium, provided the original author(s) and source are credited.

References

1. Dietel M (2007) Predictive medicine: incipient reality or fata morgana? J Pathol 212:353–355
2. Paik S, Tang G, Shak S et al (2006) Gene expression and benefit of chemotherapy in women with node-negative, estrogen receptor-positive breast cancer. J Clin Oncol 24:3726–3734
3. van Dongen JJ, Langerak AW, Bruggemann M et al (2003) Design and standardization of PCR primers and protocols for detection of clonal immunoglobulin and T-cell receptor gene recombinations in suspect lymphoproliferations: report of the BIOMED-2 Concerted Action BMH4-CT98-3936. Leukemia 17:2257–2317
4. Nardon E, Donada M, Bonin S et al (2009) Higher random oligo concentration improves reverse transcription yield of cDNA from bioptic tissues and quantitative RT-PCR reliability. Exp Mol Pathol 87:146–151
5. Masuda N, Ohnishi T, Kawamoto S et al (1999) Analysis of chemical modification of RNA from formalin-fixed samples and optimization of molecular biology applications for such samples. Nucleic Acids Res 27:4436–4443
6. McKinney MD, Moon SJ, Kulesh DA et al (2009) Detection of viral RNA from paraffin-embedded tissues after prolonged formalin fixation. J Clin Virol 44:39–42
7. Srinivasan M, Sedmak D, Jewell S (2002) Effect of fixatives and tissue processing on the content and integrity of nucleic acids. Am J Pathol 161:1961–1971
8. Groenen PJTA, Langerak AW, van Dongen JJM et al (2008) Pitfalls in TCR gene clonality testing: teaching cases. J Hematopathol 1:97–109
9. van Beers EH, Joosse SA, Ligtenberg MJ et al (2006) A multiplex PCR predictor for aCGH success of FFPE samples. Br J Cancer 94:333–337
10. Abramovitz M, Ordanic-Kodani M, Wang Y et al (2008) Optimization of RNA extraction from FFPE tissues for expression profiling in the DASL assay. Biotechniques 44:417–423
11. Chung JY, Braunschweig T, Hewitt SM (2006) Optimization of recovery of RNA from formalin-fixed, paraffin-embedded tissue. Diagn Mol Pathol 15:229–236

12. Manchester KL (1996) Use of UV methods for measurement of protein and nucleic acid concentrations. Biotechniques 20:968–970
13. Wilfinger WW, Mackey K, Chomczynski P (1997) Effect of pH and ionic strength on the spectrophotometric assessment of nucleic acid purity. Biotechniques 22(474–476):478–481
14. von Ahlfen S, Missel A, Bendrat K et al (2007) Determinants of RNA quality from FFPE samples. PLoS ONE 2:e1261
15. Ribeiro-Silva A, Zhang H, Jeffrey SS (2007) RNA extraction from ten year old formalin-fixed paraffin-embedded breast cancer samples: a comparison of column purification and magnetic bead-based technologies. BMC Mol Biol 8:118
16. Abrahamsen HN, Steiniche T, Nexo E et al (2003) Towards quantitative mRNA analysis in paraffin-embedded tissues using real-time reverse transcriptase-polymerase chain reaction: a methodological study on lymph nodes from melanoma patients. J Mol Diagn 5:34–41
17. Li J, Smyth P, Cahill S et al (2008) Improved RNA quality and TaqMan Pre-amplification method (PreAmp) to enhance expression analysis from formalin fixed paraffin embedded (FFPE) materials. BMC Biotechnol 8:10

Virchows Arch (2010) 457:319–328
DOI 10.1007/s00428-010-0943-3

ORIGINAL ARTICLE

Reciprocal correlation between the expression of cyclooxygenase-2 and E-cadherin in human bladder transitional cell carcinomas

Tae Jung Jang · Woo Heon Cha · Kyung Seob Lee

Received: 24 March 2010 / Revised: 4 May 2010 / Accepted: 7 June 2010 / Published online: 26 June 2010
© Springer-Verlag 2010

Abstract Carcinoma cells become more motile and invasive via downmodulation of E-cadherin. Cyclooxygenase-2 (COX-2) expression is associated with tumor invasion and metastasis. The aim of this study is to investigate the relationship between the expression of COX-2 and E-cadherin in a bladder cancer cell line and human bladder transitional cell carcinoma (TCCs). Phorbol 12-myristate 13-acetate (PMA) treatment for 5637 bladder cancer cells increased COX-2 expression, slightly induced Slug expression, and decreased E-cadherin expression. Ectopic expression of COX-2 or prostaglandin E_2 (PGE_2) treatment for 5637 cells reduced E-cadherin expression. This finding was confirmed by the result that knockdown of COX-2 expression or indomethacin administration increased the expression of E-cadherin. When compared with cells' motility in serum-free medium, the treatment of PMA and PGE_2 increased cell motility, and indomethacin treatment slightly decreased cell motility. In the tissues of bladder TCCs, COX-2 expression was inversely correlated with membranous E-cadherin expression and positively correlated with nuclear β-catenin expression. The expression of COX-2 and nuclear β-catenin expression was significantly higher in TCCs of high grade and invasive growth than in TCCs of low grade and noninvasive growth. In contrast, membranous E-cadherin expression was more decreased in tumors of high grade and invasive growth. In addition, nuclear β-catenin expression was significantly related to tumor recurrence. We suggest that COX-2 pathway reduces membranous E-cadherin expression in bladder TCCs and their expression pattern may provide important information in predicting the clinical behavior of bladder TCCs.

Keywords Bladder transitional cell carcinoma · Cyclooxygenase-2 · E-cadherin · β-Catenin

T. J. Jang (✉)
Department of Pathology, College of Medicine,
Dongguk University,
Sukjang-dong 707,
Gyeongju, Gyeongbuk 780-714, South Korea
e-mail: taejung@mail.dongguk.ac.kr

W. H. Cha · K. S. Lee
Departments of Urology, College of Medicine,
Dongguk University,
Gyeongju, South Korea

Introduction

Transitional cell carcinoma (TCC) of the urinary bladder accounts for about 3.2% of all the types of cancers, and TCC is the seventh most common cancer worldwide with an estimated 260,000 new cases occurring each year in men and 76,000 new cases occurring in women [1]. The most important process related to the prognosis of TCC is the invasion of lamina propria and proper muscular layer [2].

Cell–cell adhesion mediated by E-cadherin is required for the maintenance of epithelial tissue architecture in adult organisms [3]. Downmodulation of E-cadherin is observed during the later stages of tumorigenesis [4]. This down-regulation of E-cadherin is accompanied by a loss of epithelial characteristics and the acquisition of mesenchymal properties, a process often referred to as the epithelial-to-mesenchymal transition (EMT) [4]. During EMT, carcinoma cells become more motile and invasive by acquiring characteristics similar to embryonic mesenchymal cells, thereby allowing penetration of the stroma surrounding the initial neoplastic focus [5]. EMT has been also suggested to be related to bladder cancer invasion and metastasis [6]. Several studies have demonstrated that the reduction of E-cadherin expression in bladder TCCs was closely associated

with high grade and advanced stage as well as poor survival [2, 7, 8]. The loss of E-cadherin occurring during carcinoma progression can take place through gene mutations, hypermethylation of its promoter, and transcriptional repression [9]. E-cadherin repressors that have been implicated in EMT are the Snail family, the basic helix-loop-helix factors E47 and Twist, and the two-handed zinc factors zinc finger E-box-binding homeobox 1 (ZEB1) and smad-interacting protein 1 (SIP1) [5, 10]. β-Catenin is bound to membrane-associated E-cadherin and is essential for its correct position and function [11]. The reduction of membranous E-cadherin leads to the translocation of β-catenin to nucleus from cell membrane. This nuclear β-catenin activates genes necessary for cell proliferation and invasive growth [12].

Cyclooxygenase-2 (COX-2) is transiently induced by proinflammatory cytokines and growth factors [13]. Prostaglandin E_2 (PGE_2) is related to carcinogenesis through immunosuppression, inhibiting apoptosis, increasing the metastatic potential of epithelial cells, and promoting angiogenesis [14, 15]. COX-2 overexpression was observed in various tumors as well as in bladder TCCs [16–21]. Our previous study has reported that COX-2 overexpression in bladder TCCs was significantly associated with high grade and invasion of tumors [22]. Moreover, a large case–control study demonstrated an overall decreased risk of bladder cancer in regular users of nonsteroidal anti-inflammatory drugs [23]. Tsujii and DuBois have demonstrated that the COX-2 overexpression was linked to inactivation of E-cadherin [13]. A recent study showed that COX-2-dependent PGE_2 in lung cancer cells reduced E-cadherin expression via a ZEB1 and Snail and that inhibition of COX-2 resulted in rescue of E-cadherin expression [24]. Our previous study also showed a similar result in human colon cancer cells [25]. Recently, etodolac, a COX-2 inhibitor, induces upregulation of E-cadherin in bladder cancer cells [26].

Here, we extend our previous study on COX-2 expression in bladder TCCs. The aim of this study is to investigate the relationship between the expression of COX-2 and E-cadherin in a bladder cancer cell line and human bladder TCCs.

Materials and methods

Cell culture and reagents

Two bladder cancer cell lines (T24, 5637) were obtained from the Korean Cell Line Bank (Seoul, Korea) and grown in RPMI 1640 (Life Technologies, Inc., Gaithersburg, MD, USA) supplemented with 10% fetal bovine serum (Life Technologies, Inc.) and gentamicin (10 μg/ml) in a 5% CO_2 humidified atmosphere. Indomethacin, PGE_2, and phorbol 12-myristate 13-acetate (PMA) were purchased from Sigma (St. Louis, MO, USA) and dissolved in absolute ethanol or dimethyl sulfoxide, respectively.

Transfection of COX-2 cDNA

Five thousand six hundred thirty-seven cells (2×10^5 in 2 ml of RPMI 1640 without gentamicin) were plated in six-well plates. Twenty-four hours later, the cells were transfected with vector alone or with pCB7-rat COX-2 (a gift of Dr. DuBois, Vanderbilt University, TN, USA) using Lipofectamine 2000 (Life Technologies, Inc.) according to the manufacturer's instructions. Briefly, 4 μg of DNA was mixed with 250 μl of Opti-MEM I (Life Technologies, Inc.). The diluted DNA was combined with 10 μl of Lipofectamine 2000 diluted by 250 μl of Opti-MEM I (Life Technologies, Inc.) and incubated for 20 min at room temperature. This mixture was added to cells that had attained 90% confluence in six-well plates. After 48 h, the cells were harvested for Western blot analysis.

COX-2 siRNA

Five thousand six hundred thirty-seven cells (2×10^5 in 2 ml of RPMI 1640 without gentamicin) were plated in six-well plates. Twenty-four hours later, the cells were transfected with control siRNA alone or with COX2-2 siRNA (Santa Cruz Biotechnology, Inc., Santa Cruz, CA, USA) using siRNA transfection reagent (Santa Cruz Biotechnology, Inc.) according to the manufacturer's instructions.

Western blot analysis

Cells were washed with cold phosphate buffered saline (PBS) and suspended in lysis buffer (1× PBS, 1% Triton X-100) supplemented with complete miniprotease inhibitor mixture tablets (Boehringer Mannheim, Mannheim, Germany) on ice for 30 min. After removing cell debris by centrifugation, cell lysate protein concentrations were determined using bicinchoninic acid protein assay reagent (Pierce, Rockford, IL, USA) with bovine serum albumin as a standard. Twenty micrograms of protein was separated by 10% sodium dodecyl sulfate (SDS)-polyacrylamide gel and transferred to a nitrocellulose membrane. The membranes were blocked with 5% skim milk in Tris-buffered saline (TBS) for 1 h at room temperature and probed with antibodies overnight at 4°C. The antibodies used were anti-COX-2 (1:500; Cayman Chemical, Ann Arbor, MI, USA), anti-E-cadherin (1:1,000, Transduction Laboratories, Lexington, KY, USA), anti-Slug (1:750, Abcam plc., Cambridge, UK), and antiglyceraldehydes 3-phosphate dehydrogenase (anti-GAPDH; 1:200, Santa Cruz Biotechnology, Inc.). After washing with TBS–0.05% Tween 20, the blots were treated with a horseradish peroxidase-conjugated antirabbit IgG antibody (1:5,000; Zymed Labora-

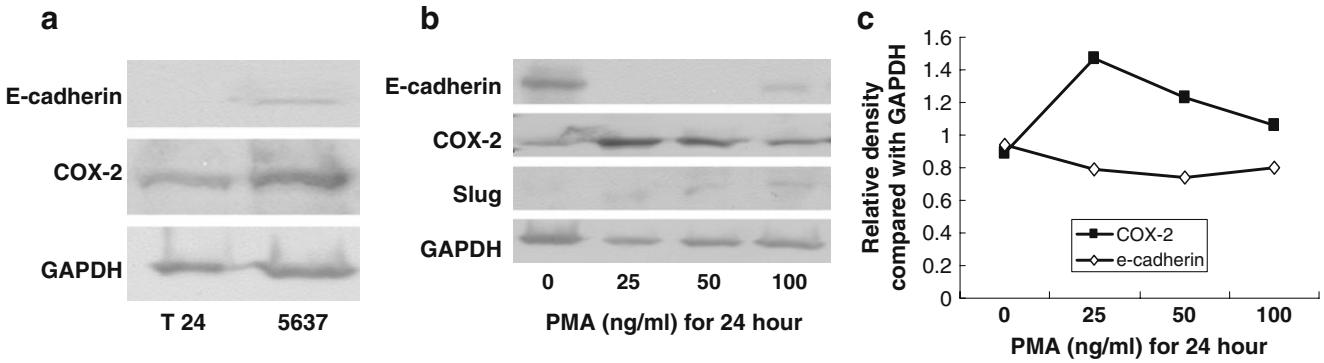

Fig. 1 Western blot analyses of E-cadherin, COX-2, and Slug in T24 and 5637 cells. **a** Endogenous expression of E-cadherin and COX-2 in T24 and 5637 cells. **b** Expression of E-cadherin, COX-2, and Slug in 5637 cells treated with PMA at the indicated doses for 24 h. Twenty micrograms of protein was separated by 10% SDS-polyacrylamide gel electrophoresis and transferred to a nitrocellulose membrane. The bottom represents GAPDH, which was used as a loading control. **c** There was an inverse correlation between the expression of COX-2 and E-cadherin in 5637 cells treated with PMA

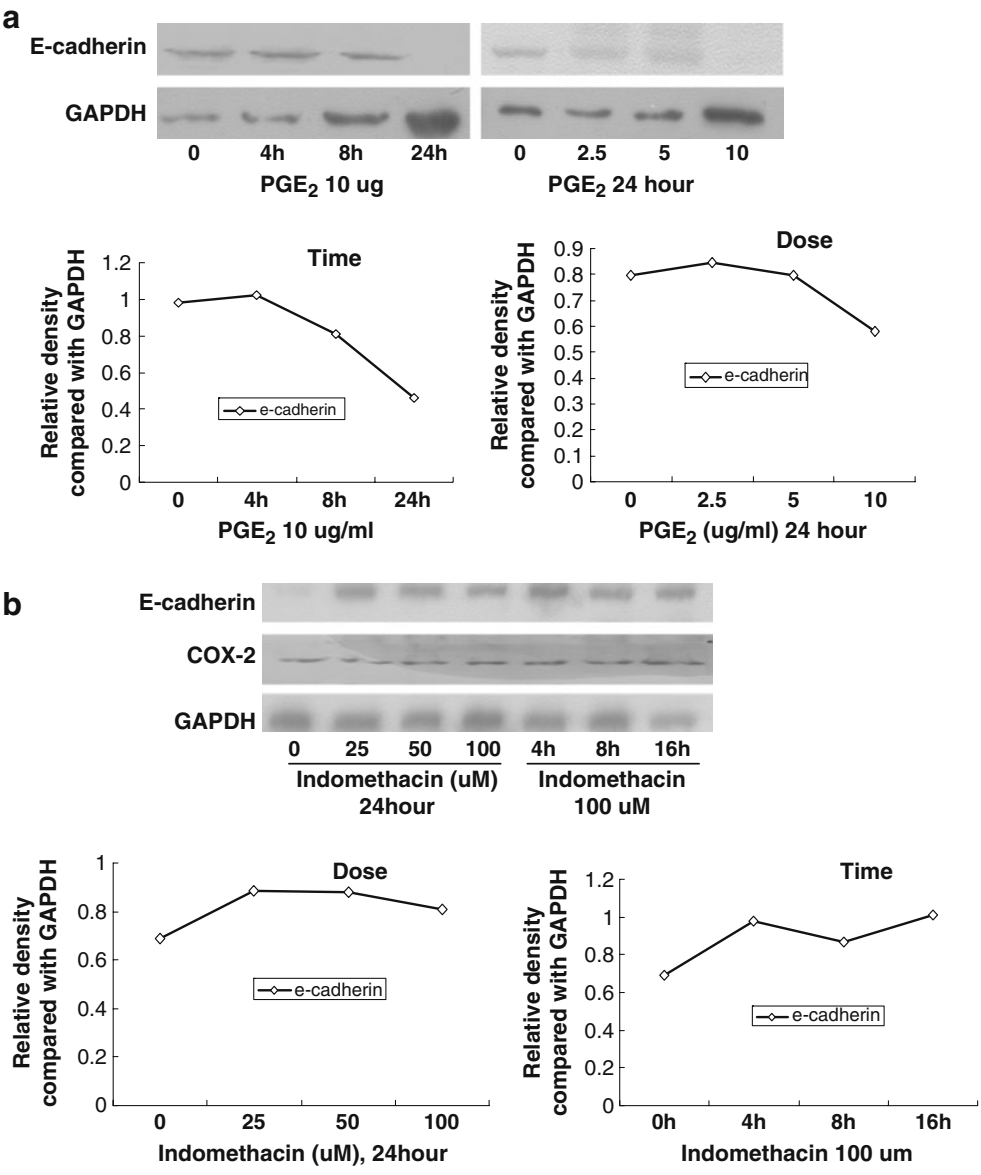

Fig. 2 Western blot analyses of E-cadherin and COX-2 in 5637 cells. **a** E-cadherin expression decreased as the dose or exposure time of PGE_2 increased. **b** E-cadherin expression increased as the dose or time of indomethacin increased. Twenty micrograms of protein was separated by 10% SDS-polyacrylamide gel electrophoresis and transferred to a nitrocellulose membrane. The *bottom* represents GAPDH, which was used as a loading control

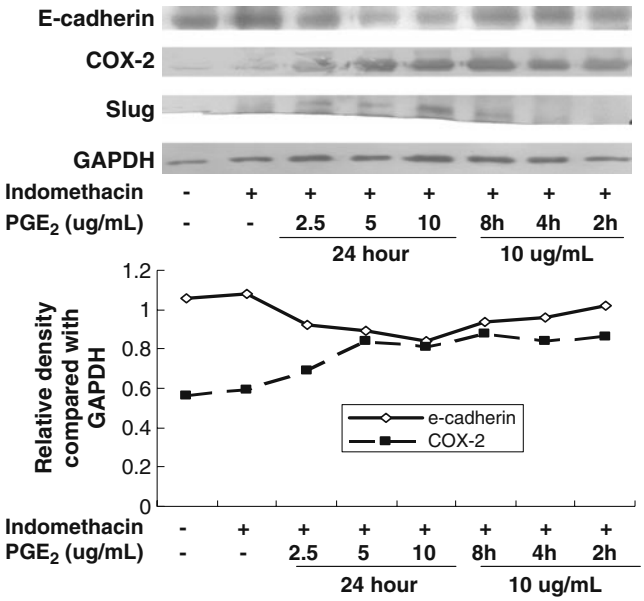

Fig. 3 Western blot analyses of E-cadherin, COX-2, and Slug according to the dose and exposure time of PGE_2 in 5637 cells pretreated with 100 μM indomethacin for 30 min. As the dose and exposure time of PGE_2 increased, E-cadherin expression mildly decreased, COX-2 expression increased, and Slug was induced. Twenty micrograms of protein was separated by 10% SDS-polyacrylamide gel electrophoresis and transferred to a nitrocellulose membrane. The *bottom* represents GAPDH, which was used as a loading control

tories Inc., San Francisco, CA, USA) or an antimouse IgG antibody (1:5,000; Zymed Laboratories Inc.) for 1 h at room temperature. Detection was performed by enhanced chemiluminescence (Pierce) and autoradiography. We examined optical density compared with GAPDH using Scion image.

Wound healing assay

Confluent cell monolayers were wounded by manually scraping the cells with a pipette tip. Debris was removed from the culture by washing it twice with PBS. The cells were then incubated with serum-free medium including either PGE_2 (10 μg/ml), indomethacin (100 μM), or PMA (50 ng/ml) and allowed to migrate into the wounded area for up to 24 h at 37°C. Images were immediately acquired at 24 h after wounding. This test was performed in triplicate.

Tissue samples and the patient population

We used 80 paraffin-embedded bladder TCCs and five normal bladder tissues obtained from the Department of Pathology at Dongguk University Kyongju Hospital. The cancer tissues were obtained from transurethral resection of bladder TCCs. In addition, the normal bladder epithelial tissues were obtained from cases of chronic cystitis. The tumor was graded in accordance with the WHO-ISUP classification [27], and the pathological T stage (pT; depth of invasion) was also determined. Thirty-two tumors were stage pTa, 24 were pT1, and 24 were more or equal to pT2. Thirty-four patients had low-grade tumors, while 46 patients had high-grade tumors. The age distribution of the patients whose tumors we were using was between 30 and 87 years old, and the male and female ratio was 5.7:1. Disease recurrence was defined as any evidence of tumor in a retained bladder at least 3 months after treatment. Twenty-six patients had recurrent tumor.

Immunohistochemistry

Urinary bladder sections of 4 μm thickness were made, and they were spread on poly-L-lysine coated slides. The paraffin sections were immersed in three changes of xylene, and they were hydrated using a graded series of alcohol solutions. Antigen retrieval was routinely performed by immersing the sections in 0.01 M citrate buffer (pH 6.0) in a pressure cooker and performing autoclaving for 15 min. The endogenous peroxidase activity was blocked with 3% hydrogen peroxide for 15 min, and then the sections were incubated with primary antibody for 2 h at room temperature. The primary antibodies used were anti-COX-2 (1:500; Cayman Chemical), anti-E-cadherin (1:1,000, Transduction Laboratories), and anti-β-catenin (1:500, Transduction Laboratories). Staining was achieved with an EnVision kit (DAKO, Santa Barbara, CA, USA) and developed with 3, 3′-diaminobenzidine tetrahydrochloride (Zymed Laboratories, Inc.) as a chromogen. The sections were counterstained for 3 min with Meyer's hematoxylin and then they were mounted. As a negative control, rabbit or mouse IgG isotype was used instead of the primary antibody. As a positive control, the tissue section of colonic adenocarcinoma was used. The immunoreactivity for cytoplasmic COX-2 expression was evaluated by assessing the percentage of positive cells, and this was graded as

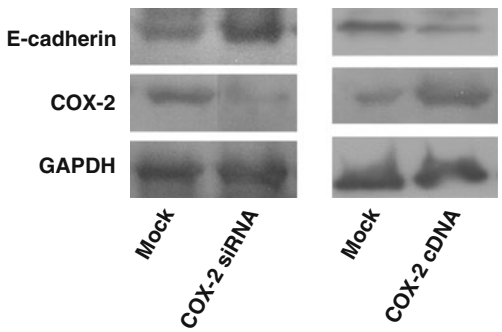

Fig. 4 Western blot analyses of E-cadherin and COX-2 in 5637 cells after the transfection of COX-2 cDNA and COX-2 siRNA. Twenty micrograms of protein was separated by 10% SDS-polyacrylamide gel electrophoresis and transferred to a nitrocellulose membrane. The *bottom* represents GAPDH, which was used as a loading control

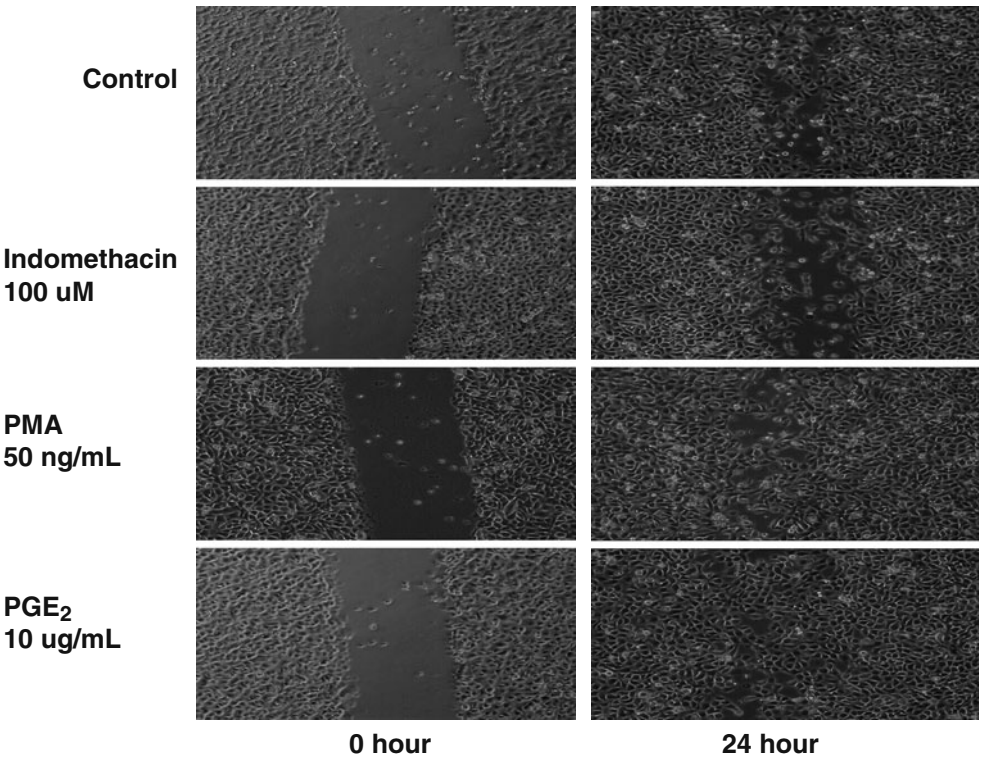

Fig. 5 Examination of cells' motility at 24 h in 5,637 cells after the administration of indomethacin (100 μM), PMA (50 ng/mL), and PGE_2 (10 μg/mL). When compared with cells' motility in serum-free medium, the treatment of PMA or PGE_2 increased cells' motility, whereas indomethacin decreased it

negativity (0–5%) or positivity (>5%). Membranous E-cadherin expression was graded according to the proportion of positive cells and classified into a positive group (>90%) and an abnormal group (0–90%). Nuclear β-catenin was interpreted to be positive when nuclear staining was present in tumor cells.

Statistical analysis

Chi-square tests, Fisher's exact test, and *t* tests were used. Statistical significance was assumed if a *p* value was less than 0.05.

Results

As shown in Fig. 1a, endogenous E-cadherin and COX-2 expressed more strongly in 5637 cells compared with T24 cells. Therefore, 5637 cells were thought to be more suitable for the purpose of our study. PMA treatment for 24 h increased COX-2 expression, slightly induced Slug expression, and decreased E-cadherin expression (Fig. 1b). There was an inverse correlation between the expression of COX-2 and E-cadherin in 5637 cells treated with PMA as shown in Fig. 1c. Figure 2 reveals E-cadherin expression in 5637 cells treated with PGE_2 or indomethacin. E-cadherin expression decreased as the dose or exposure time of PGE_2 increased, whereas E-cadherin expression increased with dose or time of indomethacin. Figure 3 reveals the expression of E-cadherin, COX-2, and Slug according to the dose and exposure time of PGE_2 in cells pretreated with 100 μM indomethacin for 30 min. As the dose and exposure time of PGE_2 increased, E-cadherin expression mildly decreased, COX-2 expression increased, and Slug was induced. The decrease rate of E-cadherin expression level was mild compared with that of 5637 cells treated with only PGE_2 as shown in Fig. 2a. Figure 4 reveals E-cadherin expression after the transfection of COX-2 cDNA and COX-2 siRNA. Ectopic expression of COX-2 reduced E-cadherin expression, whereas the knockdown of COX-2 increased it. As shown in Fig. 5, we examined cells' motility at 24 h after the administration of indomethacin (100 μM), PMA (50 ng/mL), and PGE_2 (10 μg/mL). When compared with cells' motility in serum-free medium, the treatment of PMA and PGE_2 increased cell motility, and indomethacin treatment slightly decreased cell motility.

We performed immunohistochemical staining for COX-2, E-cadherin, and β-catenin in the tissues of bladder TCCs in order to examine their clinical significance. COX-2-positive rate was 48% (38 out of 80). Figure 6 reveals that membranous E-cadherin expression was lost (Fig. 6b), and nuclear β-catenin expression was induced in TCCs (Fig. 6c) with positive COX-2 expression (Fig. 6a). Positive rate of membranous E-cadherin expression was 55% (21 out of 38) in TCCs with COX-2 expression and 86% (36 out of 42) in TCCs without COX-2 expression. Positive rate of nuclear β-catenin expression was 39% (14 out of 38) in TCCs with COX-2 expression and 12% (five out of 42) without COX-2

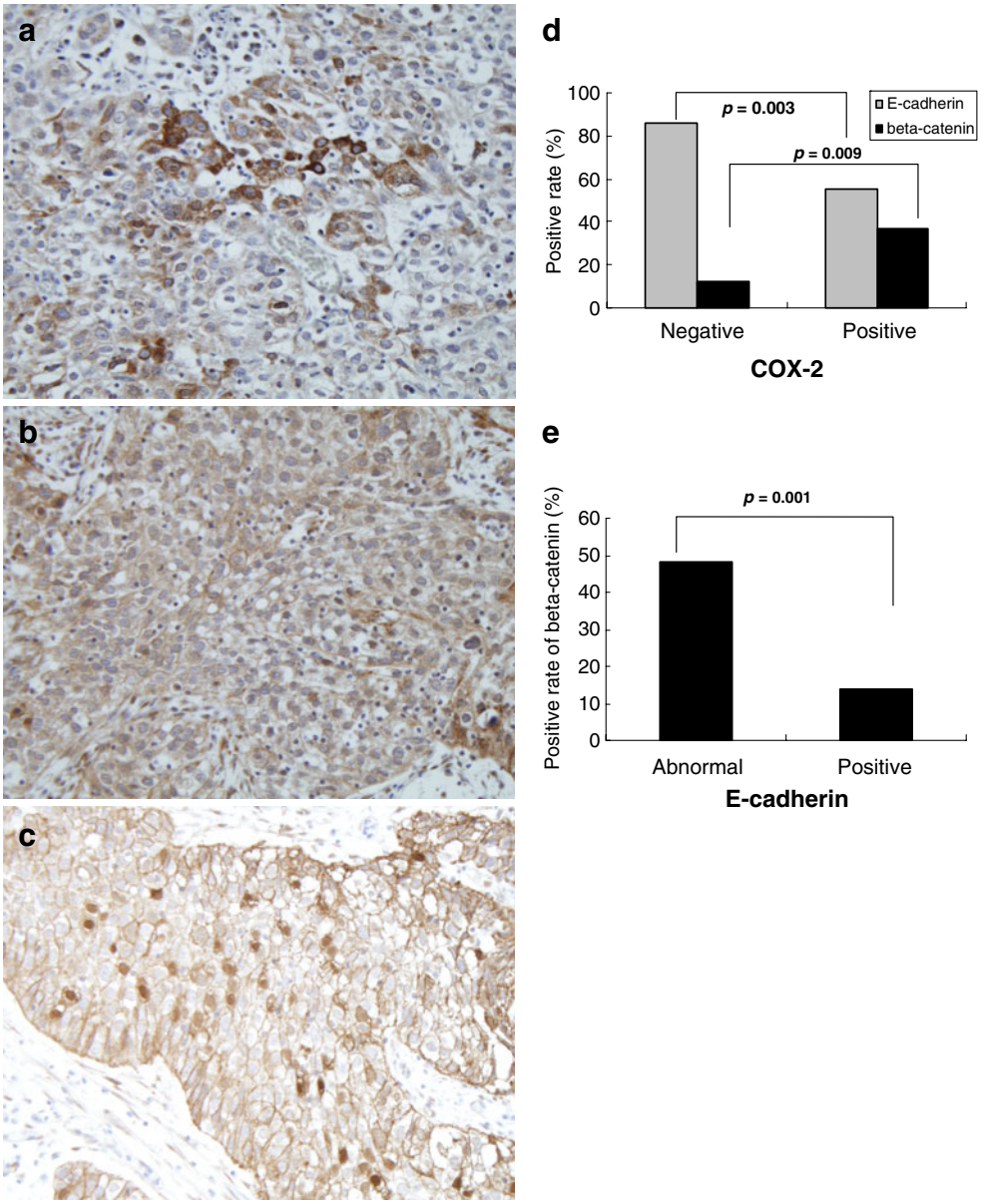

Fig. 6 Immunohistochemical staining of COX-2 (**a**), E-cadherin (**b**), and β-catenin (**c**) in TCCs. Membranous E-cadherin expression was lost, and nuclear β-catenin expression was induced in TCCs with positive COX-2 expression. **d** COX-2 expression was inversely correlated to membranous E-cadherin expression (p=0.003) and positively correlated to nuclear β-catenin expression (p=0.009). **e** There was an inverse correlation between the expression of nuclear β-catenin and membranous E-cadherin (p=0.001). **a**–**c** ×400

expression. As shown in Fig. 6d, COX-2 expression was inversely correlated to membranous E-cadherin expression (p=0.003) and positively correlated to nuclear β-catenin expression (p=0.009). In addition, there was an inverse correlation between the expression of nuclear β-catenin and membranous E-cadherin as shown in Fig. 6e (p=0.001).

Table 1 shows relationship between immunohistochemical results for COX-2, E-cadherin, and β-catenin and clinicopathologic parameters such as grade, tumor depth, and recurrence. COX-2 expression was significantly higher in TCCs of high grade and invasive growth than in TCCs of low grade and noninvasive growth. Figure 7 reveals that membranous E-cadherin expression was lost in TCCs with high grade (Fig. 7b) and invasive growth (Fig. 7c) compared with TCCs of low grade and noninvasive growth (Fig. 7a). Positive rate of membranous E-cadherin expression was 94% (32 out of 34) in low-grade TCCs, 54% (25 out of 46) in high-grade TCCs, 86% (28 out of 32) in pTa TCCs, 63% (15 out of 24) in pT1 TCCs, and 58% (14 out of 24) in more or equal to pT2 TCCs. As shown in Fig. 7d, membranous E-cadherin expression was significantly lost in TCCs with high grade (p=0.001) and invasive growth (p<0.003). Figure 8 reveals that nuclear β-catenin expression was induced in TCCs with high grade (Fig. 8b) and invasive growth (Fig. 8c) compared with TCCs of low grade and noninvasive growth (Fig. 8a). Positively rate of nuclear β-catenin expression was 6% (two out of 34) in low-grade TCCs, 37% (17 out of 46) in high-grade TCCs, 3% (one out of 32) in pTa TCCs, 17% (four out of 24) in pT1 TCCs, and 58% (14 out of 24) in more or equal to pT2 TCCs. As shown in Fig. 8d, nuclear β-catenin expression was significantly induced in high-grade (p=0.001) and invasive tumors (p<

Table 1 Positive rate of COX-2, E-cadherin, and β-catenin according to tumor grade, tumor depth, and recurrence in urinary bladder transitional cell carcinomas

	Positive rate (%)		
	COX-2	E-cadherin	β-Catenin
Tumor grade			
Low	5/34 (15)	32/34 (94)	2/34 (6)
High	33/46 (72)	25/46 (54)	17/46 (37)
Tumor depth			
pTa	4/32 (13)	28/32 (86)	1/32 (3)
pT1	17/24 (71)	15/24 (63)	4/24 (17)
More or equal to pT2	17/24 (71)	14/24 (58)	14/24 (58)
Recurrence			
Absence	25/54 (46)	40/54 (74)	9/54 (17)
Presence	13/26 (50)	17/26 (65)	10/26 (38)

0.004). Figure 9 reveals that tumor recurrence was significantly associated with nuclear β-catenin expression (p= 0.031). Positive rate of nuclear β-catenin was 17% (nine out of 54) in nonrecurrent tumors and 38% (ten out of 26) in recurrent tumors. There was no significant association between tumor recurrence and expression of COX-2 and membrane E-cadherin (data not shown).

Discussion

A defining characteristic of EMT is the loss of E-cadherin [4]. Transcriptional repression is a predominant mechanism controlling the expression of E-cadherin in most carcinomas [28]. Several transcriptional repressors, which include Snail, Slug, SIP1/ZEB1, E12/E47, and Twist, have been characterized [5, 10]. Recent studies of nonsmall cell lung cancer and colon cancer have shown that augmentation of PGE_2 by COX-2 activation or PGDH inactivation repressed E-cadherin expression through the induction of Snail and ZEB1 [23, 25, 29]. E-cadherin expression was sequentially reduced via PGE_2-EP_2 signaling pathway during ultraviolet-induced squamous cell carcinoma progression [30]. E-cadherin was upregulated and localized at intercellular junctions and the cytoplasmic membrane in etodolac-stimulated colon cancer cells [31]. A previous study has

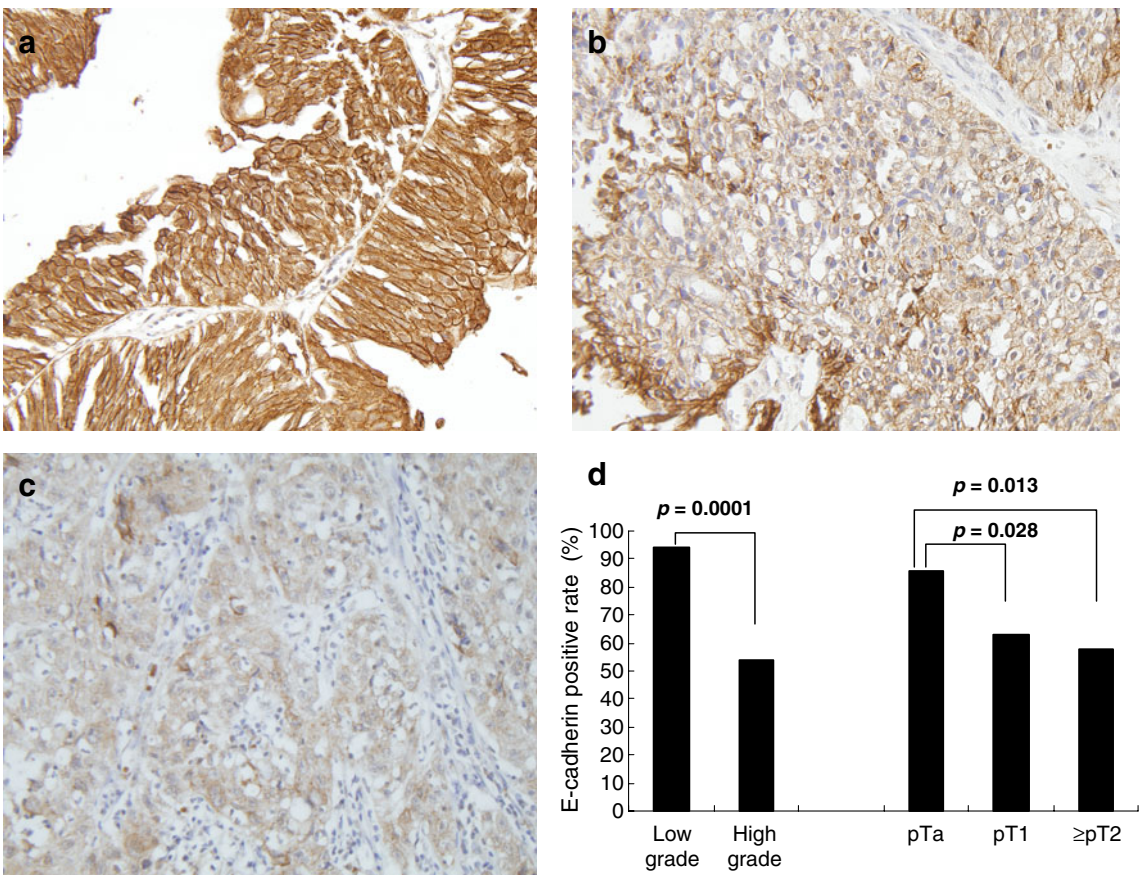

Fig. 7 Immunohistochemical staining of E-cadherin in TCCs. E-cadherin expression was lost in TCCs with high grade (**b**) and invasive growth (**c**) compared with TCCs of low grade and noninvasive growth (**a**). (**d**) Membranous E-cadherin expression was significantly lost in TCCs with high grade (p=0.001) and invasive growth (p<0.003). **a**–**c** ×400

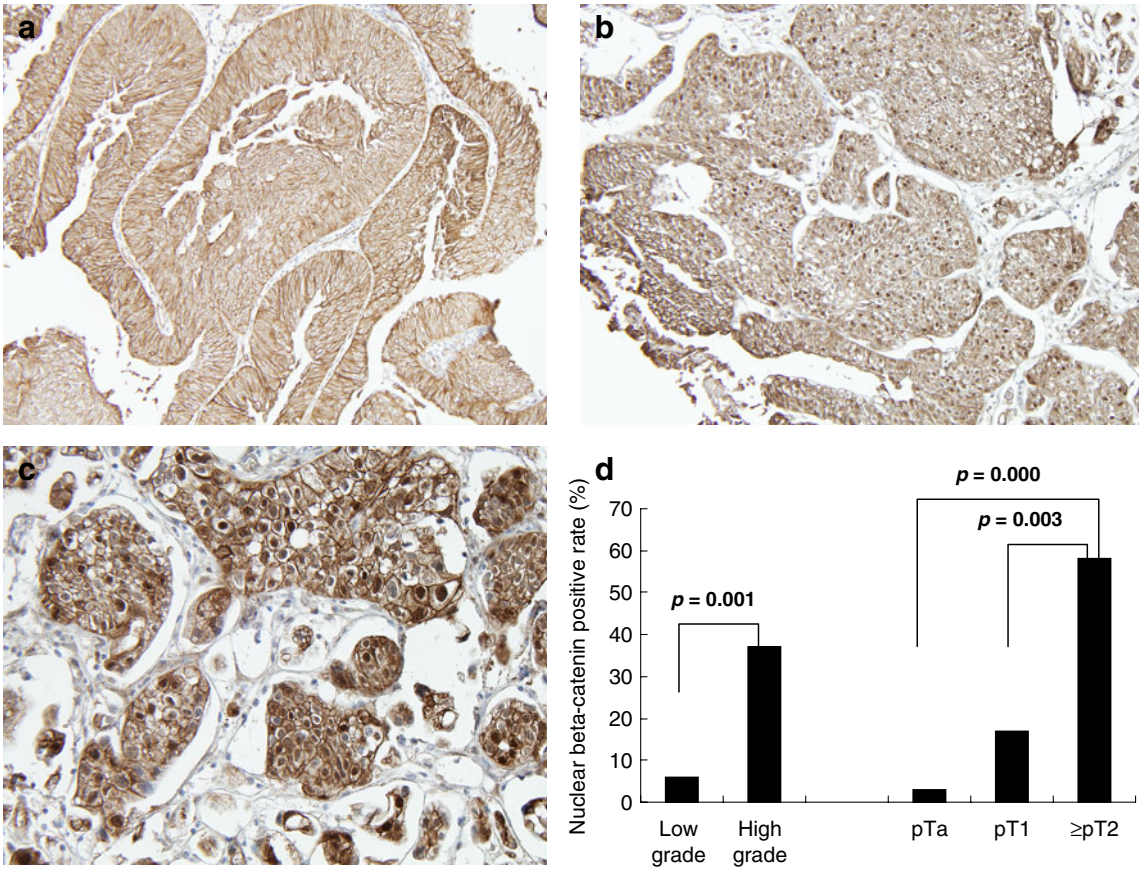

Fig. 8 Immunohistochemical staining of β-catenin in TCCs. Nuclear β-catenin expression was induced in TCCs with high grade (**b**) and invasive growth (**c**) compared with TCCs of low grade and noninvasive growth (**a**). **d** Nuclear β-catenin expression was significantly induced in high-grade (p=0.001) and invasive tumors (p< 0.004). **a**, **b** ×200; **c** ×400

reported that a selective COX-2 inhibitor increased E-cadherin expression in bladder cancer cells [26]. In the present study, we have demonstrated that ectopic expression of COX-2 or PGE_2 treatment for 5637 bladder cancer cells reduced E-cadherin expression. This finding was confirmed as follows: First, knockdown of COX-2 expression or indomethacin administration increased the expression of E-cadherin. Second, the reduction rate of E-cadherin expression after addition of PGE_2 was slight in 5637 cells pretreated with indomethacin compared with that of cells treated with only PGE_2. Third, PMA treatment or PGE_2 exposure for 5637 cells induced Slug expression. Fourth, our immunohistochemical staining in the tissues of bladder TCCs has revealed that COX-2 expression was inversely correlated with membranous E-cadherin expression. It thus appears that COX-2-dependent signaling pathway also reduces E-cadherin expression in bladder TCCs as well.

Carcinoma cells become more motile and invasive during EMT [5]. COX-2 stimulated the RhoA/Rho kinase pathway which disrupted adherens junction formation by reducing the levels of E-cadherin and α-catenin and increased cell motility [32]. In the present study, 5637 cells became more motile after addition of PMA or PGE_2. In contrast, its motility was decreased after indomethacin administration. Our previous study showed that COX-2 expression was closely related to the invasion of TCCs and was marked at the invasive front of tumors [22]. This was supported by several previous studies [18–21]. Here, we showed that abnormal E-cadherin expression was more frequently observed in invasive TCCs. This finding

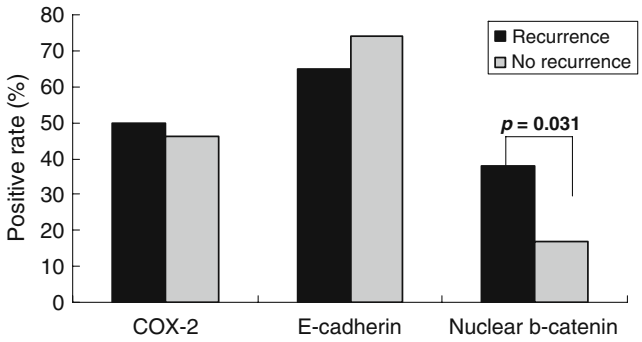

Fig. 9 Relationship between the recurrence of TCCs and the expression of COX-2, E-cadherin, and nuclear β-catenin. Tumor recurrence was significantly associated with nuclear β-catenin expression (p=0.031) and did not related to expression of COX-2 and membrane E-cadherin

supports several studies showing that the reduction of E-cadherin expression in TCC was closely associated with advanced stage as well as poor survival [2, 7, 8].

β-Catenin is bound to the cytoplasmic domain of E-cadherin, in which it enables E-cadherin to function as a cell–cell adhesion molecule and mediates the interplay of adherens junction molecules with the actin cytoskeleton [11]. Aberrations of E-cadherin expression can lead to abundant cytoplasmic β-catenin and its subsequent nuclear localization. Nuclear β-catenin activates genes necessary for cell proliferation, differentiation, and invasive growth [12]. Most of studies regarding the significance of β-catenin expression in TCCs contain no mention of its nuclear staining [2, 8, 33]. In those studies, the reduction or loss of β-catenin was related to high grade and advanced stage of TCCs as well as poor survival. A recent study has reported that nuclear β-catenin was observed in 3.5% of TCCs [7]. However, its meaning was not given in the study. In the present study, nuclear β-catenin was 23.8%, and it was significantly correlated with abnormal E-cadherin expression and positive COX-2 expression. Furthermore, nuclear β-catenin was significantly related to high-grade and invasive TCCs as well as tumor recurrence. Here, the high percentage of nuclear β-catenin appears to originate from our immunohistochemical score system. Our study also showed that nuclear β-catenin was significantly related to poor clinical course. We suggest that its presence may provide important information in predicting the prognosis of TCCs irrespective of expression level.

In conclusion, COX-2 expression was inversely correlated with membranous E-cadherin expression and positively correlated with nuclear β-catenin expression in bladder TCCs. We suggest that COX-2 pathway reduces E-cadherin expression in bladder TCCs and their expression pattern may provide important information in predicting the clinical behavior of bladder TCCs.

Conflict of interest The authors declare that they have no conflict of interest.

References

1. Jemal A, Siegel R, Ward E et al (2007) Cancer statistics, 2007. CA Cancer J Clin 57:43–66
2. Bryan RT, Atherfold PA, Yeo Y et al (2008) Cadherin switching dictates the biology of transitional cell carcinoma of the bladder: ex vivo and in vitro studies. J Pathol 215:184–194
3. Vleminckx K, Kemler R (1999) Cadherins and tissue formation: integrating adhesion and signaling. Bioessays 21:211–220
4. Thiery JP (2002) Epithelial–mesenchymal transitions in tumour progression. Nat Rev Cancer 2:442–454
5. Guarino M, Rubino B, Ballabio G (2007) The role of epithelial–mesenchymal transition in cancer pathology. Pathology 39:305–318
6. McConkey DJ, Choi W, Marquis L et al (2009) Role of epithelial-to-mesenchymal transition (EMT) in drug sensitivity and metastasis in bladder cancer. Cancer Metastasis Rev 28:335–344
7. Baumgart E, Cohen MS, Neto BS et al (2007) Identification and prognostic significance of an epithelial–mesenchymal transition expression profile in human bladder tumors. Clin Cancer Res 13:1685–1694
8. del Muro XG, Torregrosa A, Munoz J et al (2000) Prognostic value of the expression of E-cadherin and β-catenin in bladder cancer. Eur J Cancer 36:357–362
9. Hirohashi S (1998) Inactivation of the E-cadherin-mediated cell adhesion system in human cancer. Am J Pathol 153:333–339
10. Peinado H, Portillo F, Cano A (2004) Transcriptional regulation of cadherins during development and carcinogenesis. Int J Dev Biol 48:365–375
11. Barth AI, Näthke IS, Nelson WJ (1997) Cadherins, catenins and APC protein: interplay between cytoskeletal complexes and signaling pathways. Curr Opin Cell Biol 9:683–690
12. Brembeck FH, Rosário M, Birchmeier W (2006) Balancing cell adhesion and Wnt signaling, the key role of beta-catenin. Curr Opin Genet Dev 16:51–59
13. Hershman HR (1996) Prostaglandin synthase 2. Biochim Biophys Acta 1299:125–140
14. Tsujii M, DuBois RN (1995) Alterations in cellular adhesion and apoptosis in epithelial cells overexpressing prostaglandin endoperoxide synthase 2. Cell 83:493–501
15. Tsujii M, Kawano S, DuBois RN (1997) Cyclooxyenase-2 expression in human colon cancer cells increases metastatic potential. Proc Natl Acad Sci USA 94:3336–3340
16. Mohammed SI, Knapp DW, Bostwick DG et al (1999) Expression of cyclooxygenase-2 (COX-2) in human invasive transitional cell carcinoma (TCC) of the urinary bladder. Cancer Res 59:5647–5650
17. Shariat SF, Kim JH, Ayala GE, Kho K, Wheeler TM, Lerner SP (2003) Cyclooxygenase-2 is highly expressed in carcinoma in situ and T1 transitional cell carcinoma of the bladder. J Urol 169:938–942
18. Komhoff M, Guan Y, Sharppell HW et al (2000) Enhanced expression of cyclooxygenase-2 in high grade human transitional cell bladder carcinomas. Am J Pathol 157:29–35
19. Wadhwa P, Goswami AK, Joshi K, Sharma SK (2005) Cycooxygenase-2 expression increases with the stage and grade in transitional cell carcinoma of the urinary bladder. Int Urol Nephrol 37:47–53
20. Okajima E, Uemura H, Ohnishi S (2003) Expression of cyclooxygenase-2 in primary superficial bladder cancer tissue may predict risk of its recurrence after complete transurethral resection. Aktuelle Urol 34:256–258
21. Kim SI, Kwon SM, Kim YS, Hong SJ (2002) Association of cyclooxygenase-2 expression with prognosis of stage T1 grade 3 bladder cancer. Urology 60:816–821
22. Jang TJ, Lee KS (2009) The expression of cyclooxygenase-2 and surviving in urinary bladder transitional cell carcinoma. Kor J Pathol 43:206–211
23. Castelao JE, Yuan JM, Gago-Dominguez M, Yu MC, Ross RK (2000) Non-steroidal anti-inflammatory drugs and bladder cancer prevention. Br J Cancer 82:1364–1369
24. Dohadwala M, Yang SC, Luo J et al (2006) Cyclooxygenase-2-dependent regulation of E-cadherin: prostaglandin E_2 induces transcriptional repressors ZEB1 and snail in non-small cell lung cancer. Cancer Res 66:5338–5345
25. Jang TJ (2009) Cyclooxgenase-2 expression is related to the epithelial-to-mesenchymal transition in human colon cancers. Yon Med J 50:818–824
26. Okamoto A, Shirakawa T, Bito T et al (2008) Etodolac, a selective cyclooxgenase-2 inhibitor, induces upregulation of E-cadherin and has antitumor effect on human bladder cancer cells in vitro and in vivo. Urology 71:156–160

27. Epstein JI, Amin MB, Reuter VR, Mosofi FK (1998) The World Health Organization/International Society of Urology Pathology consensus classification of urothelial (transitional cell) neoplasms of the urinary bladder. Am J Surg Pathol 22:1435–1448
28. Park SH, Cheung LW, Wong AS, Leung PC (2008) Estrogen regulates Snail and Slug in the down-regulation of E-cadherin and induces metastatic potential of ovarian cancer cells through estrogen receptor alpha. Mol Endocrinol 22:2085–2098
29. Mann JR, Backlund MG, Buchanan FG et al (2006) Repression of prostaglandin dehydrogenase by epidermal growth factor and snail increases prostaglandin E_2 and promotes cancer progression. Cancer Res 66:6649–6656
30. Brouxhon S, Kyrkanides S, O'Banion MK et al (2007) Sequential down-regulation of E-cadherin with squamous cell carcinoma progression: loss of E-cadherin via a prostaglandin E_2-EP_2-dependent posttranslational mechanism. Cancer Res 67:7654–7664
31. Noda M, Tatsumi Y, Tomizawa M et al (2002) Effects of etodolac, a selective cyclooxygenase-2 inhibitor, on the expression of E-cadherin–catenin complexes in gastrointestinal cell lines. J Gastroenterol 37:896–904
32. Chang YW, Marlin JW, Chance TW, Jakobi R (2006) RhoA mediates cyclooxygenase-2 signaling to disrupt the formation of adherens junctions and increase cell motility. Cancer Res 66:11700–11708
33. Shimazui T, Schalken JA, Giroldi LA et al (1996) Prognostic value of cadherin-associated molecules (α-, β-, γ-catenins and $p120^{cas}$) in bladder tumors. Cancer Res 56:4154–4158

Virchows Arch (2010) 457:329–336
DOI 10.1007/s00428-010-0948-y

ORIGINAL ARTICLE

Autoimmune pancreatitis-related diabetes: quantitative analysis of endocrine islet cells and inflammatory infiltrate

Alton B. Farris III · Gregory Y. Lauwers · Vikram Deshpande

Received: 18 May 2010 / Revised: 19 June 2010 / Accepted: 30 June 2010 / Published online: 15 July 2010
© Springer-Verlag 2010

Abstract In autoimmune pancreatitis (AIP), mechanism(s) of paradoxical glycemic control improvement (GCI) often occurring after pancreatic resection and steroid therapy are not fully elucidated. Using image quantitation, AIP cases (n =10) with pre- and post-surgical glucose values were compared with chronic pancreatitis (CP) and normal pancreas (NP) regarding percent chromogranin immunohistochemistry (IHC) positivity as a surrogate marker of endocrine endowment; intra-islet T and B lymphocyte and plasma cell enumeration with CD3, CD20, and IgG4 IHC; and CD34 IHC islet vascularity quantitation. Postsurgical GCI, noted in 8/10 (80%) AIP cases, approached statistical significance (P=0.07) compared to CP. Endocrine endowment reduction, noted by a lower percent of chromogranin + pancreatic parenchyma, was seen in AIP (4.54%) and CP (3.20%) compared to NP (7.95%); only the CP decrease was statistically significant (P=0.02) since AIP often had ductular endocrine neogenesis. Regression suggested an inverse correlation between endocrine endowment and GCI in AIP (R=0.62, P=0.06). AIP islets were smaller and disrupted by inflammatory cell infiltration. Compared to CP, AIP islets had higher CD3 + and CD20 + cell densities. IgG4 + plasma cells were often present at a high density in AIP but typically preserved the islets. Intra-islet CD34 staining showed a lower average vascularity in AIP compared to NP (P=0.05). This study reaffirms postsurgical GCI in AIP. Prominent intra-islet inflammation and decreased vascularity in AIP may contribute to diabetogenic effects. Endocrine cell neogenesis and relative islet preservation despite islet inflammatory infiltration may explain the paradoxical GCI in AIP.

Keywords Autoimmune pancreatitis · Diabetes · Immunohistochemistry · Morphometry · IgG4

A. B. Farris III (✉)
Department of Pathology, Emory University Hospital,
1364 Clifton Road NE, Room H-188,
Atlanta, GA 30322, USA
e-mail: abfarri@emory.edu

A. B. Farris III · G. Y. Lauwers · V. Deshpande
Pathology Service, Massachusetts General Hospital,
Boston, MA, USA

Introduction

Autoimmune pancreatitis (AIP) is a steroid-responsive inflammatory pancreatobiliary-centric disease, which is frequently mass-forming. According to some studies, AIP represents the final diagnosis of approximately one quarter of Whipple resections performed for benign conditions in North America [1–4]. It affects mainly elderly individuals, and affected patients frequently present with obstructive jaundice, vague abdominal pain, and occasionally other autoimmune diseases [5]. Serologically, AIP is characterized by elevated levels of serum immunoglobulin G4 (IgG4) [5]. A non-tissue diagnosis can sometimes be rendered using a combination of clinical symptoms, radiologic features, including a diffuse enlargement of the pancreas ("sausage sign"), elevated serum IgG4 levels, ultrasound-guided fine-needle aspiration biopsy, and response to steroids [2, 6].

Histologically, AIP is characterized by a dense lymphoplasmacytic parenchymal infiltrate with secondary fibrosis and acinar atrophy. The hallmarks of AIP include a periductal collar of chronic inflammation around both small and large interlobular ducts and obliterative phlebitis [2, 6–10]. The lymphoplasmacytic infiltrate is characteristically composed of numerous IgG4-positive

plasma cells [2, 6, 7, 11, 12]. The disease can involve the bile ducts (sclerosing cholangitis), gallbladder (lymphoplasmacytic sclerosing cholecystitis), and kidney (interstitial nephritis and pseudotumor-like lesions) and the lungs (forming inflammatory masses), as well as many other organs, such as aorta and salivary glands [2, 6, 7]. Today, this multiorgan involvement is believed to be part of a systemic IgG4-related disease, which has been termed "IgG4-associated immune complex multiorgan autoimmune disease" (IMAD) [13].

In patients with AIP, paradoxical improvements in glycemic control have been observed not only after pancreatic resection, but also following steroid therapy [14–17]. It has been hypothesized that an inflammatory damage to the pancreatic islets could have a role in the apparent impaired glycemic control [14, 17]. The volume of β cells has been shown to be decreased in AIP [17]. Immunohistochemical studies have indicated that CD8+ T cells may play a role in the selective destruction of islet β cells in AIP [17, 18]. Cytokeratin 19-positive cells containing insulin and glucagon have also been identified in pancreata affected by AIP, suggesting a secondary neogenesis of islets from ductal cells [16, 17, 19].

Although the etiology of the glycemic control derangement seen in AIP remains unclear, the involvement of the islets shows similarities to what is seen in type 1A diabetes, also known as immune-mediated diabetes. In type 1A diabetes, anti-islet antibodies can be found, specifically islet cell antibody (ICA), glutamic acid decarboxylase (GAD65) autoantibody, insulin autoantibody (IAA), and insulinoma antigen-2 autoantibody [13, 20]. Somewhat similarly, carboxyanhydrase II antibodies and anti-nuclear autoantibodies have been found in AIP [9, 21]. Islet antibodies have also been demonstrated in some cases of type 2 diabetes (sometimes referred to as latent autoimmune diabetes in adults or slowly progressive insulin-dependent diabetes mellitus [SPIDDM]), and epidemiological studies have indicated that about 10% of patients with apparent type 2 diabetes have at least one autoantibody against an islet-specific antigen [20]. Also, again like type 1 diabetes, AIP shows a relationship to particular human leukocyte antigen (HLA) haplotypes. AIP produces increases in peripheral T cells expressing particular HLA-DR haplotypes (specifically DRB1*0405-DQB1*0401) [22]. Likewise, an HLA association has been demonstrated in cases of SPIDDM including the same DRB1*0405-DQB1*0401 allele [20]. Therefore, we hypothesize that a specific autoimmune phenotype may be very important in the development of the diabetes of AIP.

In this study, we investigated glucose control in a cohort of AIP patients with both preoperative and postoperative glucose values, and we examined the relationship of glucose control to endocrine endowment, intra-islet inflammatory infiltrate, and islet vascularity.

Materials and methods

Selection of cases

A series of 10 AIP cases with available pre- and post-surgical glucose values were selected and evaluated together with cases of chronic pancreatitis, not otherwise specified (NOS) (CP) (n=3) and normal pancreatic tissue (NP) (n=3). NP was selected from pancreatic tissue away from lesional tissue in individuals with pancreatic ductal adenocarcinoma (n=2 cases) and a case of a benign unilocular cyst. None of the CP patients were alcoholic. In all cases, multiple levels of glucose values were obtained for the year prior to and after surgery.

Immunohistochemical analysis

After surgery, sections of the resected pancreatic glands were fixed in 10% phosphate-buffered formalin, embedded in paraffin, sectioned at 5 μm, and stained with hematoxylin and eosin (H&E). A series of immunostains were performed using Ventana-Benchmark automated immunostainers. Primary antibodies included chromogranin, CD3 (T cells), CD20 (B cells), and CD34 (Ventana, Tuscon, AZ, USA) and IgG4 (Zymed, Carlsbad, CA, USA). Intra-islet T and B lymphocytes were enumerated using CD3 and CD20 immunohistochemical stains. CD34 immunohistochemistry was performed on selected AIP and NP cases. IgG4 staining

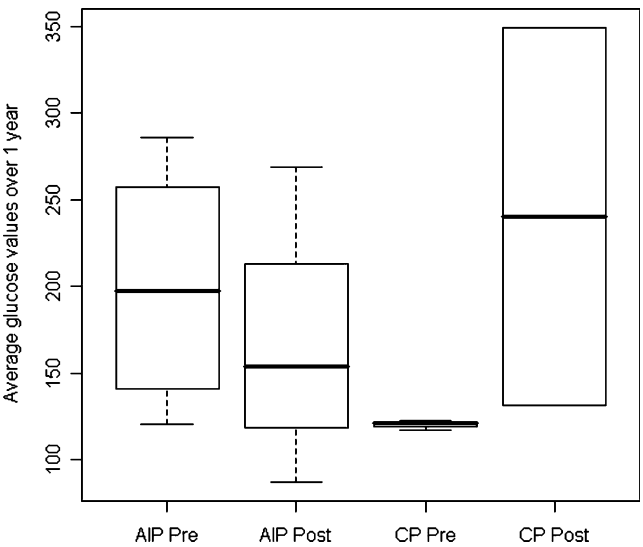

Fig. 1 Glucose values (in milligrams per deciliter) averaged over the 1 year pre- and post-surgery in cases of AIP (n=10) and CP (n=3 for pre-surgery values and 2 for post-surgery values)

was conducted at a 1:50 dilution and scored as the number of IgG4 positive plasma cells per 20× field as previously performed: 0=0, 1=1–5, 2=6–10, 3=11–20, 4=21–30, 5=31–40, 6=41–50, and 7=>50 [1].

Morphometric analysis

Slides were scanned using the Aperio ScanScope® CS system (Aperio Technologies, Vista, CA, USA), and quantitative analyses were performed with the Aperio ImageScope program [23]. The Positive Pixel Count Algorithm was used to count the number of pixels staining with chromogranin and CD34 on an entire slide of pancreatic tissue in at least 10 islet areas per case, and the IHC (ImmunoHistoChemistry) Nuclear Algorithm was used to determine the number of CD3 and CD20 positive cells in at least 10 islets per case [24]. The percent of tissue staining positive for chromogranin in an entire representative section of the most severely involved pancreatic tissue (as measured with the Aperio system) was used as a surrogate marker of endocrine cell endowment.

Statistical analysis

Data collection and preliminary data analysis was performed in Microsoft Excel (Redmond, WA, USA), and more comprehensive statistical analysis was performed using the statistical package R, version 2.6.2 [25].

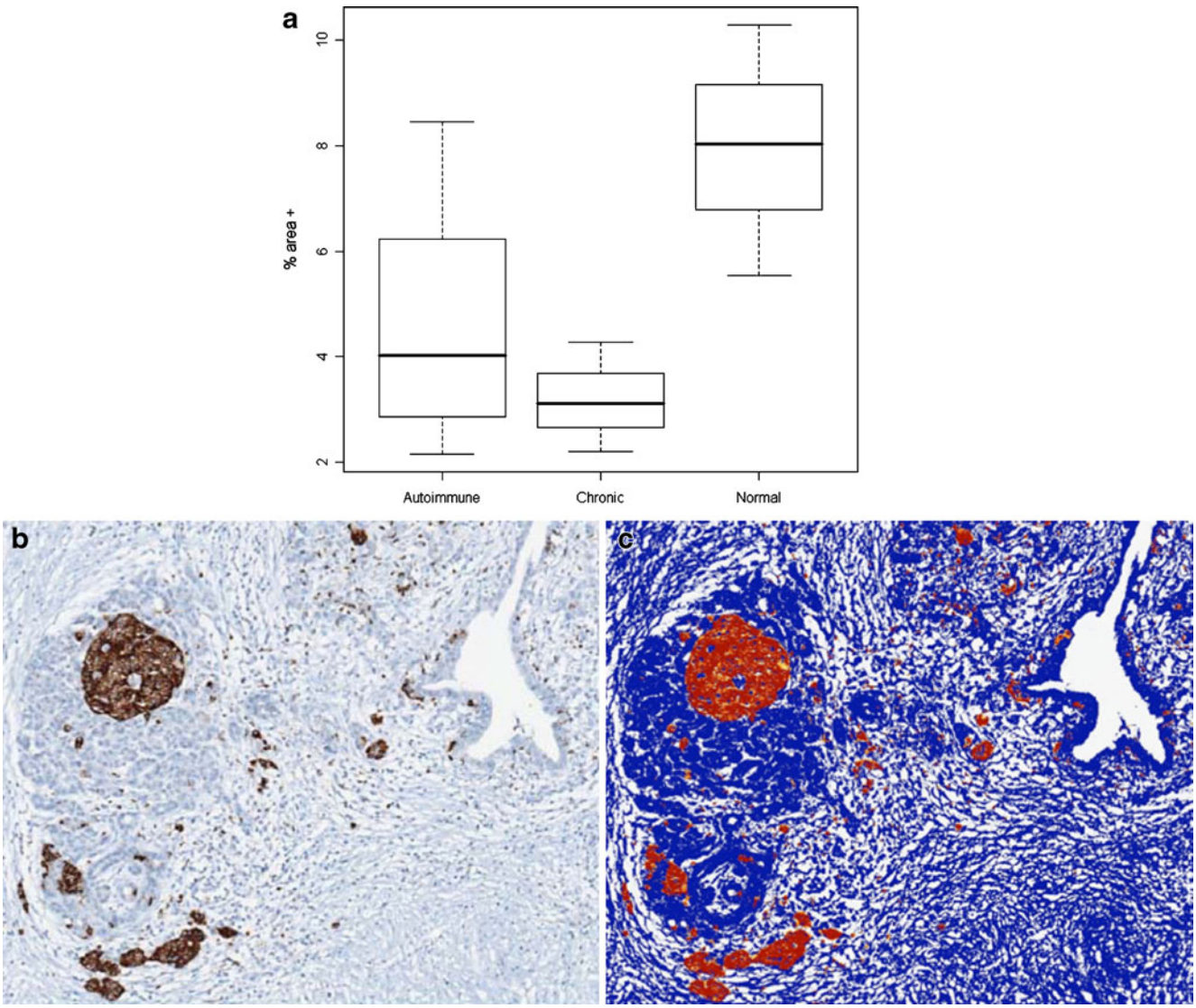

Fig. 2 **a** Percent of pancreatic tissue positive for chromogranin in cases of autoimmune (n=10) and CP (n=3) and normal controls (n=3) and **b** example of chromogranin staining islets and a ductal endocrine cell proliferation and **c** quantitation of tissue positive chromogranin. P=0.02 for the difference between normal and both AIP and CP. The difference between AIP and CP was not statistically significant

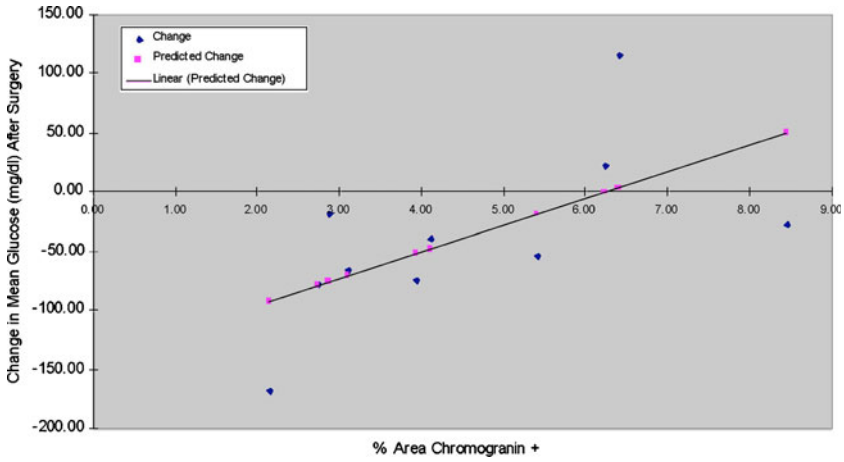

Fig. 3 Linear regression analysis of change in glucose values (in milligrams per deciliter) after surgery and percent of pancreatic tissue staining with chromogranin in cases of AIP (a surrogate marker of endocrine endowment) (n=10, R=0.62, P=0.06)

Results

Cases

A Whipple procedure was performed in all AIP cases. The patients with AIP consisted of six males and four females (average age: 55.4 years; range: 20.6–79.3 years). Comparison was made with tissue from patients with CP (n=3) and normal pancreas (n=3) with average ages of 60.1 and 57.8 years, respectively.

Endocrine endowment and glycemic control

Prior to surgery, the patients with AIP showed, on average, impaired glucose control with an average random glucose value of 200 mg/dl. Comparatively, CP cases showed an average random glucose value of 122 mg/dl for the year prior to surgery. Following surgery, improvement in glycemic control was noted in 8/10 (80%) AIP patients with an average glucose value of 162 mg/dl during the year post surgery, a difference which when compared to pre-operative values approaches statistical significance (P=0.07). In two cases of AIP treated with corticosteroids before and after surgery, glycemic control also improved after surgery. Post-surgery glucose data were not available for one CP patient, but both of the CP cases with both pre- and post-surgery glucose values showed worsened glycemic control following surgery with an average glucose value of 241 mg/dl (Fig. 1).

A decrease in the percent of pancreatic parenchyma composed of endocrine cells was documented in both AIP (4.54%) and CP cases (3.20%) compared to normal (7.95%), and the decreases in both were statistically significant (P=0.02 for both). However, the difference of the percent of pancreatic parenchyma staining with chromogranin in AIP and CP was not statistically significant (Fig. 2). Notably, part of the AIP endocrine component was accounted for by a ductular endocrine cell proliferation. The density of ductular endocrine cell proliferations was determined for AIP, CP, and normal. AIP had 0.15 foci of ductular endocrine proliferations per square millimeter, and CP and normal had 0.07 and 0.09, respectively. The difference between the values for each of these groups was not statistically significant. Regression analysis suggested a correlation between less pre-operative endocrine endowment and greater postoperative improvement in glycemic control (i.e., decreased average glucose values) in AIP cases (R=0.62, P=0.06) (Fig. 3).

Islet morphology and inflammatory infiltrate

Compared to controls, the islets in AIP were smaller, disrupted, and infiltrated by inflammatory cells (Fig. 4)

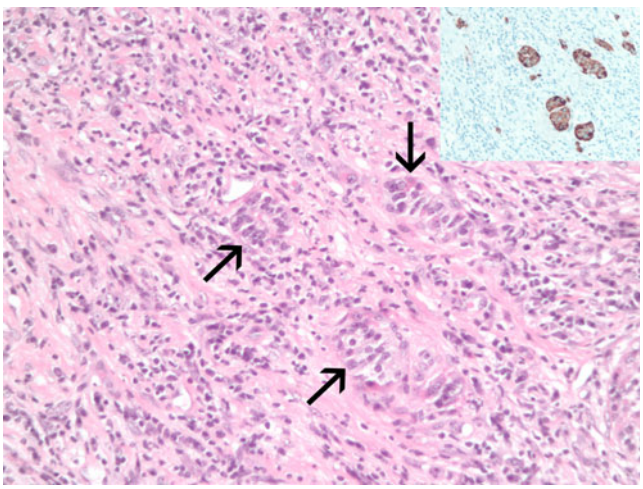

Fig. 4 Routine histology of islets disrupted (*arrows*) by inflammation in AIP (hematoxylin and eosin). The *inset* shows the corresponding area stained with chromogranin immunohistochemistry, confirming that these are small, disrupted islets

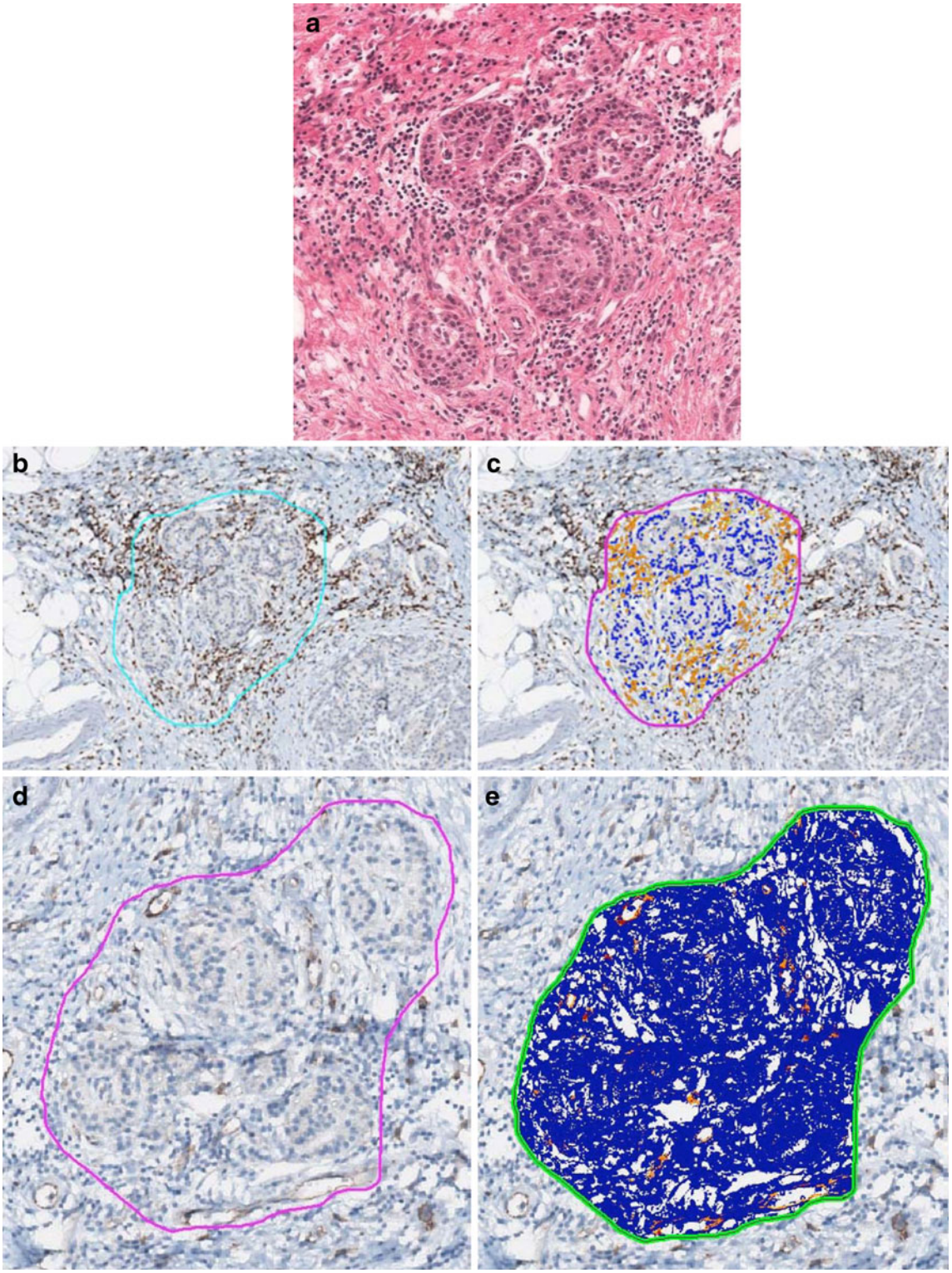

Fig. 5 Illustration of algorithm used to quantitate immunohistochemistry of an islet **a** on hematoxylin and eosin using a **b** CD3 stain **c** with CD3 + cells quantitated and **d** CD34 stain **e** with CD34 + pixels highlighted

Although the islets were disrupted, there was no evidence of necrosis or apoptosis of islet cells. The inflammatory infiltrate was composed of CD3 + T cells (Figs. 5 and 6), which predominated over CD20 + B cells. Furthermore, CD20 + cells were principally present in follicles outside of the islets, whereas CD3 + cells were present throughout the pancreatic parenchyma, including islets (Fig. 5). When compared to CP, AIP islets presented with the highest

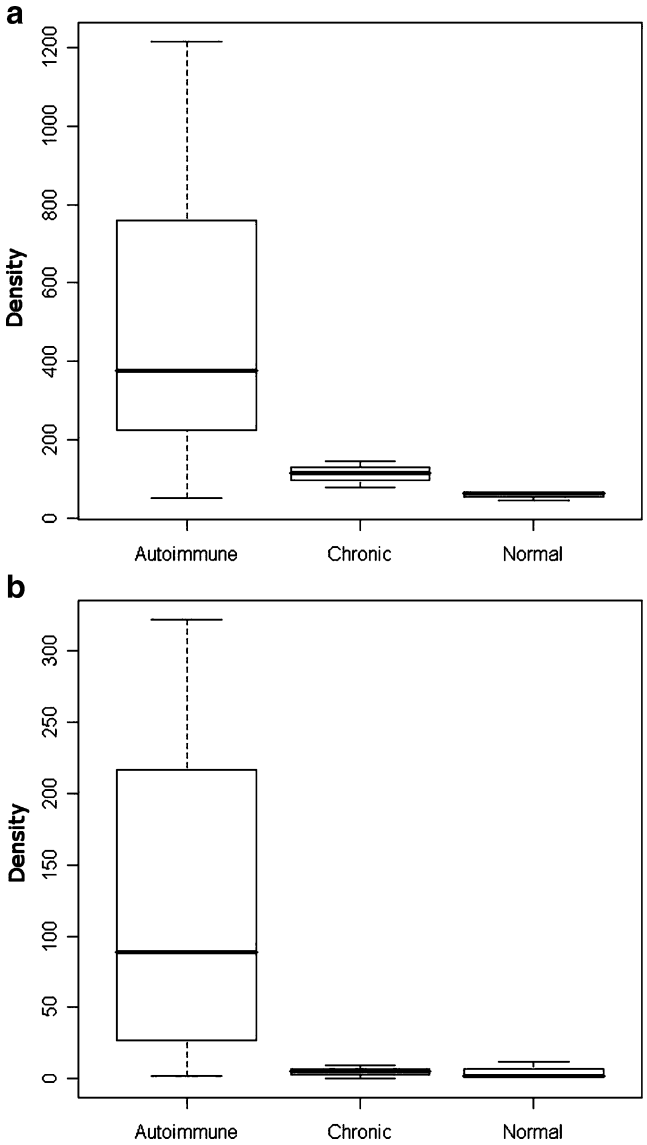

Fig. 6 Density (# of cells/mm^2) of intra-islet CD3 and CD20 cells in cases of AIP (n=10), CP (n=3), and normal controls (n=3) [P<0.05 for CD3 (between all groups), and for CD20 (only approaching significance for AIP vs CP and normal [P=0.05 and 0.06, respectively])] **a** CD3. **b** CD20

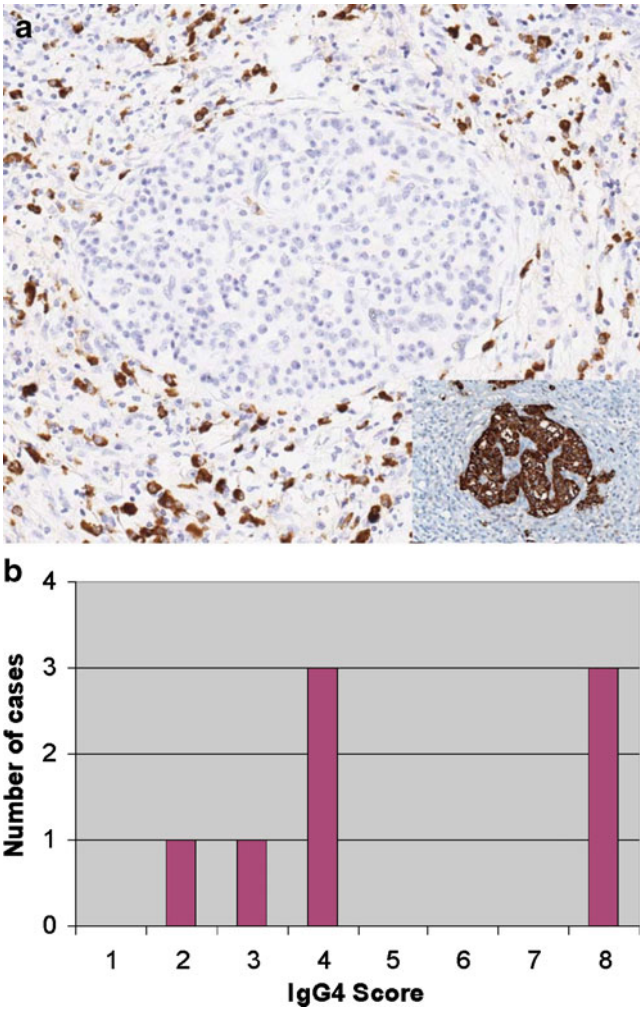

Fig. 7 **a** Islet highlighted with chromogranin (*inset*) and accompanying islet with IgG4 immunohistochemical stain and **b** Scoring of IgG4 staining (0=0 IgG4 positive plasma cells per 20× field; 0=0, 1=1−5, 2=6−10, 3=11−20, 4=21−30, 5=31−40, 6=41−50, and 7=>50)

density of infiltrating CD3 and CD20 inflammatory cells (Fig. 6) The difference between the density of CD3 positive cells between all groups was statistically significant (P< 0.05); however, the difference between CD20 positive cells in AIP, CP, and the normal groups only approached statistical significance for AIP vs the CP and normal groups (P=0.05 and 0.06, respectively).

Eight cases stained with IgG4 showed diffusely infiltrative IgG4 stained plasma cells throughout the pancreas. Seven cases showed at least greater than five positive plasma cells per 20× field, and three cases showed greater than 50 positive plasma cells per 20× field. Notably, IgG4-positive plasma cells surrounded but did not infiltrate the islets (Fig. 7).

Islet vascularity

Quantitative analysis of CD34 stained intra-islet microvasculature performed on selected cases of AIP (n=6) and normal pancreas (n=2) showed an overall decrease in intra-islet vascularity in AIP compared to normal (Fig. 8).

Discussion

In this study, impaired glycemic control was noted preoperatively in all 10 AIP cases. Impaired preoperative glycemic control was noted in two CP cases. Furthermore, in AIP cases, paradoxical glycemic control improvements were noted after surgery, whereas in CP cases, improve-

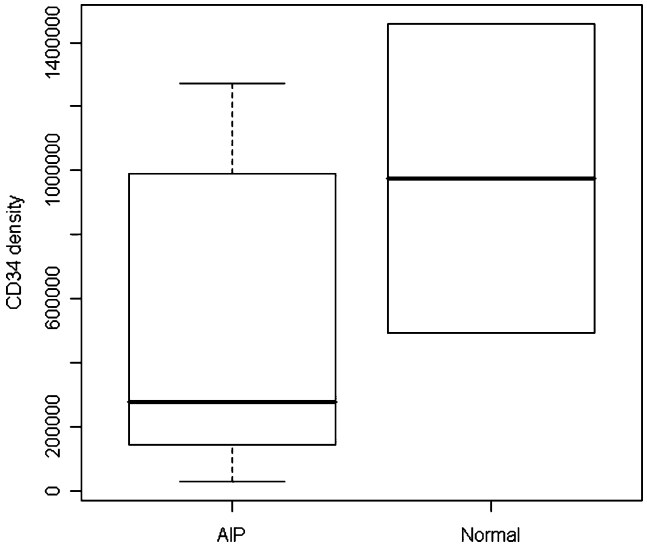

Fig. 8 Density of intra-islet CD34 positivity per unit area (measured in positive pixels per unit area [mm^2]) in cases of AIP (n=6) and **NP** (n=2) (P=0.05)

ments were not seen. Endocrine endowment in AIP cases was decreased from normal, similar to the decrease seen in CP. Preservation of the majority of the islets in AIP despite a prominent islet inflammatory infiltrate and endocrine cell neogenesis may help explain how these individuals normalize their blood glucose levels following surgery. Corticosteroids, which typically worsen glycemic control, were used in two cases of AIP, yielding a paradoxical improvement in glycemic control. Regression analysis (Fig. 3) showed more substantial improvements of glycemic control in AIP cases having lesser endocrine endowments. Significantly, individuals with the highest preoperative endocrine cell endowment did not achieve glycemic control. Paradoxical glycemic control improvement has been observed in other series of pancreatectomies [14–17]. In a series of CP, glucose tolerance improved after pancreatic head resection despite decreased insulin secretion, although improvements were transient [26]. Paradoxical improvements after surgery are somewhat difficult to explain. Possible mechanisms for the improvement in glycemic control following surgery observed include: (1) removal of the inflammatory cell nidus (following a pancreatoduodenectomy) and possible aberrant cytokine signals leading to suppression of insulin production and (2) alleviation of inflammatory and edematous duct and islet compression, allowing restoration of both endocrine and exocrine function.

Our cases typically involved quantitation of the pancreatic head endocrine endowment, and it has been shown that islet density varies within the pancreas. Islets were typically thought to be more frequent in the pancreatic tail in past studies [27, 28], although other investigations have suggested that endocrine mass is higher in the ventrally derived posterior head than the dorsal pancreas [29, 30]. However, since this study relies on a direct comparison of cases that were typically sampled from the head of the pancreas after Whipple surgeries, then relationships can likely be drawn in a meaningful manner.

As in prior studies, immunohistochemical stains do confirm inflammatory involvement of the islets in AIP [16, 17]. Quantitative immunohistochemical analysis shows that CD3 + T cells predominate over CD20 + B cells in AIP, confirming prior studies [17]. IgG4 immunohistochemistry demonstrated that a larger density of positive plasma cells were present in all cases of AIP. These IgG4 plasma cells usually did not infiltrate the islets. Although a regression analysis did not show a direct relationship between the density of CD3 cells and change in glucose values, the inflammatory intra-islet milieu is likely more complex than this simple relationship, and it is likely that other inflammatory mediators play a role.

One putative explanation for the paradoxical improvement in AIP is that the remaining pancreatic tissue is able to better compensate in the absence of inflammation, possibly through the reduction of detrimental cytokine signals. Animal models have given some insight into possible etiologies of AIP, suggesting involvement of cytokine and other molecular mediators in the pathogenesis of AIP, some of which produce involvement of the islets and some of which do not [18, 21, 31–34]. The diabetogenic effects seen in AIP could be due to aberrant regulation of the islets by T cells, restored through treatment with corticosteroids or pancreatectomy. Our study confirms, in a quantitative manner, the inflammatory involvement of the islets by T-cells demonstrated in prior studies [7, 14, 15, 35]. CD4 + and CD8 + T cell insulitis leading to β cell destruction, as well as autoantibodies against islet cells, are known to be important processes in type 1 diabetes. Inflammatory mediators such as interferon gamma (IFN-γ), tumor necrosis factor (TNF), interleukin-1 (IL-1), and IL-2 are also thought to be important in this process [9, 20, 21, 36, 37]. Similar mediators could play a role in the insulitis seen in AIP.

Alterations to pancreatic vasculature, accompanied by inflammation and edema, could be an explanation for impaired AIP endocrine and exocrine function. Although not universal, most of our AIP cases showed decreased islet vascularity. Angiogenesis mediators, produced as a result of inflammation, may in part explain the alterations in intra-islet vascularity. Interestingly, obliterative phlebitis is an almost universal finding in AIP.

In conclusion, we reaffirm paradoxical improvements in glycemic control following surgical resection in AIP. Despite intra-islet T-cell infiltrates, the majority of the islets are preserved and, in conjunction with the endocrine cell neogenesis and islet preservation, may in some measure explain the paradoxical behavior of glycemic levels in AIP. IgG4-positive plasma cells were present, often at a high

density, in cases of AIP; however, the IgG4 cells often did not infiltrate the islets, suggesting that IgG4-positive cells do not directly contribute to the decreased endocrine cell endowment in AIP. Overall, interplay between inflammatory cells and pancreatic endocrine and exocrine function is complex, and further studies evaluating the role of cytokines, the effects of various inflammatory cell subsets, and other such mechanisms may help elucidate the pathogenesis of the diabetogenic effect of AIP.

Acknowledgements The authors would like to acknowledge the laboratory assistance of the James Homer Wright Pathology Laboratories of the Massachusetts General Hospital. The authors have no disclosures or conflicts of interest.

References

1. Deshpande V, Chicano S, Finkelberg D et al (2006) Autoimmune pancreatitis: a systemic immune complex mediated disease. Am J Surg Pathol 30:1537
2. Deshpande V, Mino-Kenudson M, Brugge W et al (2005) Autoimmune pancreatitis: more than just a pancreatic disease? A contemporary review of its pathology. Arch Pathol Lab Med 129:1148
3. Sarles H, Sarles JC, Camatte R et al (1965) Observations on 205 confirmed cases of acute pancreatitis, recurring pancreatitis, and chronic pancreatitis. Gut 6:545
4. Sarles H, Sarles JC, Muratore R et al (1961) Chronic inflammatory sclerosis of the pancreas—an autonomous pancreatic disease? Am J Dig Dis 6:688
5. Hamano H, Kawa S, Horiuchi A et al (2001) High serum IgG4 concentrations in patients with sclerosing pancreatitis. N Engl J Med 344:732
6. Deshpande V, Mino-Kenudson M, Brugge WR et al (2005) Endoscopic ultrasound guided fine needle aspiration biopsy of autoimmune pancreatitis: diagnostic criteria and pitfalls. Am J Surg Pathol 29:1464
7. Mino-Kenudson M, Lauwers GY (2005) Histopathology of autoimmune pancreatitis: recognized features and unsolved issues. Journal of Gastrointestinal Surgery: Official Journal of the Society for Surgery of the Alimentary Tract 9:6
8. Notohara K, Burgart LJ, Yadav D et al (2003) Idiopathic chronic pancreatitis with periductal lymphoplasmacytic infiltration: clinicopathologic features of 35 cases. Am J Surg Pathol 27:1119–1127
9. Kloppel G, Sipos B, Zamboni G et al (2007) Autoimmune pancreatitis: histo- and immunopathological features. J Gastroenterol 42(Suppl 18):28–31
10. Zamboni G, Luttges J, Capelli P et al (2004) Histopathological features of diagnostic and clinical relevance in autoimmune pancreatitis: a study on 53 resection specimens and 9 biopsy specimens. Virchows Arch 445:552–563
11. Zhang L, Notohara K, Levy MJ et al (2007) IgG4-positive plasma cell infiltration in the diagnosis of autoimmune pancreatitis. Mod Pathol 20:23–28
12. Kojima M, Sipos B, Klapper W et al (2007) Autoimmune pancreatitis: frequency, IgG4 expression, and clonality of T and B cells. Am J Surg Pathol 31:521–528
13. Cornell LD, Chicano SL, Deshpande V et al (2007) Pseudotumors due to IgG4 immune-complex tubulointerstitial nephritis associated with autoimmune pancreatocentric disease. Am J Surg Pathol 31:1586
14. Ketikoglou IG, Elefsiniotis IS, Vezali EV et al (2004) Diabetes mellitus responsive to corticosteroids in autoimmune pancreatitis. J Clin Gastroenterol 38:910
15. Tanaka S, Kobayashi T (2002) Diabetes mellitus associated with autoimmune pancreatitis. Nippon Rinsho Japanese Journal of Clinical Medicine 60(Suppl 9):821
16. Tanaka S, Kobayashi T, Nakanishi K et al (2000) Corticosteroid-responsive diabetes mellitus associated with autoimmune pancreatitis. Lancet 356:910
17. Tanaka S, Kobayashi T, Nakanishi K et al (2002) Corticosteroid-responsive diabetes mellitus associated with autoimmune pancreatitis: pathological examinations of the endocrine and exocrine pancreas. Ann NY Acad Sci 958:152
18. Davidson TS, Longnecker DS, Hickey WF (2005) An experimental model of autoimmune pancreatitis in the rat. Am J Pathol 166:729
19. Graber I, Chavaillon A, Pilleul F et al (2006) Autoimmune pancreatitis: beneficial effects of corticosteroid therapy on biliary and metabolic complications. Gastroentérol Clin Biol 30:911
20. Kobayashi T, Tanaka S, Harii N et al (2006) Immunopathological and genetic features in slowly progressive insulin-dependent diabetes mellitus and latent autoimmune diabetes in adults. Ann NY Acad Sci 1079:60
21. Okazaki K, Uchida K, Ohana M et al (2000) Autoimmune-related pancreatitis is associated with autoantibodies and a Th1/Th2-type cellular immune response. Gastroenterology 118:573
22. Toomey DP, Swan N, Torreggiani W et al (2007) Autoimmune pancreatitis. Br J Surg 94:1067
23. Aperio Technologies (2009) Image Analysis|Aperio. Aperio Technologies, Vista, CA
24. Aperio Technologies (2009) Aperio|Support|Documentation. Aperio Technologies, Vista, CA
25. Team RDC (2006) R: A Language and Environment for Statistical Computing. R Foundation for Statistical Computing, Vienna
26. Menge BA, Schrader H, Breuer TG et al (2009) Metabolic consequences of a 50% partial pancreatectomy in humans. Diabetologia 52:306–317
27. Kloppel G, Gepts W, In't Veld PA (1992) Morphology of the Pancreas in Normal and Diabetic States. In: Alberti KGMM, DeFronzo RA, Keen H, Zimmet P (eds) International Textbook of Diabetes Mellitus. Wiley, New York, pp 224–259
28. Lazarus SS, Volk BW (1962) The pancreas in human and experimental diabetes. Grune and Stratton, New York
29. Rahier J, Goebbels RM, Henquin JC (1983) Cellular composition of the human diabetic pancreas. Diabetologia 24:366–371
30. Stefan Y, Orci L, Malaisse-Lagae F et al (1982) Quantitation of endocrine cell content in the pancreas of nondiabetic and diabetic humans. Diabetes 31:694–700
31. Aleksic T, Baumann B, Wagner M et al (2007) Cellular immune reaction in the pancreas is induced by constitutively active IkappaB kinase-2. Gut 56:227
32. Hahm KB, Im YH, Lee C et al (2000) Loss of TGF-beta signaling contributes to autoimmune pancreatitis. J Clin Investig 105:1057
33. Qu WM, Miyazaki T, Terada M et al (2002) A novel autoimmune pancreatitis model in MRL mice treated with polyinosinic: polycytidylic acid. Clin Exp Immunol 129:27
34. Uchida K, Okazaki KANT, Uose S et al (2002) Experimental immune-mediated pancreatitis in neonatally thymectomized mice immunized with carbonic anhydrase II and lactoferrin Laboratory investigation. Journal of Technical Methods and Pathology 82:411
35. Kamisawa T, Yoshiike M, Egawa N et al (2005) Treating patients with autoimmune pancreatitis: results from a long-term follow-up study. Pancreatology: Official Journal of the International Association of Pancreatology (IAP) 5:234
36. Abbas AK, Lichtman AH, Pillai S (2007) Cellular and molecular immunology. Saunders, Philadelphia
37. Eisenbarth GS (2007) Update in type 1 diabetes. J Clin Endocrinol Metab 92:2403

Virchows Arch (2010) 457:337–345
DOI 10.1007/s00428-010-0950-4

ORIGINAL ARTICLE

Myoepithelial carcinoma of the breast: a clinicopathological and immunohistochemical study of 15 diagnostically challenging cases

Natalia Buza · Nazila Zekry · Colette Charpin · Fattaneh A. Tavassoli

Received: 24 March 2010 / Revised: 14 June 2010 / Accepted: 7 July 2010 / Published online: 24 July 2010
© Springer-Verlag 2010

Abstract Myoepithelial carcinoma (MEC) is a rare type of breast cancer composed purely of myoepithelial cells. Most often it presents with a spindle cell morphology that can mimic several benign and malignant lesions and may be misdiagnosed by the pathologist. We report 15 cases of MEC, which were sent to our consultation practice: Five of them were initially diagnosed as benign. The patients, all female, ranged from 45 to 86 years in age (mean 69.5) and—with one exception—presented with a breast mass. The tumor size measured between 1 and 4.8 cm (mean 2.6 cm). Microscopically, the tumors had infiltrative growth pattern most frequently with thin anastomosing cords of tumor cells associated with an intimately admixed reactive spindle cell stroma. The neoplastic myoepithelial cells were emanating from the myoepithelial cell layer of entrapped ductules in every case. The nuclei showed mild to moderate pleomorphism, and the mitotic activity ranged from 0 to 9/10 high power field. Immunohistochemical stains for p63, CD10, CK903, and CK5/6 reacted strongly and diffusely with the tumor cells, and mainly the reactive stroma had weak positivity for calponin, S-100, and smooth muscle actin. Estrogen receptor, progesteron receptor, and Her2 immunostains were negative, but strong epidermal growth factor receptor expression was observed. Follow-up was available for seven patients: All of them were alive at last contact; one patient had local recurrence, and one developed pulmonary metastases. MEC is a potentially aggressive malignant neoplasm sharing many features with metaplastic carcinomas. Morphologically, it is often difficult to distinguish it from benign spindle cell proliferations.

Keywords Myoepithelial carcinoma · Breast · Spindle cell proliferation · Metaplastic carcinoma

N. Buza (✉) · F. A. Tavassoli
Department of Pathology, Yale University School of Medicine,
PO Box 208023, New Haven, CT 06520, USA
e-mail: natalia.buza@yale.edu

N. Zekry
Newport Harbor Pathology Medical Group Inc, Hoag Hospital,
Newport Beach, CA, USA

C. Charpin
Pathology Department, School of Medicine,
University of Aix-Marseille II,
Marseille, France

Introduction

Myoepithelial carcinoma (MEC; malignant myoepithelioma) of the breast is a rare malignant neoplasm composed entirely of myoepithelial cells with predominantly spindle cell morphology [1, 2]. It represents the malignant end of the spectrum of myoepithelial lesions in the breast, and it may arise de novo or in a preexisting benign adenomyoepithelioma [1]. Due to its rarity and deceptive morphologic features, the diagnosis of MEC is often a difficult one, especially for the general pathologist. Several benign and malignant lesions may mimic its microscopic appearance, and certain similarities and overlaps with other groups of breast carcinomas (metaplastic spindle cell adenocarcinoma or spindle cell squamous carcinoma) can make the terminology and classification somewhat confusing. In addition, due to the small number of cases presented in the literature, there is still relatively little known about the clinical course and prognosis of MECs.

Fifteen MECs, which were a major diagnostic dilemma for the primary pathologist and were sent to us for a second opinion, are reported. The microscopic and immunohistochemical features of these cases are described in detail, and

treatment and follow-up information is provided along with a discussion of the differential diagnosis and potential diagnostic pitfalls. The discussion will also focus on predictive markers (hormone receptors, Her2, EGFR) and basal-like breast carcinomas, incorporating recent immunohistochemical markers and molecular genetics of breast carcinomas.

Materials and methods

The study was approved by the Institutional Review Board at Yale University. During a 6-year period between 2004 and 2010, 15 cases of MEC of the breast were identified in the personal consultation files of one of the authors (F.T.). All hematoxylin and eosin (H&E) slides were reviewed along with the available clinical information. To qualify as a MEC, emanation of the spindled tumor cells from the myoepithelial cell layer of ducts within or at the periphery of the lesion was required. The immunohistochemical markers that were used to aid and confirm the diagnosis included p63, CD10, calponin, S-100, alpha smooth muscle actin (SMA), cytokeratin (CK) 903 (a cocktail of CK1, 5, 10, 14), and CK5/6. Estrogen receptor (ER), progesteron receptor (PR), Her2, and epidermal growth factor receptor (EGFR) immunostains were performed in 12 cases. The source of antibodies used and the immunohistochemical methods are summarized in Table 1. Her2 and EGFR immunostains were performed per kit instructions. For all immunostains, Dako EnVision detection system and Dako Autostainer were used. Appropriate positive and negative controls were performed with each case.

Results

Clinical features

All patients were female between 45 and 86 years of age (mean 69.5 years). Fourteen patients presented with a breast mass, one patient had bilateral breast hypertrophy, and the tumor was an incidental finding in the breast reduction specimen. Nine tumors were located in the left, and six tumors in the right breast. Two patients had prior history of hormone replacement therapy. One patient had family history of breast cancer. The clinical data, including treatment and follow-up, are presented in Table 2.

Macroscopic features

The diagnostic specimen was a lumpectomy/partial mastectomy in ten cases, mastectomy in three cases, mammotome biopsy in one case, and reduction mammoplasty in one patient. The tumor size was known in 14 cases, and it ranged from 1.0 to 4.8 cm (mean 2.6 cm). In the majority of cases, the gross examination revealed an ill-defined, firm, tan, white, or gray mass in the breast parenchyma (Fig. 1). Four of the tumors appeared well circumscribed macroscopically. One tumor presented as a 3.5-cm cyst with a 1.7-cm intracystic solid nodule.

Microscopic and immunohistochemical characteristics

On microscopic examination, 12 tumors were purely composed of myoepithelial cells, while three tumors originated in adenomyoepithelioma (Fig. 2). All tumors had an infiltrative growth pattern—at least focally—with thin anastomosing cords or nests of tumor cells intimately admixed with a reactive spindle cell stroma. Four of 15 cases—including three tumors arising in adenomyoepitheliomas—were predominantly circumscribed microscopically, with only focal infiltrative growth. The invasive tumor often proliferated around normal ducts and lobules incorporating them into the lesion. In some of the cases, the tumor cells were arranged in a storiform pattern with thick collagen bands between them. One tumor showed a pseudo-angiomatous pattern, reminiscent of an angiosarcoma. Necrosis and hemorrhage were uncommon features: Two tumors had small

Table 1 Immunohistochemical methods

Antibody	Source	Clone	Dilution	Antigen retrieval
P63	Dako	4A4	1:2,400	Low pH, steam
CD10	Vector	56C6	1:80	High pH, steam
Calponin	Dako	CALP	1:1,000	Low pH
S-100	Dako	Poly	1:8 prediluted	None
SMA	Dako	IA4	Prediluted	None
CK903	Dako	34βE12	1:50	Low pH, steam
CK5/6	Dako	D5/16B4	1:160	High pH, steam
ER	Dako	1D5	Prediluted	Low pH, steam
PR	Dako	PGR636	Prediluted	Low pH, steam
Her-2	Dako HercepTest Kit	NA	NA	Waterbath
EGFR	Dako PharmDx Kit	NA	NA	Protease

SMA smooth muscle actin, *ER* estrogen receptor, *PR* progesteron receptor, *NA* not applicable

Table 2 Clinical data

No.	Age at dg (years)	Specimen type	Family history	Past medical history	Side	Clinical presentation	Size (cm)	Treatment	Axillary LNs	TNM stage	Follow-up (months)	Outcome
1	78	Lumpect	na	na	L	Mass	1.5	Lumpect	ND	pT1cNx	3	NED
2	45	Breast reduction	na	na	L	Bilateral hypertrophy	1	Breast reduction	ND	pT1bNx	na	na
3	55	Lumpect	Yes	On HRT	R	Palpable mass	na	Lumpect, rad	ND	na	20	NED
4	56	Lumpect	No	On HRT, 4 years prior bx: myofibroblastic proliferation	R	Mass on mammography	2	Lumpect, chemo-rad	ND	pT1cNx	8	AWD
5	81	Lumpect	na	na	L	Mass	2.8	Lumpect, chemo	ND	pT2Nx	12	NED
6	64	Mastectomy	na	na	L	Mass	3.8	Mastectomy, ALND	Neg (0/16)	pT2N0	10	NED
7	73	Lumpect	na	Prior bx: phyllodes tumor	R	Palpable mass	2.5	Lumpect	ND	pT2Nx	3	NED
8	59	Mastectomy	na	na	L	Mass	3.5	Mastectomy, ALND	Neg (0/10)	pT2N0	na	na
9	77	Lumpect	na	na	L	Mass	3.5	Lumpect	ND	pT2Nx	na	na
10	64	Lumpect	na	na	R	Mass	1.5	Lumpect, re-excision	ND	pT1cNx	na	na
11	72	Mammotome bx	na	na	R	Mass	2.4	Mastectomy, SLN	Neg (0/4)	pT2N0	na	na
12	76	Lumpect	na	na	L	Mass	3	Lumpect, Re-excision	ND	pT2Nx	31	AWD

Dg diagnosis, *Lumpect* lumpectomy, *bx* biopsy, *na* not available, *HRT* hormone replacement therapy, *L* left, *R* right, *chemo* chemotherapy, *Rad* radiation, *ALND* axillary lymph node dissection, *SLN* sentinel lymph node, *LN* lymph node, *Neg* negative, *ND* not done, *NED* no evidence of disease, *AWD* alive with disease

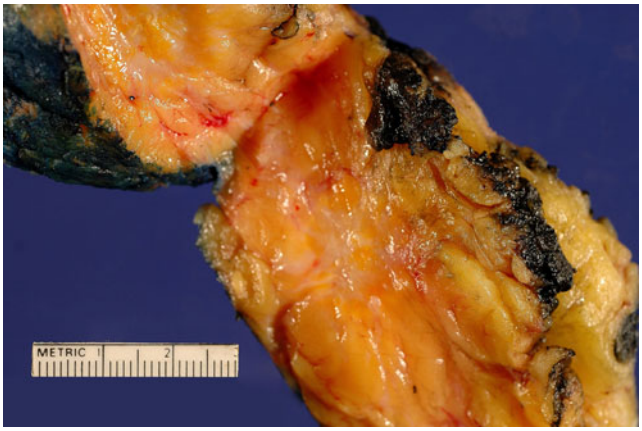

Fig. 1 Gross image of a myoepithelial carcinoma: Most tumors appear as ill-defined, firm, tan-white, or gray masses in the breast parenchyma

foci of necrosis, and three exhibited areas of hemorrhage, in one of which it was associated with the biopsy site. None of the cases had intratumoral calcifications. The tumor cells varied from spindle to ovoid to occasionally round and epithelioid in configuration; the cytoplasm was frequently indistinct. In some cases, the cytoplasm was vacuolated, and the cells closely resembled normal, non-neoplastic myoepithelial cells. There was morphologic evidence in all tumors—at least focally—that the neoplastic myoepithelial cells were emanating from the myoepithelial cell layer of entrapped ductules, often those located at the periphery of the tumor (Fig. 3a–d). In one case, the tumor cells appeared to form lumens as they emanated from the ME cell layer, but this feature was lost as the invasive cells extended into the surrounding stroma (Fig. 3d). The nuclei showed moderate pleomorphism in most cases, one tumor had areas with marked nuclear atypia. The number of mitotic figures ranged from 0 to 9/10 high power field (HPF), with five mitoses or less per ten HPF in eleven of the tumors. Two tumors showed focal squamous differentiation, in one of which it was associated with the biopsy site. The former displayed a squamous morule just as the tumor cells emanated from the myoepithelial cell layer (Fig. 2e). True glandular differentiation or heterologous mesenchymal components were not seen in any of the tumors. In several cases, a prominent lobular lymphocytic infiltrate was evident in the lobules entrapped in the lesion and those in the surrounding uninvolved breast tissue.

Various combinations of epithelial and myoepithelial markers were utilized to confirm the diagnosis. Among these, p63, CD10, CK903, and CK5/6 immunoreacted strongly and diffusely with the tumor cells in most cases; hence, they appeared to be the most helpful markers (Fig. 3c–e). Calponin, S-100, and SMA immunostains were only performed on three cases, in which the reactive stromal cells were weakly and focally to diffusely positive while the tumor cells were non-reactive. Twelve cases were evaluated for hormone receptors and Her2 status by immunohistochemistry: All of them were triple negative. EGFR, performed on 12 cases, was strongly (3+) expressed in 11 tumors (Fig. 3f), and one case showed weaker (2+) expression.

Other lesions found in association with the tumors included ductal intraepithelial neoplasia 1 (DIN 1; atypical intraductal hyperplasia and ductal carcinoma in situ, grade 1), low-risk DIN (intraductal hyperplasia), atypical papilloma, and prominent lymphocytic lobulitis.

The wide range of original diagnoses prior to consultation clearly demonstrates the diagnostic challenge these tumors often pose: Five cases were initially diagnosed as benign—adenomyoepithelioma, inflammatory myofibroblastic tumor, radial scar, atypical complex sclerosing lesion. Five cases had a general, descriptive preliminary diagnosis (poorly differentiated infiltrative neoplasm, spindle cell neoplasm, malignant neoplasm with spindle cell component, malignant spindle cell neoplasm, spindle cell stromal proliferation), one lesion was called phyllodes tumor, and two tumors were diagnosed as metaplastic carcinoma. There was only one case in which the initial diagnosis of MEC arising in an adenomyoepithelioma was confirmed on consultation.

The original diagnoses, microscopic features, and results of hormone receptor, Her2, and EGFR studies are summarized in Table 3.

Treatment and follow-up

Seven patients were treated with lumpectomy alone. One patient received radiation following lumpectomy, one patient underwent lumpectomy and chemotherapy, and one patient had a combination of lumpectomy, radiation, and chemotherapy. Four patients underwent mastectomy, three of which were combined with axillary lymph node dissection and one with sentinel lymph node biopsy. In these four cases, all lymph nodes were negative for carcinoma. One patient had reduction mammoplasty as the initial procedure and was lost to follow-up thereafter. Follow-up was available for seven patients, and it ranged from 3 to 31 months (mean 12.4 months). All patients were alive at last contact—five of them had no evidence of disease, one patient had local recurrence 19 months after the initial diagnosis, and one patient developed pulmonary metastases within 8 months of the diagnosis (Table 2).

Discussion

Myoepithelial cells in the breast form a discontinuous outer cell layer between the luminal epithelial cells and the

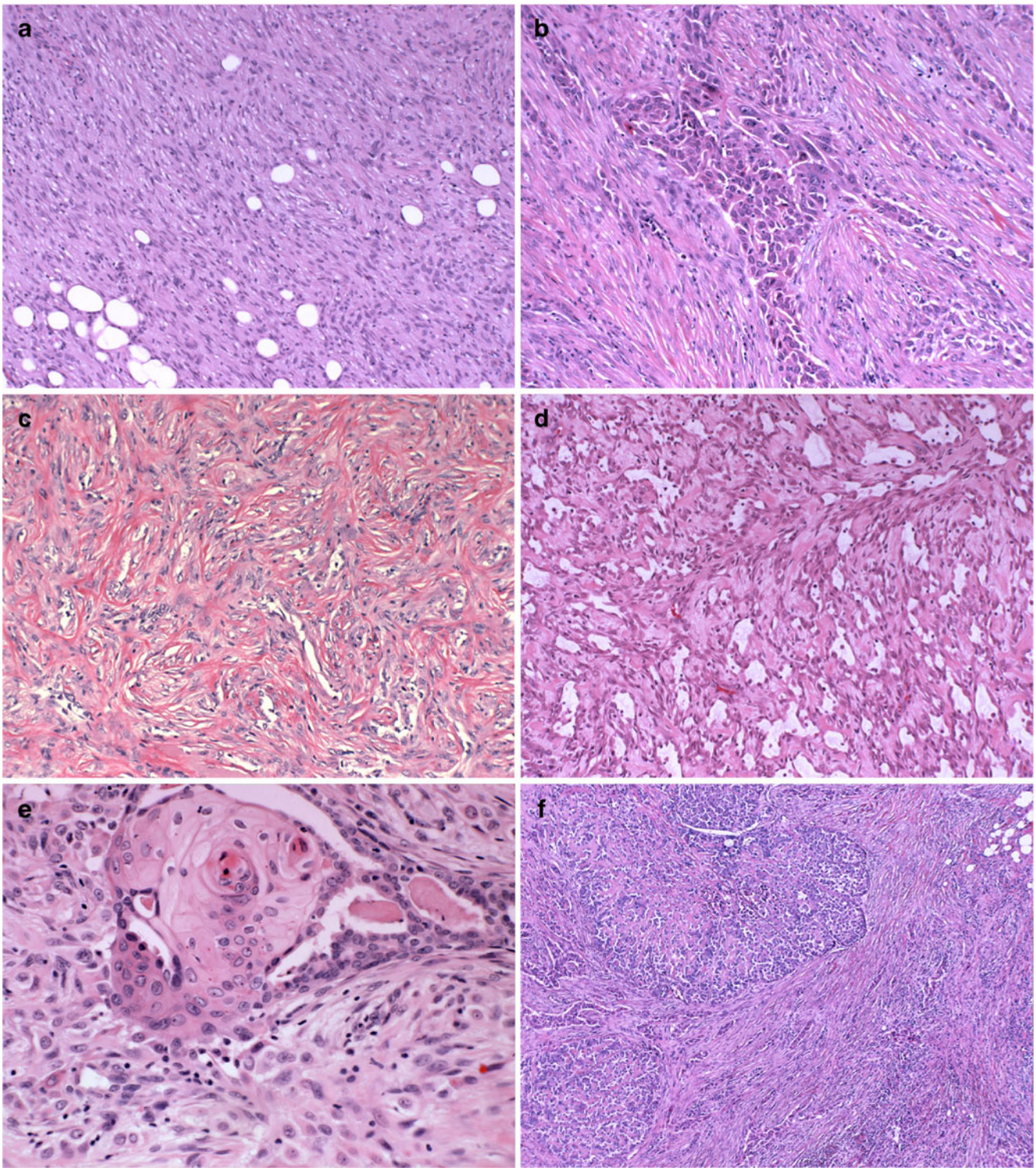

Fig. 2 a–f H&E stain. Myoepithelial carcinoma may assume several different microscopic morphological patterns. The most common pattern in our series was the fascicular arrangement of spindled tumor cells (**a**); less commonly we encountered epithelioid (**b**), storiform (**c**), and pseudoangiomatous (**d**) morphology. Focal squamous differentiation was seen in two cases (**e**), and three tumors were arising in an adenomyoepithelioma (**f**)

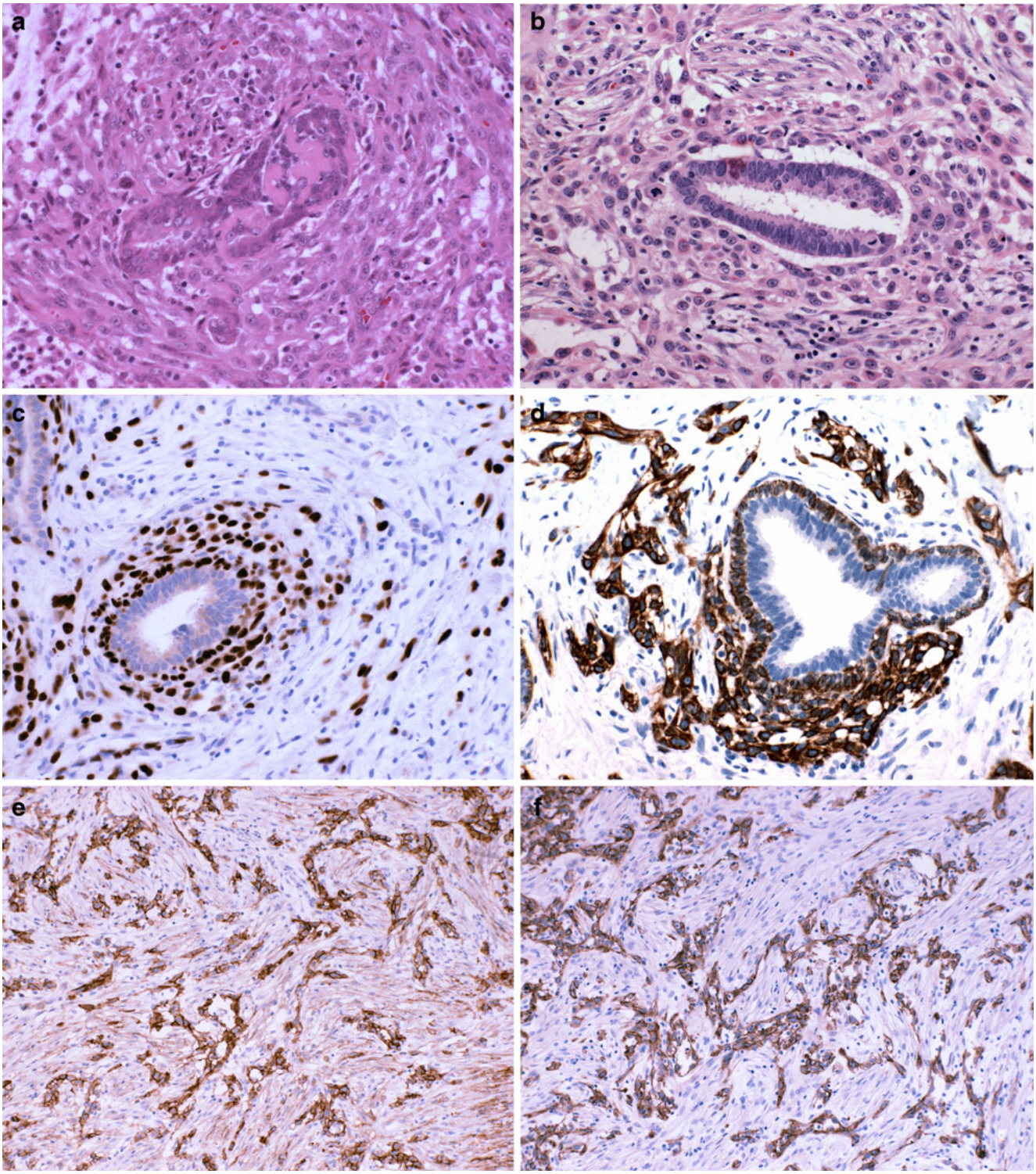

Fig. 3 Characteristically, the neoplastic myoepithelial cells are emanating from the myoepithelial cell layer of entrapped ductules (**a–b**, H&E stain). The tumor cells are intensely positive for p63 (**c**), CK903 (**d**), CD10 (**e**), and EGFR (**f**) immunohistochemical markers

basement membrane [3]. On H&E sections, they can usually be identified by their small, elongated, or ovoid nuclei and often vacuolated cytoplasm. They characteristically stain with myoepithelial immunohistochemical markers: SMA, CD10, S-100, calponin, p63, high molecular weight CKs (CK5, CK14) [4–8].

MEC is composed purely of neoplastic myoepithelial cells—most often with spindle cell morphology—and is

Table 3 Microscopic features

No.	Consult Dg	Original Dg	NG	MI	Hem	Nec	Ca++	Associated lesions	ER	PR	Her2	EGFR
1	Myoep ca	Poorly differentiated infiltrative neoplasm	2	6/10 HPF	N	N	N	LR-DIN/IDH	0	0	0	3+
2	Myoep ca (arising in AME)	Myoep ca in AME	2	5/10 HPF	N	Y	N	AME	0	0	0	3+
3	Myoep ca	Radial scar	2	0/10 HPF	N	N	N	Lymphocytic mastitis	0	0	0	3+
4	Myoep ca	IMT	2	1/10 HPF	N	N	N		0	0	0	3+
5	Myoep ca	Metaplastic carcinoma	2	6/10 HPF	N	N	N	Atypical papilloma	0	0	0	2+
6	Myoep ca	Atypical complex sclerosing lesion	2	0/10 HPF	N	N	N	DIN1/AIDH	na	na	na	ND
7	Myoep ca	Spindle cell neoplasm	2	9/10 HPF	N	N	N		0	0	0	3+
8	Myoep ca	Metaplastic carcinoma	2	5/10 HPF	N	N	N		0	0	0	3+
9	Myoep ca (arising in AME)	Malignant neoplasm with spindle cell component	3	4/10 HPF	Y	N	N	AME	na	na	na	ND
10	Myoep ca (arising in AME)	Phyllodes tumor	2	8/10 HPF	N	N	N	AME, DIN1/DCIS 1	na	na	na	ND
11	Myoep ca	Spindle cell stromal proliferation	2	0/10 HPF	N	N	N		0	0	0	3+
12	Myoep ca	AME	2	1/10 HPF	N	N	N		0	0	0	3+
13	Myoep ca	Malignant spindle cell neoplasm	2	5/10 HPF	Y	Y	N		0	0	0	3+
14	Myoep ca	no Dg	2	0/10 HPF	N	N	N		0	0	0	3+
15	Myoep ca	AME	2	0/10 HPF	Y	N	N		0	0	0	3+

Dg diagnosis, *Myoep ca* myoepithelial carcinoma, *AME* adenomyoepithelioma, *IMT* inflammatory myofibroblastic tumor, *NG* nuclear grade, *MI* mitotic index, *HPF* high power field, *Hem* hemorrhage, *Nec* necrosis, *Ca++* calcifications, *LR-DIN/IDH* low-risk ductal intraepithelial neoplasia/intraductal hyperplasia, *DIN1/ADH* ductal intraepithelial neoplasia 1/atypical intraductal hyperplasia, *DIN1/DCIS 1* ductal intraepithelial neoplasia 1/ductal carcinoma in situ grade 1, *na* not available, *ND* not done, *Y* yes, *N* no

frequently accompanied by a prominent fibroblastic stromal reaction and lymphocytic lobulitis. The tumor cells may form irregular fascicles or thicker anastomosing cords, and they often appear to be emanating from the myoepithelial cell layer of entrapped ductules within the tumor. The nuclear atypia is usually mild to moderate, and the mitotic activity is less than 10/10 HPF. Necrosis and hemorrhage may occur, but they are uncommon. Focal squamous differentiation/metaplasia can occasionally be seen. True glandular differentiation and heterologous mesenchymal elements are absent. Similar to normal myoepithelial cells, MECs variably express high molecular weight CKs, p63, calponin, SMA, CD10, and S-100 [2, 9–12]. However, as none of these markers is absolutely specific, a combination of immunostains is recommended to confirm the diagnosis. Depending on the functional status of the cells, not all of these markers are expressed by all tumors or even normal myoepithelial cells.

As illustrated in our case series, the diagnosis of MEC may be quite difficult as it can mimic several different benign and malignant lesions. Due to the prominent stromal myo/fibroblastic reaction and the spindled morphology of tumor cells that can easily blend with the background stroma, the tumor may resemble reactive fibrosis, radial scar, fibromatosis, or myofibroblastic lesions (inflammatory myofibroblastic tumor, myofibroblastoma). On thorough microscopic examination, however, one can usually distinguish the slightly more plump tumor cells from the background stroma and a CK cocktail (CKAE1/AE3), or high molecular weight CK immunostain should be ordered even if the index of suspicion is relatively low. The cells in fibromatosis characteristically form interlacing fascicles that irregularly infiltrate the breast parenchyma and in between normal structures, whereas MEC usually presents as a dominant nodule with often more shallow infiltration at the periphery. Fibromatosis is negative for CK immunostains and other myoepithelial markers. Myofibroblasts on the other hand are usually positive for SMA and CD34 immunostains but do not express CKs; positivity for desmin is variable and often patchy when present. Sarcomas (e.g., leiomyosarcoma, angiosarcoma) are also in the differential diagnosis and can be ruled out by immunohistochemical stains for high molecular weight CK, p63, and endothelial markers (for angiosarcoma).

Adenomyoepitheliomas can also undergo a malignant change—in either the myoepithelial or the epithelial component, or both—and give rise to a MEC, an adenocarcinoma, adenomyoepithelial carcinoma, sarcoma, or carcinosarcoma [1]. In these cases, the underlying adenomyoepithelioma usually helps to establish the correct diagnosis.

Some specific variants of metaplastic carcinoma (spindle cell squamous and spindle cell adenocarcinomas) closely resemble MECs. Spindle cell adenocarcinomas are negative for high molecular weight CKs, positive for CK7, and are often clearly admixed with typical adenocarcinoma [13]. Spindle cell squamous carcinomas are even more difficult to distinguish from MEC based on morphology, and the immunoprofile of the two tumor types also overlaps (both tumors are positive for high molecular weight CKs and p63). Spindle cell squamous carcinomas, however, generally show foci of clearly recognizable squamous differentiation. We believe that either both MEC and spindle cell squamous carcinoma are derived from the myoepithelial cell layer, or they have a common stem cell. The presence of squamous differentiation as the tumor cells emanated from the myoepithelial cell layer in one of our cases supports the close relationship or the common origin of these two tumors. Therefore, at present, the only morphologically distinctive feature that distinguishes MEC is its clear-cut emanation from the myoepithelial cell layer [2, 14], as this has never been described in spindle cell squamous cell carcinomas or other types of metaplastic carcinomas of the breast. Furthermore, a common cell of origin does not preclude subtyping of various patterns of carcinoma derived from myoepithelial cells. Similarly, carcinomas of luminal epithelial origin are also separated into ductal, lobular, mucinous, tubular, etc., variants because of established differences in behavior and/or patterns of metastases. A pure spindle cell carcinoma without foci of squamous or glandular differentiation requires consideration of a different set of lesions in the differential diagnosis. It is important to recognize and separate these distinctive patterns in order to learn about their behavior and compare their response to various therapies and outcome with other carcinomas of myoepithelial origin.

A myoepithelial origin for metaplastic carcinomas was initially proposed based on morphologic studies [15], and more recent immunohistochemical evidence seems to support that theory [16, 17]. In addition, both myoepithelial carcinoma and squamous carcinoma (in all its phenotypic presentations) are triple negative and express EGFR, features characteristic of basal-like breast carcinomas [12, 18–23]. Interestingly, normal myoepithelial cells are also known to demonstrate strong EGFR expression in contrast to the luminal epithelial cells [23]. We also noted EGFR expression in the normal myoepithelial cells adjacent to the tumor in all of our cases where normal tissue was present on the immunostained sections, supporting that EGFR expression may indeed be another marker of myoepithelial derivation in breast carcinomas. EGFR overexpression—due to polyploidy or gene amplification—has been shown to correlate with clinical response to anti-EGFR tyrosine kinase inhibitors in patients with non-small cell lung cancer, suggesting that patients with myoepithelial and metaplastic breast carcinomas may also benefit from targeted therapy against EGFR [24, 25].

Due to the small number of MECs reported in the literature, our data are still limited concerning their clinical behavior. A review paper analyzed 21 cases from previous studies and found that seven patients had local recurrence, six patients developed axillary lymph node metastases, and five patients had evidence of hematogenous spread (lung, bone, and brain metastases) [21]. Overall, it appears that nearly half of the reported cases of MEC had an aggressive clinical course [2, 11, 12, 18, 26–28]. However, none of these prior reports used the emanation of tumor cells from the normal myoepithelial cell layer among their morphologic criteria. In our series, only one patient had local recurrence 19 months after initial misinterpretation as a reactive stromal change, and one developed pulmonary metastases within 8 months of diagnosis. The follow-up period, however, was relatively short in most of the cases. Although the information on the efficacy of different treatment options is scarce, wide local excision with sentinel lymph node biopsy seems logical as the first step in management of these tumors. The role and type of chemotherapy, as well as the efficacy of radiation therapy, are not well established. Given the origin of these tumors from myoepithelial cells, a cell population with both mesenchymal and epithelial features, we are concerned—possibly unnecessarily—that the use of radiation therapy in management of these tumors may trigger a mesenchymal/sarcomatous differentiation in any residual tumor stem cells. Endocrine therapy and Herceptin® (trastuzumab) are usually not an option, as MECs are almost invariably triple negative.

In conclusion, MEC of the breast is a rare tumor with a deceptively bland and challenging morphology and a potentially aggressive behavior. It is most likely that the cell of origin for both MEC and squamous carcinoma—in all its phenotypic presentations—is the same: either the myoepithelial cell itself or a common basal stem cell. The presence of a few squamous morules in two of our cases—with one showing clear-cut derivation from the myoepithelial cell layer—supports this theory. Expression of mesenchymal myoepithelial markers (SMA, S-100) in the reactive stroma should be distinguished from expression of these markers in the tumor cells; a similar reactive stroma is also present in the microcystic and some spindle cell variants of squamous carcinomas. It is also possible that squamous carcinomas reflect a more differentiated form of neoplastic myoepithelial cells with preference for the more epithelial phenotype of the cells. Further studies would be helpful to refine the relationship between these rare and unique tumors. It is important for the general pathologist to be aware of the diagnostic pitfalls and lesions that can mimic MEC.

References

1. Tavassoli FA, Soares J (2003) Myoepithelial lesions. In: Tavassoli FA, Devilee P (eds) Tumours of the breast and female genital organs. Pathology and genetics. WHO classification of tumours. IARC Press, Lyon, pp 86–88
2. Tavassoli FA (1991) Myoepithelial lesions of the breast. Myoepitheliosis, adenomyoepithelioma, and myoepithelial carcinoma. Am J Surg Path 15:554–568
3. Ahmed A (1974) The myoepithelium in human breast carcinoma. J Pathol 113:129–135
4. Barbareschi M, Pecciarini L, Cangi MG, Macrì E, Rizzo A, Viale G, Doglioni C (2001) P63, a p53 homologue, is a selective nuclear marker of myoepithelial cells of the human breast. Am J Surg Pathol 25:1054–1060
5. Joshi MG, Lee AK, Pedersen CA, Schnitt S, Camus MG, Hughes KS (1996) The role of immunocytochemical markers in the differential diagnosis of proliferative and neoplastic lesions of the breast. Mod Pathol 9:57–62
6. Jarasch ED, Nagle RB, Kaufmann M, Maurer C, Böcker WJ (1988) Differential diagnosis of benign epithelial proliferations and carcinomas of the breast using antibodies to cytokeratins. Hum Pathol 19:276–289
7. Gusterson BA, Ross DT, Heath VJ, Stein T (2005) Basal cytokeratins and their relationship to the cellular origin and functional classification of breast cancer. Breast Cancer Res 7:143–148
8. Moll R, Franke WW, Schiller DL, Geiger B, Krepler R (1982) The catalog of human cytokeratins: patterns of expression in normal epithelia, tumors and cultured cells. Cell 31:11–24
9. Hungermann D, Buerger H, Oehlschlegel C, Herbst H, Boecker W (2005) Adenomyoepithelial tumours and myoepithelial carcinomas of the breast—a spectrum of monophasic and biphasic tumours dominated by immature myoepithelial cells. BMC Cancer 5:92
10. Jones C, Foschini MP, Chaggar R, Lu YJ, Wells D, Shipley JM, Eusebi V, Lakhani SR (2000) Comparative genomic hybridization analysis of myoepithelial carcinoma of the breast. Lab Invest 80:831–836
11. Lakhani SR, O'Hare MJ, Monaghan P, Winehouse J, Gazet JC, Sloane JP (1995) Malignant myoepithelioma (myoepithelial carcinoma) of the breast: a detailed cytokeratin study. J Clin Pathol 48:164–167
12. Han B, Mori I, Nakamura M, Wang X, Ozaki T, Nakamura Y, Kakudo K (2006) Myoepithelial carcinoma arising in an adenomyoepithelioma of the breast: case report with immunohistochemical and mutational analysis. Pathol Int 56:211–216
13. Ellis IO, Schnitt SJ, Sastre-Garau X et al (2003) Invasive breast carcinoma. In: Tavassoli FA, Devilee P (eds) Tumours of the breast and female genital organs. Pathology and genetics. WHO classification of tumours. IARC Press, Lyon, pp 37–40
14. Tavassoli FA (1992) Classification of metaplastic carcinomas of the breast. Pathol Annu 27(Pt 2):89–119
15. Wargotz ES, Deos PH, Norris HJ (1989) Metaplastic carcinomas of the breast. II. Spindle cell carcinoma. Hum Pathol 20:732–740
16. Reis-Filho JS, Milanezi F, Paredes J, Silva P, Pereira EM, Maeda SA, de Carvalho LV, Schmitt FC (2003) Novel and classic myoepithelial/stem cell markers in metaplastic carcinomas of the breast. Appl Immunohistochem Mol Morphol 11:1–8
17. Leibl S, Gogg-Kammerer M, Sommersacher A, Denk H, Moinfar F (2005) Metaplastic breast carcinomas: are they of myoepithelial differentiation? Immunohistochemical profile of the sarcomatoid subtype using novel myoepithelial markers. Am J Surg Pathol 29:347–353
18. Jolicoeur F, Seemayer TA, Gabbiani G, Robidoux A, Gaboury L, Oligny LL, Schurch W (2002) Multifocal, nascent, and invasive myoepithelial carcinoma (malignant myoepithelioma) of the breast: an immunohistochemical and ultrastructural study. Int J Surg Pathol 10:281–291
19. Weigelt B, Kreike B, Reis-Filho JS (2009) Metaplastic breast carcinomas are basal-like breast cancers: a genomic profiling analysis. Breast Cancer Res Treat 117:273–280
20. Leibl S, Moinfar F (2005) Metaplastic breast carcinomas are negative for Her-2 but frequently express EGFR (Her-1): potential relevance to adjuvant treatment with EGFR tyrosine kinase inhibitors? J Clin Pathol 58:700–704
21. Behranwala KA, Nasiri N, A'Hern R, Gui GP (2004) Clinical presentation and long-term outcome of pure myoepithelial carcinoma of the breast. Eur J Surg Oncol 30:357–361
22. Bossuyt V, Fadare O, Martel M, Ocal IT, Burtness B, Moinfar F, Leibl S, Tavassoli FA (2005) Remarkably high frequency of EGFR expression in breast carcinomas with squamous differentiation. Int J Surg Pathol 13:319–327
23. Santini D, Ceccarelli C, Tardio ML, Taffurelli M, Marrano D (2002) Immunocytochemical expression of epidermal growth factor receptor in myoepithelial cells of the breast. Appl Immunohistochem Mol Morphol 10:29–33
24. Tan EH, Ramlau R, Pluzanska A, Kuo HP, Reck M, Milanowski J, Au JS, Felip E, Yang PC, Damyanov D, Orlov S, Akimov M, Delmar P, Essioux L, Hillenbach C, Klughammer B, McLoughlin P, Baselga J (2010) A multicentre phase II gene expression profiling study of putative relationships between tumour biomarkers and clinical response with erlotinib in non-small-cell lung cancer. Ann Oncol 21:217–222
25. Mendelsohn J, Baselga J (2006) Epidermal growth factor receptor targeting in cancer. Semin Oncol 33:369–385
26. Foschini MP, Eusebi V (1998) Carcinomas of the breast showing myoepithelial cell differentiation. A review of the literature. Virchows Arch 432:303–310
27. Schurch W, Potvin C, Seemayer TA (1985) Malignant myoepithelioma (myoepithelial carcinoma) of the breast: an ultrastructural and immunocytochemical study. Ultrastruct Pathol 8:1–11
28. Lingamfelter D, Chen Y, Kure K, Lankachandra K (2008) Infiltrating myoepithelial carcinoma of the breast, a case report and cytologic-histologic correlation. Diagn Pathol 3:7

Virchows Arch (2010) 457:347–357
DOI 10.1007/s00428-010-0951-3

ORIGINAL ARTICLE

Histologically confirmed intracranial germ cell tumors; an analysis of 62 patients in a single institute

Dakeun Lee · Yeon-Lim Suh

Received: 27 March 2010 / Revised: 5 July 2010 / Accepted: 7 July 2010 / Published online: 23 July 2010
© Springer-Verlag 2010

Abstract This study was undertaken to document the clinicopathologic characteristics of histologically verified, primary intracranial germ cell tumors (GCTs), determine treatment outcomes, and to identify prognostic factors. The records of 62 patients (45 males and 17 females) with a primary intracranial GCT were retrospectively analyzed. Mean patient age was 18 years, and median follow-up was 41 months. The most common histological subtypes were germinoma (48.4%), followed by mixed GCT (27.4%), and teratoma (19.4%). In 23 patients (37.1%), disease onset occurred between 16 and 20 years. Germinomas and malignant non-germinomatous germ cell tumors were most prevalent in the pineal gland, suprasellar region, and basal ganglia, whereas teratomas dominated at other sites. Synchronous bifocal GCTs were found in six patients. Five-year overall survival (OS) rates according to a therapeutic classification proposed by Sawamura were 82.93%, 83.08%, and 64.71% in the good, intermediate, and poor prognosis groups, respectively (P=0.2839). Five-year OSs in patients with normal tumor marker (αFP or βHCG) and patients with elevated marker were 85.26% and 66.96%, respectively (P=0.0568). Five of six patients with alpha-fetoprotein (α-FP) of >1,000 ng/ml succumbed to disease, whereas all five patients with a beta-human chorionic gonadotropin of >1,000 mIU/ml survived. Mixed GCTs are more common in Korea than in the West. Sawamura's classification of intracranial GCT may be a fine tool for stratifying patients' survival. Patients with elevated tumor marker levels may appear to have poorer OS independent of histology. In particular, high titers of α-FP seem to impact prognosis.

Keywords Central nervous system · Germ cell tumor · Prognosis · Tumor marker

D. Lee · Y.-L. Suh (✉)
Departments of Pathology, Samsung Medical Center,
Sungkyunkwan University School of Medicine,
50 Irwon-dong, Gangnam-gu,
Seoul 135-710, Republic of Korea
e-mail: ylsuh76@skku.edu

Introduction

Primary intracranial germ cell tumors (GCTs) are a unique class of rare tumors that frequently affect children and young adults. The reported incidences of intracranial GCTs among children with a brain tumor are higher in the Far East than in the West, e.g., Canada (3.3%) [1], France (3.5%) [2], and the United States of America (4.1%) [3], but Japan (10.3%) [4], Korea (11.2%) [5], and Taiwan (14%) [6], which suggest that genetic and/or environmental factors are responsible for the tumorigenesis of GCTs. Though the incidence of these tumors is still low, their relative proportions among brain tumors appear to be increasing year-on-year worldwide [5, 7].

GCT encompasses several histological subcategories, which are usually classified as germinomatous and non-germinomatous germ cell tumors (NGGCTs) [8]. Furthermore, the distributions of intracranial GCTs with respect to tumor site and histology depend on age. Although these tumors may present similar clinical manifestations and radiological features, their treatment responses and prognoses differ greatly. Accordingly, histological verification has been advocated to enable the tailoring of therapy [9, 10].

In the Republic of Korea, several studies have described intracranial GCTs, but these studies were limited to brain

tumor statistics or patients with a clinically diagnosed GCT [5, 11, 12]. In this retrospective study, we analyzed the archived records and excised tissue samples of 62 patients with a histologically confirmed primary intracranial GCT to define the clinicopathologic characteristics of this rare group of tumors in a Korean population. In addition, we assessed treatment outcomes and prognostic factors.

Patients and methods

General considerations

The records of 62 patients with a primary intracranial GCT, diagnosed and treated at the Samsung Medical Center (Seoul) from March 1995 to January 2009 were retrospectively analyzed. Clinical information, such as, age, gender, tumor location, pathologic diagnosis, tumor marker findings, and follow-up data were retrieved. A histological diagnosis was established for all 62 patients before initial treatment. There were 45 male and 17 female patients of mean age 18 years (ranging from newborn to 48 years). Serum alpha-fetoprotein (α-FP) levels exceeding 20 ng/ml or beta-human chorionic gonadotropin (β-HCG) levels exceeding 5 mIU/ml were considered elevated. Histopathological subclassifications were determined using the World Health Organization Classification system [8].

Patients were classified into three groups based on prognosis, namely, to a good prognosis group (pure germinoma, mature teratoma), an intermediate prognosis group (germinoma with an elevated β-HCG level, extensive/multifocal/germinoma, immature teratoma, mixed tumors composed mainly of germinoma or teratoma), and a poor prognosis group (choriocarcinoma, yolk sac tumor (YST), embryonal carcinoma, mixed tumors composed mainly of choriocarcinoma, YST, and embryonal carcinoma) according to the therapeutic classification devised by Sawamura et al. [10].

Histological examination

A total of 73 intracranial GCTs from the 62 patients were reviewed histologically by a neuropathologist to confirm the diagnoses. Immunohistochemical studies were performed using formalin-fixed, paraffin-embedded tumor tissues and the labeled streptavidin-biotin method and microwave-induced antigen retrieval methods. The antibodies used to confirm diagnoses were as follows: placental alkaline phosphatase (8A9, 1:40, Novocastra) or D2-40 (D2-40, 1:130, DakoCytomation) for germinoma, α-FP (Polyclonal, 1:200, DakoCytomation) for YST, β-HCG (ZSH17, 1:50, Invitrogen) for choriocarcinoma, and CD30 (BER-H2, 1:50, DakoCytomation) for embryonal carcinoma.

Follow-up process

Patients enrolled in this study were followed up by serial magnetic resonance imaging (MRI) and by monitoring α-FP and β-HCG serum levels (median follow-up period 41 months; range 8 days to 150 months). Cytological examinations were also conducted on cerebrospinal fluid (CSF) obtained by lumbar puncture. One of the patients with germinoma in this series was initially treated at other hospital and subsequently presented at our hospital with symptoms related to recurrence. This patient was then treated according to our standard treatment protocol. All of the other 61 patients were first diagnosed and treated in our hospital.

Treatment modalities

Thirty-four patients only received stereotactic biopsy as a surgical procedure (28 had germinoma, two mixed GCT, 2 YST, one immature teratoma, and one embryonal carcinoma). Subtotal tumor resection was performed in six patients (two with germinoma, two mixed GCT, one immature teratoma, and one mature teratoma), and gross total resection in 15 patients (seven with mature teratoma and eight with mixed GCT). In addition, seven patients received an initial stereotactic biopsy and subsequently underwent subtotal (one with immature teratoma and one with mixed GCT) or total tumor resection (one with immature teratoma and four with mixed GCT). After histological verification, patients were treated according to the Korean Intracranial Germ Cell Tumor Protocol. Based on this protocol, patients with germinoma (serum β-HCG ≤50 mIU/ml) received neo-adjuvant chemotherapy and subsequent radiotherapy (19.5~24 Gy of craniospinal irradiation and 10.8~19.8 Gy of local radiation). On the other hand, patients with pure germinoma (serum β-HCG >50 mIU/ml) or another NGGCT subtype (except mature teratoma) were categorized as high-risk and received more intensive chemo- and radiotherapy (36~39 Gy of craniospinal radiation and 14.4~23.4 Gy of local radiation). The regimens used for neo-adjuvant chemotherapy were etoposide (VP-16), carboplatin, bleomycin, or cyclophosphamide. Bleomycin was only given to high-risk patients and the cyclophosphamide dosage doubled in high-risk patients. However, six patients in the series (five with germinoma, one with mixed GCT (composed of immature teratoma and germinoma)) received radiotherapy without chemotherapy. All patients with mature teratoma enrolled in this series underwent surgical resection (gross total resection for seven tumors, subtotal resection for one tumor) without adjuvant treatment.

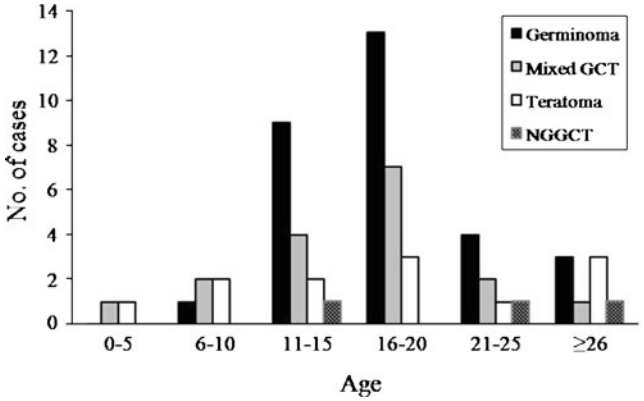

Fig. 1 Distribution of cases by age and histologic subtype

Statistical analysis

Statistical analyses were performed using SPSS for Window (version 12.0). All 62 cases were enrolled in the survival analysis. Overall survival (OS) was measured from date on study to the date of death from any cause, and event-free survival (EFS) was defined as the minimal interval from date on study to date of first disease progression, disease recurrence, or death from any cause. Survival curves were calculated using the Kaplan-Meier method, and the differences between survivals were analyzed using the log-rank test. Univariate and multivariate analyses were performed using a Cox proportional hazards regression model. *P* values of <0.05 were considered statistically significant, and all reported *P* values are two-sided.

Results

Patients

Immature teratoma was found in younger patients of mean age 11 years, whereas mature teratoma was found in older patients of mean age 24.1 years. Pure malignant NGGCT were not found in patients less than 11 years old and germinoma was only found in one patient in this age group (Fig. 1). The occurrence of intracranial GCTs peaked in 16-20 year olds (23 cases, 37.1%), and 62.9% of these patients were aged between age 11 and 20. There were 24 adult patients (≥19 years), and these comprised more than one third (40.3%) of the series. A male predominance was found in most histological subcategories, and the overall gender ratio was 2.5:1. However, mature teratoma showed a female predominance (ratio 0.6:1), and the numbers of male and female patients with immature teratoma were equal (Table 1). No associated clinical syndrome, such as Klinefelter syndrome, was present in any of our patients.

Histological diagnosis

Germinoma accounted for about a half of our 62 cases (48.4%), followed by mixed GCT (27.4%), and teratoma (19.4%). Figure 2 shows representative MR images and histological photomicrographs in a case with mixed GCT. Of the 30 germinoma cases, only one was diagnosed as germinoma with syncytiotrophoblastic giant cells (STGCs), and of the 17 mixed GCTs, three were composed of only germinoma and teratoma, and the other 14 were composed of germinoma or teratoma with other malignant NGGCT elements, which included YST (eight patients), choriocarcinoma (four patients), and embryonal carcinoma (four patients). The component most frequently encountered in mixed GCTs was germinoma (11 patients, 64.7%), followed by immature teratoma (eight patients, 47%), and YST (eight patients, 47%). Pure malignant NGGCT constituted only 4.8% of the series, but no case of pure choriocarcinoma or teratoma with malignant transformation was encountered.

Table 1 Characteristics of the 62 patients with a primary intracranial germ cell tumor with respect to the age, sex, tumor location, and histological subtype

			Tumor location (male/female)						
Histology	No. of pts (%)	Mean age	Pineal	Suprasellar	BG	Cerebellum	Multiple	Others	Total (ratio)
Germinoma	30 (48.4)	18.2	12 (12/0)	6 (2/4)	6 (6/0)	-	4 (4/0)	2 (2/0)	26/4 (6.5:1)
Mixed GCT	17 (27.4)	15.6	7 (6/1)	5 (2/3)	1 (1/0)	1 (0/1)	2 (1/1)	1 (1/0)	11/6 (1.8:1)
YST	2 (3.2)	21.5	2 (2/0)	-	-	-	-	-	2/0
EC	1 (1.6)	23	1 (1/0)	-	-	-	-	-	1/0
Teratoma									
Mature	8 (12.9)	24.1	-	-	-	4 (1/3)	-	4 (2/2)	3/5 (0.6:1)
Immature	4 (6.5)	11	2 (2/0)	1 (0/1)	-	-	-	1 (0/1)	2/2 (1:1)
Total	62 (100)	18	24 (23/1)	12 (4/8)	7 (7/0)	5 (1/4)	6 (5/1)	8 (5/3)	45/17 (2.5:1)

BG basal ganglia, *EC* embryonal carcinoma, *GCT* germ cell tumor, *YST* yolk sac tumor

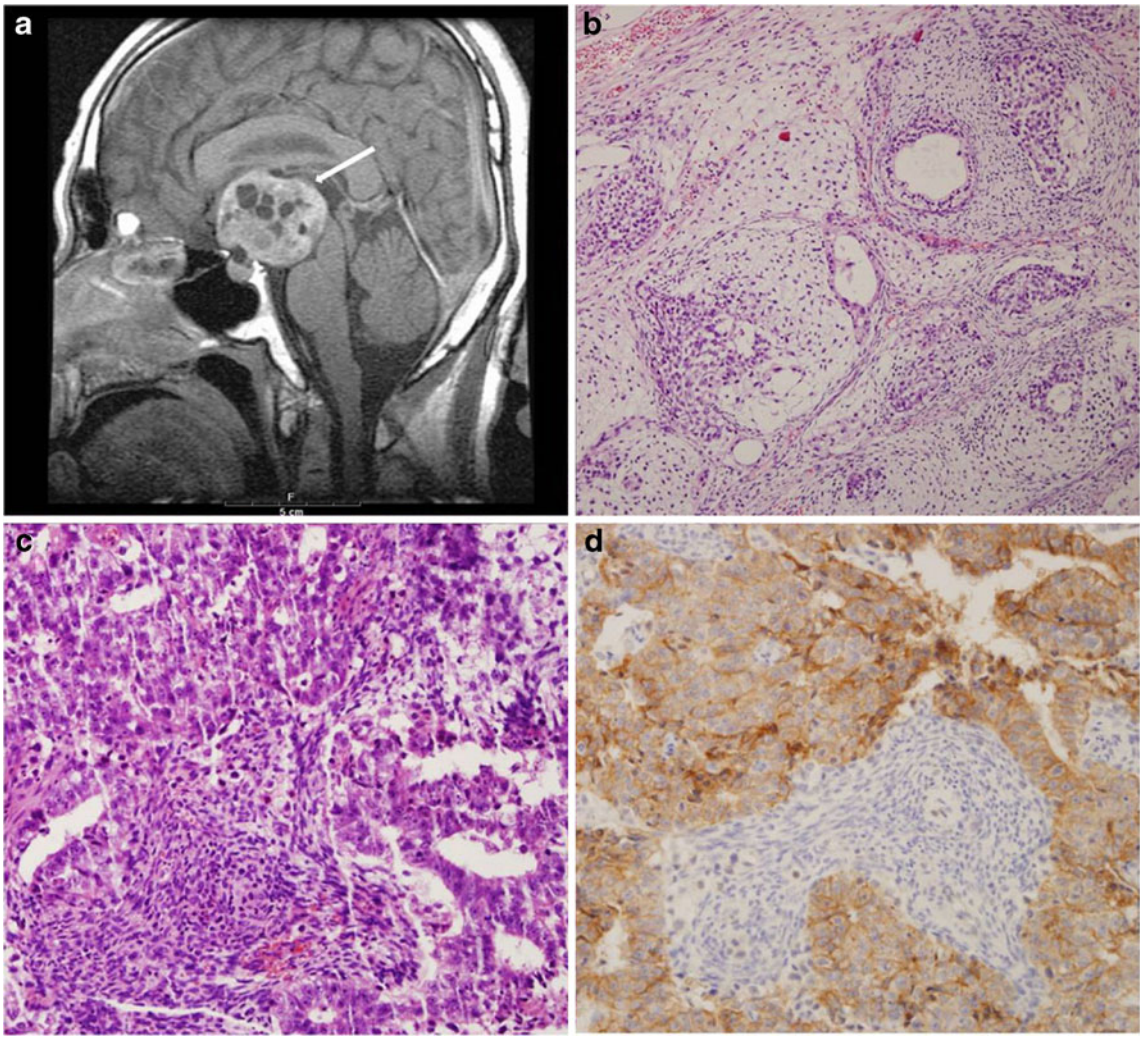

Fig. 2 Representative photomicrographs of a case with a mixed germ cell tumor. **a** Sagittal post-contrast T1-weighted magnetic resonance image demonstrating a relatively well-demarcated, solid, cystic mass with heterogeneous enhancement (*arrow*) in the suprasellar region. **b** Immature epithelial nests in loose, myxoid, immature mesenchymal tissue representing immature teratoma. **c** Cohesive nests composed of large cells with prominent nucleoli forming irregular, gland-like spaces representing embryonal carcinoma. A minute yolk sac tumor component (not shown) was also present in this tumor. **d** CD30 was well expressed in the membrane and the cytoplasm of embryonal carcinoma

Tumor locations

Patients demonstrated a wide variety of tumor locations. The pineal gland and suprasellar region were the most common sites of intracranial GCTs, and accounted for 38.7% and 19.4%, respectively. The basal ganglia and cerebellum were also common tumor locations. The cerebellum was a relatively common site for mature teratoma (50%). Other locations included; the lateral ventricle (three cases), thalamus (one case), frontal lobe (two cases), and temporal lobe (two cases). A female predominance was observed in the suprasellar region and cerebellum, whereas all other locations showed a male predominance. Germinomas were found to affect the pineal gland twice as much as the suprasellar region.

Patients with two distinct brain lesions of similar radiographic characteristics were considered as having synchronous bifocal GCTs if the two lesions were completely separate at the time of diagnosis. Minute, multifocal-enhanced lesions were considered to be metastatic tumor deposits. Six cases presented with synchronous bifocal lesions (Fig. 3). The characteristic features of these cases are summarized in Table 2.

Tumor markers

The number of patients with elevated serum tumor markers and the ranges of tumor markers by histology are summarized in Table 3. Tumor markers were not evaluated in four of the 62 patients (three with mature teratoma, one

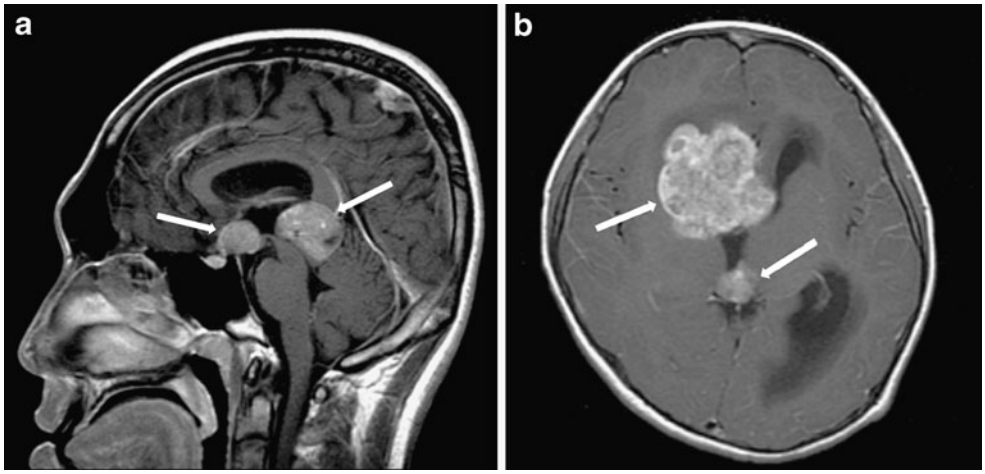

Fig. 3 Representative magnetic resonance images in cases with synchronous bifocal lesions **a** Sagittal post-contrast T1-weighted MR image demonstrating homogenous, modest enhancement of synchronous pineal and suprasellar region masses, respectively (*arrowed*). A stereotactic biopsy of the suprasellar mass confirmed a diagnosis of germinoma. **b** Axial post-contrast T1-weighted MR image demonstrating a huge, heterogeneous, hyperintense mass in the right frontal horn of the lateral ventricle and a smaller pineal mass with similar appearance (*arrowed*). This case was confirmed as mixed germ cell tumor. A moderate degree of hydrocephalus is also shown in (**b**)

with a mixed tumor). Of the remaining 58 patients, 28 (48.3%) demonstrated elevated serum titers of α-FP or β-HCG. Nine patients (30%) with germinoma revealed β-HCG elevation, and only one demonstrated STGCs in a biopsy sample. The remaining eight cases showed neither STGCs nor β-HCG-positive cells by immunohistochemistry. Patients with YST or choriocarcinoma, whether pure or not, had a highly elevated serum α-FP or β-HCG level. None of the five patients with mature teratoma had an elevated tumor marker level.

Performance status

The 62 study subjects were reviewed at initial diagnostic work-up and last follow-up, to assess Karnofsky performance statuses. These are summarized by prognostic group in Table 4. At the point of initial work-up, most patients (45 of the 62 patients, 72.6%) showed a 80-90% performance status. Only 27.4% (17 of 62) patients had a performance status of less than 80%. At last follow-ups, nine (18.75%) of the 48 survivors had no physical or neurological deficit and a performance status of 100%. Whereas 13 (27.08%) had a low performance status level (less than 80%). Severe motor paresis or cognitive dysfunction was the mainstay issue among these patients. Twenty-six (54.17%) patients with a 80-90% performance status were able to carry on nearly normal activity; most of these patients suffered from visual or endocrinological deficits.

Treatment outcomes

Four patients had CSF seeding at the time of diagnosis. Among them, one developed intracerebral metastatic lesions as well as spinal seeding, and another had a positive CSF cytology but negative spinal imaging findings at diagnosis. Intracranial multiple tumor metastasis without CSF seeding was observed in one patient at diagnosis. Eight relapses occurred among the study subjects; three patients relapsed locally, two developed local relapses accompanied with leptomeningeal seeding, one presented with multiple intracranial metastases, one developed leptomeningeal seeding only, and the other one presented with leptomeningeal and spinal seeding. Four patients experienced disease progression during treatment and 3 of these died. One patient with mixed GCT (composed of YST and immature teratoma) showed tumor enlargement by MRI

Table 2 Summary of cases that presented with synchronous bifocal lesions

Number	Sex	Age	Histology	Tumor location	Current status
1	M	18	Germinoma	P, S	Alive
2	M	19	Germinoma	Frontal horn of LV, thalamus	Alive
3	M	19	Germinoma	P, S	Alive
4	M	23	Germinoma	P, S	Alive
5	M	9	Mixed GCT	P, frontal horn of LV	Alive
6	F	17	Mixed GCT	P, S	Alive

GCT germ cell tumor, *LV* lateral ventricle, *P* pineal gland, *S* suprasellar region

Table 3 Numbers of patients with an elevated serum tumor marker level and the ranges of tumor markers levels for different histologies

Histology	α-FP		β-HCG		Normal	Total
	No.	Titer (ng/ml)	No.	Titer (mIU/ml)	No.	No.
Germinoma	0	-	8	5.3-1,528.6	21	29
Germinoma with STGCs	0	-	1	199	0	1
Mature teratoma	0	-	0	-	5	5
Immature teratoma	3(1)[a]	23-99,677	1	35.2	1	4
YST	2(1)[a]	41-22,600	1	26.1	0	2
EC	0	-	1	155.2	0	1
Mixed tumors						
Germinoma and teratoma	0	-	1	5.4	2	3
With mainly YST	5(2)[a]	905-7,300	2	31-156	1	6
With mainly EC	3(2)[a]	23-273.1	2	181.3-215	0	3
With mainly CC	0	-	4	2,440-37,510	0	4
Total	13(6)[a]	23-99,677	21	5.3-37,510	30	58

STGC syncytiotrophoblastic giant cell, *YST* yolk sac tumor, *EC* embryonal carcinoma, *CC* choriocarcinoma

[a] The number in parentheses refers to the number of cases with elevated levels of both α-FP and β-HCG

during treatment despite of a normalized serum α-FP level. Second-look surgery (gross total resection) demonstrated only a mature teratoma component, and this case was considered to show growing teratoma syndrome. Treatment associated complications were found in several patients. Intracerebral bleeding and postoperative cerebral nerve palsy occurred in two out of 41 patients who underwent stereotactic biopsy. Two patients experienced radiation-associated complications; one of them showed focal radiation-induced cerebral necrosis and the other presented with diffuse cerebral infarction. Finally, 14 patients died during follow-up periods (six with germinoma, two with immature teratoma, four with mixed GCT, and two with YST).

Table 4 Performance statuses of the 62 patients at their initial work-ups and last follow-ups by prognostic group

Karnofsky performance status (%)	Number of patients					
	Good PG		Intermediate PG		Poor PG	
	Initial	Last	Initial	Last	Initial	Last
100	0	6	0	2	0	1
90	6	4	4	4	5	4
80	13	6	9	6	8	2
70	2	4	1	1	2	3
60	2	1	1	2	1	0
50	2	0	1	0	0	1
40	0	1	1	0	0	0
30	1	0	0	0	1	0
20	0	0	1	0	0	0
10	0	0	1	0	0	0
0	0	4	0	4	0	6
Total	26	26	19	19	17	17

PG prognosis group; good prognosis group (pure germinoma, mature teratoma); intermediate prognosis group (germinoma with elevated levels of β-HCG, extensive/multifocal/germinoma, immature teratoma, mixed tumors composed mainly of germinoma or teratoma); poor prognosis group (choriocarcinoma, YST, embryonal carcinoma, mixed tumors composed mainly of choriocarcinoma, YST, or embryonal carcinoma)

The 5-year OS and EFS rates of patients with germinoma vs. NGGCT were 80.47% vs. 75% (P=0.5660) and 67.8% vs. 63.84% (P=0.4548), respectively. Five-year OS rates in the good, intermediate, and poor prognosis groups were 82.93%, 83.08%, and 64.71%, respectively (P=0.2839) (Fig. 4, Table 5). The survival times of the patients according to histologic subclassification in these three groups are summarized in Table 6. On the other hand, 5-year EFS rates in the good, intermediate, and poor prognosis groups were 82.93%, 49.85%, and 58.82%,

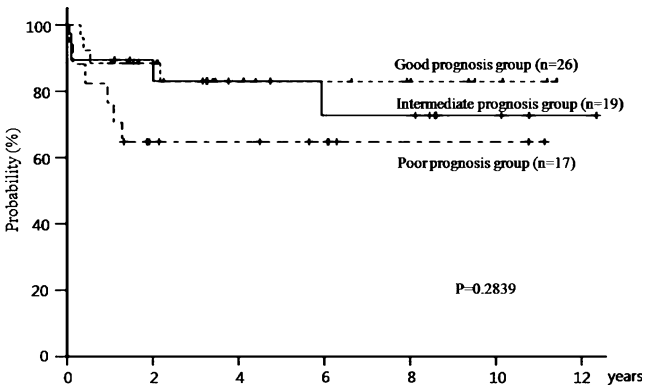

Fig. 4 Kaplan-Meier survival curves for overall survival in different prognosis groups. Good prognosis group (pure germinoma, mature teratoma); intermediate prognosis group (germinoma with elevated levels of β-HCG, extensive/multifocal/germinoma, immature teratoma, mixed tumors composed mainly of germinoma or teratoma); poor prognosis group (choriocarcinoma, YST, embryonal carcinoma, mixed tumors composed mainly of choriocarcinoma, YST, or embryonal carcinoma)

Table 5 Overall survival rates according to the histopathologic subclassification in each prognosis group

	No.	Overall survival rates (%)	
		Two years	Five years
Good prognosis group	26	88.46	82.93
Pure germinoma	18	83.33	74.07
Mature teratoma	8	100	100
Intermediate prognosis group	19	89.47	83.08
HCG-producing or multifocal germinoma	12	100	76.19
Immature teratoma	4	50	50
Mixed germinoma and teratoma	3	100	100
Poor prognosis group	17	64.71	64.71
Embryonal carcinoma	1	100	100
Yolk sac tumor	2	0	0
Malignant mixed germ cell tumor	14	71.43	71.43

respectively (P=0.0807). The 5-year OS rates of patients with normal tumor marker were higher than those of patients with an elevated tumor marker (85.26% vs. 66.96%, respectively) (Fig. 5), but this difference did not reach statistical significance (P=0.0568). The 5-year EFS rates for patients with normal marker compared to elevated marker was 74.18% and 53.15% (P=0.1216). Five of six patients with a high α-FP (>1,000 ng/ml) titer died of disease, whereas all five patients with a β-HCG titer of >1,000 mIU/ml survived. Survival rates by age (0-9, 10-18, ≥19 years; P=0.8583), genders (P=0.8031), and tumor locations (pineal gland, suprasellar region, and others; P=0.1307) were not found to differ significantly. We analyzed 17 patients in the poor prognosis group to examine the effect of gross total tumor resection on survival. In this group, two of nine (22.2%) patients that underwent gross total resection died, whereas four of eight (50%) patients who underwent stereotactic biopsy (five patients) or subtotal resection (three patients) died (P=0.2398). Univariate and multivariate analyses for OS and EFS using a Cox proportional hazards model are summarized in Table 7. Patients with an elevated marker had a higher risk of death than patients with normal marker by uni- (P=0.069) and multivariate analyses (P=0.251), but it only showed a trend. Tumors arising in suprasellar region had a higher hazard ratio for OS and EFS than tumors arising in pineal gland through uni- and multivariate analyses, but the differences did not reach significance.

Table 6 Survival times of patients in the different prognosis groups

	Good prognosis group (n=26)			Intermediate prognosis group (n=19)			Poor prognosis group (n=17)		
		Survival time (month)			Survival time (month)			Survival time (month)	
	No.	Mean	Range	No.	Mean	Range	No.	Mean	Range
Biopsy only	18	55	4-139	11	69	8 days-150	5	23	2-74
Subtotal or gross total resection	8	63	20-124	8	52	1-123	12	53	19 days-136
Radiotherapy only	4[a]	71	4-136	2	36	13-58	0	-	-
Chemo- and radiotherapy	14[a]	50	5-139	17	65	8 days-150	17	44	19 days-136
With recurrence	0	-	-	4	111	72-150	3	28	13-58
Without recurrence	26	57	4-139	15	49	8 days-131	14	48	19 days-136
Dead	4	10	4-26	4	25	8 days-72	6	8	19 days-16
Alive with disease	2	39	27-50	0	-	-	2	19	16-23
Alive without disease	20	68	13-139	15	72	13-150	9	74	23-136

Good prognosis group (pure germinoma, mature teratoma); intermediate prognosis group (germinoma with elevated levels of β-HCG, extensive/multifocal/germinoma, immature teratoma, mixed tumors composed mainly of germinoma or teratoma); poor prognosis group (choriocarcinoma, YST, embryonal carcinoma, mixed tumors composed mainly of choriocarcinoma, YST, or embryonal carcinoma)

[a]Eight patients with mature teratoma in the good prognosis group underwent surgical resection without chemo- or radiotherapy

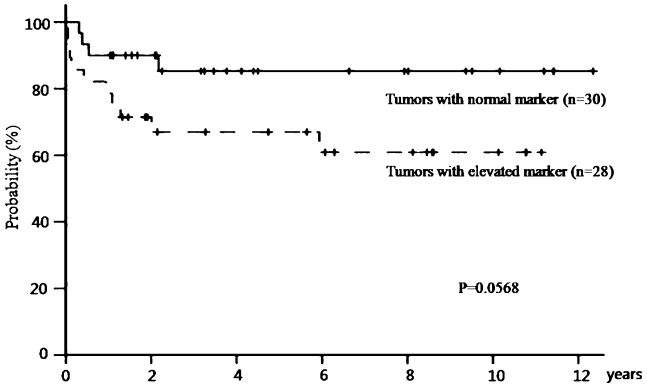

Fig. 5 Kaplan-Meier survival curves for overall survival in patients with normal tumor marker versus patients with elevated marker

Discussion

Primary intracranial GCTs are composed of several different tumor types and show varying degrees of malignancy. The clinical features of these tumors depend on location and size, whereas their histopathological and biological profiles resemble those of germ cell neoplasms arising in the gonads or other extragonadal sites [8].

A Korean multicenter study of central nervous system (CNS) tumors conducted over a period of 2 years (1997-1998) found that GCTs comprised 1.7% of the 3,221 documented cases [12], and that approximately 70% of GCTs were germinomas, followed by mature and immature teratomas (23.6%), YSTs (5.5%), mixed GCTs (3.6%), and embryonal carcinomas (1.8%). However, the present study reveals a remarkable increase in mixed GCTs (27.4%) and a relative decrease in germinomas (48.4%), and these results are rather similar to those reported in a study of Korean pediatric patients, which found that 26.3% were mixed GCTs [5]. Reports issued in the Far East, vary widely with respect to the proportions of mixed GCTs found. Higher figures have been reported by some [5, 9, 13], and markedly lower proportions by others. For example, Sawamura et al. [10] found only 14 mixed GCTs among 111 intracranial GCTs in a Japanese population, and a study performed in Taiwan reported that 13.8% were mixed GCTs, and thus, we are not sure whether this remarkable increase of mixed GCTs found in the present study represents the actual incidence of this subtype in the Korean population, even our institute have a primary third-level neurosurgical center for patients referred from throughout Korea.

Treatment and prognosis differ greatly for the various histological subgroups of intracranial GCTs. Since the 1980s, chemotherapy has been viewed as an important

Table 7 Cox proportional hazards model for overall survival and event free survival

	Overall survival				Event-free survival			
	Univariate analyses		Multivariate analyses		Univariate analyses		Multivariate analyses	
Variables	HR (95% CI)	*P*	HR (95% CI)	*P*	HR (95% CI)	*P*	HR (95% CI)	*P*
Age								
0-9	1		1		1		1	
10-18	0.678 (0.140, 3.273)	0.628	0.719 (0.131, 3.940)	0.704	0.315 (0.095, 1.048)	0.060	0.383 (0.103, 1.422)	0.152
≥19	0.639 (0.123, 3.309)	0.594	0.912 (0.144, 5.791)	0.922	0.376 (0.110, 1.286)	0.119	0.624 (0.155, 2.505)	0.506
Sex								
Male	1		1		1		1	
Female	1.159 (0.362, 3.711)	0.803	0.688 (0.142, 3.331)	0.642	1.30 (0.494, 3.423)	0.595	0.930 (0.222, 3.892)	0.921
Histology								
Germinomas	1		1		1		1	
Non-germinomas	1.362 (0.472, 3.932)	0.568	1.324 (0.405, 4.326)	0.642	1.414 (0.568, 3.519)	0.457	1.322 (0.454, 3.844)	0.690
Tumor marker								
Normal	1		1		1		1	
Elevated	2.932 (0.919, 9.357)	0.069	2.150 (0.581, 7.959)	0.251	2.056 (0.809, 5.225)	0.130	1.548 (0.526, 4.557)	0.428
Location								
Pineal	1		1		1		1	
Suprasellar	2.336 (0.674, 8.099)	0.181	2.080 (0.400, 10.816)	0.384	2.214 (0.713, 6.875)	0.169	1.643 (0.314, 8.601)	0.557
Other	0.672 (0.180, 2.504)	0.553	0.729 (0.179, 2.978)	0.660	1.002 (0.336, 2.983)	0.998	0.912 (0.282, 2.957)	0.879

Multivariate analyses were conducted using the Cox Proportional Hazards Model after adjusting for the other variables shown

CI confidence interval, *HR* hazard ratio

adjuvant treatment, and current treatment concepts embrace various combinations of surgery, chemotherapy, and radiotherapy. Furthermore, the introductions of these multimodal treatments have markedly reduced mortality and morbidity, particularly, among patients with NGGCT [9], and the traditional dichotomous classification of germinoma or NGGCT no longer stratifies patient survival adequately; in fact, the 5-year OS rates of patients with NGGCT or germinoma in present study were similar (75% vs. 80.47%). For this reason, another classification system was proposed previously that allocates histologic variants to therapeutic groups based on prognosis [9, 10]. Using this classification, we divided our patients into three groups; the good, the intermediate, and the poor prognosis groups, and we found that their survival curves differed, though not significantly different. Nevertheless, our findings confirm that this classification provides a better means of stratifying patient survival, and that it possibly provides more information for tailoring therapy in intracranial GCT patients.

Recently, Kim et al. [14] in a study of 117 CNS germ cell tumor patients treated by chemotherapy alone, reported that patients with elevated marker appeared to have poorer survival independently of tumor histology. In the present study, we found that patients with elevated marker had tended to have poorer survival (66.96% vs. 85.26%) with borderline significance (P=0.0568). Furthermore, although the effect of marker elevation on the risk of death was diluted after adjusting for other factors, such as tumor histology, marker elevation was still found to be associated with a greater risk for death (hazard ratio=2.150). This finding suggests a relationship between markers and outcome that is independent of histology. Furthermore, patients with a high α-FP titers (>1,000 ng/ml) appeared to have a poorer prognosis (five of six succumbed to the disease). This result concurs with those of studies on extracranial GCT, in which α-FP levels of >1,000 or >10,000 ng/ml were found to have prognostic significance [15, 16]. On the other hand, in the present study, five patients with a β-HCG level to >1,000 mIU/ml survived.

In the present study, as was expected, the pineal gland and suprasellar region were the most frequent locations of intracranial GCTs (except for teratoma), although basal ganglia, ventricles, cerebellum, and cerebrum were also frequently involved. Wong et al. [6] reported that 25 (18.1%) of 138 intracranial GCTs were located in the basal ganglia in a Taiwanese population, and several studies conducted in the Far East have reported GCTs showed a preference for basal ganglia and thalamus [17–19], which suggests that intracranial GCTs are more frequent in these locations in the Far East. The characteristics of each intracranial GCT subtype with regard to age, gender, and location, as observed in the present study, are generally in accord with that report in a Japanese population [9]. However, patients with mature teratoma in the present study were substantially older (mean age 24.1 vs. 11.6 years), showed a female predominance, and had unusual tumor locations. Intracranial mature teratoma is usually located in the pineal gland and its occurrence in the posterior fossa is rare [20]. However, in the present study, half of our mature teratomas were in the cerebellum, and no mature teratoma case occurred in the pineal gland. Other locations were the frontal lobe (two cases), lateral ventricle (one case), and temporal lobe (one case). A comparison between these findings and those of a previous study conducted in South Korea [5] suggests that these observations were caused by selection bias.

Multifocal lesions are sometimes observed in intracranial GCTs. For example, bifocal lesions synchronously involving the pineal gland and suprasellar region are common. Swischuk and Bryan [21] first referred to this entity as “double midline atypical teratoma”, and described it as a noncontiguous tumor in the anterior and posterior parts of the third ventricle. In the present study, there were six cases of synchronous bifocal intracranial GCTs (9.7%), which is a slightly lower prevalence than has been reported in Japanese and Taiwanese studies (12.8~13.7%) [22, 23] but which is nonetheless higher than prevalences reported in Europe and North America (approximately 6%) [24–26]. Synchronous intracranial GCTs are usually germinomas, but their histologies could be as diverse as those of intracranial GCTs [13, 27]; and in the present study, we found two mixed GCTs in this group. All of our six patients with synchronous bifocal intracranial GCT were alive at last follow-up, which suggests that synchronous tumor occurrence does not influence prognosis.

In keeping with previous surveys [5, 6, 9, 10, 24], an overall male predominance was observed in the present study, and this was most obvious for germinoma with a male to female ratio of 6.5:1, which is rather high, because the majority of previous studies have reported ratios of less than 4:1 [2, 5, 6, 9, 13, 24, 28]. In the present study, mature teratoma was the only histological subtype to show female predominance (five of eight patients), and interestingly, these five female patients were 19 years old or more. In the present study, the suprasellar region was the only anatomical site demonstrating a female predominance, which concurs with previous reports [5, 9, 13, 24].

Intracranial GCT is usually diagnosed based on tumor markers, neuroimaging characteristics, and histological assessments. However, the radiographic characteristics of all types of intracranial GCTs are similar [29], and tumor marker proteins can be produced by almost any type of GCT [9, 30]. Therefore, diagnosis usually requires histological verification. In the present study, one patient with germinoma had a high serum level of β-HCG

(1,528.6 mIU/ml), and thus, clinicians suspected mixed GCT. However, this case did not demonstrate either a choriocarcinomatous element or STGCs in the stereotactic biopsy specimen. Despite the remaining possibility of a mixed tumor, we categorized this case as germinoma, since many pure germinomas can also produce β-HCG, sometimes at high levels [31]. For the same reason [32], we followed the pathologic diagnosis in a case of immature teratoma with a high α-FP serum level, although the titer was excessive. During a meticulous slide review, we identified two diagnostic errors. Both cases had been misdiagnosed as mature teratomas because immature mesenchymal components had not been recognized.

Stereotactic biopsy is a well-established surgical technique that provides accurate access to almost any region of the intracranial space and tissue for histologic diagnosis. Stereotactic biopsy is generally regarded as a safe procedure, with minimal associated morbidity and mortality as compared to other cranial surgical modalities [33, 34]. In the present study, two patients experienced a biopsy-associated complication (4.87%), and this morbidity rate is similar to those of previous reports [34]. Stereotactic biopsy also has its limitations. First, because it is a closed procedure, no direct feedback is provided to the surgeon during the manipulation of brain tissue. Second, biopsy of well-vascularized tumors, such as, metastatic renal cell carcinoma and choriocarcinoma, should not be conducted due to risk of catastrophic intracranial hemorrhage [33]. Third, stereotactic biopsy specimens, and therefore, findings, sometimes do not represent actual tumor compositions. Two cases of mixed GCT in our series were initially misdiagnosed as YST and immature teratoma, respectively, for this reason. In our institute, we routinely perform intraoperative monitoring during brain biopsies, including stereotactic biopsies, to confirm optimal sampling. Germinomas can be promptly and definitively diagnosed by intraoperative consultation. Cytologic smears for frozen are not usually helpful for diagnosing germ cell tumors. However, they are helpful for the intraoperative diagnosis of intracranial germinomas, because scant germ cells are easily recognized and distinguished from intermingled inflammatory cells.

Growing teratoma syndrome is a rare clinical phenomenon and even rarer among intracranial GCTs [35]. It involves mature teratoma enlargement during or after chemotherapy for NGGCT with normal α-FP and β-HCG serum levels [36]. In our series, one patient with a mixed GCT (composed of YST and immature teratoma) developed this syndrome. This patient remains alive with no experience of an adverse event after second-look radical surgery. Thus, when a residual mass enlarges during or after treatment, growing teratoma syndrome should be considered in the differential diagnosis of tumor relapse or progression if there is a mismatch between radiographic and serum marker results.

Some previous reports have suggested that HCG-producing and/or STGC-containing germinomas have a greater tendency to recur [10, 13, 28, 37, 38]. Therefore, in many current protocols, patients with germinoma showing a β-HCG level of >50 mIU/ml are classified as the same group of NGGCT, and are administered higher intensity treatments than those with non-secreting germinomas. In contrast, others have reported that a β-HCG level of >50 mIU/ml has no adverse impact [39, 40]. In our series, 30% (nine out of 30) of germinoma cases had an elevated marker level, and these including four with a β-HCG level exceeding 50 mIU/ml; however, only two of these nine patients (22.2%) died of disease, whereas five of 21 (23.8%) germinoma patients with normal marker levels died during follow-up. Based on our results, β-HCG elevation in biopsy proven germinomas does not alter prognosis. However, the more intense treatments afforded patients with a β-HCG serum level of >50 mIU/ml possibly obscured actual survival differences.

Summarizing, in our Korean cohort, intracranial GCTs was found to arise in various anatomical locations and mixed GCTs were found to be more common than in the West. The therapeutic classification proposed by Sawamura for intracranial GCT based on prognosis appears to better stratify survival than a simple dichotomous split between germinoma and NGGCT. Furthermore, patients with elevated tumor marker appeared to have poorer OSs independently of tumor histology, although this did not reach statistical significance. In particular, high α-FP serum titers (>1,000 ng/ml) appear to influence survival, whereas serum β-HCG levels do not appear to impact the prognosis of biopsy proven germinoma.

Conflict of interest statement The authors have no conflict of interest to declare.

References

1. Felix I, Becker LE (1990) Intracranial germ cell tumors in children: an immunohistochemical and electron microscopic study. Pediatr Neurosurg 16:156–162
2. Bauchet L, Rigau V, Mathieu-Daude H et al (2009) Clinical epidemiology for childhood primary central nervous system tumors. J Neurooncol 92:87–98
3. CBTRUS, Central Brain Tumor Registry of the United States (2009) Statistical Report 2004-2005. Available at http://www.cbtrus.org
4. Mori K, Kurisaka M (1986) Brain tumors in childhood: statistical analysis of cases from the Brain Tumor Registry of Japan. Childs Nerv Syst 2:233–237
5. Cho KT, Wang KC, Kim SK et al (2002) Pediatric brain tumors: statistics of SNUH, Korea (1959-2000). Childs Nerv Syst 18:30–37

6. Wong TT, Ho DM, Chang KP et al (2005) Primary pediatric brain tumors: statistics of Taipei VGH, Taiwan (1975-2004). Cancer 104:2156–2167
7. Rickert CH, Paulus W (2001) Epidemiology of central nervous system tumors in childhood and adolescence based on the new WHO classification. Childs Nerv Syst 17:503–511
8. Louis DN, Ohgaki H, Wiestler O (2007) WHO classification of tumours of the central nervous system, 3rd edn. WHO Publication Center, Albany, NY
9. Matsutani M, Sano K, Takakura K et al (1997) Primary intracranial germ cell tumors: a clinical analysis of 153 histologically verified cases. J Neurosurg 86:446–455
10. Sawamura Y, Ikeda J, Shirato H et al (1998) Germ cell tumours of the central nervous system: treatment consideration based on 111 cases and their long-term clinical outcomes. Eur J Cancer 34:104–110
11. Choi JU, Kim DS, Chung SS et al (1998) Treatment of germ cell tumors in the pineal region. Childs Nerv Syst 14:41–48
12. Suh YL, Koo H, Kim TS et al (2002) Tumors of the central nervous system in Korea: a multicenter study of 3,221 cases. J Neurooncol 56:251–259
13. Sano K (1995) So-called intracranial germ cell tumours: are they really of germ cell origin? Br J Neurosurg 9:391–401
14. Kim A, Ji L, Balmaceda C et al (2008) The prognostic value of tumor markers in newly diagnosed patients with primary central nervous system germ cell tumors. Pediatr Blood Cancer 51:768–773
15. Baranzelli MC, Kramar A, Bouffet E et al (1999) Prognostic factors in children with localized malignant nonseminomatous germ cell tumors. J Clin Oncol 17:1212
16. (1997) International Germ Cell Consensus Classification: a prognostic factor-based staging system for metastatic germ cell cancers. International Germ Cell Cancer Collaborative Group J Clin Oncol 15:594-603
17. Kim DI, Yoon PH, Ryu YH et al (1998) MRI of germinomas arising from the basal ganglia and thalamus. Neuroradiology 40:507–511
18. Tamaki N, Lin T, Shirataki K et al (1990) Germ cell tumors of the thalamus and the basal ganglia. Childs Nerv Syst 6:3–7
19. Yasue M, Tanaka H, Nakajima M et al (1993) Germ cell tumors of the basal ganglia and thalamus. Pediatr Neurosurg 19:121–126
20. Beschorner R, Schittenhelm J, Bueltmann E et al (2009) Mature cerebellar teratoma in adulthood. Neuropathology 29:176–180
21. Swischuk LE, Bryan RN (1974) Double midline intracranial atypical teratomas: a recognizable neuroendocrinologic syndrome. Am J Roentgenol Radium Ther Nucl Med 122:517–524
22. Huang PI, Chen YW, Wong TT et al (2008) Extended focal radiotherapy of 30 Gy alone for intracranial synchronous bifocal germinoma: a single institute experience. Childs Nerv Syst 24:1315–1321
23. Sugiyama K, Uozumi T, Kiya K et al (1992) Intracranial germ-cell tumor with synchronous lesions in the pineal and suprasellar regions: report of six cases and review of the literature. Surg Neurol 38:114–120
24. Jennings MT, Gelman R, Hochberg F (1985) Intracranial germ-cell tumors: natural history and pathogenesis. J Neurosurg 63:155–167
25. Hoffman HJ, Otsubo H, Hendrick EB et al (1991) Intracranial germ-cell tumors in children. J Neurosurg 74:545–551
26. Jellinger K (1973) Primary intracranial germ cell tumours. Acta Neuropathol 25:291–306
27. Scheithauer BW (1985) Neuropathology of pineal region tumors. Clin Neurosurg 32:351–383
28. Yoshida J, Sugita K, Kobayashi T et al (1993) Prognosis of intracranial germ cell tumours: effectiveness of chemotherapy with cisplatin and etoposide (CDDP and VP-16). Acta Neurochir (Wien) 120:111–117
29. Echevarria ME, Fangusaro J, Goldman S (2008) Pediatric central nervous system germ cell tumors: a review. Oncologist 13:690–699
30. Packer RJ, Cohen BH, Cooney K (2000) Intracranial germ cell tumors. Oncologist 5:312–320
31. Bjurlin MA, August CZ, Weldon-Linne M et al. (2007) Histologically pure stage I seminoma with an elevated beta-hCG of 4497 IU/l Urology 70:1007 e1013-1005
32. Yamashita N, Kanai H, Kamiya K et al (1997) Immature teratoma producing alpha-fetoprotein without components of yolk sac tumor in the pineal region. Childs Nerv Syst 13:225–228
33. Krieger MD, Chandrasoma PT, Zee CS et al (1998) Role of stereotactic biopsy in the diagnosis and management of brain tumors. Semin Surg Oncol 14:13–25
34. Kongkham PN, Knifed E, Tamber MS et al (2008) Complications in 622 cases of frame-based stereotactic biopsy, a decreasing procedure. Can J Neurol Sci 35:79–84
35. Yagi K, Kageji T, Nagahiro S et al (2004) Growing teratoma syndrome in a patient with a non-germinomatous germ cell tumor in the neurohypophysis–case report. Neurol Med Chir (Tokyo) 44:33–37
36. Logothetis CJ, Samuels ML, Trindade A et al (1982) The growing teratoma syndrome. Cancer 50:1629–1635
37. Balmaceda C, Heller G, Rosenblum M et al (1996) Chemotherapy without irradiation—a novel approach for newly diagnosed CNS germ cell tumors: results of an international cooperative trial. The First International Central Nervous System Germ Cell Tumor Study. J Clin Oncol 14:2908–2915
38. Utsuki S, Kawano N, Oka H et al (1999) Cerebral germinoma with syncytiotrophoblastic giant cells: feasibility of predicting prognosis using the serum hCG level Acta Neurochir (Wien) 141:975-977; discussion 977-978
39. Sawamura Y, Shirato H, Ikeda J et al (1998) Induction chemotherapy followed by reduced-volume radiation therapy for newly diagnosed central nervous system germinoma. J Neurosurg 88:66–72
40. Shibamoto Y, Takahashi M, Sasai K (1997) Prognosis of intracranial germinoma with syncytiotrophoblastic giant cells treated by radiation therapy. Int J Radiat Oncol Biol Phys 37:505–510

Virchows Arch (2010) 457:359–368
DOI 10.1007/s00428-010-0942-4

ORIGINAL ARTICLE

Association of a p73 exon 2 GC/AT polymorphism with colorectal cancer risk and survival in Tunisian patients

Amira Toumi Arfaoui · Lilia Ben Mahmoud Kriaa · Olfa El Amine El Hadj · Majid A. Ben Hmida · Myriam Khiari · T. Khalfallah · Lasaad Gharbi · Sabeh Mzabi · Sadaa Bouraoui

Received: 26 October 2009 / Revised: 2 June 2010 / Accepted: 8 June 2010 / Published online: 20 July 2010
© Springer-Verlag 2010

Abstract We examined the association of one linked GC/AT polymorphism at p73 with the risk of colorectal cancer. In the present study, we investigated whether this polymorphism was related to the risk of colorectal cancer, and whether there were relationships between the polymorphism and LOH, protein expression or clinicopathological variables. The p73 genotypes were determined by PCR-restriction fragment length polymorphism in 150 Tunisians patients with colorectal cancer and in 204 healthy control subjects. Immunohistochemistry was performed on normal mucosa, primary tumour and metastasis. The frequencies of the genotypes were 52% for wild-type (GC/GC), 31% for heterozygotes (GC/AT) and 17% for variants (AT/AT) in patients, and 54%, 35% and 11% in controls, respectively. There were no significant differences of the frequencies of the three genotypes between the patients and controls (p=0.11). We did not find any relationship of the genotypes with clinicopathological features of patients. We found that patients with the AT/AT genotype had a significantly worse clinical outcome than those with the GC/AT and GC/GC genotype. There were no significant differences between tumoural immunostaining of the total p73 and p73 polymorphism (p=0.16). However, we found a significant difference between the expression profile of ΔNp73 isoform and frequencies of the three genotypes (p=0.0001). No LOH was observed at p73 locus. Our results suggest that the AT/AT genotype is significantly associated with poor prognosis in colorectal cancer. All these findings suggest that p73 polymorphism analysis may provide useful prognostic information for colorectal cancer patients.

Keywords Colorectal Cancer · p73 polymorphism · Prognosis

A. T. Arfaoui · L. B. M. Kriaa · M. Khiari · S. Bouraoui
Laboratory of Colorectal Cancer Research UR03ES04,
Science University Tunis,
Tunis, Tunisia

L. B. M. Kriaa
e-mail: Liliakria77@yahoo.fr

O. E. A. El Hadj · S. Mzabi · S. Bouraoui
Department of Pathology and Cytology,
Mongi Slim Hospital La Marsa,
Tunis, Tunisia

O. E. A. El Hadj
e-mail: olfaelamine@yahoo.fr

M. A. Ben Hmida
Department of Epidemiology and Preventive Medicine,
Medecine University Tunis,
Tunis, Tunisia

T. Khalfallah · L. Gharbi
Department of General Surgery, Mongi Slim Hospital La Marsa,
Tunis, Tunisia

A. T. Arfaoui (✉)
Department of Pathology and Cytology, Mongi Slim Hospital,
Sidi Daoud,
2047 Tunis, Tunisia
e-mail: arfaouiamira@hotmail.com

A. T. Arfaoui
4-1 Res Semiramis Apt Bader El Boudour Borj El Wezir,
2036 La Soukra, Tunisia

Introduction

The TP73 gene, map to chromosome 1p36, was first described by Kaghad et al. [1]. The authors identified a gene with remarkable sequence similarity to the DNA-binding, transactivation and oligomerization domains of the tumour suppressor gene TP53 [2, 3]. However, extensive mutational analysis of p73 in diverse tumours has demonstrated that

mutations in this gene are rare, being reported in fewer than 2% of all cancers screened [4–6], suggesting that this gene does not function as a traditional tumour-suppressor gene. Recently, a p73-knockout mouse model has been developed; these mice manifested various neurohormonal deficits and also inflammatory defects, in particular, the mice exhibited severe haemorrhagic inflammation and erosion of the gastrointestinal tract, but they were not susceptible to spontaneous tumours [7]. Therefore, p73 is now excluded as a classic tumour suppressor [8, 9]. However, conflicting scenarios have been described. Recently, it has been shown that the p73 gene codes for two different protein isoforms which come from the use of different promoters and alternative splicing. In general, TAp73 proteins produced from the first promoter P1 are considered to act in a manner similar to p53, responding to certain genotoxic and other stresses and activating genes involved in growth arrest and apoptosis. Thus, like p53, TAp73 is part of the complex protective response to genotoxic stress, although TAp73 can activate genes not regulated by p53 and vice versa, presumably accounting for their overlapping but not identical functions. In contrast, ΔNp73 isoforms produced from P2 promoter or from alternative splicing of exons 2 and 3 inhibit apoptosis during normal development and in cancer cell lines. This effect is mediated through two distinct actions: competition for DNA binding inhibits p53-mediated transcription, while inhibition of TAp73 transcriptional activity is achieved by direct protein-protein interactions. Theoretically, therefore, TP73 expression can be either pro-or anti-oncogenic, depending on whether anti-or pro-apoptotic (TAp73 or ΔNp73, respectively) isoforms are expressed [10].

Loss of heterozygosity (LOH) at the p73 locus has been reported with varying frequency in different tumours; 5.3% of prostatic cancers [4], 19% of neuroblastomas [11], 42% of lung cancers [12] and 8% [13] and 64% [14] of oesophageal cancers. Over-expression of the p73 protein has been seen in benign and malignant tumours including colorectal cancer (CRC), when compared with the matched normal tissues. Furthermore, p73 over-expression was correlated with a poor prognosis in colorectal, hepatocellular and breast cancers [15–18]. Notwithstanding the epidemiological evidence, very little is known about implication of the molecular and cellular mechanisms on the CRC risk, which could be modulated by diet, lifestyle as well as polymorphism. In this study, we investigate the association of p73 GC/AT polymorphism with risk and survival of CRC. Two linked, single nucleotide polymorphisms, forming a compound polymorphism at positions 4 (G→A) and 14 (C→T) have been identified in the 5′ untranslated region, of exon 2 of the p73 gene [1], and have been designated the AT and GC alleles, respectively. This polymorphism lies just upstream of the initiating AUG of exon 2, in a region which may theoretically form a stem-loop structure. It has been suggested that this could potentially affect gene expression, perhaps through alteration of the efficiency of translation initiation [1].

In this frame, many authors have already evaluated the association between p73 GC/AT polymorphism and risk of several types of cancer development including CRC. However, their findings were very conflicting according to populations [19–22].

In this present study, we sought to investigate whether the GC/AT polymorphism in the p73 gene may play a role in CRC and whether there were relationships between this polymorphism and LOH, protein expression or clinicopathological variables.

Materials and methods

Clinical and pathological data

In this case–control study, we performed a retrospective analysis from 1995 to 2008 concerning 150 patients with CRC, collected in the laboratory of Pathology of the Mongi Slim Hospital of Tunis. There were 68 cases with matched normal mucosa and primary and metastatic tumours. In the 150 cases included in this study, samples were taken not only from the tumoural area but also from margin, corresponding to distant resection, and were histologically free from precancer and cancer. The clinicopathological features (age, sex, clinical symptoms, macroscopic features, histological type, differentiation and TNM stage) were identified for each patient from surgical and pathological records. Sixty-three patients died because of cancer. Furthermore, all tumours initially reported as mucinous carcinomas were reviewed by two pathologists and those in whom histological mucinous extracellular pattern was 50% or greater of their volume were included in the mucinous group. There was no information available on patient's sex in nine cases, age in five cases, tumour location in 12 cases, TNM stage in eight cases and growth pattern in eight.

Controls comprised 204 healthy blood donors, who were in the same residential area as the patients. The individuals had neither gastrointestinal diseases nor a history of tumours.

DNA extraction

The genomic DNA was extracted from 20 mg of normal mucosa and tumour tissues by means of the Wizard SV Genomic DNA Purification System according to the manufacturer's instructions (Promega, Madison, WI). The concentration and purity of the DNA were measured with a spectrophotometer. The genomic DNA from the controls was extracted from peripheral leukocytes using the same Purification Kit (Promega).

Polymerase chain reaction and restriction fragment length polymorphism

Genomic DNA of normal and tumour samples was amplified with p73 primers: 5′-CAGGAGGACAGAGCACGAG-3′and 5′-CGAAGGTGGCTGAGGCTAG-3′. The polymerase chain reaction (PCR) mixture contained ~25 ng chromosomal DNA, 1×PCR buffer (Promega), 1.5 mM MgCl2 (Promega), 0.2 mM dNTP, 0.5 mM of each primer (SGS, Köping, Sweden), 2.5×10^{-4} U/ml Taq polymerase (Promega) and H_2O in the final reaction volume of 20 µl. Reactions were started under the following conditions: (a) 94°C for 5 min; (b) 30 cycles of 94°C for 30 s, 65°C for 30 s, 72°C for 30 s and (c) a final extension for 10 min at 72°C. The 229 bp PCR-products were checked on a 3% agarose gel, stained with ethidium bromide, in UV-light.

Of the 20 µl of PCR mixture, 1 µl was digested with StyI (Fermentas, Vilnius, Lithuania) restriction enzyme for 4 h, according to conditions specified by the manufacturer. The presence of the AT polymorphism creates a StyI digestion site, yielding products of 157 and 72 bp. The wild-type, GC allele, remained uncleaved by StyI, yielding a 229 bp product.

Analyses of loss of heterozygosity by on-chip electrophoresis

PCR on DNA from tumours and the matched DNA from normal mucosa (that was heterozygous for the polymorphism) was performed at the same PCR run, using the same protocol as mentioned above for the detection of the loss of heterozygosity. The fragments amplified were cleaved by StyI (Fermentas). For the separation of PCR products of digestion, we used DNA 1000 LabChip kits, which are manufactured for research purposes only. In brief, the chips were prepared with gel-dye mix, pressurised, and then marker solution and DNA 1500 ladder were added. For this process, 1 µl of each PCR reaction was pipetted into one out of 11 sample wells of a prepared chip. After vortexing, the chip was placed in the BioRad Experion bioanalyzer. The electrophoresis of samples lasted approximately 30–40 min. Fragment analysis was carried out using BioRad Experion software, and an overlay of two electropherograms was used to compare PCR patterns derived from tumour and non-tumour tissues. Differences in the peak patterns of the overlaid electropherograms were evaluated. Two overlays were used per patient in order to identify allelic expression and lost of heterozygosity of p73. If the three bands (72, 157 and 229 bp) were visible, the cases were considered as heterozygotes. We repeated the experiments at least two times, including PCR and enzyme cleavage, to ensure the results, and the data were consistent (Fig. 1).

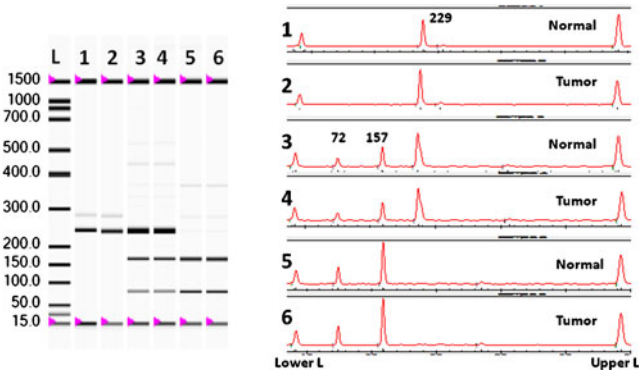

Fig. 1 PCR restriction by StyI enzyme: *Lane L*, ladder 1,500 pb. *Lane 1*, normal sample of patient with only 229-bp band. *Lane 2*, tumoural sample with GC/GC genotype. *Lane 3*, normal sample with GC/AT genotype with 229-bp, 157-bp and 72-bp bands. *Lane 4*, tumoural sample with GC/AT genotype. *Lane 5*, normal sample with AT/AT genotype with 157-bp and 72-bp bands. *Lane 6*, normal sample with AT/AT genotype. The patterns of the electropherograms representing PCR-restriction digests products derived from normal tissue, and tumoural tissue are perfectly matching and demonstrate no loss of heterozigisity

Immunohistochemistry staining

The p73 antibody used was an affinity-purified goat polyclonal antibody (Santa Cruz Biotechnology, Santa Cruz, CA, diluted 1/150) against a peptide in the C-terminus of the human isoform p73b. The antibody reacts with both p73a and p73b of human origin and it recognises the total p73 protein including full length and truncated isoforms. However, TAp73 and ΔNp73 antibodies are isoform-specific. The TAp73 is a mouse monoclonal p73 antibody (KAM-CC242F, clone 5B429; Stressgen, Victoria, Canada, diluted 1/100) epitope corresponding to the NH2-terminal region (this antibody recognises the TAp73 isoforms but does not detect the ΔNp73 variant or p53) and the ΔNp73 is a mouse monoclonal ΔNp73 antibody (clone number 38C674; abcam Inc; Cambridge, UK; diluted 1/2000) developed against a peptide corresponding to amino acids 2–13 of human ΔNp73 (LYVGDPARHLAT). This antibody does not cross-react with any TAp73 isoform or p53. Sections from paraffin-embedded tissue blocks were incubated in an oven at 37°C over night and were then deparaffinized in Toluene and hydrated in descending concentrations of ethanol and finally in double distilled H_2O. The activity of endogenous peroxidase was blocked in 3% H_2O_2 in distilled water for 10 min. To expose masked epitopes, the sections were microwaved in citrate buffer (pH 6.0) for 2×5 min, and then kept at room temperature for 20 min, followed by a Tris-wash for 2 min, and then the sections were washed three times in Tris. The primary antibodies were added and then incubated at 4°C over night. After washing with Tris, the antibodies binding was detected by incubating the sections at room temperature with the peroxidase-labelled DAKO Envision System (Dual

Link System Peroxidase, DakoCytomation Envision +) for 30 min, using DAB as a chromogene for 20 min. After washing with distilled water, the sections were then counterstained with haematoxylin. Two pathologists interpreted the results without knowledge of clinical and pathological information. To avoid artificial effect, cells in areas with necrosis, poor morphology or in the margins of sections were not counted. Total p73, TAp73 and ΔNp73 proteins were considered positive in tissue samples exhibiting nuclear or cytoplasmic staining in >10% of epithelial cells. The staining intensity was closely compared between the samples of normal mucosa, primary tumour and metastasis, from the same patient. Furthermore, we correlate p73 expression with clinicopathological features.

Statistical analysis

χ^2 and McNemar's methods were used to test significance of the difference in frequency of genotypes/alleles between normal samples and primary tumour and metastases and for testing the frequency of genotypes/alleles between colorectal cancer patients and controls or association of p73 GC/AT polymorphism with clinical and pathological factors. Cox's proportional hazards model was used to estimate the relationship between the p73 GC/AT polymorphism and survival. The curves describing survival were computerised according to Kaplan and Meier using software developed by SPSS (v17). Tests were two sided, and $p<0.05$ was considered statistically significant.

Results

The p73 polymorphism in colorectal cancer patients and healthy controls

There were no significant differences of the frequencies of the three genotypes: GC/GC, GC/AT and AT/AT, between the patients and controls ($p=0.11$, Table 1). The patients had a higher frequency of AT/AT (17 versus 11%) but a lower frequency of GC/AT genotype (31 versus 35%), compared with that of the controls. There was no statistically significant difference in the allele frequency between cases and controls ($p=0.61$, data not shown). Forty-seven cases were heterozygotic, and we did not show LOH of the p73 gene.

Table 1 Frequencies of p73 genotype in colorectal cancer patients and healthy controls

Genotype	Patients *n* (%)	Controls *n* (%)	OR (95% CI)
GC/GC	77 (52)	109 (54)	1.0
GC/AT	47 (31)	73 (35)	0.91 (0.56–1.50)
AT/AT	26 (17)	22 (11)	1.67 (0.84–3.33)
			$p=0.11$

Immunostaining of total p73, TAp73 and ΔNp73 in normal mucosa and primary and metastatic tumours

As shown in Table 2, 26% of normal mucosa exhibited p73 positive characteristics, 75% in primary tumours and 97% in metastasis. In matched samples, the frequency and the intensity of the total-p73 immunostaining were increased markedly from normal tissue to primary tumour and to metastasis ($p<10^{-8}$, Fig. 2). In most of the negative primary tumours, the corresponding metastatic tumours were p73 positive. Furthermore, the expression of p73 in primary tumours revealed in all the cases a stronger immunostaining than normal mucosa. Moreover, Both TAp73 and ΔNp73 forms were found to be significantly up-regulated from normal tissue to primary tumour and to metastasis (Fig. 3). TAp73 immunoreactivity was observed intense and diffuse in 25%, 73% and 58% in normal mucosa, in primary tumours and in metastasis, respectively ($p<10^{-8}$, Table 2). Expression of ΔNp73 protein was intense and diffuse, like TAp73, in 21%, 68% and 94% in normal mucosa, in primary tumours and in metastasis, respectively ($p<10^{-8}$, Table 2).

The relationship between the expression of the three proteins and patient's survival

The patients with total p73 positive tumours had significantly shorter survival than those with p73 negative tumours ($p=0.0001$; Fig. 4a). Furthermore, the patients with ΔNp73 positive tumours had significantly shorter survival than those with ΔNp73 negative tumours ($p=0.029$; Fig. 4b). However, there were no significant differences in the survival of patients between TAp73 positive or negative tumours ($p=0.69$; Fig. 4c).

The relationship between the p73 polymorphism and immunohistochemical staining of the three proteins

The genotypes of the polymorphism and the staining intensity of the three p73 antibodies in tumours were analysed and summarised in Table 3. We were unable to find any significant difference between tumoural immunostaining of total p73 and frequencies of the three genotypes ($p=0.16$). However, we observed that the samples with the AT/AT genotype showed a slight tendency towards stronger expression of the p73 protein in tumour. Moreover, the heterozygotic samples express a lower level of the p73 protein compared with samples with AT/AT genotype but a stronger expression than those with GC/GC genotype.

Table 2 Expression of the three proteins; total p73, TAp73 and ΔNp73 in normal mucosa, and primary and metastatic tumours from patients with colorectal adenocarcinoma

	Normal mucosa *n* (%)	Primary tumour *n* (%)	Metastatic tumour *n* (%)	*p*
Total p73				
Positive	39 (26)	113 (75)	66 (97)	$<10^{-8}$
Negative	111 (74)	37 (25)	2 (3)	
TAp73				
Positive	38 (25)	110 (73)	58 (58)	$<10^{-8}$
Negative	112 (75)	40 (27)	10 (15)	
ΔNp73				
Positive	32 (21)	102 (68)	64 (94)	$<10^{-8}$
Negative	118 (79)	48 (32)	4 (6)	

Interestingly, when we analysed the two isoforms of p73, we found a significant correlation between ΔNp73 tumoural immunostaining and frequencies of the three genotypes (p=0.0005) but not between TAp73 immunoreactivity and the genotypes (p=0.13).

The relationship between the p73 polymorphism and clinical and pathological variables

We did not find any relationship of the genotypes with gender, age, tumour site, TNM stage, growth pattern, histological subtype and differentiation (Table 4).

The relationship between the p73 polymorphism and patient's survival

A significant association between the genotypes and survival was found in the patients (p=0.0001, Fig. 5). The patients with the AT/AT genotype had a worse prognosis compared with those with both GC/AT and GC/GC variants. Further, patients with GC/GC genotype had a more favourable survival than those with GC/AT genotype.

Discussion

The mechanisms how p73 GC/AT polymorphism influences cancer development and progression is currently unknown, including CRC. Herein, we report an investigation study concerning the involvement of this polymorphism in CRC risk. Besides, the role of this polymorphism in cancer risk has been investigated extensively in a variety of cancers and the results are inconsistent. Indeed, some studies even fail to find any association between this polymorphism and risk of several types of cancer. We note as example, the early Japanese studies that did not find evidence for an association with risk of cancer: one study included 192 histologically confirmed non-small-cell lung cancer cases and 241controls [23]; one included 200 breast cancer patients and 282 controls [24]; and another included 102 esophageal cancer patients, 144 stomach cancer patients and 241 patient controls [19]. However, other studies found a significant association between this polymorphism and cancer risk, although their suggestions are very controversial not only from a population to the other one but also from cancer to other type of cancer. Indeed, one recent Japanese study with 112 cervical cancer patients found that this p73 GC/AT

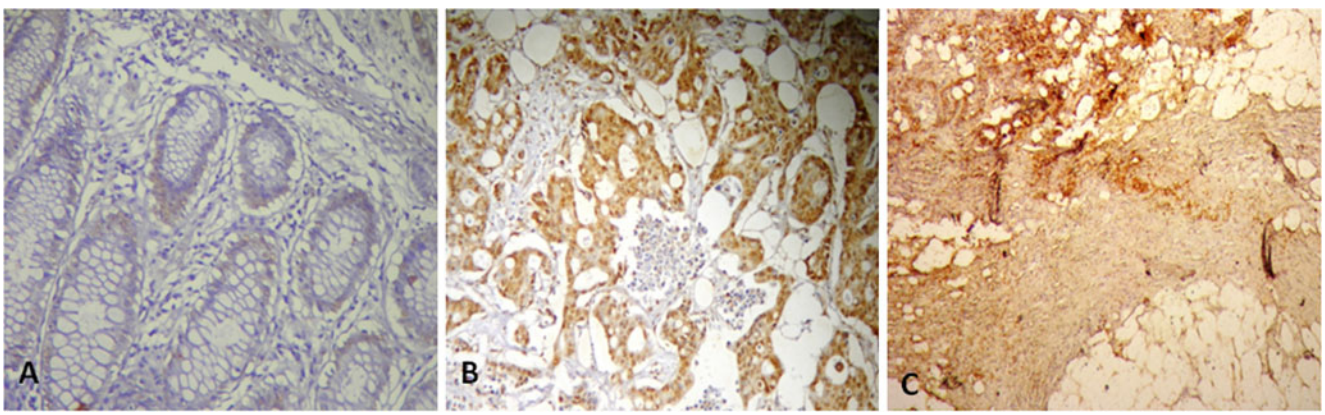

Fig. 2 The immunohistochemical staining of p73. **a** The normal mucosa weakly expressed p73 protein (original magnification, ×400). **b** The corresponding primary tumour shows p73-nuclear-positive staining in the tumour cells (original magnification, ×200). **c** Corresponding metastases reveals even stronger p73 staining throughout the tumour cells (original magnification, ×200)

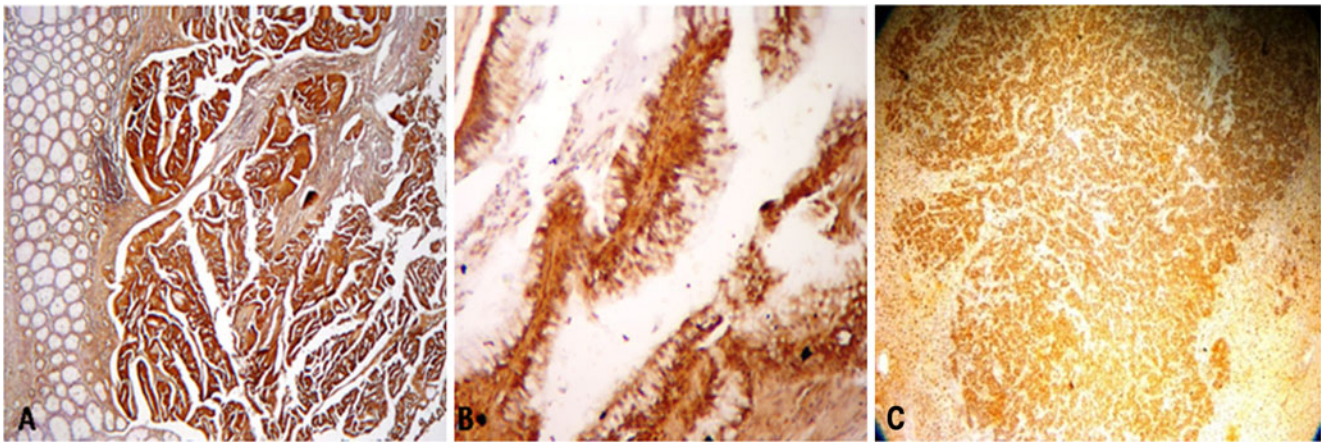

Fig. 3 The immunohistochemical staining of p73 isoform. **a** ΔNp73 protein was over-expressed in primary tumour compared with normal mucosa (original magnification, ×40). **b** Strong immunostaining of TAp73 isoform in tumour (original magnification, ×200). **c**. Strong immunostaining of ΔNp73 isoform in metastasis (original magnification, ×200)

polymorphism was associated with a borderline increased risk (OR, 1.57; 95% CI, 0.99–2.48) [25]. Moreover, in Chinese population, Hongxia Li et al. showed that the GC/GC genotype is significantly associated with poor prognosis of 526 patients with breast cancer [26]. Guojun Li et al. reviewed a much larger samples size composed of 1,056 cases patients and 1140 control subjects and showed that p73 variants AT alleles was associated with increasing risk of lung cancer in non-Hispanic white population [27]. Also, opposite suggestions were available concerning CRC. In fact, with respect to prognostic study, there is only one study evaluating the significant association of the p73 GC/AT polymorphism with overall survival in CRC from Swedish population, Pfeifer et al. reported that patients with the GC/GC genotype had worse outcome than those with the AT variants (AT/AT+GC/AT) [22]. However, Hamajima et al. did not find any relationships between this polymorphism and the risk of the digestive tract cancers including CRC in a Japanese population [19].

In this frame, this study is the first p73 GC/AT polymorphism report in Tunisian population that may represent the Maghreb's population since they have the same environmental and social factors. In the present study, we investigated the prognostic value of the p73 polymorphism in CRC. We showed here, for the first time, that the AT/AT genotype was significantly associated with poor prognosis in Tunisian patients with CRC unlike Pfeifer's study. These conflicting data and the varying results lead to suggest a different role for this p73 GC/AT polymorphism in different ethnic groups, possibly based on race, gender, age, environmental and social factors, and even clinicopathological characteristics of the patients. In fact, there were statistical differences of the genotype frequency between populations. Indeed, the genotype frequencies in Tunisian population were significantly different from American (p=0.04), Swedish (p=0.001) and Japanese populations (p=0.009) and the genotypes frequency in these four populations are; GC/GC, GC/AT and AT/AT were 54%, 35% and 11% in Tunisian, 61%, 37% and 2% in Swedish [22], 63%, 32% and 6% in American [21] and 55.3%, 40.4% and 4% in Japanese [19].

Here, we report a more elevated frequency of the AT/AT genotype in both patients and controls subjects, 17% and 11%, respectively, compared with the other world sets. Similarly to the other studies on the different cancer types, we also observed that the patients had a high frequency of AT/AT genotypes (17 versus 11%), compared with that of the controls. Furthermore, we found a significant association between the genotypes and survival. The AT/AT genotype was significantly associated with poor prognosis and shorter survival. The patients with the GC/AT genotype had a more favourable survival than those with AT/AT genotype, but showed to have shorter survival than those with GC/GC genotype. In order to know whether the GC/AT genotype was also associated with poor prognosis, we first analysed the association of survival of GC/AT and GC/GC and secondly those of GC/AT and AT/AT. Indeed, there were no significant difference between the two genotypes (GC/AT, GC/GC) and survival (p=0.108, Fig. 6a). However, we found a significant difference between GC/AT and AT/AT (p=0.0001, Fig. 6b). Thus, only the AT/AT genotype appears to be associated with a pejorative prognosis and development of the CRC, although there were no significant differences in the frequencies of the three genotypes between the patients and controls (p=0.11).

Besides, our results further support the evidence that the over-expression of the p73 protein was related to development and poor prognosis in cancer patients. Indeed, we found in this study, like many other ones [15, 16], an increased p73 expression in frequency and intensity from the normal samples to primary tumours and to metastasis. Moreover, the patients with p73-positive tumours had significantly

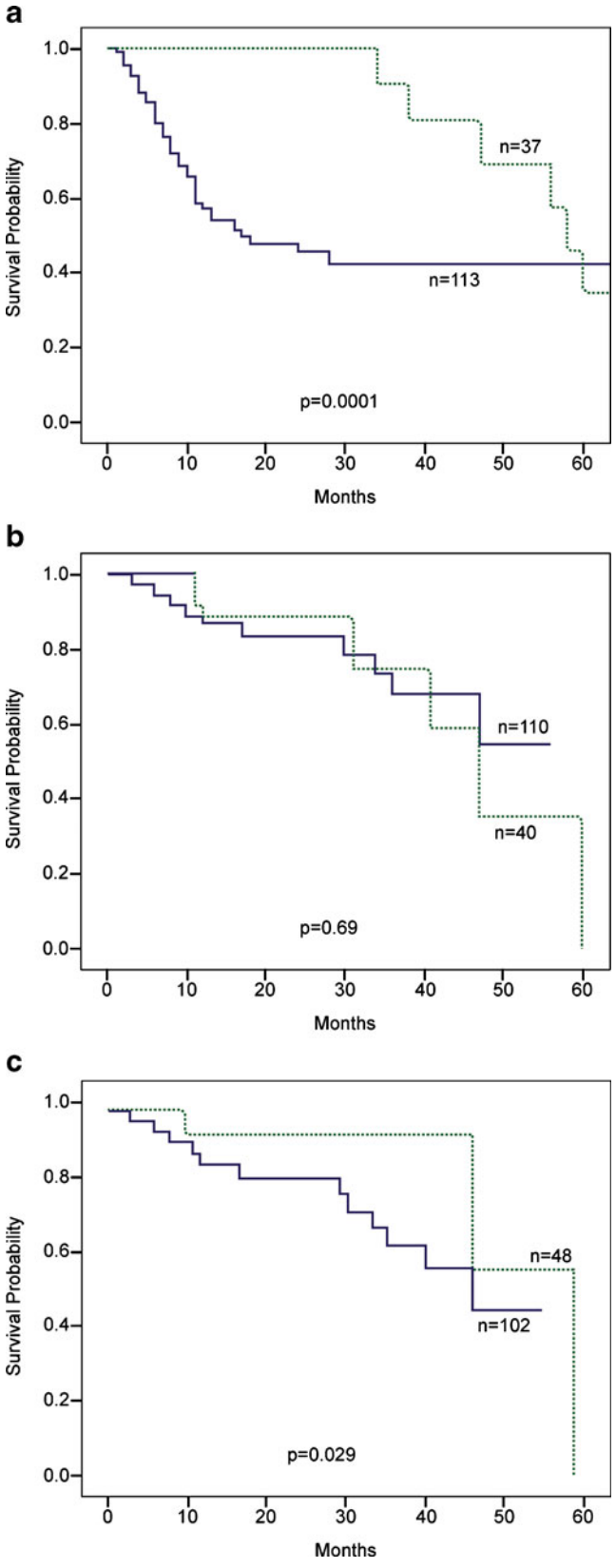

◀ **Fig. 4** The expression of the three proteins in relation to survival in colorectal cancer patients: **a** patients with total p73-positive tumours had shorter survival than those with p73-negative tumours (p=0.0001). **b** No significant difference between TAp73 immunostaining and patient's survival (p=0.69). **c** Patients with ΔNp73-positive tumours had shorter survival than those with p73-negative tumours (p=0.029)

shorter survival than those with p73-negative tumours (p= 0.0001). We note as remark that, among the p73 positive cases, some ones with AT/AT genotype showed to be more stained than those with GC/AT and GC/GC. But this observation can not be supported by statistical analyses because there are a weak number of observed cases. However, In CRC it has been shown that patients with the AT/AT genotype exhibited a slightly lower p73 expression in their tumours than those with the GC/GC genotype, but the difference did not reach statistical significance, moreover, the antibody used cannot discriminate TAp73 or ΔNp73 [22].

Indeed, the p73 gene has two protein isoforms with functionally different properties, coming to the use of different promoters and alternative splicing [28]. The transactivation proficient isoform TAp73 shows pro apoptotic effects, while the NH2-terminally truncated isoform ΔNp73 has anti-apopototic function [29, 30]. In the present study, we also explore for the first time, whether the p73 GC/AT polymorphism was associated with the expression of TAp73 and/or ΔNp73 to elucidate the functional consequences of this important polymorphism in CRC.

We found firstly, that suppressor TAp73 and putative oncogenic ΔNp73 are co-expressed in tumour samples. Thus, we suggest that even though TAp73 variants are up-regulated, the oncogenic isoforms may cancel their suppressor function, resulting in a prevalent oncogenic activity. It is possible that the presence of ΔNp73 variants, completely suppresses the transactivating activity of TAp73, with the consequent

Table 3 Relationship between p73 GC/AT polymorphism and tumoural staining of the three proteins

Staining	Genotype *n* (%)			*p*
	GC/GC	GC/AT	AT/AT	
Total p73				
Positive	52 (67)	39 (83)	19 (73)	0.16
Negative	25 (33)	8 (17)	7 (27)	
TAp73				
Positive	51 (66)	39 (83)	19 (73)	0.13
Negative	26 (34)	8 (17)	7 (27)	
ΔNp73				
Positive	40 (52)	43 (91)	19 (73)	0.0005
Negative	37 (48)	4 (9)	7 (27)	

Table 4 Relationship between characteristics of the patients and p73 genotypes

Genotype *n* (%)				
Characteristics	GC/GC	GC/AT	AT/AT	*p*
Sex				
Male	43 (58)	20 (49)	17 (65)	0.38
Female	31 (42)	21 (51)	9 (35)	
Age (year)				
<70	35 (47)	25 (53)	8 (33)	0.28
≥70	39 (53)	22 (47)	16 (67)	
Site				
Left Colon	40 (55)	30 (71)	13 (55)	0.19
Right Colon	33 (45)	12 (29)	10 (45)	
TNM Stage				
pT1	7 (9)	3 (7)	2 (9)	0.55
pT2	24 (33)	8 (19)	5 (22)	
pT3	36 (49)	30 (67)	15 (60)	
pT4	7 (9)	3 (7)	2 (9)	
Growth pattern				
Infiltrating	48 (65)	23 (52)	11 (45)	0.17
Expanding	26 (35)	21 (48)	13 (55)	
Differentiation				
Well	36 (47)	30 (63)	13 (49)	0.40
Moderately	12 (15)	6 (14)	5 (20)	
Poorly	29 (38)	11 (23)	8 (31)	
Histological type	36 (47)	30 (63)	13 (49)	
Non-mucinous	45 (59)	34 (73)	16 (63)	0.29
Mucinous	32 (41)	13 (27)	10 (37)	

There was no information available on patient's sex in nine cases, age in five cases, tumour location in 12 cases, TNM stage in eight cases and growth pattern in eight

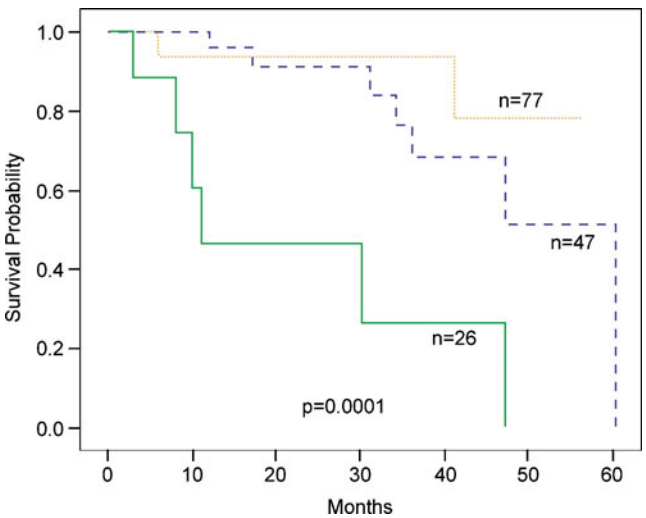

Fig. 5 The genotype of the p73 in relation to survival in colorectal cancer patients: the patients with the AT/AT genotype had a shorter survival than those who carried the other genotypes

elimination of essential TAp73 anti-tumorigenic function. In addition, at the protein level, ΔNp73 isoforms have been described to be more stable than those of TAp73 [29–31]. Thus, upregulation of ΔNp73 variants indicates that they may be of value as molecular prognostic markers. In this frame, we confirmed in the present study that elevated level of ΔNp73 is associated to poor prognosis in patient with CRC, since, we shown an increased ΔNp73 expression in frequency and intensity from the normal samples to primary tumours and to metastasis. Moreover, the patients with ΔNp73 positive tumours had significantly shorter survival than those with ΔNp73 negative tumours (p=0.029). Whereas, there were no significant difference between TAp73 immunostaining and patient's survival (p=0.69).

Secondly, we found a significant association between ΔNp73 tumoural immunostaining and the p73 GC/AT

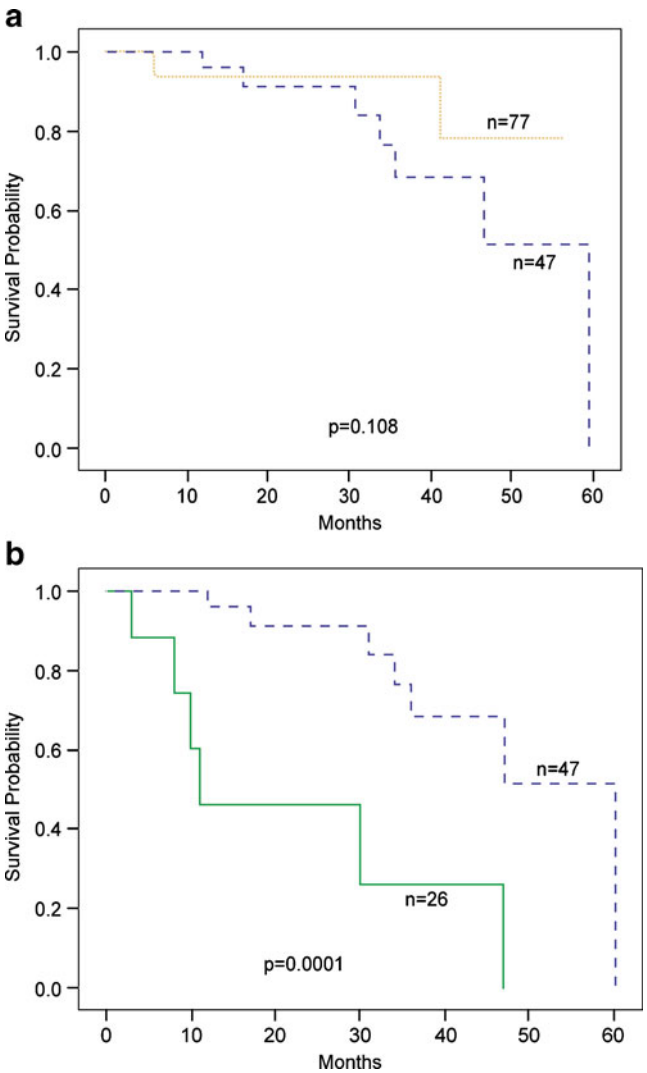

Fig. 6 The genotype of the p73 in relation to survival in colorectal cancer patients. **a** No significant difference between the two genotypes (GC/AT, GC/GC) and survival (p=0.108). **b** A significant difference between (GC/AT, AT/AT) and survival (p=0.0001)

polymorphism (p=0.0001). We found that patient with GC/AT and AT/AT genotype expressed 73% and 91% of the ΔNp73 variants, respectively, compared to GC/GC genotype with 52%. Thus, certain genotypes may therefore alter the balance between the p73 isoforms, favouring the expression of a certain isoform possibly disturbing the otherwise tightly regulated balance between pro- and anti-apoptotic signals.

Therefore, the p73 GC/AT polymorphism especially the presence of the AT allele may be considered as a valuable prognostic marker to predict poor outcome for the patients with CRC. Very recently, Lööf et al. suggested that rectal cancer patients treated with radiotherapy with the GC/GC genotype had better disease-free survival than those carrying the AT allele and shows that the p73 GC/AT polymorphism might be a factor influencing the response to preoperative radiotherapy [32].

However, this polymorphism is not the only factor involved in CRC development, but it might act as an enhancer of the progress, since p73 especially ΔNp73 variants, has been seen to interact with many genes involved in cancer development. It has, for example, been seen to interact with oncogenic ras in cellular transformation [33, 34] and with E2F-1, which increases the abundance of p73 mRNA. The levels of p73 then fluctuate through the cell cycle as a response to the E2F-1 activity [35].

On the other hand, in our present work, LOH of the p73 locus was not observed in all informative (GC/AT heterozygote) CRC cases, although the 1p36 locus is a site observed to have frequent loss of heterozygosity in various human cancers [36]. Pfeifer et al. support our finding, since they did not show LOH of the p73 gene in 54 heterozygotic cases [22]. However, in the most recent report including prostatic [5], noroblastoma [11], lung [12] and oesophageal cancers [13], they found LOH in 64% of all heterozygotic cases, in 82% of instances, there was loss of the AT allele [14], contrary to that observed in our current study. In fact, we only looked at the 229 bp surrounding the polymorphism. Our findings therefore might support that LOH of the p73 was not a frequent event in CRC, at least not in the area around the polymorphism. In the other hand, we did not exclude a possibility of contamination of tumour DNA with DNA derived from non-neoplastic cells that is known to affect the accuracy of molecular analyses. However, according to the immunohistochemical staining, the heterozygotic samples did not express a lower level of the p73 protein comparing with the samples with other genotypes if an allele is really lost. But, the immunohistochemical analysis only, could not inform us about the allelic loss in the homozygous cases because the protein expression does not change even if the LOH occurred. So, we need further quantitative molecular investigation for a better evaluation of the exact frequency of the loss of heterozygosity.

Conclusion

In summary, in the present study we found that the AT/AT genotype is strongly associated with poor clinical outcome in CRC. Thus, analysis of p73 GC/AT polymorphism may be useful in identifying the CRC patients that have a higher potential to progress towards a bad issue of the disease.

Acknowledgment This study was supported by a grant from the Ministry of the technology and the scientific research.

Conflict of interest The authors declare that they have no conflict of interest.

References

1. Kaghad M, Bonnet H, Yang A et al (1997) Monoallelically expressed gene related to p53 at 1p36, a region frequently deleted in neuroblastoma and other human cancers. Cell 90:809–819
2. Flores ER, Tsai KY, Crowley D et al (2002) p63 and p73 are required for p53-dependent apoptosis in response to DNA damage. Nature 416:560–564
3. Wang XQ, Ongkeko WM, Lau AW, Leung KM, Poon RY (2001) A possible role of p73 on the modulation of p53 level through MDM2. Cancer Res 61:1598–1603
4. Mai M, Yokomizo A, Qian C et al (1998) Activation of p73 silent allele in lung cancer. Cancer Res 58:2347–2349
5. Takahashi H, Ichimiya S, Nimura Y et al (1998) Mutation, allelotyping and transcription analyses of the p73 gene in prostatic carcinoma. Cancer Res 58:2076–2077
6. Yokomizo A, Mai M, Tindall DJ et al (1999) Overexpression of the wild type p73 gene in human bladder cancer. Oncogene 18:1629–1633
7. Yang A, Walker N, Bronson R et al (2000) p73-deficient mice have neurological, pheromonal and inflammatory defects but lack spontaneous tumours. Nature 404:99–103
8. Moll UM, Erster S, Zaika A (2001) p53, p63 and p73—solos, alliances and feuds among family members. Biochim Biophys Acta 1552:47–59
9. Benard J, Douc-Rasy S, Ahomadegbe JC (2003) TP53 family members and human Cancers. Hum Mutat 21:182–191
10. Coates PJ (2006) Regulating p73 isoforms in human tumours. J Pathol 210:385–389
11. Ichimiya S, Nimura Y, Kageyama H et al (1999) p73 at chromosome 1p36.3 is lost in advanced stage neuroblastoma but its mutation is infrequent. Oncogene 18:1061–1066
12. Nomoto S, Haruki N, Kondo M, Konishi H, Takahashi T (1998) Search for mutations and examination of allalic expression imbalance of the p73 gene at 1p36.33 in human lung cancers. Cancer Res 58:1380–1383
13. Nimura Y, Mihara M, Ichimiya S et al (1998) P73, a gene related to p53, is not mutated in esophageal carcinomas. Int J Cancer 78:437–440
14. Cai Y, Yang GY, Nie Y et al (2000) Molecular alterations of p73 in human esophageal squamous cell carcinomas: loss of heterozygosity occurs frequently; loss of imprinting and elevation of p73 expression may be related to defective p53. Carcinogenesis 21:683–689
15. Sun XF (2002) p73 Overexpression is a prognostic factor in patients with colorectal adenocarcinoma. Clin Cancer Res 8:165–170

16. Guan M, Peng HX, Yu B, Lu Y (2003) p73 overexpression and angiogenesis in human colorectal carcinoma. Jpn J Clin Oncol 33:215–220
17. Herath NI, Kew MC, Whitehall VL et al (2000) p73 is up-regulated in a subset of hepatocellular carcinomas. Hepatology 31:601–605
18. Zaika AI, Kovalev S, Marchenko ND et al (1999) Overexpression of the wild type p73 gene in breast cancer tissues and cell lines. Cancer Res 59:3257–3263
19. Hamajima N, Matsuo K, Suzuki T et al (2002) No association of p73 G4C14-to-A4T14 at exon 2 and p53 Arg72Pro polymorphism with the risk of digestive tract cancers in Japanese. Cancer Lett 181:81–85
20. Ryan BM, McManus R, Daly JS et al (2001) A common p73 polymorphism is associated with a reduced incidence of oesophageal carcinoma. Br J Cancer 85:1499–1503
21. Li G, Sturgis EM, Wang LE et al (2004) Association of a p73 exon 2 G4C14-to-A4T14 polymorphism with risk of squamous cell carcinoma of the head and neck. Carcinogenesis 25:1911–1916
22. Pfeifer D, Arbman G, Sun X-F (2005) Polymorphism of the p73 gene in relation to colorectal cancer risk and survival. Carcinogenesis 26:103–107
23. Hiraki A, Matsuo K, Hamajima N et al (2003) Different risk relations with smoking for non–small-cell lung cancer: comparison of TP53 and TP73 genotypes. Asian Pac J Cancer Prev 4:107–112
24. Huang XE, Hamajima N, Katsuda N et al (2000) Association of p53 codon Arg72Pro and p73 G4C14-to-A4T14 at exon 2 genetic polymorphisms with the risk of Japanese breast cancer. Breast Cancer 10:307–311
25. Niwa Y, Hamajima N, Atsuta Y et al (2004) Genetic polymorphisms of p73 G4C14-to-A4T14 at exon 2 and p53 Arg72Pro and the risk of cervical cancer in Japanese. Cancer Lett 205:55–60
26. Li H, Yao L, Ouyang T et al (2007) Association of p73 G4C14-to-A4T14 (GC/AT) polymorphism with breast cancer survival. Carcinogenesis 28:372–377
27. Li G, Wang Li-E, Chamberlain RM, Amos CI, Spitz MR, Wei Q (2004) p73 G4C14-to-A4T14 Polymorphism and Risk of Lung Cancer. Cancer Res 64:6863–6866
28. Melino G, De Laurenzi V, Vousden KH (2002) P73: friend or foe in tumorigenesis. Nat Rev Cancer 2:605–615
29. Grob TJ, Novak U, Maisse C et al (2001) Human delta Np73 regulates a dominant negative feedback loop for TAp73 and p53. Cell Death Differ 8:1213–1223
30. Ishimoto O, Kawahara C, Enjo K et al (2002) Possible oncogenic potential of DeltaNp73: a newly identified isoform of human p73. Cancer Res 62:636–641
31. Stiewe T, Theseling CC, Putzer BM (2002) Transactivation-deficient Delta TA-p73 inhibits p53 by direct competition for DNA binding: implications for tumorigenesis. J Biol Chem 277:14177–14185
32. Lööf J, Pfeifer D, Adell G, Sun X-F (2009) Significance of an exon 2 G4C14-to-A4T14 polymorphism in the p73 gene on survival in rectal cancer patients with or without preoperative radiotherapy. Radiother Oncol 92:215–220
33. Petrenko O, Zaika A, Moll UM (2003) deltaNp73 facilitates cell immortalization and cooperates with oncogenic Ras in cellular transformation in vivo. Mol Cell Biol 23:5540–5555
34. Fernandez-Garcia B, Vaque JP, Herreros-Villanueva M et al (2007) p73 cooperates with Ras in the activation of MAP kinase signaling cascade. Cell Death Differ 14:254–265
35. Melino G, Lu X, Gasco M, Crook T, Knight RA (2003) Functional regulation of p73 and p63: development of cancer. Trends Biochem Sci 28:663–670
36. Shan L, Yang Q, Nakamura M et al (2001) Frequent loss of heterozygosity at 1p36.3 and p73 abnormality in parathyroid adenomas. Mod Pathol 14:273–278

Virchows Arch (2010) 457:369–380
DOI 10.1007/s00428-010-0949-x

ORIGINAL ARTICLE

Obliterative airway remodelling in transplanted and non-transplanted lungs

Danny Jonigk · Katharina Theophile · Kais Hussein · Oliver Bock · Ulrich Lehmann · Clemens L. Bockmeyer · Jens Gottlieb · Stefan Fischer · Andre Simon · Tobias Welte · Lavinia Maegel · Hans Kreipe · Florian Laenger

Received: 22 April 2010 / Revised: 28 June 2010 / Accepted: 6 July 2010 / Published online: 15 July 2010
© Springer-Verlag 2010

Abstract Obliterative airway remodelling is a morphological sequence in a variety of pulmonary diseases. Notably, bronchiolitis obliterans represents one of the key complications of lung transplantation, induced by (immigrating) myofibroblasts. A comparative expression analysis of obliterative airway remodelling in transplanted and non-transplanted patients has not been reported so far. Obliterated and unremodelled airways from explanted lungs (n=19) from patients suffering from chronic allograft dysfunction, infection, graft-versus-host disease and toxic exposure were isolated by laser-assisted microdissection. Airways from lung allografts harvested shortly before and after transplantation (n=4) as well as fibroblastic foci from lungs with interstitial pulmonary fibrosis (n=4) served as references. Pre-amplified cDNA was analysed by quantitative real-time RT-PCR for expression of fibrosis, inflammation and apoptosis-associated genes. Composition of infiltrating cells and protein expression were assessed by conventional histology and immunohistochemistry. Bronchiolitis obliterans in transplanted patients showed a significant increase of BMP-7 expression (p=0.0141 compared with controls), while TGF-β1 and FGF-2 as well as BMP-4 and BMP-7 were up-regulated in fibroblastic foci in interstitial pulmonary fibrosis (p<0.0424 compared with controls). Regarding other fibrosis-associated genes (BMP-6, SMAD-3, CASP-3 and CASP-9, FASLG, NF-KB1, IL-1 and IL-2) as well as cellularity and cellular composition, no significant differences between obliterative airway remodelling in transplanted and non-transplanted patients could be shown. Obliterative airway remodelling in lung allografts and in non-transplanted patients share many morphological and genetic traits. BMPs, especially BMP-7, warrant further investigation as possible markers for the aggravation of airway remodelling.

Keywords Bronchiolitis obliterans · Lung transplantation · Fibrosis · Airway remodelling

D. Jonigk (✉) · K. Theophile · K. Hussein · O. Bock · U. Lehmann · C. L. Bockmeyer · L. Maegel · H. Kreipe · F. Laenger
Institute of Pathology, Hannover Medical School,
Carl-Neuberg-Str. 1,
30625 Hannover, Germany
e-mail: jonigk.danny@mh-hannover.de

J. Gottlieb · T. Welte
Department of Pneumology, Hannover Medical School,
Carl-Neuberg-Str. 1,
30625 Hannover, Germany

S. Fischer · A. Simon
Department of Cardiothoracic and Vascular Surgery,
Hannover Medical School,
Carl-Neuberg-Str. 1,
30625 Hannover, Germany

Introduction

Fibrous obliterative airway remodelling (OAR) of the bronchioli can be found in a variety of pulmonary conditions: post-lung transplant obliterative bronchiolitis, infectious processes, toxic exposure, idiopathic fibrotic lung disease (IPF) and collagen vascular disease with pulmonary involvement [1]. OAR occurs in two major forms differing in their distribution in the lung parenchyma as well as in their clinical setting: (1) the slowly progressing obliteration of bronchioles by plugs of collagenous stroma called bronchiolitis obliterans (BO). It is the most significant contributing factor to late mortality after allogeneic lung transplantation. While patient survival in the first year following lung transplantation (LTx) has significantly

increased due to improvements in surgical approach and clinical management, the 5-year survival does not exceed 50% on a worldwide scale, the main reason being BO, the hallmark of chronic graft dysfunction [2]. (2) Obliteration involving the distal bronchioles and adjacent alveoli by granulation tissue like mesenchymal proliferation is referred to as cryptogenic organising pneumonia (COP, formerly known as BOOP).

Though primarily a disease of the lung interstitium, the usual interstitial pneumonia (UIP) pattern of idiopathic fibrosing lung disease comprises interstitial, peribronchial and intrabronchial proliferations of myofibroblasts, so-called fibroblastic foci. These represent the forefront of remodelling that ultimately leads to interstitial scarring and end-stage lung disease and can exhibit a BO-like pattern.

In all of the above-mentioned disease processes, airway and interstitial remodelling involves the excess deposition of extracellular matrix (ECM), which is mainly produced by activated myofibroblasts [3, 4]. These are capable of fabricating more than 5,000 molecules of procollagen per minute, can exert active contraction on the surrounding tissue and have been shown to derive from three different sources: (1) transformation of local fibroblasts to a myofibroblast phenotype, (2) immigration and incorporation of circulating myofibroblasts (or their precursors) from the bloodstream and (3) epithelial–mesenchymal transition. Previously, we were able to demonstrate that substantial numbers of myofibroblasts involved in the formation of BO in transplanted patients derive from the bone marrow of the recipients [5]. In fibrous remodelling of the lung, the balance of collagen turnover is toppled in favour of ECM deposition. Physiologically, this equilibrium is controlled by matrix metalloproteinases, their inhibitors and various cytokines, like bone morphogenetic proteins (BMPs) and other members of the transforming growth factor-beta (TGF-β) superfamily [6]. Especially, TGF-β1 and its downstream Sma and Mad-related protein (SMAD) cascade are the pivotal proteins in the regulation of ECM production. Induction of TGF-β1 and post-receptor SMADs is a very common finding in active fibrosing lesions, as it is a converging pathway that incorporates other pro-fibrotic mediators such as fibroblast growth factor-2 (FGF-2), tumour necrosis factor-alpha and nuclear factor kappa-B (NF-kappa-B) [7–9].

While it has been shown that some of these underlying pathways are identical in different fibrotic diseases of the lung, the morphological process of remodelling manifests itself in divergent compartments and patterns. As outlined above, BO, COP and UIP all involve remodelling of distal airways, and so far, most research on airway remodelling has been performed in animal models, in vitro studies or analysis of total tissue samples from explanted human lungs. Therefore, our aim was to focus on the affected small airways in a unique collective of transplanted and non-transplanted lung explants to further elucidate and compare the cellular composition and mediatory cytokine milieu contributing locally to fibrous remodelling. Cytokine profiles of airway obliteration in the human setting might point to the identification of possible markers of disease manifestation and aggravation and would be of great clinical value, especially in lung transplantation.

Materials and methods

Specimens

We examined a total of 23 lung specimens. Of these, 12 were explanted allografts exhibiting BO (time between transplantation and subsequent explantation of allograft, 1,707 days [arithmetic mean, standard deviation 1,002.1]; age at transplantation, 37.1 years [arithmetic mean, standard deviation 8.8]). In addition, samples from seven explanted native lungs (age at transplantation, 32.7 years [arithmetic mean, standard deviation 14.8]) with non-transplantation-associated OAR were analysed. Underlying diseases included COP pattern, BO as sequelae of graft-versus-host disease after bone marrow transplantation, radiation-induced airway fibrosis (RF) following Hodgkin lymphoma, idiopathic pulmonary fibrosis (focal BO pattern) and organising pneumonia following inhalation injury due to massive ammonia exposure in an occupational injury. Vital, unagitated distal bronchial tissue samples (n=4) taken from an allograft lung lobe, which had to be explanted due to a perfusion deficit of the distal parenchyma within 8 days after transplantation, served as a reference for mRNA and protein expression analysis in transplanted lungs. Distal bronchial tissue from surgically downsized donor lungs (n=3) resected before transplantation served as control for the non-transplanted setting. In addition, we analysed fibroblastic foci from four explanted lungs with IPF and a predominant usual interstitial pneumonia pattern (age at transplantation, 60.5 years [arithmetic mean, standard deviation, 8.9]), as an example of an extremely aggressive fibrosing lung disease. The formalin-fixed, paraffin-embedded samples (FFPE) were retrieved from the archives of the Institute of Pathology of Hannover Medical School and handled anonymously, following the requirements of the local ethics committee (Table 1).

Light microscopy and immunohistochemistry

Chronic inflammation was graded in obliterated bronchial lesions and adjacent non-obliterated bronchioli. A score ranging from 0 (no lymphohistiocytic infiltrate), 1 (singular lymphohistiocytic cells in the airway mucosa), 2 (circumferential band of lymphocytes/histiocytes) to 3 (broad circumferential band of lymphocytes/histiocytes with epi-

Table 1 Patient data

Patients n=23	Sex	Age at Tx date (years)	Time between Tx and explantation (days)	Explanted Tx—lung	Recipient lung	Underlying disease[a]
1	♀	38	1,777	X		CF
2	♂	33	1,845	X		CF
3	♂	30	2,247	X		CF
4	♀	31	4,083	X		CF
5	♂	36	1,141	X		CF
6	♀	36	1,015	X		CF
7	♀	23	423	X		CF
8	♀	30	2,389	X		CF
9	♂	50	33	X		AT1
10	♀	37	1,434	X		PH
11	♂	55	1,867	X		IPF
12	♀	46	2,230	X		BE
13	♀	31	n.a.		X	GvHD
14	♀	32	n.a.		X	GvHD
15	♀	63	n.a.		X	COP
16	♂	16	n.a.		X	COP
17	♂	41	n.a.		X	OI
18	♂	17	n.a.		X	IPF/BO
19	♀	29	n.a.		X	RF
20	♀	47	n.a.		X	IPF/UIP
21	♂	61	n.a.		X	IPF/UIP
22	♂	72	n.a.		X	IPF/UIP
23	♀	62	n.a.		X	IPF/UIP

CF cystic fibrosis, *AT1* alpha 1-antitrypsin deficiency, *PH* primary pulmonary hypertension, *IPF/BO* interstitial pulmonary fibrosis with distinct BO, *BE* bronchiectasis, *GvHD* graft-versus-host disease, *COP* cryptogenic organising pneumonia, *OI* occupational injury, *RF* radiation fibrosis, *IPF/UIP* interstitial pulmonary fibrosis with predominant UIP pattern, *n.a.* not applicable

[a] Disease leading to transplantation

thelial inflammation/necrosis) was assigned according to microscopic findings.

Serially cut slides from the samples which had been used for mRNA expression analysis (see above) were immunohistochemically stained for various fibrosis and inflammation-associated targets (SMADs 1, 2 and 3, phospho-SMAD 1/5 and 2/3, TGF-β1, BMP 1 and 7, VEGF-α, smooth-muscle actin (sma), smooth-muscle myosin heavy chain (smmhc), caldesmon, desmin, leukocyte antigens CD 45 and CD 68), using monoclonal antibodies following a standard ABC protocol (Table 2). Staining of the obliterated and non-obliterated small airways was scored semiquantitatively, ranging from no apparent reaction (score 0), positivity in less than 30% (score 1), in more than 30% and less than 60% (score 2) and in more than 60% of cells (score 3). Staining intensity was graded as weak, intermediate or strong. For negative controls, the primary antibody was replaced by BSA.

Laser-assisted microdissection and RNA extraction

FFPE tissue sections 5 μm thick were mounted on a poly-L-lysin-coated membrane fixed onto a metal frame. After deparaffinization and haemalum staining, the CellCut Plus system (MMI Molecular Machines & Industries AG, Glattbrugg, Switzerland) was used for laser-assisted microdissection. Anatomical structures (obliterated bronchioli [BO, Fig. 1a], non-obliterated bronchioli, hilus lymph nodes and peribronchial fibroblastic foci [from IPF, Fig. 1b]) were isolated using a no-touch technique, essentially as described (Fig. 2) [10]. Approximately 1,000 cells were harvested from serial sections in each compartment. Microdissected material was suspended in a proteinase K digestion buffer by placing it directly in the adhesive cap. After overnight digestion, RNA was isolated using phenol–chloroform extraction and subsequent precipitation following our established procedure [11].

Table 2 Antibodies

Antibody	Company	Dilution	Detection System
SMAD 1	Abnova	1:25	DAB Zytomed HRP kit
SMAD 2	Abnova	1:100	DAB Zytomed HRP kit
SMAD 3	Abnova	1:100	DAB Zytomed HRP kit
Phospho-SMAD 1/5	Cell Signalling	1:25	DAB Zytomed HRP kit
Phospho-SMAD 2/3	Cell Signalling	1:25	DAB Zytomed HRP kit
TGF-β1	Acris	1:500	DAB Zytomed HRP kit
BMP-1	R & D	1:50	DAB Zytomed HRP kit
BMP-7	Abnova	1:25	DAB Zytomed HRP kit
VEGF-A	Santa Cruz	1:50	DAB Zytomed HRP kit
Smooth-muscle actin	Dako	1:25	DAB Zytomed HRP kit
Smooth-muscle myosin heavy chain	US Biological	1:100	DAB Zytomed HRP kit
Caldesmon	Dako	1:60	DAB Zytomed HRP kit
Desmin	Dako	1:75	DAB Zytomed HRP kit
CD 45	Zytomed	1:50	DAB Zytomed HRP kit
CD 68	Dako	1:100	DAB Zytomed HRP kit

cDNA synthesis and pre-amplification

cDNA was synthesised, using the High Capacity cDNA Reverse Transcription Kit (Applied Biosystems, Foster City, CA, USA), following the manufacturer's protocol. This cDNA was pre-amplified in 14 PCR cycles with non-random PCR primers, thus increasing the sensitivity of the subsequent real-time PCR analysis several thousand-fold (decrease of C_T, 14 cycles; PreAmp Master Mix Kit, Applied Biosystems), as previously shown by us [11].

Real-time PCR and expression analysis

The pre-amplified cDNA from the laser-microdissected samples was evaluated by real-time PCR (TaqMan 7500 Real-Time PCR system, Applied Biosystems, Carlsbad, CA, USA). Quantification was performed in reactions containing pre-amplified cDNA, TaqMan Gene Expression Master Mix and the individual TaqMan Gene Expression Assay (both from Applied Biosystems). A panel of fibrosis-, anti-fibrosis-, apoptosis- and inflammation-associated genes was selected and analysed, following the manufacturer's protocol (transforming growth factor-beta 1 [TGF-β1], Sma and Mad-related protein-3 [SMAD-3], FGF-2, vascular endothelial growth factor-alpha VEGF-α, bone morphogenetic protein-4, -6 and -7 [BMP-4, BMP-6 and BMP-7], interleukin-1 and interleukin-2 [IL-1 and IL-2], FAS ligand [FASL], nuclear factor kappa-B [NF-kappa-B], lymphotoxin alpha [LTA], caspase-3 and caspase-9 and ribosomal protein 13a). For negative controls, cDNA was replaced by water. C_T values were calculated by normalization to the mean expression of three endogenous controls (POLR2A, β-GUS and β-actin) and converted into $2^{-\Delta\Delta C_T}$ values with Excel 8.0 (Microsoft, Redmond, WA, USA) which in turn were statistically analysed with Prism 5.0 using the Kruskal–Wallis and Dunn's post tests (GraphPad Software, San Diego, CA, USA) [12]. For calculation of relative expression levels, the weakest signal in the control group was set equal to 1, and all other values were calculated relative to this level.

Results

Upregulation of BMP-7 characterises bronchiolitis obliterans in transplant lungs

We employed laser-assisted microdissection to analyse anatomically defined structures, not just total tissue sections. Thus, we were able to generate specific quantitative mRNA expression profiles of the pathologically affected cellular compartments and to correlate them with the results of immunohistochemistry.

We found significant upregulation of BMP-7 mRNA in BO lesions in pulmonary allografts ($p=0.0141$), compared with unremodelled bronchioli in the same organs. Likewise, BMP-7 in this clinical setting showed the strongest cytoplasmic staining in the mesenchymal cells and the remaining respiratory epithelium of the BO lesions (Fig. 3a, Table 3). In contrast, OAR in non-transplanted lungs showed no significant differences in BMP-7 mRNA expression or staining intensity when compared with endogenous or exogenous controls ($p>0.05$, unremodelled bronchioli from the same explants and native bronchioli from downsized lungs; Fig. 3a, Table 3). However, TGF-β1 was significantly increased in OAR, compared with endogenous controls from the same explants ($p=0.048$, Fig. 3b, Table 3). Otherwise, there were no significant

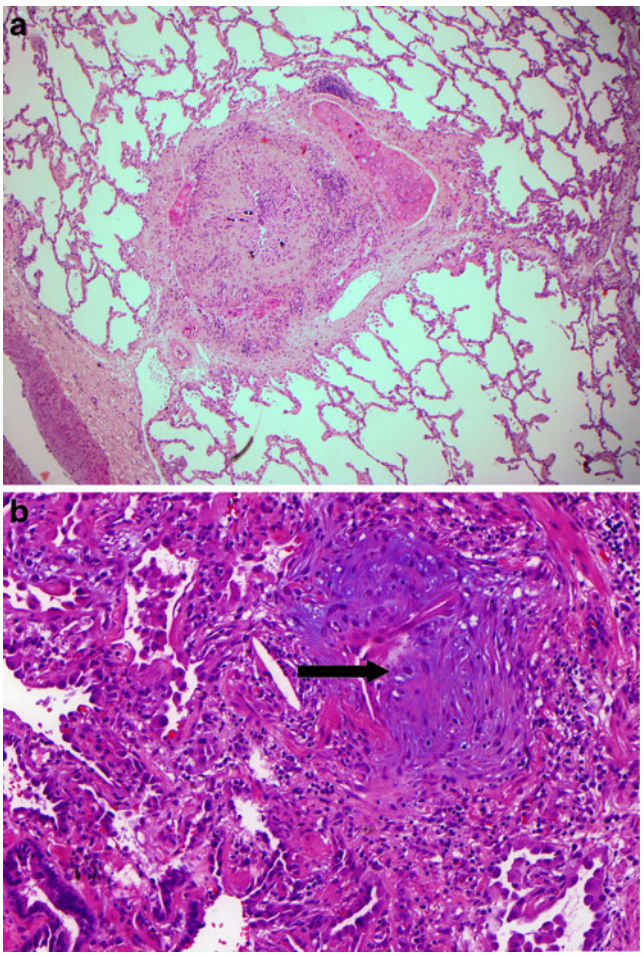

Fig. 1 **a** Obliterated airway in an advanced stage. Note the subtotal occlusion of the lumen: former dimension of the airway is outlined by smooth-muscle layer and cartilage. H & E staining. Original magnification, ×100. BX41 microscope (Olympus Germany). **b** Dense fibrosis in usual interstitial pneumonia (UIP pattern) variant of idiopathic pulmonary fibrosis. *Arrow* indicates fibroblastic focus of loosely organised connective tissue and (myo)fibroblasts. H & E staining. Original magnification, ×600. BX41 microscope (Olympus Germany)

differences between the two groups of obliterative airway lesions in transplanted and non-transplanted lungs regarding BMP-1, BMP-4, BMP-6, FGF-2, SMAD-3, CASP-3 and CASP-9, FASLG, NF-kappa-B, IL-1, IL-2, VEGF-α, LTA mRNA and protein expression ($p>0.05$).

Upregulation of BMP-4, BMP-7, TGF-β1 and FGF-2 characterises fibroblastic foci in IPF lung explants

In lung explants of patients with IPF, peribronchial fibroblastic foci displayed significant mRNA upregulation of the pro-fibrotic cytokines TGF-β1 and FGF-2 as well as BMPs 4 and 7, compared with unremodelled bronchioli ($p<0.0424$). This concurs with the complementary immunohistochemistry, where the strongest positivity for TGF-β1 and BMP-7 was found in the (myo)fibroblasts of the fibroblastic foci and in the adjacent respiratory epithelium, compared with unremodelled bronchioli (Fig. 4a–c, Table 3). No significant differences were found between the fibroblastic foci and the unremodelled bronchioli in transplanted and non-transplanted lungs regarding BMP-1, BMP-6, SMAD-3, CASP-3 and CASP-9, FASLG, NF-kappa-B, IL-1, IL-2 and VEGF-α mRNA and protein expression ($p>0.05$).

LTA was up-regulated in BO lesions in transplanted patients compared with unremodelled bronchioli ($p<0.0332$). Proangiogenic VEGF-α was over-expressed in non-obliterated bronchioli from non-transplanted lungs, compared with BO lesions in transplanted lungs and to non-transplanted controls ($p<0.0424$). Infiltrating macrophages showed a strong positivity for VEGF-α in immunohistochemical staining. Unremodelled bronchioli from transplanted lungs showed a trend to upregulation when compared with controls ($p>0.05$, Figs. 5a, b, Table 3).

SMAD protein expression in remodelled airways

Of the (phosphorylated) SMADs examined by immunohistochemistry, phospho-SMAD 2/3 showed the strongest nuclear staining in remodelled airways in transplanted as well as in non-transplanted lungs (BO and OAR) and fibroblastic foci in IPF, compared with controls (native bronchioli in the same organs, transplanted and non-transplanted reference lungs; Fig. 5d, Table 3).

Cellularity of airways in transplanted and non-transplanted lungs

As expected, remodelled airways in transplanted as well as in non-transplanted patients showed significantly more inflammatory infiltration than patent bronchioli ($p=0.0077$)—regardless of the time passed since transplantation ($p>0.05$). In particular, the CD 68-positive population of macrophages/mononuclear cells (obliterated airways mean, up to 60% of infiltrating leukocytes positive for CD 68, $p=0.0003$, Fig. 5e, Table 3) and myofibroblasts were significantly increased in obliterated airways. Myofibroblasts were identified by morphology and expression of smooth-muscle actin (obliterated airways mean, >60% of mesenchymal cells positive for sma; unremodelled bronchioli mean, up to 30% positive for sma; $p<0.0001$, Fig. 5c, Table 3). Remodelled airways in transplanted versus non-transplanted patients did not differ significantly in regard to cellularity and cellular composition ($p>0.05$).

Unremodelled small airways in transplanted and non-transplanted lung explants were also mainly infiltrated by CD 68-positive macrophages, compared with controls

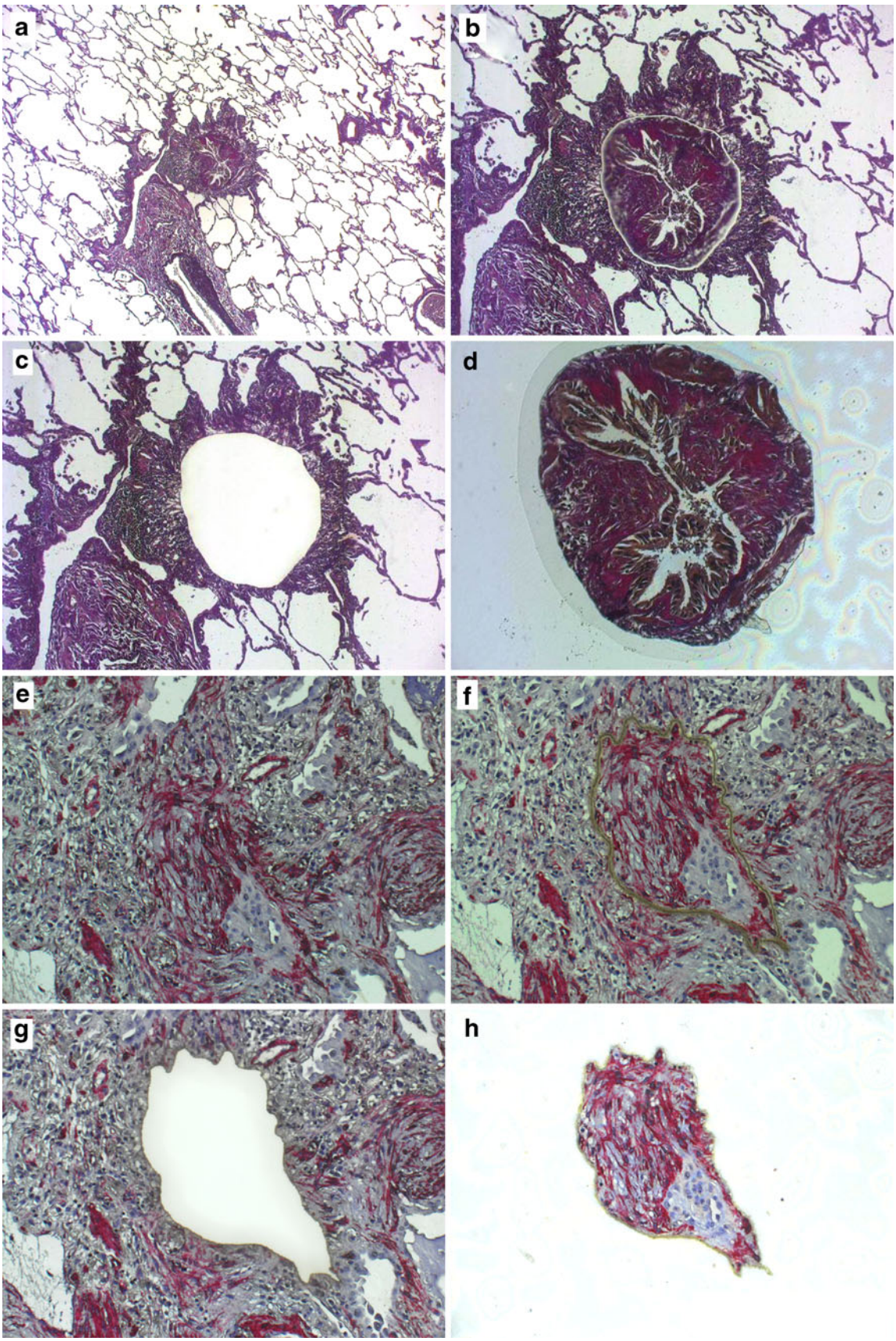
a
b
c
d
e
f
g
h

◀ **Fig. 2** **a–d** Isolation of an obliterated bronchiolus from the surrounding, unagitated lung tissue by laser-assisted microdissection (laser cut is visible in **b**; **d** shows isolated BO lesion in cap). Trichrome staining was used to highlight fibrotic changes in the remodelled airway. Haemalaun staining was routinely used for all samples from which mRNA was extracted. Original magnification: **a** ×40, **b** and **c** ×100, **d** ×200. IX 71 microscope (Olympus Germany) with CellCut Plus system for laser-assisted microdissection. **e–h** Isolation of a peribronchial fibroblastic focus is demonstrated (in UIP pattern IPF; laser cut is visible in **f**; **h** shows isolated fibroblastic focus in cap). Red smooth-muscle actin immunohistochemistry was used to demonstrate the layered composition of the fibroblastic focus. Haemalaun staining was routinely used for all samples from which mRNA was extracted. Original magnification, ×200. IX 71 microscope (Olympus Germany) with CellCut Plus system for laser-assisted microdissection

(mean unremodelled bronchioli, up to 30% of infiltrating leukocytes positive for CD 68, $p<0.05$).

Peribronchial fibroblastic foci in IPF cases consisted mainly of myofibroblasts (mean, >60% of cells positive for sma).

Discussion

BO represents one of the leading causes of death in lung-transplanted patients. The clinical outcome of BO patients who have not undergone transplantation varies, depending on the underlying cause/disease and responsiveness to steroids. Overall, only a small minority of these patients develops terminal respiratory insufficiency. Our collective of lung explants with advanced airway obliteration due to a multitude of different causes showed no major differences between transplanted and non-transplanted specimens in regard to chronic inflammation, cellularity and local microenvironment. The only significant exception was the BMP-7 upregulation in the small remodelled airways in transplanted lungs.

Our findings suggest a certain extent of similarity between the airway fibrosis in chronically rejected allografts and

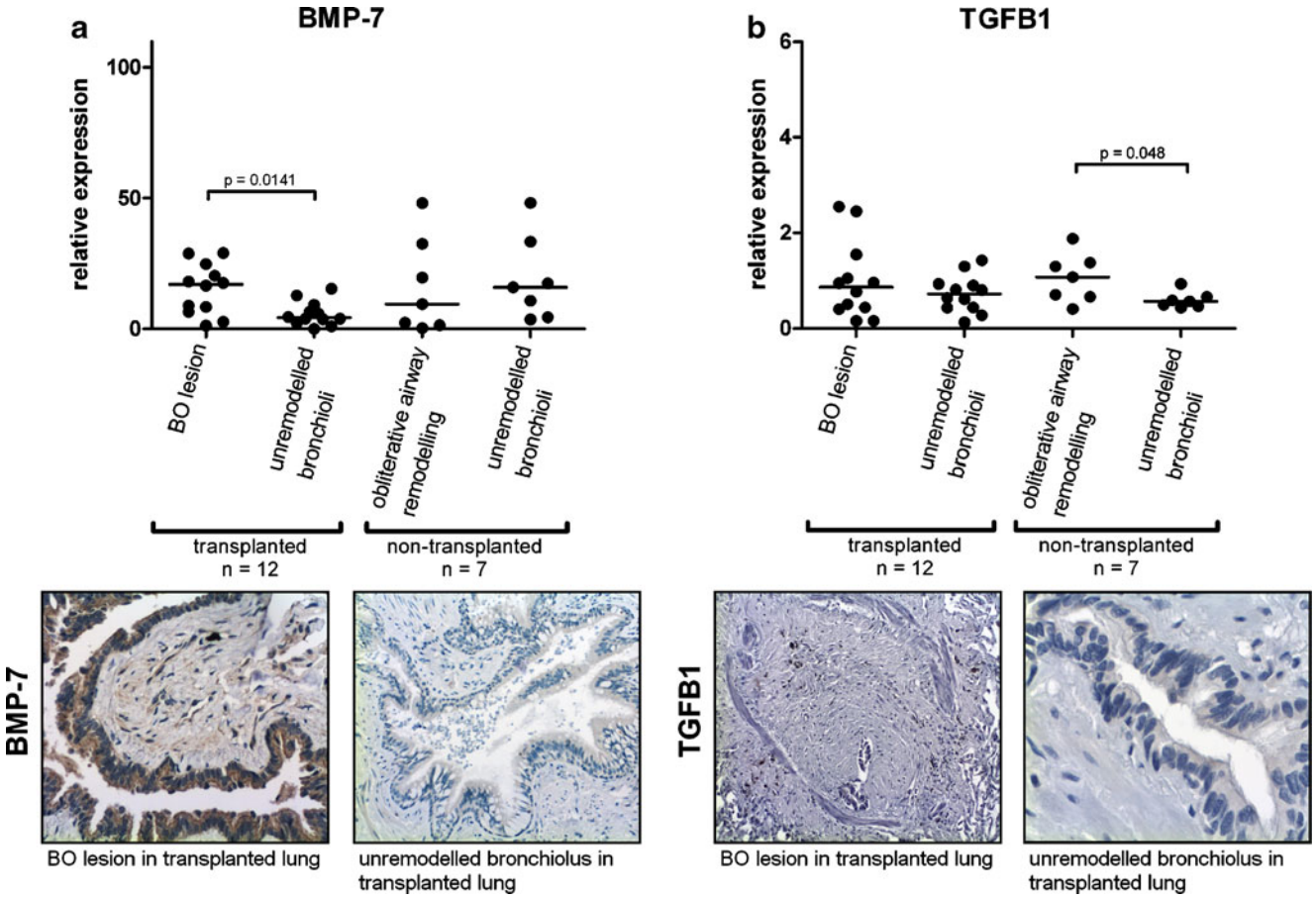

Fig. 3 mRNA and protein expression of pro-fibrotic (TGF-β1) and anti-fibrotic (BMP-7) factors in BO lesions: comparison of mRNA expression of BMP-7 (**a**) and TGF-β1 (**b**) in OAR and corresponding unremodelled bronchioli in transplanted and non-transplanted lungs. Expression of target genes was calculated using the $\Delta\Delta$ C_T-method (see "Materials and methods" for details). *Lines* indicate median, *p* values indicate significance. Note correlation of increase in immunohistochemical staining intensity and mRNA expression for BMP-7 (**a**) in OAR compared with unremodelled bronchioli from the same organs. A significant difference of mRNA expression and immunohistochemical staining intensity for TGF-β1 was only found in OAR in non-transplanted lungs but not in BO lesions in transplanted specimen (**b**)

Table 3 Immunohistochemical staining

Antibody	BO	OAR	FF	Unremodelled airways
SMAD 1	2	2	1	1
	Intermediate	Intermediate	Intermediate	Weak
SMAD 2	2	2	2	1
	Intermediate	Intermediate	Intermediate	weak
SMAD 3	1	1	1	0
	Weak	Weak	Weak	
Phospho-SMAD 1/5	1	1	1	1
	Weak	Weak	Weak	Weak
Phospho-SMAD 2/3	3	3	3	1
	Strong	Strong	Strong	Weak
TGF-β1	2	2	3	1
	Intermediate	Strong	Strong	Weak
BMP-1	1	1	1	1
	Weak	Weak	Weak	Weak
BMP-7	3	1	3	1
	Strong	Weak	Intermediate	Weak
VEGF-A	1	1	1	2
	Intermediate	intermediate	Weak	Strong
Smooth-muscle actin	3	3	2	0
	Strong	Strong	Strong	
Smooth-muscle myosin heavy chain	3	2	2	0
	Intermediate	Strong	Strong	
Caldesmon	1	1	1	0
	Weak	Weak	Weak	
Desmin	2	2	2	0
	Intermediate	Intermediate	Intermediate	
CD 45	2	2	1	1
	Strong	Strong	Intermediate	Strong
CD 68	2	2	1	1
	Strong	Strong	Weak	Strong

Immunohistochemical staining results in different anatomical/pathological compartments. The semiquantitative score indicates number of positive cells. Staining intensity is indicated as weak, intermediate or strong

BO bronchiolitis obliterans lesions in lung allografts, *OAR* obliterative airway remodelling in non-transplanted lungs, *FF* fibroblastic foci in UIP-pattern IPF lungs, *Unremodelled airways* bronchioli from the same lung explants without apparent remodelling, *score 0* no apparent reaction, *score 1* positivity in less than 30%, *score 2* positivity in more than 30% and less than 60%, *score 3* positivity in more than 60%

chronically failing, non-transplanted lungs. Furthermore, the elevation of BMP-7 in BO lesions in allografts as well as in IPF lungs requires further elucidation as a potential biomarker for ongoing BO in lung transplants.

Airway remodelling in transplanted lungs is thought to be the sequelae of a combination of alloimmune-dependent and alloimmune-independent mechanisms that eventually lead to fibrosis of the (smaller) airways. Generally speaking, it can be referred to as an "excessive reaction to injury" [13, 14]. Our lung specimens represent end-stage organs with advanced airway obliteration, as lung (re) transplantation is usually postponed to a later date out of necessity, due to a shortage of suitable grafts and the limited life expectancy of transplanted patients [15]. Consequently, in these final stages of obliteration, there were only scarce remains of the damaged epithelium that could provide both an immunological and non-immunological stimulus or act as a source for ongoing epithelial–mesenchymal transition. This "stalling" or "burning-out" of the fibrotic process and the local tissue turnover is supported by weakly expressed caspases, FAS ligand and pro-fibrotic cytokines like FGF-2 and pivotal TGF-β1 in BO lesions [16, 17].

OAR in non-transplanted patients showed TGF-β1 upregulation and rather more heterogeneous expression results than BO lesions in allografts. This most likely reflects the inhomogeneous collection of underlying

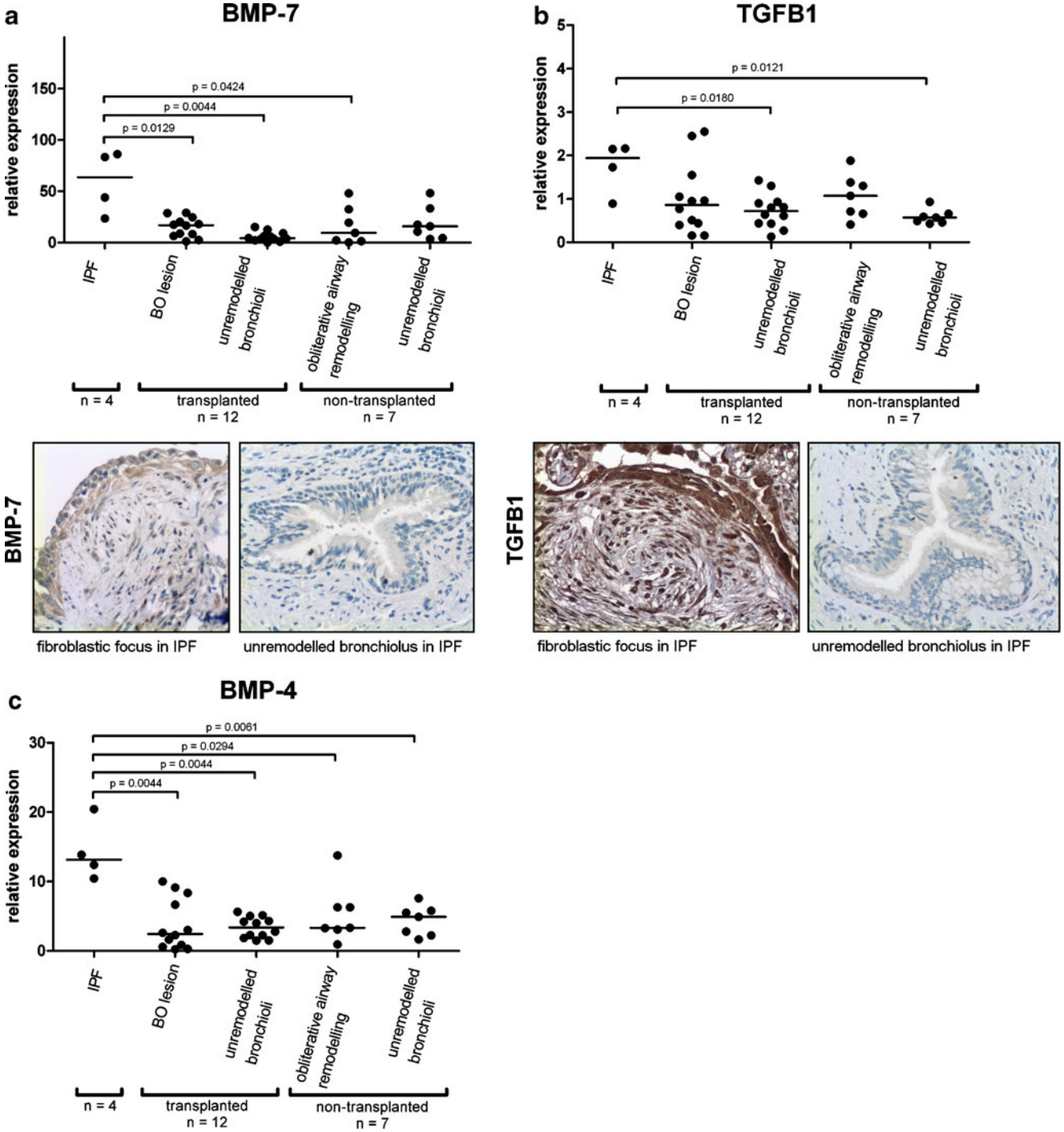

Fig. 4 mRNA and protein expression of pro-fibrotic (TGF-β1) and anti-fibrotic (BMP-4, BMP-7) factors in fibroblastic foci in IPF: comparison of mRNA expression of BMP-7 (**a**), TGF-β1 (**b**) and BMP-4 (**c**) in peribronchial fibroblastic foci in IPF (UIP pattern) with OAR and corresponding unremodelled bronchioli from the same organs, in transplanted and non-transplanted lungs. Expression of target genes was calculated using the $\Delta\Delta C_T$ method (see "Materials and methods" for details). *Lines* indicate median, *p* values indicate significance. For reasons of clarity, not all *p* values are shown (see Fig. 3). Note correlation of increase in immunohistochemical staining intensity and mRNA expression for BMP-7 (**a**) and TGF-β1 in fibroblastic foci (**b**) compared with unremodelled bronchioli from the same organs

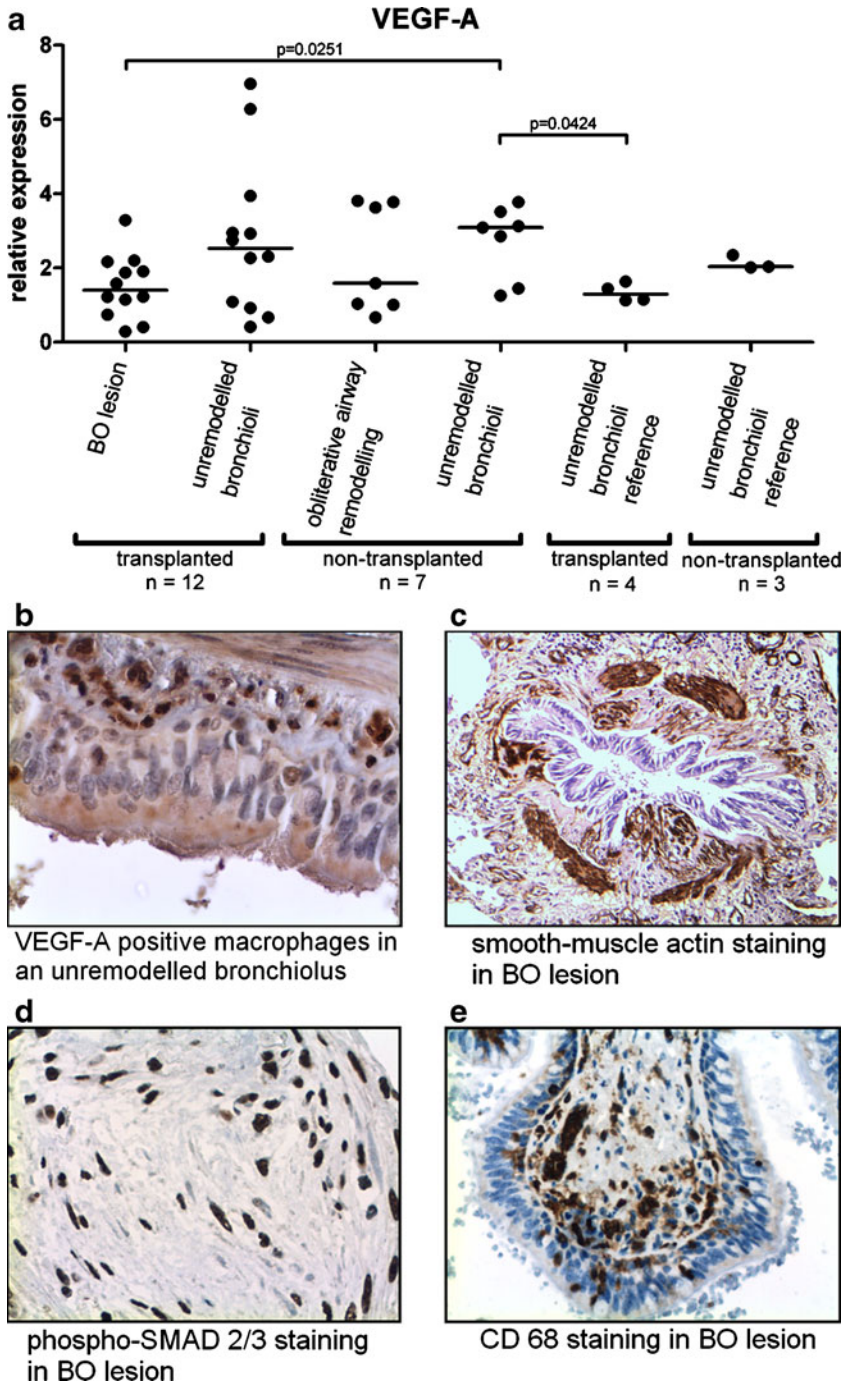

Fig. 5 VEGF-α and related parameters in OAR: comparison of mRNA expression of VEGF-α in OAR and corresponding unremodelled bronchioli in transplanted and non-transplanted lungs (**a**). Expression of target genes was calculated using the ΔΔ C_T method (see "Materials and methods" for details). *Lines* indicate median, *p* values indicate significance. Note correlation of increase in mRNA expression and immunohistochemical staining intensity in unremodelled bronchioli (**b**). BO lesions showed a marked positivity for smooth-muscle actin (**c**). Note strong nuclear staining for phospho SMAD 2/3 in BO lesion (**d**). Dense infiltrate of CD 68-positive mononuclear cells in BO lesion (**e**)

diseases and the varying time periods between the onset of respiratory impairment and transplantation in our collective of non-transplanted lung specimens. Furthermore, the majority of COP patients responds well to corticosteroid therapy and consequently does not undergo transplantation. Hence, our COP cases represent a biased subset with poor outcome [18].

The expected high expression levels of pro-fibrotic TGF-β1 and FGF-2 in the fibroblastic foci in UIP-pattern IPF lungs demonstrate the successful function of our

method. Here, fibroblastic foci represent the main site of ongoing injury, and TGF-β remains elevated even in honeycombing end-stage lungs, as fibrotic scarring is propagated until the total loss of the original architecture [19].

BMPs are elevated in BO lesions in the transplanted lung as well as in fibroblastic foci. While originally named for their ability to facilitate bone and cartilage formation, more recent experiments have shown the importance of BMP signalling balance in lung development and TGF-β pathway regulation [20]. The BMPs can be divided into two classes: the "first class" is made up of BMP-1 (tolloid-like proteinase in humans), which is directly involved in the activation of the pro-fibrotic TGF-β from its dormant precursor state [21]. The "second class" of BMPs (BMP-2 to BMP-15) bind to specific BMP receptors, which regulate the transcription of target genes further downstream by (phospho) SMAD protein complexes, which translocate into the nucleus and exert anti-fibrotic as well as other effects [22, 23].

While we found BMP-7 (and BMP-4) to be elevated in specific fibrosing lung compartments, findings in other solid organs vary: Reduced BMP-7 levels in patients with chronic fibrosing kidney diseases correlate with a bad outcome However, BMP-7 is found permanently elevated in serum and hepatocytes of patients with cirrhotic liver disease [24, 25]. Thus, the local increase in expression may be interpreted as sequelae of decreased sensitivity of BMP receptors due to continuous (autocrine) stimulation or as a result of the—at least in part—fibrogenic potential of BMPs [26–29]. BMP-7 in particular has been shown to antagonise TGF-β-induced myofibroblast generation and activation—so an upregulation may indeed represent a failed attempt of fibrosis inhibition [30, 31]. Because of this loose attribution with protective, anti-fibrotic properties, BMP infusions have been used inter alia in animal experiments and preclinical trials for the treatment of bone marrow and solid organ fibrosis [32–36]. This approach is not likely to be (as) successful in the lung, as here, not only matrix deposition but also structural changes would have to be prevented or even reversed [37].

VEGF-α was over-expressed in non-obliterated small airways in transplanted and in non-transplanted lungs alike, with the vast majority of infiltrating leukocytes being CD 68-positive, mononuclear cells. These were not actively involved in a cytokine-mediated immune response, with interleukins, NF-kappa-B and LTA showing (almost) no measurable differences between unremodelled and remodelled bronchioli. This concurs with results in animal experiments, where VEGF-α was found to have a limiting influence on fibrotic remodelling of the lung. This is most likely because of its positive effect on the recruitment of macrophages, as these contribute significantly to "airway clearance" of necrotic/apoptotic cells and infectious agents and thus reduce local inflammation and subsequent fibrosis [38–41].

As BO in end-stage organs represents the final stage of remodelling, future research should focus on the route leading there. However, the possibilities are hampered by the lack of sensitivity of transbronchial biopsies in regard to BO in transplanted patients, due to the patchy, discontinuous nature of small airway remodelling. Transbronchial biopsies are thus of limited use in the morphological study of the development of BO lesions in allografts and an ideal animal model for obliterative bronchiolitis is still waiting to be established [42]. In this situation, the molecular characteristics in remodelled and patent distal airways might serve nonetheless as a platform to perform continuous molecular profiling in lung biopsies including the study of BMP-7 in transplanted lungs.

Acknowledgements The authors would like to thank Gillian Teicke and Dr. Ho-Yen for editing the text.

Disclosure/conflicts of interest This work is supported by a grant from the Deutsche Forschungsgemeinschaft (DFG, KFO 123 LTx, to Danny Jonigk and Hans Kreipe) and by the Integriertes Forschungs- und Behandlungszentrum Transplantation (BMBF, IFB-Tx). The authors have no conflicts of interest to disclose.

References

1. Bergeron C, Al-Ramli W, Hamid Q (2009) Remodeling in asthma. Proc Am Thorac Soc 6:301–305
2. Belperio JA, Weigt SS, Fishbein MC, Lynch JP 3rd (2009) Chronic lung allograft rejection: mechanisms and therapy. Proc Am Thorac Soc 6:108–121
3. Laurent GJ, Chambers RC, Hill MR, McAnulty RJ (2007) Regulation of matrix turnover: fibroblasts, forces, factors and fibrosis. Biochem Soc Trans 35:647–651
4. Eyden B (2008) The myofibroblast: phenotypic characterization as a prerequisite to understanding its functions in translational medicine. J Cell Mol Med 12:22–37
5. Brocker V, Langer F, Fellous TG, Mengel M, Brittan M, Bredt M, Milde S, Welte T, Eder M, Haverich A, Alison MR, Kreipe H, Lehmann U (2006) Fibroblasts of recipient origin contribute to bronchiolitis obliterans in human lung transplants. Am J Respir Crit Care Med 173:1276–1282
6. Rosendahl A, Pardali E, Speletas M, Ten Dijke P, Heldin CH, Sideras P (2002) Activation of bone morphogenetic protein/Smad signaling in bronchial epithelial cells during airway inflammation. Am J Respir Cell Mol Biol 27:160–169
7. Wynn TA (2008) Cellular and molecular mechanisms of fibrosis. J Pathol 214:199–210
8. Liu Y (2006) Renal fibrosis: new insights into the pathogenesis and therapeutics. Kidney Int 69:213–217
9. Aris RM, Walsh S, Chalermskulrat W, Hathwar V, Neuringer IP (2002) Growth factor upregulation during obliterative bronchiolitis in the mouse model. Am J Respir Crit Care Med 166:417–422
10. Jonigk D, Lehmann U, Stuht S, Wilhelmi M, Haverich A, Kreipe H, Mengel M (2007) Recipient-derived neoangiogenesis of

arterioles and lymphatics in quilty lesions of cardiac allografts. Transplantation 84:1335–1342
11. Theophile K, Jonigk D, Kreipe H, Bock O (2008) Amplification of mRNA from laser-microdissected single or clustered cells in formalin-fixed and paraffin-embedded tissues for application in quantitative real-time PCR. Diagn Mol Pathol 17:101–106
12. Livak KJ, Schmittgen TD (2001) Analysis of relative gene expression data using real-time quantitative PCR and the 2(-Delta Delta C(T)) Method. Methods 25:402–408
13. Sato M, Keshavjee S (2008) Bronchiolitis obliterans syndrome: alloimmune-dependent and -independent injury with aberrant tissue remodeling. Semin Thorac Cardiovasc Surg 20:173–182
14. Ward C, De Soyza A, Fisher AJ, Pritchard G, Forrest I, Corris P (2005) A descriptive study of small airway reticular basement membrane thickening in clinically stable lung transplant recipients. J Heart Lung Transplant 24:533–537
15. Van Raemdonck D, Neyrinck A, Verleden GM, Dupont L, Coosemans W, Decaluwe H, Decker G, De Leyn P, Nafteux P, Lerut T (2009) Lung donor selection and management. Proc Am Thorac Soc 6:28–38
16. Kuwano K (2008) Involvement of epithelial cell apoptosis in interstitial lung diseases. Intern Med 47:345–353
17. Mizuta M, Nakajima H, Mizuta N, Kitamura Y, Nakajima Y, Hashimoto S, Matsuyama H, Shime N, Amaya F, Koh H, Ishizaka A, Magae J, Tanuma SI (2008) Fas ligand released by activated monocytes causes apoptosis of lung epithelial cells in human acute lung injury model in vitro. Biol Pharm Bull 31:386–390
18. Sara AG, Hamdan AJ, Hanaa B, Nawaz KA (2008) Bronchiolitis obliterans organizing pneumonia: pathogenesis, clinical features, imaging and therapy review. Ann Thorac Med 3:67–75
19. Strieter RM (2005) Pathogenesis and natural history of usual interstitial pneumonia the whole story or the last chapter of a long novel. Chest 128:526–532
20. Warburton D, Bellusci S (2004) The molecular genetics of lung morphogenesis and injury repair. Paediatr Respir Rev 5(Suppl A):283–287
21. Ge G, Greenspan DS (2006) BMP1 controls TGFbeta1 activation via cleavage of latent TGFbeta-binding protein. J Cell Biol 175:111–120
22. Hopkins DR, Keles S, Greenspan DS (2007) The bone morphogenetic protein 1/tolloid-like metalloproteinases. Matrix Biol 26:508–523
23. Langenfeld EM, Calvano SE, Abou-Nukta F, Lowry SF, Amenta P, Langenfeld J (2003) The mature bone morphogenetic protein-2 is aberrantly expressed in non-small cell lung carcinomas and stimulates tumor growth of A549 cells. Carcinogenesis 24:1445–1454
24. Nguyen TQ, Goldschmeding R (2008) Bone morphogenetic protein-7 and connective tissue growth factor: novel targets for treatment of renal fibrosis? Pharm Res 25:2416–2426
25. Tacke F, Gabele E, Bataille F, Schwabe RF, Hellerbrand C, Klebl F, Straub RH, Luedde T, Manns MP, Trautwein C, Brenner DA, Scholmerich J, Schnabl B (2007) Bone morphogenetic protein 7 is elevated in patients with chronic liver disease and exerts fibrogenic effects on human hepatic stellate cells. Dig Dis Sci 52:3404–3415
26. Koli K, Myllarniemi M, Vuorinen K, Salmenkivi K, Ryynanen MJ, Kinnula VL, Keski-Oja J (2006) Bone morphogenetic protein-4 inhibitor gremlin is overexpressed in idiopathic pulmonary fibrosis. Am J Pathol 169:61–71
27. Molloy EL, Adams A, Moore JB, Masterson JC, Madrigal-Estebas L, Mahon BP, O'Dea S (2008) BMP4 induces an epithelial-mesenchymal transition-like response in adult airway epithelial cells. Growth Factors 26:12–22
28. Kariyawasam HH, Xanthou G, Barkans J, Aizen M, Kay AB, Robinson DS (2008) Basal expression of bone morphogenetic protein receptor is reduced in mild asthma. Am J Respir Crit Care Med 177:1074–1081
29. Board TN, Rooney P, Kay PR (2008) Strain imparted during impaction grafting may contribute to bony incorporation: an in vitro study of the release of bmp-7 from allograft. J Bone Joint Surg Br 90:821–824
30. Saika S, Ikeda K, Yamanaka O, Flanders KC, Nakajima Y, Miyamoto T, Ohnishi Y, Kao WW, Muragaki Y, Ooshima A (2005) Therapeutic effects of adenoviral gene transfer of bone morphogenic protein-7 on a corneal alkali injury model in mice. Lab Invest 85:474–486
31. You L, Kruse FE (2002) Differential effect of activin A and BMP-7 on myofibroblast differentiation and the role of the Smad signaling pathway. Invest Ophthalmol Vis Sci 43:72–81
32. Hayashi M, Muneta T, Ju YJ, Mochizuki T, Sekiya I (2008) Weekly intra-articular injections of bone morphogenetic protein-7 inhibits osteoarthritis progression. Arthritis Res Ther 10:R118
33. Wang S, de Caestecker M, Kopp J, Mitu G, Lapage J, Hirschberg R (2006) Renal bone morphogenetic protein-7 protects against diabetic nephropathy. J Am Soc Nephrol 17:2504–2512
34. Zeisberg M, Kalluri R (2008) Reversal of experimental renal fibrosis by BMP7 provides insights into novel therapeutic strategies for chronic kidney disease. Pediatr Nephrol 23:1395–1398
35. Weiskirchen R, Meurer SK, Gressner OA, Herrmann J, Borkham-Kamphorst E, Gressner AM (2009) BMP-7 as antagonist of organ fibrosis. Front Biosci 14:4992–5012
36. Sun J, Chen H, Chen C, Whitsett JA, Mishina Y, Bringas P Jr, Ma JC, Warburton D, Shi W (2008) Prenatal lung epithelial cell-specific abrogation of Alk3-bone morphogenetic protein signaling causes neonatal respiratory distress by disrupting distal airway formation. Am J Pathol 172:571–582
37. Murray LA, Hackett TL, Warner SM, Shaheen F, Argentieri RL, Dudas P, Farrell FX, Knight DA (2008) BMP-7 does not protect against bleomycin-induced lung or skin fibrosis. PLoS ONE 3:4039
38. Krebs R, Tikkanen JM, Nykanen AI, Wood J, Jeltsch M, Yla-Herttuala S, Koskinen PK, Lemstrom KB (2005) Dual role of vascular endothelial growth factor in experimental obliterative bronchiolitis. Am J Respir Crit Care Med 171:1421–1429
39. Shin JH, Shim JW, Kim DS, Shim JY (2009) TGF-beta effects on airway smooth muscle cell proliferation, VEGF release and signal transduction pathways. Respirology 14:347–353
40. Hollmen M, Tikkanen JM, Nykanen AI, Koskinen PK, Lemstrom KB (2008) Tacrolimus treatment effectively inhibits progression of obliterative airway disease even at later stages of disease development. J Heart Lung Transplant 27:856–864
41. Bartlett JA, Fischer AJ, McCray PB Jr (2008) Innate immune functions of the airway epithelium. Contrib Microbiol 15:147–163
42. Panoskaltsis-Mortari A, Tram KV, Price AP, Wendt CH, Blazar BR (2007) A new murine model for bronchiolitis obliterans post-bone marrow transplant. Am J Respir Crit Care Med 176:713–723

Virchows Arch (2010) 457:381–388
DOI 10.1007/s00428-010-0946-0

ORIGINAL ARTICLE

Distribution and possible role of PDGF-AA and PDGFR-α in the gastrointestinal tract of adult guinea pigs

Fangxiao Chan · Yong Liu · Haimei Sun · Xiaoshuang Li · Hongwei Shang · Dongying Fan · Jing An · Deshan Zhou

Received: 12 April 2010 / Revised: 23 June 2010 / Accepted: 27 June 2010 / Published online: 15 July 2010
© Springer-Verlag 2010

Abstract It was reported that a signaling pathway of platelet-derived growth factors (PDGFs) and their receptors (PDGFRs) played a critical role in the developing gut of mice. Overexpression of the PDGFR-α gene in gastrointestinal stromal tumors (GISTs) indicated that parts of tumor cells originated from PDGFR-α-positive cells, but a more detailed distribution of PDGFR-α and possible role in the adult mammalian gut are still unclear. In the present study, we examined the expression of both PDGF-AA and its receptor PDGFR-α in the gastrointestinal (GI) tract of adult guinea pigs using western blotting and immunohistochemistry. PDGF-AA-immunoreactive cells were mainly distributed in the mucosal epithelium of the stomach, small intestine, and large intestine. Only a few PDGF-AA-positive cells were seen in the longitudinal muscle layer of the large intestine. In contrast, PDGFR-α-positive cells were widely distributed throughout the GI tract, including the lamina propria, muscular layer, and subserosa. Double staining showed that the distribution of the PDGFR-α-positive cells in the muscular layer were similar to those of the interstitial cells of Cajal (ICCs), and they were associated with ICCs and enteric nerves, but no double-labeled cells were observed by anti-PDGFR or Kit antibody. It was noted that PDGFR-α-positive cells were also stained with a vimentin monoclonal antibody. Based on the double staining and morphological features, we consider the PDGFR-α-positive cells belong to a subtype of fibroblast. Our results not only provide a roadmap for understanding the function of the PDGF/PDGFR signaling pathway in both normal adult mammals and during gut injury and repair but also might help in understanding the growth and development of GISTs in the clinic.

Keywords Platelet-derived growth factor · PDGF receptor · Interstitial cells of Cajal · Fibroblast · Gastrointestinal tract

F. Chan · Y. Liu · H. Sun · X. Li · H. Shang · D. Zhou (✉)
Department of Histology and Embryology,
School of Basic Medical Sciences, Capital Medical University,
Beijing 100069, China
e-mail: zhoudeshan2008@163.com

D. Fan · J. An
Department of Microbiology, School of Basic Medical Sciences,
Capital Medical University,
Beijing 100069, China

Introduction

Platelet-derived growth factors (PDGFs) composed of four subtypes (A, B, C, and D), and their receptors, PDGFRs, has two subtypes (α and β) [1–3]. It is known that PDGFs exist in epithelial cells, endothelial cells, and fibroblasts of adult mammals and play important roles in cell proliferation, survival, and migration. PDGFs are also present in the extracellular matrix and participate tissue remodeling. It has been demonstrated that the PDGFs/PDGFRs signaling pathway plays a crucial role in embryonic development, especially in organogenesis, including alveogenesis, glomerulogenesis, angiogenesis, oligodendrogenesis, and spermatogenesis [4–6]. This signaling pathway is also essential for interstitial cell and mesenchymal cell proliferation.

PDGFR-α is expressed in the mesenchymal cells and smooth muscle cells of the gut during the embryonic stage and receives PDGFs from adjacent cells to regulate morphogenesis of the villus in the mouse; PDGF-A/PDGFR-α signaling is necessary for building normal epithelium of the gastrointestinal (GI) tract and PDGFR-α is also involved in the regulation of proliferation and differentiation of some mesenchymal cells by paracrine

PDGFs [7]. In the mature GI tract, PDGFRs are found in subepithelial fibroblasts and vascular pericytes [6]. A recent study indicated that PDGFR-α-positive cells widely distributed in the GI musculature of adult mice [8]. However, the detailed expression pattern and the role of PDGFs/PDGFRs signaling in the mature GI tract of other mammals have not been reported.

C-Kit, which is structurally similar to PDGFRs, is mainly expressed in the ICCs of the GI tract [9]. C-Kit and PDGFR-α are both receptor tyrosine kinases expressed in the adult GI tract. ICCs are the enteric pacemaker cells, mediators of neurotransmission, and important regulators of GI motility. Based on their location and morphological features, ICCs are divided into four subtypes: ICC in the myenteric layer (ICC-MY), within the longitudinal and circular smooth muscle layers (ICC-IM), associated with the deep muscular plexus (ICC-DMP), and at the inner surface of the colonic circular muscle layer (ICC-SM) [10–12]. Gastrointestinal stromal tumors (GISTs) are considered to be mostly originated from ICCs that have gain-of-function mutations of c-Kit. However, a recent study reported that some GISTs acquired gain-of-function mutations of PDGFR-α gene. This result raises the possibility that PDGFR-α may also be involved in GISTs development. Clarifying the relationship between PDGFR-α-positive cells and ICCs has important significance for investigating the origin of GISTs. Therefore, in the present study, we identified the expression pattern of PDGF-AA and PDGFR-α in the GI tract of adult guinea pigs. We also analyzed the cell type and features of the PDGFR-α-expressing cells and the differences and similarities between PDGFR-α- positive cells and ICCs.

Materials and methods

Animals

Ten guinea pigs of either sex, aged 4~6 weeks, were purchased from the Animal Center of Capital Medical University (Beijing, China). All of the experimental animals were killed by an overdose of pentobarbital. All procedures were performed in accordance with the Health Guide for the Care and Use of Laboratory Animals of our University, and the Institutional Animal Care Committee approved the work.

Immunohistochemistry

Whole GI tracts, including stomach, entire small intestine, and large intestine were removed, and enteric contents were washed away with 0.01 M phosphate-buffered saline (PBS, pH 7.2). For cryo-sections, 10-mm pieces from each organ were immersed in 30% sucrose/PBS overnight at 4°C, and then embedded in an optimal cutting temperature compound and quickly frozen with liquid nitrogen. Cryosections (10 μm thickness) were cut with a cryostat (Leica CM3050S) and collected on poly-L-lysine-coated glass slides. After fan drying, the sections were fixed with Zamboni's fixative (2% paraformaldehyde/1.5% saturated picric acid solution/0.1 M phosphate buffer, pH 7.3) for 1 h at 25°C to stain for PDGFR-α or PDGF-AA.

To obtain whole-mount preparations, tissues were washed with PBS and then inflated with either acetone for 30 min at 4°C to stain for c-Kit or Zamboni's fixative for 1 h at 25°C to stain for PDGFR-α, PDGF-AA, or Vimentin. After washing with PBS, opened along the mesenteric border, the mucosas were removed to separate the longitudinal muscle layer with the serosa containing the ICC-MY and the circular muscle layer containing the ICC-DMP in the small intestine or ICC-SM in the large intestine, respectively, with the aid of a dissecting microscope.

For immunostaining, specimens were washed with PBS containing 0.3% Triton X-100 (PBST) for 20 min. After incubation in normal goat serum (5% in PBST) for 1 h (25°C), all specimens were incubated, respectively, with following primary antibodies for 24 h (4°C): rabbit anti-PDGFR-α (ab61219, Abcam; 1:300), rat anti-c-Kit (14-1172, Ack2, eBioscience; 1:100), rabbit anti-PDGF-AA (ab36744, Abcam; 1:500), or mouse anti-vimentin (M0725, Dako; 1:100). After washing with PBS, the specimens were incubated with appropriate secondary antibodies: Cy3-labeled goat anti-rat IgG (Zymed; 1:200), Cy3-labeled goat anti-mouse IgG (Zymed; 1:200), or FITC-labeled goat anti-rabbit IgG (Zymed; 1:100) for 1 h (25°C). After washing, the specimens were counter-stained with DAPI (Molecular Probes) to detect nuclei and mounted with Fluorescent Mounting Medium (Thermo Electron Co). Control specimens were prepared in the same manner, but each primary antibody was omitted. Slides were examined using a fluorescence microscope (Nikon 80i, Japan) or with a TCS SP5 confocal laser scanning microscope (Leica, Germany) with an excitation wavelength appropriate for FITC (488 nm) or Cy3 (552 nm).

Immunoblot analysis

Whole GI tracts were washed with PBS, and the muscular layers and mucosas were prepared, respectively, and then homogenized in 20 mM Tris–HCl (pH 7.5), 1 mM ethylenediamine tetraacetic acid, and 1 mM phenyl methyl sulfonyl fluoride. Homogenates were centrifuged at 1,000×*g* for 30 min at 4°C, and the supernatants were collected. Proteins were separated by sodium dodecyl sulfate polyacrylamide gel electrophoresis using a 7.5% polyacrylamide gel and transferred to a polyvinylidene fluoride membrane (Immobilon-P, Millipore Co. USA).

Membranes were blocked with 5% fat-free powdered milk in PBS containing 0.05% Tween-20 and then incubated with rabbit anti-PDGFR-α (1:2,000), rabbit anti-PDGF-AA (1:1,000) , rabbit anti-α-actin(ab5694, Abcam; 1:1,000), or rabbit anti-β-actin (ab8227, Abcam; 1:1,000), respectively. Membranes were washed in TBST and then incubated with a HRP-conjugated anti-rabbit IgG (1:2,000). Proteins were visualized with a chemiluminescence system (ECL Plus, Applygen Technologies Inc.) according to the manufacturer's instructions. α-Actin and β-actin were probed as a loading control for PDGFR-α or PDGF-AA, respectively.

Results

Immunoblot results showed a single immunoreactive band representing PDGFR-α, of approximately 180 kDa, in the GI musculatures of the adult guinea pigs (Fig. 1a); this specific immunoreactive band was not detected in the ECV304 cell line. In contrast, a single band of approximately 24 kDa was recognized by the anti-PDGF-AA antibody only in the mucosa of the stomach, small intestine, and large intestine of the adult guinea pigs (Fig. 1b).

Using immunohistochemistry, PDGF-AA-immunoreactive cells were mainly found in the mucosa of the GI tract. In the stomach (Fig. 2a), these cells were distributed in the fundic glands, whereas in the small and large intestines, PDGF-AA was expressed in the epithelial cells (Fig. 2b and c). A few PDGF-AA-immunoreactive cells were also detected in the longitudinal muscle layer of large intestine (Fig. 2d) but were not seen in other regions of the smooth muscle layers of the GI tract.

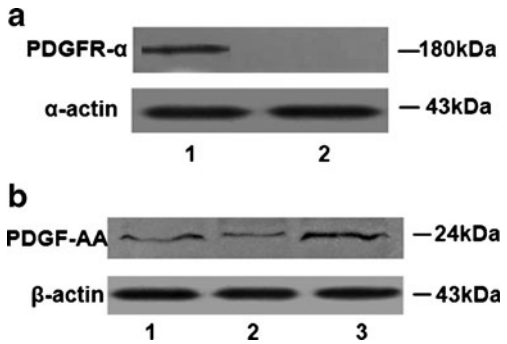

Fig. 1 Immunoblot analysis showing expression of PDGFR-α and PDGF-AA in the GI tract of adult guinea pigs. **a** PDGFR-α is seen as a single band of approximately 180 kDa in the musculature of the small intestine (*lane 1*). In the control group, no specific immunoreactive band of PDGFR-α is detected in the ECV304 cell line (*lane 2*). **b** The anti-PDGF-AA antibody recognized a single band of approximately 24 kDa in the mucosa of the stomach (*lane 1*), small intestine (*lane 2*), and large intestine (*lane 3*). α-Actin and β-actin were probed as a loading control for PDGFR-α or PDGF-AA, respectively. Molecular markers (kDa) are shown on the *right*

In contrast, PDGFR-α was expressed in the entire GI tract. The intensive PDGFR-α immunoreactive cells were often seen in the subepithelial layer and in the interstitial space of the GI muscle layers (Figs. 4a and 5a). In the stomach (Fig. 3), a number of PDGFR-α-positive cells with extended, thick cytoplasmic processes were distributed in the myenteric plexus region to form a cellular network with each other. PDGFR-α-positive cells with bipolar long processes were often seen within the muscle layers, whereas in the subserosal layer, PDGFR-α-positive cells were usually observed as multipolar shape with intense immunostaining.

In the small intestine, PDGFR-α-positive cells were often observed in the circular muscle layer, the myenteric plexus region, and the subserosal layer (Fig. 4). In the circular muscle layer, the PDGFR-α-positive cells had relatively slender bodies with bipolar thin and long cytoplasmic processes. In the myenteric plexus region, numerous PDGFR-α-positive cells surrounded the ganglia and nerve fibers, and their processes often ran parallel to the nerve fibers to form a cellular network with each other. In the subserosal layer, these positive cells showed a wider cell body with a number of extended, longer cytoplasmic processes to form an isolated cellular network.

PDGFR-α-positive cells in the large intestine were similar to those in other regions of the GI tract. They were mainly distributed in the myenteric plexus region, the smooth muscle layers, and the subserosal layer (Fig. 5a, b, c, e, f). Whole-mount preparations clearly showed that the PDGFR-α-positive cells had slender cell bodies with thin and long processes within the smooth muscle layers, but some short processes extending from the cell body were also seen. In the myenteric plexus region, these cells exhibited a round or oval cell body with some extended, thicker cytoplasmic processes, and they also formed a cellular network with each other. In the subserosal layer, PDGFR-α-positive cells showed a multipolar shape with several thin and long processes extending in all directions to form an isolated cellular network.

Another very important group of cells for regulating GI motility, ICCs, were also examined in the present study, and their distributions and morphologies were the same as our previous observations (see [13] and Fig. 5d). To identify differences and similarities between ICCs and PDGFR-α-positive cells in the smooth muscle layers, we performed double immuno-fluorescent stainings on whole-mount preparations and demonstrated that PDGFR-α-positive cells were not co-stained with c-Kit (a labeling marker for ICCs). The distribution patterns of PDGFR-α-positive cells were similar to those of ICCs (Fig. 5b–e). It needed to note that PDGFR-α-positve cells had a wider body and more irregular processes compared to ICCs.

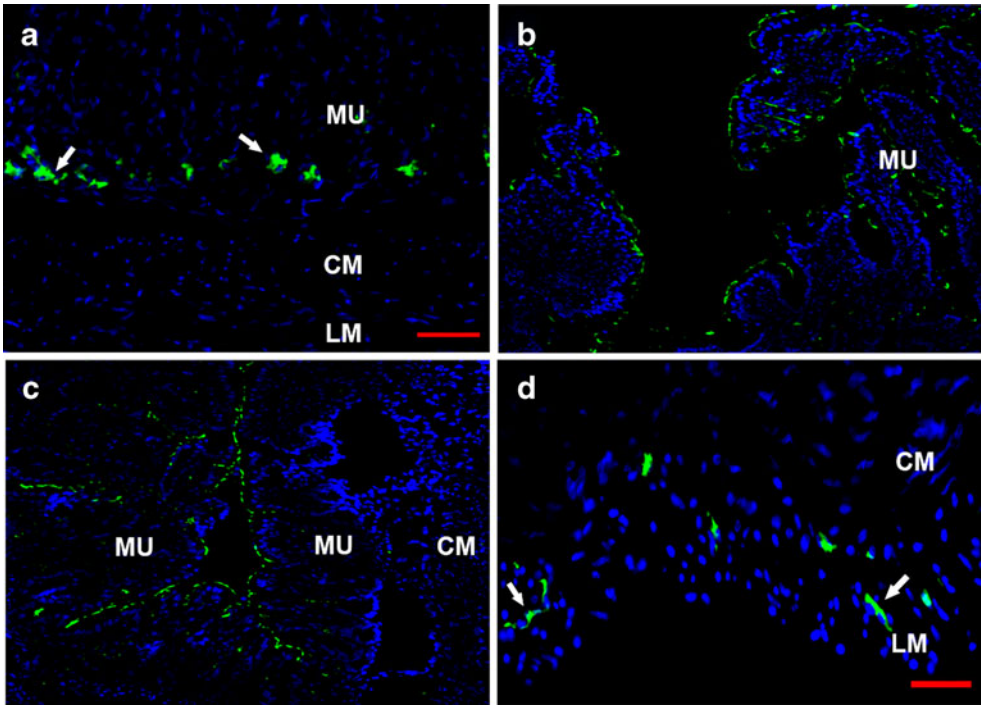

Fig. 2 Immuno-fluorescent staining for PDGF-AA was performed on cryo-sections to show the distribution of PDGF-AA (*green*) immunoreactivity in the GI tract. PDGF-AA expression was restricted to the gastric glands (*arrows*) in the stomach (**a**). Intense PDGF-AA immunoreactivity was observed in the free surface of epithelial cells both in the small intestine (**b**) and large intestine (**c**). A small number of PDGF-AA-positive cells (*arrows*) are also visible in the longitudinal muscle layer of the large intestine (**d**). The nuclei were stained with DAPI (*blue*). *MU* mucosa; *CM* circular muscle layer; *LM* longitudinal muscle layer. *Bars* 80 μm (**a**–**c**); *Bars* 40 μm (**d**)

To confirm the cell types of the PDGFR-α-positve cells, we also performed double immunostaining on whole-mount preparations using the anti-PDGFR-α antibody and the anti-vimentin monoclonal antibody, which is a marker of fibroblasts and determined that PDGFR-α-positive cells also showed vimentin immunoreactivity in the small intestine (Fig. 6), i.e., the PDGFR-α-positive cells were also labeled with the fibroblast marker. It should be noted that the same results were also obtained in the whole GI tract (data not shown).

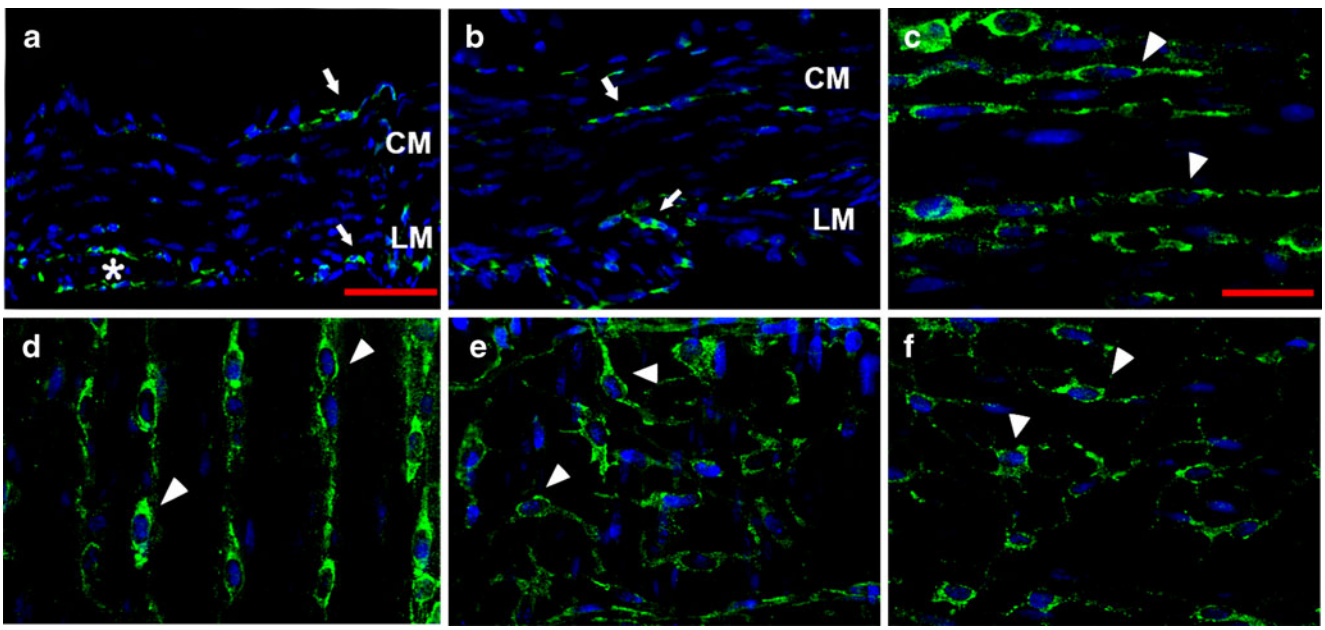

Fig. 3 A set of photographs showing immuno-fluorescent staining for PDGFR-α (*green*) in the stomach from cryo-sections (**a**, **b**) and whole-mount preparations (**c**–**f**). In gastric corpus (**a**) and gastric fundus (**b**), intensive PDGFR-α immunoreactivity was observed in the smooth muscle layers and the myenteric plexus region (*arrows*). There are numerous PDGFR-α-positive cells around the myenteric ganglion (*asterisk*). In the gastric fundus, PDGFR-α-positive cells with bipolar cell processes (*arrowheads*) were observed in the circular (**c**) and longitudinal (**d**) muscle layers, but the cells with a multipolar shape are often seen in the myenteric plexus region (**e**). Whereas PDGFR-α-positive cells with highly branched multipolar processes were observed in the subserosal layer (**f**) of the stomach. The nuclei were stained by DAPI (*blue*). *MU* mucosa; *CM* circular muscle layer; *LM* longitudinal muscle layer. *Bars* 40 μm (**a**, **b**); *Bars* 20 μm (**c**–**f**)

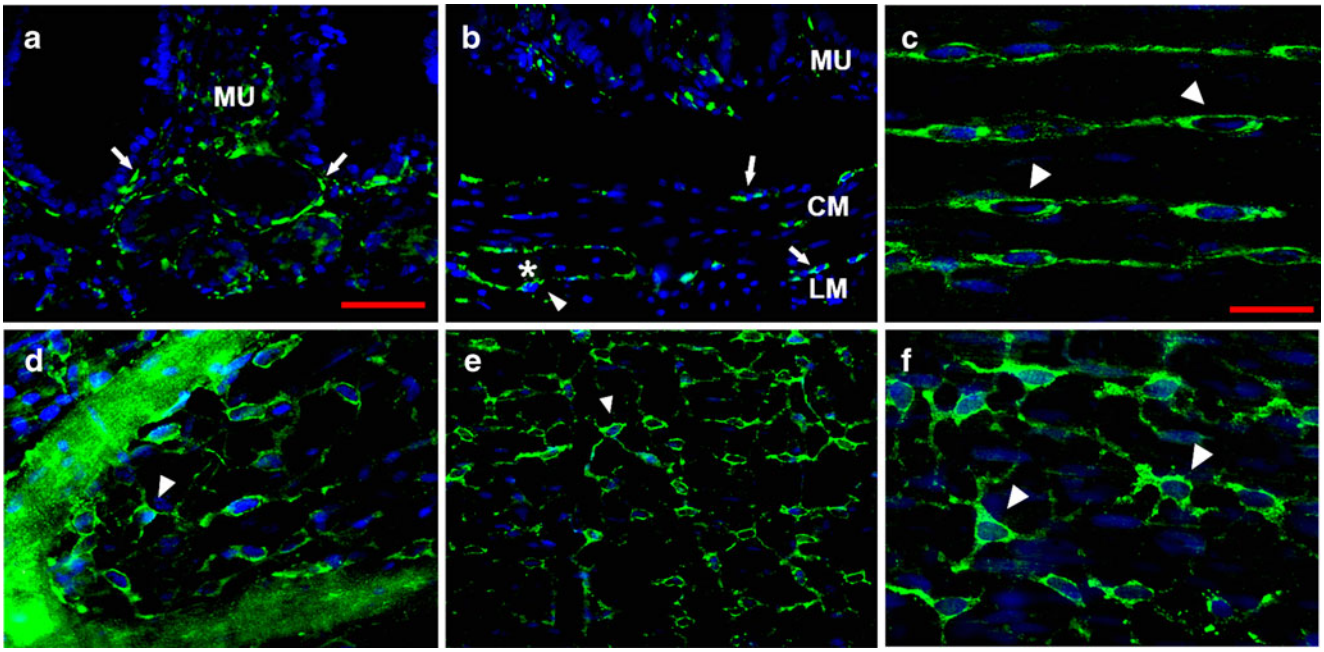

Fig. 4 The plate showing the PDGFR-α-positive cells (*green*) stained by immunocytochemistry on cryo-sections (**a**, **b**) and whole-mount preparations (**c**–**f**) of the small intestine. PDGFR-α-positive cells (*arrows*) are widely distributed in the subepithelial layer, smooth muscle layers, and myenteric plexus region. The myenteric ganglion (*asterisk*) is surrounded by PDGFR-α-positive cells. Slender-shaped PDGFR-α-positive cells with thin and long processes (*arrowheads*) were observed in the circular muscle layers (**c**). In the myenteric plexus region (**d**), PDGFR-α-positive cells with multipolar processes (*arrowheads*) were found to be associated with each other, and their processes ran parallel to the nerve fibers. Multipolar PDGFR-α-positive cells with some ramified processes (*arrowheads*) often are visible in the subserosal layer of lower magnification (**e**) and higher magnification (**f**). The nuclei were stained with DAPI (*blue*). *MU* mucosa; *CM* circular muscle layer; *LM* longitudinal muscle layer. *Bars* 40 μm (**a**, **b**, **e**); *Bars* 20 μm (**c**, **d**, **f**)

Discussion

The present study revealed the distributions of PDGF-AA and PDGFR-α in the GI tract of adult guinea pigs using immunohistochemistry and immunoblot analysis. PDGF-A was first characterized by cDNA cloning [14], and in vitro studies have demonstrated that most tumor cell lines express and secrete PDGF-AA homodimers [15]. Gene knockout studies have already shown that PDGFs plays an important role in the development of lung alveoli [16, 17], oligodendrocytes [18, 19], hair follicles [20], and neural crest cells [21]. Previous studies demonstrated that PDGFs are crucial for regulating the differentiation of some mesenchymal cells and are necessary for the normal development of the mucosal lining of the GI tract [7]. In the developing murine gut, PDGFs are expressed in premature circular smooth muscle cells and the epithelium, but they are restricted to intestinal glands in mature mice [22]. Our study clearly showed a distinct population of PDGF-AA-positive cells principally distributed in the mucosa of the GI tract in adult guinea pigs; a few of these positive cells were also observed in the longitudinal muscle layer of the large intestine. This distribution pattern indicated that PDGFs might be involved in epithelial growth, survival, and proliferation as well as in wound healing in the mature GI tract.

PDGFR-α-positive cells in the smooth muscle layers showed a similar distribution pattern to those of ICCs in all regions of the GI tract. We noticed that PDGFR-α-positive cells were often adjacent to and surrounded ICCs and the enteric nerve fibers in the myenteric plexus region and within the muscle layers. Although the distribution pattern and morphological features of PDGFR-α-positive cells were similar to those of ICCs, double immunostaining did not reveal PDGFR-α-positive cells co-expressing c-Kit (a labeling marker for ICCs). PDGFR-α-positive cells had a wider body and shorter processes, indicating that these cells distinct from ICCs. Our results suggest that PDGFR-α-positive cells might play a protective role in the normal physiological function of ICCs.

Vimentin is a cytoskeletal protein in some mesenchymal cells and is considered to be a marker for fibroblasts. Our results demonstrated that vimentin immunoreactivity co-existed in PDGFR-α-positive cells. Several studies using immunohistochemistry have shown that PDGFR-α often co-localizes with other proteins such as CD34 [23–25] or SK3 [8, 26, 27] in fibroblasts. CD34 and SK3 are also markers for fibroblasts or fibroblast-like cells. Komuro et

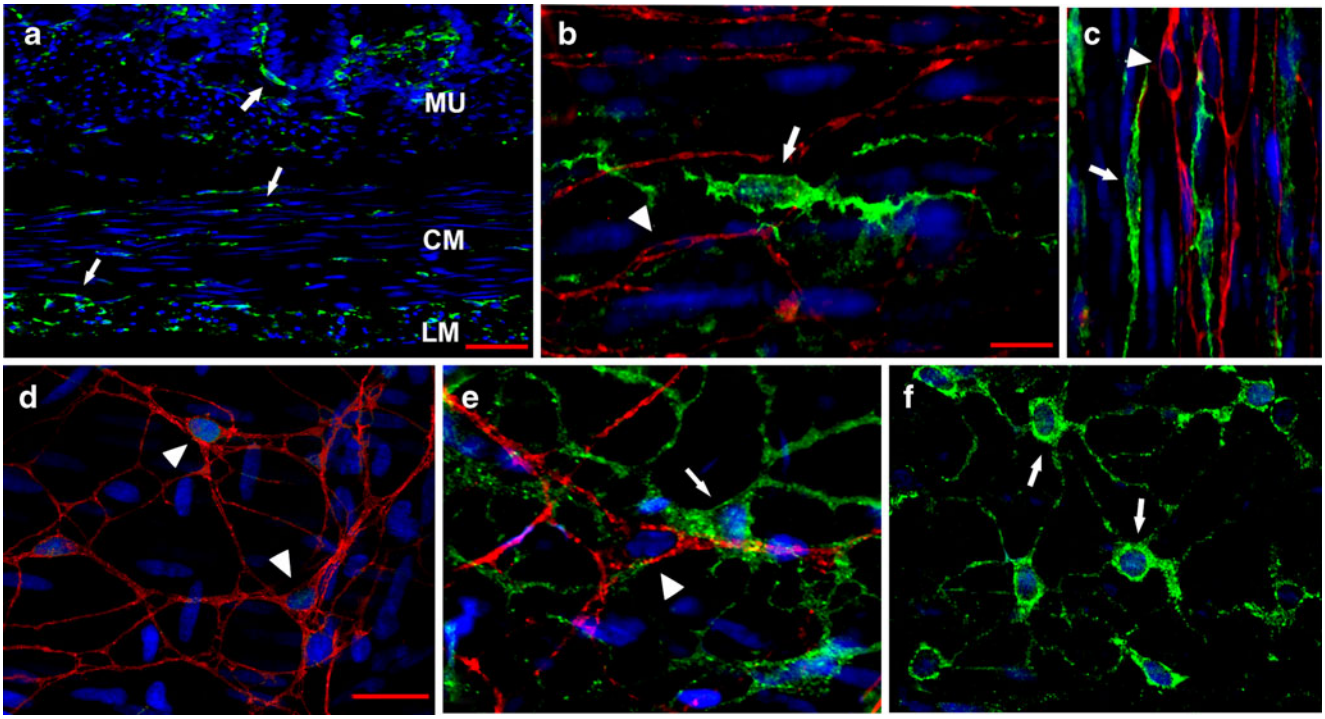

Fig. 5 This set of photographs stained by immuno-fluorescence shows PDGFR-α- positive cells (*green*) in the large intestine. In cryo-sections (**a**), numbers of PDGFR-α-positive cells (*arrows*) were found in the subepithelial layer, smooth muscle layers, and myenteric plexus region. Whole-mount preparations (**b**–**f**) with double staining show the PDGFR-α-positive cells (*green*) and c-Kit-positive cells or ICCs (*red*). PDGFR-α-positive cells (*arrows*) with bipolar processes are parallel to ICC-IM (*arrowheads*) in the circular (**b**) and longitudinal (**c**) muscle layers. ICC-MY (*arrowheads*) with long processes form a cellular network in the myenteric plexus region (**d**). The different distributions of the ICC-MY (*arrowheads*) and PDGFR-α-positive cells (*arrows*) with a few thicker processes are clearly seen in this area (**e**). Multipolar PDGFR-α-positive cells (*arrows*) with thin and long processes often form a cellular network with each other in the subserosal layer (**f**). The nuclei are stained with DAPI (*blue*). *MU* mucosa; *CM* circular muscle; *LM* longitudinal muscle. *Bars* 40 μm (**a**); *Bars* 30 μm (**d**); *Bars* 20 μm (**b**, **c**, **e**, **f**)

al. [28] concluded that fibroblasts in the muscular layers could be divided into different types according to electron microscopic observation; they might exhibit different shapes in different locations of the GI tract. Based on the morphological features and double-staining results, we consider that PDGFR-α-positive cells belong to a subtype of fibroblast or fibroblast-like cells (FLC), which are widely distributed in the GI tract.

Expression of PDGFR-α in a population of fibroblasts may have an important biological significance in the adult GI tract. It was reported that PDGFRs and c-Kit are co-expressed in the same precursor cells that differentiate into smooth muscle cells or ICCs during the embryonic period in the murine gut [22], indicating that PDGFRs and c-kit co-expressing precursor cells could differentiate into different cell types during gut development. There is the

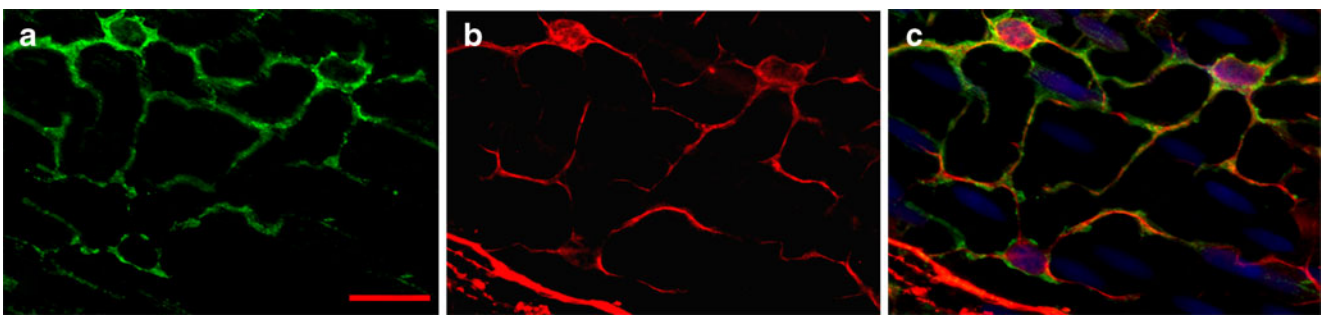

Fig. 6 The double immunostaining of PDGFR-α (*green*) and vimentin (*red*) in the subserosal layer of the small intestine. It is clearly seen that PDGFR-α-positive cells also contain the cytoskeleton filaments of vimentin (*red*) in the subserosal layer, indicating that PDGFR-α-positive cells belong to a subtype of fibroblast. *Bars* 20 μm (**a**–**c**)

possibility that these precursors could also differentiate into fibroblasts. We speculated that during embryonic periods, the loss of PDGFRs expression would cause precursors to differentiate into ICCs that consistently express c-kit. Precursors that lose c-Kit expression will become fibroblasts that consistently express PDGFRs. With a loss of both proteins, c-Kit and PDGFRs expression, the precursors will differentiate into smooth muscle cells.

Our hypothesis will help to explain the development of GISTs, the most common mesenchymal tumors in the GI tract [29, 30]. Previous studies demonstrated that most GISTs exhibit an activating mutation of the c-kit gene, but approximately 30% of GISTs lacking c-kit mutations showed activating mutations of the PDGFR-α gene [31, 32]. The existence of PDGFR-α gene mutations suggests that parts of GISTs originate from PDGFR-α precursor cells. It has been reported that PDGFRs are also expressed in other tumors such as skin, breast, colorectal, lung, pancreas, prostate, and ovarian cancers [33]. Experimental studies in animal models have demonstrated that PDGFRs expressed in the stromal cells of tumors contribute to both the recruitment of fibroblasts and angiogenesis for supporting the growth of tumor cells [34–36]. A fibroblast expressing PDGFR-α activated by PDGFs will stimulate its proliferation and provide micro-environment for producing extracellular matrix, some growth factors, and tumor growth necessary nutritional factors to directly or indirectly promote tumor growth, blood supply, and metastasis. Therefore, our results provided a new potential to target PDGFR-α for treating the GISTs and other tumors in the clinic.

In conclusion, the present immunohistochemical observations indicated that PDGFR-α-positive cells were widely distributed in the GI tract of adult guinea pigs. Their distribution pattern was similar to ICCs in the smooth muscle layers. Double staining revealed that PDGFR-α-positive cells were not stained by an ICC marker (anti-c-kit antibody) but were labeled by a fibroblast marker (anti-vimentin antibody), indicating that PDGFR-α-expressing cells belong to a subtype of fibroblast or FLC, which are basic cellular elements throughout the GI musculature. Our results, thus, might provide a roadmap not only for further understanding the functions of PDGF/PDGFR signaling pathway in the GI tract but also for comprehending the growth and development of GISTs in the clinic.

Acknowledgements This work was supported in part by grants No. 30971349 and 30871310 from the National Science Foundation of China (NSFC) and by grant No. PHR201007113 from the Funding Project for Academic Human Resources Development in Institutions of Higher Learning Under the Jurisdiction of Beijing Municipality (IHLB).

Conflict of interest statement The authors declare that they have no conflict of interest.

References

1. Fredriksson L, Li H, Eriksson U (2004) The PDGF family: four gene products form five dimeric isoforms. Cytokine Growth Factor Rev 15:197–204
2. Heldin CH, Westermark B (1999) Mechanism of action and in vivo role of platelet growth factor. Physiol Rev 79:1283–1316
3. Tallquist M, Kazlauskas A (2004) PDGF signaling in cells and mice. Cytokine Growth Factor Rev 15:205–213
4. Hoch RV, Soriano P (2003) Roles of PDGF in animal development. Development 130:4769–4784
5. Betsholtz C (2004) Insight into the physiological functions of PDGF through genetic studies in mice. Cytokine Growth Factor Rev 15:215–228
6. Andrae J, Gallini R, Betsholtz C (2008) Role of platelet-derived growth factors in physiology and medicine. Genes Dev 22:1276–1312
7. Karlsson L, Lindahl P, Heath JK, Betsholtz C (2000) Abnormal gastrointestinal development in PDGF-A and PDGFR-(alpha) deficient mice implicates a novel mesenchymal structure with putative instructive properties in villus morphogenesis. Development 127:3457–3466
8. Iino S, Horiguchi K, Horiguchi S, Nojyo Y (2009) C-Kit-negative fibroblast-like cells express platelet-derived growth factor receptor α in the murine gastrointestinal musculature. Histochem Cell Biol 131:691–702
9. Maeda H, Yamgata A, Nishikawa S (1992) Requirement of c-kit for development of intestinal pacemaker system. Development 116:369–375
10. Sanders KM (1996) A case for interstitial cells of Cajal as pacemakers and mediators of neurotransmission in the gastrointestinal tract. Gastroenterology 111:492–515
11. Iino S, Horiguchi K (2006) Interstitial cells of Cajal are involved in neurotransmission in the gastrointestinal tract. Acta histochem cytochem 39:145–153
12. Rumessen JJ, Vanderwinden JM (2003) Interstitial cells in the musculature of the gastrointestinal tract: Cajal and beyond. Int Rev Cytol 229:115–208
13. Mei F, Han J, Zhou DS et al (2009) Plasticity of interstitial cells of Cajal: a study in the small intestine of adult guinea pigs. Anat Rec 292:985–993
14. Betsholtz C, Johnsson A, Heldin CH et al (1986) cDNA sequence and chromosomal localization of human platelet-derived growth factor A-chain and its expression in tumour cell lines. Nature 320:695–699
15. Heldin CH, Johnsson A, Wennergren S et al (1986) A human osteosarcoma cell line secretes a growth factor structurally related to a homodimer of PDGF A-chains. Nature 319:511–514
16. Boström H, Willetts K, Pekny M et al (1996) PDGF-A signaling is a critical event in lung alveolar myofibroblast development and alveogenesis. Cell 85:863–873
17. Lindahl P, Karlsson L, Hellström M et al (1997) Alveogenesis failure in PDGF-A deficient mice is coupled to lack of distal spreading of alveolar smooth muscle cell progenitors during lung development. Development 124:3943–3953
18. Calver AR, Hall AC, Yu WP et al (1998) Oligodendrocyte population dynamics and the role of PDGF in vivo. Neuron 20:869–882
19. Fruttiger M, Karlsson L, Hall AC et al (1999) Defective oligodendrocyte development and severe hypomyelination in PDGF-A knockout mice. Development 126:457–467
20. Karlsson L, Bondjers C, Betsholtz C (1999) Roles for PDGF-A and sonic hedgehog in development of mesenchymal components of the hair follicle. Development 126:2611–2621

21. Soriano P (1997) The PDGF alpha receptor is required for neural crest cell survival and for normal patterning of the somites. Development 124:2691–2700
22. Kurahashi M, Niwa Y, Cheng J et al (2008) Platelet-derived growth factor signals play critical roles in differentiation of longitudinal smooth muscle cells in mouse embryonic gut. Neurogastroenterol Motil 20:521–531
23. Robinson TL, Sircar K, Hewlett BR et al (2000) Gastrointestinal stromal tumors may originate from a subset of CD34-positive interstitial cells of Cajal. Am J Pathol 156:1157–1163
24. Vanderwinden JM, Rumessen JJ, De Laet MH et al (1999) CD34+cells in human intestine are fibroblasts adjacent to, but distinct from, interstitial cells of Cajal. Lab invest 79:59–65
25. Vanderwinden JM, Rumessen JJ, De Laet MH et al (2000) CD34 immunoreactivity and interstitial cells of Cajal in the human and mouse gastrointestinal tract. Cell Tissue Res 302:145–153
26. Fujita A, Takeuchi T, Jun H, Hata F (2003) Localization of Ca^{2+}-activated K^+ channel, SK3, in fibroblast-like cells forming gap junctions with smooth muscle cells in the mouse small intestine. J Pharmacol Sci 92:35–42
27. Vanderwinden JM, Rumessen JJ, Schiffmann SN et al (2002) Kit negative fibroblast like cells expressing SK3, a Ca^{2+}-activated K^+channel, in the gut musculature in health and disease. Cell Tissue Res 310:349–358
28. Komuro T, Seki K, Horiguchi K (1999) Ultrastructural characterization of the interstitial cells of Cajal. Arch Histol Cytol 62:295–316
29. Hirota S, Isozaki K, Moriyama Y et al (1998) Gain-of-function mutations of c-kit in human gastrointestinal stromal tumors. Science 279:577–580
30. Nishida T, Hirota S (2000) Biological and clinical review of stromal tumors in the gastrointestinal tract. Histol Histopathol 15:1293–1301
31. Heinrich MC, Corless CL, Duensing A et al (2003) PDGFRα activating mutations in gastrointestinal stromal tumors. Science 299:708–710
32. Hirota S, Ohashi A, Nishida T et al (2003) Gain-of-function mutations of platelet derived growth factor receptor alpha gene in gastrointestinal stromal tumors. Gastroenterology 125:660–667
33. Fleming TP, Saxena A, Clark WC et al (1992) Amplification and/or overexpression of platelet-derived growth factor receptors and epidermal growth factor receptor in human glia tumors. Cancer Res 52:4550–4553
34. Forsberg K, Valyi-Nagy I, Heldin C et al (1993) Platelet-derived growth factor (PDGF) in oncogenesis: Development of a vascular connective tissue stroma in xenotransplanted human melanoma producing PDGF-BB. Proc Natl Acad Sci 90:393–397
35. Skobe M, Fusenig NE (1998) Tumorigenic conversion of immortal human keratinocytes through stromal cell activation. Proc Natl Acad Sci 95:1050–1055
36. Shao ZM, Nguyen M, Barsky SH (2000) Human breast carcinoma desmoplasia is PDGF initiated. Oncogene 19:4337–4345

Virchows Arch (2010) 457:389–395
DOI 10.1007/s00428-010-0944-2

ORIGINAL ARTICLE

CD99-positive large cell neuroendocrine carcinoma with rearranged EWSR1 gene in an infant: a case of prognostically favorable tumor

Vicki S. Malone · Sheila M. Dobin · Kathleen A. Jones · Ludvik R. Donner

Received: 3 May 2010 / Revised: 14 June 2010 / Accepted: 17 June 2010 / Published online: 9 July 2010
© Springer-Verlag 2010

Abstract The first case of large cell neuroendocrine carcinoma arising in an infant is presented. The tumor arose at the anal verge of a 1-year-old girl. The diagnosis of this CD99-positive tumor was supported by expression of epithelial (keratins, EMA, and Ep-CAM) and neuroendocrine (chromogranin A, synaptophysin, and neuron-specific enolase) markers and absence of immunoreactivity for Fli-1. No fusion of EWSR1 with FLI-1 or ERG was detected by polymerase chain reaction. However, the split of the *EWSR1* gene was demonstrated by fluorescence in situ hybridization. This case adds to the few epithelial tumors in which an EWSR1 rearrangement was demonstrated. Because the tumor was initially misclassified as an extraskeletal Ewing's sarcoma, the patient was treated according to the Ewing's sarcoma treatment protocol. She remains free of tumor 8 years after initial diagnosis.

Keywords Neuroendocrine carcinoma · Anus · Infancy · EWSR1

V. S. Malone · S. M. Dobin · K. A. Jones · L. R. Donner (✉)
Department of Pathology,
Scott and White Memorial Hospital and Clinic,
2401 South 31st Street,
Temple, TX 76508, USA
e-mail: ldonner@swmail.sw.org

V. S. Malone · S. M. Dobin · K. A. Jones · L. R. Donner
Scott, Sherwood and Brindley Foundation,
Temple, TX, USA

V. S. Malone · S. M. Dobin · K. A. Jones · L. R. Donner
The Texas A&M Health Science Center College of Medicine,
Temple, TX, USA

Introduction

Neuroendocrine epithelial neoplasms are rarely encountered in children below the age of 10 years [1–5]. The youngest reported patient was a 6-year-old child with appendiceal carcinoid [2]. The rare incidence of neuroendocrine epithelial neoplasms contrasts with the incidence of extraskeletal Ewing's sarcomas. For example, out of 49 patients with extraskeletal Ewing's sarcomas entered in the Kiel Pediatric Tumor Registry, two patients were less than a year of age, and four patients were 1–5 years old [6]. We describe the first case of an infant with large cell neuroendocrine carcinoma. The clinical course was unexpectedly excellent, and she remains free of tumor for 8 years.

Clinical history

A 12-month-old white girl was seen in April 2002 for a recent 2-cm non-tender nodule of the left lateral aspect of the anal verge. Because the nodule was initially considered to represent a benign cyst, it was partially enucleated, partially bluntly dissected from adherent surrounding tissue 7 weeks later. An outside diagnosis of primitive neuroectodermal tumor was rendered, and the patient was registered in the Ewing's sarcoma treatment study and received vincristine, doxorubicin, and cyclophosphamide followed by ifosfamide, etoposide, mesna, and G-CSF starting July 2002.

The tumor site was re-excised in September 2002 and biopsied in October 2003. These procedures yielded perianal skin, anal and rectal tissue, and skeletal muscle. No residual tumor was found. She remains free of tumor for 8 years after excision. The magnetic resonance imaging of the abdomen and pelvis, and chest radiograms remain normal.

Materials and methods

Immunohistochemistry Immunohistochemical staining was performed on formalin-fixed, paraffin-embedded sections using EnVision + DAB system (Dako, Carpinteria, CA, USA). The tissue sections were pretreated by steaming in Dako Target Retrieval Solution, high pH except for tissue sections to be incubated with antibodies against MOC-31, Ber-EP4, GFAP, Fli-1, microtubule-associated protein 1B, and alpha-internexin, which were pretreated in citrate buffer pH 6.1 (Dako). The tissue section incubated with antibody against muscle-specific actin was not pretreated. The monoclonal antibodies used and their manufacturers are listed in Table 1.

Table 1 List of antibodies

Antibody	Source
AE-1/AE-3	Dako
Keratins 5/6	Dako
Keratin 7	Dako
Keratin 20	Dako
EMA	Dako
MOC-31	Dako
Ber-EP4	Dako
E-cadherin	Dako
CD99	Dako
Chromogranin A	Dako
Synaptophysin	Dako
Neuron-specific enolase	Dako
GFAP	Dako
Neurofilaments	Dako
S100	Dako
WT1	Dako
HHF35	Dako
Desmin	Dako
CD30	Dako
CD56	Novocastra[a]
Peripherin	Novocastra
NeuN	Chemicon[b]
Nestin	Chemicon
α-Internexin	Chemicon
Fli-1	Santa Cruz[c]
Microtubule-associated protein 1B	Sigma[d]
Prostate acid phosphatase	Convance[e]

[a] Novocastra, Bannockburn, IL, USA

[b] Chemicon International, Temeculla, CA, USA

[c] Santa Cruz Biotechnology, Santa Cruz, CA, USA

[d] Sigma, St. Louis, MO, USA

[e] Convance Research Products, Emeryville, CA, USA

Electron microscopy Portions of tumor tissue were fixed in 2.5% glutaraldehyde and postfixed in 1% osmium tetroxide. Thin sections were stained with uranyl acetate and lead citrate and were examined using a Hitachi H-600 electron microscope.

Molecular pathology Reverse transcription–polymerase chain reaction for the presence of EWSR1–FLI-1 and EWSR1–ERG was performed using total RNA extracted from paraffin-embedded tumor tissue by Dolores H. Lopez-Terrada, M.D., Ph.D., Department of Pathology, Texas Children's Hospital, Houston, TX, USA. The primers for beta-actin were used for amplification control.

Fluorescence in situ hybridization The analysis was performed on formalin-fixed, paraffin-embedded sections using LSI EWSR1 and LSI FUS dual color break-apart probes (Abbott Molecular/Vysis, Des Plaines, IL, USA) according to the manufacturer's instructions. The hybridization efficiency was 100%.

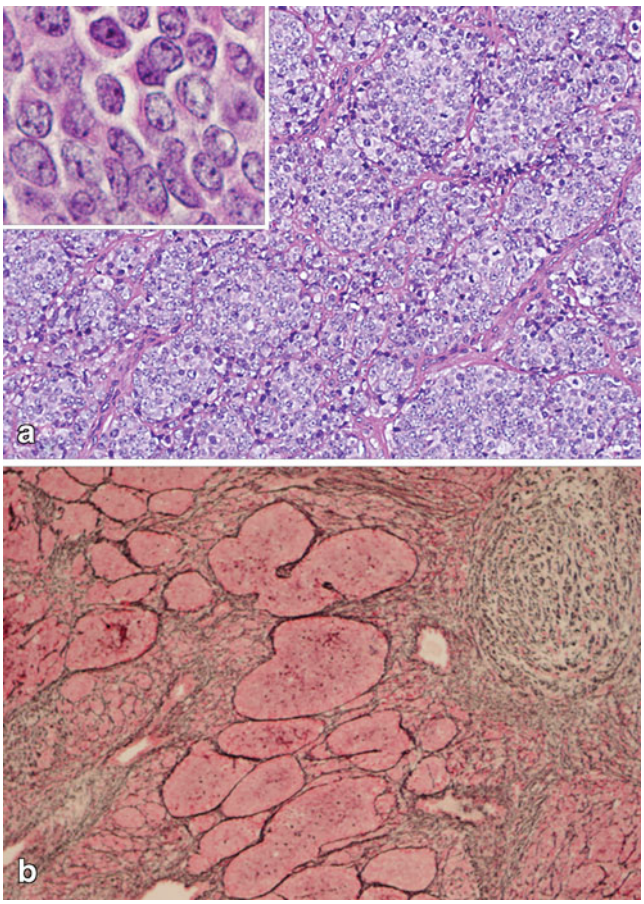

Fig. 1 Micronodular arrangement of tumor cells (**a**) that is accentuated by silver stain for reticulin fibers (**b**)

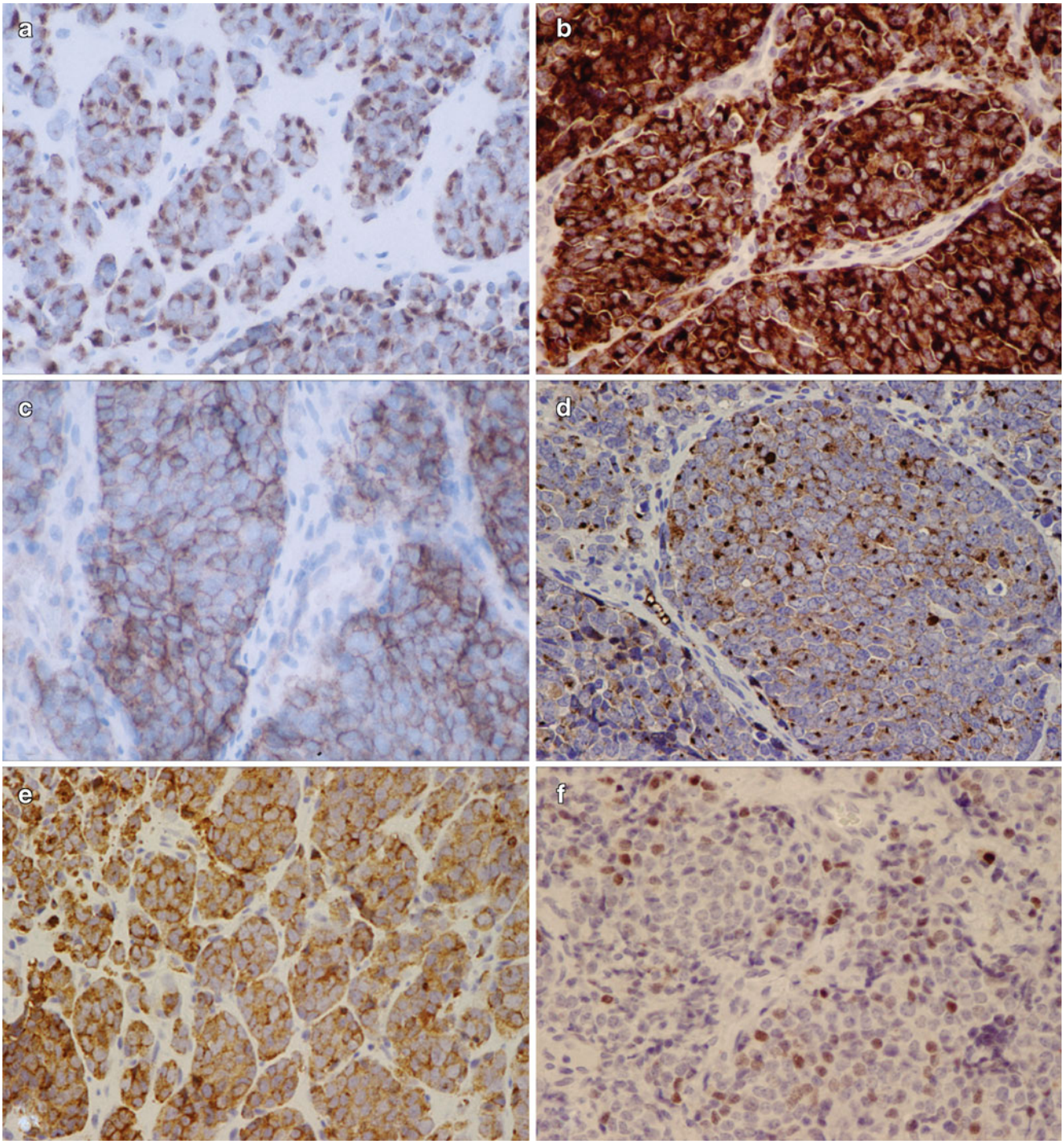

Fig. 2 Strong dot-like immunoreactivity for keratin (**a**), strong immunoreactivity for EMA (**b**), membranous positivity for CD99 (**c**), expression of chromogranin A (**d**) and synaptophysin (**e**), and multifocal nuclear expression of NeuN (**f**)

Pathologic findings

Gross and microscopic findings The tumor was received without any mucosa or skin. It measured 2.7×2.3×2.0 cm, was round and rubbery, and had a fleshy pink tan, focally necrotic parenchyma. It invaded the fibroadipose tissue, smooth and skeletal muscle. Focal perineural invasion was identified at the periphery of the tumor, but no vascular invasion was found. The margins were involved. Micronodular arrangement of the tumor cells was accentuated by Gordon and Sweets silver stain for reticulin fibers. The tumor was highly cellular, and the nuclei were round and medium sized, with dispersed chromatin and distinct nucleoli. The cytoplasm was scanty, amphophilic, or faintly eosinophilic.

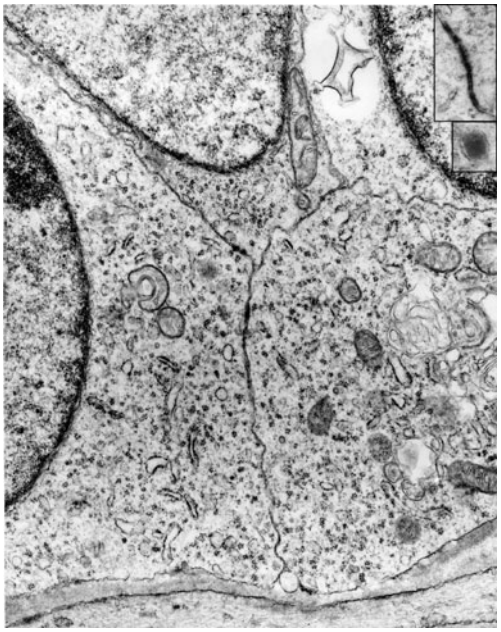

Fig. 3 Ultrastructure of the tumor. Note that in contrast to Ewing's sarcomas, the cytoplasm is quite organelle rich. Negative magnification, ×10,000. Note in *insets* a dense-core granule (negative magnification, ×5,000) and desmosome-like junction (negative magnification, ×8,000)

No glycogen was detected by periodic acid-Schiff stain. Fourteen mitoses were identified in ten high-power fields (Fig. 1).

Immunohistochemical findings All neoplastic cells were strongly positive in a dot-like pattern for pan-keratin. They were also strongly positive for EMA, MOC-31, chromogranin A, synaptophysin, neuron-specific enolase, and CD56 and were moderately positive for Ber-Ep4, CD99, NeuN, and microtubule-associated protein 1B. Not detected were keratins 5/6, keratin 7, keratin 20, E-cadherin, GFAP, neurofilaments, S100 protein, nestin, peripherin, alpha-internexin, CD30, WT1, muscle-specific actin, desmin, and prostate acid phosphatase. Sixteen percent of cells were Ki-67 positive (Fig. 2).

Ultrastructural findings The cytoplasm was rich in polyribosomes and contained prominent rough endoplasmic reticulum and moderate numbers of mitochondria. The cell membranes were straight and contained occasional primitive cell junctions and desmosome-like junctions. The intermediate filaments were scanty. Only rare 200-nm dense-core granules consistent with neuroendocrine granules were identified (Fig. 3).

Molecular pathology No EWSR1–FLI1 and EWSR1–ERG fusions were detected by polymerase chain reaction.

Fluorescence in situ hybridization study Two hundred nuclei each were analyzed. Rearrangement of the *EWSR1* gene was detected in 62% of nuclei scored. No cells with a rearranged *FUS* gene were observed (Fig. 4a, b).

Discussion

Our diagnosis of large cell neuroendocrine carcinoma is based on immunohistochemical, ultrastructural, and molecular genetic data. While up to one third of Ewing's sarcomas express keratin, the expression is typically focal and exceptionally multifocal [7–12]. Synaptophysin, neuron-specific enolase, and CD56 are expressed in a small minority of Ewing's sarcomas, but these tumors are chromogranin A negative [13, 14]. CD99, a characteristic Ewing's sarcoma marker, is also expressed in 20% of neuroendocrine carcinomas [15, 16]. Fli-1, a marker expressed in the majority of Ewing's sarcomas [17], was not expressed in our tumor. NeuN is expressed in the majority of normal

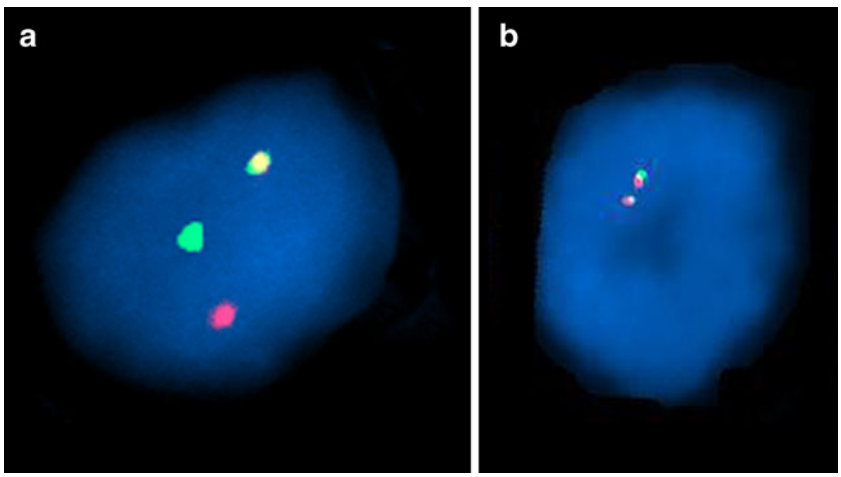

Fig. 4 Interphase FISH study using break-apart EWSR1 and FUS probes. **a** One fusion, one red, and one green signal indicate rearrangement of *EWSR1* gene. **b** *FUS* gene is not rearranged

neurons, a minority of neuroblastomas, and tumors that are not of neuronal derivation, like ependymomas, rhabdomyosarcomas, and even neuroendocrine carcinomas [10, 18, 19]. The ultrastructural features of our tumor, particularly its relatively organelle-rich cytoplasm, are also not consistent with Ewing's sarcoma [20]. Although fusion of the *EWSR1* gene with *FLI-1* or *ERG* genes was not detected in our tumor by polymerase chain reaction, the fluorescence in situ hybridization (FISH) study revealed that the *EWSR1* gene was rearranged. Ewing's sarcomas carry characteristic fusion of the 5′ portion of the *EWSR1* gene with the 3′ portion of one of the following genes of the ETS family of transcription factors: FLI-1 (in 90–95% of tumors), ERG (in 5–10% of tumors), and rarely with ETV1, E1AF, and FEV [21]. Very rare cases of fusion with NFATc2, which codes for another transcription factor that shares sequences with the ETS family [22] and ZSG, which codes for a putative zinc finger protein with transcriptional repressor-like domain [23], were described. In a handful of cases, the *EWSR1* gene remained intact and was functionally substituted by FUS–ERG or FUS–FEV fusions [24–26].

Weinreb et al. [27] recently described a soft tissue tumor of the neck in a 29-year-old man with light microscopic, immunophenotypic, and ultrastructural features of squamous cell carcinoma. EWSR1–FLI-1 fusion was detected in the tumor by polymerase chain reaction and by FISH. Although the authors chose to classify the tumor as Ewing's sarcoma, their finding indicates that EWSR1–FLI-1 fusion could occur in a wider range of tumors than currently thought.

Most importantly, rearrangement of the *EWSR1* gene is not restricted to Ewing's sarcomas but occurs also in desmoplastic small round cell tumors, clear cell sarcomas, extraskeletal myxoid chondrosarcomas, angiomatoid fibrous histiocytomas, and myxoid/round cell liposarcomas [28, 29], and was described in a case of embryonal rhabdomyosarcoma [30]. It was also detected in several epithelial tumors: in five of six hidradenomas, a mucoepidermoid carcinoma of the submandibular gland [31], a soft tissue myoepithelioma [32], and a soft tissue myoepithelial carcinoma [33]. Unfortunately, the cell cultures derived from our tumor yielded only diploid cells, and the partner gene of the translocated EWSR1 remains unknown.

Large cell neuroendocrine carcinoma of the anal canal is a rarity—approximately 20 cases have been reported, none of them in children [34, 35]. Large cell neuroendocrine carcinomas of the rectum are also rare and highly malignant neoplasms that typically arise in elderly patients. A 12-year-old girl with poorly differentiated adenocarcinoma with neuroendocrine differentiation of the left colon was included in the National Tumor Institute, Milan, Italy study of seven children with colorectal carcinomas. The patient succumbed to her disease after 26 months despite 12 cycles of 5-fluorouracil therapy [36]. Approximately 70% of adult patients already present with metastases, and their overall survival is only 7–10 months [35, 37]. There are few reports in the literature about chemotherapy of neuroendocrine tumors of the gut, and experience is limited. Chemotherapy should be used only in metastatic disease. The combination of streptozotocin plus 5-fluorouracil/doxorubicin is recommended in metastatic less aggressive tumors and cisplatin/carboplatin in poorly differentiated tumors of the foregut. Cisplatin plus etoposide have proven to be effective in fast growing midgut and hindgut tumors [38]. A 67% response rate to etoposide and cisplatin was reported in a single study for poorly differentiated neuroendocrine carcinomas of the gut. Unfortunately, the median duration of remissions lasted less than 8 months [39]. Thus, the excellent clinical course of our patient is intriguing and seems to be without a parallel. Although the margins of the excision specimen were heavily involved by the tumor, no remaining tumor was found in the re-excision and biopsy specimens. It is uncertain whether the residual neoplastic cells were killed by chemotherapy or by cauterization. Prognostic significance of mitotic count and Ki-67 index were proposed for neuroendocrine tumors of the foregut [40]. Although our tumor was histologically poorly differentiated, both parameters were lower than required for grade 3 tumors. It may indicate a certain degree of limitation of its biological aggressiveness.

Acknowledgments Consultation with Professor Dr. Gunter Kloppel, Institute of Pathology, and Professor Dr. Ivo Leuschner, Institute of Pediatric Pathology, University of Kiel, Kiel, Germany is gratefully acknowledged.

Conflict of interest statement We declare that we have no conflict of interest.

References

1. Broaddus RR, Herzog CE, Hicks MJ (2003) Neuroendocrine tumors (carcinoid and neuroendocrine carcinoma) presenting at extra-appendiceal sites in childhood and adolescence. Arch Pathol Lab Med 127:1200–1203
2. Corpron CA, Black CT, Herzog CE, Sellin RV, Lally KP, Andrassy RJ (1995) A half century of experience with carcinoid tumors in children. Am J Surg 170:606–608
3. Moertel CL, Weiland LH, Telander RL (1990) Carcinoid tumor of the appendix in the first two decades of life. J Pediatr Surg 25:1073–1075
4. Schmid CH, Beham A, Feichtinger J, Aubock L, Dietze O (1992) Recurrent and subsequently metastasizing Merkel cell carcinoma in a 7-year-old girl. Histopathology 20:437–439
5. Spunt SL, Pratt CB, Rao BN, Pritchard M, Jenkins JJ, Hill DA, Cain AM, Pappo AS (2000) Childhood carcinoid tumors: the St Jude Children's Research Hospital experience. J Pediatr Surg 35:1282–1286
6. Harms D (1995) Soft tissue sarcomas in the Kiel Pediatric Tumor Registry. In: Harms D, Schmidt D (eds) Current topics in pathology. Springer, Berlin, pp 31–45

7. Collini P, Sampietro G, Bertulli R, Casali PG, Luksch R, Mezzelani A, Sozzi G, Pilotti S (2001) Cytokeratin immunoreactivity in 41 cases of ES/PNET confirmed by molecular diagnostic studies. Am Surg Pathol 25:273–274
8. Folpe AL, Goldblum JR, Rubin BP, Shehata BM, Liu W, Dei Tos AP, Weiss SW (2005) Morphologic and immunophenotypic diversity in Ewing family tumors: a study of 66 genetically confirmed cases. Am J Surg Pathol 29:1025–1033
9. Gu M, Antonescu CR, Guiter G, Huvos AG, Ladanyi M, Zakowski MF (2000) Cytokeratin immunoreactivity in Ewing's sarcoma: prevalence in 50 cases confirmed by molecular diagnostic studies. Am J Surg Pathol 24:410–416
10. Shuangshoti S, Mujananon S, Chaipipat M, Keetacheeva K, Shuangshoti S (2005) Expression of neuronal nuclear antigen (NeuN) in epithelial neuroendocrine carcinoma. Appl Immunohistochem Mol Morphol 13:265–267
11. Vakar-Lopez F, Ayala AG, Raymond AK, Czerniak B (2000) Epithelial phenotype in Ewing's sarcoma/primitive neuroectodermal tumor. Int J Surg Pathol 8:59–65
12. Srivastava A, Rosenberg AE, Selig M, Rubin BP, Nielsen GP (2005) Keratin-positive Ewing's sarcoma: an ultrastructural study of 12 cases. Int J Surg Pathol 13:43–50
13. Gardner LJ, Polski JM, Fallon R, Dunphy CH (1998) Identification of CD56 and CD57 by flow cytometry in Ewing's sarcoma or primitive neuroectodermal tumor. Virchows Arch 433:35–40
14. Wick MR (2000) Immunohistology of neuroendocrine and neuroectodermal tumors. Semin Diagn Pathol 17:194–203
15. Ali A, Serra S, Asa SL, Chetty R (2006) The predictive value of CK19 and CD99 in pancreatic endocrine tumors. Am J Surg Pathol 30:1588–1594
16. Pelosi G, Rraggetta F, Sonzogni A, Fazio N, Cavallon A, Viale G (2000) CD99 immunoreactivity in gastrointestinal and pulmonary neuroendocrine tumours. Virchows Arch 437:270–274
17. Folpe AL, Hill CE, Parham DM, O'Shea PA, Weiss SW (2000) Immunohistochemical detection of FLI-1 protein expression: a study of 132 round cell tumors with emphasis on CD99-positive mimics of Ewing's sarcoma/primitive neuroectodermal tumor. Am J Surg Pathol 24:1657–1662
18. Parker JR, Armstrong DL, Strother D, Rudman DM, Dauser RC, Laurent JP, Deyd J, Rouah PE (2001) Anti-neuronal nuclei immunohistochemical staining pattern in childhood ependymomas. J Child Neurol 16:548–552
19. Willoughby V, Sonawala A, Werlang-Perurena A, Donner LR (2008) A comparative immunohistochemical analysis of small round cell tumors of childhood: utility of peripherin and α-internexin as markers for neuroblastomas. Appl Immunohistochem Mol Morphol 16:344–348
20. Mackay B, Donner L, Ordonez NG (1986) Small round cell tumors. In: Russo J, Sommers SC (eds) Tumor diagnosis by electron microscopy, 3rd edn. Field, Rich, and Associates, New York, pp 281–313
21. Sandberg AA, Bridge JA (2000) Updates on cytogenetics and molecular genetics of bone and soft tissue tumors: Ewing sarcoma and peripheral primitive neuroectodermal tumors. Cancer Genet Cytogenet 123:1–26
22. Szuhai K, Ijszenga M, de Jong D, Karseladze A, Tanke HJ, Hogendoorn PC (2009) The NFATc2 gene is involved in a novel cloned translocation in a Ewing sarcoma variant that couples its function in immunology to oncology. Clin Cancer Res 15:2259–2268
23. Mastrangelo T, Modena P, Tornielli S, Bullrich F, Testi MA, Mezzelani A, Radice P, Azzarelli A, Pilotti S, Croce CM, Pierotti MA, Sozzi G (2000) A novel zinc finger gene is fused to EWS in small round cell tumor. Oncogene 19:3799–3804
24. Berg T, Kalsaas AH, Buechner J, Busund LT (2009) Ewing sarcoma–peripheral neuroectodermal tumor of the kidney with a FUS–ERG fusion transcript. Cancer Genet Cytogenet 194:53–57
25. Ng TL, Nielsen T, Hayes M et al (2007) Novel Ewing sarcoma translocation identified in a case lacking EWS gene rearrangement. Pediatr Dev Pathol 10:83A
26. Shing DC, McMullan DJ, Roberts P, Smith K, Chin SF, Nicholson J, Tillman RM, Ramani P, Cullinane C, Coleman N (2003) FUS/ERG gene fusion in Ewing's tumors. Cancer Res 63:4568–4576
27. Weinreb I, Goldstein D, Perez-Ordonez B (2008) Primary extraskeletal Ewing family tumor with complex epithelial differentiation: a unique case arising in the lateral neck presenting with Horner syndrome. Am J Surg Pathol 32:1742–1748
28. Romeo S, Dei Tos AP (2010) Soft tissue tumors associated with EWSR1 translocation. Virchows Arch 456:219–234
29. Tanas MR, Goldblum JR (2009) Fluorescence in situ hybridization in the diagnosis of soft tissue neoplasms: a review. Adv Anat Pathol 16:838–391
30. Sirvent N, Trassard M, Ebran N, Attias R, Pedeutour F (2009) Fusion of EWSR1 with the DUX4 facioscapulohumeral muscular dystrophy region resulting from t(4;22)(q35;q12) in a case of embryonal rhabdomyosarcoma. Cancer Genet Cytogenet 195:12–18
31. Moller E, Stenman G, Mandahl N, Hamberg H, Molne L, van den Oord JJ, Brosjo O, Mertens F, Panagopoulos I (2008) POU5F1, encoding a key regulator of stem cell pluripotency, is fused to EWSR1 in hidradenoma of the skin and mucoepidermoid carcinoma of the salivary glands. J Pathol 215:78–86
32. Brandal P, Panagopoulos I, Bjerkehagen B, Gorunova L, Skjeldal S, Micci F, Hein S (2008) Detection of a t(1;22)(q23;q12) translocation leading to an EWSR1–PBX1 fusion gene in a myoepithelioma. Genes Chromosom Cancer 47:558–564
33. Brandal P, Panagopoulos I, Bjerkehagen B, Heim S (2009) T(19;22)(q13;q12) translocation leading to the novel fusion gene EWSR1–ZNF444 in soft tissue myoepithelial carcinoma. Genes Chromosom Cancer 48:1051–1056
34. Balachandra B, Marcus V, Jass JR (2007) Poorly differentiated tumours of the anal canal: a diagnostic strategy for the surgical pathologist. Histopathology 50:163–174
35. Bernick PE, Klimstra DS, Shia J, Minsky B, Saltz L, Shi W, Thaler H, Guillem J, Paty P, Cohen AM, Wong WD (2004) Neuroendocrine carcinomas of the colon and rectum. Dis Colon Rectum 47:163–169
36. Ferrari A, Rognone A, Casanova M, Zaffignani E, Piva L, Collini P, Bertario L, Sala P, Leo E, Belli F, Gallino G (2008) Colorectal carcinoma in children and adolescents: the experience of the Istituto Nazionale Tumori of Milan, Italy. Pediatr Blood Cancer 50:588–593
37. Ahlman A, Nilsson DO, McNicol AM, Ruszniewski P, Niederle B, Ricke J, Jensen R, Kos-Kudla B, Oberg K, O'Connor JM, Pavel ME, Vullierme MP, Frascati Consensus Conference participants (2008) Poorly differentiated endocrine carcinomas of midgut and hindgut origin. Neuroendocrinology 87:40–46
38. Plockinger U, Rindi G, Arnold R, Eriksson B, Krenning EP, de Herder WW, Goede A, Caplin M, Oberg K, Reubi JC, Nilsson O, Delle Fave G, Ruszniewski P, Ahlman H, Weidenmann B, Society European Neuroendocrine Tumour (2004) Guidelines for the diagnosis and treatment of neuroendocrine gastrointestinal tumours. A consensus statement on behalf of the European

Neuroendocrine Tumour Society (ENETS). Neuroendocrinology 80:394–424
39. Moertel CG, Kvols LK, O'Connell MJ, Rubin J (1991) Treatment of neuroendocrine carcinomas with combined etoposide and cisplatin. Evidence of major therapeutic activity in the anaplastic variants of these neoplasms. Cancer 68:227–232
40. Rindi G, Kloppel G, Ahlman H, Caplin M, Couvelard A, de Herder WW, Erikssson B, Falchetti A, Falconi M, Komminoth P, Korner M, Lopes JM, McNicol AM, Nilsson O, Perren A, Scarpa A, Scoazec JY, Wiedenmann B, Frascati Consensus Conference participants (2006) TNM staging of foregut (neuro)endocrine tumors: a consensus proposal including a grading system. Virchows Arch 449:395–401

Virchows Arch (2010) 457:397–404
DOI 10.1007/s00428-010-0937-1

ORIGINAL ARTICLE

Strength of molecular cytogenetic analyses for adjusting the diagnosis of renal cell carcinomas with both clear cells and papillary features: a study of three cases

Juliette Haudebourg · Benjamin Hoch · Thibault Fabas · Nathalie Cardot-Leccia · Fanny Burel-Vandenbos · Annick Vieillefond · Jean Amiel · Jean-François Michiels · Florence Pedeutour

Received: 1 February 2010 / Revised: 7 May 2010 / Accepted: 18 May 2010 / Published online: 22 June 2010
© Springer-Verlag 2010

Abstract Histological features are usually sufficient for providing an accurate diagnosis of renal cell carcinomas (RCC). However, the morphological appearance might sometimes be misleading. For instance, RCC with papillary areas and extensive clear cell changes may be difficult to classify either as clear cell renal carcinoma or as papillary renal cell carcinoma (pRCC). We used the combination of immunohistochemistry, conventional cytogenetics, fluorescence in situ hybridization (FISH), bacterial artificial chromosomes comparative genomic hybridization arrays and high-density single nucleotides polymorphism arrays (SNP arrays) to characterize three cases of RCC showing a predominant cytology of cells with clear cytoplasm and variable amounts of papillary areas. In accordance with the 2004 World Health Organization (WHO) classification, we initially assessed the diagnosis of clear cell RCC for one of the cases and unclassified RCC for the two remaining cases. However, because of a strong immunohistochemical labeling for α-methylacyl-CoA racemase, as well as the presence of a gain of chromosomes 7 and 17, we concluded that two of these tumors were actually pRCC. As for the third case, because of the presence of both pCCR and ccCCR molecular cytogenetic aberrations, including gains of chromosomes 7 and 17, loss of chromosome Y and whole chromosome 3 loss of heterozyosity (isodisomy), the final diagnosis was hybrid tumor cc-pRCC, so-called "unclassified RCC" according to the WHO classification. Our observations demonstrate the necessity to use immunohistochemical and cytogenetic tools in all cases of RCC showing unusual features. The combination of FISH and SNP arrays is prevailing for characterizing cases with hybrid features.

Keywords Clear cell renal carcinoma · Papillary renal cell carcinoma · AMACR · FISH · CGH array · SNP array

Supported by the French Institut National du Cancer

J. Haudebourg (✉) · N. Cardot-Leccia · F. Burel-Vandenbos · J.-F. Michiels
Department of Pathology, Nice University Hospital, Nice, France
e-mail: juliette.haudebourg@nice.fnclcc.fr

B. Hoch · T. Fabas · F. Pedeutour
Laboratory of Solid Tumors Genetics, Nice University Hospital, Nice, France

B. Hoch · T. Fabas · F. Pedeutour
Faculty of Medicine, University of Nice Sophia-Antipolis, CNRS, UMR 6543, Nice, France

A. Vieillefond
Department of Pathology, Cochin Hospital, Paris, France

J. Amiel
Department of Urology, Nice University Hospital, Nice, France

Introduction

The classification of renal cell carcinomas (RCC) includes several histological subtypes among which clear cell carcinomas (ccRCC) and papillary renal cell carcinomas (pRCC) are the most common [1]. According to the 2004 World Health Organization (WHO) classification [1], ccRCC show a solid alveolar growth pattern composed of clear cells, while pRCC are characterized by papillae recovered by small basophilic cells (type 1 pRCC) or by large eosinophilic cells (type 2

pRCC). Immunohistochemical analysis is helpful for distinguishing ccRCC from pRCC [2]. Indeed, ccRCC typically show immunoreactivity to antibodies against CD10, whereas they lack immunoreactivity for α-methylacyl-CoA racemase (AMACR) and cytokeratin 7 (CK7). In contrast, pRCC show a characteristic positivity for AMACR and CK7 and less frequently for CD10. The immunoreactivity for CK7 is more frequent in type 1 pRCC (80%) than in type 2 pRCC (20%). Considering that ccRCC are more aggressive than type 1 pRCC and that type 2 pRCC, which account for 33% of papillary tumors, are characterized by a poor prognosis, it is important to identify precisely the RCC subtypes in order to provide the most appropriate care to the patient. The emergence of targeted therapies, such as antiangiogenic drugs and mTOR inhibitors, has dramatically improved the survival of patients affected by ccRCC. However, according to the WHO 2004 classification [1] criteria, 4–5% of RCC presenting unusual morphological features are reported as "unclassified". In particular, the presence of mixed morphological components in the same tumor is puzzling for the pathologist and may cause misdiagnoses. For instance, tumors with both clear cells and papillae may be the cause of diagnostic difficulties and subsequent inappropriate treatments.

Most common types of RCC are characterized by recurrent chromosomal abnormalities, the detection of which is very useful for confirming or completing the diagnosis. In fact, approximately 60–80% of ccRCC are characterized by a complete or partial loss of chromosome 3 when studied by classic molecular cytogenetic methods [3] and as much as 100% by high-density single nucleotide polymorphism-based oligonucleotide arrays (SNP arrays) [4]. In contrast, most type 1 pRCC show gains of chromosomes 7 and 17, and loss of chromosome Y in tumor cells from male patients [5].

We report three cases of RCC, with predominant clear cell features and variable proportions of papillary architecture. In accordance with the 2004 WHO classification [1], we initially proposed the diagnosis of ccCCR for one of the cases and unclassified RCC for the two remaining cases. However, complementary immunohistochemical and molecular studies, including conventional cytogenetics, fluorescence in situ hybridization (FISH), comparative genomic hybridization on bacterial artificial chromosomes arrays (BAC CGH array) plus SNP arrays allowed us to establish alternative diagnoses for these three cases we analyzed.

Materials and methods

Histological and immunohistochemical analysis

Tumor material was fixed in 10% phosphate-buffered formalin and embedded in paraffin. Histological sections were stained with hematoxylin–eosin–saffron. Immunohistochemical analysis was done using the following monoclonal antibodies: CK7 (clone OV-TL12/30, Dako, Glostrup, Denmark), CD10 (clone 56C6, 1/20 dilution, Novocastra, Newcastle, UK), AMACR (clone 13H4, 1/100 dilution, Dako), TFE3 (SC-5958, 1/300 dilution, Santa Cruz, CA, USA) and TFEB (Santa Cruz SC-11004, 1/400 dilution, Santa Cruz, CA, USA). Immunolabeling and detection were performed using the Dako autostainer automate and the EnVision system (Dako), according to the manufacturer's recommendations. Antigen retrieval was performed using target retrieval solution PH6 (reference K8010, Dako) for EMA and target retrieval solution PH9 (reference K8015, Dako) for AMARC, CD10, CK7, TFE3 and TFEB. The detection was performed using the Envision Flex Kit (Dako) with 3-3 diaminobenzidine as a chromogen.

Cytogenetic and FISH analysis

Fresh fragments of the tumors were prepared for cytogenetic analysis. Tumor tissues were disaggregated and cells from short-term cultures (4–10 days) were used for metaphase chromosome preparations according to standard methods [6]. Metaphase search and karyotyping were performed using the Metafer M-Search Metaphase Finder and Ikaros softwares (Metasystems, Althusseim, Germany). Karyotypes were described in accordance to the International System for Human Cytogenetic Nomenclature [7].

Preparations of metaphase cells for FISH analyses, labeling of probes and evaluation of results were done as described previously [8]. FISH analysis was performed on interphase cell suspensions obtained from a fresh sample and fixed by methanol/acetic acid (1:3) for cases 1 and 2 and extracted from 50-µm-thick tissue sections fixed in formalin and paraffin-embedded for case 3. The probes used for this study are described in Table 1. Microscopic analysis was completed using a DM6000B microscope (Leica Microsystems, Wetzlar, Germany). FISH images were processed using the ISIS software (MetaSystems).

BAC CGH array and SNP array analyses

DNA from cases 1 and 2 was extracted from frozen fragments of the tumors, according to standard methods. DNA was quantified using the PicoGreen system (Invitrogen, San Diego, CA)). One microgram of tumor DNA labeled with Cy5 and 1 µg of DNA obtained from a pool of 25 sex-matched reference samples (Coriell Institute for Medical Research, Camden, NJ) labeled with Cy3 were hybridized to the BAC CGH arrays IntegraCHIP V.7.2 (5244 BAC clones spaced along the genome, median gap of 0.5 Mb between clones) (IntegraGen, Evry, France). The

Table 1 Probes used for FISH analysis

Probe name	Locus/chromosomal position	Origin
UroVysion®	Centromeric probes CEP 3, CEP 7, CEP 17 and locus 9p21	Vysis[a]
AneuVysion®	(1) Centromeric probes CEP 18, CEP X, CEP Y and locus Yq12 (2) LSI 13 (locus 13q14) and LSI 21 (locus 21q22.13-q22.2)	Vysis®[a]
RP11-438 J1 and RP11-642E22	Probe distal to *VHL*/(3p25.3) (chr3:10,158,319-10,168,746 and chr3:8,746,429-8,841,478)[b]	CHORI[c]
CEP® 2	Centromere 2	Vysis[a]
LSI® p16/CEP® 9	Locus 9p21 (CDKN2A and CDKN2B) and centromere 9	Vysis[a]
LSI® CyclinD1	Locus 11q13 and Centromere 11	Vysis[a]

[a] Downers Grove, IL, USA

[b] http://genome.ucsc.edu

[c] Children's Hospital Oakland Research Institute; http://bacpac.chori.org/

BAC CGH arrays data were analyzed using the GenoCensus® software (IntegraGen). Cy5/Cy3 ratios of background-corrected intensities were normalized by a block-by-block loess regression procedure, and mean ratios were obtained from the spot replicates of each clone. We removed from the analysis clones with less than three morphologically acceptable replicates or with a coefficient of variation of the mean of the replicates that exceeded 0.2 .

The SNP BeadChip Human370CNV-Quad (Illumina, San Diego, CA) was used for the SNP array analyses. Data were analyzed using the BeadStudio v3.0 software (Illumina), which allows for the visualization of several variables relevant to the detection of copy number alterations, including the B-allele frequency (BAF) and log R ratio (LRR). The BAF for a sample shows the theta value for a SNP, corrected for cluster position. Cluster positions were generated from a large set of normal individuals. "Normal" diploid DNA is expected to have three BAF clusters: two for the homozygous SNPs (AA and BB) with BAF close to 0 and 1, respectively, and one for the heterozygous SNPs (AB) with BAF centred at approximately 0.5. The BAF=0 if theta<tAA;=0.5×(theta−tAA)/(tAB−tAA) if theta<tAB;=0.5+0.5×(theta−tAB)/(tBB−tAB) if theta<tBB;=1 if theta>or=tBB (tAA, tAB and tBB are the mean theta values of all genotypes in the AA, AB and BB clusters plotted in polar normalized coordinates, respectively). The LRR graph shows the log normalized intensity ratio for each SNP in the test sample compared with a reference DNA sample. The LRR is based on normalized intensity data. The LRR for a sample is the log (base 2) ratio of the normalized *R* value for the SNP divided by the expected normalized *R* value. We should note that the presence of the expected two copies of any given SNP in a normal, diploid state would result in a LRR of approximately 0. Also, statistically significant deviations from 0 are interpreted as copy number changes. Then, a positive LRR suggests gain in copy number and a negative LRR suggests a loss in copy number. Because anomalies of the ploidy may be overlooked by the normalization, the thresholds for detection of single copy alterations were adapted according to the level of ploidy as previously determined by interphase FISH analysis (and by karyotype for case 2).

Clinical and histopathological observations

Case 1

The patient was a 77-year-old man who presented with abdominal pain. He had a previous history of hypertension, obesity [body mass index (BMI), 32] and dyslipidemia. Computed tomography (CT) scan revealed a 6-cm heterogeneous mass in the right kidney. A right nephrectomy was performed. Gross examination showed an encapsulated tumor of 6 cm located in the inferior pole of the kidney. The cut surface showed a solid golden yellow tumor. Microscopically, 70% of the neoplastic cells had predominantly clear cytoplasms, while 30% of them had eosinophilic cytoplasms. The tumor cells were arranged predominantly in an alveolar and trabecular pattern and separated by fibrovascular septae. Areas of papillary pattern accounted for approximately 5% of the tumor (Fig. 1). Papillae were recovered by eosinophilic cells and rarely by clear cells. Foamy macrophages were not observed. The Fürhman nuclear grade was III and the stage was pT1b. According to the 2004 WHO classification, the diagnosis was ccRCC. After a follow-up period of 2 years, the patient showed no evidence of disease.

Case 2

A 53-year-old woman with previous history of hypertension and obesity (BMI, 35) presented with a pain in the right flank. CT scan showed a 4.5-cm enhancing solid mass of the right kidney. A right nephrectomy was performed. Gross examination of the kidney showed an encapsulated

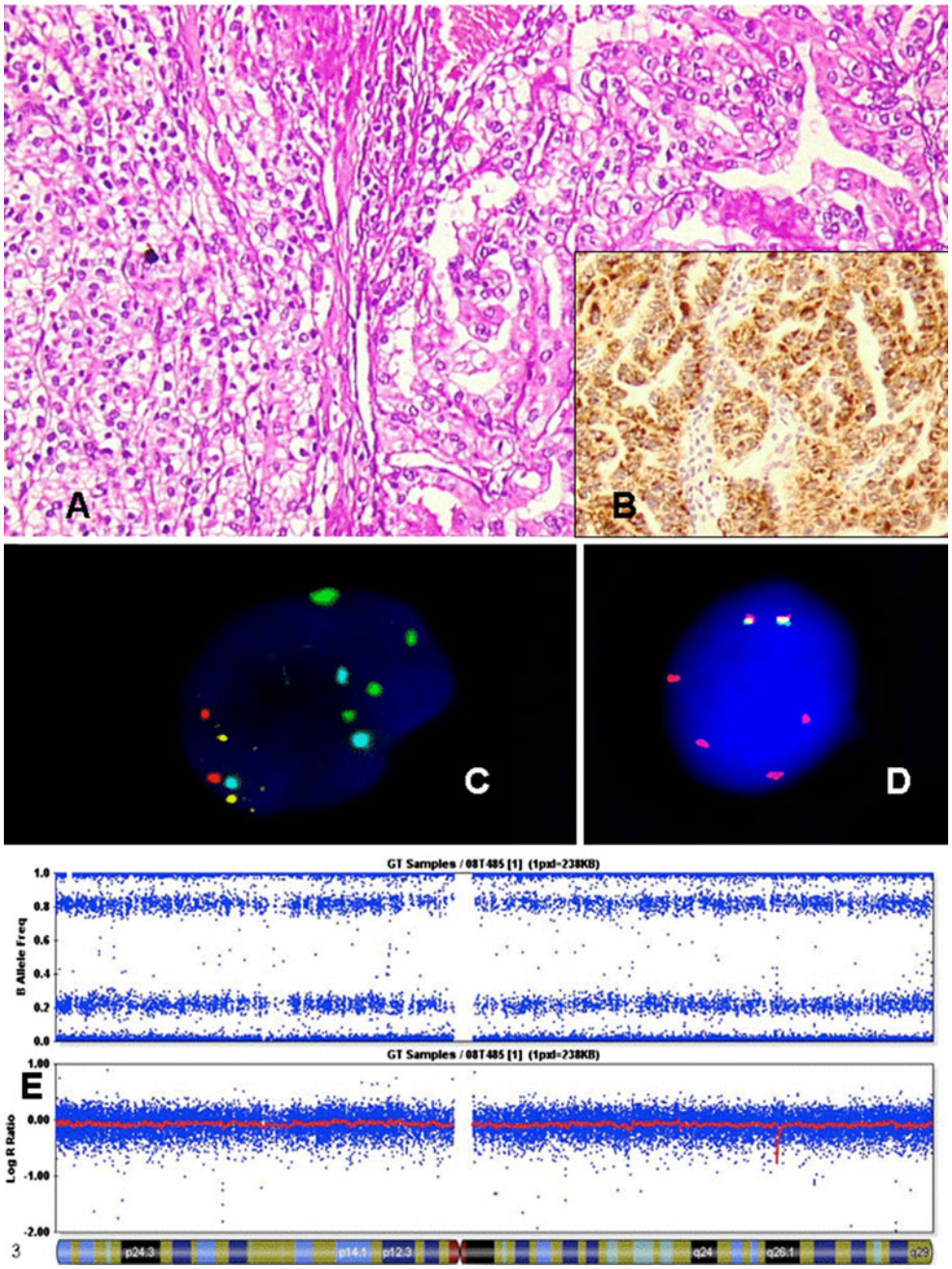

Fig. 1 Immunohistochemical and genetic features of case 1. **a** Microscopic field showing renal cell carcinoma with both clear cells in the solid area at the left side and papillae area at the right side (hematoxylin–eosin–saffron, magnification ×100). **b** Immunostaining for AMACR showing diffuse reactivity (magnification ×100). **c** Fluorescence in situ hybridization using centromeric probes for chromosome 3 (*red signals*), chromosome 7 (*green signals*), chromosome 17 (*blue signals*) and subtelomeric probe 9p21 (*gold signals*) showing a representative nucleus with disomy 3, tetrasomy 7, trisomy 17 and disomy 9p21. **d** Fluorescence in situ hybridization with a probe specific for the *VHL* gene and a neighbor locus at 3p25.3 (coupled red/green signals) and a centromeric probe of chromosome 7 (red signals) showing two signals for *VHL* (absence of deletion) and a tetrasomy 7 (four red signals). **e** SNP array showing loss of heterozygosity (isodisomy) for chromosome 3. The lower box shows LRR graph: the log normalized intensity ratio for each SNP in case 1 sample compared with a reference DNA sample is at 0. This indicates no loss or gain of chromosome 3 (disomy 3). The upper box shows B-allelic frequency (*BAF*: allelic copy ratio for the genomic SNPs). No cluster for the heterozygous SNPs (AB) with BAF centered at approximately 0.5 is observed in this case, whereas two clusters are observed for the homozygous SNPs (AA and BB) with BAF close to 0 and 1, respectively. This indicates a loss of heterozygosity (isodisomy) for chromosome 3. The presence of SNP showing BAF at 0.8 and 0.2 corresponds to DNA from stromal cells (slight contamination by nontumoral tissue)

tumor of 4.5 cm of the inferior pole. The cut surface was solid, yellow, and showed haemorrhagic changes. Microscopically, the architecture was nested, solid and papillary (Fig. 2). The nests were separated by delicate fibrovascular septae. The cells were large with predominantly clear cytoplasms (80%) and rarely eosinophilic cytoplasms (20%) (Fig. 2). The areas of papillary pattern represented 40% of the tumor volume. Foamy macrophages were observed. The papillae were recovered by clear cells and eosinophilic cells. The Fürhman nuclear grade was III and the stage was pT1b. According to the 2004 WHO classification [1], the diagnosis was "unclassified RCC". After a follow-up period of 3 years, the patient showed no evidence of disease.

Case 3

A 43-year-old female patient with unremarkable medical history presented with abdominal pain. CT scan showed a 2.8-cm solid mass of the inferior pole of the right kidney. A right partial nephrectomy was performed for excision of the tumor. Gross examination of kidney showed a well-

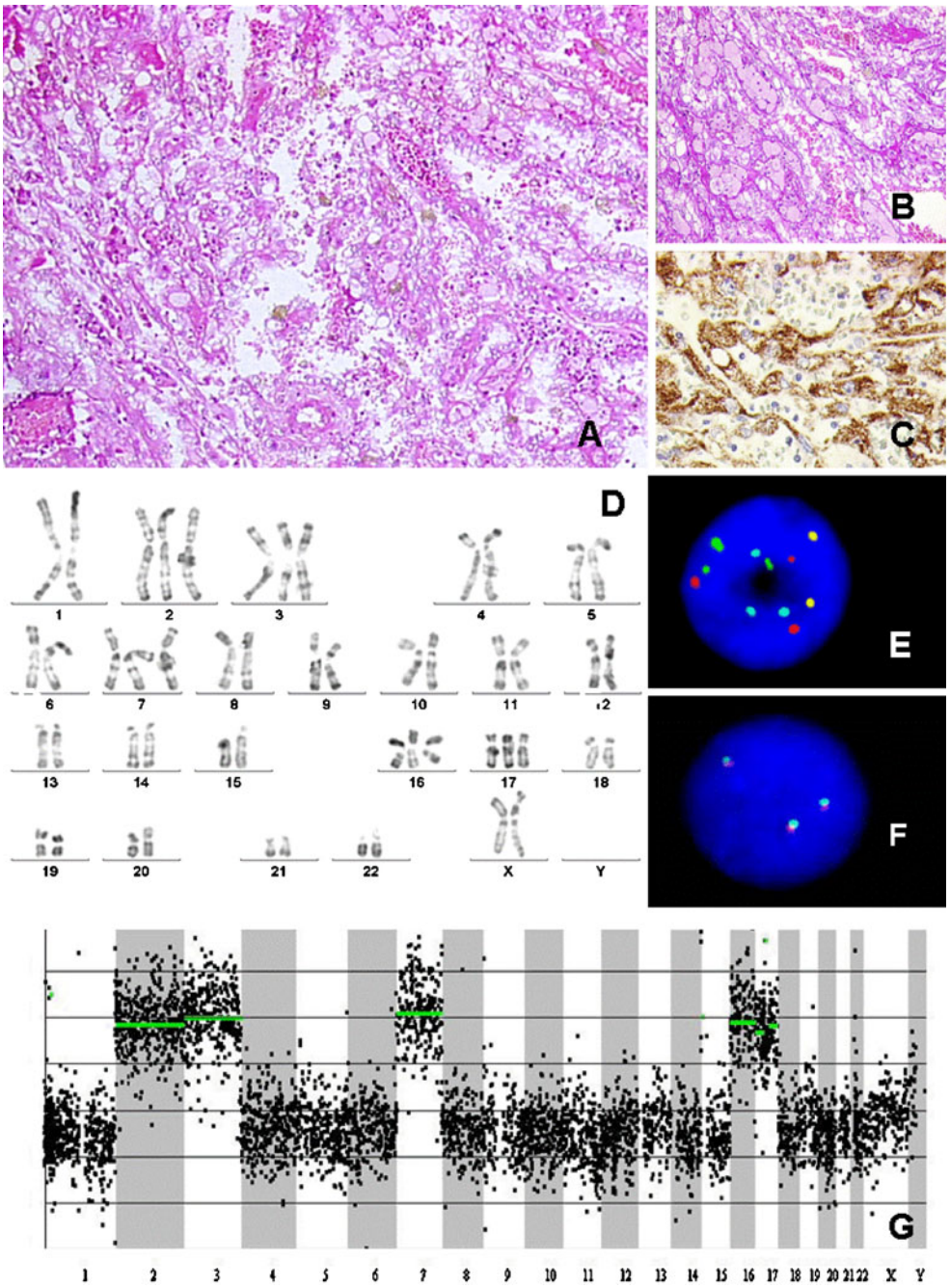

Fig. 2 Immunohistochemical and genetic features of case 2. **a** Microscopic field showing renal cell carcinoma with papillary areas (hematoxylin–eosin–saffron, magnification ×100). **b** The papillae are covered by clear cells (hematoxylin–eosin–saffron, magnification ×200). **c** Immunostaining for AMACR showing diffuse reactivity (magnification ×200). **d** Fluorescence in situ hybridization with centromeric probes for chromosome 3 (*red signals*), chromosome 7 (*green signals*), chromosome 17 (*blue signals*) and subtelomeric probe 9p21 (*gold signals*) showing nuclei with trisomy 3, trisomy 7, trisomy 17 and trisomy 9p21 **e** Fluorescence in situ hybridization with a couple of subtelomeric probes for 3p25 including the *VHL* gene at 3p25.3 and a control probe close to *VHL* (*fused red/green signals*). Three red/green signals per nucleus are observed, indicating a trisomy 3 and that *VHL* is not deleted. **f** RHG banded karyotype showing trisomy 2, 3, 7, 16, 17. **g** BAC array-CGH profile showing gains of chromosomes 2, 3, 7, 16 and 17. The tumor/control log2 ratios were plotted for all clones on the basis of their chromosome positions. Clones are ordered from chromosomes 1 to 22 and XY within each chromosome on the basis of the March 2006 UCSC human reference sequence HG18, NCBI Build 36.1 (http://www.genome.ucsc.edu/cgi-bin/hgGateway). Gains are indicated by *green lines*

encapsulated tumor measuring 2.8 cm. The cut surface was predominantly solid and yellowish. Microscopically, the tumor was well delimited by a fibrous capsule and its architecture was entirely papillary (Fig. 3). Also, tumor cells presented an abundant clear cytoplasm surrounded by a thin membrane. The papillae contained fibrovascular axis and aggregates of foamy macrophages. The Fürhman nuclear grade was III and the stage was pT1a. According to the 2004 WHO classification[1], the diagnosis was "unclassified RCC". After a follow-up period of 5 years, the patient showed no evidence of disease.

Results

Immunohistochemical findings

A positive staining for AMACR and CD10 and a negative staining for TFE3 and TFEB were observed in the three cases (Figs. 1–3). The staining for CK7 was positive in cases 2 and 3 and negative in case 1.

Cytogenetic and molecular findings

Case 1

Conventional cytogenetic analysis was unsuccessful because of absence of in vitro cell proliferation. Interphase FISH analysis was performed on uncultured tumor cells with probes which showed gain of chromosomes 7 (tetrasomy and pentasomy) as well as trisomies 2, 9, 17 and 18 and loss of chromosome Y (Fig. 1). We did not detect numerical abnormality of chromosome 3 or deletion of the *VHL* gene (3p25) (Fig. 1). We observed three fluorescent signals per cell with the centromeric probe of chromosome 9 but only two signals with the *CDKN2A/CDKN2B* probe, indicating a trisomy 9 with a deletion of the 9p21 region for one of the chromosomes 9. Both BAC CGH array and SNP array analyses showed gains of chromosomes 2, 4, 5, 7, 9, 11, 12, 13, 16, 17, 18, 20, 21, 22 and loss of chromosome Y (Fig. 1). Moreover, the SNP array analysis showed complete loss of heterozyogosity (LOH), or isodisomy, for the chromosomes 3 (Fig. 1) and 15.

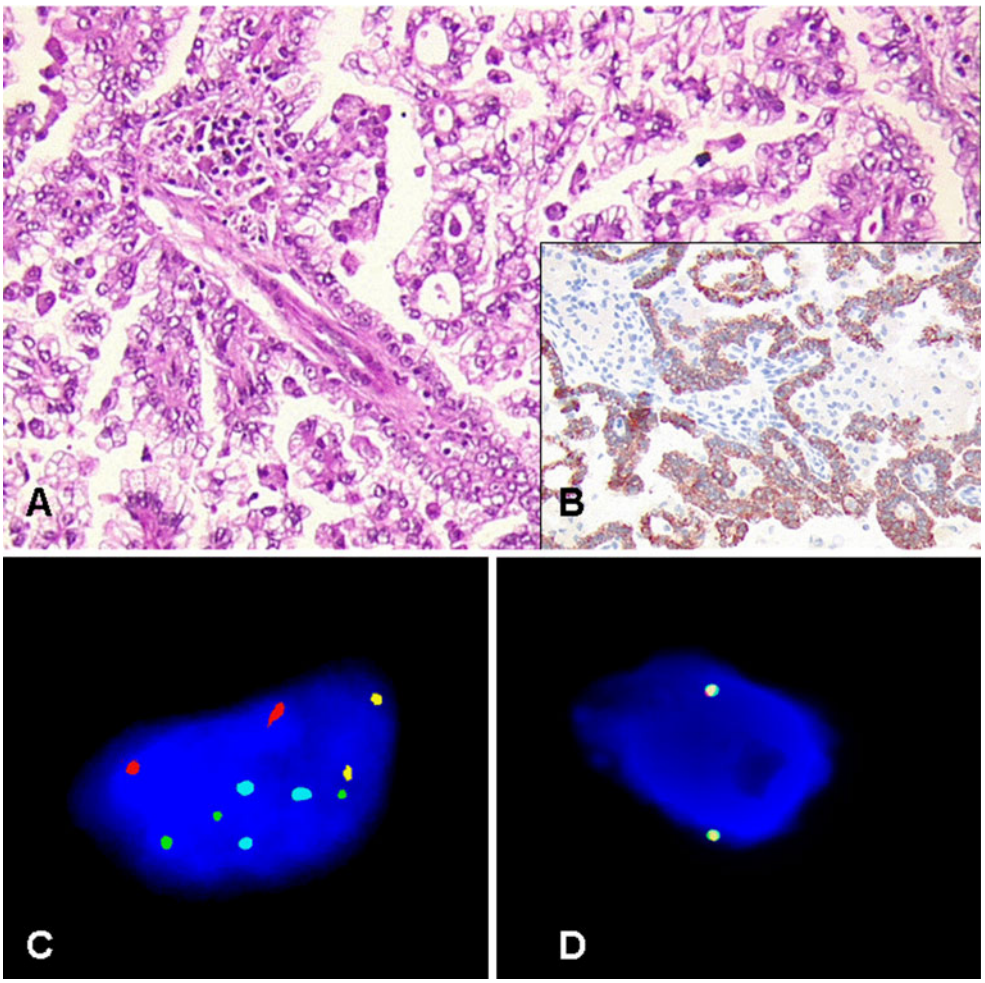

Fig. 3 Immunohistochemical and genetic features of case 3. **a** Microscopic field showing renal cell carcinoma with papillary areas covered by clear cells (hematoxylin–eosin–saffron, magnification ×200). **b** Immunostaining for AMACR showing diffuse reactivity (magnification ×200). **c** Fluorescence in situ hybridization with centromeric probes for chromosome 3 (*red signals*), chromosome 7 (*green signals*), chromosome 17 (*blue signals*) and subtelomeric probe 9p21 (CDKN2A/CDKN2B) (*gold signals*) showing nuclei with disomy 3, disomy 9p21, trisomy 7 and trisomy 17. **e** Fluorescence in situ hybridization with a couple of subtelomeric probes for 3p25 including the *VHL* gene at 3p25.3 and a control probe close to *VHL* (*fused red/green signals*). Two red/green signals per nucleus are observed, indicating that *VHL* is not deleted

Case 2

Eight metaphases were analyzed by reverse banding using heat and Giemsa (RHG). Trisomies for chromosomes 2, 3, 7, 16 and 17 were detected in all cells (Fig. 2). The karyotype was: 51, XX, +2, +3, +7, +16, +17. The FISH analysis performed on noncultured interphase cells using centromeric probes for chromosomes 3, 7, 9 and 17 confirmed the trisomies 3, 7 and 17. Additionally, three signals per cell corresponding to the *VHL* probe were observed, indicating that this gene was not deleted. No numerical abnormality was detected for chromosome 9. Both BAC CGH array and SNP array analyses showed gains of chromosomes 2, 3, 7, 16 and 17 (Fig. 2). Furthermore, SNP array analysis showed isodisomies for regions1p31, 1q31, 3q13–21, 8q24, 14q31.3, 16q21, 17q22, 17q24.3 and 19p13–q13.2. Because of their large sizes, and because they were completely homozygous (no difference between tumor cells and contaminating stromal cells), these isodisomies were highly suspected to be of constitutional origin rather than being specific to the tumor cells.

Case 3

The interphase FISH analysis showed trisomies 7 and 17, disomy for chromosomes 3 and 9 as well as no deletion of the *VHL* gene.

Discussion

We report three cases of RCC with a predominant proportion of clear cells and variable amounts of papillary areas. Following complementary immunohistochemical and genomic analyses, the profiles of these tumors were not concordant with ccRCC. Instead, the features were those of pRCC. Cases 2 and 3 showed immunoreactivity for AMARC as well as gains of chromosome 7 and 17 and no loss of 3p. To note, polysomy 7 and loss of chromosome Y are not fully specific anomalies. In particular, they have also been observed in ccRCC [9–11]. However, in the context a RCC, the association of chromosomes 7 and 17 gains, chromosome Y loss and absence of chromosome 3 loss is consistent with a pCCR genomic profile. We therefore modified the diagnosis of these two cases in pRCC. The immunohistochemical and molecular cytogenetic profiles of case 1 presented also numerous elements consistent with a pRCC, such as immunoreactivity for AMACR and CK7, gains of chromosome 7 and 17 and loss of chromosome Y. Nevertheless, both the LOH for chromosome 3 and the fact that the papillary pattern was not predominant in this case led us to conclude to a hybrid tumor made up of both ccRCC and pRCC components. This kind of tumor is denominated “unclassified” in the 2004 WHO classification [1].

These three cases illustrate the difficulties of making a proper diagnosis without using complementary molecular tools. A few reports describing RCC with both clear cells and papillary component are available in the literature. A new subtype of RCC, characterized by both a papillary pattern and the presence of clear cells, was described in five patients [12]. This entity showed a particular immunohistochemical profile characterized by positivity for CK7 and negativity for CD10 and AMACR. The authors called these tumors “clear cell papillary RCC”. However, the genomic characteristics of these five cases were different from our three cases since FISH analysis did not detect trisomies 7 and 17 or 3p deletion. The RCC associated with Xp11 translocations are also composed of cells with clear cytoplasm to faintly eosinophilic cytoplasm, arranged in nest and papillary structures [13]. These tumors are generally observed in teenagers and young adults and show positive immunostaining for TFE3 or TFEB [14]. No TFE3 or TFEB staining was detected in our cases. Fuzesi et al. [15] and Salama et al. [16] described three and seven cases of RCC [16] with both papillary architecture and clear cells, respectively. Following molecular analysis the final diagnosis of these ten cases was ccRCC [15, 16]: in the three cases described by Fusezi et al., a deletion of the short arm of chromosome 3 and no trisomy 7 or 17 were observed, while Salama et al. detected a LOH of the 3p region and no gain of chromosomes 7 and 17. Gobbo et al. [17] analyzed 14 cases of unclassified RCC characterized by papillary architecture and variable amounts of clear cells. Immunohistochemistry using CK7, AMACR and TFE3 antibodies and FISH analysis allowed them to be separated in two groups, ccRCC and pRCC. Two cases remained unclassified due to a discrepancy between results of molecular cytogenetic analysis and immunohistochemistry.

Our results confirm and complete the observations by Gobbo et al. [17]. However, in addition to the combination of FISH and immunohistochemical analyses, we also performed array studies in cases 1 and 2. Notably, the use of SNP arrays in case 1 showed LOH for chromosome 3. If we had only performed immunohistochemical and FISH analysis, as described in the series of Gobbo et al. [17], we would have conluded that the tumor was a pRCC. In fact, LOH for chromosome 3, a feature not detectable by FISH analysis (since two chromosome 3 are present), is a characteristic feature of ccRCC, while the gain of chromosomes 7 and 17 and the loss of chromosome Y are characteristic of pRCC. Our data highlight the strength of using several complementary methods, including SNP arrays.

Virtual karyotyping with SNP arrays was shown to be a valuable tool for increasing diagnosis accuracy in morphologically challenging or unclassified RCC [18–20]. Kim et

al. have analyzed 21 challenging renal epithelial tumors including four tumors with morphologic features mixing clear cells with papillary architecture. In three cases, the SNP arrays analysis showed 3p loss consistent with a ccCCR. In the study by Monzon et al., one case of RCC with papillary architecture and clear cell features showed 3p loss, leading to its classification as ccCCR.

Trisomies for chromosomes other than chromosomes 7 and 17 were also detected in cases 1 and 2. Such trisomies are not unusual in pRCC and are considered as secondary anomalies [5]. In case 1, the high number of these trisomies put the total number of chromosomes up to 59. This is at the limit between a hyperdiploid and hypotriploid genome. In such cases, the results of arrays are difficult to interpret if no complementary analyses are done concomitantly to determine the ploidy level and adapt the arrays thresholds, such as karyotype or interphase FISH analysis.

Our results suggest that some RCC that are diagnosed only on the basis of morphological analysis are probably misdiagnosed. The genomic analysis is of crucial importance for establishing the final diagnosis and subsequently giving the most appropriate treatment to the patient. Several methods including conventional karyotype, FISH, BAC CGH array and SNP array can be used for the detection of genomic alterations of renal neoplasms. We showed here that using the combination of these methods was efficient for characterizing our cases. However, such a combination is not always possible for routine diagnosis. The possibility to use only one of these methods, or a combination of several, depends on the type of biological sample available for diagnosis. FISH probes specific for the centromeres of chromosomes 3, 7, 17 and Y as well as the *VHL* gene are useful for identifying the main features of cCCR or pRCC. SNP-array analysis is a powerful tool for the detection of genomic gains and losses and is the only method for detecting LOH over the whole genome. However, array results might be difficult to interpret if not completed by interphase FISH analysis.

Conflict of interest statement We declare that we have no conflict of interest.

References

1. Eble JN, Sauter G, Epstein JI, Sesterhenn IA (2004) Pathology and Genetics of Tumours of the Urinary System and Male Genital Organs . World Health Organization Classification of Tumours ed. Lyon: IARC Press; 359
2. Allory Y, Bazille C, Vieillefond A et al (2008) Profiling and classification tree applied to renal epithelial tumours. Histopathology 52:158–166
3. Yoshida MA, Ohyashiki K, Ochi H et al (1986) Cytogenetic studies of tumor tissue from patients with nonfamilial renal cell carcinoma. Cancer Res 46:2139–2147
4. Toma MI, Grosser M, Herr A et al (2008) Loss of heterozygosity and copy number abnormality in clear cell renal cell carcinoma discovered by high-density affymetrix 10 K single nucleotide polymorphism mapping array. Neoplasia 10:634–642
5. Kovacs G, Fuzesi L, Emanual A et al (1991) Cytogenetics of papillary renal cell tumors. Genes Chromosom Cancer 3:249–255
6. Limon J, Dal Cin P, Sandberg AA (1986) Application of long-term collagenase disaggregation for the cytogenetic analysis of human solid tumors. Cancer Genet Cytogenet 23:305–313
7. Shaffer L, Tommerup N (2005) ISCN: An International System for Human Cytogenetic Nomenclature. S Karger, Basel
8. Sirvent N, Forus A, Lescaut W et al (2000) Characterization of centromere alterations in liposarcomas. Genes Chromosom Cancer 29:117–129
9. Van den berg E, Dijkhuisen T, Stôrkel S et al (1995) Chromosomal abnormalities in non-neoplastic renal tissue. Cancer Genet Cytogenet 85(2):152–154
10. Granata P, Portentoso P, Minelli E et al (1992) Clonal chromosom changes in renal carcinoma do not correlate with clinical stages and histopathologic grades. Cancer Genet Cytogenet 64(1):30–34
11. Klatte T, Rao PN, Martino D et al (2009) Cytogenetic profile predicts prognosis of patients with clear cell renal cell carcinoma. J Clin Oncol 27(5):746–753
12. Gobbo S, Eble JN, Grignon DJ et al (2008) Clear cell papillary renal cell carcinoma: a distinct histopathologic and molecular genetic entity. Am J Surg Pathol 32:1239–1245
13. Argani P, Olgac S, Tickoo SK et al (2007) Xp11 translocation renal cell carcinoma in adults: expanded clinical, pathologic, and genetic spectrum. Am J Surg Pathol 31:1149–1160
14. Argani P, Ladanyi M (2005) Translocation carcinomas of the kidney. Clin Lab Med 25:363–378
15. Fuzesi L, Gunawan B, Bergmann F, Tack S, Braun S, Jakse G (1999) Papillary renal cell carcinoma with clear cell cytomorphology and chromosomal loss of 3p. Histopathology 35:157–161
16. Salama ME, Worsham MJ, DePeralta-Venturina M (2003) Malignant papillary renal tumors with extensive clear cell change: a molecular analysis by microsatellite analysis and fluorescence in situ hybridization. Arch Pathol Lab Med 127:1176–1181
17. Gobbo S, Eble JN, Maclennan GT et al (2008) Renal cell carcinomas with papillary architecture and clear cell components: the utility of immunohistochemical and cytogenetical analyses in differential diagnosis. Am J Surg Pathol 32:1780–1786
18. Monzon FA, Hagenkord JM, Lyons-Weiler MA et al (2008) Whole genome SNP arrays as a potential diagnostic tool for the detection of characteristic chromosomal aberrations in renal epithelial tumors. Mod Pathol 21:599–608
19. Kim HJ, Shen SS, Ayala AG et al (2009) Virtual-karyotyping with SNP microarrays in morphologically challenging renal cell neoplasms: a practical and useful diagnostic modality. Am J Surg Pathol 33:1276–1286
20. Hagenkord JM, Parwani AV, Lyons-Weiler MA et al (2008) Virtual karyotyping with SNP microarrays reduces uncertainty in the diagnosis of renal epithelial tumors. Diagn Pathol 3:44

Virchows Arch (2010) 457:405–414
DOI 10.1007/s00428-010-0935-3

INVITED COMMENTARY

From anatomy to surgery to pathology: eighteenth century London and the Hunterian schools

Clive R. Taylor

Received: 19 April 2010 / Accepted: 6 May 2010 / Published online: 23 May 2010
© Springer-Verlag 2010

Keywords John Hunter · Anatomy · Pathology · Surgery · William Hunter · Matthew Baillie · Autopsy · Pathology museums · Experimental Pathology · Translational research · Evidence based medicine

John Hunter, extolled for his pioneering contributions to surgery, was a surgeon as much by default as by design. By default, in that in spite of the urgings of his brother, William Hunter, M.D., John Hunter showed no interest in pursuit of a Doctorate in Medicine; and by default, in that he did not pursue training as a pathologist. There was good reason for the latter for in John Hunter's day, Pathology did not exist as a discipline [1] and pathologists had not then been invented [2]. John Hunter had yet to take those first steps in a career that was later to contribute materially to the beginnings of the discipline of Pathology. Nonetheless, if some latter day title must be chosen to represent John Hunter's abiding passion for investigation of disease by dissection, then the title 'morbid anatomist' fits as well as any (Fig. 1).

Beginnings

John Hunter was born in February, 1928, on a Scottish farm, the youngest of ten children [3–5]. Only three survived into later adult life, William, Dorothea and John. Curiously all three were to impact the discipline of Pathology, in different ways.

C. R. Taylor (✉)
Department of Pathology, HMR 311, Keck School of Medicine of the University of Southern California,
2011 Zonal Avenue,
Los Angeles, CA 90033, USA
e-mail: cltaylor@usc.edu

William, an older brother by 10 years (b. 1718), attended lectures at the University of Edinburgh in 1740 by Alexander Monro ("Primus"): "There I learned a good deal by my ears; but almost nothing by my eyes;….The defect was, that the professor was obliged to demonstrate all the parts…..upon one dead body." [6] Shortly thereafter, William Hunter reappeared in London, where his rise to prominence was rapid, announcing his own anatomy school by advertisement in the London Post in September 1746, "Gentlemen may have the opportunity of learning the Art of Dissecting during the whole winter session in the same manner as at Paris" [7]. He was admitted to the Corporation of Surgeons on August 6th of 1748, awarded a Doctorate in Medicine by the University of Glasgow in 1850, and soon after switched his allegiance to the Royal College of Physicians. Dorothea's contribution to Pathology was indirect, through her son Matthew Baillie (b. 1761), who trained with both of his uncles and in 1793 authored the first systematic Pathology text, built upon that experience; "Morbid Anatomy of Some of the Most Important Parts of the Human Body" [8] (See Fig. 5).

John Hunter, in contrast to William, had no love for books or formal learning, and little respect for either: "When I was a boy it was little about reading and writing… I wanted to know about the clouds and the grasses, why the leaves change colour in the autumn. I watched the ants, bees, birds, tadpoles, and caddis worms." (recollections of John Hunter) [9, p 16]. Hunter also later recalled that he "totally rejected books"—preferring to take up the "volume of the human body." [10].

London; definitely not Oxford

William Hunter was well established in London in 1748 when John, at the age of 20 years, arrived to assist in his

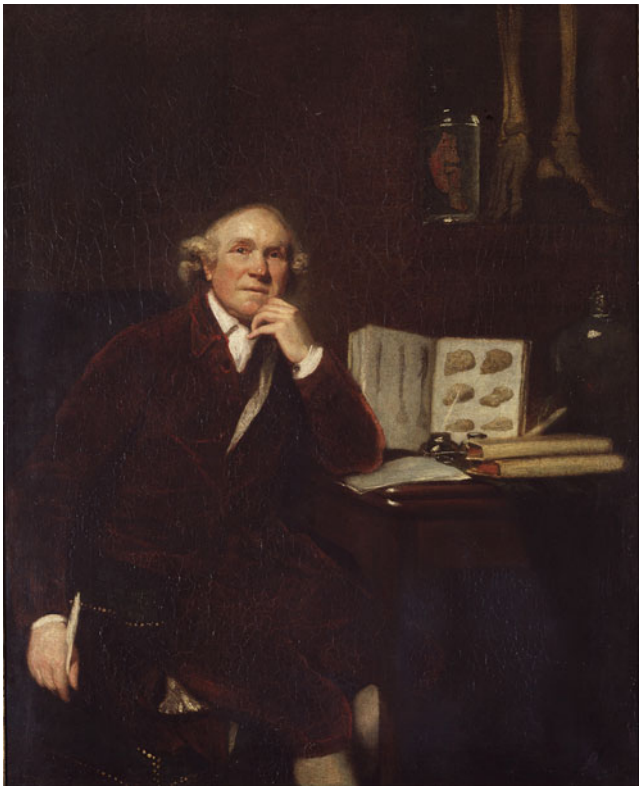

Fig. 1 Portrait of John Hunter 1786 by Sir Joshua Reynolds (1723–1792) in the collection of Royal College of Pathologists of England, London. Courtesy of the College. Copies of the portrait by John Jackson (1813) and an unknown artist are to be found in the National Gallery and Oriel College, Oxford. An engraved mezzotint of the Reynolds portrait was produced by William Sharp (1788). Notably, Hunter conducted the autopsy dissection of Reynolds, just 18 months before his own death

brother's dissection room in the somewhat seedy Covent Garden area of the City [3–5]. A brief foray to Oxford University as a Gentleman Commoner at St. Mary's Hall (1753), flirting with Latin and the notion of becoming a physician, was just that, brief: "They wanted to make an old woman of me; or that I should stuff Latin and Greek at the University." (speaking to Sir Thomas Carlisle, cited by Ottley) [4, p 14]. After a single semester, he left the hallowed halls of Oxford and returned to hands on dissection at the school in London.

Anatomy; the school and the museums

At the Covent Garden Anatomy School, William Hunter lectured, using fresh dissections and preserved specimens, the preparation of which became John Hunter's primary passion (Fig. 2). The crucial and unique attraction of the "Hunter School" was that every student dissected a body of their own, "after the manner of Paris". Given exposure to this "wealth" of material, insatiable curiosity, and acute observational skills honed by those childhood forays with caddis flies, it is scarcely surprising that John Hunter soon became "master of what was already known, as well as making some addition to that knowledge" (Everard Home) [3, p xvii].

In many ways, John Hunter was the right man, in the right place, at the right time. London in the eighteenth century was almost unique among the major cities of Europe in having no medical school for the training of physicians, or for that matter, surgeons. The latter received such training as was available through trade guilds, dating from mediaeval times, in this instance the Company of Barber Surgeons, from which, according to Ottley, the Company of Surgeons "was happily dissolved" in 1745 [4, p 5]. The Company of Barber Surgeons had "the right of claiming annually four executed felons" for public dissection [4, p 5]. Otherwise, dissection of the human body was illegal for any purpose, including the education of students; "any surgeon dissecting a body out of their Hall was liable to a fine of ten pounds" [4, p 5]. Specimens retained from these dissections were often put on display in show rooms [9, 11–16], the most notorious of which was Benjamin Rackstraw's "Museum of Anatomy and Curiosities" at 197, Fleet Street [17]. This desire of the public to view the dead and parts thereof, smacks of ghouls, of "un-civilized" times gone by. However, it is not so different from the recent "Body Worlds" exhibits of "plastinated" bodies, human and animal, presented by Gunther von Hagen [18] that have drawn crowds around the World, "carrying on the traditions of the Renaissance Anatomists." If imitation is the sincerest form of flattery, John Hunter would have been much pleased by this belated recognition of his work.

Resurrection men

Out of necessity, John Hunter acquired other skills, related less directly to pathology, or to surgery for that matter. He became adept at procuring bodies from the gallows in competition with other anatomists [3–5, 9, 11–16] (The "Tyburn Tree" gibbet reputedly could dispose of a score of miscreants at a time, the last hanging recorded in 1783; a marker plaque exists on the traffic roundabout at the junction of Bayswater and Edgeware Roads, close to Marble Arch). Biographers agree that when criminals were in short supply Hunter would resort to engaging "resurrection men" or "body snatchers," to lift newly dead corpses from newly dug graves [3–5] at prices from one guinea upwards. In the eighteenth century, grave robbing was a fact of life, rather of death for medical students worldwide, [3, 4, 15, 16], continuing well into the nineteenth century in the fledgling medical schools of the USA [19]. This

Fig. 2 Typically detailed dissections of crural and carotid arteries from Palmer's 'Works of John Hunter' (Pl.XXIV; Palmer JF. Ed. Longman, London, 1837) Credit: Wellcome Library, London

practice was only to abate when anatomical dissection was "legalized" in Britain, after the Warburton Anatomy Act of 1832, precipitated by Burke and Hare, who, in obtaining bodies for the surgeon John Knox in Edinburgh, preempted the grave. Burke was convicted of multiple murders and publically dissected by Professor Monro ("Tertius"), as part of the punishment. The term "burking" endures today in the lexicon of forensics, another possible link with Pathology for the Hunter brothers in the light of speculation that they may have resorted to "burking" for certain "hard to get" specimens, such as gravid uteri [20].

Surgery

Beginning in 1749, John Hunter walked the "cutting wards" behind William Cheselden at Chelsea Hospital and then Percivall Pott at St. Bartholomew's, both eminent surgeons of the day. There was a wealth of pathologic material, broken limbs, aneurysms, infections, venereal diseases, ruptures, stones and the like; for each of which John Hunter observed the standard surgical approaches of the day, and for each asked the questions; why, and how, and how better? Then, for reasons of ill health, "that threatened to end in consumption … he was advised to seek a more southerly climate" [4, p xx]. Hunter therefore obtained a commissioned as Staff Surgeon on the British Expedition to take Belleisle from the French during the Seven Year's War, continuing on to the Portugal Campaign of 1762. During this period of military service Hunter had opportunity to operate on many critically wounded soldiers, and famously began to question the "laudable pus" doctrine, eventually casting it aside, albeit that his reasoning did not find expression in print until 1794, with publication of "A Treatise on the Blood, Inflammation and Gun Shot Wounds." [21]. Returning to England Hunter founded his own anatomy school in 1764, was elected to the Royal Society in 1767 [3, p xix], became a member of the Corporation of Surgeons, and was appointed Surgeon-extraordinary to His Majesty in 1776 [3, p xxvii].

The legacy to pathology

The number and variety of bodies dissected by Hunter allowed preparation of numerous preserved specimens (Fig. 2), establishing principles and practices that for two centuries were to form the core of anatomy and gross pathology teaching at medical schools everywhere. Parts of the body that could be preserved by drying, were dissected, cleaned, "painted with dilute arsenical solution," dried, by hanging from the beams, then varnished [3–5, 9, 21]. This method served adequately for bone, nerves, some muscles, vessels and the like, but was of limited value for larger body parts. For the latter, alcohol in the form of spirits of wine was preferred among anatomists. To this method John Hunter added precise techniques employing injection of vessels, seminiferous tubules and hollow viscera with fluids of varying viscosity, to preserve form and add color. He used concoctions of waxes, tallow, oils, animal fats and plant resins, plus sometimes mercury, with artist's pigments for color. In some instances, with infinite care and precise timing, solid tissues were "digested away" in acid (the "corrosion" method) to leave displays of wax filled vasculature, or bronchial trees. Sealed in glass jars, covered with waxed pig's bladders and lead, many of these specimens may be seen today, 250 years later, in the Hunterian Museum at the Royal College of Surgeons in London, a virtual tour of which may be accessed online [22] (see Fig. 6).

Particular challenges involved studies of the bodies of pregnant women and their fetuses, leading, after a suitably long gestation, to publication by William Hunter in 1774 of "The Anatomy of the Human Gravid Uterus Exhibited in Figures" [23]. Although this was a long term project of William's, who also was an "accoucheur," much of the dissection and deductive work that established the existence of a separate placental circulation was performed by John Hunter. William Hunter, in his "Preface," does reference his brother John, "whose accuracy in anatomical researches is so well known, that to omit this opportunity of thanking him, would be in some measure to disregard the future reputation of the work itself" [24]. Nonetheless, there is a lingering belief that John felt he had received insufficient credit; one of the wedges that eventually separated the brothers to the death [3, 4].

The autopsy

The autopsy was legitimized by Hunter, as knowledge extended beyond anatomy to examination and precise recording of the response of the body to injury and disease. Having completed several thousand dissections (autopsies) John Hunter was an advocate of "anatomization." Increasingly, he was approached to examine the cause of death of patients, and even notable public figures. Such a case was the dissection conducted on 24th Feb 1792, on the prominent artist Sir Joshua Reynolds, who had painted the portrait of John Hunter that hangs in the College of Surgeons. "In the cavity of the belly the only diseased part was the liver, which was of a magnitude very uncommon…….and was of a consistence which is usually called scirrhous. It had lost its natural colour and become pale yellow." [4, p 121]. Hunter's advocacy extended so far as to urge that his own body should be anatomized after his death; and indeed it was. Everard Home provided a detailed report of the findings in his "Short Account of the Life of the Author" [3, p lxii]: "…..The coronary arteries…..bony tubes, which were with difficulty divided by the knife….the aorta immediately beyond the semilunar valves had its cavity larger than usual, putting on the appearance of an incipient aneurism….and was studded over with opaque white spots, raised higher than the general surface."

Pathology museums and the "first pathologists"

John Hunter's reputation for innovative and effective surgery grew and with it his practice, and his access to funds. According to Everard Home [3], much of the money that Hunter made went into the acquisition of specimens for dissection. By 1783, when he moved into larger premises in Leicester Square, his collection was both enormous and incredibly diverse [3, p xxxviii], spanning numerous human specimens, and those from animals, insects, birds and fossils; catalogued in Paget's "John Hunter" at a total of 13,682 [5, p 248]. Surviving parts are to be found at the Hunterian Museum of the Royal College of Surgeons in London (Fig. 3, see also Fig. 6). (William's specimens, a number prepared by John, are in the Hunterian Museum of the University of Glasgow). Listed among the specimens at Leicester Square were 1,084 pathological specimens in spirit, 3,745 physiological preparations in spirit, 1,242, dry specimens, plus zoological specimens, and even 215 "microscopic preparations" [5. p248]. "He collected 'everything"—and thus became—as no one else in his time—a comparative anatomist and pathologist;" (Sir James Paget) [25, p 13] (See Fig. 4).

The systematic arrangement of specimens in museums for education and research, provided models that all would eventually follow, such that in the nineteenth and twentieth centuries almost every medical school boasted such a museum, albeit ever so modest by comparison. Not only did these museums give shape to medical education, especially in Pathology, but their influence extended into research and far beyond. The "curators" of these early "Hunterian" museums at medical schools in London,

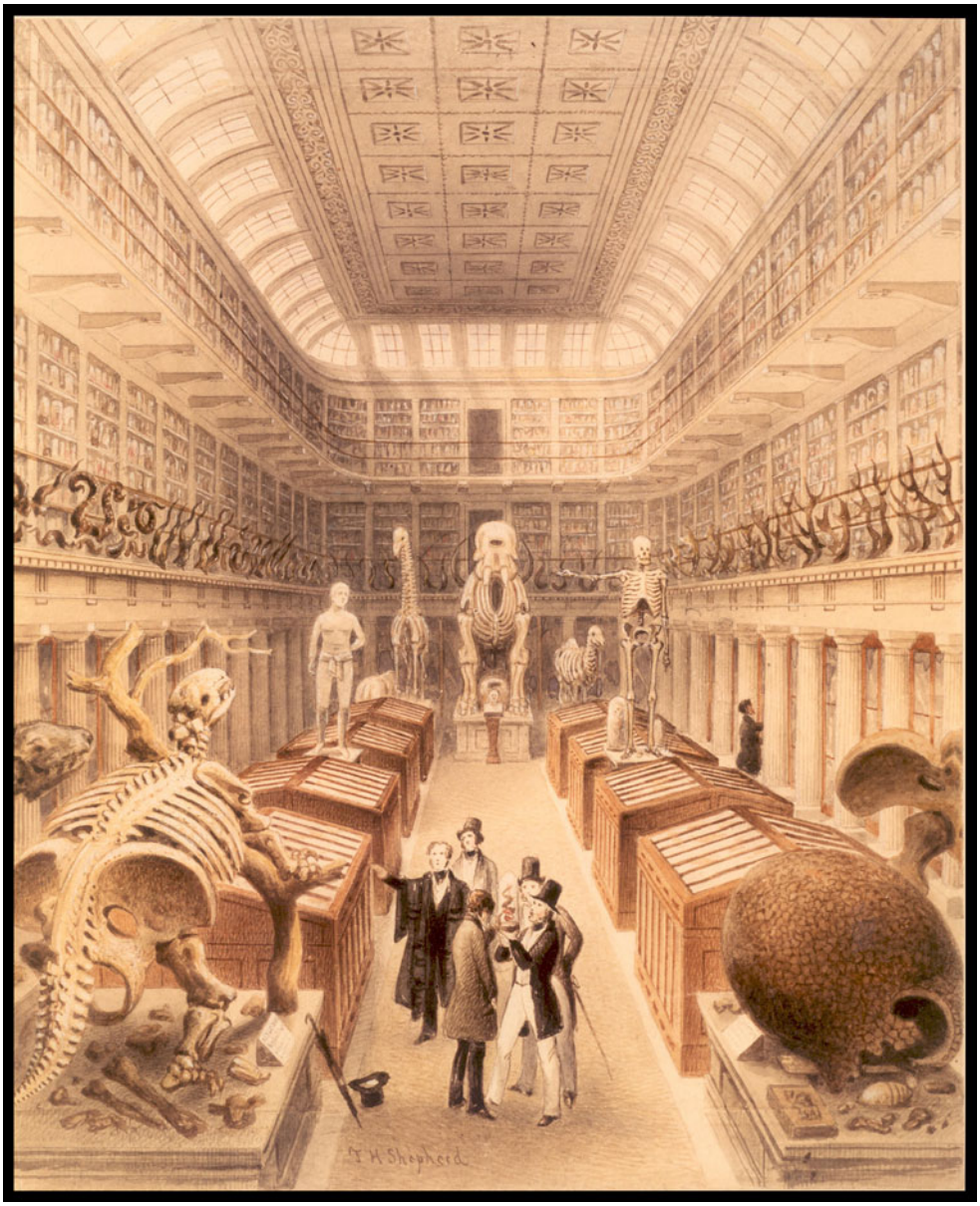

Fig. 3 The Hunterian Museum at the Royal College of Surgeons, London, as seen in 1842. Illustration by Thomas Hosmer Shepherd. Reproduced by kind permission of the President and Council of the Royal College of Surgeons of England. *Black* and *white* image appeared in the London Illustrated News of 1844

Edinburgh and elsewhere, evolved from "inspectors of the dead," to lecturers in "morbid anatomy," and to the first named "Professors of Pathology" [1, 2].

Experimental and comparative pathology

In a remarkable prelude to two productive centuries of "experimental pathology," John Hunter turned also to dissection of animals. Frank "vivisection" was not, of course, possible in humans, surgical techniques notwithstanding. But John Hunter certainly performed experiments on live animals [3–5, 9], as described in "A Treatise on Blood, Inflammation and Gunshot Wounds" [21]. In addition, he conducted countless dissections of diverse animals, 500 or more different species by the reckoning of various biographers [3–5, 14]. According to Home, "Comparative Anatomy may be considered as the pursuit in which Mr. Hunter was constantly employed. No opportunity escaped him." [3, p xxv]. It was this curiosity that drove him to the procurement or purchase of rare beasts of great variety, as for example from the menagerie at the Tower of London. Ottley [4, p 30] records one notable transaction: "Pray George," said he one day to Mr. Nicol the bookseller, "have you got any money in your pocket?" Mr. N. replied in the affirmative. "Have you got five guineas? Because if you have, and will lend it to me, you shall go halves." "Halves in what?" inquired his friend. "Why, halves in a magnificent tiger which is now dying in Castle Street." [see also 5, p 222]. Many of John Hunter's papers to the Royal Society or in the Philosophical Transactions described findings in animals, birds, fishes,

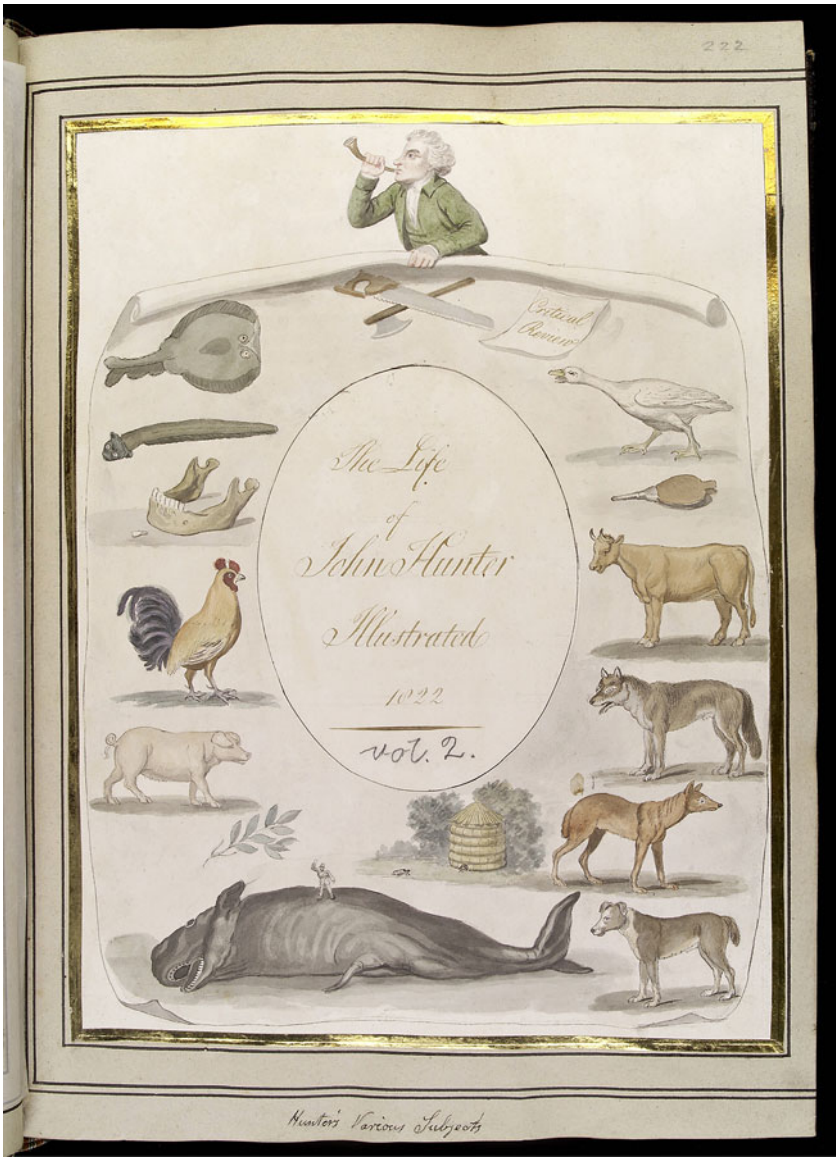

Fig. 4 Title page from The Life of John Hunter, volume 2, published in 1822 by Jesse Foot a contemporary (14): 'Hunter's Various Subjects', illustrating the diversity of Hunter's interests and specimens. The words 'Critical Review' also appear in the montage, indicative of Foot's position as a relentless critic of much of Hunter's work. Image credit: The Wellcome Library, London

insects, or even vegetables, rather than human anatomy [3, p xxv; 14, p 87] (Fig. 4).

Hunter's work also anticipated by some two centuries the current trend in "evidence based medicine." "He was aware that his continuous programme of research meant his views were always changing, so that whatever he told the students would be out of date before long" [26]. Famously, when his pupil, Edward Jenner, asked his advice on treating a certain patient, Hunter replied: "I think your solution is just. But why think, why not trie the experiment?" [27] This advice became a mantra. "Don't think, try; be patient, be accurate;" (cited by Sir James Paget) [25, p 14]. The concept and use of planned controls also extends throughout Hunter's work, using animals as models for man, comparing animal to man, and animal to animal. "To make comparative experiments (upon the digestive powers), the different animals destined for that purpose should be under similar circumstances…equal in age….equal in fatness…. equal in health" [28, p 87]. In this design, Hunter foresaw the essential role of "matched" controls in biological experiments. Hunter was impatient to put theories to test, and bring tested theories into practice; "I think we may set it down as an axiom, that ….the next step should be, the application of that principle to useful purposes." [28, p 86]. This of course is the germ of "translational research," yet another lesson from John Hunter for us today; for Hunter from idea, to experiment, to practical application in patients, could be counted in days or weeks, not years [5, 21, 28].

In another connection with pathology, Hunter utilized a primitive microscope for his work on developing chick embryos in opened fertilized eggs. He was not overly impressed with the resolution afforded and, as usual, was not restrained in offering opinions as to how microscopes

should be used, and by whom. In "A Treatise on Blood, Inflammation and Gun-shot Wounds," when discussing the "Red Globules" as one of three components of blood, Hunter wrote, "Malpighi was probably the first who employed a microscope for this purpose, and he, in 1668, wrote a description of the appearance of the globules in the blood vessels of the omentum, which he mistook, however, for globules of fat." [21, p 40]. Hunter continued; "Microscopical obervations were pursued with great ardour by Antonius Van Leeuwenhoeck, who saw the red globules, August the 15th, 1673." Hunter could not resist a final comment; "These early observers probably imagined more than they saw." [21, p 41]. Hunter expressed even greater concern over the validity of microscopic findings of those lacking appropriate experience; "To look through a microscope….is a presumption….to expect to throw light on subjects that they have not taken the previous steps to understand." [28, p 83]. In these sentiments Hunter anticipated events that were to occur over half a century later, when improvements in manufacture of microscopes led to increased availability, "forcing" the emergence of a new generation of physicians, who perforce dedicated the time necessary to acquire experience in their use – the first histopathologists [2].

The pathology literature

John Hunter was prolific in written descriptions of his specimens, and of his thoughts and research. Parts appeared in letters to friends and students; "The measly pork are hydatids." (letter to Edward Jenner, December, 1790; cited by Ottley, [4], p 118]. Other parts were presented to the Royal Society, or cited by early biographers [3–5, 14]. In one instance Hunter was long in coming to press. Thus "A Treatise on Blood, Inflammation and Gunshot Wounds," had its genesis during Hunter's military service in1760, but did not appear in print until 1793–1794 [21]. At 575 pages, it is an impressive work, but 34 years in gestation. Much of Hunter's non-published work was gathered long after his death and printed in 1835 in multiple volumes [28, 29]. Volume 1 included "The Life of John Hunter F.R.S." by Drewry Ottley [4], plus key elements of Hunter's philosophy:

- "In the present lectures it is my intention to begin with the physiology of the animal oeconomy in its natural or healthy state; and then to come to pathology, ….which may be called the perversion of the natural actions…" [29, p 211];
- "….in studying diseases we ought not only to understand the effect, as inflammation, suppuration, &c., but also the cause of that effect;…" [29, p 208];
- "Tumours may be divided into solid and encysted, which are very different diseases……They commonly arise from one fixed point, as a root, and then spread out in all directions, if the surrounding parts allow of it." [29, p 568].

While these volumes contain detailed reports of many of Hunter's experiments, there is a persisting belief that much may have been lost; "In the course of numberless dissections which he had prosecuted during thirty years of unwearied diligence, he necessarily made a great variety of isolated observations….always carefully recorded….; but by Sir Everard Home's extraordinary destruction of his manuscripts science has been deprived of the fruits of his industry." [4, p 137]. Drewry Ottley [4], Stephen Paget [5] and others have pondered this "inexplicable" burning of Hunter's papers by Everard Home. Upon persistent inquiry,

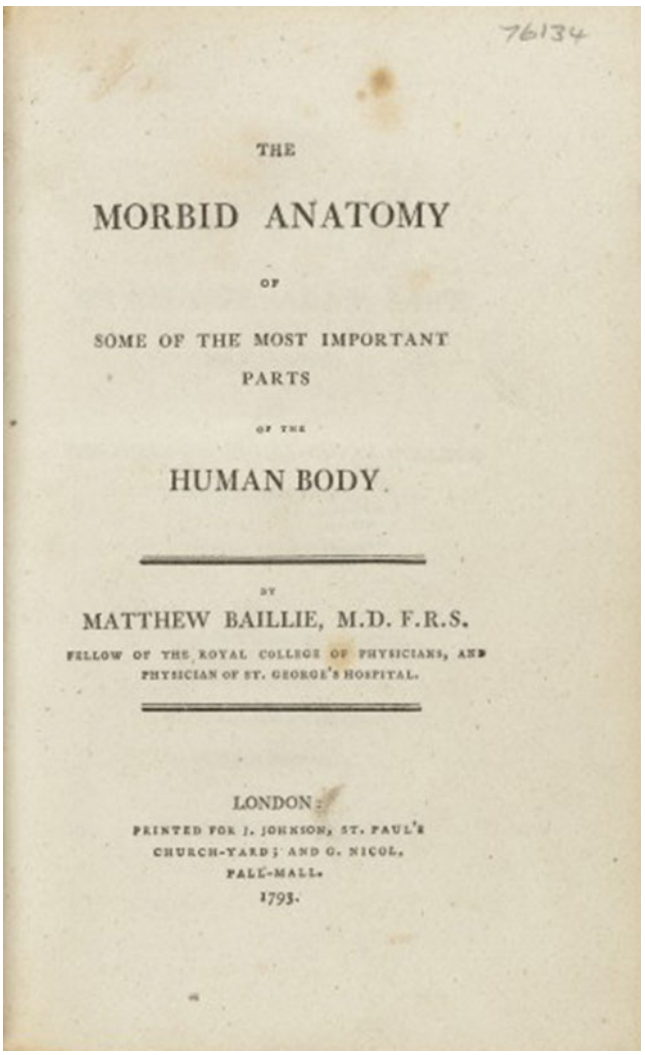

Fig. 5 Matthew Baillie. Title page to 'Morbid Anatomy of Some of the Most Important Parts of the Human Body. 1892 (8). Credit: Wellcome Library, London

Home responded to the Board of Curators of the College to the effect that, "Mr. Hunter desired that, after his death, his manuscripts should not be entrusted to anybody, but were to be destroyed, being in too imperfect a state for the public eye" (Paget, [5, p 254]). Whatever the truth, the outcome is that some of Hunter's work was lost, exactly which parts is neither known, nor now knowable. Speculation has it that parts of Hunter's work may in fact have been published, under a kind of posthumous "nom de plume," for Everard Home, custodian of Hunter's records, presented more papers to the Royal Society in the decades following Hunter's death than any other individual. Thus the "fruits of Hunter's industry" feared lost [4, 5], may not so much have been lost as disguised.

Publish or perish

Rivalry for primacy in discovery, with the attendant pressures and emotions, was no less in the eighteenth century than now. Almost from the day of John Hunter's arrival in London, there were spirited contests for right of discovery, pitting the Hunter brothers against the Monros of Edinburgh for identification of the lachrymal ducts, injection of the seminiferous tubules, and definition of the absorbent system (lacteals and lymphatics), during which young Alexander Monro (Secondus) attended lectures in London at the Hunter School; inside information. Then there was the race against Percivall Pott for demonstration of origin of congenital hernia [5, p 60]. In these contests, William was the public voice and John the practical hands behind the scenes, compiling the evidence. The contest took a different and more destructive turn with respect to proving the existence of a separate placental circulation, leading to friction between the two brothers for credit (William the "voice"; John the "hands"), contributing to their estrangement noted previously [5, p 70].

Edward Jenner and Matthew Baillie

John Hunter "trained" more than 1,000 students in his 45-year career, many of whom, as individuals, are lost to history. A number were to make their individual marks, including Astley Cooper, Abernathy, Jenner and Baillie.

Fig. 6 John Hunter's Museum as it is today—The Crystal Gallery of the Royal College of Surgeons of England, London. Photograph courtesy of the College

Collectively, these students brought to surgery, and to medicine at large, Hunter's new spirit of observation and inquiry.

Hunter's influence on Edward Jenner was critical; they maintained an active correspondence and exchange of specimens. The collected letters have been published in various forms, and recount diverse interests and experiments across many species, including notably cuckoos [4, 5]; (Jenner was elected to the Royal Society for the demonstration in 1788 that young cuckoos in a foreign nest evict the native hatchlings.) The critical "vaccination experiments," though not effected by Jenner until after Hunter's death, nonetheless derive from that spirit of active scientific inquiry inculcated by Hunter in his young protégée. Again there are lessons to be learned. The paper describing this remarkable work was initially rejected by the Royal Society, and when finally published in 1798, still remained controversial for years.

John Hunter left more than 13,000 specimens, innumerable pages of notes and papers and, as his single greatest legacy to Pathology, he left Matthew Baillie.

The nephew of William and John Hunter, Matthew Baillie possessed many talents, not least an ability to find a way to continue working with both of his uncles during their progressive estrangement. With the support of William Hunter, Baillie was "appointed to an Exhibition at Balliol College," Oxford, in 1780 (letter from Archbishop Cornwallis to William Hunter)[5, p 237], and gained the D.M. degree in 1789. Baillie's book, "The Morbid Anatomy of Some of the Most Important Parts of the Human Body" [8] (Fig. 5), was published within a year of John Hunter's death. It included multiple references (to "Hunter," "Dr. Hunter" and "Dr. J. Hunter") and case materials from work with both of his illustrious uncles; "My situation has given me more than the ordinary opportunities of examining morbid structure…Dr. Hunter's collection contains a very large number of preparations exhibiting morbid appearances which I can have recourse to at any time for examination." (Baillie, 1794, Preface to First Edition) [8].

"Morbid Anatomy" put Pathology on the map as a discipline: "The object of this work is to explain more minutely than has hitherto been done the changes of structure arising from morbid actions in some of the most important parts of the human body." [8]. It influenced the development of Medicine and Pathology everywhere, with 11 English editions, three American editions, and translations into German, French, Italian, and Russian [30]. Beginning in 1799, ten fasciculi of accompanying engravings also were published [31]. "The order of the Engravings will correspond very much with that of…my book upon Morbid Anatomy." [30, p 449]. Baillie died in 1823; his portrait is to be found in the Reading Room of Balliol College, Oxford.

The end

In 1793, frustrated with colleagues who were, in his opinion, not sharing in the effort of teaching students, Hunter "announced his intention to discontinue the practice of dividing equally among the surgeons the admissions fees of all pupils attending the hospital." [4, p 127]. In the ensuing controversy, at a meeting of the Board on October 16th, Hunter became aggravated to the extent that he left abruptly, collapsed, and died in the hallway, in spite of efforts by Everard Home and Matthew Baillie to revive him [4, p 131]; in the context of the times, 200 miles away, the same day, Marie Antoinette was condemned by the Revolutionary Tribunal in Paris and at 12.15 p.m. met her death on the guillotine.

Matthew Baillie and Everard Home were named executors of the will, a major charge being to offer the "museum" to the British Government (or failing that a foreign government or to individuals). This charge proved difficult to fulfill; Mr. Pitt the Prime Minister, at war with France, responded, "What buy preparations! Why I have not money enough to buy gunpowder." [5, p 240] Eventually, after years of effort by Sir Joseph Banks and Lord Auckland, Parliament voted a sum for procurement of the collection (15,000 pounds; about 1 pound per specimen), which was offered first to the Royal College of Physicians, and declined, then to the Corporation of Surgeons, who accepted on December 23rd 1799, coincident with the granting of a new charter from the Crown, to become the Royal College of Surgeons: a posthumous contribution by Hunter. Today the Hunterian Museum remains under the care of the College having been damaged during the London Blitz, but reconstituted and supplemented with other materials [22] (Fig. 6).

The mortal remains of John Hunter were re-interred in Westminster Abbey in 1759. His portrait by Sir Joshua Reynolds (Fig. 1) is with the Royal College of Surgeons of England.

References

1. Foster WD (1981) Pathology as a Profession in Great Britain, and the Early History of the Royal College of Pathologists. Royal College of Pathologists, undated, circa 1981
2. Taylor CR, DeYoung BR, Cohen MB (2008) Pathology Education: Quo vadis? Hum Pathol 39:1555–1561
3. Home E (1794) A Short Account of the Life of the Author. In: Hunter J. A treatise on the blood, inflammation and gunshot wounds. J Richardson for G Nicol, Pall-Mall, London. (Reprinted by Classics of Medicine Library. Gryphon. Birmingham, Al, 1982). (American Edition Ed. Palmer JF. Haswall, Barrington and Haswall, Philadelphia, 1840 available at Google Books). Available at http://books.google.com/books?id=

5wdAAAAAYAAJ&dq=A+Treatise+on+Blood+Inflammation+and+gunshot+wounds&printsec Accessed 12 January 2010
4. Ottley D (1835) The Life of John Hunter F.R.S. In Palmer JF. The Works of John Hunter. F.R.S.: with Notes". Volume 1. Longman, Rees, Orme, Brown, Green and Longman. Paternoster Row, London. Available at Google books. http://books.google.com/books?id=UwQHAAAAcAAJ&dq=palmer+the+works+of+john+hunter. Accessed 20 December 2009
5. Paget S (1897) John Hunter. Man of Science and Surgeon. T Fisher Unwin, London. Reprinted by BiblioLife LLC. 2009. Available at www.bibliolife.com. Accessed 10 October 2009
6. Hunter W (1784) Two Introductory Lectures delivered by Dr William Hunter to his last course of anatomical lectures at his theatre in Windmill-Street. J Johnson, St. Paul's Church-yard, London, pp 88–89. Available at Google books. http://books.google.com/books?id=eVIOAAAAQAAJ&printsec=frontcover&dq=william+hunter+introductory+lectures. Accessed 20 December 2009
7. Finch E (1957) The Influence of the Hunters on Medical Education. Ann R Coll Surg Engl 20:205–248
8. Baillie M (1793) 'Morbid Anatomy of Some of the Most Important Parts of the Human Body'. Printed for J Johnson, St. Paul's Church-yard; and G. Nicol, Pall-Mall, London. (Second American Edition NH Walpole. Printed by GW.Nichols for Fessenden, Brattleborough. VT. 271 pages, 1808. Available at Google Books). http://books.google.com/books?id=AE8SAAAAYAAJ&dq=Morbid+Anatomy+of+Some+of+the+Most+Important+Parts+of+the+Human+Body. Accessed 1 January 2010
9. Moore W (2005) The Knife Man. The Extraordinary Life and Times of John Hunter Father of Modern Surgery. Broadway Books, New York
10. Abernethy J (1825) from the original in the European Journal of 1782, as reprinted in Abernethy, J Physiological Lectures, London, Longman, pp 341–352. Cited by Moore W, 2005, p17 [9]
11. Oppenheimer JM (1946) New Aspects of John and William Hunter. Henry Schuman, New York
12. Kobler J (1960) The Reluctant Surgeon. A biography of John Hunter. Doubleday, New York
13. Rogers G (1958) Brother Surgeons. Corgi Transworld Publishers, London
14. Foot J (1794) The Life of John Hunter. Becket, Pall-Mall, London. Available at Google Books. http://books.google.com/books?id=Z24EAAAAYAAJ&dq=john+hunter+jesse+foot&printsec. Accessed 1 January 2010
15. Chaplin S (2005) The body snatchers' legacy to medicine. Simon Chaplin, Curator of the Hunterian Museum of the Royal College of Surgeons, cited by Jane Elliott, BBC News. December 12, 2005. Available at www.bbc.com. Accessed 29 November 2009
16. Dimmer F (1992) The Body Snatchers. Citadel (Carol Publishing Group), Secaucus
17. Antiques Digest (2010). Fleet Street. Originally published early 1900s). Available at http://www.oldandsold.com/articles33n/fleet-street-1.shtml. Accessed 7 January 2010
18. von Hagen G (2010). Body Worlds. Available at (http://www.bodyworlds.com/en.html). Accessed 1 January 2010
19. Tward AD, Patterson HA (2002) From Grave Robbing to Gifting: Cadaver Supply in the United States. JAMA 287:1183
20. Shelton DC (2010) The Emperor's New Clothes. JR Soc Med 103:46–50
21. Hunter J (1794) A treatise on the blood, inflammation and gun-shot wounds. London: J. Richardson for G Nicol, Pall-Mall, London. (Reprinted by Classics of Medicine Library. Gryphon. Birmingham, Al, 1982). American Edition Ed Palmer JF. Haswall, Barrington and Haswall, Philadelphia 1840. Available at Google Books). http://books.google.com/books?id=5wdAAAAAYAAJ&dq=A+Treatise+on+Blood+Inflammation+and+gunshot+wounds&printsec. Accessed 12 January 2010
22. Royal College of Surgeons of England. Available at http://www.rcseng.ac.uk/museums. Accessed 11 January 2010
23. Hunter W (1774) Edited by Baillie, M. 'The Anatomy of the Human Gravid Uterus Exhibited in Figures' Baskerville. Birmingham. Reprinted second edition. H. Renshaw, London, 1843. Available at Google books. http://books.google.com/books?id=M3gEAAAAQAAJ&printsec. Accessed 5 December 2009
24. Mitchell R (1927) William Hunter's Anatomy of the Human Gravid Uterus. Can Med Assoc J 17:1379–1383
25. Paget Sir J. (1897) Introduction to 'John Hunter' in Paget S John Hunter. Man of Science and Surgeon. T. Fisher Unwin, London, 1897. Reprinted by BiblioLife LLC. 2009. Available at www.bibliolife.com. Accessed 10 October 2009
26. Moore W (2009) John Hunter: learning from natural experiments, 'placebos', and the state of mind of a patient in the 18th century. Journal Royal Society of Medicine 102:394-396. Available at The James Lind Library www.jameslindlibrary.org. Accessed 5 January 2010
27. Cornelius EH, Harding Rains AJ (1976) John Hunter to Edward Jenner, 2 August (no year), Letters from the Past from John Hunter to Edward Jenner, p 9. Cited by Moore W 2009. (28)
28. Hunter J. In Palmer. J.F. Ed. The Works of John Hunter. F.R.S.: with Notes". Volume 4. Longman, Rees, Orme, Brown, Green and Longman. Paternoster Row, London. 1835. Available at Google Books. http://books.google.com/books?id=UwQHAAAAcAAJ&dq=palmer+the+works+of+john+hunter. Accessed 5 January 2010
29. Hunter J (1835) In Palmer JF Ed. The Works of John Hunter. F.R.S.: with Notes". Volume 1. Longman, Rees, Orme, Brown, Green and Longman, Paternoster Row, London, 1835. Available at Google Books. http://books.google.com/books?id=UwQHAAAAcAAJ&dq=palmer+the+works+of+john+hunter. Accessed 20 December 2009
30. Crainz F (1982) The editions and translations of Dr Matthew Baillie's Morbid Anatomy. Med Hist 26:443–452, obtainable at the Welcome Trust Centre for the History of Medicine, London
31. Baillie M (1799–1802) A series of engravings, accompanied with explanations, which are intended to illustrate the morbid anatomy of some of the most important parts of the human body. Fasciculus I–X. W. Bulmer and Co., London (sold by J. Johnson, St. Paul's Church-yard; and G Nicol, Pall-Mall).

Virchows Arch (2010) 457:415–422
DOI 10.1007/s00428-010-0962-0

ORIGINAL ARTICLE

CpG island hypermethylator phenotype in gastric carcinoma and its clinicopathological features

Seog-Yun Park · Myeong Cherl Kook · Young Woo Kim · Nam-Yun Cho · Namhee Jung · Hyeong-Ju Kwon · Tae-You Kim · Gyeong Hoon Kang

Received: 16 June 2010 / Revised: 4 August 2010 / Accepted: 5 August 2010 / Published online: 25 August 2010
© Springer-Verlag 2010

Abstract Gastric carcinoma (GC) is one of the human cancers in which promoter CpG island hypermethylation is frequently found. CpG island methylator phenotype (CIMP) refers to a subset of GCs which harbor concordant methylation of multiple promoter CpG island loci. However, little is known regarding clinicopathological features of CIMP-positive (CIMP-high) GC. Our study aimed to characterize clinicopathological features of CIMP-high GC. We analyzed 196 cases of GCs for their methylation status in 16 cancer-specific CpG island loci using MethyLight assay and arbitrarily defined CIMP-high GC as those with methylation at 13 or more CpG island loci. With exclusion of microsatellite instability-positive GC and EBV-positive GC from the analysis, CIMP-high GC (n=10, 6.7%) demonstrated tendency toward higher cancer stage, infiltrative growth type, poor differentiation, and diffuse or mixed type of Lauren classification. CIMP-high GC showed significantly shortened survival compared with that of CIMP-negative GC. When CIMP-negative GC (methylation at 12 or less) was divided into CIMP-intermediate and CIMP-low (methylation at one or none), CIMP-low exhibited better clinical outcome than CIMP-intermediate. Hypermethylation at 14 CpG island loci or more was closely associated with poor clinical outcome and found to be an independent prognostic factor. Our findings that CIMP-high GCs were featured with characteristic clinicopathological parameters, including poor prognosis are distinct from previous studies. More extensive, large-scaled study is necessary to validate the findings of the present study.

Keywords CpG island · CpG island methylator phenotype · Gastric cancer · Methylation

S.-Y. Park · M. C. Kook
Department of Pathology,
National Cancer Center,
Goyang, Gyeonggi-do, South Korea

Y. W. Kim
Department of General Surgery,
National Cancer Center,
Goyang, Gyeonggi-do, South Korea

N.-Y. Cho · N. Jung · G. H. Kang
Laboratory of Epigenetics, Cancer Research Institute,
Seoul National University College of Medicine,
Seoul, South Korea

H.-J. Kwon · G. H. Kang
Department of Pathology,
2nd Stage Brain Korea Project
and Seoul National University College of Medicine,
Seoul, South Korea

T.-Y. Kim
Department of Internal Medicine,
Seoul National University College of Medicine,
Seoul, South Korea

G. H. Kang (✉)
Department of Pathology,
Seoul National University College of Medicine,
28 Yongon-dong, Chongno-gu,
Seoul 110-744, South Korea
e-mail: ghkang@snu.ac.kr

Promoter CpG island hypermethylation is an important mechanism in tumorigenesis of human cancers and can act as an alternative to genetic mutations for the inactivation of tumor suppressor genes or tumor-related genes. CpG island methylator phenotype (CIMP) refers to a subset of malignancies that show widespread hypermethylation of multiple promoter CpG island loci. Since CIMP concept was first introduced to the molecular pathways of colorectal cancers (CRCs) by Dr. Issa group [1], many investigators have attempted to characterize the clinicopathological and molec-

ular features of CIMP-positive CRCs and found their close associations with proximal colon location, older age at onset, poor differentiation, microsatellite instability (MSI), and *BRAF* mutation [2–4]. Similarly, the presence of CIMP-positive gastric carcinoma (GC) has been reported by the same group [5], which did not find distinct clinicopathologic features of CIMP-positive GCs except for a close association with MSI. Since then, several investigators have strived to find out additional clinicopathological features of CIMP-positive GCs and close associations with Epstein-Barr virus (EBV) infection and diffuse-type histology were added [6–11].

Unlike normal colon mucosae, gastric mucosae show frequent hypermethylation of many promoter CpG island loci because *Helicobacter pylori* infection, prevalent in Asian countries, induces enhanced CpG island hypermethylation of many susceptible genes in normal gastric epithelial cells [12, 13]. In contrast to the universal application of reference microsatellite markers for the diagnosis of MSI in human cancers regardless tissue types [14], CIMP marker panels of CRCs cannot be applied to the determination of CIMP in GCs because some of the markers are hypermethylated in non-neoplastic gastric mucosae harboring *H. pylori* infection at levels or frequencies comparable to those of GCs and are not cancer-specific methylaton markers [15, 16]. Thus, it is necessary to develop GC's own CIMP marker panels. Several investigators have used their own CIMP marker panels and cut-off values for the determination of CIMP status and characterization of features distinct in CIMP-positive GCs, producing variable and inconsistent findings [6–11].

Through our previous studies [15, 17] in which we screened 170 DNA methylation markers against gastric cancers and non-neoplastic gastric mucosae for their cancer specificity using the MethyLight assay, we developed 16 cancer-specific markers which showed significantly higher levels or frequencies of methylation in GCs than in non-neoplastic gastric mucosae regardless of *H. pylori* infection status. These 16 DNA methylation markers showed strong concordance in methylation of each individual marker in GCs [18]. In order to identify whether GCs with methylation at most of these markers have distinct clinicopathologic features, we analyzed 196 cases of advanced gastric cancer (AGC) for their methylation status in 16 DNA methylation markers and then arbitrarily set cut-off values (the number of methylated markers) to diagnose CIMP-positive GC. Subsequently, we attempted to analyze clinicopathologic features of CIMP-positive GCs defined by various cut-off values of 8–14. However, we did not find cut-off values to define CIMP-positive GCs which showed significantly different clinical outcomes from those of CIMP-negative GCs. Then, we excluded EBV-positive GCs and MSI-positive GCs from the analysis because these two subtypes have been known to harbor their own distinct clinicopathologic features. After determination of an optimal cut-off value to diagnose CIMP, we characterized distinct clinicopathologic features of CIMP-positive GCs.

Material and methods

From the files of the Department of Pathology, we retrieved formalin-fixed, paraffin-embedded archival tissues from 196 AGC patients who underwent curative surgery and extended lymphadenectomy in National Cancer Center, Ilsan, Korea between 2002 and 2003. We excluded patients who had any of the following: R1 surgery, neo-adjuvant therapy, other primary malignancy, or death of other causes. The age of cancer patients ranged 22–79 years (mean, 56.8 years; median, 59 years) and male to female ratio was 133:63. Through gross and microscopic examination, tumor cases were evaluated for their pathological parameters: gross type (Borrmann's classification), tumor differentiation, histological type (Lauren classification), and TNM stage (American Joint Committee on Cancer). Tumor differentiation was categorized as poorly differentiated (≤50% glandular area) or differentiated (>50% glandular area). Tumors were classified as mixed-type GC when tumors showed both intestinal-type and diffuse-type components in excess of 40%. *H. pylori* infection status was determined through three different tests, including serum *H. pylori* IgG test (Genedica *H. pylori* ELISA; Green Cross Sang A Co., Seoul, South Korea), a rapid urease test (CLO test, Delta West, Bentley, Australia) and histological evaluation of *H. pylori* using Giemsa staining. The study was approved by the Institutional Review Board.

DNA preparation

After tumor areas were identified on light microscopy, areas where tumor cells occupied >40% of total cells and represented the most prevalent histological type of the individual case, were marked and scraped from the tissue slide with a knife blade. For the MSI test, non-tumorous portions in matched GC were obtained from normal gastric mucosae which were confirmed to be tumor-free on light microscopic examination. The dissected tissues were placed into microtubes containing tissue lysis buffer (100 mM Tris–HCl (pH 8.0), 10 mM EDTA (pH 8.0), 1 mg/ml proteinase K, and 0.05 mg/ml tRNA) and the microtubes were incubated on 50°C for 2 days.

DNA methylation analysis

The sodium bisulfite conversion of genomic DNA was performed as described [15]. The 16 genes were *BCL2*, *BDNF*, *CACNA1G*, *CALCA*, *CHFR*, *CYP1B1*, *DLEC1*,

GRIN2B, *RUNX3*, *SEZ6L*, *SFRP4*, *TERT*, *THBS1*, *TIMP3*, *TP73*, and *TWIST1*. Primers and probes used for the MethyLight assay target promoter sequences or the first exon of the corresponding genes and their oligonucleotide sequences have been described [2]. Real-time PCR-based DNA methylation assay (MethyLight assay) was validated and performed as described earlier [19, 20]. We used a percentage of methylated reference (PMR) cut-off value of 4 to define methylation-positive vs. -negative and determined DNA methylation frequencies (PMR>4) for each CpG island locus.

Microsatellite instability

The MSI status of each tumor sample was determined using a consensus panel of five reference microsatellite markers (BAT25, BAT26, D2S123, D3S546, and D17S250) by a previously described method [15]. A tumor was considered to be MSI+if two or more of the five markers showed novel alleles compared to normal DNA.

Epstein-Barr virus-encoded RNA in situ hybridization

In situ hybridization was performed to detect Epstein-Barr virus-encoded small RNA (EBER) 1–2 mRNAs using a fluorescein-conjugated EBV (EBER) peptide nucleic acid probe (Dako, Glostrup, Denmark) on paraffin tissue section. Subsequent steps used a detection kit for fluorescein-labeled probes (Dako). Slides were washed in stringency wash buffer and then an alkaline phosphatase-linked antibody to fluorescein was applied for 20 min at room temperature. For visualization, the chromogen solution 5-bromo-4-chloro-3-indolyl-phosphatase/4-nitroblue tetrazolium was applied.

Statistical analysis

Associations between clinicopathological parameters and CIMP status were analyzed using Pearson's chi-square test. Survival was measured from the date of resection of GC to the date of death or the last clinical follow-up time before 31 December 2007. The average follow-up time (from surgery to death or the last follow-up) was 46 months (range, 1–72 months). Overall survival rates were assessed using the Kaplan–Meier log-rank test, and using Cox proportional-hazards regression models, multivariate analysis was performed in a background manner to determine association between survival and CIMP, adjusting for variable suggested to be prognostic factors on Univariate analysis. All statistical analyses were conducted using SPSS software (SPSS, Ver. 15.0; SPSS Inc., Chicago, IL). P values of <0.05 were accepted as being statistically significant.

Results

We analyzed 196 AGC samples for their methylation status in 16 cancer-specific DNA methylation markers using MethyLight technology and PMR values were calculated for each sample and MethyLight reaction (Fig. 1). Of 16 CpG island loci, *TWIST1* showed the highest methylation frequency (88%), whereas *TP73* exhibited the lowest methylation frequency (15%). Six loci, including *TWIST1*, *SFRP4*, *BCL2*, *TIMP3*, *SEZ6L*, and *CALCA*, showed methylation frequencies of 50% or more. The number of genes methylated in an individual cancer varied from 0 to 16 (average, 7.5) and was distributed in a continuous pattern. Ten cases were negative for three tests for *H. pylori* infection but no differences were found in the number of methylated genes between *H. pylori*-negative GCs and *H. pylori*-positive GCs (data not shown).

Poor survival of CpG island methylator phenotype-positive GCs

Because hypermethylation of one specific locus tends to be concordant with that of the other individual loci, a better or worse survival observed in GCs with hypermethylation of the individual loci could not be attributed to the hypermethylation of the locus. Rather, the survival may be related to concordant hypermethylation of multiple CpG island loci, namely CIMP. With application of varying cut-off values of 8–14 to EBV-negative/MSI-negative GCs, we found that cut-off values of 13 or 14 defined CIMP-positive GCs which showed worse clinical outcome than CIMP-negative GCs (Fig. 2). By multivariate analysis, we found that CIMP-positive GCs defined by cut-off values of 13 was not an independent prognostic parameter but that CIMP-positive GCs defined by cut-off values of 14 was an independent prognostic parameter heralding poor prognosis (Table 1).

Pathological features of CIMP-positive GCs

Then we trichotomized EBV-negative/MSI-negative GCs into CIMP-high (defined as GCs with methylation at 14 or more), CIMP-intermediate (defined as GCs with methylation at less than 14 and more than 1), and CIMP-low (methylation at 1 or 0) and analyzed their survival with Kaplan–Meier method, CIMP-low showed the best prognosis while CIMP-intermediate exhibited survival curve between those of CIMP-high and CIMP-low (Fig. 3). When these three subtypes were correlated with clinicopathological parameters, CIMP-positive (or CIMP-high) GCs tended to show poor differentiation, diffuse type or mixed type of Lauren classification, infiltrative gross type, and higher tumor stage (Table 2).

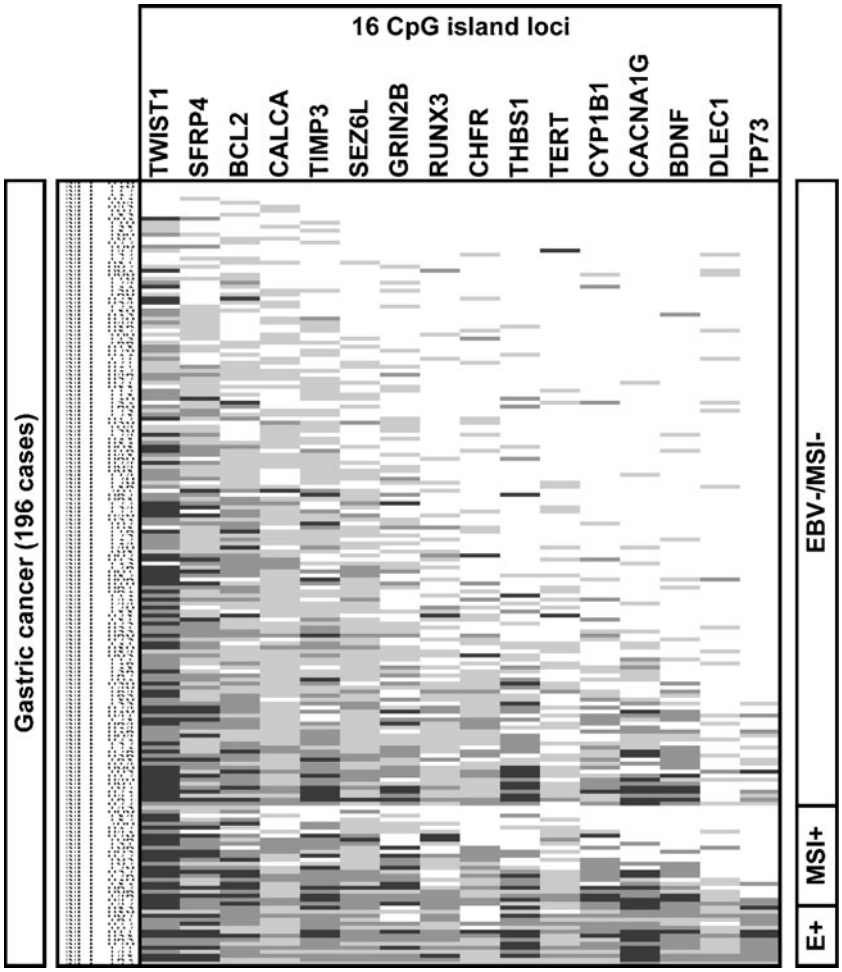

Fig. 1 Methylation map of the PMR values obtained for each CpG island locus in gastric cancer samples (n=196). *Gray-scaled boxes* represent four classes of methylation levels (0≤PMR<4 (*white*), 4≤PMR<20 (*light gray*), 20≤PMR<50 (*dark gray*), PMR≥50 (*black*)). *E+*, EBV-positive; *MSI+*, microsatellite instability-positive; *EBV−/MSI−*, EBV-negative/MSI-negative

Discussion

In the present study, we have analyzed a series of GCs (n=196) for their methylation status in 16 cancer-specific DNA methylation markers using the MethyLight assay. The distribution of GCs regarding the number of genes methylated was of continuous pattern, not of discrete, bimodal pattern, which means absence of absolute cut-off points to define CIMP-positive GCs. Thus, we tried variable cut-off values to define CIMP-positive GC in order to find an optimal cut-off

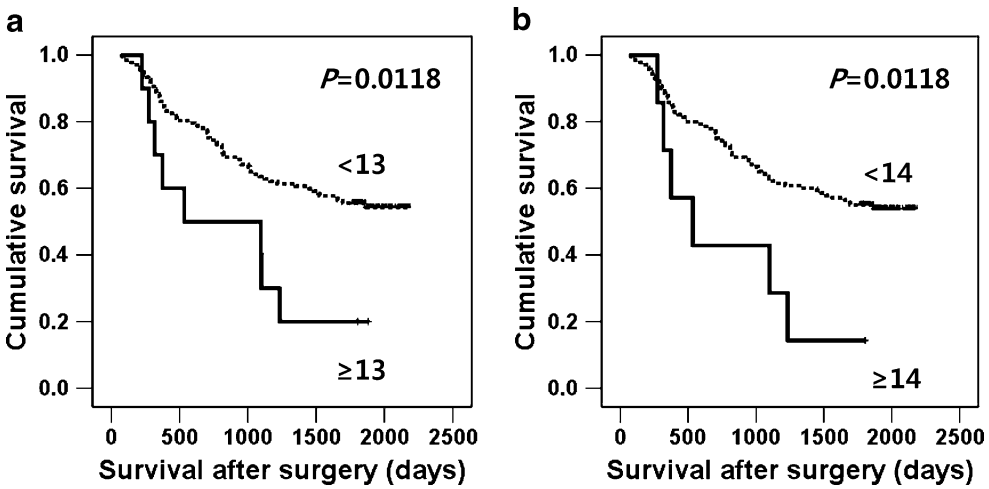

Fig. 2 Survival curves of CpG island methylator phenotype (CIMP)-positive and -negative groups were compared using Kaplan–Meier procedure and log-rank test. Cut-off values to define CIMP-positive gastric cancer were applied differently for A and B (13 and 14, respectively)

Table 1 Univariate and multivariate survival analysis in 147 gastric cancer patients[a] (excluding EBV+or MSI+gastric cancers)

Parameters	*n*	Univariate analysis		Multivariate analysis	
		Mean survival time (months; 95% confidence interval)	*P* value	Hazard ratio (95% confidence interval)	*P* value
Age					
58 years or less	71	49 (42–55)	0.957	–	
59 years or more	76	50 (44–56)		–	
Gross					
Borrmann I, II	21	59 (50–68)	0.134	–	
Borrmann III, IV	126	48 (43–52)		–	
Lauren					
Intestinal	58	53 (46–59)	0.569	–	
Diffuse	69	45 (39–51)		–	
Mixed	16	52 (39–66)		–	
Differentiation					
Low grade	34	54 (46–62)	0.461	–	
High grade	113	48 (43–53)		–	
TNM					
IB	24	69 (64–74)	<0.001	Reference	
II	31	62 (56–68)		3.904 (0.843–18.088)	0.082
IIIa	31	57 (49–65)		4.599 (1.007–21.007)	0.049
IIIb	18	44 (32–56)		11.959 (2.635–54.278)	0.001
IV	43	25 (19–31)		27.245 (6.513–113.963)	<0.001
CIMP					
Negative	140	50 (46–55)	0.012	Reference	
Positive	7	27 (13–34)		2.958 (1.238–7.066)	0.015

[a] Survival was analyzed in 147 patients, excluding three patients because of follow-up loss

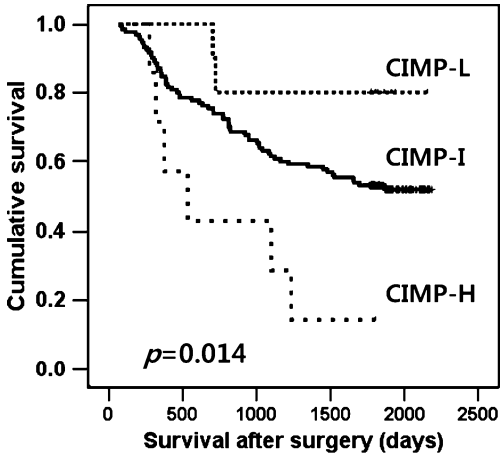

Fig. 3 Kaplan–Meier survival curves in MSI-negative/EBV-negative gastric cancers (n=147) according to CIMP status. I CIMP-low, II CIMP-intermediate, III CIMP-high or (CIMP-positive). CIMP-intermediate tumor was defined as a tumor with methylation at two to 13 genes

value which can define CIMP-positive GCs which should carry a prognostic implication. We found out that EBV-negative/MSI-negative GCs with methylation at 14 or more genes were closely associated with poor prognosis and the association remained significant against multivariable analysis. Such defined CIMP-positive GCs tended to show distinct clinicopathologic features, including proclivity toward diffuse- or mixed-type histology, poor differentiation, infiltrative gross types, and higher cancer stage.

CIMP refers to a subset of epithelial malignancies which show concurrent promoter CpG island hypermethylation of multiple genes and is well characterized in colorectal cancers. In contrast to colorectal cancers, little is known regarding clinicopathological features of CIMP-positive GC. In the literature, several researchers attempted to characterize clinicopathological features of CIMP-positive GC using variable methodologies of DNA methylation analysis and their own CIMP marker panels, and produced controversial results (Table 3) [6–11]. Despite variable findings, relatively common findings include close associations of CIMP-positive GCs with diffuse type and better clinical outcome. In the present study, CIMP-positive GCs tended to show an association with not only diffuse type but also mixed type of Lauren's classification. None of the intestinal-type GCs was CIMP-positive, whereas 5.7% of the diffuse-type GCs and 18.8% of the mixed-type GCs were CIMP-positive. Most previous studies reported that CIMP was associated with better prognosis but not an independent prognostic factor on multivariable analysis. In contrast, the present study showed that CIMP was closely associated with poor prognosis of GC patients and CIMP was an independent prognostic marker. The discrepancy might be attributed to the differences in DNA methylation markers to define CIMP, use of qualitative or quantitative methodologies to analyze DNA methylation, and utilization of microdissection. However, in the present study, the number of CIMP-positive GCs was too small to decide whether CIMP is a prognostic marker. What is worth of being addressed is that our approach was able to detect a subset of GCs which were highly methylated and such a defined GC showed a poor prognosis in an independent manner. A large-scaled study is necessary to determine whether CIMP defined by 16 DNA methylation markers and cut-off value of 14 is an independent biomarker heralding poor prognosis of gastric cancer patients.

In the present study, of the three subtypes defined by the methylation frequencies, CIMP-low, defined as tumors with methylation at one gene or none, showed the best clinical outcome. Although CIN and CIMP have been reported to be mutually exclusive in CRCs [21], little is known regarding

Table 2 Clinicopathological features of CpG island methylator phenotype-positive gastric cancers

		CIMP-high (n=7)	CIMP-intermediate (n=132)	CIMP-low (n=11)	p value
Gender	M	3 (42.9%)	90 (68.2%)	10 (90.9%)	0.095
	F	4 (67.1%)	42 (31.8%)	1 (9.1%)	
Gross	Borrmann I or II	0	17 (12.9%)	4 (36.4%)	0.054
	Borrmann III or IV	7 (100%)	115 (87.1%)	7 (63.6%)	
Lauren	Intestinal	0	51 (38.9%)	8 (72.7%)	0.006
	Diffuse	4 (57.1%)	64 (48.9%)	2 (18.2%)	
	Mixed	3 (42.9%)	13 (9.9%)	0	
	Unclassified	0	5 (2.8%)	1 (9.1%)	
Differentiation	Low grade	0	29 (22.0%)	6 (54.5%)	0.016
	High grade	7 (100%)	103 (78.0%)	5 (45.5%)	
TNM	I, II	2 (28.6%)	46 (34.8%)	8 (72.7%)	0.039
	III, IV	5 (71.4%)	86 (65.2%)	3 (27.3%)	
Survival	3 year survival rate	28.6%	61.5%	80%	0.0138
	5 year survival rate	14.3%	53.1%	80%	

Table 3 Scientific papers reporting CIMP-positive gastric cancers

	Method[a]	CIMP marker panel	Cut-off value	Features
Toyota M, et al. Cancer Res 1999	COBRA	*MINT1*, *MINT2*, *MINT12*, *MINT25*, *MINT31*	CIMP+(3 or more), CIMP-intermediate (2), CIMP- (1 or negative)	Lower stage in CIMP+; otherwise no specific findings for CIMP+
Oue N, et al. Cancer 2006	COBRA	*MINT1*, *MINT2*, *MINT12*, *MINT25*, *MINT31*	CIMP+(3 or more), CIMP- (2 or less). Other 12 genes (methylation-high, 5 or more)	no specific findings for CIMP+but methylation-high group showing higher tissue and nodal stages
An C, et al. Clin Cancer Res 2005	MSP, microdissection	*MINT1*, *MINT2*, *MINT25*, *MINT31*, *MLH1*	CIMP-high (3 or more), CIMP-low (2 or less), CIMP-negative (0)	CIMP-high showing association with MSI, better prognosis (not independent factor)
Chang MS, et al. Clin Cancer Res 2006	MSP	*LOX*, *HRASLS*, *FLNc*, *HAND1*, *TM*	CIMP-high (4–5), CIMP-intermediate (1-3), CIMP-negative (0)	CIMP-high showing better prognosis (not independent factor)
Kusano M, et al. Cancer 2006	COBRA	*MINT1*, *MINT2*, *MINT12*, *MINT25*, *MINT31*	CIMP-high (4–5), CIMP-intermediate (1–3), CIMP-negative (0)	CIMP-high closely associated with proximal location, diffuse type, less-advanced tumor stage (multivariable), better prognosis (univariable)
Enomoto S, et al. Cancer Sci 2007	Q-MSP	*LOX*, *HRASLS*, *FLNc*, *HAND1*, *THBD*, *F2R*, *NT5E*, *GREM1*, *ZNF177*, *CLDN3*, *PAX6*, *CTSL*	CIMP-high (5 or more), CIMP-low (1–4), CIMP-negative (0)	CIMP-high closely associated with diffuse type, better prognosis (univariable)

[a] *COBRA* combined bisulfite restriction analysis, *MSP* methylation-specific PCR, *Q-MSP* quantitative MSP

their relationship in GCs. Based on similarities of molecular alterations between CRC and GC, most of CIMP-low GCs are expected to be CIN-positive GCs because all of these were MSI-negative in our GC samples. Or, other unknown molecular pathways may be the driving the progression of this CIMP-low/MSI-negative GC subtype. CIMP-low tumors were distinct from CIMP-high tumors by male dominance, low-grade differentiation, intestinal type, fungating gross type, and lower TNM stage. The present study analyzed *H. pylori*-infected GC samples only and at present it is difficult to understand the fact that CIMP-low tumors occur in the background of *H. pylori*-infected gastric mucosa which are usually enhanced at hypermethylation in multiple CpG island loci because of *H. pylori* infection and subsequent inflammatory reaction. Although we did not analyze the methylation status of 16 genes in the adjacent non-neoplastic gastric mucosa, in our previous study [17] we analyzed the same 13 genes in *H. pylori*-infected chronic gastritis and intestinal metaplasia of GC patients and the number of genes methylated was 4.8 and 9.1, respectively. These numbers are much higher than that of CIMP-low tumors. At present, we cannot provide explanation about the development of CIMP-low tumors in the background of *H. pylori*-infected gastric mucosa. Ushijima team's study has demonstrated that CIMP-high GCs were not accompanied with higher number of genes methylated in the background mucosa [6].

In conclusion, we have analyzed 196 cases of GC for their methylation status in 16 CpG island loci and correlated their hypermethylation with clinicopathological features. Novel findings include that mixed-type histology was found to be associated with enhanced hypermethylation and EBV-negative/MSI-negative GCs with hypermethylation at 14 or more genes showed worse clinical behaviors.

Acknowledgement Supported by a grant of the Korea Healthcare Technology R&D Project, Ministry for Health, Welfare and Family Affairs, Republic of Korea (A091081).

Disclosure The authors declare that they have no conflict of interest.

References

1. Toyota M, Ahuja N, Ohe-Toyota M et al (1999) CpG island methylator phenotype in colorectal cancer. Proc Natl Acad Sci USA 96:8681–8686
2. Weisenberger DJ, Siegmund KD, Campan M et al (2006) CpG island methylator phenotype underlies sporadic microsatellite instability and is tightly associated with BRAF mutation in colorectal cancer. Nat Genet 38:787–793
3. Ogino S, Goel A (2008) Molecular classification and correlates in colorectal cancer. J Mol Diagn 10:13–27
4. Kim JH, Shin SH, Kwon HJ, Cho NY, Kang GH (2009) Prognostic implications of CpG island hypermethylator phenotype in colorectal cancers. Virchows Arch 455:485–494

5. Toyota M, Ahuja N, Suzuki H et al (1999) Aberrant methylation in gastric cancer associated with the CpG island methylator phenotype. Cancer Res 59:5438–5442
6. Enomoto S, Maekita T, Tsukamoto T et al (2007) Lack of association between CpG island methylator phenotype in human gastric cancers and methylation in their background non-cancerous gastric mucosae. Cancer Sci 98:1853–1861
7. Kang GH, Lee S, Kim WH et al (2002) Epstein-barr virus-positive gastric carcinoma demonstrates frequent aberrant methylation of multiple genes and constitutes CpG island methylator phenotype-positive gastric carcinoma. Am J Pathol 160:787–794
8. Chang MS, Uozaki H, Chong JM et al (2006) CpG island methylation status in gastric carcinoma with and without infection of Epstein-Barr virus. Clin Cancer Res 12:2995–3002
9. Oue N, Oshimo Y, Nakayama H et al (2003) DNA methylation of multiple genes in gastric carcinoma: association with histological type and CpG island methylator phenotype. Cancer Sci 94:901–905
10. An C, Choi IS, Yao JC et al (2005) Prognostic significance of CpG island methylator phenotype and microsatellite instability in gastric carcinoma. Clin Cancer Res 11:656–663
11. Kusano M, Toyota M, Suzuki H et al (2006) Genetic, epigenetic, and clinicopathologic features of gastric carcinomas with the CpG island methylator phenotype and an association with Epstein-Barr virus. Cancer 106:1467–1479
12. Chan AO, Peng JZ, Lam SK et al (2006) Eradication of *Helicobacter pylori* infection reverses E-cadherin promoter hypermethylation. Gut 55:463–468
13. Chan AO, Lam SK, Wong BC et al (2003) Promoter methylation of E-cadherin gene in gastric mucosa associated with *Helicobacter pylori* infection and in gastric cancer. Gut 52:502–506
14. Boland CR, Thibodeau SN, Hamilton SR et al (1998) A National Cancer Institute Workshop on Microsatellite Instability for cancer detection and familial predisposition: development of international criteria for the determination of microsatellite instability in colorectal cancer. Cancer Res 58:5248–5257
15. Kang GH, Lee S, Cho NY et al (2008) DNA methylation profiles of gastric carcinoma characterized by quantitative DNA methylation analysis. Lab Invest 88:161–170
16. Yoo EJ, Park SY, Cho NY et al (2008) Helicobacter pylori-infection-associated CpG island hypermethylation in the stomach and its possible association with polycomb repressive marks. Virchows Arch 452:515–524
17. Park SY, Yoo EJ, Cho NY, Kim N, Kang GH (2009) Comparison of CpG island hypermethylation and repetitive DNA hypomethylation in premalignant stages of gastric cancer, stratified for Helicobacter pylori infection. J Pathol 219:410–416
18. Park SY, Kook MC, Kim YW et al (2010) Mixed-type gastric cancer and its association with high-frequency CpG island hypermethylation. Virchows Arch 456(6):625–633
19. Ogino S, Cantor M, Kawasaki T et al (2006) CpG island methylator phenotype (CIMP) of colorectal cancer is best characterised by quantitative DNA methylation analysis and prospective cohort studies. Gut 55:1000–1006
20. Ogino S, Kawasaki T, Brahmandam M et al (2006) Precision and performance characteristics of bisulfite conversion and real-time PCR (MethyLight) for quantitative DNA methylation analysis. J Mol Diagn 8:209–217
21. Goel A, Nagasaka T, Arnold CN et al (2007) The CpG island methylator phenotype and chromosomal instability are inversely correlated in sporadic colorectal cancer. Gastroenterology 132:127–138

Virchows Arch (2010) 457:423–432
DOI 10.1007/s00428-010-0956-y

ORIGINAL ARTICLE

Loss of WW domain-containing oxidoreductase expression in the progression and development of gastric carcinoma: clinical and histopathologic correlations

Naoko Maeda · Shuho Semba · Shunji Nakayama · Kazuyoshi Yanagihara · Hiroshi Yokozaki

Received: 14 June 2010 / Revised: 25 July 2010 / Accepted: 26 July 2010 / Published online: 25 August 2010
© Springer-Verlag 2010

Abstract The purpose of this study is to investigate the role of the WW domain-containing oxidoreductase (WWOX) tumor suppressor that maps to the common fragile site *FRA16D* (16q23.3-24.1) during the development of gastric carcinoma (GC), we examined the altered expression of WWOX in GC cell lines and tissue samples as well as the effects of restoration of the *WWOX* gene into WWOX-deficient GC cells. All GC cell lines (HSC-45, HSC-57, HSC-59, MKN-7, and MKN-74) showed reduced WWOX expression at the mRNA and protein levels and hypermethylation at the *WWOX* regulatory site was detected in HSC-45 and HSC-59 cells. Interestingly, treatment with the deacetylating agent trichostatin A and the demethylating agent 5-aza-2′-deoxycytidine restored endogenous WWOX expression levels in HSC-59 cells. Restoration of the *WWOX* gene with Ad-WWOX into HSC-59 cells effectively suppressed cell growth and increased the population of cells in subG$_1$ DNA content. In GC tissue samples, the loss of WWOX expression was detected in 24 (33%) of 73 GC cases in accordance with the hypermethylation at the *WWOX* regulatory site. Surprisingly, negative immunoreactivity against WWOX showed a significant relationship with several clinicopathologic findings, including histology (P=0.0001), depth of invasion (P=0.0004), lymph node metastasis (P=0.0003), vessel infiltration (lymphatic vessels, P=0.0167 and venous vessels, P=0.0005), and clinicopathologic stage (P=0.001). These findings suggest that repression of WWOX expression may play an important role in stomach carcinogenesis. WWOX thus appears to be a good biomarker for molecular diagnosis of the grade of malignancy of GCs.

Keywords WW domain-containing oxidoreductase · Gastric carcinoma · CpG island methylation · Tumor suppressor · Clinicopathologic findings

N. Maeda · S. Semba (✉) · S. Nakayama · H. Yokozaki
Division of Pathology, Department of Pathology,
Kobe University Graduate School of Medicine,
7-5-1 Kusunoki-cho, Chuo-ku,
Kobe 650-0017, Japan
e-mail: semba@med.kobe-u.ac.jp

K. Yanagihara
Laboratory of Health Sciences, Department of Life Sciences,
Faculty of Pharmacology, Yasuda Women's University,
6-13-1 Yasuhigashi, Asaminami-ku,
Hiroshima 731-0153, Japan

Introduction

Common chromosome fragile sites in the human genome are particularly susceptible to damage by environmental carcinogens. Common fragile sites have been observed at or near structural chromosome defects recognized in various cancers, and such genomic instability contributes to neoplasia by virtue of altered expression of the associated genes [1]. Homozygous deletion and chromosomal breakage at the *FRA3B* (3p14.2) have been shown to result in a loss of gene expression of the fragile histidine triad (FHIT) tumor suppressor in various human malignancies [1, 2]. Similarly, the WW domain-containing oxidoreductase (WWOX) has been isolated as a candidate tumor suppressor that maps to the common fragile site *FRA16D* (16q23.3-24.1) [3]. The WWOX protein contains two WW domains in the NH_2-terminal region (WW1 and WW2) and a short chain dehydrogenase/reductase domain, and the WW1 domain is involved in the protein–protein interactions with Ap2γ [4], Ap2α [4], ErbB-4 [5], p73 [6], and p53 [7]. Therefore, loss of function of WWOX triggered by frequent deletion of the *WWOX* locus and resultant loss of

WWOX expression is considered to have some oncogenic effects in the development of human malignancies, including those of the breast [8, 9], esophagus [10], lung [11], and pancreas [12, 13]. Supporting the possible tumor suppressor function of WWOX, restoration of the *WWOX* expression into the WWOX-deficient cancer cells effectively suppresses cell growth and induces caspase-dependent apoptosis in vitro and in vivo [13–15].

In gastric carcinoma (GC) cases, frequent reduction of WWOX expression and loss of heterozygosity (LOH) has been documented [16]; whereas, the roles of WWOX in GC cells still remain unknown. In this study, we therefore conducted adenoviral gene delivery into GC cells to confirm the tumor-suppressive effects of the WWOX protein. Furthermore, WWOX expression in the GC tissues was analyzed to investigate the correlations with the methylation status of the WWOX regulatory CpG sites and clinicopathologic findings.

Materials and methods

Cell lines and tissue samples

Human GC cell lines HSC-45, HSC-57, and HSC-59 were established by Kazuyoshi Yanagihara (Yasuda Women's University, Hiroshima, Japan) [17, 18]. MKN-7 and MKN-74 cells were gifts from Prof. Toshiyuki Suzuki (Fukushima Medical University, Fukushima, Japan) [19, 20]. All cell lines were maintained in RPMI-1640 with 10% fetal bovine serum (FBS). HSC-59 cells were treated with the deacetylating agent trichostatin A (TSA, 1 μM) and the demethylating agent 5-aza-2′-deoxycytidine (AZA, 5 μM) [13]. A total of 73 formalin-fixed and paraffin-embedded GC tissue samples [Wel (well-differentiated type), 24 cases; Mod (moderately differentiated type), 33 cases; and Por (poorly differentiated type), 16 cases] surgically removed at Kobe University Hospital (Kobe, Japan) were employed. Informed consent was obtained from all patients and the study was approved by the Kobe University Institutional Review Board. None of these cases had received adjuvant chemotherapy or radiotherapy before surgery. Histological examination was performed according to the classification of gastric carcinoma [21].

Adenoviral gene transduction, cell growth test, and flow cytometry

Adenoviruses carrying the *WWOX* (Ad-WWOX) and *GFP* gene (Ad-GFP) were prepared, amplified, and titrated as described elsewhere [14]. Cells were transduced with Ad-WWOX and Ad-GFP at an appropriate multiplicity of infection (MOI) for 4 h before addition of culture medium. Over 95% transduction efficiency was assessed by visualization of GFP-expressing cells using fluorescence microscopy. For the cell growth test, HSC-59 cells were plated in a 100-mm dish at a density of 1.0×10^5 cells and infected with Ad-WWOX and Ad-GFP at a desired MOI. Viable cells were counted at each time point. For flow cytometry, 1.0×10^4 cells were infected with Ad-WWOX or Ad-GFP. Forty-eight hours after viral infection, the cells were fixed in ethanol, collected by centrifugation, and stained with propidium iodide. The analysis was performed with a FACSCalibur cytometer (BD Biosciences, San Jose, CA, USA).

Reverse transcription-PCR and quantitative real-time RT-PCR

Total RNA was isolated using the RNeasy Mini Kit (Qiagen, Hilden, Germany). Reverse transcription-PCR (RT-PCR) was performed using the following primer sets: *WWOX*, 5′-AGT TCC TGA GCG AGT GGA CC-3′/5′-TTA CTT TCA AAC AGG CCA CCA C-3′; and *β-actin*, 5′-GCA CTC TTC CAG CCT TCC TTC-3′/5′-GGA GTA CTT GCG CTC AGG AGG-3′ [13]. After an initial incubation at 50°C for 30 min and denaturation at 95°C for 15 min, the following cycling conditions (40 cycles) were used for PCR: denaturation at 94°C for 15 s, annealing at 60°C for 30 s, and extension at 72°C for 1 min. Quantitative real-time RT-PCR was performed using a QuantiTect SYBR Green PCR kit (Qiagen) in triplicates with primer sets specific to *WWOX* (forward, 5′-TGC CTC TTC ATG TGC TTG TG-3′; reverse, 5′-GGT GGT CTC CAG GCC ATC T-3′), with *β-actin* as a housekeeping gene. Thermal cycling was performed with an ABI StepOne real-time PCR system (Applied Biosystems). The C_T values were determined by plotting the observed fluorescence against the cycle number. Each C_T value was analyzed using the comparative threshold cycle method and normalized to the C_T values of *G3PDH*. The relative gene expression levels were estimated using the following formula: relative expression $=2^{-(\mathrm{CT}[target\ gene]-\mathrm{CT}[G3PDH])}$.

Methylation-specific PCR

Genomic DNA was treated with sodium bisulfite (EpiTect Bisulfite kit; Qiagen) and was analyzed by methylation-specific PCR (MSP) using primer sets located within the *WWOX* regulatory site [13]: methylated, 5′-GCG AGT GGA TTC GGT AGC GGG CGA-3′/5′-CCG TAT CGT CCA ACC CCG CGT-3′ and unmethylated, 5′-GTG AGT GGA TTT GGT AGT GGG TGA-3′/5′-CCA TAT CAT CCA ACC CCA CAT-3′. The PCR amplification consisted of 35 cycles (denaturation at 94°C for 30 s, annealing at 62°C for 30 s, and extension at 72°C for 1 min).

Microsatellite analysis

Four microsatellite markers within the *WWOX* locus were analyzed [10, 16]. The forward primers were fluorescein labeled with 6-FAM (D16S3029), HEX (D16S3096), VIC (D16S504), and TAMRA (D16S518). PCR was performed in 15 μl of reaction volumes containing 1 μl of template DNA, 0.56 μM of each primer, 74.7 μM of dNTP, 4.5 μM of $MgCl_2$, and 0.075 U of AmpliTaq Gold (Applied Biosystems, Foster City, CA, USA). The PCR amplification consisted of 45 cycles (94°C for 45 s, 55°C for 45 s, and 72°C for 45 s) followed by a final extension for 10 min at 72°C. Polymerase chain reaction products were electrophoresed in ABI PRISM 310 Genetic Analyzer (Applied Biosystems). Alleles were defined as the two highest peaks (tumor DNA alleles, T1, T2; normal DNA alleles, N1, N2) and a ratio of (T1/T2)/(N1/N2) of <0.10 or >10 was scored as an LOH.

Western blot

Cells were lysed in a lysis buffer [50 μM of Tris–HCl (pH 7.4), 125 μM of NaCl, 0.1% Triton X, and 5 μM of EDTA]. Proteins were separated by SDS-polyacrylamide gel electrophoresis electrotransferred onto an Immunobilon-P membrane (Millipore, Billerica, MA, USA) and then immunoblotted with antibodies against WWOX (Imgenex, San Diego, CA, USA) and β-actin (Sigma, St. Louis, MO, USA). Horseradish peroxidase-conjugated donkey anti-mouse IgG and sheep anti-rabbit IgG (GE Healthcare, Piscataway, NJ, USA) were used as secondary antibodies. Proteins were visualized using enhanced chemiluminescence.

Immunofluorescence and immunohistochemistry

Cells were grown on glass cover slips and then fixed with methanol. Staining patterns obtained with antibody against WWOX were visualized with Cy2-conjugated antibody against rabbit IgG (GE Healthcare). The nuclei were stained with 4,6-diamidino-2-phenylindole (DAPI). A modified version of the immunoglobulin enzyme bridge technique with an LSAB kit (Dako, Glostrup, Denmark) was used. Briefly, deparaffinized and rehydrated sections were autoclaved to retrieve antigenicity. After blocking of endogenous peroxidase and non-specific reactions, the primary antibodies against WWOX which were diluted 1:5,000 were applied to the sections, which were then incubated with biotinylated monkey anti-rabbit IgG. Detection was done with streptavidin–biotin–peroxidase system with diaminobenzidine. Immunoreactivity of WWOX was graded according to the number of stained cells and the staining intensity in individual cells as follows: (–), almost no positive cells; (+), 5–50% of tumor cells showed weak immunoreactivity; and (++), >50% of tumor cells showed moderate to intense immunoreactivity.

Statistical analysis

Relationship between WWOX immunoreactivity and the clinicopathologic findings were investigated by Chi-square test. Survival curves were plotted using the Kaplan–Meier method. Patients with stage I GC were excluded and 39 patients who underwent curative surgery and who received follow-up care at Kobe University Hospital were examined. *P* values less than 0.05 were considered statistically significant.

Results

Hypermethylation-mediated repression of WWOX expression in GC cell lines

Analysis of the WWOX expression pattern in normal human tissues showed that expression was highest in the reproductive organs but was moderate in the alimentary tract, including the stomach [3, 16, 22]. First, the WWOX expression levels in the five GC cell lines (HSC-45, HSC-57, HSC-59, MKN-7, and MKN-74) were analyzed by RT-PCR and Western blot. Compared with HSC-45, HSC-57 and MKN-74 cells, the *WWOX* mRNA expression was undetectable in HSC-59 and MKN-7 cells, a finding compatible with the protein levels detected by Western blot (Fig. 1a, b). Since the levels of WWOX expression in these cell lines were much lower than that in normal gastric mucosa (Fig. 1a, b), we divided these cell lines into WWOX-low (HSC-45, HSC-57, and MKN-74) and WWOX-deficient (HSC-59 and MKN-7) according to their endogenous WWOX levels. By immunofluorescence, we confirmed the results in GC cell lines of the HSC (Fig. 1c) and MKN series (data not shown).

Hypermethylation of the *WWOX* promoter plays a central role in the resultant reduction of WWOX expression in various human malignancies [23, 24]. We thereby performed MSP to evaluate the methylation status at the *WWOX* regulatory CpG sites. Methylation-specific bands were found in the HSC-45 and HSC-59 cells; the intensity of the methylation-specific band in the HSC-45 cells was weak, but that in HSC-59 cells was strong in comparison with the unmethylated bands (Fig. 2a). Although HSC-57, MKN-7, and MKN-74 cells expressed low or absent WWOX expression, the *WWOX* regulatory CpG sites were unmethylated (Fig. 2a). In HSC-59 cells, we confirmed that treatment with the deacetylating agent TSA and demethylating agent AZA resulted in restoration of WWOX

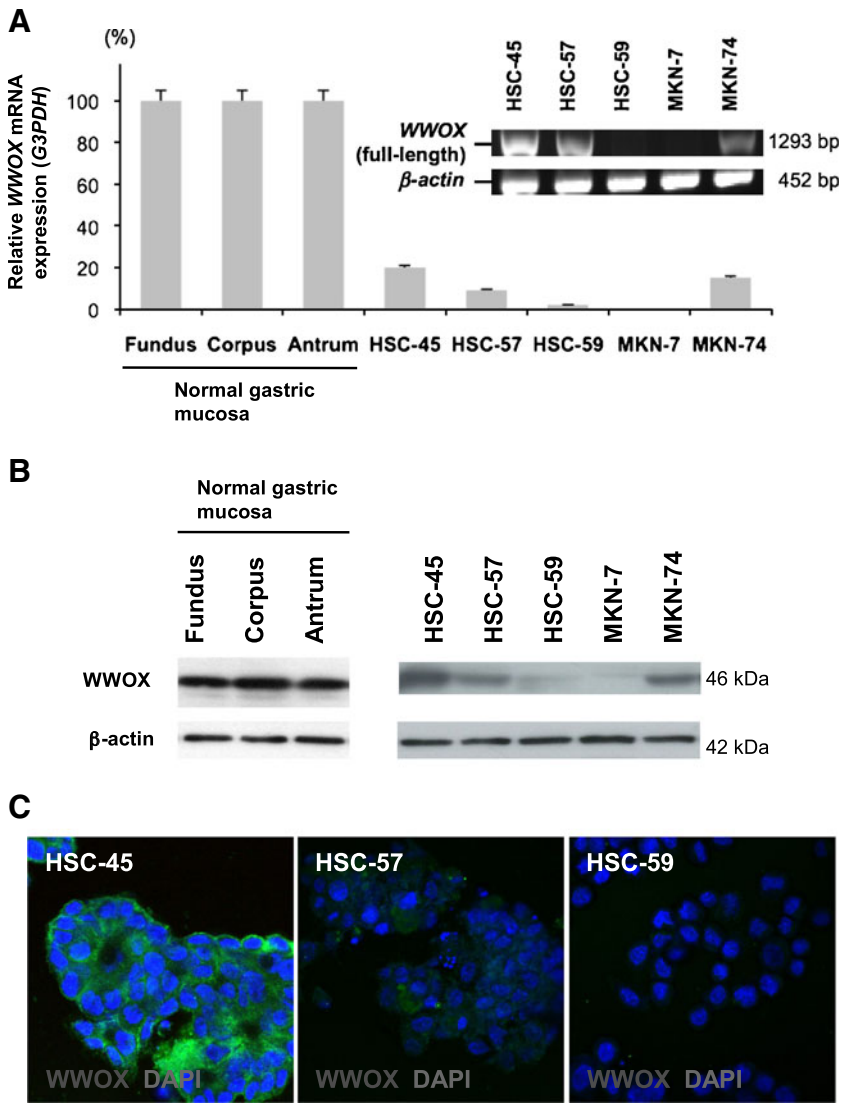

Fig. 1 Reduced WWOX expression at the mRNA and protein levels in GC cell lines. **a** Results of RT-PCR and quantitative RT-PCR. Human normal gastric mucosa used as a reference of *WWOX* mRNA levels. The mRNA levels of *G3PDH* expression were analyzed as a control. β-Actin was used as a loading control. **b** Results of Western blot. *β-actin* was used as a control. **c** Representative illustration of WWOX expression in the HSC series of GC cell lines (HSC-45, HSC-57, and HSC-59). Nuclei were stained with DAPI

expression (Fig. 2b). Restoration of the WWOX expression by treatment with TSA and AZA did not cause morphological changes (Fig. 2c) but decreased cell proliferation activity in HSC-59 cells (Fig. 2d).

Tumor-suppressive effects of restoration of the *WWOX* gene in GC cells

We attempted to investigate the tumor suppressor effects of WWOX in HSC-59 cells by carrying the *WWOX* gene with adenoviral gene delivery (Fig. 3a). Since the Ad-WWOX was designed to co-express GFP when transduced into mammalian cells, over 95% of the infectivity of Ad-WWOX in the HSC-59 cells was observed by the detection of GFP signals under a fluorescence microscope 24 h post-infection (data not shown). Restoration of the *WWOX* gene increased the sub-G_1 population in an MOI-dependent manner, serving as an indicator of cell death (Fig. 3b); moreover, cell counts showed a significant inhibition of cell growth by Ad-WWOX infection in dose- and time-dependent manners (Fig. 3c, d).

Reduction of WWOX is a significant biomarker for the grade of malignancy of human GC tissues

The expression levels of WWOX protein in non-neoplastic gastric mucosa and 73 GC tissue samples were determined by immunohistochemistry. An abundant cytoplasmic WWOX expression was detected in normal gastric epithelium in the presence or absence of intestinal metaplasia; whereas, no significant expression was detected in fibroblasts, smooth muscle cells, endothelial cells, or inflammatory cells (Fig. 4a). In a total of 73 GC cases, high (++) and weak (+) levels of WWOX expressions were observed in 16 (22%) and 33 (45%) of the 73 GC cases, respectively. Loss of the WWOX expression was detected in 24 (33%) of

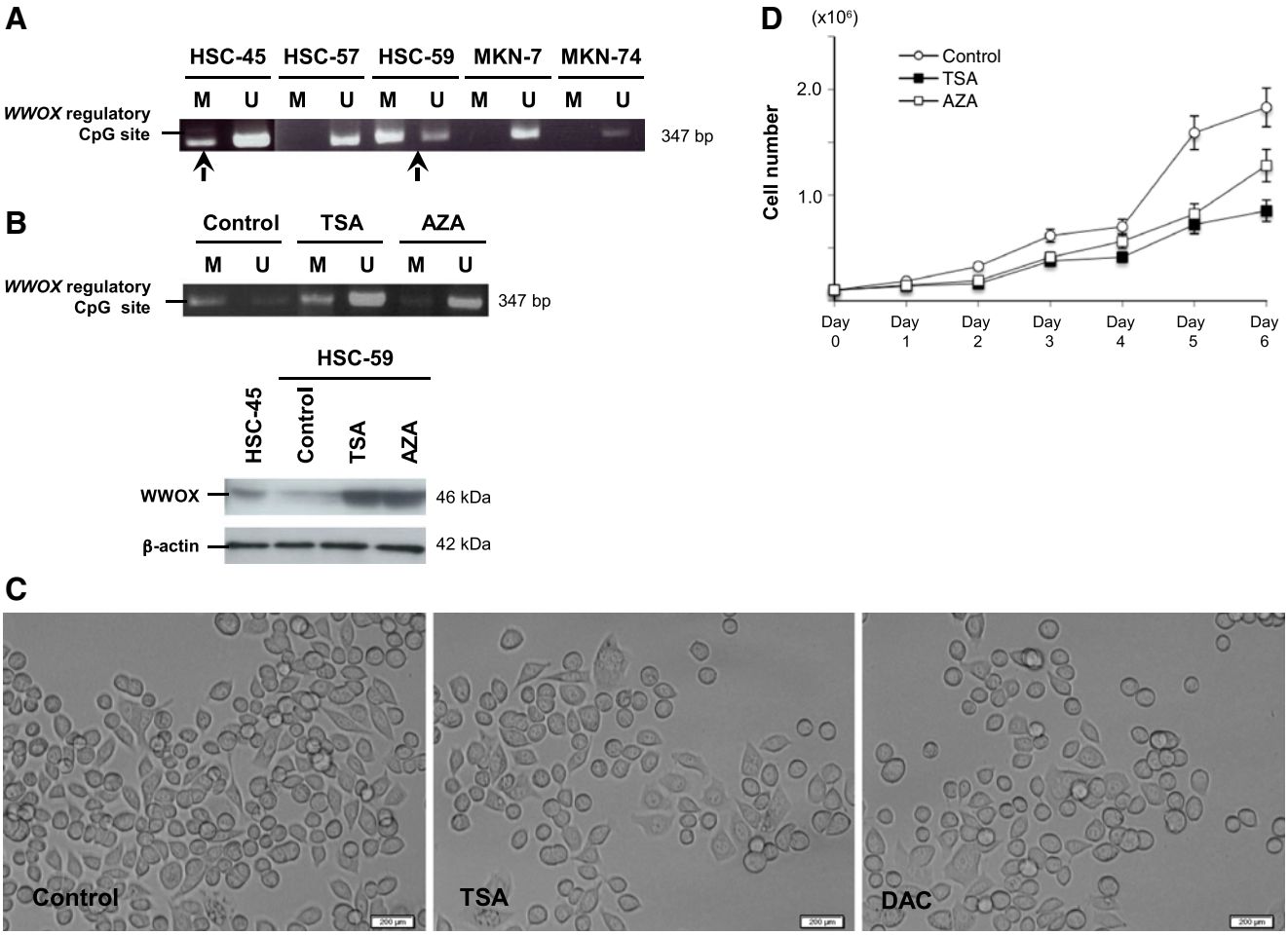

Fig. 2 Hypermethylation of the *WWOX* regulatory CpG site in GC cell lines and restoration of WWOX expression by treatment with deacetylating agent TSA and demethylating agent AZA. **a** The methylation status at the *WWOX* promoter region. *Arrows* indicate the methylation-specific bands. *M* methylated and *U* unmethylated. **b** Restoration of WWOX expression in HSC-59 cells at the protein levels. Treatment with TSA and AZA was performed as described in the text. β-Actin was used as a loading control. **c** Representative illustration of HSC-59 cells in the presence or absence of treatment with TSA and AZA (72 h). **e** Growth test in the HSC-59 cells after treatment with TSA and AZA

the GC cases examined, which was detected more frequently in the cases with poorly differentiated adenocarcinoma (P= 0.0001; Table 1). In addition, WWOX(−) GC cases showed significant correlations with the depth of invasion (P= 0.0004) and the incidence of lymph node metastasis (P= 0.0005). Furthermore, the frequency of the loss of WWOX expression in cases with vessel infiltration was statistically higher than that in cases without vessel infiltration (lymphatic vessels, P=0.0167 and venous vessels, P=0.0005), resulting in a correlation with a clinicopathologic stage (P= 0.001); however, the levels of WWOX expression showed no correlation with any other clinicopathologic features such as age, gender, or location of the tumor (data not shown). Although we investigated LOH at the WWOX locus (D16S3029, D16S3096, D16S504, and D16S518) in these GC cases, the incidence of LOH was detected only in one (8%) of 13 WWOX(−) GCs at D16S3029 (Fig. 4a). We also performed MSP to investigate the epigenetic backgrounds of the WWOX(−) GCs. Representative results are shown in Fig. 4b. Nine cases showed methylation-specific bands at the *WWOX* regulatory CpG site (Fig. 4b). Among 13 WWOX (−) GCs, seven (54%) cases were related to promoter methylation, which was detected in two (13%) GC cases with WWOX(+, ++) (P=0.0290; Table 2). There were no associations between the WWOX methylation status and other clinical variables (data not shown).

Finally, we performed a prognosis study to determine whether WWOX could be used as a biomolecular marker to monitor risks after curative surgery for primary GC. However, by Kaplan–Meier analysis, there was no statistical difference between WWOX(–) and WWOX (+, ++) GC cases despite the fact that patients with GC that were negative for WWOX immunoreactivity tended to have a worse prognosis (Fig. 5).

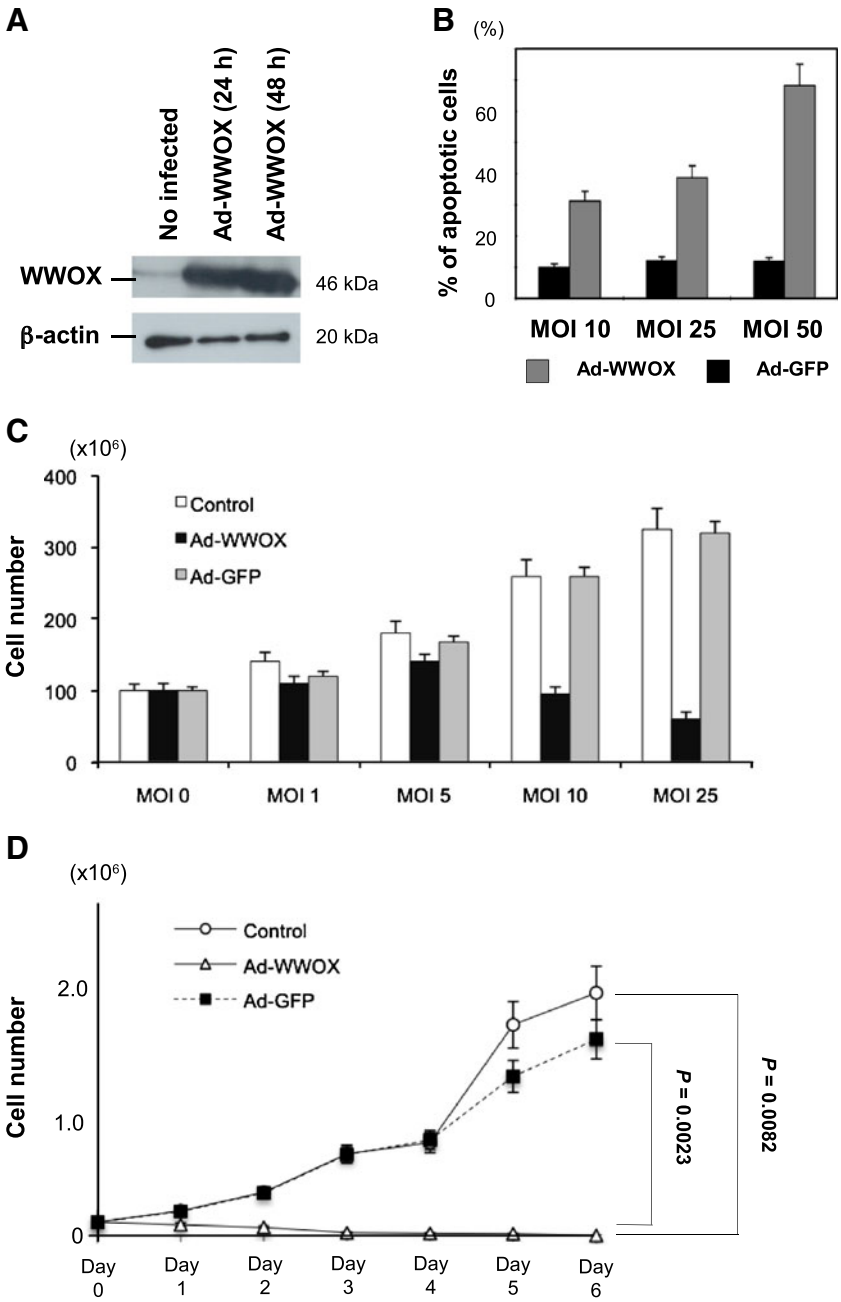

Fig. 3 Restoration of the *WWOX* gene effectively induces apoptosis and suppresses cell growth in HSC-59 cells. **a** Detection of recombinant WWOX protein by Western blot. The cells were infected with Ad-WWOX and Ad-GFP at an MOI of 25. β-Actin was used as a loading control. **b** Ad-WWOX induced apoptosis in an MOI-dependent manner. Forty-eight hours after infection of Ad-WWOX, the cells were collected for flow cytometric analysis. Ad-GFP was used as a negative control. **c**, **d** The growth-inhibitory effect of transduction of the recombinant *WWOX* gene (MOI 25)

Discussion

A very high frequency of LOH at the *WWOX* locus (*FRA16D*) has been documented in multiple types of human cancer [5, 10–12]. Another mechanism of reducing *WWOX* transcriptional levels that has been widely studied is the CpG island hypermethylation at the *WWOX* promoter and coding region. Iliopoulos et al. [23] studied on the methylation status of the *WWOX* promoter, exon 1 and part of intron 1, and revealed that methylation of 25–30% of the CpG islands in the *WWOX* regulatory site was basically enough to decrease WWOX protein expression levels. Nakayama et al. [24] reported that hypermethylation of the *WWOX* regulatory site was detected in WWOX-negative intraductal papillary-mucinous adenomas (33%) and intraductal papillary-mucinous carcinomas (53%) of the pancreas. Thus, hypermethylation may possibly play an important role in the suppression of WWOX expression. Our results show that the *WWOX* gene is inactivated in the majority of GCs and suggest that carcinogens could exert their carcinogenic potential on the gastric mucosa by affecting, directly or indirectly, the fragile region contained in the *WWOX* gene, thus causing breakage and/or deletion within this gene. Evidence of frequent reduction of the

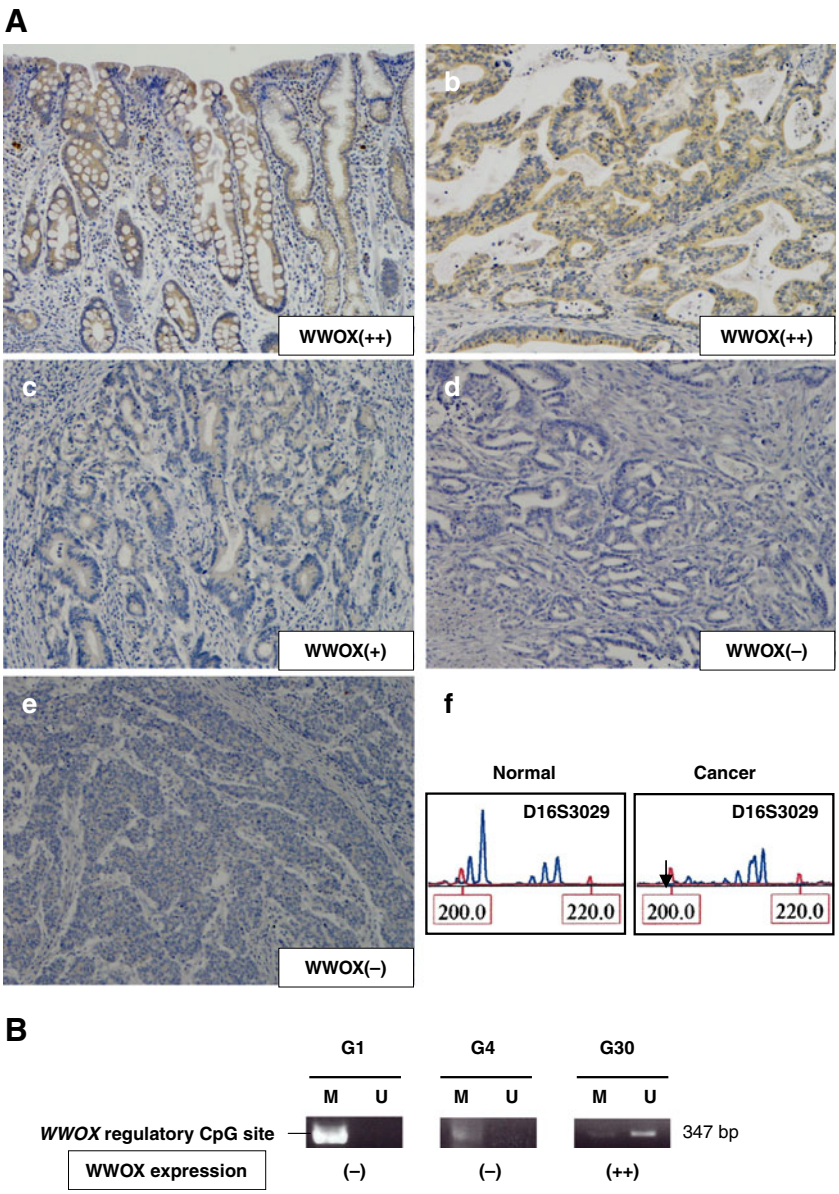

Fig. 4 Hypermethylation-mediated downregulation of WWOX expression in human GC cases. **a** Immunoreactivity against WWOX in normal gastric mucosa (*a*, ×200) and GCs (*b–e*, ×200). (*f*) Representative results of LOH analysis at D16S3029 in a WWOX(–) GC case. **b** MSP analysis in GC cases (G1, G4, and G30). The status of WWOX expression is also shown. *M* methylated and *U* unmethylated

WWOX expression by promoter hypermethylation and suppression of tumor growth by restoration of the *WWOX* gene strongly indicates that WWOX plays an important role in stomach carcinogenesis.

Since all cell lines analyzed in this study expressed low levels of WWOX in comparison with normal gastric mucosa, reduction of the WWOX expression is likely to be one of the common events in GC cells. In the previous report by Aqeilan et al. [16], LOH at the *WWOX* locus has documented to be responsible for the alteration of *WWOX* levels; nevertheless, we could not detect frequent LOH in these GC tissues. The discrepancy is probably due to the criterion of LOH. We decided LOH only when an allele peak signal from tumor DNA was reduced by *10%* compared with the normal counterpart to avoid overestimation. In the present study, we have demonstrated the significance of treatment with TSA and AZA for the restoration of the WWOX expression in HSC-59 cells (Fig. 2b), supporting the previous data that revealed promoter methylation as an important mechanism that downregulates the transcriptional activity of the *WWOX* gene [13, 15]; however, we could not find the methylation-mediated negative regulation of the *WWOX* gene in HSC-57, MKN-7, and MKN-74 cells (Fig. 2b). This may be due to other mechanisms that suppress WWOX expression in the process of GC. In addition to the genetic and epigenetic background of the *WWOX* gene, posttranscriptional regulation of the WWOX protein levels has been elucidated. Activated Cdc42-associated kinase (ACK1) has been identified as the WWOX-interacting protein, which phos-

Table 1 Correlation with the expression of WWOX and clinicopathological parameters

	WWOX expression			*P* value[a]
	(–) *n*=24 (33%)	(+) *n*=33 (45%)	(++) *n*=16 (22%)	
Histology[b]				
Wel (%)	1 (5)	5 (28)	12 (67)	0.0001*
Mod (%)	5 (16)	22 (71)	4 (13)	
Por (%)	18 (75)	6 (25)	0 (0)	
Depth of invasion[c]				
T1 (%)	0 (0)	14 (61)	9 (39)	0.0004*
T2 (%)	5 (26)	9 (48)	5 (26)	
T3 (%)	13 (59)	7 (32)	2 (9)	
T4 (%)	6 (67)	3 (33)	0 (0)	
Lymph node metastasis				
Positive (%)	22 (49)	18 (40)	5 (11)	0.0003*
Negative (%)	2 (7)	15 (54)	11 (39)	
Lymphatic vessels infiltration				
Positive (%)	23 (42)	22 (40)	10 (18)	0.0167*
Negative (%)	1 (6)	11 (61)	6 (33)	
Venous vessels infiltration				
Positive (%)	24 (46)	20 (39)	8 (15)	0.0005*
Negative (%)	0 (0)	13 (62)	8 (38)	
Clinicopathogic stage				
I (%)	0 (0)	14 (61)	9 (39)	0.001*
II (%)	1 (11)	5 (56)	3 (33)	
III (%)	9 (43)	10 (48)	2 (9)	
IV (%)	14 (70)	4 (20)	2 (10)	

[a] *P* values less than 0.05 were considered to be statistically significant

[b] Histological types were classified into three groups according to the Japanese classification of gastric carcinomas [20]: Wel, well-differentiated type including papillary (pap) and tubular adenocarcinoma (tub1); Mod, moderately differentiated type including tubular adenocarcinoma (tub2); Por, poorly differentiated adenocarcinoma including solid type (por1), non-solid type (por2) and signet-ring cell carcinoma (sig).

[c] Depth of invasion and clinicopathological stage were classified according to the TNM classification of the International Union Against Cancer

*P <0.05

phorylates WWOX and subsequently leads to rapid dissociation of the WWOX-ACK1 complex and WWOX polyubiquitination followed by degradation [25].

Our data highlights a pivotal role for the WWOX in suppressing cell proliferation and increasing the population of cells with sub-G_1 DNA contents in GC cells (Fig. 3). Taking together the evidence that WWOX functions to induce caspase-dependent apoptosis and suppress cell growth [13–15] and that all GC cell lines analyzed in this study show loss or genetic alteration of p53 (unpublished data), WWOX-mediated tumor suppression is thought to be independent of the p53 status. Also, knockdown or knockout experiments should have been done in normal gastric epithelial cells or in cells that express abundant endogenous WWOX in order to prove the specific function of WWOX as a tumor suppressor and the significance of WWOX reduction in patients with GC. In previous studies, silencing of WWOX by the RNA

Table 2 Correlation with the expression of WWOX and the methylation status at the *WWOX* regulatory CpG site

	WWOX expression status		*P* value[a]
	(–) *n*=13	(+, ++) *n*=14	
The methylation status			
Methylated (complete + partial)	7	2	0.0290*
Unmethylated	6	12	

[a] *P* values less than 0.05 were considered to be statistically significant

*P <0.05

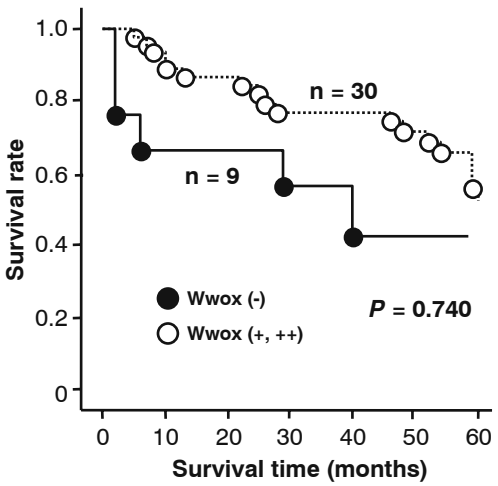

Fig. 5 Kaplan–Meier survival curves by the expression of WWOX in patients with GC

interference increased resistance to UV-induced apoptosis [26] and adhesiveness to fibronectin [27]. In addition, $Wwox^{-/-}$ develop osteosarcomas and $Wwox^{\pm/-}$ develop spontaneous lung papillary carcinomas, and when challenged with *N*-nitrosomethylbenzylamine (NMBA) carcinogen, $Wwox^{-/-}$ mice develop a higher incidence of forestomach tumors as compared to wild-type control mice [28, 29]. These findings support the tumor-suppressing effect of WWOX not only in tumorigenicity but also in resistance to various therapies and cell migration. Further investigation will be needed to clarify the other mechanism(s) by which WWOX expression levels can be downregulated in GC cells.

In a previous report, loss of WWOX protein expression was observed in 33% of GC cell lines and 65% of GC cases [3]. The data on GC cell lines were almost equivalent to the data in the present study (Fig. 1a, b); however, the incidence of loss of WWOX expression in GC cases was quite different. This may be caused by the difference of the specificity of each antibody and the criterion of WWOX immunoreactivity. Indeed, in this study, the sum of the frequencies of the lost and decreased WWOX expression was 78% [WWOX(–), 33% and WWOX(+), 45%], which was nearly equal to the previous results [16]. This, together with the finding that the loss of the WWOX expression is closely associated with several clinicopathologic parameters, including histology, depth of invasion, lymph node metastasis, vessel infiltration, and clinicopathologic stage (Table 1), WWOX expression is likely to be a good criterion for the diagnosis of the grade of malignancy of GCs, but not of the prognosis.

Acknowledgements This work was supported by a grant-in-aid for scientific research (C-19590347, C-20590341, and C-21590370) from the Japan Society for Promotion of Science.

Conflict of interest statement We declare that we have no conflict of interest.

References

1. Ohta M, Inoue H, Cotticelli MG et al (1996) The *FHIT* gene, spanning the chromosome 3p14.2 fragile site and renal carcinoma-associated t(3;8) breakpoint, is abnomal in digestive tract cancers. Cell 84:587–597
2. Huebner K, Croce CM (2003) Cancer and the *FRA3B/FHIT* fragile locus: it's a HIT. Br J Cancer 88:1501–1506
3. Bednarek AK, Laflin KJ, Daniel RL et al (2000) *WWOX*, a novel WW domain-containing protein mapping to human chromosome 16q23.3-24.1, a region frequently affected in breast cancer. Cancer Res 60:2140–2145
4. Aqeilan RI, Palamarchuk A, Weigel RJ et al (2004) Physical and functional interactions between the Wwox tumor suppressor protein and the AP-2γ transcription factor. Cancer Res 101:4401–4406
5. Aqeilan RI, Donati V, Palamarchuk A et al (2005) WW domain-containing proteins, WWOX and YAP, compete for interaction with ErbB-4 and modulate its transcriptional function. Cancer Res 65:6764–6772
6. Aqeilan RI, Pekarsky Y, Herrero JJ et al (2004) Functional association between Wwox tumor suppressor protein and p73, a p53 homolog. Proc Natl Acad Sci USA 101:4401–4406
7. Chang NS, Doherty J, Ensign A et al (2005) WOX1 is essential for tumor necrosis factor-UV, light-, staurosporine-, and p53-mediated cell death, and its tyrosine 33-phospholrylated form binds and stabilizes serine 46-phosphorylated p53. J Biol Chem 280:43100–43108
8. Paige AJ, Taylor KJ, Taylor C et al (2001) WWOX: a candidate tumor suppressor gene involved in multiple tumor types. Proc Natl Acad Sci USA 98:11417–11422
9. Driouch K, Prydz H, Monese R et al (2002) Alternative transcripts of the candidate tumor suppressor gene, WWOX, are expressed at high levels in human breast tumors. Oncogene 21:1832–1840
10. Kuroki T, Trapasso F, Shiraishi T et al (2002) Genetic alterations of the tumor suppressor gene WWOX in esophageal squamous cell carcinoma. Cancer Res 62:2258–2260
11. Yendamuri S, Kuroki T, Trapasso F et al (2003) WW domain containing oxidoreductase gene expression is altered in non-small cell lung cancer. Cancer Res 63:878–881
12. Kuroki T, Yendamuri S, Trapasso F et al (2004) The tumor suppressor gene *WWOX* at *FRA16D* is involved in pancreatic carcinogenesis. Clin Cancer Res 10:2459–2465
13. Nakayama S, Semba S, Maeda N et al (2008) Role of the *WWOX* gene, encompassing fragile region *FRA16D*, in suppression of pancreatic carcinoma cells. Cancer Sci 99:1370–1376
14. Fabbri M, Iliopoulos D, Trapasso F et al (2005) *WWOX* gene restration prevents lung cancer growth in vitro and in vivo. Proc Natl Acad Sci USA 102:15611–15616
15. Qin HR, Iliopoulos D, Semba S et al (2006) A role for the WWOX gene in prostete cancer. Cancer Res 66:6477–6481
16. Aqeilan RI, Kuroki T, Pekarsky Y et al (2004) Loss of WWOX expression in gastric carcinoma. Clin Cancer Res 10:3053–3058
17. Yanagihara K, Ito A, Toge T et al (1993) Antiproliferative effects of isoflavones on human cancer cell lines established from the gastrointestinal tract. Cancer Res 53:5815–5821
18. Yanagihara K, Seyama T, Tsumuraya M et al (1991) Establishment and characterization of human signet ring cell gastric carcinoma cell lines with amplification of the c-myc oncogene. Cancer Res 51:381–386
19. Hojo H (1977) Establishment of cultured cell lines of human stomach cancer—origin and their morphological characteristics. (in Japanese) Niigata Igakukai Zassi 91:737–752
20. Motoyama T, Hojo H, Watanabe H (1986) Comparison of seven cell lines derived from human gastric carcinomas. Acta Pathol Jpn 36:65–83
21. Japanse Gastric Cancer Association (2010) Japanese classification of gastric carcinoma, 14th edn. Kanehara Ltd, Tokyo
22. Watanabe A, Hippo Y, Taniguchi H et al (2003) An opposing view on WWOX protein function as a tumor suppressor. Cancer Res 63:8629–8633
23. Iliopoulos D, Guler G, Han SY et al (2005) Fragile genes as biomarkers: epigenetic control of *WWOX* and *FHIT* in lung, breast and bladder cancer. Oncogene 24:1625–1633
24. Nakayama S, Semba S, Maeda N et al (2009) Hypermethyaltion-mediated reduction of WWOX expression in intraductal papillary mucinous neoplasms of the pancreas. Br J Cancer 100:1438–1443
25. Mahajan NP, Whang TE, Mohler JL et al (2005) Activated tyrosine kinase Ack1 promotes prostate tumorigenesis: role of Ack1 in polyubiquitination of tumor suppressor Wwox. Cancer Res 65:10514–10523
26. Lai FJ, Cheng CL, Chen ST et al (2005) WOX1 is essential for UVB irradiation-induced apoptosis and down-regulated via translational

blockade in UVB-induced cutaneous squamous cell carcinoma in vivo. Clin Cancer Res 11:5769–5777
27. Gourley C, Paige AJW, Taylor KJ et al (2009) *WWOX* gene expression abolishes ovarian cancer tumorigenicity in vivo and decreases attachment to fibronectin via Integrin α_3. Cancer Res 69:4835–4842
28. Aqeilan RI, Trapasso F, Hussain S et al (2007) Targeted deletion of Wwox reveals a tumor suppressor function. Proc Natl Acad Sci USA 104:3949–3954
29. Aqeilan RI, Hagan JP, Aqeilan HA et al (2007) Inactivation of the *Wwox* gene accelerates forestomach tumor progression in vivo. Cancer Res 67:5606–5610

Virchows Arch (2010) 457:433–441
DOI 10.1007/s00428-010-0958-9

ORIGINAL ARTICLE

DNA methylation changes in ex-adenoma carcinoma of the large intestine

Hyeong-Ju Kwon · Jung Ho Kim · Jeong Mo Bae · Nam-Yun Cho · Tae-You Kim · Gyeong Hoon Kang

Received: 3 May 2010 / Revised: 20 July 2010 / Accepted: 31 July 2010 / Published online: 14 August 2010
© Springer-Verlag 2010

Abstract Ex-adenoma carcinoma (EAC) is a carcinoma with contiguous adenoma element in its vicinity which provides a morphological evidence for adenoma–carcinoma sequence. During multistep colorectal carcinogenesis, promoter CpG island hypermethylation has been known to increase in a stepwise manner whereas diffuse genomic hypomethylation has been known to be an early event and not progress. However, some controversies exist. EAC is a good model to study the timing of hypermethylation and hypomethylation changes during multistep carcinogenesis, which this study aimed to elucidate. We analyzed 39 cases of EAC for their methylation status in eight DNA methylation markers of CpG island methylator phenotype (CIMP) panel, ten CIMP-nonrelated, cancer-specific markers, and three repetitive DNA elements (*ALU*, *LINE-1*, and *SAT2*) using MethyLight assay or combined bisulfite restriction analysis. Twenty-two cases of cancers had contiguous tubulovillous adenomas and 17 cases had contiguous tubular adenomas. Regardless of CIMP markers or nonrelated markers, a significant increase in the number of methylated genes was found from normal mucosa to adenoma, whereas no increase was found from adenoma to carcinoma. Both *ALU* and *LINE-1* showed a significant decrease of methylation levels from normal mucosa to adenoma ($p<0.05$), but there is no difference between adenoma and cancer. However, *SAT2* methylation level exhibited a stepwise decrease from normal mucosa to adenoma to cancer. Our findings suggest that morphological progression from traditional adenoma to carcinoma does not appear to be accompanied by increases in promoter CpG island hypermethylation or repetitive DNA hypomethylation, except for *SAT2* hypomethylation which showed continuous progression during multistep carcinogenesis.

Keywords CpG island · Hypermethylation · DNA methylation changes · Ex-adenoma carcinoma

Electronic supplementary material The online version of this article (doi:10.1007/s00428-010-0958-9) contains supplementary material, which is available to authorized users.

H.J. Kwon and J.H. Kim contributed equally to this work.

H.-J. Kwon · J. H. Kim · J. M. Bae · G. H. Kang (✉)
Department of Pathology,
Seoul National University College of Medicine,
28 Yongon-dong, Chongno-gu,
Seoul 110-744, South Korea
e-mail: ghkang@snu.ac.kr

N.-Y. Cho · G. H. Kang
Laboratory of Epigenetics,
Cancer Research Institute and 2nd Stage Brain Korea,
Seoul National University College of Medicine,
Seoul, South Korea

T.-Y. Kim
Department of Internal Medicine,
Seoul National University College of Medicine,
Seoul, South Korea

Introduction

Colorectal cancer (CRC) is a heterogeneous disease entity on the aspect of molecular carcinogenesis [1, 2], and three different main molecular pathways are involved: chromosomal instability (CIN), microsatellite instability (MSI), and epigenetic instability pathways. CIN is the main pathway accounting for about 50–80% of CRCs, characterized by alterations in the structure and number of chromosomes and accompanying genetic mutations of oncogenes and tumor suppressor genes [2–4]. MSI is characterized by concordant frameshift mutations in microsatellites located within the coding exons and accounts for about 13% of CRCs. The third pathway, epigenetic instability pathway, is featured with

concurrent hypermethylation of multiple genes in their promoter CpG island loci and resultant inactivation of the genes. CpG island methylator phenotype (CIMP) refers to a subset of CRCs which occur through epigenetic instability pathway. MSI+ CRCs and CIMP+ CRCs overlap and are considered to be in an exclusive relationship with CIN+ CRCs [5, 6].

Promoter CpG island hypermethylation acts as an alternative to genetic mutations for the inactivation of tumor suppressor genes or tumor-related genes and is now recognized as an important mechanism in molecular carcinogenesis. Recent studies of CRCs have demonstrated that the number of genes inactivated by promoter CpG island hypermethylation is four-times higher than the number of genes undergoing genetic mutations [1, 7]. Generalized genomic hypomethylation is a common finding in human cancers, regardless of tissue type, and has been shown to be closely associated with genomic instability [8]. Repetitive DNA elements, including *ALU*, *LINE-1*, and *SAT2*, comprise about 45% of genomic DNAs, and their methylation levels have been known to correlate well with 5-methylcytosine content in the human genome [9].

Because most CRCs develop from traditional adenomatous polyps (tubular adenomas with or without villosity) and show morphological and genetic progression through an adenoma–carcinoma sequence [10–12], promoter CpG island hypermethylation, an important mechanism of colorectal carcinogenesis, was expected to be found in traditional adenomatous polyps, and some studies have demonstrated that CpG island hypermethylation occurs in adenomatous polyps [13–15]. In a previous study [16] in which we analyzed colon adenoma and CRC samples for their methylation status in 12 genes using methylation-specific PCR, we found that the number of genes methylated in colon adenoma samples was significantly higher than that of normal colon samples but significantly lower than that of CRC samples. This finding led us to believe that CpG island hypermethylation accumulates with progression of the lesion along the multistep colorectal carcinogenesis. However, our previous study has a problem in study sample collection: the collected CRC samples were heterogeneous on the aspect of molecular pathway and included not only CIN-positive CRCs but also CIMP-positive or MSI-positive CRCs, whereas the collected adenomas were traditional adenomatous polyps which occur through CIN pathway. Adenoma and carcinoma components of ex-adenoma carcinoma samples are of the same molecular pathway and thus ex-adenoma carcinoma samples provide a platform to test whether promoter CpG island hypermethylation accumulates with the progression of the lesion from adenoma to carcinoma.

The fact that CIN and CIMP lie in a mutually exclusive relationship does not mean that promoter CpG island hypermethylation does not occur and contribute to the tumor progression in CIMP-negative tumors because *MGMT* methylation is known to be tightly associated with C-to-T transition-type mutation of *KRAS* which is a frequent event in CIMP-negative CRCs and a considerable number of genes are inactivated by promoter CpG island hypermethylation in CIMP-negative CRCs [17]. A transgenic mouse experiment has demonstrated that an induction of *dnmt3b* overexpression caused hypermethylation of some genes and an increase in the number and size of adenomas in APC^{min} mice [18]. These findings suggest that genetic changes and epigenetic changes contribute to tumorigenesis through concert effects. However, information is limited regarding the timing of promoter CpG island hypermethylation in multistep colorectal carcinogenesis and whether promoter CpG island hypermethylation is a progressive event. In the present study, we analyzed 39 cases of ex-adenoma CRC (CRC with contiguous tubular or tubulovillous adenomas in the marginal portion of the same tumor lesion) for their methylation status in eight CIMP-specific markers [19] and ten cancer-specific markers using MethyLight technology and measured the methylation levels of the 18 markers in carcinoma, contiguous adenoma, and adjacent colon mucosa portions of the same patients. The ten markers (*APC*, *CHFR*, *DLC1*, *ITGA3*, *MGMT*, *RASSF1A*, *SCGB3A1*, *SEZ6L*, *SFRP1*, and *SFRP5*) were selected because they were methylated in a cancer-specific manner but did not show an association with CIMP in a preliminary study. Through determination of methylation status of CIMP-related markers and CIMP-nonrelated markers in normal mucosa, adenoma, and carcinoma components of ex-adenoma carcinoma samples, we aimed to elucidate whether a significant change of promoter CpG island hypermethylation is accompanied in the transformation of traditional adenoma to adenocarcinoma. We analyzed 30 cases of serrated polyps and 92 cases of CRC which did not show any identifiable contiguous adenoma, for their methylation status in the 18 markers in order to compare the methylation status of ex-adenoma carcinoma samples. In addition, we performed methylation analyses of repetitive DNA elements, including *ALU*, *LINE-1*, and *SAT2*, using combined bisulfite restriction analysis (COBRA) or MethyLight technology to elucidate the timing of hypomethylation events of repetitive DNA elements and to elucidate whether there is a marked change of repetitive DNA hypomethylation between adenoma stage and carcinoma stage.

Material and methods

Tissue samples

After reviewing the electronic medical records of CRC patients who underwent colonoscopic mucosal resection or

curative resection for CRCs in Seoul National University Hospital, Seoul, Korea from 2006 January to 2006 December, we found 42 cases of ex-adenoma CRC in which tumor glands invaded more than muscularis mucosae. Intramucosal adenocarcinoma with a contiguous adenoma was not included in the study material. Of 42 cases, 39 contiguous adenomas were traditional adenomas, whereas three adenoma cases were mixed serrated adenoma (n=2) and traditional serrated adenoma (n=1). These three serrated cases were excluded from the study. Through light microscopic examination, we marked tumor areas meeting two criteria (1) tumor cells are most dense and (2) a tumor area represents the main histology and differentiation of the tumor. As a control group for ex-adenoma carcinoma samples, we retrieved 30 cases of polypectomy specimen of serrated polyp (hyperplastic polyp (n=10), sessile serrated adenoma (n=10), and traditional serrated adenoma (n=10)) and a consecutive series of 92 cases of curatively resected CRC which did not show contiguous adenoma. Ten serial 10-μm-thick histological slides of formalin-fixed tumor and normal tissue blocks were used for manual microdissection. Clinicopathological features of these cases are summarized in Supplementary Table 1. The study was approved by the Institutional Board of Ethics Committee.

DNA extraction and bisulfite modification

After light microscopic examination of tissue slides, carcinoma, adenoma, and normal mucosa portions were marked cautiously to avoid the contamination of cancer tissues into adenoma tissues. Then manual microdissection was performed with knife blades, and the scraped tissues were collected into 1.5 mL micro tubes containing 50 μL tissue lysis buffer (0.5% Tween 20 (Sigma, St. Louis, MO), 100 mM of Tris–HCl buffer (pH 7.6), 1 mM of EDTA, and 20 μg of proteinase K (Sigma)). Samples were incubated at 55°C overnight. Proteinase K was then inactivated by incubating at 95°C for 10 min, and the extracted DNA was stored at −20°C until use. Bisulfite conversion was performed using the Zymo EZ DNA methylation kit (Zymo Research Co, Orange, CA) according to the manufacturer's protocol.

Hypermethylation and hypomethylation assays

After bisulfite conversion of the same amount of DNA solution, *ALU*-based MethyLight control reaction was done to quantify the number of input target DNA, and the threshold cycle values were confirmed to be comparable among DNA samples. MethyLight assay to measure DNA methylation of 18 individual genes was performed as previously [20]. Primers and probes specific for methylated DNA and used for MethyLight reactions are listed in Supplementary Table 2. The percentage of methylated reference (PMR) at a specific gene was calculated by dividing the *GENE*/*ALU* ratio of a sample by the *GENE*/*ALU* ratio of in vitro fully methylated placental DNA and multiplying by 100. Although there was no standard cutoff value for classifying methylated and unmethylated loci using DNA methylation analyses, a CpG island locus was considered methylated if the PMR value was >4 [21]. The methylation status in repetitive DNA elements was analyzed using MethyLight technology (for *SAT2*) or combined bisulfite restriction analysis (for *LINE-1* and *ALU*) as described [20, 22].

Statistics

All statistical analyses were conducted using SPSS software version 15.0 (SPSS, Inc., Chicago, IL, USA). The two-tailed Student's t test was used to evaluate the significance of the differences between two means. However, for the comparison of means on the same patients, the paired t test was used. All reported p values are two-sided, and p values of less than 0.05 were considered to indicate significance.

Results

Methylation analysis of eight CIMP markers in ex-adenoma carcinoma samples and control samples

We did MethyLight analysis of eight CIMP-specific markers on three-paired normal colon mucosa, adenoma, and cancer samples from 39 ex-adenoma carcinoma cases and determined PMR values for each sample and each CpG island locus (Fig. 1). Two loci, *NEUROG1* and *CDKN2A* (*p16*), were significantly methylated in colon adenoma samples at levels higher than those of adjacent normal colon mucosa samples ($p<0.05$, Fig. 2). Four loci, *CACNA1G*, *CRABP1*, *IGF2*, and *SOCS1*, showed higher methylation level in colon adenoma samples than in normal colon mucosa samples, but the difference was of marginal significance ($0.05<p$ value<0.066). The remaining three loci did not show any difference in the methylation levels between normal colon samples and paired adenoma samples. The remaining two loci did not show any difference in the methylation levels between normal colon samples and paired adenoma samples. No difference was found in the methylation levels of the examined eight CpG island loci between cancer samples and contiguous adenoma samples. The mean number of methylated loci (PMR>4) in adenoma samples was 0.9, higher than that of normal adjacent colon samples (0.2, p=0.001, paired t test), but similar to that of carcinoma samples (0.7, Fig. 3). Colon cancer samples did not show any difference in the number

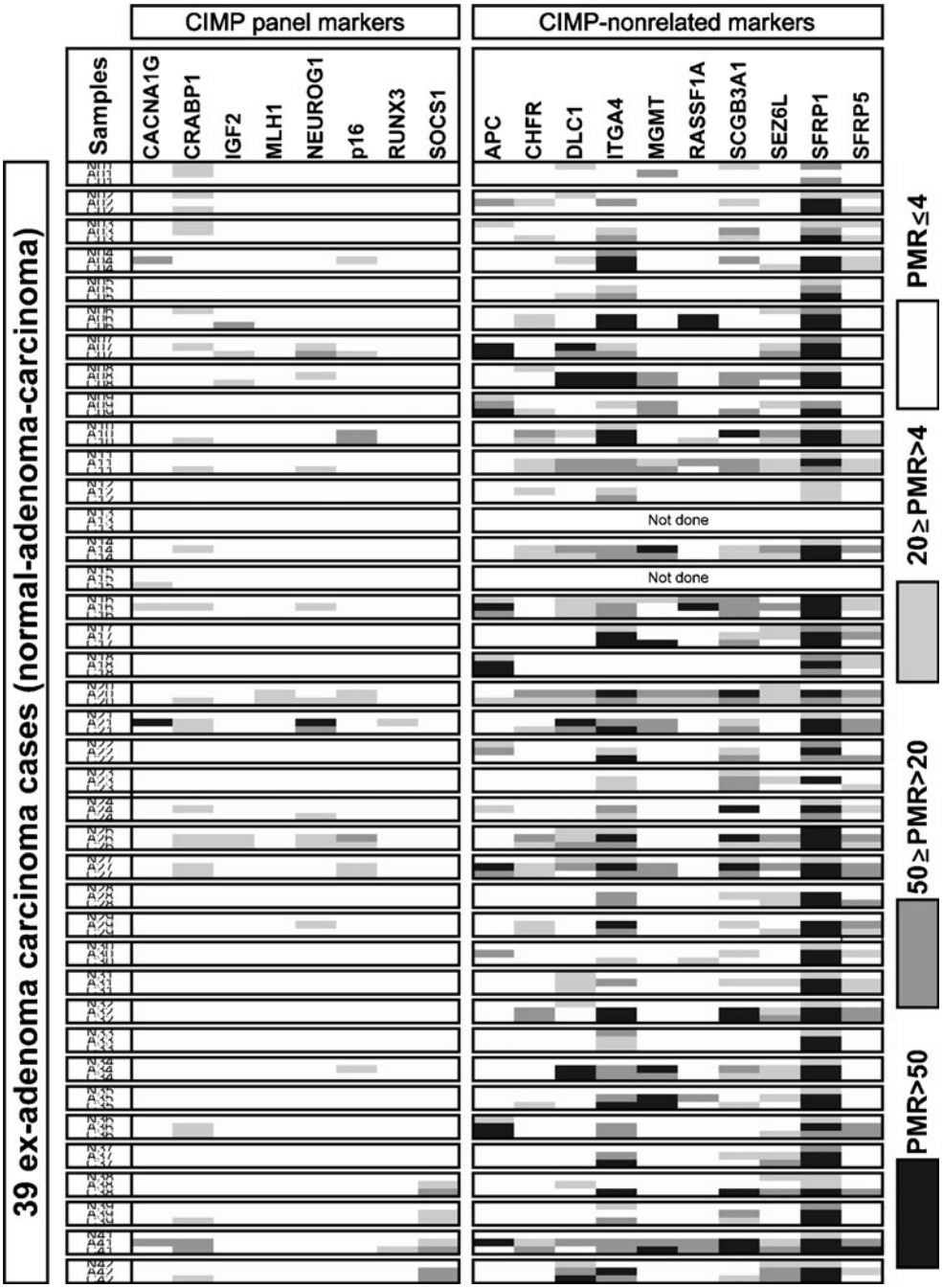

Fig. 1 Methylation map of eight CIMP markers and ten CIMP-nonrelated markers in 39 ex-adenoma carcinoma samples and paired normal samples. One outlined row consists of three rows in which paired normal mucosa–adenoma–carcinoma samples were arranged in *parallel* (*upper*, *middle*, and *lower row*, respectively)

of methylated genes with regards to AJCC cancer stage or tumor differentiation (Table 1). Contiguous adenoma samples did not exhibit any difference in the number of methylated genes in terms of dysplasia grade (low vs. high) or adenoma morphology (degree of villosity, Table 1). None of the contiguous adenoma or carcinoma samples were positive for CIMP which was defined as tumors with hypermethylation of five or more genes.

For the comparison of the methylation status of CIMP-specific genes between traditional adenomas and serrated polyps, we analyzed serrated polyps (hyperplastic polyp (n=10), sessile serrated adenoma (n=10), and traditional serrated adenoma (n=10)) for their methylation status in eight CIMP panel markers. We found that 60% of sessile serrated adenomas and 80% of traditional serrated adenomas were positive for CIMP, whereas 20% of hyperplastic polyps were positive for CIMP (Fig. 4). The mean number of methylated genes was 4.0, 4.8, and 2.0 for sessile serrated adenomas, traditional serrated adenomas, and hyperplastic polyps, respectively.

In order to identify whether CRCs without contiguous adenoma are heterogeneous in the aspect of CpG island

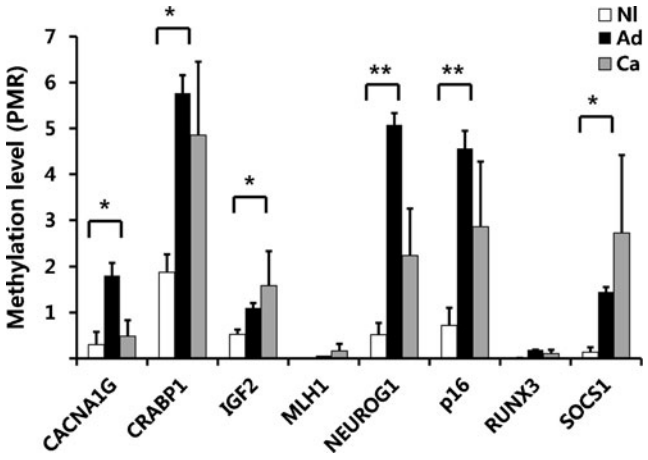

Fig. 2 Comparisons of methylation levels (PMR) of eight CIMP markers among individual components (normal–adenoma–carcinoma) of ex-adenoma carcinoma samples. *Double asterisks* indicate significant difference between normal and adenoma samples (p value <0.05) and *single asterisk* indicates marginally significant difference between normal and adenoma samples ($0.05<p$ value<0.065)

hypermethylation, we analyzed another set of CRCs without contiguous adenoma (n=92) for eight CIMP panel markers and compared the results with those of ex-adenoma carcinomas. In contrast to the fact that none of the ex-adenoma carcinoma samples were positive for CIMP, ten cases of CRCs without contiguous adenoma were positive for CIMP. The distribution of CRC cases without contiguous adenoma regarding the number of methylated genes was different from that of ex-adenoma carcinoma samples and showed somewhat bimodal pattern (Fig. 5). The number of methylated genes was 1.6, significantly higher in CRCs without contiguous adenoma than in carcinoma or adenoma components (0.7 and 0.9, respectively) of ex-adenoma carcinomas (p<0.02, Student t test).

Methylation analysis of CIMP-nonrelated markers in ex-adenoma carcinoma samples and control samples

In order to identify whether a different set of methylation markers will yield different results, we selected other ten cancer-specific methylation markers which did not show significant differences of methylation frequencies between CIMP-positive CRCs and CIMP-negative CRCs in a preliminary study. We performed MethyLight analysis of ten CpG island loci on three-paired normal colon mucosa, adenoma, and cancer samples from 39 ex-adenoma carcinoma cases (Fig. 1). All the individual CpG island loci showed significantly higher methylation levels in adenoma samples than in paired normal samples (p< 0.05, paired t test). However, there were no differences of the methylation levels in the individual CpG island loci between adenoma samples and paired carcinoma samples. The mean number of methylated loci was 2.3, 5.2, and 4.7 for normal mucosa, adenoma, and carcinoma samples, respectively (normal vs. adenoma, paired t test, p<0.001; adenoma vs. carcinoma, paired t test, p=0.056). Furthermore, no difference was found in the number of methylated loci between low stage (stages I and II) and high stage (stage III) carcinoma samples (4.5 vs. 5.5, p= 0.201) and between well-differentiated carcinoma and moderately differentiated carcinoma samples (4.3 vs. 4.9, p=0.387).

Methylation analysis of ten CIMP-nonrelated DNA methylation markers was performed in the control samples including serrated polyps and CRCs without contiguous adenoma. No difference was found in the number of methylated markers between adenocarcinomas without contiguous adenoma and adenoma or carcinoma components of ex-adenoma carcinomas (4.7 vs. 4.7 or 5.2, p=0.981 and p=0.218). No difference was noted in the number of methylated markers between adenoma component of ex-adenoma carcinomas and traditional serrated adenomas or sessile serrated adenomas (5.2 vs. 5.8 or 5.5, p=0.385 and p=0.677).

Hypomethylation changes of repetitive DNA elements

COBRA assays were performed to determine methylation levels of *ALU* and *LINE-1*, and MethyLight assay was done to measure methylation level of *SAT2*. Methylation levels of *SAT2* tended to decrease progressively along the multistep carcinogenesis (Fig. 6) and the differences between normal colon and adenoma and between cancer and contiguous adenoma were statistically significant (p<0.001 and p=0.023, paired t test). *ALU* and *LINE-1* methylation levels in adenoma samples were significantly lower than in adjacent normal mucosa samples, but similar

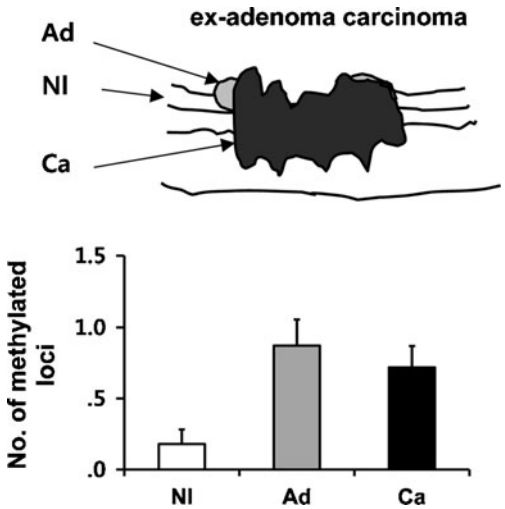

Fig. 3 Comparison of the number of methylated CIMP markers in individual components of ex-adenoma carcinoma samples. *Nl* normal mucosa, *Ad* adenoma, *Ca* carcinoma. *Error bar* indicates SEM

Table 1 Comparison of the number of methylated markers (CIMP markers) in carcinoma by cancer stage and comparison of the number of methylated markers in adenoma by dysplasia grade or villosity degree

		n	No. of genes methylated	SEM	*p* value
Cancer	Stage I	27	0.6	0.144	$p=0.153$
	Stage II	4	1.5	0.866	
	Stage III	8	0.9	0.350	
Cancer	Well	13	0.5	0.183	$p=0.235$
	Moderately	26	0.8	0.205	
	Poorly	0			
Adenoma	Low grade	21	1.0	0.253	$p=0.309$
	High grade	18	0.7	0.268	
Adenoma	Tubular	17	0.9	0.295	$p=0.758$
	Tubulovillous	19	0.8	0.248	
	Villous	3	1.3	0.881	

to the respective ones in cancer samples (Fig. 6). *ALU*, *LINE-1*, and *SAT2* did not show any difference in the methylation levels between low stage (I and II) and high stage (III) cancer samples.

Discussion

In the present study, we analyzed 39 ex-adenoma carcinoma cases for their methylation status in three repetitive DNA

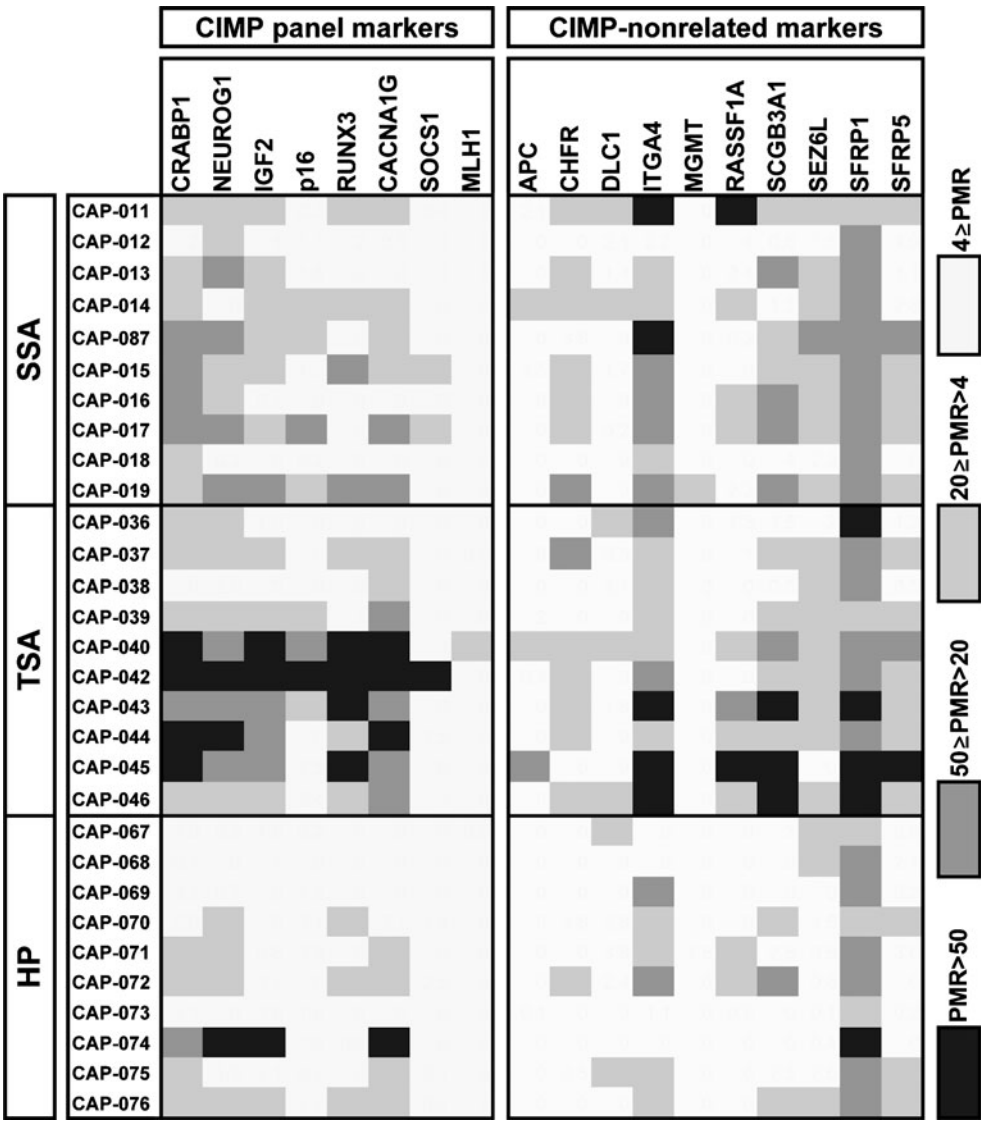

Fig. 4 MethyLight analysis results of eight CIMP-specific markers and ten CIMP-nonrelated markers in hyperplastic polyps (HP, $n=10$), traditional serrated adenomas (TSA, $n=10$), and sessile serrated adenomas (SSA, $n=10$)

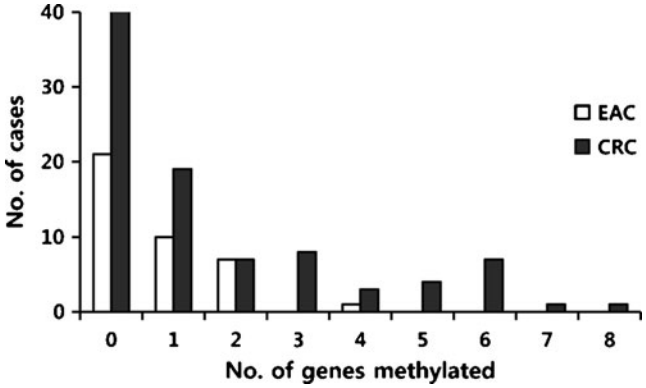

Fig. 5 A difference exists in the distribution of the number of methylated CIMP-specific markers between ex-adenoma carcinoma (*EAC*) and colorectal carcinoma without contiguous adenoma (*CRC*) samples. CpG island methylator phenotype (CIMP)-positive tumors (tumors with methylation at five or more CIMP markers) were noted in CRC samples, whereas no CIMP-positive tumor was present in ex-adenoma carcinoma samples

elements, eight CIMP panel markers, and ten CIMP-nonrelated, cancer-specific DNA methylation markers. Our findings suggest that neoplastic transformation from normal cells to traditional adenoma cells is accompanied by an increase in aberrant promoter CpG island hypermethylation but that further significant increase in promoter CpG island hypermethylation of CIMP-related genes or CIMP-nonrelated genes might not be accompanied in the malignant transformation of adenoma cells in the adenoma–carcinoma sequence and in the progression of cancer from lower TNM stage to higher TNM stage. This result is consistent with the findings of other researchers' studies [14, 23]: Hoon team performed quantitative methylation analysis of four *MINT* loci in 72 cases of ex-adenoma carcinoma of the colon and found no significant difference in the number of methylated *MINT* loci between adenoma and carcinoma samples [23]. Grady team conducted methylation-specific PCR analysis of eight CpG island loci in primary colon adenocarcinoma samples and liver metastasis samples and found no difference in the number of methylated CpG island loci between stages I–II and stages III–IV cancers and between primary colon cancers and matched liver metastases [14]. Our findings that neither adenoma components nor adenocarcinoma components of the ex-adenoma carcinoma cases were positive for CIMP and that no further significant increase of CpG island hypermethylation occurs in the malignant transformation and cancer progression suggest that CIMP-positive CRCs does not develop from traditional adenomas.

CIMP-positive CRCs, constituting about 15% of CRCs, are known to have characteristic clinicopathologic and molecular features, including female preponderance, older age at onset, proximal colon location, close association with MSI, and frequent *BRAF* mutation [2, 22, 24]. Recent studies suggested that serrated polyps, including traditional serrated adenoma, sessile serrated adenoma, and hyperplastic polyps, might be precursor lesions of CIMP-positive CRCs because they harbor concordant hypermethylation of multiple CpG island loci and high frequencies of *BRAF* mutation [25–28]. Our study also provided evidences, high frequencies of CIMP in serrated polyps but absence of CIMP in adenoma or carcinoma components of ex-adenoma carcinoma cases, supporting the relationship of serrated polyps with CIMP-positive CRCs. In addition, we analyzed *BRAF* mutation in serrated polyps and adenomatous polyps and found high frequencies of *BRAF* mutation in serrated polyps but no *BRAF* mutation in adenomatous polyps (data not shown). These results indicate that serrated polyps are more likely

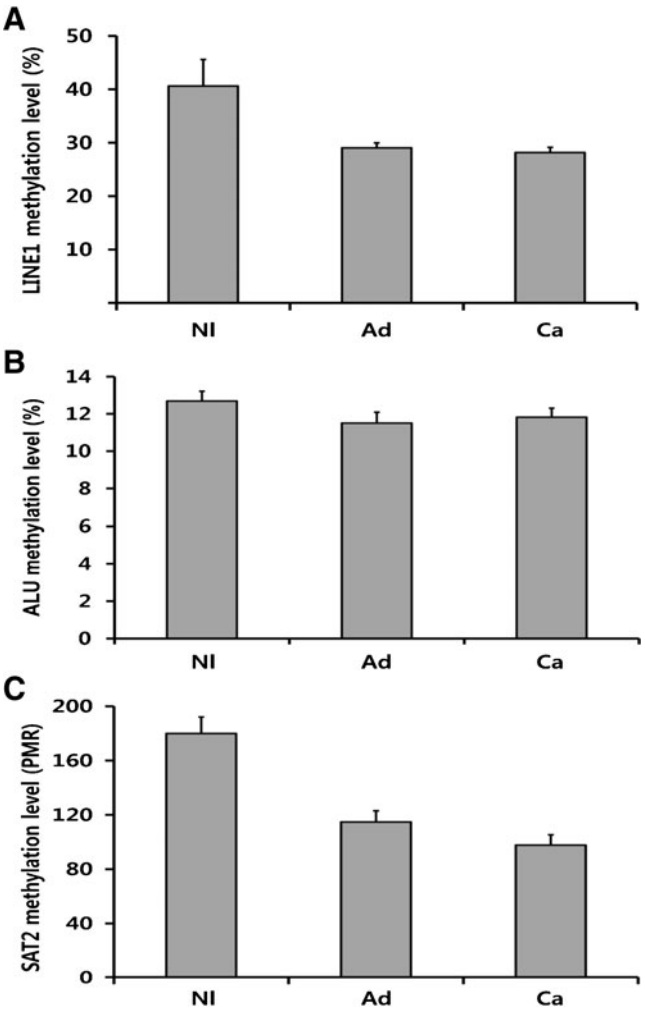

Fig. 6 Comparison of three repetitive DNA elements in three components (normal mucosa (*Nl*), adenoma (*Ad*), and carcinoma (*Ca*)) of ex-adenoma carcinoma samples. Three elements showed a significant decrease in their methylation levels from normal samples to adenoma samples. But there was no difference of *LINE1* and *ALU* methylation levels between adenoma and carcinoma samples. In contrast, *SAT2* showed a further decrease in its methylation levels from adenoma to carcinoma samples. *Error bar* indicates SEM

to be precursors of CIMP-positive CRCs. This association is further supported by the fact that CIMP-positive CRCs frequently show serrated appearances, indicating morphological continuum from serrated polyps [25, 28, 29].

DNA methylation changes occurring in cancer cells are characterized with focal promoter CpG island hypermethylation and diffuse genomic DNA hypomethylation. Epithelial malignancies which develop through multistep carcinogenesis have demonstrated a stepwise increase of CpG island hypermethylation and a stepwise decrease of methylation levels in repetitive DNA elements with the progression of the lesion along multistep carcinogenesis, including hepatocellular carcinoma [30], gastric cancer [31], prostate cancer [32], and extrahepatic cholangiocarcinoma [33]. In contrast with these malignancies, colorectal cancers in the present study showed neither further increase of promoter CpG island hypermethylation compared with those of colon adenomas nor further decrease of *LINE-1* and *ALU* methylation levels compared with those of colon adenomas. No difference of methylation levels in genomic DNA between CRCs and premalignant polyps has been shown by Bariol et al. [34]. However, in the present study, repetitive DNA elements showed different methylation behaviors depending on the type of repetitive DNA elements: no further decrease of methylation levels of *LINE-1* and *ALU* but further decrease of *SAT2* methylation levels from colon adenomas to CRCs. Because *LINE-1* and *ALU* are major components of repetitive DNA elements but *SAT2* is a minor element, changes in *SAT2* level might not be represented by the measurement of global methylation study.

The present study analyzed eight CIMP panel markers and ten CIMP-nonrelated cancer-specific DNA methylation markers for their methylation status in three components (normal mucosa, adenoma, and carcinoma samples) from ex-adenoma carcinoma samples. These two subsets of CpG island loci showed different methylation behaviors: CIMP panel markers were highly methylated in serrated polyps and rarely methylated in adenoma or carcinoma components of ex-adenoma carcinomas, whereas the ten CIMP-nonrelated markers were methylated at similar frequencies in both traditional or sessile serrated adenomas and traditional adenomas of ex-adenoma carcinomas. These results suggest that CIMP-related markers are selectively methylated in the epigenetic instability pathway (from serrated polyps to CIMP+ CRCs), whereas CIMP-nonrelated markers are commonly methylated regardless of the molecular pathways (epigenetic instability pathway or CIN pathway). However, because the selected 18 markers are not thought to represent the methylation behaviors of all the cancer-specific methylation markers, a large-scaled methylation marker study, e.g., Illumina Infinium methylation assay, will be needed to clarify the point that cancer-specific, promoter CpG island hypermethylation generally occur in the stage of adenoma and no further increases of promoter CpG island hypermethylation in adenocarcinomas developing through the CIN pathway. Another point to be considered is that adenoma components of ex-adenoma carcinoma are more likely to be genetically or epigenetically more advanced than conventional adenomas with no associated contiguous carcinoma. Thus, it is necessary to compare the number of methylated CIMP-nonrelated markers between early stage, small adenoma and late stage, large adenoma in order to identify whether there is a progressive increase of promoter CpG island hypermethylation in CIMP-nonrelated genes with progression of the adenomatous lesion.

In the present study, we did not analyze normal colon mucosa samples from tumor-free subjects for their methylation status. Several studies have demonstrated that cancer-specific DNA methylation markers are more frequently methylated in normal colon mucosa from adenoma or cancer patients than in normal colon mucosa from tumor-free subjects, indicating that colon tumor may arise in the background of colon mucosa with enhanced hypermethylation at cancer-specific DNA methylation markers [35–37]. In contrast to cancer-specific methylation markers, recent studies have indicated that aging-related DNA methylation markers tend to decrease in their methylation levels in normal colon mucosa from adenoma or cancer patients than in normal mucosa from tumor-free subjects [38, 39]. However, unlike hypomethylation in aging-related methylation markers, *LINE-1* hypomethylation has been demonstrated to be not associated with concomitant pathology [38, 40].

In conclusion, we have studied three tissue elements (normal mucosa, adenoma, and carcinoma) of ex-adenoma CRC samples for their methylation status in 18 CpG island loci (eight CIMP panel markers and ten CIMP-nonrelated markers) and three repetitive DNA elements. We found that CpG island hypermethylation was an early event but that no further increase of CpG island hypermethylation occurs from adenoma to carcinoma. Hypomethylation of *LINE-1* and *ALU* was found to occur in adenoma but did not progress after malignant transformation. In contrast, *SAT2* hypomethylation showed a continuous decrease from normal mucosa through adenoma to carcinoma.

Acknowledgments This study is supported by a grant of the Korea Healthcare Technology R&D Project, Ministry for Health, Welfare & Family Affairs, Republic of Korea (A091081), a grant from the Seoul National University Hospital Research Fund (30-2009-001-0), and a Priority Research Centers Program through the National Research Foundation of Korea (NRF) funded by the Ministry of Education, Science and Technology (2009-0093820).

Conflict of interests The authors declare that they have no conflict of interests.

References

1. Wood LD, Parsons DW, Jones S et al (2007) The genomic landscapes of human breast and colorectal cancers. Science 318:1108–1113
2. Ogino S, Shima K, Baba Y, et al. (2008) Colorectal cancer expression of PPARG (Peroxisome Proliferator-Activated Receptor-gamma) is associated with good prognosis gastroenterology
3. Jass JR (2007) Classification of colorectal cancer based on correlation of clinical, morphological and molecular features. Histopathology 50:113–130
4. Boland CR, Shin SK, Goel A (2009) Promoter methylation in the genesis of gastrointestinal cancer. Yonsei Med J 50:309–321
5. Goel A, Nagasaka T, Arnold CN et al (2007) The CpG island methylator phenotype and chromosomal instability are inversely correlated in sporadic colorectal cancer. Gastroenterology 132:127–138
6. Cheng YW, Pincas H, Bacolod MD et al (2008) CpG island methylator phenotype associates with low-degree chromosomal abnormalities in colorectal cancer. Clin Cancer Res 14:6005–6013
7. Schuebel KE, Chen W, Cope L et al (2007) Comparing the DNA hypermethylome with gene mutations in human colorectal cancer. PLoS Genet 3:1709–1723
8. Karpf AR, Matsui S (2005) Genetic disruption of cytosine DNA methyltransferase enzymes induces chromosomal instability in human cancer cells. Cancer Res 65:8635–8639
9. Weisenberger DJ, Campan M, Long TI et al (2005) Analysis of repetitive element DNA methylation by MethyLight. Nucleic Acids Res 33:6823–6836
10. Kinzler KW, Vogelstein B (1996) Lessons from hereditary colorectal cancer. Cell 87:159–170
11. Fearon ER, Dang CV (1999) Cancer genetics: tumor suppressor meets oncogene. Curr Biol 9:R62–R65
12. Chung DC (2000) The genetic basis of colorectal cancer: insights into critical pathways of tumorigenesis. Gastroenterology 119:854–865
13. Rashid A, Shen L, Morris JS, Issa JP, Hamilton SR (2001) CpG island methylation in colorectal adenomas. Am J Pathol 159:1129–1135
14. Kim YH, Petko Z, Dzieciatkowski S et al (2006) CpG island methylation of genes accumulates during the adenoma progression step of the multistep pathogenesis of colorectal cancer. Genes Chromosom Cancer 45:781–789
15. Kaz A, Kim YH, Dzieciatkowski S et al (2007) Evidence for the role of aberrant DNA methylation in the pathogenesis of Lynch syndrome adenomas. Int J Cancer 120:1922–1929
16. Lee S, Hwang KS, Lee HJ, Kim JS, Kang GH (2004) Aberrant CpG island hypermethylation of multiple genes in colorectal neoplasia. Lab Invest 84:884–893
17. Yagi K, Akagi K, Hayashi H et al (2010) Three DNA methylation epigenotypes in human colorectal cancer. Clin Cancer Res 16:21–33
18. Linhart HG, Lin H, Yamada Y et al (2007) Dnmt3b promotes tumorigenesis in vivo by gene-specific de novo methylation and transcriptional silencing. Genes Dev 21:3110–3122
19. Ogino S, Kawasaki T, Kirkner GJ et al (2007) Evaluation of markers for CpG island methylator phenotype (CIMP) in colorectal cancer by a large population-based sample. J Mol Diagn 9:305–314
20. Cho NY, Kim BH, Choi M et al (2007) Hypermethylation of CpG island loci and hypomethylation of LINE-1 and Alu repeats in prostate adenocarcinoma and their relationship to clinicopathological features. J Pathol 211:269–277
21. Ogino S, Kawasaki T, Brahmandam M et al (2006) Precision and performance characteristics of bisulfite conversion and real-time PCR (MethyLight) for quantitative DNA methylation analysis. J Mol Diagn 8:209–217
22. Weisenberger DJ, Siegmund KD, Campan M et al (2006) CpG island methylator phenotype underlies sporadic microsatellite instability and is tightly associated with BRAF mutation in colorectal cancer. Nat Genet 38:787–793
23. de Maat MF, Umetani N, Sunami E, Turner RR, Hoon DS (2007) Assessment of methylation events during colorectal tumor progression by absolute quantitative analysis of methylated alleles. Mol Cancer Res 5:461–471
24. Samowitz WS, Albertsen H, Herrick J et al (2005) Evaluation of a large, population-based sample supports a CpG island methylator phenotype in colon cancer. Gastroenterology 129:837–845
25. Jass JR, Baker K, Zlobec I et al (2006) Advanced colorectal polyps with the molecular and morphological features of serrated polyps and adenomas: concept of a 'fusion' pathway to colorectal cancer. Histopathology 49:121–131
26. Kambara T, Simms LA, Whitehall VL et al (2004) BRAF mutation is associated with DNA methylation in serrated polyps and cancers of the colorectum. Gut 53:1137–1144
27. Chan TL, Zhao W, Leung SY, Yuen ST (2003) BRAF and KRAS mutations in colorectal hyperplastic polyps and serrated adenomas. Cancer Res 63:4878–4881
28. O'Brien MJ, Yang S, Mack C et al (2006) Comparison of microsatellite instability, CpG island methylation phenotype, BRAF and KRAS status in serrated polyps and traditional adenomas indicates separate pathways to distinct colorectal carcinoma end points. Am J Surg Pathol 30:1491–1501
29. Jass JR (2005) Serrated adenoma of the colorectum and the DNA-methylator phenotype. Nat Clin Pract Oncol 2:398–405
30. Lee HS, Kim BH, Cho NY et al (2009) Prognostic implications of and relationship between CpG island hypermethylation and repetitive DNA hypomethylation in hepatocellular carcinoma. Clin Cancer Res 15:812–820
31. Cravo M, Pinto R, Fidalgo P et al (1996) Global DNA hypomethylation occurs in the early stages of intestinal type gastric carcinoma. Gut 39:434–438
32. Schulz WA, Hoffmann MJ (2009) Epigenetic mechanisms in the biology of prostate cancer. Semin Cancer Biol 19:172–180
33. Kim BH, Cho NY, Shin SH et al (2009) CpG island hypermethylation and repetitive DNA hypomethylation in premalignant lesion of extrahepatic cholangiocarcinoma. Virchows Arch 10:10
34. Bariol C, Suter C, Cheong K et al (2003) The relationship between hypomethylation and CpG island methylation in colorectal neoplasia. Am J Pathol 162:1361–1371
35. Ahlquist T, Lind GE, Costa VL et al (2008) Gene methylation profiles of normal mucosa, and benign and malignant colorectal tumors identify early onset markers. Mol Cancer 7:94
36. Paun BC, Kukuruga D, Jin Z, et al. (2010) Relation between normal rectal methylation, smoking status, and the presence or absence of colorectal adenomas. Cancer (in press)
37. Giovannucci E, Ogino S (2005) DNA methylation, field effects, and colorectal cancer. J Natl Cancer Inst 97:1317–1319
38. Worthley DL, Whitehall VL, Buttenshaw RL et al (2010) DNA methylation within the normal colorectal mucosa is associated with pathway-specific predisposition to cancer. Oncogene 29:1653–1662
39. Hiraoka S, Kato J, Horii J et al (2010) Methylation status of normal background mucosa is correlated with occurrence and development of neoplasia in the distal colon. Hum Pathol 41:38–47
40. Figueiredo JC, Grau MV, Wallace K et al (2009) Global DNA hypomethylation (LINE-1) in the normal colon and lifestyle characteristics and dietary and genetic factors. Cancer Epidemiol Biomark Prev 18:1041–1049

Virchows Arch (2010) 457:443–449
DOI 10.1007/s00428-010-0959-8

ORIGINAL ARTICLE

Mucin core protein expression in serrated polyps of the large intestine

Kohei Fujita · Minako Hirahashi · Hidetaka Yamamoto · Takayuki Matsumoto · Masaki Gushima · Yoshinao Oda · Junji Kishimoto · Takashi Yao · Mitsuo Iida · Masazumi Tsuneyoshi

Received: 5 May 2010 / Revised: 26 July 2010 / Accepted: 31 July 2010 / Published online: 28 August 2010
© Springer-Verlag 2010

Abstract Sessile serrated adenoma (SSA) has been proposed as a precursor to microsatellite-unstable colorectal carcinoma. However, histological criteria dictating how to differentiate serrated lesions have not been completely established, and a histological overlap exists between SSA and hyperplastic polyps (HPs), particularly the microvesicular type. In this study, based on a critical review of histology, we aimed to elucidate the potential utility of the mucin phenotype in the identification of SSA. We evaluated mucin core protein expression (MUC2, MUC5AC, and MUC6) by immunohistochemical stain in 65 cases of microvesicular-type HPs, 51 SSAs, and 72 traditional serrated adenomas (TSAs). SSAs had clinicopathological and morphological features distinct from those of HPs and TSAs. MUC6 was more frequently positive in SSAs (39%) than in TSAs (4%) and HPs (19%) ($P<0.001$ and $P=0.0107$, respectively). Right-sided HPs more frequently expressed MUC6 than did left-sided HPs (60% vs. 4%, respectively; $P<0.0001$), but SSAs and TSAs showed no regional differences. These findings suggest that determination of mucin core protein expression is insufficient for differentiating SSAs from other types of serrated polyps, and that microvesicular-type HPs of the right colon and SSAs may belong to the same mucin spectrum.

Keywords Sessile serrated adenoma · Hyperplastic polyp · Traditional serrated adenoma · MUC6

K. Fujita · M. Hirahashi (✉) · H. Yamamoto · M. Gushima · Y. Oda · M. Tsuneyoshi
Department of Anatomic Pathology,
Graduate School of Medical Sciences, Kyushu University,
3-1-1 Maidashi, Higashi-ku,
Fukuoka 812-8582, Japan
e-mail: mi-hira@surgpath.med.kyushu-u.ac.jp

K. Fujita · T. Matsumoto · M. Gushima · M. Iida
Department of Medicine and Clinical Science,
Graduate School of Medical Sciences, Kyushu University,
Fukuoka, Japan

J. Kishimoto
Department of Digital Medicine Initiative,
Graduate School of Medical Sciences, Kyushu University,
Fukuoka, Japan

T. Yao
Department of Human Pathology,
Juntendo University School of Medicine,
Tokyo, Japan

Introduction

Serrated polyps of the large intestine are composed of a heterogeneous group that includes hyperplastic polyps (HPs) and sessile serrated adenomas (SSAs), traditional serrated adenomas (TSAs), and mixed polyps [1]. HPs can be further classified into three subtypes based on the amount of mucin: microvesicular, goblet cell, and mucin-poor. Increasing evidence suggests that a certain proportion of colorectal cancers develop via the recently recognized "serrated polyp-neoplasia pathway," which differs from the conventional adenoma-carcinoma sequence caused by chromosomal instability. The presumed endpoint of this pathway is microsatellite-unstable carcinoma with DNA hypermethylation and BRAF mutations, predominantly in the right colon [2–4].

Clinically, SSAs tend to be sessile, right-sided in location, and large (>1 cm in maximum dimension). They are also frequently associated with BRAF mutations and abnormal DNA methylation [5–7]. SSAs are thus considered to be precursors of some populations of microsatellite instability high (MSI-H) colorectal carcinomas [1].

The distinction between SSA and other serrated polyps is clinically important because of their differences in clinicopathological and biological behaviors. According to a recent study, the incidence of subsequent colorectal cancers was significantly higher in patients with SSA (12.5%) than in those with HP (1.8%) [8]. However, the similarities in terminology and morphology of "serrated" polyps made it difficult to understand and diagnose SSA. In particular, a histological overlap exists between SSA and microvesicular-type HP. Although the disorganized architecture, extended proliferative zone, and subtle cellular atypia of SSA have been proposed to be distinctive features to separate HP, neither the diagnostic criteria nor specific marker for SSA has been completely established to date.

It has recently been reported that determination of the profile of mucin core proteins, such as MUC5AC, MUC2, and MUC6, is useful for diagnosing SSA [9, 10]. However, results should be carefully interpreted because there may be diagnostic and regional variation in the serrated polyps used in the previous literature. In this study, we performed a critical histological review of SSAs and morphological mimics, and elucidated the potential utility of mucin core protein expression to identify SSAs.

Materials and methods

Case selection

We retrospectively accumulated clinicopathologic data for 254 cases of serrated polyps that were polypectomized at our institution from 1993 to 2008. Cases in which the condition of the specimen was insufficient for a convincing diagnosis were excluded. Serrated polyps were defined as polypoid lesions of the large bowel, demonstrating a serrated or "saw-toothed" architecture due to infolding of the crypt epithelium. Clinical records of the patients were reviewed with regard to patient age, gender, clinical diagnosis, family history, and colonoscopic findings. Lesions with established diagnoses of familial adenomatous polyposis, hereditary non-polyposis colorectal carcinoma, inflammatory bowel disease, or hyperplastic/serrated polyposis syndrome as defined by the World Health Organization [11] were excluded from the analysis.

We reviewed histological specimens from all 254 cases and excluded 22 cases of mixed polyp and 44 cases of goblet cell type HP from the study (see below regarding HP sub-classification). A total of 65 cases of microvesicular HPs, 51 SSAs, and 72 TSAs were retrieved in this study. We evaluated the clinicopathological findings of these 188 polyps from 175 patients. The maximum diameter slice of each polyp was used for histology, and each polyp was categorized as large (≥10 mm) or small (<10 mm). Location was classified as the right colon (proximal to the splenic flexure) or left colon (distal to the splenic flexure). This study was approved by the Institutional Review Board of Kyushu University, Japan (no. 22–12).

Histologic diagnosis

Histologic findings of the serrated polyps were reviewed independently by two pathologists (K.F. and T.Y.) according to the following scheme.

Diagnosis of TSA was based on criteria established by Longacre and Fenoglio Preiser [12]. Briefly, TSA was defined as a neoplastic lesion with a serrated glandular pattern composed of atypical cells having elongated and/or pseudostratified nuclei and eosinophilic cytoplasm (Fig. 1a) [1].

SSA was defined as a lesion with irregularly dilated glands, serration at the bases of crypts, and horizontally and/or laterally branched crypt bases (Fig. 1b, c) [1, 5].

HP was defined as a lesion with the following characteristics: 1) no or little dysmaturational crypts, 2) crypt bases that were predominantly tapered, and 3) lower thirds of the crypts that were straight, narrow, and lined with proliferative cells. According to previous reports [5], we further classified HPs into three types based on the amount of mucin: microvesicular, goblet cell, and mucin-poor. All HPs used in this study were microvesicular; the most dilemmatic differential diagnosis seemed to be that between microvesicular-type HPs and SSAs (Fig. 1d) [13]. We compared the following histological features between SSAs and microvesicular HPs (Table 1) [5, 9, 13]: (1) horizontally and/or laterally branched crypts (upper crypts/lower crypts); (2) basal crypt dilation; (3) exaggerated luminal serration in the lower crypts; (4) increased mucin production; (5) superficial mitoses; (6) mild cytological atypia in the upper crypts, specifically characterized by enlarged vesicular nuclei with prominent nucleoli; and (7) increased epithelial-stromal ratio (>50%). In cases of disagreement regarding histological classification, the two observers reviewed the slice together until a common consensus was obtained.

Immunohistochemistry

Immunohistochemical staining was performed using monoclonal antibodies to MUC2 (NovoCastra, Newcastle-upon-Tyne, UK; diluted 1:200) as markers for goblet cells, to MUC5AC (NovoCastra; diluted 1:200) as markers for gastric foveolar differentiation, and to MUC6 (NovoCastra; diluted 1:200) as markers for gastric pyloric differentiation.

Sections were cut into thicknesses of 4 μm, deparaffinized in xylene, and dehydrated in descending dilutions of

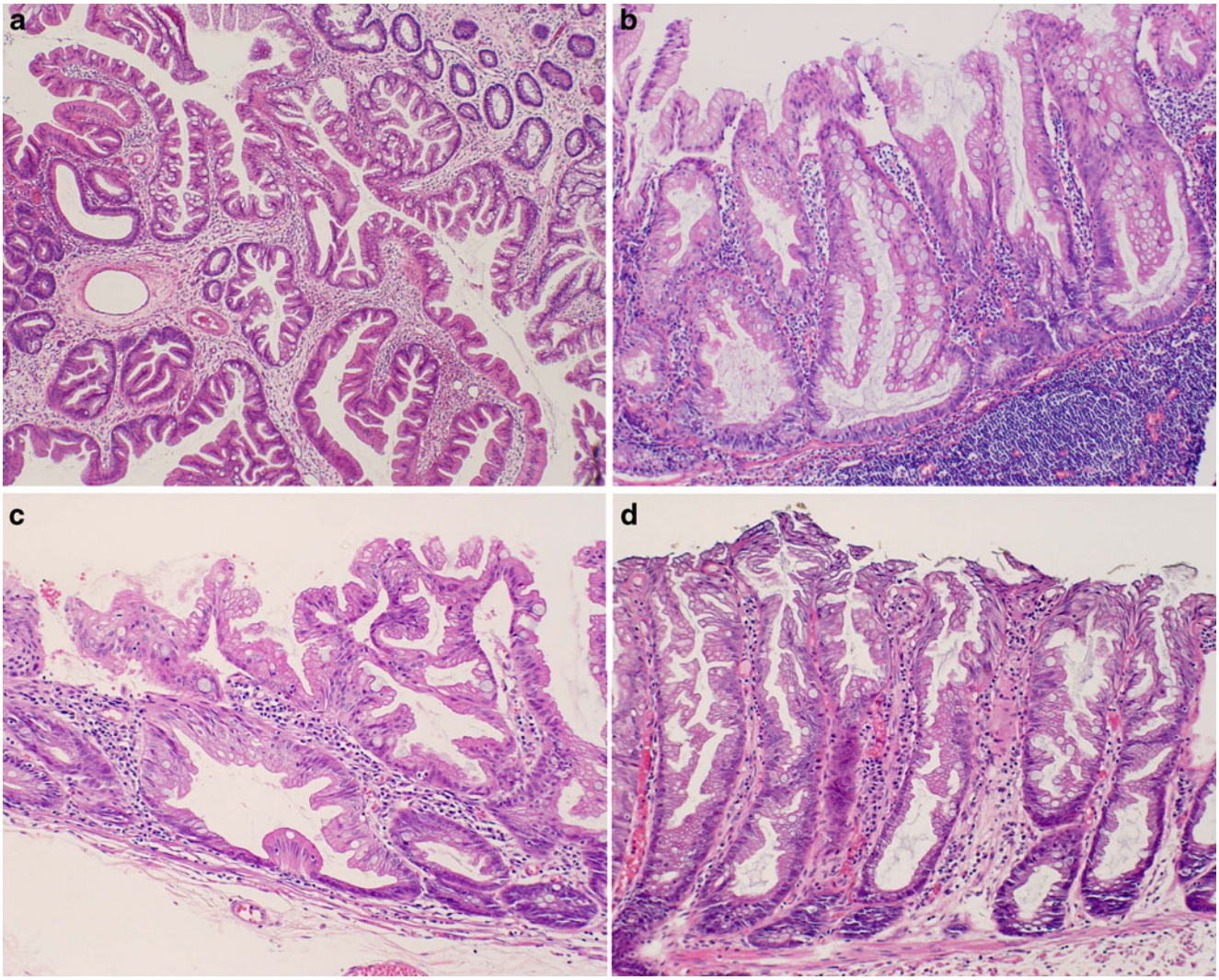

Fig. 1 Histological appearance of serrated polyps. Traditional serrated adenomas (TSAs) have serrated crypts lined by eosinophilic columnar cells with elongated nuclei (**a**). Sessile serrated adenomas (SSAs) contain dilated or laterally branched crypts without overt cytological atypia (**b**). Exaggerated luminal serration in the lower crypts is also seen in SSAs (**c**). Microvesicular-type hyperplastic polyps (HPs) have a simple crypt architecture with a narrowed base (**d**)

ethanol. For antigen retrieval, each slide was treated by microwave heating in a citrate buffer (pH 6.0) for 30 min (MUC2, MUC5AC, and MUC6). Endogenous peroxidase activity was blocked by 30 min of incubation with 0.3% hydrogen peroxidase in absolute methanol. Background staining was minimized by incubation with 1% normal rabbit serum for 10 min. Sections were incubated with a primary antibody overnight at 4°C, followed by testing with

Table 1 Morphological differences between hyperplastic polyps (HPs) and sessile serrated adenomas (SSAs)

	HPs (n=65)	SSAs (n=51)	P value
Horizontally and/or laterally branched crypts			
Upper crypts	13 (20.0%)	25 (49.0%)	0.0013
Lower crypts	0 (0%)	30 (60.8%)	<0.0001
Basal crypt dilation	2 (3.1%)	38 (74.5%)	<0.0001
Exaggerated luminal serration in the lower crypts	0 (0%)	35 (68.6%)	<0.0001
Increased mucin production	29 (44.6%)	39 (76.5%)	0.0006
Superficial mitoses	5 (7.7%)	14 (27.5%)	0.0055
Mild cytologic atypia in the upper crypts	12 (18.5%)	23 (45.1%)	0.0024
Increased epithelial/stromal ratio	43 (66.2%)	46 (90.2%)	0.0035

a streptavidin-biotin-peroxidase kit (Nichirei, Tokyo, Japan). Diaminobenzidine tetrahydrochloride was used as the chromogen. Finally, sections were counterstained with Mayer's hematoxylin.

The results of cytoplasmic staining for MUC2, MUC5AC, and MUC6 were scored to be sporadic (1+) when <5% of cells were positive, focal (2+) when 5–50% of cells were positive, and diffuse (3+) when >50% cells were positive. Immunoreactivity of 2+ or more was considered positive; otherwise, it was considered negative.

Statistical analysis

JMP Statistical Discovery Software (version 7.0.1 J; SAS Inc., Cary, NC, USA) was used for statistical analysis. Fisher's exact test was used to evaluate the association between two dichotomous variables. Student's t test was utilized to evaluate the differences in mean continuous variables (age and size). Each comparison was protected by the overall F test. Results were considered statistically significant if $p<0.05$.

Results

Clinicopathological findings

The distribution of polyps was as follows: 65 HPs (15 right-sided, 50 left-sided), 51 SSAs (39 right-sided, 12 left-sided), and 72 TSAs (13 right-sided, 59 left-sided). Clinicopathological features are summarized in Table 2. Patients with SSAs were older than those with HPs ($P=0.0068$). SSAs and TSAs were larger in size than HPs ($P<0.0001$), while the sizes of SSAs and TSAs did not differ significantly ($P=0.9454$). SSAs were more likely to be located in the right colon compared with HPs or TSAs ($P<0.0001$), and displayed a more sessile configuration compared with TSAs ($P<0.0001$).

Histological findings

Morphological differences between HPs and SSAs are summarized in Table 1. The distinction between HPs and SSAs was mainly based on the three major criteria for SSAs [14]: horizontally and/or laterally branched crypts, basal crypt dilation, and exaggerated luminal serration in the lower crypts ($P<0.001$, respectively). However, significant differences were also seen with regard to other factors, such as increased mucin production, superficial mitoses, cytologic atypia in the upper crypts, and a relatively high epithelial/stromal ratio of cells ($P=0.0006$, $P=0.005$, $P=0.0024$, and $P=0.0035$, respectively).

Immunohistochemical findings of MUC6, MUC5AC, and MUC2

Immunohistochemical results are indicated in Table 3. Eleven HPs (16.9%), 20 SSAs (39.2%), and 3 TSAs (4.2%) were positive for MUC6. The positive rate of MUC6 in SSAs was significantly higher than that in HPs or TSAs ($P=0.0107$ and $P<0.0001$, respectively), and HPs showed a higher frequency of MUC6 expression than did TSAs ($P=0.0215$). The typical expression pattern of MUC6 was immunoreactivity in the cytoplasm of the crypt-lining cells at the crypt bases in HPs, SSAs, and TSAs (Fig. 2). In SSAs, MUC6 was expressed not only in the basal portion of dilated or laterally branched crypts, but also in the basal portion of regular or straight crypts.

MUC5AC was detected within the cytoplasm of both goblet-like and non-goblet-like cells. MUC5AC was expressed throughout the entire length of the crypts in HPs and in SSAs, but MUC5AC expression tended to be decreased at the basal portion of the crypts in the TSAs even when other portions of the crypts were immunoreactive for MUC5AC. The incidence of MUC5AC expression was 75.4% (49/65) in HPs, 80.4% (41/51) in SSAs, and 43.1% (31/72) in TSAs. SSAs and HPs each showed significantly higher positive rates for MUC5AC than did TSAs ($P<0.0001$ and $P=0.0001$, respectively).

All serrated polyps diffusely exhibited MUC2 expression throughout the entire length of the crypt-lining cells, with similar staining intensities and distribution patterns.

Correlation between tumor location and pathological findings

No significant regional differences in clinicopathological findings were observed in HPs, SSAs, or TSAs (Table 4). HPs in the right side of the colon showed more frequent MUC6 expression than did those in the left side (9/15, 60.0% vs. 2/50, 4.0%; $P<0.0001$), but SSAs and TSAs showed no regional differences in MUC6 expression. As for MUC5AC and MUC2, no such regional differences were observed in HPs, SSAs, or and TSAs.

Discussion

In 2005, a panel of authorities provided a conceptual framework for the diagnosis of SSAs [1]. In that framework, "architectural dysplasia" rather than "cytological dysplasia" was the hallmark for the diagnosis of SSA. The significant features distinguishing SSAs from HPs are horizontally and/or laterally branched crypts, basal crypt dilation, exaggerated luminal serration in the lower crypts, increased mucin production, superficial mitoses, cytological

Table 2 Clinical features of serrated polyps

	HP (n=65)	SSA (n=51)	TSA (n=72)	P value (HP vs SSA)	P value (SSA vs TSA)	P value (TSA vs HP)
Age (years, means±SD)	56.9±11.2	62.6±10.2	59.6±11.7	0.0068	0.1468	0.1581
Gender (male/female)	57/8	36/15	41/31	0.0335	0.1350	<0.0001
Polyp size (mm, means±SD)	7.2±3.9	10.8±5.6	10.7±4.1	<0.0001	0.9454	<0.0001
Location (right/left)	15/50	39/12	13/59	<0.0001	<0.0001	0.5277
Gross appearance (protruded/sessile)	29/36	13/38	50/22	0.0510	<0.0001	0.0054

HP hyperplastic polyp, *SSA* sessile serrated adenoma, *TSA* traditional serrated adenoma

atypia in the upper crypts, and an increased epithelial-to-stromal ratio [5, 9, 13]. In the present study, we diagnosed SSAs and HPs on the basis of these morphological features. As a result, we showed differences in size and location of SSAs and HPs, as well as a difference in gender [5, 7, 9, 15]. The clinicopathologic features of serrated polyps found in our investigation were compatible with those reported previously.

In this study, we examined the possible role or utility of the mucin phenotype in the differential diagnosis of serrated polyps. The expression of MUC5AC and MUC6 was lower in TSAs than in HPs or SSAs, but there was no such difference between HPs and SSAs. Therefore, the mucin phenotype may be useful in distinguishing TSAs from HPs and SSAs. In addition, TSAs can be considered as an independent category of serrated polyps in terms of MUC6 and MUC5AC expressions.

Several studies have shown that the positive rate of MUC6 expression was higher in SSAs than in HPs [10, 16–18]. According to these reports, MUC6 expression was positive in 20–100% of SSAs and in 0–27% of HPs. In our study, MUC6 expression was observed in about 40% of SSAs and 17% of HPs.

The controversial results of MUC6 expression are assumed to be due in part to diagnostic variation in serrated polyps. Although in most previous studies on MUC6 [10, 16–18], as well as in the current study, a diagnostic approach similar to that proposed by Snover et al. [1, 5] was adapted to identify SSAs; however, convincing diagnostic criteria of SSAs have not been completely established. Alternatively, interpretation of SSA characteristics may be somewhat variable among pathologists. In fact, as noted in Table 1, several histologic factors can be commonly observed between microvesicular HPs and SSAs. This result is consistent with a previous report by Chung et al. [13].

Another possible reason for the relatively high prevalence of MUC6 expression in our series of HPs may be that only microvesicular-type HPs were included. In contrast, in most previous studies, the detail of sub-classification of HPs has not been described [10, 16–18].

The positive rate of MUC6 may also be influenced by the site of the lesion. The expression of MUC6 was significantly higher in right-sided HPs than in left-sided HPs in our series (see below). In contrast, in most previous reports, only limited numbers of right-sided HPs were included; thus, regional differences in the mucin phenotype of HP were not evaluated well [10, 16, 18]. Our observations suggest that HPs and SSAs, particularly in the right-sided colon, cannot be distinguished from each other by MUC6 immunostaining alone.

Bartley et al. recently reported that MUC6 expression in SSAs is associated with a proximal location [17]. In our study, MUC6 expression in SSAs did not differ based on the site of the lesion, whereas there was a trend toward similar mucin expression in right-sided colonic HPs and SSAs. Based on these observations, it can be assumed that right-sided HPs and SSAs represent a spectrum of serrated polyps that share similar mucin phenotypes. Although the molecular mechanism for aberrant expression of MUC6 in right-sided HP remains unclear, Kim et al. reported that HP in the proximal colon showed more frequent CpG island methylation of RASSF2, p16, MINT1, HIC1, and MLH1 when compared with those in the distal colon; however, no such difference was found in SSAs, TSAs, or tubular adenomas [19]. The authors also reported that right-sided

Table 3 Immunohistochemical staining results in serrated polyps

	HP (n=65)	SSA (n=51)	TSA (n=72)	P value (HP vs SSA)	P value (SSA vs TSA)	P value (TSA vs HP)
MUC6	11 (16.9%)	20 (39.2%)	3 (4.2%)	0.0107	<0.0001	0.0215
MUC5AC	49 (75.4%)	41(80.4%)	31 (43.1%)	0.6546	<0.0001	0.0001
MUC2	65 (100%)	51 (100%)	72 (100%)	1.000	1.000	1.000

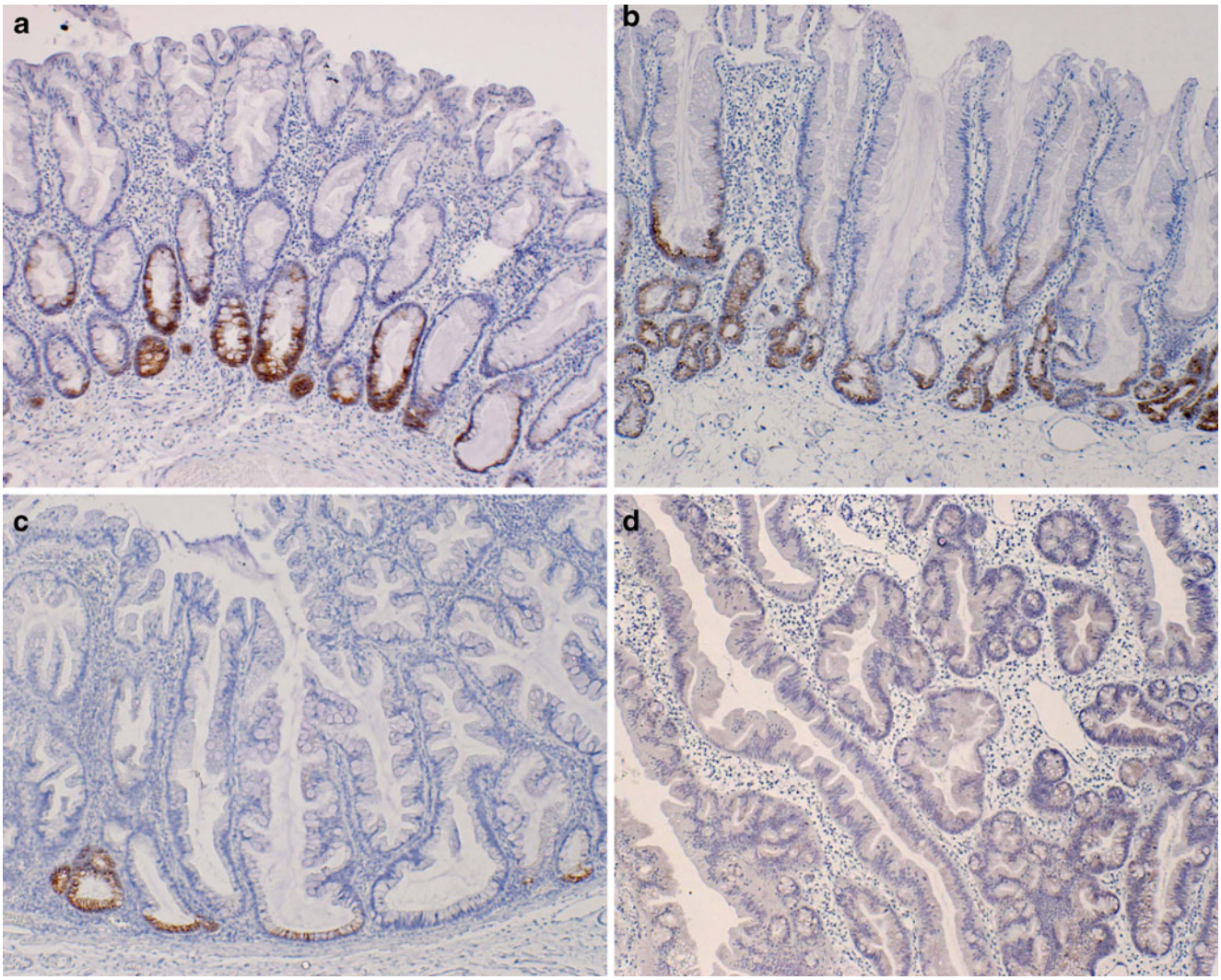

Fig. 2 Immunohistochemical staining for MUC6. MUC6 is expressed at the crypt bases in HPs (**a**) and SSAs (**b**). In this area of SSA, MUC6 is predominantly expressed at the bases of straight crypts rather than at the bases of dilated or laterally branched crypts (**c**). Negative stain for MUC6 in TSAs is noted (**d**)

Table 4 Comparison of right-sided and left-sided serrated polyps

Polyp type	HP (n=65)		P value	SSA (n=51)		P value	TSA (n=72)		P value
Location	Rt. (n=15)	Lt. (n=50)		Rt. (n=39)	Lt. (n=12)		Rt. (n=13)	Lt. (n=59)	
Age (years, means±SD)	59.4±10.0	56.1±11.5	0.3155	63.3±10.3	60.0±9.9	0.3816	60.0±11.9	59.5±11.7	0.8780
Gender (male/female)	13/2	44/6	1.000	27/12	9/3	1.000	6/7	35/24	0.5376
Polyp size (mm, means±SD)	7.2±4.1	7.2±3.9	1.000	11.4±6.0	8.6±3.3	0.0555	11.3±3.5	10.6±4.3	0.5950
Gross appearance (protruded/sessile)	4/11	25/25	0.1442	10/29	3/9	1.000	6/7	44/15	0.0923
MUC6	9 (60.0%)	2 (4.0%)	<0.0001	17 (43.6%)	3 (25%)	0.3227	1 (7.7%)	2 (3.4%)	0.4549
MUC5AC	14 (93.3%)	35 (70.0%)	0.0908	31 (79.5%)	10 (83.3%)	1.000	4 (30.8%)	27 (45.8%)	0.3709
MUC2	15 (100%)	50 (100%)	1.000	39 (100%)	12 (100%)	1.000	13 (100%)	59 (100%)	1.000

HPs and SSAs showed similar methylation status and prevalence of BRAF mutation. These findings, as well as the mucin expression profile, may also support the idea that right- and left-sided HPs differ biologically, and that the former may be more closely related to SSAs than previously anticipated.

In summary, our present investigation indicated that the type of serrated polyp cannot be determined by mucin profiles alone. We also found that SSAs and HPs in the right colon share a similar mucin phenotype, suggesting that these lesions may represent a continuous spectrum of right-sided serrated polyps. Further identification of additional molecular or immunohistochemical markers to predict the cancer risk of serrated polyps is needed.

Acknowledgments The authors thank Ms Y. Nozuka for technical assistance. The English in this manuscript was edited by Edanz.

Conflict of interest statement We declare that we have no conflict of interest.

References

1. Snover DC, Jass JR, Fenoglio-Preiser C, Batts KP (2005) Serrated polyps of the large intestine: a morphologic and molecular review of an evolving concept. Am J Clin Pathol 124:380–391
2. Kambara T, Simms LA, Whitehall VL, Spring KJ, Wynter CV, Walsh MD, Barker MA, Arnold S, McGivern A, Matsubara N, Tanaka N, Higuchi T, Young J, Jass JR, Leggett BA (2004) BRAF mutation is associated with DNA methylation in serrated polyps and cancers of the colorectum. Gut 53:1137–1144
3. Yang S, Farraye FA, Mack C, Posnik O, O'Brien MJ (2004) BRAF and KRAS Mutations in hyperplastic polyps and serrated adenomas of the colorectum: relationship to histology and CpG island methylation status. Am J Surg Pathol 28:1452–1459
4. O'Brien MJ, Yang S, Mack C, Xu H, Huang CS, Mulcahy E, Amorosino M, Farraye FA (2006) Comparison of microsatellite instability, CpG island methylation phenotype, BRAF and KRAS status in serrated polyps and traditional adenomas indicates separate pathways to distinct colorectal carcinoma end points. Am J Surg Pathol 30:1491–1501
5. Torlakovic E, Skovlund E, Snover DC, Torlakovic G, Nesland JM (2003) Morphologic reappraisal of serrated colorectal polyps. Am J Surg Pathol 27:65–81
6. Goldstein NS, Bhanot P, Odish E, Hunter S (2003) Hyperplastic-like colon polyps that preceded microsatellite-unstable adenocarcinomas. Am J Clin Pathol 119:778–796
7. Sandmeier D, Seelentag W, Bouzourene H (2007) Serrated polyps of the colorectum: is sessile serrated adenoma distinguishable from hyperplastic polyp in a daily practice? Virchows Arch 450:613–618
8. Lu FI, van de Niekerk W, Owen D, Tha SP, Turbin DA, Webber DL (2010) Longitudinal outcome study of sessile serrated adenomas of the colorectum: an increased risk for subsequent right-sided colorectal carcinoma. Am J Surg Pathol 34:927–934
9. Higuchi T, Sugihara K, Jass JR (2005) Demographic and pathological characteristics of serrated polyps of colorectum. Histopathology 47:32–40
10. Owens SR, Chiosea SI, Kuan SF (2008) Selective expression of gastric mucin MUC6 in colonic sessile serrated adenoma but not in hyperplastic polyp aids in morphological diagnosis of serrated polyps. Mod Pathol 21:660–669
11. Burt R, Jass JR (2000) Hyperplastic polyposis. In: Hamilton SR, Aaltonen LA et al (eds) Pathology and genetics of tumours of the digestive system. World Health Organization Classification of Tumours, vol. 2. IARC Press, Lyon France, p 135
12. Longacre TA, Fenoglio-Preiser CM (1990) Mixed hyperplastic adenomatous polyps/serrated adenomas. A distinct form of colorectal neoplasia. Am J Surg Pathol 14:524–537
13. Chung SM, Chen YT, Panczykowski A, Schamberg N, Klimstra DS, Yantiss RK (2008) Serrated polyps with "intermediate features" of sessile serrated polyp and microvesicular hyperplastic polyp: a practical approach to the classification of nondysplastic serrated polyps. Am J Surg Pathol 32:407–412
14. Farris AB, Misdraji J, Srivastava A, Muzikansky A, Deshpande V, Lauwers GY, Mino-Kenudson M (2008) Sessile serrated adenoma: challenging discrimination from other serrated colonic polyps. Am J Surg Pathol 32:30–35
15. Lee SK, Chang HJ, Kim TI, Kim WH, Park CK, Chang DK, Park DI, Sohn JH, Byeon JS, Yang SK, Kim JO, Lee SH, Jin SY, Park CH, Baek IH, Eun CS, Han DS, Park SJ, Chang HK, Jeen YT, Kim HS, Park DH, Shin SJ, Chang MS (2008) Clinicopathologic findings of colorectal traditional and sessile serrated adenomas in Korea: a multicenter study. Digestion 77:178–183
16. Mochizuka A, Uehara T, Nakamura T, Kobayashi Y, Ota H (2007) Hyperplastic polyps and sessile serrated 'adenomas' of the colon and rectum display gastric pyloric differentiation. Histochem Cell Biol 128:445–455
17. Bartley AN, Thompson PA, Buckmeier JA, Kepler CY, Hsu CH, Snyder MS, Lance P, Bhattacharyya A, Hamilton SR (2010) Expression of gastric pyloric mucin, MUC6, in colorectal serrated polyps. Mod Pathol 23:169–176
18. Percinel S, Savas B, Ensari A, Kuzu I, Kuzu MA, Bektas M, Cetinkaya H, Kursun N (2007) Mucins in the colorectal neoplastic spectrum with reference to conventional and serrated adenomas. Turk J Gastroenterol 18:230–238
19. Kim YH, Kakar S, Cun L, Deng G, Kim YS (2008) Distinct CpG island methylation profiles and BRAF mutation status in serrated and adenomatous colorectal polyps. Int J Cancer 123:2587–2593

Virchows Arch (2010) 457:451–456
DOI 10.1007/s00428-010-0961-1

ORIGINAL ARTICLE

Differences in the T-bet and GATA-3 expression patterns between lymphocytic colitis and coeliac disease

Korinna Jöhrens · Maria Grünbaum · Ioannis Anagnostopoulos

Received: 19 March 2010 / Revised: 30 July 2010 / Accepted: 5 August 2010 / Published online: 31 August 2010
© Springer-Verlag 2010

Abstract Lymphocytic colitis (LC) is a disease of unknown aetiology. Among other pathogenetic possibilities, an abnormal reaction to a luminal antigen has been discussed. To clarify this fact, we characterized the inflammatory infiltrate in LC and compared it with the Th1 response-related coeliac disease (CD). Biopsies from 10 LC and 10 CD patients were analyzed by immunohistochemistry for detection of T-bet, the master regulator of Th1 response and its antagonist GATA-3 in T cells employing double labellings. In LC, 10–20% of intraepithelial lymphocytes (IEL) expressed GATA-3 and the remaining T-bet, whereas in CD, all IEL were T-bet-positive. The T cells in the lamina propria of LC (65–70% CD4+; 30–35% CD8+) showed a mixed expression pattern of T-bet and GATA-3. The majority of the CD4+ T cells were GATA-3+, while T-bet and GATA-3 were expressed at a similar frequency by the CD8+ T cells. Most of the T cells in the lamina propria of CD specimens were CD4+, showing a predominant T-bet expression. Also, most of the CD8+ lamina propria T cells in CD were T-bet+. We conclude that in contrast to CD, which exhibits immunophenotypical features of a Th1-response, LC shows features of a mixed Th1/Th2 immune response.

K. Jöhrens · M. Grünbaum · I. Anagnostopoulos
Institute for Pathology, Charité, Campus Benjamin Franklin,
Medical University Berlin,
Berlin, Germany

I. Anagnostopoulos (✉)
Institute for Pathology, Charité-University Medicine Berlin,
Campus Mitte,
Charitéplatz 1,
10117 Berlin, Germany
e-mail: korinna.joehrens@charite.de

Present Address:
K. Jöhrens · I. Anagnostopoulos
Institute for Pathology, Charité, Campus Mitte,
Medical University Berlin,
Berlin, Germany

Keywords Lymphocytic colitis · Coeliac disease · Immune response · T-bet · GATA-3 · Immunohistochemistry

Introduction

Lymphocytic colitis (LC) was first mentioned in 1989 [1]. Together with collagenous colitis, it is subsumed under the term of microscopic colitis [2]. The definition of this disease includes watery diarrhoea of variable severity ranging from self-limited up to treatment refractory without endoscopically visible mucosa damage and an increased number of intraepithelial lymphocytes (IEL) in bioptic specimens [3]. In addition to the presence of more than 35 T cells for every 100 colonic epithelia, LC is characterized by a mixed inflammatory infiltrate in the lamina propria composed of lymphocytes, plasma cells, eosinophils, neutrophils and mast cells. These features are more prominent in the proximal colon in comparison with the distal areas [4, 5]. The reported incidence of LC in Europe is up to 4.0/100,000 persons per year with a slight but not significant female predominance and the recorded annual incidence in Iceland [4, 6].

Until now, the cause of LC is unknown, and different potential pathophysiologic mechanisms have been investigated. Among these, an HLA association has been discussed by several authors, but the findings are discrepant, and drawing conclusions regarding this fact is difficult. In one study, a significant seasonal incidence pattern of LC was observed [7]. An interesting point of view is the possibility of an abnormal reaction to a luminal antigen. This is supported by the reported coincidence of coeliac disease (CD) and LC and the detection of anti-gliadin, anti-endomysial and anti-tissue transglutaminase antibodies in up to 17% of the patients with LC [8–10].

As recent studies could characterize CD as a Th1 immune response [11, 12], we addressed the question whether CD and LC are two diseases manifesting in

different areas of the gastrointestinal tract with similar pathomechanism or not. Both diseases share histological features, i.e. elevated IEL and a mixed inflammatory infiltrate in the lamina propria although eosinophils are more prominent in LC. As we could already show in CD, nearly all IEL and a portion of the CD4 positive T cell infiltrate of the lamina propria express T-bet, the master regulator of the Th1 response [13]. T-bet regulates in a direct and indirect way the expression of interferon gamma (IFN-γ), one of the most important interleukins of the Th1 response, in CD4 and CD8 positive T cells [14]. The antagonist of T-bet with respect to immune response is GATA-3, a zinc-finger transcription factor abundantly expressed in the T-lymphocyte lineage thought to participate in T-cell receptor gene activation. Moreover, it is essential for the early T-cell development. GATA-3 is expressed at a high level in naïve, freshly activated and Th2 lineage cells and in lower levels in CD8 positive T cells. Additionally, GATA-3 plays a critical role in expression of the IL5 gene in the Th2 cells [15].

This immunohistochemical study was designed as to characterize the T-cell infiltrates in biopsies of patients with LC and compare this pattern with that of patients with CD. The chosen panel of antibodies consisted of T-bet and GATA-3 and double labellings for T-bet/CD4, T-bet/CD8, T-bet/CD20 as well as GATA-3/CD4, GATA-3/CD8, GATA-3/CD20 for precise characterization of GATA-3 and T-bet expressing cells.

Materials and methods

Tissue specimens

Haematoxylin and eosin (H&E) stained (Fig. 1a) as well as CD3 immunostained (Fig. 1b) sections of formalin-fixed and paraffin-embedded large bowel biopsies from 10 patients

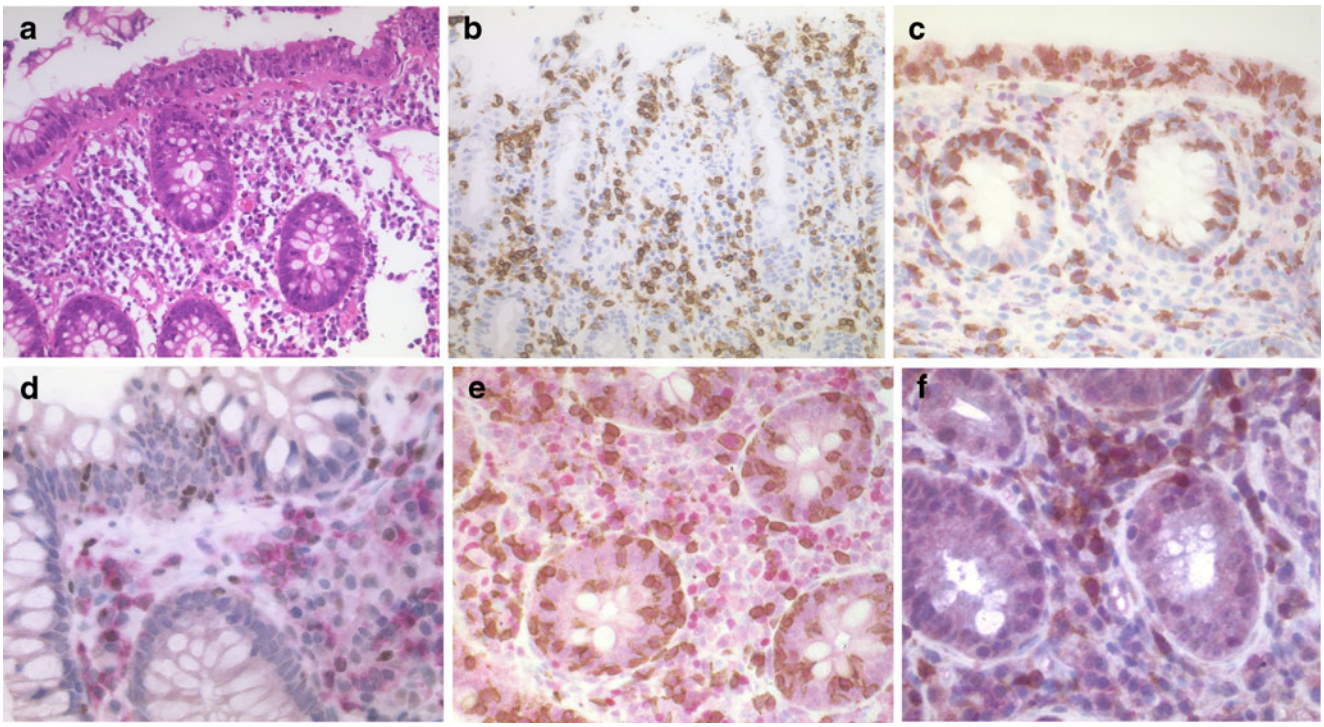

Fig. 1 **a** Histological features of lymphocytic colitis in a colonic biopsy specimen: The surface epithelium is infiltrated by numerous lymphocytes and exhibits degenerative changes. The lamina propria is infiltrated by lymphocytes, plasma cells and eosinophils (H&E stain, original magnification ×25). **b** The immunostain for CD3 highlights the large number of intraepithelial T cells and shows that the lymphocytes of the lamina propria also belong to the T-cell lineage (anti-CD3 antibody, avidin–biotin–peroxidase method, original magnification ×25). **c** Double labelling for T-bet (red nuclear immunostain) and CD8 (brown membrane immunostain) in a specimen of lymphocytic colitis shows that the majority of intraepithelial CD8+ T cells express T-bet (combination of avidin–biotin–peroxidase and APAAP methods, original magnification ×50). **d** Double labelling for T-bet (brown nuclear immunostain) and CD4 (red membrane and cytoplasmic immunostain) in a sample of lymphocytic colitis shows that a proportion of T cells in the lamina propria coexpress T-bet and CD4 (combination of avidin–biotin–peroxidase and APAAP methods, original magnification ×50). **e** Double labelling for GATA-3 (red nuclear immunostain) and CD8 (brown membrane immunostain) in a specimen of lymphocytic colitis reveals that a proportion of intraepithelial CD8+ cells also expresses GATA-3. Observe the large number of GATA-3+ lymphocytes in the lamina propria of which only a small part also expresses CD8 (combination of avidin–biotin–peroxidase and APAAP methods, original magnification ×50). **f** Double labelling for GATA-3 (red nuclear immunostain) and CD4 (brown membrane immunostain) in a specimen of lymphocytic colitis shows that several of the GATA-3+ lymphocytes in the lamina propria coexpress CD4 (combination of avidin–biotin–peroxidase and APAAP methods, original magnification ×60)

with clinical features of LC were evaluated according to the criteria of Mills et al. [16]. In addition, duodenal biopsies from 10 patients with the clinical picture of CD were evaluated according to the modified Marsh criteria and were classified as grade IIIa and IIIb (Fig. 2a, b). All samples from the 20 patients were anonymised.

Immunohistochemistry

The primary antibodies used for evaluation of T cells in the various specimens were directed against CD3 (polyclonal, DAKO, Glostrup, Denmark), CD4 (clone 1F6, Novocastra, Leica Microsystems, Newcastle, UK) and CD8 (clone C8/144B, DAKO). For T-bet detection, the monoclonal antibody clone 4B10 obtained from Santa Cruz Biotechnology (Santa Cruz, CA, USA) was used. The antibody against GATA-3 (clone HG3-31) was also from Santa Cruz Biotechnology. As T-bet and GATA-3 antibodies were of the mouse IgG1 class, a mouse isotype-specific negative control antibody (clone DAK-GO1) was used for control experiments (Fig. 3). B cells were demonstrated using a CD20 antibody (clone L26; DAKO).

Prior to incubation with the primary antibodies, the dewaxed 4-μm thick sections were subjected to an antigen-demasking procedure consisting of a brief, high-temperature heating of the sections immersed in citrate buffer (10 mM, pH 6.0) and a heating time of 2 min in a high-pressure cooker. Bound antibodies were made visible using either the streptavidin–biotin–alkaline phosphatase method (T-bet) or the alkaline phosphatase anti-alkaline phosphatase method (remaining antigens) and FastRed as chromogen. All reagents for that purpose were purchased from DAKO.

Immunostains for lineage allocation of T-bet and GATA-3 expressing cells involved double labelling for T-bet or GATA-3 and CD20, CD3, CD4 or CD8. For this purpose, the dewaxed sections were subjected to the above-mentioned antigen retrieval protocol followed by an incubation with the anti-CD20, CD3, CD4 or CD8 antibody and visualization of bound antibodies using the streptavi-

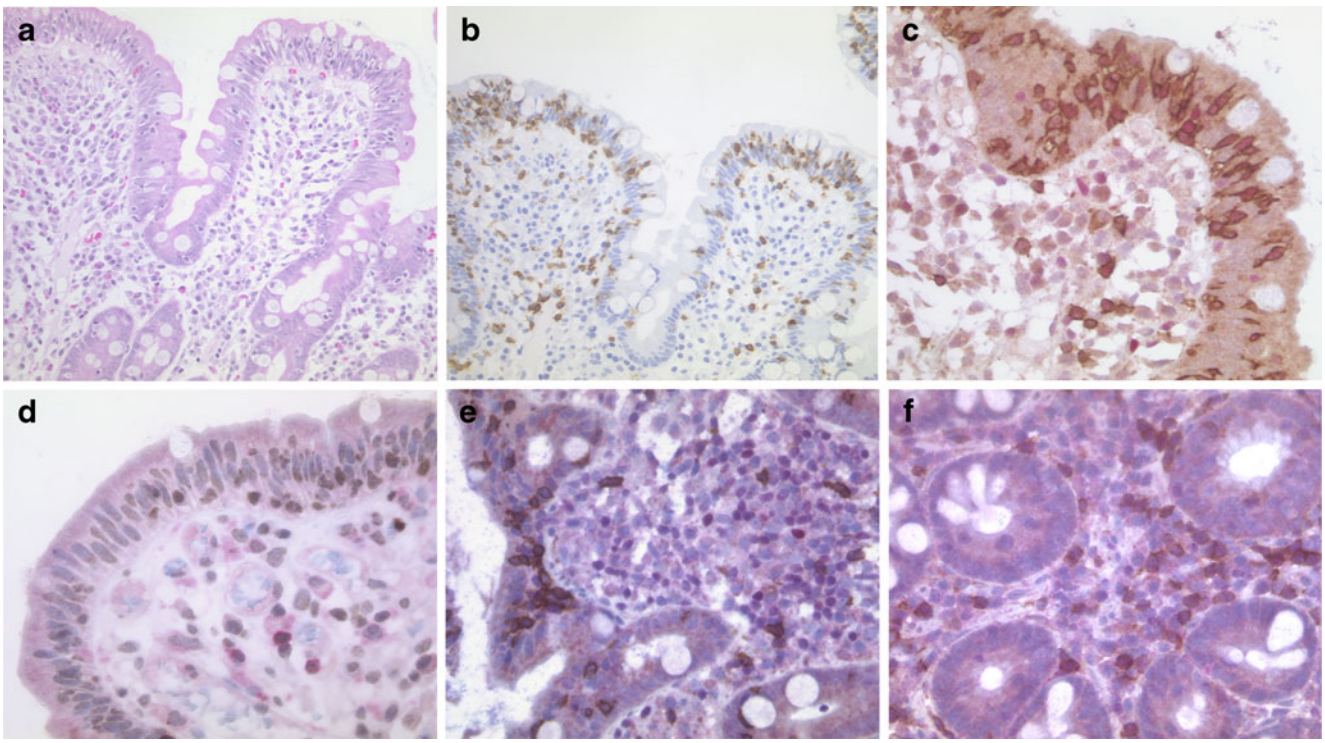

Fig. 2 **a** Histological features of coeliac disease in a duodenal biopsy specimen: The surface epithelium of the blunted shortened villi is infiltrated by numerous lymphocytes. The lamina propria is infiltrated by lymphocytes and plasma cells (H&E stain, original magnification ×25). **b** The immunostain for CD3 highlights the large number of intraepithelial T cells (anti-CD3 antibody, avidin–biotin–peroxidase method, original magnification ×25). **c** Double labelling for T-bet (red nuclear immunostain) and CD8 (brown membrane immunostain) in a specimen of coeliac disease shows that all intraepithelial cells coexpress T-bet. Also several of the CD8+ cells within the lamina propria coexpress T-bet (combination of avidin–biotin–peroxidase and APAAP methods, original magnification ×45). **d** Double labelling for T-bet (brown nuclear immunostain) and CD4 (red membrane and cytoplasmic immunostain) in a sample of coeliac disease shows that several of the CD4+ cells within the lamina propria coexpress T-bet (combination of avidin–biotin–peroxidase and APAAP methods, original magnification ×50). **e** Double labelling for GATA-3 (red nuclear immunostain) and CD8 (brown membrane immunostain) in a specimen of coeliac disease reveals that none of the intraepithelial CD8-positive cells do express GATA-3. Only single of the GATA-3+ lymphocytes in the lamina propria express CD8 (combination of avidin–biotin–peroxidase and APAAP methods, original magnification ×50). **f** Double labelling for GATA-3 (red nuclear immunostain) and CD4 (brown membrane immunostain) in a specimen of coeliac disease shows that only a low number of the CD4+ lymphocytes in the lamina propria coexpress GATA-3 (combination of avidin–biotin–peroxidase and APAAP methods, original magnification ×50)

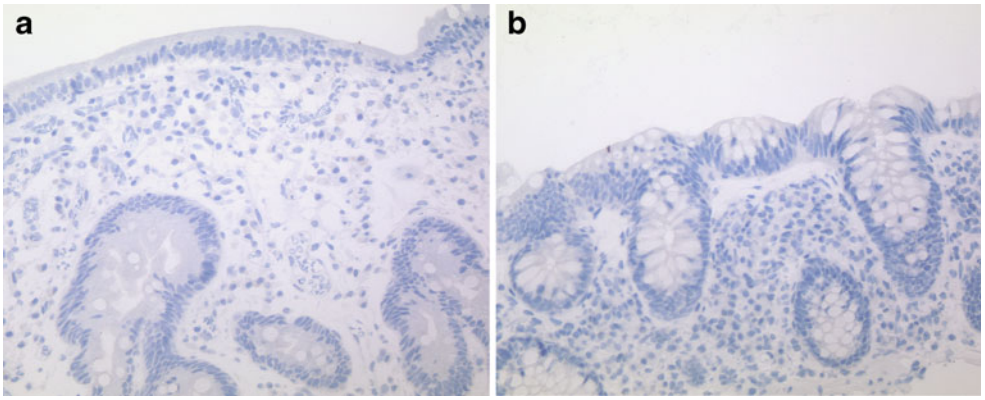

Fig. 3 **a** Labelling of a sample of coeliac disease with an IgG1 isotype control antibody (×30). **b** Labelling of a sample of lymphocytic colitis with an IgG1 isotype control antibody (×30)

din–biotin–peroxidase method and diaminobenzidine as chromogen. Subsequently, the sections were incubated with the anti-T-bet or anti-GATA-3 antibody which became visualized with the alkaline phosphatase anti-alkaline phosphatase method and FastRed as chromogen. The result was a brown membrane staining for CD20, CD3, CD4 or CD8 and a brown nucleus for T-bet or GATA-3. In some instances, T-bet and GATA-3 became visualized using the streptavidin–biotin peroxidase method and membrane bound antibodies with the alkaline phosphatase method resulting in a brown nuclear and red membrane staining. The number of positive cells was determined after respective double labellings and counting of 100 intra-epithelial or lamina propria lymphocytes in each case.

Results

Intraepithelial lymphocytes in lymphocytic colitis

All IEL belonged to the CD8+ T-cell subpopulation. No CD4+ T cells were observed. Double immunostains revealed that 80% to 90% of the CD8+ T cells expressed T-bet (Fig. 1c) and 10% to 20% GATA-3 (Fig. 1e). No intraepithelial CD20-expressing B cells were observed (data not shown).

Intraepithelial lymphocytes in coeliac disease

Double labellings showed a strong T-bet expression in the intraepithelial CD8+ T cells of all 10 investigated cases of CD (Fig. 2c). None of the IEL stained with the antibody against GATA-3 (Fig. 2e). Again, no intraepithelial B cells were detectable (data not shown).

T cells in the lamina propria of lymphocytic colitis

The T-cell infiltrate of the lamina propria varied from moderate to severe and was composed predominantly of CD4+ T cells (65–70%) and to a lesser percentage (30–35%) of CD8+ T cells. An expression of GATA-3 was detected in up to 30–40% of the T cells, whereas 30–50% expressed T-bet. According to the double labellings, up to 60% of the GATA-3+ T cells were assigned to the CD4+ (Fig. 1f) subpopulation and up to 20% to the CD8+ fraction (Fig. 1e). Of the T cells, 30–40% showed a coexpression of CD4 and T-bet (Fig. 1d) and additional 20% of CD8 (Fig. 1c) and T-bet. The number of eosinophils varied from only few cells to 30% of the inflammatory infiltrate.

T cells in the lamina propria of coeliac disease

The majority (80%) of T cells in the lamina propria of CD expressed CD4 and 10% CD8. Double labelling for CD4 and T-bet showed that 75% of the CD4 cells coexpressed T-bet with variable intensity (Fig. 2d). Three to twenty percent expressed GATA-3 (Fig. 2f). Up to 80% of the CD8+ T cells expressed T-bet (Fig. 2c) and only few cells GATA-3 (Fig. 2e). The results are summarized on Tables 1 and 2.

Table 1 T-bet and GATA-3 expression patterns by intraepithelial CD8-positive T lymphocytes

Disease entity	T-bet/CD8	GATA-3/CD8
Lymphocytic colitis	80–90%	10–20%
Coeliac disease	100%	0%

The number of positive cells was determined after respective double labellings and counting of 100 intraepithelial lymphocytes in each case

Table 2 T-bet and GATA-3 expression patterns in T-lymphocyte subpopulations of the lamina propria

Disease entity	T-bet/CD8	T-bet/CD4	GATA-3/CD8	GATA-3/CD4
Lymphocytic colitis	20%	30–40%	10–20%	50–60%
Coeliac disease	80%	75%	>5%	3–20%

The number of positive cells was determined after respective double labellings and counting of 100 lymphocytes in the lamina propria of each case

B cells in the lamina propria

In both disease entities, only a small number of CD20-positive B cells within the lamina propria was detectable. These cells did not show either T-bet or GATA-3 expression (data not shown).

Discussion

This study aimed at the comparison of the expression patterns of the master regulators of Th1 and Th2 immune response (T-bet and GATA-3 respectively) in biopsies from CD and LC patients in order to verify possible similarities in the pathogenesis of these entities. In contrast to CD with a clear cut correlation between antigen and morphological as well as clinical outcome, the pathomechanism of LC is unclear. Gluten is only in some cases responsible for the manifestation of the disease [17, 18], and drugs as well as other food components than gluten are under discussion. Furthermore, the therapy differs from that to coeliac disease. Gluten-free diet is only in some cases helpful [19], but steroids are often effective.

The situation in CD is clear as it has been established as a Th1-mediated inflammatory reaction [12, 13]. In line with the central role of T-bet in this setting [11, 14–16, 20–23], we observed in an earlier and in the present study that the majority (75%) of the CD4+ cells in the lamina propria express T-bet. In contrast, GATA-3 is found only in up to 20% of the lamina propria CD4+ cells. Activated CD8+ cells also play a critical role by supporting the Th1 response. Also in this situation, CD8+ cells express T-bet at high levels and produce IFN-γ. Therefore, almost all intraepithelial CD8+ T cells observed in CD, and most of the rare CD8+ T cells found in the lamina propria constantly express T-bet [13] while GATA-3 is practically absent from this population.

In LC, all intraepithelial T cells belong to the CD8 subpopulation similar to the situation found in CD; the T-bet and GATA-3 expression patterns are however significantly different to CD, as in all investigated cases, a 10–20% of IEL showed a constant GATA-3 expression with the remaining being T-bet positive. More prominent are the differences regarding the lamina propria infiltrate where the GATA-3+ T cells are more prominent than the T-bet+ T cells in the LC specimens. Moreover, in all cases a small proportion of CD8+ T cells expressed also GATA-3.

GATA-3 is not only necessary for the T-cell development but also essential for the Th2 response. It is able to bind the promoter region of IL-5, an interleukin, which plays a central role in growth and differentiation of eosinophils [24]. In contrast to that, T-bet represses Th2 lineage commitment through a tyrosine kinase-mediated interaction between itself and GATA-3 that interferes with the binding of GATA-3 to its target DNA [25]. In line with this data, LC showed a variable infiltrate of eosinophils ranging from only few cells up to 30%. In contrast, CD specimens contained only a minimal eosinophilic component.

Although recent studies described that early CD8+/CD4+ thymocytes lose GATA-3 expression during differentiation to CD8+ T cells [26], we observed in all cases of LC a small proportion of CD8+ T cells expressing GATA-3. In comparison with the T-bet expression profile during Th1 response [14, 27], it may be possible that CD8+ T cells in LC try to support a Th2 response by producing GATA-3.

After considering these facts, our results imply that LC represents a combined Th1/Th2 response caused either by an intra- or extracellular microorganism or by a hypersensitivity reaction to food components.

Acknowledgement The authors would like to thank Constanze Cieluch for excellent technical assistance.

Conflict of interest statement The authors declare that they have no conflict of interest.

References

1. Lazenby AJ, Yardley JH, Giardiello FM, Jessurun J, Bayless TM (1989) Lymphocytic ("microscopic") colitis: a comparative histopathologic study with particular reference to collagenous colitis. Hum Pathol 20:18–28
2. Read NW, Krejs GJ, Read MG, Santa Ana CA, Morawski SG, Fordtran JS (1980) Chronic diarrhea of unknown origin. Gastroenterology 78:264–271
3. Schiller LR (1999) Microscopic colitis syndrome: lymphocytic colitis and collagenous colitis. Semin Gastrointest Dis 10:145–155
4. Giardiello FM, Lazenby AJ, Bayless TM et al (1989) Lymphocytic (microscopic) colitis. Clinicopathologic study of 18 patients and comparison to collagenous colitis. Dig Dis Sci 34:1730–1738
5. Levison DA, Lazenby AJ, Yardley JH (1993) Microscopic colitis cases revisited. Gastroenterology 105:1594–1596
6. Agnarsdottir M, Gunnlaugsson O, Orvar KB et al (2002) Collagenous and lymphocytic colitis in Iceland. Dig Dis Sci 47:1122–1128
7. LaSala PR, Chodosh AB, Vecchio JA, Schned LM, Blaszyk H (2005) Seasonal pattern of onset in lymphocytic colitis. J Clin Gastroenterol 39:891–893
8. Bohr J, Tysk C, Yang P, Danielsson D, Jarnerot G (1996) Autoantibodies and immunoglobulins in collagenous colitis. Gut 39:73–76
9. Fine KD, Do K, Schulte K et al (2000) High prevalence of celiac sprue-like HLA-DQ genes and enteropathy in patients with the microscopic colitis syndrome. Am J Gastroenterol 95:1974–1982
10. McCashland TM, Donovan JP, Strobach RS, Linder J, Quigley EM (1992) Collagenous enterocolitis: a manifestation of gluten-sensitive enteropathy. J Clin Gastroenterol 15:45–51
11. Neurath MF, Weigmann B, Finotto S et al (2002) The transcription factor T-bet regulates mucosal T cell activation in experimental colitis and Crohn's disease. J Exp Med 195: 1129–1143
12. Weigmann B, Neurath MF (2002) T-bet and mucosal Th1 responses in the gastrointestinal tract. Gut 51:301–303
13. Johrens K, Anagnostopoulos I, Stein H (2005) T-bet expression patterns in coeliac disease, cryptic and overt enteropathy-type T-cell lymphoma. Histopathology 47:368–374
14. Hartenstein B, Teurich S, Hess J, Schenkel J, Schorpp-Kistner M, Angel P (2002) Th2 cell-specific cytokine expression and

allergen-induced airway inflammation depend on JunB. EMBO J 21:6321–6329
15. Hwang ES, Szabo SJ, Schwartzberg PL, Glimcher LH (2005) T helper cell fate specified by kinase-mediated interaction of T-bet with GATA-3. Science 307:430–433
16. Mills LR, Schuman BM, Thompson WO (1993) Lymphocytic colitis. A definable clinical and histological diagnosis. Dig Dis Sci 38:1147–1151
17. Zins BJ, Sandborn WJ, Tremaine WJ (1995) Collagenous and lymphocytic colitis: subject review and therapeutic alternatives. Am J Gastroenterol 90:1394–1400
18. Matteoni CA, Goldblum JR, Wang N, Brzezinski A, Achkar E, Soffer EE (2001) Celiac disease is highly prevalent in lymphocytic colitis. J Clin Gastroenterol 32:225–227
19. Pardi DS (2004) Microscopic colitis: an update. Inflamm Bowel Dis 10:860–870
20. Yin Z, Chen C, Szabo SJ, Glimcher LH, Ray A, Craft J (2002) T-Bet expression and failure of GATA-3 cross-regulation lead to default production of IFN-gamma by gammadelta T cells. J Immunol 168:1566–1571
21. Sullivan BM, Juedes A, Szabo SJ, von Herrath M, Glimcher LH (2003) Antigen-driven effector CD8 T cell function regulated by T-bet. Proc Natl Acad Sci USA 100:15818–15823
22. Szabo SJ, Sullivan BM, Stemmann C, Satoskar AR, Sleckman BP, Glimcher LH (2002) Distinct effects of T-bet in TH1 lineage commitment and IFN-gamma production in CD4 and CD8 T cells. Science 295:338–342
23. Robinson DS, O'Garra A (2002) Further checkpoints in Th1 development. Immunity 16:755–758
24. Wang J, Young IG (2007) Eosinophilic inflammation: mechanisms regulating IL-5 transcription in human T lymphocytes. Allergy 62:1131–1138
25. Chakir H, Wang H, Lefebvre DE, Webb J, Scott FW (2003) T-bet/GATA-3 ratio as a measure of the Th1/Th2 cytokine profile in mixed cell populations: predominant role of GATA-3. J Immunol Methods 278:157–169
26. Pai SY, Truitt ML, Ting CN, Leiden JM, Glimcher LH, Ho IC (2003) Critical roles for transcription factor GATA-3 in thymocyte development. Immunity 19:863–875
27. Lametschwandtner G, Biedermann T, Schwarzler C et al (2004) Sustained T-bet expression confers polarized human TH2 cells with TH1-like cytokine production and migratory capacities. J Allergy Clin Immunol 113(5):987–994

Virchows Arch (2010) 457:457–466
DOI 10.1007/s00428-010-0957-x

ORIGINAL ARTICLE

Hepatic progenitor cells in chronic hepatitis C: a phenomenon of older age and advanced liver disease

Johanna Delladetsima · Paraskevi Alexandrou · Konstantinos Giaslakiotis · Mina Psichogiou · Gregory Hatzis · Vana Sypsa · Dina Tiniakos

Received: 14 April 2010 / Revised: 30 July 2010 / Accepted: 30 July 2010 / Published online: 19 August 2010
© Springer-Verlag 2010

Abstract Hepatic progenitor cells (HPC) appear in a variety of liver diseases. Their occurrence in chronic hepatitis C (CHC) remains unclear, and triggering factors have to be elucidated. The presence of HPC in CHC was examined in relation to histological and virological parameters and patient age. Fifty liver biopsies of HCV-infected patients were examined. The presence of HPC was evaluated by immunohistochemical expression of keratin 7 (K7). Double immunostaining with K7 and cell proliferation marker Ki-67 was undertaken. Ductular reaction at the limiting plate, mean number of isolated progenitor cells (IPC) and isolated ductular structures (IDS) were quantified. The predominant distribution pattern of IPC and IDS and the presence of K7(+) hepatocytes were registered. Relationship between ductular reaction, IPC, IDS, presence of K7(+) hepatocytes, and patient age, hepatitis grade and stage, HCV RNA, and HCV genotype was examined. Prominent ductular reaction and increased numbers of IPC and IDS correlated significantly with older age and severe fibrosis/cirrhosis. The above HPC subtypes were not proliferating. Periportal/periseptal distribution pattern of IPC and IDS and presence of K7(+) hepatocytes were significantly more frequent in advanced hepatitis stages and in patients older than 40 years. Intraparenchymal distribution pattern correlated with younger age, lobular activity, and early fibrosis stage. K7(+) hepatocytes were encountered almost exclusively in the periportal pattern and in the presence of interface hepatitis and were more frequent among HCV genotype-1 patients. HPC activation in CHC is a common but diverse phenomenon closely related to patient age and hepatitis stage.

Keywords Hepatitis C · HCV · Progenitor cells · Age · Senescence · Cell proliferation

J. Delladetsima · P. Alexandrou · K. Giaslakiotis
First Department of Pathology, Medical School,
National & Kapodistrian University of Athens,
Athens, Greece

M. Psichogiou
First Department of Propaedeutic Medicine, Medical School,
National & Kapodistrian University of Athens,
Athens, Greece

G. Hatzis
Department of Pathophysiology, Medical School,
National & Kapodistrian University of Athens,
Athens, Greece

V. Sypsa
Department of Hygiene and Epidemiology, Medical School,
National & Kapodistrian University of Athens,
Athens, Greece

D. Tiniakos
Laboratory of Histology & Embryology, Medical School,
National & Kapodistrian University of Athens,
Athens, Greece

J. Delladetsima (✉)
First Department of Pathology,
Medical School, National & Kapodistrian University of Athens,
75 Mikras Asias Str, Goudi,
Athens 11527, Greece
e-mail: jokadelladetsima@hotmail.com

Introduction

Hepatic progenitor cells (HPC) in humans are the counterpart of oval cells in rodents, displaying the capacity of bipotential differentiation [1, 2], while their likely niches include primarily the canals of Hering [3]. HPC become visible in massive and sub-massive necrosis [4–7], as well as in a variety of chronic liver diseases forming ductular structures (DS) at the portal tract interface and in the periportal area [8–16]. It is postulated that their activation is driven by a replicative defect of the hepatocytes, which comprise the main regeneration compartment under normal

conditions [17, 18]. Inflammation [17, 19], viral factors [20], steatosis [21], and drugs [18] have been implicated as inhibitory factors leading to replication inefficiency of hepatocytes. In chronic hepatitis C (CHC), HPC activation is frequently observed predominantly as ductular reaction at the portal interface [8, 10, 12, 15, 16]. The degree of HPC expansion has been correlated with hepatitis severity and deficient hepatocyte replication [8], suggesting an accessory role in parenchymal regeneration. Involvement in fibrogenesis [8], as well as adverse prognostic significance in response to treatment [15], has also been suggested. However, the origin and function of HPC in CHC are still unclear, while limited information is available referring to pathogenesis and stimulatory factors.

In the present study, we performed a quantitative and topographical histological evaluation of HPC at the portal interface and within the parenchyma in liver biopsies of patients with CHC. The findings were correlated with different variables that may potentially interfere with the activation process of HPC such as hepatitis severity, viral load, hepatitis C virus (HCV) genotype, and patient age to better understand the nature of HPC in CHC.

Materials and methods

Material

The examined material consisted of 50 consecutive liver biopsies from 50 treatment-naïve patients with CHC; 57.1% were males and mean patient age was 43.8 years (±13.1 years). The study conformed to the ethical guidelines of the 1975 Declaration of Helsinki. Written informed consent was obtained from all patients for the use of anonymized tissue sections for research purposes following routine liver biopsy histological diagnosis.

All biopsies contained more than ten portal tracts. Histological evaluation of chronic hepatitis included grading and staging based on the scoring system proposed by Ishak et al. [22]. Grades 1 to 3 were ascribed to minimal, grades 4 through 7 as mild, and grades 8 through 12 as moderate chronic hepatitis. Hepatitis stage was assessed using Masson trichrome, van Gieson's, and Gomori stains. Stages 1–2 indicated mild fibrosis, stages 3–4 moderate fibrosis, stages 5–6 severe fibrosis/cirrhosis. The extent of steatosis was additionally evaluated and graded separately on a four-grade scale (0: no steatosis, 1: <1/3, 2: 1/3–2/3, 3: >2/3 of liver parenchyma involved).

Methods

The presence of HPC was identified by immunohistochemical expression of keratin 7 (clone OV-TL 12/30; Dako, Glostrup, Denmark). In preliminary tests on serial sections of randomly selected cases from our material, no statistically significant difference was seen between the number of keratin 7(+) HPC and that of keratin 19(+) HPC in each case. Keratin 7 (K7) was preferred over keratin 19 or other HPC-specific markers because it not only identified HPC but in addition decorated intermediate cells and K7(+) hepatocytes (2). Immunohistochemistry was performed on consecutive paraffin sections using the EnVision System (Dako) with 3,3′ diaminobenzidine (DAB) as a chromogen, according to standard protocols. Double immunostaining with K7 and Ki-67 cell proliferation marker (PA0118, Novocastra, Newcastle upon Tyne, UK) was undertaken in 29 cases with available material using the EnVision G2 Doublestain System (Dako). All liver biopsies included at least 10 high-power fields (HPF) ×400. Histological slides were evaluated by two pathologists at a double-headed microscope.

Evaluation of immunostaining

K7(+) HPC were identified as ductular reaction, as isolated progenitor cells (IPC), and as isolated ductular structures (IDS) according to the classification and terminology proposed by Roskams et al. [2] with modifications. Ductular reaction was defined as irregular cords of small cuboidal or elongated cells with or without poorly discernible lumina, located at the portal–parenchyma interface with or without some extension to the periphery of hepatic lobules or cirrhotic nodules, usually in association with interspersed small solitary K7(+) cells with scant cytoplasm and oval nuclei. IPC and IDS were observed in the parenchyma. The majority of IDS formed string-like structures with poorly formed lumina or without lumina. IPC were similar to the solitary cells of ductular reaction. K7(+) immunostaining in HPC was strongly cytoplasmic.

Ductular reaction was assessed semi-quantitatively on a three-grade scale based on its extent around the limiting plate; grade 1 represented focal discontinuous or continuous ductular reaction in less than 1/3 of the portal tract circumference. Grade 3 was defined by continuous ductular reaction rimming more than 1/3 of the circumference in ≥50% of portal tracts. The intermediate extension of ductular reaction was scored as grade 2. In the parenchyma, the number of IPC and IDS was counted in the entire section (surface area expressed in high power fields-HPF) and the mean number of IPC and IDC per 10 HPF was calculated for each case.

The presence of K7(+) hepatocytes and intermediate cells was also registered. Intermediate cells corresponded to K7(+) cells with morphological features between biliary cells and hepatocytes, while K7(+) hepatocytes showed the same morphology with mature hepatocytes and weak immunostaining. In addition, the predominant distribution pattern of all K7 (+) cell types and structures was evaluated in every case. Ki-

67 labeling index (LI) was calculated separately for hepatocytes and HPC and was expressed as the mean number of cells with positive nuclear staining per 10 HPF, respectively.

HCV genotyping and HCV-RNA assessment

HCV genotyping was performed using a commercially available assay (INNOLiPA HCV II, Innogenetics NV). Quantitative assessment of HCV-RNA was performed by branched DNA-enhanced label amplification assay (b-DNA 3.0, Bayer, Tarrytown, NY, USA) in serum samples obtained at the time of liver biopsy.

Statistical analysis

Statistical analysis of data was done using the statistical package SPSS for Windows (version 15.0; SPSS, Chicago, IL, USA). Relationship between ductular reaction, IPC, IDS, K7(+) hepatocytes, and patient age (≤40 and >40 years) hepatitis grade and stage, grade of steatosis, HCV RNA, and HCV genotype were examined by chi-square test, *t* test, Wilcoxon rank-sum test, Kruskal–Wallis test or Spearman correlation coefficient, as appropriate. Multiple logistic or linear regression was used to determine factors independently associated with the variables under study. Statistical significance was set at $p<0.05$.

Results

HPC expansion constituted a constant finding in all liver biopsies, except of one case with minimal hepatitis. HPC appeared in a combination pattern of ductular reaction at the limiting plate and IPC and IDS within the parenchyma irrespective of hepatitis grade and stage.

Ductular reaction grade 1 was observed in 18 (38.3%), grade 2 in 17 (36.2%), and grade 3 in 12 (25.5%) cases (Fig. 1a). The number of IPC ranged from 0 to 88.8, with a

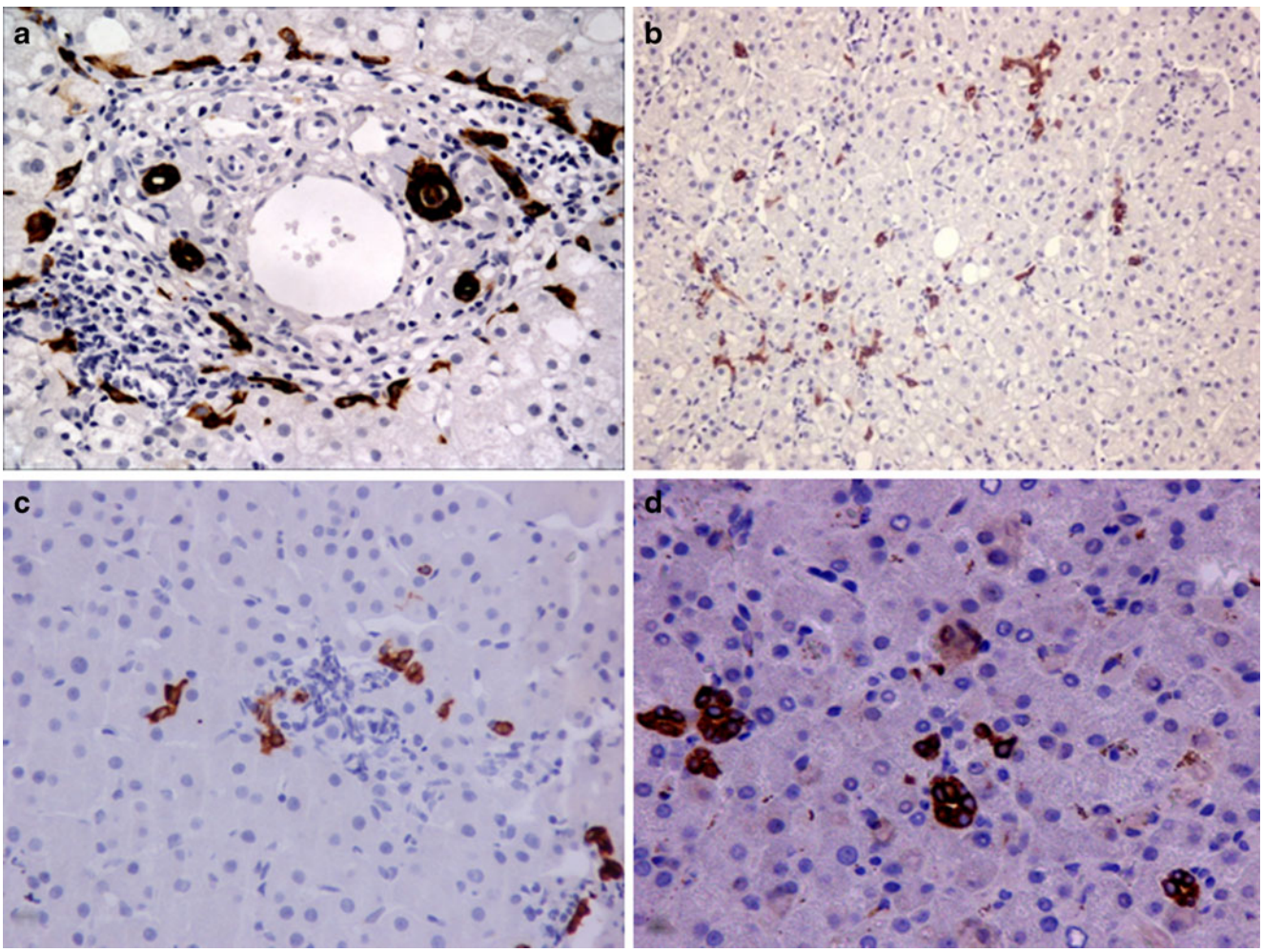

Fig. 1 **a** Ductular reaction grade 3 rimming the portal tract circumference (EnVision ×400). **b** Prominent number of IDS and IPC with spatial interrelationship and random intraparenchymal distribution (EnVision ×200). **c** IDS and IPC at the periphery of hepatocellular necrosis (EnVision ×400). **d** Keratin 7(+) IDS with signs of maturation (EnVision ×400)

median (25th, 75th) of 8.7 (3.3, 18.3). The number of IDS was lower, ranging from 0 to 161.3 with a median (25th, 75th) of 3.3 (0.9, 8.3). IPC and IDS showed significant spatial interrelationship (Fig. 1b) often adjacent to necroinflammatory foci (Fig. 1c). IDS displaying signs of maturation were also present, while differentiated ductules with cuboidal lining cells and well-formed lumina were rarely encountered (Fig. 1d).

In univariate analysis, ductular reaction was associated significantly with IPC and IDS counts (Table 1). However, in four cases with mild ductular reaction, the numbers of IPC, IDS, or both exceeded the median values. There was a significant positive association between older age and prominent ductular reaction. More specifically, the mean (SD) age of patients with ductular reaction graded as 1, 2, and 3 was 38.1 (10.9), 40.6 (10.8), and 56.7 (11.5) years, respectively ($p<0.001$). Moreover, the frequency of grade 3 ductular reaction among patients with moderate/severe fibrosis or cirrhosis was significantly higher than that of patients with no or mild fibrosis (53.9% vs 15.2%, $p=0.018$). Patients with extensive steatosis had more prominent ductular reaction (DR grade 2 and 3: 84.6% of patients with steatosis 2–3 vs 51.5% of patients with steatosis 0–1, $p=0.038$).

In multivariate analysis, the only independent factor associated with prominent ductular reaction was age; a 1-year increase in age resulted in an OR (95%CI) 1.13 (1.05, 1.21) ($p=0.001$) of having ductular reaction grade 3. This association was independent of the hepatic steatosis status.

The number of IDS was positively correlated with the number of IPC (Spearman's r: 0.778, $p<0.001$). Both variables showed significant correlation with older age and increasing hepatitis stage. In particular, the median (25th, 75th) number of IDS and IPC in patients ≤40 years of age was 1.4 (0.3, 3.5) and 4.5 (2.7, 7.4) as compared to 8.0 (3.7, 10.8) and 16.2 (9.3, 23.1) in the group of patients older than 40 years, respectively ($p<0.001$) (Table 1). Patients with moderate/severe fibrosis or cirrhosis showed significantly higher numbers of IPC and IDS as compared to patients with no or mild fibrosis (Table 1). IDS and IPC were not associated with grade of steatosis ($p=0.093$ and $p=0.1624$, respectively). The association of IPC with age and stage was confirmed in multivariate analysis [(age per year: $\beta=0.384$, $p=0.003$, stage (severe/cirrhosis vs others): $\beta=13.6$, $p=0.007$)]. No statistically significant association was found between ductular reaction, IPC, IDS, and the other variables examined (i.e. gender, HCV genotype, HCV-RNA, hepatitis grade, including portal inflammation, interface hepatitis, lobular activity), in both univariate and multivariate analyses.

K7(+) hepatocytes and intermediate cells were encountered in ten cases, seven of which were in advanced hepatitis stages (severe fibrosis/cirrhosis). They were usually located in close proximity to IPC and IDS and in higher numbers in periportal and periseptal areas (Fig. 2a). Fewer K7(+) hepatocytes were found also separately and at a distance from IPC and IDS (Fig. 2b). Univariate statistical analysis showed significant association between the presence of K7 (+) hepatocytes and interface hepatitis ($p=0.014$), advanced hepatitis stage ($p<0.001$, older age ($p=0.004$), and genotype 1 ($p=0.03$) (Table 2). Additionally, the presence of K7 (+) hepatocytes was associated with prominent ductular reaction ($p=0.001$) and higher number of IPC ($p<0.001$) and IDS ($p=0.002$) (Table 2). A marginal association was found with steatosis; K7(+) hepatocytes were present in 13.9% and 38.5% of patients with steatosis 0–1 and 2–3,

Table 1 Association of isolated ductular structures and isolated progenitor cells with patients' demographic and histological characteristics

	Isolated ductular structures		Isolated progenitor cells	
	Median (25th, 75th)	p	Median (25th, 75th)	p
Age		<0.001		<0.001
≤40 years	1.4 (0.3, 3.5)		4.5 (2.7, 7.4)	
>40 years	8.0 (3.7, 10.8)		16.2 (9.3, 23.1)	
Steatosis grade		0.428		0.257
0–1	3.3 (0.9, 8.1)		8.1 (3.3, 13.8)	
2–3	3.8 (1.1, 10.8)		10.7 (4.4, 21.5)	
Ductular reaction		0.002		<0.001
Grade 1	1.2 (0.8, 3.3)		4.3 (2.4, 7.6)	
Grade 2	3.7 (1.1, 8.1)		9.7 (4.4, 17.1)	
Grade 3	8.5 (4.6, 14)		17.8 (11.4, 23.6)	
Fibrosis		0.014		<0.001
No/mild	1.9 (0.9, 7.9)		5.3 (2.7, 10.6)	
Moderate	4.6 (0.9, 4.6)		9.3 (7.6, 10.4)	
Severe/cirrhosis	9.5 (7.4, 12.6)		26.9 (14.4, 37.8)	

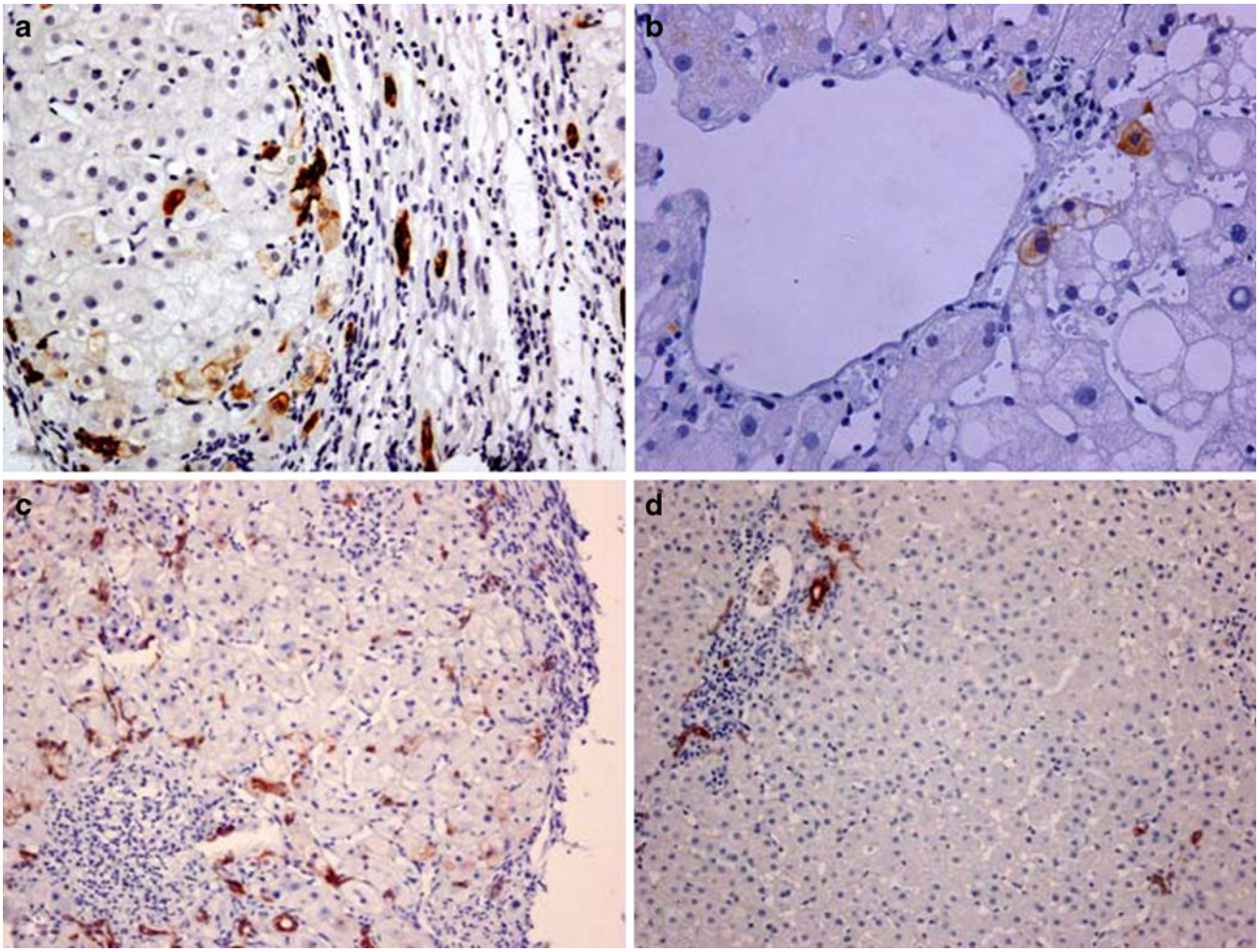

Fig. 2 **a** Keratin 7 (K7) (+) hepatocytes and intermediate cells at the periphery of a cirrhotic nodule in association with ductular structures (EnVision ×200). **b** K7(+) hepatocytes adjacent to a terminal hepatic venule in the absence of IDS and IPC (EnVision ×400). **c** Periportal distribution pattern with IDS, IPC, and K7(+) hepatocytes in the periportal area (EnVision ×200). **d** Intraparenchymal distribution pattern with a small group of HPC at a distance from the portal tract (EnVision ×100)

respectively (p=0.06). Multivariate analysis revealed strong association with advanced hepatitis stage (OR moderate, severe, cirrhosis, vs mild, no fibrosis: 1.95, p=0.003) and HCV genotype 1 (OR 1 vs other: 2.66, p=0.029). There was no association with steatosis (p=0.134).

Topographical evaluation of IPC and IDS revealed two different distribution patterns. A predominant periportal/ periseptal distribution pattern was observed in 24 (57.1%) cases and was characterized by the preferential localization of IPC and IDS in the periportal/ periseptal area (Fig. 2c). An intraparenchymal distribution pattern, in which both IPC and IDS were randomly distributed throughout the lobules or cirrhotic nodules, was found in 18 (42.9%) cases (Figs. 1b and 2d). Study of the distribution patterns of IPC and IDS showed that distinct patterns were differentially associated with different degrees of ductular reaction and numbers of IPC and IDS and correlated with patient age and hepatitis stage.

Intraparenchymal distribution pattern was more frequent in patients younger than 40 years (59.1%), whereas periportal distribution pattern was more frequently found in patients >40 years (75%) (p=0.026) (Table 3). Patients at more advanced hepatitis stages had a higher prevalence of periportal distribution pattern (p=0.029). More specifically, 75% and 100% of patients with moderate fibrosis and severe fibrosis/cirrhosis, respectively, exhibited periportal distribution pattern. The same pattern was frequently encountered in the presence of interface hepatitis in patients with early hepatitis stage (17/18, 94%) (p=0.085). On the contrary, intraparenchymal distribution pattern was frequently observed in biopsies with higher necroinflammatory activity, although this association did not reach statistical significance (p=0.059). IPC and IDS counts were higher in periportal than intraparenchymal distribution pattern groups (IPC: median 4.56 vs 12.79, p=0.003, IDS: median 1.75 vs 6.45, p=0.019). In addition, ductular

Table 2 Presence of K7(+) hepatocytes according to clinical and histological characteristics

	K7(+) hepatocytes		*p*
	Present (n=10) n (%)	Absent (n=39) n (%)	
Age			0.004
≤40 years	1 (4.0)	24 (96.0)	
>40 years	9 (37.5)	15 (62.5)	
HCV genotype			0.030
1	9 (34.6)	17 (65.4)	
3	1 (6.7)	14 (93.3)	
Other	0 (0.0)	8 (100.0)	
Fibrosis			<0.001
No fibrosis	0 (0.0)	10 (100.0)	
Mild	1 (4.2)	23 (95.8)	
Moderate	2 (28.6)	5 (71.4)	
Severe/cirrhosis	7 (87.5)	1 (12.5)	
Interface hepatitis			0.014
0	0 (0.0)	20 (100.0)	
1	4 (25.0)	12 (75.0)	
2	4 (44.4)	5 (55.6)	
3–4	2 (50.0)	2 (50.0)	
Steatosis grade			0.06
0–1	5 (13.9)	31 (86.1)	
2–3	5 (38.5)	8 (61.5)	
IPC			<0.001
Median (25th, 75th)	18.4 (12.1, 37)	5.6 (2.8, 10.7)	
IDS			0.002
Median (25th, 75th)	9.4 (4.6, 13.5)	1.9 (0.9, 6.4)	
Ductular reaction			0.001
Grade 1	0 (0.0)	18 (100.0)	
Grade 2	3 (17.7)	14 (82.4)	
Grade 3	7 (58.3)	5 (41.7)	

IPC isolated progenitor cells, *IDS* isolated ductular structures

reaction was significantly associated with the distribution pattern (p=0.02). Grade 3 ductular reaction was exclusively encountered in periportal distribution pattern (12/12, 100%), while the majority of patients with grade 1 ductular reaction frequently showed intraparenchymal distribution pattern (11/14, 78.6%). In addition, K7(+) hepatocytes were present with a high frequency in the periportal distribution pattern (41.7%), while in the intraparenchymal pattern, they were extremely rare and were considered absent (p=0.002).

HPC in 25 out of 29 cases examined by double immunostaining were negative for Ki-67. Ki-67 nuclear positivity in K7(+) HPC was extremely rare and was observed only in a total of seven cells in four cases (Fig. 3). There was no correlation between hepatocellular Ki-67 LI and grade of ductular reaction (p=0.581), presence of K7 (+) hepatocytes (p=0.464), numbers of IPC and IDS, and distribution pattern (p=0.614) (Table 4).

Discussion

The involvement of progenitor cells in hepatocarcinogenesis and in liver regeneration after chemically induced massive necrosis is well established in animals. In humans, equivalent cells have been recognized in fulminant hepatitis [4–7] and as a component of chronic liver injury, appearing as atypical ductular structures and isolated small cells in various liver diseases [1, 8, 12, 16]. In CHC, HPC expansion seems to be a very frequent phenomenon occurring even in mild and early stage disease [8, 10, 12, 15].

In our study group, the presence of HPC constituted an almost constant finding. They were encountered irrespective of hepatitis severity in a combination pattern of ductular reaction at the limiting plate and IPC and IDS within the parenchyma. HPC proliferative activity was almost absent. Prominent ductular reaction and increased counts of both intraparenchymal components demonstrated an independent significant correlation with older age and advanced hepatitis stage. The relationship of HPC with hepatitis stage in CHC has been reported in previous studies [8, 10, 15, 16, 23]. However, the potential significance of patient age in the activation process has not yet been investigated.

It is suggested that proliferation of HPC is triggered by diminished or suppressed replication capacity of mature hepatocytes which constitute the main source for restitution of liver cell loss [17, 18]. A similar tendency was observed in our study, although it did not reach statistical significance probably due to the small number of cases. Reactive oxygen species produced in fatty liver disease and chronic hepatitis have been implicated as triggering factors of HPC recruitment by suppressing the conventional regeneration pathway [21]. Another factor that has been implicated for the diminished hepatocellular proliferation in cirrhosis in humans and chronic liver injury in mice is replication senescence [24–27]. A state of senescence due to long-term hepatocyte proliferation has been postulated to be responsible for the involvement of progenitor cells in the regeneration process in cirrhotic livers [25]. The association of HPC proliferation with hepatocytic replication arrest as expressed by p21 immunoreactivity provides further indication [8, 20]. Our results are consistent with this hypothesis and imply that replication exhaustion of hepatocytes in association with diminished liver mass in severe fibrosis and cirrhosis may promote HPC activation. Moreover, they highlight patient age as a major stimulatory component of this auxiliary regeneration pathway probably through age-related senescence and dysfunction of native hepatocytes. The

Table 3 Association of IPC and IDS distribution patterns with clinical and histological parameters

	IPC/IDS distribution pattern		*p*
	Intraparenchymal (*n*=18) *n* (%)	Periportal (*n*=24) *n* (%)	
Age			0.026
≤40 years	13 (59.1)	9 (40.9)	
>40 years	5 (25.0)	15 (75.0)	
Fibrosis			0.029
No fibrosis	5 (62.5)	3 (37.5)	
Mild	12 (54.6)	10 (45.5)	
Moderate	1 (25.0)	3 (75.0)	
Severe/cirrhosis	0 (0.0)	8 (100.0)	
Lobular necroinflammatory activity			0.059
1	2 (25.0)	6 (75.0)	
2	8 (34.8)	15 (65.2)	
3–4	8 (72.7)	3 (27.3)	
IPC			0.003
Median (25th, 75th)	4.6 (2.7,10.4)	12.8 (6.7, 22.3)	
IDS			0.019
Median (25th, 75th)	1.7 (0.3,6.4)	6.4 (2.1, 10.0)	
Ductular reaction			0.001
Grade 1	11 (78.6)	3 (21.4)	
Grade 2	7 (43.8)	9 (56.3)	
Grade 3	0 (0.0)	12 (100.0)	

IPC isolated progenitor cells, *IDS* isolated ductular structures

suggested role of steatosis in HPC activation through impaired hepatocellular replication [8] is weakened in our study by the absence of an independent correlation between grade of steatosis and HPC expansion in the multivariate analysis. The contribution of HPC in fibrogenesis, postulated by Clouston et al. [8] and Richardson et al. [28], cannot be neglected due to their close relationship with the extent of fibrosis and warrants further investigation.

Data regarding phenotype and topography of HPC activation vary among different studies. A ductular reaction at the limiting plate of portal tracts and septa has been invariably identified [8, 12, 15, 16, 29]. Diverse observations have been reported regarding the intraparenchymal HPC

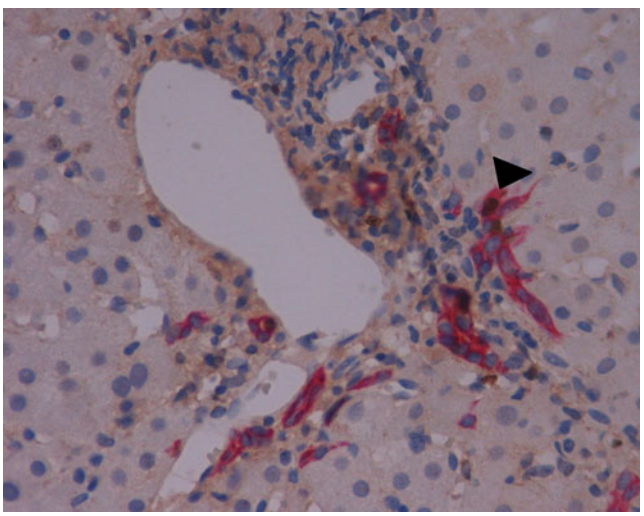

Fig. 3 Ki-67 nuclear positivity (brown-stained nuclei) in proliferating cells and keratin 7 (K7) (+) bile ductular cells and HPC (red-stained cytoplasm). A double-stained Ki-67(+)/K7(+) HPC is shown (*arrowhead*) (EnVision Doublestain ×400)

Table 4 Association of Ki-67 labeling index with ductular reaction, presence of keratin 7 (+) hepatocytes, and distribution pattern of isolated progenitor cells and isolated ductular structures

	Ki-67 labeling index	
	Median (25th, 75th)	*p*
Ductular reaction		0.581
Grade 1	10 (4, 25)	
Grade 2	16 (9, 30)	
Grade 3	36 (2, 62)	
Keratin 7 (+) hepatocytes		0.464
No	11 (4, 27)	
Yes	26 (5.5, 52)	
IPC/IDS distribution pattern		0.614
Periportal	1.2 (0.8, 3.3)	
Intraparenchymal	3.7 (1.1, 8.1)	

IPC isolated progenitor cells, *IDS* isolated ductular structures

distribution. The periportal area is referred to be the preferential region both for the extension of ductular reaction as well as for IPC expansion [8, 15, 16, 29]. However, in high grade and late stage disease, ductular structures were found to extend deep into the hepatic lobules and cirrhotic nodules [16], while Libbrecht et al. [12] reported the presence of IPC in all lobular zones in moderate and severe lobular inflammation. In our study, ductular reaction at the limiting plate was found in co-existence with intraparenchymal localization of IPC and IDS. Their quantitative interrelationship along with their intimate correlation with hepatitis stage and patient age lead primarily to the assumption of an underlying common histogenetic process. This hypothesis is weakened by the hitherto unreported recognition of two distribution patterns showing different histological and demographic features, which point towards distinct types of HPC activation. A predominant periportal distribution pattern of IDS and IPC occurred significantly more frequently in older patients and in advanced hepatitis stages. This pattern was also associated with a high degree of ductular reaction, higher counts of IPC and IDS, the presence of K7(+) hepatocytes, as well as with interface hepatitis. An intraparenchymal distribution pattern was significantly more common in younger patients and in early hepatitis stages, was associated with milder degrees of ductular reaction and lower numbers of IDS and IPC, and correlated with lobular necroinflammatory activity. The existence of two different HPC activation subgroups has not been noted previously. Some indications become perceptible in the study of Libbrecht et al., which correlated the extent of ductular reaction with the severity of interface hepatitis and the more centrally located HPC with the severity of lobular inflammation [12].

In the periportal distribution pattern, HPC expansion seems to originate from the limiting plate under the influence of interface hepatitis followed by extension deep into the periportal region. This suggestion is in accordance with previous reports regarding the source of activated progenitor cells [8, 15, 16]. However, it cannot sufficiently explain the presence of HPC at a distance from the periportal region, especially in the intraparenchymal distribution pattern, and the discordance between high intraparenchymal HPC counts and a subtle ductular reaction seen in some of our cases. Their migration into the parenchyma proposed by Libbrecht et al. [12], according to ultrastructural findings [30] and the demonstrated interconnection of HPC with migrating stellate cells [10, 31, 32], could give a plausible explanation. However, alternative possibilities such as direct origin from circulating bone marrow derived stem cells [33, 34] or derivation from dedifferentiated or metaplastic hepatocytes [2, 35, 36] may exist. In most of our cases showing an intraparenchymal distribution pattern, HPC were often found within or at the periphery of necroinflammatory foci in accordance with previous reports [12, 16]. This finding permits the speculation that elements of the inflammatory response, such as chemokines and cytokines, attract and activate organ-specific and/or bone marrow-derived stem cells [37–39]. Less probable is the origin of HPC from dedifferentiated hepatocytes due to the almost total absence of intermediate cells and K7(+) hepatocytes in this particular distribution pattern.

Another issue, which has not as yet been clarified, is the role and the fate of activated HPC. Their bi-potential nature is inherent with a differentiation capacity towards hepatocytes and biliary cells. In massive hepatic necrosis, it has not been fully clarified whether ductular hepatocytes are able to restitute the lost liver mass. At least one study provides well documented evidence in favor of this pathway [40], while a gradual differentiation to mature bile ductules has also been demonstrated [7]. In CHC, the possibility of HPC maturation towards the hepatocytic lineage has been proposed within the concept of a differentiation continuum with intermediate cells and K7 (+) hepatocytes [12, 16]. In our study, IPC were found to be adjacent to atypical IDS, the latter possibly representing a proliferation product of IPC with signs of biliary differentiation. This differentiation process is rarely accomplished, as shown by the presence of few phenotypically mature bile ductules within the parenchyma. The differentiation potential towards hepatocytes seems to vary among the two HPC distribution patterns. In the intraparenchymal pattern, the absence of K7(+) hepatocytes and intermediate cells makes hepatocellular differentiation of HPC unlikely. Their role in regeneration may thus be indirect and their future regression or fusion with native hepatocytes has to be considered as a possible outcome. On the contrary, in the periportal distribution pattern, K7(+) hepatocytes often in proximity to IPC and in association with intermediate cells may represent the end step of hepatocellular differentiation of IPC contributing directly to parenchymal reconstitution. It is of interest that the emergence of K7(+) hepatocytes is closely and independently linked with advanced liver disease, interface hepatitis, and the background of hepatocellular senescence, namely with the same factors implicated for HPC activation. On this basis, one may interpret the co-existence of HPC and K7(+) hepatocytes as the expression of successive phases of a single pathogenetic mechanism. However, we cannot rule out a histogenetic process analogous to biliary modulation of senescent dysfunctioning hepatocytes running parallel to HPC activation in an attempt of phenotypic-functional accommodation to an altered microenvironment. The additional detection of K7(+) hepatocytes spatially independent of HPC and intermediate cells in this study, as well as the identification of signs of cellular senescence and degeneration in K7(+) hepatocytes reported

by Eleazar et al. [16], may support this hypothesis. In agreement with our findings is the detection of K7(+) hepatocytes in cases of severe fibrosis and cirrhosis [10] and the relationship between K7(+) hepatocytes and hepatitis stage [16].

Poor data exist concerning the possible role of HCV genotype in HPC activation. One report correlated genotype 1 and 4 with higher HPC expression [15], while another correlated hepatocellular p21 expression with HPC and ductular reaction in patients infected with genotype 1 raising the possibility of a contributory role of the latter in liver cell dysfunction [8]. In our study, HCV genotype 1 was associated with the presence of K7(+) hepatocytes pointing towards a direct cytopathic contribution of HCV genotype 1 in the trans-differentiation process.

In conclusion, HPC activation in CHC is a common but diverse phenomenon closely related to increased patient age and fibrosis stage. A predominant periportal expansion pattern and the appearance of K7(+) hepatocytes may represent manifestations of histogenetic mechanisms intimately associated with older age and advanced hepatitis stage, thus implicating hepatocellular senescence and alterations in the microenvironment as contributory factors. In younger ages, HPC activation is usually limited and displays a lobular distribution pattern; K7(+) hepatocytes are almost absent while necroinflammation constitutes a potential triggering factor. The role and fate of activated HPC in CHC need to be further elucidated in future studies.

Acknowledgements The authors acknowledge the support of "Kapodistrias" research grants 70/4/9680 (J.D.) and 70/4/6549 (D.T.), Special Accounts Research Fund (ELKE), National and Kapodistrian University of Athens, Greece. The technical expertise of Dr. Despoina Karandrea is recognized.

Conflict of interest The authors declare that they have no conflict of interest.

References

1. Roskams T, De Vos R, Van Eyken P et al (1998) Hepatic OV-6 expression in human liver disease and rat experiments:evidence for hepatic progenitor cells in man. J Hepatol 29(3):455–463
2. Roskams TA, Theise ND, Balabaud C et al (2004) Nomenclature of the finer branches of the biliary tree: canals, ductules and ductular reactions in human livers. Hepatology 39:1739–1745
3. Kuwahara R, Kofman AV, Landis CS et al (2009) The hepatic stem cell niche: identification by label-retaining cell assay. Hepatology 47:1994–2002
4. Gerber MA, Thung SN, Shen S, Ishak KG (1983) Phenotypic characterization of hepatic proliferation. Antigenic expression by proliferating epithelial cells in fetal liver, massive hepatic necrosis, and nodular transformation of the liver. Am J Pathol 110(1):70–74
5. Demetris AJ, Seaberg EC, Wennerberg A et al (1996) Ductular reaction after submassive necrosis in humans. Special emphasis on analysis of ductular hepatocytes. Am J Pathol 149(2):439–448
6. Fujita M, Furukawa H, Hattori M et al (2000) Sequential observation of liver cell regeneration after massive hepatic necrosis in auxilliary partial orthotopic liver transplantation. Mod Pathol 13(2):152–157
7. Delladetsima J, Kyriakou V, Vafiadis I et al (1995) Ductular structures in acute hepatitis with panacinar necrosis. J Pathol 175 (1):69–76
8. Clouston AD, Powell EE, Walsh MJ et al (2005) Fibrosis correlates with a ductular reaction in hepatitis C: roles of impaired replication, progenitor cells and steatosis. Hepatology 41(4):809–818
9. Tan J, Hytiroglou P, Wieczorek R et al (2002) Immunohistochemical evidence for hepatic progenitor cells in liver diseases. Liver 22(5):365–373
10. Fotiadu A, Tzioufa V, Vrettou E et al (2004) Progenitor cell activation in chronic viral hepatitis. Liver Int 24(3):268–274
11. Roskams T (2003) Progenitor cell involvement in cirrhotic human liver diseases: from controversy to consensus. J Hepatol 39 (3):431–434
12. Libbrecht L, Desmet V, Van Damme B, Roskams T (2000) Deep intralobular extension of human hepatic "progenitor cells" correlates with parenchymal inflammation in chronic viral hepatitis:can "progenitor cells" migrate? J Pathol 192(3):373–378
13. Crosby HA, Hübscher S, Fabris L et al (1998) Immunolocalization of putative human liver progenitor cells in livers from patients with end-stage primary biliary cirrhosis and sclerosing cholangitis using the monoclonal antibody OV-6. Am J Pathol 152(3):771–779
14. Ray MB, Mendenhall CL, French SW, Gartside PS (1993) Bile duct changes in alcoholic liver disease. The veterans administration cooperative study group. Liver 13(1):36–45
15. Tsamandas AC, Syrokosta I, Thomopoulos K et al (2006) Potential role of hepatic progenitor cells expression in cases of chronic hepatitis C and their relation to response to therapy: a clinicopathologic study. Liver Int 26(7):817–826
16. Eleazar JA, Memeo L, Jhang JS et al (2004) Progenitor cell expansion: an important source of hepatocyte regeneration in chronic hepatitis. J Hepatol 41(6):983–991
17. Fausto N (2004) Liver regeneration and repair: hepatocytes, progenitor cells, and stem cells. Hepatology 39(6):1477–1487
18. Sell S (2001) Heterogeneity and plasticity of hepatocyte lineage cells. Hepatology 33(3):738–750
19. Romero-Gallo J, Sozmen EG, Chytil A et al (2005) Inactivation of TGF-beta signaling in hepatocytes results in an increased proliferative response after partial hepatectomy. Oncogene 24 (18):3028–3041
20. Wagayama H, Shiraki K, Yamanaka T et al (2001) p21WAF1/CTP1 expression and hepatitis virus type. Dig Dis Sci 46 (10):2074–2079
21. Roskams T, Yang SQ, Koteish A et al (2003) Oxidative stress and oval cell accumulation in mice and humans with alcoholic and nonalcoholic fatty liver disease. Am J Pathol 163(4):1301–1311
22. Ishak K, Baptista A, Bianchi L et al (1995) Histological grading and staging of chronic hepatitis. J Hepatol 22:696–699
23. Lowes KN, Brennan BA, Yeoh GC, Olynyk JK (1999) Oval cell numbers in human chronic liver diseases are directly related to disease severity. Am J Pathol 154(2):537–541
24. Paradis V, Youssef N, Dangere D et al (2001) Replicative senescence in normal liver, chronic hepatitis C and hepatocellular carcinoma. Hum Pathol 32(3):327–332
25. Falkowski O, An HJ, Ianus IA et al (2003) Regeneration of hepatocyte "buds" in cirrhosis from intrabiliary stem cells. J Hepatol 39(3):357–364
26. Rudolph KL, Chang S, Millard M et al (2000) Inhibition of experimental liver cirrosis in mice by telomerase gene delivery. Science 287(5456):1253–1258

27. Wiemann SU, Satynarayana A, Tsahuridu M et al (2002) Hepatocyte telomere shortening and senescence are general markers of human liver cirrhosis. FASEB J 16(9):935–942
28. Richardson MM, Johnsson JR, Powell EE et al (2007) Progressive fibrosis in non-alcoholic steatohepatitis: association with altered regeneration and a ductular reaction. Gastroenterology 133 (1):350–352
29. Hytiroglou P, Tobias H, Saxena R (2004) The canals of Hering might represent a target of methotrexate hepatic toxicity. Am J Clin Pathol 121(3):324–329
30. Sarraf C, Lalani EN, Golding M et al (1994) Cell behavior in the acetylaminofluorene-treated regenerating rat liver. Light and electron microscopic observations. Am J Pathol 145(5):1114–1126
31. Ikeda K, Wakahara T, Wang YQ et al (1999) In vitro migratory potential of rat quiescent hepatic stellate cells and its augmentation by cell activation. Hepatology 29(6):1760–1767
32. Marra F, Romanelli RG, Giannini C et al (1999) Monocyte chemotactic protein-1 as a chemoattractant for human hepatic stellate cells. Hepatology 29(1):140–148
33. Theise ND, Nimmakayalu M, Gardner R et al (2000) Liver from bone marrow in humans. Hepatology 32(1):11–16
34. Jang YY, Collector MI, Baylin SB et al (2004) Hematopoietic stem cells convert into liver cells within days without fusion. Nat Cell Biol 6(6):532–539
35. Desmet V, Roskams T, Van Eyken P (1995) Ductular reaction in the liver. Pathol Res Pract 191(6):513–524
36. Block GD, Locker J, Bowen WC et al (1996) Population expansion, clonal growth and specific differentiation patterns in primary cultures of hepatocytes induced by HGF/SF, EGF and TGF alpha in a chemically defined (HGM) medium. J Cell Biol 132(6):1133–1149
37. Bisgaard HC, Muller S, Nagy P et al (1999) Modulation of the gene network connected to interferon-gamma in liver regeneration from oval cells. Am J Pathol 155(4):1075–1085
38. Lowes KN, Croager EJ, Abraham LJ et al (2003) Upregulation of lymphotoxin beta expression in liver progenitor (oval) cells in chronic hepatitis C. Gut 52(9):1327–1332
39. Alison MR, Islam S, Lim S (2009) Stem cells in liver regeneration, fibrosis and cancer: the good, the bad and the ugly. J Pathol 217:282–298
40. Fujita M, Furukawa H, Hattori M, Todo S, Ishida Y, Nagashima K (2000) Sequential observation of liver cell regeneration after massive hepatic necrosis in auxiliary partial orthotopic liver transplantation. Mod Pathol 13:152–157

Virchows Arch (2010) 457:467–476
DOI 10.1007/s00428-010-0964-y

ORIGINAL ARTICLE

Androgen receptor is frequently expressed in HER2-positive, ER/PR-negative breast cancers

Donata Micello · Alessandro Marando · Nora Sahnane · Cristina Riva · Carlo Capella · Fausto Sessa

Received: 6 April 2010 / Revised: 9 July 2010 / Accepted: 14 August 2010 / Published online: 31 August 2010
© Springer-Verlag 2010

Abstract The estrogen receptor (ER)/progesterone receptor (PR)-negative breast carcinomas (BCs) encompass three molecular subtypes: one with human epidermal growth factor receptor 2 (HER) overexpression, one normal like, and the triple negative. The androgen receptor (AR) is expressed in 70–90% of invasive BCs. The aim of our study is to detect the expression of AR in a series of ER/PR-negative BCs to ascertain if there is clinical significance in relation to BC molecular subtypes. A immunohistochemical study for all receptors and cytokeratin expression was performed in 232 cases of ER/PR-negative BCs. According to cytokeratin expression, BCs were classified into two groups: luminal-type BCs (44.2%) and basal-like-type BCs (55.8%). According to the expression of HER2, 59.3% were triple-negative BCs (when ER, PR, and HER2 were negative) and 40.7% were HER2-positive BCs. AR expression was observed in 128 tumors (56.6%). One hundred and ten cases (48.8%) had >10% and 18 (7.8%) had <10% of positively stained cells. AR immunoreactivity was found in 31.2% basal-like BCs, while in the luminal group 71.1% of cases were positive, showing highly significant correlation ($p<10^{-8}$). Regarding HER2 status, 76.7% of HER2-positive BC cases were AR positive compared with only 30.4% of triple-negative BC types, showing a strong statistically significant correlation. In conclusion, we show that AR is frequently expressed in ER/PR-negative BCs and that expression of HER2 and AR is highly correlated ($p<0.005$). Our results point out the role of AR and HER2 in the pathogenesis of BCs and suggest the potential role of AR in clinical management of ER/PR-negative BCs.

Keywords AR · HER2 · ER/PR-negative breast cancer

Research support This study has been in part supported by a grant from the University of Insubria, Varese, Italy.

D. Micello · F. Sessa
Department of Anatomic Pathology, Multimedica IRCCS, Milan, Italy

A. Marando · N. Sahnane · C. Riva · C. Capella · F. Sessa
Department of Human Morphology, University of Insubria, Varese, Italy

F. Sessa (✉)
Department of Pathology, Multimedica IRCCS,
Via Fantoli 16/15,
20138 Milan, Italy
e-mail: fausto.sessa@uninsubria.it

Introduction

The role of estrogen receptor (ER) and the progesterone receptor (PR) in human breast carcinomas is well established, but little is known about the significance of androgen receptor (AR). The androgen receptor is expressed in 70% to 90% of invasive breast cancers: a frequency comparable to, or higher than, that reported for ER (60–80%) and PR (50–70%) [1–11]. Although ER, PR, and AR are frequently co-expressed in breast cancers, a considerable proportion of AR-positive carcinomas, ranging from 9% to 50%, are negative for both ER and PR [2, 3, 5, 7, 9, 10, 12–15]. In addition, AR was identified as the only sex steroid receptor expressed in approximately 25% of breast cancer metastases [16].

The influence of AR expression on survival of breast cancer patients is unclear. AR seemed to predict a response to hormone therapy and a better overall survival, but AR expression was not predictive of disease-free survival in ER-positive neoplasms, while ER status was an independent prognostic factor for disease-free survival [5, 13, 17]. For ER-negative tumors, AR positivity was associated with significantly better disease-free survival and with better prognosis for metastatic disease [8] and with significantly better survival after disease recurrence compared with AR-negative tumors [18].

Gene expression profiles allow breast carcinoma (BC) classification into five main groups, two of them ER+ (luminal A and luminal B) and three ER− (human epidermal growth factor receptor 2 (HER)+, basal like, and normal breast like). The main immunophenotype of the basal-like group as defined by gene expression analysis is the lack of expression of ER, PR, and HER2 and the expression of basal-associated markers such as basal cytokeratins (CK5, CK17, and CK14) and EGFR. These are currently used as surrogate immunohistochemical markers for the identification of basal-like BCs in routine practice [15, 19–23]. The normal-like gene expression pattern was typified by the high expression of gene characteristic of adipose tissue and other non-epithelial cell types. This molecular subtype is not easily defined by immunohistochemical surrogates (ER−, PR−, HER2−, CK5/6−), and thus these tumors were designated as an "unclassified group." Farmer et al. [24] have shown that AR expression level divides ER-negative tumors into two major gene expression clusters, including ER−/AR− (basal) and ER−/AR+ (molecular apocrine subtype).

HER2 is a well-known prognostic and predictive parameter [25] and represents a biologically and clinically important feature. HER2 protein overexpression has been detected in 20–30% of invasive breast carcinoma [26, 27], and it has been found both in ER+ and in ER− breast cancer [28]. Some studies have investigated the relationship between AR and HER2 immunohistochemical status in breast carcinomas with conflicting results. Narita et al. [11], in agreement with other workers [6, 14], did not find any significant correlation, but other studies reported HER2 overexpression in grade 3, AR-positive carcinomas [8, 9, 29]. In addition, a functionally significant crosstalk between androgen receptor and the HER2 pathway has been identified in ER-negative breast cancer [30].

The prevalence and role of AR expression in triple-negative ER−/PR−/HER2 have not been clearly elucidated. Rakha et al. [31], investigating 282 triple-negative consecutive invasive breast cancers, showed AR expression in 13% of the cases.

The aim of this study was to evaluate the immunohistochemical expression of AR in a series of 232 ER− and PR− breast cancer and to correlate it with HER2 expression. In addition, the AR expression has been correlated with clinicopathological parameters, histopathological features, and follow-up data.

Materials and methods

Histological study

A total of 232 cases of ER- and PR-negative invasive BCs were selected among 1,301 consecutive invasive ductal BCs collected at the Department of Pathology, Ospedale di Circolo, and University of Insubria, Varese, Italy, from 1995 to 2000. Criteria for selection included the following: the cases were primary breast cancer, the histological type was ductal invasive carcinoma, NOS, excluding the apocrine and adenoid-cystic cancer types, and the immunohistochemical expression of ER and PR was considered negative (carcinomas were completely negative in 208 cases or present in less than 10% of tumor cells in 24 cases included in our series because clinical treatment followed guidelines of completely negative BCs). A complete and intense membrane staining for HER2 in >10% of tumor cells was considered as positive (94 cases). Of these BCs, 89 cases showed HER2 positivity in >30% of tumor cells (score 3+) while the remaining five cases were scored 2+. No FISH test for HER2 amplification was done for these cases. The tumor ER, PR, and HER2 status was available from pathology reports. Clinicopathological information concerning age, tumor site, size, and local extension were obtained from patient records. The tumor pathological stage was assessed according to the TNM sixth edition recommendations [32].

Formalin-fixed paraffin-embedded sections of tissues obtained from surgical samples (226 cases) and trucut core biopsies (six cases) were routinely stained with hematoxylin and eosin (H&E) for morphological assessment. Microscopic slides of all cases were reviewed by two senior pathologists (CR and FS) in order to assess the histological type, according to the World Health Organization's recommendations [33], and the grade, applying the Elston–Ellis criteria [34].

Immunohistochemical study

For each case, immunohistochemical expression of AR was evaluated along with p53 and proliferative index (Ki-67, antibody MIB-1). In addition, basal and luminal differentiation of breast carcinomas was investigated using antibodies against CK5, CK14, CK8, and CK18 [35, 36]. In all cases, 4-μm-thick paraffin sections were deparaffinized in bioclear and rehydrated through a graded series of ethanol. Endogenous peroxidase activity was inhibited with 10% hydrogen peroxide (H_2O_2) in distilled water for 10 min. Antigen retrieval was provided using microwave for 10 min in 0.01 M sodium citrate buffer pH 6 and protease digestion. Sections were incubated overnight at 4°C with the primary antibodies and subsequently for 1 h with a 1:200 dilution of biotin-labeled secondary anti-mouse or anti-rabbit antibody followed by ABC complex (avidin, 1:100, and biotin-labeled peroxidase, 1:100) (Dako). Sections were then stained with a solution of 3,3′diaminobenzidine (Sigma) with H_2O_2 in Tris–HCl buffer, pH 7.4, lightly counterstained with Mayer's hematoxylin, dehy-

drated, and mounted. (The source and dilution of primary antibodies used are listed in Table 1.)

In all cases, immunoreactivity was semiquantitatively evaluated and recorded as the percentage of positive cells. BCs were classified as basal like when at least 5% of cancer cells were immunoreactive for CK5 and/or CK14, independent of the intensity of the immunostaining [35, 36]. For AR, we considered nuclear labeling in more than 10% of neoplastic cells as the cutoff point for positivity, similar to standardized criteria used for other steroid hormone receptors [9].

Positive controls included normal breast tissue surrounding the neoplastic lesion (for all antibodies) and normal prostatic tissue (for AR). Negative controls included the omission of primary antibodies. All the immunoreactions were separately evaluated by two senior pathologists.

Statistical analysis

The statistical analysis was performed using the χ^2 test with Yates' correction (SPSS 7.5 software). The survival analysis was performed by employing the Kaplan–Meier product limit estimate of probability of survival against time, producing a product limit survival curve for each of the following variables: age, stage, presence of lymph node metastases, and immunohistochemical expression of basal (CK5, CK14) and luminal (CK8, CK18) immunophenotype and AR.

Multivariate analysis was carried out using the Cox proportional hazard model. Variables with $p<0.15$ in the univariate analysis were entered into the multivariate analysis. For all the survival analyses, the Survan XL program, version 1.14 (copyright © 1995–1997), was employed.

Table 1 Antibodies used for the immunohistochemical study

Ab	Source	Clone	Retrieval	Dilution
ER	DAKO	1D5	CB pH6, MW5′x4	1/100
PR	YLEM	1A6	CB pH6, MW5′x4	1/20
HER2	DAKO	–[a]	CB pH6, MW5′x2	1/400
P53	DAKO	DO7	CB pH6, MW5′x2	1/500
Ki-67	DAKO	MIB1	CB pH6, MW5′x4	1/100
CK5	Novocastra	XM26	CB pH6, MW 5′x2	1/200
CK14	Novocastra	LL002	CB pH6, MW 5′x2	1/20
CK8	DAKO	35βH11	CB pH6, MW 5′x2	1/100
CK18	DAKO	DC-10	CB pH6, MW 5′x2	1/40
AR	Novocastra	AR27	CB pH6, MW 5′x2	1/20

CB citrate buffer, *MW* microwave

[a] Polyclonal rabbit antibody anti-human HER2 oncoprotein

Results

Clinicopathological data and immunoprofile

The mean age of the 232 patients at diagnosis was 58.7 years (range 24–97 years). The most frequent location of tumors was the upper-external quadrant (37%), and the diameter ranged from 0.3 to 10.5 cm (mean 2.37 cm). The pathological stage at diagnosis was known in 224 patients: 112 tumors were in stage pT1 (50%), 91 in pT2 (40.6%), five in pT3 (2.2%), and 16 in pT4 (7.1%). Lymph node status was available for 175 cases in which axillary dissection was performed, and lymph node involvement was present in 83 cases (47.4%). The series of 232 cases included 216 (93.1%) poorly differentiated (G3) and 16 (6.8%) moderately differentiated (G2) ductal BCs.

The mean percentage of Ki-67-positive nuclei was 55.7% (range 14–95). Overexpression of p53 in more than 10% of tumor cells was present in 168/231 (72.7%) cases with a mean percentage of p53-positive nuclei of 63.6%. The comprehensive results of the immunohistochemical study are reported in Table 2. According to luminal and basal cytokeratin expression, tumors were classified into two groups: 100 (44.2%) luminal-type BCs, expressing only CK8 and/or CK18, and 126 (55.8%) basal-like-type BCs positive for CK5 and/or CK14 in more than 5% of cancer cells, often also showing luminal cytokeratin expression; six cases failed. In addition, according to the expression of HER2, 137 (59.3%) cases were considered as triple-negative BCs (when ER, PR, and HER2 were negative) (Fig. 1) and 94 (40.7%) as HER2-positive BCs; one case failed.

AR immunohistochemistry

AR expression was evaluable in 226 cases, and AR positivity was observed in 128 BCs (56.6%). One hundred and ten cases (48.8%) had >10% positive cells, with an average of 59% of AR nuclear immunoreactivity (range 10–100%), and 18 (7.8%) showed <10% of positively stained cells, and 98 tumors (43.4%) were AR negative (Table 3).

Comparison of AR expression with other tumor clinicopathological features is shown in Table 4. While the pT did not show any statistically significant difference between T1 and T2–T3–T4 (45.8% of cases versus 51.8%; $p=0.38$), the correlation of lymph node status with AR expression showed statistically significant results ($p<0.034$). In fact, axillary lymph node metastases were present in 63.4% (52/82) of patients with AR-positive tumors, compared with 36.6% (30/82) of those with AR-negative lesions. On the contrary, 41 out 89 (46.1%) pN0 patients were AR positive and 48 out 89 (53.9%) were AR negative. Regarding tumor

Table 2 Clinicopathological profile of ER- and PR-negative breast carcinoma

Variable	Number	Percent
Number of cases	232	
Mean age (years ± SD)	65.8±8.67	
Immuno classification[a]		
Luminal type	100	44.2
Basal-like type	126	55.8
HER2 positive	94	40.7
HER2 negative	137	59.3
Grade of differentiation		
G2	16	6.9
G3	216	93.1
T stage (226 cases)		
1	112	50
2	91	40.6
3	5	2.2
4	16	7.1
Lymph node status (175 cases)		
N0	92	52.6
N1	50	28.6
N2	26	14.8
N3	7	4.0

[a] Number of cases may not sum to the total of 232 due to missing values on the variable of interest

grade, AR positivity was seen in eight (50%) out of 16 G2 cases and in 102 (48.6%) out of 210 G3 cases.

The basal-like-type BCs were AR positive in 31.2% (39/125) of cases, while in the luminal group 71.1% of cases (69/97) were positive, showing highly significant correlation ($p<10^{-8}$). Regarding AR immunoexpression and HER2 status, statistical analysis showed a strongly significant correlation: 76.7% (69/90) of HER2 positive BCs cases were AR positive (Fig. 2) compared with only 30.4% (41/135) of triple-negative BC types ($p<10^{-10}$).

Survival analysis

Information about overall and disease-free survival was available for 224 patients: 138 (61.6%) patients were alive after a median follow-up time of 116.4 months (range 83–173 months) while 86 (38.4%) out of 224 were dead of disease after a median follow-up time of 36.3 months (range 2–99 months). Regarding clinical evolution, 130 of the 138 alive patients (94.2%) were disease free after a median follow-up time of 116.2 months (range 83–173 months), while only eight (5.8%) experienced disease relapse after a median follow-up time of 68.3 months (range 6–119 months). For the group of the 86 dead women, 54 (62.8%) patients died with disease after a median follow-up of 33.63 months (range 2–99 months) while 32 (37.2%) developed a disease relapse after a median of 34.3 months (range 0–71 months).

No relationship between overall survival and AR expression was found ($p=0.16$). In fact, among the still-living patients, 45.3% (62/137) harbored AR-positive BCs and 54.7% (75/137) harbored AR-negative BCs, while among the 84 deceased patients, 47 (56%) harbored AR-positive BCs and 37 (44%) harbored AR-negative ones.

Also, there was no significant correlation between AR status and disease-free survival ($p=0.44$) since 22 (56.4%) of 39 patients with disease relapse harbored AR-positive BCs and 17 (43.6%) harbored AR-negative BCs. On the other hand, of the 183 patients with no evidence of distant metastasis, 86 (46.9%) women harbored AR-positive BCs while 93 (50.8%) harbored AR-negative BCs.

Survival analysis has been performed to determine a possible relationship between patient outcome and age at diagnosis, stage, presence of lymph node metastases, and immunohistochemical expression of basal (CK5, CK14) and luminal (CK8, CK18) markers and AR. Factors influencing survival in the univariate analysis were age at diagnosis (the probability of survival after a follow-up time of 144 months was 87.4% for patients ≤40 years old vs 57.5% for patients >40 years old, $p=0.006$), pT stage (median survival time of 100 months for T1 vs 84 months for T2–T3–T4, $p<0.0001$), and axillary lymph node status (median survival time of 101 months for lymph-node-negative tumors vs 70 months for lymph-node-positive tumors, $p<0.0001$) (Figs. 3 and 4).

Multivariate analysis was performed using the Cox proportional hazard model including the three variables which were statistically significant in the univariate analysis. Results showed that stage and lymph node status are independent prognostic factors ($p=0.0261$ and $p=0.0017$ respectively, Table 5).

Discussion

AR as a target for the treatment of hormone-receptor-negative breast cancer is an uncharacterized territory and targeting AR with AR androgen-based hormonal therapy in ER and PR breast cancer should be taken into consideration as potential interactions between AR and other tumor-growth-related factors [37]. Recently, there has been renewed interest in alternative hormonal treatment, including progestin medroxyprogesterone acetate, for use both in early disease and in the advanced setting when conventional therapies fail [38–40]. These studies suggest AR as a marker for the efficiency of endocrine

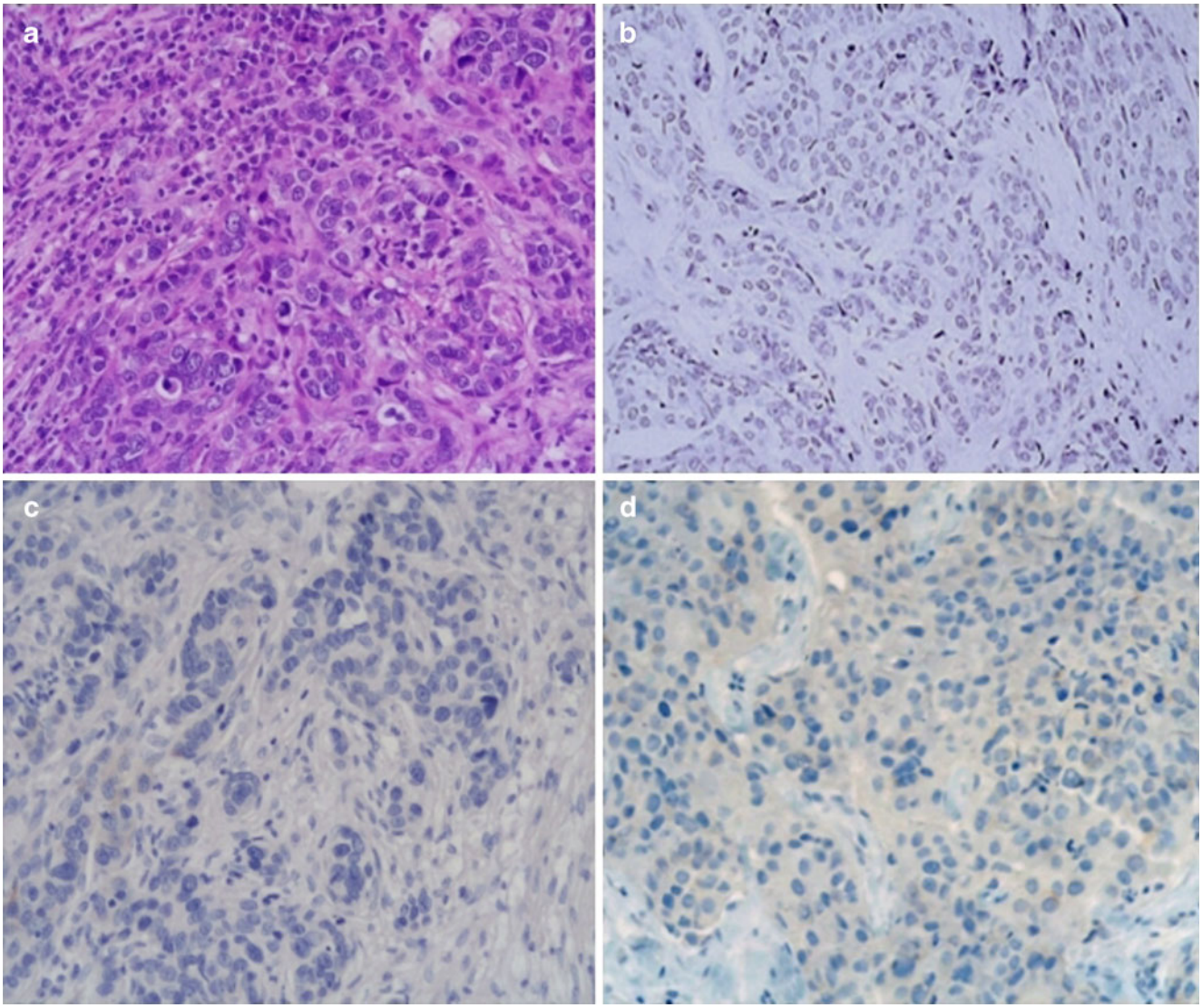

Fig. 1 Grade 3 triple-negative BC (**a** H&E staining) showing negative ER (**b**), HER2 (**c**), and AR (**d**) immunostaining

therapy and for new hormonal therapeutic strategies in women with estrogen-negative cancer.

Other studies have examined the significance of AR in breast carcinomas, usually in comparison with ER and PR status, but few immunohistochemical studies have investigated the expression of AR as the only sex steroid receptor expressed in ductal invasive breast carcinomas. In this context, our study focused on a large series of ER- and PR-negative ductal carcinomas, since most ER/PR-positive tumors are AR positive. It is clear from this study that AR expression is a frequent feature of ER- and PR-negative ductal breast carcinomas. Our results show a 56.6% incidence of AR positivity in ER- and PR-negative ductal invasive breast carcinomas, which is similar to the earlier reported percentage in previous investigations [8, 9, 41].

Table 3 Expression of AR in 226 ER- and PR-negative breast cancer

Mean positive nuclear tumor cells (%)	No. of cases	%
0	98	43.4
<10	18	7.8
≥10	110	48.8

As is commonly expected in ER- and PR-negative ductal breast carcinomas, in the present investigation, almost all tumors (93.1%) were G3, showing a higher percentage of G3 cases than those (74%) reported by Scawn and Shousha [41]. AR positivity has been shown in 48.6% of poorly differentiated carcinomas (G3), in agreement with previous immunohistochemical studies examining a smaller series of cases of ER/PR-negative breast carcinomas [5, 8, 9, 11, 14].

Table 4 Correlation between AR immunoexpression and other clinical and histopathological features

Parameter	n[a] (226)	n AR+ (%)	n AR− (%)	p
pT1	107	49 (45.8)	58 (54.2)	0.38
pT2 pT3 pT4	112	58 (51.8)	54 (48.2)	
Nodal status				
+	82	52 (63.4)	30 (36.6)	<0.034
–	89	41 (46.1)	48 (53.9)	
G1	0	0	0	0.89
G2	16	8 (50)	8 (50)	
G3	210	102 (48.6)	108 (51.4)	
Luminal type	97	69 (71.1)	28 (28.9)	$<10^{-8}$
Basal-like type	125	39 (31.2)	86 (68.8)	
HER2 positive	90	69 (76.7)	21 (23.3)	$<10^{-10}$
HER2 negative	135	41 (30.4)	94 (69.6)	
Alive	137	62 (45.3)	75 (54.7)	0.16
Dead	84	47 (56)	37 (44)	
Age				
≤ 40	26	7 (31.8)	15 (68.2)	$<10^{-3}$
> 40	198	103 (50.5)	37 (49.5)	
Disease relapse				
+	39	22 (56.4)	17 (43.6)	0.44
–	183	86 (46.4)	93 (50.8)	

[a] n number of cases; number of cases may not sum to the total of 226 due to missing values on the variable of interest. Statistically significant at $P<0.05$

Bryan et al. [17] did not find a significant correlation between AR and menopausal status in their patients, in contrast with Agoff and colleagues [8] who found that AR expression correlated with both increasing age and menopausal status. For our study, no information was available about menopausal status of the patients, but we could not find any tumor correlation of AR expression of BCs and the age of the patients.

Regarding the nodal status, which represents a reliable prognostic factor in breast carcinoma, there was a significant correlation between lymph node status and overall survival. In our study, we found that the percentage of axillary lymph node disease was 47.4%, in agreement with other investigations [41, 42] but higher than the general incidence of 20–30% commonly observed in the breast cancer [43]. One notable finding of the current study was the positive association between AR expression and lymph node metastases, in contrast with the results of other studies [6, 11]. On the other hand, we did not find a correlation of AR expression with the pT stage of the tumors, in agreement with recent studies [10].

An interesting finding of our study was the significant correlation between AR expression and HER2 status. This result is in agreement with the observations of other workers that have detected HER2 overexpression in G3-AR-positive carcinomas [8, 9, 29] but is in contrast with some other studies [6, 11, 14]. These data suggest that AR can be involved in the pathogenesis of breast carcinomas, indicating that HER2 may control the transcriptional activity of AR, the latter regulating its own transcription. The interaction of AR with the HER2-related pathway has been investigated in human prostate cancer cell lines, suggesting a crosstalk between AR and HER2 pathway and demonstrating that HER2 induces AR transactivation through the MAP kinase pathway [44–48]. These findings have potential clinical relevance since anti-androgens did not inhibit AR in the presence of HER2.

Doane et al. [28] point out the heterogeneity of AR expression as well as the complexity of AR signaling in breast cancer, showing that androgens inhibited the growth of some cell lines but stimulated the growth of other cell lines. Because of the clinical heterogeneity of ER-negative, PR-negative tumors, Doane et al. [28] speculated that molecular subsets exist in ER- and PR-negative tumors and postulated that AR may act in concert with other signal transduction pathway, and it is known that receptor tyrosine kinase pathway functions as a modulator of nuclear hormone receptor activity [49]. Very recently, similar results have been reported by Niemeier et al. [50] who, studying the AR expression in 189 consecutive BCs, outlined the close association between AR positivity and HER2 status in five out of eight HER2 BCs while Park et al. [51] reported the AR positivity in 32 out of 43 HER2 BCs. The authors suggest a potential target role for AR both in AR+ HER2 BC molecular class and in AR+ triple-negative BCs.

Carcinoma of the breast is recognized to be a heterogeneous disease consisting of phenotypically diverse population of cancer cells. Previous studies have demonstrated that BCs with basal-like phenotype is a special group of tumors that appear to be predominantly grade 3 ER and PR negative [52] and is characterized by a specific immunohistochemical profile and poor prognosis [51–53]. In our study, basal-like carcinomas represented more than half of the cases (55.8%), and they expressed AR receptors less frequently (31.2% of the cases) than luminal carcinomas (71.1% of the cases), in agreement with other investigations [15, 31, 54].

The prognostic significance of AR expression in ER- and PR-negative breast cancer has been poorly investigated, while most studies have emphasized the prognostic value of AR status in ER+/PR+ BCs [5, 7, 13, 14, 17]. Our study focused on ER- and PR-negative tumors and did not find any association between AR expression with both the overall survival and the disease-free survival (Fig. 3). Our findings are only partially in agreement with previous investigations [8] that have found an association between AR expression and disease-free survival in the subset of patients with ER-negative BCs in univariate analysis but not in multivariate.

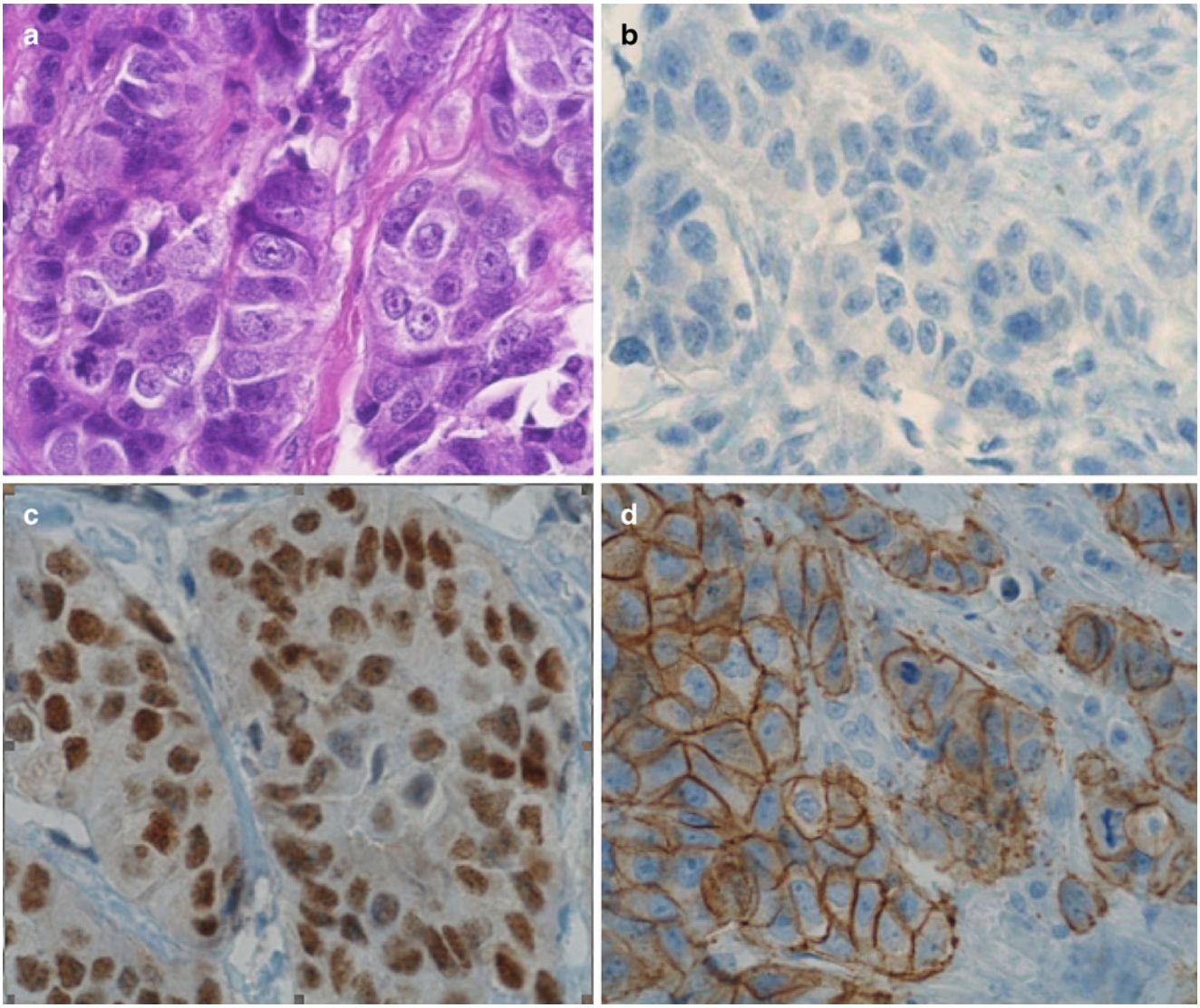

Fig. 2 Grade 3 BC (**a** H&E staining) showing negative ER immunostaining (**b**) and strong AR immunostaining (**c**) together with HER2, score 3 positivity (**d**)

Our investigation has shown that, with multivariate analysis, only lymph node status and tumor size were independent prognostic variables, while AR status was not a significant predictor of disease-free survival and overall survival as well as the luminal, basal-like, and HER2 immunohistochemical categories. These results may be explained by the fact that our study was concentrated on ER- and PR-negative tumors, which tend to be high-grade ductal carcinomas with more advanced stage at diagnosis and a high rate of proliferation. On the other hand, this study was a retrospective investigation, and our survival curves may reflect innate characteristics of the tumors since that treatment has not been influenced by AR expression, and all patients had received standard therapies. In fact, the therapeutic approach to BCs in the middle of the 1990s was non-tailored as suggested by the more recent treatment guidelines. Although AR is expressed in almost 50% of ER-negative tumors, the functional role of AR in BC remains unclear; further exploration of this area could expand the repertoire of potential treatment for patient with ER-negative breast cancer [55].

We can conclude that AR is frequently expressed in ER- and PR-negative poorly differentiated (G3) BCs and that expression of HER2 and AR is highly correlated ($p<$ 0.005). In addition, a notable finding was that the majority of AR-positive BCs were lymph node positive. The frequent expression of AR and common coexpression of AR and HER2 oncoprotein in ER- and PR-negative BCs raise the important question of the role of AR and HER2 in

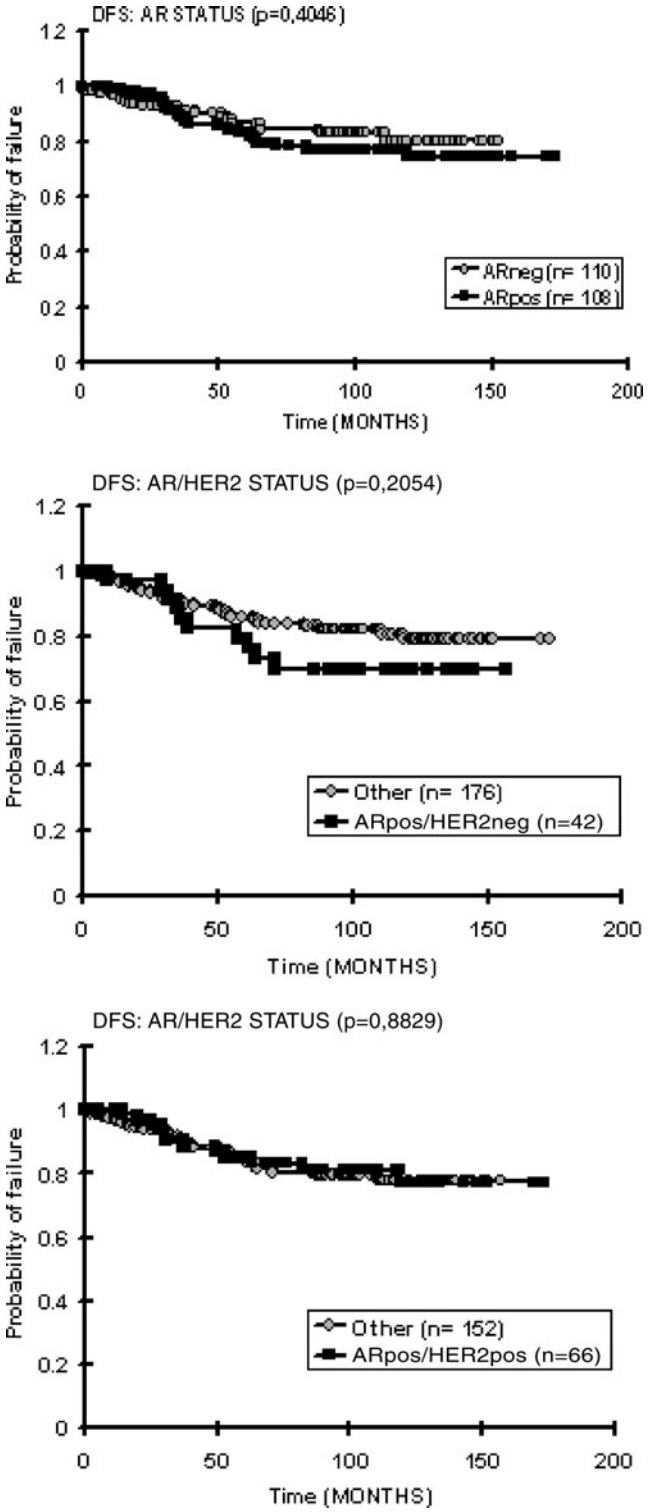

Fig. 3 Kaplan–Meier survival curves illustrating disease-free survival for patients stratified by AR status and AR/HER2 status. No significant differences was observed

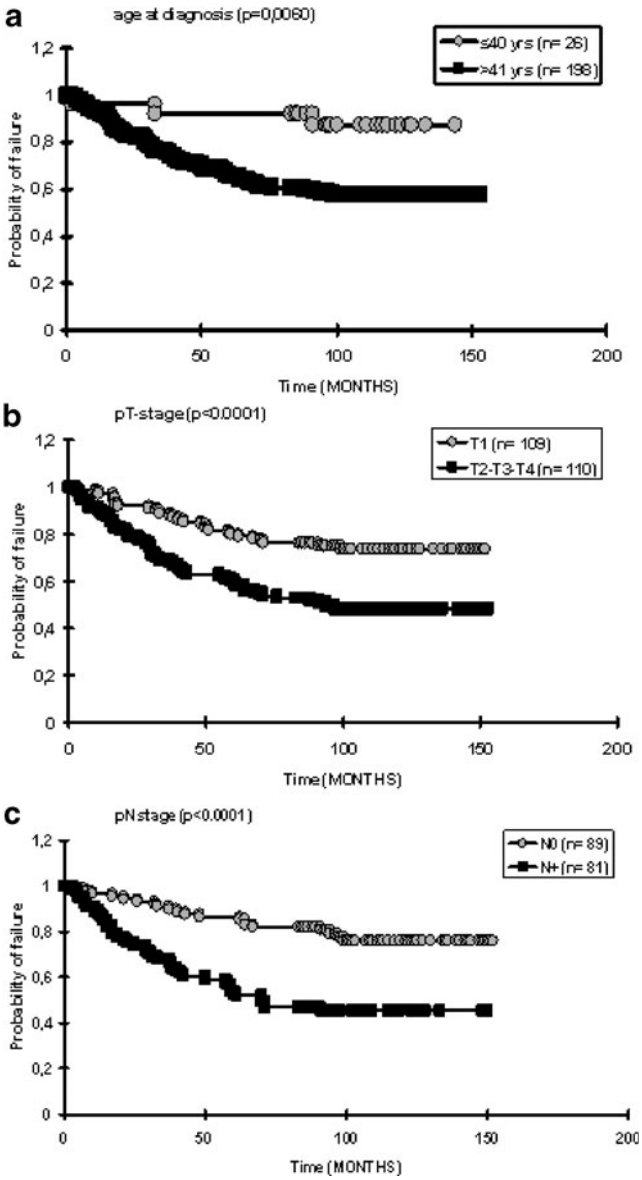

Fig. 4 Kaplan–Meier survival curves illustrating overall survival for patients stratified by age at diagnosis (**a**), pT stage (**b**), and lymph node status (**b**). Significantly worse survival rates were noticed for patients with tumors occurred after the age of 40 years, advanced pT stage and presence of lymph node metastases

the pathogenesis and treatment of ER- and PR-negative BCs. Further investigations of AR in ER- and PR-negative BCs could provide more information concerning the involvement of AR in the pathogenesis of breast cancer and the potential role in clinical management of women with ER- and PR-negative breast carcinomas.

Table 5 Results of multivariate analysis

Variable	HR	95% CI	*p* value
Age at diagnosis	3.7929	0.9296–15.4749	0.065
pT stage	1.8759	1.0806–3.2566	0.026
Lymph node status	2.4581	1.4050–4.3006	0.0017

Conflict of interest statement We declare that we have no conflict of interest.

References

1. Ellis LM, Wittliff JL, Bryant MS et al (1989) Correlation of estrogen, progesterone, and androgen receptors in breast cancer. Am J Surg 157:577–581
2. Lea OA, Kvinnsland S, Thorsen T et al (1989) Improved measurement of androgen receptors in human breast cancer. Cancer Res 49:7162–7167
3. Kimura N, Mizokami A, Oonuma T et al (1993) Immunocytochemical localization of androgen receptor with polyclonal antibody in paraffin-embedded human tissue. J Histochem Cytochem 41:671–678
4. Hall RE, Aspinall JO, Horsfall DJ et al (1996) Expression of the androgen receptor and an androgen-responsive protein, apolipoprotein D, in human breast cancer. Br J Cancer 74:1175–1180
5. Kuenen-Boumeester V, Van Der Kwast TH, Claassen CC et al (1996) The clinical significance of androgen receptors in breast cancer and their relation to histological and cell biological parameters. Eur J Cancer 32A:1560–1565
6. Bièche I, Parfait B, Tozlu S et al (2001) Quantitation of androgen receptor gene expression in sporadic breast tumors by real-time RT-PCR: evidence that MYC is an AR-regulated gene. Carcinogenesis 22:1521–1526
7. Brys M, Wojcik M, Romanowicz-Makowska H et al (2002) Androgen receptor status in female breast cancer: RT-PCR and Western blot studies. J Cancer Res Clin Oncol 128:85–90
8. Agoff SN, Swanson PE, Linden H et al (2003) Androgen receptor expression in estrogen receptor-negative breast cancer. Immunohistochemical, clinical and prognostic associations. Am J Clin Pathol 120:725–731
9. Moinfar F, Okcu M, Tsybrovskyy O et al (2003) Androgen receptors frequently are expressed in breast carcinomas. Potential relevance to new therapeutic strategies. Cancer 98:703–711
10. Riva C, Dainese E, Caprara G et al (2005) Immunohistochemical study of androgen receptors in breast carcinoma. Evidence of their frequent expression in lobular carcinoma. Virchows Arch 447:695–700
11. Narita D, Raica M, Suciu C et al (2006) Immunohistochemical expression of androgen receptor and prostate-specific antigen in breast cancer. Folia Histochem Cytobiol 44:165–172
12. Kuenen-Boumeester V, Van Der Kwast TH, Van Putten WLJ et al (1992) Immunohistochemical determination of androgen receptors in relation to oestrogen and progesterone receptors in female breast cancer. Int J Cancer 52:581–584
13. Soreide JA, Lea OA, Varhaug JE et al (1992) Androgen receptors in operable breast cancer: relation to other steroid hormone receptors, correlation to prognostic factors and predictive value for effect of adjuvant tamoxifen treatment. Eur J Surg Oncol 18:112–118
14. Isola JJ (1993) Immunohistochemical demonstration of androgen receptor in breast cancer and its relationship to other prognostic factors. J Pathol 170:31–35
15. Rakha EA, El-Sayed ME, Green AR et al (2007) Breast carcinoma with basal differentiation: a proposal for pathology definition based on basal cytokeratin expression. Histopathology 50:434–438
16. Bayer-Garner IB, Smoller B (2000) Androgen receptors: a marker of increase sensitivity for identifying breast cancer in skin metastasis of unknown primary site. Mod Pathol 13:119–122
17. Bryan RM, Mercer RJ, Bennett RC et al (1984) Androgen receptors in breast cancer. Cancer 54:2436–2440
18. Schippinger W, Regitnig P, Dandachi N et al (2006) Evaluation of the prognostic significance of androgen receptor expression in metastatic breast cancer. Virchows Arch 449:24–30
19. Perou CM, Sørlie T, Eisen MB et al (2000) Molecular portraits of human breast tumours. Nature 406:747–752
20. Sørlie T, Perou CM, Tibshirani R et al (2001) Gene expression patterns of breast carcinomas distinguish tumor subclasses with clinical implications. Proc Natl Acad Sci U S A 98:10869–10874
21. Sørlie T, Tibshirani R, Parker J et al (2003) Repeated observation of breast tumor subtypes in independent gene expression data sets. Proc Natl Acad Sci U S A 100:8418–8423
22. El-Rehim A, Ball G, Pinder SE et al (2005) High-throughput protein expression analysis using tissue microarray technology of a large well-characterised series identifies biologically distinct classes of breast cancer confirming recent cDNA expression analyses. Int J Cancer 116:340–350
23. Mattie MD, Benz CC, Bowers J et al (2006) Optimized high-throughput microRNA expression profiling provides novel biomarker assessment of clinical prostate and breast cancer biopsies. Mol Cancer 5:24
24. Farmer P, Bonnefoi H, Becette V et al (2005) Identification of molecular apocrine breast tumours by microarray analysis. Oncogene 24:4660–4671
25. Quenel N, Wafflart J, Bonichon F et al (1995) The prognostic value of c-erbB2 in primary breast carcinomas: a study on 942 cases. Breast Cancer Res Treat 35:283–291
26. Hubbard AL, Doris CP, Thompson AM et al (1994) Critical determination of the frequency of c-erbB-2 amplification in breast cancer. Br J Cancer 70:434–439
27. Ross JS, Fletcher JA (1999) HER-2/neu (c-erb-B2) gene and protein in breast cancer. Am J Clin Pathol 112:S53–S67
28. Doane AS, Danso M, Lal P et al (2006) An estrogen receptor-negative breast cancer subset characterized by a hormonally regulated transcriptional program and response to androgen. Oncogene 25:3994–4008
29. Liegl B, Horn LC, Moinfar F (2005) Androgen receptors are frequently expressed in mammary and extramammary Paget's disease. Mod Pathol 18:1283–1288
30. Naderi A, Hughes-Davies L (2008) A functionally significant cross-talk between androgen receptor and ErbB2 pathways in estrogen receptor negative breast cancer. Neoplasia 10:542–548
31. Rakha EA, El-Sayed ME, Green AR et al (2007) Prognostic markers in triple-negative breast cancer. Cancer 109:25–32
32. Greene FL, Page DL, Fleming ID et al (2002) The AJCC cancer staging manual, 6th edn. Springer, New York, pp 257–281
33. Tavassoli FA, Devilee P (2003) Pathology & genetics tumours of the breast and female genital organs. WHO, Albany
34. Elston CW, Ellis IO (2002) Pathological prognostic factors in breast cancer I The value of histological grade in breast cancer: experience from a large study with long-term follow-up. Histopathology 41(3):151–153, Histopathology 1991;403–410
35. Laakso M, Loman N, Borg A, Isola J et al (2005) Cytokeratin 5/14-positive breast cancer: true basal phenotype confined to BRCA1 tumors. Mod Pathol 18:1321–1328
36. Laakso M, Tanner M, Nilsson J et al (2006) Basoluminal carcinoma: a new biologically and prognostically distinct entity between basal and luminal breast cancer. Clin Cancer Res 12:4185–4191
37. Nahleh Z (2008) Androgen receptor as a target for the treatment of hormone receptor-negative breast cancer: an unchartered territory. Future Oncol 4:15–21
38. Zaucha R, Sosinska-Mielcarek K, Jassem J (2004) Long-term survival of a patient with primarily chemo-resistant metastatic breast cancer treated with Medroxyprogesterone acetate. Breast 13:321–324

39. Otani S, Toyota N, Nozaka K et al (2004) Successful combination therapy with 5′-DFUR and MPA for breast cancer with spinal and vertebral metastases. Gan To Kagaku Ryoho 31:2151–2153
40. Focan C, Beauduin M, Majos F et al (2004) High-dose oral medroxyprogesterone acetate or tamoxifen as adjuvant hormone therapy for node-negative early-stage breast cancer: randomized trial with 7-year update. Clin Breast Cancer 5:136–141
41. Scawn R, Shousha S (2002) Morphologic spectrum of estrogen receptor-negative breast carcinoma. Arch Pathol Lab Med 126:325–330
42. Putti TC, El-Rehim DM, Rakha EA et al (2005) Estrogen receptor-negative breast carcinomas: a review of morphology and immunophenotypical analysis. Mod Pathol 18:26–35
43. Allred DC, Harvey JM, Berardo M et al (1998) Prognostic and predictive factors in breast cancer by immunohistochemical analysis. Mod Pathol 11:155–168
44. Yeh S, Lin HK, Kang HY et al (1999) From HER/Neu signal cascade to androgen receptor and its coactivators: a novel pathway by induction of androgen target genes through MAP kinase in prostate cancer cells. Proc Natl Acad Sci U S A 96:5458–5463
45. Meng TC, Lee MS, Lin MF (2000) Interaction between protein tyrosine phosphatase and protein tyrosine kinase is involved in androgen-promoted growth of human prostate cancer cells. Oncogene 19:2664–2677
46. Liu Y, Majumder S, McCall W et al (2005) Inhibition of HER-2/neu kinase impairs androgen receptor recruitment to the androgen responsive enhancer. Cancer Res 65:3404–3409
47. Guo Z, Dai B, Jiang T et al (2006) Regulation of androgen receptor activity by tyrosine phosphorylation. Cancer Cell 66 (10):309–319
48. Mellinghoff IK, Vivanco I, Kwon A et al (2004) HER2/neu kinase-dependent modulation of androgen receptor function through effects on DNA binding and stability. Cancer Cell 6:517–527
49. Shao D, Lazar MA (1999) Modulating nuclear receptor function: may the phos be with you. J Clin Invest 103:1617–1618
50. Niemeier LA, Dabbs DJ, Beriwal S et al (2010) Androgen receptor in breast cancer: expression in estrogen receptor-positive tumors and in estrogen receptor-negative tumors with apocrine differentiation. Mod Pathol 23:205–212
51. Park S, Koo J, Park HS et al (2010) Expression of androgen receptors in primary breast cancer. Ann Oncol 21:488–492
52. Jones C, Nonni AV, Fulford L et al (2001) CGH analysis of ductal carcinoma of the breast with basaloid/myoepithelial cell differentiation. Br J Cancer 85:422–427
53. Nielsen TO, Hsu FD, Jensen K et al (2004) Immunohistochemical and clinical characterization of the basal-like subtype of invasive breast carcinoma. Clin Cancer Res 10:5367–5374
54. Rakha EA, Putti TC, Abd El-Rehim DM et al (2006) Morphological and immunophenotypic analysis of breast carcinomas with basal and myoepithelial differentiation. J Pathol 208:495–506
55. Moe RE, Anderson BO (2007) Androgens and androgen receptors: a clinically neglected sector in breast cancer biology. J Surg Ong 95:437–439

Virchows Arch (2010) 457:477–482
DOI 10.1007/s00428-010-0955-z

ORIGINAL ARTICLE

Differential expression of glu-tubulin in relation to mammary gland disease

Hajime Kuroda · Ken Saito · Mina Kuroda · Yutaka Suzuki

Received: 12 April 2010 / Revised: 17 June 2010 / Accepted: 25 July 2010 / Published online: 10 August 2010
© Springer-Verlag 2010

Abstract Tubulin is one of the molecular components that regulate cytosketal structure relating to cell differentiation, invasion, and metastasis in cancer. Recently, glu-tubulin, in which the C-terminal tyrosine of α-tubulin is removed by tubulin carboxypeptidase, overexpression has been reported in malignant tumors of the mammary gland immunohistochemically. We identified 147 cases accessioned in the Department of Pathology, International University of Health and Welfare Hospital from 2003 to 2009. Of the 78 malignant tumor cases, staining for glu-tubulin was observed in 56 (71.8%), and only 22 cases showed no significant staining. However, in benign disease, glu-tubulin staining was detected in the cytoplasm of fibroblasts and endothelial cells, but was completely absent from epithelial cells in 64 of 69 cases. When the expression of glu-tubulin was compared between malignant tumor, benign tumor, and other benign disease, a significant differentiation was found among expressions of this protein. These results indicate that glu-tubulin represents a strong selective expression for cancer cells and may be useful to identify and quantify human breast cancer.

Keywords Glu-tubulin · Histological typing · Mammary gland

H. Kuroda (✉) · K. Saito
Department of Pathology,
International University of Health and Welfare Hospital,
537-3 Iguchi, Nasushiobara,
Tochigi 329-2763, Japan
e-mail: hajimek@iuhw.ac.jp

M. Kuroda
Department of Pathology, Meikai University School of Dentistry,
Sakado, Japan

Y. Suzuki
Department of Surgery,
International University of Health and Welfare Hospital,
Tochigi, Japan

Introduction

Microtubules, which consist of an αβ-tubulin heterodimer, function in mitosis, cell motility, intracellular transport, and the maintenance of cell shape [1]. In previous reports, there was an abnormal accumulation of tubulin in cancer cells in several organs [2–6]. Recently, glu-tubulin, in which the C-terminal tyrosine of α-tubulin is removed by tubulin carboxypeptidase, overexpression has been reported in malignant tumors of the mammary gland immunohistochemically [7]. Therefore, using a protocol to detect expression of glu-tubulin may be adequate for a pathological differential diagnosis of malignant mammary gland tumors. To confirm this possibility, we undertook a strategy to examine both malignant and benign disease to determine its use in human mammary gland disease. Furthermore, to our knowledge, this is the first report to investigate immunohistochemical glu-tubulin detection in breast carcinoma compared with benign mammary disease; others have previously investigated glu-tubulin immunohistochemically only in breast cancers. The potential for biological variability even among malignant tumors has been recognized, and some researchers tested multiple parameters to ensure that the glu-tubulin would be useful in routine examinations. Here, we tested for accumulation of glu-tubulin in pathological specimens of mammary gland disease and whether tubulin expression was related to malignancy.

Materials and methods

We identified 147 cases accessioned in the Department of Pathology, International University of Health and Welfare Hospital from 2003 to 2009 for which paraffin blocks were available. There were sufficient biopsies or lumpectomy specimens of breast disease remaining in the blocks to permit the cutting of additional sections for immunohistochemical staining. For each case, all available hematoxylin and eosin–stained sections were reviewed to confirm the diagnosis of mammary disease by three observers without knowledge of either the prior histological results or the clinical outcome, and to select a representative block for immunostaining. The histological grade for invasive ductal carcinoma, which consists of three components (differentiation, pleomorphism, and mitotic index), was based on the recommendations made by Elston and Ellis [8]. Each component was scored on a scale from 1 to 3. The scores were summed and categorized as grade 1 (well differentiated), grade 2 (moderately differentiated), or grade 3 (poorly differentiated). The number of mitoses was counted in 10 consecutive fields at 400 magnification in the highest proliferative invasive area. The mitotic index was categorized as low grade (mitotic count ≤14) and high grade (mitotic count ≥15).

Glu-tubulin was evaluated by immunohistochemical analysis using a specific antibody. Five-micrometer-thick unstained sections were deparaffinized in xylene and rehydrated in a decreasing ethanol series (100–50%). After antigen retrieval with L.A.B. solution (Polyscience, Inc., Warrington, PA) for 20 min at 60°C, the endogenous peroxidase activity was quenched by exposure to 5% H_2O_2 overnight at room temperature. The sections were then permeabilized with phosphate-buffered saline containing 0.5% Triton X-100 for 6 min. After washing twice with phosphate-buffered saline containing 0.3% Triton X-100 for 10 min, unspecific antibody binding was blocked with 1% goat serum for an hour. The sections were incubated for 2 days at 4°C with a rabbit polyclonal anti-Glu-tubulin antibody (Cosmo Bio, Tokyo, Japan) at 1:1,000 dilution. After washing, the sections were further processed with a Histofine SAB-PO(R) kit (Nichirei Corp., Tokyo, Japan) following the manufacturer's instructions. A color reaction was developed with 3,3′-diaminobenzidine. After counterstaining with hematoxylin, the sections were dehydrated and mounted with mount-quick (Daido Sangyo Co. Ltd, Tokyo, Japan) and analyzed using an Olympus BX51 microscope. Nerve fibers known to express high levels of glu-tubulin were used as positive controls and were included in each staining run [9–12]. Negative controls were obtained by omission of the positive controls. Cases were considered glu-tubulin-positive if any cytoplasmic and/or membranous staining was observed in the cancer cells, even if focal. These criteria are similar to those previously used for scoring this marker in breast cancer [7].

We also examined for estrogen (ER; clone SP1), progesterone (PgR; clone 1E2), and HER2/neu (clone 4B5) protein expression using a fully automated Ventana Benchmark system. Briefly, 5-μm-thick unstained sections were placed onto an electrostatically charged glass slide and baked to allow for tissue adherence. The glass slides were pretreated with the recommended pretreatment solution provided by Ventana for tissue deparaffinization and antigen retrieval. Each immunostained slide was evaluated for the presence of ER and PgR expression, and HER2 protein overexpression, in the cancer cells. Tumor cells that showed nuclear staining for ER or PgR were ER positive and PgR positive, respectively. Of note, all ER-positive and PgR-positive cases showed staining in at least 10% of the tumor cell nuclei, whereas all ER-negative cases showed a complete absence of tumor cell staining (but with staining of normal breast epithelial cell nucle) [1]. Tumor cells were considered positive for HER2 protein overexpression when more than 30% of the cells showed strong membrane staining (equivalent to a score of 3+ on the DakoCytomation HercepTest) [13]. All immunostains were initially reviewed and scored by 2 pathologists. A χ^2 test was used to compute the statistical association among 3 variables, and the Mann–Whitney test was used to compare means. An P value of 0.05 was considered statistically significant. Statistical analysis was carried out using StatView software.

Results

The histological and clinical characteristics of the breast cancer cases identified in this study are summarized in Tables 1 and 2. All of the patients were women with breast carcinoma, and their ages ranged from 32 to 93 years (mean, 56.7 years). The mean tumor size was 2.4 cm at maximum diameter. The invasive ductal carcinomas were Elston and Ellis–modified Bloom–Richardson grade 1 in 48 cases (71.6%), grade 2 in 8 cases (11.9%), and grade 3 in 11 cases (16.4%). In 78 carcinoma cases, staining for glu-tubulin was observed in 56 (71.8%) cases (Table 2). The staining pattern of breast carcinoma was predominantly characterized by cytoplasmic staining of epithelial cells (Fig. 1a–c). In most tumors, some areas also showed cell–cell boundary staining. Only 22 cases showed no significant breast cancer staining. However, in benign tumor and other benign disease, glu-tubulin staining was detected in the cytoplasm of fibroblasts and endothelial cells, but was completely absent from epithelial cells in 64 of 69 cases (Fig. 2a–c). Very weak cytoplasmic staining was seen in only 4 (8.3%) of the 48 benign tumors and 1 (4.7%) of the 21 other benign disease cases without membranous glu-

Table 1 The relationship between the histological characteristics of carcinoma and the glu-tubulin marker

	Glu-tubulin		*P*
	Positive	Negative	
No. (78 cases)	56	22	
Age (y)	57.3	55.9	0.6305
Size (cm)	2.4	2.3	0.4591
LN metastasis-positive	6	2	0.8316
LN metastasis-negative	50	20	
Nuclear grading in invasive ductal carcinoma (67 cases)			
G1	32	16	0.4345
G2	7	1	
G3	9	2	
Invasive carcinoma	52	19	0.3839
Noninvasive carcinoma	4	3	
Hormonal and HER2 status in invasive ductal carcinoma (67cases)			
ER(+), PgR(+), HER2(−)	28	12	0.8059
ER(+), PgR(+), HER2(+)	4	1	
ER variable, PgR variable HER2(+)	5	1	
ER variable, PgR variable HER2(−)	4	3	
ER(−), PgR(−), HER2(−)	7	2	

tubulin expression. When the expression of glu-tubulin was compared in breast carcinoma versus benign tumor and other benign mammary disease, a significant association was found between expression of this protein and malignant tumor of the breast (Table 2). We also found that in normal areas of breast tissue sections, glu-tubulin staining was detected in the cytoplasm of fibroblasts and endothelial cells. The nuclei and cytoplasm of myoepithelial cells were occasionally stained, but epithelial cells were not stained.

Correlation of glu-tubulin expression with major prognostic factors in breast tumors including patient age, tumor size, axillary lymph node metastasis, nuclear grade, carcinoma invasion, steroid receptor, and HER2/neu status were examined. Based on our results, glu-tubulin expression was unrelated

Table 2 Relationship between glu-tubulin expression and mammary disease

	Histological type	No.	Glu-tubulin			*P*
			Positive	Negative	Positive/total (%)	
Malignant tumor	Invasive ductal carcinoma not otherwise specified	62	44	18	56/78 (71.8%)	
	Invasive lobular carcinoma	4	4	0		
	Tubular carcinoma	1	1	0		
	Mucinous carcinoma	3	2	1		
	Medullary carcinoma	1	1	0		
	Intracystic carcinoma	1	1	0		
	Paget disease	1	1	0		
	Ductal carcinoma in situ	5	2	3		
Benign tumor	Fibroadenoma	38	3	35	4/48 (8.3%)	<0.0001
	Papilloma	5	0	5		
	Ductal adenoma	2	1	1		
	Adenomyoepithelioma	2	0	2		
	Hemartoma	1	0	1		
Other benign disease	Mastitis	11	0	11	1/21 (4.7%)	
	Fibrocystic disease	10	1	9		
		Total 147	61	86		

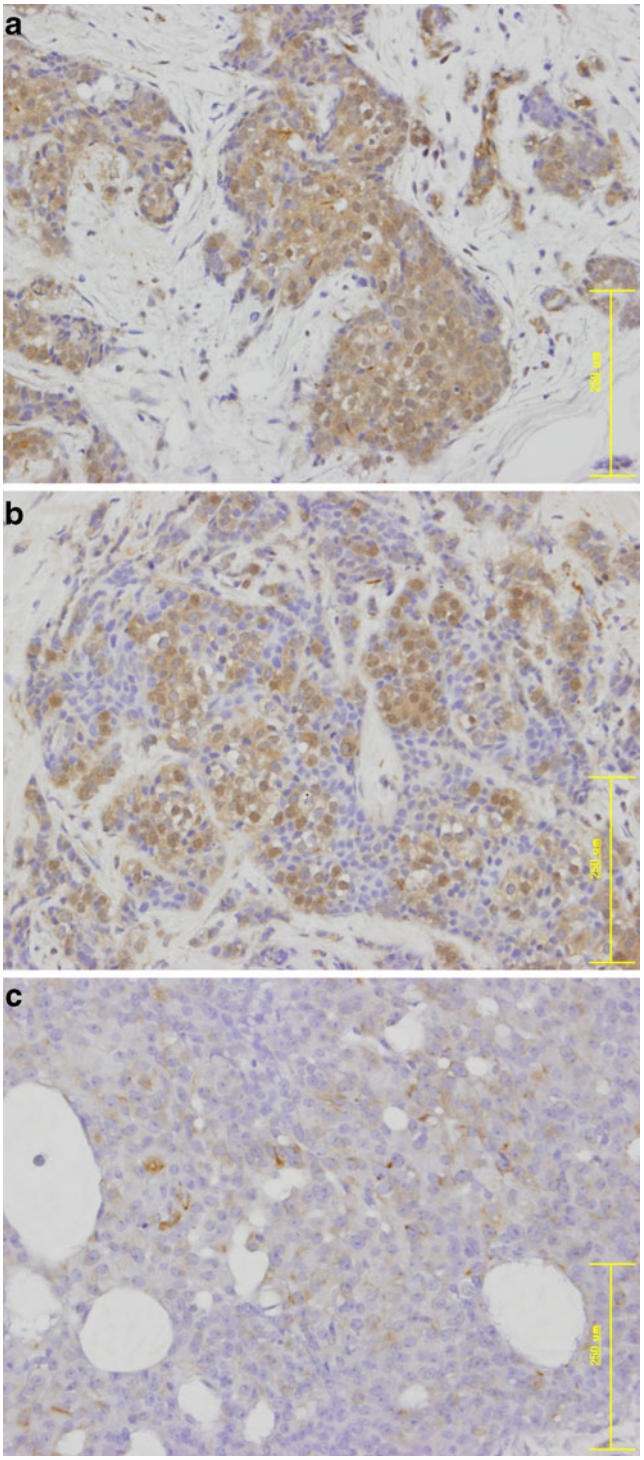

Fig. 1 **a** Carcinoma with strong and diffusely cytoplasmic reactivity of tumor cells to the glu-tubulin antibody scored as positive. **b** Carcinoma with focal and moderate cytoplasmic reactivity of tumor cells to the glu-tubulin antibody scored as positive. **c** Carcinoma with weak cytoplasmic reactivity of tumor cells to the glu-tubulin antibody scored as positive

to age, tumor size, nuclear grade, carcinoma invasion, axillary node metastasis, or hormonal receptor, and HER2/neu status.

Follow-up data were available in 54 of the 78 patients diagnosed with carcinomas. Of these 54 patients, 5 died of

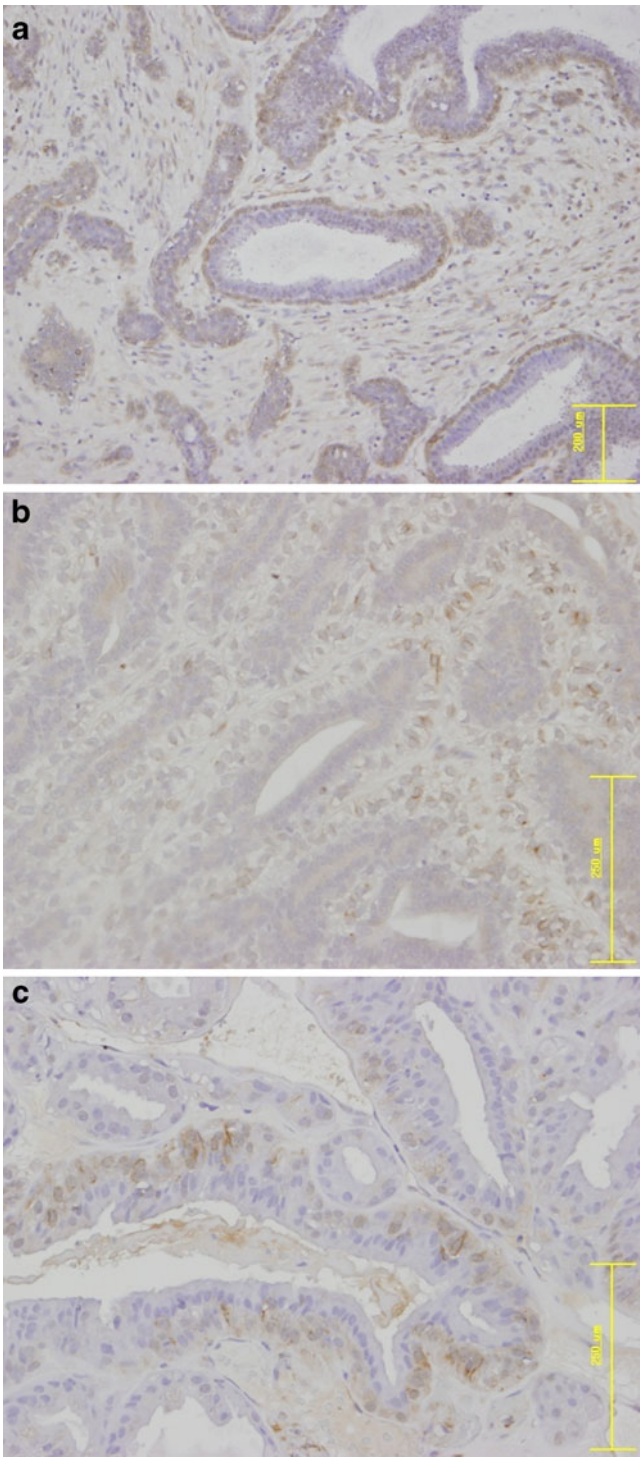

Fig. 2 **a–c** The cytoplasm of epithelial cells was negative for glu-tubulin, whereas those of fibroblasts and endothelial cells were positive in fibroadenoma (**a**), adenomyoepithelioma (**b**), and papilloma (**c**)

the disease after the initial diagnosis of the primary lesion and 49 patients were alive at 5 years after the initial diagnosis; however, 6 patients had recurrent disease. The 5-year survival rate, when corrected for intercurrent deaths, was 91.6% for glu-tubulin-positive patients and 90% for patients with glu-tubulin-negative tumors.

Discussion

Immunohistochemical techniques have proven useful in the diagnosis of cancer. However, immunohistochemistry also has its challenges in diagnosing breast cancer because of the difficulty in achieving maximum sensitivity without sacrificing specificity. A preliminary limited survey of previous reports indicated the differential expression of tubulin in several types of cancers. Carles et al. [3] reported that tubulin was present in cell lines of human colon adenocarcinoma by a reverse transcription polymerase chain reaction (RT-PCR) method. Sève et al. [4] performed immunohistochemical examination of microtubular components in tumor samples from patients with locally advanced or metastatic non-small cell lung cancer and found they were correlated with a high ratio of expression. Bernard-Marty et al. [6] examined 54 metastatic or locally advanced breast cancer patients with the expression of tubulin evaluated by immunohistochemistry and found that the majority of tumor samples expressed the tubulin protein. Furthermore, Mialhe et al. [7] examined 135 cases of breast cancer and 53% expressed glu-tubulin. More importantly, they reported that normal epithelial cells were not stained. Therefore, using a protocol to detect strong expression of glu-tubulin may be adequate for the differential diagnosis of malignant tumor in mammary glands. Similar to their findings, despite the histological variation in the carcinoma, most of our cases demonstrated expression in malignant cell components. This result was in contrast to our benign disease control group, including fibroadenoma, mastitis, and fibrocystic disease, in which expression was reduced or lost in the epithelial component.

As reported in many previous studies, microtubules are essential for cell polarization toward the direction of movement, contributing to cell migration [14–17]. Stable microtubules increase cell migration as they act as a directed membrane and in cell-organ transportation of the cell, regulating adhesion and contraction. Glu-tubulin is a form of stabilized tubulin that is expressed in the microtubules of migrating cells [18, 19]. Based on our results, the content of glu-tubulin in malignant tumors is consistent with a role for stabilized tubulin in migration and invasion. Further, based on a life table analysis, a poorer prognosis for patients with glu-tubulin expression with breast carcinoma was seen in other reports [7]. From the results above, the possibility of glu-tubulin expression as a clinically useful marker of tumor prognosis is proposed. These results are encouraging, although we found that glu-tubulin expression was unrelated to age, tumor size, nuclear grade, tumor invasion, hormonal and HER2 status and axillary node metastasis, whereas it was strongly correlated with prognosis. Furthermore, the patient's prognosis in our study was based on the analysis of small groups, and the meaning of these results is not definitive.

This study was aimed at establishing the glu-tubulin expression in mammary disease, with the hope that such information will provide a basis for studying the expression of glu-tubulin in the diseased breast. Our results with the glu-tubulin antibody suggest that glu-tubulin may be useful to identify and quantify human breast cancer. However, these results need to be replicated and expanded to many more cases and other cancers before any recommendations can be made on the use of this antibody in the routine identification of malignant tumors.

Acknowledgements The authors thank Dr. Kanji Sugiyama (Department of Anatomy, Meikai University School of Dentistry) for technical assistance with immunohistochemical staining and Dr. Megumi Takehara (Department of Surgery, Jichi Medical University) for her help and support in obtaining the clinical data.

References

1. Rodriguez OC, Schaefer AW, Mandato CA et al (2003) Conserved microtubule-actin interactions in cell movement and morphogenesis. Nat Cell Biol 5:599–609
2. Kavallaris M, Kuo DY, Burkhart CA et al (1997) Taxol-resistant epithelial ovarian tumors are associated with altered expression of specific beta-tubulin isotypes. J Clin Invest 100:1282–1293
3. Carles G, Braguer D, Dumontet C et al (1999) Differentiation of human colon cancer cells changes the expression of beta-tubulin isotypes and MAPs. Br J Cancer 80:1162–1168
4. Sève P, Isaac S, Trédan O et al (2005) Expression of class III β-tubulin is predictive of patient outcome in patients with non-small cell lung cancer receiving vinorelbine-based chemotherapy. Clin Cancer Res 11:5481–5486
5. Terry S, Ploussard G, Allory Y et al (2009) Increased expression of class III beta-tubulin in castration-resistant human prostate cancer. Br J Cancer 101:951–956
6. Bernard-Marty C, Treilleux I, Dumontet C et al (2002) Microtubule-associated parameters as predictive markers of docetaxel activity in advanced breast cancer patients: results of a pilot study. Clin Breast Cancer 3:341–345
7. Mialhe A, Lafanechère L, Treilleux I et al (2001) Tubulin detyrosination is a frequent occurrence in breast cancers of poor prognosis. Cancer Res 61:5024–5027
8. Elston CW, Ellis IO (1991) Pathological prognostic factors in breast cancer. I. The value of histological grade in breast cancer: experience from a large study with long-term follow-up. Histopathology 19:403–410
9. Gundersen GG, Bulinski JC (1986) Microtubule arrays in differentiated cells contain elevated levels of a post-translationally modified form of tubulin. Eur J Cell Biol 42:288–294
10. Kreis TE (1987) Microtubules containing detyrosinated tubulin are less dynamic. EMBO J 6:2597–2606

11. Schulze E, Asai DJ, Bulinski JC et al (1987) Posttranslational modification and microtubule stability. J Cell Biol 105:2167–2177
12. Prescott AR, Vestberg M, Warn RM (1989) Microtubules rich in modified alpha-tubulin characterize the tail processes of motile fibroblasts. J Cell Sci 94:227–236
13. Wolff AC, Hammond ME, Schwartz JN et al (2007) American Society of Clinical Oncology/College of American Pathologists guideline recommendations for human epidermal growth factor receptor 2 testing in breast cancer. J Clin Oncol 25:118–145
14. Wittmann T, Waterman-Storer CM (2001) Cell motility: can Rho GTPases and microtubules point the way? J Cell Sci 114:3795–3803
15. Nabi IR (1999) The polarization of the motile cell. J Cell Sci 112:1803–1811
16. Zheng Y (2004) G protein control of microtubule assembly. Annu Rev Cell Dev Biol 20:867–894
17. Jordan MA, Wilson L (2004) Microtubules as a target for anticancer drugs. Nat Rev Cancer 4:253–265
18. Gundersen GG, Bulinski JC (1988) Selective stabilization of microtubules oriented toward the direction of cell migration. Proc Natl Acad Sci USA 85:5946–5950
19. Wen Y, Eng CH, Schmoranzer J et al (2004) EB1 and APC bind to mDia to stabilize microtubules downstream of Rho and promote cell migration. Nat Cell Biol 6:820–830

Virchows Arch (2010) 457:483–495
DOI 10.1007/s00428-010-0963-z

ORIGINAL ARTICLE

Usefulness of tissue microarrays for assessment of protein expression, gene copy number and mutational status of EGFR in lung adenocarcinoma

Marius I. Ilie · Véronique Hofman · Christelle Bonnetaud · Katia Havet · Virginie Lespinet-Fabre · Céline Coëlle · Virginie Gavric-Tanga · Nicolas Vénissac · Jerôme Mouroux · Paul Hofman

Received: 31 May 2010 / Revised: 17 July 2010 / Accepted: 11 August 2010 / Published online: 28 August 2010
© Springer-Verlag 2010

Abstract Specific inhibitors targeting the epidermal growth factor receptor (EGFR) can increase survival rates in certain lung adenocarcinoma patients with mutations in the *EGFR* gene. Although such EGFR-targeted therapies have been approved for use, there is no general consensus among surgical pathologists on how the EGFR status should be tested in lung adenocarcinoma tissues and whether the results of immunohistochemistry (IHC), fluorescence in situ hybridization (FISH), and mutational analysis by molecular methods correlate. We evaluated the EGFR status in 61 lung adenocarcinomas by IHC (using total and mutant-specific antibodies against EGFR), by FISH analysis on tissue microarrays (TMAs), and by direct sequencing. The results of each method were compared using χ^2 and κappa statistics. The sensitivity and negative predictive value estimating the presence of abnormal EGFR for each test was calculated. The results show that, with respect to expression patterns and clinicopathological parameters, the total and mutant-specific EGFR detected by immunohistochemistry and FISH analysis on TMAs are valid and are equivalent to conventional methods performed on whole-tissue sections. Abnormal EGFR was detected in 52.4% of patients by IHC, FISH, and sequencing. The best sensitivity (100%) and negative predictive value (100%) was determined by evaluating the EGFR status with all methods. Testing for molecular changes in EGFR using a single test is likely to underestimate the presence of EGFR abnormalities. Taken together, these results demonstrate the high potential of TMAs to test for the major mechanisms of EGFR activation in patients with lung adenocarcinoma.

Keywords EGFR · Lung adenocarcinoma · Tissue microarrays · Immunohistochemistry · FISH · Sequencing

M. I. Ilie · V. Hofman · K. Havet · P. Hofman (✉)
Laboratory of Clinical and Experimental Pathology,
Louis Pasteur Hospital,
30 Avenue de la Voie Romaine,
06002 Nice Cedex 01, France
e-mail: hofman.p@chu-nice.fr

M. I. Ilie · V. Hofman · N. Vénissac · J. Mouroux · P. Hofman
INSERM ERI-21/EA 4319, Faculty of Medicine,
University of Nice Sophia Antipolis,
Nice, France

M. I. Ilie · V. Hofman · C. Bonnetaud · V. Lespinet-Fabre · C. Coëlle · V. Gavric-Tanga · P. Hofman
Human Tissue Biobank Unit/CRB INSERM,
Louis Pasteur Hospital,
Nice, France

N. Vénissac · J. Mouroux
Department of Thoracic Surgery, Louis Pasteur Hospital,
Nice, France

Epidermal growth factor receptor (EGFR) tyrosine kinase inhibitors (TKIs) such as gefitinib (Iressa®, Astra-Zeneca, UK) and erlotinib (Tarceva®, OSI/ Genentech, USA) show objective responses in 10% to 27% of patients with advanced non-small-cell lung cancer (NSCLC) after failure of standard chemotherapy [1, 2]. Moreover, recent clinical trials demonstrated substantial benefit of gefitinib administration in selected patients with advanced NSCLC with *EGFR* mutation-positive tumors [3]. Therefore, the European Medicines Agency (EMEA) supported the approval of gefitinib for patients with locally advanced or metastatic NSCLC with activating mutations of EGFR, across all lines of therapy (http://www.ema.europa.eu/

humandocs/Humans/EPAR/iressa/iressa.htm. Accessed 24 April 2010). In this regard, the French National Institute of Cancer (INCa) launched, at the end of 2009, a national program financing the detection by sequencing of *EGFR* mutations in patients with lung adenocarcinoma.

EGFR (HER-1/ErbB1) is a TK receptor of the ErbB family that plays a major role in tumor development and progression [4]. EGFR activation on the surface of cancer cells promotes the activation of the Ras-antiapoptotic cascade, cell growth, survival, and cell cycle progression, differentiation, and angiogenesis [5–7]. Together with its ligands, it is expressed in 40–80% of patients with NSCLC [8]. However, it appears that certain patients obtain more benefit from EGFR-TKIs than others. A higher probability of response appears to be associated with clinical characteristics, such as gender (female), never smoking status, Asian ethnic origin, and adenocarcinoma sub-type [9]. Nevertheless, strategies for patient selection using molecular diagnostics of EGFR activation increase the efficacy of EGFR-targeted therapies and greatly optimize response to treatment in patients with lung adenocarcinoma. Various mechanisms of EGFR activation in cancer cells have been demonstrated: overexpression of ligands and receptors, gene amplification, and activating mutations [10]. For these reasons, selection of patients who will benefit from EGFR inhibition according to their genetic status is an important issue in EGFR-targeted therapy in NSCLC.

The relationship between EGFR protein expression and tumor sensitivity to TKIs is currently unclear [11–15]. Retrospectives studies failed to demonstrate a predictive value for EGFR overexpression measured by immunohistochemistry (IHC) in patients with NSCLC who are treated with TKIs [12, 13]. However, other recent trials found a relationship between EGFR protein expression and better overall survival in patients with relapsed or refractory NSCLC who received TKI therapy [11, 14, 15]. Conversely, some studies showed that high polysomy or amplification of the *EGFR* gene analyzed by fluorescence in situ hybridization (FISH) tended to be the best predictor of response, even better than detection of gene mutations in *EGFR* [11, 16, 17]. Finally, other studies assert the superiority of the detection of *EGFR* mutations for prediction [18, 19]. The two most frequent *EGFR* mutations are short in-frame deletions of exon 19 and a point mutation (CTG to CGG) in exon 21 at nucleotide 2573, which results in substitution of leucine by arginine at codon 858 (L858R) [20]. Together, these two mutations account for almost 90% of all *EGFR* mutations in NSCLC [20]. Response rates to EGFR-TKIs range from 48% to 90% for patients with *EGFR* mutations, while responses are less common in patients without a mutation (5–31%) [21]. Interestingly, two mutant-specific antibodies directed against the most common mutant forms of the EGFR oncoprotein have been recently developed for IHC use: 15-bp deletion (E746_A750del) in exon 19 and the L858R point mutation in exon 21 [22].

Limited studies have analyzed the possible correlation between different EGFR abnormalities measured by IHC, for total protein expression or for the two mutants (specific antibodies), FISH and sequencing [23–27]. The variability in the results of trials that tested these methods of detection of the EGFR status may reflect variations in the methodology and the interpretation of the test results, as well as patient demographics and cohorts [26, 28, 29].

This study was conducted to demonstrate the potential interest of the tissue microarray (TMA) method to assess protein expression, gene amplification, and mutational status of EGFR in a retrospective cohort of lung adenocarcinoma patients. For this purpose, the relationship between protein expression, gene copy number, and mutational status of EGFR (using mutant-specific antibodies) was evaluated in TMA built with 61 lung adenocarcinomas. Results were then compared with direct sequencing of exons 19, 20, and 21 of *EGFR*, performed in parallel from DNA extracted from mirror frozen tumor tissues. Finally, the correlation between the genetic status and clinicopathological parameters of patients was evaluated. The results show that the TMA method could be useful in detecting EGFR overexpression, mutational status, or gene amplification and may be suitable in a larger series of NSCLC patients.

Patients and methods

Patients

Selected paraffin blocks of formalin-fixed tissues from 61 patients diagnosed with lung adenocarcinoma from January 2007 to November 2009 were retrieved from the archives of the Laboratory of Clinical and Experimental Pathology (Pasteur Hospital, Nice, France). Patients were all Caucasians and were matched for gender and smoking status. The median age was 67 years (range, 42–83 years). Tumors were histologically classified according to WHO guidelines [30]. They included 29 mixed adenocarcinomas with a bronchioloalveolar component, 27 mixed adenocarcinomas, and 5 bronchioloalveolar carcinomas. All tumors were staged according to the international Tumor–Node–Metastasis (TNM) classification [31]. There were 32 I-stage, 9 II-stage, 15 III-stage, and 5 IV-stage tumors. To build TMAs, selection of the cases to be included in the study was based on parameters such as collection by rigorous adherence to banking protocols [32], the absence of neoadjuvant treatment, and the availability of sufficient tissue to examine molecular abnormalities and protein expression by IHC. A well-qualified sample is one where

there is over 60% cancer cells and no necrosis [33]. The study was done with the approval of the ethics committee (CHU of Nice). The patients received the necessary information concerning the study, and informed signed consent was obtained from each patient.

Preparation of tissue microarrays

Representative tumor regions were selected for building TMAs after thorough evaluation of H&E slides, and arrays were designed as previously described [34]. Three core tissue biopsies, 600 μm in diameter, corresponding to the selected morphologically representative region of each paraffin-embedded tumor, were transplanted onto a recipient block using an automated tissue arrayer (Beecher Instruments, Silver Spring, MD, USA and Alphelys, Paris, France). Moreover, the cores were selected from different tumor regions, including the center and the periphery of the lesion. Three additional core tissue biopsies were selected from morphologically normal lung tissue adjacent to each tumor and served as a negative control.

Immunohistochemistry

IHC for total EGFR was performed on serial 4 μm deparaffinized TMA sections, as described [34], using an automated single-staining procedure (Benchmark XT, Ventana Medical Systems, Roche Group, Inc., Tucson, AZ). A mouse monoclonal antibody anti-EGFR (clone 3C6; Ventana, Strasbourg, France) was used according to the manufacturer's instructions. Sections were blindly and independently analyzed by two observers (MI and VH) at low magnification (×200). Total EGFR protein overexpression was evaluated on TMA cores using an IHC scoring system as described: 0, no membrane staining; 1+, faint, partial membrane staining; 2+, weak, complete membrane staining in >10% of tumor cells; 3+, intense complete membrane staining in >10% of tumor cells [25].

IHC with the two mutation-specific antibodies, one recognizing the exon 21 L858R *EGFR* mutation and the other the E746-750 15-bp deletion in exon 19, was done manually as described [22]. Briefly, after deparaffinization, antigen retrieval was performed using EDTH pH 9 (Dako, Glostrup, Denmark) for 30 min, and the primary antibody (1:100, rabbit, monoclonal, Cell Signalling, Danvers, USA) was applied. For detection, the EnVision FLEX kit (Dako) was used. The intensity of EGFR mutant-specific IHC was scored as previously described: 0 = no or faint staining in <10% of tumor cells; 1+ = faint staining in >10% of tumor cells; 2+ = moderate staining; 3+ = strong staining [35]. Total EGFR overexpression was considered as 2+ and 3+ and positive mutant-specific EGFR expression as between 1+ and 3+. Whole-tissue sections from tumor blocks of all cases were stained for total EGFR and compared with the corresponding TMAs spots using the above-mentioned scoring criteria. IHC with the mutant-specific antibodies was performed on whole sections of all positive cases by direct sequencing. In parallel, seven randomly selected negative cases were evaluated on whole-tissue sections.

Fluorescence in situ hybridization

Fluorescence in situ hybridization (FISH) was performed on paraffin-embedded TMAs and whole-tissue 4-μm sections according to a protocol described previously [36]. At least 100 non-overlapping interphase nuclei per core were analyzed blindly and independently by two pathologists (MI and VH). Patients were classified into two strata according to previously described criteria [16]: (1) FISH-negative, with no or low genomic gain (≤4 copies of EGFR in >40% of cells) or (2) FISH-positive with either high polysomy (≥4 copies of EGFR in >40% of cells) or with gene amplification. Gene amplification was considered positive when tight gene clusters were present and a gene/chromosome ratio per cell of ≥2 or homogenously staining regions with ≥15 copies in ≥10% of cells were detected. A FISH analysis was performed in parallel on whole-tissue sections corresponding to all the positive cases and on seven randomly selected negative cases on TMA and compared with the corresponding TMA spots using the above-mentioned scoring criteria.

DNA extraction and direct sequencing of the *EGFR* gene

Genomic DNA was extracted from frozen tissue samples with >60% tumor cells using the MagNA Pure Compact Nucleic Acid Isolation Kit Large Volume (Roche Group, Inc., Tucson, AR) according to the manufacturer's instructions. After initial denaturation at 94°C for 5 min, gDNA (100 ng) for exons 19, 20, and 21 of EGFR analysis was subjected to 35 cycles of polymerase chain reaction (PCR) (94°C for 30 s, 56°C for EGFR exon 20, 60°C for EGFR exons 19 and 21 for 30 s, and 72°C for 30 s) using Taq platinum (Invitrogen), followed by a final extension at 72°C for 10 min. Primer pairs used for amplification were those described by Choong et al. [37]. Aliquots of all PCR products were examined by 2% agarose gel electrophoresis. After amplification, post-PCR purification was performed using ExoSAP-IT (GE Healthcare Life Sciences) according to the manufacturer's procedures. All samples were bidirectionally sequenced on an ABI Prism 310 sequencer using the Applied Big Dye Terminator v1.1 kit (Applied Biosystems, Inc., Foster City, CA). Mutations in the *EGFR* gene in patients were reanalyzed with the BioEdit software program [38] by additional amplification and sequencing.

Statistical analysis

Analyses were performed using SPSS 16.0 statistical software (SPSS Inc., Chicago, IL). The degree of agreement between data from whole-tissue sections and the mean value of the three spots corresponding to each case on TMAs was assessed using the Cohen's κ coefficient. The optimal sensitivity and the negative predictive value of t he EGFR test were determined by ROC curve analysis. The χ^2 and Mann–Whitney tests were used to explore the association between EGFR test results and the clinicopathological variables of patients. All statistical tests were two-sided, and a significant p value was set at 0.05.

Results

EGFR mutations were detected by direct sequencing in 16.4% (10 of 61) of cases. All cases had an exon 19 mutation (100%). Among the ten *EGFR* mutations in exon 19, there were 15-bp deletions (n=8), 18-bp deletions (n=1), and insertion/duplication of 18 bp (n=1) (Fig. 1). No mutation was identified in exons 20 and 21 of *EGFR*.

Positive immunolabeling for total EGFR detected by IHC on TMAs was noted in 36% (22 of 61) of all cases and in 40% (4 of 10) of mutant cases (Fig. 2a; Table 1). The EGFR expression levels observed on the TMA spots faithfully reflected the staining intensity of the protein on whole-tissue sections from corresponding tumor blocks (κ=0.92). Although total EGFR overexpression strongly correlated with the mutational positive status detected by direct sequencing (p=0.024), there was poor agreement between these two latter methods (κ=0.03; Table 1). Six mutant tumor samples (60%) stained faintly on IHC, whereas 35% (18 of 51) of wild-type cases overexpressed EGFR (Table 1).

Thirteen of 61 (21.3%) cases demonstrated high polysomy and amplification by FISH analysis in both whole-tissue sections and corresponding TMA cores (Fig. 3; Table 2). The κappa index was used to measure the agreement between these two methods, and a total concordance was found (κ=1; p<0.0001). Moreover, the

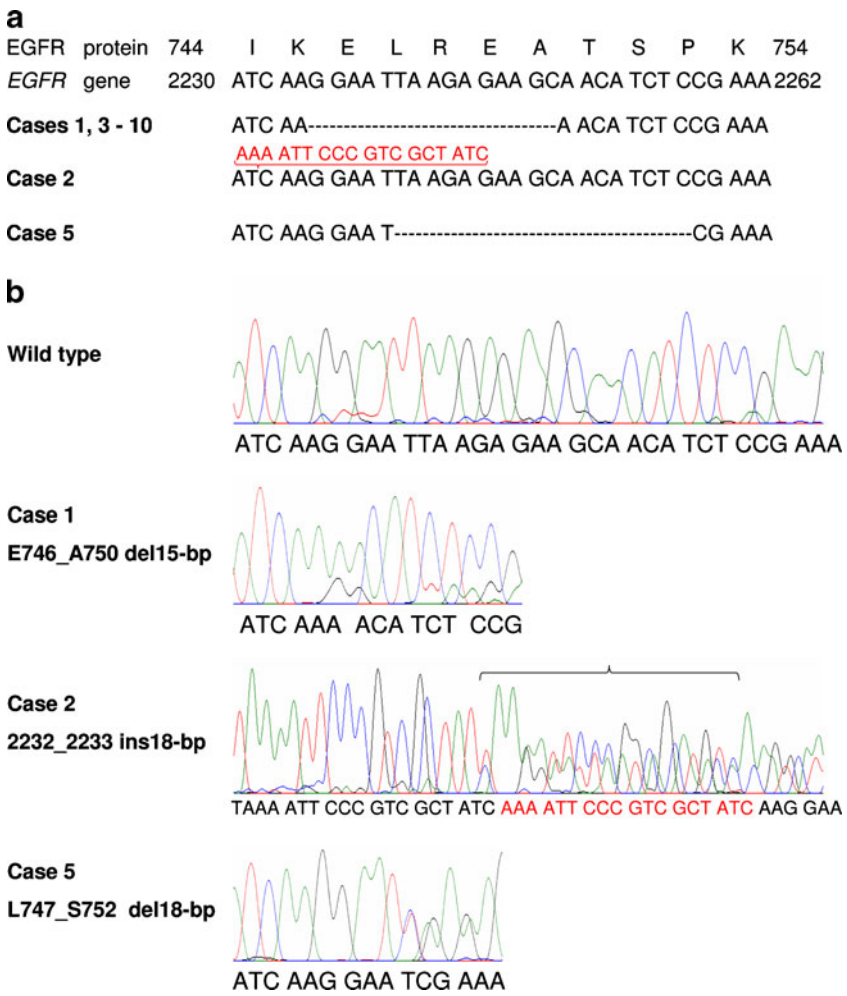

Fig. 1 Mutations in the *EGFR* gene detected by direct sequencing of the cohort. **a** Three representative nucleotide patterns of mutations in *EGFR* exon 19. **b** Three representative electropherograms of mutations in *EGFR* exon 19

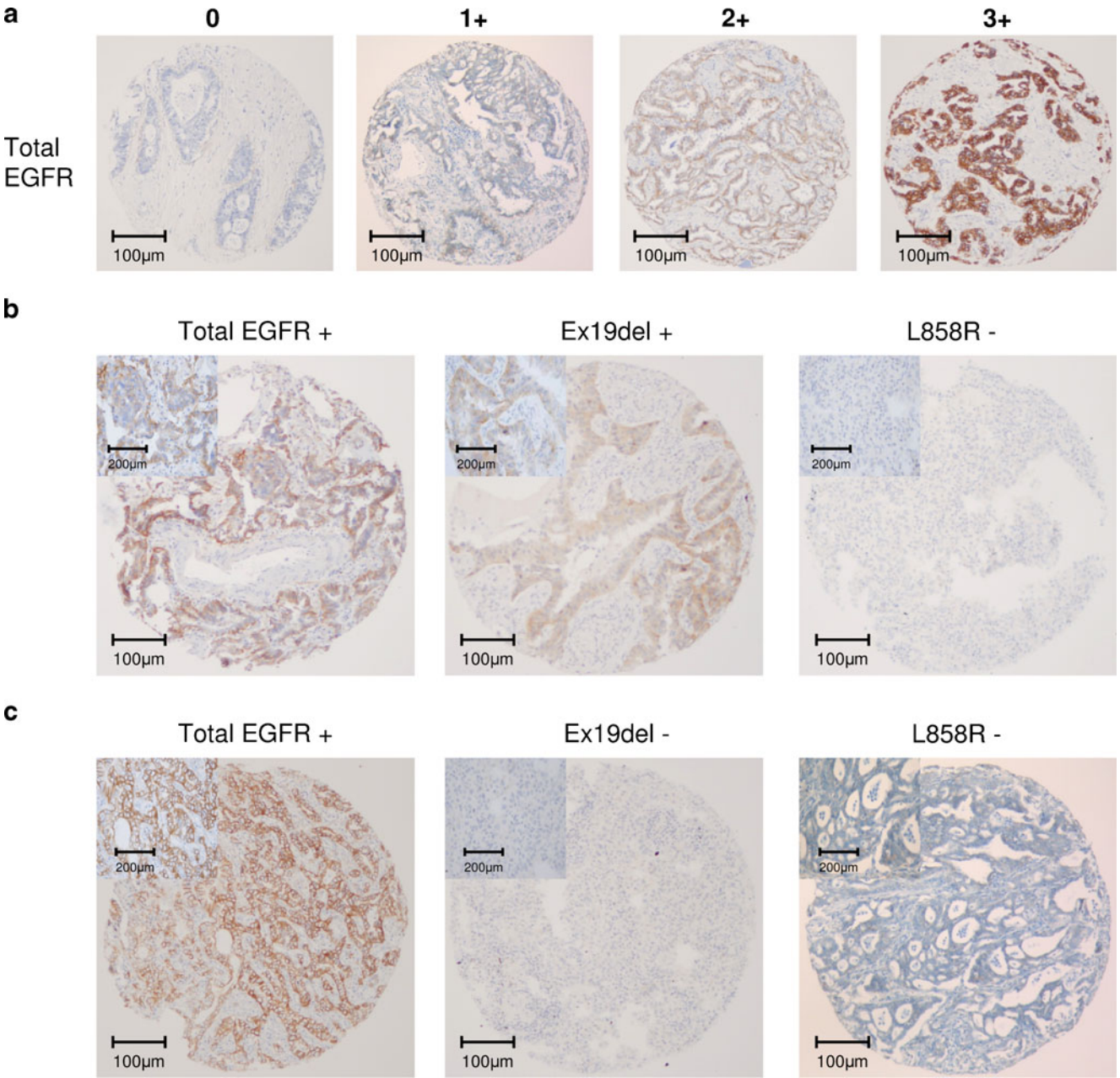

Fig. 2 Lung adenocarcinomas with different levels of immunohistochemical staining. **a** From absent to high total EGFR protein expression. **b** A tumor sample showing positive immunolabelling to the exon 19 mutant-specific and total EGFR antibodies and negative staining to the *EGFR* L858R mutant-specific antibody. **c** Wild-type tumor sample showing positive staining to total EGFR and negative staining to the two mutant-specific antibodies (exon 21, L858R and exon 19, E746-750 15-bp deletion). *Scale bar* in **a**–**c**, 100 μm and in **b** and **c** inserts, 200 μm

Table 1 Correlation between the mutational status of *EGFR* obtained by direct sequencing and of total EGFR protein expression obtained by immunohistochemistry on TMAs

Sequencing	Total EGFR IHC				*K* index	*p* value*
	0	1+	2+	3+		
Wild-type (n=51)	15 (29.4%)	18 (35.2%)	14 (27.4%)	4 (7.8%)	0.03	0.024
Exon 19 mutations (n=10)	3 (30%)	3 (30%)	0 (0%)	4 (40%)		

*p=0.05; a χ^2 test was used

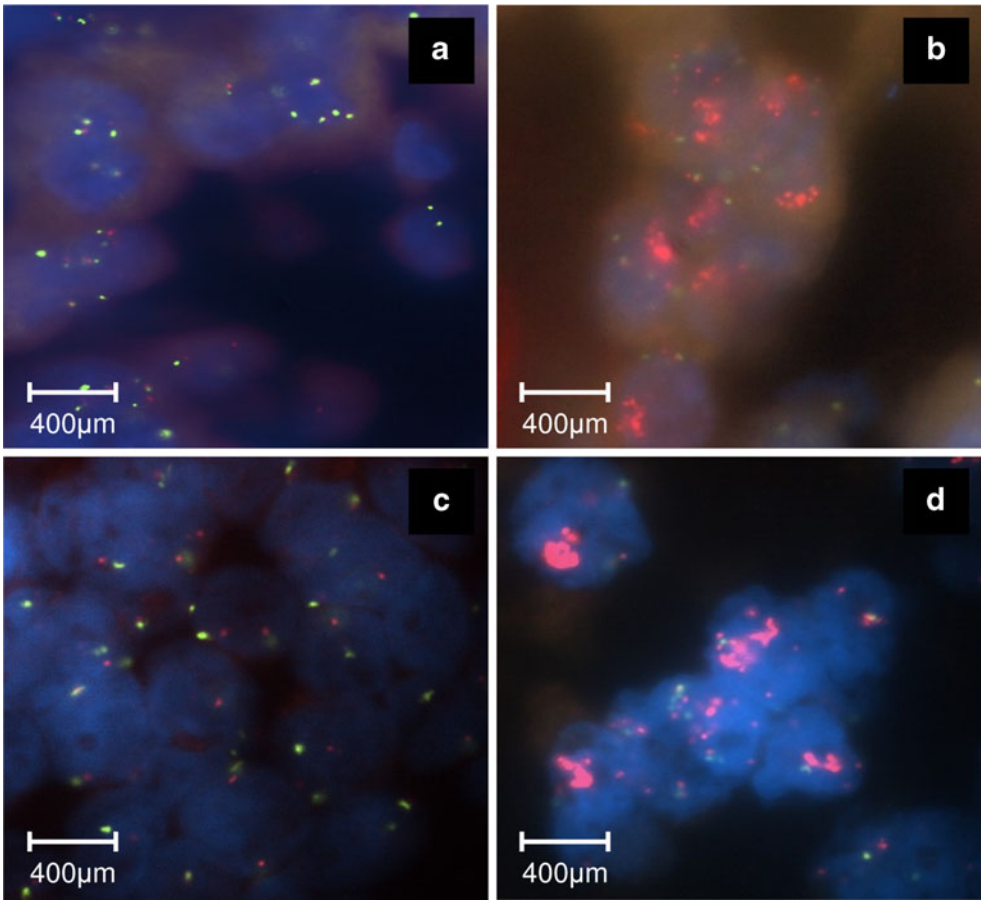

Fig. 3 Detection of the copy number of the *EGFR* gene by FISH (*red signal EGFR*, *green signal* CEP 7) in lung adenocarcinomas. Negative FISH test (**a**) and clustered gene amplification (**b**) on a whole-tissue section (*top*). Negative FISH analysis (**c**) and increased copy numbers of *EGFR* (**d**) showing gene amplification on TMA cores (*bottom*). *Scale bar* 400 µm

FISH-positive status was strongly related to total EGFR overexpression when performed on TMAs (p=0.013), and we found fair agreement between the two tests (κ=0.33; Table 2). The relationship between mutational status obtained by direct sequencing and *EGFR* gene copy number analyzed by FISH on TMAs was evaluated. There was a significant correlation between these two methods (p=0.045) and fair agreement between them (κ=0.30; Table 3).

Out of all cases, 13 were positive with the exon 19 *EGFR* mutant-specific antibody when performed on TMAs (Fig. 2b, c; Table 4). Similar expression levels were observed in whole-tissue sections from corresponding tumor blocks in a subset of 20 tumors (κ=0.91). The staining was both cytoplasmic and membranous. There was no significant correlation to total EGFR protein overexpression (p=0.23) and the κappa index showed slight agreement (κ=0.18; Table 4). All the eight cases (100%) with a 15-bp deletion in exon 19, detected by direct sequencing, were positive for IHC with the EGFR mutant-specific antibody (Table 5). However, positive immunostaining with the exon 19 mutant-specific antibody was also observed in four cases without mutations and in one case with an 18-bp deletion. The EGFR exon 19

Table 2 Correlation between the total EGFR protein expression obtained with TMAs by immunohistochemistry and the *EGFR* gene copy number obtained by FISH analysis

Total EGFR IHC	FISH		*K* index	*p* value*
	FISH + (*n*)	FISH − (*n*)		
Positive	9	13	0.33	0.013
Negative	4	35		

*p=0.05; a χ^2 test was used

Table 3 Correlation between the mutational status obtained by direct sequencing and the *EGFR* gene copy number obtained with TMAs by FISH analysis

Sequencing	FISH		*K* index	*p* value*
	FISH + (*n*)	FISH − (*n*)		
Wild-type	5	5	0.30	0.045
Exon 19 mutations	8	43		

*p=0.05; a χ^2 test was used

Table 4 Relationship between *EGFR* exon 19 mutant-specific TMA immunohistochemistry and total TMA EGFR protein expression

EGFR mutant-specific IHC	Total EGFR IHC		*K* index	*p* value*
	Positive (*n*)	Negative (*n*)		
Positive	7	6	0.18	0.23
Negative	15	33		

*$p=0.05$; a χ^2 test was used

mutant-specific antibody detected 90% of exon 19 mutants with a specificity of 92%. Furthermore, these two methods demonstrated strong statistical correlation ($p<0.001$) and substantial concordance ($\kappa=0.73$ and $\kappa=0.76$, respectively; Table 5). Finally, we found a significant relationship ($p=0.004$) with fair agreement ($\kappa=0.41$) between a high *EGFR* gene copy number and an exon 19 mutational status as determined by mutant-specific IHC, where both analyses were performed on TMAs (Table 6). However, when the 15-bp deletion cases were considered for analysis, the κappa index was lower ($\kappa=0.26$), and there was only a tendency for association with the positive FISH status ($p=0.09$; Table 6).

Among the 61 cases, 26 of 61 (43%) were negative with all four methods. Using the method described by Gupta et al. to define a "true positive result" by identifying a positive result with any of these methods, we found that total EGFR IHC demonstrated the highest percentage of positivity (36%) when EGFR tests were individually considered (Fig. 4a). By adding the results of the gene copy number analysis to the mutational status, we found larger benefit, which was higher when IHC for total EGFR was performed with either three of the methods (Fig. 4b). Finally, the highest percentage of positive EGFR tests was obtained with all four methods taken together (Fig. 4c).

Table 5 Relationship between *EGFR* exon 19 mutant-specific TMA immunohistochemistry and mutational status obtained by direct sequencing

EGFR mutant-specific IHC	Sequencing		*K* index	*p* value*
	Exon 19 mutations (*n*)	Wild-type (*n*)		
Exon 19 mutations				
Positive	9	4	0.73	<0.001
Negative	1	47		
15-bp deletion cases				
Positive	8	4	0.76	<0.001
Negative	0	47		

*$p=0.05$; a χ^2 test was used

Table 6 Relationship between *EGFR* exon 19 mutant-specific TMA immunohistochemistry and the *EGFR* gene copy number as detected by FISH analysis of TMAs

EGFR mutant-specific IHC	FISH		*K* index	*p* value*
	FISH + (*n*)	FISH − (*n*)		
Exon 19 mutations				
Positive	7	6	0.41	0.004
Negative	6	42		
15-bp deletion cases				
Positive	4	4	0.26	0.09
Negative	9	44		

*$p=0.05$; a χ^2 test was used

When the results of a single method were evaluated, IHC had the highest sensitivity (62.86%; Table 7). EGFR protein expression detected by IHC and the mutational status determined either by direct sequencing or by mutant-specific IHC together demonstrated an acceptable sensitivity (80%) and a negative predictive value (79%; Table 7). Finally, we found a total sensitivity (100%) and a total negative predictive value (100%) when all methods were evaluated (Table 7).

We performed statistical analysis to evaluate a possible relationship between the results of these three methods and the clinicopathological variables of patients. The results obtained by direct sequencing alone were used to define the mutational status, with regard to its strong correlation with mutant-specific IHC. The proportion of EGFR exon 19 deletions detected by direct sequencing was significantly associated with the never smoking status ($p=0.01$) and with female sex ($p=0.01$; Table 8). No other correlation was found with age, histological sub-type, or pathologic tumour-node-metastasis (pTNM) stage.

Discussion

There is urgent need for methods that allow the high-throughput analysis of the EGFR status in biopsy samples using IHC markers and FISH analysis based markers. Some studies have focused on validation of immunohistochemical analysis of EGFR expression on TMAs, while only limited reports have validated FISH analysis or recently developed mutant EGFR-specific antibodies for IHC using TMAs in several types of cancer [35, 36, 39]. We are aware of the limited interest in TMA technology as a daily routine test. However, given the rising interest in new prognostic and theranostic biomarkers, our study, although quite limited in the number of cases, demonstrates the potential of detecting such biomarkers in larger studies for efficient translational research [40].

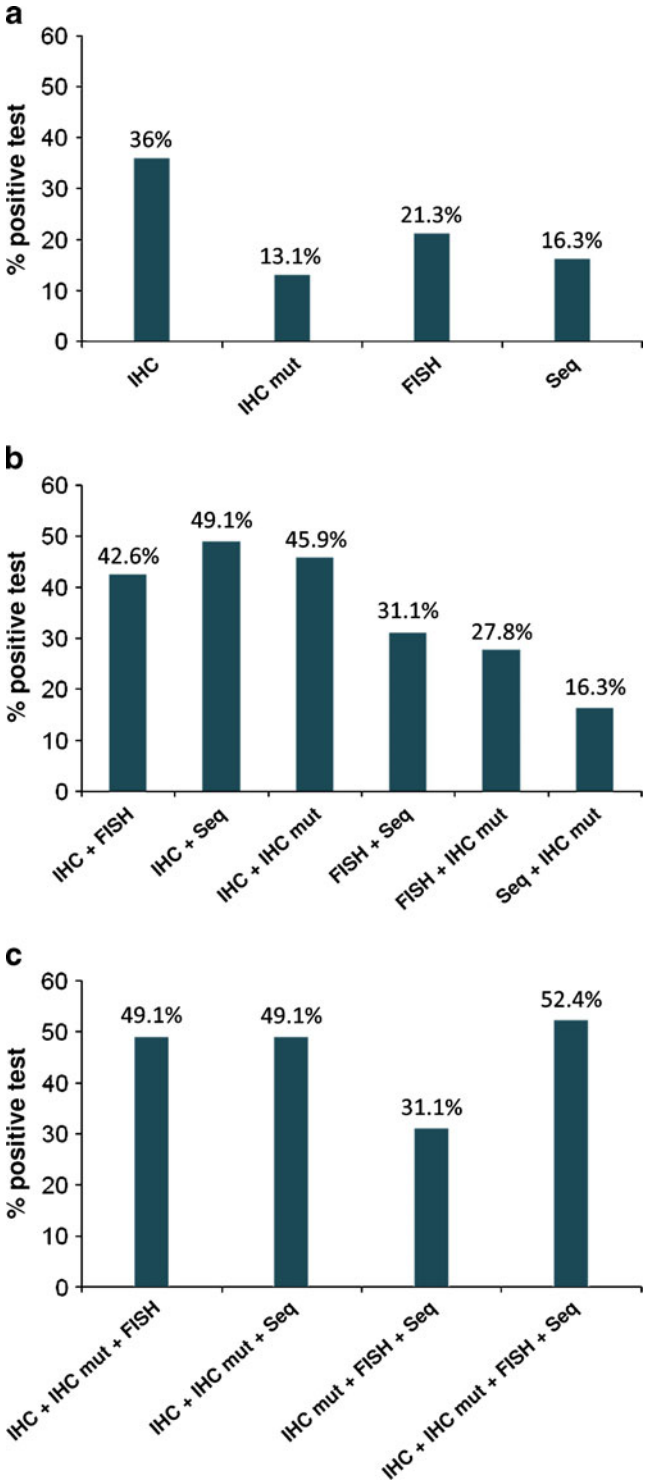

Fig. 4 Percentage of EGFR-positive tests obtained by immunohistochemistry with total EGFR and *EGFR* exon 19 mutant-specific antibodies, fluorescence in situ hybridization, and direct sequencing in 61 lung adenocarcinomas. **a** Test results with one method. **b** Test results with two methods. **c** Test results with three or all methods together

We show that total EGFR IHC, mutant-specific IHC, and FISH analyses performed on whole-tissue sections can be performed with TMAs. Previous studies revealed a variable level of concordance between whole-tissue sections and assessable TMAs when other markers, like HER2, MYC, CCND1, and MDM2, were tested by FISH [41–43]. Since the intratumor heterogeneity would have the most significant impact on the results in tumors with low levels of protein expression or gene amplification, we compared both whole sections and TMA. We recently validated the TMA methodology in lung oncology for analysis of the expression of other proteins in a large series of 555 NSCLC cases [44]. We found an excellent correlation between FISH analysis on whole-tissue sections in comparison with corresponding TMAs. Intratumor variation in the EGFR gene copy number can be more dramatic at higher levels of EGFR gene amplification. However, this variation would have a minimal impact on the designation of a tumor as being EGFR amplified or not amplified in most cases on whole-tissue sections [43]. EGFR-FISH analysis on TMAs in lung adenocarcinoma may therefore be suitable for evaluation of the EGFR gene copy number in a large series of lung adenocarcinoma. In addition, we found fair concordance between total EGFR IHC staining and FISH analysis on TMAs, as EGFR protein overexpression is often associated with *EGFR* gene amplification [45]. Moreover, our results indicate that *EGFR* amplification, preferentially of the mutant allele, often accompanies *EGFR* mutation, as already suggested [25]. Thus, TMAs

Table 7 Sensitivity and negative predictive value of immunohistochemistry, FISH analysis, or direct sequencing for evaluation of the EGFR status

Method	Sensitivity (%)	NPV (%)
IHC	62.86	67
IHC mut	22.86	49
FISH	37.14	54
Seq	28.57	51
IHC+IHC mut	80	79
IHC+FISH	74.29	74
IHC+Seq	80	79
IHC mut+FISH	48.57	59
IHC mut+Seq	51.43	60
FISH+Seq	51.43	60
IHC+IHC mut+FISH	85.71	84
IHC+IHC mut+Seq	97.14	96
IHC mut+FISH+Seq	62.86	67
All methods	100	100

NPV negative predictive value, *IHC* total EGFR immunohistochemistry, *IHC mut* EGFR mutant-specific immunohistochemistry, *Seq* sequencing

Table 8 Clinicopathological characteristics of 61 patients with lung adenocarcinoma according to EGFR protein expression detected by TMA immunohistochemsitry, the gene copy number determined by FISH analysis, and mutational status determined by direct sequencing

Variables[a]	FISH		*p* value*	IHC		*p* value*	Seq		*p* value*
	+	−		+	−		+	−	
Age									
>65 years	7	27	0.99	13	21	0.99	7	27	0.51
≤65 years	5	22		7	20		3	24	
Sex									
Female	9	21	0.093	11	19	0.99	9	21	0.01
Male	3	28		9	22		1	30	
Smoking history									
Never smoked	7	17	0.23	10	14	0.36	9	15	0.01
Former or current smokers	5	32		10	27		1	36	
Histologic sub-type									
Mixed ADC	9	18	0.50	8	19	0.17	3	24	0.24
Mixed ADC+BAL	4	25		12	17		7	22	
BAL	0	5		0	5		0	5	
pTNM stage									
I+II	8	33	0.87	16	25	0.68	7	34	0.87
III+IV	5	15		6	14		3	17	

Seq sequencing, *ADC* adenocarcinoma, *BAL* bronchioloalveolar carcinoma, *TNM* tumor node metastasis

[a] χ^2 or Mann–Whitney tests when appropriate

**p* value significant at the 0.05 level

can be an appropriate tool for analyzing EGFR protein expression and *EGFR* gene amplification, allowing a more precise evaluation of these mechanisms of activation in a larger series of patients [46–48].

Having validated immunostaining for the total EGFR protein and FISH analysis of the *EGFR* gene copy number on TMAs, we evaluated the mutational status either by using a recently developed mutant EGFR-specific antibody on TMAs or by direct sequencing. Our results show that EGFR exon 19 mutant-specific IHC on TMAs highly correlated with whole-tissue section analysis. Because the large sections may be much more frequently considered as mutant-specific IHC-positive than TMA spots, it might be assumed that false positives on large sections may represent either biologically irrelevant focal findings or local artificial staining, as described [43]. Because of the size of the tissue area to be stained, artificial staining results can be a greater problem on large sections than on TMAs. Although there was a strong correlation between IHC staining on TMAs and results obtained by direct sequencing, false positive results (8%) and the 92% specificity emphasize the need for further molecular validation in routine use. Moreover, *EGFR* gene amplification was associated with IHC staining for mutant-specific exon 19 EGFR on TMAs but not for the 15-bp deletion. Although *EGFR* amplification occurs preferentially on the mutated allele [25], this may suggest that there is no amplification of a specific type of mutation.

We found that *EGFR* genomic gain and mutations were much less frequent cellular events than EGFR overexpression, as previously described [24]. However, the highest percentage of positive EGFR tests was obtained with all four methods taken together. Furthermore, we evaluated the sensitivity of these methods. Total EGFR IHC had the highest sensitivity, which was not surprising considering the high frequency (34–84%) of EGFR protein overexpression, as already reported in NSCLC [49–51]. Total EGFR protein expression and the mutational status gave a very good negative predictive value (96%) according to a recent report [26]. However, only the evaluation by all four methods reached a high 100% sensitivity and a 100% negative predictive value in detecting EGFR abnormalities. Therefore, great attention should be made when choosing less than three or four methods for EGFR testing in routine clinical practice. This latter finding suggests that the presence of EGFR abnormalities, which might significantly predict response to TKIs, may be underestimated when using direct sequencing alone.

Although IHC staining for total EGFR statistically correlated with a positive mutational status, there was poor agreement between these two methods. In addition, IHC could not predict the *EGFR* mutational status since, in our study, it missed 60% of mutant tumors, as previously shown [25]. Moreover, a large number of IHC-positive tumors lacked mutations. However, we believe that this test should not be completely proscribed as it demonstrated the best sensitivity (62.86%) and negative predictive value (67%). When considered along with *EGFR* molecular modifications (i.e., gene amplification and mutations), we found an even higher negative predictive value (96%). Previous studies have reported the lack of correlation between an *EGFR* mutation and IHC positivity [11, 52]

and *EGFR* mutant tumors with an absence of IHC positivity [14] in TKIs-treated NSCLC patients.

There are many published reports attempting to correlate EGFR protein overexpression and benefit of TKIs in lung adenocarcinoma patients [11–15]. However, the data regarding the role of EGFR expression in predicting the tumor sensitivity to TKIs are inconsistent and confusing [29]. In this regard, retrospective analyses of patients with NSCLC who received TKIs therapy found no obvious relationship between the amount of EGFR protein, assessed by immunohistochemistry (IHC), and the objective response rate [12, 13]. Perez-Soler et al. suggested that the detection of EGFR overexpression by IHC may not offer predictive information [13], although Tsao et al. have shown a significant correlation between EGFR overexpression detected by IHC and response to TKIs therapy [15]. Similarly, in the ISEL phase III study that compared gefitinib treatment with placebo, patients with EGFR-positive tumors who received gefitinib demonstrated significantly prolonged survival compared with patients with EGFR-negative tumors [14]. Among the patients whose tumors were negative for EGFR protein expression, a trend toward decreased overall survival was observed for the 83 patients treated with gefitinib compared with those treated with placebo. The lack of consensus regarding the predictive value of EGFR protein expression might reflect the use of a variety of antibodies, the different protocols, or the quantification criteria and the subjectivity in interpretation. In addition, this might be a result of a lack of clarity surrounding the definition and biological implication of protein expression vs overexpression, with the latter implying a pathological state.

Inconsistent results have also been reported regarding a correlation between detection of *EGFR* gene amplification/polysomy as detected by FISH and benefit of TKIs. Hirsch et al. and others have proposed that detection of polysomy and gene amplification by FISH analysis provides a valuable predictive test [23]. Sone et al., in a study of 59 patients, showed a correlation between *EGFR* mutations detected by PCR and amplification detected by FISH [53]. In contrast, Cappuzzo et al. did not show similar results [11]. Bell et al. and Endo et al. did not find a correlation between the results of FISH and molecular analysis and proposed that *EGFR* kinase mutations and gene amplification appear to identify different genetic subsets of pulmonary adenocarcinoma [17]. The study of Bell et al. is of particular interest since they used quantitative PCR, a precise method to evaluate the *EGFR* gene copy number and to distinguish specific amplification from non-specific aneuploidy [17]. However, this study did not evaluate the results with statistical methods [17]. A recent study by Li et al. using PCR to detect deletions within exon 19 and the L858R mutation in exon 21, IHC for expression of EGFR, and chromogenic in situ hybridization for *EGFR* amplification showed that *EGFR* amplification is often associated with an *EGFR* mutation [25]. *EGFR* mutations were predictive biomarkers in 78% of studies, but there was no consensus concerning the methodology [28]. Most studies have evaluated exon 19 in-frame deletions, exon 18 and 21 single nucleotide substitutions, and exon 20 in-frame duplications [28]. Mitsudomi et al. [54] suggested that patients with point mutations at the *EGFR* 19 locus have a lower response rate to gefitinib than individuals with deletions in the same exon, whereas Sasaki et al. have reported that exon 19 deletions offer no predictive value [55]. In addition, the mutant and wild-type EGFR could be influenced by mutations in genes coding for proteins associated with downstream EGFR pathways. Therefore, different patterns of phosphorylation are associated with EGFR mutations and may be used as surrogate markers for therapeutic decisions. Moreover, even the wild-type EGFR pathway may be active through these alternative routes, and these patients may benefit from treatment with TKIs [56]. Therefore, it may be of great interest to study the functional activity of these proteins and their relationship to a TKIs response.

Three major recent clinical trials, BR.21, IDEAL, and IPASS concluded that EGFR protein overexpression was not predictive of response to erlotinib or gefitinib therapy and that these drugs provided maximum benefit in patients with TK mutations [3, 17, 53]. However, a recent meta-analysis of 5,000 lung adenocarcinoma patients reported in 27 studies showed that IHC, FISH, and sequencing were all associated with a significant response to TKIs therapy [28]. This latter review also identified considerable variability in the methodologies used in the different studies and in the predictive value of the results for response to gefitinib and erlotinib therapy [28]. Regarding the methodology used for EGFR analysis, the TMA methodology could be a good approach to reduce such variability, as we showed that all the major mechanisms of EGFR activation can be detected and analyzed on TMAs. For this purpose, a stringent quality control of samples is needed, as awareness of the importance of preanalytical factors is becoming apparent [33, 57]. High-quality tumor tissue is the key to optimal molecular and proteomic analysis. Therefore, the collection, processing, storage, and shipment of biosamples for analysis must be performed under well-documented and rigorously quality-controlled procedures as each of one of these critical steps can modify the nucleic acid and protein structures [33]. Moreover, new fixatives may improve such analyses. A recent study addressed this issue and showed that non-aldehyde fixatives were less convenient for TMA construction [58]. Moreover this study showed that non-aldehyde fixatives can increase the DNA integrity of fixed samples [58]. Intratumoral heterogeneity is the major issue for

consideration when using TMAs to analyze for biomarkers. The key to obtaining a high concordance between analysis of whole paraffin sections and TMA core samples is the selection of representative tumor material (>60% tumor cells, non-tumor zone or stromal reaction removal, lack of necrosis) by the surgical pathologist. Loss of material during pretreatment stages can be another limitation. For this purpose, a minimum of three cores from each tumor sample is recommended [59].

Considering the complexity and redundancy of the EGFR pathway, it is natural to assume that one cannot expect a sole determinant for clinical benefit of EGFR-TKIs [60]. In the present study we evaluated the EGFR status in 61 patients with lung adenocarcinoma by IHC staining for total EGFR and for exon 19 mutant-specific EGFR by FISH on TMAs and by direct sequencing. We demonstrate the high potential of the TMA methodology in detecting the abnormal EGFR status. We showed that the test results are independent variables, suggesting that there is a need to develop evidence-based and consensus standardization guidelines for the performance and interpretation of EGFR tests in routine clinical practice.

Acknowledgement M.I. Ilie was supported by a fellowship from Institut National du Cancer (INCa). P. Hofman, V. Hofman, and J. Mouroux were supported by a PHRC 2003 Grant (CHU of Nice).

Conflict of interest statement We declare that we have no conflict of interest.

References

1. Hirsch FR, Witta S (2005) Biomarkers for prediction of sensitivity to EGFR inhibitors in non-small cell lung cancer. Curr Opin Oncol 17:118–122
2. Reck M (2009) Gefitinib in the treatment of advanced non-small-cell lung cancer. Expert Rev Anticancer Ther 9:401–412. doi:10.1586/era.09.1
3. Mok TS, Wu YL, Thongprasert S et al (2009) Gefitinib or carboplatin-paclitaxel in pulmonary adenocarcinoma. N Engl J Med 361:947–957
4. Jorissen RN, Walker F, Pouliot N, Garrett TP, Ward CW, Burgess AW (2003) Epidermal growth factor receptor: mechanisms of activation and signalling. Exp Cell Res 284:31–53. doi:10.1016/S0014-4827(02)00098-8
5. Sato M, Shames DS, Gazdar AF, Minna JD (2007) A translational view of the molecular pathogenesis of lung cancer. J Thorac Oncol 2:327–343. doi:10.1097/01.JTO.0000263718.69320.4c
6. Ono M, Kuwano M (2006) Molecular mechanisms of epidermal growth factor receptor (EGFR) activation and response to gefitinib and other EGFR-targeting drugs. Clin Cancer Res 12:7242–7251. doi:10.1158/1078-0432.CCR-06-0646
7. Herbst RS, Heymach JV, Lippman SM (2008) Lung cancer. N Engl J Med 359:1367–1380. doi:10.1056/NEJMra0802714
8. Mendelsohn J, Baselga J (2003) Status of epidermal growth factor receptor antagonists in the biology and treatment of cancer. J Clin Oncol 21:2787–2799
9. Ciardiello F, Tortora G (2008) EGFR antagonists in cancer treatment. N Engl J Med 358:1160–1174. doi:10.1056/NEJMra0707704
10. Sequist LV, Lynch TJ (2008) EGFR tyrosine kinase inhibitors in lung cancer: an evolving story. Annu Rev Med 59:429–442. doi:10.1146/annurev.med.59.090506.202405
11. Cappuzzo F, Hirsch FR, Rossi E et al (2005) Epidermal growth factor receptor gene and protein and gefitinib sensitivity in non-small-cell lung cancer. J Natl Cancer Inst 97:643–655. doi:10.1093/jnci/dji112
12. Parra HS, Cavina R, Latteri F, Zucali PA, Campagnoli E, Morenghi E, Grimaldi GC, Roncalli M, Santoro A (2004) Analysis of epidermal growth factor receptor expression as a predictive factor for response to gefitinib ('Iressa', ZD1839) in non-small-cell lung cancer. Br J Cancer 91:208–212. doi:10.1038/sj.bjc.6601923
13. Perez-Soler R, Chachoua A, Hammond LA et al (2004) Determinants of tumor response and survival with erlotinib in patients with non-small-cell lung cancer. J Clin Oncol 22:3238–3247. doi:10.1200/JCO.2004.11.057
14. Hirsch FR, Varella-Garcia M, Bunn PA Jr et al (2006) Molecular predictors of outcome with gefitinib in a phase III placebo-controlled study in advanced non-small-cell lung cancer. J Clin Oncol 24:5034–5042. doi:10.1200/JCO.2006.06.3958
15. Tsao MS, Sakurada A, Cutz JC et al (2005) Erlotinib in lung cancer—molecular and clinical predictors of outcome. N Engl J Med 353:133–144
16. Hirsch FR, Varella-Garcia M, McCoy J et al (2005) Increased epidermal growth factor receptor gene copy number detected by fluorescence in situ hybridization associates with increased sensitivity to gefitinib in patients with bronchioloalveolar carcinoma subtypes: a Southwest Oncology Group Study. J Clin Oncol 23:6838–6845. doi:10.1200/JCO.2005.01.2823
17. Bell DW, Lynch TJ, Haserlat SM et al (2005) Epidermal growth factor receptor mutations and gene amplification in non-small-cell lung cancer: molecular analysis of the IDEAL/INTACT gefitinib trials. J Clin Oncol 23:8081–8092. doi:10.1200/JCO.2005.02.7078
18. Han SW, Kim TY, Hwang PG et al (2005) Predictive and prognostic impact of epidermal growth factor receptor mutation in non-small-cell lung cancer patients treated with gefitinib. J Clin Oncol 23:2493–2501. doi:10.1200/JCO.2005.01.388
19. Morita S, Okamoto I, Kobayashi K et al (2009) Combined survival analysis of prospective clinical trials of gefitinib for non-small cell lung cancer with EGFR mutations. Clin Cancer Res 15:4493–4498. doi:10.1158/1078-0432.CCR-09-0391
20. Sharma SV, Bell DW, Settleman J, Haber DA (2007) Epidermal growth factor receptor mutations in lung cancer. Nat Rev Cancer 7:169–181. doi:10.1038/nrc2088
21. Ellis PM, Morzycki W, Melosky B et al (2009) The role of the epidermal growth factor receptor tyrosine kinase inhibitors as therapy for advanced, metastatic, and recurrent non-small-cell lung cancer: a Canadian national consensus statement. Curr Oncol 16:27–48
22. Yu J, Kane S, Wu J et al (2009) Mutation-specific antibodies for the detection of EGFR mutations in non-small-cell lung cancer. Clin Cancer Res 15:3023–3028. doi:10.1158/1078-0432.CCR-08-2739
23. Hirsch FR, Varella-Garcia M, Cappuzzo F et al (2007) Combination of EGFR gene copy number and protein expression predicts outcome for advanced non-small-cell lung cancer patients treated with gefitinib. Ann Oncol 18:752–760. doi:10.1093/annonc/mdm003
24. Hirsch FR, Varella-Garcia M, Bunn PA Jr, Di Maria MV, Veve R, Bremmes RM, Baron AE, Zeng C, Franklin WA (2003) Epidermal growth factor receptor in non-small-cell lung carcinomas: corre-

lation between gene copy number and protein expression and impact on prognosis. J Clin Oncol 21:3798–3807. doi:10.1200/JCO.2003.11.069
25. Li AR, Chitale D, Riely GJ, Pao W, Miller VA, Zakowski MF, Rusch V, Kris MG, Ladanyi M (2008) EGFR mutations in lung adenocarcinomas: clinical testing experience and relationship to EGFR gene copy number and immunohistochemical expression. J Mol Diagn 10:242–248. doi:10.2353/jmoldx.2008.070178
26. Gupta R, Dastane AM, Forozan F, Riley-Portuguez A, Chung F, Lopategui J, Marchevsky AM (2009) Evaluation of EGFR abnormalities in patients with pulmonary adenocarcinoma: the need to test neoplasms with more than one method. Mod Pathol 22:128–133. doi:10.1038/modpathol.2008.182
27. El-Zammar OA, Zhang S, Katzenstein AL (2009) Comparison of FISH, PCR, and immunohistochemistry in assessing EGFR status in lung adenocarcinoma and correlation with clinicopathologic features. Diagn Mol Pathol 18:133–137. doi:10.1097/PDM.0b013e3181857ea9
28. Gupta R, Dastane AM, McKenna R Jr, Marchevsky AM (2009) The predictive value of epidermal growth factor receptor tests in patients with pulmonary adenocarcinoma: review of current "best evidence" with meta-analysis. Hum Pathol 40:356–365. doi:10.1016/j.humpath.2008.08.008
29. Eberhard DA, Giaccone G, Johnson BE (2008) Biomarkers of response to epidermal growth factor receptor inhibitors in non-small-cell lung cancer working group: standardization for use in the clinical trial setting. J Clin Oncol 26:983–994. doi:10.1200/JCO.2007.12.9858
30. Travis WD, Brambilla E, Muller-Hermelink HK, Harris CC (2004) World health organization classification of tumours. Pathology and genetics of tumours of the lung, pleura, thymus and heart. IARC Press, Lyon
31. Mountain CF (1997) Revisions in the international system for staging lung cancer. Chest 111:1710–1717. doi:10.1378/chest.111.6.1710
32. Betsou F, Lehmann S, Ashton G et al (2010) Standard preanalytical coding for biospecimens: defining the sample PREanalytical code. Cancer Epidemiol Biomark Prev 19:1004–1011. doi:10.1158/1055-9965.EPI-09-1268
33. Hofman V, Ilie M, Gavric-Tanga V et al (2010) Rôle du laboratoire d'anatomie pathologique dans l'approche pré-analytique des examens de biologie moléculaire réalisés en pathologie tumorale. Ann Pathol 30:85–93
34. Hofman P, Butori C, Havet K, Hofman V, Selva E, Guevara N, Santini J, Van Obberghen-Schilling E (2008) Prognostic significance of cortactin levels in head and neck squamous cell carcinoma: comparison with epidermal growth factor receptor status. Br J Cancer 98:956–964. doi:10.1038/sj.bjc.6604245
35. Brevet M, Arcila M, Ladanyi M (2010) Assessment of EGFR mutation status in lung adenocarcinoma by immunohistochemistry using antibodies specific to the two major forms of mutant EGFR. J Mol Diagn 12:169–176. doi:10.2353/jmoldx.2010.090140
36. Koynova DK, Tsenova VS, Jankova RS, Gurov PB, Toncheva DI (2005) Tissue microarray analysis of EGFR and HER2 oncogene copy number alterations in squamous cell carcinoma of the larynx. J Cancer Res Clin Oncol 131:199–203. doi:10.1007/s00432-004-0627-y
37. Choong NW, Dietrich S, Seiwert TY et al (2006) Gefitinib response of erlotinib-refractory lung cancer involving meninges—role of EGFR mutation. Nat Clin Pract Oncol 3:50–57. doi:10.1038/ncponc0400
38. Hall TA (1999) BioEdit: a user-friendly biological sequence alignment editor and analysis program for Windows 95/98/NT. Nucl Acids Symp Ser 41:95–98
39. Park K, Han S, Shin E, Kim HJ, Kim JY (2007) EGFR gene and protein expression in breast cancers. Eur J Surg Oncol 33:956–960. doi:10.1016/j.ejso.2007.01.033
40. Sauter G, Simon R, Hillan K (2003) Tissue microarrays in drug discovery. Nat Rev Drug Discov 2:962–972
41. Al-Kuraya K, Schraml P, Torhorst J et al (2004) Prognostic relevance of gene amplifications and coamplifications in breast cancer. Cancer Res 64:8534–8540. doi:10.1158/0008-5472.CAN-04-1945
42. Giltnane JM, Molinaro A, Cheng H, Robinson A, Turbin D, Gelmon K, Huntsman D, Rimm DL (2008) Comparison of quantitative immunofluorescence with conventional methods for HER2/neu testing with respect to response to trastuzumab therapy in metastatic breast cancer. Arch Pathol Lab Med 132:1635–1647
43. Bhargava R, Lal P, Chen B (2004) Feasibility of using tissue microarrays for the assessment of HER-2 gene amplification by fluorescence in situ hybridization in breast carcinoma. Diagn Mol Pathol 13:213–216
44. Ilie M, Mazure NM, Hofman V et al (2010) High levels of carbonic anhydrase IX in tumour tissue and plasma are biomarkers of poor prognostic in patients with non-small cell lung cancer. Br J Cancer 102:1627–1635
45. Suzuki S, Dobashi Y, Sakurai H, Nishikawa K, Hanawa M, Ooi A (2005) Protein overexpression and gene amplification of epidermal growth factor receptor in non small cell lung carcinomas. An immunohistochemical and fluorescence in situ hybridization study. Cancer 103:1265–1273. doi:10.1002/cncr.20909
46. Bubendorf L, Nocito A, Moch H, Sauter G (2001) Tissue microarray (TMA) technology: miniaturized pathology archives for high-throughput in situ studies. J Pathol 195:72–79. doi:10.1002/path.893
47. Sato-Kuwabara Y, Neves JI, Fregnani JH, Sallum RA, Soares FA (2009) Evaluation of gene amplification and protein expression of HER-2/neu in esophageal squamous cell carcinoma using Fluorescence in situ Hybridization (FISH) and immunohistochemistry. BMC Cancer 9:6. doi:10.1186/1471-2407-9-6
48. Nocito A, Kononen J, Kallioniemi OP, Sauter G (2001) Tissue microarrays (TMAs) for high-throughput molecular pathology research. Int J Cancer 94:1–5. doi:10.1002/ijc.1385
49. Brabender J, Danenberg KD, Metzger R, Schneider PM, Park J, Salonga D, Holscher AH, Danenberg PV (2001) Epidermal growth factor receptor and HER2-neu mRNA expression in non-small cell lung cancer is correlated with survival. Clin Cancer Res 7:1850–1855
50. Nakamura H, Kawasaki N, Taguchi M, Kabasawa K (2006) Survival impact of epidermal growth factor receptor overexpression in patients with non-small cell lung cancer: a meta-analysis. Thorax 61:140–145. doi:10.1136/thx.2005.042275
51. Franklin WA, Veve R, Hirsch FR, Helfrich BA, Bunn PA Jr (2002) Epidermal growth factor receptor family in lung cancer and premalignancy. Semin Oncol 29:3–14. doi:10.1053/sonc.2002.31520
52. Pinter F, Papay J, Almasi A et al (2008) Epidermal growth factor receptor (EGFR) high gene copy number and activating mutations in lung adenocarcinomas are not consistently accompanied by positivity for EGFR protein by standard immunohistochemistry. J Mol Diagn 10:160–168. doi:10.2353/jmoldx.2008.070125
53. Sone T, Kasahara K, Kimura H et al (2007) Comparative analysis of epidermal growth factor receptor mutations and gene amplification as predictors of gefitinib efficacy in Japanese patients with nonsmall cell lung cancer. Cancer 109:1836–1844. doi:10.1002/cncr.22593
54. Mitsudomi T, Kosaka T, Endoh H et al (2005) Mutations of the epidermal growth factor receptor gene predict prolonged survival after gefitinib treatment in patients with non-small-cell lung cancer with postoperative recurrence. J Clin Oncol 23:2513–2520. doi:10.1200/JCO.2005.00.992

55. Sasaki H, Endo K, Okuda K et al (2008) Epidermal growth factor receptor gene amplification and gefitinib sensitivity in patients with recurrent lung cancer. J Cancer Res Clin Oncol 134:569–577
56. VanMeter AJ, Rodriguez AS, Bowman ED et al (2008) Laser capture microdissection and protein microarray analysis of human non-small cell lung cancer: differential epidermal growth factor receptor (EGPR) phosphorylation events associated with mutated EGFR compared with wild type. Mol Cell Proteomics 7:1902–1924
57. Yu YY, Zhu ZG (2010) Significance of biological resource collection and tumor tissue bank creation. World J Gastrointest Oncol 2:5–8. doi:10.4251/wjgo.v2.i1.5
58. Lassalle S, Hofman V, Marius I et al (2009) Assessment of morphology, antigenicity, and nucleic acid integrity for diagnostic thyroid pathology using formalin substitute fixatives. Thyroid 19:1239–1248
59. Piqueras M, Navarro S, Castel V, Canete A, Llombart-Bosch A, Noguera R (2009) Analysis of biological prognostic factors using tissue microarrays in neuroblastic tumors. Pediatr Blood Cancer 52:209–214
60. Uramoto H, Mitsudomi T (2007) Which biomarker predicts benefit from EGFR-TKI treatment for patients with lung cancer? Br J Cancer 96:857–863. doi:10.1038/sj.bjc.6603665

Virchows Arch (2010) 457:497–507
DOI 10.1007/s00428-010-0954-0

ORIGINAL ARTICLE

TTF1 expression in normal lung neuroendocrine cells and related tumors: immunohistochemical study comparing two different monoclonal antibodies

Stefano La Rosa · Anna Maria Chiaravalli · Claudia Placidi · Nikolaos Papanikolaou · Michele Cerati · Carlo Capella

Received: 15 April 2010 / Revised: 17 July 2010 / Accepted: 19 July 2010 / Published online: 6 August 2010
© Springer-Verlag 2010

Abstract Thyroid transcription factor-1 (TTF1) regulates lung morphogenesis and differentiation, and its immunohistochemical expression is used for identifying lung neoplasms. The 8G7G3/1 antibody has been used in previous studies, but a different and more sensitive anti-TTF1 antibody, named SPT24, has become commercially available. Since the immunohistochemical expression of TTF1 in normal lung neuroendocrine (NE) cells has not been previously investigated and its utility in the diagnosis of lung NE tumors is a controversial issue, we studied the TTF1 expression in normal adult and fetal lungs, in 83 pulmonary NE neoplasms, in 131 non-lung NE tumors and in 36 metastases from these neoplasms using these two antibodies. A TTF1 immunoreactivity was demonstrated in normal fetal and adult NE cells when using the SPT24 clone. Conversely, using the 8G7G3/1 antibody, only rare fetal neuroendocrine cells were TTF1 positive while adult NE cells were negative. The SPT24 clone identified TTF1 expression in more carcinoids, most of them peripherally located, and poorly differentiated NE carcinomas than the 8G7G3/1 clone. Non-pulmonary well-differentiated NE tumors were negative for both antibodies. Among the 45 non-pulmonary poorly differentiated NE carcinomas 11% were positive for 8G7G3/1 and 18% for SPT24. TTF1 expression in metastases perfectly reflected that detected in the related primary tumors. Our results indicate that the SPT24 antibody is more sensitive than the 8G7G3/1 clone for labeling lung carcinoids and it appears particularly useful in detecting peripheral neoplasms. In addition, the expression of TTF1 in normal NE cells suggests a possible role for the transcription factor in their development and differentiation.

Keywords Thyroid transcription factor-1 · Lung · Carcinoid · Immunohistochemistry

S. La Rosa (✉) · A. M. Chiaravalli · M. Cerati · C. Capella
Department of Pathology, Ospedale di Circolo,
Viale Borri 57,
21100 Varese, Italy
e-mail: anapat@ospedale.varese.it

C. Placidi · N. Papanikolaou · C. Capella
Department of Human Morphology, University of Insubria,
Varese, Italy

Introduction

Thyroid transcription factor-1 (TTF1) is a tissue-specific transcription factor involved in the development and morphogenesis of the lung, thyroid, and ventral forebrain [1]. In normal adult tissues it is expressed in epithelial thyroid cells, in Clara cells, and type 2 pneumocytes of the lung and in pituicytes [1–3]. Consequently, the expression of TTF1 in tumors originating in the thyroid, lungs, and neurohypophysis is not surprising. Among thyroid tumors, with the exception of anaplastic/undifferentiated carcinomas, TTF1 is widely expressed as demonstrated by the fact that medullary carcinomas and neoplasms of follicular derivation are generally TTF1 positive [1, 2, 4]. TTF1 expression has been reported to be positive in most lung adenocarcinomas and non-mucinous bronchioloalveolar carcinomas. For this reason, TTF1 immunohistochemistry seems particularly useful for the differential diagnosis between primary and metastatic adenocarcinomas of the lung [5].

Although it is well known that TTF1 regulates the morphogenesis and development of respiratory cells of the lung [6], there are no data indicating the expression of TTF1 in fetal and/or adult pulmonary neuroendocrine (NE)

cells where it might play a role in their differentiation and development. Moreover, the usefulness of TTF1 immunohistochemical detection in the diagnosis of lung NE tumors is a controversial issue [5]. Poorly differentiated NE carcinomas (PDNECs) of the lung express TTF1, but this finding does not permit a differential diagnosis with lung metastases from PDNECs located elsewhere, since they are frequently TTF1 positive, with the sole exception of Merkel cell carcinoma of the skin [7–9]. The utility of TTF1 immunohistochemistry in the diagnosis of pulmonary carcinoids is a matter of ongoing debate, and published results from different groups have often been contradictory. Some authors suggested a high specificity and sensitivity of TTF1 immunohistochemistry in detecting lung carcinoids [10] while other groups did not find any TTF1 expression in typical and atypical carcinoids [5, 11–13]. Between these two extremes, other investigators have reported an expression of TTF1 ranging from 17% to 69% of cases [14–21]. In most of the published studies only the monoclonal antibody 8G7G3/1 was used. However, a different clone of the anti-TTF1 antibody, SPT24, is now commercially available and it has been found to be more sensitive than the 8G7G3/1 clone in recognizing lung adenocarcinomas [20, 22]. Matoso et al. [20] demonstrated that the specificity of the two clones was identical while Comperat et al. [22] found that the SPT24 clone, while more sensitive, was a little bit less specific than the 8G7G3/1 antibody. The usefulness of the SPT24 antibody in the diagnosis of lung carcinoids and of lung NE carcinomas in general has not been widely investigated, but some recent results seem to indicate a higher sensitivity of the SPT24 clone compared to the 8G7G3/1 antibody [20] which warrants further investigation.

In the present study we have investigated, using both the 8G7G3/1 and SPT24 antibodies, a series of 83 NE tumors of the lung and, for comparison, a series of 131 NE neoplasms of different sites in order to verify their diagnostic usefulness in detecting primary lung NE neoplasms. Moreover, we investigated 19 metastases from pulmonary NE tumors and 17 metastases from non-pulmonary NE tumors. In addition, we also studied a series of normal adult and fetal lungs to verify whether pulmonary NE cells express TTF1. Finally, we have reviewed the literature on TTF1 expression in well and poorly differentiated NE tumors of the lung and of other sites to give to the reader a comprehensive overview of this controversial topic.

Materials and methods

Cases

Ten normal adult lungs, seven normal fetal lungs (gestational age ranging from 14 to 33 weeks), four tumorlets, one of them associated with NE hyperplasia in the surrounding pulmonary parenchyma, and 83 NE tumors of the lung were collected from the files of the Department of Pathology of the Ospedale di Circolo in Varese. Tumors were classified according to the WHO classification of pulmonary neoplasms [23] into 41 typical carcinoids (TCs), ten atypical carcinoids (ACs), 13 large cell NE carcinomas (LCNECs), and 19 small cell NE carcinomas (SCNECs). Moreover, 131 NE neoplasms (86 well differentiated and 45 poorly differentiated) located outside the lung were studied for comparison. The 86 non-pulmonary well-differentiated NE tumors consisted of six gastric, 54 intestinal and 26 pancreatic tumors. The non-lung PDNECs were located in the esophagus (five cases), stomach (eight cases), intestine (12 cases), pancreas (two cases), gallbladder (one case), skin (four cases), uterus (two cases), prostate (six cases), urinary bladder (one case), and the head and neck region (four cases). The study also included 17 metastases from non-lung well-differentiated NE tumors (two gastric, one duodenal, ten ileal, one rectal, and three pancreatic) and 19 metastases from lung NE tumors: three from TCs (one in the liver, one in a lymph node and one in the thyroid), one from AC (liver), eight from LCNECs (six nodal and two pleural), and seven from SCNECs (one cerebral, one cerebellar, one cutaneous and four nodal). All tissues were fixed in buffered formalin (formaldehyde 4% and acetate buffer 0.05 M) for 24 h and routinely embedded in paraffin wax. Five-micrometer-thick sections were stained with hematoxylin–eosin (H & E) and Grimelius' silver stain for the histopathological examination.

Immunohistochemistry

Three-micrometer-thick sections were mounted on poly-L-lysine coated slides, deparaffinized and hydrated through graded alcohols to water. After endogenous peroxidase activity inhibition, performed by dipping sections in 3% hydrogen peroxide for 10 min, sections were treated in EDTA buffer pH 8 in a microwave oven at 750 W for 10 min for antigen retrieval. This treatment gave the best result in terms of staining intensity when compared with treatment using citrate buffer pH 6. Successively, sections were incubated with primary monoclonal anti-TTF1 antibodies (SPT24 or 8G7G3/1 clone) at 4°C for 18–20 h followed by the avidin–biotin complex (ABC) procedure. Immunoreactions were developed using 0.03% 3,3′-diaminobenzidine tetrahydrochloride and then sections were counterstained with Harris' hematoxylin. Colocalization studies were performed using double label immunohistochemical stains as previously described [24] and employing the two anti-TTF1 antibodies and the monoclonal anti-chromogranin A antibody LK2H10 (Ventana, Tucson, AZ, USA). The SPT24 antibody (Novocastra, Newcastle, UK; used at

1:100 dilution) was raised against a prokaryotic recombinant protein corresponding to the 123 amino acid fragment of the N-terminal region of the TTF1 molecule. The 8G7G3/1 antibody (NeoMarkers, Fremont, CA, USA; used at 1:2 dilution) was raised against a rat TTF1 recombinant protein [25]. Only nuclear immunoreactivity was considered while faint cytoplasmic staining, sometimes observed with the 8G7G3/1 antibody, was considered a negative result [26]. Specificity controls consisted of substitution of the primary antibody with non-immune serum of the same species at the same dilution and use of control tissues with or without the pertinent antigen.

To exclude equivocal reactions and in agreement with the criteria adopted in several previous studies [7, 11, 12, 14, 15, 18, 27] tumors were considered negative (0) when there was no immunoreactivity or if immunoreactivity was observed in less than 10% of tumor cells. Positive tumors were scored as follows: weak (1+) when the intensity of the reaction was weak and frequently observed in 10% to 40% of tumor cells; intense (3+) when it was strong and generally present in more than 70% of cells; moderate (2+) when it showed features between scores 1+ and 3+.

The specificity and sensitivity of anti-TTF1 antibodies in detecting NE neoplasms of the lung was calculated as follows: specificity = truenegatives/(true negatives + false positives); sensitivity = true positives/(true positives + false negatives) [28, 29]. For detecting lung NE tumors, false positives were defined as non-pulmonary NE tumors showing TTF1 immunoreactivity while false negatives were lung NE tumors lacking TTF1. True positives were defined as lung tumors showing TTF1 immunoreactivity while true negatives were non-lung neoplasms lacking TTF1.

Statistical analysis

The different expression of TTF1 detected with both antibodies among various tumor types was evaluated using the Fisher's exact test.

Results

Normal adult and fetal lungs

In adult normal lungs, we identified a TTF1 immunoreactivity in several cells using both antibodies but with some differences between them (Fig. 1). With the 8G7G3/1 clone, the immunoreactivity was nuclear and intense in several alveolar and bronchiolar cells while it was lacking in epithelial cells of bronchi lobares and segmentales and of submucosal glands. Using the SPT24 antibody we identified a nuclear TTF1 immunoreactivity in a higher number of alveolar and bronchiolar cells than with the 8G7G3/1 antibody. In addition, we also observed a strong nuclear TTF1 immunoreactivity in several cells of bronchi lobares and segmentales mainly located in the basal layer and in cells of submucosal glands.

In fetal lungs, a TTF1 immunoreactivity was demonstrated with both antibodies already at the 14th gestational

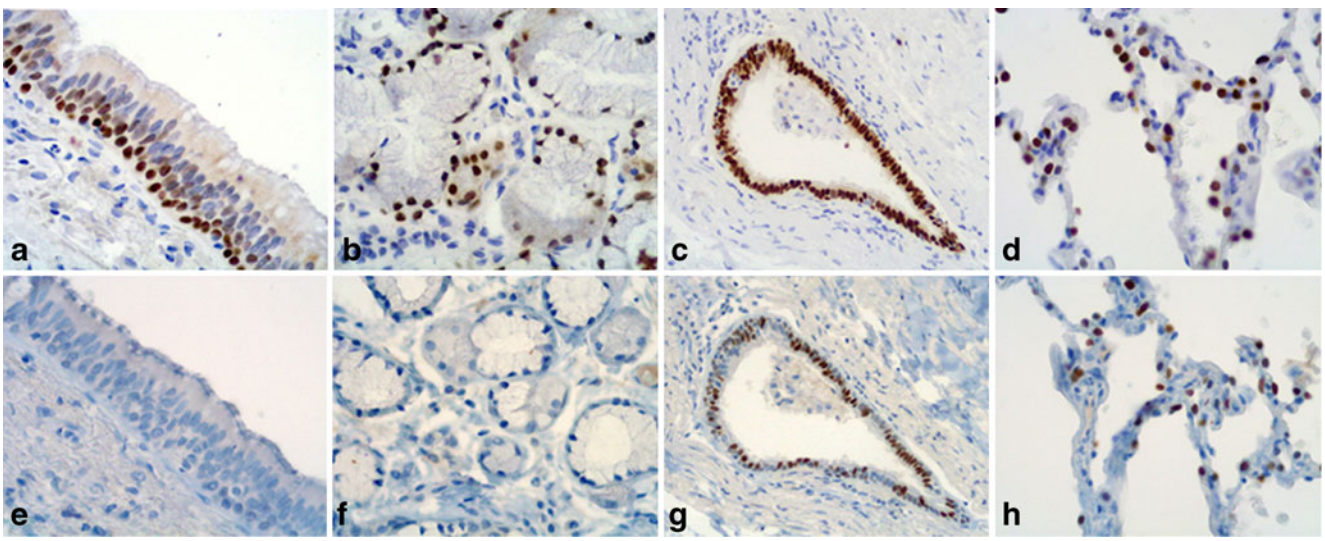

Fig. 1 TTF1 expression in normal adult lung. The SPT24 antibody identified a strong nuclear TTF1 immunoreactivity in several basal bronchial cells (**a**) and in submucosal glands (**b**) which were conversely negative when tested with the 8G7G3/1 antibody (**e**, **f**). Although bronchiolar and alveolar cells were stained by both antibodies, TTF1 positive cells were more numerous and more intensely stained by the SPT24 antibody (**c**, **d**) than by the 8G7G3/1 one (**g**, **h**)

week and it was present in all phases (pseudoglandular, canalicular, and saccular) of the fetal life until birth. As in adult lungs, we observed a TTF1 immunoreactivity in more cells when using the SPT24 antibody than when using the 8G7G3/1 clone and this difference became more evident at a later gestational stage (Fig. 2).

Using double label immunohistochemistry (Fig. 3), we investigated the TTF1 and chromogranin A expression in normal pulmonary NE cells. NE cells present in the mucosa of principal bronchi or peripherally located in both adult and fetal lungs were TTF1 immunoreactive when investigated with the SPT24 antibody. In addition, NE cells forming NE bodies (NEBs) in fetal lungs as well as NE cells forming linear hyperplastic lesions and NEBs in the lung of an adult patient with tumorlets were also positive for the SPT24 antibody. Using the 8G7G3/1 clone, we only found a TTF1 immunoreactivity in rare fetal NE cells especially at an earlier stage of lung development while TTF1 immunoreactivity was lacking in normal or hyperplastic NE cells of adult lungs.

Endocrine tumors

The immunohistochemical nuclear expression of TTF1 in lung NE tumors (Fig. 4), detected using both the 8G7G3/1 and SPT24 antibody, is summarized in Table 1. Although both antibodies showed 100% specificity in detecting lung carcinoids, the SPT24 antibody was more sensitive than the 8G7G3/1 (Table 2). In addition, the number of TTF1-positive cells and intensity of the staining was stronger

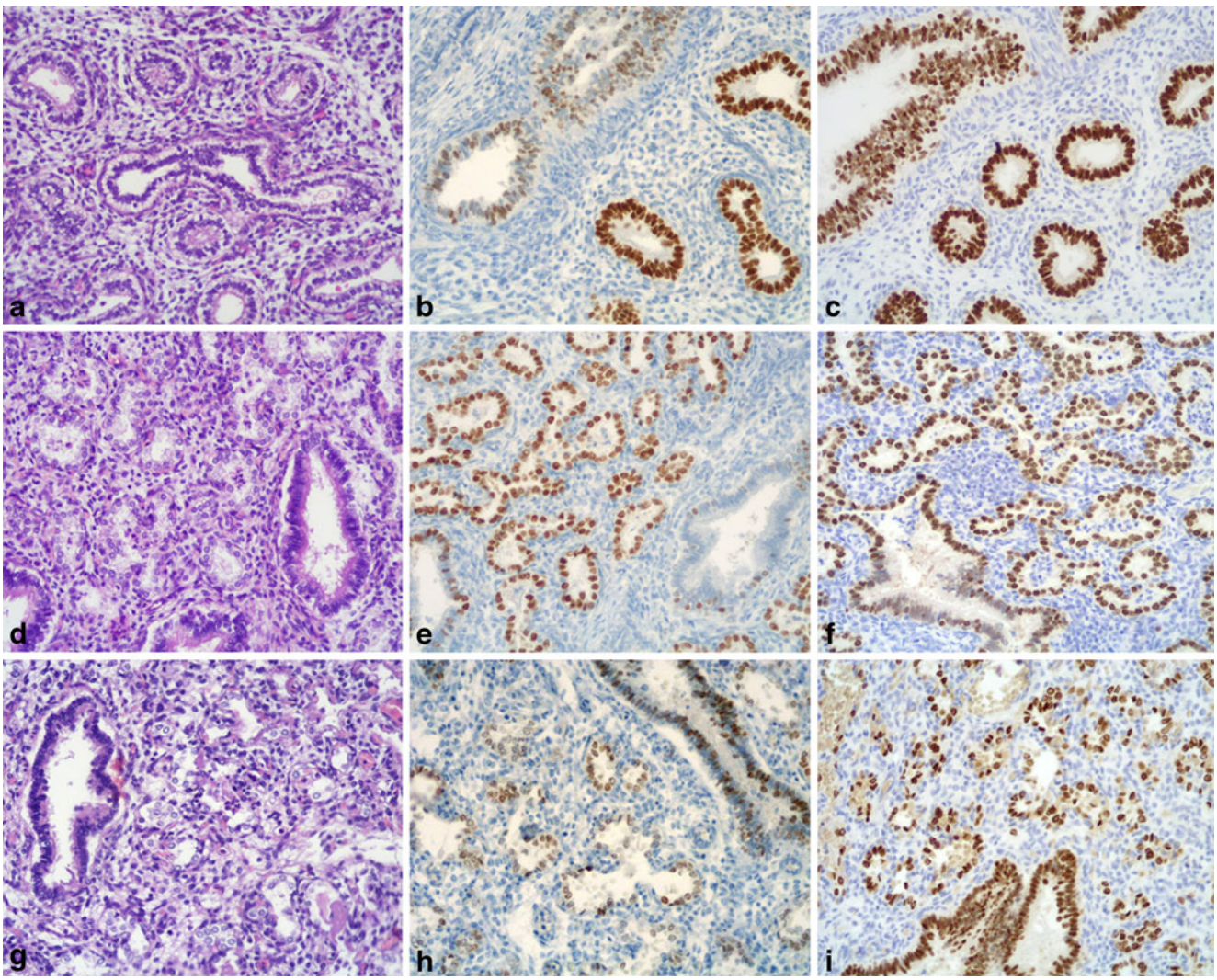

Fig. 2 TTF1 expression in normal fetal lungs at 14th (**a**–**c**), 21st (**d**–**f**), and 27th (**g**–**i**) week of gestation. TTF1 immunoreactivity was found using both antibodies, but the 8G7G3/1 antibody (**b**, **e**, **h**) identified fewer positive cells which also showed a weaker immunoreactivity than the SPT24 antibody (**c**, **f**, **i**)

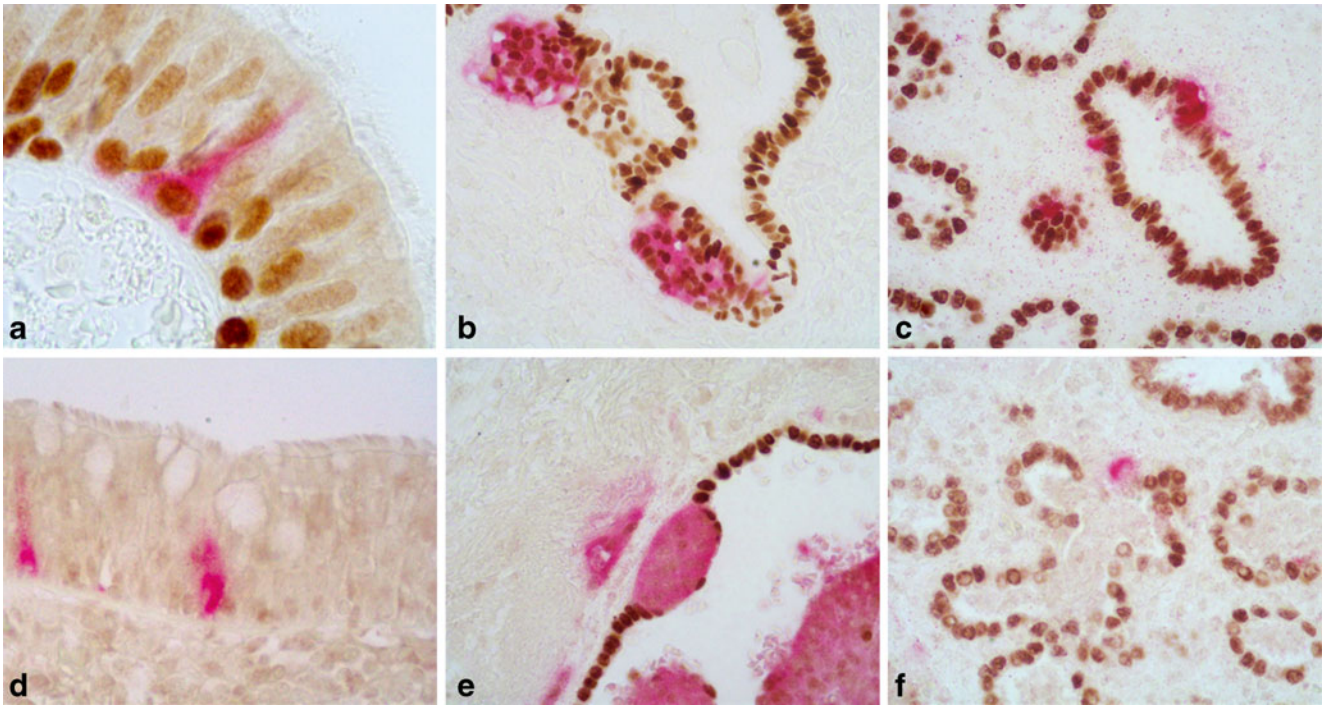

Fig. 3 Double label immunostainings demonstrated that chromogranin A positive NE cells present in main bronchi (**a**) and in peripheral NEBs (**b**) of adult lungs show an intense nuclear TTF1 immunoreactivity when the SPT24 antibody was used. Conversely, these cells lack TTF1 expression when the 8G7G3/1 antibody was employed (**d**, **e**). The same result was observed in fetal lungs, where NE cells where positive for the SPT24 antibody (**c**), but negative for the 8G7G3/1 one (**f**). Chromogranin A is stained in red and TTF1 in brown

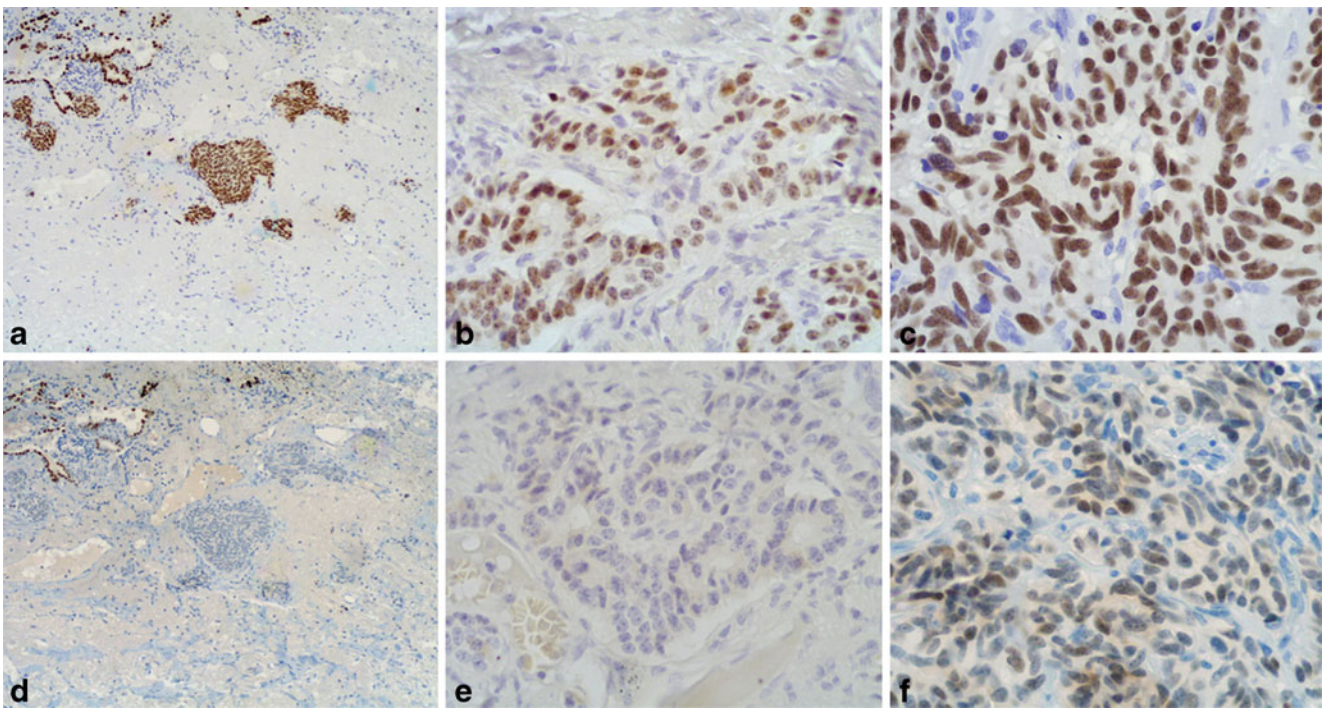

Fig. 4 The SPT24 antibody demonstrated a strong TTF1 immunoreactivity in tumorlets (**a**) and carcinoids (**b**, **c**) which were negative (**d**, **e**) or weak positive (**f**) when tested with the 8G7G3/1 antibody

Table 1 TTF1 expression in lung NE tumors evaluated using 8G7G3/1 and SPT24 antibodies

	Typical carcinoids		Atypical carcinoids		LCNECs		SCNECs	
	8G7G3/1 (%)	SPT24 (%)	8G7G3/1 (%)	SPT24 (%)	8G7G3/1 (%)	SPT24 (%)	8G7G3/1 (%)	SPT24 (%)
Central	0/30	7/30 (23.3)	0/9	1/9 (11)	4/12 (33.3)	9/12 (75)	14/19 (73.3)	16/19 (84.2)
Peripheral	4/11 (36)	8/11 (72.7)	0/1	1/1 (100)	0/1	1/1 (100)		
Total	4/41 (9.7)	15/41 (36.6)	0/10	2/10 (20)	4/13 (30.7)	10/13 (76.9)	14/19 (73.3)	16/19 (84.2)

LCNECs large cell NE carcinomas, *SCNECs* small cell NE carcinomas

using the SPT24 antibody (Table 3). Thirty seven out of forty three (86%) lung endocrine tumors showed an immunohistochemical score 2+/3+ using the SPT24 antibody, and while using the 8G7G3/1 clone the intensity score 2+/3+ was found in 15/22 (68%) tumors. Among TCs the percentage of TTF1 positive neoplasms detected with the SPT24 antibody was 36.6%, statistically significantly higher ($p<0.01$) than the percentage of cases (9.7%) identified with the 8G7G3/1 antibody. However, it is interesting to note that the SPT24 antibody was very sensitive in detecting peripherally located carcinoids. In fact, the percentage of TTF1-positive TCs increased from 23.3% to 72.7% ($p=0.01$), passing from centrally to peripherally located tumors, respectively. This finding also appeared to be true for ACs even if the number of cases was small. The SPT24 antibody was also more sensitive than the 8G7G3/1 one ($p=0.04$) in identifying LCNECs. Conversely, although the SPT24 identified a higher number of SCNECs than the 8G7G3/1 antibody, the difference was not statistically significant.

TTF1 expression in metastases from lung NE tumors perfectly reflected the expression of TTF1 in the related primary neoplasms independent of the antibody used (Table 4).

Well-differentiated digestive NE tumors and related metastases were all negative for TTF1 with the 8G7G3/1 and with the SPT24 antibody. Non-pulmonary PDNECs were positive for TTF1 in five of 45 (11%) cases (two gastric, two prostatic, and one of the urinary bladder) when the 8G7G3/1 antibody was used and in eight of 45 (18%) cases (two gastric, one intestinal, two pancreatic, one gallbladder, and two prostatic) when the SPT24 was used, but this difference was not statistically significant.

All tumorlets investigated showed intense nuclear immunoreactivity for the SPT24 antibody while the immunoreactivity was negative or very weak with the 8G7G3/1 one (Fig. 4).

Table 2 Sensitivity and specificity of SPT24 and 8G7G3/1 antibodies in detecting lung NE tumors

	SPT24		8G7G3/1	
	Sensitivity	Specificity	Sensitivity	Specificity
Carcinoids (%)	33	100	7	100
PDNECs (%)	81	82	56	89
Carcinoids+ PDNECs (%)	52	93	26	96

PDNECs poorly differentiated NE carcinomas

Discussion

In this study we have performed an accurate investigation of TTF1 expression in normal and neoplastic NE cells of the lung using two different antibodies, the clones SPT24 and 8G7G3/1. To the best of our knowledge, we describe for the first time that normal human NE cells of both fetal and adult lungs are TTF1 immunoreactive, either when centrally located in the bronchi lobares and segmentales or peripherally in the lung parenchyma. Using the SPT24 antibody, we were indeed able to identify a TTF1 immunoreactivity in NE cells of fetal lungs starting at the 14th gestational week of life and in those of adult pulmonary parenchyma suggesting that TTF1 may play a role in the development and differentiation of lung NE cells in both fetuses and adults. The 8G7G3/1 antibody stained several alveolar cells but identified TTF1 in only rare fetal NE cells, missing those of adult lungs in agreement with previous findings [11]. In general, the 8G7G3/1 clone showed a lower TTF1 detection capability than the SPT24 antibody, also in non-NE cells, as demonstrated by the fact that using the SPT24 clone we found TTF1 immunoreactivity in more alveolar cells and also in basal cells of larger bronchi and in cells of submucosal glands which were negative for the 8G7G3/1 antibody. The mechanism through which TTF1 may modulate the development and differentiation of lung NE cells is still unknown.

This study is also the first to compare the diagnostic usefulness of SPT24 and 8G7G3/1 antibodies in a large series of NE tumors of the lung. The results obtained

Table 3 Comparison of TTF1 expression between the two antibodies in relation to the cutoff values

Percentage of positive tumor cells	Score	8G7G3/1[a]				SPT24[a]			
		TCs	ATs	LCNECs	SCNECs	TCs	ATs	LCNECs	SCNECs
<10	0	37	10	9	5	26	8	3	3
10–40	1+	3	0	1	3	5	0	1	0
40–70	2+	1	0	1	9	3	1	4	6
≥70	3+	0	0	2	2	7	1	5	10

TCs typical carcinoids, *ACs* atypical carcinoids, *LCNECs* large cell NE carcinomas, *SCNECs* small cell NE carcinomas

[a] The numbers indicate the number of tumors

demonstrate that the SPT24 clone is more sensitive than the 8G7G3/1 antibody for diagnosing lung NE tumors, especially when peripherally located. This finding is important if we consider that the utility of TTF1 immunohistochemistry in the diagnosis of lung NE neoplasms is a controversial issue. The diagnostic usefulness of TTF1 expression in lung carcinoids has been a matter of debate in recent years, and data published in the literature have often been contradictory (Table 5). While some authors have suggested that TTF1 is highly specific and sensitive in identifying lung carcinoids [10], other groups did not confirm this observation [5, 11–13]. Moreover, the expression of TTF1 in lung carcinoids reported in other series ranged from 17% to 69% of cases [14–21]. With the exception of only three investigations [30–32], all published papers described findings obtained using the 8G7G3/1 monoclonal antibody and the discrepancy in the results may be largely explained by different tissue processing, different antigen retrieval protocols, and different selection of cases. In addition, the different cutoff values used to define a tumor as positive should also be considered as an additional element to justify the different results reported in the literature. Indeed, different scoring systems have been used for the quantification of TTF1. In agreement with several previous investigations [7, 11, 12, 14, 15, 18, 27] we believe that focal positivity, corresponding to less than 10% of immunoreactive cells, is not significant. For this reason we used this cutoff value to discriminate between negative and positive tumors. However, it is worth noting that some authors considered tumors negative when no staining was observed [8, 10, 19, 20, 33–38] while in other studies a cutoff of 5% was used to discriminate between negative and positive neoplasms [16, 22].

Table 4 Comparison of TTF1 expression between primary lung NE tumors and related metastases

	8G7G3/1		SPT24	
	Primary	Metastasis	Primary	Metastasis
TCs	0/3	0/3	1/3	1/3
ACs	0/1	0/1	0/1	0/1
LCNECs	3/8	4/8	6/8	6/8
SCNECs	5/7	5/7	6/7	6/7
Total (%)	8/19 (42)	9/19 (47)	13/19 (68)	13/19 (68)

TCs typical carcinoids, *ACs* atypical carcinoids, *LCNECs* large cell NE carcinomas, *SCNECs* small cell NE carcinomas

Our study has demonstrated, in a large series of lung NE neoplasms, that the SPT24 antibody is more sensitive than the 8G7G3/1. Although the general sensitivity did not seem particularly high (Table 2), it is worth noting that the SPT24 antibody was more sensitive in detecting peripherally located carcinoids and this finding is in agreement with results reported by Du and coworkers [16]. In this regard it is interesting to underline that peripherally located tumorlets of our series were also intensely stained by the SPT24 antibody. The specificity of the SPT24 antibody was very high (100%) in detecting lung carcinoids; indeed we did not find any positive cases among 86 well-differentiated endocrine tumors of the digestive system. Although less sensitive, the 8G7G3/1 antibody showed the same high grade of specificity and this finding is in agreement with previously published results (Table 6). By reviewing the literature, we found that only four of 604 (0.7%) gastroenteropancreatic NE tumors investigated were TTF1 positive and they were located in the stomach (two cases) [15, 19], ileum (one case), and pancreas (one case) [21].

The expression of TTF1 in PDNECs of the lung (LCNECs and SCNECs) has been previously well demonstrated (Table 5). However, TTF1 immunohistochemistry does not appear to be reliable for the differential diagnosis between PDNECs of the lung and those located elsewhere because several cases of PDNECs arising in the digestive and urogenital system have been found to be TTF1 positive (Table 7). The only exception is Merkel cell carcinomas of the skin which were TTF1 negative in all studies,

Table 5 Literature review: TTF1 expression in NE tumors of the lung determined using both the 8G7G3/1 and SPT24 antibodies

References	8G7G3/1				SPT24				Carcinoid	
	TC (%)	AT (%)	LCNEC (%)	SCNEC (%)	TC (%)	AT (%)	LCNEC (%)	SCNEC (%)	8G7G3/1 (%)	SPT24 (%)
Holzinger et al. [25]	ne	ne	ne	5/6 (83)						
Myong et al. [35]	ne	ne	ne	14/16 (88)						
Byrd-Gloster et al. [27]	ne	ne	ne	35/36 (97)						
Ordonez et al. [8]	ne	ne	ne	27/28 (96)						
Cheuk et al. [9]	ne	ne	ne	43/52 (83)						
Leech et al. [39]	ne	ne	ne	10/10 (100)						
Nakamura et al. [36]	ne	ne	ne	16/18 (89)						
Wang et al. [37]	ne	ne	ne	5/6 (83)						
Carlson et al. [33]	ne	ne	ne	20/22 (90)						
Yang et al. [40]	ne	ne	ne	9/9 (100)						
Hanly et al. [34]	ne	ne	ne	28/33 (85)						
Barbareschi et al. [41]	ne	ne	6/8 (75)	3/5 (60)						
Folpe et al. [14]	18/51 (35)	9/9 (100)	6/8 (75)	20/21 (95)					27/60 (45%)	
Kaufman et al. [15]	4/9 (44)	2/3 (67)	2/4 (50)	30/37 (81)					6/12 (50)	
Oliveira et al. [10]	16/17 (80)	3/3 (100)	ne	ne					19/20 (95)	
Zamecnik et al. [12]	0/6	ne	ne	8/9 (89)					0/6	
Sturm et al. [11]	0/27	0/23	31/64 (49)	47/55 (85)					0/50	
Du et al. [16]	10/36 (28)	5/17 (29)	6/16 (37)	ne					15/53 (28)	
Saqi et al. [17]	6/12 (50)	2/3 (67)	ne	ne					8/15 (53)	
Lin et al. [18]	8/22 (36)	5/8 (63)	ne	27/30 (90)					13/30 (43)	
Chang et al. [5]	0/8	0/3	ne	19/36 (53)					0/11	
Hiroshima et al. [13]	0/7	0/2	4/17 (24)	13/23 (57)					0/9	
Bobos et al. [42]								11/13 (85)		
Present study	4/41 (10)	0/10	4/13 (31)	14/19 (74)	15/41 (37)	2/10 (20)	10/13 (77)	16/19 (84)	4/51 (8)	17/51 (33)
Total	66/236 (28)	26/81 (32)	59/130 (45)	393/471 (83)	15/41 (37)	2/10 (20)	10/13 (77)	27/32 (84)		
Cai et al. [19] (%)[a]	11/16 (69)								11/16 (69)	
Schmitt et al. [21] (%)[a]	16/31 (52)								16/31 (52)	
Matoso et al. [20] (%)[a]	4/23 (17)				14/23 (61)				4/23 (17)	14/23 (61)
								Total	123/387 (32)	31/74 (42)

TC typical carcinoid, *AT* atypical carcinoid, *LCNEC* large cell NE carcinoma, *SCNEC* small cell NE carcinoma, ne not evaluated

[a] In these studies lung carcinoids were considered together, not differentiated in typical and atypical

independent of the clone used (Table 7). On the basis of these findings, the expression of TTF1 in our non-lung PDNECs is not surprising and is in agreement with other reports in the literature.

The good correlation of TTF1 expression between primary and metastatic NE tumors of the lung that we have found indicates that metastatic tissues retain the same phenotype of the related primary neoplasms and suggests a role of TTF1 immunohistochemistry in the diagnostic pathway of metastatic NE tumors as also indicated by the review of the literature (Table 8). Based on this evidence, TTF1 may appear useful for diagnosing metastases of well-differentiated neuroendocrine tumors of unknown origin [18].

The higher TTF1 detection capability of the SPT24 clone in comparison to the 8G7G3/1 clone has been previously reported [20, 22] and this is in agreement with the higher sensitivity that we have observed in our series of lung carcinoids. The reason why this should be so is not clear and it may perhaps be due to technical aspects as above described and to the different immunogens used for making the antibodies. The SPT24 antibody was raised against a prokaryotic recombinant protein corresponding to a 123-amino acid fragment of the N-terminal region of the TTF1 molecule. The 8G7G3/1 antibody was raised against a rat TTF1 recombinant protein [25], but the exact amino acid sequence recognized by this specific clone has never been specified. However, it is conceivable that the epitopes recognized by the two antibodies are different and that the epitope detected by the SPT24 clone is less modified by tissue processing. In conclusion, our study shows that the specificity and sensitivity of the TTF1 expression for detecting lung NE tumors depends on the clone used. The SPT24 is more sensitive than the 8G7G3/1 antibody for diagnosing lung carcinoids and it appears particularly

Table 6 Literature review: TTF1 expression in non-lung well-differentiated NE tumors

	Gastrointestinal	Pancreas	Thymus
Agoff et al. [7]	0/48	0/15	
Oliveira et al. [10]	0/48	0/10	0/3
Cai et al. [19]	1/46[a]	0/12	
Lin et al. [18]	0/60	0/30	0/1
Schmitt et al. [21]	1/63[b]	1/87	
Present study	0/60	0/26	
Kaufman et al. [15][c]	1/19[a]		0/1
Du et al. [16][c]	0/17		0/11
Saqi et al. [17][c]	0/63		
Total	4/604 (0.7%)		0/16

In all studies the 8G7G3/1 antibody was employed

[a] The positive case was located in the stomach

[b] The positive case was located in the ileum

[c] In these studies gastrointestinal and pancreatic well-differentiated NE tumors were considered together

Table 8 Literature review: TTF1 expression in metastases from lung and non-lung well-differentiated NE tumors

	Gastrointestinal	Pancreas	Lung
Oliveira et al. [10]	0/24	0/10	8/10
Lin et al. [18]	0/10	0/1	2/2
Schmitt et al. [21]	0/28	0/18	
Present study	0/14	0/3	0/4[a]
Total (%)	0/76	0/32	10/16 (63)

Findings obtained with the 8G7G3/1 antibody

[a] When using the SPT24 antibody we found that one out four metastases was TTF1 positive

useful to detect peripherally located neoplasms. PDNECs of the lung widely express TTF1 independently of the clone used. However, the utility of TTF1 immunohistochemistry for diagnosing PDNECs seems to be of limited value because PDNECs located elsewhere, with the exception of Merkel cell carcinomas, are frequently TTF1 positive. In addition, the expression of TTF1 in normal fetal and adult NE cells suggests that it may play a role in their development and differentiation.

Table 7 Literature review: TTF1 expression in non-pulmonary poorly differentiated NE carcinomas

	Esophagus	Gastrointestinal	Pancreas	Kidney	Urinary bladder	Prostate	Uterus	Skin	Clone
Byrd-Gloster et al. [27]								0/21	8G7G3/1
Hanly et al. [34]								0/21	8G7G3/1
Leech et al. [39]								0/11	8G7G3/1
Yang et al. [40]								0/22	8G7G3/1
Lin et al. [18]								0/3	8G7G3/1
Kaufman et al. [15]					3/4	8/8	0/1	0/16	8G7G3/1
Ordonez et al. [8]		2/12	0/1		1/5	0/3	1/3	0/18	8G7G3/1
Cheuk et al. [9]		8/53			1/3	1/3	7/18	0/23	8G7G3/1
Agoff et al. [7]				0/1	2/4	4/4	1/7	0/6	8G7G3/1
Barbareschi et al. [41]		3/13			2/10	5/5	2/3		8G7G3/1
La Rosa et al. [43]				0/1					8G7G3/1
Carlson et al. [33]							3/8		8G7G3/1
Soriano et al. [44]					2/10				8G7G3/1
Jones et al. [45]					17/44				8G7G3/1
Yao et al. [46]						15/18			8G7G3/1
Wang et al. [47]						23/44			8G7G3/1
Yun et al. [38]	15/21								8G7G3/1
Present study	0/5	2/20	0/2		1/1	2/6	0/2	0/4	8G7G3/1
Total	15/26 (58%)	15/98 (15%)	0/3	0/2	29/81 (36%)	58/91 (64%)	14/42 (33%)	0/145	
Bobos et al. [42]								0/13	SPT24
Serrano et al. [48]					13/46				SPT24
Present study	0/5	3/20	2/2		0/1	2/6	0/2	0/4	SPT24
Total	0/5	3/20 (15%)	2/2		13/47 (28%)	2/6 (33%)	0/2	0/17	

Acknowledgments This study was supported in part by a grant from the University of Insubria, Varese.

Conflict of interest statement We declare that we have no conflict of interest.

References

1. Lau SK, Luthringer DJ, Eisen RN (2002) Thyroid transcription factor-1: review. Appl Immunohistochem Mol Morphol 10:97–102
2. Katoh R, Kawaoi A, Miyagi E, Li X, Suzuki K, Nakamura Y, Kakudo K (2000) Thyroid transcription factor-1 in normal, hyperplastic, and neoplastic follicular thyroid cells examined by immunohistochemistry and nonradioactive in situ hybridization. Mod Pathol 13:570–576
3. Lee EB, Tihan T, Scheithauer BW, Zhang PJ, Gonatas NK (2009) Thyroid transcription factor 1 expression in sellar tumors: a histogenetic marker? J Neuropathol Exp Neurol 68:482–488
4. Miettinen M, Franssila KO (2000) Variable expression of keratins and nearly uniform lack of thyroid transcription factor 1 in thyroid anaplastic carcinoma. Hum Pathol 31:1139–1145
5. Chang YL, Lee YC, Liao WY, Wu CT (2004) The utility and limitation of thyroid transcription factor-1 protein in primary and metastatic pulmonary neoplasms. Lung Cancer 44:149–157
6. Maeda Y, Davé V, Whitsett JA (2007) Transcriptional control of lung morphogenesis. Physiol Rev 87:219–244
7. Agoff SN, Lamps LW, Philip AT, Amin MB, Schmidt RA, True LD, Folpe AL (2000) Thyroid transcription factor-1 is expressed in extrapulmonary small cell carcinomas but not in other extrapulmonary neuroendocrine tumors. Mod Pathol 13:238–242
8. Ordonez NG (2000) Value of thyroid transcription factor-1 immunostaining in distinguishing small cell lung carcinomas from other small cell carcinomas. Am J Surg Pathol 24:1217–1223
9. Cheuk W, Kwan MY, Suster S, Chan JK (2001) Immunostaining for thyroid transcription factor 1 and cytokeratin 20 aids the distinction of small cell carcinoma from Merkel cell carcinoma, but not pulmonary from extrapulmonary small cell carcinomas. Arch Pathol Lab Med 125:228–231
10. Oliveira AM, Tazelaar HD, Myers JL, Erickson LA, Lloyd RV (2001) Thyroid transcription factor-1 distinguishes metastatic pulmonary from well-differentiated neuroendocrine tumors of other sites. Am J Surg Pathol 25:815–819
11. Sturm N, Rossi G, Lantuejoul S, Papotti M, Frachon S, Claraz C, Brichon PY, Brambilla C, Brambilla E (2002) Expression of thyroid transcription factor-1 in the spectrum of neuroendocrine cell lung proliferation with special interest in carcinoids. Hum Pathol 33:175–182
12. Zamecnik J, Kodet R (2002) Value of thyroid transcription factor-1 and surfactant apoprotein A in the differential diagnosis of pulmonary carcinomas: a study of 109 cases. Virchows Arch 440:353–361
13. Hiroshima K, Iyoda A, Shida T, Shibuya K, Iizasa T, Kishi H, Tanizawa T, Fujisawa T, Nakatani Y (2006) Distinction of pulmonary large cell neuroendocrine carcinoma from small cell lung carcinoma: a morphological, immunohistochemical, and molecular analysis. Mod Pathol 19:1358–1368
14. Folpe AL, Gown AM, Lamps LW, Garcia R, Dail DH, Zarbo RJ, Schmidt RA (1999) Thyroid transcription factor-1: immunohistochemical evaluation in pulmonary neuroendocrine tumors. Mod Pathol 12:5–8
15. Kaufmann O, Dietel M (2000) Expression of thyroid transcription factor-1 in pulmonary and extrapulmonary small cell carcinomas and other neuroendocrine carcinomas of various primary sites. Histopathology 36:415–420
16. Du EZ, Goldstraw P, Zacharias J, Tiffet O, Craig PJ, Nicholson AG, Weidner N, Yi ES (2004) TTF-1 expression is specific for lung primary in typical and atypical carcinoids: TTF1-positive carcinoids are predominantly in peripheral location. Hum Pathol 35:825–831
17. Saqi A, Alexis D, Remotti F, Bhagat G (2005) Usefulness of CDX2 and TTF-1 in differentiating gastrointestinal from pulmonary carcinoids. Am J Clin Pathol 123:394–404
18. Lin X, Saad RS, Luckasevic TM, Silverman JF, Liu Y (2007) Diagnostic values of CDX2 and TTF-1 expressions in separating metastatic neuroendocrine neoplasms of unknown origin. Appl Immunohistochem Mol Morphol 15:407–414
19. Cai YC, Banner B, Glickman J, Odze RD (2001) Cytokeratin 7 and 20 and thyroid transcription factor 1 can help distinguish pulmonary from gastrointestinal carcinoid and pancreatic endocrine tumors. Hum Pathol 32:1087–1093
20. Matoso A, Singh K, Jacob R, Greaves WO, Tavares R, Noble L, Resnick MB, DeLellis RA, Wang LJ (2010) Comparison of thyroid transcription factor-1 expression by 2 monoclonal antibodies in pulmonary and nonpulmonary primary tumors. Appl Immunohistochem Mol Morphol 18:142–149
21. Schmitt AM, Riniker F, Anlauf M, Schmid S, Soltermann A, Moch H, Heitz PU, Klöppel G, Komminoth P, Perren A (2008) Islet 1 (Isl1) expression is a reliable marker for pancreatic endocrine tumors and their metastases. Am J Surg Pathol 32:420–425
22. Compérat E, Zhang F, Perrotin C, Molina T, Magdeleinat P, Marmey B, Régnard JF, Audouin J, Camilleri-Broet S (2005) Variable sensitivity and specificity of TTF-1 antibodies in lung metastatic adenocarcinoma of colorectal origin. Mod Pathol 18:1371–1376
23. Travis WD, Brambilla E, Muller-Hermelink HK, Harris CC (2004) World Health Organization classification of tumours. Pathology and genetics of tumours of the lung, pleura, thymus and heart. IARC Press, Lyon
24. Lan HY, Mu W, Nikolic-Paterson DJ, Atkins RC (1995) A novel, simple, reliable, and sensitive method for multiple immunoenzyme staining: use of microwave oven heating to block antibody crossreactivity and retrieve antigens. J Histochem Cytochem 43:97–102
25. Holzinger A, Dingle S, Bejarano PA, Miller M, Weaver TE, Di Lauro R, Whitsett JA (1996) Monoclonal antibody to thyroid transcription factor-1: production, characterization, and usefulness in tumor diagnosis. Hybridoma 15:49–53
26. Bejarano PA, Mousavi F (2003) Incidence and significance of cytoplasmic thyroid transcription factor-1 immunoreactivity. Arch Pathol Lab Med 127:193–195
27. Byrd-Gloster AL, Khoor A, Glass LF, Messina JL, Whitsett JA, Livingston SK, Cagle PT (2000) Differential expression of thyroid transcription factor 1 in small cell lung carcinoma and Merkel cell tumor. Hum Pathol 31:58–62
28. La Rosa S, Rigoli E, Uccella S, Chiaravalli AM, Capella C (2004) CDX2 as a marker of intestinal EC-cells and related well-differentiated endocrine tumors. Virchows Arch 445:248–254
29. La Rosa S, Franzi F, Marchet S, Finzi G, Clerici M, Vigetti G, Chiaravalli AM, Sessa F, Capella C (2009) The monoclonal anti-BCL10 antibody (clone 331.1) is a sensitive and specific marker of pancreatic acinar cell carcinoma and pancreatic metaplasia. Virchows Arch 454:133–142
30. Fabbro D, Di Loreto C, Stamerra O, Beltrami A, Lonigro R, Damante G (1996) TTF-1 gene expression in human lung tumours. Eur J Cancer 32A:512–517
31. Di Loreto C, Di Lauro V, Puglisi F, Damante G, Fabbro D, Beltrami CA (1997) Immunocytochemical expression of tissue specific transcription factor-1 in lung carcinoma. J Clin Pathol 50:30–32

32. Harlamert HA, Mira J, Bejarano PA, Baughman RP, Miller MA, Whitsett JA, Yassin R (1998) Thyroid transcription factor-1 and cytokeratins 7 and 20 in pulmonary breast carcinoma. Acta Cytol 42:1382–1388
33. Carlson JW, Nucci MR, Brodsky J, Crum CP, Hirsch MS (2007) Biomarker-assisted diagnosis of ovarian, cervical and pulmonary small cell carcinomas: the role of TTF-1, WT-1 and HPV analysis. Histopathology 51:305–312
34. Hanly AJ, Elgart GW, Jorda M, Smith J, Nadji M (2000) Analysis of thyroid transcription factor-1 and cytokeratin 20 separates Merkel cell carcinoma from small cell carcinoma of the lung. J Cutan Pathol 27:118–120
35. Myong N (2003) Thyroid transcription factor-1 (TTF-1) expression in human lung carcinomas: its prognostic implication and relationship with expression of p53 and Ki67 proteins. J Korean Med Sci 18:494–500
36. Nakamura N, Miyagi E, Murata S, Kawaoi A, Katoh R (2002) Expression of thyroid transcription factor-1 in normal and neoplastic lung tissues. Mod Pathol 15:1058–1067
37. Wang LJ, Greaves WO, Sabo E, Noble L, Tavares R, Ng T, DeLellis RA, Resnick MB (2009) GCDFP-15 positive and TTF-1 negative primary lung neoplasms. A tissue microarray study of 381 primary lung tumors. Appl Immunohistochem Mol Morphol 17:505–511
38. Yun J, Zhang M, Hou J, Tian Q, Fu J, Liang X, Wu Q, Rong T (2007) Primary small cell carcinoma of the esophagus: clinicopathological and immunohistochemical features of 21 cases. BMC Cancer 7:38
39. Leech SN, Kolar AJO, Barrett PD, Sinclair SA, Leonard N (2001) Merkel cell carcinoma can be distinguished from metastatic small cell carcinoma using antibodies to cytokeratin 20 and thyroid transcription factor 1. J Clin Pathol 54:727–729
40. Yang DT, Holden JA, Florell SR (2004) CD117, CK20, TTF-1, and DNA topoisomerase II-α antigen expression in small cell tumors. J Cutan Pathol 31:254–261
41. Barbareschi M, Roldo C, Zamboni G, Capelli P, Cavazza A, Macri E, Cangi MG, Chilosi M, Doglioni C (2004) *CDX-2* homeobox gene product expression in neuroendocrine tumors. Its role as a marker of intestinal neuroendocrine tumors. Am J Surg Pathol 28:1169–1176
42. Bobos M, Hytiroglou P, Kostopoulos I, Karkavelas G, Papadimitriou C (2006) Immunohistochemical distinction between Merkel cell carcinoma and small cell carcinoma of the lung. Am J Dermatopathol 28:99–104
43. La Rosa S, Bernasconi B, Micello D, Finzi G, Capella C (2009) Primary small cell neuroendocrine carcinoma of the kidney: morphological, immunohistochemical, ultrastructural, and cytogenetic study of a case and review of the literature. Endocr Pathol 20:24–34
44. Soriano P, Navarro S, Gil M, Llombart-Bosh A (2004) Small cell carcinoma of the urinary bladder. A clinico-pathological study of ten cases. Virchows Arch 445:292–297
45. Jones TD, Kernek KM, Yang XJ, Lopez-Beltran A, MacLennan GT, Eble JN, Lin H, Pan C, Tretiakova M, Baldrige LA, Cheng L (2005) Thyroid transcription factor 1 expression in small cell carcinoma of the urinary bladder: an immunohistochemical profile of 44 cases. Hum Pathol 36:718–723
46. Yao JL, Madeb R, Bourne P, Lei J, Yang X, Tickoo S, Liu Z, Tan D, Cheng L, Hatem F, Huang J, di Sant'Agnese PA (2006) Small cell carcinoma of the prostate: an immunohistochemical study. Am J Surg Pathol 30:705–712
47. Wang W, Epstein JA (2008) Small cell carcinoma of the prostate. A morphologic and immunohistochemical study of 95 cases. Am J Surg Pathol 32:65–71
48. Serrano FA, Sanchez-Mora N, Arranz JA, Hernandez C, Alvarez-Fernandez E (2007) Large cell and small cell neuroendocrine bladder carcinoma. Immunohistochemical and outcome study in a single institution. Am J Clin Pathol 128:733–739

Virchows Arch (2010) 457:509–511
DOI 10.1007/s00428-010-0965-x

LETTER TO THE EDITOR

Occupational problems with microscopy in the pathology laboratory

Richard John Flavin · Mark Guerin · Donal Sean O'Briain

Received: 28 April 2010 / Revised: 4 August 2010 / Accepted: 18 August 2010 / Published online: 31 August 2010
© Springer-Verlag 2010

Dear Sir:

In the clinical laboratory, many workers spend prolonged periods at microscopy, but there is little appreciation of the range and severity of the work-related problems that may ensue. We administered a questionnaire to assess the magnitude of occupational problems associated with microscope use in the pathology laboratory.

Laboratory personnel in Ireland were interviewed through an anonymized questionnaire. Ethical approval for the study was obtained from the St. James's and Federation of Dublin Voluntary Hospitals Ethics Committee. There were 62 respondents with equal numbers of males and females. The response rate was approximately 40%. Personnel were predominately histopathologists or cytopathologists working at consultant level. The majority were less than 50 years of age. Table 1 is a summary of the main results.

This study reports a high incidence of visual and musculoskeletal problems (some serious) in the pathology laboratory associated with microscopy use. Three quarters reported episodic musculoskeletal problems involving predominately the neck, back, and shoulder and 20% noted repetitive strain injuries. More than half of those affected required some therapy and 5% had taken sick leave. Visual problems, predominately eye fatigue, were indicated by more than half the respondents. Interestingly quite a significant number of respondents who performed routine microscopy less than the median number of hours per week (20.5h) still reported quite a high incidence of either occupationally associated visual or musculoskeletal problems (39% and 26%, respectively). As expected, there was an increase in the reported visual and musculoskeletal problems once the median number of hours is exceeded (71% and 55%, respectively). Furthermore, the number of years working with a microscope did not have a major impact on the type of occupational injury sustained: Those respondents who worked less than the median number of years (14.5 years) reported a high incidence of either visual or musculoskeletal problems (65% and 32%, respectively) as did those who worked above the median number of years (45% and 42%, respectively).

Microscopists should be aware for the potential for work-related illness. Previous studies, involving cytotechnologists and part-time microscopists, have reported similar high rates of neck, shoulder and back pain, eye strain, or headache as a result of working long hours with a conventional light microscope, and related these to the use of non-ergonomic workstations [1–3]. It is interesting that there is little fall in the number reporting occupational injuries compared with the older studies. Although specifics on microscope types was not assessed in the questionnaire, it is likely that newer generation microscopes were in use

R. J. Flavin · D. S. O'Briain
Department of Histopathology,
St. James's Hospital and Trinity College Dublin,
Dublin, Ireland

R. J. Flavin (✉)
The Department of Pathology,
National University of Ireland Galway,
Galway, Ireland
e-mail: richard.flavin@nuigalway.ie

M. Guerin
The Department of Opthalmology,
The Mater Misericordiae University Hospital,
Dublin, Ireland

Table 1 Summary of survey

	Total
No. of respondents	62
Median hours of microscopy per week	20.5 [1–45]
Median years working in a microscopy discipline[a]	14.5 [2–41]
Musculoskeletal problems	
No. of respondents with episodic musculoskeletal problems associated with microscopy	27 (75%)
Of those	
No. with repetitive strain injuries	10 (37%)
No. whose ability to work at microscope affected	9 (33%)
No. requiring treatment	16 (59%)
No. requiring sick leave	3 (11%)
Problem areas: neck (13), back (11), shoulder (8), wrist (4), hand (1)	
Visual problems	
No. of respondents with visual problems associated with microscopy	35 (56%)
Problems include[b]: eye fatigue (25), eye discomfort (6), headache (5), dry eye (4), dizziness and nausea (4)	
No. of respondents with both visual and musculoskeletal problems associated with microscopy	18 (29%)
Prevention	
No. of respondents with visual problems associated with microscopy who:	
Take visual breaks every 15–30 min	1 (3%)
Have routine 2 yearly ophthalmic check up[c]	17 (49%)
Had ergonomic modification of microscope	4 (11%)
No. of respondents with visual or musculoskeletal problems associated with microscopy (44) who:	
Have received ergonomic instruction	7 (16%)
Are not satisfied with their ergonomic workstation ± microscope[d]	19 (43%)

[a] There was no difference in the number of older (greater than 50 years of age) versus younger pathologists who had occupational problems associated with microscopy (73% versus 72%). There was minimal difference between the genders for the same problems (68% males versus 71% females). Those who performed routine microscopy less than the median number of hours per week or had worked with a microscope less than the median number of years still reported quite a high incidence of occupationally associated visual or musculoskeletal problems: 39% and 26%, respectively (less than the median hours); 65% and 32% (less than the median years)

[b] Some experienced more than one problem

[c] All of these respondents wear glasses for visual problems such as myopia, astigmatism, and presbyobia

[d] Fifteen of 27 (56%) had not adjusted their microscopy suite to accommodate for musculoskeletal problems

and might be expected to produce less problems. However, it is also possible that injured microscopists may be more likely to respond to the current questionnaire.

Ergonomic microscopes and workstations, ergonomic observation (neutral neck, straight back, supported elbows, and padded surface) and instruction, and regular eye examination have all been advocated as preventative measures in reducing occupational injury related to microscopy [4, 5]. Intuitively, these measures would be expected to improve the injury rate but specific evidence is scare. One study found that an ergonomic microscope may reduce sick leave days and furthermore increase productivity to an expected range of 5–25% [1]. Our study indicates, however, that few of the injured microscopists had received any ergonomic instruction, and indeed a large percentage were dissatisfied with the ergonomics of their workstation and microscope. Notwithstanding, the role of ergonomic and regular visual checkups in helping reduce the high frequency of microscopy-related injury merits further assessment in well-powered studies.

In conclusion, our results indicate that the risk of acquiring microscopy-related problems will remain as long as preventative strategies are not being implemented by individually affected pathologists.

Conflict of interest The authors declare that they have no conflict of interest.

References

1. Haines H, McAtamney L (1993) Applying ergonomics to improve microscopy work. USA Microsc Anal 1:17–19
2. Kalavar SS, Hunting KL (1996) Musculoskeletal symptoms among cytotechnologists. Lab Med 27:765–769
3. Sillanpaa J, Nyberg M, Laippala P (2003) A new table for work with a microscope, a solution to ergonomic problems. Appl Ergon 34:621–628
4. Vratny M (1999) Considerations in microscope design to avoid cumulative trauma disorder in clinical laboratory applications. Am Clin Lab 18(3):18
5. Kofler M, Kreczy A, Gschwendtner A (2002) Occupational backache–surface electromyography demonstrates the advantage of an ergonomic versus a standard workstation. Eur J Appl Physiol 86:492–497

Virchows Arch (2010) 457:513–520
DOI 10.1007/s00428-010-0983-8

REVIEW AND PERSPECTIVE

A moulage museum is not just a museum

Wax models as teaching instruments

Robin A. Cooke

Received: 30 August 2010 / Accepted: 8 September 2010 / Published online: 5 October 2010
© Springer-Verlag 2010

Abstract The technique of making moulages (wax models) for the teaching of anatomy was introduced in Florence from the late 1600s. Studying the moulages was a much more pleasant way of learning anatomy than the alternative of dissecting dead bodies, when the tissues were undergoing postmortem decay. The technique spread to other medical schools in Europe as well as to England, Russia, North and South America, and Japan. The introduction of photography in the late 1800s made the moulageurs redundant. However, all of these countries now have historical museums that exhibit the specimens that remain from this period. A few moulageurs did continue to make specimens, mainly of dermatological conditions, right into the late 1900s. In 2005, the University of Zurich opened a new museum to showcase some such moulages made by local artists.

Keywords History · Museums · Moulage · Wax models · Teaching · Anatomy

In past centuries, a number of different techniques have been used to present anatomical and pathological features for the education of students of art and medicine. One of the more artistic of these was the creation of wax models (moulages). Although the technique of wax modeling was already known to the Greeks and Romans, the first documented evidence that it was used in anatomy teaching was in the early fourteenth century by a young prosector Allessandra Giliani in Bologna, where she was a master in (vascular) wax injection techniques. About a century later, Andrea del Verrocchio (1435–1488) was the first to make casts of the living body as models for schools, and this apparently stimulated his pupil Leonardo de Vinci (1452–1519) to make wax casts of the ventricles of the brain. Furthermore, the great Michelangelo Buonarroti (1475–1564) created many wax models as base for his marble figures. Other famous painters also had training in anatomy because most wax models were made by artists for students of art, not medicine. However, these moulages were not produced on a large scale

When in 1537, the Flemish physician Andreas Vesalius (1514–1564) was appointed Professor in Surgery at the University of Padua in Italy, one of his duties was to conduct anatomical dissections to demonstrate human anatomy to medical students. Unlike his predecessors, he performed these himself. However, the dissections could only last for a short time because of postmortem changes. To overcome this problem, and to give his students something lasting to take away from his lectures and dissections, Vesalius made drawings of the dissections. To improve their quality, he soon employed an artist to make the drawings and a printer to reproduce them by the newly invented technique of printing invented by Johannes Gutenberg (about 1401–1468) in Mainz, Germany [1]. In 1543 his, "De Humani Corporis Fabrica" became the first printed textbook of human anatomy and established Anatomy as a scientific discipline.

R. A. Cooke (✉)
Pathology Queensland, Royal Brisbane Hospital,
Herston Rd,
Brisbane, QLD 4029, Australia
e-mail: cooker@ozemail.com.au

Italy: the cradle of anatomical wax models

In the 100 years after Vesalius published his "Fabrica," the use of life sized colored wax models was perfected in the

art schools of Northern Italy. Since then, production of moulages took place on a larger scale, especially to serve medical students in the study of human anatomy. The pioneers in perfecting this to the illustration of human anatomy were the painter Lodovico Cigoli (1559–1613) and, a generation later, the wax model artist Gaetano Zumbo (1656–1701), who is known for his wax models of decomposing bodies. (Fig. 1).

However, others also added to this development.. In the eigteenth century, restrictions still existed on human dissections. Fortunately, the Archbishop of Bologna Cardinal Lambertini (1675–1768, the later Pope Benedict XIV) took a special interest in the University, particularly in the work of the anatomist Ercole Lelli (1702–1766). He granted a special dispensation, which allowed anatomical dissections to be performed and the models to be made using these dissections. As a pope, he establised, at his own expense, a wax museum of which Lelli became the custodian. As a result of this, Ercole Lelli was able to perfect the wax methodology for the application to human anatomy [2] (Fig. 2). In 1743, he hired an ambitious young sculptor Giovanna Manzoline (1700–1755), to help him with his work for the pope. The student soon surpassed this master and married his student Anna Morandi (1716–1774), who in turn surpassed her husband in the art of making wax models. After her husband's death, she was given the chair of Anatomy in Bologna. Anna Manzolini and the Florentine sculptor Clemente Susini (1754–1814) brought the Italian School to its zenith [3]. Clemente Susini was supported by the anatomists Felice Fontana (1730–1805) and Paolo Mascagni (1755–1815). Not only was he a master craftsman, he was also a prolific worker. Most of the human anatomical specimens housed in La Specola—the Zoological Museum of the University of Florence—were made by him: 19 life size bodies and 1,400 specimens of

Fig. 1 Florence late 1600s. Victims of a plague epidemic made by Gaetano Zumbo. In relation to the spread of plague by the rat flea (a finding made in 1894), note the rat on the chest of one victim

Fig. 2 Bologna mid-1700s. Life size model of a pregnant woman with the anterior abdominal wall removed to show the anatomy of the internal organs

limbs and organs. Although most of these models are now over 200 years old, they still look fresh and realistic. Each model is presented in a specially made wooden case with a glass front. In the base of each case, there is a drawer, which contains water color drawings of the model with arrows identifying each anatomical structure.

Lelli's earliest works were fixed to a wooden board. A number of these, for example, a horse-shoe kidney, form part of his collection which is now displayed in the museum of the University of Bologna. To provide stability for his life-size whole bodies, he used human bones and added the other tissues in wax. On the other hand, Susini used metal rods inside the wax to support his life size models.

These people were artists as well as anatomists, and their models were studied by students of art as well as of medicine. Their aim was to have their creations aesthetically pleasing as well as being anatomically accurate. To this end, their life size models were always made to adopt an artistic pose. The making and perfection of wax models become a profession, and their students went to many universities in Italy; that is why there are still wax models in many medical schools throughout Italy.

In 1785, Joseph II, Emperor of Austria, inspired by a visit to Anna Manzolini, established in Vienna an Academy for training his army surgeons, which became known as the Josephinum. One of the important teachers he recruited to the staff of his Academy was the Italian surgeon Giovanni Brambilla (1728–1800) from the University of Pavia, a city to the South of Milan. Brambilla was well aware of the teaching potential of the wax anatomical models and suggested that some should be acquired.

The Emperor approached his cousin, Peter Leopold, Grand Duke of Lorraine, who said that his workshops in Florence could not cope with such a large order. However, his court phycisian Felice Fontana took up the commission

and installed the necessary craftsmen in his own house. Therefore, under the supervision of the masters, approximately 1,200 specimens were made. The contract price was 30,000 Austrian florins.

In 1786, the specimens were transported across the Brenner Pass on the backs of mules and then shipped down the Danube from Linz to Vienna. There, they were installed in the Josephinum and contributed to the anatomical knowledge of hundreds of army surgeons. Just as in the original museum in Florence, each specimen was housed in a glass fronted wooden case and accompanied by an annotated water color drawing (Fig. 3).

Included in the consignment was a series of specimens illustrating the normal development and delivery of the fetus and some of the possible obstetrical complications (a similar collection of wax obstetrical models is housed in the Science Museum in Florence). These specimens have been very well cared for and remain one of the prized treasures of the Institute of the History of Medicine housed in the Josephinum in Vienna [4]. Like the wax models in Italy, they still look fresh and life-like, even though they were made over 200 years ago.

Wax models for pathology teaching in Europe

The pathologists in Bologna in the 1800's commissioned wax models to be made of features of pathological anatomy. These included quite a few specimens of congenital abnormalities and teratology. Some of these are matched with a wax model of the fetus beside a preparation of the corresponding skeleton. About 1,600 of these specimens were gathering dust in the Institute of Anatomic Pathology in the University of Bologna until 1988, when a restoration programme was begun to prepare them for display at the 900th centenary of the University. They are now housed in the Museum of the University of Bologna.

Florence was soon to follow. In 1824, the members of the Florentine Accademia Medico-Fisica founded a Pathology Museum. Within a year, the museum treasures had outgrown their original premises, and the museum was moved to another location. In 1837, it was moved to the Careggi Hospital of the University of Florence. Inspired by this success, in 1840, the first Chair of Pathology in Italy was created in Florence. The Professor chose to use the wax models of pathological anatomy to teach his students. Many of these models are now housed in the Museo dell'Istituto Fiorentino di Anatomia Patologica (Fig. 4). In recent years, these models have been cleaned and restored [5].

In Austria, the Medical School of Vienna became pre-eminent in the mid-1800's [6]. One of the prominent members of the staff at that time was the pathologist, Carl Rokitansky (1804–1878). One of his contemporaries, Ferdinand von Hebra (1816–1880) was a pioneer in founding the clinical discipline of Dermatology. Like so many teachers before him, von Hebra found that he could not assemble enough patients at any one time to demonstrate all the variations of a subject that he wished to cover in a lecture. Therefore, in 1860, he produced an "Atlas of Portraits of Diseases of the Skin." This contained 104 plates

Fig. 3 Vienna 1786. Specimen of a head and neck dissection in the Josephinum. It was made in Florence. Note the drawing with the anatomical features labelled. It is housed in a wooden case with a glass front

Fig. 4 Florence about 1840. In the 1830s wax models began to be made of pathological conditions. This is an advanced carcinoma of the breast from the Museo dell'Istituto Fiorentino di Anatomia Patologica artist: E. Tortori. Photograph taken by Marijke van den Tweel

drawn by the artist Anton Elfinger (1821–1864). This artist then turned to making colored wax models of skin diseases. He only made a small number, but he was followed by Karl Henning (1860–1917) who, between 1890 and 1917, made over 1,500 colored wax models of different types of skin diseases. These were prepared in collaboration with von Hebra's successor, Moritz Kaposi (1837–1902), and other dermatologists at the General Hospital in Vienna. Henning's son, Theodor, continued making wax models, but by this time, photography had been introduced, and it began to supersede this technology. Wax models were made in Berlin, too, at this time, but most of them seem to have been lost [7].

In various other countries in Europe, there are museums that contain significant numbers of wax models of medical conditions. Two of the biggest and best preserved are in the Gordon Museum in Guy's Hospital in London [8] and in the Museum and Library of the Hopital St. Louis in Paris [9]. The wax models in the Gordon Museum were created by Joseph Towne (1808–1879). Joseph was 18 years old when he submitted an approximately 18 in. (45 cm) tall wax model of a skeleton in a competition arranged by the Royal Society of Arts. They were offering a gold and a silver medal as prizes for the best anatomical wax models. Towne won the silver medal, but more importantly, this led to his meeting the surgeon Astley Cooper, who hired him as a wax modeler for Guy's Hospital, a position he occupied until his death 53 years later.

At first, Joseph Towne was employed to make anatomical models from human dissections performed by John Hilton (1805–1878), a famous London anatomist and surgeon. He made a number of beautiful anatomical models, but after the passing of the Anatomy Act in 1832, it became possible to obtain bodies for medical students to dissect themselves, and there was no further need for wax anatomical models. Thomas Addison (1793–1860), one of the famous physicians at Guy's then encouraged him to start making models of dermatological conditions—including the hyperpigmentation of patients with adrenal insufficiency (Addison's disease; Fig. 5)

The Gordon Museum at Guy's Hospital has about 50 anatomical models and about 650 dermatological ones made by Towne. The former are now of historical interest, but the latter are still used for teaching dermatology. Towne worked alone, never allowed anyone to watch him at work, and never showed anyone his technique. It appears that none of his specimens contained any internal support and that he used very simple sculpting instruments. Presumably, he made sketches of his subject matter and then sculpted the model from a solid block of wax. His colors are quite different from those of the continental modelers. In addition to his wax modeling, he sculpted marble busts of a number of the famous doctors of Guy's Hospital, including his patron, Astley Cooper.

In 1984, the Gordon Museum was refurbished so that it could combine the functions of an historical museum comprising the wax models of Joseph Towne, the specimens of the original cases of Addison's disease, Bright's disease, and Hodgkin's disease, and a working museum for the teaching of pathology. It also became the center of the audio-visual teaching facility for Guy's Hospital Medical School. As a result, this Museum plays an active and important role in the teaching of today's students while preserving something from the past.

In France, one of the famous surgeons of the Medical School of the University of Paris was Guillaume Dupuytren (1777–1835). In his will, he left money to the Faculty of Medicine to establish the first Chair of Anatomical Pathology. The money was not quite sufficient for this

Fig. 5 London about 1850. Gordon Museum, Guy's Hospital. Addison's disease made by Joseph Towne

purpose, so it was spent on developing a Pathology Museum, which bears his name—the Musée Dupuytren—situated within the Ecole de Medicine in Paris. This Museum has a large collection of modern pathology specimens as well as a considerable number of historical ones. There are quite a number of wax models of clinical conditions—for example, phocomelia, carcinoma of the penis, gout, turban tumour, and Madura foot (Fig. 6). The specimens in this museum have been sorted and catalogued in the past few years, and it is now being refurbished so that it will play a part in teaching in the twenty-first century (Dr. Paul de Saint Maur, personal communication).

The Hopital Saint Louis is situated a few kilometers from the center of Paris. It is one of the oldest hospitals in the city, having been built in 1616. From the early 1800s, it specialised in skin diseases and venereal diseases. The leading physician of this period was Jean-Louis Alibert (1768–1837), who, with von Hebra, was one of the "fathers" of modern dermatology. In one of the inner courtyards of the hospital, there is an old library and museum building. The museum contains a large number of colored wax models of various dermatological conditions, including many which demonstrate the cutaneous manifestations of syphilis. Some of the models are housed on the ground floor, while others are in galleries which rise above this floor level. The main room is used for teaching dermatology and for meetings of the Dermatology Society. With the introduction of antibiotics and other modern treatments, many of these diseases are no longer seen in technologically advanced countries.

Well over 2,000 of these models were made by the artist, Jules Baretta (1834–1928) [9]. He worked in a studio in the hospital from 1865–1914. The dermatologists at the hospital would send him patients. He made a cast of the part of the body to be depicted, and while waiting for the cast to dry (to set) and to guarantee their cooperation, he would entertain them by chatting to them about their condition, or by playing the piano.

The models in the museum still retain their beautiful, natural color and provide a faithful record of skin diseases prevalent at that time (Fig. 7). Baretta became world famous in his time. The first International Congress of Dermatology was held in the Hopital St. Louis Museum in 1889, and his moulages were shown. In 1892, he exhibited some of his models at the Dermatology Congress in Vienna. He received orders from all over the world and sold specimens for an average of 50 Francs.

Russia was not left behind. The Department of Skin and Venereal Diseases of the I.M. Sechenov Moscow Medical Academy was founded in 1869, and a museum was established in 1895 by Professor A.I. Pospelov. He was probably influenced in this by watching Jules Baretta demonstrate his moulages at the Dermatology Congress in Vienna in 1892. Pospelov purchased some Baretta models to be the foundation specimens for his proposed museum. He appointed the wax modeler, S. P. Fiviesky (1856–1934) to prepare dermatological models for him. Fiviesky copied Baretta's technique and won many prizes for his work. He taught his son, S. P. Fiviesky (1896–1971) and his daughter-in-law, Anna F. Fivieskaya. The museum now has about 1,300 wax models, which were all made by the three Fivieskys (Fig. 8). The models are housed in cupboards that line the walls of the lecture theaters in the Dermatology Institute. They are in active use in teaching dermatology.

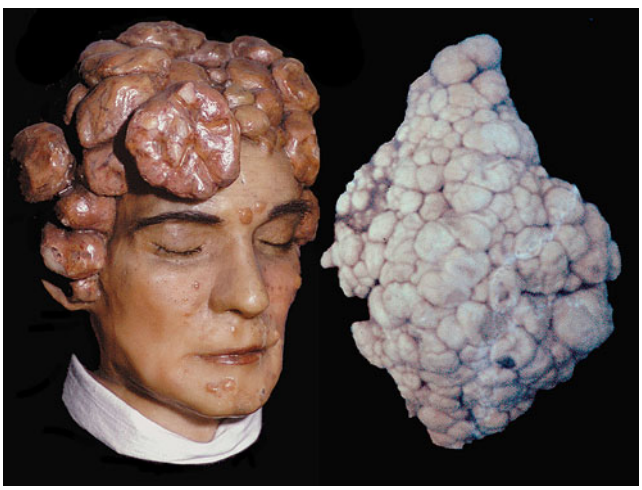

Fig. 6 Paris Dupuytren Museum, Ecole de Medicine mid 1800s. On the *left* is a wax model that shows a patient with a 'Turban tumour'—a benign sweat gland tumour photographed in 1983. On the *right* is a similar tumour removed from the scalp of a patient in Charite Hospital, Berlin in about 1990 when it was photographed

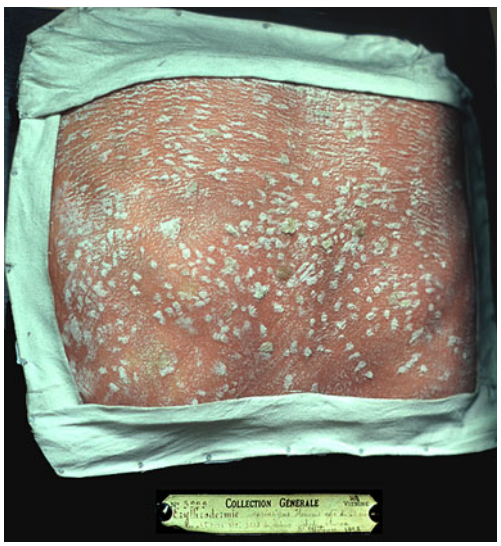

Fig. 7 Paris. Hôpital St Louis. Late 1800s and early 1900s. Erythroderma made by Jules Baretta

Fig. 8 Moscow 1998. Madame Fivieskaya with some of the dermatological wax models she made

Moulage museums outside Europe

In the second half of the nineteenth century, many medical schools in the USA [10] sent well-funded delegations to Europe to purchase teaching materials. These included quite a number of wax anatomical and dermatological models. In 1850, the State of Louisana bought 80 wax dermatological models from Towne in London. In the same year, the first batch of about 300 dermatological wax models for the University of Pennsylvania was also purchased from Towne. Further batches of models were purchased after 1870 from London, Paris, and other European centers and added to the collection in the university. Other universities, such as Harvard in Boston, St. Louis, MO, and Augusta, GA also purchased wax models.

Perhaps the largest surviving collection of wax anatomical and dermatological models in the USA is in the Scott and White Memorial Hospital in the city of Temple, TX [11]. The museum houses about 1,300 specimens from an original collection of 3,000. They were crafted by the husband and wife team, Kenneth and Margaret Phillips between 1932 and 1955.

From Japan [12], Keizo Dohi (1866–1931), a founder of Dermatology in Japan went to study in the Dermatology Clinic of Moritz Kaposi in Vienna in 1895. There, he met Karl Henning from whom he learned the technique of making moulages. On his return to Japan as Professor of Dermatology at the University of Tokyo, he employed an artist whom he had known since early school days—Yu Ito (1864–1934). He instructed him in the art of wax modeling, and in the next 30 years, Ito made over 2,000 moulages. Ito taught the technique to many students, with the result that a number of universities developed collections of wax models of dermatological conditions. The moulage collections were badly damaged and neglected for many years after the introduction of photography. It is estimated that there are well over 3,000 moulages preserved in various medical museums throughout Japan. The biggest collections are reported to be in the following universities—Tokyo, Hokkaido, Chiba, Nigata, Nagoya, Kyoto, and Nagasaki (Fig. 9).

Australian Universities, too, purchased wax models for teaching purposes. The Pathology Museum of the University of Melbourne has one of Baretta's models. It was purchased in Paris by the foundation professor of pathology, anatomy, and physiology who was recrutied from London in 1860. He was given a small amount of money to purchase appropriate teaching aids before he left England.

The University of Queensland Medical School in Brisbane has three models from Vienna. They were purchased by the first professor of pathology in 1935 during a fact finding tour in preparation for the teaching of pathology in the medical school, which was opened in 1936.

South America has a few small collections of wax models. In Brazil, the Museum of Medical History in Recife carries a few terra cotta models of dermatological diseases. These were made by a modeler in Rio de Janeiro. He probably visited Europe in the hey day of the modeling era and brought the technique home with him.

The role of wax model museums in teaching was made obsolete by the Frenchman, Louis Daguerre, who introduced the first practical camera in 1839. In 1888, the

Fig. 9 Nagasaki 2008. University of Nagasaki historical museum. Two of the large cabinets containing wax models probably made by Ryuji Takahira, a pupil of Yu Ito in the early 1900s

American, George Eastman, put photography into the hands of the "masses," when he marketed the Kodak camera. The introduction of Kodachrome film in 1935 made this the best means of illustrating lectures for students. Whereas Vesalius could only demonstrate to a small audience of students, and the moulage museums were only accessible by small numbers of students, using 35 mm kodachrome slides, it was possible for a lecturer to have a live audience of more than 1,000. Since the beginning of this millenium using digital images, a lecturer could reach a much larger live audience. Using transmitting technology, lectures can be viewed in "real time" in auditoria at a distance. They can also be reproduced an infinite number of times by means of various data storage devices.

Despite these revolutionary advances in technology, the art of the moulageur has been preserved in some places, notably in Zurich, Switzerland [13]. Moulages began to be made in the Dermatology Clinic at the University in 1917. The first moulageur was Lotte Volger. In the 1970s, another moulageur, Elsbeth Stoiber, joined the staff. Elsbeth spent a number of years in a leprosy clinic in India where she made many wax models of leprosy. All of these moulages were combined into one collection of about 1,400 specimens. They are now on display in the Moulagenmuseum in the University of Zurich, which opened in 2005 (Fig. 10).

The exquisite craftsmanship of these artists produced artistically beautiful and accurate representations of normal anatomy and of diseases that were prevalent at the time. Many of the diseases demonstrated were shown in an advanced stage because there was no effective treatment available. Because of the treatment that is readily available in countries with well-funded health services, many of these diseases are no longer seen there. However, sadly, some of them still occur in countries that do not have well-funded health services.

The moulage (wax model) museums are worth visiting and preserving not only for their intrinsic artistic value but also for their value as repositories of medical history.

Fig. 10 Zurich 2010. Moulagenmuseum University of Zurich. Chicken pox. These moulages were made in the mid and late 1900s by Lotte Volger and Elsbeth Stoiber

Acknowledgments The author would like to thank the curators of the many museums he has visited around the world for their unstinted assistance in providing factual information about their exhibits. Just as interesting have been the anecdotes about the material and the people who made the original specimens. Thanks also for allowing me to photograph some of the exhibits and for giving me permission to publish them.

Disclaimer The author claims no conflict of interests.

References

1. Krawietz P (2000) Gutenberg man of the millennium—from a secret enterprise to the first media revolution. Verlag Hermann Schmidt, Mainz
2. Armaroli M (1981) Le Cere Anatomiche Bolognesi del Settecento. CLUEB, Bologna
3. Azzaroli ML (1975) La Specola—the zoological museum of Florence University. Leo S. Olschki Editore, Firenze
4. Skopec GH (2000) Anatomie als Kunst—Anatomische Wachsmodelle des 18. Jahrhunderts im Josephinum in Wien. Christian Brandstätter Verlag, Wien
5. Nesi G, Santi R, Taddei GL (2009) Art and the teaching of pathological anatomy at the University of Florence since the nineteenth century. Virchows Arch 455:15–19
6. Lesky E (1977) The Vienna medical school of the 19th century. The Johns Hopkins University Press (JHUP), Baltimore
7. Schnalke T (1995) Diseases in wax—the history of the medical moulage. Quintessence, Berlin
8. Daws J (1979) The remarkable Joseph Towne (1806–1879). Guy's Hospital Medical Students' Magazine
9. Tilles G, Wallach D (1996) Le musee des moulages de l'hôpital Saint-Louis. Doin Editeurs/Assistance Publique Hôpitaux de Paris, Paris
10. Haviland T, Parish LC (1970) A brief account of the use of wax models in the study of medicine. J Hist Med 1970:52–75
11. Mears MM, Feaster V (1994) The wax medical moulage collection at Scott and white memorial hospital. Int J Dermatol 11:446–447
12. Imaizumi T, Nagatoya Y (1995) Dermatologic moulage in Japan. Int J Dermatol 14:817–821
13. Geiges ML (2006) Moulagenmuseum UniversitätsSpital und Universität. Universität Zürich, Zürich

Virchows Arch (2010) 457:521–527
DOI 10.1007/s00428-010-0967-8

ORIGINAL ARTICLE

Increased neuroendocrine cells in resected metastases compared to primary colorectal adenocarcinomas

Marco Volante · Valerio Marci · Snezana Andrejevic-Blant · Veronica Tavaglione · Maria Carla Sculli · Marco Tampellini · Mauro Papotti

Received: 29 June 2010 / Revised: 17 August 2010 / Accepted: 18 August 2010 / Published online: 2 September 2010
© Springer-Verlag 2010

Abstract Neuroendocrine differentiation has been described in rectal adenocarcinomas receiving neoadjuvant therapy prior to radical surgery, but its clinical relevance is controversial and no data are currently available in colorectal carcinoma metastases as compared to primary tumors. The presence of chromogranin A positive tumor cells was investigated by means of immunohistochemistry on surgical specimens from 54 primary colorectal carcinomas and their corresponding metastases, resected at diagnosis or during tumor progression. In 47 patients, tumor metastases were resected 1 month to 12 years after chemotherapy and/or radiotherapy, while in the remaining seven patients no additional therapy after primary surgery was performed. In primary tumors, neuroendocrine differentiation was found in 12/54 cases (22.2%) as compared to 25/54 metastatic lesions (46.3%; $p=0.01$). The presence of neuroendocrine phenotype was not correlated with any clinical pathological parameter nor with a different proliferation index. However, patients having neuroendocrine cells in the primary tumor had a significantly shorter survival from the time of metastatic spread than those having not (33.3 vs. 55.5 months; $p=0.04$). In summary, our data show that colorectal carcinoma metastases contain a higher percentage of neuroendocrine differentiated cells as compared to their corresponding primaries, a finding possibly related to the influence of chemotherapy in neuroendocrine differentiation during colorectal carcinoma progression.

Keywords Colorectal carcinoma · Metastases · Neuroendocrine differentiation · Chemotherapy

M. Volante · V. Marci · V. Tavaglione · M. Papotti
Division of Pathology, University of Turin at San Luigi Hospital, Orbassano,
Torino, Italy

M. C. Sculli · M. Tampellini
Division of Oncology, Department of Clinical & Biological Sciences, University of Turin at San Luigi Hospital, Orbassano,
Torino, Italy

S. Andrejevic-Blant
Institute of Pathology CHUV and University of Lausanne,
Lausanne, Switzerland

M. Volante (✉)
Department of Clinical and Biological Sciences,
University of Turin at San Luigi Hospital,
Regione Gonzole 10,
10043 Orbassano, Torino, Italy
e-mail: marco.volante@unito.it

Introduction

Neuroendocrine differentiation has been described in human adenocarcinomas of the prostate, breast, stomach, lung, and colorectum, among others [1–8]. The clinical significance of this finding is debated and in any case differs among the various organs. In the prostate, neuroendocrine differentiation has been demonstrated in therapy naïve cases but it has been specifically associated to hormone refractory cancers and indeed found associated to tumor progression and a worse prognosis [5]. At variance, in breast cancer neuroendocrine differentiation has been consistently demonstrated to lack any prognostic significance [9], whereas its association with a more aggressive disease is still controversial in lung [7, 10] and stomach carcinomas [6].

In colorectal carcinoma, neuroendocrine cells were identified in up to 77% of cases, largely depending on the method used to assess the neuroendocrine cell population [1, 11, 12]. Classically, chromogranin A immunohisto-

chemistry is the most common technique, although it is generally considered that a panel of neuroendocrine markers, including synaptophysin, CD56 and others, has to be preferred in order to increase the sensitivity. Nevertheless, the clinical relevance of neuroendocrine differentiation in colorectal carcinoma is still debated being either associated to poor survival [13] or not [11].

The mechanisms leading to neuroendocrine differentiation in colorectal carcinoma are incompletely understood and are currently accepted as belonging to divergent differentiation processes that might be modulated by therapeutic interventions. In fact, Shia et al. [14] described a significant increase of chromogranin A positive cells in resected rectal adenocarcinomas after neo-adjuvant chemotherapy alone or combined to radiotherapy; comparing endoscopic biopsies with the corresponding rectal surgical specimen, it was shown that 68% of resected rectal carcinomas after chemotherapy had chromogranin A positive tumor cells, as compared to 30% of cases in pre-treatment endoscopic biopsies and to 17% of cases in a control series of conventional, untreated cases. This observation suggests that pharmacological intervention may have potential effects on the selection of specific cell types that are not sensitive (or not as sensitive) to conventional treatment strategies. This phenomenon is well known in prostatic adenocarcinoma treated with androgen deprivation therapy: an increase of chromogranin A immunoreactive cells in tumor tissue (in association to raised chromogranin A serum levels) has been correlated to the onset of hormonal refractory disease. In addition, the presence of a neuroendocrine cell component in therapy naïve prostate cancer patients was found predictive of androgen deprivation treatment failure [5].

When re-evaluating the morphological features of a rectal adenocarcinoma that occurred in a young woman that is following a long disease free survival after complete resection and medical treatment of a local pelvic recurrence, we observed a significant increase in the amount of chromogranin A positive cells in the recurrent pelvic tumor compared to the primary carcinoma specimen. In between the two operations, the patient received several courses of chemotherapy, as described elsewhere [15]. This observation, in agreement with the data reported by Shia et al. [14], prompted us to investigate if chemotherapy can also affect the extent of neuroendocrine differentiation in resected metastases of relapsing colorectal carcinomas, compared to their primary tumor. We here show that neuroendocrine differentiation, as detected by chromogranin A immunoreactivity, is significantly higher in resected pulmonary, liver, or abdominal metastases of colorectal cancer compared to the corresponding primaries. In addition, median survival was shorter for colorectal carcinomas with a neuroendocrine differentiated population in the primary tumor, indicating that the neuroendocrine cell population may respond differently to current medical treatment for colorectal cancer and may possibly affect survival.

Materials and methods

Patients From the colorectal carcinoma database established at the Oncology Unit of the San Luigi Hospital and University of Turin, 54 patients were retrospectively collected in the period from 1996 to 2008, having a radically resected colorectal adenocarcinoma and also a resection of a synchronous (21 cases) or metachronous (33 cases) metastasis of the same tumor, from the lung, liver, or peritoneum. All but seven patients received adjuvant chemotherapy after resection of the primary, and eight rectal carcinomas had also radiotherapy administrated. The chemotherapy protocols administrated to the 47 patients included oxaliplatin-based chemotherapy (FOLFOX or XELOX or chronomodulated FFL 4/10 regimens) in 39, irinotecan-based chemotherapy (FOLFIRI) in 2, and 5-FluoroUracil based chemotherapy (De Gramont's schema or protracted continuous infusion of 5FloroUracil) in six of them.

Tissues Representative paraffin blocks from both primary and metastatic tumors as well as complete follow-up information were available for all cases. Metastatic lymph nodes were also analyzed in 20 cases, as a control group. All pathological material was anonymized by a pathology staff member not involved in the current project and tissues from primary and metastatic tumors of the same patient were coded to allow the comparison in each anonymized case.

Immunohistochemistry Chromogranin A was selected as a reliable marker of neuroendocrine differentiation based on extensive literature data [14], and the immunohistochemical reactions were performed on sections collected onto charged slides serial to those stained with conventional hematoxylin and eosin. A standard immunohistochemical technique was used, including microwave oven antigen retrieval (15 min in 10 mmol/L citrate buffer solution at pH 6.0) and incubation with the primary chromogranin A antibody (clone LK2H10, diluted 1:800; Novocastra laboratories, Newcastle Upon Tyne, UK). The immunoreactions were revealed by a dextran-chain (biotin-free) detection system (EnVysion, DakoCytomation, Glostrup, Denmark), using 3,3′-diaminobenzidine (DAB, Dako) as a chromogen. The slides were then counterstained with hematoxylin, dehydrated, and mounted. Neuroendocrine cells of the surrounding colorectal mucosa in primary tumors served as positive internal control. Sections of pancreatic islet cells served as external positive controls for chromogranin A in each immunohistochemical run. Chromogranin A reactivity was scored as reported by Shia [14] in a

three-tie system, including score 0: no staining in tumor cells; score 1+: 1–20% of tumor cells stained, and score 2+: >20% of cells stained. In all cases, the proliferative activity was assessed by means of Ki-67 immunostaining (clone MIB1, Dako, diluted 1:300), using the above described procedure. The proliferative fraction was expressed as percentage of Ki-67 reactive nuclei, after counting positive cells out of a thousand. In all cases with a chromogranin A-positive population, both in primary and metastatic samples, Ki-67 and chromogranin A were investigated by double immunohistochemical reactions, using immunoperoxidase procedure for Ki-67, followed by immunoalkaline phosphatase method Envision-AP (Dako) with Vector blue alkaline phosphatase substrate kit III (from Vector Laboratories, CA, USA) for chromogranin A, at the same conditions reported above.

Statistical analysis Differences between chromogranin A expression and clinical pathological variables were analyzed by the chi-square test with Yates' correction, when appropriate, whereas mean Ki-67 indexes within different groups were compared using Student's *t* test. Survival curves were plotted using the Kaplan–Meier method and were statistically evaluated using the log-rank test. These statistical computations were performed using the SPSS for Windows and STATISTICA for Windows software. The significance level was set at $p<0.05$.

Results

Patients The present case series of 54 cases (Table 1) included 23 females and 31 males having a median age of 60.5 years (range 28–79). The primary tumors were located in the right colon (12 cases), left colon (25 cases), and rectum (17 cases). Conventional adenocarcinoma was observed in 48 cases, while the remaining six cases were mucinous carcinomas. With regard to tumor grade, three cases were well differentiated, 40 moderately and 11 poorly differentiated. According to the 2010 TNM 7th edition staging system, 48 cases were staged pT3–T4, being the remaining six tumors staged pT1–T2. Most cases (43/54, 79.6%) had lymph node metastases at the time of diagnosis. The site of distant metastasis examined in the present study was liver in 33 patients, peritoneum in 11 patients, lung in nine patients, and ovary in one patient.

Neuroendocrine differentiation Positive chromogranin A immunostaining, including both scores 1 and 2, was observed in 12 of the 54 primary colorectal carcinomas (22.2%) and in 25/54 metastases (46.3%). This difference

Table 1 Clinico-pathological data of 54 colorectal carcinomas that underwent surgical resection of a metastasis at diagnosis or along tumor progression

Number of patients	54	
Median age (years) (range)	60.5 (28–79)	
Male/Female ratio	31/23	
Primary tumor location	R/colon: 12, L/colon: 25, Rectum: 17	
Tumor grade	G1: 3, G2: 40, G3: 11	
Tumor stage	T1: 1, T2: 5, T3: 37, T4: 11; N0: 11, N1-2: 43	
Surgically resected metastasis	Liver: 33, Lung: 9, Peritoneal: 11, Ovarian: 1	
Chemotherapy administrated	47	
No chemotherapy administrated	7 (5 at diagnosis and 2 during tumor progression)	
Chromogranin A expression	12/54 (22.2%) in primary CRC	
	25/54 (46.3%) in CRC metastases	
	Chi-square $p=0.01$	
Ki-67 proliferation index	67.1% (primary CRC) and 62.4% (metastases)	
Median survival from first diagnosis	CgA negative in primary CRC	59.9 months (42 pats)
	CgA positive in primary CRC	35.9 months (12 pats)
	Log rank $p=0.08$	
Median survival from metastatic spread	CgA negative in primary CRC	55.5 months (42 pats)
	CgA positive in primary CRC	33.3 months (12 pats)
	Log rank $p=0.04$	
	CgA negative in CRC metastasis	53.8 months (29 pats)
	CgA positive in CRC metastasis	38.3 months (25 pats)
	Log rank $p=0.18$	

R right, *L* left, *CRC* colorectal carcinoma, *CgA* chromogranin A

was statistically significant (p=0.01 by chi-square test). In primary colorectal carcinomas, chromogranin A-positive cases were equally distributed between those with synchronous metastases (six cases, 26.3%) and those that developed metastases at follow up (the other six, 20%).

When comparing chromogranin A staining between primary tumor and metastasis of the same patient, in 37 cases (68.5%) we failed to show any change (27 double negative and ten double positive, without any increase in the extent of positivity in the latter group), whereas an increase was evident in 15/54 (27.8%), including 13/47 chemotherapy-treated, and 2/7 chemo-naïve patients. In ten of these 15 cases, the chromogranin A-positive population was detected in the metastatic tissue only (Fig. 1a–b), whereas in the remaining five it was already focally present in the primary tumor (immunohistochemical score 1) but was increased in the metastasis (immunohistochemical score 2; Fig. 1c–d). The remaining two cases could not be analyzed due to the presence of extensive mucin lakes with very few neoplastic cells in the metastases. Synchronous metastatic lymph nodes were analyzed in 20 cases, from one to three metastatic lymph nodes for each case. Among these, ten cases corresponded to chromogranin A positive and ten cases to chromogranin A negative primary tumors. All lymph node samples showed no chromogranin A immunoreactivity, except for two cases (both having a positive chromogranin A in the primary tumor, score 1) with rare scattered positive cells.

The presence of neuroendocrine-differentiated primary colorectal cancers was associated to shorter overall survival (35.9 versus 59.9 months) and shorter survival from the time of metastatic spread (33.3 versus 55.5 months), being the latter statistically significant in univariate analysis (log rank p= 0.04; Fig. 2); a similar trend was observed considering those cases having chromogranin A positive cells in the metastases as opposed to negative cases (38.3 versus 53.8 months from the time of metastatic spread; log rank p=0.18).

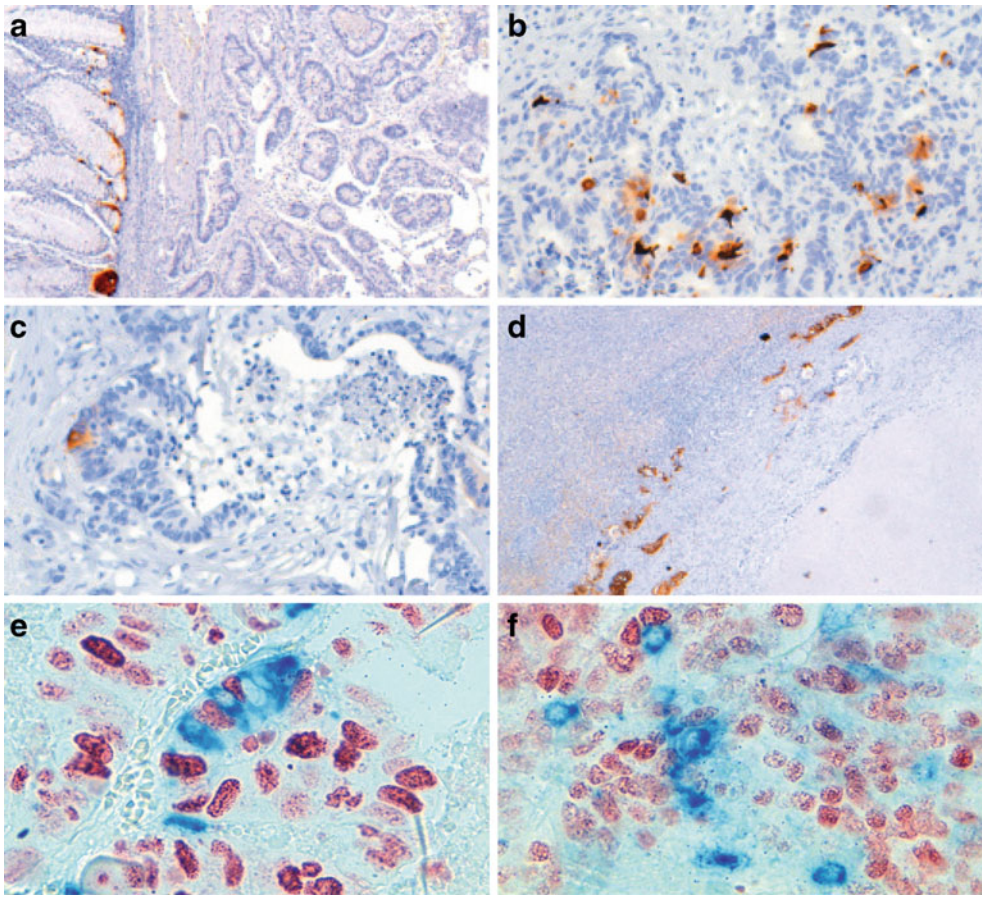

Fig. 1 Primary rectal adenocarcinoma (**a**, case 4) with no evidence of neuroendocrine differentiation (normal colonic mucosa in the left). After 18 months and following 5-FU treatment, a liver metastasis eventually developed (**b**), showing numerous scattered neuroendocrine cells (score 2). Primary colonic adenocarcinoma (**c**, case 18), with focal neuroendocrine differentiation (score 1), with subsequent (9 months later) extensively necrotic liver metastasis (**d**), following 5-FU and oxaliplatin treatment, showing diffuse neuroendocrine differentiation (score 2; normal liver in the upper left corner). Double immunostaining for chromogranin A (*blue*) and Ki-67 (*brown*) in a primary colonic adenocarcinoma (**e**) and in a liver metastasis (**f**) showing numerous proliferating tumor cells and few neuroendocrine cells in a resting phase (**a**–**d** chromogranin A staining, immunoperoxidase; **e** and **f** double sequential immunoperoxidase for Ki-67 and immunoalkaline phosphatase for chromogranin A; original magnifications **a** and **d** 100×; **b** and **c** 200×; **e** and **f** 400×)

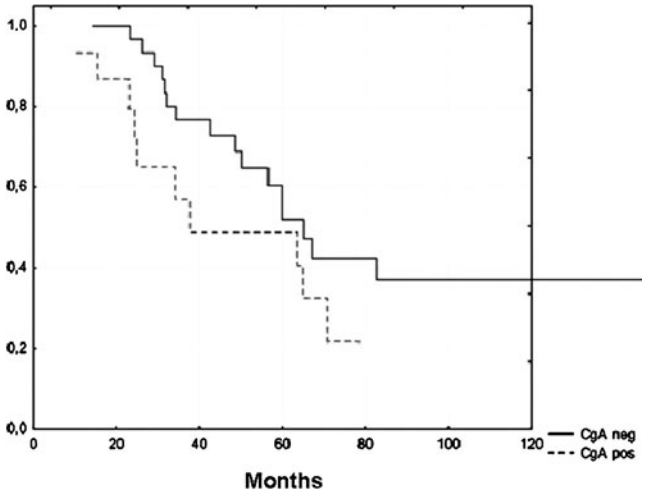

Fig. 2 Survival of colorectal carcinoma patients from the time of metastatic progression, grouped according to chromogranin A reactivity (positivity including immunohistochemical scores 1 and 2) in the primary tumors (log rank test, $p=0.04$)

The proliferative activity was assessed by means of Ki-67 immunostaining in all cases of colorectal carcinoma, both in the primary and in the metastatic locations (means 67.1% and 62.4%, respectively). No statistically significant difference was observed between the mean Ki-67 proliferative index of colorectal carcinomas with neuroendocrine differentiation and negative cancers (78.5% versus 64%, respectively). The proliferative activity of metastatic tissues was also similar in neuroendocrine and non- neuroendocrine differentiated tumor groups (Ki-67 index of 59.1% and 65.3%, respectively). Double immunostainings combining chromogranin A and Ki-67 showed that the neuroendocrine cell population generally was not actively proliferating, both in primary tumors and metastases (Fig. 1e–f).

When the presence of neuroendocrine differentiation was compared with primary tumor location (right and left colon and rectum), tumor histotype (conventional versus mucinous), tumor stage and grade of differentiation, site of metastasis (liver versus peritoneum and lung), and response to chemotherapy (stable disease versus partial or complete response), no significant correlation was observed between any of the above considered parameters and chromogranin A expression, neither in primary nor in metastatic specimens.

Discussion

In this study, we have shown that distant metastases of colorectal carcinoma contain a significantly higher amount of neuroendocrine cells compared to the corresponding primary tumors, as detected by chromogranin A immunostaining in surgical specimens. This may be part of the natural history of colorectal cancer progression or be related to the effects of chemotherapy, which generally preceded the surgical removal of distant metastases.

Since it is virtually impossible to analyze a control group of surgically resected colorectal carcinomas with no subsequent chemotherapy (only seven cases were recruited in the current series), the demonstration of a direct effect of chemotherapy on the increase of neuroendocrine cells is not possible. However, this was already demonstrated in a study on rectal adenocarcinoma preoperatively treated by chemo and/or radiotherapy [14]. The authors restricted their analysis to primary tumors, comparing the neuroendocrine cell density in pre-treatment biopsies versus the corresponding surgical specimen of rectal cancer, and found a significantly higher amount of neuroendocrine cells in treated rectal carcinomas compared to the control group of adenocarcinomas that did not undergo neoadjuvant therapy.

Based on this report, we therefore expanded the analysis to colonic and rectal carcinomas and to their metastatic locations, which are now increasingly being resected especially from lung and liver, to assess the phenotypic profile of cancer cell populations in the setting of metastatic and progressing disease. Indeed, distant metastases were found to contain a higher amount of neuroendocrine cells, as compared to their primaries, and this may be the result of relative selection of tumor clones not responsive to conventional chemotherapy protocols, or to direct effects of chemotherapy agents on a fraction of neoplastic cells differentiated along the neuroendocrine lineage. Moreover, we analyzed synchronous metastatic lymph nodes in 20 cases, both from chromogranin A negative and positive primaries, and failed to demonstrate any significant chromogranin A immunoreactivity. Although the limited bulk of tumor tissue in lymph nodes as compared to primaries or distant metastases might be a bias, this finding seems to suggest that the selection of neuroendocrine tumor cell clones is more likely related to anti-neoplastic treatments rather than to metastatic progression.

The role of chemotherapy in favoring the increase and the selection of neuroendocrine differentiated neoplastic cell clones is controversial. Shia et al. [14] demonstrated a role of neoadjuvant treatments in inducing a significant increase of the neuroendocrine cell population in primary colorectal carcinoma specimens. The same may well be the case in metastatic locations, although a statistical validation of this event is currently not possible. The very few cases (seven) that did not (or could not) undergo chemotherapy had a variable amount of neuroendocrine cells in their metastases, but the extremely limited number of cases hampers any statistical analysis and definite conclusion. In addition, in some cases, the development of distant metastases occurred many years after surgery and subsequent chemotherapy, suggesting that the different tumor cell populations, exocrine (mucinous), and neuroendocrine may

play complex reciprocal interactions. In this respect, the expression of transcription factors known to drive neuroendocrine differentiation in the embryonic life, such as human achaete-scute-homologue type 1 (hASH1) may be involved in the occurrence of neuroendocrine differentiation [16]. Unfortunately, in the present series, no hASH1 expression was observed (data not shown) suggesting that at least in the intestinal area, the development of neuroendocrine differentiated cells may follow alternative pathways, compared to other models such as the prostate [17].

In this context, it is of interest that the neuroendocrine population both in primary tumors and metastases showed a very low proliferative activity, in agreement with earlier observations in gastric carcinoma [18] that pointed out that neuroendocrine cells are terminally differentiated cells, devoid of any proliferative potential. Moreover, in our cases, the mean Ki-67 proliferation index was similar in primary and metastatic cancers, as well as in colorectal carcinomas with or without neuroendocrine features.

A second issue is related to the prognostic influence of neuroendocrine differentiation in colorectal carcinoma. In the present series, cases having a neuroendocrine differentiated component in the primary tumors had a slightly shorter survival both from the time of diagnosis and the time from metastatic spread but statistical significance was reached for the latter case only, possible due to the relatively small sample size. Other literature data are in line with this observation [13, 19, 20], although some authors found no prognostic differences between neuroendocrine differentiated and conventional colorectal carcinoma [21]. No correlation was also observed with any clinical pathological parameter. In conclusion, we herein reported an increased detection on neuroendocrine tumor cells in metastatic tissues of chemotherapy-treated colorectal cancer patients, as compared to the corresponding primary tumors, associated to reduced patients' survival; the biological and predictive meaning of this observation would deserve further elucidation but is possibly related to the positive selection by chemotherapy of neuroendocrine tumors clones that are characterized by a very low proliferative activity.

Acknowledgments This work is partially supported by grants from the Italian Ministry of University (ex-60%, Rome) to MV, MT, and MP.

Conflict of interest statement We declare that we have no conflict of interest.

References

1. Pagani A, Papotti M, Abbona GC, Bussolati G (1995) Chromogranin gene expression in colorectal adenocarcinomas. Mod Pathol 8:626–632
2. Abbona G, Papotti M, Viberti L, Macrì L, Stella A, Bussolati G (1998) Chromogranin A gene epression in non-small cell lung carcinomas. J Pathol 186:151–156
3. Righi L, Sapino A, Marchiò C, Papotti M, Bussolati G (2010) Neuroendocrine differentiation in breast cancer: established facts and unresolved problems. Semin Diagn Pathol 27:69–76
4. López-Bonet E, Alonso-Ruano M, Barraza G, Vazquez-Martin A, Bernadó L, Menendez JA (2008) Solid neuroendocrine breast carcinomas: incidence, clinico-pathological features and imunohistochemical profiling. Oncol Rep 20:1369–1374
5. Berruti A, Bollito E, Cracco CM, Volante M, Ciccone G, Porpiglia F, Papotti M, Scarpa RM, Dogliotti L (2010) The prognostic role of immunohistochemical chromogranin A expression in prostate cancer patients is significantly modified by androgen-deprivation therapy. Prostate 70:718–726
6. Jiang SX, Mikami T, Umezawa A, Saegusa M, Kameya T, Okayasu I (2006) Gastric large cell neuroendocrine carcinomas: a distinct clinicopathologic entity. Am J Surg Pathol 30:945–953
7. Howe MC, Chapman A, Kerr K, Dougal M, Anderson H, Hasleton PS (2005) Neuroendocrine differentiation in non-small cell lung cancer and its relation to prognosis and therapy. Histopathology 46:195–201
8. Segawa Y, Takata S, Fujii M, Oze I, Fujiwara Y, Kato Y, Ogino A, Komori E, Sawada S, Yamashita M, Nishimura R, Teramoto N, Takashima S (2009) Immunohistochemical detection of neuroendocrine differentiation in non-small-cell lung cancer and its clinical implications. J Cancer Res Clin Oncol 135:1055–1059
9. van Krimpen C, Elferink A, Broodman CA, Hop WC, Pronk A, Menke M (2004) The prognostic influence of neuroendocrine differentiation in breast cancer: results of a long-term follow-up study. Breast 13:329–333
10. Pelosi G, Pasini F, Sonzogni A, Maffini F, Maisonneuve P, Iannucci A, Terzi A, De Manzoni G, Bresaola E, Viale G (2003) Prognostic implications of neuroendocrine differentiation and hormone production in patients with stage I nonsmall cell lung carcinoma. Cancer 97:2487–2497
11. Mori M, Mimori K, Kamakura T, Adachi Y, Ikeda Y, Sugimachi K (1995) Chromogranin positive cells in colorectal carcinoma and transitional mucosa. J Clin Pathol 48:754–758
12. Cho YB, Yang SS, Lee WY, Song SY, Kim SH, Shin HJ, Yun SH, Chun HK (2010) The clinical significance of neuroendocrine differentiation in T3–T4 node-negative colorectal cancer. Int J Surg Pathol 18:201–206
13. Grabowsky P, Schindler I, Anagnostopoulos I, Foss HD, RieckenEO MU, Stein H, Berger G, Buhr HJ, Scherubl H (2001) Neuroendocrine differentiation is a relevant prognostic factor in stage III–IV colorectal cancer. Eur J Gastroenterol Hepatol 13:405–411
14. Shia J, Tickoo SK, Guillem JG, Qin J, Nissan A, Hoos A, Stojadinovic A, Ruo L, Wong WD, Paty PB, Weiser MR, Minsky BD, Klimstra DS (2002) Increased endocrine cells in treated rectal adenocarcinomas. A possible reflection of endocrine differentiation in tumor cells induced by chemotherapy and radiotherapy. Am J Surg Pathol 26:863–872
15. Tampellini M, Brizzi MP, Bitossi R, Alabiso I, Sculli CM, Chiusa L, Papotti M, Dogliotti L (2007) Six-year stabilisation of a relapsed pelvic mass from rectal cancer after oxaliplatin-containing chemotherapy. J Cancer Res Clin Oncol 133:783–785
16. Borges M, Linnoila RI, van de Velde HJ, Chen H, Nelkin BD, Mabry M, Baylin SB, Ball DW (1997) An achaete-scute homologue essential for neuroendocrine differentiation in the lung. Nature 386:852–855
17. Rapa I, Ceppi P, Bollito E, Rosas R, Cappia S, Bacillo E, Porpiglia F, Berruti A, Papotti M, Volante M (2008) Human

ASH1 expression in prostate cancer with neuroendocrine differentiation. Mod Pathol 21:700–707
18. Ooi A, Hayashi H, Katsuda S, Nakanishi I (1992) Gastric carcinoma cells with endocrine differentiation show no evidence of proliferation. Hum Pathol 23:736–741
19. Hamada Y, Oishi A, Shoji T, Takada H, Yamamura M, Hioki K, Yamamoto M (1992) Endocrine cells and prognosis in patients with colorectal carcinoma. Cancer 69:2641–2646
20. De Bruine AP, Wiggers T, Beek C, Volovics A, von Meyenfeldt M, Arends JW, Bosman FT (1993) Endocrine cells in colorectal adenocarcinomas: incidence, hormone profile and prognostic relevance. Int J Cancer 54:765–771
21. Ferrero S, Buffa R, Pruneri G, Siccardi AG, Pelagi M, Lee AK, Coggi G, Bosari S (1995) The prevalence and clinical significance of chromogranin A and secretogranin II immunoreactivity in colorectal adenocarcinomas. Virchows Arch 426:587–592

Virchows Arch (2010) 457:529–536
DOI 10.1007/s00428-010-0968-7

ORIGINAL ARTICLE

Immunohistochemical analysis of pyloric gland adenomas using a series of Mucin 2, Mucin 5AC, Mucin 6, CD10, Ki67 and p53

Michael Vieth · Ryoji Kushima · Ken-ichi Mukaisho · Rie Sakai · T. Kasami · Takanori Hattori

Received: 6 June 2010 / Revised: 18 August 2010 / Accepted: 21 August 2010 / Published online: 9 September 2010
© Springer-Verlag 2010

Abstract A pyloric gland adenoma (PGA) of the stomach was first described in a book chapter in 1976 by Kurt Elster and has been rarely reported in the literature. We expanded the current immunohistochemical data of these adenomas in a detailed series to further analyse the immunhistochemical status of PGA. From 60 patients with PGA with and without adenocarcinomas of the gastrointestinal tract, an immunhistochemical panel of Mucin 2, Mucin 5AC, Mucin 6, CD10, Ki67 and p53 was used to define the expression of these markers. All PGA were positive for Mucin 6 (deep mucoid glands), which they express over the whole lesion up to the surface. Mucin 5AC expression varies from case to case. A transition from gastric to intestinal differentiation can be observed focally as depicted by Mucin 2 and CD10 in 65% of the cases. The gastric corpus mucosa of elderly patients with either *Helicobacter pylori* gastritis or autoimmune gastritis is highly affected. Almost 47% of all PGA already underwent malignant transformation into adenocarcinoma. Significant immunohistochemical differences could be detected between PGA with and without adenocarcinoma regarding ki67 and p53. The diagnosis of PGA can be confirmed immunohistochemically by staining against apomucin 6 and apomucin 5AC. Focal intestinal differentiation supports the hypothesis that gastric adenocarcinomas can initially develop from carcinomas of the gastric type and transform into intestinal type later on. The high frequency of malignant transformation of PGA underlines its high potential for invasive malignancy.

Keywords Pyloric gland adenoma · Immunohistochemistry · Adenocarcinoma · Gastro-intestinal tract

Introduction

The majority of gastric polyps are non-neoplastic tumour-like lesions [1]. Only about 10% of all gastric polyps are adenomas [2]. Adenomas of the gastrointestinal tract are, for the most part, benign lesions [3, 4]. Besides the most frequent type of gastric adenoma in form of the tubular adenoma depicting classical signs of intraepithelial neoplasia/dysplasia, there are other rare variants, e.g. foveolar adenoma that can be diagnosed from time to time.

Among the various types of adenoma of the gastric mucosa is an adenoma with gastric differentiation—a so-called pyloric gland adenoma (PGA), which is a rare variant [5–7] (approx. 2.7% of all gastric polyps [2]). This lesion was first described by Kurt Elster [8] in 1976 in a book chapter, but was interpreted as adenoma-like hyperplasia of mucoid glands. Precise data on the frequency of locations of PGA other than stomach are not known since these lesions are very rare. The first PGA with transition to adenocarcinoma has been presented by Borchard [9] during

M. Vieth and R. Kushima share first authorship. MV is supported by a grant of the Japanese Society of Pathology for a scholarship at the Shiga University of Medical Science, Department of Pathology, Ohtsu, Japan.

M. Vieth (✉)
Institute of Pathology, Klinikum Bayreuth,
Preuschwitzerstr. 101,
95445 Bayreuth, Germany
e-mail: vieth.lkpathol@uni-bayreuth.de

R. Kushima
Division of Pathology, National Cancer Center Hospital,
Tokyo, Japan

K.-i. Mukaisho · R. Sakai · T. Kasami · T. Hattori
Department of Pathology, Shiga University of Medical Science,
Otsu, Japan

Table 1 Demographic data of 60 patients with PGA

	PGA with adenocarcinoma	PGA without carcinoma
Gender (male/female)	15/13	15/17
Age in years		
All	70.50 ±10.72	71.81±14.2
Female	75.23±9.02	71.47±14.8
Male	66.40±10.64	72.20±13.99
Gastritis status		
Normal	0%	4%
hp	20%	24%
ex-hp	33.3%	12%
c-gastritis	26.7%	12%
Autoimmune gastritis	20%	48%
No information	15 cases	12 cases
Size in mm	15.19±9.51	9.25±5.83
Depth of infiltration		
Mucosal (pT1a)	24	
pT1b sm1	2	
pT1b sm2	0	
pT1b sm3	2	
Grading		
g1	26	
g2	2	

a slide seminar for pathologists in 1986 and 1987. The first characterisation of two cases by mucin analysis has been carried out by Borchard et al. [5] in 1990. In the same year, Watanabe [7] mentioned PGA in the WHO classification of gastric tumours. Rarely does the histological work-up of a specimen other than gastric reveal heterotopic gastric mucosa. More often, gastric metaplasia of different types of gastrointestinal epithelium can be observed (e.g. gastric metaplasia of duodenal bulb). Tumours arising in such heterotopias or metaplasias should, however, always reveal a differentiation of the 'tissue of origin'. Since then, similar adenomas have been described elsewhere in the gastrointestinal tract [6, 10–15] and even in the uterine cervix [16, 17]. Most are believed to develop on such gastric metaplasias. Recently, our group published clinical data of a series of 90 PGA mainly arisen from gastric mucosa [18]. Despite some immunohistochemical analyses, mainly all described by Borchard et al. [5] and Kushima et al. [19, 20] in single cases, only one further report on a series of

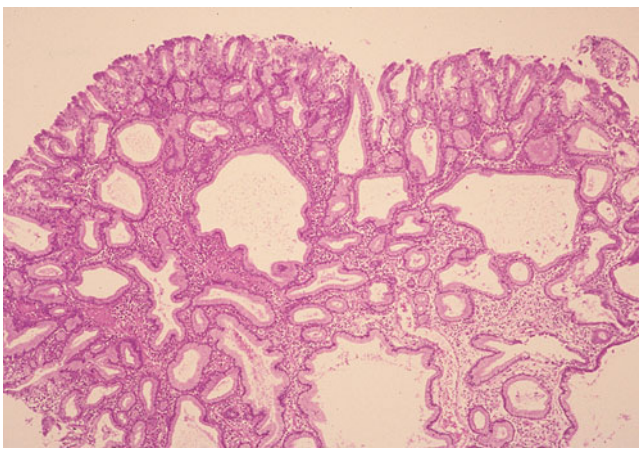

Fig. 1 Low-power view of PGA of gastric corpus mucosa with closely packed tubules with varying diameter and ectasia of some glands (HE, ×25)

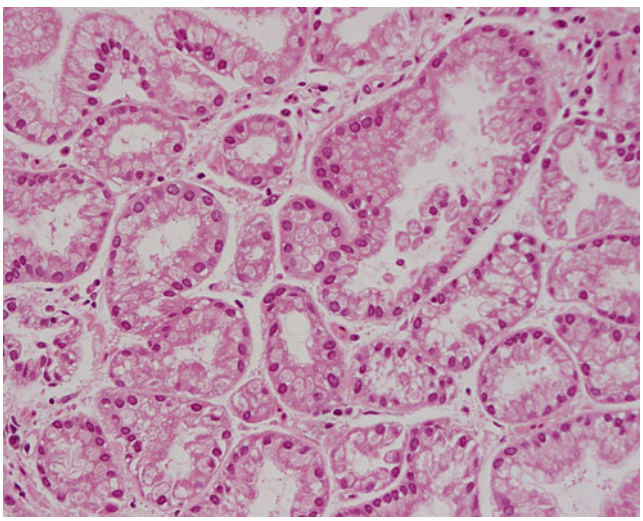

Fig. 2 High-power view of Fig. 1: nuclei are round and slightly above the basal membrane. The cytoplasm is pale to eosinophilic (HE, ×100)

Table 2 Location of PGA of the gastrointestinal tract

Location	*n* (%)	Transition to adenocarcinoma, *n* (%)
Descending duodenum	1 (1.7)	1 (100)
Papilla vateri	2 (3.3)	2 (100)
Gallbladder	5 (8.33)	1 (20)
Common bile duct	2 (3.3)	1 (50)
Cardia	19 (31.8)	11 (57.9)
Fundic mucosa	27 (45)	10 (37)
Antrum	2 (3.3)	1 (50)
Duodenal bulb	2 (3.3)	1 (50)
Total	60	28 (46.7)

immunohistological workup of PGA has been carried out so far. For this reason, we carried out a clinico-pathological immunohistochemical analysis of 60 consecutive patients with PGA and expanded the immunoprofile to Ki67 and p53. It needs to be stressed that immunohistochemical workup is not needed in routine diagnostics [18] but allows us to expand our knowledge on gastric differentiated neoplasia and might help in routine diagnostics if in doubt to identify such lesions by staining against apomucin 6 and apomucin 5AC [18]. In the past, PGAs have been regarded as hyperplasia or hamartoma, and this entity has not been accepted especially in the Anglo-American literature. However, our group has suggested the unstable and precancerous nature of PGA by first successful demonstration of a 'pyloric gland adenoma-adenocarcinoma sequence' by analyses of CGH [21]. Most recently, PGA was recognised in the international literature by Chen et al. [22], although we cannot agree with their diagnosis of some presented figures that seem to show immature gastric epithelium rather than foveolar adenoma or PGA.

Patients and methods

For the present analysis, we included 60 consecutive patients with PGA (see Table 1) (Figs. 1 and 2). Follow-up data were available between 6 months and 6 years after first diagnosis. No recurrence was noted after complete removal of the tumour. These patients were not included in our first series published in 2003 [18]. In the present analysis, 50% were male and 50% were female patients. The diagnosis of PGA was made according to the criteria proposed by Watanabe [7]: PGAs are mainly composed of closely packed pyloric type glands. The glands are lined by cuboidal or columnar mucus-secreting cells. The nuclei are round or oval, relatively small, hyperchromatic with a parabasal location and do not show the classical form of intraepithelial neoplasia/dysplasia with elongated and palisading nuclei. Adenocarcinoma was diagnosed whenever a so called lateral expansion or fusion of neighbouring fovelae can be observed [18]. It is known that well differentiated adenocarcinoma can build their own basal membrane and, thus, break through the

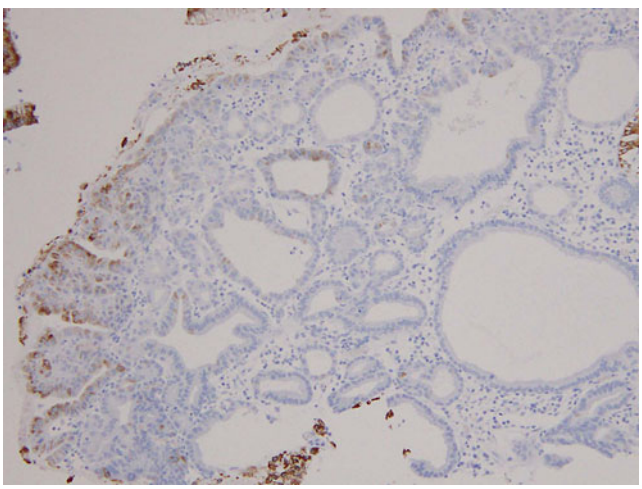

Fig. 3 Apomucin 5AC is only detected in luminal foveolar epithelium of a PGA (please see Fig. 5) (×25)

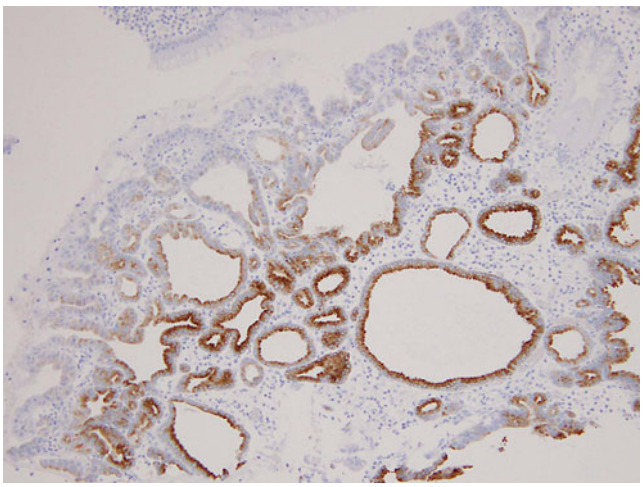

Fig. 4 Marked immunohistochemical reaction against apomucin 6 within a pyloric gland andenoma (please see Fig. 5). Only most luminal glands are negative (×25)

Table 3 Immunohistochemical marker for the detection of gastric and/or intestinal differentiation in PGAs with and without transition to adenocarcinoma

	Gastric foveolar type	Pyloric gland type	Intestinal goblet cells	Small bowel		
Staining	Apomucin 5AC	Apomucin 6	Apomucin 2	CD10	Ki 67	p53
Clone distributor	CLH2 Novocastra, Newcastle, UK Immunotech Marseille, F	CLH5 Novocastra, Newcastle, UK PAb1801 Oncogene Cambridge, MA, USA	Ccp58 Novocastra, Newcastle, UK	56C6 Novocastra, Newcastle, UK	MIB-1	
Specificity	Human Apomucin 5AC	Human Apomucin 6	Human Apomucin 2	CD10 glycoprotein	Proliferation index	p53
Positivity	Gastric surface epithelium, mucous cells and neck cells	Pyloric gland cells, mucous neck cells, cardia gland cells, Brunner's gland and pseudopyloric gland cells	Goblet cells and pre-goblet cells	enterocytes	Proliferating cells	p53 overexpression
Staining pattern	Intracytoplasmatic and non-luminal membranous	Intracytoplasmatic and non-luminal membranous intracytoplasmatic	Intracytoplasmatic and non-luminal membranous Nuclear staining	Striated border and rarely Nuclear staining		
Dilution used	1:100	1:50	1:500	1:200	1:100	1:400

basal membrane or single tumour cells are not to be expected in early adenocarcinomas. The cytology even of adenocarcinoma in PGA is known to show rather mild abnormalities [18] due to the gastric differentiation since these neoplastic lesions show different characteristics from the classical signs of intraepithelial neoplasia/dysplasia. The cytological abnormalities of nuclei in PGA adenoarcinoma are mild but differ clearly from the non-carcinomatous part by transition from round or oval nuclei to more elongated, pleomorphic nuclei with loss of polarity compared to the monotonous nuclei in PGA without adenocarcinoma. The WHO classification from 2000 [4] does not discuss such lesions in detail. For location of the present series of PGA, please see Table 2.

Table 4 Definition of immunoreactive score used in this analysis according to Remmele et al. [23]

Immunoreactive score (IRS)
IRS=PP x SI
PP=percentage of positive cells
SI=staining intensity
SI grading
0=no reaction
1=slight reaction
2=moderate reaction
3=marked reaction
PP grading
0=no positive cells
1=<10% positive cells
2=10–50% positive cells
3=51–80% positive cells
4=>80% positive cells

Immunohistochemistry

Specific antibodies to the various kinds of mucins are used to define gastric and intestinal phenotypes and include MUC 5AC specific for gastric surface foveolar-type mucin, MUC 6 for pyloric gland type mucin (pyloric glands, mucous neck cell, pseudopyloric gland cells and cardia gland cells) (Figs. 3 and 4), MUC 2 for goblet cells and their precursors, CD10 for the striated border on the apical surface of small bowel absorptive cells (enterocytes). Reactions against Ki67 and p53 were carried out also (for specific details, please see Table 3). For retrieval of

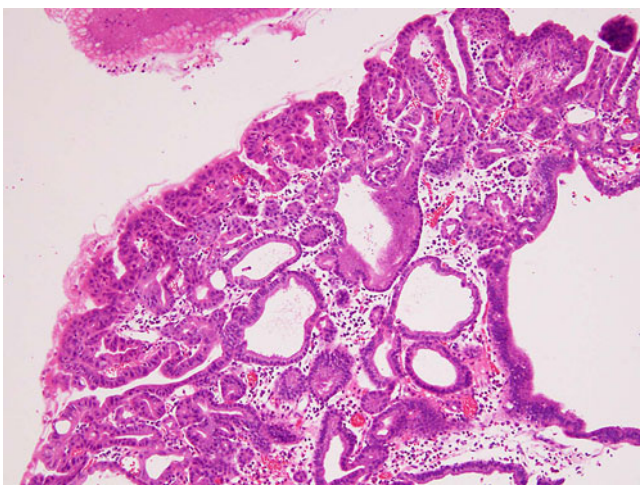

Fig. 5 PGA (*upper right half*) with transition into a well differentiated mucosal gastric adenocarcinoma (*lower left half*). Note the typically slight morphological nuclear changes and slight changes of the glandular architecture but lateral expansion of the carcinomatous glands (HE, ×25)

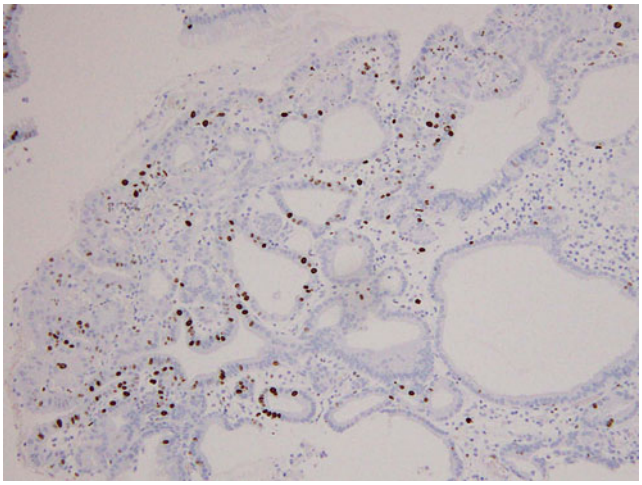

Fig. 6 PGA (Fig. 5) with focal enhanced staining of Ki67 in the carcinomatous part compared to negativity in the adjacent adenomatous glands (×25)

antigens, deparaffinised sections were heated in citrate buffer (pH 6.0) using a microwave for 20 min. Also, endogenous peroxidase was blocked by 20-min incubation with 0.3% hydrogen peroxidase in absolute methanol. Sections were washed and non-specific binding was blocked by the use of normal serum (Nichirei, Tokyo, Japan). Overnight incubation at 4°C was carried for binding of the primary antibody. Afterwards, 30-min incubation with biotinylated secondary antibody was performed, followed by substrate binding by using streptavidin–biotin–peroxidase method. Counterstaining with haemalaun was carried out additionally in all cases. For all stains, negative and positive controls were carried out, and staining was only accepted if evaluable results of controls showed the expected results. If not, staining was repeated until internal controls showed appropriate results.

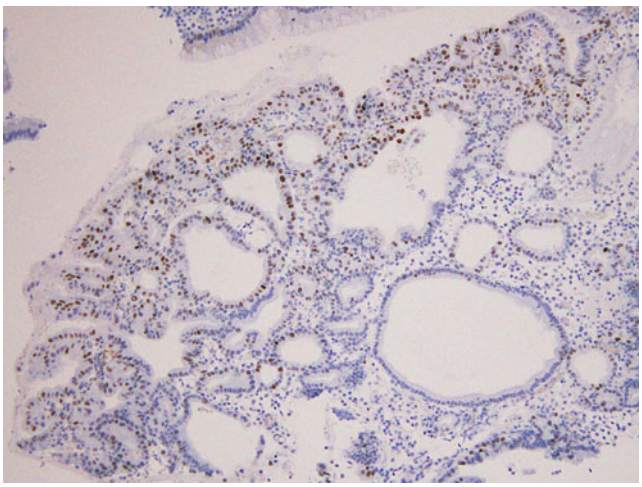

Fig. 7 Rare case of PGA (Fig. 5) with focal marked staining of p53 in the carcinomatous part. Normally, such adenocarcinomas are negative for p53 (×25)

Grading of positivity

Positivity was semiquantitatively graded according to the Remmele score [23] (see Table 4). The percentage of positive cells was divided in to five grades: 0–4 (0%, <10%, 10–50%, 51–80%, >80%) multiplied with the grade of intensity (graded from 0 to 3) of the immunohistochemical reaction. Intestinal differentiation was diagnosed whenever lesions MUC 2 showed positivity and CD10-positive cells were detected. In case MUC 2 staining was not associated with positive CD10 reaction, a gastric phenotype was diagnosed regardless of the intensity or grade of MUC 2 positivity.

In PGA with transition to adenocarcinoma (Fig. 5) of the gastric type, the analysis was based on the non-carcinomatous area of the PGA. Ki67 and p53 were used as additional markers for transition to adenocarcinoma (Figs. 6 and 7). Characteristically, most cases of PGA adenocarcinoma show an increased proliferation (Ki67) but mainly negative or weak reaction against p53 (see Tables 5 and 6). Very often, the carcinomatous areas were very small to draw valid conclusions from these very circumscribed areas. The phenotype of carcinoma was determined according to Shiroshita et al. [24].

Statistical analysis

All analyses were carried out using the SPPS Software package (SPPS for Windows 9.0, SPPS Munich, Germany), using U test Mann–Whitney test. Values for $p<0.05$ were considered significant.

Results

In 32 patients with PGA without evidence of adenocarcinoma and 28 individuals with transition to adenocarcinoma, MUC 5AC and MUC 6 were positive in 100% of the cases, but showing case-dependent varying intensities and varying size of areas detected by the MUC 5AC and MUC 6. MUC 5AC positivity compared to MUC 6 in lesions without malignant transformation showed that nine cases vs three cases had a slight positivity (<10% positive cells), eight vs four cases a positivity of 10–50% of the cells, 13 vs 16 cases a positive reaction in 51–80% of the cells and two vs nine cases a marked reaction in >80% of the cells, respectively. In cases with adenocarcinoma, six cases of MUC 5AC had a slight expression vs seven cases against MUC6 (<10% positive cells), eight vs five cases (10–50% positive cells), 14 vs 10 cases (51–80% positivity) and zero vs six cases with positivity noted in >80% of the cells, respectively.

Table 5 Grading by presence of reactive cells for each mucin antibody separated into PGA without and with transition to adenocarcinoma

	PGA without adenocarcinoma					Diagnosis pyloric gland adenom with adenocarcinoma				
Grade	0	1	2	3	4	0	1	2	3	4
Mucin Antibody										
CD10	21	6	5	0	0	15	9	4	0	0
MUC 2	11	15	6	0	0	12	11	5	0	0
MUC 5AC	0	9	8	13	2	0	6	8	14	0
MUC 6	0	3	4	16	9	0	7	5	10	6
P53	11	5	7	7	0	5	8	7	8	0
Ki67	1	8	12	11	0	0	5	8	13	2

CD10 positive cells were detected in 11 cases (34.4%) in PGA without transition to adenocarcinoma and 13 (46.4%) in cases with transition to adenocarcinoma. CD10 expression in 21 cases (65.6%) without carcinoma was negative, six cases (18.7%) showed a very focal weak expression (<10% of the cells) and five cases (10.7%) a moderate (10–50% of all cells) reaction against CD10. In cases with transition to carcinoma, 15 cases 53.6% were negative, nine cases (32.1%) showed a slight focal positivity against CD10 and in four cases (14.3%), a moderate staining was detected. CD10 for the most stained luminal antigens and was rarely observed for showing a slight intracytoplasmatic reaction. MUC 2 reactivity in PGA without carcinoma was noted in 21 cases (65.6%) but described as very focal, 15 cases (46.8%) were slightly positive, whereas only six cases (18.8%) showed a moderate reaction against MUC 2. MUC 2 was positive in goblet cell and in precursor non-goblet cells. In carcinomatous areas, MUC 2 was observed in and above the proliferation zone of the tumour. Among these cases with transition to adenocarcinoma, 16 cases (57.1%) were positive for MUC 2; 11 cases (39.3%) were slightly and five cases (17.9%) moderately positive (see Table 5 and 6). Paradoxical staining with Mucin 3 (Con A) was noted in none of the cases. A positive reaction against p53 was noted in 19 cases (59.3%) without adenocarcinoma and in 23 (82.1%) cases with transition to adenocarcinoma. Ki67 staining was noted in 31 of 32 cases (96.8%) without transition to carcinoma and in 100% of the cases with carcinoma. Ki67 was noted to be slightly positive in eight cases (25%) without carcinoma, compared to five cases (17.6%) with carcinoma, 12 cases (37.5%) compared to eight cases (28.6%) were moderately positive, 11 cases (34.4%) compared to 13 cases (46.4%) showed a positivity of nuclear staining in 51–80% of the cells and no case compared to two cases (7.1%) showed a positivity greater than 80%. Only the immunoreactive score according to Remmele [23] showed significant differences between Ki67 ($p=0.0026$) and p53 ($p=0.0058$) expression between PGA with and without transition to adenocarcinoma. All cases, despite one that showed intestinal type of carcinoma, showed a transition into gastric phenotype of adenocarcinoma, according to the criteria by Shiroshita et al. [24].

Discussion

In the present immunhistochemical analysis, we were able to demonstrate the importance of the presence of Mucin 6 in the diagnosis of PGA since this type of mucin underlines the pathogenesis of PGAs from deep mucoid glands. Interestingly, expression of Mucin 5, which is present in luminal foveolar type of columnar epithelium, varied in its intensity from case to case. Some cases even showed a bidirectional expression of Mucin 5AC and Mucin 6.

Table 6 Grading by immunoreactive score (IRS) for each mucin separated into PGA without and with transition to adenocarcinoma

PGA without adenocarcinoma										Diagnosis pyloric gland adenom with adenocarcinoma								
IRS	0	1	2	3	4	6	8	9	12	0	1	2	3	4	6	8	9	12
Mucin Antibody																		
CD10	21	6	5	0	0	0	0	0	0	15	9	4	0	0	0	0	0	0
MUC 2	11	15	6	0	0	0	0	0	0	12	11	5	0	0	0	0	0	0
MUC 5AC	0	1	6	2	6	5	0	10	2	0	0	5	1	6	6	0	9	1
MUC 6	0	0	0	3	2	3	1	15	8	0	0	0	7	0	5	0	10	6
P53	11	5	7	7	0	0	0	0	0	5	8	7	8	0	0	0	0	0
Ki67	1	7	9	4	3	2	0	6	0	0	2	1	5	5	4	1	9	1

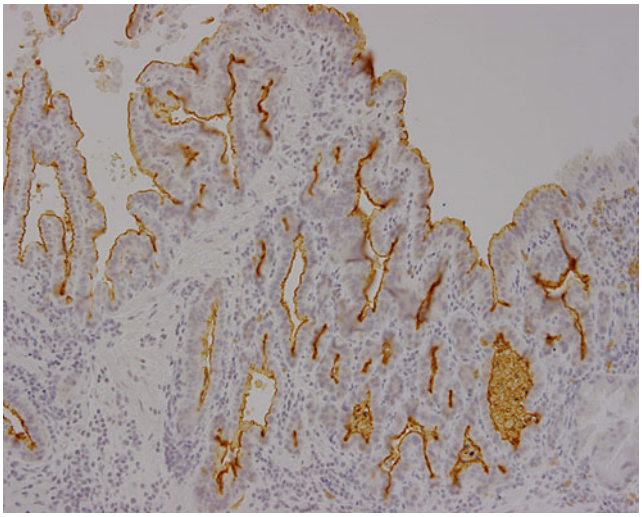

Fig. 8 Staining by CD10 of the brush border of a PGA indicating small bowel differentiation (lesion different from Fig. 5)

Additionally, these cases showed a higher Ki67 proliferation index. This might underline the immature character of these lesions. Higher proliferation rate, especially in connection with positive staining for p53, does indicate a greater rate of malignant transformation in PGA. On the other hand, it has to be noted that a reaction against p53 in early PGA adenocarcinoma is often weak or negative. Malignant transformation was 42.7% in these cases, which is comparable to the whole study cohort. However, it has to be noted that there are clear criteria available [5, 19] that allow the diagnosis of PGA with routine H&E staining. Immunohistochemistry is confirming the diagnosis and can be used to document the different types of differentiation more clearly.

As suggested by Shiroshita et al. [24], we subdivided the presence of intestinal mucin into MUC 2 (large bowel type mucin) and CD10 (Fig. 8) positive phenotype (small bowel type mucin). MUC 2 (Fig. 9) and CD10 presence was always very focal; thus, it did not change the phenotype of the whole lesion but indicated that an intestinal differentiation is not uncommon in PGAs. Our findings support the findings of others [23–25], indicating that a relatively large proportion of early gastric carcinomas initially arise as gastric carcinomas of the gastric type that secondarily convert into a gastric carcinoma of the intestinal type. Which, and how many, antibodies should be used to define the phenotypes of gastric carcinomas has recently been clearly defined by Shiroshita et al. [24, 25].

In the present series of PGA of the gastrointestinal tract, 46.7% of these lesions showed a transition to adenocarcinoma. This result represents an even greater percentage of malignant transformation but is comparable to our first series of 90 cases published recently [18]. The differences might be due to the smaller patient number in the present series. In the present analysis, there was a smaller number of gastric lesions available compared to extra-gastric lesions than in our first series. In extra-gastric lesions, a slightly higher frequency of malignant transformation is observed than in gastric lesions (50% vs 45.8%) [26, 27]. The high frequency of malignant transformation can be explained by the fact that PGA is still an unknown entity and is therefore often diagnosed at the stage of invasive carcinoma [28]. The small number of extra-gastric lesions supports this hypothesis. As in our first series, these tumours were mostly confined to the mucosa and were well differentiated, which is in favour of early endoscopic detection. Again, the most lesions were found in old patients in their eighth decade predominantly in cardia and fundic mucosa in *Helicobacter pylori* or autoimmune gastritis. PGA with transition to adenocarcinoma showed a higher Ki67 proliferation index and immunohistochemical positivity for p53, thus underlining the malignant potential of these lesions. Since only the immunohistochemistry score according to Remmele [23] showed the significant results, our analyses demonstrate the usefulness of this score also.

Conclusion

A diagnosis of PGA can already be made on basis of routine H&E staining. Immunohistochemistry can confirm the diagnosis of PGA by staining against apomucin 6 and apomucin 5AC. Immunhistochemically, it is possible to unreveal focal intestinal differentiation, thus supporting the hypothesis that gastric adenocarcinomas can initially develop from carcinomas of the gastric type and transform into intestinal type later on. The high frequency of

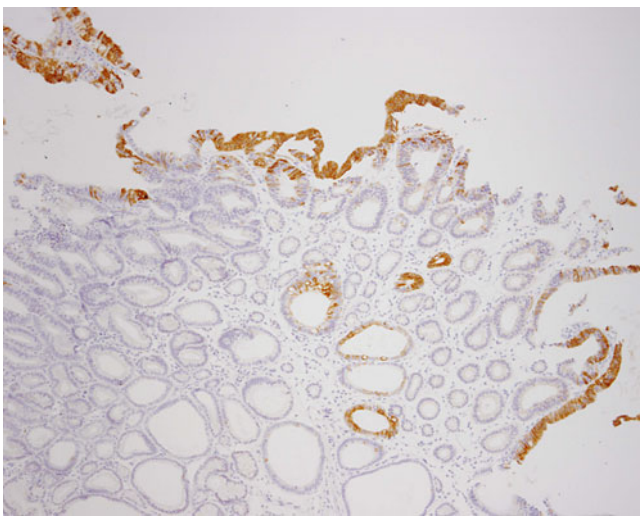

Fig. 9 Very focal staining by Mucin 2 indicating an intestinal differentiation (large bowel) (lesion different from Fig. 5)

malignant transformation of PGA underlines its high potential for invasive malignancy.

Acknowledgement This manuscript is dedicated to Professor Manfred Stolte on occasion of his 70th birthday. The authors declare no conflict of interest.

References

1. Eidt S, Stolte M (1989) Gastric glandular cysts–investigations into their genesis and relationship to colorectal epithelial tumors. Z Gastroenterol 27:212–7
2. Oberhuber G, Stolte M (2000) Gastric polyps: an update of their pathology and biological significance. Virchows Arch 437:581–590
3. Kushima R, Müller W, Stolte M, Borchard F (1996) Differential p53 protein expression in gastric adenomas of gastric and intestinal types: possible sequence of p53 alteration in the stomach carcinogenesis according to histological and mucin histochemical phenotypes. Virchows Arch 428:223–227
4. Hamilton SR, Aaltonen LA (eds) (2000) WHO classification of tumours. Tumours of the digestive system. IARC, Lyon
5. Borchard F, Ghanei A, Koldovsky U, Hengels KJ, Bückmann FW (1990) Gastrale Differenzierung in Adenomen der Magenschleimhaut Immunhistochemische und elektronenmikroskopische Untersuchungen. Verh Dtsch Ges Pathol 74:528
6. Kato N, Akiyama S, Motoyama T (2002) Pyloric gland-type tubular adenoma superimposed on intraductal papillary mucinous tumor of the pancreas. Pyloric gland adenoma of the pancreas. Virchows Arch 440:205–8
7. Watanabe H, Gass JF, Sobin LH (1990) Histological typing of oesophageal and gastric tumours. Spinger, Berlin
8. Elster K (1976) Histologic classification of gastric polyps. In: Morson BC (ed) Pathology of the gastro-intestinal tract. Springer, Berlin, pp 78–92
9. Borchard F (1987) 16. Tutorial IAP, Tumoren des oberen Gastrointestinaltraktes, Düsseldorf
10. Kushima R, Rüthlein HJ, Stolte M, Hattori T, Borchard F (1999) Pyloric gland-type adenoma arising in heterotopic gastric mucosa of the duodenum with dysplastic progression of the gastric type. Virch Arch 435:452–7
11. Bakotic BW, Robinson MJ, Sturm PD, Hruban RH, Offerhaus GJ, Albores-Saavedra J (1999) Pyloric gland adenoma of the main pancreatic duct. Am J Surg Pathol 23:227–231
12. Itoi T, Watanabe H, Ajioka Y, Ooohashi Y, Takei K, Nishikura K, Nakamura Y, Horic A, Saito T (1996) APC, K-ras codon 12 mutations and p53 gene expression in carcinoma and adenoma of the gall-bladder suggest two genetic pathways in gall-bladder carcinogenesis. Pathol Int 46:333–340
13. Kushima R, Remmele W, Stolte M, Borchard F (1996) Pyloric gland type adenoma of the gallbladder with squamoid spindle cell metaplasia. Pathol Res Pract 192:963–969
14. Takei K, Watanabe H, Itoi T, Saito T (1996) p53 and Ki-67 immunoreactivity and nuclear morphometry of "carcinoma-in-adenoma" and adenoma of the gall bladder. Pathol Int 46:908–917
15. Michal M, Crurik R, Matler K, Benes Z (2003) Regarding the paper by Vieth et al. Virchows Archiv 443/4:317-321. Virchows Archiv 443:589–590
16. Ishii K, Hidaka E, Katsuyama T, Ota H, Shiozawa T, Tsuchiya S (1999) Ultrastructural features of adenoma malignum of the uterine cervix: demonstration of gastric phenotypes. Ultrastruct Pathol 23:375–81
17. Mikami Y, Hata S, Fujiwara K, Imajo Y, Kohno I, Manabe T (1999) Florid endocervical glandular hyperplasia with intestinal and pyloric gland metaplasia: worrisome benign mimic of "adenoma malignum". Gynecol Oncol 74:504–11
18. Vieth M, Kushima R, Borchard F, Stolte M (2003) Pyloric gland adenoma: a clinico-pathological analysis of 90 cases. Virchows Arch 442:317–321
19. Kushima R, Mukaisho K, Vieth M, Borchard F, Stolte M, Hattori T (2003) Pyloric-gland-type adenomas of the stomach. Stomach and Intestine (Tokyo) 38:1377–1387
20. Kushima R (2004) Pyloric gland adenoma. Pathology and Clinical Medicine 22:634–635
21. Kushima R, Vieth M, Borchard F et al (2006) Gastric-type well-differentiated adenocarcinoma and pyloric gland adenoma of the stomach. Gastric Cancer 9:177–184
22. Chen ZM, Scudiere JR, Abraham SC, Montgomery E (2009) Pyloric gland adenoma: an entity distinct from gastric foveolar type adenoma. Am J Surg Pathol 33:186–93
23. Remmele W, Stegner HE (1987) Vorschlag zur einheitlichen Definition eines Immunreaktiven Score (IRS) für den immunhistochemischen Östrogenrezeptor-Nachweis (ER-ICA) im Mammakarzinomgewebe. Pathologe 8:138–140
24. Shiroshita H, Watanabe H, Ajioka Y, Watanabe G, Nishikura K, Kitano S (2004) Re-evaluation of mucin phenotypes of gastric minute well-differentiated-type adenocarcinomas using a series of HGM, MUC 5AC, M-GGMC, MUC 2 and CD10 stains. Pathol Int 54:311–321
25. Kushima R, Jancic S, Hattori T (1993) Association between expression of sialosyl-Tn antigen and intestinalization of gastric carcinomas. Int J Cancer 55:904–8
26. Hattori T, Kushima R (2001) Gastric differentiated stomach adenocarcinoma. Pathologe 22:97–104
27. Bamba M, Sugihara H, Kushima R, Okada K, Tsukashita S, Hattori T (2001) Time dependent expression of intestinal phenotype in signet ring cell carcinomas of the human stomach. Virchows Arch 438:49–56
28. Kushima R, Vieth M (2010) Tubular adenoma of the stomach with special reference to the Japanese criteria and pyloric gland adenoma. Pathologe 31:177–81

Virchows Arch (2010) 457:537–545
DOI 10.1007/s00428-010-0972-y

ORIGINAL ARTICLE

Comparison of six immunohistochemical markers for the histologic diagnosis of neoplasia in Barrett's esophagus

Andreas Weimann · Anja Rieger · Mathias Zimmermann · Monica Gross · Peter Hoffmann · Hortense Slevogt · Lars Morawietz

Received: 15 July 2010 / Revised: 20 August 2010 / Accepted: 24 August 2010 / Published online: 16 September 2010
© Springer-Verlag 2010

Abstract In esophageal neoplasms, the histopathologic differentiation between Barrett's esophagus with or without intraepithelial neoplasia and adenocarcinoma is often challenging. Immunohistochemistry might help to differentiate between these lesions. The expression of CDX2, LI-cadherin, mucin 2 (MUC2), blood group 8 (BG8, Lewis^y), claudin-2, and villin was investigated in normal gastroesophageal (n=23) and in Barrett's (n=17) mucosa, in low-grade (n=12) and high-grade (n=9) intraepithelial neoplasia (IEN) as well as in esophageal adenocarcinoma (n=16), using immunohistochemistry. For CDX2 and LI-cadherin, the immunoreactivity score was highest in IEN while for MUC2, BG8, and villin, it dropped gradually from Barrett's via IEN to adenocarcinoma, and expression of Claudin-2 was only weak and focal in all lesions. The expression of MUC2 and LI-cadherin differed significantly between all examined lesions except between low-grade and high-grade IEN. MUC2 and LI-cadherin are useful immunohistochemical markers for the differentiation between normal glandular mucosa, Barrett's mucosa, IEN, and invasive carcinoma of the esophagus; however, none of the examined markers was helpful for the differentiation between low-grade and high-grade IEN.

Keywords Barrett's esophagus · Intestinal metaplasia · Intraepithelial neoplasia · Mucin 2 · LI-cadherin · Immunohistochemistry

Introduction

Barrett's esophagus, first described by the surgeon Norman Barrett in 1950 [1] and refined in 1957 [2], is defined as a columnar metaplasia of the distal esophagus that develops as a result of chronic gastroesophageal reflux disease. The squamous epithelium of the distal esophagus is replaced by metaplastic intestine-like columnar epithelium with goblet cells, which may progress to esophageal ulcer, stricture, intraepithelial neoplasia (IEN), or even adenocarcinoma. Esophageal adenocarcinoma is a tumor with a rapidly increasing incidence in most western countries [3]. The cell of origin for Barrett's esophagus is unknown, but potential candidates include cells in the basal layer of the esophageal squamous epithelium or multipotent stem cells located in the squamous epithelium or within the ducts of submucosal esophageal glands. A recent study in rats has even raised the possibility that, under certain circumstances, the progenitor cell for Barrett's esophagus might be derived from circulating stem cells of bone marrow origin [4].

The specialized columnar epithelium is composed of both goblet and columnar non-goblet cells, but only the former are considered as the hallmark of Barrett's esophagus [5–8]. The rapidly rising incidence of esophageal adenocarcinoma over the past two decades has driven efforts to identify patients with Barrett's esophagus [9, 10]. The sensitivity and positive

Andreas Weimann and Anja Rieger contributed equally to this work

A. Weimann · M. Zimmermann · M. Gross · P. Hoffmann
Institute for Laboratory Medicine and Pathobiochemistry,
Charité–University Medical Center,
Berlin, Germany

A. Rieger · L. Morawietz (✉)
Institute of Pathology, Charité–University Medical Center,
Charitéplatz 1,
10117 Berlin, Germany
e-mail: lars.morawietz@charite.de

H. Slevogt
Department of Internal Medicine/Infectious Diseases,
Charité–University Medical Center,
Berlin, Germany

predictive value of standard upper endoscopy for diagnosing Barrett's esophagus have been reported as 82% and 34%, respectively [11]. This is secondary to the patchy and mosaic distribution of intestinal metaplasia within the columnar-lined esophagus. Thus, the diagnosis could be missed when goblet cells are inconspicuous or when even small biopsies with crush artifacts are sent for examination. Accordingly, the availability of markers capable of detecting intestinal differentiation in the absence of goblet cells could be of high clinical importance.

The caudal-type homeobox transcription factor (*cdx*) genes (CDX1 and CDX2, respectively) are important during the early differentiation and maintenance of intestinal epithelium via regulation of intestine-specific gene transcription [12, 13]. CDX2, especially, has attracted recent interest as an early marker for dysplastic epithelium because its expression has been demonstrated in Barrett's metaplasia, esophagitis, and intestinal metaplasia of the stomach in human beings [14–16]. The CDX2 gene is physiologically expressed throughout the small and large intestine, with the proximal limit occurring at the gastroduodenal junction. Ectopic CDX2 expression is considered to play a critical role in the development of intestinal metaplasia.

Cadherins belong to the family of transmembrane glycoproteins responsible for Ca^{2+}-dependent cell–cell adhesion [17]. Furthermore, cadherins are involved in the maintenance of tissue structure and morphogenesis [17, 18]. Today, there is increasing evidence that cadherin-mediated cell adhesion additionally plays a pivotal role in carcinoma cell behavior [19, 20]. Liver–intestine (Li)-cadherin is a structurally unique member of the cadherin superfamily as it contains seven instead of five molecular domains as a hallmark [21, 22]. LI-cadherin is one of the transcriptional targets of CDX2 [21–23]. It is selectively expressed on the basolateral surface of enterocytes and goblet cells in the small and large intestine but not in the upper gastric tract. In contrast to rats, LI-cadherin is not expressed in the liver of humans [24]. Aberrant LI-cadherin expression has been shown to be a sensitive marker for early detection of gastric intestinal metaplasia and well differentiated adenocarcinomas [24] as well as a marker of hepatocellular carcinomas [25] and pancreatic ductal adenocarcinomas [26]. Ko et al. detected overexpression and co-localization of CDX2 and LI-cadherin in gastric intestinal metaplasia and adenocarcinoma and presumed that aberrant up-regulation of CDX2 and consequently the activation of different intestinal genes might be one of the possible mechanisms linked to the induction of intestinal metaplasia [16].

Villin is an actin-binding cytoskeletal protein in the microvillus core of the brush border. Its expression can be induced by long-term acid exposure and is correlated with the development of differentiated polarized cells that contain a brush border and microvillus inclusions [27]. Villin is an end-differentiated marker of intestinal cells, and the protein needs to be of a sufficient quantity to result in a mature brush border [28]. An in vitro study demonstrated the rate of villin synthesis to be dramatically increased in the course of enterocyte differentiation, remaining remarkably stable after synthesis. Immunofluorescence and immunogold labeling showed villin diffusely distributed in undifferentiated cells [29].

Claudins, the recently identified multigene transmembrane protein family, are thought to be the major constituents of tight junctions, the most apical components of cell sealing complexes responsible for cell–cell adhesion, cell polarity, and control of paracellular ion transport [30, 31]. Several recent studies have detected changes in claudin expression during carcinogenesis, as in cervical neoplasia, breast, ovarian, pancreatic, colorectal, prostate, and other cancers. Tight junction proteins have even been suggested as potential antibody targets for pancarcinoma therapy [32, 33].

Mucins are high molecular weight glycoproteins synthesized by a broad range of epithelial tissues and are coded for by mucin (MUC) genes. Mucins are subdivided into two groups: secreted mucins (e.g., MUC2, MUC5, and MUC6) and membrane-bound mucins (e.g., MUC1, MUC3, and MUC4). Mucins play a key role in the gastrointestinal tract by constituting a physical barrier and a protective diffusion barrier for the underlying epithelium. Altered expression patterns of mucin epitopes have been described in colon and stomach cancers and are correlated with decreased survival. One hypothesizes that these aberrant expression patterns lead to continued epithelial damage, increased cell growth, and metastatic ability especially in the esophagus [34, 35].

Additionally, cell-surface carbohydrates play an outstanding role in tumor growth, progression, and metastases [36]. The blood group $Lewis^y$ antigen [particularly blood group 8 (BG8)] is strongly associated with increased cell growth and metastatic potential in a variety of cancers, including human breast, colon, lung, and ovarian carcinomas [36]. Furthermore, the $Lewis^y$ molecular structure is one tumor-associated carbohydrate structure being explored as a target for monoclonal antibody-based imaging and therapy.

Barrett's epithelium expresses several marker proteins of both intestinal and gastric differentiation. Because of the above mentioned properties of these six potential markers, aim of the present study was to investigate if any of these proteins could emerge as useful markers in routine histopathologic diagnosis, especially for the differentiation between Barrett's mucosa with and without IEN, and between IEN and invasive neoplasia, which is often difficult using histomorphology alone. Accordingly, we focused on specialized columnar epithelium in Barrett's

mucosa without IEN, with low- and high-grade intraepithelial neoplasia as well as on invasive adenocarcinoma and on normal gastroesophageal tissue in order to gain detailed insight into the complex metaplasia–dysplasia–adenocarcinoma sequence.

Material and methods

Patients and samples

The present study was retrospectively conducted on samples from 70 patients, which had primarily been examined at the Institute of Pathology at the University Hospital Charité, Berlin, in the years 2004 (n=4), 2005 (n=16), and 2006 (n=50). The mean patient age was 64 years (minimum, 32; maximum, 97; standard deviation, 12.5 years), 19 were female and 51 were male. The tissue had been obtained as biopsies (n=50), mucosectomy specimens (n=6), or as esophageal resections (n=14). The H&E-stained slides were reviewed to verify the initial diagnoses and to select suitable areas for immunohistochemical stainings, then the formalin-fixed, paraffin-embedded tissue was selected from the archive of the institute. When available, adjacent non-neoplastic epithelium was evaluated in samples from intraepithelial or invasive neoplasia, so the total number of evaluated tissues was n=77. These covered the whole spectrum from normal gastroesophageal mucosa (n=23) through Barrett's mucosa without IEN (n=17), with low-grade (LG-IEN, n=12) and high-grade intraepithelial neoplasia (HG-IEN, n=9) to invasive adenocarcinoma (n=16). The diagnoses were based on the histomorphology according to the criteria of the WHO classification of tumors 2000 [37]. All patients had given informed consent to the use of the tissue samples in this study, in accordance with the Helsinki Declaration of the World Medical Association.

All tissue samples had been evaluated in our previous study about the significance of CDX2 and LI-cadherin expression [38]; however, since in 11 of the previously used 88 tissue blocks the respective lesions were almost used up, no results of the MUC2, BG8, claudin-2, and villin stainings could be collected, so the present collection and also the results regarding CDX2 and LI-cadherin differ slightly from our previously demonstrated findings.

Immunohistochemistry

Microsections of 2-μm thickness were deparaffinized with xylene. Antigen retrieval was performed in boiling sodium citrate buffer (0.01 mM; pH 6.0). Endogenous peroxidase was quenched by incubation with peroxidase block (DAKO, Glostrup, Denmark) for 10 min. The antibodies and dilutions were as follows: anti-LI-cadherin goat polyclonal at 1:1,000 (Santa Cruz Biotechnology, Santa Cruz, CA, USA), anti-CDX2 at 1:100 (Biogenetics, Padua, Italy), anti-MUC2 mouse clone Ccp58 at 1:100 (Santa Cruz), anti-BG8 mouse clone F3 at 1:40 (Signet, Dedham, MA, USA), anti-claudin rabbit polyclonal ready-to-use (Panomics, Redwood City, CA, USA), and anti-villin goat polyclonal at 1:50 (Santa Cruz).

For antibody detection, the LSAB plus HRP kit (DAKO) was used according to the manufacturer's protocol. DAB was used as chromogen, and the sections were then counterstained with haematoxylin for 2 min.

A negative control, which was obtained by omitting the primary antibody, accompanied each staining run and was confirmed to be negative in order to exclude unspecific tissue reactions with the detection kit.

Histopathologic evaluation

All stained slides were evaluated on a standard light microscope (LaborLux, Leitz, Bensheim, Germany) at ×25, ×100, ×200, and ×400 magnification. Microphotographs were captured by a 3-CCD camera (KY-F75U, JVC Professional Products Company, Wayne, NJ, USA).

The staining intensity was graded semiquantitatively from 0 (absent) to 1 (slight), 2 (moderate) to 3 (strong). Also, the relative number of positively stained cells compared to all epithelial cells of the target lesion was estimated in measures of 10%. The accuracy of this percentage is limited for the evaluation of LG-IEN and HG-IEN because on the immunohistochemically stained slides the histomorphology was more ambiguous when compared to H&E morphology, and therefore the range of the lesions could not be determined exactly. Another limitation to the preciseness of our evaluation was the variability of the immunohistochemical expression within one lesion. They exhibited areas of no, moderate, and strong expression side by side, which were combined to a single score.

In analogy to Remmele and Stegner [39], an immunoreactivity score (IRS) was calculated as the product of the value for staining intensity (from 0 to 3) and a value for the percentage of positive cells, the latter defined as follows: 0, less than 10% positive cells; 1, 10–19% positive; 2, 20–59% positive; 3, 60–89% positive; and 4, 90–100% positive, the total IRS ranging from 0 to 12.

Statistical analysis

For descriptive statistics, arithmetic mean and median were acquired. The correlations between the six markers were calculated using Pearson's correlation coefficient. To analyze significances between the different kinds of lesions, at first the Kruskal–Wallis test was used, and for detailed

analysis, the Mann–Whitney test was applied. Significance was assumed when $p<0.05$. All calculations were performed using an SPSS 16.0 software (SPSS Inc., Chicago, IL, USA).

Results

Staining properties of the antibodies

Using the described staining techniques, CDX2 showed a nuclear staining reaction in cells at the luminal surface and in the foveolae. LI-cadherin displayed a membranous stain, accentuated at the luminal side of the epithelium. MUC2 showed a cytoplasmic staining reaction with a perimembranous accentuation. BG8 could be detected in the cytoplasm in squamous and cylindric epithelium, especially in mucin-secreting cells. Claudin-2 staining was membranous, although an aberrant nuclear reaction could be observed too. Villin staining was restricted to the brush border, so it was only detected at the luminar side of the cell membrane. Examples of all staining reactions are given in Fig. 1.

Staining intensities in the different esophageal lesions

CDX2 was not expressed in normal cardiac mucosa. A moderate staining was observed in Barrett's mucosa and a stronger staining in LG-IEN and HG-IEN, whereas the staining was weaker again in invasive adenocarcinoma. A similar distribution could be observed for LI-cadherin, MUC2, and villin, with certain differences; MUC2 showed the strongest staining in Barrett's mucosa but only very focal staining in invasive carcinoma, and villin was already weakly expressed in the normal mucosa and also strongly in Barrett's mucosa. The distribution of BG8 was different; it was strongly positive in normal and Barrett's mucosa and decreased gradually from LG-IEN to invasive carcinoma. Claudin-2 immunoreactivity was very weak and focal in all examined lesions. The details of the immunohistochemical evaluation are given in Table 1.

Statistical analysis of the different expression levels

The first statistical evaluation of the marker expression in the different lesions, using the Kruskal–Wallis test, revealed that all markers except claudin-2 showed significant differences between the lesions (Table 2). A detailed analysis was clarified between lesions the markers could significantly differentiate and between those they could not. This revealed MUC2 (both IRS and percentage of positive cells) as the marker which differed significantly among all the lesions, except between low- and high-grade IEN. In fact, no marker was able to differentiate between the different grades of IEN. Also, LI-cadherin was able to differentiate between most of the lesions, but no significance was found between Barrett's mucosa without IEN and invasive carcinoma, which is due to the fact that in carcinoma the expression dropped under the level of LG-IEN and HG-IEN. A detailed depiction of the levels of significance is given in Table 3.

Correlations between the examined markers

Pearson's correlation coefficient revealed a highly significant ($p<0.001$) correlation between CDX2, LI-cadherin, BG8, and villin stainings, and also a significant ($p<0.05$) correlation between MUC2, CDX2, LI-cadherin, and villin regarding the staining intensity as well as the percentage of positive cells and the IRS (correlation coefficients for IRS in Table 4, data for staining intensity and percentage are not shown).

Discussion

This study analyzed the complex expression pattern of CDX2, LI-cadherin, MUC2, BG8, claudin-2, and villin during the development of Barrett's epithelium to adenocarcinoma according to the metaplasia–dysplasia–adenocarcinoma sequence. Barrett's esophagus is a complication of long-standing gastroesophageal reflux which often remains asymptomatic. It is considered a risk factor for esophageal adenocarcinoma, which has a poor prognosis unless detected at an early stage [40, 41]. Therefore, the presence of Barrett's mucosa is used as a marker for the identification of those patients who are at higher risk for development of esophageal cancer and therefore need regular screening. At present, the best predictor of the future development of a carcinoma in a given patient with Barrett's esophagus is still the histomorphologic identification of IEN. The high-grade IEN carries the highest relative risk (33%) for a malignant progression in Barrett's esophagus with a 5-year incidence for adenocarcinoma of 59% [42, 43].

In vivo studies described CDX2 as being a regulator of intestine-specific gene transcription, as evidenced by its binding to several intestine-specific promoters followed by activation of transcription. This is the case for LI-cadherin, an intestine-specific adhesion molecule with aberrant expression in intestinal metaplasia and well-differentiated adenocarcinomas of the stomach [23, 24]. A previous study by Ko et al. compared LI-cadherin expression in human gastric adenocarcinomas with clinicopathological findings, prognosis, and CDX2 expression. They were able to observe a strong association between these parameters and the aggressiveness of gastric carcinoma. Ko et al. described

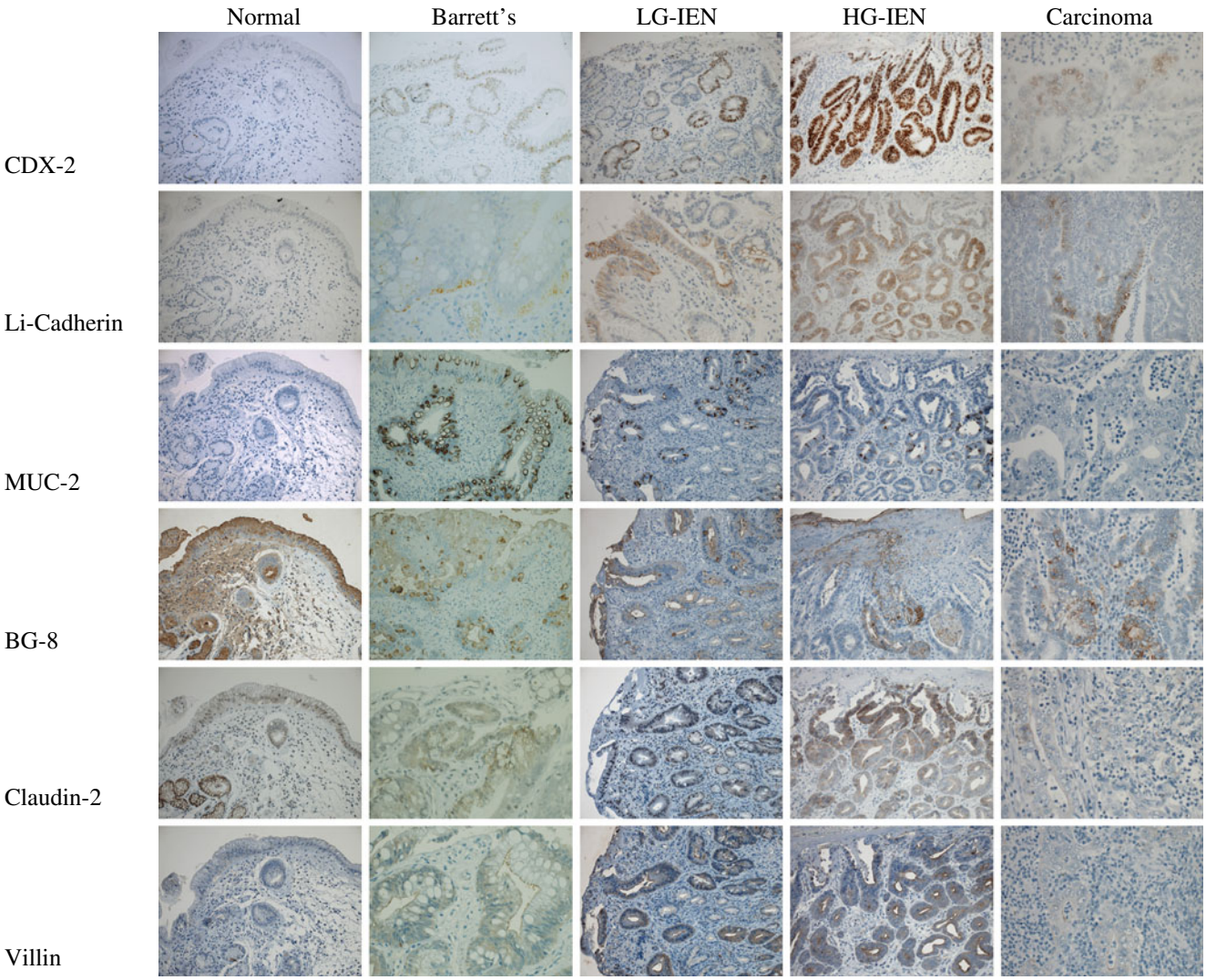

Fig. 1 Examples of the immunohistochemical staining properties of all examined markers (*rows*) in all examined types of lesions (*columns*). CDX2 staining is confined to the nucleus while LI-cadherin and claudin-2 display a membranous and MUC2 a cytoplasmic stain, and villin reaction is restricted to the brush border. BG8 staining is strongest in mucin-secreting cells. The examples show the differences in staining intensity between the distinct lesions. Original magnification, ×200; except carcinoma, ×400

LI-cadherin as being an excellent marker for high-grade malignancies [44]. Several studies have been done, so far, based on the hope that in the future, specific molecular changes might serve as reliable markers for the early identification of patients who are likely to develop carcinoma. Eda et al. [15] demonstrated that CDX2 already emerged at the stage of esophagitis in inflammatory squamous mucosa, using the reverse transcriptase-polymerase chain reaction (RT-PCR) technique. There was a 100% concordance between the CDX2 expression determined by RT-PCR and immunohistochemistry. Eda et al. clarified the expression of CDX2 in chronic gastritis and concluded that inflammation might play an important role in the induction of CDX2 expression and its downstream actions [14]. According to their findings, CDX2 expression is an early event in intestinal differentiation, its presence and that of LI-cadherin indicate that the molecular signal cascade for intestinal differentiation is in place and therefore the expression of these two proteins might actually be more sensitive for the diagnosis of Barrett's esophagus and its upstream lesions than routine histologic evaluation for the presence of goblet cells.

In our study, we observed nuclear positivity for CDX2 (39%) coupled with membranous expression of LI-cadherin (40%) of the epithelial cells of Barrett's mucosa, and the intensity of staining and the distribution of expression was increased and relatively stable for both markers within the sequential steps from low-grade (62% resp. 63%) to high-grade IEN (68% resp. 70%) while only the normal cylindric epithelium lacked of the expression of both (0%). The staining was weaker again in invasive adenocarcinoma (48% resp. 33%). A possible explanation for this phenom-

Table 1 Arithmetic means (median values in parentheses) for staining intensity, percentage of positive cells, and immunoreactivity score (IRS) for each marker in each kind of lesion

	Histopathologic type of lesion				
	Normal	Barrett	Low-grade IEN	High-grade IEN	Carcinoma
CDX2					
Intensity	0.4 (0)	2.0 (2)	1.9 (2)	2.6 (3)	2.1 (2)
Percentage	2 (0)	39 (30)	62 (70)	68 (70)	48 (45)
IRS	0.4 (0)	4.7 (4)	5.3 (5)	7.6 (6)	5.1 (4)
LI-cadherin					
Intensity	0.1 (0)	2.0 (0)	2.3 (2.5)	2.4 (2)	1.8 (2)
Percentage	0 (0)	40 (30)	63 (70)	70 (70)	33 (20)
IRS	0.1 (0)	4.5 (4)	7.3 (6)	7.3 (6)	4.0 (4)
MUC2					
Intensity	0. (0)	3.0 (3)	3.0 (3)	2.3 (3)	2.3 (3)
Percentage	0 (0)	92 (100)	22 (20)	16 (10)	9 (0)
IRS	0.0 (0)	11.3 (12)	4.4 (6)	3.7 (3)	1.4 (0)
BG8					
Intensity	2.4 (2)	1.8 (2)	1.6 (2)	1.2 (1)	1.2 (1)
Percentage	83 (100)	75 (100)	65 (80)	48 (50)	44 (30)
IRS	8.5 (8)	6.6 (8)	4.6 (4)	3.3 (3)	3.2 (3)
Claudin-2					
Intensity	0.5 (0)	0.1 (0)	0.6 (0)	0.5 (0)	1.0 (0)
Percentage	5 (0)	2 (0)	5 (0)	7 (0)	16 (0)
IRS	0.9 (0)	0.1 (0)	1.0 (0)	1.0 (0)	2.5 (0)
Villin					
Intensity	1.2 (1)	2.7 (3)	2.3 (2)	2.4 (3)	1.9 (2)
Percentage	25 (20)	88 (90)	75 (80)	78 (80)	36 (30)
IRS	2.5 (2)	9.5 (9)	7.4 (7)	8.1 (6)	4.2 (4)

enon might be that cancer cells become less differentiated during disease progression, resulting in a loss of CDX2 and its downstream-located transcription targets, respectively. In contrast to Phillips et al. [45], we did not observe decreased CDX2 staining in high-grade IEN.

Noguchi et al. first investigated, in 1989, the use of BG8 antigen as a marker for distinguishing between non-epithelial lesions (mesothelioma) and adenocarcinomas of the lung using the NCC-ST-433 monoclonal antibody on formalin-fixed, paraffin-embedded tissue specimens. They reported expression of BG8 antigen in 20 (95%) of 21 pulmonary adenocarcinomas and in four (44%) of nine mesotheliomas. Based on these results, the authors concluded that BG8 immunostaining was not a useful marker to discriminate between these two malignancies [46]. In contrast to these findings, Riera et al. reported, in 1997, a BG8 expression in 114 (92.7%) of 123 pulmonary adenocarcinomas, whereas only five (8.8%) of 57 mesotheliomas reacted focally and weakly for this marker. In that publication, the authors emphasized that BG8 was one of the best immunohistochemical markers currently available to assist in the diagnosis of epithelial mesotheliomas [47]. In our study, the BG8 staining pattern was closely related to the degree of cellular differentiation; normal and Barrett's mucosa were strongly positive for BG8 expression (83% resp. 75% positivity for BG8) with a gradual decrease from LG-IEN (65%) to HG-IEN (48%) to invasive carcinoma (44%). This could be explained by a decrease in differentiation during the dysplastic transformation of the mucosa.

Another downstream target of CDX2 is the MUC2 protein. MUC2 is secreted from goblet cells in Barrett's esophagus. MUC2 has been shown to be present in and

Table 2 Levels of significance (Kruskal–Wallis test) for the ability of each marker to discriminate between all different types of lesions

	CDX2	LI-cadherin	MUC2	BG8	Claudin-2	Villin
Intensity	0.000	0.000	0.000	0.000	0.286	0.000
Percentage	0.000	0.000	0.000	0.006	0.533	0.000
IRS	0.000	0.000	0.000	0.000	0.454	0.000

Table 3 Levels of significance for each marker (rows) to discriminate between two types of lesions (columns)

Tissue marker	Normal Barrett	Normal LG-IEN	Normal HG-IEN	Normal CA	Barrett LG-IEN	Barrett HG-IEN	Barrett CA	LG-EIN HG-IEN	LG-IEN CA	HG-IEN CA
CDX2										
Intensity	**0.000**	**0.000**	**0.000**	**0.000**	0.705	0.067	0.877	0.094	0.657	0.161
Percentage	**0.000**	**0.000**	**0.000**	**0.000**	0.061	**0.021**	0.318	0.541	0.106	0.104
IRS	**0.000**	**0.000**	**0.000**	**0.000**	0.590	**0.029**	0.728	0.117	0.851	0.062
LI-cadherin										
Intensity	**0.000**	**0.000**	**0.000**	**0.000**	0.173	0.081	0.860	0.875	0.219	0.181
Percentage	**0.000**	**0.000**	**0.000**	**0.000**	**0.034**	**0.007**	0.197	0.640	**0.018**	**0.007**
IRS	**0.000**	**0.000**	**0.000**	**0.000**	**0.029**	**0.003**	0.448	0.970	**0.026**	**0.011**
MUC2										
Intensity	**0.000**	**0.000**	**0.000**	**0.000**	0.240	0.054	**0.046**	0.108	0.095	0.963
Percentage	**0.000**	**0.000**	**0.000**	**0.040**	**0.000**	**0.000**	**0.000**	0.390	**0.008**	**0.048**
IRS	**0.000**	**0.000**	**0.000**	**0.040**	**0.000**	**0.000**	**0.000**	0.532	**0.006**	**0.033**
BG8										
Intensity	**0.029**	**0.003**	**0.001**	**0.000**	0.294	**0.021**	**0.024**	0.056	0.113	0.689
Percentage	0.873	0.109	**0.033**	**0.003**	0.147	0.055	**0.006**	0.459	0.208	0.689
IRS	0.178	**0.006**	**0.004**	**0.000**	0.050	**0.025**	**0.004**	0.156	0.126	0.912
Claudin-2										
Intensity	**0.030**	0.710	0.746	0.581	0.156	0.266	**0.022**	1.000	0.451	0.577
Percentage	0.050	0.629	0.787	0.949	0.200	0.266	0.087	0.926	0.653	0.710
IRS	**0.034**	0.656	0.746	0.899	0.169	0.266	0.074	1.000	0.617	0.655
Villin										
Intensity	**0.000**	**0.002**	**0.007**	0.079	0.301	0.630	0.087	0.748	0.354	0.319
Percentage	**0.000**	**0.000**	**0.001**	0.155	0.396	0.582	**0.000**	1.000	**0.001**	**0.016**
IRS	**0.000**	**0.000**	**0.002**	0.076	0.313	0.308	**0.000**	0.852	**0.014**	**0.047**

Significant values ($p<0.05$) are printed in bold

CA carcinoma

relatively specific to human Barrett epithelium, and it likely plays an important role in the cytoprotection against reflux of gastroduodenal contents, including bile acids, the latter being a candidate etiologic factor for the development of Barrett's esophagus [48]. Furthermore, it is well-known that the intestinal differentiation gene CDX2 is an important transcriptional regulator of the MUC2 expression [49]. Immunohistochemical studies have revealed that MUC2 is not expressed in normal esophageal squamous epithelium but is commonly found in goblet cells of colonic, intestinal, and Barrett epithelium. The expression and secretion of MUC2 in Barrett's esophagus is a feature of cellular differentiation as secretory mucins are normally produced by highly differentiated cells. In concordance to the findings of other groups, our data showed an absent MUC2 expression in normal gastroesophageal mucosa but a 92% positivity in Barrett's mucosa followed by a significant decrease from LG-IEN (22%) to HG-IEN (16%) to invasive carcinoma (9%) due to the increase in cellular atypia and decrease of the number of goblet cells.

Villin is a candidate gene of CDX2 further downstream and an end-differentiated marker of intestinal cells [50]. The

Table 4 Pearson's correlation coefficients for the IRS between the different markers

	CDX2	LI-cadherin	MUC2	BG8	Claudin-2	Villin
CDX2		**0.773**	**0.264**	**−0.383**	0.141	**0.381**
LI-cadherin	**0.773**		**0.300**	**−0.332**	0.077	**0.437**
MUC2	**0.264**	**0.300**		0.031	−0.127	**0.635**
BG8	**−0.383**	**−0.332**	0.031		−0.135	−0.186
Claudin-2	0.141	0.077	−0.127	−0.135		−0.086
Villin	**0.381**	**0.437**	**0.635**	−0.186	−0.086	

Large and bold, significant at $p<0.01$: bold, significant at $p<0.05$; not bold, not significant

protein needs to be of sufficient quantity to result in a mature brush border [28]. We found villin to be present in 25% of normal mucosa and in 88% of the Barrett's mucosa cases. Besides goblet cells, villin was expressed in the brush border and cytoplasm of superficial columnar epithelium and luminal borders of glands containing goblet cells. Its expression was quite high in LG-IEN (75%) and in HG-IEN (78%) but showed a clear decrease to 36% positive cells in invasive carcinoma. Further immunohistochemical analyses of gastric intestinal metaplasia and cancer revealed that villin and CDX2 expressions are tightly coupled. Moreover, Yamamichi et al. were able to demonstrate that CDX2 regulates the intestinal villin expression through recruiting the Brm-type SWI/SNF complex to the villin promoter [50].

Previous studies reported contradictive results regarding the expression patterns of claudin-2 proteins in Barrett's esophagus and in invasive adenocarcinomas [51, 52]. Our results showed only a very weak and focal expression of claudin-2 in all examined lesions.

The significance of our study is limited because it is not a prospective study and because we could not correlate the expression of the examined markers with the clinical outcome. Follow-up biopsies from patients with Barrett's mucosa without and with IEN were not available in most cases, so no statement can be made about the progression of the disease. This study is a description of the expression of six different markers, some of which will be helpful in routine histopathologic diagnosis.

In summary, all used markers except claudin-2 were detectable with varying intensities in the different lesions, and most showed significant differences between the examined disease stages. MUC2 was the marker that differed significantly among all lesions, except between low- and high-grade IEN. In fact, no marker was able to differentiate between the two grades of IEN. Additionally, LI-cadherin was able to differentiate between most of the lesions, too, but no significance was found between Barrett's mucosa without IEN and invasive carcinoma. We would like to recommend both MUC2 and LI-cadherin as additional markers for the histopathologic evaluation of glandular esophageal lesions, especially for the differentiation between Barrett's esophagus with and without IEN and between IEN and adenocarcinoma.

Acknowledgments The excellent technical assistance of Mrs. Gabriele Fernahl is gratefully acknowledged.

Conflict of interest statement The authors declare that they have no conflict of interest.

References

1. Barrett NR (1950) Chronic peptic ulcer of the oesophagus and 'oesophagitis'. Br J Surg 38:175–182
2. Barrett NR (1957) The lower esophagus lined by columnar epithelium. Surgery 41:881–894
3. Haggitt RC (1992) Adenocarcinoma in Barrett's esophagus: a new epidemic? Hum Pathol 23:475–476
4. Sarosi G, Brown G, Jaiswal K et al (2008) Bone marrow progenitor cells contribute to esophageal regeneration and metaplasia in a rat model of Barrett's esophagus. Dis Esophagus 21:43–50
5. Sampliner RE (1998) Practice guidelines on the diagnosis, surveillance, and therapy of Barrett'sesophagus. The Practice Parameters Committee of the American College of Gastroenterology. Am J Gastroenterol 93:1028–1032
6. Weinstein WM, Ippoliti AF (1996) The diagnosis of Barrett's esophagus: goblets, goblets, goblets. Gastrointest Endosc 44:91–95
7. Batts KP (2001) Barrett esophagus—more steps forward. Hum Pathol 32:357–359
8. Goldblum JR (2003) Barrett's esophagus and Barrett's-related dysplasia. Mod Pathol 16:316–324
9. Blot WJ, Devesa SS, Kneller RW, Fraumeni JF Jr (1991) Rising incidence of adenocarcinoma of the esophagus and gastric cardia. JAMA 265:1287–1289
10. Vizcaino AP, Moreno V, Lambert R, Parkin DM (2002) Time trends incidence of both major histologic types of esophageal carcinomas in selected countries, 1973–1995. Int J Cancer 99:860–868
11. Eloubedi MA, Provenzale D (1999) Does this patient have Barrett's esophagus? The utility of predicting Barrett's esophagus at the index endoscopy. Am J Gastroenterol 94:937–943
12. Freund JN, Domon-Dell C, Kedinger M, Duluc I (1998) The Cdx-1 and Cdx-2 homeobox genes in the intestine. Biochem Cell Biol 76:957–969
13. Suh E, Traber PG (1996) An intestine-specific homeobox gene regulates proliferation and differentiation. Mol Cell Biol 16:619–625
14. Eda A, Osawa H, Yanaka I, Satoh K, Mutoh H, Kihira K, Sugano K (2002) Expression of homeobox gene CDX2 precedes that of CDX1 during the progression of intestinal metaplasia. J Gastroenterol 37:94–100
15. Eda A, Osawa H, Satoh K, Yanaka I, Kihira K, Ishino Y, Mutoh H, Sugano K (2003) Aberrant expression of CDX2 in Barrett'sepithelium and inflammatory esophageal mucosa. J Gastroenterol 38:14–22
16. Ko S, Chu KM, Luk JM, Wong BW, Yuen ST, Leung SY, Wong J (2005) CDX2 co-localizes with liver-intestine cadherin in intestinal metaplasia and adenocarcinoma of the stomach. J Pathol 205:615–622
17. Ranscht B (1994) Cadherins and catenins: interactions and functions in embryogenic development. Curr Opin Cell Biol 6:740–746
18. Takeichi M (1995) Morphogenetic roles of classic cadherins. Curr Opin Cell Biol 7:619–627
19. Takeichei M (1993) Cadherins in cancer: implications for invasion and metastasis. Curr Opin Cell Biol 5:806–811
20. Hirohashi S (1998) Inactivation of the E-cadherin-mediated cell adhesion system in human cancers. Am J Pathol 153:333–339
21. Berndorff D, Gessner R, Kreft B, Schnoy N, Lajous-Petter AM, Loch N, Reutter W, Hotsch M, Tauber R (1994) Liver–intestine cadherin: molecular cloning and characterization of a novel Ca^{2+}-dependent cell adhesion molecule expressed in liver and intestine. J Cell Biol 125:1353–1369
22. Gessner R, Tauber R (2000) Intestinal cell adhesion molecules. Liver–intestine cadherin. Ann NY Acad Sci 915:136–143
23. Hinoi T, Lucas PC, Kuick R, Hanash S, Cho KR, Fearon ER (2002) CDX2 regulates liver intestine-cadherin expression in normal and malignant colon epithelium and intestinal metaplasia. Gastroenterology 123:1565–1577

24. Grötzinger C, Kneifel J, Patschan D, Schnoy N, Anagnostopoulos I, Faiss S, Tauber R, Wiedenmann B, Gessner R (2001) LI-cadherin: a marker of gastric metaplasia and neoplasia. Gut 49:8
25. Wong BW, Luk JM, Ng IO, Hu MY, Liu KD, Fan ST (2003) Identification of liver–intestine cadherin in hepatocellular carcinoma—a potential disease marker. Biochem Biophys Res Commun 311:618–624
26. Takamura M, Sakamoto M, Ino Y, Shimamura T, Ichida T, Asakura H, Hirohashi S (2003) Expression of liver–intestine cadherin and its possible interaction with galectin-3 in ductal adenocarcinoma of the pancreas. Cancer Sci 94:425–430
27. Fitzgerald RC, Omary MB, Triadafilopoulos G (1997) Acid modulation of HT29 cell growth and differentiation: an in vitro model for Barrett's esophagus. J Cell Sci 110:663–671
28. Niwa T, Ikehara Y, Nakanishi H et al (2005) Mixed gastric- and intestinal-type metaplasia is formed by cells with dual intestinal and gastric differentiation. J Histochem Cytochem 53:75–85
29. Dudouet B, Robine S, Huet C et al (1987) Changes in villin synthesis and subcellular distribution during intestinal differentiation of HT29-18 clones. J Cell Biol 105:359–369
30. Furuse M, Sasaki H, Tsukita S (1999) Manner of interaction of heterogeneous claudin species within and between tight junction strands. J Cell Biol 147:891–903
31. Sawada N, Murata M, Kikuchi K, Osanai M, Tobioka H, Kojima T, Chiba H (2003) Tight junctions and human diseases. Med Electron Microsc 36:147–156
32. Offner S, Hekele A, Teichmann U, Weinberger S, Gross S, Kufer P, Itin C, Baeuerle PA, Kohleisen B (2004) Epithelial tight junction proteins as potential antibody targets for pancarcinoma therapy. Cancer Immunol Immunother 54:431–445
33. Michl P, Buchholz M, Rolke M, Kunsch S, Lohr M, McClane B, Tsukita S, Leder G, Adler G, Gress TM (2001) Claudin-4: a new target for pancreatic cancer treatment using *Clostridium perfringens* enterotoxin. Gastroenterology 121:678–684
34. Ho SB, Niehans GH, Lyftogt C, Yan PS, Cherwitz DL et al (1993) Heterogeneity of mucin gene expression in normal and neoplastic tissues. Cancer Res 53:641–651
35. Burjonrappa SC, Reedimasu S, Nawaz Z et al (2009) Mucin expression profile in Barrett´s, dysplasia, adenocarcinoma sequence in the esophagus. Indian J Cancer 44:1–5
36. Blaszczyk-Thurin M, Ramachandran M, Westerink MAJ et al (1996) Molecular recognition of the Lewis Y antigen by monoclonal antibodies. Prot Engineering 5:447–459
37. Werner M, Flejou JF, Hainaut P, Hoefler H, Lambert R, Keller G, Stein HJ (2000) Adenocarcinoma of the oesophagus. In: Hamilton SR, Aaltonen LA (eds) WHO classification of tumours, pathology & genetics, tumors of the digestive system. IARC Press, Lyon, pp 20–26
38. Weimann A, Zimmermann M, Gross M, Slevogt H, Rieger A, Morawietz L (2010) CDX2 and LI-cadherin expression in esophageal mucosa: use of both markers can facilitate the histologic diagnosis of Barrett's esophagus and carcinoma. Int J Surg Pathol. doi:10.1177/1066896910364428
39. Remmele W, Stegner HE (1987) Recommendation for uniform definition of an immunoreactive score (IRS) for immunohistochemical estrogen receptor detection (ER-ICA) in breast cancer tissue. Pathologe 8:138–140
40. Conio M, Lapertosa G, Blanchi S, Filiberti R (2003) Barrett's esophagus: an update. Crit Rev Oncol Hematol 46:187–206
41. Falk GW (2002) Barrett's esophagus. Gastroenterology 122:1569–1591
42. Menke-Pluymers MB, Mulder AH, Hop WC, van Blankenstein M, Tilanus HW (1994) Dysplasia and aneuploidy as markers of malignant degeneration in Barrett's oesophagus. The Rotterdam Oesophageal Tumour Study Group. Gut 35:1348–1351
43. Reid BJ, Levine DS, Longton G, Blount PL, Rabinovitch PS (2000) Predictors of progression to cancer in Barrett's esophagus: baseline histology and flow cytometry identify low- and high-risk patient subsets. Am J Gastroenterol 95:1669–1676
44. Ko S, Chu KM, Luk JM, Wong BW, Yuen ST, Leung SY, Wong J (2004) Overexpression of LI-cadherin in gastric cancer is associated with lymph node metastasis. Biochem Biophys Res Commun 319:562–568
45. Phillips RW, Frierson HF Jr, Moskaluk CA (2003) Cdx2 as a marker of epithelial intestinal differentiation in the esophagus. Am J Surg Pathol 27:1442–1447
46. Noguchi M, Nakajima T, Hirohashi S, Akiba T, Shimosato Y (1989) Immunohistochemical distinction of malignant mesothelioma from pulmonary adenocarcinoma with anti-surfactant apoprotein, anti-Lewisa, and anti-Tn antibodies. Hum Pathol 20:53–57
47. Riera JR, Astengo-Osuna C, Longmate JA, Battifora H (1997) The immunohistochemical diagnostic panel for epithelial mesothelioma. A reevaluation after heat-induced epitope retrieval. Am J Surg Pathol 21:1409–1419
48. Kauer WK, Peters JH, DeMeester TR, Ireland AP, Bremner CG, Hagen JA (1995) Mixed reflux of gastric and duodenal juices is more harmful to the esophagus than gastric juice alone: the need for surgical therapy re-emphasized. Ann Surg 222:525–531
49. Yamamoto H, Bai YQ, Yuasa Y (2003) Homeodomain protein CDX2 regulates goblet-specific MUC2 gene expression. Biochem Biophys Res Commun 300:813–818
50. Yamamichi N, Inada KI, Furukawa C, Sakurai K et al (2009) Cdx2 and the Brm-type SWI/SNF complex cooperatively regulate villin expression in gastrointestinal cells. Exp Cell Res 315:1779–1789
51. Jovov B, Van Itallie CM, Shaheen NJ, Carson JL et al (2007) Claudin-18: a dominant tight junction protein in Barrett's esophagus and likely contributor to its acid resistance. Am J Physiol Gastrointest Liver Physiol 293:1106–1113
52. Györffy H, Holczbauer A, Nagy P, Szabó Z et al (2005) Claudin expression in Barrett's esophagus and adenocarcinoma. Virchows Arch 447:961–968

Virchows Arch (2010) 457:547–553
DOI 10.1007/s00428-010-0971-z

ORIGINAL ARTICLE

Measurements of cancer extent in a conservatively treated prostate cancer biopsy cohort

Ramzi Rajab · Gabrielle Fisher · Michael W. Kattan · Christopher S. Foster · Tim Oliver · Henrik Møller · Victor Reuter · Peter Scardino · Jack Cuzick · Daniel M. Berney · on behalf of the Transatlantic Prostate Group

Received: 28 July 2010 / Revised: 23 August 2010 / Accepted: 29 August 2010 / Published online: 9 September 2010
© Springer-Verlag 2010

Abstract The optimal method for measuring cancer extent in prostate biopsy specimens is unknown. Seven hundred forty-four patients diagnosed between 1990 and 1996 with prostate cancer and managed conservatively were identified. The clinical end point was death from prostate cancer. The extent of cancer was measured in terms of number of cancer cores (NCC), percentage of cores with cancer (PCC), total length of cancer (LCC) and percentage length of cancer in the cores (PLC). These were correlated with prostate cancer mortality, in univariate and multivariate analysis including Gleason score and prostate-specific antigen (PSA). All extent of cancer variables were significant predictors of prostate cancer death on univariate analysis: NCC, hazard ration (HR)=1.15, 95% confidence interval (CI)=1.04–1.28, P=0.011; PPC, HR=1.01, 95% CI=1.01–1.02, P<0.0001; LCC, HR=1.02, 95% CI=1.01–1.03, P=0.002; PLC, HR=1.01, 95% CI=1.01–1.02, P=0.0001. In multivariate analysis including Gleason score and baseline PSA, PCC and PLC were both independently significant P=0.004 and P=0.012, respectively, and added further information to that provided by PSA and Gleason score, whereas NNC and LCC were no longer significant (P=0.5 and P=0.3 respectively). In a final model, including both extent of cancer variables, PCC was the stronger, adding more value than PLC (χ^2 (1df)=7.8, P=0.005, χ^2 (1df)=0.5, P=0.48 respectively). Measurements of disease burden in needle biopsy specimens are significant predictors of prostate-cancer-related death. The percentage of positive cores appeared the strongest predictor and was stronger than percentage length of cancer in the cores.

Keywords Prostate biopsy · Prostate cancer · Biopsy prognostic factors · Tumour extent

R. Rajab · T. Oliver · D. M. Berney
Centre for Molecular Oncology and Imaging,
Barts and The London School of Medicine and Dentistry,
Queen Mary University of London,
London, UK

G. Fisher · J. Cuzick
Cancer Research UK Department of Epidemiology, Mathematics and Statistics, Wolfson Institute of Preventive Medicine,
Queen Mary University of London,
London, UK

M. W. Kattan
Department of Biostatistics and Epidemiology,
Cleveland Clinic Foundation,
Cleveland, OH, USA

C. S. Foster
Department of Cellular Pathology and Molecular Genetics,
Liverpool University Hospital,
Liverpool, UK

H. Møller
King's College London, Thames Cancer Registry,
London, UK

V. Reuter · P. Scardino
Departments of Pathology and Urology,
Memorial Sloan Kettering Cancer Centre,
New York, USA

D. M. Berney (✉)
Centre for Molecular Oncology and Imaging St. Bartholomew's Medical School, Queen Mary, University of London,
Charterhouse Square,
London EC1M 6BQ, UK
e-mail: D.Berney@bartsandthelondon.nhs.uk

Introduction

The advent of prostate-specific antigen (PSA) screening has resulted in an increase in the detection of early stage tumours [1–3]. However, the benefits of radical therapy in patients with low- or intermediate-risk disease are not clear cut, and many of these patients may benefit from a more conservative approach [4]. Nomograms based on preclinical parameters have been devised to guide clinical management [5–8], but these do not routinely include measures of cancer extent.

Pathological data from biopsy specimens other than Gleason score have increasingly been used to improve the predictive accuracy of outcome models that guide clinical management, by identifying factors associated with an increased risk of disease progression in terms of PSA failure and metastatic disease post-radical prostatectomy [6, 9–14].

A cohort study by the Transatlantic Prostate Group developed a model using Gleason score and PSA to stratify patients with localised prostate cancer managed conservatively into three groups with 10-year cancer-specific mortalities of <10%, 10–30% and >30% [6]. After Gleason score and PSA, the extent of cancer in the biopsy specimen showed a strong association with prostate-cancer-related deaths on univariate and multivariate analysis. However, there are different methods of measuring cancer extent in prostate needle core biopsies. In this study, we determine which pathological assessment of the "extent of cancer" in diagnostic prostate biopsies best predicts long-term survival.

Methods

Study population, follow-up and end points

The protocol for patient selection and data collection methodology has been detailed in a previous report by the Transatlantic Prostate Group [6] and is summarised below. Patients diagnosed with biopsy-proven, localised prostate cancer between 1990 and 1996 were identified by participating UK cancer registries. Exclusion criteria included age >76 years, no baseline PSA, invasive carcinoma within 5 years prior to diagnosis, hormone treatment prior to biopsy and a follow-up period of less than 6 months. Patients were also excluded if they underwent radical prostatectomy or radiotherapy within 6 months of diagnosis or had evidence of metastasis, a baseline PSA >100 ng/ml or died within 6 months of diagnosis.

The clinical end point was defined as death from prostate cancer. Survival outcomes were ascertained from medical records and cancer registry data. Last follow-up was via the cancer registries, and the last review took place in December 2006.

Pathological assessment of biopsy specimens

Diagnostic needle core biopsy specimens were reviewed by an expert panel of urological pathologists to confirm the diagnosis and Gleason grading. Extent of cancer in biopsy specimens was determined by multiple methods (Table 1): data available included total number of cores (TNC) and number of cores with cancer (NCC) as well as the total length of all cores (TLC) and length of cancer in cores (LCC). Apart from the NCC and LCC, these data allowed calculation of the percentage of cancer-positive cores (PCC = NCC/TNC) and secondly the percentage length of cancer (PLC) in the cores (PLC = LCC/TLC). Measurements of cancer length and core lengths were all made by an expert uropathologist (DB) with microscope-mounted Vernier's scales and rulers, respectively. Measurements of linear cancer length within individual cores did not include intervening non-tumour tissue. Gleason grading conformed to modern ISUP criteria [15].

Statistics

The primary end point for this study was death from prostate cancer. Univariate and multivariate analyses were performed by proportional hazard models. All *P* values were two-sided and 95% confidence intervals were based on normal distribution.

Results

Patient selection identified a cohort of 2,333 eligible men. Centrally reviewed, Gleason grading results were available for 1,656 (71%) cases, 474 cases were excluded on histological grounds (missing histology 284, incorrect pathological specimen 43, histologically negative 135, no

Table 1 Measurements of cancer extent made including abbreviations and calculations

Different measurements of cancer extent on prostate core biopsies	Abbreviations and calculations
Total number of cores	TNC
Number of cores with cancer	NCC
Total length of cores	TLC
Length of cancer in all cores	LCC
Percentage of cancerous cores	PCC = NCC/TNC×100
Percentage length of cancer	PLC = LCC/TLC×100

tissue left in the block 6 and six cases were histologically ungradable for Gleason score) and for 203 cases the histology specimen was not requested for review. Cases diagnosed from prostate chips were not included in this study, and analysis was confined to the 744 cases diagnosed on the basis of needle core biopsies. The mean age at diagnosis was 69.2 years (range 44–76 years). Median follow-up was 106 months (range 6–197 months).

The total number of cores per patient ranged from one to nine, and the proportion positive is shown (Fig. 1). In univariate analysis, NCC was a significant predictor of prostate cancer death (hazard ratio (HR)=1.15, 95% confidence interval (CI)=1.04–1.28, χ^2 (1*df*)=6.4, *P*=0.011) but was less informative than the PCC (HR=1.01, 95% CI=1.01–1.02, χ^2 (1*df*)=27.1, *P*<0.0001). The KM survivor curve for PPC analysed in three groups (<50%, 50 to <100% or 100%) is shown in Fig. 2a.

In multivariate analysis, in the standard model including Gleason score (≤5, 6, 7, 8, 9 or 10) and PSA (ng/ml) (0–4, >4–10, >10–25, >25–50, >50–100), PCC was significant independently of Gleason score and PSA and provided additional prognostic value ($\Delta\chi^2$ (1*df*)=8.1, *P*=0.04). In contrast, NCC provided almost no additional prognostic value ($\Delta\chi^2$ (1*df*)=0.45, *P*=0.5), Table 2.

The extent of cancer measured as the absolute (LCC) and percentage length of cancer in the needle cores (PLC) was recorded for 737 cases. In univariate analysis, PLC was a significant predictor of prostate cancer death, when assessed as a continuous variable (HR=1.01, 95% CI=1.01–1.02 χ^2 (1*df*)=21.26, *P*=0.0001) or as a grouped variable. The most informative grouping was based on quintiles (χ^2 (1*df*)=27, *P*<0.0001) (Fig. 2b), but this was only slightly more informative than a simpler variable based on two groups (≤30%, >30%) (HR=2.21, 95% CI=1.6–3.1, χ^2 (1*df*)=25, *P*<0.0001) (Fig. 2c). Although LCC was also a significant predictor of prostate cancer death, it was less informative (HR=1.02, 95% CI=1.01–1.03, χ^2 (1*df*)=9.8, *P*=0.002).

In multivariate analysis, PLC was significant independently of Gleason score and PSA and provided some additional prognostic value to the standard model. The added value of the PLC variable based on two groups (≤30%, >30%) was very similar to that based on quintiles ($\Delta\chi^2$ (1*df*), 5.6, *P*=0.018, and $\Delta\chi^2$ (1*df*), 6.3, *P*=0.012 respectively), but LCC provided almost no additional prognostic value ($\Delta\chi^2$ (1*df*), 0.96, *P*=0.33) (Table 2).

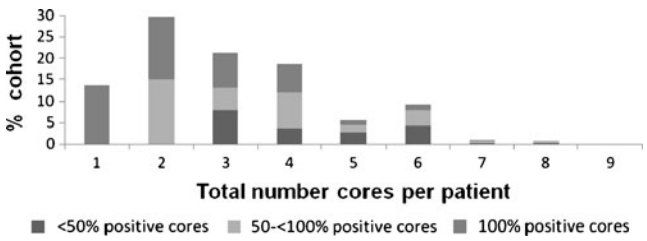

Fig. 1 Distribution of cancer-positive cores according to the total number of cores reviewed, in cases diagnosed by needle biopsy (*n*=727)

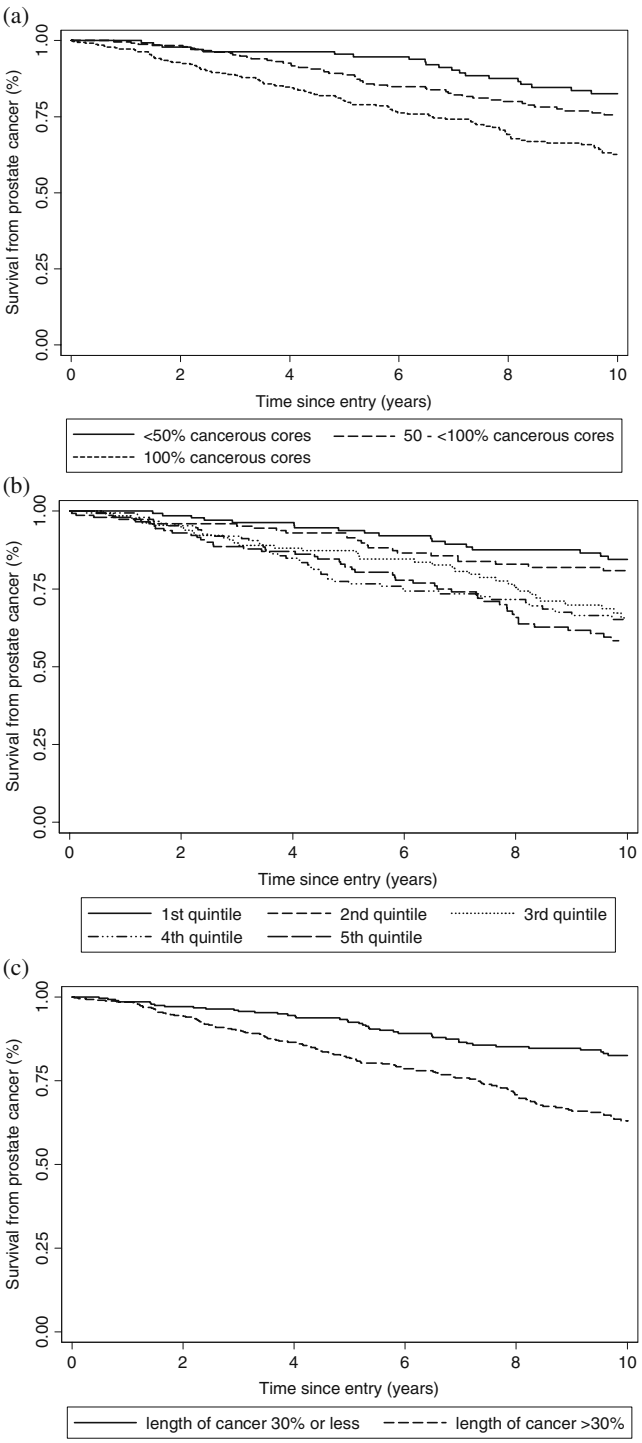

Fig. 2 Kaplan–Meir plot estimating prostate cancer cause-specific survival according to the extent of cancer in the biopsy: **a** percentage cancer-positive cores *n*=727; percentage length of cancer in the cores, **b** quintiles, **c** 30% cutoff point (*n*=737) for men diagnosed by needle biopsy

Table 2 The added value of pathological assessments of the extent of cancer (PCC, NCC, PLC, LCC) in a multivariate model including Gleason score (G) and baseline PSA level for predicting prostate cancer mortality in men with conservatively treated prostate cancer diagnosed by needle biopsy

Variable	Number	χ^2 (1*df*)[h]	$\Delta\chi^2$	*P* value
Positive cores (%)				
G[a]	727	59.8	–	
G + PSA[b]	727	71.3	11.6	<0.001
G + PSA + PCC[c]	727	79.5	8.1	0.004
G + PSA + NCC[d]	727	71.4	0.45	0.50
Length of cancer (%)				
G	737	63	–	
G + PSA	737	73.1	10.1	0.002
G + PSA + PLC quintiles[e]	737	78.7	5.6	0.018
G + PSA + PLC binary[f]	737	79.5	6.4	0.012
G + PSA + LCC[g]	737	74.1	0.96	0.3
Combined model				
G	723	59.7	–	
G + PSA	723	70.5	10.8	0.001
G + PSA + PCC	723	78.3	7.8	0.005
G + PSA + PLC binary	723	75.1	4.5	0.03
G + PSA + PLC quintiles	723	74.7	4.2	0.04
G + PSA + PCC + PLC binary	723	78.8	0.5	0.5

G Gleason score, *PSA* prostate-specific antigen, *PCC* percentage of cancer-positive cores, *NCC* number of cancer-positive cores, *PLC* percentage length of cancer, *PLC* percentage length of cancer, *LCC* length of cancer

[a] G score groups: ≤5, 6, 7, 8, ≥9

[b] PSA (ng/ml) groups: 0–4, >4–10, >10–25, >25–50, >50–100

[c] PCC (%) groups: < 50, 50 to <100, 100

[d] NCC (1, 2, 3, ≥4)

[e] PLC (%) quintiles: 1.8–14.1,14.2–29.5, 30–49.5, 50–76, 76.1–100

[f] PLC binary: ≤30, >30, cut off

[g] LCC (mm) continuous

[h] All chi-squared values (χ2) are for trend and are all on one degree of freedom (*df*)

An analysis of the 723 cases with both extent of cancer variables (PCC and PLC) available allowed a direct comparison of their predictive power. The predictive power of the variable PCC (<50%, 50% to <100% or 100%) was greater than that of PLC measured either as a two- or five-group variable ($\Delta\chi^2$ (1*df*)=7.8, *P*=0.005, $\Delta\chi^2$ (1*df*)=4.5, *P*=0.03, $\Delta\chi$2 (1*df*), 4.2, *P*=0.04), respectively (Table 2).

Detailed multivariate analysis for the final model including PCC, Gleason score (<7, =7, >7) and baseline PSA (ng/ml) (0–4, >4–10, >10–25, >25–50, >50–100) is shown in Table 3.

Discussion

The present dilemma arising out of the advent of PSA screening is how best to manage the increasing proportion of patients with intermediate- and low-risk prostate cancer, as defined by standard models using age, PSA and Gleason score. This is recognition that many of these patients have indolent disease in whom the benefits of radical prostatectomy do not outweigh the surgical morbidity. The parameters that define these two groups are becoming more stringent as clinicians adopt more conservative management protocols [16, 17]. However, even with standard models of prognostication, there is heterogeneity within the low–intermediate-risk (Gleason 6 and 7 and low PSA) patient groups and a recognition that a proportion of patients will develop progressive disease in whom radical treatment is then warranted [18].

This has driven the exploration of pathological factors in preoperative specimens to predict poor outcome. In the absence of validated molecular markers of prognostic valve, which are practical in large screening populations, many studies have focused on measurements of disease burden in needle core biopsies.

The number of positive cores in sextant biopsies have been shown to correlate with tumour stage [19–22] and

Table 3 Multivariate analysis of pathological assessments of the extent of cancer measured as PCC, in a model including G and baseline PSA level for predicting prostate cancer mortality in men with conservatively treated prostate cancer diagnosed by needle biopsy (n=727)

Variable	N (%)	Hazard ratio (95% CI)	χ^2 (1df)[a] contribution	P value
Gleason score				
<7	262 (36)	1 (ref)	38	<0.0001
7	271 (37)	1.78 (1.17–2.73)		
>7	194 (27)	3.47 (2.26–5.31)		
PSA (ng/ml)				
0–4	52 (7)	1 (ref)	11	0.001
4–10	138 (19)	0.68 (0.35–1.36)		
10–25	261 (36)	0.68 (0.37–1.26)		
25–50	160 (22)	1.5 (0.82–2.75)		
50–100	116 (16)	1.35 (0.72–2.51)		
PCC (%)				
<50	138 (19)	1 (ref)	7	0.008
50 to <100	255 (35)	1.38 (0.82–2.33)		
100	334 (46)	1.74 (1.06–2.85)		

χ^2 chi-squared, *df* degrees of freedom, *CI* confidence interval, *ref* reference category, *PSA* prostate-specific antigen, *PCC* percentage of cancer-positive cores, *PLC* percentage length of cancer in the cores

[a] All chi-square values (χ2) are for trend and are all on one degree of freedom (df)

surgical margin status in radical prostatectomy specimens [23, 24] and the presence pelvic lymph node metastasis [25]. Similarly, the percentage of positive cores has been shown to be predictive of stage [26], extra-capsular extension [27, 28], distant metastasis, biochemical progression and death following radical prostatectomy [29].

In addition, the percentage cancer involvement of biopsies is predictive of capsular perforation and seminal vesicle involvement [30]. The total length of cancer has also been shown to correlate with stage, positive surgical margins and biochemical recurrence following radical prostatectomy, respectively [24]. Brimo et al. showed that the greatest percentage of cancer, the total percentage of cancer and the greatest millimetric length of cancer in the needle cores were closely associated with clinical stage [31].

A systematic review by Harnden et al. determined the significance of measurements of disease burden in biopsy specimens for predicting risk of progression after radial prostatectomy [32]. The authors were unable to make firm conclusions on absolute measurements made of tumour burden. Tumour burden represented as a percentage was found to be more consistent, and most studies they reviewed showed that the percentage of cancer involvement was an independent predictor of PSA recurrence following radical prostatectomy.

In the current study, the percentage of positive cores (FC) was strongly predictive of prostate cancer death over the long follow-up period (median follow-up 117 months) despite the heterogeneity of the study population with regard to standard prognostic indicators (age, PSA and Gleason score at presentation) and treatment-related factors (initial hormone treatment). These findings are consistent with previous studies in which the percentage of positive cores was predictive of stage, surgical margin status [33] and biochemical recurrence [10, 34–37].

The utility of the percentage of positive cores is dependant on the number of cores taken to sample disease extent, which acts as a corrective factor for the size of the gland. Thus, the accuracy of this measure increases with the number of cores taken. In this sense, the measure is likely to overestimate disease extent when the core number is low.

Conversely, when the core number is high (approaching 21 biopsies) and the fraction of positive cores is low, the measurement will more accurately predict low disease burden which is especially important during selection of patients for active surveillance programmes [38]. As only 10% of the cohort was composed of sextant biopsies, there were too few cases to analyse adequately. There was no heterogeneity within this subset of cases. It is hoped that a more contemporary cohort conforming more to modern practice will be published in the future.

Similar principles apply with measurements of the total fractional length of cancer in biopsy specimens. In this study, the power of the total fractional length of cancer in needle biopsies was almost uninformative. This may be explained by the measurement underestimating the size of large tumours when the biopsy number is low and thus may not reflect its true clinical usefulness in predicting prognosis. In fact, several studies have shown that the total percentage length of cancer was predictive of pathological stage and PSA recurrence post-radical prostatectomy [11, 24, 39]. However, other studies also failed to demonstrate a correlation between the percentage of prostate cancer in the biopsy and clinical stage or biochemical recurrence following radical prostatectomy [40, 41].

Limiting factors in this study include its retrospective nature, low biopsy numbers compared to contemporary series and the heterogeneity of the study population when analysing the significance of disease burden in the biopsies. However, despite the aforementioned confounding factors, no contemporary series, let alone one with in which patients

are managed by watchful waiting, has enough follow-up to make long-term measurements of this nature. Furthermore, direct comparisons of predicted PSA failure after radical prostatectomy and prostate-cancer-related death in patients managed by watchful waiting or active surveillance need to be made with caution, as PSA failure does not necessarily imply clinical progression without correction for PSA doubling time [42–44].

Conclusions

This study is unique in correlating measurements of disease burden in diagnostic specimens with long-term survival in patients managed by watchful waiting. The percentage of positive cores was strongly predictive of prostate-cancer-related death on multivariate analysis and added additional information to models utilising PSA and Gleason score to refine management decision in patients with low-risk disease who would qualify for conservative management.

Acknowledgements This study was supported by Cancer Research UK, a Specialised Programme of Research Excellence (SPORE) grant from the US National Cancer Institute (USA), Orchid and The David Koch Foundation. Funding bodies had no involvement in the design and conduct of the study; in collection management, analysis and interpretation of the data; or in preparation, review and approval of the paper.

Conflict of interest statement We declare that we have no conflict of interest.

References

1. Pelzer AE, Colleselli D, Bektic J et al (2008) Clinical and pathological features of screen vs non-screen-detected prostate cancers: is there a difference? BJU Int 102:24–27
2. Smith DS, Humphrey PA, Catalona WJ (1997) The early detection of prostate carcinoma with prostate specific antigen: the Washington University experience. Cancer 80:1852–1856
3. Bartsch G, Horninger W, Klocker H et al (2008) Tyrol prostate cancer demonstration project: early detection, treatment, outcome, incidence and mortality. BJU Int 101:809–816
4. Loeb S, Roehl KA, Helfand BT et al (2008) Complications of open radical retropubic prostatectomy in potential candidates for active monitoring. Urology 72:887–891
5. Makarov DV, Trock BJ, Humphreys EB et al (2007) Updated nomogram to predict pathologic stage of prostate cancer given prostate-specific antigen level, clinical stage, and biopsy Gleason score (Partin tables) based on cases from 2000 to 2005. Urology 69:1095–1101
6. Cuzick J, Fisher G, Kattan MW et al (2006) Long-term outcome among men with conservatively treated localised prostate cancer. Br J Cancer 95:1186–1194
7. D'Amico AV, Whittington R, Malkowicz SB et al (1999) Pretreatment nomogram for prostate-specific antigen recurrence after radical prostatectomy or external-beam radiation therapy for clinically localized prostate cancer. J Clin Oncol 17:168–172
8. Epstein JI, Walsh PC, Carmichael M et al (1994) Pathologic and clinical findings to predict tumor extent of nonpalpable (stage T1c) prostate cancer. JAMA 271:368–374
9. Nelson CP, Dunn RL, Wei JT et al (2003) Contemporary preoperative parameters predict cancer-free survival after radical prostatectomy: a tool to facilitate treatment decisions. Urol Oncol 21:213–218
10. Freedland SJ, Aronson WJ, Terris MK et al (2003) Percent of prostate needle biopsy cores with cancer is significant independent predictor of prostate specific antigen recurrence following radical prostatectomy: results from SEARCH database. J Urol 169:2136–2141
11. Freedland SJ, Aronson WJ, Csathy GS et al (2003) Comparison of percentage of total prostate needle biopsy tissue with cancer to percentage of cores with cancer for predicting PSA recurrence after radical prostatectomy: results from the SEARCH database. Urology 61:742–747
12. Goto Y, Ohori M, Arakawa A et al (1996) Distinguishing clinically important from unimportant prostate cancers before treatment: value of systematic biopsies. J Urol 156:1059–1063
13. Graefen M, Noldus J, Pichlmeier U et al (1999) Early prostate-specific antigen relapse after radical retropubic prostatectomy: prediction on the basis of preoperative and postoperative tumor characteristics. Eur Urol 36:21–30
14. Gretzer MB, Epstein JI, Pound CR et al (2002) Substratification of stage T1C prostate cancer based on the probability of biochemical recurrence. Urology 60:1034–1039
15. Epstein JI, Allsbrook WC Jr, Amin MB et al (2005) The 2005 International Society of Urological Pathology (ISUP) consensus conference on Gleason grading of prostatic carcinoma. Am J Surg Pathol 29:1228–1242
16. Suardi N, Capitanio U, Chun FK et al (2008) Currently used criteria for active surveillance in men with low-risk prostate cancer: an analysis of pathologic features. Cancer 113:2068–2072
17. Conti SL, Dall'era M, Fradet V et al (2009) Pathological outcomes of candidates for active surveillance of prostate cancer. J Urol 181:1628–1633, discussion 1633–1624
18. Isbarn H, Karakiewicz PI, Ahyai SA et al (2009) Differences in histopathological and biochemical outcomes in patients with low Gleason score prostate cancer. BJU International 105:818–823
19. Peller PA, Young DC, Marmaduke DP et al (1995) Sextant prostate biopsies. A histopathologic correlation with radical prostatectomy specimens. Cancer 75:530–538
20. Wills ML, Sauvageot J, Partin AW et al (1998) Ability of sextant biopsies to predict radical prostatectomy stage. Urology 51:759–764
21. Huland H, Hammerer P, Henke RP et al (1996) Preoperative prediction of tumor heterogeneity and recurrence after radical prostatectomy for localized prostatic carcinoma with digital rectal, examination prostate specific antigen and the results of 6 systematic biopsies. J Urol 155:1344–1347
22. Badalament RA, Miller MC, Peller PA et al (1996) An algorithm for predicting nonorgan confined prostate cancer using the results obtained from sextant core biopsies with prostate specific antigen level. J Urol 156:1375–1380
23. Tigrani VS, Bhargava V, Shinohara K et al (1999) Number of positive systematic sextant biopsies predicts surgical margin status at radical prostatectomy. Urology 54:689–693
24. Ravery V, Chastang C, Toublanc M et al (2000) Percentage of cancer on biopsy cores accurately predicts extracapsular extension and biochemical relapse after radical prostatectomy for T1–T2 prostate cancer. Eur Urol 37:449–455
25. Conrad S, Graefen M, Pichlmeier U et al (1998) Systematic sextant biopsies improve preoperative prediction of pelvic lymph node metastases in patients with clinically localized prostatic carcinoma. J Urol 159:2023–2029

26. Yoon JH, Chen MH, Renshaw AA et al (2002) Predictive factor analysis as the basis for the clinical utility of percent positive prostate biopsies in patients with intermediate-risk prostate cancer. Urology 60:454–457
27. Ravery V, Boccon-Gibod LA, Dauge-Geffroy MC et al (1994) Systematic biopsies accurately predict extracapsular extension of prostate cancer and persistent/recurrent detectable PSA after radical prostatectomy. Urology 44:371–376
28. Mortensen MM, Mortensen PS, Borre M (2009) Percentage of tumour-positive biopsy cores: an independent predictor of extraprostatic disease. Scand J Urol Nephrol 43:109–113
29. Lotan Y, Shariat SF, Khoddami SM et al (2004) The percent of biopsy cores positive for cancer is a predictor of advanced pathological stage and poor clinical outcomes in patients treated with radical prostatectomy. J Urol 171:2209–2214
30. Bostwick DG, Qian J, Bergstralh E et al (1996) Prediction of capsular perforation and seminal vesicle invasion in prostate cancer. J Urol 155:1361–1367
31. Brimo F, Vollmer RT, Corcos J et al (2008) Prognostic value of various morphometric measurements of tumour extent in prostate needle core tissue. Histopathology 53:177–183
32. Harnden P, Shelley MD, Naylor B et al (2008) Does the extent of carcinoma in prostatic biopsies predict prostate-specific antigen recurrence? A systematic review. Eur Urol 54:728–739
33. Bismar TA, Lewis JS Jr, Vollmer RT et al (2003) Multiple measures of carcinoma extent versus perineural invasion in prostate needle biopsy tissue in prediction of pathologic stage in a screening population. Am J Surg Pathol 27:432–440
34. Briganti A, Chun FK, Hutterer GC et al (2007) Systematic assessment of the ability of the number and percentage of positive biopsy cores to predict pathologic stage and biochemical recurrence after radical prostatectomy. Eur Urol 52:733–743
35. D'Amico AV, Whittington R, Malkowicz SB et al (2000) Clinical utility of the percentage of positive prostate biopsies in defining biochemical outcome after radical prostatectomy for patients with clinically localized prostate cancer. J Clin Oncol 18:1164–1172
36. D'Amico AV, Whittington R, Malkowicz SB et al (2000) Combination of the preoperative PSA level, biopsy Gleason score, percentage of positive biopsies, and MRI T-stage to predict early PSA failure in men with clinically localized prostate cancer. Urology 55:572–577
37. Presti JC Jr, Shinohara K, Bacchetti P et al (1998) Positive fraction of systematic biopsies predicts risk of relapse after radical prostatectomy. Urology 52:1079–1084
38. Ploussard G, Xylinas E, Salomon L et al (2009) The role of biopsy core number in selecting prostate cancer patients for active surveillance. Eur Urol 56:891–1104
39. Freedland SJ, Terris MK, Csathy GS et al (2004) Preoperative model for predicting prostate specific antigen recurrence after radical prostatectomy using percent of biopsy tissue with cancer, biopsy Gleason grade and serum prostate specific antigen. J Urol 171:2215–2220
40. Ravery V, Schmid HP, Toublanc M et al (1996) Is the percentage of cancer in biopsy cores predictive of extracapsular disease in T1–T2 prostate carcinoma? Cancer 78:1079–1084
41. Linson PW, Lee AK, Doytchinova T et al (2002) Percentage of core lengths involved with prostate cancer: does it add to the percentage of positive prostate biopsies in predicting postoperative prostate-specific antigen outcome for men with intermediate-risk prostate cancer? Urology 59:704–708
42. Okotie OT, Aronson WJ, Wieder JA et al (2004) Predictors of metastatic disease in men with biochemical failure following radical prostatectomy. J Urol 171:2260–2264
43. Miyake H, Hara I, Kurahashi T et al (2006) Clinicopathological features of patients with biochemical recurrence after radical prostatectomy without progressive rise in serum prostate-specific antigen. Urol Int 77:200–204
44. Taplin ME (2003) Biochemical (prostate-specific antigen) relapse: an oncologist's perspective. Rev Urol 5(Suppl 3):S3–S13

Virchows Arch (2010) 457:555–561
DOI 10.1007/s00428-010-0969-6

ORIGINAL ARTICLE

Cyclin D3 gene amplification in bladder carcinoma in situ

Antonio Lopez-Beltran · Jose L. Ordóñez · Ana P. Otero · Ana Blanca · Vicky Sevillano · Marta Sanchez-Carbayo · Elisa Muñoz · Liang Cheng · Rodolfo Montironi · Enrique de Alava

Received: 21 July 2010 / Revised: 20 August 2010 / Accepted: 21 August 2010 / Published online: 7 September 2010
© Springer-Verlag 2010

Abstract Carcinoma in situ (CIS) is a non-papillary high-grade, potentially aggressive, and unpredictable manifestation of bladder urothelial carcinoma. The aim of this study was to assess patterns of *Cyclin D3* gene amplification in Bacillus Calmette-Guerin (BCG)-treated CIS and correlate gene status with recurrence-free and progression-free survival. A sequential cohort series of 28 primary (isolated) or secondary (concomitant) bladder CIS samples in which there was enough tissue material to assess *Cyclin D3* gene status by fluorescent in situ hybridization was the study group. *Cyclin D3 gene* amplification was present in 29% of secondary CIS; none of primary CIS samples had *Cyclin D3* gene amplification. *Cyclin D3* amplification was related to recurrence- (p=0.046) and progression-free survival (p=0.002). Type of bladder CIS (primary vs. secondary) was unrelated to recurrence- or progression-free survival in the current series. Cox's regression analysis selected Cyclin D3 as an independent predictor of progression-free survival (p=0.041, relative risk=61.503, 95% confidence interval= 1.1–274.710). None of primary CIS cases recurred on follow-up; nine secondary CIS recurred and four of them progressed to invasive bladder carcinoma HG T1 (n=1), T2b N0M0 (n=1), T3b N1M0 (n=1) and T4aN1M1 (n=1). Mean recurrence±SD (months) occurred at 19.5±2.06 (95% (confidence interval (CI)), 15.5–23.6); mean progression (months) occurred at 23.8±1.46 (95% (CI), 20.9–26.7). Our study suggests that *Cyclin D3* gene amplification might be a predictor of aggressiveness in BCG-treated CIS.

Keywords Bladder · Cyclin D3 · Carcinoma in situ · Gene amplification

A. Lopez-Beltran
Department of Pathology, Cordoba University Medical School, Cordoba, Spain

J. L. Ordóñez · A. P. Otero · V. Sevillano · E. de Alava
Laboratory of Molecular Pathology, Centro de Investigación del Cáncer-IBMCC, University of Salamanca-CSIC, Salamanca, Spain

E. de Alava
e-mail: edealava@usal.es

A. Blanca
Biomedical Research Unit, University Hospital, Cordoba, Spain

M. Sanchez-Carbayo
National Cancer Institute CNIO, Madrid, Spain

E. Muñoz
Biostatistics Unit, University Hospital, Cordoba, Spain

L. Cheng
Department of Pathology and Laboratory Medicine, Indiana University School of Medicine, Indianapolis, USA

R. Montironi
Institute of Pathological Anatomy and Histopathology, Polytechnic University of the Marche Region, Ancona, Italy

A. Lopez-Beltran (✉)
Faculty of Medicine, Unit of Anatomical Pathology, 14004 Cordoba, Spain
e-mail: em1lobea@uco.es

Introduction

Carcinoma in situ (CIS) of the urinary bladder is a distinct entity, which is defined as a flat (e.g., non-papillary) high-grade non-invasive urothelial carcinoma [1, 2]. The untreated natural history indicates more than 50% 5-year progression rate and a higher recurrence rate [3–14]. In case of concomitant high-grade pT1 papillary tumors, the chance of progression seems even worse [3–14]. The clinical problem in CIS is not only the difficult diagnosis but also the therapy. In Bacillus Calmette-Guerin (BCG)-non-responding patients the risk of tumor progression is substantial [3–5, 7, 10–14]. Clinical factors are of little help as predictors of tumor progression in CIS patients. Markers such as COX-2 or anomalies of the *TP53* suppressor gene have been investigated, but their value in recurrence and progression of CIS patients remains uncertain. Other molecular markers (in particular gene profiles) currently still do not seem powerful enough to predict progression or response to therapy in CIS patients. Recent reports, however clearly indicate that a combined p53/p21 expression, *TP53* mutation and loss of chromosome 9 and 9p21 or loss of E-cadherin have potential to be associated with progression and cancer-specific survival in CIS patients [15–23]. The value of other markers for progression in CIS patients, like oncogenes, cell-cycle regulator genes, proliferation, neovascularization markers and growth factors remains to be determined [15–19]

Cyclin D3 plays a pivotal role in controlling physiological progression from the G1 to the S phase of the cell cycle. *Cyclin D3* gene may be deregulated in a number of human malignant tumors [24–28]. Recent reports suggest that *Cyclin D3* gene is deregulated in bladder urothelial carcinoma with no reports concerning CIS [24, 25, 27]. The status of *Cyclin D3* gene in bladder CIS remains unknown.

The aim of this study was to assess patterns of *Cyclin D3* gene amplification in BCG-treated bladder CIS and correlate *Cyclin D3* status with patient's outcome.

Material and methods

Patients and clinical follow-up

The present study was approved by the committee on ethical standards of the University of Cordoba, Spain. A sequential cohort series of 28 patients with newly diagnosed bladder CIS (primary (pure) CIS, $n=3$; secondary (concomitant) CIS, $n=25$) was the study group. Additionally, in three cases there was normal urothelium adjacent to CIS, and in five cases of secondary CIS frozen samples were available at the tissue bank; these specimens were used for additional *Cyclin D3* gene and protein validation studies.

The patients underwent random bladder biopsies (primary CIS) or complete transurethral resection (TURB) and random bladder biopsies (secondary cases) and were seen at the University Hospital of Cordoba in 2005. Male patients received additional biopsies from the prostatic urethra. A re-TURB was performed when appropriate. The patients received BCG therapy (Tice strain, $2–5\times10^8$ colony-forming units weekly for six consecutive weeks) followed by maintenance according to the EAU guidelines for at least 1 year [5]. Cystectomy was offered to patients with BCG failure. Patient's follow-up, calculated as the number of months from the date of the diagnostic procedure to the date of the most recent cystoscopy (or to the date of the last visit or death), was (mean±SD) 38.82±3.59 months. Tumor recurrence was defined as reappearance of tumor after the initial treatment. Tumor stage progression was defined as shift to any higher stage (T1, T2–T4) in recurrent tumors or the appearance of metastases. Preoperative excretory urography was performed to exclude cases with evidence of upper urinary tract disease.

All available hematoxylin and eosin stained slides including primary tumors as well as their recurrences were re-evaluated by two dedicated pathologists without knowledge of the clinical status, and were diagnosed and graded in accordance with the most recent World Health Organization grading system. Clinical and pathologic staging was determined in accordance with the TNM, 2002 revision.

Tissue microarray

Twenty-eight bladder CIS specimens were collected in a tissue microarray (TMA) using a custom-built precision instrument (Tissue Arrayer-Beecher Instruments, Silver Spring, MD). Representative tumor areas were identified and encircled on H&E-stained slides from each block. Two 0.6-mm tissue cylinders corresponding to the selected areas were removed from each paraffin donor block and placed side by side in an empty recipient paraffin block measuring 27×20 mm. Hematoxylin and eosin stained slides of the TMA allowed to verify the adequacy of the samples.

Fluorescent in situ hybridization

A specific *Cyclin D3* locus probe (PAC clone RP5-973 N23) labeled with Spectum red-dUTP (red signal) (Vysis, Downers Grove, IL) was made. Briefly, isolated PAC DNA was labeled with Spectrum red-dUTP (Vysis) by nick translation (Vysis) and purified after adding 10 μg of COT-1 (Invitrogen, Carlsbad, CA, USA). A commercially available (CEP 6) probe (Vysis) labeled with spectrum green (green signal) was also used. To check the specificity of the home made probe, co-hybridizations using both

commercial CEP6 and *Cyclin D3* specific probes were performed over metaphases of peripheral blood cells.

Fluorescent in situ hybridization (FISH) analysis was done on 2-μm-thick sections obtained from the tissue microarray. Negative controls were samples of unrelated tumors and adjacent normal mucosa or normal tissues of unrelated organs from 20 additional patients. A volume of 10 μl of the diluted probes was applied to the slides. The slide was covered with a glass coverslip and sealed with rubber cement. Using a Hybrite machine (Vysis), denaturation was 75°C for 5 min and hybridization was at 37°C for at least 16 h. After removing the coverslips posthybridization washing was done at 46°C in 2XSSC, 50% formamide for 5 min and stained with DAPI ((6-diamidino-2-phenylindole) and mounted with Vectashield H-1000 medium (Vector). Digital images were obtained using a Zeiss Axioplan2 epifluorescence microscope (Carl Zeiss Oberkochen, Germany) equipped with a digital camera (ORCA-ER-1394, Hamamatsu Photonics KK, Hamamatsu, Japan). In all cases, 100 nuclei were counted for each punch. The number of red signals (*Cyclin D3*) and green signals (CEP6 centromeric) were counted for each nucleus and the average was recorded. We established a ratio red signal/green signal of 2 or greater as an evidence of *Cyclin D3* gene amplification.

Western blot analysis

Protein was extracted from five bladder CIS samples using Qproteome Cell Compartiment kit (Qiagen, GmbH, Hilden) following the manufacturer's instructions. The protein concentration was determined using the Bradford assay (Bio-Rad Laboratories). Then, 25 μg nuclear protein was separated in 4–12% Bis-Tris gels (Bio-Rad Laboratories, Inc. Hercules CA) and transferred (Transfers systems: Bio-Rad, Hercules, CA, USA) to nitrocellulose membranes (Bio-Rad Laboratories). Equal loading of samples was checked by staining membranes with Ponceau-S. Membranes were blocked in 5% non-fat dried milk in TTBS-L (Tris–HCl 20 mM pH 7.6, 0.2% Tween 20, 150 mM NaCl) and incubated for 2 h at room temperature with anti-cyclin D3 antibody (cyclin D3–D7; sc-6283; Santa Cruz Biotechnology Inc, Santa Cruz, CA, USA) at 1:1,000 dilution. The signal was detected using enhanced chemiluminescence (ECLTM Plus Western Blotting Detection Reagents and Hyperfilm ECLTM, Amersham Bioscien-

Table 1 Patient's characteristics

Variable	Number (%)
Gender	
Female	4 (14)
Male	24 (86)
Age in years	
Mean±SD	72±7.84
Median	70.5
Range	57–86
CIS	
Primary (pure)	3 (11)
Secondary (concomitant)	25 (89)
Associated tumor in secondary CIS	
TaG3	6 (24)
T1G3	15 (60)
T2(at least)G3	4 (16)
BCG treatment	28 (100)
CIS recurrence	
Primary	0 (100)
Secondary	9 (36)
Time[a] to CIS recurrence (mean±SD (95% CI))	19.5±2.06 (15.5–23.0)
CIS progression	
Primary	0 (100)
Secondary	4 (16)
Time[a] to CIS progression (mean±SD (95% CI))	23.8±1.46 (20.9–26.7)
Cyclin D3 gene status in CIS	
No amplification	20 (71)
Amplification	8 (29)

CIS urothelial carcinoma in situ, *SD* standard deviation, *CI* confidence interval

[a] In months

ces Corp., Piscataway, NJ, USA). Full-range rainbow (Amersham Life Science, UK) was run on each gel as a standard molecular weight marker.

Statistical analysis

The endpoint of the study were recurrence- and progression-free survival. Univariate survival analysis was conducted using the Kaplan–Meier method, and differences among groups were tested for significance using the Log-rank test. Significant parameters in the univariate analysis entered a multivariate analysis of independent prognostic factors using Cox's proportional hazard regression analysis, and the relative risk with 95% confidence interval was calculated. All the statistical analyses were performed using the SPSS for Windows Software (SPSS Inc, Chicago, IL). A p value of less than or equal to 0.05 was considered indicative of a statistically significant difference.

Results

Table 1 shows patients' characteristics. A total of 28 patients (24 men) with bladder CIS were the study cohort. Their mean age was 72 years (±SD, 7.84 years). Primary CIS was diagnosed in three patients (11%) and secondary CIS in 25 patients (89%). Associated tumor in secondary CIS were TaG3 in six patients, T1G3 in 15 patients, and T2 (at least) G3 in four patients that were part of a bladder preservation program. These patients received TURB and re-TURB followed in all cases by BCG with maintenance (Table 1).

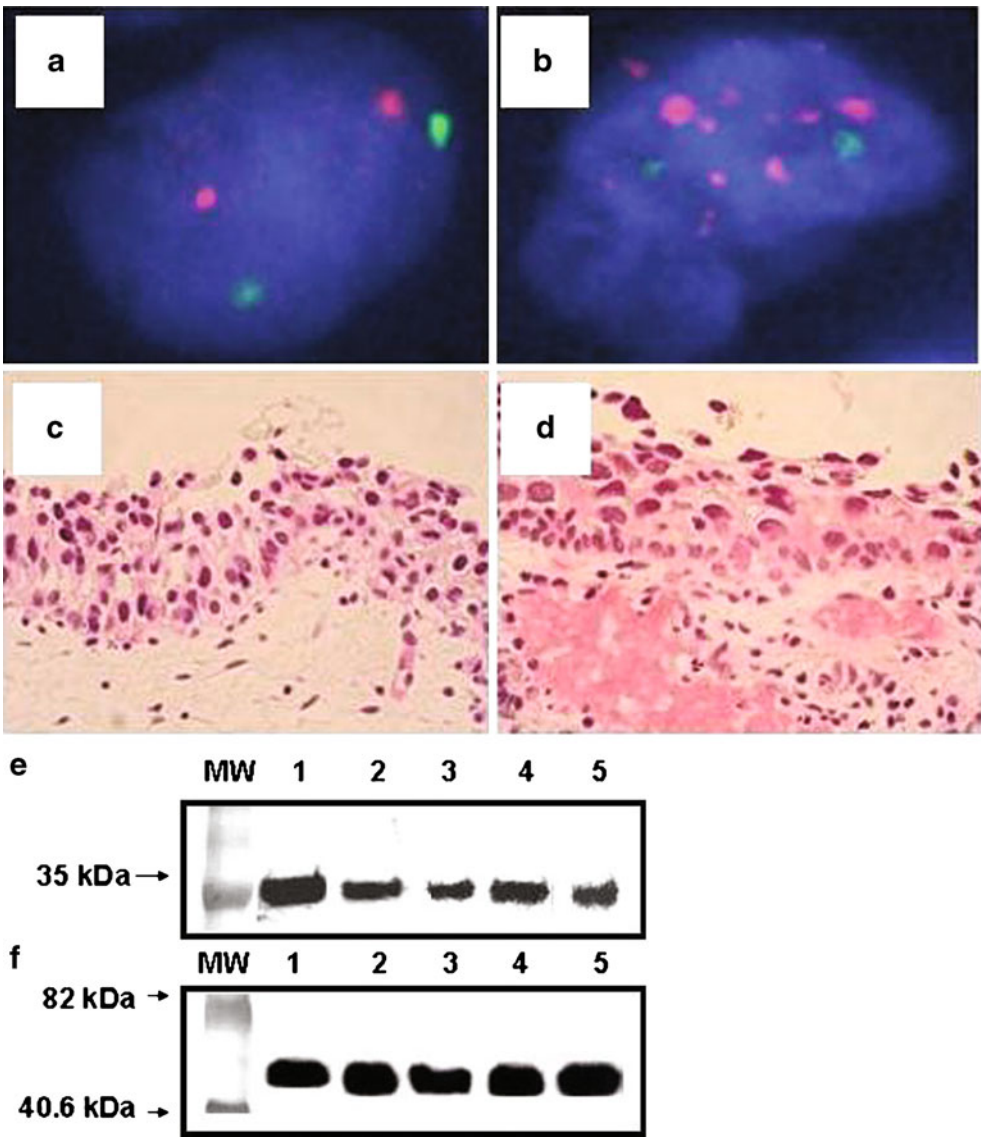

Fig. 1 Cyclin D3 gene normal expression (not amplified) showing two red signals and two centromeric green signals on chromosome 9 (normal expression) in CIS (case 3) (**a**) as compared with Cyclin D3 gene amplification (polysomy) characterized by multiple red signals in contrast to two centromeric green signals on chromosome 9 (normal expression) in CIS (case 11) (**b**). Examples of CIS with non-amplified (**c**) or amplified (**d**) Cyclin D3 gene. Protein bands by western blot analysis characteristics of Cyclin D3 (**e**) and the loading control ß-Actin (**f**). *MW* molecular weight, *KDa* kilodalton

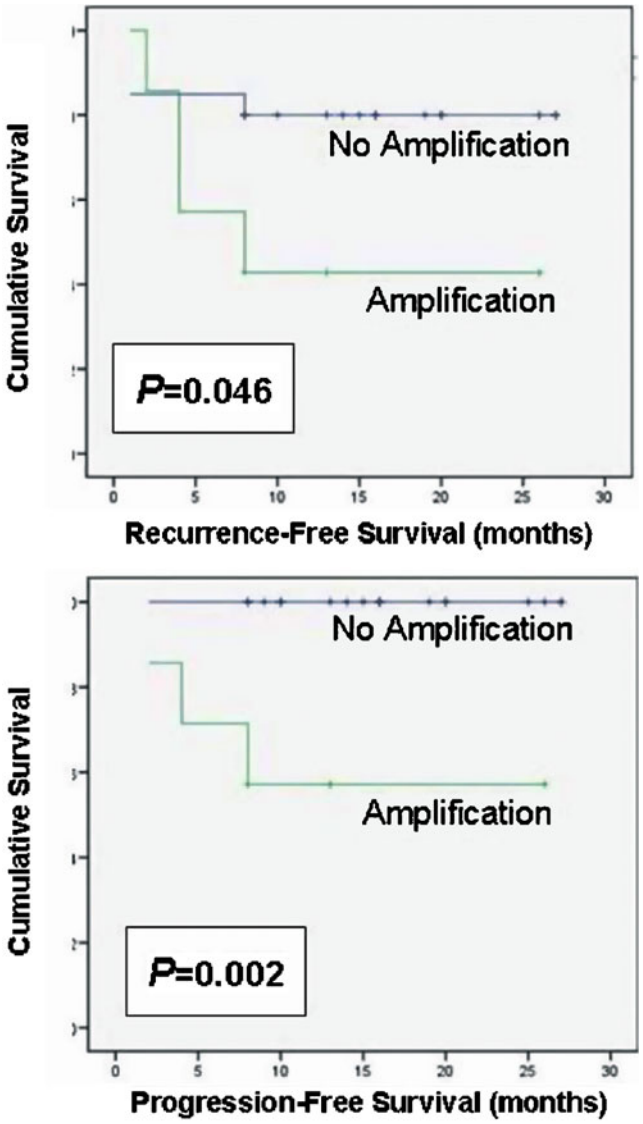

Fig. 2 Kaplan–Meier plots illustrating the association between Cyclin D3 gene status and recurrence- (*up*) or progression-free survival (*bottom*)

Cyclin D3 gene amplification seen by FISH as multiple scattered or grouped red signals was present in 29% of secondary CIS; none of primary CIS or control samples had *Cyclin D3* gene amplification (Fig. 1). *Cyclin D3* gene amplification was related to recurrence- (p=0.046) and progression-free survival (p=0.002) (Fig. 2); type of bladder CIS (primary vs. secondary) was unrelated to recurrence- or progression-free survival (Table 2). Cox's regression analysis selected Cyclin D3 as an independent predictor of progression-free survival (p=0.041, relative risk=61.503, 95% confidence interval=1.1–274.710) (Table 3). None of primary CIS cases recurred on follow-up period; nine secondary CIS recurred and four of them progressed to invasive bladder carcinoma HG T1 (n=1), T2b N0M0 (n=1), T3b N1M0 (n=1) and T4aN1M1 (n=1). Mean recurrence±SD (months) occurred at 19.5±2.06 (95% (confidence interval (CI)), 15.5–23.6); mean progression (months) occurred at 23.8±1.46 (95% (CI), 20.9–26.7). Normal urothelium control specimens had no *Cyclin D3* amplified signals. Western blot Cyclin D3 protein expression analysis showed bands in five CIS cases that had *Cyclin D3* gene amplified indicating that Cyclin D3 gene amplification may lead to *Cyclin* D3 protein expression in these cases (Fig. 1).

Discussion

Carcinoma in situ of the urinary bladder is a distinct entity which frequently shows an unpredictable course. The untreated natural history indicates a more than 50% 5-year progression rate and an even higher recurrence rate [3–14]. Current BCG protocols have improved substantially the prognosis of these patients, but in non-responding patients the risk of tumor progression is high [3–14].

Clinical factors are of little help as predictors of aggressiveness. Some recent reports, however, clearly indicate the value of p53, and Shariat et al. [15] showed that a combined p53/p21Waf1 expression was associated

Table 2 Recurrence- and progression-free survival in CIS patients according to CIS type (primary vs. secondary) and Cyclin D3 gene status (not amplified vs. amplified)

	Overall (N=28)	Recurrence-free (%)	Log-rank	P value	Progression-free (%)	Log-rank	P value
CIS			1.29	0.255		0.487	0.485
Primary	3	3 (100)			3 (100)		
Secondary	25	16 (64)			21 (84)		
Cyclin D3 gene status in CIS			3.93	0.046		10.07	0.002
Not amplification	20	16 (80)			20 (100)		
Amplification	8	3 (37.5)			4 (50)		

CIS urothelial carcinoma in situ

Table 3 Cox's multivariate analysis showing independent variables related to recurrence- and progression-free survival in patients with urothelial carcinoma in situ

Variable	RR	95% CI	*P* value
Recurrence-free survival			
Cyclin D3 gene amplification	3.159	0.785–12.704	0.105
Type of CIS (primary vs. secondary)	24.535	0.4–154.062	0.057
Progression-free survival			
Cyclin D3 gene amplification	61.503	1.1–274.710	0.041
Type of CIS (primary vs. secondary)	23.945	0.9–240.458	0.065

with progression and cancer-specific survival in CIS patients. Hopman et al. [16] also found an association between *TP53* mutation, loss of chromosome 9 and 9p21, and invasive bladder cancer in CIS patients. Loss of E-cadherin expression was reported as another risk factor for progression and disease-specific survival in patients with CIS [17]. Likewise, for COX-2 immunohistochemistry, for example, a correlation with expression and progression in CIS patients could not be confirmed. Other molecular markers do not seem powerful enough to predict response to therapy or progression in CIS patients in daily practice [20, 21]. Therefore, studies on newer molecular markers to define patterns of aggressiveness in CIS are needed.

Cyclin D family, mainly Cyclin D1 and Cyclin D3, form complexes with cyclin dependent kinases 4 and 6 which promote phosphorylation and inactivation of the retinoblastoma protein, thus releasing the promoter factor E2F-1. This, in turn activates genes involved in DNA synthesis, thereby mediating the progression of cells from G1-to-S phase of cell cycle.

In the present study, *Cyclin D3* gene status has been found to be related to recurrence- and progression-free (independent predictor) survival in BCG-treated CIS patients. This is an original finding not previously reported. We found up-regulation of *Cyclin D3* gene to be present in about one third of secondary CIS cases. This result agrees with our previous work showing Cyclin D3 protein up-regulation in high-grade bladder carcinoma [24, 25, 27]. In addition, we have observed that none of primary CIS cases entering the current study had *Cyclin D3* gene amplification, raising the question if the known differences in aggressiveness between primary and secondary CIS cases could be explained by differences in genetic alterations between these two forms of bladder CIS; this could be related to a higher cell-cycle regulatory genes alteration in secondary CIS. Likewise, the small number of primary CIS cases included represents a limitation of our study. This fact needs to be demonstrated in further studies, but could be supported by the absence of *Cyclin D3* gene up-regulation in primary CIS cases in the current study.

Moreover, a recent study based on quantitative gene expression profiles showed that *Cyclin D3* gene was a significant predictor or recurrence (97% sensitivity) in high-grade stage Ta bladder cancer, [27] thus supporting our findings on *Cyclin D3* gene amplification in bladder CIS; CIS is considered a high-grade tumor both at clinical and molecular level. Our finding of a strong association of *Cyclin D3* gene amplification with recurrence-free and mainly with progression-free survival could indicate that there is an important deregulation of *Cyclin D3* gene and protein over-expression in high-grade bladder cancer [24, 25, 27]. Moreover, it seems that Cyclin D3 alteration is a potentially relevant finding since the use of cell-cycle regulatory proteins as therapeutic targets of their modulators, represents an active field of research [24]. Available modulators of Cyclin D3 expression such Interferon-α and flavopiridol, that can induce cell-cycle arrest by directly inhibiting cyclin dependent kinases and by down-regulation of Cyclin D3, might represent a future alternative to other conventional therapeutic approaches in a subset of bladder CIS patients at higher risk of aggressive behavior.

In addition, over-expression of Cyclin D3, as specific G1-S aberration, was associated in former studies with increased proliferation and down-regulation of p27Kip1 and p21Waf1 in high-grade bladder carcinoma, thus suggesting that different aberrations of G1-S phase are linked in high-grade bladder carcinoma including CIS [25]. In fact, increased proliferation and down-regulation of p27Kip1 and p21Waf1 are common in bladder CIS [18, 23, 25].

In conclusion, the apparent role of *Cyclin D3* gene up-regulation in selecting tumors at higher risk of developing invasive disease warrants further prospective studies on the expression of these cell-cycle regulatory genes and proteins in bladder CIS.

Acknowledgment Supported by the grants SAF2007-64942 (Ministry of Education and Research, Madrid, Spain), P07-CVI-02974 and PI0003/2007 (Junta de Andalucia, Seville, Spain). Work at CIC is also funded by Instituto de Salud Carlos III (PI081828, RD06/020/0059). JLO is supported by ISCIII (Contratos Postdoctorales Sara Borrell CD6/00001).

Conflict of Interest Statement No potential conflicts of interest

References

1. Lopez-Beltran A (2008) Bladder cancer: clinical and pathological profile. Scand J Urol Nephrol Suppl 218:95–109
2. Nese N, Gupta R, Bui MH, Amin MB (2009) Carcinoma in situ of the urinary bladder: review of clinicopathologic characteristics with an emphasis on aspects related to molecular diagnostic techniques and prognosis. J Natl Compr Canc Netw 7:48–57
3. Andius P, Damm O, Holmäng S (2004) Prognostic factors in patients with carcinoma in situ treated with intravesical Bacille Calmette-Guérin. Scand J Urol Nephrol 38:285–290
4. Witjes JA (2004) Bladder carcinoma in situ in 2003: state of the art. Eur Urol 45:142–146
5. van der Meijden AP, Sylvester R, Oosterlinck W (2005) EAU guidelines on the diagnosis and treatment of urothelial carcinoma in situ. Eur Urol 48:363–371
6. Sylvester RJ, van der Meijden A, Witjes JA (2005) High-grade Ta urothelial carcinoma and carcinoma in situ of the bladder. Urology 66(Suppl 1):90–107
7. Shariat SF, Palapattu GS, Karakiewicz PI (2007) Concomitant carcinoma in situ is a feature of aggressive disease in patients with organ-confined TCC at radical cystectomy. Eur Urol 51:152–160
8. Montironi R, Lopez-Beltran A, Scarpelli M, Mazzucchelli R, Cheng L (2009) 2004 World Health Organization Classification of the Noninvasive Urothelial Neoplasms: Inherent Problems and Clinical Reflections. Eur Urol Suppl 8:453–457
9. Cheng L, Cheville JC, Neumann RM (1999) Survival of Patients with Carcinoma In Situ of the Urinary Bladder. Cancer 85:2469–2474
10. Gonzalez-Campora R, Davalos-Casanova G, Beato-Moreno A, Lopez-Beltran A (2007) BCL-2, TP53 and BAX protein expression in superficial urothelial bladder carcinoma. Cancer Lett 250:292–299
11. Gofrit ON, Pode D, Pizov G (2009) The natural history of bladder carcinoma in situ after initial response to bacillus Calmette-Gúerin immunotherapy. Urol Oncol 27:258–262
12. Wolf H, Melsen F, Pedersen SE, Nielsen KT (1994) Natural history of carcinoma in situ of the urinary bladder Scand. J Urol Néphrol Suppl 157:147–151
13. Palou J, Laguna P, Millan-Rodriguez F, Hall RR, Salvador-Bayarri J, Vicente-Rodriguez J (2001) Control group and maintenance treatment with bacillus Calmette-Guerin for carcinoma in situ and/or high grade bladder tumors. J Urol 165:1488–1491
14. Ribal MJ, Alcaraz A, Mengual L (2004) Chromosomal High-Polysomies Predict Tumour Progression in T1 Transitional Cell Carcinoma of the Bladder. Eur Urol 45:593–599
15. Shariat SF, Kim J, Raptidis G, Ayala GE, Lerner SP (2003) Association of p53 and p21 expression with clinical outcome in patients with carcinoma in situ of the urinary bladder. Urology 61:1140–1145
16. Hopman AH, Kamps MA, Speel EJ, Schapers RF, Sauter G, Ramaekers FC (2002) Identification of chromosome 9 alterations and p53 accumulation in isolated carcinoma in situ of the urinary bladder versus carcinoma in situ associated with carcinoma. Am J Pathol 161:1119–1125
17. Shariat SF, Pahlavan S, Baseman AG (2001) E-cadherin expression predicts clinical outcome in carcinoma in situ of the urinary bladder. Urology 57:60–65
18. Zlotta AR, Noel JC, Fayt I (1999) Correlation and prognostic significance of p53, p21WAF1/CIP1 and Ki-67 expression in patients with superficial bladder tumors treated with bacillus Calmette-Guerin intravesical therapy. J Urol 161:792–798
19. Hartmann A, Schlake G, Zaak D (2002) Occurrence of chromosome 9 and p53 alterations in multifocal dysplasia and carcinoma in situ of human urinary bladder. Cancer Res 62:809–818
20. Dyrskjøt L, Kruhøffer M, Thykjaer T (2004) Gene expression in the urinary bladder: a common carcinoma in situ gene expression signature exists disregarding histopathological classification. Cancer Res 64:4040–4048
21. Zieger K, Marcussen N, Borre M, Orntoft TF, Dyrskjøt L (2009) Consistent genomic alterations in carcinoma in situ of the urinary bladder confirm the presence of two major pathways in bladder cancer development. Int J Cancer 125:2095–2103
22. Lopez-Beltran A, Cheng L, Mazzucchelli R, Blanca A, Montironi R (2008) Morphological and Molecular Profiles and Pathways in Bladder Neoplasms. Anticancer Res 28:2893–2900
23. Schrier BP, Vriesema JL, Witjes JA, Kiemeney LA, Schalken JA (2006) The predictive value of p53, p27(kip1), and alpha-catenin for progression in superficial bladder carcinoma. Eur Urol 50:76–82
24. Lopez-Beltran A, Requena MJ, Luque RJ, Alvarez J, Montironi R (2006) Cyclin D3 expression in primary Ta/T1 bladder cancer. J Pathol 209:106–113
25. Lopez-Beltran A, Luque RJ, Alvarez-Kindelan J, Montironi R (2004) Prognostic Factors in StageT1Grade 3 Bladder Cancer Survival: The Role of G1+S Modulators (p53, p21Waf1, p27kip1, Cyclin D1, and Cyclin D3) and Proliferation Index (ki67-MIB1). Eur Urol 45:606–612
26. Bartkova J, Zemanova M, Bartek J (1996) Abundance and subcellular localization of cyclin D3 in human tumors. Int J Cancer 65:323–327
27. Birkhahn M, Mitra AP, Williams AJ (2010) Predicting recurrence and progression of noninvasive papillary bladder cancer at initial presentation based on quantitative gene expression profiles. Eur Urol 57:12–20
28. Pruneri G, Pignataro L, Valentini S (2005) Cyclin D3 immunoreactivity is an independent predictor of survival in laryngeal squamous cell carcinoma. Clin Cancer Res 11:242–248

Virchows Arch (2010) 457:563–575
DOI 10.1007/s00428-010-0976-7

ORIGINAL ARTICLE

Integrin-linked kinase (ILK) in pulmonary fibrosis

Panagiotis Kavvadas · Katerina P. Kypreou · Evdokia Protopapadakis · Evangelia Prodromidi · Paschalis Sideras · Aristidis S. Charonis

Received: 19 July 2010 / Revised: 30 August 2010 / Accepted: 7 September 2010 / Published online: 21 September 2010
© Springer-Verlag 2010

Abstract Pulmonary fibrosis is a common feature of a large group of lung diseases. The molecular mechanisms underlying pulmonary fibrosis and the key macromolecules involved are not fully understood yet. In an effort to better understand aspects of pulmonary fibrosis, the established bleomycin injection model in mice was used and the focus of the present study was on integrin-linked kinase (ILK) expression. ILK is an intracellular protein involved in the regulation of integrin-mediated processes. In fibrosis, ILK has been examined in the kidney and in the liver where it mediates epithelial to mesenchymal transition (EMT) and hepatic stellate cell activation, respectively. However, information on ILK's involvement in lung fibrosis is missing. In order to examine ILK's role in pulmonary fibrosis, we used both an in vivo and an in vitro approach. In vivo, the bleomycin model was used in order to examine ILK's expression and localization in the fibrotic lung. In vitro, transforming growth factor-β1 was used to induce fibrotic characteristics and EMT in alveolar epithelial cells. ILK's role in alveolar EMT was studied by siRNA. Our results demonstrate that in the animal model used, ILK exhibits a decrease in expression at early stages of the fibrotic process and that a specific subset of fibroblasts is expressing ILK. The in vitro experiments suggested that ILK is not directly involved in E-cadherin downregulation and initiation of EMT (as is the case in renal fibrosis) but is involved in upregulation of vimentin. These results suggest that ILK is involved in lung fibrosis in a tissue-specific manner and raise the possibility to use it as a specific therapeutic target for lung fibrosis in the future.

Keywords Lung · Fibrosis · ILK · EMT

P. Kavvadas · K. P. Kypreou · A. S. Charonis (✉)
Section of Histology, Center for Basic Research I,
Biomedical Research Foundation of the Academy of Athens,
4, Soranou Efessiou Street,
Athens 115 27, Greece
e-mail: acharonis@bioacademy.gr

E. Protopapadakis · E. Prodromidi · P. Sideras
Center for Immunology and Transplantation,
Biomedical Research Foundation of the Academy of Athens,
4, Soranou Efessiou Street,
Athens 115 27, Greece

Introduction

Pulmonary fibrosis is a late feature of a diverse group of lung diseases, named interstitial lung diseases (ILDs). There are over 200 ILDs that can be classified into two categories: ILDs with a known and ILDs with an unknown etiology. The later are known with the general term idiopathic pulmonary fibrosis (IPF) [1]. IPF accounts for about 45% of all ILD cases [2] in the USA with the incidence being as high as 30/100,000 in the US population [3]. IPF is characterized by alveolar epithelial cell injury and hyperplasia, deposition of extracellular matrix and scar formation. The end result is the loss of lung elasticity and alveolar surface area leading to impairment of gas exchange and pulmonary function [4].

Molecular mechanisms underlying the development of fibrosis among different tissues exhibit basic common features as well as significant differences. As basic common features of the fibrotic response, we usually consider the need of continuous exposure of the tissue to an initial insult or stimulus, the excessive synthesis and decreased degradation of collagen and the central role of cytokines such as transforming growth factor-β1 (TGF-β1) in the regulation of the fibrotic process [5]. A key aspect in fibrogenesis that

appears to exhibit tissue specificity is the origin of myofibroblasts [6]. Myofibroblasts are the key cellular components of fibrogenesis since they produce and secrete large amounts of collagen. Although it was originally believed that myofibroblasts derive from local fibroblasts [7], it is now widely accepted that myofibroblasts can derive from at least two additional sources including epithelial cells through a process known as epithelial to mesenchymal transition (EMT), and bone marrow-derived cells [8, 9].

EMT is a process that normally occurs during embryogenesis and organogenesis allowing cells to switch between epithelial and mesenchymal phenotypes [8]. Recent studies have indicated that in lungs undergoing fibrosis, epithelial cells undergo EMT and transform into fibroblasts and/or myofibroblasts [10–12]. However, in terms of tissue specificity, the role of proteins mediating EMT and myofibroblasts activation and accumulation has not yet been studied.

Integin-linked kinase (ILK) is a protein discovered in 1996 in a yeast two-hybrid screen using the cytoplasmic tail of β1 integrin as bait [13]. It is an intracellular serine/threonine protein kinase located in focal adhesions. It consists of an N-terminal domain that contains four ankyrin repeats, a central pleckstrin homology-like domain and a C-terminal kinase domain. The ankyrin repeats of ILK bind to particularly interesting new cysteine-histidine protein (PINCH) while the C-terminal domain interacts with parvins, forming a ternary complex that allows ILK to stabilize and survive in the cytoplasm [14]. Through its interactions with β-integrins, PINCH, and parvins, ILK is involved in the regulation of a number of integrin-mediated processes that include cell adhesion, cell shape changes, gene expression, and extracellular matrix deposition [15]. Moreover, it has been proposed that ILK regulates the phosphorylation of Akt at Ser473 and of glycogen synthase kinase 3β in various cell types [16, 17] thus involving ILK in fundamental cell processes such as survival.

The role of ILK in fibrosis has been mainly examined in the kidney and in the liver. In the kidney, it is believed to mediate EMT in response to TGF-β1 and induce expression of matrix metalloproteinases [18, 19]. In particular, it has been reported that ILK mediates the initial and therefore key step of EMT, the loss of E-cadherin which results in the loss of the close contact that characterizes cells in epithelia sheets. In the liver, ILK is necessary for the survival of hepatocytes in vivo and in vitro [20] while in liver fibrosis it mediates hepatic stellate cells activation into myofibroblasts, a process that resembles EMT in several aspects [21]. These studies suggest that ILK is a multifunctional protein that can regulate several key cellular processes as well as myofibroblast accumulation in the fibrotic kidney and liver. However, its role in pulmonary fibrosis and alveolar EMT has not yet been examined.

In order to examine the involvement of ILK in pulmonary fibrosis and alveolar EMT, we performed both an in vivo and an in vitro analysis. In vivo, the bleomycin model of pulmonary fibrosis was used. Despite the differences in morphology and cells involved between the various IPF forms and the bleomycin model, this model was used in the present study since it is widely used and well characterized. Moreover, it is also proposed that EMT occurs in the bleomycin model, rendering it even more suitable in order to examine ILK's role in pulmonary fibrosis [10–12]. In vitro, the A549 alveolar epithelial cell line was used in combination with TGF-β. TGF-β is a key mediator of the fibrotic response in all tissues and is widely used in vitro in order to induce fibrotic characteristics and EMT in cells.

Materials and methods

Antibodies

The rabbit polyclonal anti-ILK antibod was purchased from Sigma-Aldrich (St. Louis, MO, USA) and used for western blotting, immunohistochemistry, and immunofluorescence. Anti-Vimentin was purchased from Thermo scientific (Astmoor Runcoor, Cheshire, UK), anti E-cadherin from BD Transduction Laboratories (San Jose, CA, USA), anti-Fibronectin from Santa-Cruz biotechnology Inc (Santa Cruz, CA, USA), anti-type I cell alpha protein and anti-fibroblast specific protein 1 (FSP1) from Developmental Studies Hybridoma Bank (Iowa City, IA, USA) and anti-surfactant protein B from Abcam (Cambridge, MA, USA), anti-β-actin and anti-α smooth muscle from Sigma-Aldrich. Secondary horseradish peroxidase (HRP)-conjugated antibodies were purchased from Sigma-Aldrich while secondary fluoresceine-conjugated antibodies from Jackson Immunoresearch laboratories (West Grove, PA, USA).

Bleomycin model

Female C57/B16 mice at the age of 8–12 week old were used. They were purchased from Charles River Breeding Laboratories and housed in the Animal facility of our institution. They were anesthetized by a combination of ketamine, xylazine, and atropine and 10–15 min later they were administered intratracheally with either 150 mg/kg of bleomycin (bleocin, Nippon Kayaku Co Ltd, Tokyo, Japan) or phosphate-buffered saline (PBS). Mice were sacrificed 2, 4, 9, 15 and 23 days post administration and lungs were collected. For biochemical experiments, right lungs were snap-frozen in liquid nitrogen and stored at −80°C. For morphological experiments, left lungs were fixed by 10% formalin, dehydrated, and paraffin embedded.

Cell culture and cytokine treatment

Human alveolar epithelial cells (A549) were purchased from DSMZ (German Collection of Microorganisms and Cell Cultures, Braunschweig, Germany). Cells were cultured in DMEM low glucose supplemented with 10% fetal bovine serum (FBS), 2 mM L-glutamine, and 1% penicillin–streptomycin. Cells were seeded at approximately 80% confluence in FBS containing medium. After 24 h, cells were changed to serum free medium (0.1% FBS) and cultured overnight. Then, cells were incubated with 5 ng/ml human recombinant TGF-β1 (Peprotech, Paris, France) for various periods of times. In a group of experiments, before incubation with TGF-β1, cells were pre-incubated with 10 μM of FR167653 (Astellas Pharma, Markham, ON, Canada) or 10 μM SB-431542 (Sigma-Aldrich) or 10nM U0126 (Promega, Madison, WI, USA) or 100 nM Wortmannin (Sigma-Aldrich).

Silencing of ILK

Small interference RNA against ILK was purchased by Qiagen (Valencia, CA, USA) while negative control small interfering RNA (siRNA) was purchased from Dharmacon (siGenome non-targeting siRNA #1, Thermo scientific, Dharmacon). At 60% confluence, cells were washed with Optimem and transfected with targeted or control siRNA as described by the manufacturer at a final concentration of 25 nM. Six hours post-transfection, Optimem was replaced with normal medium and cells were further incubated for 24 or 48 h.

Sequence of siRNA for ILK: 5′-AGCUUAACUUCC UGACGAA dTdT
3′-UUCGUCAGGAAGUUAAGCU dGdT

Protein extraction and western blotting

Animals Tissue samples from control and bleomycin-treated mice (two to five animals from each group) were homogenized in 0.5 ml of lysis buffer (50 mM Tris–HCl, 1% NP40, 0.25% sodium deoxycholate, 150 mM NaCl, 1 mM Na_2EDTA, 2% Sodium pyrophosphate, 2% NaF, 0,25% Na_3VO_4, 1 mM PMSF, 4% protease inhibitors cocktail (Sigma-Aldrich)), left on ice for 30 min and then centrifuged for 15 min at 13,000 rpm at 4°C. Supernatants were collected.

Cell culture Cells were washed twice with PBS, collected, and centrifuged for 15 min at 2,500 rpm. Then, cells were lysed in 100 μl of RIPA buffer (50 mM Tris–HCl, 1% NP40, 0.25% Sodium Deoxycholate, 150 mM NaCl, 1 mM Na_2EDTA, 1 mM PMSF, 1% protease inhibitors cocktail (Sigma-Aldrich)) and left on ice for 45 min. Then, they were centrifuged for 15 min at 12,500 rpm at 4°C and supernatants were collected.

All protein extracts were quantified with Bradford protein assay and equal amounts of protein samples were loaded on 10% polyacrylamide gels. Samples were then transferred to a nitrocellulose membrane which was pre-treated with 5% skimmed milk for 1 h and then incubated with primary antibodies overnight at 4°C. The bound antibodies were labeled with horseradish peroxidase-conjugated secondary antibodies for 90 min in room temperature. Detection was done with the Western Lightning Chemiluminescence Reagent of Perkin Elmer. Western blots were scanned with GS-800 calibrated densitometer and images were analyzed with Quantity One image processing software (Bio-Rad). Beta-actin was used to verify all protein loads and data were normalized to actin load.

Immunohistochemistry

Tissue sections (5 μm) were deparafinezed and rehydrated. After endogenous peroxidase inactivation with 5% H_2O_2 in methanol for 30 min at room temperature in the dark, section were treated in 0.01 M citric acid at 400 W in a microwave for 10 min. Then, sections were incubated with the Background Block solution (Cell Merque) for 5 min. Tissue sections were incubated with either a rabbit polyclonal anti-ILK antibody or with rabbit IgG in a similar concentration with that of anti-ILK antibody as a negative control for 1 h at room temperature. Then, sections were washed and incubated with anti-rabbit HRP-conjugated antibody (Sigma-Aldrich) for 45 min at room temperature. The detection reaction was developed with 3′, 3′ diaminobenzidine (Vector Laboratories, Peterborough, UK). Nuclei were counterstained with hematoxylin before examination. Sections were finally dehydraded in graded alcohols and xylene and embedded in mounting solution (DPX).

Immunofluorescence

Animals Tissue sections were deparafinezed, rehydrated, and pretreated in 0.01 M citric acid at 80°C for 20 min. Then sections were blocked with 5% horse serum in PBS for 90 min in room temperature and then incubated with primary antibodies at 4°C overnight. Then sections were washed, incubated with fluoresceine-conjugated secondary antibodies and DAPI. Finally, sections were dehydrated in graded alcohols and xylene and embedded in DPX.

Cell culture A549 cells were grown on poly-L-lysine-coated coverslips and incubated at 37°C. Cells were then fixed with 4% paraformaldehyde in PBS for 20 min at room temperature. Permeabilization and blocking were performed

with 0.1% Triton X-100, 5% FBS in PBS buffer for 30 min in room temperature. Subsequently, cells were incubated with primary antibodies overnight at 4°C, followed by incubation with fluoresceine-conjugated secondary antibodies and DAPI.

Picro-sirius red staining

Tissue sections were deparafinized and rehydrated and stained with picro-sirius red solution (0.5 g of picro-sirius red in 500 ml of aqueous solution of picric acid) for 1 h at room temperature. Then, sections were washed in acidified water (5 ml of acetic acid in 1 l of distilled water), dehydrated in alcohol and xylene, and mounted with DPX.

Results

Fibrosis progression in the bleomycin model

In order to investigate the potential involvement of ILK in pulmonary fibrosis, we used the bleomycin model which is one of the best-characterized murine models in use today. In our experimental protocol, either bleomycin (150 mg/kg) or PBS (for control animals) was delivered via the intratracheal route and animals were sacrificed 2, 4, 9, 15, and 23 days post-administration. Intratracheal administration resulted in an initial damage of alveolar epithelial cells, followed by neutrophil and macrophage infiltration. Collagen expression and thus fibroblast accumulation, remains low until day 9 and peaks at days 15 and 23 [4, 22, 23]. The extent of extracellular matrix accumulation in our model is presented in Fig. 1. The

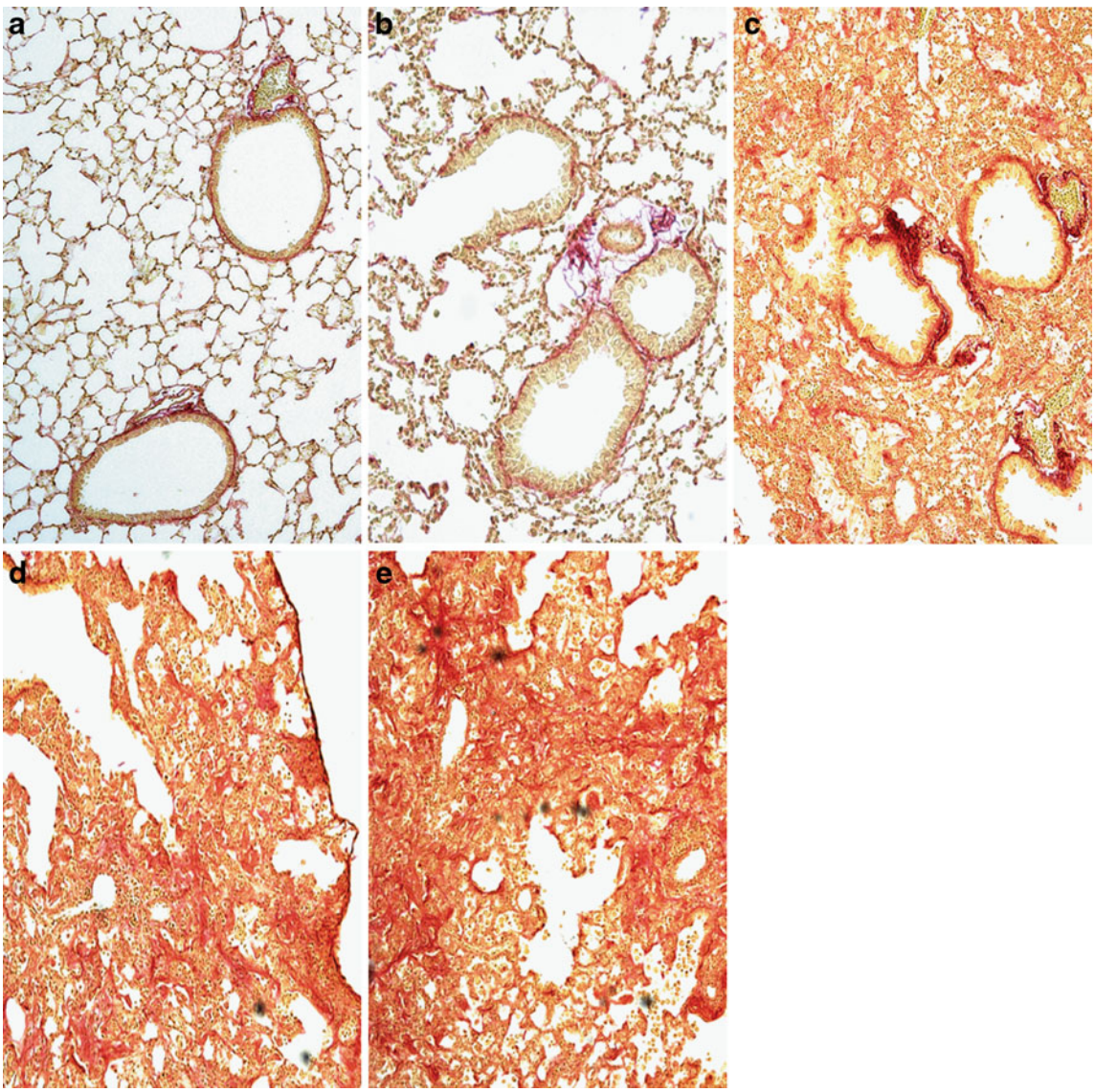

Fig. 1 Extracellular matrix accumulation at the bleomycin model measured with the picro-sirius red staining method that stains all collagen types red. Sections from a PBS-treated animal (**a**) and bleomycin-treated animals for 2 (**b**), 9 (**c**), 15 (**d**), and 23 (**e**) days are presented

method of staining with picro-sirius red identifies all collagen types and highlights the extent of collagen production during the different time intervals used. As can be seen from Fig. 1, the amount of collagen in the lung is practically unaltered in day 2 but starts to increase in a time-dependant manner starting from day 9. At days 15 and 23 collagen is uniformly distributed and accompanied by loss of alveolar structures. Therefore, the course of collagen accumulation in our model and under the experimental conditions used is in agreement with the findings of previously published work on the bleomycin model [23].

ILK quantification in the bleomycin model

Western blot analysis for ILK in days 2, 4, 9, 15, and 23 revealed that protein levels of ILK were increased at days 2 and 4 while they were decreased, compared to PBS, in day 9 (Fig. 2a). At later time intervals, including days 15 and 23, protein levels showed a tendency to increase again compared to day 9. As can been seen in Fig. 2b, during day 15, protein levels are still lower compared to control levels but are higher than the levels in day 9. In day 23, protein levels have reached control levels. In conclusion, in the bleomycin model of pulmonary fibrosis, an initial increase of ILK is followed by a dramatic decrease during day 9. From this time point and on, ILK protein levels slowly elevate till they reach the control levels at day 23. Real-time RT-PCR experiments also confirmed these observations at the mRNA levels (data not shown). The above data suggested that differences exists between ILK expression in other organ fibrosis models (like renal and liver fibrosis) and the bleomycin lung fibrosis model and prompted us to further investigate this phenomenon.

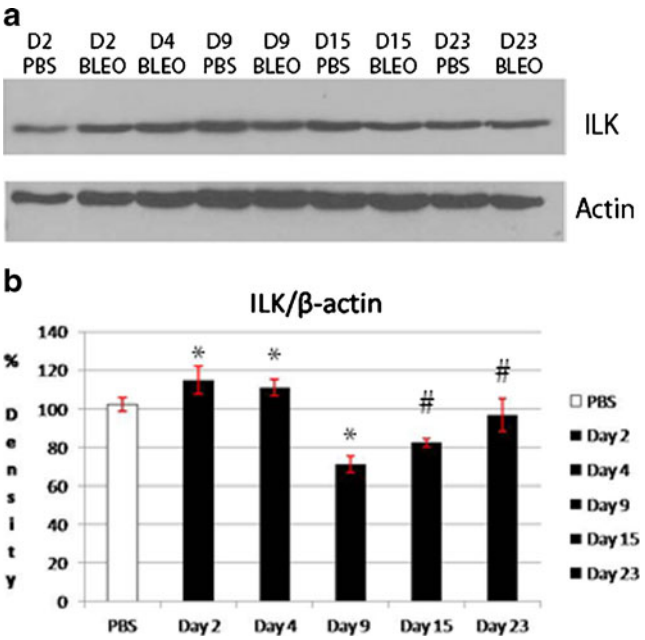

Fig. 2 Biochemical quantification of ILK in the murine bleomycin model of pulmonary fibrosis. **a** Western for ILK in control and bleomycin-treated animals. Pooled samples from five animals from each time interval were used since hematoxylin staining of tissue of every animal revealed no significant differences between animals of the same group. Beta-actin is used as a reference protein. **b** Densitometric analysis and quantification of the expression of ILK compared to β-actin. Since PBS samples showed no significant differences, only one of them is presented. Data are expressed as means±SD from three independent experiments. *$P<0.05$, #$P>0.05$

ILK distribution in the bleomycin model

In order to understand the observed changes of ILK expression, it was imperative to study the distribution of ILK in the normal lung and during the development of fibrosis in the bleomycin model.

Immunohistochemistry experiments for ILK revealed that in the normal lung it is expressed in the bronchial epithelium (Fig. 3c), in vascular smooth muscle cells (data not shown), and in the alveolar wall (Fig. 3b). The main cell types present in the alveolar wall are type I and II pneumocytes, endothelial cells, and pericytes (and to a lesser extent, alveolar macrophages, interstitial fibroblasts, and other cell types). Lung parenchyma at day 2 after bleomycin administration does not exhibit significant histological differences from control lungs. At day 9, the first fibrotic areas have already formed but are still low in number and size. The main characteristics at day 9 is the extensive loss of ILK positive cells within the alveolar walls (Fig. 3e) and the partial destruction of bronchial epithelial cells which also express ILK (Fig. 3f). Double immunofluorescence experiments for ILK and type I pneumocytes α-protein (data not shown), confirmed that ILK is expressed in type I cells which are the main target of bleomycin within the alveolar wall. Taken together, these two results indicate that the decrease in ILK levels, observed during day 9, could be attributed, to a certain extent, to the destruction of epithelial cell populations. At days 15 and 23 (Fig. 3h, i), normal lung architecture is extensively compromised. The tissue is characterized by large fibrotic lesions with great heterogeneity, as far as ILK is concerned, since there are areas with no ILK-positive cells next to areas with significant staining for ILK.

ILK and alveolar EMT

Type II alveolar cells survive bleomycin, proliferate and eventually differentiate into type I cells [24]. Moreover, they are considered as the key source of EMT-derived fibroblasts in the lung [10–12]. To evaluate ILK in alveolar EMT, we performed double immunofluorescence experiments for ILK and surfactant protein B which is a protein

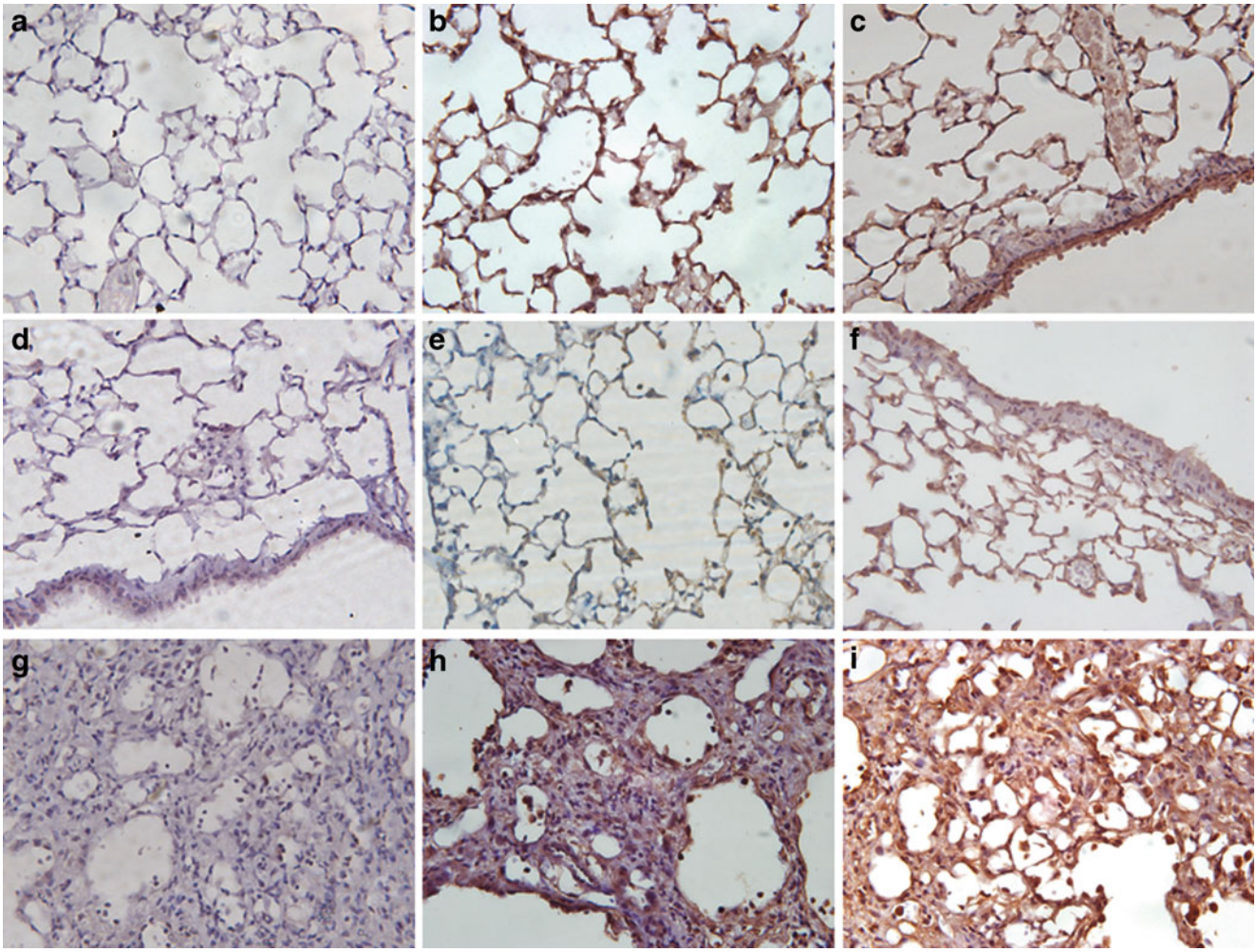

Fig. 3 Immunohistochemistry for ILK in the bleomycin model. **a**, **b**, **c**.ILK in the normal lung. ILK stains bronchial epithelial cells (**c**) and cells in the alveolar walls (**b**), probably alveolar epithelial and endothelial cells. IgG staining is used as negative control (**a**). **d**, **e**, **f** ILK in the 9 days treated with bleomycin lung. ILK staining in the alveolar wall (**e**) is dramatically decreased due to alveolar epithelial cell destruction by bleomycin. Bronchial epithelial cells (**f**) are also partially destroyed in response to bleomycin. IgG staining is used as negative control (**d**). **g**, **h**, **i** ILK in the 15 days treated with bleomycin lung. Lung architecture is completely destroyed and normal parenchyma has been substituted by extensive fibrotic lesions consisting of connective tissues. ILK staining is highly heterogenic since there are ILK negative (**h**) and ILK positive (**i**) areas. IgG staining is used as negative control (**g**)

used as a type II cell marker. FSP1 is a protein frequently used to identify fibroblast subpopulations [25]; therefore, we decided to check the presence and distribution of FSP1 in the bleomycin model. Our results showed no staining for FSP1 in the normal alveoli (data not shown). In the fibrotic lung, from as early as day 9, we observed a significant increase of FSP1 staining. In the remaining of the alveolar walls at day 9 post-injection, the majority of the FSP1 expressing cells co-express ILK (Fig. 4e–h), suggesting the possibility that type II alveolar cells are undergoing EMT.

ILK and lung myofibroblasts

It has recently been proposed that lung myofibroblasts are rarely derived from EMT [10]. In order to estimate the extent to which ILK is expressed in lung myofibroblasts, we performed double staining for ILK and α-smooth muscle actin (α-SMA) which is considered as a myofibroblasts marker. In the normal lung, α-SMA is expressed in vascular and bronchial smooth muscle cells. However in the fibrotic lung, it is highly expressed in the fibrotic lesions indicating the presence of myofibroblasts. ILK exhibited limited co-expression with α-SMA (Fig. 4i–l) indicating that ILK is mainly expressed in the fibroblast subpopulation that expresses FSP1.

Induction of EMT in A549 cells

To gain better understanding of the involvement of ILK in alveolar EMT, we performed in vitro EMT studies using the

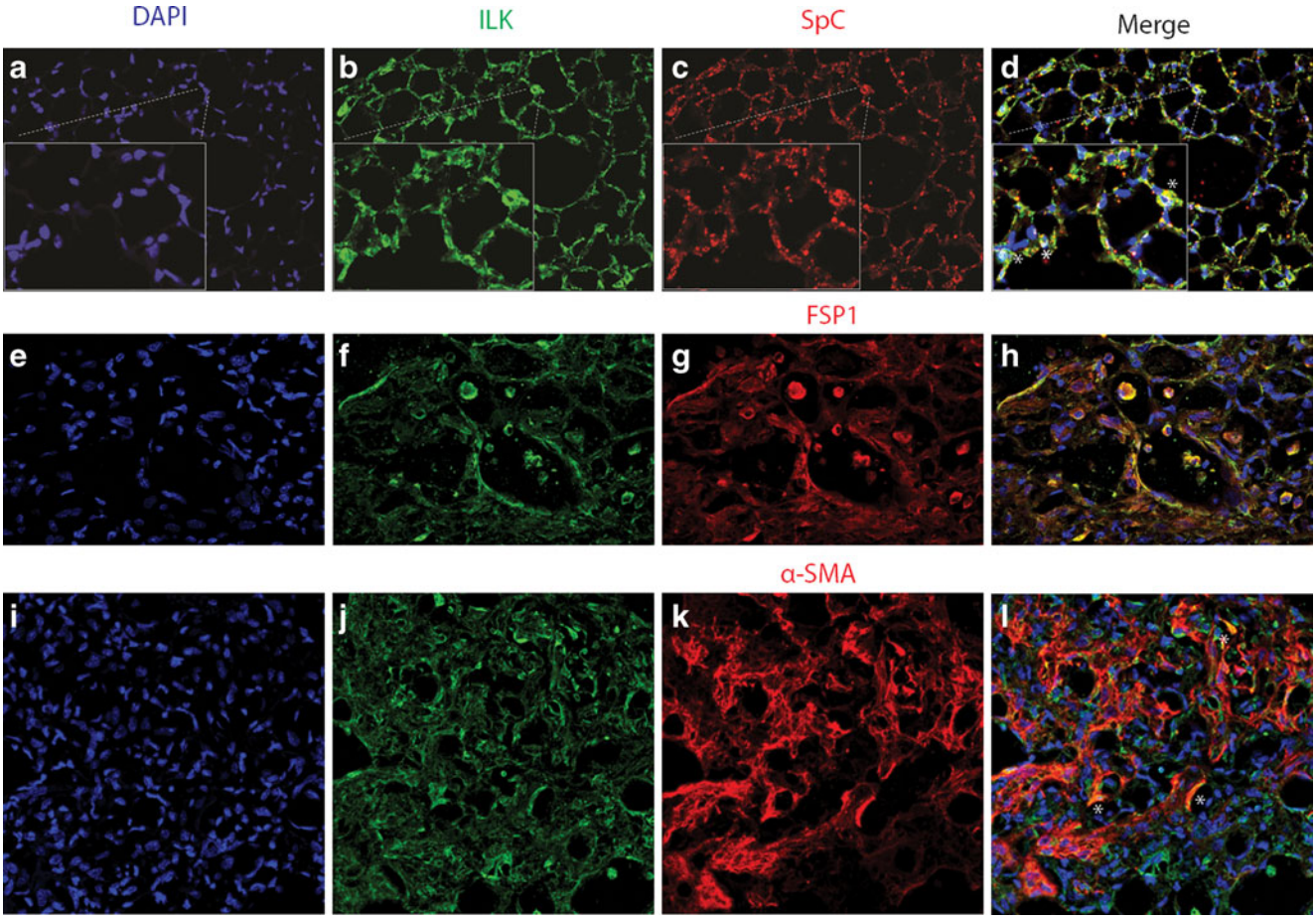

Fig. 4 Double immunofluorescence experiments for ILK and Surfactant protein B, FSP1 and α-SMA. **a**–**d** Double immunofluorescense for ILK and the type II cell marker surfactant protein B (SpB) at day 9. **a** DAPI, **b** ILK, **c** SpB, **d** merged image. ILK is expressed in cells producing surfactant protein B (examples are pointed by *asterisks* in the magnified field on the *left*), thus verifying that type I pneumocytes express ILK. **e**–**h** Double immunofluorescense for ILK and the fibroblast marker FSP1 at day 15. **e** DAPI, **f** ILK, **g** FSP1, **h** merged image. ILK and FSP1 are widely co-expressed, indicating that ILK is expressed in fibroblasts subpopulations expressing FSP1. **i**–**l** Double immunofluorescense for ILK and α-SMA at day 15. **i** DAPI, **j** ILK, **k** α-SMA, **l** merged image. ILK and α-SMA exhibit limited co-expression indicating that ILK is expressed in a small subset of myofibroblasts (characteristic examples are pointed with *astericks*)

A549 alveolar epithelial cell line. In order to induce EMT in the A549 cell line, cells were incubated for various time intervals with 5 ng/ml human recombinant TGF-β1. To evaluate the phenotypic changes, several markers for EMT were used. After 24 h, E-cadherin, an epithelial phenotype marker, was 60% downregulated and reached the lowest level at 48 h. Vimentin, a mesenchymal marker, was almost undetectable in control cells, appeared upregulated from as early as 4 h and peaked at 48 h while FSP1 increased after 12-h incubation with TGF-β1 (Fig. 5a). After 48 h, cell–cell contact and cluster formation were lost, while cells begun to acquire a spindle like morphology (Fig. 5e). Since in fibrosis, specific cells increase their α-SMA and fibronectin expression, we examined whether in our TGF-β1-induced culture system these proteins were also upregulated. Therefore, we performed immunofluorescence experiments which showed that these two proteins were also upregulated at 48 h (Fig. 6a–d and e–h for α-SMA and fibronectin, respectively). Based on these findings, we have selected to use the time interval of 48 h in most of our experiments.

ILK is induced during EMT in alveolar epithelial cells

In order to examine the changes in ILK expression following incubation with TGF-β1 in A549 cells, we performed western blotting experiments. It is apparent from Fig. 7 that ILK is upregulated in response to TGF-β1. The upregulation is observed from as early as 4 h (slight upregulation) and peaks at 48 h.

TGF-β induces ILK through a SMAD-dependent mechanism

It is well known that TGF-β1 can activate numerous intracellular signaling pathways. These include SMAD-dependent and SMAD-independent pathways such as the mitogen-activated protein kinase (MAPK) pathway,

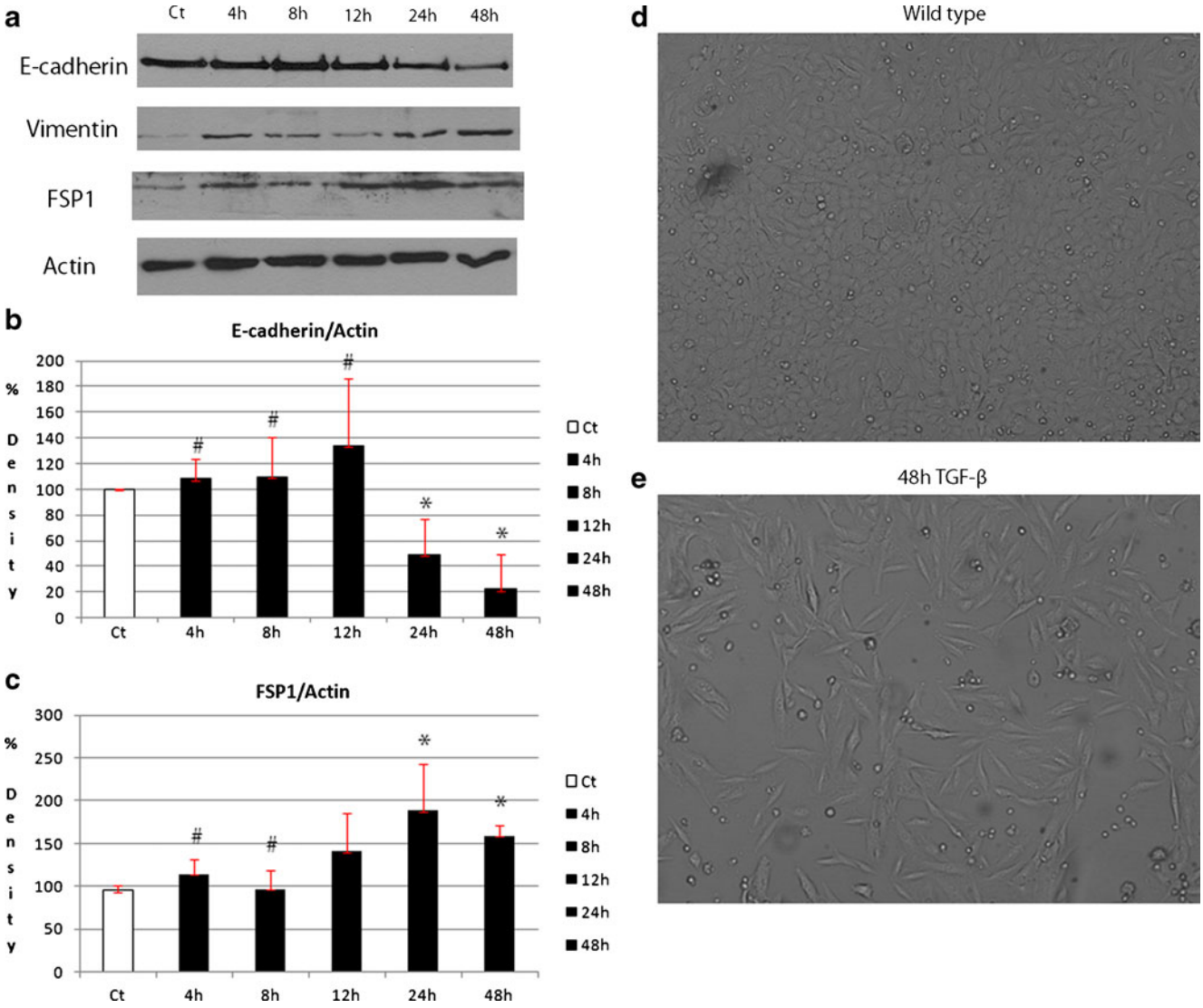

Fig. 5 TGF-β induces EMT in alveolar epithelial cells. **a** Western blotting for E-cadherin and vimentin after incubation for 24, 48, and 72 h with human recombinant TGF-β1. Beta-actin is used as a reference protein. **b**, **c** Densitometric analysis and quantification of the expression of and E-cadherin and FSP1 compared to β-actin, respectively. Results are expressed as means±SD from three independent experiments. Vimentin levels were practically undetectable, not allowing further statistical analysis. *$P<0.05$. **d** Normal epithelial cells maintain close cell–cell adhesion and form clusters. **e** After 48 h incubation with TGF-β cells acquire a spindle like morphology and begin to detach from each other

phosphatidylinositol-3-kinase (Pi3k) pathway, and pathways driven by Rho-like GTPases, etc. In order to unravel the mechanism through which TGF-β1 upregulates ILK, we have used specific chemical inhibitors for several pathways including SB-431542 for the SMAD2/3 pathway, FR167653 for the p38 MAPK pathway, U0126 for the ERK 1/2 pathway, and Wortmannin for the Pi3k pathway. Our results (Fig. 8) demonstrate that TGF-β1 upregulates ILK through a Smad2/3-dependent mechanism since preincubation with SB-431542, completely abolishes ILK upregulation. SB-431542 is an ALK5 (the TGF-β1 type I receptor) inhibitor which prevents activation of Smad2/3. Preincubation with wortmannin, a Pi3k inhibitor, showed that ILK upregulation is independent of Pi3k signaling since ILK upregulation by TGF-β1 was not abolished by wortmannin preincubation (Fig. 8c). As for MAPK pathways, the p38 MAPK kinase pathway does not affect ILK (Fig. 4d) while the Erk1/2 pathway seems to downregulate ILK (Fig. 8b). In conclusion, the above results indicate that TGF-β upregulates ILK through a Smad2/3-dependent mechanism.

Downregulation of ILK and EMT

In order to further understand the role of ILK in lung fibrosis and more specifically in the phenomenon of EMT in alveolar epithelial cells, we examined the effects of ILK

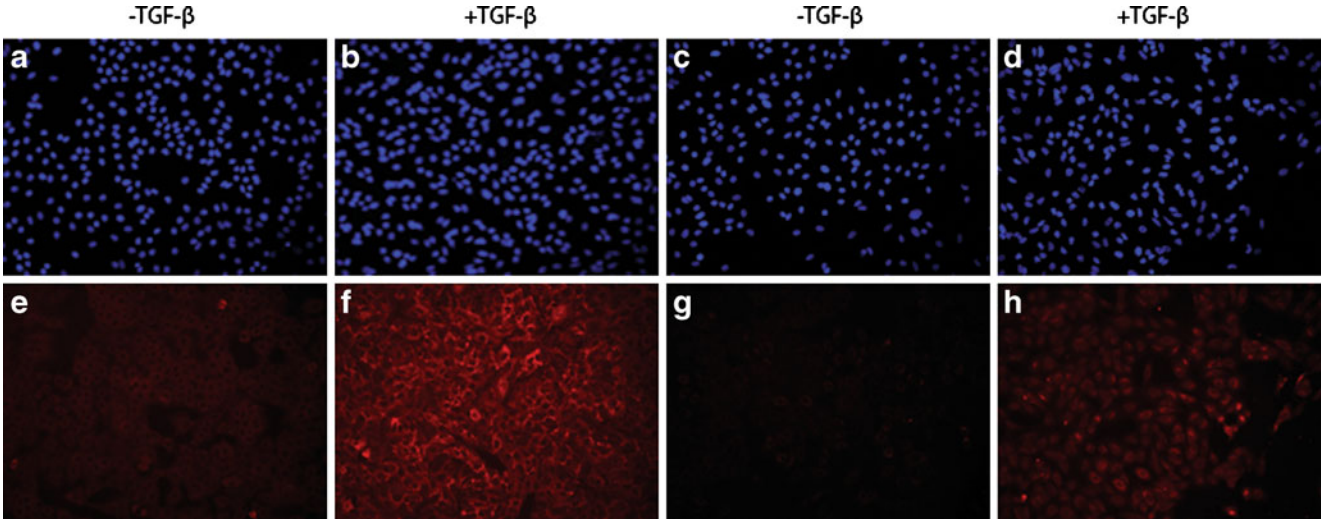

Fig. 6 TGF-β induces expression of mesenchymal and fibrotic markers in alveolar epithelial cells such as α-SMA (**a**–**d**) and fibronectin (**e**–**h**). In normal alveolar epithelial cells, α-SMA (**c**) and fibronectin (**g**) are almost undetectable. After incubation with TGF-β for 48 h (**d**, **h**, respectively) they are dramatically increased. Nuclei are stained with DAPI

downregulation by siRNA, in cells undergoing EMT following TGF-β1 treatment. The technique used for siRNA allowed a 75–80% reduction of ILK as seen in Fig. 5a. We have concentrated on the two EMT markers used before, E-cadherin and vimentin, since these markers are characteristic of early (E-cadherin) and late (vimentin) stages of EMT. Our results using western blot analysis, demonstrate that downregulation of ILK did not restore E-cadherin expression; however, it did affect vimentin since its upregulation by TGF-β1 was reduced by 50% (Fig. 9c,d). Therefore, our results indicate that ILK is not primarily involved in the early stages of EMT, for which E-cadherin is a characteristic marker, whereas it interferes with later stages of EMT related to cell migration, for which vimentin can be considered as a representative marker.

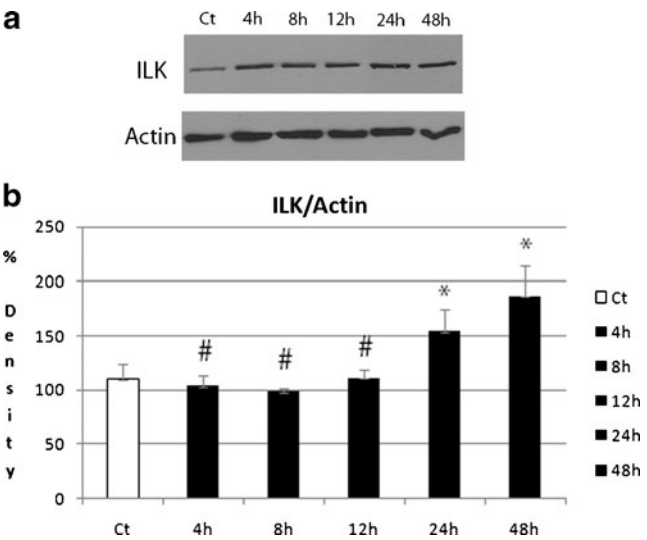

Fig. 7 ILK increases in response to TGF-β. **a** Western blotting for ILK after incubation for 24, 48, and 72 h with human recombinant TGF-β1. Beta-actin is used as a reference protein. **b** Densitometric analysis and quantification of the expression of ILK compared to β-actin. Results are expressed as means±SD from three independent experiments. *$P<0.05$, #$P>0.05$

Discussion

In order to design efficient and targeted treatments for any fibrotic condition, it is necessary to understand the mechanism(s) underlying the fibrotic processes. It has been proposed that among the mechanisms involved in the generation of extarcellular matrix producing cells, EMT plays an important role in several organs, including the lung [10, 12]. Furthermore, in order to gain a better understanding and develop specific targets for efficient treatment, we need to specify macromolecules that play a crucial role in the development of fibrosis. In the present report, we focus on one such macromolecule, ILK and we explore its expression and role in lung fibrosis.

The involvement of ILK in lung fibrosis was examined, using an animal model and a cell culture system. ILK's role has been extensively studied in renal [18, 19, 26] and in liver fibrosis [21]. However, its role in pulmonary fibrosis has not been studied so far. Our data first establish alterations of ILK expression during lung fibrosis, second highlight differences regarding ILK's role in alveolar EMT compared to its role in EMT in other organs and third, suggest that ILK may be differentially expressed in different types of (myo)fibroblasts.

In order to examine ILK's role in pulmonary fibrosis, we used both an in vivo and an in vitro approach. For the in vivo study we used the murine, bleomycin model of

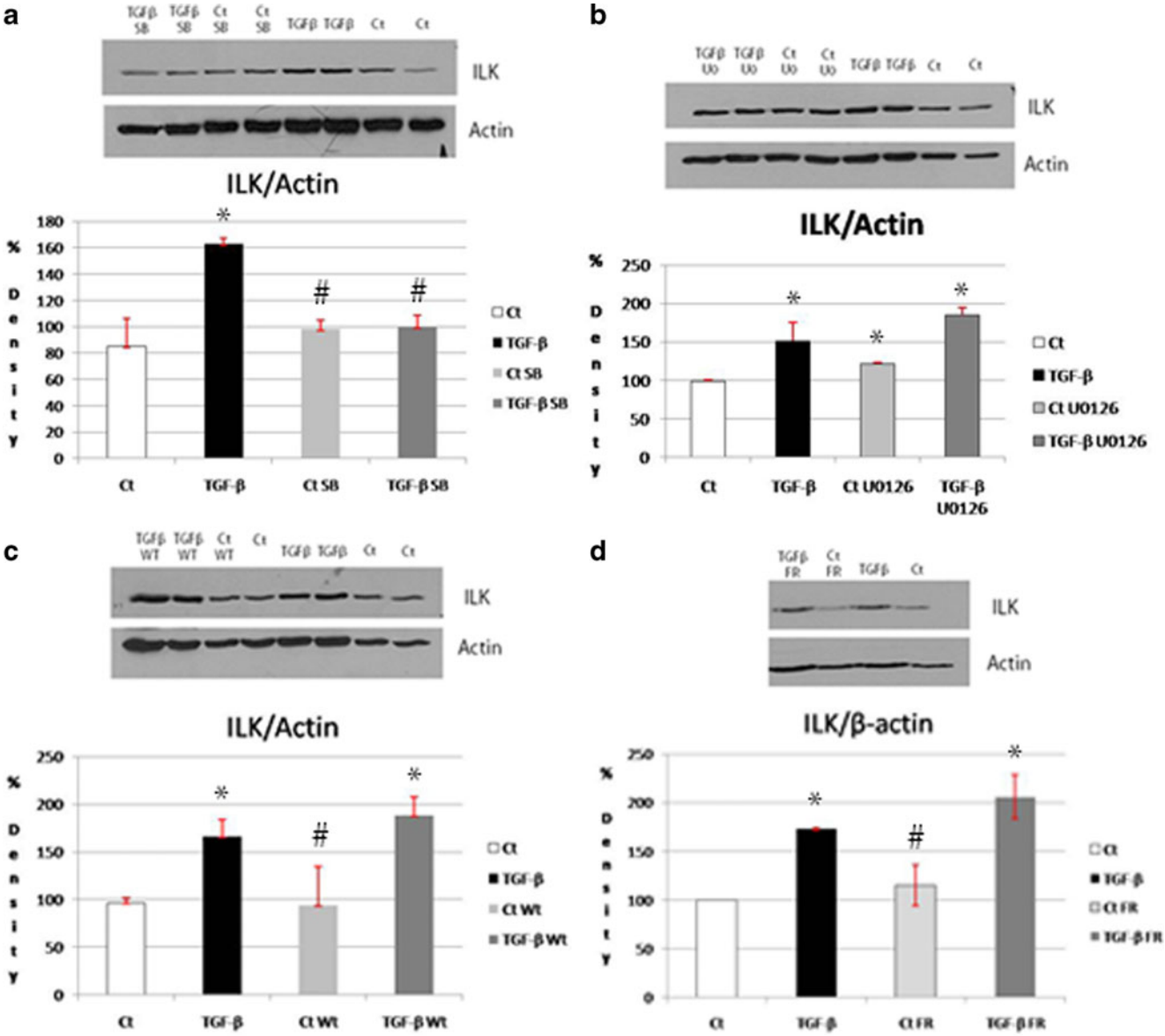

Fig. 8 TGF-β upregulates ILK in a Smad 2,3-dependent manner. **a** Western for blotting for ILK in the absence or in the presence of the ALK5/smad 2,3 pathway inhibitor SB-431542 (SB). Incubation with TGF-β for 48 h upregulates ILK but preincubation with SB-431542 completely abolishes this upregulation. Beta-actin is used as a reference protein. All samples are presented as duplicates while results are expressed as means±SD from the independent samples. **b**, **c**, **d** Western blotting for ILK in the presence or in the absence of the erk1/2 pathway inhibitor U0126 (U0), of wortmannin (WT) which is a Pi3K inhibitor and of FR167653 (FR), a p38 MAPK inhibitor respectively. Preincubation with these chemical inhibitors had no effect on ILK upregulation. Beta-actin is used as a reference protein. Wortmannin and U0126 treated samples are presented as duplicates and results are expressed as means±SD from the two independent samples. Data from FR167653-treated samples are expressed as means±SD from two independent experiments. *$P<0.05$, #$P>0.05$

pulmonary fibrosis since it is well characterized and EMT has been proposed to occur in response to bleomycin-induced lung destruction. Evaluation of the level of expression of ILK by biochemical approaches indicated a pattern of expression drastically different from renal fibrosis models [18, 19] since ILK was downregulated during days 9 and 15. In order to better understand these changes, morphological approaches were further used. Immunohistochemistry experiments demonstrated generation of fibrotic lesions and infiltration of several cell types with marked heterogeneity in the level of expression of ILK. Therefore, these findings strongly suggest that overall biochemical quantification of ILK expression in the fibrotic lung is not very meaningful. Indeed, quantification of the immunohistochemistry experiments revealed that although by percent, ILK was decreased at days 9 and 15 exhibiting a similar pattern to that of the western blotting, the total amount of ILK was increased during the late time intervals

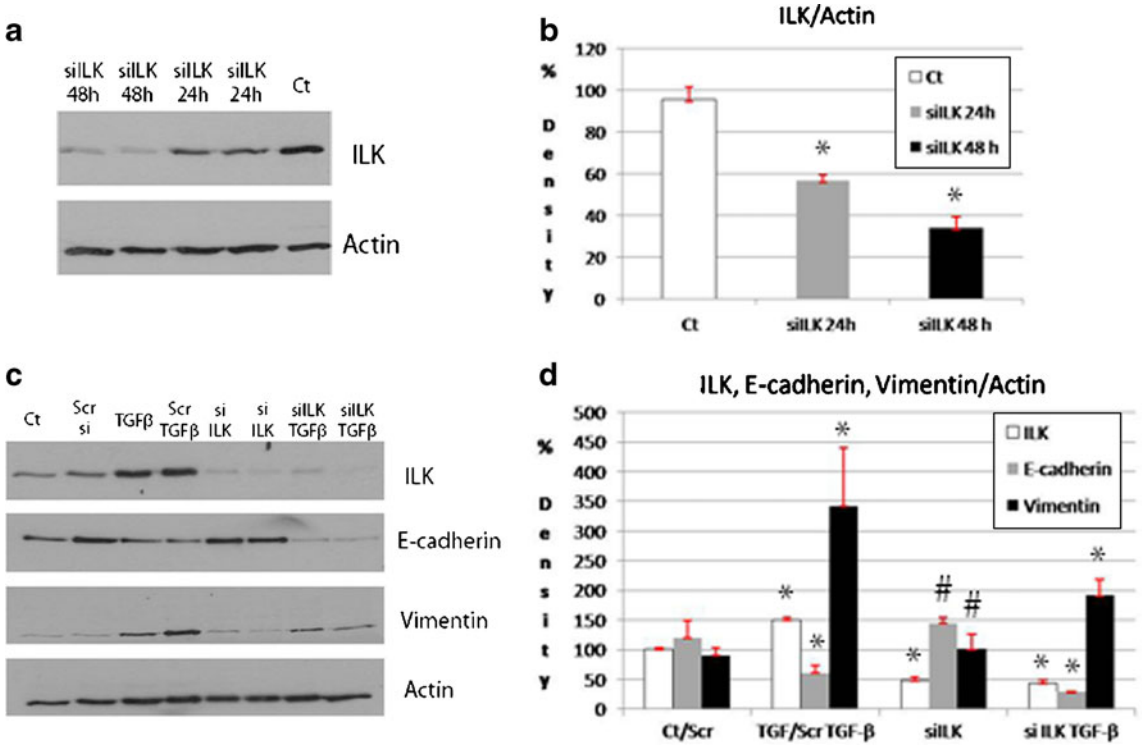

Fig. 9 Silencing of ILK and its role in alveolar EMT. **a** Western for ILK after 24 and 48 h incubation with siRNA (25 nM) specific for ILK. Beta-actin is used as a reference protein. **b** Densitometric analysis and quantification of the expression of ILK compared to β-actin. Results are expressed as means±SD from three independent experiments. **c** Western for ILK, E-cadherin and vimentin in the presence (*lanes 5–8*) or in the absence (*lanes 1–4*) of siRNA for ILK in combination with TGF-β treatment (*lanes 3, 4, 7, 8*) for 48 h. Beta-actin is used as a reference protein. siRNA-treated and siRNA/TGF-β-treated samples are presented as duplicates. Untransfected (*lane 1*) or transfected with scramble siRNA (*lane 2*) cells are used as controls. **d** Densitometric analysis and quantification of the expression of ILK, E-cadherin, and vimentin compared to β-actin. **P*<0.05, #*P*>0.05

(days 15 and 23). Based on these observations, we focused on the characterization of cell populations expressing ILK in normal and fibrotic lung.

Our data showed that ILK localizes in type I pneumocytes and bronchial epithelial cells. These data suggest that downregulation of ILK during day 9, is probably due to the dramatic decrease of these epithelial populations. During days 15 and 23, where ILK levels show a tendency to increase towards control values, the lung is characterized by great heterogeneity and infiltration of numerous cell populations. Co-localization experiments for ILK and the pan-leukocyte marker CD45 (data not shown) revealed that ILK is expressed in subsets of cells of the immune system, most probably macrophages. Infiltration of immune cells that express ILK could justify the increase in the levels of ILK observed during day 15 compared to day 9 while co-localization of ILK with leucocytes could justify the overall increase observed in day 2 which is mainly characterized by inflammation and not fibrosis.

As far as EMT-related cell populations are concerned, double immunofluorescence experiments revealed that ILK is expressed in type II pneumocytes and in the fibrotic lung, in cells expressing FSP1. Type II cells are the progenitors of type I cells so they have the capacity to proliferate, migrate, and differentiate into type I cells in order to repopulate the alveolar surface after injury [24, 27]. However, it should be noted that several other mechanisms contribute to the regeneration of the injured lung parenchyma [28]. Moreover, it has been reported that in response to tissue injury, type II cells undergo EMT and contribute to the increased fibroblast/myofibroblast populations in fibrosis [10–12]. FSP1, a protein that belongs to the calmodulin-S100-troponin C superfamily, has been proposed as a fibroblast marker, usually used to characterize EMT-derived fibroblasts [25, 29]. Finally, our data showed a limited expression of ILK in α-SMA positive cells which based on cell shape and distribution, appear to be myofibroblasts. Since it has been reported that although EMT occurs in the fibrotic lung but it has little contribution to the myofibroblasts accumulation [10, 11] our findings raise the possibility that ILK is mainly expressed in EMT-derived fibroblasts and myofibroblasts and it could be used as an EMT marker. However, more experimental work is needed to confirm this hypothesis. In addition, the bleomycin murine model of pulmonary fibrosis exhibits differences compared to the lung pathology in human IPF.

These differences are both stimulus-related and species-related. In this context, it is expected that crucial differences may exist in the origin and the phenotype of the populations of fibroblasts and myofibroblasts present in each specific condition [30, 31].

In order to better understand ILK's potential involvement in alveolar EMT, we used the alveolar epithelial A549 cell line. TGF-β, which is a key mediator of fibrotic events, including EMT was used to induce EMT—which in renal fibrosis is triggered through a TGF-β-Smad-ILK dependent mechanism—and fibrotic characteristics to the cells. Our results showed that incubation of A549 cells with TGF-beta leads to acquisition of fibrotic characteristics and initiation of EMT while ILK is upregulated in a Smad 2,3-dependent mechanism.

ILK's siRNA-mediated downregulation failed to rescue E-cadherin levels while it partially affected the upregulation of vimentin, an intermediate filaments protein, used as a mesenchymal marker [32]. Vimentin is implicated in migration and invasion of transformed and tumor cells [33]. Since it has been shown that ILK mediates TGF-β-induced E-cadherin repression and therefore initiation of EMT in renal tubular epithelial cells, our results indicate that ILK is not involved or its action can be substituted in the initiation of alveolar EMT. Moreover, since ILK affects the levels of vimentin, a protein involved in later stages of EMT such as migration this could mean that ILK participates in alveolar EMT but in a different way than that in renal EMT. Taken together, these data reinforce the concept that mediators of basic fibrotic processes may act in a tissue specific manner and their role in fibrotic events cannot be extrapolated from one organ to the other.

Acknowledgments The present work was supported by funds from Biomedical Research Foundation of the Academy of Athens and PENED 03ED245 from the Greek Secretariat for Research and Technology. We are grateful to Dr. Stavros Giaglis for help with RT-RT-PCR, Dr. Stamatis N. Pagakis and Dr. Eleni Rigana for their help with confocal microscopy, Anna Agapaki for help with histological techniques, and to the members of Department of Histology for the excellent cooperation. We are also thankful to Dr. Dimitrios Kouretas for his support and interaction.

Declaration of interest The authors declare they have no conflict of interest.

References

1. Green F (2002) Overview of pulmonary fibrosis. Chest 122:334–339
2. Coultas DB, Zumwalt RE, Black WE, Sobonya RE (1994) The epidemiology of interstitial lung diseases. Am J Respir Crit Care Med 150:967–972
3. American Thoracic Society ERS (2000) Idiopathic pulmonary fibrosis: diagnosis and treatment. International consensus statement. Am J Respir Crit Care Med 161:646–664
4. Moore BB, Hogaboam CM (2008) Murine models of pulmonary fibrosis. Am J Physiol Lung Cell Mol Physiol 294:L152–L160
5. Mutsaers SE, Bishop JE, McGrouther G, Laurent GJ (1997) Mechanisms of tissue repair: from wound healing to fibrosis. Int J Biochem Cell Biol 29:5–17
6. Kisseleva T, Brenner DA (2008) Mechanisms of fibrogenesis. Exp Biol Med 233:109–122
7. Kumar V, Abbas AK, Fausto N (2005) Tissue renewal and repair: regeneration, healing and fibrosis. In: Kumar V, Abbas AK, Fausto N (eds) Pathologic basis of disease, 7th edn. Elsevier, Saunders, pp 87–118
8. Kalluri R, Neilson EG (2003) Epithelial–mesenchymal transition and its implications for fibrosis. J Clin Invest 112:1776–1784
9. Bucala R, Spiegel LA, Chesney J, Hogan M, Cerami A (1994) Circulating fibrocytes define a new leukocyte subpopulation that mediates tissue repair. Mol Med 1:71–81
10. Tanjore H, Xu XC, Polosukhin VV, Degryse AL, Li B, Han W, Sherrill TP, Plieth D, Neilson EG, Blackwell TS, Lawson WE (2009) Contribution of epithelial derived fibroblasts to bleomycin induced lung fibrosis. Am J Respir Crit Care Med 180(7):657–665
11. Wu Z, Yang L, Cai L, Zhang M, Cheng X, Yang X, Xu J (2007) Detection of epithelial to mesenchymal transition in airways of a bleomycin induced pulmonary fibrosis model derived from an α-smooth muscle actin-Cre transgenic mouse. Respir Res 8:1–11
12. Kim KK, Kugler MC, Wolters PJ, Robillard L, Galvez MG, Brumwell AN, Sheppard D, Chapman HA (2006) Alveolar epithelial cell mesenchymal transition develops in vivo during pulmonary fibrosis and is regulated by the extracellular matrix. PNAS 103(35):13180–13185
13. Hannigan GE, Leung-Hagesteijn C, Fitz-Gibbon L, Coppolino MG, Radeva G, Filmus J (1996) Regulation of cell adhesion and anchorage-dependent growth by a new beta 1-integrin-linked protein kinase. Nature 379:91–96
14. Legate KR, Montanez E, Kudlacek O, Fassler R (2006) ILK, PINCH and parvin: the Tipp of integrin signaling. Nature 7:20–31
15. Wu C, Keightly SY, Leung-Hagesteijn C, Radeva G, Coppolino M, Goicoechea S, McDonald JA, Dedhar S (1998) Integrin-linked protein kinase regulates fibronectin matrix assembly, E-cadherin expression and tumorigenenicity. J Biol Chem 273: 528–536
16. Persad S, Attwell S, Gray V, Mawji N, Deng JT, Leung D (2001) Regulation of protein kinase B/Akt-serine 473 phosphorylation by integrin-linked kinase: critical roles for kinase activity and amino acids arginine 211 and serine 343. J Biol Chem 276:27462–27469
17. Delcommenne M, Tan C, Gray V, Rue L, Woodgett J, Dedhar S (1998) Phosphoinositide-3-OH kinase-dependent regulation of glycogen synthase kinase 3 and protein kinase B/Akt by the integrin-linked kinase. Proc Natl Acad Sci 95:11211–11216
18. Li Y, Yang J, Dai C, Wu C, Liu Y (2003) Role for integrin-linked kinase in mediating tubular epithelial to mesenchymal transition and renal interstitial fibrogenesis. J Clin Investig 112:503–516
19. Li Y, Dai C, Wu C, Liu Y (2007) PINCH-1 promotes tubular epithelial-to-mesenchymal transition by interacting with integrin-linked kinase. J Am Soc Nephrol 18:2534–2543
20. Gkretsi V, Mars WM, Bowen WC, Barua L, Yang Y, Guo L, St-Arnaud R, Dedhar S, Wu C, Michalopoulos GK (2007) Loss of integrin-linked kinase from mouse hepatocytes in vitro and in vivo results in apoptosis and hepatitis. Hepatology 45(4):1025–1034
21. Zhang Y, Ikegami T, Honda A, Miyazaki T, Bouscarel B, Rojkind M, Hyodo I, Matsuzaki Y (2006) Involvement of integrin-linked kinase in carbon tetrachloride-induced hepatic fibrosis in rats. Hepatology 44(3):612–622
22. Chaudhary NI, Schnapp A, Park JE (2005) Pharmacological differentiation of inflammation and fibrosis in the rat bleomycin model. Am J Respir Crit Care Med 173:769–776

23. Izbicki G, Segel MJ, Christensen TG, Conner MW, Breuer R (2002) Time course of bleomycin-induced lung fibrosis. Int J Exp Path 83:111–119
24. Adamson IY, Bowden DH (1974) The type 2 cell as progenitor of alveolar epithelial regeneration. A cytodynamic study in mice after exposure to oxygen. Lab Invest 30:35–42
25. Lawson WE, Polosukhin VV, Stathopoulos GT, Zoia O, Han W, Plieth D, Loyd JE, Neilson EG, Blackwell TS (2005) Characterization of fibroblast-specific protein 1 in pulmonary fibrosis. Am J Respir Crit Care Med 171:889–907
26. Li Y, Tan X, Dai C, Stolz DB, Wang D, Liu Y (2009) Inhibition of integrin-linked kinase attenuates renal interstitial fibrosis. J Am Soc Nephrol 20(9):1907–1918
27. Bowden DH (1981) Alveolar response to injury. Thorax 36:801–804
28. Hegab AE, Kubo H, Fujino N, Suzuki T, He M, Kato H, Yamaha M (2010) Isolation and characterization of murine multipotent lung stem cells. Stem Cells Dev 19(4):523–526
29. Flier SN, Tanjore H, Kokkotou EG, Sugimoto H, Zeisberg M, Kalluri R (2010) Identification of epithelial to mesenchymal transition as a novel source of fibroblasts in intestinal fibrosis. J Biol Chem 285(26):20202–20212
30. Moeller A, Ask K, Warburton D, Gauldie J, Kolb M (2008) The bleomycin animal model: a useful tool to investigate treatment options for idiopathic pulmonary fibrosis? Int J Biochem Cell Biol 40(3):362–382
31. Hardie WD, Glasser SW, Hagood JS (2009) Emerging concepts in the pathogenesis of lung fibrosis. Am J Pathol 175(1):3–16
32. Gilles G, Polette M, Piette J, Delvigne AC, Thompson EW, Foidart JM, Birembaut P (1996) Vimentin expression in cervical carcinomas: association with invasive and migratory potential. J Pathol 180(2):175–180
33. Paccione RJ, Miyazaki H, Patel V, Waseem A, Gutkind JS, Zehner ZE, Yeudall WA (2008) Keratin down-regulation in vimentin-positive cancer cells is reversible by vimentin RNA interference, which inhibits growth and motility. Mol Cancer Ther 7(9):2894–2903

Virchows Arch (2010) 457:577–583
DOI 10.1007/s00428-010-0975-8

ORIGINAL ARTICLE

TLE1 expression in malignant mesothelioma

Atsuji Matsuyama · Masanori Hisaoka · Mahoko Iwasaki · Mao Iwashita · Sachi Hisanaga · Hiroshi Hashimoto

Received: 7 May 2010 / Revised: 29 July 2010 / Accepted: 7 September 2010 / Published online: 21 September 2010
© Springer-Verlag 2010

Abstract Malignant mesothelioma, an aggressive and often lethal tumor commonly associated with asbestos exposure, has been morphologically classified into epithelial, biphasic, and sarcomatoid subtypes. Histological distinction between biphasic or sarcomatoid mesothelioma and synovial sarcoma may be problematic in certain circumstances of intrathoracic location because of their similar clinicopathologic features, including not only their morphology but also occasional positive immunoreaction of mesothelioma markers. TLE1, which plays an important role in Wnt pathway, has been shown to be a specific marker for synovial sarcoma and diagnostically is useful; however, TLE1 expression in malignant mesotheliomas has not been fully evaluated. We immunohistochemically examined the expression of TLE1, factors related to the Wnt pathway including β-catenin and cyclin D1, and mesothelioma markers including calretinin, HBME-1, cytokeratin 5/6, and thrombomodulin in 29 malignant mesotheliomas. TLE1 was variably expressed in 28 malignant mesotheliomas regardless of histomorphological subtype with >25% of positive cells in 20 cases (69.0%). There was no evidence of association of TLE1 expression with immunoreactivity to other markers. Our study showed no or limited value of the immunohistochemical TLE1 expression in distinguishing malignant mesothelioma and synovial sarcoma.

A. Matsuyama · M. Hisaoka · M. Iwasaki · M. Iwashita · S. Hisanaga · H. Hashimoto (✉)
Department of Pathology and Oncology, School of Medicine, University of Occupational and Environmental Health, 1-1 Iseigaoka, Yahatanishi-ku, Kitakyushu 807-8555, Japan
e-mail: hiroshi@med.uoeh-u.ac.jp

A. Matsuyama
e-mail: amatsu@med.uoeh-u.ac.jp

Keywords Malignant mesothelioma · Synovial sarcoma · TLE1 · Differential diagnosis · Immunohistochemistry

Introduction

Malignant mesothelioma is an aggressive, often lethal tumor commonly associated with asbestos exposure [1]. The 2004 World Health Organization classification broadly classifies malignant mesothelioma into three subtypes: epithelial, biphasic, and sarcomatoid mesothelioma [1]. In contrast to epithelioid mesothelioma, which may have histological features reminiscent of carcinoma, biphasic, and sarcomatoid mesotheliomas should be histologically differentiated from a variety of tumors, including sarcomatoid carcinoma or mesenchymal tumors. Synovial sarcoma is one of the most problematic differential diagnoses of biphasic or sarcomatoid malignant mesothelioma in certain circumstances of pleural and pulmonary locations [2, 3] because of their overlapping monophasic fibrous or biphasic epithelioid and sarcomatoid morphology and occasional positive immunoreaction of some mesothelioma markers [4]. Demonstration of the reciprocal translocation t(X;18)(p11;q11) or the resulting SS18–SSX gene fusion by cytogenetics, reverse transcription-polymerase chain reaction or fluorescence in situ hybridization has proven specific for synovial sarcoma and diagnostically useful [1]; however, assessments for these genetic aberrations require an apparatus or certain techniques for genetic or molecular assays, which are not always available in pathological departments or laboratories. It may be practically valuable to make a correct diagnosis without such an ancillary molecular technique. TLE1, which plays an important role in the Wnt pathway [5], has been shown to be a specific and diagnostically useful immunohistochemical

marker for synovial sarcoma [6]. Subsequently, TLE1 expression has been demonstrated even in a subset of soft tissue tumors other than synovial sarcoma [7–9] and might play a limited role in diagnosing synovial sarcoma; however, there have been few reports of the status of TLE1 in malignant mesotheliomas [8].

In the present study, we immunohistochemically evaluated the expression of TLE1 in a series of malignant mesothelioma to assess its value in differentiating malignant mesothelioma from synovial sarcoma. Expressions of mesothelioma markers and factors associated with the Wnt pathway were also examined in both types of tumors.

Materials and methods

Twenty-nine lesions of malignant mesothelioma were retrieved from the files of the Department of Pathology, University of Occupational and Environmental Health Hospital, and of the Department of Pathology and Oncology, School of Medicine, University of Occupational and Environmental Health, Kitakyushu, Japan. They were clinicopathologically and immunohistochemically re-evaluated, and subclassified into the three histological variants: epithelioid, sarcomatoid, and biphasic. Biphasic mesothelioma was defined as tumor with more than 10% of each epithelioid or sarcomatoid component [1].

For the immunohistochemical analysis, Histofine Simple Stain MAX PO (Nichirei, Tokyo, Japan) employing the universal immunoenzyme amino acid polymer method was used. The TLE1 antibody (sc-9121, rabbit polyclonal, 1:20; Santa Cruz, CA, USA) used and its dilution were described in previous studies [6, 8, 9]. We preliminarily tested several standard pretreatment methods, including those used in the previous studies. As a result, heating in 10 mmol/L citrate buffer at pH 6.0 by a pressure cooker for 10 min was adopted because of its most constant and intense staining results. Other antibodies used were as follows: β-catenin (14/beta-catenin, monoclonal, 1:100; BD Transduction Laboratories, San Diego, CA, USA), cyclin D1 (SP4, rabbit monoclonal, 1:50; Nichirei), calretinin (DC8, rabbit polyclonal, 1:1; Zymed, south San Francisco, CA, USA), cytokeratins 5/6 (D5/16 B4, monoclonal, 1:50; Dako, Glostrup, Denmark), thrombomodulin (TM-1009, monoclonal, 1:25; Dako), and HBME-1 (monoclonal, 1:100; Dako). For antigen retrieval, heating in 10 mmol/L citrate buffer (pH 6.0) by a pressure cooker was performed for 10 min before the immunoreaction for β-catenin and cyclin D1 or in 1 mM ethylenediamine tetraacetic acid (EDTA) solution at pH 8.0 for calretinin and cytokeratin 5/6. A protease treatment was performed for thrombomodulin. After the incubation with the primary antibodies at room temperature, the reaction products were visualized by soaking sections in 0.2 mg/mL diaminobenzidine in 0.05 mol/L Tris–HCl buffer, pH 7.6, containing 0.003% hydrogen peroxide. For an evaluation of the TLE1 expression in malignant mesotheliomas, we examined 114 slides derived from 20 biopsy, 20 surgical, and two autopsy specimens (one to seven slides per specimen), including those of recurrent or metastatic tumors because TLE1 expression was reported to be potentially heterogeneous within the same tumor [9]. We evaluated the immunoreactivity of the markers in each of the epithelioid and sarcomatoid components of the mesotheliomas as follows: 3+, positive in >50% of tumor cells; 2+, positive in 25–50% of tumor cells; 1+, positive in 5–25% of tumor cells; and −, positive in <5% of tumor cells. In the evaluation of TLE1 immunohistochemistry, only intranuclear staining was considered to be positive. We also examined immunoreactivity of TLE1, β-catenin, and cyclin D1 in five cases of synovial sarcoma, all of which were confirmed to possess SS18–SSX fusion transcripts by reverse transcription-polymerase chain reaction [10], and nine non-neoplastic mesothelial lesions (seven organizing or fibrinous pleuritis, one mesothelial cyst, and one peritonitis due to appendicitis), and TLE1 in seven lung carcinomas (four adenocarcinomas, two sarcomatoid carcinomas, one squamous cell carcinoma). As negative controls, the reaction with non-immuned serum obtained from the normal mouse and the commercially available rabbit serum (Nichirei) was also examined with the heating antigen retrieval in citrate buffer or EDTA in specimens of malignant mesotheliomas. Correlation of the immunohistochemical expression between TLE1 and each marker examined was determined by Spearman's rank correlation coefficient. Probability values of <0.05 were considered significant.

Results

The 29 patients with malignant mesotheliomas examined in this study consisted of 27 men and two women whose ages ranged from 51 to 85 years (mean, 63.3 years; median, 66 years). Of the 29 tumors, 27 tumors were located in the pleura, one in the peritoneum and one in the pericardium. Twenty-one patients had occupational history of asbestos exposure, although such clinical information was not available in two other cases. On the basis of a histological review, 12 (41.4%) tumors were subclassified as epithelioid type (Fig. 1a), ten (34.5%) as biphasic type, and seven (24%) as sarcomatoid type (Fig. 1e). The sarcomatoid components in ten biphasic mesotheliomas accounted for 20–80%. Information regarding the clinical outcome was available in 22 cases, and 20 patients died in 1–87 months (median, 7 months; mean, 14.2 months) after diagnosis. The other two patients were alive at 3 months after diagnosis.

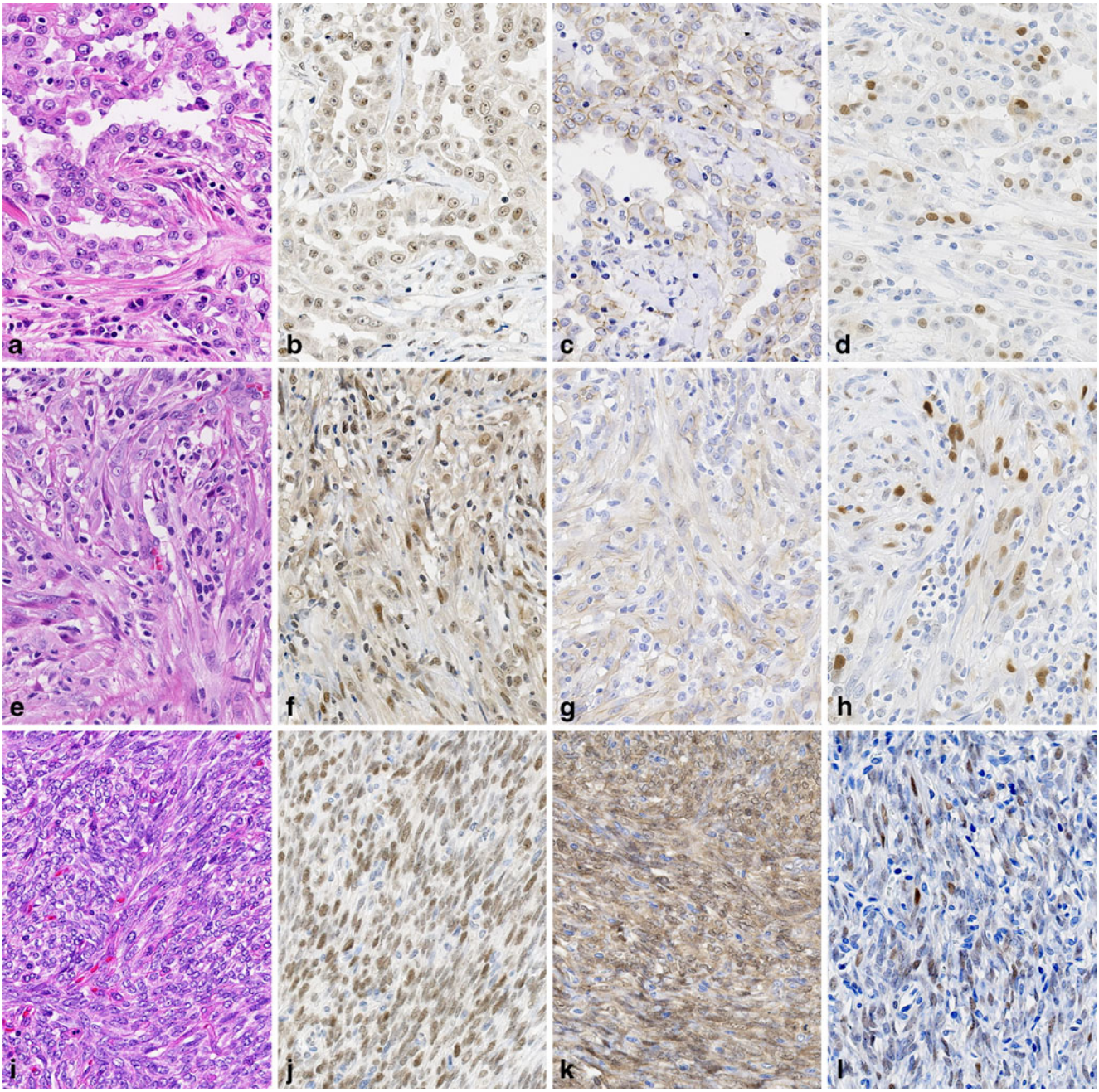

Fig. 1 Hematoxylin & eosin staining (**a**, **e**, **i**) and immunohistochemical findings in epithelioid (case 7, **a**–**d**), and sarcomatoid (case 26, **e**–**h**) mesotheliomas and synovial sarcoma (**i**–**l**). TLE1 (**b**, **f**) and cyclin D1 (**d**, **h**) are expressed irrespective of the histologic subtypes of mesothelioma, whereas both subtypes lack nuclear expression of β-catenin (**c**, **g**). Many tumor cells in a synovial sarcoma are positively reactive to TLE1 (**j**), β-catenin (**k**), and cyclin D1 (**l**)

The immunohistochemical results of malignant mesotheliomas are shown in Table 1 and Fig. 1. TLE1 expression was variably observed in 28 of the 29 (96.6%) cases of malignant mesothelioma, displaying 2+ or 3+ positivity in 20 cases (69.0%), although the intensity of the immunoreaction was somewhat weaker than that in synovial sarcomas (Fig.1b, f, j). According to the histomorphological subtypes, eight of 12 epithelioid mesotheliomas and the epithelioid component of five of ten biphasic mesotheliomas [total, 13 of 22 (59.1%) mesotheliomas with epithelioid features] displayed 2+ or 3+ TLE1 positivity, whereas six of seven sarcomatoid mesotheliomas and the sarcomatoid component of six of ten biphasic mesotheliomas [total, 12 of 17 (70.6%) mesotheliomas with sarcomatoid features] showed 2+ or 3+ positivity. Only one tumor regarded as TLE1 negative was epithelioid mesothelioma. The expression of calretinin was seen in all 29 (100%) malignant mesotheliomas. HBME-1 was positive in 21

(72.4%) mesotheliomas, cytokeratin 5/6 in 20 (69.0%), and thrombomodulin in 24 (82.8%). The expression status of these markers was not correlated with TLE1 expression (Table 1). Nuclear β-catenin expression was confined to less than 5% of tumor cells in all the mesotheliomas, although its variable cytoplasmic and almost constant membranous expression was observed (Fig. 1c, g). Cyclin D1 was expressed in 26 (89.7%) mesotheliomas with 16 (55.2%) cases of 2+ or 3+ reactivity (Fig. 1d, h). TLE1 (3+, four cases; 2+, one case) and cyclin D1 (3+, two cases; 2+, one case; 1+, two cases) were immunoreactive in all five synovial sarcomas examined, and nuclear β-catenin expression was also variably recognized in four cases (3+, two cases; 2+, one case; 1+, one case; negative, one case) (Fig. 1i–l). Nuclei of non-neoplastic mesothelial cells were constantly positive for TLE1 (Fig. 2) but negative for β-catenin and cyclin D1. Among the seven lung carcinomas examined, six were negative for TLE1. The remaining one adenocarcinoma focally expressed TLE1.

Discussion

TLE1 is a member of the *TLE* gene family that encodes human transcriptional repressors, which bind to Tcf/Lef family transcription factors resulting in displacing β-catenin

Table 1 Histological types and immunohistochemical results of the 29 malignant mesotheliomas

Case	Histologic type	Sarcomatoid component (%)	TLE1	β-Catenin[a]	Cyclin D1	Calretinin	CK 5/6	TM	HBME-1
1	Epithelioid	0	3	0	2	3	1	2	2
2	Epithelioid	0	3	0	3	3	2	3	3
3	Epithelioid	<5	1	0	0	3	3	1	3
4	Epithelioid	<5	1	0	2	3	3	2	3
5	Epithelioid	<5	1	0	0	3	3	1	1
6	Epithelioid	<5	3	0	2	3	3	1	3
7	Epithelioid	<5	3	0	2	3	2	0	3
8	Epithelioid	<5	3	0	1	3	2	2	3
9	Epithelioid	<10	0	0	3	3	1	0	3
10	Epithelioid	<10	3	0	1	3	3	1	3
11	Epithelioid	<10	3	0	3	3	1	3	3
12	Epithelioid	<10	3	0	2	3	2	3	1
13	Biphasic[b]	20	1/1	0/0	1/1	3/1	3/2	1/1	2/0
14	Biphasic	20	3/3	0/0	1/1	3/3	1/1	1/2	3/2
15	Biphasic	30	3/3	0/0	3/2	1/0	1/0	2/2	1/0
16	Biphasic	40	3/3	0/0	3/3	3/3	1/0	0/1	1/0
17	Biphasic	50	1/3	0/0	1/1	3/3	1/0	1/1	3/0
18	Biphasic	50	1/1	0/0	2/2	2/2	0/0	0/0	0/0
19	Biphasic	50	3/3	0/0	1/1	3/3	3/1	1/1	3/1
20	Biphasic	70	1/1	0/0	1/0	3/0	2/0	3/1	2/0
21	Biphasic	80	1/0	0/0	0/0	3/1	1/0	1/1	3/0
22	Biphasic	80	2/2	0/0	1/2	3/3	0/0	0/1	0/0
23	Sarcomatoid	>90	3	0	2	3	0	2	2
24	Sarcomatoid	>95	1	0	1	2	0	0	0
25	Sarcomatoid	>95	3	0	2	2	0	0	0
26	Sarcomatoid	>95	3	0	3	3	0	1	0
27	Sarcomatoid	100	3	0	1	1	0	1	0
28	Sarcomatoid	100	3	0	1	2	0	1	0
29	Sarcomatoid	100	3	0	2	1	0	1	0
Probability value[c]				>0.999	0.0662	0.610	0.468	0.101	0.857

TM thrombomodulin, *CK 5/6* cytokeratin 5/6

[a] Only nuclear β-catenin expression is scored as positive

[b] Each immunohistochemical result of biphasic mesotheliomas is shown as an epithelioid component/sarcomatoid component

[c] Correlation with TLE1 expression

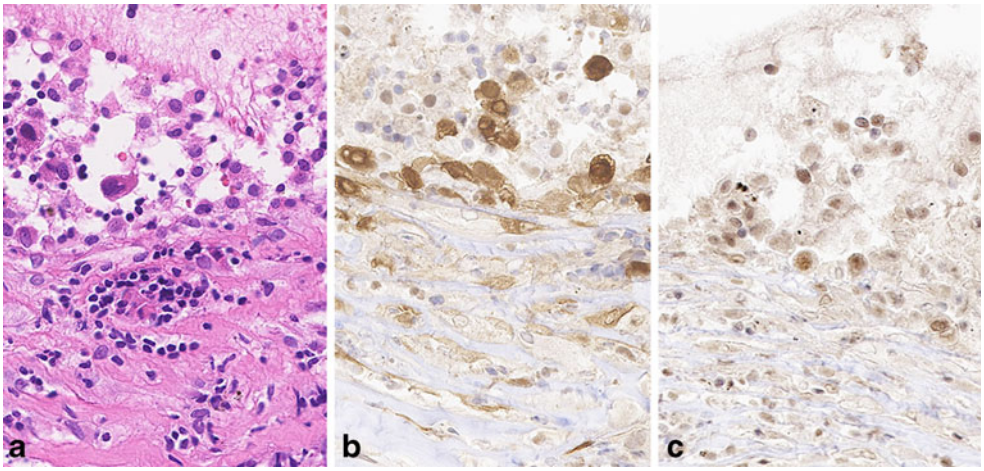

Fig. 2 Hematoxylin & eosin staining (**a**) and immunostaining for calretinin (**b**), and TLE1 (**c**) in non-neoplastic, reactive mesothelial cells. Non-neoplastic mesothelial cells are constantly immunoreactive to TLE1 (**c**)

and repressing the Wnt/β-catenin signaling pathway [5]. The expression of TLE1 in synovial sarcomas has been demonstrated by several DNA microarray studies [11–14] and immunohistochemical studies [6–9, 15]. Because of its sensitivity and specificity, TLE1 was initially demonstrated to be a diagnostically useful immunohistochemical marker in synovial sarcoma [6]; however, Kosemehmetoglu et al. [9] showed that TLE1 expression is not specific for synovial sarcoma, being variably immunoreactive in 37% of soft tissue tumors other than synovial sarcoma. The TLE1-positive tumors included a malignant peripheral nerve sheath tumor, which may be one of the most important differential diagnoses of synovial sarcoma, solitary fibrous tumor, schwannoma, epithelioid sarcoma, acral myxoinflammatory fibroblastic sarcoma, chordoma, endometrial stromal sarcoma, leiomyosarcoma, liposarcoma, lipoma, myxofibrosarcoma, neurofibroma, rhabdomyosarcoma, undifferentiated pleomorphic sarcoma, Ewing sarcoma, gastrointestinal stromal tumor, chondrosarcoma, clear cell sarcoma, carcinosarcoma, fibroxanthoma, hemangiopericytoma, fibrosarcoma, and spindle epithelial tumor with thymus-like differentiation [6–9]. On the other hand, TLE1 expression is also seen in non-neoplastic mesothelial cells [9], but the expression of TLE1 in malignant mesotheliomas has not been fully evaluated [8]. It is sometimes difficult to distinguish malignant mesothelioma from synovial sarcoma originating in the thoracic cavity because they occasionally have overlapping clinicopathologic characteristics, including the biphasic epithelioid and sarcomatoid histomorphology, and expression of mesothelioma markers [2, 16]. The expression of calretinin, a calcium-binding protein expressed in both neural tissue and non-neural cell types, including mesothelium [17], has been recognized in not only most malignant mesotheliomas [4, 16, 17] but also in 60% of synovial sarcomas [4]. In addition, other markers sensitive to mesothelioma such as HBME-1, cytokeratin 5/6, and thrombomodulin are not specific for mesothelioma [4, 16] and may be expressed in a subset of synovial sarcoma [4]. In the present study, we examined the immunohistochemical expression of TLE1 in malignant mesotheliomas and compared its expression pattern with other markers that are typically known to be expressed in malignant mesotheliomas. In our results, 28 of 29 cases exhibited positive immunoreaction to TLE1, irrespective of their histological subtypes or of expression of other mesothelioma-related immunohistochemical markers. Despite the different detection systems (Envision system employing dextran polymer method or the Ventana automated immunostainer was utilized in the previous studies) and the different antigen retrieval methods used in the previous studies [6, 8, 9], the constant immunohistochemical expression of TLE1 in synovial sarcomas both in previous studies and ours suggest that these technical differences have not influenced the staining results. The difference of intensity of TLE1 expression between malignant mesotheliomas and synovial sarcoma was small and might be arbitrary. Immunoreactivity for TLE1 is by no means specific for synovial sarcoma and seems to have no use or, if any, only a supplementary role in differentiating synovial sarcoma from mesothelioma.

We also examined the immunohistochemical expression of β-catenin and cyclin D1, which may be associated with TLE1 via the Wnt signaling pathway, to assess the role of TLE1 in tumorigenesis or cell cycle regulation in malignant mesotheliomas. Our results demonstrated that most mesotheliomas exhibited a low or moderate level of nuclear expression of cyclin D1, whereas β-catenin was limited to membranous or cytoplasmic localization with no or quite limited nuclear accumulation [18]. In synovial sarcoma, SS18–SSX fusion protein has been shown to lead nuclear accumulation of β-catenin [14], and it has been speculated that TLE1 overexpression may represent a compensatory response to excessive β-catenin signaling or serve to limit transcriptional activation to certain genes, and that the nuclear expression of TLE1 and β-catenin resulting in

transcriptional activation of target genes plays an important role in the pathogenesis of this tumor [6]. Previous studies showed that the SS18–SSX-mediated nuclear accumulation of cyclin D1 in synovial sarcomas was mediated by the PI3K-Akt-GSK3β pathway [19, 20] or aberrant β-catenin nuclear expression [21]. In general, cyclin D1 may also be activated without nuclear β-catenin overexpression via many different transcription signalings such as the MAPK pathway [22], JAK–STAT pathway [19, 23], and Notch–CSL pathway [20]. In malignant mesothelioma, MAPK is frequently expressed and activated with phosphorylation of the extracellular-regulated kinase, the c-Jun amino-terminal kinase, and p38 [24, 25]. The activation of cyclin D1 in malignant mesotheliomas seems to be induced via different mechanisms from synovial sarcoma and may be unrelated to TLE1 or the Wnt pathway. The constant TLE1 expression in non-neoplastic mesothelial cells suggests that TLE1 expression is not essential for malignant transformation of mesothelial cells. Further studies are required to clarify the exact role of TLE1 in these tumors.

In conclusion, our study showed that most of the malignant mesotheliomas expressed TLE1, and that immunohistochemistry for TLE1 is not useful or may have only a limited role in distinguishing between malignant mesothelioma and synovial sarcoma. The nuclear accumulation of β-catenin was not seen in malignant mesothelioma in contrast to synovial sarcoma, although both tumors frequently exhibited cyclin D1 overexpression, suggesting distinct biological significance of TLE1 in these tumors.

Conflict of interest statement We declare that we have no conflict of interest.

References

1. Churg A, Roggli V, Galateau-Salle F et al (2004) Mesothelioma. In: Travis WD, Brambilla E, Müller-Hermelink HK, Harris C (eds) Pathology and genetics of tumours of the lung, pleura, thymus and heart. IARC, Lyon, pp 128–136
2. Nicholson AG, Goldstraw P, Fisher C (1998) Synovial sarcoma of the pleura and its differentiation from other primary pleural tumours: a clinicopathological and immunohistochemical review of three cases. Histopathology 33:508–513
3. Okamoto S, Hisaoka M, Daa T, Hatakeyama K, Iwamasa T, Hashimoto H (2004) Primary pulmonary synovial sarcoma: a clinicopathologic, immunohistochemical, and molecular study of 11 cases. Hum Pathol 35:850–856
4. Miettinen M, Limon J, Niezabitowski A, Lasota J (2001) Calretinin and other mesothelioma markers in synovial sarcoma: analysis of antigenic similarities and differences with malignant mesothelioma. Am J Surg Pathol 25:610–617
5. Daniels DL, Weis WI (2005) β-catenin directly displaces Groucho/TLE repressors from Tcf/Lef in Wnt-mediated transcription activation. Nat Struct Mol Biol 12:364–371
6. Terry J, Saito T, Subramanian S, Ruttan C, Antonescu CR, Goldblum JR, Downs-Kelly E, Corless CL, Rubin BP, van de Rijn M, Ladanyi M, Nielsen TO (2007) TLE1 as a diagnostic immunohistochemical marker for synovial sarcoma emerging from gene expression profiling studies. Am J Surg Pathol 31:240–246
7. Folpe AL, Lloyd RV, Bacchi CE, Rosai J (2009) Spindle epithelial tumor with thymus-like differentiation: a morphologic, immunohistochemical, and molecular genetic study of 11 cases. Am J Surg Pathol 33:1179–1186
8. Jagdis A, Rubin BP, Tubbs RR, Pacheco M, Nielsen TO (2009) Prospective evaluation of TLE1 as a diagnostic immunohistochemical marker in synovial sarcoma. Am J Surg Pathol 33:1743–1751
9. Kosemehmetoglu K, Vrana JA, Folpe AL (2009) TLE1 expression is not specific for synovial sarcoma: a whole section study of 163 soft tissue and bone neoplasms. Mod Pathol 22:872–878
10. Tsuji S, Hisaoka M, Morimitsu Y, Hashimoto H, Shimajiri S, Komiya S, Ushijima M, Nakamura T (1998) Detection of SYT-SSX fusion transcripts in synovial sarcoma by reverse transcription-polymerase chain reaction using archival paraffin-embedded tissues. Am J Pathol 153:1807–1812
11. Baird K, Davis S, Antonescu CR, Harper UL, Walker RL, Chen Y, Glatfelter AA, Duray PH, Meltzer PS (2005) Gene expression profiling of human sarcomas: insights into sarcoma biology. Cancer Res 65:9226–9235
12. Beck AH, West RB, van de Rijn M (2010) Gene expression profiling for the investigation of soft tissue sarcoma pathogenesis and the identification of diagnostic, prognostic, and predictive biomarkers. Virchows Arch 456:141–151
13. Ng TL, Gown AM, Barry TS, Cheang MC, Chan AK, Turbin DA, Hsu FD, West RB, Nielsen TO (2005) Nuclear beta-catenin in mesenchymal tumors. Mod Pathol 18:68–74
14. Pretto D, Barco R, Rivera J, Neel N, Gustavson MD, Eid JE (2006) The synovial sarcoma translocation protein SYT-SSX2 recruits β-catenin to the nucleus and associates with it in an active complex. Oncogene 25:3661–3669
15. Knösel T, Heretsch S, Altendorf-Hofmann A, Richter P, Katenkamp K, Katenkamp D, Berndt A, Petersen I (2010) TLE1 is a robust diagnostic biomarker for synovial sarcomas and correlates with t(X;18): analysis of 319 cases. Eur J Cancer 46:1170–1176
16. Lucas DR, Pass HI, Madan SK, Adsay NV, Wali A, Tabaczka P, Lonardo F (2003) Sarcomatoid mesothelioma and its histological mimics: a comparative immunohistochemical study. Histopathology 42:270–279
17. Gotzos V, Vogt P, Celio MR (1996) The calcium binding protein calretinin is a selective marker for malignant pleural mesotheliomas of the epithelial type. Pathol Res Pract 192:137–147
18. Abutaily AS, Collins JE, Roche WR (2003) Cadherins, catenins and APC in pleural malignant mesothelioma. J Pathol 201: 355–362
19. Sakamoto K, Creamer BA, Triplett AA, Wagner KU (2007) The Janus kinase 2 is required for expression and nuclear accumulation of cyclin D1 in proliferating mammary epithelial cells. Mol Endocrinol 21:1877–1892

20. Stahl M, Ge C, Shi S, Pestell RG, Stanley P (2006) Notch1-induced transformation of RKE-1 cells requires up-regulation of cyclin D1. Cancer Res 66:7562–7570
21. Horvai AE, Kramer MJ, O'Donnell R (2006) Beta-catenin nuclear expression correlates with cyclin D1 expression in primary and metastatic synovial sarcoma: a tissue microarray study. Arch Pathol Lab Med 130:792–798
22. Ortiz J, Funk C, Schäfer A, Lechner J (2009) Stu1 inversely regulates kinetochore capture and spindle stability. Genes Dev 23:2778–2791
23. Wang C, Li Z, Fu M, Bouras T, Pestell RG (2004) Signal transduction mediated by cyclin D1: from mitogens to cell proliferation: a molecular target with therapeutic potential. Cancer Treat Res 119:217–237
24. Sekido Y (2008) Molecular biology of malignant mesothelioma. Environ Health Prev Med 13:65–70
25. Vintman L, Nielsen S, Berner A, Reich R, Davidson B (2005) Mitogen-activated protein kinase expression and activation does not differentiate benign from malignant mesothelial cells. Cancer 103:2427–2433

Virchows Arch (2010) 457:585–595
DOI 10.1007/s00428-010-0970-0

ORIGINAL ARTICLE

An additional long-term mechanism of NF-κB regulation after cytokine treatment in a human hepatoma cell line

Patricia Kohlhof

Received: 18 May 2010 / Revised: 26 August 2010 / Accepted: 27 August 2010 / Published online: 23 September 2010
© Springer-Verlag 2010

Abstract The eukaryotic transcription factor nuclear factor-κB (NF-κB) is mainly involved in the regulation of immune response and inflammation. A prolonged activation of NF-κB has been reported in context with chronic diseases. What leads to a prolongation of NF-κB activity is not well understood. Here, an increase in total intracellular NF-κB protein and mRNA levels as well as a temporary colocalization of NF-κB with proteasomes in human hepatocytes after treatment with TNF-α or IL-1β is reported. This indicates that beside an instantaneous activation of NF-κB and partly autoregulated inactivation by breakdown and synthesis of the inhibitors of NF-κB (IκBs), there are also mechanisms for a long-term regulation by de novo-synthesis and degradation of NF-κB protein.

Keywords NF-κB regulation · NF-κB synthesis · NF-κB degradation · Proteasomal degradation · Inflammatory cytokines · TNF-α · IL-1β · HepG2 cells

Introduction

Nuclear factor-κB (NF-κB) is a family of eukaryotic transcription factors with a common N-terminal region. The Rel homology domain consists of about 300 amino acids [1] and recognizes a common DNA sequence motive [2]. It is responsible for dimerization and binding of inhibitors of NF-κB, the IκBs, [3] and contains a nuclear localization signal. The NF-κB family consists of several distinct proteins [1]. They are expressed ubiquitously, usually exist as homo- or heterodimers and are involved in development, cell growth control [1], the modulation of apoptosis [2, 3], and acute immune and inflammatory response [3, 4]. NF-κBs are activated by a wide range of stimuli, including exposure to bacterial lipopolysaccharide (LPS) or inflammatory cytokines such as TNF-α or IL-1β [5–12]. Some NF-κB family members, especially the p65/p50 heterodimer, are inducible by a release from the NF-κB–IκB complex. This complex mediates a tight regulation of NF-κB activity.

The IκBs share the ankyrin repeat motif mediating NF-κB–IκB interaction [13]. In most cell types, NF-κB is inactivated by IκBs, and activation is achieved by rapid phosphorylation, ubiquitination, and proteasomal degradation of the inhibitors. The IκBα gene contains an NF-κB binding site in its promoter region, and IκBα is directly upregulated by NF-κB. A study of the activation of hepatocytes by cytokines reports a time course of NF-κB activation for about 360 min and a biphasic return to the inactivated state, reflecting different modes of IκB resynthesis and different stability of the different IκB–NF-κB complexes [10, 14].

This downregulation of NF-κB activity via autoregulation has been reported for a range of stimuli and cell types [15, 16–19]. Prolonged NF-κB activity, partly achieved by de novo-synthesis of NF-κB, on the other hand, has so far only been described in two settings: (1) In endothelial cells and white blood cells of diabetic rats, binding of advanced glycosylation end products (AGEs) to AGE receptors (RAGEs) results in synthesis of NF-κB (p65) and a prolonged activation of NF-κB which lasts longer than 1 week. Simultaneously, there is a new synthesis of IκBs, associated with an imbalance, which seems to contribute to sustained NF-κB activation [20]. (2) In fibroblasts infected with human cytomegalovirus, an activation of NF-κB

P. Kohlhof
Institute of Anatomy and Cell Biology II,
University of Heidelberg,
Heidelberg, Germany

Present Address:
P. Kohlhof (✉)
Institute of Pathology, Klinikum Stuttgart,
Kriegsbergstrasse 60,
70174 Stuttgart, Germany
e-mail: P.Kohlhof@klinikum-stuttgart.de

(p105/p50 and p65) promoters was reported, as well as an increase of NF-κB mRNA. Protein levels were not investigated. The increase in p65 mRNA levels in this model occurred 8 h post-induction and could be suppressed by pretreatment with cycloheximide [21–24].

It is interesting, in this context, that the p65 promoter does not contain NF-κB binding sites, but potential SP1 and HIP1 binding sites [25]. One study [26] described a distal (about 2. 2 kb upstream of the promoter region) NF-κB-dependent enhancer region in the MCP-1 gene in monocytes. This gene has an SP1-dependent promoter that, after induction with TNF-α, is only activated after NF-κB-induced modification of the distal enhancer. This process additionally involves the cofactors CBP and p300.

A stabilization of NF-κB by overexpression of Pin-1 and increased polyubiquitination and proteasomal degradation mediated through SOCS-1 has been reported. Pin-1 has been shown to be upregulated in certain types of cancer that constitutively overexpress NF-κB [27–29]. SOCS-1, on the other hand, is down- regulated in some types of cancer [30, 31].

Our findings show NF-κB activation in context with acute inflammation suggesting an additional mechanism of NF-κB regulation after stimulation with cytokines which results in a prolonged activation of about 24 h and involves protein synthesis and proteasomal degradation. This activation is more persistent than the rapid NF-κB activation usually associated with inflammation, but less persistent than in context with degeneration and chronic disease.

Materials and methods

Cell culture and treatment and cellular fractionation

Human hepatoma (HepG2) cells were maintained routinely in minimal essential medium-α supplemented with L-glutamine, penicillin/streptomycin (all from Gibco/Life Technologies) and 9% (*v*/*v*) heat-inactivated fetal calf serum (PAA). They were grown to about 80% confluence before further investigation.

For Western blot analysis, cells were adapted to serum-free conditions [32] before stimulants were added (as indicated below). Cells were harvested and centrifuged and pellets treated depending on desired fraction. For immunofluorescence staining, cells were disseminated in a density of 1×10^5 cells/well on cover glasses plated with type I collagen (Gibco) in 24-well microtiter plates (Falcon). For cellular fractions, whole cell lysates were obtained by rupturing pellets in TVBE containing 0.2% Triton X-100 with a Potter homogenizer. Nuclear extracts were prepared, and the purity and integrity of nuclei were assessed microscopically after methylene blue staining, according to a standard protocol by Rickwood et al. [33].The isolation of enriched proteasomal fractions was performed according to a protocol modified after [34, 35]. In short, cells grown in cell line flasks with 18% FCS in the culture chamber for 5 days and harvested with accutase were centrifuged twice in PBS, resuspended, homogenized, and centrifuged for 20 min at 15,000×*g*. The supernatant was laminated on top of a linear (19–46% glycerol in proteasome buffer) gradient and centrifuged in a swing-out bucket rotor (VTi50 in a L5-B65 ultracentrifuge, Beckmann) at 200,000×*g* for 270 min. Five fractions of 3 ml each and onwards of 1.5 ml each were collected from top to bottom, and fractions of similar protein content (shown by electrophoresis and silver impregnation) were pooled and concentrated using VivaSpin columns. For RNA isolation, cells were stored in RNAlater (Qiagen) after harvesting.

Stock solutions of 2 μg/mL of IL-1β or TNF-α (R&D Systems) were prepared in PBS/0.2% FCS. Concentrations and time courses of cytokines and *N*-acetylcysteine (NAC), cycloheximide, and puromycin (Sigma) were established according to standard protocols and tested to be effective without cytotoxicity.

Western blotting

The protein concentration of each sample was measured according to Bradford (Bio-Rad) and a Kontron spectrophotometer. Samples were denaturated with SDS sample buffer containing 5% α-mercaptoethanol at 95°C for 10 min and electrophoresed on 12.5% Tris–HCl gels (Bio-Rad), followed by electrophoretic transfer to polyvinylidene difluoride (PVDF) membranes (Millipore). Western blot analysis of whole cell lysates was carried out with specific primary antibody against NFκBp65 (Santa Cruz, 1:200) on whole cell lysates and nuclear extracts. In experiments carried out regularly to assess tolerable concentrations of cytokeratins and other agents and to compare cells of higher passages to freshly thawed specimen, whole cell lysates of treated and untreated cells were separated electrophoretically, stained (Coumassie Brilliant Blue and silver impregnation according to Blum) and lanes compared with regard to relative protein content (data not shown). One extract of each cellular compartment was used as a control in each gel electrophoresis preceding Western blotting. Membranes were exposed to a horse radish peroxidase-conjugated species-specific secondary antibody (Santa Cruz) and ECL solution (Bio-Rad) and proteins made visible by detecting chemifluorescence emission with a Kodak Image Station. Student's T-test of 3 different experiments was performed for statistical analysis.

Northern blotting

RNA was isolated using an RNeasy Mini kit, mRNA using an Oligotex-mRNA kit (Qiagen), according to protocol. Concentration and purity were assessed photometrically.

The cDNA synthesis was performed using a SuperScript One-Step RT-PCR System (Invitrogen). Primers were: 5′-CGG CAT GGA CGA ACT GTT C-3′ (forward) and 5′-CAG CTT GGC AAC AGC TTT AT-3′ (reverse). DNA was separated electrophoretically and extracted with a QIAquick gel extraction kit (Qiagen), according to manufacturer's instructions. Ligation was obtained using a TOPO TA cloning kit (Invitrogen). Blue/white selection of transformed cells was carried out after incubation at 37°C for 1 h on agar plates containing ampicillin and coated with X-Gal (5-bromo-4-chlor-3-indolyl-β-D-galactopyranosid). Clones were picked and plasmids isolated using a Nucleospin Plasmid isolation kit (Macherey-Nagel). One of these clones was linearized and amplified with m13 primers (TOPO TA cloning kit, Invitrogen). In vitro transcription was accomplished with a DIG-RNA labeling mix (Roche) for 2 h at 37°C; EDTA was added to a concentration of 20 mM and cRNA precipitated with ethanol and resuspended in RNase-free water. A negative probe was generated by omitting labeled UTP. A short section of the labeled probes was sequenced (SeqLab). RNA was separated under denaturing agarose gel conditions, transferred to a nylon membrane by Northern blotting and crosslinked (Stratagene). Hybridization was carried out overnight at 68°C (Techne hybridization oven) under RNase-free conditions with 100 ng of linearized antisense probe per milliliter buffer. Membrane treatment was performed with anti-digoxigenin Fab fragments linked to alkaline phosphatase (1:10,000 in maleate buffer) and chemiluminescence substrate (Roche). Detection of chemiluminescence signals of Western and Northern blots was effective with a digital scanner (Kodak image station). The signal was analyzed using NIH Image 6.1 and Microsoft Excel 7.0. Student's T-test of 3 different experiments was performed for statistical analysis.

Immunocytochemistry

For indirect immunofluorescence staining, cells were fixed in 4% paraformaldehyde solution and incubated with goat anti-NFκBp65 antibody (Santa Cruz), fluorescence-labeled donkey anti-goat IgG (Alexa/Molecular Probes) and counterstained with DAPI (0.5 μg/ml). Cover glasses were mounted on microscope slides in moviol containing an anti-bleaching agent and assessed with a Leitz fluorescence microscope system with an analog camera, using a 100× magnifying oil immersion lens, pictures scanned (Nikon) and digitally processed with Adobe Photoshop. Cover slides not submitted to primary antibody, but otherwise treated equally, served as negative control.

Electron microscopy

For transmission electron microscopy, cells were grown on Melinex foil (Plano, Marburg, Germany) and fixed in 4% paraformaldehyde. Enriched proteasomal fractions were fixed in 0.25% glutaraldehyde, adsorbed to a membrane filter and embedded in agar. Further embedding for immunoelectron microscopy was performed in LRwhite. Ultra thin sections (50–60 nm, Reichert microtome) were transferred to nickel grids and contrasted with uranyl acetate. Antibodies against human NF-κB p65 (goat, Santa Cruz) and the 20S subunit of mammalian proteasomes (rabbit, Calbiochem) were labeled with species-specific secondary antibody linked with 10-nm gold particles or the protein A gold method with 5-nm gold particles, respectively. For negative staining, drops of the enriched proteasomal fractions were transferred to deionized grids and contrasted with 1% phosphotungstic acid, followed by 2% uranyl acetate. All grids were filmed with formvar and investigated with a LEO 906 electron microscope with a digital camera.

Results

Induction with proinflammatory cytokines can cause a late activation of NF-κB

Cells grown on cover slides were continuously treated with TNF-α (90 μg/mL) or IL-1β (5 ng/mL) for 30 min or 24 h, respectively. They were stained immunocytochemically with an NF-κB (p65) antibody and a fluorescent secondary antibody and counterstained with DAPI. Immunofluorescence at both intervals showed a nuclear translocation in treated cells as compared to a predominantly cytosolic staining in control cells (Fig. 1).

In parallel, cells treated with TNF-α or untreated cells were grown in culture flasks as described and harvested after 24 h. Nuclear extracts were prepared, separated electrophoretically and blotted on PVDF membranes. Immunoblotting was performed with NF-κB (p65) antibody and a horseradish peroxidase conjugated secondary antibody. With immunoblotting, an increase of about 50% of NF-κB signal could be detected in nuclear extracts of TNF-α- treated cells as compared to those of untreated cells. (Fig. 2).

The nuclear localization of NF-κB can be antagonized by the antioxidative reagent *N*-acetylcysteine

To investigate if nuclear localization induced by TNF-α is antagonized by an antioxidative reagent, cells grown on cover slides for 24 h were treated with different combinations of NAC and TNF-α and immunostained for NF-κB with a fluorescent probe. There were five sample preparations, namely, untreated cells, cells treated with TNF-α alone, cells treated with 10 mMol NAC alone, and cells treated with TNF-α combined with NAC in concentrations of 2 or 10 mMol. Three times, 100

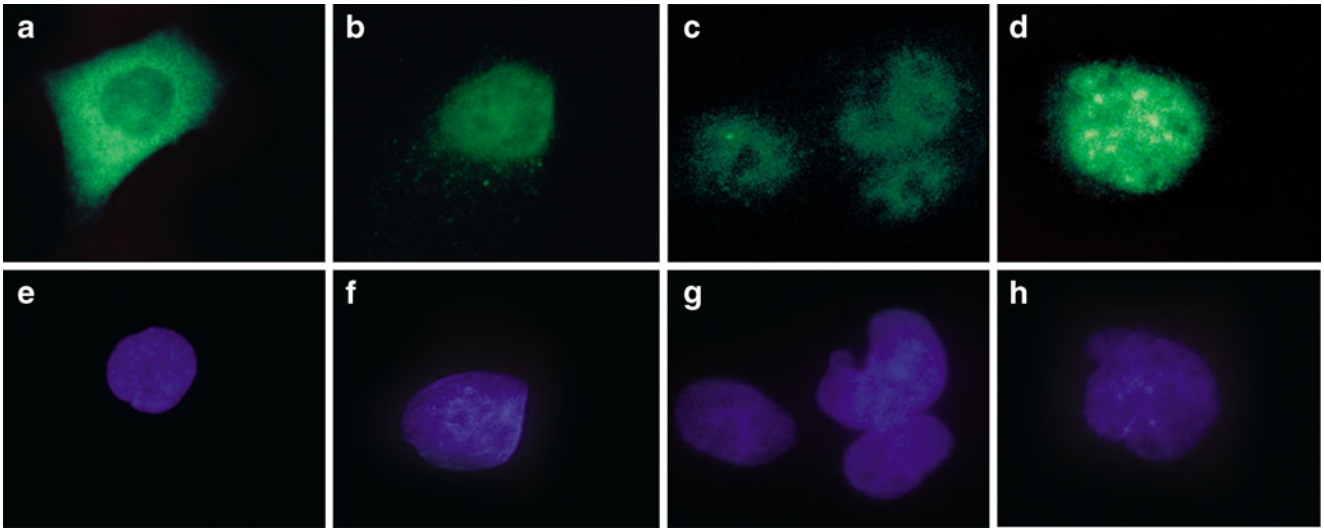

Fig. 1 Increased nuclear localization of NF-κB after 22 h of treatment with proinflammatory cytokines shown by immunofluorescence microscopy. In untreated cells (**a**, **b**), a mainly cytosolic localization of NF-κB is seen, whereas in cells treated with TNF-α for 22 h (**c**, **d**) or 30 min (**e**, **f**) or IL-1β, localization was predominantly nuclear

cells at a time of each group were investigated with a fluorescence microscope, and the results were averaged. Cells were categorized depending on whether the cytosolic signal exceeded the nuclear one or vice versa.

A predominantly cytosolic localization in 100% of investigated cells could be observed for cells not treated with TNF-α, with or without NAC, and for cells cotreated with TNF-α and 10 mMol NAC. In preparations treated solely with TNF-α, there was an outbalance of nuclear signal in 73% of cells. The cotreatment with 2 mMol NAC almost abolished this effect, with an average of 5% activated cells (Fig. 3)

TNF-α and IL-1β induce total cellular amount of NF-κB after long-time stimulation

To investigate whether HepG2 cells induced with TNF-α and IL-1β contain a greater amount of NF-κB protein than untreated cells, total cellular extracts of treated cells or

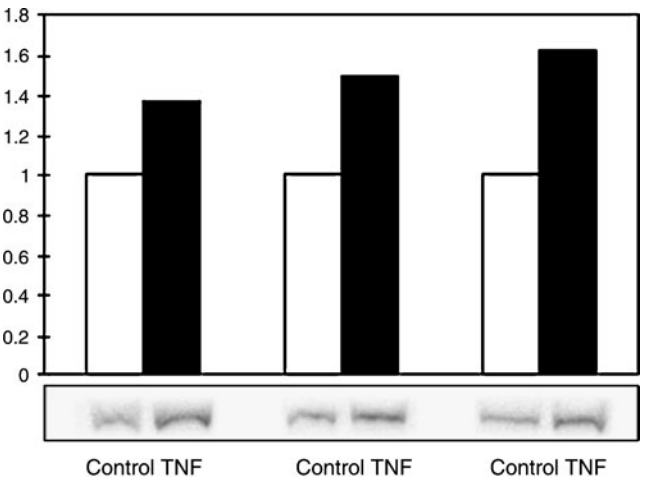

Fig. 2 Increased nuclear localization of NF-κB after 22 h of treatment with proinflammatory cytokines, as revealed by Western blotting. In nuclear extracts of TNF-α-induced cells (22 h), a distinct increase of NF-κB levels, compared to controls, could be detected. Three different blots are shown. *Upper panel*: quantitative analysis of protein levels of TNF- α treated cells (*black*) compared to controls (*white*, equaling 1); *lower panel*: Western blot results, controls (*lanes 1*, *3*, *5*), treated cells (*lanes 2*, *4*, *6*)

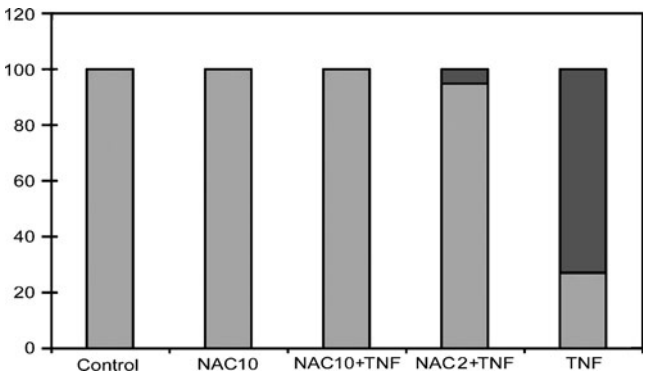

Fig. 3 Inhibition of TNF-α induced NF-κB activation by NAC in a dose-dependent manner. Cells grown on cover slides and treated with NAC alone or combined with TNF-α were incubated with a p65 antibody and labeled with a fluorescing secondary antibody. One hundred cells each were divided in two groups, those with predominantly cytosolic (shown as *light gray*) or nuclear (*dark gray*) signal. The average of three counts is shown here. While a higher dose of NAC inhibits TNF-α induced activity totally, with a lower dose, individual cells are activated

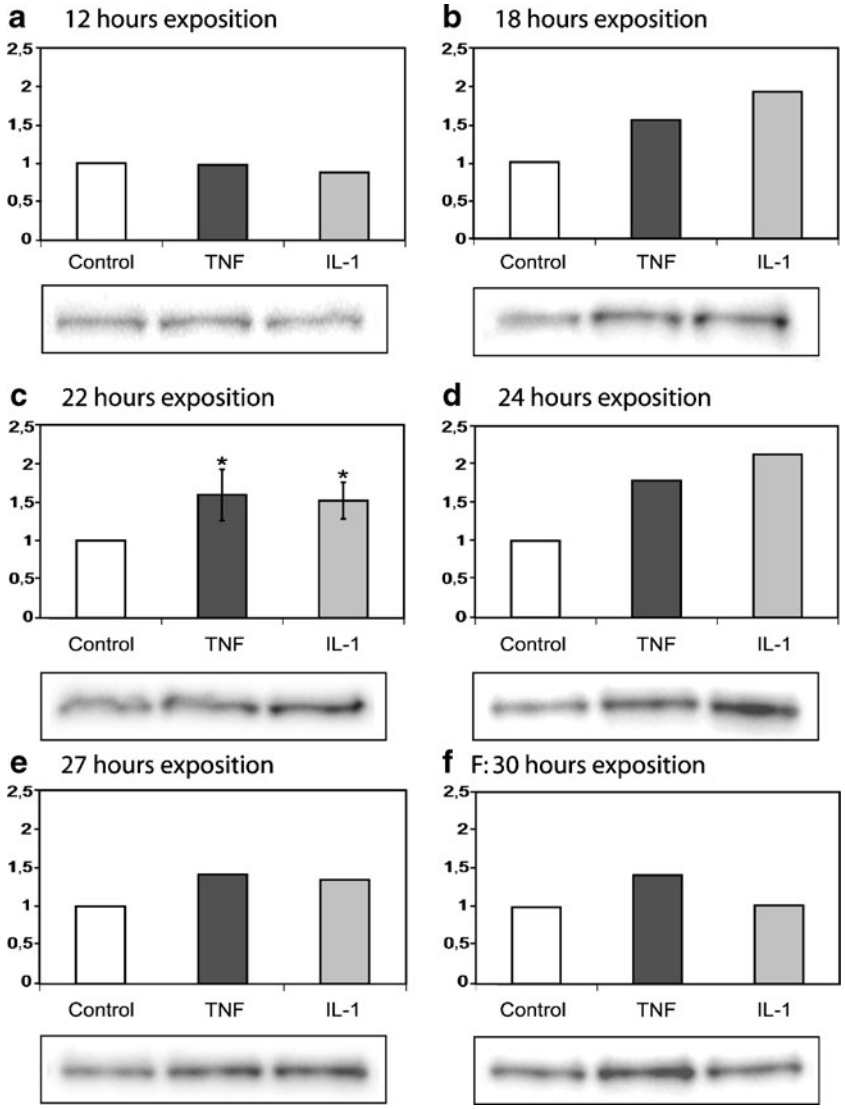

Fig. 4 Increase in total cellular amount of NF-κB protein levels. To investigate if HepG2 cells induced with TNF-α and IL-1β contain a greater amount of NF-κB protein than untreated cells, total cellular extracts of treated cells or control cells were separated electrophoretically and immunoblotted with an NF-κB (p65) antibody. Stimulation with both cytokines led to increased NF-κB protein levels. The increase in NF-κB as compared to controls is significant for 22-h treatment with TNF-α as well as IL-1β (**c**, n=3). The time course is similar for both cytokines; at 3, 6, 9, and 12 h post induction, no effect was detectable (**a**, 12 h). An increase was first seen 18 h post-induction (**b**, 18 h). A maximum increase was visible after 22 to 24 h (**c**, **d**), followed by a decrease after 27 h (**e**). After this, time courses diverge slightly. Whereas NF-κB protein returns to the original level for cells treated with IL-1β, TNF-α treated cells show a slightly persisting effect for up to 30 h (**f**)

control cells were separated electrophoretically and immunoblotted with an NF-κB (p65) antibody (Fig. 4). Stimulation with both cytokines led to increased NF-κB protein levels. The increase in NF-κB as compared to controls is significant for 22-h treatment with TNF-α as well as IL-1β (Fig. 4c). The time course is similar for both cytokines; after 3, 4, 9, and 12 h post-induction, no effect was detectable (Fig. 4a, 12 h). An increase was first seen after 18 h of induction (Fig. 4b, 18 h). A maximum increase was visible after 22 to 24 h (Fig. 4c, d), followed by a decrease after 27 h (Fig. 4e). After this, time courses diverge slightly. Whereas NF-κB protein returns to the original level for cells treated with IL-1β, TNF-α treated cells show a slightly persisting effect for up to 30 h (Fig. 4f).

The TNF-α- and IL-1β-induced increase of NF-κB is the result of an augmented transcription and translation

To test whether the induction of NF-κB reported above is the result of an increased transcription, HepG2 cells were treated with TNF-α or IL-1β, respectively, and compared to

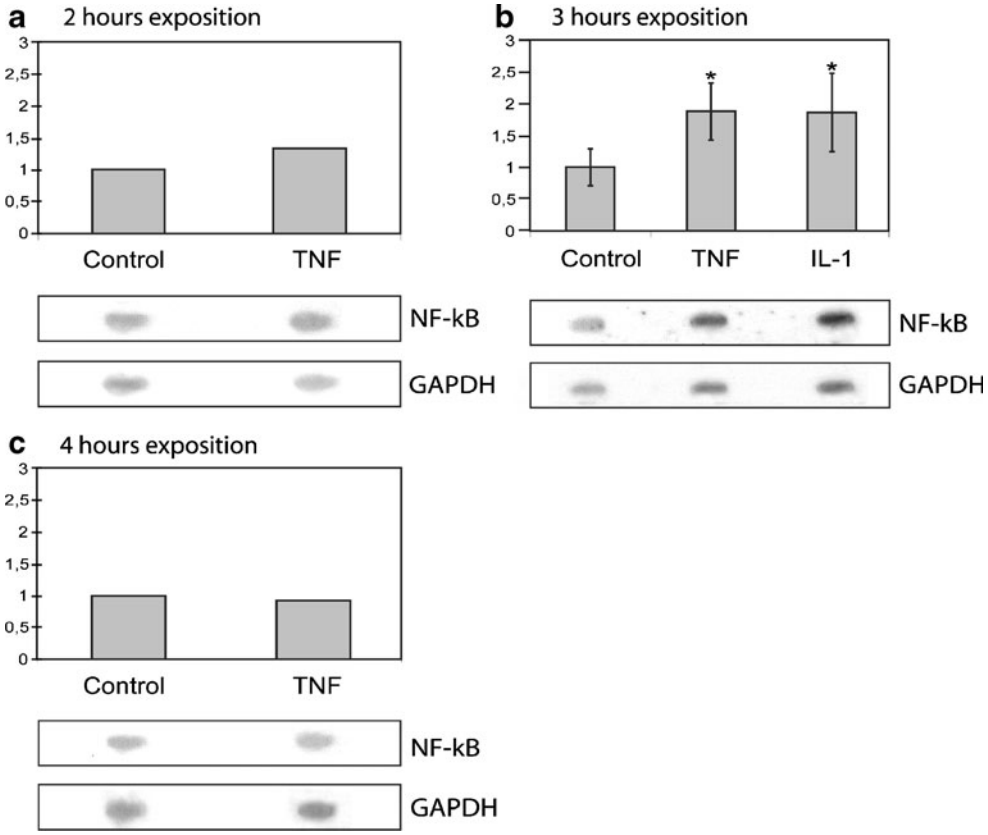

Fig. 5 Increase in NF-κB mRNA levels. HepG2 cells were adapted to serum-free conditions and treated, respectively, and compared to untreated cells. Northern blot analysis of mRNA extracted from HepG2 cells treated with TNF-α or IL-1β as compared to control cells. An increase in NF-κB mRNA could be observed after 2 h of induction (**a**), reaching a maximum after 3 h (**b**) and returning to control levels after 4 h (**c**). This induction in mRNA levels was significant for 3 h of treatment with both cytokines as compared with control cells (**b**, n=3)

untreated cells. Northern blot analysis was performed on nuclear extracts (Fig. 5).

An increase in NF-κB mRNA could be observed after 2 h of induction (Fig. 5a), reaching a maximum after 3 h (Fig. 5b) and returning to control levels after 4 h (Fig. 5c). This induction in mRNA levels was significant after 3 h of treatment with both cytokines (Fig. 5b).

Translation was investigated by adding cycloheximide (CHX) or puromycin (PM) in addition to cytokines. The effects of CHX and PM were visualized by Western blotting of total cellular extracts (Fig. 6). Both PM (Fig. 6a) and CHX (Fig. 6b) antagonized a rise in NF-κB levels of treated cells, suggesting de novo protein synthesis of NF-κB.

NF-κB is colocalized with proteasomes

To investigate the possibility of an increased proteasomal degradation of NF-κB after maximal increase in cellular NF-κB levels, immunoelectron microscopy of cells grown in a monolayer was performed with p65 and anti-20S proteasome (α unit) antibodies and 5- or 10-nm immunogold, respectively. A colocalization of 5- and 10-nm

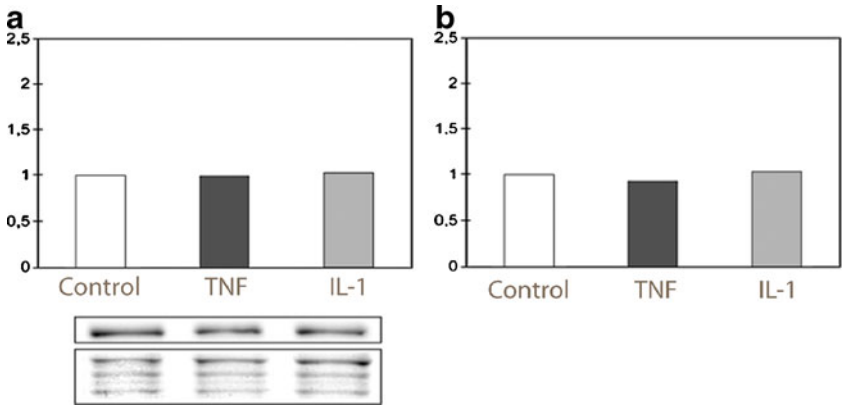

Fig. 6 Inhibition of increase in NF-κB protein levels by CHX or PM. Western blots of total cellular extracts of cells treated with TNF or IL-1 alone or combined with CHX or PM, using an NF-κB p65 antibody. Addition of both CHX and PM showed NF-κB levels equal to controls (*white*) after 22-h treatment with TNF (*black*) or IL-1 (*gray*)

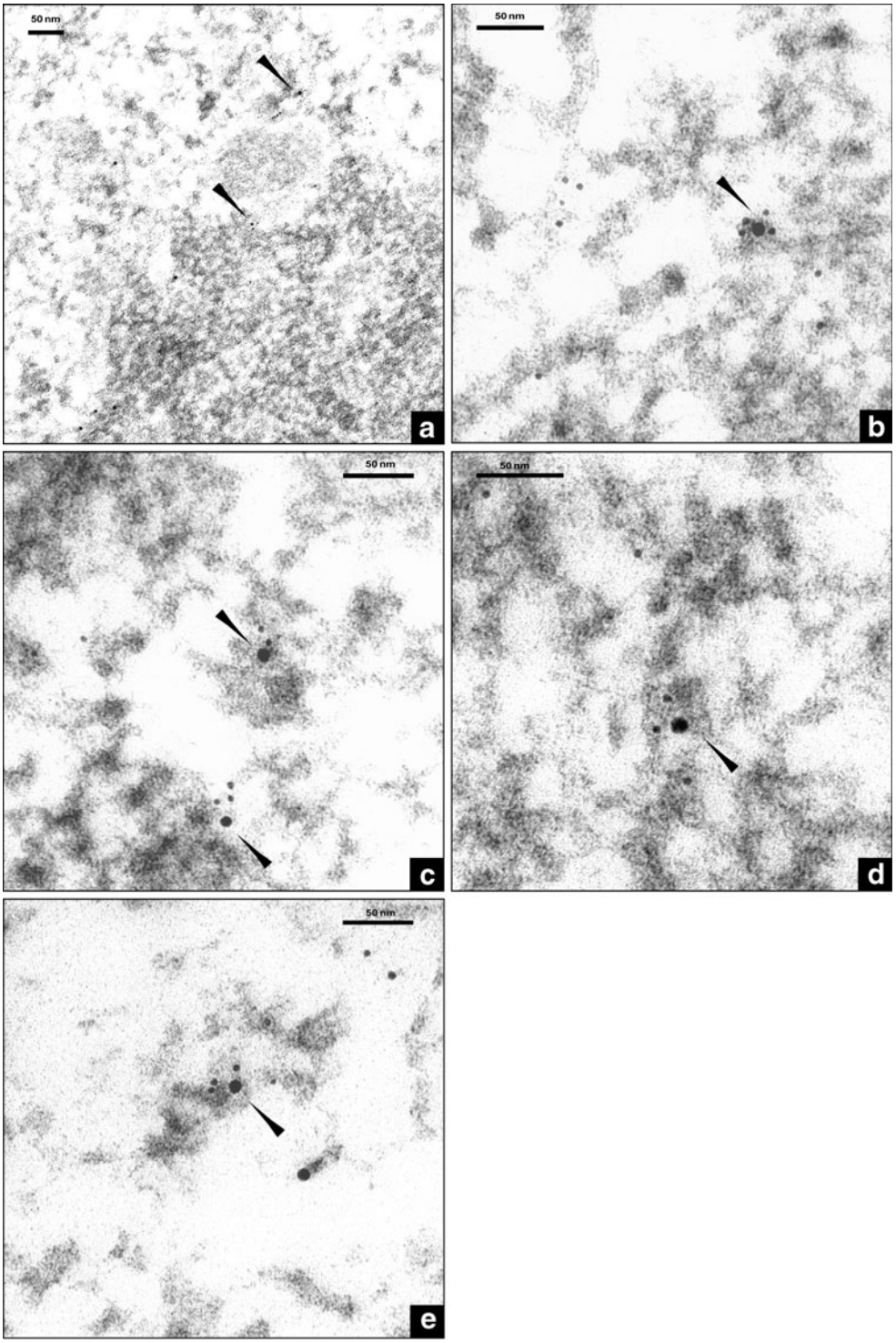

Fig. 7 Intranuclear localization of NF-κB and proteasomal subunits. Cells grown on Mellinex foil and treated with IL-1β for 27 h investigated by immunoelectron microscopy show a colocalization of 5 nm gold delineating the 27S proteasomal subunit and 10-nm gold particles highlighting p65 in the cytoplasm and nucleus of treated cells quite regularly, while it only rarely occurs in control cells (data not shown)

immunogold particles in immediate vicinity (distance between gold particles not more than 20 nm) was investigated in nuclei of cells treated with IL-1β for 27 h (Fig. 7a–e) or control cells. In treated cells, an increase of about fourfold could be observed, as seen in the ratio of immunogold detecting p65 to gold particles tagging α20S. Furthermore, in enriched proteasomal fractions of treated cells embedded for immunoelectron microscopy, NF-κB immunogold could be detected, contrary to proteasomal fractions of untreated cells (Fig. 8).

Western dot blot investigation of cell fractions obtained by density gradient centrifugation with primary antibodies specific for α20S, p65, or IκBα revealed a marked elevation of signal for NF-κB as well as IκBα in fractions

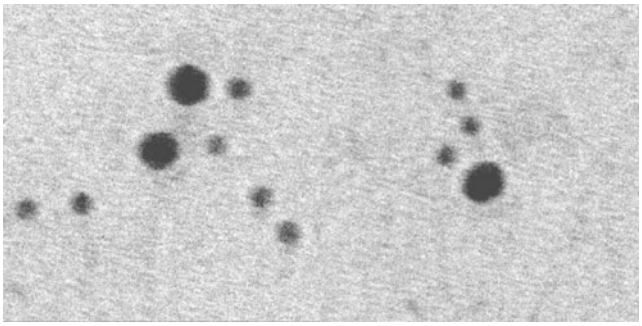

Fig. 8 Colocalization of NF-κB with proteasomes. Enriched proteasomal fractions of cytokine treated cells (IL-1β, 27 h) with immunogold labeling of 20S (5 nm) and NF-κB (10 nm) shows a colocalization of the proteasomal subunit and NF-κB immunogold in the nuclear compartment

that contain the vast majority of the cells' proteasomal content (Fig. 9).

Discussion

Hepatoma cells were shown to have characteristics of hepatocytes and thus are similar to cells that physiologically participate in the acute phase reaction and are a common in vitro model of liver cell reaction in acute inflammation. One of the cancer cell lines in which SOCS-1 is shown to be silenced is the human hepatoma cell line Hep3B. This cell line is related to the cell line used in the experiments presented here, HepG2, but Hep3B, in contrast to HepG2, contains hepatitis B virus. In a different experimental setting, SOCS-1 was silenced in HepG2 cells expressing the hepatitis C virus core protein, but not in wild-type cells [36], so HepG2 cells can be used as a model for NF-κB activation.

Another work [37] investigated SOCS gene expression in HepG2 cells after induction with IL-1β, IL-6, and/or growth hormone. SOCS-1 was not upregulated, whereas SOCS-3 was. Thus, HepG2 cells are a valid model for investigating the influence of acute phase mediators, while liver cells and livers of diverse genetically altered mice are established as models for the interface between inflammation and cancer [38, 39]. While the carcinogenic potential of chronic inflammation on liver parenchymal cells has been shown before, the 'switch' from acute to chronic inflammation remains yet elusive, not only regarding liver, but other organ systems as well. Among the most important mediators of acute inflammation are cytokines, mainly TNF-α and IL-1β. These affect the acute phase response, which mainly involves the liver and results in a thoroughly changed metabolism focused on non-specific immune response. This process usually expires as immediately as it is started and is regulated tightly. The same can be said about the mediators, namely, NF-κB.

Since Bierhaus et al. [20] demonstrated a sustained NF-κB activation in a model of a certain chronic inflammatory disease (diabetes), it seemed to stand to reason that this is one possible dysregulation that can result in chronic inflammation. This was investigated here by several experiments.

In a first set of experiments, a prolonged activation of NF-κB for up to 27 or 30 h after continuous treatment with IL-1β or TNF-α, respectively, could be observed.

This was at least in part a result of a de novo-synthesis of NF-κB p65. Involvement of translation was shown by a total increase of NF-κB (p65) protein content in cell lysates which could be antagonized by the protein synthesis inhibitors puromycin and cycloheximide. Transcriptional activity was demonstrated by an increase of p65 mRNA in RNA extracts of treated compared to untreated cells. This is the first description of an upregulation of NF-κB in context with acute cytokine-mediated inflammation by de novo-synthesis. Furthermore, a putative downregulation by increased proteolysis was hinted by a colocalization of NF-κB with proteasomes. This effect was strongly increased after 27 h of treatment with IL-1β. Although a degradation of NF-κB in the cause of protein turnover is to be expected to take place in proteasomes, this is something not investigated before. Furthermore, the peak shown shortly before and around the time NF-κB protein levels

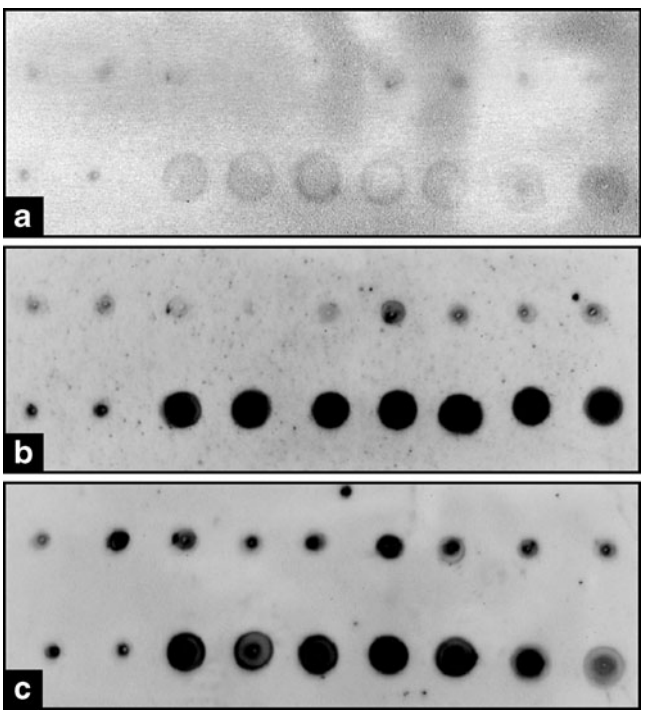

Fig. 9 Localization of NF-κB and I-κB within proteasomal fractions. Western dot blot analysis of fractions of HepG2 cells (IL-1β, 27 h) obtained by ultracentrifugation demonstrates an increased signal of I-κB (**c**) and NF-κB (**b**) in the fractions containing the proteasomal subunit as shown in **a**. Primary antibodies: **a** anti-20S proteasomal subunit, **b** anti-NF-κB (p65), **c** anti-I-κB

return to values without induction makes an "on demand" degradation of NF-κB very plausible.

Altogether, these findings can be regarded as indications for a further mechanism of NF-κB regulation. So far, work on NF-κB activation was mainly focused on its interaction with the IκBs and the rapid activation by proteolysis of its inhibitors and the self-limiting mechanism by synthesis of the IκBs [40]. Especially the rapid inducibility is one of the qualities of NF-κB that distinguish it from other transcription factors and make it a participant in the acute phase response. Another distinct feature of NF-κB is its activation by a wide range of stimuli. These cause differential changes of cell metabolism, and this is only in part due to the dimeric character of NF-κB and the several combinations of NF-κB subunits. Several pathways and modulations are described so far, such as costimulation of several signal cascades or second messengers, modulation by special proteins, posttranscriptional or posttranslational modification, or transcriptional coactivation. Also, translocated NF-κB subunits can be modified by nuclear kinases, acetylases, or phosphatases, resulting in co-activator or co-repressor activities [41–46].

After induction with LPS that utilizes similar signaling pathways as IL-1, an activation of up to 36 h could be observed in monocytic cells that are among the few cells with a constitutive NF-κB activity, in contrast to TNF-mediated activation that lasts for 4 to 6 h. These are the usual time courses after acute activation; the difference between the cytokines is mainly due to a different utilization of the IκBs [47]. In liver cells, the activation time is usually up to 6 h for both cytokines. Some reports of different time courses of NF-κB activity exist in context with chronic inflammation and cancer. An oscillation of NF-κB between cytoplasm and nucleus after 24 h of continuous treatment with TNF-α has been reported in single carcinoma and neuroblastoma cells [48], whereas a prolonged NF-κB activation for at least about a week was observed in monocytic cells of diabetic rats and depends on RAGE-mediated synthesis of NF-κB p65 [20].

In the non-monocytic cell model used here, NF-κB activation times as reported are exceeding the autoregulatory feedback loop observed after inflammatory stimuli by far. Since hepatocytes in vivo play an important role in secretion of acute phase proteins, every prolongation of NF-κB activation not only has consequences on the liver, but also systemic effects.

Taken together with the abovementioned reports, the results presented here can contribute to the understanding of the progress of acute immunologic processes to chronic inflammation and, possibly, cancer. It is proposed that NF-κB cannot only be regulated indirectly, as widely reported for a lot of mainly inflammatory stimuli, by breaking down the inhibitors, almost invariably followed by resynthesis in an autoregulatory fashion. In addition, there seems to be a direct, also partially automediated mechanism regulating protein synthesis and degradation of subunits of the transcription factor itself, shown here by application of TNF-α and IL-1β and which could contribute to chronification of acute inflammation.

It is implied that termination of NF-κB signaling by IκB synthesis and a resulting return of NF-κB–IκB homoeostasis to pre-induction levels after several hours doesn't necessarily have to occur. Rather, under certain circumstances, this homoeostasis can be shifted towards predominance of NF-κB for a longer time. Exact time frames remain to be established, as well as the possible coincidence of sustained NF-κB activity with other chronic inflammatory conditions besides diabetes and with carcinogenesis. A corroboration of the hypothesis that NF-κB is partly regulated by degradation comes from the observation that signaling-dependent proteins in cancer cell lines with constitutive NF-κB activity influence NF-κB protein stability.

Acknowledgements The author thanks Prof. Dr. H. Dariush Fahimi (Institute of Anatomy and Cell Biology II, University of Heidelberg) for the possibility to work on this topic, Prof. Dr. Fahimi and Prof. Dr. Dr. Alfred Völkl (Institute of Anatomy and Cell Biology II, University of Heidelberg) for the theoretical and technical advice, Ms. Gabriele Krämer (Institute of Anatomy and Cell Biology II, University of Heidelberg) for the excellent technical assistance, Dr. C. Kuhn (ZMBH, Heidelberg) for the HepG2 cells, Mr. Daniel Kühn for graphic expertise, and Dr. Dietmar Techel (Institute of Pathology, Klinikum Stuttgart) for the critical reading.

Conflict of interest None

References

1. Baldwin AS Jr (1996) The NF-kappa B and I kappa B proteins: new discoveries and insights. Annu Rev Immunol 14:649–683
2. Karin M, Ben-Neriah Y (2000) Phosphorylation meets ubiquitination: the control of NF-[kappa]B activity. Annu Rev Immunol 18:621–663
3. Karin M (1999) How NF-kappaB is activated: the role of the IkappaB kinase (IKK) complex. Oncogene 18(49):6867–6874
4. Pomerantz JL, Baltimore D (2002) Two pathways to NF-kappaB. Mol Cell 10(4):693–695
5. Stilmann M, Hinz M, Arslan SC, Zimmer A, Schreiber V, Scheidereit C (2009) A nuclear poly(ADP-ribose)-dependent signalosome confers DNA damaga-induced IκB kinase activation. Mol Cell 36:365–378
6. Karin M (1999) The beginning of the end: IkappaB kinase (IKK) and NF-kappaB activation. J Biol Chem 274(39):27339–27342
7. Bouwmeester T, Bauch A, Ruffner H, Angrand PO, Bergamini G, Croughton K, Cruciat C, Eberhard D, Gagneur J, Ghidelli S, Hopf C, Huhse B, Mangano R, Michon AM, Schirle M, Schlegl J, Schwab M, Stein MA, Bauer A, Casari G, Drewes G, Gavin AC, Jackson DB, Joberty G, Neubauer G, Rick J, Kuster B, Superti-Furga G (2004) A physical and functional map of the human

TNF-alpha/NF-kappa B signal transduction pathway. Nat Cell Biol 6(2):97–105
8. Donald R, Ballard DW, Hawinger J (1995) Proteolytic processing of NF-kappa B/I kappa B in human monocytes. ATP-dependent induction by pro-inflammatory mediators. J Biol Chem 270(1):9–12
9. Dumitru CD, Ceci JD, Tsatsanis C, Kontoyoannis D, Stamatakis K, Lin JH, Patriotis C, Jenkins NA, Copeland NG, Kollias G, Tsichlis PN (2000) TNF-alpha induction by LPS is regulated posttranscriptionally via a Tpl2/ERK-dependent pathway. Cell 103(7):1071–1083
10. Han Y, Brasier AR (1997) Mechanism for Biphasic Rel A NF-kappa B1 Nuclear Translocation in TNF-alpha -stimulated Hepatocytes. J Biol Chem 272(15):9825–9832
11. Han Y, Weinman S, Boldogh I, Walker RK, Brasier AR (1999) Tumor necrosis factor-alpha-inducible IkappaBalpha proteolysis mediated by cytosolic m-calpain. A mechanism parallel to the ubiquitin-proteasome pathway for nuclear factor-kappab activation. J Biol Chem 274(2):787–794
12. Matsuda A, Suzuki Y, Honda G, Muramatsu S, Matsuzaki O, Nagano Y, Doi T, Shimotohno K, Harada T, Nishida E, Hayashi H, Sugano S (2003) Large-scale identification and characterization of human genes that activate NF-kappaB and MAPK signaling pathways. Oncogene 22(21):3307–3318
13. Baeuerle PA, Baltimore D (1988) I kappa B: a specific inhibitor of the NF-kappa B transcription factor. Science 242(4878):540–546
14. Han Y, Meng T, Murray NR, Fields AP, Brasier AR (1999) Interleukin-1-induced nuclear factor-kappa B-Ikappa B alpha autoregulatory feedback loop in hepatocytes. A role for protein kinase C alpha in post-transcriptional regulation of Ikappa B alpha resynthesis. J Biol Chem 274(2):939–947
15. Sun SC, Ganchi PA, Beraud C, Ballard DW, Greene WC (1994) Autoregulation of the NF-kappa B transactivator RelA (p65) by multiple cytoplasmic inhibitors containing ankyrin motifs. Proc Natl Acad Sci USA 91(4):1346–1350
16. Chiao PJ, Miyamoto S, Verma IM (1994) Autoregulation of I {kappa}B{alpha} activity. Proc Natl Acad Sci 91(1):28–32
17. Brown K, Park S, Kanno T, Franzoso G, Siebenlist U (1993) Mutual regulation of the transcriptional activator NF-kappa B and its inhibitor, I kappa B-alpha. Proc Natl Acad Sci USA 90 (6):2532–2536
18. Arenzana-Seisdedos F, Thompson J, Rodriguez MS, Bachelerie F, Thomas D, Hay RT (1995) Inducible nuclear expression of newly synthesized I kappa B alpha negatively regulates DNA-binding and transcriptional activities of NF-kappa B. Mol Cell Biol 15 (5):2689–2696
19. Arenzana-Seisdedos F, Turpin P, Rodriguez M, Thomas D, Hay RT, Virelizier JL, Dargemont C (1997) Nuclear localization of I kappa B alpha promotes active transport of NF-kappa B from the nucleus to the cytoplasm. J Cell Sci 110 (Pt 3):369–378
20. Bierhaus A, Schiekofer S, Schwaninger M, Andrassy M, Humpert PM, Chen J, Hong M, Luther T, Henle T, Kloting I, Morcos M, Hofmann M, Tritschler H, Weigle B, Kasper M, Smith M, Perry G, Schmidt AM, Stern DM, Haring HU, Schleicher E, Nawroth PP (2001) Diabetes-associated sustained activation of the transcription factor nuclear factor-{kappa}B. Diabetes 50(12):2792–2808
21. Kowalik TF, Wing B, Haskill JS, Azizkhan JC, Baldwin AS Jr, Huang ES (1993) Multiple mechanisms are implicated in the regulation of NF-kappa B activity during human cytomegalovirus infection. Proc Natl Acad Sci USA 90(3):1107–1111
22. Yurochko AD, Kowalik TF, Huong SM, Huang ES (1995) Human cytomegalovirus upregulates NF-kappa B activity by transactivating the NF-kappa B p105/p50 and p65 promoters. J Virol 69 (9):5391–5400
23. Yurochko AD, Hwang ES, Rasmussen L, Keay S, Pereira L, Huang ES (1997) The human cytomegalovirus UL55 (gB) and UL75 (gH) glycoprotein ligands initiate the rapid activation of Sp1 and NF-kappaB during infection. J Virol 71(7):5051–5059
24. Yurochko AD, Mayo MW, Poma EE, Baldwin AS Jr, Huang ES (1997) Induction of the factor Sp1 during human cytomegalovirus infection mediates upregulation of the p65 and p105/p50 NF-kappaB promoters. J Virol 71(6):4638–4648
25. Ueberla K, Lu Y, Chung E, Haseltine WA (1993) The NF-kappa B p65 promoter. J Acquir Immune Defic Syndr 6(3):227–230
26. Teferedegne B, Green MR, Guo Z, Boss JM (2006) Mechanism of action of a distal NF-{kappa}B-dependent enhancer. Mol Cell Biol 26(15):5759–5770
27. Ryo A, Liou YC, Lu KP, Wulf G (2003) Prolyl isomerase Pin1: a catalyst for oncogenesis and a potential therapeutic target in cancer. J Cell Sci 116(5):773–783
28. Ryo A, Suizu F, Yoshida Y, Perrem K, Liou YC, Wulf G, Rottapel R, Yamaoka S, Lu KP (2003) Regulation of NF-[kappa]B signaling by Pin1-dependent prolyl isomerization and ubiquitin-mediated proteolysis of p65/RelA. Mol Cell 12(6):1413–1426
29. Wulf GM, Ryo A, Wulf GG, Lee SW, Niu T, Petkova V, Lu KP (2001) Pin1 is overexpressed in breast cancer and cooperates with Ras signaling in increasing the transcriptional activity of c-Jun towards cyclin D1. EMBO J 20(13):3459–3472
30. Yoshikawa H, Matsubara K, Qian GS, Jackson P, Groopman JD, Manning JE, Harris CC, Herman JG (2001) SOCS-1, a negative regulator of the JAK/STAT pathway, is silenced by methylation in human hepatocellular carcinoma and shows growth-suppression activity. Nat Genet 28(1):29–35
31. Rottapel R, Ilangumaran S, Neale C, La Rose J, Ho JM, Nguyen MH, Barber D, Dubreuil P, de Sepulveda P (2002) The tumor suppressor activity of SOCS-1. Oncogene 21(28):4351–4362
32. Semenkova LN, Dudich EI, Dudich IV, Shingarova LN, Korobko VG (1997) Alpha-fetoprotein as a TNF resistance factor for the human hepatocarcinoma cell line HepG2. Tumour Biol 18(1):30–40
33. Rickwood D, Messent A, Patel D (1997) Isolation and characterization of nuclei and nuclear subfractions. Subcellular fractionation – a practical approach. Oxford University Press, pp 71–77
34. Enenkel C, Lehmann A, Kloetzel PM (1998) Subcellular distribution of proteasomes implicates a major location of protein degradation in the nuclear envelope-ER network in yeast. Embo J 17(21):6144–6154
35. Wilkinson CR, Wallace M, Morphew M, Perry P, Allshire P, Javerzat JP, McIntosh JR, Gordon C (1998) Localization of the 26S proteasome during mitosis and meiosis in fission yeast. Embo J 17(22):6465–6476
36. Miyoshi H, Fujie H, Shintani Y, Tsutsumi T, Shinzawa S, Makuuchi M, Kokudo N, Matsuura Y, Suzuki T, Miyamura T, Moriya K, Koike K (2005) Hepatitis C virus core protein exerts an inhibitory effect on suppressor of cytokine signaling (SOCS)-1 gene expression. J Hepatol 43(5):757–763
37. Wu X, Herndon DN, Wolf SE (2003) Growth hormone down-regulation of Interleukin-1beta and Interleukin-6 induced acute phase protein gene expression is associated with increased gene expression of suppressor of cytokine signal-3. Shock 19(4):314–320
38. Haybaeck J, Zeller N, Wolf MJ, Weber A, Wagner U, Kurrer MO, Bremer J, Iezzi G, Graf R, Clavien P-A, Thimme R, Blum H, Nedospasov SA, Zatloukal K, Ramzan M, Ciesek S, Pietschmann T, Marche PN, Karin M, Kopf M, Browning JL, Aguzzi A, Heikenwalder M (2009) A lymphotoxin-driven pathway to hepatocellular carcinoma. Cancer Cell 16:295–308
39. Maeda S, Kamata H, Luo J-L, Leffert H, Karin M (2005) IKKβ couples hepatocyte death to cytokine-driven compensatory proliferation that promotes chemical hepatocarcinogenesis. Cell 121:977–990

40. Perkins ND (2007) Integrating cell-signalling pathways with NF-kappaB and IKK function. Nat Rev Mol Cell Biol 8(1):49–62
41. Craig R, Larkin A, Mingo AM, Thuerauf DJ, Andrews C, McDonough PM, Glembotski CC (2000) p38 MAPK and NF-kappa B collaborate to induce interleukin-6 gene expression and release. Evidence for a cytoprotective autocrine signaling pathway in a cardiac myocyte model system. J Biol Chem 275(31):23814–23824
42. Zhong H, SuYang H, Erdjument-Bromage H, Tempst P, Ghosh S (1997) The transcriptional activity of NF-kappaB is regulated by the IkappaB-associated PKAc subunit through a cyclic AMP-independent mechanism. Cell 89(3):413–424
43. Vlahopoulos S, Boldogh I, Casola A, Brasier AR (1999) Nuclear factor-kappaB-dependent induction of interleukin-8 gene expression by tumor necrosis factor alpha: evidence for an antioxidant sensitive activating pathway distinct from nuclear translocation. Blood 94(6):1878–1889
44. You M, Flick LM, Yu D, Feng GS (2001) Modulation of the nuclear factor kappa B pathway by Shp-2 tyrosine phosphatase in mediating the induction of interleukin (IL)-6 by IL-1 or tumor necrosis factor. J Exp Med 193(1):101–110
45. Perkins ND (1997) Achieving transcriptional specifity with NF-kappaB. Int J Biochem Cell Biol 29(12):1433–1448
46. Zhong H, Voll R, Ghosh S (1998) Phosphorylation of NF-kappaB p65 by PKA stimulates transcriptional activity by promoting a novel bivalent interaction with the coactivator CBP/300. Mol Cell 1(5):661–671
47. Thompson JE, Phillips RJ, Erdjument-Bromage H, Tempst P, Ghosh S (1995) I[kappa]B-[beta] regulates the persistent response in a biphasic activation of NF-[kappa]B. Cell 80 (4):573–582
48. Nelson DE, Ihekwaba AE, Elliott M, Johnson JR, Gibney CA, Foreman BE, Nelson G, See V, Horton CA, Spiller DG, Edwards SW, McDowell HP, Unitt JF, Sullivan E, Grimley R, Benson N, Broomhead D, Kell DB, White MR (2004) Oscillations in NF-kappaB signaling control the dynamics of gene expression. Science 306(5696):704–708

Virchows Arch (2010) 457:597–608
DOI 10.1007/s00428-010-0979-4

ORIGINAL ARTICLE

Mucosal carcinoma of the fallopian tube coexists with ovarian cancer of serous subtype only: a study of Japanese cases

Daichi Maeda · Satoshi Ota · Yutaka Takazawa · Kenichi Ohashi · Masaya Mori · Tetsuo Imamura · Shunsuke Nakagawa · Tetsu Yano · Yuji Taketani · Masashi Fukayama

Received: 1 June 2010 / Revised: 7 September 2010 / Accepted: 10 September 2010 / Published online: 25 September 2010
© Springer-Verlag 2010

Abstract Previous studies in Western countries have revealed that mucosal carcinoma of the fallopian tube frequently coexists with pelvic (ovarian, tubal, and peritoneal) serous carcinomas, and early tubal carcinoma is now regarded as a possible origin of these tumors. However, the relationship between early tubal carcinoma and non-serous ovarian cancer, such as clear cell adenocarcinoma, has not been studied in detail. In this study, we sought to examine the coexistence of mucosal carcinoma of the fallopian tube in Japanese ovarian cancer cases. We submitted the fallopian tubes in toto for histological examination in 52 ovarian carcinoma cases and three peritoneal serous carcinoma cases. The ovarian tumors included 12 serous adenocarcinomas, 23 clear cell adenocarcinomas, nine endometrioid adenocarcinomas, three mucinous adenocarcinomas, and four mixed epithelial carcinomas. Mucosal carcinoma of the fallopian tube did not coexist with non-serous adenocarcinoma (n=40). In contrast, mucosal carcinoma of the fallopian tube was observed in six cases of ovarian serous adenocarcinoma and one case of peritoneal serous adenocarcinoma. In these cases, the p53 immunophenotypes were similar in tubal lesions and invasive ovarian or peritoneal carcinomas. Tumors were negative for p53 in four of seven cases, and one of the p53-negative serous adenocarcinomas showed low-grade morphology. We believe that some ovarian and peritoneal serous adenocarcinomas develop from early tubal carcinomas. However, it should be noted that early tubal carcinomas are not always p53-positive immunohistochemically. Finally, it is unlikely that early tubal lesions are involved in the carcinogenesis of clear cell adenocarcinoma and other non-serous adenocarcinomas.

Keywords Ovarian carcinoma · Fallopian tube · Mucosal carcinoma · p53

D. Maeda · S. Ota · Y. Takazawa · M. Fukayama (✉)
Department of Pathology, Graduate School of Medicine,
The University of Tokyo,
7-3-1 Hongo Bunkyoku,
Tokyo 113-0033, Japan
e-mail: mfukayama-tky@umin.net

K. Ohashi
Department of Pathology, Toranomon Hospital,
2-2-2 Toranomon Minato-ku,
Tokyo, Japan

M. Mori
Department of Pathology, Mitsui Memorial Hospital,
1 Kandaizumicho Chiyoda-ku,
Tokyo, Japan

T. Imamura
Department of Pathology, Teikyo University Hospital,
2-11-1 Kaga Itabashi-ku,
Tokyo, Japan

S. Nakagawa · T. Yano · Y. Taketani
Department of Obstetrics and Gynecology,
Graduate School of Medicine, The University of Tokyo,
7-3-1 Hongo Bunkyo-ku,
Tokyo, Japan

Introduction

The pathogenesis of primary ovarian carcinomas has long been controversial, and it remains a topic of debate. Ovarian surface epithelium or intracortical inclusion cysts have been considered to be the origin of most ovarian carcinomas, and thus, the term "malignant surface epithelial tumor" has been used to represent ovarian carcinoma [1]. It is also known that some endometrioid adenocarcinomas

and clear cell adenocarcinomas arise from endometriotic lesions [2–4]. At this point, regarding mucinous adenocarcinomas and low-grade serous adenocarcinomas, stepwise carcinogenesis from borderline tumor to invasive carcinoma has been suggested. In contrast, high-grade serous adenocarcinoma, which often presents in an advanced stage with multiple peritoneal disseminations, is believed to arise de novo, and *TP53* mutation is known to play a key role in its progression [5, 6].

In recent years, accumulating evidence suggests that the fallopian tube epithelium is the origin of the tumors conventionally diagnosed as ovarian high-grade serous adenocarcinomas [7–15]. This novel theory has attracted much attention in the field of gynecological research. Three major findings were essential to establishing this theory. First, extensive sectioning of salpingo-oophorectomy specimens from women with BRCA mutations has shown that the fallopian tube, especially its fimbriated end, is a preferred site for early adenocarcinoma [9, 16–18]. These early forms of tubal adenocarcinoma were usually in situ lesions, and Crum et al. referred to them as "tubal intraepithelial carcinomas" (TICs) [7, 10]. Second, histological examination of the whole fallopian tube has demonstrated that TICs frequently coexisted with ovarian and peritoneal high-grade serous adenocarcinomas in the general population [8, 10]. Finally, analyses of TICs and ovarian carcinomas for p53 protein accumulation, *TP53* mutations, and chromosomal instability revealed similar genetic alterations in both tubal and ovarian lesions [8, 10, 11]. Indeed, these key findings provide evidence for designating TICs as preceding lesions of high-grade serous cancers. Nonetheless, previous reports on the association between fallopian tube lesions and ovarian and peritoneal cancers are from limited institutions in North America, and they focus primarily on serous carcinogenesis and the involvement of *TP53* gene alterations.

In the current study, we examined the coexistence of mucosal carcinoma of the fallopian tube among Japanese cases of ovarian and peritoneal cancer. The distribution of ovarian carcinoma cases according to their histological subtypes is different between Japan and Western countries. In Japan, the incidence of clear cell adenocarcinoma is much higher [19–21]. Consequently, we were able to include not only serous adenocarcinomas but also a large number of clear cell adenocarcinoma cases in this study. Our main objective was to assess whether the coexistence of mucosal carcinoma of the fallopian tube is a specific event in p53-positive high-grade serous carcinoma cases. In this report, we refrain from using the term "tubal intraepithelial carcinoma" (TIC) because it is now used widely as a term representing an early cancer that develops to form pelvic high-grade serous carcinoma, and some researchers emphasize p53 positivity as its key feature [7]. Instead, we use the term "mucosal carcinoma of the fallopian tube" to represent all histologically malignant tubal lesions that show intraepithelial growth, regardless of their immunophenotype.

Materials and methods

Case selection

We prospectively analyzed cases diagnosed as ovarian carcinoma or peritoneal serous carcinoma in four major hospitals in Tokyo, Japan (the University of Tokyo Hospital, Toranomon Hospital, Mitsui Memorial Hospital, and Teikyo University Hospital) between 2007 and 2009. The definitions of peritoneal and ovarian carcinomas were based on criteria adapted from the International Federation of Gynecology and Obstetrics (FIGO) and the World Health Organization [22, 23]. Cases with predominantly peritoneal tumor and minimal ovarian surface or tubal involvement were classified as peritoneal carcinomas. The diagnosis of ovarian carcinoma was confirmed when the bulk of the neoplasm was identified in the parenchyma of the ovary. Histological classification of the ovarian and peritoneal carcinomas was based on the most recent criteria of the World Health Organization [23]. Ovarian carcinomas diagnosed as serous adenocarcinomas were subcategorized as either low- or high-grade, according to a two-tier grading system (adapted from the MD Anderson Cancer Center grading system) [24]. Tumor staging was performed in accordance with the standards of FIGO, based on clinical information and pathological findings.

Section preparation and examination of resected specimens

For salpingo-oophorectomy specimens, we attempted to submit the fallopian tube, including the fimbria, in toto. The fallopian tubes were sectioned serially, approximately every 3 mm. The histological diagnosis of mucosal (in situ) carcinoma of the fallopian tube was based solely on morphology. Mucosal carcinoma was characterized by replacement of the normal tubal epithelium by malignant glandular epithelial cells with pleomorphic nuclei [23]. Stratification, loss of epithelial polarity, and lack of stromal invasion are other features of mucosal carcinoma of the fallopian tube. When peritoneal dissemination was sampled and submitted separately to the Department of Pathology, we evaluated its representative sections. The presence or absence of peritoneal dissemination was recorded in all the cases.

Completeness of tubal sectioning

We graded the completeness of the in toto tubal sectioning using a four-tier system, as described in Table 1. Of the 71

Table 1 Grading of completeness of in toto sectioning of the fallopian tubes and case distribution

	Submitted adnexa	Tumor involvement	In toto sectioning	Cases (n=71)
A (perfect)	Bilateral	Ovary: unilateral/bilateral Peritoneal dissemination: +/−	Completely performed bilaterally	40
B (satisfactory)	Unilateral	Ovary: clinically unilateral Peritoneal dissemination: –	Completely performed unilaterally (affected side)	8
	Bilateral	Ovary: histologically unilateral Peritoneal dissemination: –	Completely performed unilaterally (affected side)	1
C (adequate)	Bilateral/ unilateral	Ovary: histologically or clinically unilateral Peritoneal dissemination: +	Completely performed unilaterally (affected side)	3
		Ovary: histologically or clinically bilateral Peritoneal dissemination: +/−	Completely performed unilaterally (ipsilateral to the dominant ovarian mass)	3
D (inadequate)	Bilateral/ unilateral	Ovary: unilateral/bilateral Peritoneal dissemination: +/−	Incompletely performed in the tube ipsilateral to the dominant ovarian mass	16

MCFT mucosal carcinoma of the fallopian tube

ovarian and peritoneal cancer cases retrieved, we were able to perform appropriate sectioning in 55 cases (Grades A to C). As for peritoneal cancer cases, sectioning was considered appropriate only when bilateral fallopian tubes were perfectly sectioned. Three peritoneal serous adenocarcinoma cases were classified in the Grade A category. Reasons for incomplete sectioning (Grade D) included an unidentifiable fallopian tube due to replacement by tumor and inadequate sections made in the initial settings. Further clinicopathological analyses including a survey for mucosal carcinoma of the fallopian tube were performed on cases classified as Grades A to C.

Clinical survey of patients with serous adenocarcinoma

We examined the medical records of 15 serous adenocarcinoma (12 ovarian and three peritoneal) patients and their demographics: data including age, tumor site, preoperative diagnosis, survival status, and follow-up period were obtained. None of the patients underwent preoperative chemotherapy or radiotherapy. The follow-up period was calculated from the date of surgery to the date of death or last clinical evaluation. The mean follow-up interval was 11.9 months (range, 1-33). Medical records of non-serous adenocarcinoma patients were not investigated in this study.

Immunohistochemistry

Tissue samples were fixed in formalin and embedded in paraffin. For the serous adenocarcinoma cases, sections (4 μm) were cut from paraffin-embedded blocks containing ovarian or peritoneal tumor tissue and mucosal carcinoma of the fallopian tube, when present. Immunohistochemistry was performed with the following antibodies: mouse monoclonal anti-p53 antibody (1:100, Clone DO-7, Novocastra Laboratories, Newcastle Upon Tyne, UK), mouse monoclonal anti-Ki67 antibody (1:100, Clone MIB-1, Dako, Glostrup, Denmark), and mouse monoclonal anti-Wilms' tumor 1 (WT-1) protein (1:25, Clone 6F-H2, Dako). Immunohistochemical staining was performed according to standard techniques using a Ventana Benchmark® XT autostainer (Ventana Medical Systems Inc, Tucson, AZ, USA). Appropriate controls were included. p53 immunoreactivity was classified as completely negative (CN) when no cells showed any positive nuclear immunoreactivity, negative (N) when nuclear immunoreactivity was observed in <10% of cells, and positive (P) if ≥10% of cells showed strong nuclear immunoreactivity [25]. The percentage of cells with positive Ki-67 nuclear staining was interpreted as the proliferation index (MIB-1 index) for each lesion. MIB-1 index was quantified by counting at least 200 cells in the most immunoreactive area in each sample. As for minute lesions that consisted of less than 200 cells, all the cells were subjected to analysis. WT-1 immunoreactivity was assessed based on nuclear staining, and its intensity was classified subjectively as weak or strong. WT-1 immunoreactivity was scored as follows: 0 (totally negative or <10% of cells strongly/weakly positive), 1+ (≥10% of cells weakly positive and/or 10–50% of cells strongly positive), or 2+ (>50% of cells strongly positive). Additionally, the immunoreactivity of benign epithelium on the same sections, but away from mucosal carcinoma of the fallopian tube, was assessed with all three antibodies.

Examination of fallopian tubes for p53 signatures

To clarify the incidence of benign epithelium showing linear p53 immunopositivity (p53 signature) in the background tubal mucosa of serous adenocarcinoma cases and non-serous adenocarcinoma cases, we performed immunohistochemistry

for p53 in all the fallopian tube tissues sectioned in all of the serous adenocarcinoma cases (n=15) and in 15 cases of clear cell adenocarcinoma chosen as a control group. We made the diagnosis of p53 signature when greater than 75% of benign-looking tubal epithelial cells showed strong immunoreactivity for p53 in a linear manner, exceeding 12 cells in length, in accordance with a previous report [26].

Statistical analysis

Statistical analysis was performed using the χ^2 test. Statistical analyses were performed with StatView 5.0 software (SAS Institute, Cary, NC, USA), and $P<0.05$ was considered statistically significant.

Results

Ovarian and peritoneal carcinoma case distribution and presence of mucosal carcinoma of the fallopian tube

The distribution of the ovarian and peritoneal carcinoma cases and frequency of coexisting mucosal carcinoma of the fallopian tube are summarized in Table 2. Of the 55 cases properly examined for tubal lesions, three were peritoneal high-grade serous carcinoma cases and 52 were ovarian carcinoma cases. Histologically, our series consisted of 15 serous adenocarcinomas (14 high-grade serous adenocarcinomas and one low-grade serous adenocarcinoma), 23 clear cell adenocarcinomas, nine endometrioid adenocarcinomas, two mucinous adenocarcinomas, one mucinous borderline tumor with intraepithelial carcinoma, four mixed epithelial carcinomas, and one undifferentiated carcinoma. Perfect sectioning of the fallopian tubes (Grade A) was performed in 13/15 serous adenocarcinoma cases, and in 27/40 non-serous adenocarcinoma cases (P=0.155). Mucosal carcinoma of the fallopian tube was present only in the serous adenocarcinoma cases (7/15) and not in the non-serous adenocarcinoma cases (0/40; P=0.0001). We observed coexisting mucosal carcinoma of the fallopian tube in five ovarian high-grade serous adenocarcinoma cases, one ovarian low-grade serous adenocarcinoma case, and one peritoneal serous adenocarcinoma case. Perfect sectioning of the fallopian tubes (Grade A) was performed in all seven serous adenocarcinoma cases that had coexisting tubal lesions. Of the eight serous adenocarcinomas without coexisting tubal carcinoma, six were in the Grade A (perfect) sectioning category and two were in the Grade C (adequate) sectioning category. Statistically, grade of sectioning was not significantly different between serous adenocarcinoma cases with coexisting tubal lesions and those without (P=0.155).

Clinicopathological features of serous adenocarcinoma patients

Since early tubal carcinomas were associated only with ovarian/peritoneal serous adenocarcinomas, we specifically examined medical records of serous adenocarcinoma cases. The clinicopathological features including the immunophenotypes of 15 serous adenocarcinomas are summarized in Table 3. Cases 1–7 are cases with mucosal carcinomas of the fallopian tube, and cases 8–15 are those without. Histologically, all of the serous carcinomas except for case 1 were high-grade serous adenocarcinomas.

In case 1, the ovarian tumor showed features of low-grade serous adenocarcinoma, such as mild nuclear atypia, low mitotic activity (7 per 10 HPFs), coexistence of serous borderline (atypical proliferative) tumor component, and p53-negative (N) immunophenotype (Fig. 1). Its predominant architectural pattern was glandular and papillary pattern. A solid component was present, but focal.

In all ovarian serous adenocarcinoma cases with mucosal carcinomas of the fallopian tube, coexisting tubal lesions were found in the fimbriae ipsilateral to the dominant ovarian tumor. Mucosal carcinomas of the fallopian tube were multifocal in cases 1 and 2. In case 1, another mucosal carcinoma was found in non-fimbriated tubal mucosa ipsilateral to the dominant ovarian tumor. In case 2, ovarian carcinoma showed bilateral involvement, and minute mucosal carcinoma of the fallopian tube was also found in the fimbria contralateral to the dominant ovarian mass. With regard to patient age, tumor stage, and survival, we found no obvious difference between cases with and without mucosal carcinoma of the fallopian tube.

Histologically, in cases 2–4, the mucosal carcinomas of the fallopian tube in the ipsilateral side of the dominant

Table 2 Coexistence of mucosal carcinoma of the fallopian tube in ovarian and peritoneal cancer cases

Histology	Serous (n=15)	Non-serous (n=40)			
		Clear cell	Endometrioid	Mucinous	Others
Number of cases	15	23	9	3	5
Peritoneal dissemination (+)	13	7	0	0	1
Mucosal carcinoma of the fallopian tube (+)	7	0	0	0	0

Table 3 Clinicopathological and immunohistochemical features of serous adenocarcinoma cases

Case	Diagnosis	Age	Histological grade	Stage	Survival	PD	Sig	MCFT	p53 status	WT-1 status	MIB-1 index
1	OC	46	Low	III	NED (20 months)	+	−	+	N/N/N[a]	1+/2+/2+[a]	18/9/1[a]
2	OC	38	High	III	DOD (7 months)	+	−	+	P/P/N[a]	−/−/2+[a]	76/72/2[a]
3	OC	48	High	III	NED (2 months)	+	−	+	N/N/N[a]	2+/2+/2+[a]	71/54/1[a]
4	OC	46	High	III	AWD (15 months)	+	−	+	CN/CN/N[a]	2+/2+/1+[a]	56/55/1[a]
5	OC	47	High	III	NED (4 months)	+	−	+	CN/CN/N[a]	2+/2+/1+[a]	76/40/1[a]
6	OC	57	High	III	AWD (3 months)	+	+	+	P/P/N[a]	1+/2+/2+[a]	34/14/3[a]
7	PC	66	High	III	AWD (1 months)	+	+	+	P/P/N[a]	1+/2+/2+[a]	75/29/0[a]
8	OC	55	High	III	NED (19 months)	−	−	−	P[b]	1+[b]	46[b]
9	OC	59	High	I	NED (17 months)	−	−	−	P[b]	2+[b]	51[b]
10	OC	49	High	III	NED (15 months)	+	−	−	P[b]	2+[b]	44[b]
11	OC	35	High	IV	AWD (8 months)	+	−	−	P[b]	2+[b]	11[b]
12	OC	58	High	III	NED (9 months)	+	−	−	P[b]	2+[b]	42[b]
13	OC	38	High	III	NED (7 months)	+	+	−	N[b]	1+[b]	49[b]
14	PC	49	High	III	NED (18 months)	+	+	−	CN[b,c]	2+[b]	47[b]
15	PC	66	High	IV	AWD (33 months)	+	−	−	CN[b]	2+[b]	78[b]

PD peritoneal dissemination, *Sig* p53 signature, *MCFT* mucosal carcinoma of the fallopian tube, *WT-1* Wilms' tumor 1, *IT* invasive (ovarian or peritoneal) tumor, *BTE* benign tubal epithelium, *OC* ovarian carcinoma, *PC* peritoneal carcinoma, *NED* no evidence of disease, *AWD* alive with disease, *DOD* died of disease, *CN* completely negative, *N* negative, *P* positive

[a] IT/MCFT/BTE

[b] IT

[c] Completely negative except for one tubal lesion showing diffuse p53 positivity

ovarian tumor were in situ lesions by themselves, and no invasive carcinoma was found in continuity with them. In cases 1, 5, and 7, invasive tubal carcinoma was found in continuity or adjacent to the in situ lesions. Histology of the mucosal carcinoma of the fallopian tube was similar to that of the coexisting dominant invasive carcinoma mass in the ovary or peritoneum.

In case 1, the tubal lesion also had low-grade morphological features (Fig. 2). Uniform tumor cells with mild nuclear atypia replaced the tubal mucosa, and they displayed a prominent papillary growth pattern. Its histology was quite similar to that of a typical ovarian serous borderline tumor. Mucosal carcinomas of the fallopian tube in cases 2–7 were composed of tumor cells with marked nuclear atypia (Fig. 3). The presence of prominent nucleoli and frequent mitotic activity were also observed. In cases 3-7, mild to moderate inflammatory cell infiltration was observed in the stroma beneath the mucosal carcinomas of the fallopian tube. In some of these cases, there were histologically obvious cancer implantations in nearby tubal mucosa that were surrounded by desmoplastic stroma.

Immunohistochemical features of serous adenocarcinoma cases

Immunohistochemically, mucosal carcinomas of the fallopian tube that coexisted with ovarian/peritoneal serous adenocarcinomas showed higher MIB-1 index, compared with the benign fallopian tube epithelium (Figs. 2b and 3f). In all seven cases with coexisting mucosal carcinoma of the fallopian tube, both tubal lesions and invasive ovarian/peritoneal carcinomas showed similar immunophenotypes for p53 and WT-1. In case 1, the immunophenotype was only assessable in one of two coexisting mucosal carcinomas of the fallopian tube because the other tubal lesion disappeared in sections for immunohistochemistry. In case 2, two mucosal carcinomas of the fallopian tube showed similar immunophenotypes. Surprisingly, diffuse nuclear staining for p53 protein was observed only in three cases of ovarian/peritoneal carcinomas with coexisting tubal carcinomas (cases 2, 6, and 7; Fig. 3d). In the rest four cases, both invasive ovarian cancer and coexisting tubal carcinoma showed negative (either CN, completely negative; or N, negative) immunoreactivity for p53. Among them, cases 4 and 5 revealed completely negative (CN) immunophenotype for p53, and cases 1 and 3 showed negative (N) immunoreactivity (i.e., only scattered positive cells) for p53 (Figs. 1d and 2a).

Among eight ovarian and peritoneal serous carcinomas that had no coexisting mucosal carcinoma of the fallopian tube, five cases showed positive immunoreactivity for p53, one case revealed p53-completely negative (CN) immunophenotype, and one case was p53-negative (N). However, one remaining case (case 14) revealed an exceptional p53 immunophenotype. Case 14 was diagnosed as peritoneal high-grade serous adenocarcinoma. Along with many

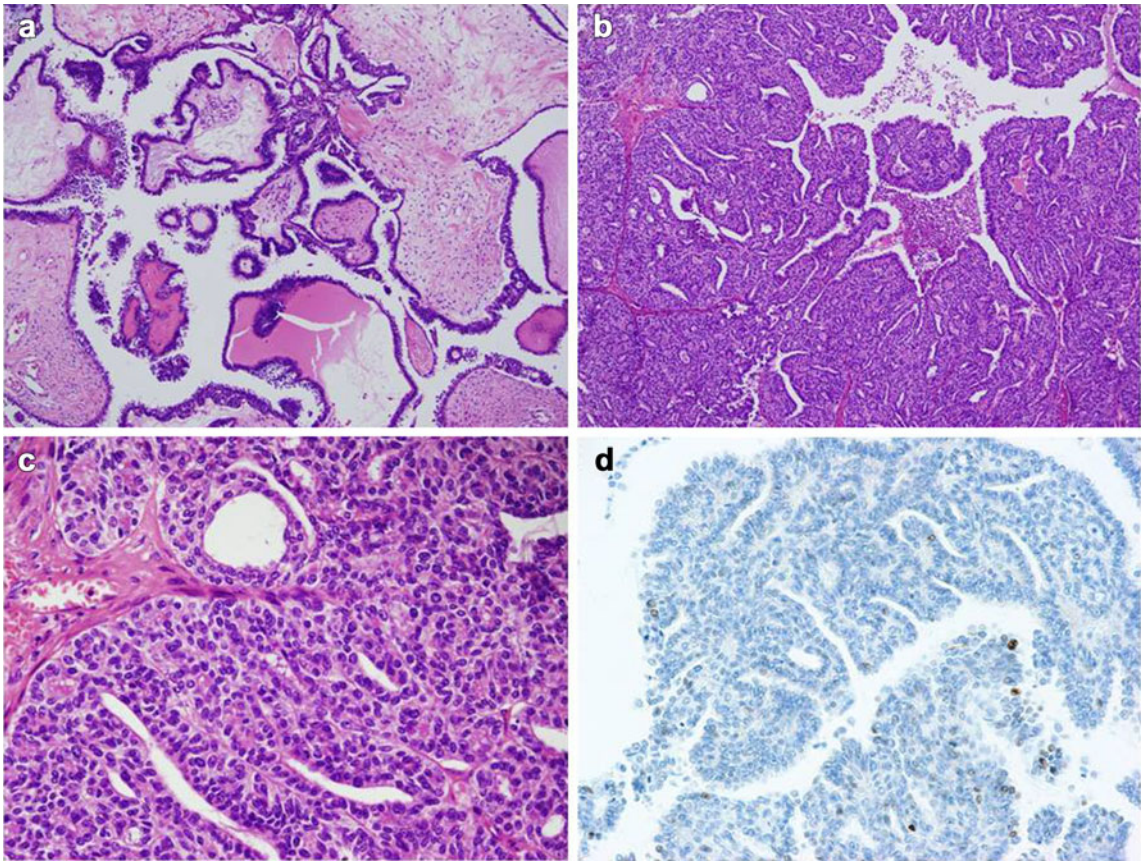

Fig. 1 Histology of ovarian tumor in case 1. **a** Serous borderline tumor component that coexisted with low-grade serous adenocarcinoma. **b** Majority of the ovarian mass was composed of low-grade serous adenocarcinoma showing papillary and glandular patterns of growth. **c** High-power view of the low-grade serous adenocarcinoma. Tumor cells are monotonous and their atypia is mild. **d** Low-grade serous adenocarcinoma showing only scattered immunoreactivity for p53

tumor foci in the omentum (Fig. 4a), we observed superficial involvement of bilateral ovaries (Fig. 4b) and a round discrete tumor nest in the submucosal stroma of the left tube (Fig. 4c). Although these tumor foci (omental, ovarian, and tubal) revealed similar morphological features, the p53 immunophenotype was significantly different between the omental/ovarian carcinoma and the left tubal carcinoma. After immunostaining all the slides that contained carcinoma, we found that all omental and ovarian carcinoma foci were completely negative (CN) for p53 (Fig. 4a, b) and that the left tubal carcinoma focus was diffusely positive for p53 (Fig. 4c). We then made serial sections of the left tubal lesion to examine whether mucosal carcinoma was in adjacent tubal mucosa. Deeper sections revealed tumor exposure in the tubal mucosal (Fig. 4d), but no in situ carcinoma component was identified.

p53 signature in the background tubal mucosa of serous and clear cell adenocarcinoma cases

The p53 signature was present in four of 15 cases of serous adenocarcinoma (Table 3). Of the cases with p53 signatures, two (cases 6 and 7) had coexisting mucosal carcinoma of the fallopian tube. Among the control group of clear cell adenocarcinoma cases, p53 signatures were found in seven of 15 cases (Fig. 5). The p53 signatures were often multifocal and, in some cases, bilateral. Of the 17 p53 signatures (five in serous adenocarcinoma cases and 12 in clear cell adenocarcinoma cases) detected in our series, 14 were located in the non-fimbriated tubal mucosa, and only three were in the fimbriated ends. The MIB-1 indices of the p53 signatures were very low, mostly below 5%, and no increase was observed in comparison with the index of the adjacent tubal mucosa.

Discussion

A newly introduced theory that designates the origin of ovarian cancer to the tubal epithelium has attracted significant attention. The theory is expected to explain, at least to some extent, the ovarian carcinogenesis that had for the most part been a mystery. However, it should be noted that only a few studies have assessed the association

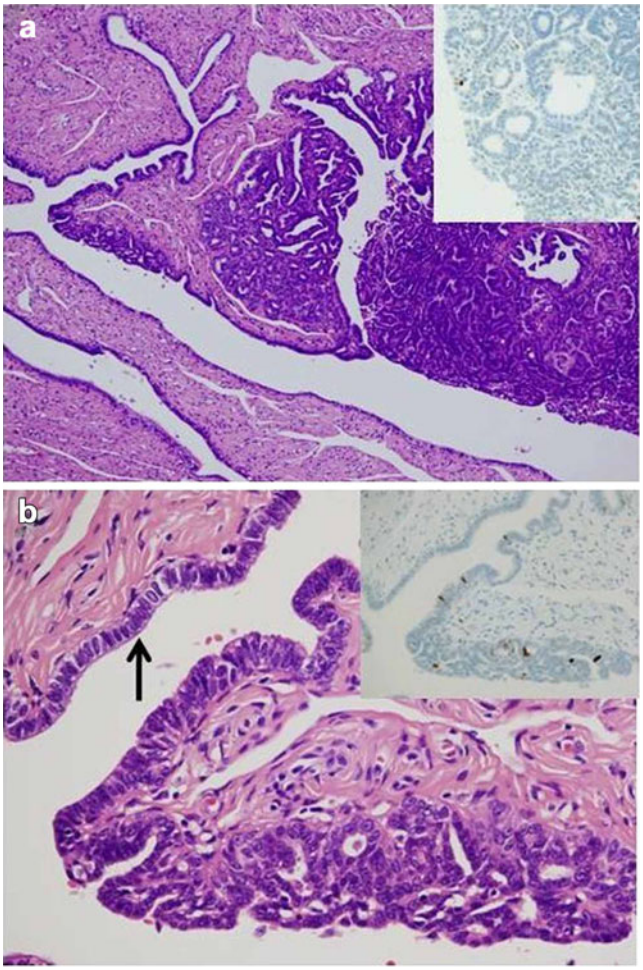

Fig. 2 Mucosal carcinoma of the fallopian tube detected in case 1. **a** Low-power view of the tubal low-grade serous adenocarcinoma. Predominant component of the tumor was noninvasive (in situ). However, some foci of microinvasion were observed. Tubal carcinoma was negative for p53 (*inset*). **b** High-power view of the tubal low-grade serous carcinoma and benign background tubal mucosa (*arrow*). Tumor cells with only mild atypia grew in complexed glandular structures and papillary structures. Immunostaining for Ki-67 is shown in the *inset*. Although the tubal carcinoma showed higher MIB-1 index in comparison with the benign tubal epithelium, its MIB-1 index was no more than 5%

between mucosal carcinomas of the fallopian tube and ovarian carcinomas in general populations to date [8, 10, 11, 15]. In these reports, the authors focused primarily on high-grade serous carcinogenesis and p53 alterations involved in the process. Other histological subtypes of ovarian cancer have not been studied in detail for coexisting tubal lesions. In fact, none of the past series included ovarian clear cell adenocarcinomas, which sometimes resemble serous adenocarcinoma histologically and pose difficult problems to surgical pathologists. In this study, we examined Japanese ovarian and peritoneal cancer cases, which included a large number of ovarian non-serous adenocarcinomas. The high prevalence of clear cell adenocarcinomas in our series should be attributed to the Japanese patient background. By comparing four major histological subtypes of ovarian carcinoma (serous, clear cell, endometrioid, and mucinous), we demonstrated that the coexistence of mucosal carcinoma of the fallopian tube was specific to cases of serous adenocarcinoma. The results of our study suggest that tubal lesion is unlikely to be associated with the development of ovarian clear cell adenocarcinomas and other non-serous adenocarcinomas. Thus, with regard to the origin of non-serous ovarian cancer, attention should rather be paid to the ovarian surface epithelium, inclusion cysts, and endometriotic lesions.

In our study, coexisting mucosal carcinoma of the fallopian tube was found in seven of 15 serous adenocarcinoma cases. The incidence of coexisting mucosal carcinoma and frequency of fimbrial involvement were similar to the values reported previously [8, 10, 15]. However, the p53 immunophenotype of mucosal carcinomas of the fallopian tube in our series was different from those in previous reports. In contrast to the previous series, which showed that nearly all mucosal carcinomas of the fallopian tube were immunohistochemically p53-positive [8, 10], more than half of the tubal lesions in our series were p53-negative. In this report, we hope to emphasize the existence of p53-negative mucosal carcinomas of the fallopian tube. Considering that more than 30% of high-grade serous adenocarcinomas are p53-negative immunohistochemically [26], it is reasonable that we encounter occasional p53-negative early tubal carcinomas that coexist with p53-negative high-grade ovarian/peritoneal serous adenocarcinomas. In general, a cautious approach is necessary in the evaluation of p53 immunoreactivity, especially when assessing the involvement of *TP53* mutations. It is well known that diffuse nuclear p53 immunoreactivity suggests the presence of such mutations. Importantly, studies have revealed that protein-truncating *TP53* mutations can lead to completely negative immunoreactivity [27]. On the other hand, a few scattered p53-positive cells by immunohistochemistry suggest that the lesion harbors wild-type *TP53*. In our series, most of the high-grade serous adenocarcinoma cases, including their coexisting tubal lesions, scored either as P (positive) or CN (completely negative) in immunoreactivity for p53. Therefore, it is highly likely that these tumors harbor *TP53* mutations, and we believe *TP53* alterations play a significant role in the tumorigenesis of many tubal mucosal carcinomas.

Another striking finding in our study was the presence of tubal mucosal carcinoma coexisting with ovarian low-grade serous adenocarcinoma. Currently, not much is known about tubal low-grade serous adenocarcinoma, and there has been no report on the coexistence of tubal mucosal carcinoma in an ovarian low-grade serous adenocarcinoma

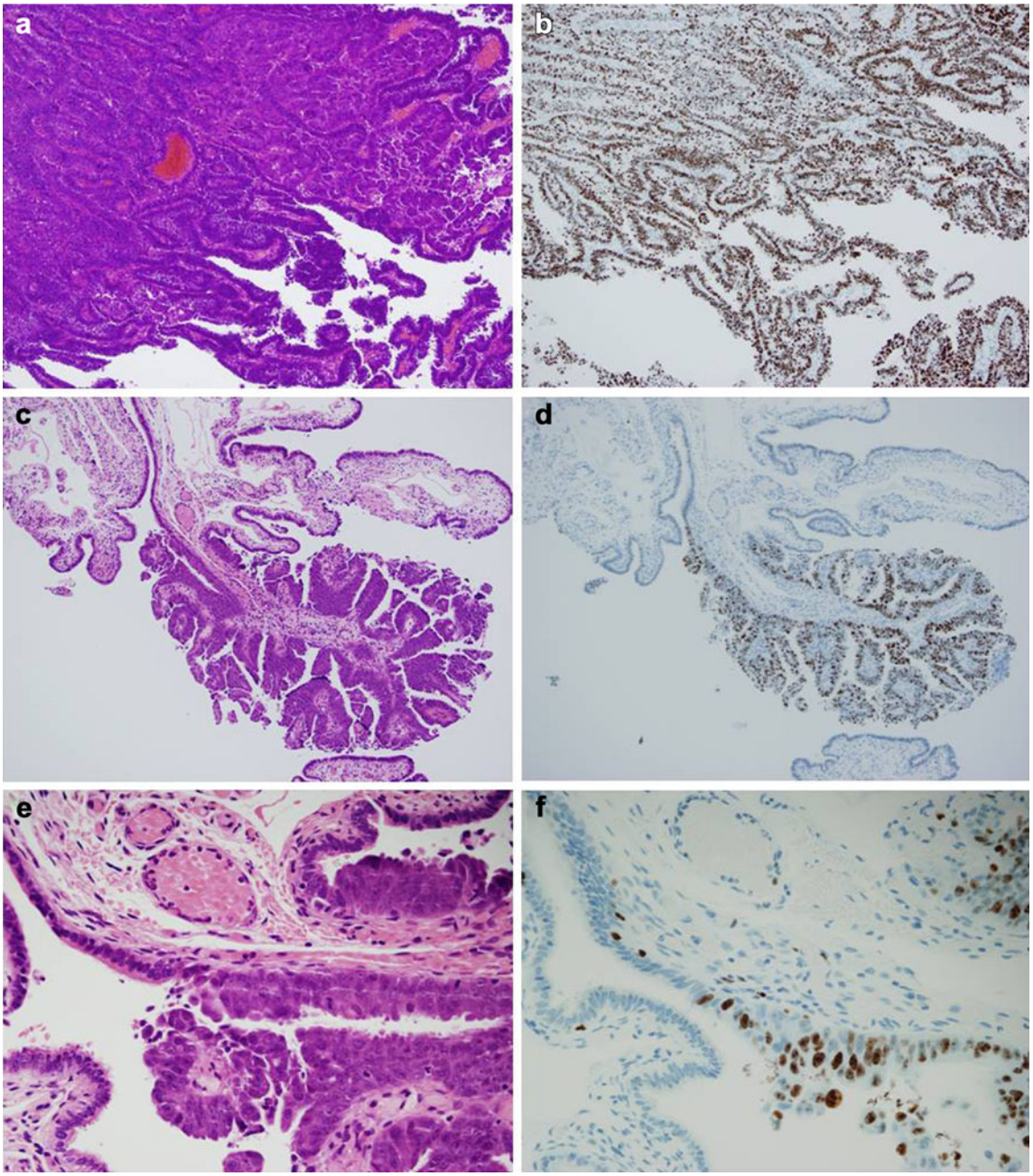

Fig. 3 Histology of ovarian tumor and coexisting mucosal carcinoma of the fallopian tube in case 2. **a** Ovarian carcinoma was high-grade serous adenocarcinoma showing papillary pattern of growth. **b** Ovarian high-grade serous adenocarcinoma showing diffuse immunoreactivity for p53. **c** Mucosal carcinoma of the fallopian tube detected in the fimbriae. **d** Mucosal carcinoma of the fallopian tube was p53-positive. **e** High-power view of the mucosal carcinoma of the fallopian tube. Tumor cells with moderate to severe atypia showing intraepithelial growth. **f** MIB-1 index of the mucosal carcinoma of the fallopian tube was elevated markedly (>50%), compared to adjacent benign mucosa

case. In our case, the tubal lesion showed prominent papillary growth and was large enough to be readily recognized upon microscopic examination. However, cytological atypia of this low-grade tubal carcinoma was very mild, and only a slight increase in MIB-1 index was seen. In addition, p53 immunohistochemistry revealed a wild-type *TP53* phenotype. Based on our experience, we believe that such low-grade tubal lesions can be diagnosed only by means of thorough histological examination, as immunohistochemistry may not always be helpful. Initially, surgical pathologists should be made aware of the occurrence of tubal low-grade serous adenocarcinoma. Accumulation of information about low-grade tubal carcinomas will provide more insights into the pathogenesis of early tubal cancers,

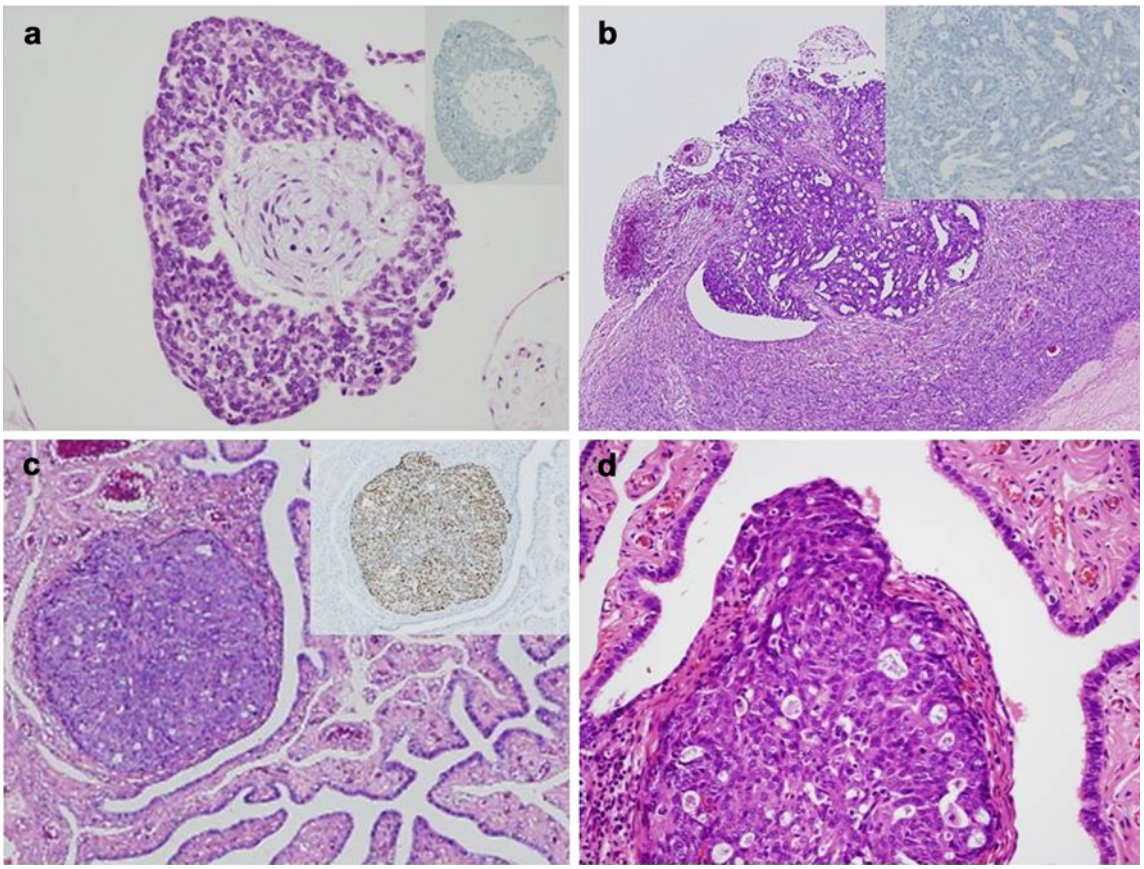

Fig. 4 Histological features of pelvic serous adenocarcinomas of case 14. **a** Nests of serous adenocarcinoma in the omentum, and p53 immunostaining (*inset*). Adenocarcinoma in the omentum is completely negative for p53. **b** Serous adenocarcinoma involving the ovarian surface and p53 immunostaining (*inset*). Adenocarcinoma in the ovary is also completely negative for p53. **c** A well-circumscribed nodule of serous adenocarcinoma detected in the submucosa of the left fallopian tube, and p53 staining (*inset*). The tubal lesion is diffusely positive for p53. **d** A deeper section of the left tubal carcinoma revealed tumor exposure in the tubal mucosa. However, no intraepithelial carcinoma was detected in the adjacent tubal mucosa

including their potential association with ovarian low-grade serous adenocarcinomas.

Regarding p53 alterations in the fallopian tube, we also evaluated the existence of p53 signatures in the background tubal mucosa. The p53 signature has been recognized as a lesion that will evolve to p53-positive mucosal carcinoma of the fallopian tube [14]. Studies have emphasized its importance as an initial change that occurs in pelvic serous carcinogenesis [11, 28]. Interestingly, the p53 signature has been reported to be equally prevalent in benign tubes of BRCA+ and control women [11]. In this series, the prevalence of p53 signatures was not significantly different between serous adenocarcinoma cases and clear cell adenocarcinoma cases. Based on this result, we assume that the presence of the p53 signature itself does not constitute a risk for developing p53-positive pelvic serous carcinoma. Rather, events that take place between the p53 signature and p53-positive mucosal carcinoma of the fallopian tube should be regarded as key steps in the carcinogenesis of p53-positive pelvic serous adenocarcinomas.

Theoretically, there are three ways of interpreting mucosal carcinoma of the fallopian tube: most importantly, as an "early carcinoma (preceding lesion) that progresses to form pelvic serous carcinoma," as a "disseminated serous carcinoma showing intraepithelial spread," or as a part of "multifocal (multiclonal) neoplastic lesions in the pelvis." Each theory has its strong points and weak points. Recent studies have provided evidence in support of the "preceding lesion" theory [7–11, 15]. The frequent presence of early tubal lesions in prophylactically removed specimens from BRCA carriers is an important rationale for designating mucosal carcinoma of the fallopian tube as a "preceding lesion," not just a "coexistent lesion." However, BRCA carriers comprise only about 10% of ovarian cancer patients [29–31], and incidence of mucosal carcinoma of the fallopian tube in patients without BRCA mutations remains unclear. In addition, the precise events that take place between the evolution of initial early tubal carcinoma and the development of mass-forming ovarian or peritoneal serous carcinoma have yet to be clarified. Thus, although

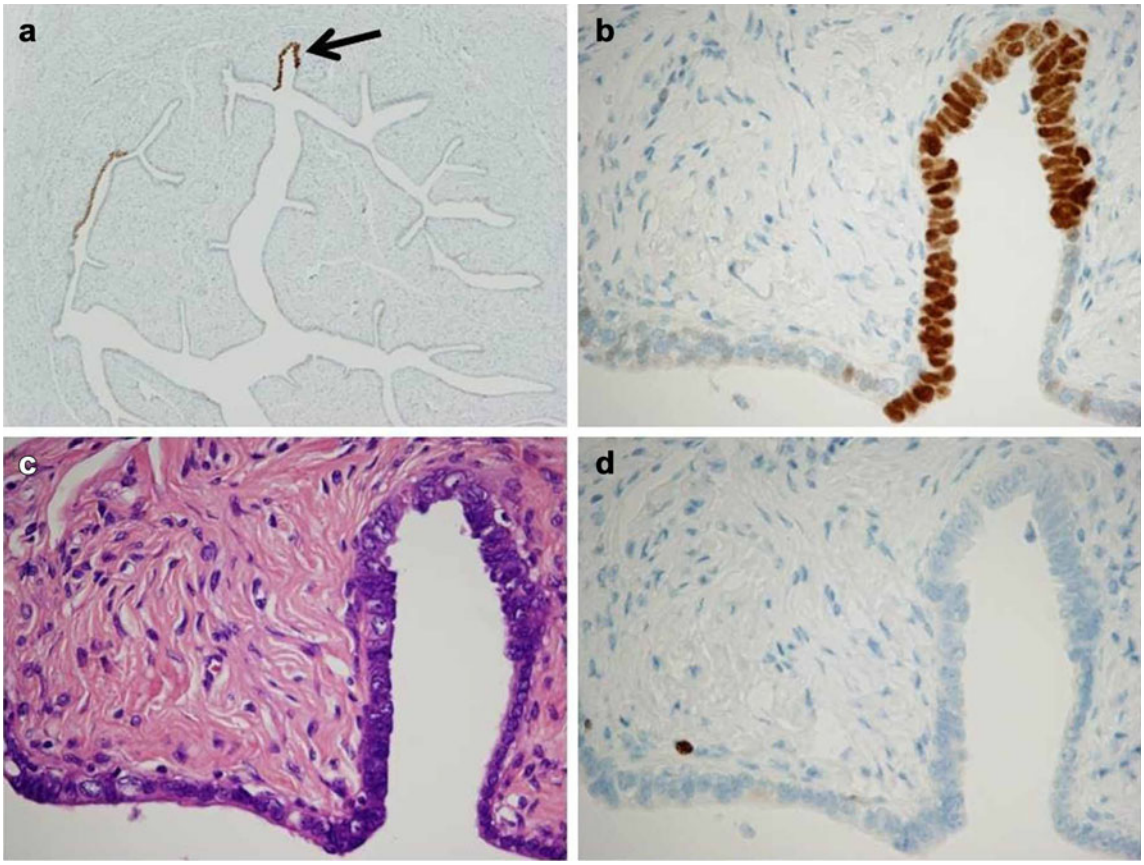

Fig. 5 p53 signatures in the background tubal epithelium of an ovarian clear cell adenocarcinoma case. **a** Immunostaining for p53. Multifocal p53 signatures were found in non-fimbriated tubal mucosa. **b** High-power view of a p53 signature (*arrow* in **a**), (**c**) its hematoxylin and eosin staining, and (**d**) its Ki-67 immunostaining. MIB-1 index of the p53 signature was 0%

we believe, based on the results of our study, that mucosal carcinoma of the fallopian tube is a candidate preceding lesion of pelvic serous adenocarcinoma, additional evidence is necessary to strengthen this hypothesis.

The possibility of some tubal mucosal carcinomas being cancer disseminations from remote tumors should also be discussed. In our series, seven of 13 serous adenocarcinomas with peritoneal disseminations had coexisting mucosal carcinomas of the fallopian tube. On the other hand, mucosal carcinoma of the fallopian tube was not identified in any of the eight non-serous adenocarcinomas with peritoneal disseminations. This result suggests that, in general, ovarian cancer dissemination rarely shows tubal intraepithelial spread. Consequently, it is rather unlikely that a significant number of mucosal carcinomas of the fallopian tube are disseminated carcinoma showing intraepithelial spread. However, in some of our cases, we experienced certain difficulties in making a strict histological distinction between primary intraepithelial neoplasm of the fallopian tube and cancer implantation involving the tubal mucosa. The distinction was especially problematic when the lesions were accompanied by inflammatory stroma and adjacent invasive carcinoma. Ancillary tests, such as immunohistochemistry and genetic studies, are not helpful in making such a distinction.

Finally, mucosal carcinoma of the fallopian tube might be viewed as a part of multifocal (multiclonal) pelvic tumors. Although previous molecular studies on mucosal carcinomas of the fallopian tube have indicated monoclonal origin of the tubal and ovarian tumors in most cases [8, 10, 11], the numbers of cases studied were small, and there were some exceptions. In a series by Salvador et al. [8], fluorescence in situ hybridization (FISH) analysis revealed the possible multiclonal origin of carcinomas involving the ovary and the fallopian tube in one of the cases. In another series, by Kindelberger et al. [10], a case of ovarian serous adenocarcinoma accompanied by two multiclonal tubal carcinomas was included. We have also seen a case of bilateral early tubal carcinomas with an intraepithelial component in the past, which suggested multifocal carcinogenesis in the fallopian tubes [32]. In addition, there has been a report on multiclonal origin for some peritoneal serous carcinomas in patients with BRCA1 mutation [30]. In the present study, the possibility of multiclonal serous

carcinogenesis was seriously considered in case 14, in which we evaluated numerous serous adenocarcinoma foci in the pelvis and found only one minute nodule in the left tube that was p53-positive. We did not identify a definite TIC component adjacent to the left tubal lesion. However, it is likely that the left tubal lesion is a primary p53-positive tubal serous adenocarcinoma that is not associated with p53-negative peritoneal and ovarian serous adenocarcinoma within the same patient. Another case in which we suspected multifocal carcinogenesis was case 1. In case 1, the transition between the serous borderline tumor component and the low-grade serous adenocarcinoma component was observed in the ovary. Given that a serous borderline tumor is a well-known precursor of ovarian low-grade serous adenocarcinoma, the histological findings of the ovarian tumor in case 1 are indicative of primary ovarian origin, and there is a significant chance that the coexisting early tubal carcinoma has arisen independently. Further molecular investigations including mutation analysis of genes involved in carcinogenesis of high-grade/low-grade serous adenocarcinomas (e.g., *TP53*, *BRAF*, and *KRAS*), LOH (loss of heterozygosity), and DNA copy number analysis are needed to assess the clonality of these multifocal pelvic carcinomas.

In conclusion, we demonstrated that mucosal carcinomas of the fallopian tube often coexist with the serous subtype of ovarian cancer, but not with clear cell adenocarcinoma and other non-serous adenocarcinomas of the ovary, in the Japanese population. In comparison with previous studies, tubal lesions in our series showed p53 protein overexpression less frequently. We also encountered a rare case of ovarian low-grade serous adenocarcinoma that coexisted with low-grade tubal carcinoma. Mucosal carcinoma of the fallopian tube is certainly a candidate origin (i.e., early manifestation) of ovarian and peritoneal serous carcinomas. However, to truly demonstrate its role as a preceding lesion, there are obstacles to overcome. Our observations indicate the possible heterogeneity of the lesions currently regarded as TICs or mucosal carcinomas of the fallopian tube on a histological basis. In other words, a few of them may represent a part of multiclonal pelvic serous tumors, and a very few others may be cancer dissemination showing tubal intraepithelial spread. We hope that larger studies from around the world will provide fresh and more comprehensive views on this issue. Finally, the fact that about half of the ovarian serous adenocarcinomas do not have coexisting tubal lesions should not be disregarded. At this point, the conventional de novo pathway that considers the origin of serous adenocarcinoma to be in the ovarian surface epithelium cannot be completely eliminated from the list.

Acknowledgements The authors thank the faculty and resident staff in the Department of Pathology at the University of Tokyo Hospital and Mitsui Memorial Hospital, especially Hideki Miyazaki and Masako Ikemura, for their assistance with the extensive sectioning of the fallopian tubes.

Conflict of interest None.

References

1. Seidman JD, Russell P, Kurman RJ (2002) Surface epithelial tumors of the ovary. In: Kurman RJ (ed) Blaustein's pathology of the female genital tract, 5th edn. Springer, New York, pp 873–878
2. Fukunaga M, Nomura K, Ishikawa E et al (1997) Ovarian atypical endometriosis: its close association with malignant epithelial tumours. Histopathology 30:249–255
3. Okuda T, Otsuka J, Sekizawa A et al (2003) p53 mutations and overexpression affect prognosis of ovarian endometrioid cancer but not clear cell cancer. Gynecol Oncol 88:318–325
4. Modesitt SC, Tortolero-Luna G, Robinson JB et al (2002) Ovarian and extraovarian endometriosis-associated cancer. Obstet Gynecol 100:788–795
5. Malpica A (2008) Grading of ovarian cancer: a histotype-specific approach. Int J Gynecol Pathol 27:175–181
6. Shih IM, Kurman RJ (2004) Ovarian tumorigenesis: a proposed model based on morphological and molecular genetic analysis. Am J Pathol 164:1511–1518
7. Lee Y, Medeiros F, Kindelberger D et al (2006) Advances in the recognition of tubal intraepithelial carcinoma: applications to cancer screening and the pathogenesis of ovarian cancer. Adv Anat Pathol 13:1–7
8. Salvador S, Rempel A, Soslow RA et al (2008) Chromosomal instability in fallopian tube precursor lesions of serous carcinoma and frequent monoclonality of synchronous ovarian and fallopian tube mucosal serous carcinoma. Gynecol Oncol 110:408–417
9. Medeiros F, Muto MG, Lee Y et al (2006) The tubal fimbria is a preferred site for early adenocarcinoma in women with familial ovarian cancer syndrome. Am J Surg Pathol 30:230–236
10. Kindelberger DW, Lee Y, Miron A et al (2007) Intraepithelial carcinoma of the fimbria and pelvic serous carcinoma: evidence for a causal relationship. Am J Surg Pathol 31:161–169
11. Lee Y, Miron A, Drapkin R et al (2007) A candidate precursor to serous carcinoma that originates in the distal fallopian tube. J Pathol 211:26–35
12. Crum CP, Drapkin R, Miron A et al (2007) The distal fallopian tube: a new model for pelvic serous carcinogenesis. Curr Opin Obstet Gynecol 19:3–9
13. Jarboe E, Folkins A, Nucci MR et al (2008) Serous carcinogenesis in the fallopian tube: a descriptive classification. Int J Gynecol Pathol 27:1–9
14. Levanon K, Crum C, Drapkin R (2008) New insights into the pathogenesis of serous ovarian cancer and its clinical impact. J Clin Oncol 26:5284–5293
15. Roh MH, Kindelberger D, Crum CP (2009) Serous tubal intraepithelial carcinoma and the dominant ovarian mass: clues to serous tumor origin? Am J Surg Pathol 33:376–383
16. Powell CB, Kenley E, Chen LM et al (2005) Risk-reducing salpingo-oophorectomy in BRCA mutation carriers: role of serial sectioning in the detection of occult malignancy. J Clin Oncol 23:127–132
17. Finch A, Shaw P, Rosen B et al (2006) Clinical and pathologic findings of prophylactic salpingo-oophorectomies in 159 BRCA1 and BRCA2 carriers. Gynecol Oncol 100:58–64
18. Colgan TJ, Murphy J, Cole DE et al (2001) Occult carcinoma in prophylactic oophorectomy specimens: prevalence and association

with BRCA germline mutation status. Am J Surg Pathol 25:1283–1289
19. Sugiyama T, Kamura T, Kigawa J et al (2000) Clinical characteristics of clear cell carcinoma of the ovary: a distinct histologic type with poor prognosis and resistance to platinum-based chemotherapy. Cancer 88:2584–2589
20. Itamochi H, Kigawa J, Terakawa N (2008) Mechanisms of chemoresistance and poor prognosis in ovarian clear cell carcinoma. Cancer Sci 99:653–658
21. Katabuchi H, Takano M, Udagawa Y (2008) Clinical conference: clear cell adenocarcinoma of the ovary. Nippon Sanka Fujinka Gakkai Zasshi 60:224–228
22. Benedet JL, Bender H, Jones H 3rd et al (2000) FIGO staging classifications and clinical practice guidelines in the management of gynecologic cancers. FIGO committee on gynecologic oncology. Int J Gynaecol Obstet 70:209–262
23. Tavassoli FA, Devilee P (eds) (2003) Pathology and genetics of tumours of the breast and female genital organs. IARC Press, Lyon
24. Malpica A, Deavers MT, Lu K et al (2004) Grading ovarian serous carcinoma using a two-tier system. Am J Surg Pathol 28:496–504
25. Anttila MA, Ji H, Juhola MT et al (1999) The prognostic significance of p53 expression quantitated by computerized image analysis in epithelial ovarian cancer. Int J Gynecol Pathol 18:42–51
26. Kobel M, Kalloger SE, Carrick J et al (2009) A limited panel of immunomarkers can reliably distinguish between clear cell and high-grade serous carcinoma of the ovary. Am J Surg Pathol 33:14–21
27. Holstege H, Joose SA, van Oostrom CTM et al (2009) High incidence of protein-truncating TP53 mutations in BRCA1-related breast cancer. Cancer Res 69:3625–3633
28. Shaw PA, Rouzbahman M, Pizer ES et al (2009) Candidate serous cancer precursors in fallopian tube epithelium of BRCA1/2 mutation carriers. Mod Pathol 22:1133–1138
29. Boyd J (2003) Specific keynote: hereditary ovarian cancer: what we know. Gynecol Oncol 88:S8–S10
30. Shaw PA, McLaughlin JR, Zweemer RP et al (2002) Histopathologic features of genetically determined ovarian cancer. Int J Gynecol Pathol 21:407–411
31. Schorge JO, Muto MG, Welch WR et al (1998) Molecular evidence for multifocal papillary serous carcinoma of the peritoneum in patients with germline BRCA1 mutations. J Natl Cancer Inst 90:841–845
32. Maeda D, Takazawa Y, Ota S et al (2010) Bilateral microscopic adenocarcinoma of the fallopian tubes detected by an endometrial cytologic smear. Int J Gynecol Pathol 29:273–277

Virchows Arch (2010) 457:609–618
DOI 10.1007/s00428-010-0974-9

ORIGINAL ARTICLE

Murine immune response induced by *Leishmania major* during the implantation of paraffin tablets

Maria Letícia Costa Reis · Vanessa Martins Ferreira · Xia Zhang · Ricardo Gonçalves · Leda Quércia Vieira · Washington Luiz Tafuri · David M. Mosser · Wagner Luiz Tafuri

Received: 29 March 2010 / Revised: 16 July 2010 / Accepted: 7 September 2010 / Published online: 21 September 2010
© Springer-Verlag 2010

Abstract We carried out a model of chronic inflammation using a subcutaneous paraffin tablet in mice experimentally infected with *Leishmania major*. It was previously reported that the parasite load following paraffin implantation occurred at a peak of 21 days in both BALB/c and C57BL/6 mice. At the present study, we have investigated what cytokines and chemokines are directly related to the parasite load in C57BL/6 mice. All mice were divided in four groups: mice implanted with paraffin tablets; mice experimentally infected with *L. major;* mice implanted with paraffin tablets and experimentally infected with *L. major*; and mice submitted only to the surgery were used for the Real-Time Polymerase Chain Reaction (RT-PCR) controls. Fragments of skin tissue and the tissue surrounding the paraffin tablets (inflammatory capsule) were collected for histopathology and RT-PCR studies. By 21 days, a diffuse chronic inflammatory reaction was mainly observed in the deep dermis where macrophages parasitized with *Leishmania* amastigotes were also found. RT-PCR analysis has shown that BALB/c mice showed strong IL-4 and IL-10 mRNA expression than controls with very little expression of IFN-γ. In contrast, both IFN-γ and IL-10 mRNA was found in higher levels in C57BL/6 animals. Moreover, in C57BL/6 mice the expression of chemokines mRNA of CCL3/MIP-1α was more highly expressed than CCL2/MCP-1. We conclude that the Th1 immune response C57BL/6 did not change to a Th2 response, even though C57BL/6 animals presented higher parasitism than BALB/c mice 21 days after infection and paraffin implantation.

Keywords *Leishmania major* · Paraffin tablets · Chronic inflammation · Cytokines · C57BL/6 and BALB/c mice

M. Letícia Costa Reis · V. Martins Ferreira · W. Luiz Tafuri (✉)
Departamento de Patologia Geral, Universidade Federal de Minas Gerais, Instituto de Ciências Biológicas,
Av Antonio Carlos, Campus Pampulha,
Belo Horizonte 6627 MG, Brazil
e-mail: wagner@icb.ufmg.br

M. Letícia Costa Reis
e-mail: marialeticia@ufmg.br

V. Martins Ferreira
e-mail: vmferreirabio@yahoo.com.br

X. Zhang · D. M. Mosser
Department of Cell Biology and Molecular Genetics,
Univeristy of Maryland,
Microbiology Bldg,
College Park, MD 20742, USA

X. Zhang
e-mail: xiazhang@umd.edu

D. M. Mosser
e-mail: dmosser@umd.edu

R. Gonçalves
Instituto de Ciências Exatas e Biológicas,
Núcleo de Pesquisas em Ciências Biológicas (NUPEB),
Universidade Federal de Ouro Preto,
Morro do Cruzeiro, Bauxita,
Ouro Preto, MG, Brazil
e-mail: ricardo@nupeb.ufop.br

L. Quércia Vieira
Departamento de Bioquímica e Imunologia, Universidade Federal de Minas Gerais, Instituto de Ciências Biológicas,
Av Antonio Carlos, Campus Pampulha,
Belo Horizonte 6627 MG, Brazil
e-mail: lqvieira@icb.ufmg.br

W. Luiz Tafuri
Departamento de Anatomia Patológica e Medicina Legal,
Universidade Federal de Minas Gerais, Faculdade de Medicina,
Av Alfredo Balena 90,
Belo Horizonte, MG, Brazil
e-mail: washington.tafuri@cnpq.br

Introduction

Leishmania parasites are obligatory intracellular pathogens that replicate primarily within macrophages, and also in dendritic cells (DCs) and fibroblasts [1, 2]. The initial step in protective host defense against *Leishmania* is confinement of the parasite to the site of infection. Infected macrophages are stimulated to produce antimicrobial molecules by interferons [3]. Twenty-four hours after infection, migrating NK cells at the site of the infection up-regulate IFN-γ, which amplifies the host immune defense [4, 5]. Immature DCs in the skin (*Langerhans* cells) then take up *Leishmania* promastigotes and migrate to the regional lymph nodes where they differentiate into mature antigen-presenting DCs [6]. These DCs have two main functions: they present antigens to naïve T cells and they produce interleukin (IL)-12, the cytokine most crucial for the development of a Th1 adaptive immune response [7]. IFN-γ is produced in large amounts by activated Th1 cells, enhancing anti-*Leishmania* activity at the infection site [8]. In consequence, resolution of the infection depends on the early presence of macrophages and the activation of these cells by IFN-γ. Activated Th1 cells enhance parasite killing by macrophages, when they release IFN-γ [9]. However, these immunological processes differ in effectiveness among human individuals. In fact, *Leishmania* parasites can cause a wide spectrum of cutaneous diseases, including: (1) localized cutaneous leishmaniasis (LCL); (2) mucocutaneous leishmaniasis involving erosive lesions of the oral and nasal mucosa; (3) diffuse cutaneous leishmaniasis (DCL) characterized by multiple non-healing lesions; and (4) a distinct clinical form called disseminated cutaneous leishmaniasis [10–12].

In recent years, the regulation of cell migration to the site of inflammation has been intensively investigated. Chemokines, small chemotactic cytokines, are responsible for coordinating leukocyte trafficking with immune cell differentiation and effector functions [13, 14]. LCL lesions show strong expression of Th1-associated chemokines such as CCL2/MCP-1, CXCL9/MIG, and CXCL10/IP10. In contrast, chronic DCL entails lower expression of Th1-associated chemokines and higher levels of CCL3/MIP-1α [9].

The mouse is generally considered a valuable model for human disease. For cutaneous leishmaniasis, it provides an excellent model for identifying the factors involved in developing T helper subsets, since Th1 cells confer protection in resistant strains of mice (C57BL/6), whereas Th2 cells are associated with a fatal outcome in susceptible mice (BALB/c) [15]. Despite technological advances in characterizing the influx of different monocyte–macrophage subpopulations at the molecular level [16, 17], the role of inflammatory macrophages in leishmaniasis remains relatively poorly defined. In 2000, Tafuri et al. [18] described a model of monocytic inflammation using a subcutaneous paraffin tablet. This inert irritant induces the recruitment of monocytes to the site of inflammation and the localized immobilization of macrophages around the tablet. Monocyte infiltration and macrophage accumulation following paraffin implantation was similar in BALB/c and C57BL/6 mice. When paraffin implantation was coupled with *Leishmania major* infection, both strains of mice had large numbers of parasites associated with these inflammatory macrophages at 21 days post-infection. Thus, the early accumulation of parasites in macrophages occurs in both genetically susceptible (BALB/c) and resistant (C57BL/6) strains of mice. Despite these heavy early parasite burdens, the C57BL/6 mouse is able to resolve infection, whereas the BALB/c mouse does not. In that time, based on Murray et al. [19], we discussed that the heavy parasitism that we observe is dependent on the type of macrophages recruited into lesions, and that paraffin implantation can recruit a population of permissive macrophages even in the genetically resistant C57BL/6 mouse. However, in the previous histological examination, the nature of cytokines and chemokines that were produced by these inflammatory cells was not determined [18].

Considering that C57BL/6 mice presented a parasite load similar to BALB/c mice 21 days after infection during the implantation of paraffin tablets, the aim of this study was to determine the chemokines that are produced in this tissue. We hypothesized that the chemokines could be directly related to the parasite load increasing in C57BL/6 mice after paraffin implantation associated to the *Leishmania* infection. We show that over the first 3 weeks post-implantation, there was a remarkable similarity in the histological features and the degree of parasitism in these two mouse strains. However, unlike the BALB/c mouse that is unable to clear infection, the parasite infection was transient in C57BL/6 mice, which had begun to clear the infection by 30 days. Real-time PCR analysis has shown that both IFN-γ and IL-10 mRNA was found in higher levels in the skin and inflammatory capsule of C57BL/6 animals that were infected with *L. major* when compared to paraffin implant alone. In addition, in C57BL/6 mice the expression of chemokines mRNA of CCL2/MCP-1, CCL3/MIP-1α, CCL5/RANTES, CXCL9/MIG, and CXCL10/IP-10 were found in the infected tissues. Particularly, CCL3/MIP-1α was more highly expressed than CCL2/MCP-1, suggesting a differential and important role for them in the recruitment and activation of different immune cells that can define a permissive profile at the site of infection with *L. major*.

Materials and methods

Subcutaneous implantation of paraffin tablets

Paraffin tablets (220.0 mg;Queel-Indústrias Químicas Ltda, São Paulo, Brazil) with the dimensions - 1.0x0.5 cm (HXL) were prepared as described previously. These tablets have a

smooth surface and are maintained under aseptic conditions. To implant them, mice were anesthetized and shaved, and then a skin incision (1.5 cm) was made on the dorsum using blunt point scissors. Tablets were inserted into a small subcutaneous cavity, and the wound was stitched [18].

Mice

Section "Mice"

One hundred mice, 4–6 weeks old, obtained from our animal facility at ICB/UFMG, were divided into two groups: 50 C57BL/6 and 50 BALB/C mice where they were subdivided in four groups.

Group 1 (P) This group comprised mice implanted with paraffin tablets (n=30; 15 of each mice strain);

Group 2 (L) This group comprised mice experimentally infected with *L. major* promastigotes (n=30; 15 of each mice strain)

Group 3 (P+L) This group comprised mice implanted with paraffin tablets and infected with promastigotes immediately thereafter (n=30; 15 of each mice strain);

Group 4 (Group sham–"Wound Healing Surgery Group") This group comprised of ten mice that were submitted only to the surgery (skin incision) where the wound was stitched (wound healing). We collected the skin samples from dorsal area. (n=10; 5 of each mice strain)

These animals were sacrificed at 7, 21 and 30 days.

Day 7–20 mice were distributed in groups 1, 2, 3 and 4 (five mice in each group)

Day 21–15 mice were distributed in groups 1, 2 and 3 (five mice in each group)

Day 30–15 mice were distributed in groups 1, 2 and 3 (five mice in each group)

Experimental infection

C57BL/6 mice were injected with 1×10^6 *L. major* promastigotes in 100 μl (subcutaneous) in the dorsum nearest the paraffin tablet, but not inside of the paraffin tablets and immediately after implantation. Control mice (without paraffin) were infected at the same time. BALB/c mouse experiments followed the same protocol.

Parasites

The Friendlin strain of *L. major* clone IV (MHOM/IL/80/Friedlin) was used in all experiments. Promastigotes were grown at 25°C in Grace's insect cell culture medium (GIBCO Laboratories, Grand Island, NY, USA) supplemented with 20% heat-inactivated fetal bovine serum, glutamine (2 mM), penicillin G (100 U/ml) and streptomycin (100 μg/ml). Stationary-phase promastigotes, obtained from 7- to 9-day cultures, were used for all experimental infections.

Disease progression and collection of tissue samples for histopathology

Five animals from each group were sacrificed at 7, 21 and 30 days after the experimental infection. At each of the designated days, fragments of skin tissue and the tissue surrounding the paraffin tablets (inflammatory capsule) were collected for histopathology [18]. Tissues were fixed in 10% buffered formalin, dehydrated, cleared, embedded in paraffin, cut (3–4 μm thick) and stained with Hematoxylin and Eosin (HE).

Microtitration

Parasites were quantified by limiting dilution, as previously [20]. The inflammatory capsule formed by the paraffin implantation was homogenized using a glass tissue grinder in sterile PBS. Tissue debris was removed by centrifugation at 150×g and the cells were concentrated by centrifugation at 2,000×g. Pellets were resuspended in 400 ml supplemented Grace's culture medium (see above). Samples were plated on to culture plates and serially diluted 1:10 in supplemented Grace's insect tissue culture medium. Each sample was plated in duplicate and read 5 days after the start of culture. Pipette tips were discarded after each dilution to avoid carrying adhering parasites from one well to another. Results are expressed as the negative log of the titer (i.e., the dilution corresponding to the last positive well).

Tissue extraction and determination of *N*-acetyl-β-D-glucosaminidase activity

Fragments of the inflammatory capsule were collected, weighed and homogenized (vortex) in 1.9 ml of 0.1 M NaCl, 0.02 M NaH_2PO_4 0.015 M sodium EDTA, pH 4.7, 4°C, per 100 mg tissue. Infiltration of mononuclear cells was quantified by measuring the levels of the lysosomal enzyme *N*-acetylglucosaminidase (NAG), which is present at high levels in activated macrophages [21]. Part of the pellet remaining after hemoglobin measurement was retained for this assay. These pellets were weighed, homogenized in 0.9% w/v NaCl containing 0.1% v/v Triton X-100 (Promega, Madison, WI, USA) and centrifuged (10,000×g, 10 min, 4°C). Samples of the resulting

supernatant (100 μl) were incubated for 10 min with 100 μl of 2.24 mM *p*-nitrophenyl-*N*-acetyl-h-D-glucosaminide (Sigma-Aldrich, St. Louis, MO, USA), prepared in 0.1 M citrate/phosphate buffer (pH 4.5). The reaction was terminated by adding 100 μl 0.2 M glycine buffer, pH 10.6. Hydrolysis of the substrate was determined by measuring the absorption at 405 nm. NAG activity was expressed as the change in OD per gram wet tissue.

Quantitative real-time polymerase chain reaction

Fragments of the inflammatory capsule were collected and Total RNA was extracted using a single-step phenol/chloroform procedure (TRIZOL®) according to the manufacturer's instructions (Invitrogen, Carlsbad, CA, USA). Briefly, the tissue was soaked with TRIZOL solution and homogenized using a PowerGen Generator (Fisher Scientifics, Franklin, MA,USA). Chloroform (0.25 ml) was added to 1 ml of TRIZOL homogenate and mixed thoroughly. After centrifugation, the upper aqueous phase was transferred to a fresh tube and 0.7 ml of isopropyl alcohol was added to precipitate the RNA. The RNA pellet was washed once with 70% ethanol and air-dried for no more than 10 min at room temperature. Contaminating genomic DNA was eliminated by dissolving the RNA pellet in 10 mM Tris-HCl, pH 7.5, containing RNase-free DNase and 1 mM $MgCl_2$ and incubating for 30 min at room temperature. TRIZOL® solution was then added to stop the reaction and the total RNA was further purified as described above. The final RNA pellet was dissolved in RNase-free water and the A260/280 ratio was measured to evaluate quality [22].

First-strand cDNA synthesis by reverse-transcription reaction: First strand cDNA was generated using ThermoScript® Reverse Transcriptase (Invitrogen,). A 5 μg of genomic DNA-free total RNA and oligo$(dT)_{20}$ primer were used; the detailed procedure is described in the manufacturer's instructions (Invitrogen).

Quantitative-PCR: This was performed using a LightCycler®480 Real-time PCR System (Roche Applied Science, Indianapolis, IN, USA) with SYBR Green PCR reagents purchased from BioRad. Melting curve analyses were carried out to ensure that a single product with the expected melting curve characteristics was obtained. The relative differences among samples were analyzed using the ΔΔCt method described previously. A ΔCt value was determined for each sample using the Ct value for GAPDH to normalize loading differences. A ΔΔCt value was then obtained by subtracting the ΔCt value for the mice submitted only to the surgery (group sham-without paraffin and Leishmania infection) from the corresponding experimental ΔCt. The fold difference over the value for the sham mice was calculated as $2^{\Delta\Delta Ct}$.

Statistical analysis: GraphPad Prism software was used. Data were analyzed statistically by the Student *t* test. Data are expressed as mean±SD. The level of significance was set at $p<0.05$.

Results

Histology

C57BL/6 and BALB/c mice implanted with paraffin alone (Group P)

Sterile paraffin tablets were implanted subcutaneously in the back of C57BL/6 and BALB/c mice. According to Tafuri et al. (2000) [18], both strains of mice had an inflammatory capsule of tissue formed around the paraffin tablets as a result of granulomatous tissue formation.

C57BL/6 and BALB/c mice experimentally infected with Leishmania alone (Group L)

By 21 days, the inflammatory reaction in the BALB/c mice was intense and large numbers of parasitized macrophages were present throughout the lesion. In C57BL/6 mice, a discrete chronic inflammatory process in the deep dermis was observed. Only a few macrophages parasitized with *L. major* were observed (Fig. 1a, b).

C57BL/6 and BALB/c mice experimentally infected with Leishmania and implanted with paraffin (Group P+L)

By 21 days, a diffuse chronic inflammatory reaction was mainly observed in the deep dermis and hypodermis (Fig. 1c, d, and e). Macrophages parasitized with *Leishmania* amastigotes were also found in the dermis (Fig. 1e). Moreover, a new formation of blood vessels and fibroblast proliferation with mature collagen deposition were observed mainly in the capsules (Fig. 1f). However, collagen deposition was observed in both strains of mice, and the degree of deposition was not substantially different between the two strains. Some formation of giant cells was observed, and some of these cells had parasites within their cytoplasm (Fig. 1g, h).

C57BL/6 and BALB/c mice submitted only to the surgery without Leishmania and paraffin implanted (sham group)

Macroscopical lesions were not observed in the dorsum of all mice as an extension of the wound healing. In fact, microscopically skin sections of all mice did not show any histological alteration in the epidermis or dermis of all the samples at 21 days post-surgery assay.

Tissue parasite load

According to Tafuri et al. [18], higher parasite load was observed at 21 days post-infection in BALB/c mice and C57BL/6 when compared to the other groups, at 7 and 21 days. Interestingly, C57BL/6 mice showed higher parasitism than BALB/c mice in the tissue capsules ($p \leq 0.01$). By 30 days, the parasite load had decreased in C57BL/6 but not in BALB/c (Fig. 2).

N-acetyl-β-D-glucosaminidase activity

We had shown by histological examination that the capsule tissue obtained from C57BL/6 presented an intense chronic

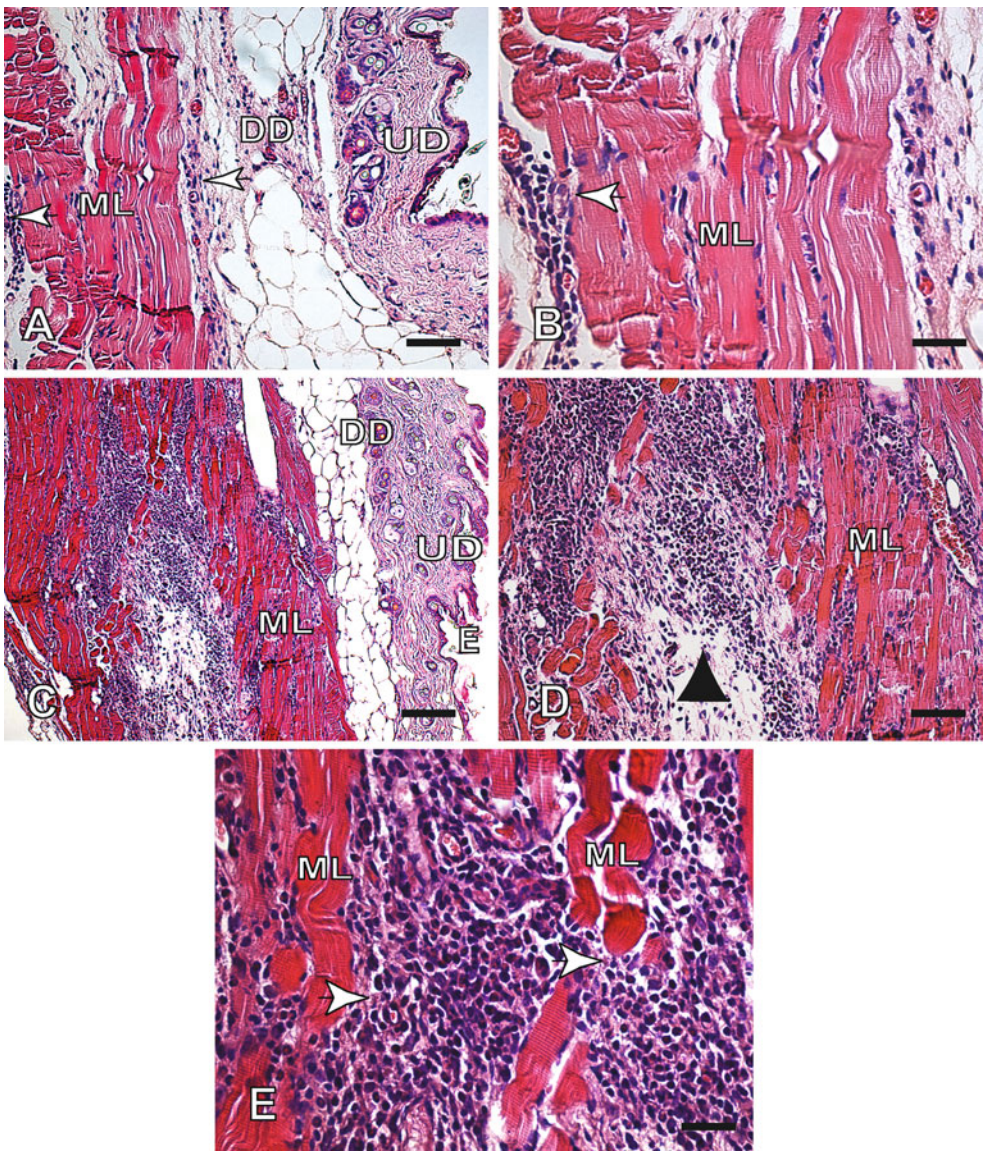

Fig. 1 a–e: a, b Skin fragment of C57BL/6 mice infected with *L. major* (21 days). **a** Note the presence of a discrete chronic inflammatory exudate in the deep dermis (*DD; white arrows*). Hematoxylin and eosin (HE) stain. *Bar*=32 μm. *E* Epidermis; *UD* Upper dermis; *DD* Deep dermis; *ML* Muscular layer. **b** High magnification showing mononuclear cells and some macrophages with amastigotes forms of *Leishmania* (*white arrow*). HE stain. *Bar*=16 μm. **c–e** Skin fragment of C57BL/6 implanted with paraffin tablets and infected with *L. major* (21 days). **c** There is an intense chronic inflammatory exudate dissecting the muscular layer (*ML*) in the deep dermis. HE stain. *Bar*=62 μm. **d, e** Higher magnification showing inflammatory mononuclear cells also provoking tissue damage (*black triangle*). Amastigotes forms of *Leishmania* can be observed inside macrophages (*white arrows*). HE stain. *Bar*=32 and 16 μm, respectively. **f–h** Inflammatory capsule of C57BL/6 implanted with paraffin tablets and infected with *L. major* (21 days). **f** Granulomatous tissue formation with blood vessels (*arrowheads*), collagen and mononuclear exudate can be noted. HE stain. *Bar*=16 μm. **g** Giant cell formation (*white arrowheads*) and macrophages parasitized with *Leishmania* amastigotes were readily observed (*white arrows*). HE stain. *Bar*=16 μm. **h** Granuloma formation with giant cells (*white arrowhead*) and epithelioid cells (*white arrows*). HE stain. *Bar*=16 μm

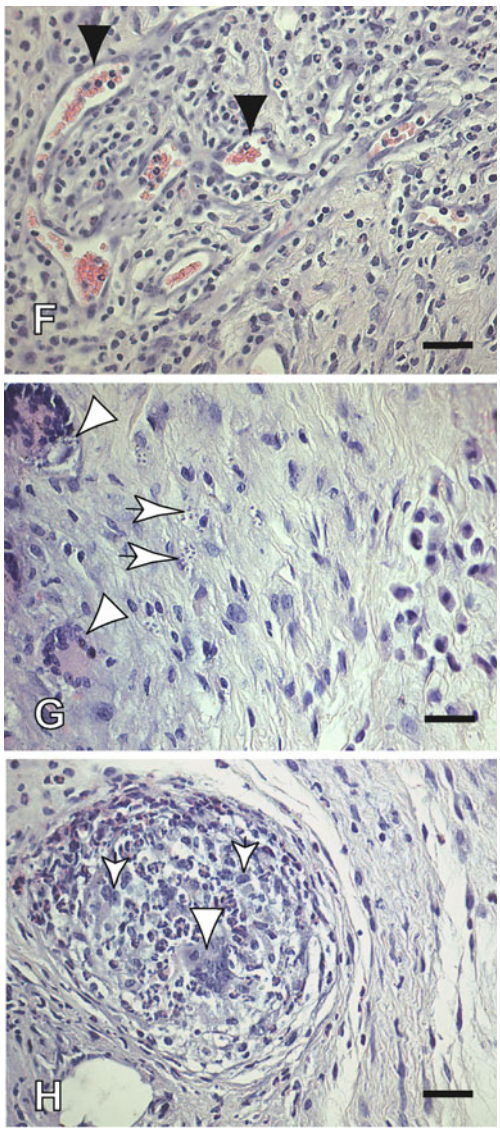

Fig. 1 (continued)

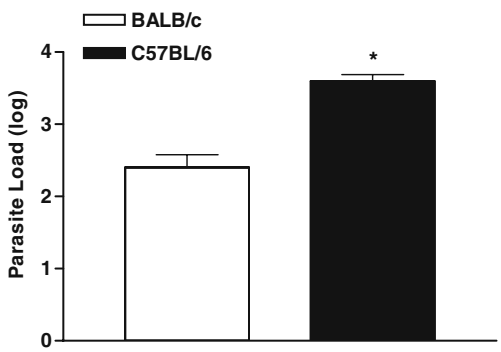

Fig. 2 Parasite load of inflammatory capsule of C57BL/6 and BALB/c implanted with paraffin tablets and infected with *L. major* (21 days). Statistical difference was noted by 21 days (*Bars*, mean±SD; *asterisk*, $p<0.01$ compared to BALB/c group)

inflammatory reaction by 21 days. We therefore investigated the accumulation of activated inflammatory macrophages by an indirect method, NAG activity. At the site of the lesion (capsule tissue) induced by the paraffin implantation associated with *L. major*, NAG activity was significantly increased ($p \leq 0.05$) at 21 days after experimental infection, compared to paraffin-implantation group (Fig. 3).

Cytokines and chemokines at the site of infection

mRNA expression of the cytokines IL-12, TNF-α, and IFN-γ, which are associated with the resistant phenotype to *L. major* infection (C57BL/6 mice), and IL-4 and IL-10, which are associated with the susceptible phenotype (BALB/c), were determined by real-time polymerase chain reaction (RT-PCR). Expression of chemokines related to monocyte-macrophage (CCL2/MCP-1, CCL3/MIP-1α and CCL5/RANTES) and lymphocyte (CXCL9/MIG and CXCL10/IP-10) recruitment was also investigated. For these studies, all capsule samples from BALB/c and C57BL/6 mice were obtained 21 days after paraffin implantation concurrent with *Leishmania* infection. This time point was chosen because the kinetics of the inflammatory response peaked and the parasite load was prominent in both BALB/c and C57BL/6 mice. Skin tissue samples of sham group were used as controls to compare the cytokine levels. Figure 4a shows that C57BL/6 mice have a resistant phenotype marked by the higher expression of IFN-γ and IL-12 mRNA. Both of these expressions were increased in mice receiving parasites plus paraffin (gray bars), relative to mice receiving paraffin implantation alone (black bars). TNF-α and IL-10 mRNA were detected in lower levels in these mice, and there was no increase relative to paraffin alone. BALB/c mice, on the other hand, expression higher levels of IL-10 and IL-4 mRNA than C57BL/6 mice, and these levels were higher in mice receiving both parasites and paraffin implantation (Fig. 4b).

C57BL/6 mice from the P+L group showed higher levels of CCL3/MIP-1α, CCL5/RANTES, CXCL9/MIG and CXCL10/IP-10 mRNA when compared to the paraffin alone group (Fig. 5a). In particular, CXCL9/MIG level in the P+L group was dramatically increased. BALB/c mice, in contrast, expressed higher levels of CCL2/MCP-1 and CCL3/MIP-1α than C57BL/6 (Fig. 5b).

Discussion

In these paraffin implantation model, both C57BL/6 and BALB/c mouse strains showed an early increase in the numbers of parasites in the lesions accompanies the inflammation. This increase in parasite numbers was

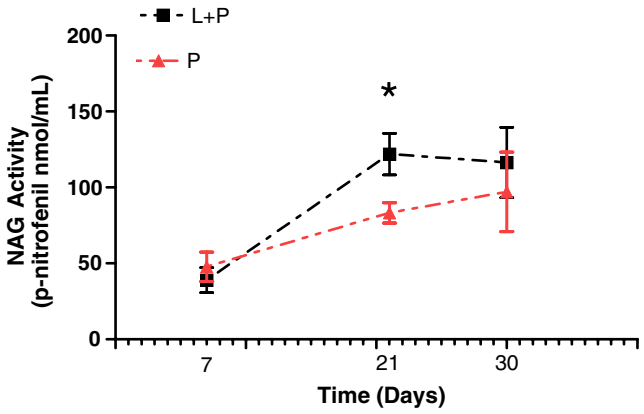

Fig. 3 *N*-acetyl-β-D-glucosaminidase activity in C57BL/6 mice: Fragments of a granulomatous tissue formation (inflammatory capsule) were obtained from 7, 21, and 30 days after the infection and implantation. The NAG activity was determined individually and each *symbol* represents the average and standard deviation of five animals for each group. *L+P* represents mice with the paraffin-tablet implantation and infection with *L. major*; *P* represents mice with paraffin-tablets implantation only.). Statistical difference was noted by 21 days (*Bars*, mean±SD; *asterisk*, $p<0.05$ compared to paraffin group)

observed over the first 3 weeks of infection with a peak at 21 days. In fact, these results were the same observed by Tafuri et al. (2000) [18] following the same experimental protocol. The increase in parasite burden due to paraffin implantation was associated with an intense and diffuse chronic inflammatory reaction, with macrophages heavily loaded with parasites. Moreover, NAG activity was higher at 21 days in the inflammatory capsule of C57BL/6 mice than BALB/c. However, this increase in parasites was transient and these mice subsequently began to resolve their infections. In fact, 30 days after infection, the number of parasites in their lesions begun to be reduced relative to those in the BALB/c mice.

C57BL/6 mice produce IFN-γ, TNF-α and IL-12 in response to *Leishmania* infection, and are able to resolve their infection and develop long-lasting immunity. BALB/c mice, in contrast, produce IL-4 and IL-10 rather than IFN-γ and fail to resolve their lesions, ultimately succumbing to fulminating infection [15, 23]. In this work, C57BL/6 implanted with paraffin concurrently with *L. major* infection showed a marked expression of IFN-γ mRNA by 25 times greater than controls. Small amounts of IL10 (10 ng/ml) inhibit IL-12, TNF-α, and IFN-γ production by macrophages and also render the macrophages refractory to the activating effect of IFN-γ have shown by Kane and Mosser [24]. In consequence, IL-10 prevents macrophages from eliminating intracellular parasites. IL-10 mRNA was also expressed concomitantly with IFN-γ expression. In addition to macrophages, one subset of CD4+CD25-Foxp3-Th1 cells with IFN-γ production produces high amounts of IL-10. IL-10 derived from these Th1 cells and macrophages play a

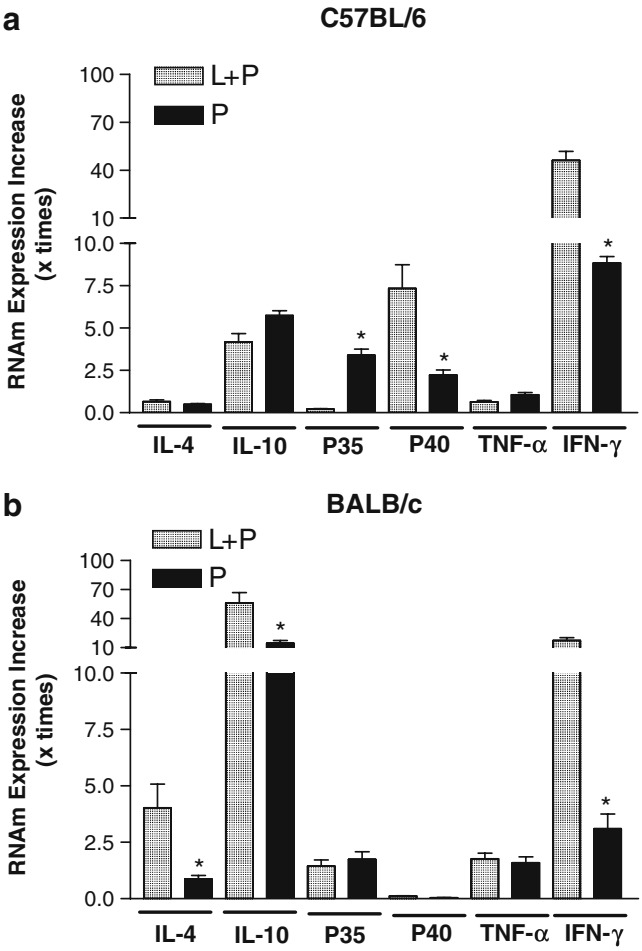

Fig. 4 **a** mRNA expression by RT-PCR of cytokines in C57BL/6 mice: Fragments of a granulomatous tissue formation (inflammatory capsule) were obtained from 21 days after the infection and implantation. The results are expressed of increasing numbers in relation to skin tissue samples from animals that were submitted only to the surgery, group sham (considered zero-axis graph). Each *bar* represents the average and standard deviation of five animals for each group. *L+P* represents mice with the paraffin-tablet implantation and infection with *L. major*; *P* represents mice with paraffin-tablets implantation only.). Statistical difference was noted by 21 days (*Bars*, mean±SD; *asterisk* $p<0.05$ compared to L+P group). **b** mRNA expression by RT-PCR of cytokines in BALB/c mice: Fragments of a granulomatous tissue formation (inflammatory capsule) were obtained from 21 days after the infection and implantation. The results are expressed of increasing numbers in relation to skin tissue samples from animals that were submitted only to the surgery, group sham (considered zero-axis graph). Each *bar* represents the average and standard deviation of five animals for each group. *L+P* represents mice with the paraffin-tablet implantation and infection with *L. major*; *P* represents mice with paraffin-tablets implantation only. Statistical difference was noted by 21 days (*Bars*, mean±SD, *asterisk*, $p<0.05$ compared to L+P group)

pathologic role in the pathogenesis of *Leishmania* infection, as reported by Anderson [25]. Thus, our data are consistent with these earlier studies and could explain the increased tissue parasite load at 21 days (transient susceptibility), related to higher IL-10 mRNA expression at the site of

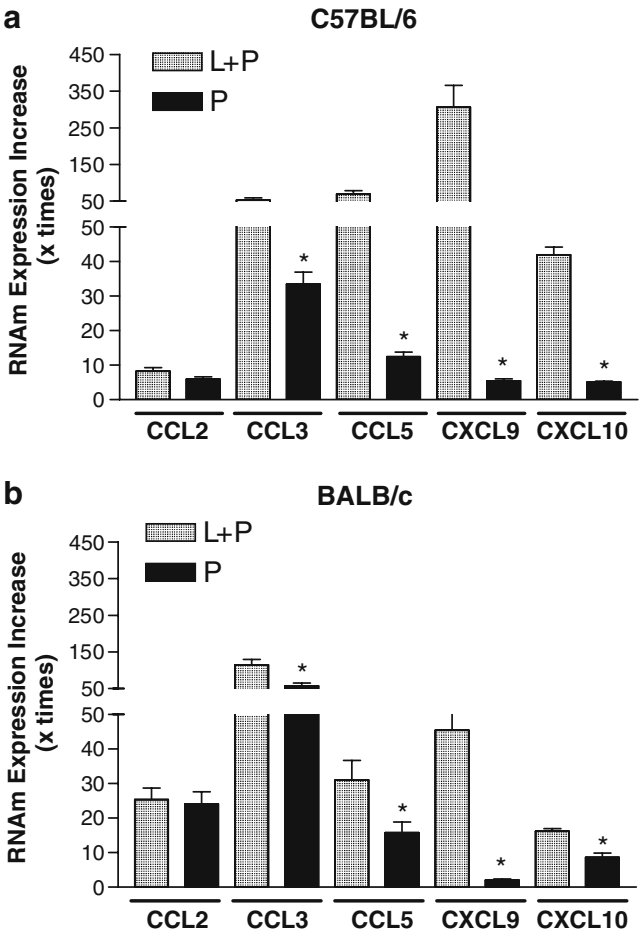

Fig. 5 **a** mRNA expression by RT-PCR of chemokines in C57BL/6 mice: Fragments of a granulomatous tissue formation (inflammatory capsule) were obtained from 21 days after the infection and implantation. The results are expressed of increasing numbers in relation to skin tissue samples from animals that were submitted only to the surgery, group sham (considered zero-axis graph). Each *bar* represents the average and standard deviation of five animals for each group. *L+P* represents mice with the paraffin-tablet implantation and infection with *L. major*; *P* represents mice with paraffin-tablets implantation only. Statistical difference was noted by 21 days (*Bars*, mean±SD; *asterisk*, $p<0.05$ compared to L+P group). **b** mRNA expression by RT-PCR of chemokines in BALB/c mice: Fragments of a granulomatous tissue formation (inflammatory capsule) were obtained from 21 days after the infection and implantation. The results are expressed of increasing numbers in relation to skin tissue samples from animals that were submitted only to the surgery, group sham (considered zero-axis graph). Each *bar* represents the average and standard deviation of five animals for each group. *L+P* represents mice with the paraffin-tablet implantation and infection with *L. major*; *P* represents mice with paraffin-tablets implantation only. Statistical difference was noted by 21 days (*Bars*, mean±SD; *asterisk*, $p<0.05$ compared to L+P group

infection, probably without changing the systemic Th1 profile in C57BL/6. In contrast, BALB/c mice showed strong IL-10 mRNA expression by 51 times higher than controls with very little expression of IFN-γ; IL-4 message was also mainly detected in BALB/c mice. IL-4 production induces Th2 differentiation and progressive leishmaniasis in susceptible mice, but the persistence of infection in these mice could be related to an overproduction of IL-10, which inhibits Th1 cells, and not by exacerbation of the Th2 response [26]. In addition to the Th2 cell-polarizing conditions that underlie the susceptibility of BALB/c mice to cutaneous *Leishmania* infection, overproduction of endogenous IL-10 by the host has been well recognized as a central factor that compromises Th1 response to efficiently clean parasites, not only in a variety of mouse models but also in human beings.

On the other hand, IL-12 is essential for an effective polarization of naïve Th cells to the Th1 phenotype characterized by the expression of IFN-γ. IL-12 is composed of two subunit, p35 and p40. IL-12p40 expression is readily detectable in C57BL/6 strain with higher expression in paraffin-*Leishmania* group than paraffin one. However, IL-12p40 expression is hardly detected in BALB/c strain. Scharton-Kersten and Scott found that BALB/c mice lose the capacity to produce IL-12 in the initial phases of *L. major* infection owing to genetic defect [27]. Furthermore, IL-12p40 reduction can also be due to the inhibitory effect of Fcγ-mediated signaling induced by interaction of opsonized parasites on the macrophages [22].

Matte and Olivier found that *L. major* is a strong inducer of an early inflammatory response, and this immunological scenario could potentially restrain the parasite to the inoculation site, favoring the development of local swelling and cutaneous lesions [28]. In our paraffin model, we found increased expression of all chemokines investigated in the skin inflammatory capsule tissue (CCL2, CCL3, CCL5, CXCL9 and CXCL10), especially those induced by IFN-γ and directly involved in the Th1 response, such as CCL3/MIP1-α, CXCL9/MIG and CXCL10/IP-10. These last two chemokines are chemoattractants for CXCR3 T lymphocytes [13]. The onset of *Leishmania donovani*-induced hepatic inflammation and granuloma formation was found to be delayed in CXCR3-/-C57BL/6 mice [29]. The increased expressions of CXCL9/MIG and CXCL10/IP-10 may attract regulatory T cell populations with subsequent IL-10 production at the site of inflammation [30, 31].

CCL5/RANTES up-regulates IL-12, IFN-γ and migration of Th1 cells, particularly memory T cells to the site of infection [32, 33]. Here, we observed significantly greater production of the chemokine CCL5/RANTES in the skin capsules of C57BL/6 mice implanted with paraffin concurrently with experimental infection with *L. major* promastigotes compared to mice that had received only paraffin implantation. ELISA assays (data not shown) revealed a notably greater production of CCL5/RANTES in the initial phases of experimental infection (7 days), especially in mice with both paraffin implantation and *L. major* infection. Consistently with the kinetics of this experimen-

tal protocol (LP) in C57BL/6 mice, the CCL5/RANTES mRNA levels decreased by 21 days and fell to the levels found in non-infected mice by 30 days. Thus, the decrease in CCL5/RANTES might be directly correlated with the inflammatory response at the site of experimental *Leishmania* infection in C57BL/6 mice. Santiago and co-authors have demonstrated that treatment with Met-RANTES or anti-CCL5/RANTES rendered C57BL/6 animals more susceptible to *L. major* and skewed the immune response from type 1 to type 2 by diminishing IFN-γ production by draining lymph node cells and increasing IL-4 mRNA expression in the lesions [33].

CCL2/MCP-1 is known to attract monocytes, DCs, natural killer cells, and memory T lymphocytes [32]. It has been suggested that CC chemokine receptor 2 (CCR2), the receptor that binds CCL2/MCP-1, increases monocyte recruitment, whereas CCL2/MCP-1 plays a variety of roles in host defense against *Leishmania* [34–36]. It has been reported that high doses of CCL2/MCP-1 activate anti-*Leishmania* macrophage killing mechanisms, either directly by inducing reactive oxygen intermediates [6], or indirectly via nitric oxide production [37]. Recently, a subset of CCR2-positive monocytes has been identified and shown to migrate into inflammatory sites. This population of cells may play a role in pathogen clearance [16]. Here, C57BL/6 mice showed low levels of CCL2/MCP-1 at 21 days after infection. Thus, the lower levels of CCL2/MCP-1 detected in C57BL/6 mice may be consistent with the intense tissue parasite load in the skin capsules. In fact, Conrad and others, working with CCL2/MCP-1 transgenic *L. major* promastigotes, considered that CCL2/MCP-1 is the main chemoattractant recruiting a restrictive CCR2-positive macrophage subset to the site of infection in resistant mouse strains [38]. These macrophages may assist in resolving the lesions when coactivated with CCL2/MCP-1, whereas the lack of CCL2/MCP-1 production may preclude any such recruitment of CCR2-positive monocytes/macrophages in susceptible BALB/c mice. In our work, BALB/c mice showed no statistical difference from controls in CCL2/MCP-1 production. It has been reported in humans that CCL2/MCP-1 is present in self-healing lesions but absent in non-healing diffuse cutaneous leishmaniasis [9].

Ritter and Heinrich-Korner described divergent expression of inflammatory dermal chemokines in self-healing localized cutaneous leishmaniasis and progressive diffuse cutaneous leishmaniasis [9]. LCL is characterized by strong expression of Th1-associated chemokines such as CCL2/MCP-1, CXCL9/MIG and CXCL10/IP-10, and small amounts of CCL3/MIP-1α. Chronic DCL is associated with the opposite expression pattern: CCL3/MIP-1α is dominant and CCL2/MCP-1, CXCL9/MIG and CXCL10/IP-10 are expressed at low levels. In our model, C57BL/6 mice concurrently implanted with paraffin and infected with *Leishmania* dominantly expressed CXCL9/MIG whereas in BALB/c mice, CCL3/MIP-1 is the highest expressed chemokines. In parallel with Th1-phenotype in C57BL/6 and Th2-phenotype in BALB/c as demonstrated by the expression pattern of cytokines and chemokines, the lesion in C57BL/6 is transient and healed after 30 days whereas BALB/c mice have a persistent and non-healing lesion. It has been suggested that immigrating monocytes–macrophages act more like host cells that are permissive for *Leishmania* growth than as effector cells that restrict parasite replication [17]. This permissiveness exists even in the face of the intense inflammatory reaction that occurs in response to paraffin. In fact, Tafuri et al. (2000) [18], in a morphological study, showed that *L. major* lesions were more intense when induced along with the inert inflammatory agent. In both the BALB/c and C57BL/6 strains of mice, an early increase in the numbers of parasites in lesions accompanied this inflammation. This increase in parasite numbers in the lesion was observed over the first 3 weeks of infection. In this present study, we have attempted to determine the immunological response in C57BL/6 during this transiently susceptibility picture related to the highest tissue parasite load. We conclude that the Th1 immune response C57BL/6 did not change to a Th2 response, even though C57BL/6 animals presented higher parasitism than BALB/c mice 21 days after infection and paraffin implantation. Importantly, our models of C57BL/6 mice implanted with paraffin and infected with *Leishmania* vs. BALB/c strain with same manipulation will be useful models to mimic self-healing localized cutaneous leishmaniasis (LCL) vs. progressive diffuse cutaneous leishmaniasis (DCL) in human beings.

Conflict of interest statement We declare that we have no conflict of interest.

References

1. Alexander J, Russell DG (1992) The interaction of *Leishmania* species with macrophages. Adv Parasitol 31:175–254. doi:10.1016/S1471-4922(02)02352-8
2. Bogdan C, Donhauser N, Döring R, Röllinghoff M, Diefenbach A, Rittig MG (2000) Fibroblasts as host cells in latent leishmaniosis. J Exp Med 191:2121–2130. doi:10.1016/j.ijid.2008.11.008
3. Diefenbach A, Schindler H, Donhauser N, Lorenz E, Laskay T, MacMicking J, Rollinghoff M, Gresser I, Bogdan C (1998) Type 1 interferon (IFNalpha/beta) and type 2 nitric oxide synthase regulate the innate immune response to a protozoan parasite. Immunity 8:77–87. doi:10.1016/S1074-7613(00)80460-4
4. Bogdan C, Rollinghoff M (1998) The immune response to *Leishmania*: mechanisms of parasite control and evasion. Int J Parasitol 28:121–134. doi:10.1016/S0020-7519(97)00169-0

5. Vester B, Muller K, Solbach W, Laskay T (1999) Early gene expression of NK cell-activating chemokines in mice resistant to *Leishmania major*. Infect Immun 67:3155–3159
6. Moll H (2000) The role of dendritic cells at the early stages of *Leishmania* infection. Adv Exp Med Biol 479:163–173. doi:10.1007/0-306-46831-X_14
7. Von Stebut E, Belkaid Y, Jakob T, Sacks DL, Udey MC (1998) Uptake of *Leishmania major* amastigotes results in activation and interleukin 12 release from murine skin-derived dendritic cells: implications for the initiation of anti-*Leishmania* immunity. J Exp Med 188:1547–1552
8. Liew FY, Li Y, Millott S (1990) Tumor necrosis factor-alpha synergizes with IFN-gamma in mediating killing of *Leishmania major* through the induction of nitric oxide. J Immunol 145:4306–4310
9. Ritter U, Korner H (2002) Divergent expression of inflammatory dermal chemokines in cutaneous leishmaniasis. Parasite Immunol 24:295–301
10. Ashford RW (2000) The leishmaniases as emerging and reemerging zoonoses. Int J Parasitol 30:1269–1281. doi:10.1016/S0020-7519(00)00136-3
11. Silveira FT, Lainson R, Corbett CE (2005) Further observations on clinical, histopathological, and immunological features of borderline disseminated cutaneous leishmaniasis caused by *Leishmania (Leishmania) amazonensis*. Mem Inst Oswaldo Cruz 100:525–534
12. Sousa AQ, Pompeu MML, Sólon FRN, Frutuoso MS, Teixeira MJ, Silva TMJ (2006) Disseminated cutaneous leishmaniasis: a patient with 749 lesions. Braz J Infect Dis 10:230–230
13. Roychoudhury K, Roy S (2004) Role of chemokines in *Leishmania* infection. Curr Mol Med 4:691–696
14. Zlotnik A, Yoshie O, Nomiyama H (2006) The chemokine and chemokine receptor superfamilies and their molecular evolution. Genome Biol 7:243.1–243.10. doi: 10.1186/gb-2006-7-12-243
15. Scott P (1991) IFN-gamma modulates the early development of Th1 and Th2 responses in a murine model of cutaneous leishmaniasis. J Immunol 147:3149–3155
16. Gordon S, Taylor PR (2005) Monocyte and macrophage heterogeneity. Nat Rev Immunol 5:953–964. doi:10.1038/nri1733
17. Mosser DM, Edwards JP (2008) Exploring the full spectrum of macrophage activation. Nat Rev Immunol 8(12):958–969. doi:10.1038/nri2448
18. Tafuri WL, Melo MN, Paiva MC, Mosser DM, Tafuri WL (2000) Kinetics of an experimental inflammatory reaction induced by *Leishmania major* during the implantation of paraffin tablets in mice. Virchows Arch 437:429–435. doi:10.1007/s004280000231
19. Murray HW (1994) Blood monocytes: differing effector role in experimental visceral versus cutaneous leishmaniasis. Parasitol Today 10:220–223. doi:10.1016/0169-4758(94)90117-1
20. Vieira LQ, Goldschmidt M, Nashleanas M, Pfeffer K, Mak T, Scott P (1996) Mice lacking the TNF receptor p55 fail to resolve lesions caused by infection with *Leishmania major*, but control parasite replication. J Immunol 157:827–835
21. Bailey PJ (1988) Sponge implants as models. Methods Enzymol 162:327–334
22. Yang Z, Mosser DM, Zhang X (2007) Activation of the MAPK, ERK, following *Leishmania amazonensis* infection of macrophages. J Immunol 178:1077–1085
23. Sacks D, Noben-Trauth N (2002) The immunology of susceptibility and resistance to *Leishmania major* in mice. Nat Rev Immunol 2:845–858. doi:10.1038/nri933
24. Kane MM, Mosser MD (2001) The role of IL-10 in promoting disease progression in leishmaniasis. J Immunol 166:1141–1147
25. Anderson CF, Oukka M, Kuchroo VJ, Sacks D (2007) CD4(+)CD25(-)Foxp3(-) Th1 cells are the source of IL-10-mediated immune suppression in chronic cutaneous leishmaniasis. J Exp Med 204:285–297. doi:10.1084/jem.20061886
26. Anderson CF, Mendez S, Sacks DL (2005) Nonhealing infection despite Th1 polarization produced by a strain of *Leishmania major* in C57BL/6 mice. J Immunol 174:2934–2941
27. Scharton-Kersten T, Scott P (1995) The role of the innate immune response in Th1 cell development following *Leishmania major* infection. J Leukoc Biol 57:515–522
28. Matte C, Olivier M (2002) Leishmania-induced cellular recruitment during the early inflammatory response: modulation of proinflammatory mediators. J Infect Dis 185:673–681
29. Barbi J, Ogumu S, Rosas LE, Carlson T, Lu B, Gerard C, Lezama-Davila CM, Satoskar AR (2007) Lack of CXCR3 delays the development of hepatic inflammation but does not impair resistance to *Leishmania donovani*. J Infect Dis 195:1713–1717
30. Daly C, Rollins BJ (2003) Monocyte chemoattractant protein-1 (CCL2) in inflammatory disease and adaptive immunity: therapeutic opportunities and controversies. Microcirculation 10:247–257
31. Peters N, Sacks D (2006) Immune privilege in sites of chronic infection: *Leishmania* and regulatory T cells. Immunol Rev 213:159–179. doi:10.1111/j.1600-065X.2006.00432.x
32. Aliberti J, Reis e Sousa C, Schito M, Hieny S, Wells T, Huffnagle GB, Sher A (2000) CCR5 provides a signal for microbial induced production of IL-12 by CD8 alpha+dendritic cells. Nat Immunol 1:83–87
33. Santiago HC, Oliveira CF, Santiago L, Ferraz FO, de Souza DG, de-Freitas LA, Afonso LC, Teixeira MM, Gazzinelli RT, Vieira LQ (2004) Involvement of the chemokine RANTES (CCL5) in resistance to experimental infection with *Leishmania major*. Infect Immun 72:4918–4923. doi:10.1128/IAI.72.8.4918-4923.2004
34. Murdoch C, Finn A (2000) Chemokine receptors and their role in inflammation and infectious diseases. Blood 95:3032–3043
35. Sato N, Ahuja SK, Quinones M, Kostecki V, Reddick RL, Melby PC, Kuziel WA, Ahuja SS (2000) CC chemokine receptor (CCR)2 is required for langerhans cell migration and localization of T helper cell type 1 (Th1)-inducing dendritic cells. Absence of CCR2 shifts the *Leishmania major*-resistant phenotype to a susceptible state dominated by Th2 cytokines, b cell outgrowth, and sustained neutrophilic inflammation. J Exp Med 192:205–218
36. Conrad SM, Strauss-Ayali D, Field AE, Mack M, Mosser DM (2007) *Leishmania*-derived murine monocyte chemoattractant protein 1 enhances the recruitment of a restrictive population of CC chemokine receptor 2-positive macrophages. Infect Immun 75:653–665. doi:10.1128/IAI.01314-06
37. Ritter U, Moll H (2000) Monocyte chemotactic protein-1 stimulates the killing of *Leishmania major* by human monocytes, acts synergistically with IFN-gamma and is antagonized by IL-4. Eur J Immunol 30:3111–3120. doi:10.1002/1521-4141(200011)30:11<3111::AID-IMMU3111>3.0.CO;2-O
38. Brandonisio O, Panaro MA, Fumarola I, Sisto M, Leogrande D, Acquafredda A, Spinelli D, Mitolo V (2002) Macrophage chemotactic protein-1 and macrophage inflammatory protein-1 alpha induce nitric oxide release and enhance parasite killing in *Leishmania infantum*-infected human macrophages. Clin Exp Med 2:125–129. doi:10.1007/s102380200017

Virchows Arch (2010) 457:619–622
DOI 10.1007/s00428-010-0966-9

CASE REPORT

A non-catecholamine-producing sympathetic paraganglioma of the spermatic cord: the importance of performing candidate gene mutation analysis

Despoina Alataki · A. Triantafyllidis · José Gaal · C. Rodiou · J. Vouros · A. Papathanasiou · A. Papanicolaou · V. Rombis · Ronald R. de Krijger

Received: 7 May 2010 / Revised: 13 August 2010 / Accepted: 18 August 2010 / Published online: 15 September 2010
© The Author(s) 2010. This article is published with open access at Springerlink.com

Abstract
Background Catecholamine-producing tumours are called pheochromocytomas when they are located in the adrenal gland and sympathetic paragangliomas when they are located elsewhere in the abdomen. Rarely these tumours do not produce catecholamines and even more rarely they arise in the spermatic cord. Over the past decade, systematic mutation analysis of apparently sporadic cases of pheochromocytomas and paragangliomas has elucidated the frequent presence of germ line mutations in one of five candidate genes, including *RET*, *VHL*, *SDHB*, *SDHC*, and *SDHD*.
Clinical history and methods We describe a 45-year-old man with a non catecholamine-producing paraganglioma of the spermatic cord. We performed SDHB immunohistochemistry and performed mutation analysis of the *SDHB*, *SDHC*, and *SDHD* genes.
Results There was no staining of tumour cells with SDHB immunohistochemistry, indicative of an *SDH* mutation. Mutation analysis demonstrated a germ line *SDHD* mutation (p.Val147Met).
Conclusions Systematic mutation analysis is required in paraganglioma patients for the detection of germ line mutations. This should be preceded by SDHB immunohistochemistry to limit the number of genes to be tested.

Keywords Sympathetic paraganglioma · Spermatic cord · SDHD · Immunohistochemistry

Precis Candidate gene mutation analysis on a paraganglioma of the spermatic cord

D. Alataki · A. Papanicolaou
Department of Pathology,
Hippokration General Hospital of Thessaloniki,
Thessaloniki, Greece

A. Triantafyllidis · C. Rodiou · J. Vouros · A. Papathanasiou · V. Rombis
Department of Urology,
Hippokration General Hospital of Thessaloniki,
Thessaloniki, Greece

J. Gaal · R. R. de Krijger (✉)
Department of Pathology, Josephine Nefkens Institute,
Erasmus MC-University Medical Center Rotterdam,
P.O. Box 2040, 3000 CA Rotterdam, The Netherlands
e-mail: r.dekrijger@erasmusmc.nl

Introduction

Extra-adrenal tumours originating from chromaffin cells are called sympathetic paragangliomas and arise from paraganglia that are distributed along the pre- and paravertebral sympathetic chains and the sympathetic nerve fibres, which innervate the pelvic and retroperitoneal organs. In contrast, tumours originating from the adrenal medulla are called pheochromocytomas [1]. Between 25% and 79% of sympathetic paragangliomas and about 90% of pheochromocytomas are associated with clinical signs of excess catecholamine secretion, while the remaining cases represent clinically non-functional tumours [2]. Most of these tumours produce but do not secrete catecholamines and may therefore evade detection for many years.

The majority of sympathetic paragangliomas occur in various abdominal sites, mostly in a paravertebral location, or in the organ of Zuckerkandl, a sympathetic paraganglion that plays an important role early in life. More rarely, sympathetic paragangliomas have been described in the bladder wall, which may elicit micturition-related complaints of excess catecholamine secretion [3, 4]. An even less frequent location is in the spermatic cord, where until

now eight cases had been described in the international literature [5–12]; however, none of these have been investigated for mutations in sympathetic paraganglioma-related genes. An overview of the clinical data of these previous eight patients is presented in Table 1.

Between 12% and 24% of apparently sporadic paragangliomas have been shown over the past decade to have a hereditary basis, involving mutations in one of five different genes: the REarranged during Transfection (*RET*) proto-oncogene, the von Hippel–Lindau (*VHL*) gene, and the succinate dehydrogenase subunits B (*SDHB*), C (*SDHC*), and D (*SDHD*) genes [13], [14].

In the present study, we report the first case of a spermatic cord sympathetic paraganglioma in which the tumour tissue was investigated by SDHB immunohistochemistry. This was shown to be a useful tool in diagnosing paraganglioma patients with *SDHx* mutations; negative immunostaining was seen in paragangliomas with *SDHx* mutations, whereas paragangliomas without mutations are positive with SDHB immunohistochemistry [15]. In this spermatic cord sympathetic paraganglioma, the negative immunostaining gave an important clue for the presence of an *SDHx* mutation, which was subsequently shown to be a previously unknown germ line *SDHD* mutation.

Clinical history

A 45-year-old man presented with a painless lump in his left hemiscrotum of months' duration. In his past medical history, an episode of acute left epididymitis, which subsided with antibiotics, was recorded 20 years earlier. On physical examination, a palpable, painless, firm mass was revealed in the upper pole of this left testicle. With a provisional diagnosis of a testicular neoplasm, a left inguinal orchiectomy was recommended and subsequently performed. His blood pressure was stable during and after surgery. The orchiectomy specimen displayed a tumour mass confined to the spermatic cord measuring 4.8×3.3×2.5 cm, weighing 71 g, surrounded by a capsule. The cut surface showed homogeneously reddish-white tumour tissue with an elastic consistency, while both the testis and epididymis were of normal colour, shape, and consistency (Fig. 1a).

Microscopically, there was a solid-looking tumour, with well-defined nests or trabeculae of tumour cells, separated by highly vascularized septa, focally thickened and hyalinized (Fig. 1b). Immunohistochemically, the tumour cells displayed strong and diffuse reactivity for vimentin, chromogranin A (Fig. 1c), synaptophysin, and neuron-specific enolase. Moreover, sustentacular cells were immunoreactive for S-100 protein. Taken together, a diagnosis of an abdominal, presumably sympathetic, paraganglioma was proffered. Following this histological diagnosis, the urologists performed an additional 24-h urinary analysis of catecholamines and their metabolites, which was shown to be normal. Three years after surgery, the patient is healthy, free of disease, and without tumours at other anatomic sites. There were no other family members known to the patient that had one or more pheochromocytomas or paragangliomas.

Material and methods

DNA was isolated from formalin fixed paraffin-embedded (FFPE) material. A region of at least 80% tumour cells was micro-dissected, and DNA was isolated using the Puregene DNA isolation kit (Gentra, Minneapolis, USA) according to manufacturer's protocol. An SDHB immunohistochemistry was performed using the rabbit polyclonal antibody HPA002868 (Sigma-Aldrich Corp, St. Louis, MO; 1:500) according to the method described by van Nederveen et al. [15]. Subsequently, mutation analysis was performed by direct sequencing of tumour tissue.

Results

The SDHB immunohistochemistry did not show any reactivity of the neoplastic cells (Fig. 1d). The mutation

Table 1 Clinical data of the previous eight patients with spermatic cord PGL

	Age	Symptoms	Hormonally active	Additional tumours	Reference
1	37	Painless mass right scrotal sac for 10 years	No	No	Eusebi et al. [5]
2	52	Painless mass left scrotal sac for 10 years/elevated blood pressure at operation	Yes	No	Soejima et al. [6]
3	18	Painless mass in right scrotal sac for 2 years	No	No	Bacchi at al. [7]
4	37	Painful mass in right scrotal sac	No	No	Mashat et al. [8]
5	40	Painless mass in left scrotal sac	No	No	Attaran et al. [9]
6	52	Lump within the right spermatic cord	No	No	Young et al. [10]
7	55	Painless left scrotal mass	Yes	Bilateral carotid body paragangliomas and bilateral pheochromocytomas	Abe et al. [11]
8	69	Weight loss, malaise, and mass in right testicle	No	No	Garaffa et al. [12]

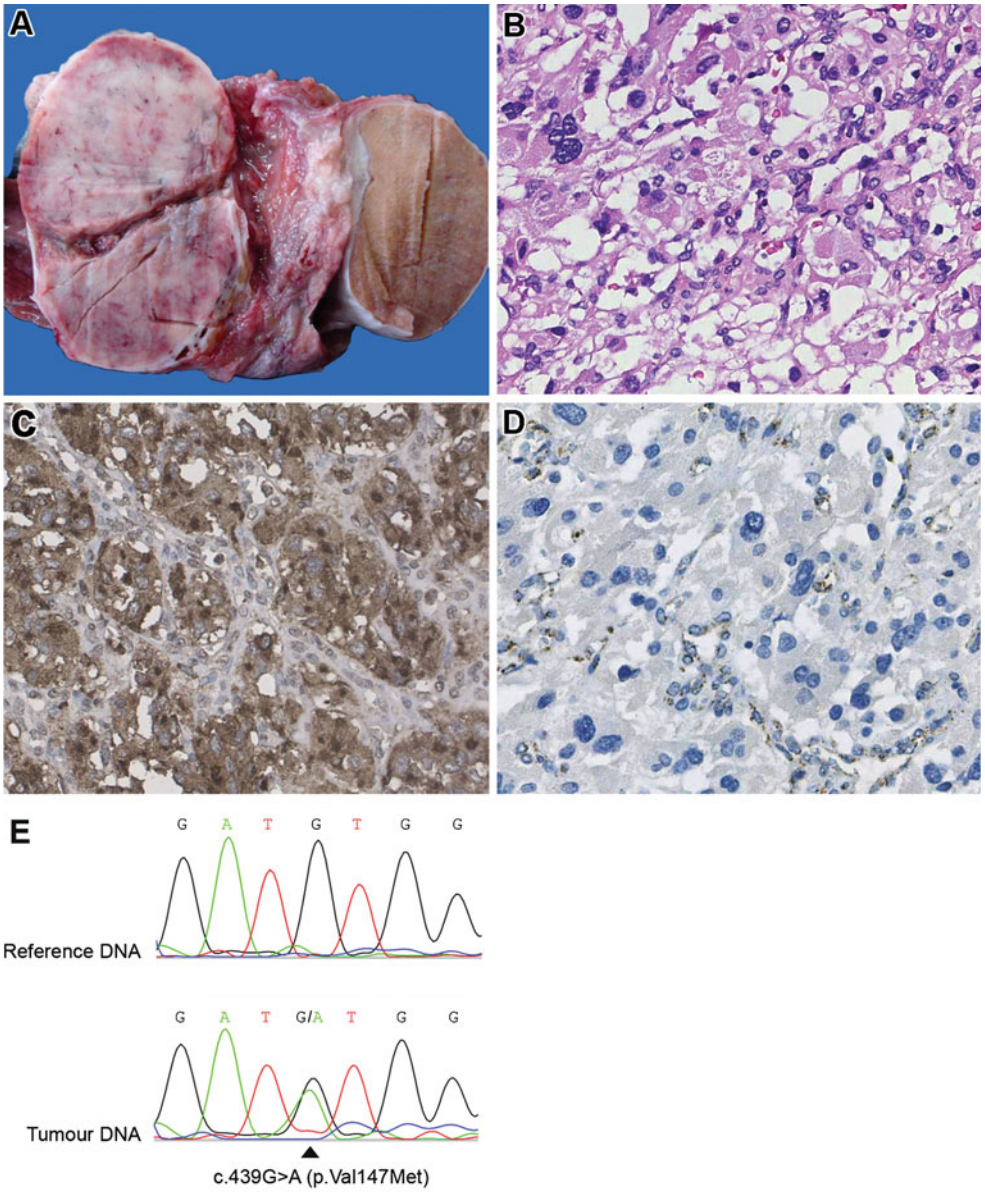

Fig. 1 **a** Gross aspect of spermatic cord paraganglioma. **b** Typical histology of the tumour showing large polygonal cells with ample amphophilic cytoplasm and moderate nuclear pleomorphism. **c** Chromogranin A immunohistochemistry showing positive staining in the tumour cells. **d** SDHB immunohistochemistry showing negative staining in tumour cells, while endothelial cells are immunoreactive. **e** Mutation analysis showing a p.Val147Met mutation in the tumour DNA compared with normal reference DNA

analysis that was performed by direct sequencing, on tumour tissue of this patient, showed an *SDHD* mutation in exon 4 (c.439 G→T, p.Val147Met) (Fig. 1e).

Discussion

In the present case report, we have described, for the first time in an individual case the use of SDHB immunohistochemistry for the guidance of subsequent DNA mutation analysis. Because of negative immunostaining, an *SDHx* mutation was predicted and eventually shown to be a p.Val147Met *SDHD* mutation.

This patient represents the ninth patient in the English literature with a spermatic cord paraganglioma, which was detected by its local mass effect, as it did not appear to produce catecholamines. The latter has not been formally proven, as no biochemical analyses had been carried out prior to surgery; however, the patient did not report any complaints that could be related to high blood pressure and/or catecholamine excess. The unusual location for a paraganglioma in the spermatic cord has been attributed to migration of neural crest progenitor cells, which are known to be present in the paraganglia throughout the abdomen, as is reflected by the various locations of abdominal sympathetic paraganglioma [16]. It is entirely conceivable that these progenitor cells migrate along with the developing male gonad and give rise to paragangliomas at low frequency.

Thus far, these paragangliomas have been described in middle-aged men, none of whom has had genetic testing, although one patient clearly had evidence of multiple tumours, for which we would strongly recommend systematic candi-

date gene mutation analysis [11]. Until about 10 years ago, pheochromocytomas and paragangliomas were known to occur in the context of various tumour syndromes, including multiple endocrine neoplasia type 2 (MEN 2), VHL disease, and NF1. Since the beginning of this decade, four additional genes (*SDHB*, *SDHC*, *SDHD, and SDHAF2*) have been added, causing the pheochromocytoma–paraganglioma syndrome, characterized by the occurrence of multiple pheochromocytoma and/or paraganglioma in the same patient and his or her family members. Whereas originally the frequency of germ line mutations in pheochromocytomas and paragangliomas was estimated at 10%, based upon patients from clearly recognizable familial tumour syndromes, systematic analysis of all genes (with the exception of *NF1*) has shown that an additional 15–25% of pheochromocytoma and paraganglioma patients are carriers of germ line mutations in each of these genes [13, 14]. Although somatic mutations in some of these genes have been described, they are quantitatively insignificant [4].

The finding of this mutation has important implications for further patient management, as it is known that patients with *SDHD* germ line mutations are at increased risk to develop further paragangliomas, either abdominal or head and neck, or even pheochromocytomas. In addition, other family members may also be affected, so they should be screened too.

Taken together, we show here that the spermatic cord can be a rare location for the occurrence of paragangliomas in male patients and that a stepwise immunohistochemical and genetic approach can be employed for the diagnosis of inherited paraganglioma, even in the absence of a positive family history.

Acknowledgements We are grateful to Frank van der Panne for the help in preparing the figures.

Conflict of interest statement We declare that we have no conflict of interest.

Funding José Gaal is supported by a grant of Erasmus MC.

Open Access This article is distributed under the terms of the Creative Commons Attribution Noncommercial License which permits any noncommercial use, distribution, and reproduction in any medium, provided the original author(s) and source are credited.

References

1. Timmers HJ, Gimenez-Roqueplo AP, Mannelli M, Pacak K (2009) Clinical aspects of SDHx-related pheochromocytoma and paraganglioma. Endocr Relat Cancer 16(2):391–400
2. Erickson D, Kudva YC, Ebersold MJ, Thompson GB, Grant CS, van Heerden JA, Young WF Jr (2001) Benign paragangliomas: clinical presentation and treatment outcomes in 236 patients. J Clin Endocrinol Metab 86(11):5210–5216
3. Im SH, Kim NH (2008) Thunderclap headache after micturition in bladder pheochromocytoma. Headache 48(6):965–967
4. van Nederveen FH, Korpershoek E, Lenders JW, de Krijger RR, Dinjens WN (2007) Somatic *SDHB* mutation in an extraadrenal pheochromocytoma. N Engl J Med 357(3):306–308
5. Eusebi V, Massarelli G (1971) Phaeochromocytoma of the spermatic cord: report of a case. J Pathol 105(4):283–284
6. Soejima H, Ogawa O, Nomura Y, Ogata J (1977) Pheochromocytoma of the spermatic cord: a case report. J Urol 118(3):495–496
7. Bacchi CE, Schmidt RA, Brandao M, Scapulatempo R, Costa JC, Schmitt FC (1990) Paragangliomaof the spermatic cord. Report of a case with immunohistochemical and ultrastructural studies. Arch Pathol Lab Med 114(8):899–901
8. Mashat F, Meccawi A, Garg S, Christian E (1993) Paraganglioma of the spermatic cord. Ann Saudi Med 13(2):208–210
9. Attaran SY, Shakeri S, Sobhani AR (1996) Paraganglioma of the spermatic cord: report of a case. J Urol 155(2):651
10. Young IE, Nawroz IM, Aitken RJ (1999) Phaeochromocytoma of the spermatic cord. J Clin Pathol 52(4):305–306
11. Abe T, Matsuda H, Shindo J, Nonomura K, Koyanagi T (2000) Ectopicpheochromocytoma arising in the spermatic cord 5 years after removal of bilateral carotid body tumors and adrenal pheochromocytomas. Int J Urol 7(3):110–111
12. Garaffa G, Muneer A, Freeman A, Abdel Raheem AM, Ralph DJ, Minhas S, Rees RW (2008) Paraganglioma of the spermatic cord: case report and review of the literature. Sci World J 8:1256–1258
13. Amar L, Bertherat J, Baudin E, Ajzenberg C, Bressac-de Paillerets B, Chabre O, Chamontin B, Delemer B, Giraud S, Murat A, Niccoli-Sire P, Richard S, Rohmer V, Sadoul JL, Strompf L, Schlumberger M, Bertagna X, Plouin PF, Jeunemaitre X, Gimenez-Roqueplo AP (2005) Genetic testing in pheochromocytoma or functionalparaganglioma. J Clin Oncol 23(34):8812–8818
14. Neumann HP, Bausch B, McWhinney SR, Bender BU, Gimm O, Franke G, Schipper J, Klisch J, Altehoefer C, Zerres K, Januszewicz A, Eng C, Smith WM, Munk R, Manz T, Glaesker S, Apel TW, Treier M, Reineke M, Walz MK, Hoang-Vu C, Brauckhoff M, Klein-Franke A, Klose P, Schmidt H, Maier-Woelfle M, Peczkowska M, Szmigielski C (2002) Germ-line mutations in nonsyndromic pheochromocytoma. N Engl J Med 346(19):1459–1466
15. van Nederveen FH, Gaal J, Favier J, Korpershoek E, Oldenburg RA, de Bruyn EM, Sleddens HF, Derkx P, Riviere J, Dannenberg H, Petri BJ, Komminoth P, Pacak K, Hop WC, Pollard PJ, Mannelli M, Bayley JP, Perren A, Niemann S, Verhofstad AA, de Bruine AP, Maher ER, Tissier F, Meatchi T, Badoual C, Bertherat J, Amar L, Alataki D, Van Marck E, Ferrau F, Francois J, de Herder WW, Peeters MP, van Linge A, Lenders JW, Gimenez-Roqueplo AP, de Krijger RR, Dinjens WN (2009) An immunohistochemical procedure to detect patients with paraganglioma and phaeochromocytoma with germline *SDHB*, *SDHC*, or *SDHD* gene mutations: a retrospective and prospective analysis. Lancet Oncol 10(8):764–771
16. Jaffer S, Harpaz N (2002) Mesenteric paraganglioma: a case report and review of the literature. Arch Pathol Lab Med 126 (3):362–364

Virchows Arch (2010) 457:623–625
DOI 10.1007/s00428-010-0987-4

LETTER TO THE EDITOR

A novel primary *KIT* exon 9 single nucleotide substitution c.1427G>T (p.Ser476Ile) in a gastrointestinal stromal tumor

Florian Grabellus · Sien-Yi Sheu · Sebastian Bauer · Norbert Speich · Kurt W. Schmid · Karl Worm

Received: 21 July 2010 / Revised: 11 September 2010 / Accepted: 24 September 2010 / Published online: 5 October 2010
© Springer-Verlag 2010

Dear Sir:

Gastrointestinal stromal tumors (GISTs) are mesenchymal tumors that originate from the interstitial cells of Cajal. These neoplasms are characterized by the expression of the receptor tyrosine kinase KIT (CD117, c-Kit), and mutations in the c-kit proto-oncogene resulting in constitutive activation of the receptor are associated with the tumorigenesis of most GISTs [1]. For unresectable and metastatic tumors, the multi-targeted tyrosine kinase inhibitor imatinib mesylate is considered the first choice of treatment.

We report the case of a 44-year-old male who initially presented with a GIST of the stomach measuring 16.0 cm in August 2007 at his local hospital. The tumor was incompletely resected by partial gastrectomy, and adjuvant imatinib at 400 mg/d was started in September 2007. Following 15 months of imatinib, the patient developed hepatic and peritoneal metastases (January 2009). He then asked for a recommendation for further treatment at our sarcoma center.

F. Grabellus (✉) · S.-Y. Sheu · K. W. Schmid · K. Worm
Institute of Pathology and Neuropathology,
University Hospital Essen, University of Duisburg-Essen,
Hufelandstrasse 55,
45122 Essen, Germany
e-mail: florian.grabellus@uk-essen.de

S. Bauer
Department of Internal Medicine and Cancer Research,
University Hospital Essen, University of Duisburg-Essen,
Hufelandstrasse 55,
45122 Essen, Germany

N. Speich
GenOPath GbR,
Heilsbachstrasse 17,
53123 Bonn, Germany

We recommended a dose escalation of imatinib to 800 mg/d. Computed tomography showed disease stabilization at first follow-up in March 2009 but a progression of the disease 3 months later. The patient's treatment regimen was changed to 37.5 mg/d of sunitinib in a continuous daily schedule, which resulted in disease stabilization for 6 months and, subsequently, progressive hepatic disease.

The histopathological analysis revealed a mixed type GIST (Fig. 1a, b) with a mitotic index of ten mitoses/50 high-power fields (1HPF = 0.23 mm^2). Immunohistochemical staining of the GIST showed a positive reaction with antibodies against c-KIT, CD34, and DOG1. The assessment of tumor behavior, which was performed following the NIH consensus guidelines [2] or the classification proposed by Miettinen and Lasota [3], revealed a "high-risk" for malignancy.

We performed a sequence analysis of *KIT* exons 9, 11, 13, and 17 as well as *PDGFRα* exons 12 and 18 in the primary tumor (central tumor section) and adjacent non-neoplastic formalin-fixed and paraffin-embedded tissue. The analysis was carried out by PCR amplification (Primus 25 Thermocycler, MWG, Ebersberg, Germany) followed by direct sequencing of both the forward and reverse strands with an ABI 3130 Genetic Analyzer (Applied Biosystems, Foster City, CA, USA).

We used two independent PCR reactions for sequence analysis, which was additionally confirmed by a second test in a different institution (GenOPath GbR Bonn, Germany).

As a result of the genetic analysis of the tumor tissue, we identified a novel primary *KIT* exon 9 single nucleotide substitution c.1427G>T (p.Ser476Ile) that was not detectable in the adjacent normal tissue (Fig. 2). The electropherogram of the tumor tissue showed almost no wild-type component, so that a homozygous mutation status is very likely. It was shown that the loss of the wild-type allele may be present at

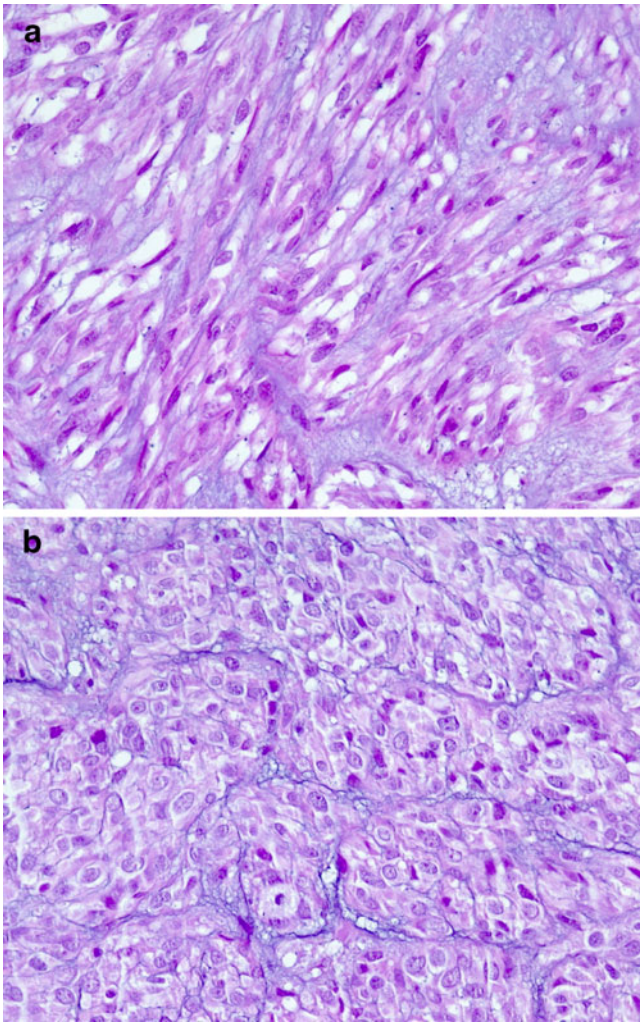

Fig. 1 Histopathology of the mixed type gastrointestinal tumor (H&E, ×200). **a** Spindle cell features. **b** Epithelioid tumor cells

primary diagnosis or may occur during tumor progression. Generally, *KIT* mutation homozygosity is associated with a more aggressive tumor behavior, which may be applied to the reported *KIT* exon 9 mutation.

Mutations in the exon 11 of *KIT*, which encodes the juxtamembrane domain, especially deletions or single nucleotide substitutions, are by far the most frequent primary genetic alterations in GISTs. In contrast, primary mutations in exon 9 of *KIT*, which encodes the extracellular domain near the transmembrane domain are rare and almost all of these mutations consist of c.1525_1530dupGCCTAT (p.Ala502_Tyr503dup) [4]. At present, only a few primary *KIT* exon 9 single nucleotide substitutions (e.g., Glu490Gly) have been reported and published [5].

Precise genotyping of GISTs allows the prediction of the biological behavior, prognosis, and tumor response to treatment [4]. Establishing a correlation between GIST genotypes and the outcome of treatment can improve modern targeted therapy, especially in light of the rising choice of tyrosine kinase inhibitors. The publication of large GIST genotyping studies, as well as of case reports on novel mutations, could therefore contribute to a better understanding of tumorigenesis, behavior, and therapy of GISTs.

The significance of the reported *KIT* exon 9 single nucleotide substitution c.1427G>T (p.Ser476Ile) is not yet clear; however, the assessment of the adjacent tissue, which showed a wild-type sequence, identified this genetic alteration as being tumor specific, excluding the possibility of a single nucleotide polymorphism. Previously, *KIT* exon 9-mutated GISTs (with the c.1525_1530dupGCCTAT) were found to be associated with an intestinal location (>90%), large size, spindle cell type, and aggressive clinical behavior. In this regard, the case reported in the present work clearly differs from the prototypical *KIT* exon 9-mutated GIST.

Generally, imatinib response, as well as progression-free and overall survival of tumors with *KIT* exon 9 mutations, was found to be intermediate between GIST with exon 11 mutation and wild-type GIST. Regarding *KIT* exon 9-mutated GIST, the presented patient had quite a long progression-free interval (PFS) of 15 months under imatinib standard therapy, since median PFS of patients with the usual *KIT* exon 9 mutation is less than 1 year. Unfortunately, information regarding the benefits of an initial higher dose of imatinib as frontline therapy for patients with the *KIT* exon 9 mutations, as has recently been

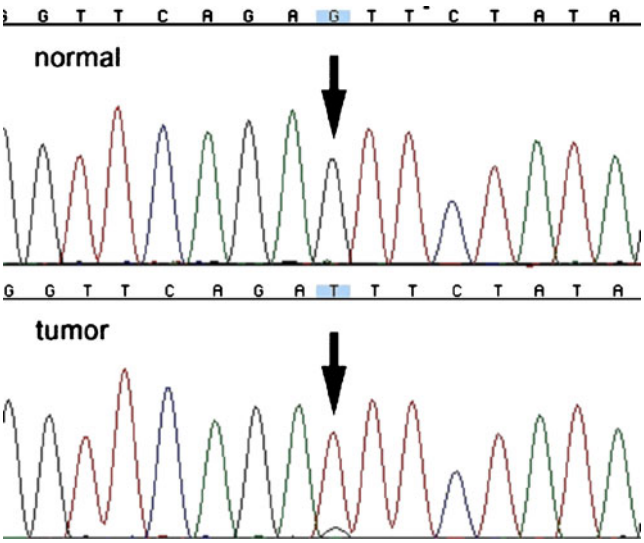

Fig. 2 Sequencing of tumor tissue identified the *KIT* exon 9 single nucleotide substitution c.1427G>T, which leads to Ser476Ile in the KIT protein. The adjacent normal tissue showed a wild-type sequence

recommended, was not available at the start of the present patient's treatment. Whether initial treatment with 800 mg/d of imatinib would have resulted in an improved PFS remains unanswered.

References

1. Hirota S, Isozaki K, Moriyama Y et al (1998) Gain-of-function mutations of c-kit in human gastrointestinal stromal tumors. Science 279:577–580
2. Fletcher CD, Berman JJ, Corless C et al (2002) Diagnosis of gastrointestinal stromal tumors: a consensus approach. Hum Pathol 33:459–465
3. Miettinen M, Lasota J (2006) Gastrointestinal stromal tumors: pathology and prognosis at different sites. Semin Diagn Pathol 23:70–83
4. Lasota J, Miettinen M (2008) Clinical significance of oncogenic KIT and PDGFRA mutations in gastrointestinal stromal tumours. Histopathology 53:245–266
5. Martin J, Poveda A, Llombart-Bosch A et al (2005) Deletions affecting codons 557-558 of the c-KIT gene indicate a poor prognosis in patients with completely resected gastrointestinal stromal tumors: a study by the Spanish Group for Sarcoma Research (GEIS). J Clin Oncol 23:6190–6198

Virchows Arch (2010) 457:627–633
DOI 10.1007/s00428-010-0996-3

ORIGINAL ARTICLE

MTHFR C677T polymorphism and differential methylation status in gastric cancer: an association with *Helicobacter pylori* infection

Eduardo Henrique Cunha Neves Filho · Markenia Kelia Santos Alves · Valeska Portela Lima · Silvia Helena Barem Rabenhorst

Received: 25 June 2010 / Revised: 1 October 2010 / Accepted: 5 October 2010 / Published online: 19 October 2010
© Springer-Verlag 2010

Abstract *MTHFR* C677T and *Helicobacter pylori* infection are believed to play critical roles in the DNA methylation process, an epigenetic feature frequently found in gastric cancer. The aim of this study was to verify the associations between the *MTHFR* C677T polymorphism and the methylation status of three gastric cancer-related genes. The influence of *H. pylori* strains was also assessed. DNA extracted from 71 gastric tumor samples was available for *MTHFR* C677T genotyping by PCR-RFLP, promoter methylation identification by MS-PCR and *H. pylori* detection and posterior subtyping (*cag*A and *vac*A genes) by PCR. In the distal tumors, a positive correlation was found between the methylation of *CDKN2A* and the allele T carriers (r=0.357; p=0.009). Considering the eldest patients (age≥60 years old), this correlation was even higher (r=0,417; p=0.014). *H. pylori* infection by highly pathogenic strains (*cag*A+/*vac*As1m1) was also found correlated to promoter methylation of *CDKN2A* and the allele T carriers in distal tumors (r=0.484; p=0.026). No significant correlation was verified between *MTHFR* C677T genotype and promoter methylation status when we analyzed the general sample. DNA methylation in *CDKN2A* associated to the *MTHFR* 677T carrier is suggested to be a distal tumor characteristic, especially in those 60 years old or older, and it seems to depend on the infection by *H. pylori cag*A/*vac*As1m1 strains.

Keywords *MTHFR* C677T · DNA methylation · *Helicobacter pylori* · Gastric cancer

E. H. C. Neves Filho · M. K. S. Alves · V. P. Lima · S. H. B. Rabenhorst
Department of Pathology and Forensic Medicine—Genetic Section, Universidade Federal do Ceará,
Rua Alexandre Baraúna, 949, Porangabussu,
CEP 60183-630 Fortaleza, Brazil

E. H. C. Neves Filho (✉)
Departamento de Patologia e Medicina Legal,
Universidade Federal do Ceará—Faculdade de Medicina,
Rua Alexandre Baraúna, 949, Porangabussu,
CEP 60183-630 Fortaleza, CE, Brazil
e-mail: edu0689@yahoo.com.br

Introduction

Gastric adenocarcinoma is one of the most frequent malignancies worldwide and it is globally the second leading cause of cancer-related deaths [1]. Brazil is one of the countries with a higher incidence, mainly in the Southeast and Northeast regions [2]. Gastric cancer has multifactorial etiology, being caused by environmental, genetic and epigenetic factors, which may interact to the tumor promotion and progression [3]. Epidemiological studies have shown an association between disturbances of folate metabolism and increased risk of gastric cancer, including low intake of folate, low levels of folate in blood or genetic factors affecting folate metabolism, such as polymorphisms in folate-metabolizing genes [4–6].

Methylenetetrahydrofolate reductase (MTHFR) acts centrally in folate metabolism, catalyzing the 5-methylenetetrahydrofolate synthesis reaction, the predominant circulatory form of folate and carbon donor for the remethylation of homocysteine to methionine. This pathway leads to the production of *S*-adenosylmethionine, the universal donor of methyl radical in human, which is required for DNA methylation [7]. Thus, polymorphisms that reduce the MTHFR activity could influence the status of DNA

methylation and would explain individual susceptibility to gastric cancer [8]. A C/T nucleotide change at 677 position of the *MTHFR* gene (*MTHFR* C677T), resulting in an alanine-to-valine substitution in the MTHFR protein, was found to produce a thermolabile variant of the MTHFR and significantly reduces the enzyme activity [9]. Furthermore, a recent meta-analysis carried out by Boccia et al. reported a significant positive correlation between gastric cancer and the *MTHFR* 677TT genotype [10].

DNA methylation is an important epigenetic feature of DNA that plays critical roles in gene regulation and cellular differentiation mechanisms. Methylation of promoter, especially in the CpG islands, culminates in gene silencing. Gastric cancer is one of the human tumors with higher number of silenced genes by methylation of their CpG islands [11]. Currently, the available data about the role of *MTHFR* C677T polymorphism in relation to the aberrant DNA methylation in gastric cancer is inconsistent and incomplete. It has been suggested that this polymorphism plays a dual role on the methylation status of promoter regions depending on the target gene [8, 12].

Another important etiological factor in gastric cancer is *Helicobacter pylori* infection. Bacterial virulence factors are characteristics present in some bacteria which enable them to cause disease. These are, mainly, vacuolating cytotoxin production associated to certain types of *vacA* (vacuolating cytotoxin gene A) alleles and *cagA* (cytotoxin associated gene product A) [13]. *H. pylori* strains expressing *cagA* and more active forms of *vacA*, such as the s1m1 genotype, are more likely to cause disease [14].

Despite of some advances, the molecular mechanisms associated with *H. pylori* in gastric carcinogenesis remains poorly understood. One of the promoting effects has been attributed to the induction of inflammation and aberrant methylation. It has been reported that frequencies or levels of CpG islands methylation of certain genes correlate with *H. pylori* infection, histological or serological severity of gastritis, and gastric cancer occurrence [12]. The observation that *H. pylori*-induced methylation is reversed after *H. pylori* eradication therapy supports this hypothesis [14]. Thus, the aim of this study was to verify the associations between the *MTHFR* C677T polymorphism genotype and the DNA methylation of three candidates genes (*COX-2*, *CDKN2A*, and *HMLH1*), largely associated with gastric carcinogenesis, and the influence of *H. pylori* strains in this process.

Materials and methods

Clinical specimens

The present study was approved by the Hospital Ethics Committee in the Federal University of Ceará and all subjects signed the informed consent form before inclusion. Samples from 71 patients with gastric adenocarcinoma who had undergone gastrectomy were collected from Walter Cantídio University Hospital and Santa Casa de Misericórdia Hospital, both located in Fortaleza, the Ceará state capital. The histological classification was done according to Lauren's classification by our team of pathologists.

DNA extraction

Genomic DNA was extracted from frozen tumor tissue using the cetyltrimethyl ammonium bromide (CTAB) technique, adapted from Foster and Twell [15]. The DNA extraction was done only in fragments that showed more than 80% of tumor cells. The DNA quality was analyzed by 1% agarose gel electrophoresis and the amount was determined using the NanoDropTM® 3300 fluorospectrometer (Wilmington, DE, USA).

Sodium bisulfite treatment and methylation-specific PCR (MS-PCR)

Extracted DNA of tumor tissue was modified by sodium bisulfite to determine the methylation status of the *CDKN2A, HMLH1*, and *COX-2* genes by MS-PCR, as previously described by Ferrasi et al. [16]. The primers targeted to the studied promoter gene regions are described in Table 1. PCR was performed in 25 μL reaction volume, containing 1× Platinum *Taq* buffer, 3.0 mM $MgCl_2$ (*CDKN2A*) or 1.5 mM $MgCl_2$ (*HMLH1* and *COX-2*), 0.4 mM of each dNTPs, 0.64 μM (*CDKN2A*), 0.24 mM (*HMLH1*) or 0.4 mM (*COX-2*) of each primer set, 1U of Platinum *Taq* DNA Polymerase® (Invitrogen, Foster, CA, USA), and 1 μL of treated DNA. DNA methylated in vitro by Sss-I methylase® (New England Biolabs, Beverly, MA, USA) was used as a positive control. Water and DNA from peripheral lymphocytes of healthy donors were used as negative controls. The PCR products were separated in 6% non-denaturing polyacrylamide gel and subsequently submitted to silver staining (Fig. 1).

For confirmation of the reaction specificity, MS-PCR products from *CDKN2A*, *HMLH1*, and *COX-2* genes analyzed were cloned with a TOPO TA Cloning Kit® (Invitrogen, California, USA) and both the methylated and unmethylated PCR products were sequenced using an ABI PRISM® BigDye Terminator v.3.0 Cycle Sequencing Kit® (Applied Biosystems, Foster, CA, USA) and ABI Prism 3100 DNA Sequencer® (Applied Biosystems).

Determination of MTHFR C677T genotypes

MTHFR C677T genetic polymorphism was detected by PCR-RFLP as previously described by Frosst et al. [17].

Table 1 PCR primer sets used for MS-PCR

Gene	Primer sequences (5′ - 3′)		Annealing (°C)	Size of PCR product (bp)	Ref.
	Forward	Reverse			
CDKN2A	M TTATTAGAGGGTGGGGCGGATCGC	GACCCCGAACCGCGACCGTAA	70	150	[32]
	U TTATTAGAGGGTGGGGTGGATTGT	CAACCCCAAACCACAACCATAA	70	151	
HMLH1	M TATATCGTTCGTAGTATTCGTGT	TCCGACCCGAATAAACCCAA	66	153	[33]
	U TTTTGATGTAGATGTTTTATTAG GGTTGT	ACCACCTCATCATAACTACCCACA	64	124	
COX-2	M TTAGATACGGCGGCGGCGGC	TCTTTACCCGAACGCTTCCG	59	161	[34]
	U ATAGATTAGATATGGTGGTGGTGGT	CACAATCTTTACCCAAACACTTCCA	65	171	

M methylated; *U* unmethylated

The PCR products of 198 bp were digested with restriction endonuclease *Hinf* I, producing a 175 and a 23 bp fragments if the polymorphism was present. The digestive products were resolved by electrophoresis in 6% polyacrylamide gel with silver staining. Random samples were reanalyzed for laboratory procedures control (Fig. 2).

Detection of *H. pylori* and vacA alleles and the presence of cagA gene

H. pylori infection was detected by PCR of the *ure*C gene. The primers for the *H. pylori* studied genes and their annealing temperature are described in Table 2. For confirmation of the reaction specificity, PCR products from *ure*C gene were cloned with TOPO TA Cloning Kit® (Invitrogen, California, USA) and sequenced using the ABI PRISM® BigDye Terminator v.3.0 Cycle Sequencing Kit® (Applied Biosystems, Foster, CA, USA) and ABI Prism 3100 DNA Sequencer® (Applied Biosystems).

The *ure*C, *cag*A, *vac*A s1/s2, *vac*A m1/m2 genes were amplified in a 25-μL volume containing 2.5 μL of 10× PCR buffer® (Invitrogen, Cergy Pontoise, France); 1% Tween 20, 1.5 mM of $MgCl_2$ (Invitrogen), 200 μM (each) of dNTPs (Invitrogen), 1U of Platinum *Taq* polymerase® (Invitrogen); 0.4 μM (*ure*C, *cag*A, *vac*A s1/s2, *vac*A m1), 0.3 μM (*vac*A m2) for each primer and 1 μL of DNA. DNAse-free water was used as negative control. The PCR products were analyzed by 1% agarose gel electrophoresis with ethidium bromide staining (Fig. 3). v*ac*A and *cag*A genes were considered positive when a specific fragment was detected (Table 2). Random samples were reanalyzed to confirm the results. DNA preservation has been confirmed by amplification of different genes in other approaches under study in our laboratory.

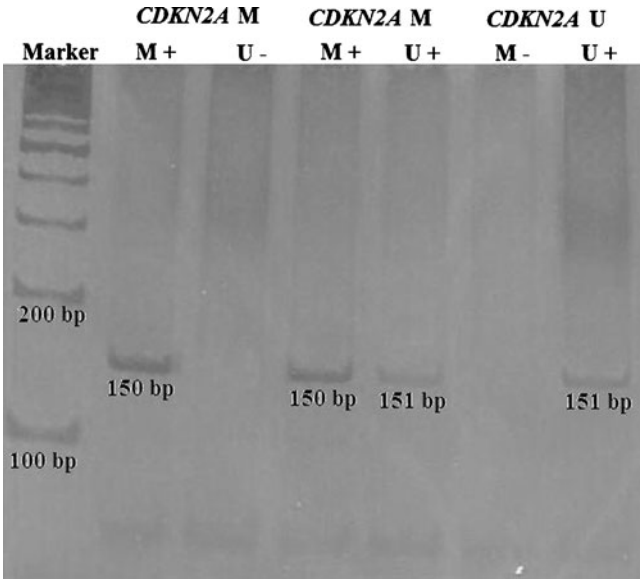

Fig. 1 Representative electrophoresis of the *CDKN2A* MS-PCR in 6% polyacrylamide gel with silver staining

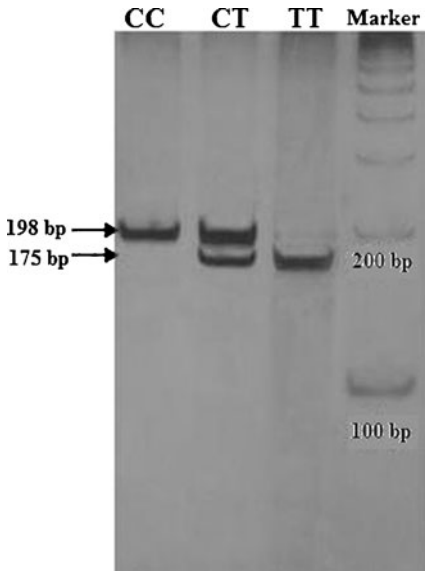

Fig. 2 Representative electrophoresis of the *MTHFR* C677T polymorphism in 6% polyacrylamide gel with silver staining

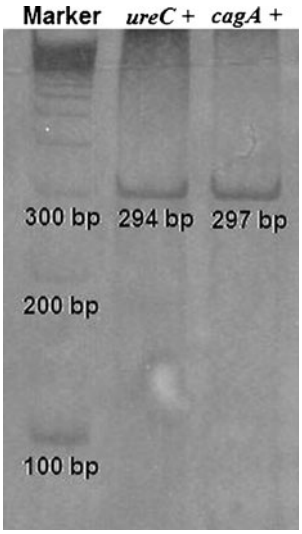

Fig. 3 Representative electrophoresis of the *ure*C and *cag*A genes amplification in 6% polyacrylamide gel with silver staining

Statistical analyses

These were carried out using the statistical program SPSS® version 15.0 (Chicago, IL, USA). Statistically significant differences were evaluated by the chi-square test (χ^2). Correlations were analyzed by Spearman's rank correlation coefficient. The results were considered statistically significant when p values were less than 0.05.

Results

Study population

Among the 71 cases analyzed, 45 (63.4%) were males and 26 (36.6%) females. The average age was 64.2, ranging from 23 to 92 years old. The most frequent site was the gastric non cardia [52/71 (73.2%)×19/71 (26.8%)]. Intestinal and diffuse subtypes presented 43 (60.5%) and 28 (39.5%) frequencies, respectively.

Frequency of promoter methylation of three CpG islands and MTHFR genotypes

All 71 tumor samples were available for MS-PCR analysis and for *MTHFR* genotyping. CpG island methylation was found in 30 of the tumors samples (42.2%) for *CDKN2A*, 38 (53.5%) for *COX-2* and 22 (30.9%) for *HMLH1*. The *MTHFR* C677T genotype shows similar frequency for the homozygous CC (34/71; 47.8%) and heterozygous CT (31/71; 43.6%) carriers. Homozygous carries for *MTHFR* 677TT was found in only 8.6% of the patients.

Association between MTHFR C677T, promoter methylation and clinicopathological parameters

The association of each *MTHFR* C677T genotype to the promoter CpG islands methylation status is shown in Table 3. No significant correlation was found between the promoter methylation for all the studied genes, age (cutoff of 60 years old), histological subtypes (intestinal and diffuse), and *MTHFR* genotype (Table 3).

When the tumors were analyzed according to its localization, in the distal tumors a positive correlation was found between the promoter methylation of *CDKN2A* and the allele T carriers (CT and TT genotypes; r=0.357, p=0.009) (Table 4). Considering the patients age with 60 years old or older, this correlation was even higher (r=0.417, p=0.014).

Influence of *H. pylori* genotype in the methylation process

H. pylori infection was present in 68 of the patients (95.8%). Among them, 31 (45.5%) were *cagA*+/*vacA*s1m1. As most of the patients were *H. pylori* positive, we verify if there was an association between the *H. pylori* strains and the *MTHFR* genotype in gene methylation, considering clinicopathological parameters. From these analysis, we

Table 2 PCR primer sets used for genotyping *H. pylori*

Gene	Primer sequence	Annealing (°C)	Size (bp) of PCR product	Reference number
ureC	F—5′ AAGCTTTTAGGGGTGTTAGGGGTTT 3′ R—5′ AAGCTTACTTTCTAACACTAACGC 3′	55	294	[35]
vacA				
s1/s1	F—5′ ATGGAAATACAACAAACACAC 3′ R—5′ CTGCTTGAATGCGCCAAAC 3′	55	259/286	[36]
m1	F—5′ GGTCAAAATGCGGTCATGG 3′ R—5′ CCATTGGTACCTGTAGAAAC 3′	55	290	
m2	F—5′ GGAGCCCCAGGAAACATTG 3′ R—5′ CATAACTAGCGCCTTGCAC 3′	52	192	
cagA	F—5′ ATAATGCTAAATTAGACAACTTGAGCGA 3′ R—5′ TTAGAATAATCAACAAACATAACGCCAT 3′	56	297	[37]

F forward; *R* reverse

Table 3 Association between the MTHFR C677T genotype, the clinicopathological parameters, and the promoter methylation status for the three studied genes

Variables	MTHFR genotype			Alelle T carriers
	CC	CT	TT	
Sex				
Male	22	18	5	23
Female	12	13	1	14
Age				
<60	13	7	2	9
≥60	21	24	4	28
Lauren's histotype				
Diffuse	13	13	2	15
Intestinal	21	18	4	22
Anatomical site				
Proximal	9	8	2	10
Distal	25	23	4	27
CDKN2A				
Methylated	23	15	3	18
Unmethylated	11	16	3	19
COX-2				
Methylated	17	13	3	16
Unmethylated	17	18	3	21
HMLH1				
Methylated	24	21	4	25
Unmethylated	10	10	2	12

found a high association between the promoter methylation of *CDKN2A* and the *MTHFR* 677T carrier (r=0.484, p=0.026) in the distal tumors infected by *H. pylori cagA*+/*vacA*s1m1.

Association between number of methylated CpG islands and MTHFR genotype

To investigate whether the *MTHFR* genotype might be associated with methylation of multiple CpG sites we grouped all the 71 subjects according to the numbers of methylated genes: none, 1, 2, and 3. No promoter methylated gene was present in 20 (28.2%) of the cases while the presence of 1, 2, and 3 was observed in 19 (26.8%), 25 (35.2%), and 7 (9.8%) of the cases, respectively. The mean number of methylated CpG sites according to the *MTHFR* genotype was 1.12 for CC, 1.42 for CT, 1.33 for TT and 1.40 for T carrier. No significant association was found between *MTHFR* genotype and number of methylated CpG sites and no statistical difference was verified between the number mean of methylated CpG sites over the different *MTHFR* genotypes.

Discussion

The relationship between the hypermethylation of tumor suppressor genes or DNA repair genes with the gastric carcinogenesis process has been pointed in many studies; however, the factors involved in the induction of this process are still unknown [18, 19]. Some studies indicate that DNA methylation depends on environmental factors such as *H. pylori* infection and may also vary according to the presence of polymorphisms involved in this process as those of enzymes involved in the folate cycle [8, 12, 13]. However, there are only few studies focusing these aspects and they present controversial results. So that, in the present study, the association between the methylation status of *CDKN2A*, *HMLH1*, and *COX-2,* the *MTHFR* C677T polymorphism and the influence of high pathogenic *H. pylori* strains in gastric cancer were analyzed.

The first analysis focused the association between the presence of promoter methylation and the *MTHFR* C677T polymorphism. Some studies demonstrated that genetic and epigenetic changes in gastric carcinoma differ depending on the tumor localization and on its histological subtype [20, 21]. Based on that, the data were analyzed according to these aspects. Although no difference was observed regarding to histological subtype, differences were identified according to the tumor anatomic site. In the distal tumors, an unexpected positive correlation was found between the CpG island methylation of *CDKN2A* and the allele T carriers. In fact, this correlation was even higher when we considered the 60 years old or older patients. Tahara et al. [12] also observed a similar correlation between the hypermethylation of *CDKN2A* and the *MTHFR* 677TT genotype, but these authors did not associate it to the tumor anatomic site. Both ours and Tahara et al.'s studies disagree with Weng et al. [22],

Table 4 Association between MTHFR polymorphism and methylation status of three promoter CpG islands on the distal tumors

Variables	MTHFR genotype			Alelle T carriers
	CC	CT	TT	
CDKN2A				
Unmethylated	6	14	2	16
Methylated	9	9	2	11*
COX-2				
Unmethylated	13	14	2	16
Methylated	12	9	2	11
HMLH1				
Unmethylated	10	9	1	10
Methylated	15	14	3	17

*p=0.009

which found a promoter hypermethylation of *CDKN2A* in patients with the *MTHFR* 677CC genotype. Various studies have been associating the *MTHFR* C677T polymorphism to gastric cancer risk in a specific anatomic localization. Wang et al. [23], evaluating the association of *MTHFR* C677T and thymidylate synthase promoter polymorphisms with genetic susceptibility found a gastric cardia adenocarcinoma risk related to the *MTHFR* 677TT and 2R2R genotypes. Likewise, Miao et al. [5] observed that subjects with the *MTHFR* 677TT variant genotype had a twofold increased risk of gastric cardia adenocarcinoma. These studies suggested that the common functionally polymorphism *MTHFR* C677T plays a substantial influence in the gastric cardia adenocarcinoma carcinogenesis. However, both studies did not evaluate the methylation pattern of specific genes associated to this polymorphism. Related to methylation status associated with tumor region there are some controversy. Vo et al. [24] found no distinct methylation status for *CDKN2A* regarded to the tumor localization, while recent studies carried out in Turkey [25] and Germany [26] correlate methylation of promoter *CDKN2A* to cardiac tumors, but the *MTHFR* C677T polymorphism influence was not assessed. We suggest that in distal tumors, the silencing of tumor suppressor genes by their promoter CpG islands methylation, especially when influenced by *MTHFR* polymorphism, might be an important carcinogenic pathway.

It has been well established over the literature that, in general, the methylation status of promoter CpG islands tends to increase with age [27]. From that standpoint, we found that the correlation between methylation of *CDKN2A* and *MTHFR* 677T carrier subjects in distal tumors is higher in an older generation (60 years old or older). It seems that the *MTHFR* polymorphism may have a greater influence on the methylation status as time goes by. Additionally, in the present study, *MTHFR* C677T polymorphism does not act homogeneously over all the studied genes. *MTHFR* 677TT genotype seems to be related to the hypermethylation of *CDKN2A*; on the other hand, it does not show an involvement regarding to *HMLH1* and *COX-2* methylation status. Some studies have been reporting this dual behavior of *MTHFR* C677T polymorphism regarding to methylation or unmethylation of promoter regions depending on the target gene [8, 12]. Our data suggests that this differential methylation status influenced by *MTHFR* C677T genotype depends on the tissue, specifically on the tumor localization. Probably the induction of the methylation process of some genes, like *HMLH1* and *COX-2,* is independent on the *MTHFR* C677T polymorphism.

Although the hypermethylation of promoter regions in genes involved on gastric carcinogenesis has been well accepted and some studies associate it with *MTHFR* C677T polymorphism, the influence of *H. pylori* in this process is still not understood. In the present study, the infection by a highly pathogenic *H. pylori* strain (*cagA*+and *vacA* s1m1 genotype) was associated to the methylation of *CDKN2A* in the distal stomach in patients with *MTHFR* 677TT genotype.

Recently, there have been reports showing that *H. pylori* infection is the most predisposing factor for gene methylation in the stomach [28–30]. It is well known that *H. pylori* induces chronic inflammation, resulting in down-regulation of the some genes that maintain gastric mucosal homeostasis [14]. Also, the inflammation induced by *H. pylori* infection seems to promoter methylation of certain genes [31], which could justify an increased risk of tumor formation, mainly associated with the risk of noncardia gastric cancer.

In conclusion, the DNA methylation in promoter regions of *CDKN2A* associated to the *MTHFR* 677T carrier is suggested to be a distal tumor characteristic, especially in those 60 years old or older, and depends on the infection by *H. pylori cag*A/*vac*As1m1 strains. More studies with large sample size involving the folate enzymes polymorphisms, DNA methylation and *H. pylori* infection are needed to extend our understanding of gastric carcinogenesis.

Conflict of interest statement We attest the inexistence of conflicts of interest, corporate involvement, or patent holdings.

References

1. Lao-Sirieix P, Caldas C, Fitzgerald RC (2010) Genetic predisposition to gastro-oesophageal cancer. Curr Opin Genet Dev 20 (3):210–217
2. Ministério da Saúde do Brasil. Instituto Nacional de Câncer (2009) Estimativa 2010: incidência de câncer no Brasil. INCA, Rio de Janeiro
3. Cotran RS et al (2000) Robbins—patologia estrutural e funcional. Guanabara Koogan, Rio de Janeiro
4. Choi SW, Mason JB (2000) Folate and carcinogenesis: an integrated scheme. J Nutr 130:129–132
5. Miao X, Xing D, Tan W, Qi J, Lu W, Lin D (2002) Susceptibility to gastric cardia adenocarcinoma and genetic polymorphism in methylenetetrahydrofolate reductase in an at-risk Chinese population. Cancer Epidemiol Biomark Prev 11(11):1454–1458
6. Götze T, Röcken C, Röhl FW et al (2007) Gene polymorphisms of folate metabolizing enzymes and the risk of gastric cancer. Cancer Lett 251(2):228–236
7. Shen H, Xu Y, Zheng Y et al (2001) Polymorphisms of 5, 10-methylenetetrahydrofolate reductase and risk of gastric cancer in a Chinese population: a case-control study. Int J Cancer 5:332–336
8. Wang J, Sasco AJ, Fu C et al (2008) Aberrant DNA methylation of P16, MGMT, and hMLH1 genes in combination with MTHFR C677T genetic polymorphism in esophageal squamous cell carcinoma. Cancer Epidemiol Biomark Prev 17(1):118–125
9. Graziano F, Kawakami K, Ruzzo A et al (2006) Methylenetetrahydrofolate reductase 677C/T gene polymorphism, gastric cancer susceptibility and genomic DNA hypomethylation in an at-risk Italian population. Int J Cancer 118(3):628–632

10. Boccia S, Hung R, Ricciardi G et al (2008) Meta- and pooled analyses of the methylenetetrahydrofolate reductase C677T and A1298C polymorphisms and gastric cancer risk: a huge-GSEC review. Am J Epidemiol 167(5):505–516
11. Perri F, Cotugno R, Piepoli A et al (2007) Aberrant DNA methylation in non-neoplastic gastric mucosa of *H. pylori* infected patients and effect of eradication. Am J Gastroenterol 102 (7):1361–1371
12. Tahara T, Shibata T, Nakamura M et al (2009) MTHFR 677T carrier influences the methylation status of *H. pylori*-infected gastric mucosa in older subjects. Dig Dis Sci 54(11):2391–2398
13. Atherton JC (1998) *H. pylori* virulence factors. Br Med Bull 54 (1):105–120
14. Atherton JC (2006) The pathogenesis of *Helicobacter pylori*-induced gastro-duodenal diseases. Annu Rev Pathol 1:63–96
15. Foster GD, Twell DJ (1996) Plant gene isolation: principles and practice. Wiley, England
16. Ferrasi AC, Pinheiro NA, Rabenhorst SH et al (2010) *Helicobacter pylori* and EBV in gastric carcinomas: methylation status and microsatellite instability. World J Gastroenterol 16(3):312–319
17. Frosst P, Blom HJ, Milos R et al (1995) A candidate genetic risk factor for vascular disease: a common mutation in methylenetetrahydrofolate reductase. Nat Genet 10:111–113
18. Kim H, Kim YH, Kim SE, Kim NG, Noh SH, Kim H (2003) Concerted promoter hypermethylation of hMLH1, p16INK4A, and E-cadherin in gastric carcinomas with microsatellite instability. J Pathol 200(1):23–31
19. Shim YH, Kang GH, Ro JY (2000) Correlation of p16 hypermethylation with p16 protein loss in sporadic gastric carcinomas. Lab Invest 80(5):689–695
20. Driessen A, Nafteux P, Lerut T et al (2004) Identical cytokeratin expression pattern CK7+/CK20− in esophageal and cardiac cancer: etiopathological and clinical implications. Mod Pathol 17 (1):49–55
21. Tahara E (2004) Genetic pathways of two types of gastric cancer. IARC Sci Publ 157:327–349
22. Weng YR, Sun DF, Fang JY, Gu WQ, Zhu HY (2006) Folate levels in mucosal tissue but not methylenetetrahydrofolate reductase polymorphisms are associated with gastric carcinogenesis. World J Gastroenterol 12(47):7591–7597
23. Wang LD, Guo RF, Fan ZM et al (2005) Association of methylenetetrahydrofolate reductase and thymidylate synthase promoter polymorphisms with genetic susceptibility to esophageal and cardia cancer in a Chinese high-risk population. Dis Esophagus 18(3):177–184
24. Vo QN, Geradts J, Boudreau DA, Bravo JC, Schneider BG (2002) CDKN2A promoter methylation in gastric adenocarcinomas: clinical variables. Hum Pathol 33(12):1200–1204
25. Ksiaa F, Ziadi S, Amara K, Korbi S, Trimeche M (2009) Biological significance of promoter hypermethylation of tumor-related genes in patients with gastric carcinoma. Clin Chim Acta 404(2):128–133
26. Sarbia M, Geddert H, Klump B, Kiel S, Iskender E, Gabbert HE (2004) Hypermethylation of tumor suppressor genes (p16INK4A, p14ARF and APC) in adenocarcinomas of the upper gastrointestinal tract. Int J Cancer 111(2):224–228
27. van Rijnsoever M, Grieu F, Elsaleh H, Joseph D, Iacopetta B (2002) Characterisation of colorectal cancers showing hypermethylation at multiple CpG islands. Gut 51(6):797–802
28. Nardone G, Compare D, De Colibus P, de Nucci G, Rocco A (2007) Helicobacter pylori and epigenetic mechanisms underlying gastric carcinogenesis. Dig Dis 25(3):225–229
29. Kitajima Y, Ohtaka K, Mitsuno M et al (2008) *Helicobacter pylori* infection is an independent risk factor for Runx3 methylation in gastric cancer. Oncol Rep 19(1):197–202
30. Maekita T, Nakazawa K, Mihara M et al (2006) High levels of aberrant DNA methylation in *Helicobacter pylori*-infected gastric mucosae and its possible association with gastric cancer risk. Clin Cancer Res 12(3 Pt 1):989–995
31. Katayama Y, Takahashi M, Kuwayama H (2009) *Helicobacter pylori* causes runx3 gene methylation and its loss of expression in gastric epithelial cells, which is mediated by nitric oxide produced by macrophages. Biochem Biophys Res Commun 388(3):496–500
32. Herman JG, Graff JR, Myöhänen S, Nelkin BD, Baylin SB (1996) Methylation-specific PCR: a novel PCR assay for methylation status of CpG islands. Proc Natl Acad Sci 93:9821–9826
33. Kang GH, Shim YH, Ro JY (1999) Correlation of methylation of the *HMLH1* promoter with lack of expression of HMLH1 in sporadic gastric carcinomas with replication error. Lab Invest 79 (7):903–909
34. Akhtar M, Cheng Y, Magno RM et al (2001) Promoter methylation regulates *Helicobacter pylori*-stimulated cyclooxygenase-2 expression in gastric epithelial cells. Cancer Res 61(6):2399–2403
35. Lage AP, Godfroid E, Fauconnier A et al (1995) Diagnosis of *Helicobacter pylori* infection by PCR: comparison with other invasive techniques and detection of cagA gene in gastric biopsy specimens. J Clin Microbiol 33:2752–2756
36. Atherton JC, Cao P, Peek RMJR, Tummuru MK, Blaser MJ, Cover TL (1995) Mosaicism in vacuolating cytotoxin alleles of *Helicobacter pylori*. Association of specific vacA types with cytotoxin production and peptic ulceration. J Biol Chem 270:17771–17777
37. Domingo D, Alarcon T, Pietro N, Sanchez I, Lopez-Brea M (1999) cagA and vacA status of Spanish *Helicobacter pylori* clinical isolates. J Clin Microbiol 37:2113–2114

Virchows Arch (2010) 457:635–642
DOI 10.1007/s00428-010-0990-9

ORIGINAL ARTICLE

Loss of cell polarity protein Lgl2 in foveolar-type gastric dysplasia: correlation with expression of the apical marker aPKC-zeta

Mikhail Lisovsky · Fumihiro Ogawa · Karen Dresser · Bruce Woda · Gregory Y. Lauwers

Received: 23 August 2010 / Revised: 23 September 2010 / Accepted: 25 September 2010 / Published online: 13 October 2010
© Springer-Verlag 2010

Abstract Recognition of gastric epithelial dysplasia, although a key to cancer prevention, can be challenging. In this study, we evaluated whether Lgl2 can serve as a marker of gastric foveolar-type dysplasia. Since atypical protein kinase C (aPKC) is a partner of Lgl2 in the control of apical–basal polarity we also investigated whether aPKC-zeta can compliment Lgl2 as a marker of dysplasia. Routinely processed specimens included 64 normal mucosa, 35 reactive gastropathies, 31 chronic gastritides, 65 gastric dysplasias (25 foveolar; 40 adenomatous), and 34 gastric adenocarcinomas. Twenty (80%) foveolar-type dysplasias showed absence of Lgl2 immunoreactivity, while normal basolateral expression of Lgl2 was consistently seen in normal gastric epithelium (n=20) and chronic gastritis (n=22; p<0.00001). Loss of Lgl2 was similar in the groups with low-grade and high-grade foveolar-type dysplasia, 79% and 83%, respectively. Linear apical anti-aPKC-zeta immunoreactivity was consistently present in the normal epithelium and was preserved in 91% of reactive gastropathies and 87% of chronic gastritides. In contrast, loss of apical aPKC-zeta staining was observed in 47% and 65% of low-grade dysplasias of foveolar and adenomatous types, respectively (p<0.005) and in nonsignificantly higher percentage of high-grade dysplasias. Apical aPKC-zeta staining was lost in 97% of gastric adenocarcinomas. Our data suggest a role of Lgl2 immunohistochemistry as an adjunct in the diagnosis of foveolar-type gastric dysplasia. aPKC-zeta had moderate sensitivity as a marker of gastric dysplasia and additional studies are needed to establish its role in the diagnosis of dysplasia.

Keywords Foveolar-type · Gastric dysplasia · Lgl2 · aPKC · Adenocarcinoma · Stomach

M. Lisovsky · K. Dresser · B. Woda
Department of Pathology, UMassMemorial Medical Center and University of Massachusetts Medical School,
Worcester, MA, USA

M. Lisovsky · F. Ogawa · G. Y. Lauwers
Department of Pathology, Massachusetts General Hospital and Harvard Medical School,
Boston, MA, USA

M. Lisovsky (✉)
Department of Pathology, Dartmouth Hitchcock Medical Center,
One Medical Center Drive,
Lebanon, NH, USA
e-mail: mikhail.lisovsky@hitchcock.org

Introduction

Gastric epithelial dysplasia is a noninvasive neoplastic lesion associated with increased risk of synchronous and metachronous adenocarcinoma of the stomach [1]. It may arise in either metaplastic mucosa (i.e., intestinal metaplasia; pseudopyloric metaplasia), or in native mucosa. It can be non-polypoid, depressed or polypoid [2]. Histologically, gastric dysplasia is divided into adenomatous (intestinal) type, which is most common, and the rarer foveolar (hyperplastic) type. The latter should not be confused with non-neoplastic hyperplastic polyps. While adenomatous dysplasia shows similarities with colonic adenomas, foveolar-type dysplasia is reminiscent of normal gastric superficial epithelium. The majority of foveolar-type dysplasias arise in the background of fundic gland polyps and familial adenomatous polyposis (FAP). Recently, about 30% of gastric dysplasias were reported to have a hybrid phenotype, defined as having at least 10% of the alternative histologic type [3]. Adenomatous and, arguably, foveolar-type dysplasias (see Discussion) are precursors of gastric

adenocarcinoma of the intestinal type and are classified into two grades: low grade and high grade [4, 5].

The histologic diagnosis of gastric dysplasia can be challenging due to multiple causes including interobserver variability, orientation of the specimen, sampling issues, and difficulty in distinguishing dysplasia from reactive atypia. While multiple architectural and cytologic features are used in combination to reach a diagnosis of dysplasia, most criteria taken in isolation suffer from low specificity. Abnormal cell polarity is among the more specific markers of dysplasia. It is defined as loss of perpendicular orientation of the nuclei in relation to the basal membrane and/or as apical–basal stratification of the nuclei. However, these features may be limited. Furthermore, any reparative process can show similar alterations. Therefore, availability of a biomarker specific for dysplasia could increase the accuracy of the diagnosis of gastric dysplasia.

Molecular and genetic characterization has established loss of cell polarity as one of the intrinsic mechanisms of malignant transformation of the epithelial cell [6, 7]. This discovery opened an opportunity to characterize dysplasia and carcinoma on the basis of alteration of cell polarity markers. Among these is the product of *Lethal giant larvae* (*lgl*) gene, first discovered in *Drosophila* and shown to control basolateral polarity and asymmetric cell division [2]. Lgl is a downstream target of atypical protein kinase C (aPKC) that is involved in the control of apical cell polarity. aPKC is a class of kinases within the protein kinase C superfamily which includes isoforms zeta, and iota/lambda. aPKCs require neither diacylglycerol nor Ca^{+2} but phosphatidylinositides for activation. Once phosphorylated by apically located aPKC, Lgl is excluded from the apical cell domain and accumulates in the basolateral cell domain, associating with the submembranous actin cytoskeleton [8–11]. Mutual inhibition of aPKC and Lgl has been shown to control the extent and integrity of the apical and basolateral cell domains [12, 13]. While the function of Lgl is still being elucidated, some data suggests its role in exocytosis [14]. Homozygous mutation of *lgl* in *Drosophila* leads to simultaneous disruption of cell polarity and malignant transformation, suggesting a role for *lgl* as a tumor suppressor gene [6, 15, 16]. Two homologs, *lgl1* and *lgl2* (also known as *hugl-1* and *hugl-2*), have been described in humans. *lgl1* mRNA is downregulated or absent in more than 60% of studied human solid tumors comprised of breast, lung, prostate, ovarian, and colonic carcinomas and melanomas [17, 18]. Recently, we have reported that Lgl2 is an immunohistochemical marker of gastric epithelium that is expressed in the basolateral submembranous cell domain. We have also reported that immunohistochemistry for Lgl2 is a useful adjunct to rule out gastric dysplasia, because Lgl2 expression is disrupted in gastric dysplasia and adenocarcinoma [19]. The primary focus of that study was on gastric dysplasia of the *adenomatous* type. In the current study, we sought to evaluate whether loss of Lgl2 expression can be used as a marker of *foveolar*-type gastric dysplasia. In addition, we wanted to evaluate whether apical polarity protein aPKC could compliment basolateral protein Lgl2 as a marker of dysplasia.

Materials and methods

Case selection

Paraffin blocks of normal, reactive, and neoplastic mucosa of digestive organs from resection, endoscopic mucosal resection, or biopsy specimens were obtained from the surgical pathology files of UMass Memorial Medical Center (Worcester, MA) and Massachusetts General Hospital (Boston, MA). Our control group included specimens of normal gastric mucosa (antrum: 14; corpus/fundus: 14; and cardia: 13), of normal duodenum (n=11), normal colon (n=12), reactive gastropathy (n=35) and chronic gastritis (n=31). The group of gastric epithelial dysplasia included 25 cases of foveolar dysplasia (13 sporadic and 12 associated with fundic gland polyps in the setting of FAP). Seven sporadic cases were low grade and six were high grade. Conversely, all dysplasias in fundic gland polyps were low grade. We also collected 40 cases of adenomatous gastric dysplasia (17 gastric adenomas and 23 foci of non-polypoid dysplasia adjacent to adenocarcinoma). Twenty-three cases were low grade (16 adenomas and seven non-polypoid dysplasias) and 17 were high grade (one gastric adenoma and 16 non-polypoid dysplasias). Finally, we also collected 34 gastric adenocarcinomas of the intestinal type. Five adenocarcinomas were well differentiated, 19 were moderately differentiated and ten were poorly differentiated. All specimens had been formalin-fixed, paraffin-embedded, and processed routinely. Approval for the study was obtained from the Institutional Review Boards of UMassMemorial Medical Center and Massachussetts General Hospital.

Histological and immunohistochemical analysis

Reactive gastropathy was diagnosed using widely accepted criteria [20, 21]. Gastric epithelial dysplasia was classified as adenomatous or foveolar type. Adenomatous dysplasia resembles colonic adenomas showing crowded tubular glands lined by columnar cells with dense eosinophilic cytoplasm, overlapping hyperchromatic and pseudostratified pencillate nuclei with inconspicuous nucleoli [22]. Foveolar-type dysplasia resembles gastric foveolar epithelium and shows glandular branching and epithelial intraluminal infoldings. Dysplastic cells have pale eosinophilic cytoplasm with a variable pink apical mucinous cap and hyperchromatic ovoid-to-round nuclei with mild pseudostratifica-

tion. Both types of dysplasia were subclassified as low grade or high grade. In high-grade dysplasia, crowding, branching, and budding of glands were prominent; cells were low columnar or cuboidal with round to oval vesicular nuclei and prominent nucleoli. There was also distinct loss of nuclear polarity. In contrast to adenomatous high-grade dysplasia that showed scant amphophilic cytoplasm, foveolar-type high-grade dysplasia displayed moderate to abundant eosinophilic cytoplasm [4, 5, 22]. Lauren's classification was used to categorize gastric adenocarcinomas as intestinal or diffuse type [23]. Intestinal-type adenocarcinomas were subclassified into well differentiated (well-formed glands or papillae), moderately differentiated (irregularly branching glands or complex and incomplete papillae), and poorly differentiated (ill-formed glands or single infiltrative cells) [24].

To evaluate the expression of aPKC protein, the staining protocol was optimized using several different tissues. Normal samples from liver, kidney, colon, duodenum, and stomach were first used to explore the distribution of the protein throughout organ systems. An anti-aPKC-zeta antibody (see below) was titrated out to achieve the best resolution of apical staining from the background. Titration was performed using normal and hyperplastic antral mucosa with the cut-off being where apical staining started to be lost. For each case, one to three blocks were selected for immunostaining. Immunohistochemistry was performed on 5-μm tissue sections. Antigen retrieval was carried out with 0.01 M citrate buffer pH 6.0 in a 770-W microwave oven for 14 min. The slides were stained on the Dako Autostainer (Dako Corporation, Carpinteria, CA) using the EnVision+ (Dako) staining reagents. The sections were first blocked for endogenous non-specific protein and peroxidase activity with an application of Dual Endogenous Block (Dako) for 10 min, followed by a buffer wash. They were incubated with either Lgl2 antibody at 1:750 (mouse monoclonal, clone 4G2, Novus Biologicals, Littleton, CO) [19], or PKC-zeta at 1:500 (rabbit polyclonal, catalog #sc-216, Santa Cruz Biotechnology, Santa Cruz, CA), for 30 min, followed by a buffer wash. After incubation with the EnVision+ Dual Link (Dako) detection reagent (a polymer conjugated with goat-anti-mouse-Ig, goat-anti-rabbit-IgG, and horseradish peroxidase) for 30 min, the sections were washed, and treated with a solution of diaminobenzidine and hydrogen peroxide for 10 min. After rinsing, a toning solution (DAB Enhancer, Dako) was used for 5 min to enrich the final coloration. Counterstaining was achieved with hematoxylin. Negative controls were stained using the same procedure, but with antibody diluent only in place of the primary antibody. Immunohistochemical staining was evaluated by two of the authors (M.L. and G.Y.L). Patterns of Lgl2 expression were reported as basolateral, cytoplasmic, or negative (no immunoreactivity present). Patterns of aPKC-zeta expression were noted as apical, cytoplasmic, focal cytoplasmic or negative. When more than one pattern of expression was observed in a specimen, major and minor patterns of staining were recorded. An immunoreactivity pattern was qualified as major when it was present in 50% or more of the cells of interest; a minor pattern—when present in less than 50% of the cells of interest. The intensity of staining was not graded.

Statistical analysis

Differences in the proportion of specimens with specific staining patterns were evaluated using Fisher's Exact Test. P value less than 0.05 was considered significant.

Results

Loss of Lgl2 expression in gastric foveolar-type dysplasia

We evaluated Lgl2 expression in a series of 25 gastric foveolar-type dysplasias consisting of 19 low-grade lesions (seven sporadic and 12 associated with FAP) and six high-grade lesions (all sporadic). A series of 20 normal stomach mucosae and 22 chronic gastritides served as control. While all normal stomach mucosae and chronic gastritides specimens showed basolateral Lgl2 immunoreactivity, as previously reported [19], total of 20 (80%) foveolar-type dysplasias showed absence of anti-Lgl2 immunostaining ($p<0.00001$, Fig. 1a–d). Low-grade and high-grade dysplasias showed similar loss of Lgl2 expression, in 79% and 83% of cases, respectively (Table 1). Within the group of low-grade dysplasia, both sporadic and FAP-associated dysplasias had similar loss of Lgl2 immunoreactivity (in 83% and 86% of cases, respectively). There were no cases of high-grade dysplasia associated with fundic gland polyps/FAP. These results show that loss of Lgl2 expression is present in the majority of cases of gastric foveolar-type dysplasia.

Expression of aPKC-zeta in normal gastrointestinal mucosa

Linear apical anti-aPKC-zeta immunoreactivity was present in the foveolar epithelium of normal gastric mucosa including the antrum ($n=14$), the corpus ($n=14$), and the cardia ($n=13$; Fig. 2a). Oxyntic glands of all 14 corpus mucosae also showed consistent apical staining (Fig. 2b). Antral and cardiac glands did not have a reproducible pattern of staining. In comparison, 11 duodenal and 12 colonic mucosae had diffuse cytoplasmic aPKC-zeta immunoreactivity (Fig. 2c, d). Gastric lamina propria, submucosa, and muscularis propria were uniformly negative for anti-aPKC-zeta immunoreactivity. These findings demonstrate that aPKC-zeta is selectively expressed in the apical domain of the cells of the foveolar epithelium and the corpus glands.

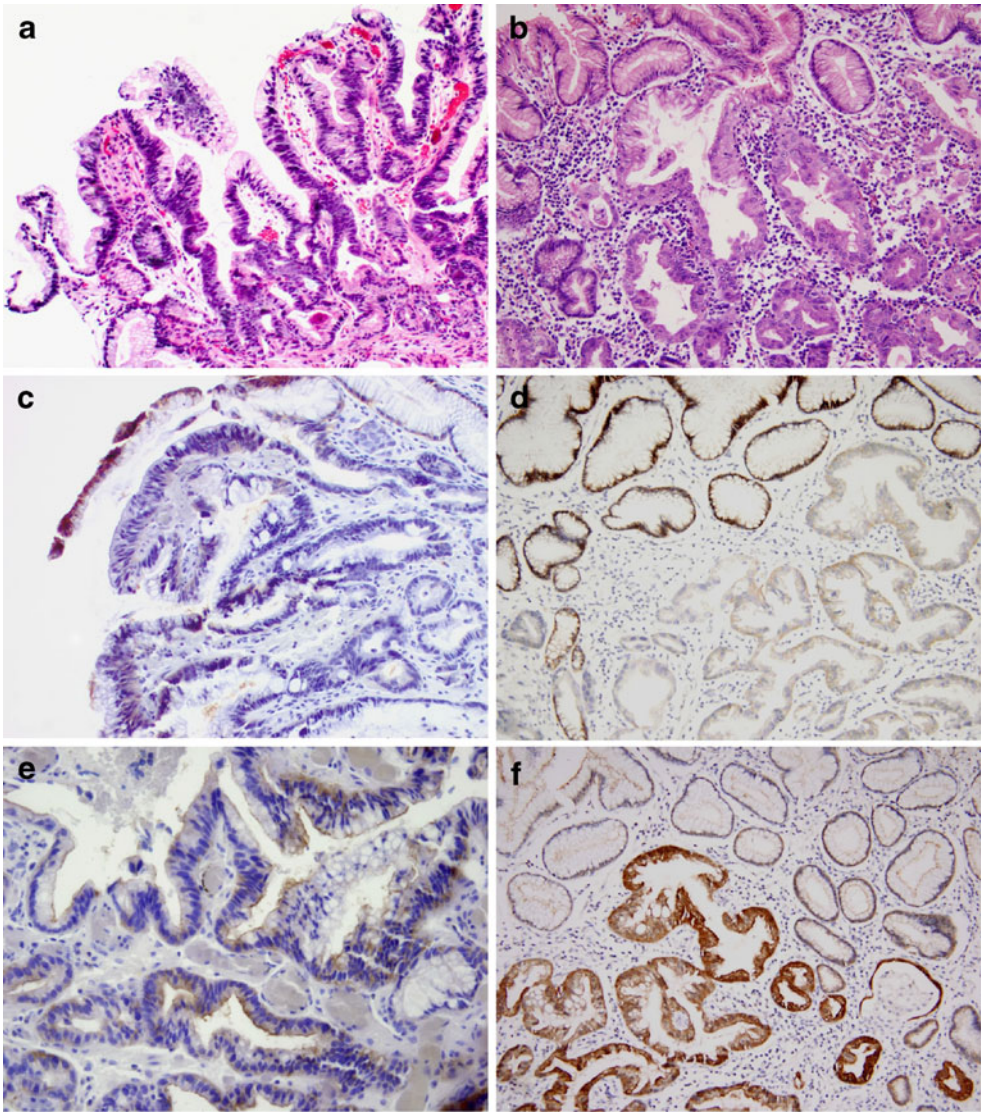

Fig. 1 Expression of Lgl2 and aPKC-zeta in low-grade and high-grade foveolar-type dysplasia. **a, c, e** Low-grade foveolar-type dysplasia; **b, d, f** high-grade foveolar-type dysplasia. **a** Low-grade foveolar-type dysplasia, H&E staining. **b** High-grade foveolar-type dysplasia, H&E staining. **c** Loss of Lgl2 expression in low-grade foveolar-type dysplasia. Normal basolateral staining is preserved in nondysplastic mucosa, which has upside-down orientation (*upper left*; same specimen as in **a**). **d** Loss of Lgl2 in high-grade foveolar-type dysplasia. Normal basolateral staining is preserved in nondysplastic mucosa (*upper part*, the same specimen as in **b**). **e** Preserved apical expression of aPKC-zeta in low-grade foveolar-type dysplasia. **f** Aberrant cytoplasmic aPKC-zeta in high-grade foveolar-type dysplasia. Normal apical staining is preserved in nondysplastic mucosa (*upper part* of the image; same specimen as in **b** and **d**)

Expression of aPKC-zeta in reactive gastropathy and chronic gastritis

Expression of aPKC-zeta was evaluated in 35 reactive gastropathies and 31 cases of chronic gastritis. Similar to normal mucosa, apical aPKC-zeta staining was present in 32 (91%) reactive gastropathies and 27 (87%) chronic gastritides (Fig. 2e, f; Table 2). These results suggest that apical localization of aPKC-zeta is preserved in gastric reactive and inflammatory conditions.

Loss of apical expression of aPKC-zeta in gastric dysplasia and adenocarcinoma

Gastric foveolar-type dysplasia Loss of apical aPKC-zeta immunoreactivity was present in 47% (n=10) of low-grade

Table 1 Lgl2 staining patterns in gastric foveolar-type dysplasia

Staining patterns		Foveolar-type dysplasia (n=25)		Chronic gastritis (n=22)	Normal epithelium (n=20)
Major	Minor	Low grade (n=19)	High grade (n=6)		
Basolateral	n/a	2 (11%)	0	22 (100%)	20 (100%)
Basolateral	Cytoplasmic	1 (5%)	0	0	0
Negative	n/a	15 (79%)	5 (83%)	0	0
Negative	Cytoplasmic	1 (5%)	1 (17%)	0	0

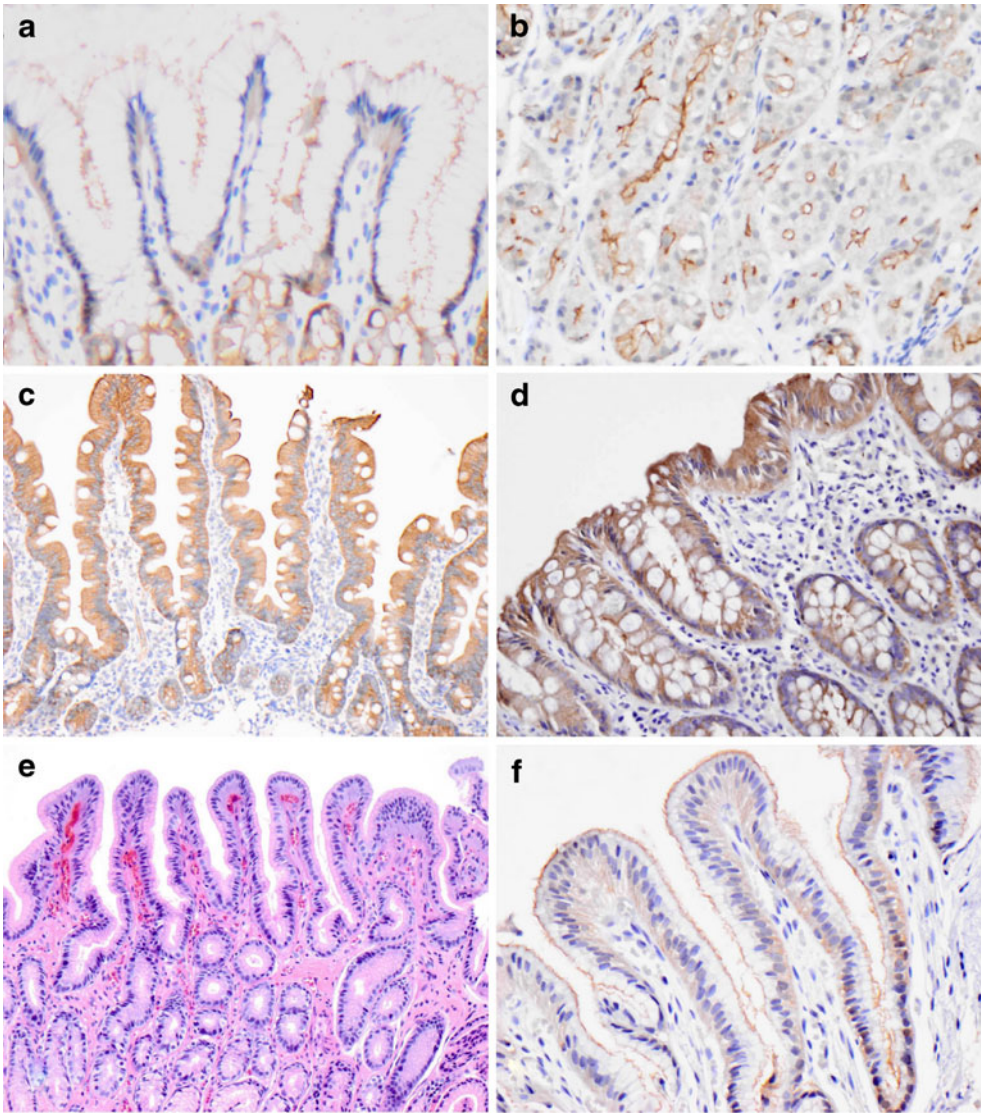

Fig. 2 Expression of aPKC-zeta in normal gastric mucosa and reactive gastropathy. **a** Apical localization of anti-aPKC immunoreactivity in the normal foveolar epithelium. **b** Apical localization of anti- aPKC-zeta immunoreactivity in gastric corpus glands. **c** Cytoplasmic anti- aPKC-zeta immunoreactivity in the duodenum. **d** Cytoplasmic anti-aPKC-zeta immunoreactivity in the colon. **e, f** Preserved apical aPKC-zeta expression in reactive gastropathy (**e** H&E staining; **f** anti- aPKC-zeta immunohistochemistry)

foveolar-type dysplasias and in 83% (n=5) of high-grade dysplasias (p=0.14, not significant; Table 2; Figs. 1e, f and 3d). Apical aPKC-zeta was more frequently lost in adenocarcinoma compared to low-grade dysplasia, involving 97% (n=33) of cases (p<0.00001, Fig. 3c).

Gastric adenomatous dysplasia The cohort of gastric adenomatous dysplasias and adenocarcinomas selected for aPKC-zeta studies was previously reported [19]. In total, 23 low grade and 17 high-grade adenomatous dysplasias and 34 adenocarcinomas of the intestinal type were evaluated.

Table 2 aPKC-zeta staining patterns in chemical gastropathy, gastric dysplasia and gastric adenocarcinoma

Staining pattern	Reactive gastropathy (n=35)	Chronic gastritis (n=31)	Gastric epithelial dysplasia				Gastric adenocarcinoma (n=34)
			Adenomatous		Foveolar		
			Low grade (n=23)	High grade (n=17)	Low grade (n=19)	High grade (n=6)	
Apical	32 (91%)	27 (87%)	8 (35%)	2 (12%)	10 (53%)	1 (17%)	0
Cytoplasmic	0		8 (35%)	12 (71%)	3 (16%)	4 (66%)	33 (97%)
Mixed apical and cytoplasmic	0		4 (17%)	3 (17%)	5 (26%)	1 (17%)	1 (3%)
Focal cytoplasmic	0		0	0			0
Negative	3 (9%)	4 (13%)	3 (13%)	0	1 (5%)		0

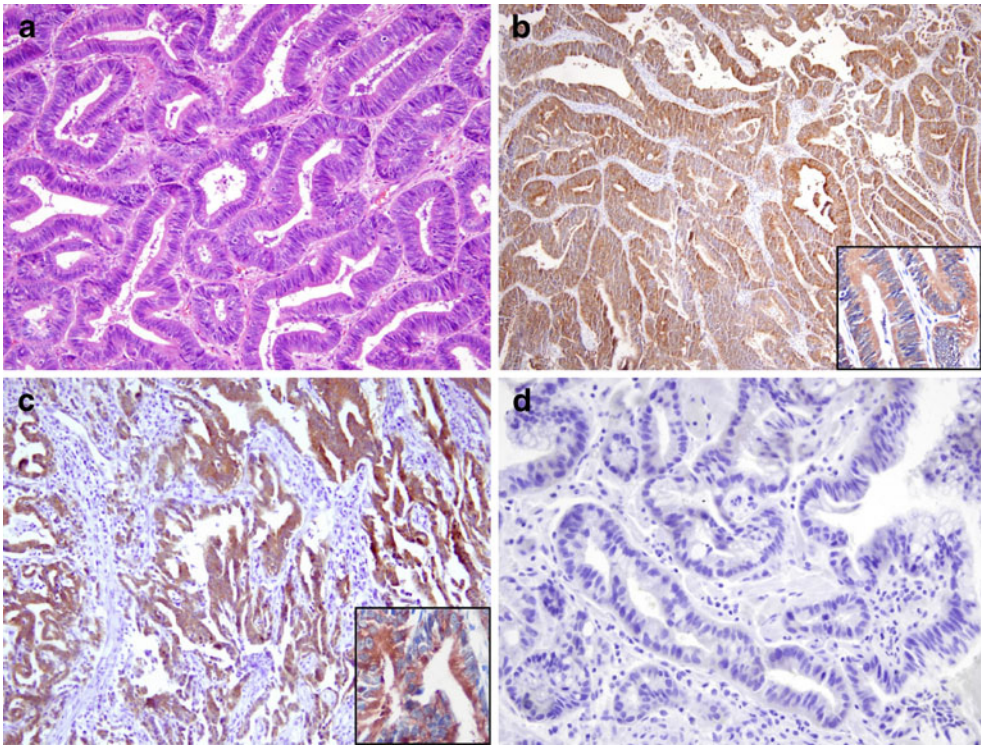

Fig. 3 **a**, **b** Aberrant cytoplasmic anti- aPKC-zeta immunoreactivity in low-grade adenomatous dysplasia **a** H&E staining, **b** aPKC-zeta immunohistochemistry. *Inset* in **b** shows loss of apical localization of aPKC-zeta at higher magnification. **c** Aberrant cytoplasmic anti-aPKC-zeta immunoreactivity in gastric adenocarcinoma. *Inset* shows loss of apical localization of aPKC-zeta at higher magnification. **d** Loss of aPKC-zeta expression in low-grade foveolar-type gastric dysplasia

Apical anti-aPKC-zeta staining was lost in 65% (n=15) of low-grade dysplasias, in 88% (n=15) of high-grade dysplasias (p=0.096, borderline significant). Overall, the data suggest that apical aPKC-zeta is lost in gastric dysplasia of both foveolar and adenomatous types.

Discussion

Gastric foveolar-type dysplasia, a previously underdiagnosed entity also known as type II or hyperplastic dysplasia, has been increasingly recognized as a precursor of gastric adenocarcinoma. In contrast to adenomatous dysplasia, it resembles normal gastric epithelium, variably retaining eosinophilic apical mucin and showing little elongation or stratification of the nuclei and lack of goblet or Paneth cells. Foveolar-type dysplasia correlates with expression of gastric mucin, such as Muc5AC, supporting the view that foveolar-type dysplasia arises in the epithelium with gastric differentiation. In contrast, adenomatous gastric dysplasia correlates with the expression of intestinal markers CDX2 and MUC2, consistent with its intestinal differentiation [3, 25–27]. Approximately 30% of gastric dysplasias were recently reported to have a hybrid adenomatous/foveolar phenotype, defined as having at least 10% of the alternative histologic type [3]. Foveolar-type dysplasia has been also reported in Barrett's esophagus and was linked to adenocarcinoma of the esophagus [28–30]. The major differential diagnosis of gastric foveolar-type dysplasia is with reactive or regenerative atypia. Mucosal regeneration or reparative process due to active inflammation, erosions or ulcers may demonstrate cytological atypia with severe mucin depletion, nuclear hyperchromasia and increased mitotic activity mimicking dysplasia. Features that favor reactive nature of these changes are vascular congestion and edema of the lamina propria, evenly spaced nuclei without crowding or pseudostratification, gradual transition from the atypical to normal cells and maturation of the epithelium towards the surface [4, 31]. Sometimes making a distinction can be challenging or impossible on morphological grounds suggesting that a biomarker of dysplasia could be a useful diagnostic adjunct.

We have recently reported that a cell polarity protein Lgl2 is a marker of gastric epithelium that is useful in ruling out gastric adenomatous dysplasia [19]. In the current study, we sought to evaluate Lgl2 as a marker of foveolar-type gastric dysplasia. Lgl2 expression was lost in 80% of gastric foveolar-type dysplasias. Both sporadic dysplasias (low and high grade) and dysplasias associated with FAP (all low grade), had similar loss of Lgl2 expression indicating that it is an early phenomenon in neoplastic progression. Molecular mechanisms of Lgl2 loss in gastric dysplasia are unknown; however constitutive activation of the Wnt signaling pathway is a possible explanation. Activated Wnt signaling has been implicated in gastric carcinogenesis and it interferes with the Lgl function in experimental conditions [32–35].

Based on these and previous findings we propose the utility of Lgl2 as an immunohistochemical adjunct for evaluation of both foveolar and adenomatous forms of gastric dysplasia [3, 19]. One limitation of using Lgl2 is its consistent lack of expression in intestinal metaplasia [19]. Consequently, negative Lgl2 staining cannot differentiate dysplasia from intestinal metaplasia with reactive change. Therefore, Lgl2 staining could be used to rule out gastric dysplasia (if the staining is positive) in situations where intestinal metaplasia with reactive change cannot be excluded.

Few studies have addressed molecular or clinicopathological features of foveolar gastric dysplasia. No significant differences in APC gene alterations, high-level MSI and K-ras mutations were found in gastric adenomas of intestinal versus foveolar type [36]. Similarly, clinicopathological significance of foveolar-type dysplasia remains uncertain and is being debated in the literature. One line of evidence suggests that gastric foveolar-type adenomas are low-grade lesions that are not associated with appreciable progression to adenocarcinoma [37, 38]. Others found that foveolar-type dysplasias are often high grade, and are more often associated with the development of a second dysplastic lesion and adenocarcinoma than adenomatous dysplasia [3]. The discrepancy is likely due to evaluation of biologically distinct groups of lesions. For instance, in the studies of Abraham et al. 2002 and Chen et al. 2009 the vast majority of foveolar-type dysplasias were polypoid lesions associated with fundic gland polyps and FAP. However, in the study of Park et al. 2009, 40% of the lesions were depressed or non-polypoid, and none were associated with FAP or fundic gland polyps [3, 36, 38]. In our study, all cases of foveolar-type dysplasia associated with FAP were low grade, while all high-grade lesions were sporadic.

We next evaluated utility of aPKC-zeta as a marker of gastric dysplasia. We reasoned that since aPKC is an apical polarity protein that antoganizes Lgl and maintains identity of the apical cell domain, it may be a candidate marker of dysplasia complimentary to Lgl2 [39]. Additionally, aPKC was reported to function as an oncogene in non-small cell lung and ovarian carcinomas and its oncogenic effect was partially attributed to abnormal cell polarity [40, 41]. We show in this study that aPKC-zeta is selectively expressed at the apical surface of normal foveolar cells and oxyntic gland cells, the localization predicted from experimental models. We next show that apical localization of aPKC-zeta is maintained in reactive gastropathy and chronic gastritis. In contrast, apical aPKC-zeta was lost in low-grade dysplasia of both foveolar and adenomatous types in 47% and 65% of cases, respectively. More frequent loss was seen in high-grade dysplasia, although the difference was not statistically significant. Lack of significance was probably due to the relatively small number of high-grade dysplasias, which is one of the limitations of our study. All but one case of adenocarcinoma showed loss of apical aPKC-zeta immunoreactivity. Altogether, the results favor incremental loss of apical aPKC-zeta during dysplasia-adenocarcinoma progression in the stomach. Still, moderate sensitivity of the aPKC-zeta loss as a marker of dysplasia may limit its use diagnostically.

In summary, we conclude that Lgl2 immunohistochemistry may be helpful in the diagnosis of gastric foveolar-type dysplasia. Our study also suggests moderate sensitivity of loss of apical aPKC-zeta as a marker of gastric dysplasia. However, additional studies are needed to further assess utility of aPKC-zeta in gastric dysplasia.

Conflict of interest The authors declare that they have no conflict of interest.

References

1. Lauwers GY, Srivastava A (2007) Gastric preneoplastic lesions and epithelial dysplasia. Gastroenterol Clin North Am 36:813–829
2. Antonioli DA (1994) Precursors of gastric carcinoma: a critical review with a brief description of early (curable) gastric cancer. Hum Pathol 25:994–1005
3. Park DY, Srivastava A, Kim GH et al (2008) Adenomatous and foveolar gastric dysplasia: distinct patterns of mucin expression and background intestinal metaplasia. Am J Surg Pathol 32:524–533
4. Lauwers GY, Riddell RH (1999) Gastric epithelial dysplasia. Gut 45:784–790
5. Rugge M, Correa P, Dixon MF et al (2000) Gastric dysplasia: the Padova international classification. Am J Surg Pathol 24:167–176
6. Bilder D (2004) Epithelial polarity and proliferation control: links from the Drosophila neoplastic tumor suppressors. Genes Dev 18:1909–1925
7. Zhan L, Rosenberg A, Bergami KC et al (2008) Deregulation of scribble promotes mammary tumorigenesis and reveals a role for cell polarity in carcinoma. Cell 135:865–878
8. Albertson R, Doe CQ (2003) Dlg, Scrib and Lgl regulate neuroblast cell size and mitotic spindle asymmetry. Nat Cell Biol 5:166–170
9. Betschinger J, Knoblich JA (2004) Dare to be different: asymmetric cell division in Drosophila. *C. elegans* and vertebrates. Curr Biol 14:R674–R685
10. Plant PJ, Fawcett JP, Lin DC et al (2003) A polarity complex of mPar-6 and atypical PKC binds, phosphorylates and regulates mammalian Lgl. Nat Cell Biol 5:301–308
11. Yamanaka T, Horikoshi Y, Sugiyama Y et al (2003) Mammalian Lgl forms a protein complex with PAR-6 and aPKC independently of PAR-3 to regulate epithelial cell polarity. Curr Biol 13:734–743
12. Chalmers AD, Pambos M, Mason J et al (2005) aPKC, Crumbs3 and Lgl2 control apicobasal polarity in early vertebrate development. Development 132:977–986
13. Hutterer A, Betschinger J, Petronczki M et al (2004) Sequential roles of Cdc42, Par-6, aPKC, and Lgl in the establishment of epithelial polarity during Drosophila embryogenesis. Dev Cell 6:845–854
14. Zhang X, Wang P, Gangar A et al (2005) Lethal giant larvae proteins interact with the exocyst complex and are involved in polarized exocytosis. J Cell Biol 170:273–283

15. Gateff E (1978) Malignant neoplasms of genetic origin in Drosophila melanogaster. Science 200:1448–1459
16. Bilder D, Li M, Perrimon N (2000) Cooperative regulation of cell polarity and growth by Drosophila tumor suppressors. Science 289:113–116
17. Grifoni D, Garoia F, Schimanski CC et al (2004) The human protein Hugl-1 substitutes for Drosophila lethal giant larvae tumour suppressor function in vivo. Oncogene 23:8688–8694
18. Schimanski CC, Schmitz G, Kashyap A et al (2005) Reduced expression of Hugl-1, the human homologue of Drosophila tumour suppressor gene lgl, contributes to progression of colorectal cancer. Oncogene 24:3100–3109
19. Lisovsky M, Dresser K, Baker S et al (2009) Cell polarity protein Lgl2 is lost or aberrantly localized in gastric dysplasia and adenocarcinoma: an immunohistochemical study. Mod Pathol 22:977–984
20. Sobala GM, King RF, Axon AT, Dixon MF (1990) Reflux gastritis in the intact stomach. J Clin Pathol 43:303–306
21. Quinn CM, Bjarnason I, Price AB (1993) Gastritis in patients on non-steroidal anti-inflammatory drugs. Histopathology 23:341–348
22. Srivastava A, Lauwers GY (2008) Gastric epithelial dysplasia: the Western perspective. Dig Liver Dis 40:641–649
23. Lauren P (1965) The two histological main types of gastric carcinoma: diffuse and so-called intestinal-type carcinoma. An attempt at a histo-clinical classification. Acta Pathol Microbiol Scand 64:31–49
24. Fenoglio-Preser C, Carneiro F, Correa P et al (2000) Tumors of the stomach. In: Hamilton SR, Aaltonen LA (eds) World Health Organization classification of tumours: pathology and genetics of tumours of the digestive system. IARC Press, Lyon, pp 37–52
25. Tsukashita S, Kushima R, Bamba M (2001) MUC gene expression and histogenesis of adenocarcinoma of the stomach. Int J Cancer 94:166–170
26. Tajima Y, Yamazaki K, Makino R (2006) Gastric and intestinal phenotypic marker expression in early differentiated-type tumors of the stomach: clinicopathologic significance and genetic background. Clin Cancer Res 12:6469–6479
27. Park DY, Srivastava A, Kim GH (2010) CDX2 expression in the intestinal-type gastric epithelial neoplasia: frequency and significance. Mod Pathol 23:54–61
28. Rucker-Schmidt RL, Sanchez CA, Blount PL (2009) Nonadenomatous dysplasia in Barrett esophagus: a clinical, pathologic, and DNA content flow cytometric study. Am J Surg Pathol 33:886–893
29. Brown IS, Whiteman DC, Lauwers GY (2010) Foveolar type dysplasia in Barrett esophagus. Mod Pathol 23:834–843
30. Mahajan D, Bennett AE, Liu X (2010) Grading of gastric foveolar-type dysplasia in Barrett's esophagus. Mod Pathol 23:1–11
31. Goldstein NS, Lewin KJ (1997) Gastric epithelial dysplasia and adenoma: historical review andhistological criteria for grading. Hum Pathol 28:127–133
32. Clements WM, Wang J, Sarnaik A et al (2002) beta-Catenin mutation is a frequent cause of Wnt pathway activation in gastric cancer. Cancer Res 62:3503–3506
33. Horii A, Nakatsuru S, Miyoshi Y et al (1992) The APC gene, responsible for familial adenomatous polyposis, is mutated in human gastric cancer. Cancer Res 52:3231–3233
34. Nojima M, Suzuki H, Toyota M et al (2007) Frequent epigenetic inactivation of SFRP genes and constitutive activation of Wnt signaling in gastric cancer. Oncogene 26:4699–4713
35. Dollar GL, Weber U, Mlodzik M et al (2005) Regulation of Lethal giant larvae by Dishevelled. Nature 437:1376–1380
36. Abraham SC, Park SJ, Lee JH et al (2003) Genetic alterations in gastric adenomas of intestinal and foveolar phenotypes. Mod Pathol 16:786–795
37. Abraham SC, Montgomery EA, Singh VK et al (2002) Gastric adenomas: intestinal-type and gastric-type adenomas differ in the risk of adenocarcinoma and presence of background mucosal pathology. Am J Surg Pathol 26:1276–1285
38. Chen ZM, Scudiere JR, Abraham SC et al (2009) Pyloric gland adenoma: an entity distinct from gastric foveolar type adenoma. Am J Surg Pathol 33:186–193
39. Assémat E, Bazellières E, Pallesi-Pocachard E et al (2008) Polarity complex proteins. Biochim Biophys Acta 1778:614–630
40. Regala RP, Weems C, Jamieson L et al (2005) Atypical protein kinase C iota is an oncogene in human non-small cell lung cancer. Cancer Res 65:8905–8911
41. Eder AM, Sui X, Rosen DG et al (2005) Atypical PKCiota contributes to poor prognosis through loss of apical-basal polarity and cyclin E overexpression in ovarian cancer. Proc Natl Acad Sci USA 102:12519–12524

Virchows Arch (2010) 457:643–649
DOI 10.1007/s00428-010-0978-5

ORIGINAL ARTICLE

Vacuolated cell pattern of pancreatobiliary adenocarcinoma: a clinicopathological analysis of 24 cases of a poorly recognized distinctive morphologic variant important in the differential diagnosis

Nevra Dursun · Jining Feng · Olca Basturk · Sudeshna Bandyopadhyay · Jeanette D. Cheng · Volkan N. Adsay

Received: 5 August 2010 / Revised: 7 September 2010 / Accepted: 9 September 2010 / Published online: 8 October 2010
© Springer-Verlag 2010

Abstract Pancreatic ductal adenocarcinoma (PDCA) is characterized by well-defined tubular units in the vast majority of the cases; however, variations in this theme do occur. It is important to recognize the morphologic spectrum of PDCA to avoid misdiagnosis especially in small specimens and also in metastatic foci. Here, we document a morphologic variant of PDCA that is characterized by a distinctive pattern of infiltrating cribriform nests in a distinctive "microcystic" or "secretory" pattern. Twenty-four cases of PDCA have been identified in a review of 505 cases diagnosed with PDCA. Histologically, this pattern was characterized by infiltrating nests of tumor cells with large vacuoles and "signet-ring" like appearance imparting a cribriform growth pattern. The vacuoles were one to five cells in size, often merging to form multilocular spaces separated by a thin rim of cell membrane. Many of these spaces contained CA19.9 positive granular secretory material. The nuclei were often pushed to the periphery and compressed in a pattern resembling adipocytes, although the nuclei were often densely hyperchromatic and displayed significant atypia. Especially in biopsies from the peripancreatic fat and peritoneum, these neoplastic cells had been misdiagnosed as degenerating adipocytes, and in the lymph nodes, they had been misinterpreted as lipogranulomas. Clinical findings of the patients were similar to that of conventional PDCA, except higher incidence of history of smoking (83% vs. 60%; $p=0.034$). In conclusion, vacuolated cell adenocarcinoma is a distinct morphologic variant of PDCA, and the presence of this peculiar pattern in a metastatic site, although not specific, should raise the suspicion of a PDCA.

Keywords Pancreas · Pancreatobiliary · Ductal · Adenocarcinoma · Vacuolated · Lipoid · Signet ring · Cribriform

This study was presented in part at the annual meeting of the United States and Canadian Academy of Pathology in Atlanta, GA in 2000.

N. Dursun
Department of Pathology,
Istanbul Education and Research Hospital,
Istanbul, Turkey

J. Feng · S. Bandyopadhyay
Department of Pathology,
Karmanos Cancer Institute and Wayne State University,
Detroit, MI, USA

O. Basturk
Department of Pathology,
Memorial Sloan–Kettering Cancer Center,
New York, NY, USA

J. D. Cheng
Department of Pathology, Piedmont Hospital,
Atlanta, GA, USA

V. N. Adsay (✉)
Department of Pathology and Laboratory Medicine,
Emory University Hospital,
1364 Clifton Road NE, Room H-180B,
Atlanta, GA 30322, USA
e-mail: volkan.adsay@emory.edu
e-mail: nadsay@emory.edu

Introduction

Histopathologic diagnosis of pancreatic ductal adenocarcinoma (PDCA) is often challenging. This is partly due to the inaccessibility of the organ, which necessitates the diagnosis to be rendered in limited specimens, small biopsies, or

frozen sections [1]. In addition, benign conditions of the pancreas, especially chronic pancreatitis, can closely mimic PDCA. Conversely, PDCA typically has an abundant stromal component (hence the synonym scirrhous carcinoma) which, on one hand, hampers the tumor tissue yield in small specimens and, on the other, complicates the microscopic evaluation by morphologically mimicking chronic pancreatitis [2]. This challenge may partly be overcome by recognizing the various morphologic patterns that PDCA exhibits.

It is also important to recognize the morphologic spectrum of PDCA for its correct diagnosis in the metastatic sites. A significant proportion of the PDCA patients presents with metastatic tumors and an unsuspected primary in the pancreas. In fact, studies have shown that PDCA is one of the most common, if not the most common, sources of "carcinoma of unknown origin" [3,4].

PDCA is characterized (and defined) by infiltrating tubular units lined by cuboidal cells, embedded in desmoplastic stroma. However, there are various cytologic and architectural variations that occur on top of this basic theme, which are included under the umbrella of pancreatobiliary carcinoma [4]. In this study, a distinctive morphologic variant characterized by infiltrating cribriform units that are formed by vacuolated tumor cells (resembling adipocytes or signet-ring cells) that contain CA19-9 positive secretory material is documented. The histologic, immunophenotypic, molecular, and clinical characteristics of this variant are analyzed and compared to those of the ordinary PDCA.

Materials and methods

Patients

Five hundred and five consecutive cases of PDCA seen in the files were reviewed. Twenty-four cases (18 pancreatectomies and six biopsies) that displayed this distinctive vacuolated/cribriform pattern in more than 25% of the tumors were identified. From the resection specimens, an average of 15 slides was available (range, one to 29) for examination on these cases.

Demographic features of the group were analyzed, and the clinical history of the patients for the presumed risk factors of PDCA such as diabetes mellitus, smoking, and alcohol were recorded, where available.

The findings were contrasted with those of conventional PDCA.

Histochemical analysis

Histochemical stains, namely Mayer's mucicarmine, high iron diamine–alcian blue (to differentiate sialated mucins from sulfated mucins), periodic acid–Schiff, and alcian blue–periodic acid–Schiff (AB-PAS, for acidic mucins), were performed.

Immunohistochemistry

All tumors for which material was available were studied for the mucin-related glycoproteins and oncoproteins using immunohistochemical stains with carcinoembryonic antigen (CEA; BioGenex, San Ramon, CA; 1:200), CA19-9 (Novocastra, New Castle upon Tyne; 1:200), B72.3 (Signet, Dedham, MA; 1:40), MUC1 (Novocastra, New Castle upon Tyne; 1:160), and MUC2 (Novocastra, New Castle upon Tyne; 1:100), which have known expression patterns (and presumed diagnostic utility) in PDCA. High molecular weight cytokeratin, also known as HMWCK or CK34βE12, a marker that is positive in squamous change in pancreas tumors, was also tested to determine whether this pattern represents a form of abortive squamous differentiation.

Avidin–biotin–peroxidase method was used. Negative and positive controls were included with each batch of slides tested.

K-ras mutation analysis

Frozen tumor tissue was available in eight cases and was used to search for the mutation in codon 12 of *K-ras* oncogene, which is very common in cases of conventional PDCA.

DNA extraction and PCR amplification

DNA extraction and PCR amplification for the analysis of mutations in codon 12 of the *K-ras* gene were accomplished following methods previously published [5]. The extract containing genomic DNA (10 μl) was subjected to PCR in a total volume of 50 μl of reaction mixture using specific primers. The primer set consisted of 5′-ATGACTGAATA TAAACTTGT-3′ (forward) and 5′-CTATTGTTGGATCA TATT-3′ (reverse), and the PCR was carried out in a DNA thermal cylinder (Cetus-Perkin Elmer, Norwalk, CT) for 35 cycles. Each cycle of amplification consisted of 1 min of denaturation at 94°C, 1 min of annealing at 57°C, and 2 min of polymerization at 72°C. After the last cycle, polymerization was continued for an additional 7 min at 72°C.

Slot blotting and southern hybridization

Slot-blot southern analysis of PCR-amplified samples was carried out using ^{32}P-labeled oligonucleotide probe panel following standard procedure [5]. Amplified DNA was denatured by adding 7 μl of the PCR reaction mixture to 100 μl of 0.4 M NaOH and 25 mM EDTA. The mixture

was heated to 95°C for 2 min and placed on ice. One hundred microliters of 2 M Tris–HCl (pH 7.4) was added and slot blotted on a nylon membrane using the Schleicher & Schuell (Keane, NH) manifold-II apparatus. The membranes were prehybridized in the hybridization mixture (5× SSPE, 5× Denhardts, 0.5% sodium dodecyl sulfate (SDS), 100 mM sodium pyrophosphate, pH 7.5) for 1 h at 37°C on a shaker. 5′-end-^{32}P-labeled oligonucleotide probe (wild-type probe and six specific probes to each base mutation) was added to the hybridization mix to a final concentration of 2×10^6 cpm/ml and hybridized overnight at 37°C in a hybridization incubator. The membranes were washed with 6× SCC and 3 M tetramethylammonium chloride (TMAC) wash solution (3 m TMAC, 50 mM Tris–HCl, 2 mM EDTA, 0.1% SDS) twice at 61°C for 30 min with constant shaking and were autoradiographed. Control samples for all the studies were taken from areas without tumor from the same histologic sections.

Statistical analysis and comparison with ordinary PDCA

Available demographic data (age, location of the tumor, as well as history of smoking, diabetes, and alcohol) of the patients with vacuolated cell pattern were compared with those of ordinary PDCA identified in the same database. For the comparison of age and tumor size, *t* test was applied, and for the remaining, chi-square test was utilized. Kaplan–Meier survival curves were made to compare the clinical outcome.

Results

Clinical findings

The mean age of the patients was 61 (range, 43 to 72 years) vs. 63 in PDCA. There was slight female predominance, with nine of the patients males and 15 females (F/M=1.7 vs. 1 in PDCA; Table 1). Fifteen were Caucasians, seven were African Americans, and two were unknown (ratio= 2.1 vs. 1.5 in PDCA). The tumors ranged in size from 2.0 to 6.0 cm (mean tumor size, 3.8 vs. 3.5 cm in PDCA). Six patients had biopsy diagnosis only, and their tumor sizes were based on reports from the CT examination. Among resection specimens, 12 tumors were located in the head, five in the tail, and one in the body of the pancreas.

In the available data on the past history of the patients, 14/16 were smokers (83% vs. 59% in PDCA), four of 13 had diabetes (30% vs. 27% in PDCA), and three of 14 (21% vs. 22% in PDCA) had alcohol abuse (Fig. 1). Only the difference in history of smoking was statistically significant (p=0.034).

Histopathologic findings

Microscopically, this variant was characterized by infiltrating clusters of tumor cells that contained large vacuoles imparting them a cribriform architecture (Fig. 2). The vacuoles were one to five cells in size, often merging to form multilocular spaces separated by a thin rim of cell membrane (Figs. 2 and 3). These microcystic spaces pushed the nuclei to the periphery of the cells, compressing them and indenting the nuclear membrane. This created a pattern reminiscent of adipocytes (lipoid pattern) or signet-ring cells (Fig. 4). Many of these spaces contained material composed of cellular debris (necrotic cells, Fig. 2) and mucin (Fig. 5; positive with histochemical and immunohistochemical stains; see below). The nuclei, upon close inspection, were often densely hyperchromatic and displayed significant atypia, enlargement, and pleomorphism (Figs. 4 and 6). In two cases, in the biopsies from the peripancreatic fat and peritoneum, this pattern has been misdiagnosed as degenerating adipocytes. In two other cases, the metastatic foci in

Table 1 Clinical findings

Clinical findings	PDCA with vacuolated pattern (n=24)	PDCA with tubular pattern (n=481)
Demographic data		
Mean age (years)	61	63
Female/male	1.7	1
Race	68% Caucasian	60% Caucasian
	32% African American	40% African American
Tumor size (mean; cm)	3.8	3.5
Location	Head=67%	Head=81%
	Body/tail=33%	Tail=19%
Clinical history		
Smoker (%)	82	59 (p=0.034)
DM (%)	30	27
Alcohol abuse (%)	21	22
K-ras mutation (%)	87.5	72

DM diabetes mellitus

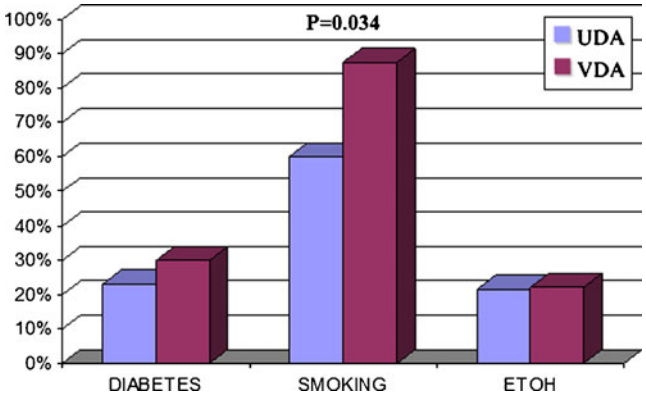

Fig. 1 When comparing the incidence of diabetes mellitus, smoking, and alcohol in vacuolated cell variant (VDA) and ordinary ductal adenocarcinoma (UDA), only the difference in history of smoking was statistically significant (p=0.034)

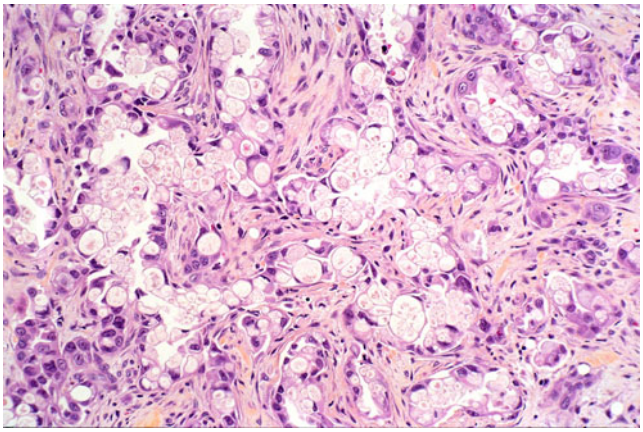

Fig. 3 In some examples, the vacuoles impart a signet-ring-like appearance to the cells and may even have targetoid mucin in some areas

the lymph nodes were missed (Fig. 7), possibly because they were misinterpreted as lipogranulomas or sinusoidal lipid, which they closely resembled.

Histochemical findings

Mucicarmine, high iron diamine (Fig. 8), and AB-PAS stains [mostly blue (sialated acidic mucin) with focal black (sulfated acidic mucin)] were all positive in the vacuolated cells of 11 cases examined (11/11).

Immunohistochemical findings

Immunohistochemical phenotype of the vacuolated pattern was similar to that of PDCA. The tumor cells were positive uniformly for CA19-9 (11/11, Fig. 8) and MUC1 (11/11) and, in some cases, also for CEA (8 of 11, two of which was focal) and B72.3 (5 of 11). CK34βE12, which is usually negative in PDCA, however, was detected in 6 of 11 cases. Only one case revealed focal MUC2 positivity, which was limited to goblet cell metaplasia area (1 of 11).

Molecular analysis

Mutation in codon 12 of *K-ras* oncogene, was detected in seven of the eight (87.5%) cases studied (vs. 56 of 78 (72%) in PDCA; p=0.676).

Survival analysis

Median survival after diagnosis was 13.7 months (vs. 13.8 months in PDCA; Fig. 9).

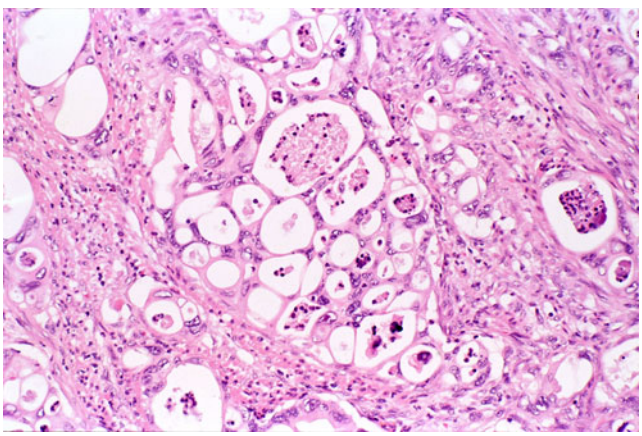

Fig. 2 In vacuolated variant of ductal adenocarcinoma, infiltrating glandular elements often form a cribriform pattern created by multiple-cell-size vacuoles that are separated by thin strands of cytoplasm. The vacuoles often contain necrotic debris admixed with neutrophils

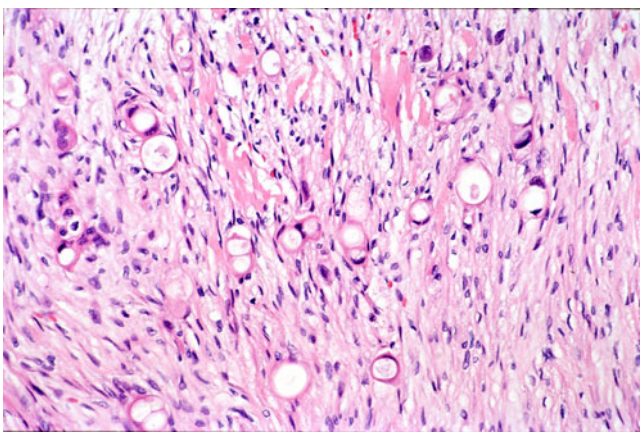

Fig. 4 In areas where the infiltrative units are smaller, tangential cut of the vacuolated glands may give the impression of individual cell infiltration mimicking diffuse infiltrative-type ("poorly cohesive cell" or "signet-ring" cell) carcinoma; however, the presence of larger cohesive glandular elements establish the diagnosis that this is merely the vacuolated variant of ductal adenocarcinoma

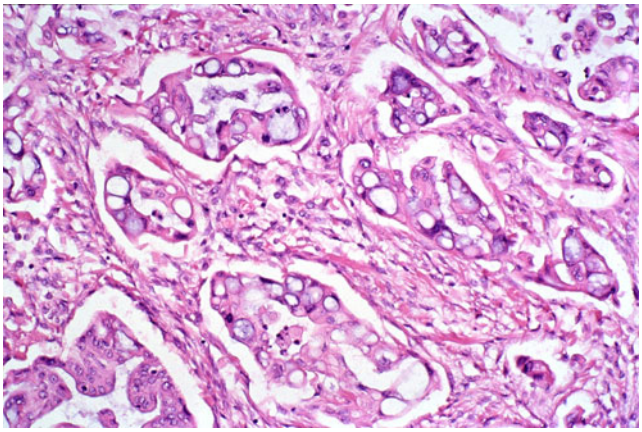

Fig. 5 In rare areas, transition from more mucin-filled vacuoles to the more characteristic empty vacuoles can be observed. In this particular case, artifactual clefting around the infiltrative glands created a pseudo-micropapillary carcinoma appearance

Discussion

Morphologic repertoire of pancreatobiliary-type adenocarcinoma originating in the pancreas (invasive ductal adenocarcinoma, PDCA) includes a hitherto unrecognized distinctive pattern characterized by infiltrating cribriform clusters of cells with microcystic formations. In this variant, the microcysts appear to result from the fusion of intracellular lumenae, many of which contain CA19-9 positive secretory material admixed with nuclear debris and mucin. These spaces compress the cytoplasmic organelles to the periphery of the cell, forming a thin bridging membrane. The nuclei are often compressed and indented, creating a picture reminiscent of signet-ring cells or adipocytes, to an extent that these tumor cells have been mistaken for lipogranulomas or sinusoidal fat, both of which are common findings in peripancreatic lymph nodes.

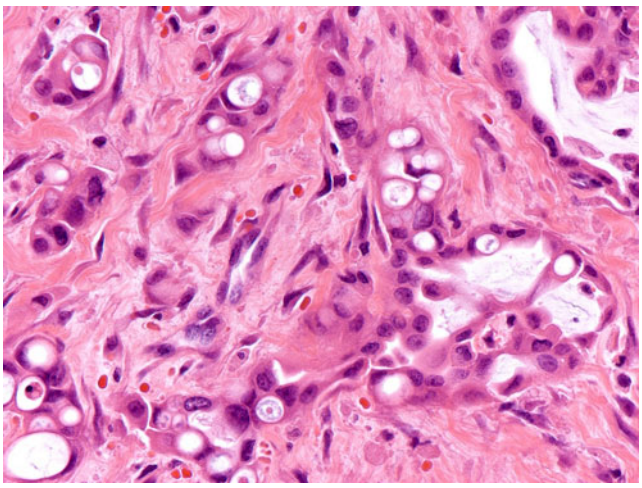

Fig. 6 In some areas, the vacuoles were smaller and overtly intracytoplasmic, some containing targetoid mucin. The nuclei were often displayed significant atypia, enlargement, and pleomorphism

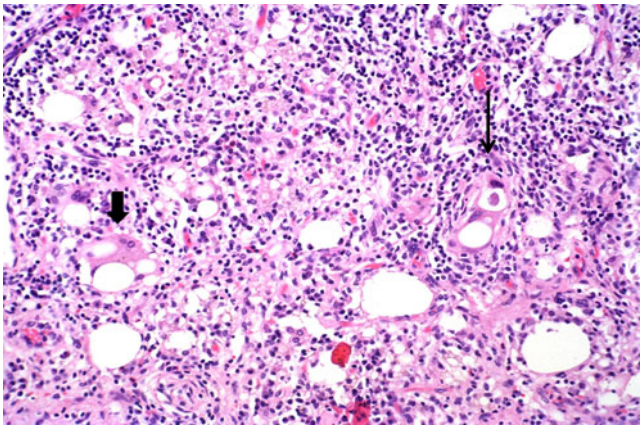

Fig. 7 Vacuolated cell adenocarcinomas (*right*, *thin arrow*) can be mistaken as lipogranulomas (*left*, *thick arrow*) because of their mimicry of fat. Close inspection, however, typically elucidates the severe degree of cytologic atypia including marked pleomorphism and hyperchromatism, which is characteristically present

They may also be mistaken for fat necrosis in biopsies from peripancreatic tissue or peritoneal surfaces to which PDCA often disseminates.

It is important to recognize this pattern because it may be diagnostically important in limited specimens or in biopsies from metastatic foci, especially since many PDCA patients present with distant tumor and an unsuspected primary in the pancreas. The authors have seen several examples in the liver and other sites including bone marrow, in which this pattern led to the correct diagnosis of otherwise unsuspected PDCA. Differential diagnosis include signet-ring cell carcinoma, tumors with lipoblast-like or signet-ring cells from other primary sites, specifically breast and stomach, and liposar-

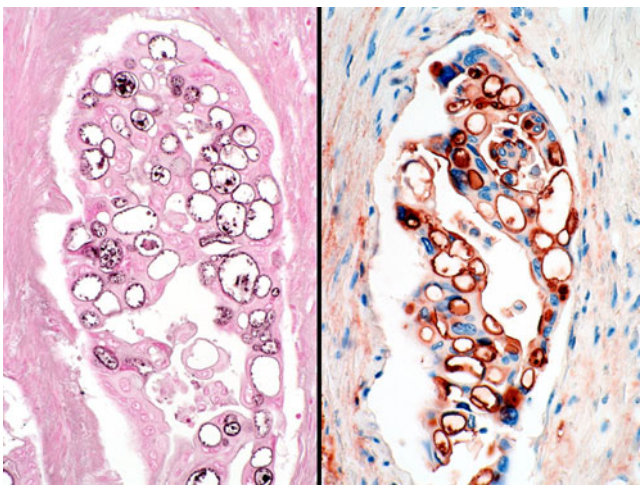

Fig. 8 Histochemical and immunohistochemical stains confirm that these vacuoles are in fact intraglandular lumen formations that are lined by secretory apparatus containing mucin (*left*, high iron diamine) and mucin-related glycoproteins (*right*, CA19-9)

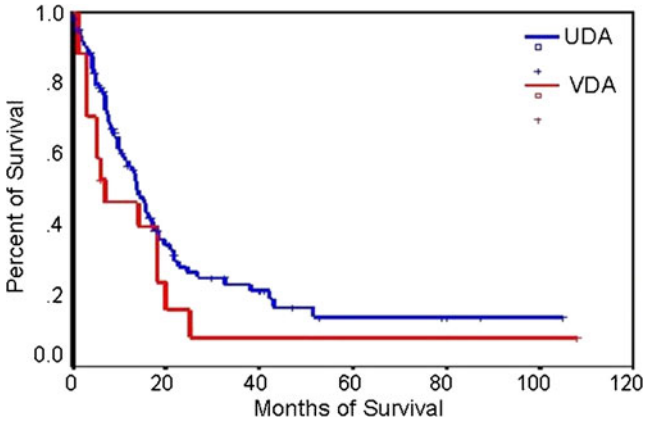

Fig. 9 Survival rates of vacuolated cell variant (VDA) and ordinary ductal adenocarcinoma (UDA)

coma (alone or as part of sarcomatoid carcinoma). All these distinctions have significant therapeutic implications.

Although uncommon, this pattern may also be encountered in tumors from other sites, especially in surface epithelial organs. The presence of distinctive large vacuoles that compress the nucleus forming a cribriform architecture is a typical finding in adenomatoid tumors (the so-called localized mesothelioma of gynecologic tract) [6,7], but may also be rarely seen in mesotheliomas [8]. This pattern is also well recognized as a variant of meningioma in the meninges [9], another site with a highly specialized "lining" properties, similar in that sense to mesothelium. The authors have also encountered this pattern in laryngeal and GE-junction carcinomas, both of which are sites with transition from a glandular to squamous epithelium, raising the question of this pattern being a result of lumen forming cells that are also showing immature squamous properties. The positivity of CK34βE12, a marker of squamous differentiation in the pancreas, in 6 of 11 cases reported here may lend further support to this possibility. On the other hand, in none of these cases was frank evidence of squamous differentiation such as keratin formation, squamous pearls, or histologic evidence of desmosomal junctions identified. Therefore, it appears that the process is likely to be recapitulating attenuated "lining" cells akin to those seen in adenomatoid tumors or mesotheliomas, rather than true squamous differentiation.

A pattern similar to the one described here may also be rarely seen in solid glandular organs including the salivary glands [10,11], and we have noted it occasionally even in the colon. In the ovary, it has been documented as a rare variant that was reported as "mixed-epithelial carcinoma with microcystic pattern and signet ring cells" [12], a term that has been coined for this pattern in the meninges [9]. Since ovarian involvement in disseminated PDCA is not uncommon [13–15] (and vice versa is also true [16]), it is important to be aware that this pattern may be exhibited by the tumors from both organs. A similar tumor type has been also noted in the urinary bladder under the same heading (microcystic transitional cell carcinomas) [5,17,18] along with the lipid cell variant of urothelial carcinoma with histologic appearance similar to lipoblasts [19–22].

The term microcystic, in the pancreas, however, is used specifically for serous cystadenomas (and its look-alikes) that are characterized by macroscopically visible small cysts (only a few millimeters in diameter) that form a distinctive sieve-like arrangement. Therefore, although "microcystic" is probably the best descriptive term for this pattern, it ought to be avoided for this variant of PDCA since it is already fully identified with a benign and distinctive tumor in this organ. Also, although the cells in this pattern have "signet-ring" appearance; we, as many others, are of the opinion that the term "signet ring" ought to be avoided outside the setting of diffuse infiltrative-type (E-cadherin related) carcinoma that is characterized by individual cell infiltration. In the void of the liberty to use these terms, the best descriptive names to designate this pattern are felt to be vacuolated or cribriform adenocarcinoma. The latter has been associated with a distinctive and well-differentiated tumor in the breast and may be misleading as well.

Fortunately, the name one chooses to describe this variant may not be that important because the findings in this study suggest that this is a morphologic variant of pancreatobiliary-type adenocarcinoma, not a separate tumor type. Its clinical characteristics are not too different from PDCA, with the exception of higher incidence of smoking history. The association with smoking may be of interest because studies in other organs are now revealing that smoking triggers different pathways of carcinogenesis [23,24] and may have closer association with certain glandular subtypes [25]. Along the same lines, although it did not reach statistical significance, the incidence of *K-ras* mutation appeared to be higher in vacuolated carcinomas in our population. Whether this has a role in the development of this distinctive secretory/vacuolated pattern needs further scrutiny because it is becoming increasingly clear that *K-ras* is an oncogene commonly involved in glandular neoplasia of various organs [26], and different types of *K-ras* mutation may be responsible for different patterns and degrees of secretory properties.

The clinical course of vacuolated variant appears to be slightly more aggressive than the average PDCA, putting it in the more poorly differentiated category. Breast carcinomas with similar pattern also reported to have worse prognosis, particularly in elderly patients [27]. While this may be surprising based on the degree of glandular secretory differentiation, it is not at all if the nuclear grade is taken into consideration because this variant is often associated with high nuclear grade; despite their compressed (attenuated) appearance, the nuclei are often very atypical, hyperchromatic, and irregular, an important clue for the diagnosis of this pattern.

In conclusion, the morphologic spectrum of PDCA includes a vacuolated (cribriform) pattern that ought to be recognized because it may be important in the often challenging differential diagnosis of this tumor type both in limited specimens from the pancreas and metastatic sites.

Acknowledgement This study is supported in part by the National Cancer Institute Specialized Program in Research Excellence (SPORE) CA101936 in Pancreas Cancer (PAR-02-068) and in part by the Georgia Cancer Coalition Distinguished Cancer Clinicians and Scientists Program.

Conflict of interest The authors have no conflict of interest.

References

1. Adsay N, Bandyopadhyay S, Basturk O, Kilinc N, Andea A, Cheng J (2005) Chronic pancreatitis or pancreatic ductal adenocarcinoma? Histopathologic criteria for the differential diagnosis. Semin Diagn Pathol 21(4):268–276
2. Adsay N, Basturk O, Klimstra D, Klöppel G (2005) Pancreatic pseudotumors: non-neoplastic solid lesions of the pancreas that clinically mimic pancreas cancer. Semin Diagn Pathol 21(4):260–267
3. Cubilla A, Fitzgerald PJ (1978) Pancreas cancer. I. Duct adenocarcinoma. A clinical-pathologic study of 380 patients. Pathol Annu 13:241–289
4. Hruban RH, Pitman MB, Klimstra DS (2007) Tumors of the pancreas. ARP, Washington
5. Sari A, Uyaroglu MA, Ermete M, Oder M, Girgin C, Dincer C (2007) Microcystic urothelial carcinoma of the urinary bladder metastatic to the penis. Pathol Oncol Res 13(2):170–173
6. Delahunt B, Eble JN, Nacey JN, Thornton A (2001) Immunohistochemical evidence for mesothelial origin of paratesticular adenomatoid tumour. Histopathology 38(5):479
7. Young RH (2008) Testicular tumors—some new and a few perennial problems. Arch Pathol Lab Med 132(4):548–564
8. Umezu H, Kuwata K, Ebe Y, Yamamoto T, Naito M, Yamato Y et al (2002) Microcystic variant of localized malignant mesothelioma accompanying an adenomatoid tumor-like lesion. Pathol Int 52(5–6):416–422
9. Kuchna I, Matyja E, Wierzba-Bobrowicz T, Mazurowski W (1994) Microcystic meningioma—a rarely occurring morphological variant of meningioma. Folia Neuropathol 32(4):259–263
10. Skalova A, Vanecek T, Sima R, Laco J, Weinreb I, Perez-Ordonez B et al (2010) Mammary analogue secretory carcinoma of salivary glands, containing the ETV6-NTRK3 fusion gene: a hitherto undescribed salivary gland tumor entity. Am J Surg Pathol 34 (5):599–608
11. Ghannoum JE, Freedman PD (2004) Signet-ring cell (mucin-producing) adenocarcinomas of minor salivary glands. Am J Surg Pathol 28(1):89–93
12. Che M, Tornos C, Deavers MT, Malpica A, Gershenson DM, Silva EG (2001) Ovarian mixed-epithelial carcinomas with a microcystic pattern and signet-ring cells. Int J Gynecol Pathol 20 (4):323–328
13. Young RH, Hart WR (1989) Metastases from carcinomas of the pancreas simulating primary mucinous tumors of the ovary. A report of seven cases. Am J Surg Pathol 13(9):748–756
14. Prat J (2005) Ovarian carcinomas, including secondary tumors: diagnostically challenging areas. Mod Pathol 18 Suppl 2:S99–S111
15. Seidman JD, Kurman RJ, Ronnett BM (2003) Primary and metastatic mucinous adenocarcinomas in the ovaries: incidence in routine practice with a new approach to improve intraoperative diagnosis. Am J Surg Pathol 27(7):985–993
16. Adsay NV, Andea A, Basturk O, Kilinc N, Nassar H, Cheng JD (2004) Secondary tumors of the pancreas: an analysis of a surgical and autopsy database and review of the literature. Virchows Arch 444(6):527–535
17. Young RH, Zukerberg LR (1991) Microcystic transitional cell carcinomas of the urinary bladder. A report of four cases. Am J Clin Pathol 96(5):635–639
18. Leroy X, Leteurtre E, De La Taille A, Augusto D, Biserte J, Gosselin B (2002) Microcystic transitional cell carcinoma: a report of 2 cases arising in the renal pelvis. Arch Pathol Lab Med 126(7):859–861
19. Lopez-Beltran A, Sauter G, Gasser T (2004) Infiltrating urothelial carcinoma. IARC, Lyon
20. Soylu A, Aydin NE, Yilmaz U, Kutlu R, Gunes A (2005) Urothelial carcinoma featuring lipid cell and plasmacytoid morphology with poor prognostic outcome. Urology 65(4):797
21. Leroy X, Gonzalez S, Zini L, Aubert S (2007) Lipoid-cell variant of urothelial carcinoma: a clinicopathologic and immunohistochemical study of five cases. Am J Surg Pathol 31(5):770–773
22. Lopez-Beltran A, Amin MB, Oliveira PS, Montironi R, Algaba F, McKenney JK et al (2010) Urothelial carcinoma of the bladder, lipid cell variant: clinicopathologic findings and LOH analysis. Am J Surg Pathol 34(3):371–376
23. Paris C, Clement-Duchene C, Vignaud JM, Gislard A, Stoufflet A, Bertrand O et al (2010) Relationships between lung adenocarcinoma and gender, age, smoking and occupational risk factors: a case–case study. Lung Cancer 68(2):146–153
24. Mountzios G, Fouret P, Soria JC (2008) Mechanisms of disease: signal transduction in lung carcinogenesis—a comparison of smokers and never-smokers. Nat Clin Pract Oncol 5(10):610–618
25. Borras J, Borras JM, Galceran J, Sanchez V, Moreno V, Gonzalez JR (2001) Trends in smoking-related cancer incidence in Tarragona, Spain, 1980–96. Cancer Causes Control 12(10):903–908
26. Porta M, Crous-Bou M, Wark PA, Vineis P, Real FX, Malats N et al (2009) Cigarette smoking and *K-ras* mutations in pancreas, lung and colorectal adenocarcinomas: etiopathogenic similarities, differences and paradoxes. Mutat Res 682(2–3):83–93
27. Tavassoli FA, Norris HJ (1980) Secretory carcinoma of the breast. Cancer 45(9):2404–2413

Virchows Arch (2010) 457:651–657
DOI 10.1007/s00428-010-0999-0

ORIGINAL ARTICLE

Pancreatic neuroma-like lesions after upper abdominal surgery: a clinicopathological postmortem study

Susumu Matsukuma · Kimiya Sato

Received: 9 September 2010 / Accepted: 8 October 2010 / Published online: 27 October 2010
© Springer-Verlag 2010

Abstract To elucidate poorly understood pancreatic neural changes after upper abdominal surgery (UAS), we histologically examined 57 postmortem pancreases after gastrectomy, esophagectomy, and esophageal transection, and also investigated each clinical manifestation. Six pancreases (10.5%) had unique histopathological lesions composed of prominently thickened and/or proliferated neural fascicles. They focally or multifocally involved the pancreatic lobules and/or interlobular septa and mimicked traumatic neuroma. Three of the six lesions were accompanied by moderate to severe chronic pancreatitis/pancreatic fibrosis. All six patients were asymptomatic, although only one exhibited a low-echoic pancreatic mass. There were no statistically significant associations between the pancreatic neural lesions and the patients' sex, age, the time interval between the surgery and the patients' death, impaired glucose tolerance, the presence of hyalinized pancreatic islets, or the presence of moderate to severe chronic pancreatitis/pancreatic fibrosis. No similar prominent neural lesions were identified in an additional 57 age- and sex-matched control pancreases. We concluded that these prominent neural lesions were pancreatic neuroma-like lesions following UAS. This study failed to demonstrate the distinct pathogenesis of the neuroma-like lesions and further investigation may be needed. However, this report is the first to delineate that asymptomatic neuroma-like lesions can occur following UAS. Consideration of this possible development would be useful for accurate follow-up of patients who undergo UAS, although its occurrence may be infrequent.

Keywords Neuroma · Traumatic neuroma · Pancreas · Gastrectomy

S. Matsukuma (✉) · K. Sato
Department of Pathology,
Japan Self-Defense Forces Central Hospital,
1-2-24 Ikejiri,
Setagaya-ku, Tokyo 154-0001, Japan
e-mail: skuma@cocoa.plala.or.jp

Introduction

Pancreas is richly innervated from the parasympathetic vagus nerve and the sympathetic splanchnic nerve via the celiac and superior mesenteric plexi [1–3]. Most of the larger nerves are found around the splenic arteries/veins and in the interlobular fibrous septa, but smaller nerves may be found in the lobule [1]. However, primary pancreatic neural neoplasms are rare [2–5]. Pathological neural changes following upper abdominal surgery (UAS) are poorly understood, although many researchers have described reactive neural proliferation in chronic pancreatic disease [1, 3, 6] and pathologic changes of pancreatic islets of Langerhans after gastrectomy [7, 8]. Traumatic neuromas of bile duct following cholecystectomy are well-known conditions [9–11]. However, previous reports describing pancreatic neuroma are rare; our review of the literature disclosed only two isolated cases [12, 13]. Therefore, this study attempted to elucidate the histopathological neural changes of postmortem pancreases following UAS, and also analyzed the clinicopathological correlations of each case showing neural changes.

Material and methods

Fifty-seven postmortem pancreases taken from patients having a past history of UAS including 51 gastrectomies

(42 distal gastrectomies, four total gastrectomies, one fundectomy, three partial gastrectomies, and one remnant stomach resection after distal gastrectomy), four esophagectomies, one esophagectomy with splenectomy, and one esophageal transection with splenectomy were examined histologically. These records were retrieved from the autopsy files of the Department of Pathology, Japan Self-Defense Forces Central Hospital, Tokyo, Japan, between January 1988 and January 2010. These 57 individuals included 49 men and eight women, with a mean age of 74.5 years (range, 41–90 years). For a control study, 83 postmortem pancreases taken from patients who had not undergone UAS and died of various diseases excluding pancreatic, gastric, and esophageal cancers, randomly retrieved from the autopsy files of the Department of Pathology, Japan Self-Defense Forces Central Hospital (from 1989 to 2009), were also examined. These control cases included 62 men and 21 women, with a mean age of 72.6 years (range, 40–93 years). All pancreases, with no extensive autolysis or prominently cancerous involvement, were fixed in 10% buffered formalin and routinely processed. The postmortem interval ranged from 1 to 21 h (mean, 8.5 h). The representative pancreatic tissues were two to five blocks from head, body, and/or tail region of the pancreas for each case in the UAS-related group, and were three to five blocks from at least three regions (head, body, and tail regions of the pancreas) for each case in the control group.

To evaluate the neural changes, we searched for neural fascicles throughout hematoxylin & eosin (H&E)-stained slides of all representative pancreases, and measured the longest dimension intersecting the axial neural fascicles with or without pathologic changes. Neural fascicles directly connected to the neurons along the splenic arteries/veins were not evaluated because they were expected to exhibit thickened features normally. We defined cases where the longest dimension of neural fascicles exceeded 300 μm as exhibiting "prominent" changes. The degree of accompanying chronic pancreatitis/pancreatic fibrosis (CP/PF) and the presence of hyalinized pancreatic islets were also investigated. In cases in which paraffin blocks were available, additional serial sections were cut and stained with H&E and Masson's trichrome stain. Selected sections were immunostained with antibodies against S-100 protein (polyclonal, Nichirei, Tokyo, Japan) and epithelial membrane antigen (EMA; monoclonal, Nichirei) using a Histofine streptavidin–biotin–peroxidase kit (Nichirei).

Clinical information, obtained from autopsy recording charts and referring clinicians, was evaluated for associations with pancreatic pathologic changes. No patients with neurofibromatosis were included in this study. Statistical analyses used unpaired *t*-test and Fisher's exact test. Statistical significance was set at $P<0.05$.

Results

Lobular and interlobular neural fascicles were found in 53 and in all 57 pancreases after UAS, respectively. The longest dimension in the lobular fascicles ranged from 23.8 to 655 μm (mean, 107.5 μm), and in the interlobular fascicles ranged from 44 to 856 μm (mean, 152.3 μm). Hyalinosis of pancreatic islets and moderate to severe CP/PF were found in 13 (22.8%) and in 33 (57.9%) of 57 pancreases after UAS, respectively.

Six of the 57 pancreases after UAS (10.5%) had prominent neural lesions composed of markedly thickened and/or proliferated neural fascicles and the longest dimension of each case ranged from 312 to 856 μm (mean, 547.8 μm). In 11 other pancreases, mildly to moderately swollen neural fascicles, ranging in the longest dimension from 85 to 253 μm (mean, 179.5 μm), were found in lobule and/or interlobular septa, but they did not show prominently thickened/proliferated features. The clinicopathological characteristics of the six patients with prominent neural lesions are summarized in Table 1. These prominent neural lesions were often found in the pancreatic head, but there was no definite favored location in pancreases that were examined. In two pancreases, the prominent neural lesions exhibited a whorled or nested focal pattern and abruptly involved the pancreatic lobule (Fig. 1) or the fibrously distended interlobular septum (Fig. 2). These focal lesions were not encapsulated and did not contain ganglion cells. In the remaining four pancreases, prominent neural lesions multifocally or diffusely involved both the lobules and the interlobular septa in a tortuous and/or arborizing arrangement (Figs. 3 and 4). These diffuse or multifocal lesions vaguely or partially retained the preexisting neural structures, scarcely contained ganglion cells, and partially showed myxoid changes. In six prominent neural lesions, three pancreases were involved by moderate to severe CP/PF, and only two pancreases showed mildly to moderately perineural lymphoid infiltration (Fig. 4d). One diffuse neural lesion (case 1, Fig. 4) was accompanied by severe fibrosis, lobular atrophy, and focally dense lymphoid infiltration, which had been detected by antemortem ultrasonography as a low-echoic pancreatic mass. However, this lesion showed no histological features of autoimmune pancreatitis characterized by diffusely and densely lymphoplasmocytic infiltration. Masson's trichrome stain clearly demonstrated fibrosis accompanied with prominent neural changes. Immunohistochemically, prominent neural lesions showed diffuse and strong positivity for S-100 protein, suggesting Schwann cell proliferation (Figs. 2b and 4b). Faintly EMA-positive spindle cells, suggesting perineural cells, always surrounded preexisting neural fascicles, and partially surrounded small neural fascicles in the marginal zone of interlobular nodular lesion.

Table 1 Clinicopathological characteristics of six cases showing prominently thickened and/or proliferated neural changes of the pancreas

Case	Age	Sex	Surgery	RP	Disease for surgery	TI (year)	Main autopsy diagnosis	AP	Degree of CP/PF	HP	Thickened and/or proliferated neural changes				
											Distribution	Location	Longest dimension of neural fascicle (μm)		Perineural lymphoid infiltrate
													Lobular	Interlobular	
1	79	M	DG	B-I	Gastric cancer	11.3	Pneumonia	None[a]	Severe	Present	Diffuse	Tail > Body	379	426	Multifocal/Moderate
2	81	M	DG	B-II	Gastric cancer	8.7	Lung cancer	None	Mild	None	Focal	Head	655	103	Focal/Mild
3	80	M	DG	B-I	Gastric ulcer	35	Interstitial pneumonia	None	Mild	None	Multifocal	Head	311	453	None
4	82	M	DG	B-I	Gastric cancer	6.4	Valvular heart disease	None	Mild	None	Focal	Body	23.8	856	None
5	65	M	PG		Gastric ulcer	24	HCC, LC	None	Moderate	None	Multifocal	Head	312	281	None
6	77	F	DG	B-I	Gastric cancer	2	Cerebral infarction	None	Moderate	None	Multifocal	Head > Body	585	123	None

DG distal gastrectomy, *PD* partial gastrectomy, *RP* reconstruction procedure, *B-I* Billroth's I anastomosis, *B-II* Billroth's II anastomosis, *TI* time interval between the surgery and the patient's death, *HCC* hepatocellular carcinoma, *LC* liver cirrhosis, *AP* abdominal pain, *CP/PF* chronic pancreatitis/pancreatic fibrosis, *HP* hyalinosis of pancreatic islets

[a] Low-echoic area was detected in the tail of the pancreas, but no abdominal pain was present

However, no distinct proliferation of EMA-positive cells was found within the prominent neural lesions.

The statistical comparison between six cases with prominent neural changes and the remaining 51 cases with no prominent neural changes is summarized in Table 2. The longest dimension of identified neural fascicles, in both lobular and interlobular neural fascicles, showed statistically significant differences between them. However, there was no statistically significant relationship between the prominent neural changes and other clinicopathological features including age, sex, time interval between the surgery and the patient's death, impaired glucose tolerance or diabetes mellitus, hyalinosis of pancreatic islets, and moderate to severe CP/PF.

As a control study of the prominent neural changes in pancreases after UAS, we used 57 age- and sex-matched control cases selected from 83 control cases on the basis of similar frequency/degree of CP/PF (including 32 cases of moderate to severe CP/PF). They consisted of 49 men and eight women, with a mean age of 74.4 years (range, 42–90 years). The longest dimension of the lobular neural fascicles ranged from 25.7 to 171 μm (mean, 62.9 μm), which were found in 56 of the 57 control cases, and the longest dimension of the interlobular neural fascicles ranged from 44.2 to 256 μm (mean, 123.0 μm), which were found in all 57 control cases; both were significantly thinner than those of 57 pancreases after UAS (unpaired *t*-test; $P=0.006$ and 0.049, respectively). However, in these 57 control cases, no prominent neural lesions were identified, although moderately swollen neural fascicles, ranging in the longest dimension from 171 to 256 μm (mean, 216.3 μm), were focally found in four pancreases. Hyalinosis of pancreatic islets was found in 13 cases (13/57, 22.8%), the frequency of which was equal to that of pancreases after UAS.

Discussion

This study identified prominently thickened/proliferated neural lesions in six (10.5%) of 57 postmortem pancreases after UAS. One lesion involved only interlobular septum, but the other five lesions invariably involved the pancreatic lobules for which only smaller neurons may be found in normal conditions [1]. They were detected not only by statistically morphometric evaluation but also by the unique histological features. They were characterized by focal or multifocal neural thickening and proliferation with or without fibrosis; focal nodular lesions were composed of globular proliferation of neural fascicles, and multifocal and/or diffuse lesions involving both lobules and interlobular septa in a torturous or arborizing fashion. S-100 protein-positive Schwann cells proliferated in these prominent neural

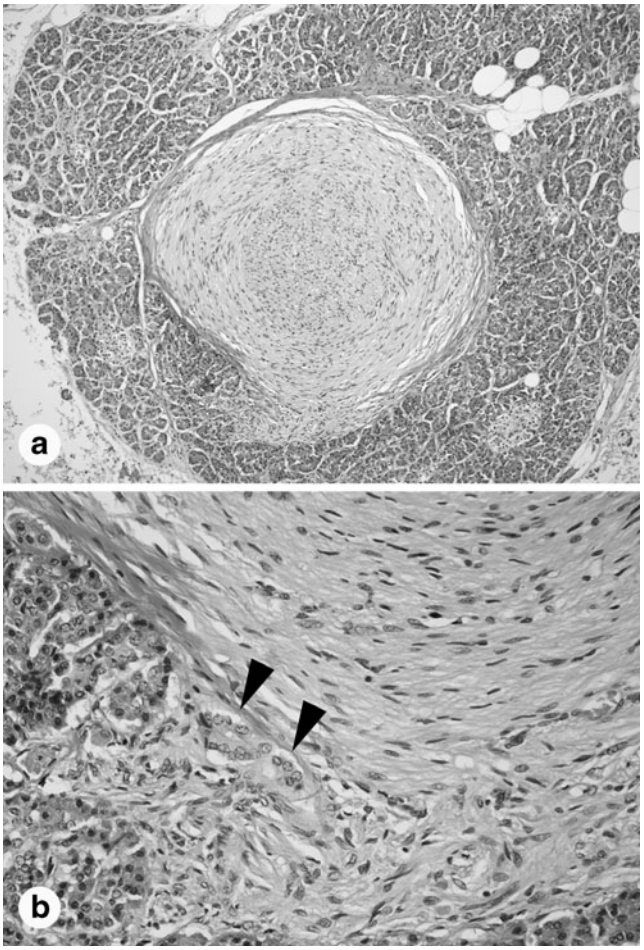

Fig. 1 Focal prominent neural lesion of the pancreas (case 2). **a** Nodular or globular proliferation of neural fascicles abruptly involving pancreatic lobule with slight to mild fibrosis (HE, ×100). **b** High magnification of the proliferating neural tissues entrapping pancreatic ductular cells (arrowheads) (HE, ×400)

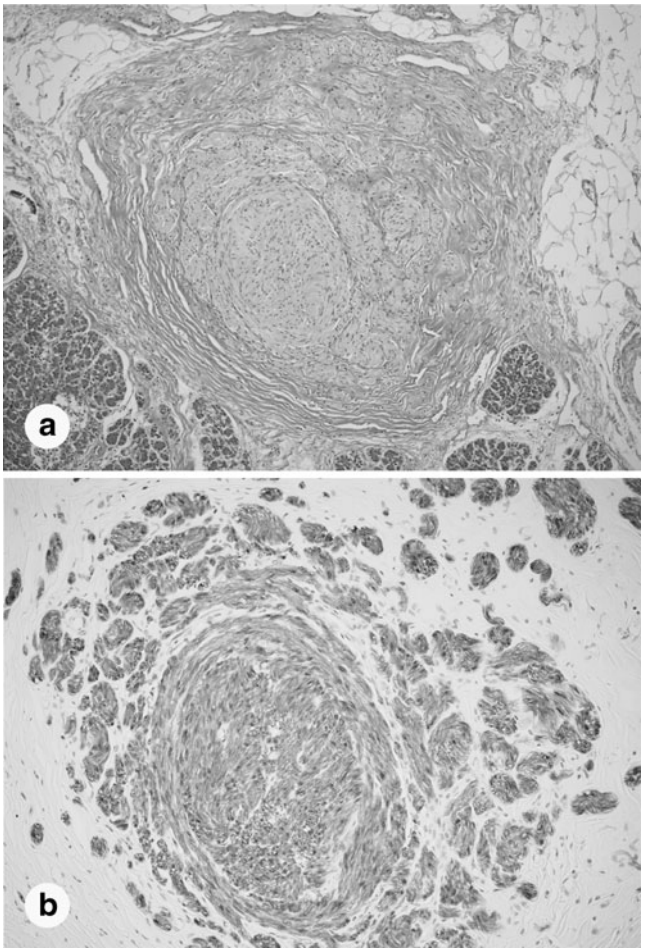

Fig. 2 Focal prominent neural lesion of the pancreas (case 4). **a** Nodular proliferation of neural fascicles in the fibrously distended interlobular septum (HE, ×100). **b** Immunostain for S-100 protein distinctly revealing Schwann cell proliferation in globular and nested fashions (immunostain, ×200)

lesions, but EMA-positive perineural cell proliferation was obscure. These features closely resembled those of traumatic or amputation neuroma, which is known to arise in the proximal ends of transected or injured nerves as a result of trauma or surgery [3, 9].

Traumatic neuroma occurs in bile duct [9–11], gallbladder [14], and intestine [15]. However, similar pancreatic lesions remain poorly understood; only two cases have been reported to date [12, 13]. One case of pancreatic traumatic neuroma after splenectomy was suggested to have developed at a surgically injured site of autonomic neuron along the splenic artery located close to the pancreas [12]. In the current study, similar lesions were not found in two pancreases after splenectomy. The other case was associated with excision of pancreatic pseudocyst [13], and its occurrence could be explained by reparative/proliferative reaction of surgically injured neurons through the pancreatic parenchyma into the pseudocyst. However, UAS would injure a

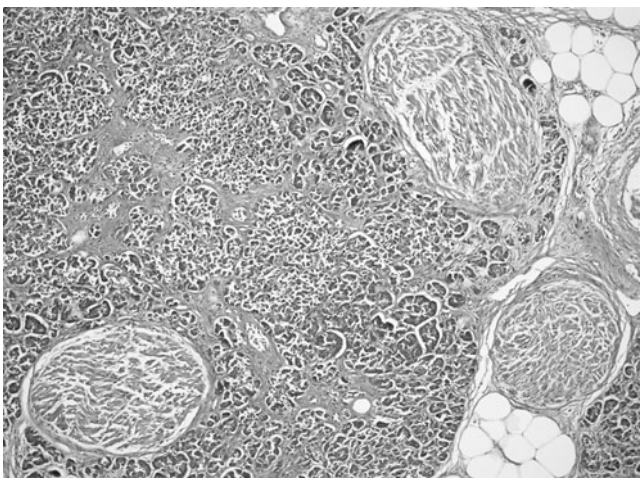

Fig. 3 Multifocal prominent neural lesions of the pancreas (case 5). Thickened neural fascicles with myxoid changes involving pancreatic lobule and interlobular septum, preserving preexisting structures of pancreatic neural tissues (HE, ×100)

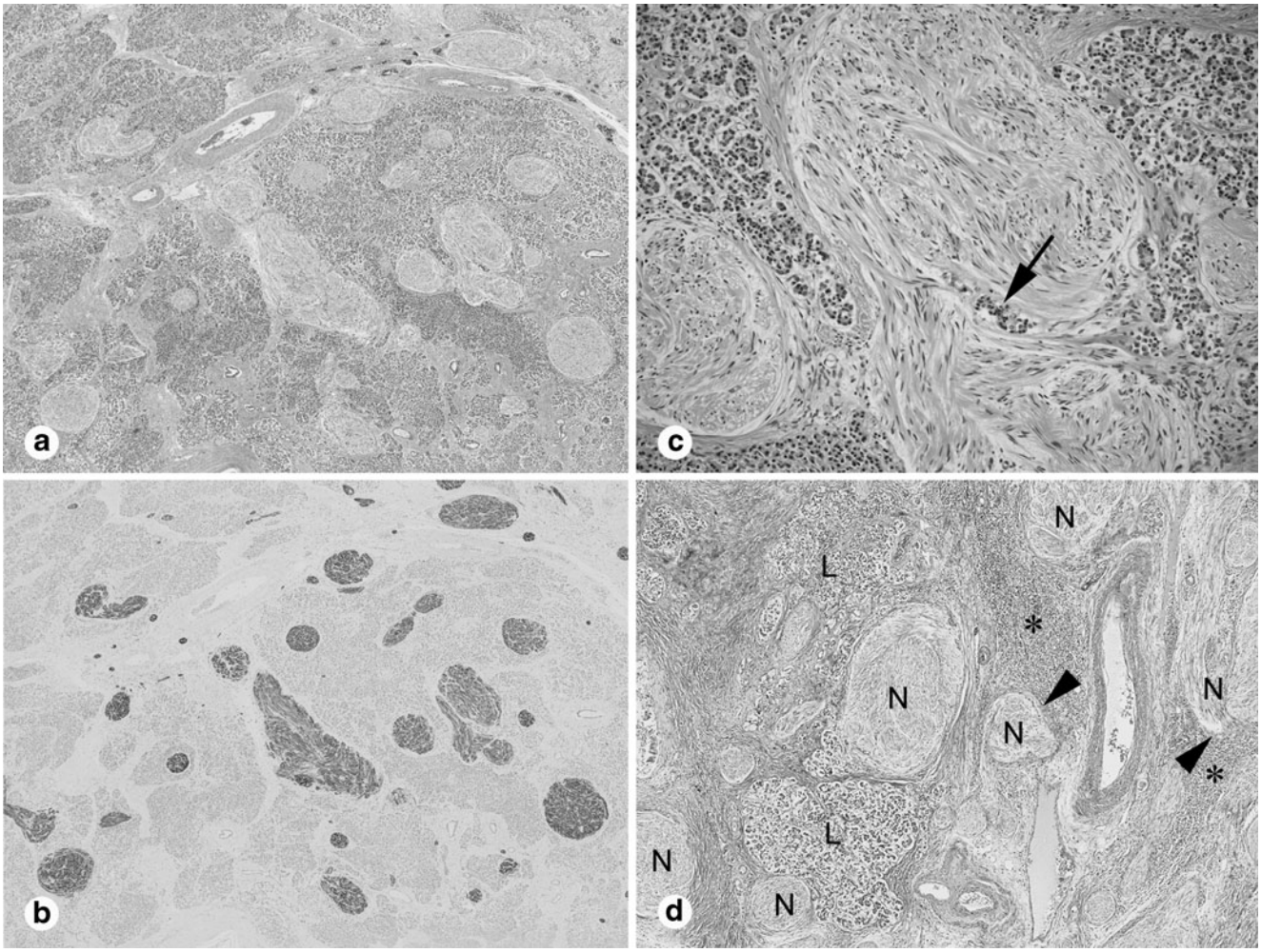

Fig. 4 Diffuse and multifocal prominent neural lesions of the pancreas (case 1). **a** Low magnification showing numerous thickened neural fascicles in the pancreatic lobules and interlobular septa (HE, ×40). **b** S-100 protein-positive Schwann cells proliferating in the thickened neural fascicles. Compare with panel a (immunostain, ×40). **c** Tortuous proliferation of neural fascicle entrapping pancreatic acinar cells (*arrow*) (HE, ×200). **d** Marked pancreatic fibrosis and lobular atrophy (*L*) with thickened neural fascicles (*N*). Lymphoid aggregates (*asterisks*) focally infiltrating the neural fascicles (*arrowheads*). (Masson's trichrome stain, ×100)

Table 2 Relationship between the prominent neural changes and various clinicopathological features

	Prominent neural changes (+) (n=6)	Prominent neural changes (−) (n=51)	P
Longest dimension of lobular neuronal fascicle (μm)	23.8–655 (mean, 377.6)	28.7–205 (mean, 73.0)	<0.01[a, b]
Longest dimension of interlobular neuronal fascicle (μm)	103–856 (mean, 373.7)	44–287 (mean, 126.3)	<0.05[a, b]
Age (years)	65–82 (mean, 77.3)	41–90 (mean, 74.1)	0.51[a]
Sex	men 5/women 1	men 44/women 7	0.67[c]
Time interval between the surgery and the patient's death (years)	2–35 (mean, 14.6)	0.08–47 (mean, 12.8)	0.71[c]
Impaired glucose tolerance or diabetes mellitus	3/6	17/51	0.65[c]
Hyalinosis of pancreatic islets	1/6	12/51	1[c]
Moderate to severe CP/PF	3/6	30/51	0.69[c]

CP/PF chronic pancreatitis/pancreatic fibrosis

[a] Unpaired *t*-test, two-tailed

[b] Statistically significant

[c] Fisher's exact test

more proximal or central portion of the vagus and/or the splanchnic nerves, and UAS-related traumatic neuroma may presumably arise in a more proximal extrapancreatic region. In fact, traumatic neuromas of lower esophagus after vagotomy [16] and around neighboring celiac trunk after gastrectomy [17] have been described. These findings raise a suspicion that the currently identified neural lesions may not be "true" traumatic neuromas. On the other hand, the thickened tortuous neural fascicles with myxoid changes resembled those of neurofibroma. Pancreatic neurofibroma is rare, and often associated with neurofibromatosis [3]. However, this study included no patients with neurofibromatosis, and showed tortuous neural proliferations occasionally entrapping the acinar or ductile cells, which were somewhat different from those of neurofibroma. Considering these findings, we concluded that the currently identified lesions were pancreatic "neuroma-like lesions" after UAS.

Many investigators have mentioned that pancreatic nerves become thicker in chronic pancreatitis [1, 3, 6, 18]. In addition, in this study, three of the six neuroma-like lesions were accompanied by moderate to severe CP/PF. These findings raise the possibility that CP/PF induces neuroma-like changes. Friess et al. [18] described a possible interaction between altered pancreatic neural tissues and perineural inflammatory cell infiltrates. Recent studies [19, 20] have also noted that enhanced neural density and hypertrophy are closely linked to the severity of perineural inflammatory infiltrate. These neural changes seem to enhance and generate pancreatic neuropathic pain [19]. However, in the current study, the other three pancreatic neuroma-like lesions were associated with a mild form of CP/PF only, and the degree of neuroma-like changes was not always linked to the severity of CP/PF. There was no statistically significant association between the pancreatic neuroma-like lesions and moderate to severe CP/PF. That severe CP/PF is secondary to the developing neuroma-like lesions rather than the pathogenetic cause cannot be ruled out. Perineural lymphoid infiltration was found in only two neuroma-like lesions. Clinically, none of the six patients having pancreatic neuroma-like lesions showed abdominal pain. In addition, the neuroma-like lesions were not found in 57 additional sex- and age-matched control cases, which were similar in frequency/degree of CP/PF to the currently examined pancreases after UAS. Furthermore, to our knowledge, pancreatic neuroma-like changes have not been clearly shown in previous reports concerning neural changes in chronic pancreatitis. These findings suggest that the currently identified pancreatic neuroma-like lesions are distinctive pathomorphological changes of pancreas after UAS rather than CP/PF-related changes or unusual senescent features.

Other investigators [7, 8] have demonstrated an increased rate of hyalinosis of pancreatic islets after gastrectomy. They have concluded that vagotomy combined with gastrectomy causes the islets to become hyperactive, and finally results in their hyalinization [7]. In the current study, the incidence of hyalinosis of pancreatic islets after UAS was almost equal to that of sex- and age-matched control cases with no past history of UAS. However, we speculate that similar neural irritation or activation due to UAS-related injury of vagus and/or splanchnic nerves could promote the pancreatic neuroma-like changes. In the present study, the longest dimension of the neural fascicle in 57 pancreases after UAS was significantly greater than that of 57 additional age- and sex-matched control cases. These findings may support our speculation that UAS-related neural injury induces the thickening of pancreatic neural fascicles. Mildly to moderately swollen neural changes, found in 11 of 57 pancreases after UAS, might be initial features of neuroma-like lesions. Concomitant CP/PF may enhance these neural changes. However, similar moderately swollen neurons were identified in four of the 57 control cases. These findings also raise the possibility that pancreatic neural changes might be influenced by additional unknown factors besides UAS-related injury and CP/PF. Further investigation is needed to explain the distinct pathogenesis of the pancreatic neuroma-like lesions after UAS.

Recent advances in imaging procedures have enabled detection of relatively small tumors including traumatic neuromas, schwannomas, or other neurogenic tumors [21]. Indeed, one patient (case 1) in the current study was found to exhibit a low-echoic mass of the pancreatic tail, suggesting recurrence or metastasis of the previously removed gastric cancer. However, autopsy revealed only benign pancreatic neuroma-like lesions and fibrosis, and did not show recurrence of gastric cancer or distinct pathologic features of autoimmune pancreatitis. Pancreas is a deeply situated organ, and percutaneous fine-needle biopsy is exceedingly difficult. Post-operative adhesive condition after UAS would lead to hesitation to perform laparoscopic pancreatic biopsy. However, upper gastrointestinal carcinoma can involve the pancreas secondarily [2]. Some authors have noted an increase in pancreatic cancer risk after gastric surgery [22]. Therefore, a patient's follow-up after UAS requires the precise assessment of imaging examination on the pancreatic lesions. We believe that consideration of the possible occurrence of pancreatic neuroma-like lesions after UAS is important in differential diagnosis of true primary or secondary pancreatic neoplasm.

In conclusion, the present study elucidated that asymptomatic pancreatic neuroma-like lesions can occur after UAS, in this case in 11.8% (6/51) of pancreases after gastrectomy. This study failed to reveal the distinct pathogenesis of the neuroma-like lesions after UAS. However, we believe that their occurrence should be

recognized in differential diagnosis of true pancreatic neoplasm on the basis of management of patients following UAS, although their occurrence may be infrequent.

Acknowledgements The authors thank Hiroaki Yamaguchi, Takeshi Okada, and Naoya Shin-mura for excellent technical assistance, and Daniel Mrozek for editing the manuscript.

Conflict of interest statement We declare that we have no conflict of interest.

References

1. Owen DA, Kelly JK (2001) Pathology of the gallbladder, biliary tract and pancreas. In: Livolsi VA (ed) Major problems in pathology, vol 39. Saunders, Philadelphia, pp 1–13, 63–101, 154–187
2. Klimstra DS, Hruban RH, Pitman MB (2007) Pancreas. In: Mills SE (ed) Histology for pathologists, 3rd edn. Lippincott Williams & Wilkins, Philadelphia, pp 325–333, 723–760
3. Hruban RH, Pitman MB, Klimstra DS (2007) Tumors of the pancreas. In: Silverberg SG, Sobin LH (eds) AFIP atlas of tumor pathology, 4th series, Fascicle 6. American Registry of Pathology, Washington, pp 1–22, 305–324
4. Suzuki S, Kaji S, Koike N et al (2010) Pancreatic schwannoma: a case report and literature review with special reference to imaging features. JOP J Pancreas (Online) 11:31–35
5. Bui TD, Nguyen T, Huerta S, Gu M, Hsiang D Pancreatic schwannoma. A case report and review of the literature. JOP J Pancreas (Online) 5:520–526
6. Bockman DE, Buchler M, Malfertheiner P, Beger HG (1988) Analysis of nerves in chronic pancreatitis. Gastroenterology 94:1459–1469
7. Suda K, Takei K, Suzuki F, Kamano T, Yamane T (1997) Histopathologic study of islets of Langerhans in patients after gastrectomy. J Clin Gastroenterol 25:546–549
8. Itoh H, Takei K (2000) Immunohistochemical and statistical studies on the islets of Langerhans pancreas in autopsied patients after gastrectomy. Hum Pathol 31:1368–1376
9. Burger PC, Scheithauer BW, Vogel FS (2002) Peripheral nervous system. In: Burger PC, Scheithauer BW, Vogel FS (eds) Surgical pathology of the nervous system and its coverings, 4th edn. Churchill Livingstone, New York, pp 579–648
10. Fujino Y, Satoh Y (1991) A case report of amputation neuroma of the common bile duct occurred two months after cholecystectomy. Jpn J Gastroenterol Surg 24:2437–2441
11. Nagata Y, Tomioka T, Chiba K, Kanematsu T (1995) Traumatic neuroma of the common hepatic duct after laparoscopic cholecystectomy. Am J Gastroenterol 90:1887–1888
12. Geddy PM, Venables CW (1991) Traumatic neuroma at the tail of the pancreas following splenectomy. Postgrad Med J 67:90–91
13. Kim JW, Choi G, Hwang JE, Kang SK, Han DJ, Jang SJ (2006) Traumatic neuroma in the pancreas head following excision of pseudocyst: a brief case report. Korean J Pathol 40:385–388
14. Elhag AM, Al Awadi NZ (1992) Amputation neuroma of the gallbladder. Histopathology 21:586–587
15. Chandrasoma P, Wheeler D, Radin DR (1985) Traumatic neuroma of the intestine. Gastrointest Radiol 10:161–162
16. Gillesby WJ, Wu KH (1965) Amputation neuromas of vagus nerves. Am J Surg 110:673–676
17. Kwon JH, Ryu SW, Kang YN (2007) Traumatic neuroma around the celiac trunk after gastrectomy mimicking a nodal metastasis: a case report. Korean J Radiol 8:242–245
18. Friess H, Shrikhande S, Shrikhande M et al (2002) Neural alterations in surgical stage chronic pancreatitis are independent of the underlying aetiology. Gut 50:682–686
19. Ceyhan GO, Bergmann F, Kadihasanoglu M et al (2009) Pancreatic neuropathy and neuropathic pain—a comprehensive pathomorphological study of 546 cases. Gastroenterology 136:177–186
20. Ceyhan GO, Demir IE, Rauch U et al (2009) Pancreatic neuropathy results in "neural remodeling" and altered pancreatic innervation in chronic pancreatitis and pancreatic cancer. Am J Gastroenterol 104:1555–1565
21. Murphey MD, Smith WS, Smith SE, Kransdorf MJ, Temple HT (1999) From the archives of the AFIP. Imaging of musculoskeletal neurogenic tumors: radiologic–pathologic correlation. Radiographics 19:1523–1580
22. Tascilar M, van Rees BP, Sturm PDJ et al (2002) Pancreatic cancer after remote peptic ulcer surgery. J Clin Pathol 55:340–345

Virchows Arch (2010) 457:659–667
DOI 10.1007/s00428-010-0992-7

ORIGINAL ARTICLE

The expression and distribution of group IIA phospholipase A2 in human colorectal tumours

Tuulia Avoranta · Jari Sundström · Eija Korkeila · Kari Syrjänen · Seppo Pyrhönen · Jukka Laine

Received: 9 June 2010 / Revised: 1 September 2010 / Accepted: 29 September 2010 / Published online: 12 October 2010
© Springer-Verlag 2010

Abstract Secretory phospholipase A2 group IIA (IIA PLA2) is a protein shown to be increased in various human malignancies. The expression profile of this protein, however, is controversial in colorectal carcinoma. The aim of this study was to examine the distribution and expression of IIA PLA2 protein in benign, premalignant and malignant colorectal tumours as well as in peritumoural mucosa. Seven hyperplastic polyps, 24 adenomas and 83 colorectal carcinomas were stained with immunohistochemistry (IHC) for IIA PLA2. Four hyperplastic polyps, 12 adenomas and nine carcinomas were also evaluated for the sites of IIA PLA2 expression using mRNA in situ hybridisation (ISH). There was no immunoreactivity for IIA PLA2 in hyperplastic polyps. A total of 79% of adenomas and 31% of carcinomas showed IIA PLA2-immunopositive tumour cells in IHC, and the expression was localised to epithelial cells with ISH. In carcinomas, IIA PLA2-immunopositive apoptotic cells and necrosis were also found. The epithelial cells in the peritumoural mucosa showed immunopositivity for IIA PLA2 in 96% of cases, with considerably stronger intensity adjacent to carcinoma than in the more distal mucosa. Moreover, IIA PLA2-immunopositive malignant epithelial cells were found in 44% of cases in the invasive front of carcinomas. Our results suggest that the IIA PLA2 protein content is dramatically decreased in malignant colorectal tumours as compared with adenomas. The protein is also found in the apoptotic cells, necrosis, peritumoural mucosa and in the invasive front of carcinomas.

Keywords Group IIA phospholipase A2 · Localisation · Colorectal adenoma · Colorectal carcinoma

T. Avoranta (✉) · E. Korkeila · K. Syrjänen · S. Pyrhönen
Department of Oncology and Radiotherapy, University of Turku and Turku University Hospital,
Savitehtaankatu 1 PB 52,
20521 Turku, Finland
e-mail: stavor@utu.fi

J. Sundström · J. Laine
Department of Pathology, University of Turku and Turku University Hospital,
Kiinamyllynkatu 10,
20520 Turku, Finland

Introduction

Phospholipase A2 (PLA2) family consists of several enzymes hydrolysing the sn-2 ester bond of membrane phospholipids, thus creating a lysophospholipid and releasing fatty acids—predominantly arachidonic acid (AA). Cyclooxygenases (COX) change free AA into eicosanoids, such as prostaglandin E2 (PGE2) [1]. Most colorectal cancers arise from pre-existing adenomas in a process called adenoma-to-carcinoma sequence. Because it takes several years for a normal cryptal cell to undergo neoplastic molecular changes and develop into clinically recognised neoplasm [2], it is important to find biological markers that are altered early in colorectal carcinogenesis. Because deregulation of the COX-2/PGE2 pathway is demonstrated to influence colorectal carcinogenesis via a number of distinct mechanisms [3], functional defects of PLA2 proteins have been regarded as potential predictive molecular markers in colorectal cancer [4–6].

Secretory phospholipase A2 group IIA (IIA PLA2) is a 14-kDa enzyme of PLA2-family found in a number of tissues and body fluids [7]. The concentration of group IIA PLA2 enzyme in blood plasma is known to increase dramatically in several diseases involving generalised inflammation [8, 9], and the content of IIA PLA2 has been demonstrated to be upregulated in a range of human

malignancies, such as prostate [10–12], gastric [13] and intestinal cancer [14, 15].

In the gastrointestinal tract, IIA PLA2 is particularly found in the Paneth cells of the small intestine and in the goblet cells of the large intestine [16, 17]. In contrast to normal colorectal mucosa, where little or no IIA PLA2 protein is present [15, 16, 18], increased expression of IIA PLA2 detected at protein and messenger RNA (mRNA) level has been reported in colorectal adenomas of familial adenomatous polyposis (FAP) patients [19]. Increased levels of IIA PLA2 protein have also been demonstrated in chronic inflammatory bowel disease [20–23] as well as in normal colorectal mucosa adjacent to adenocarcinoma [15, 18].

The expression profile of IIA PLA2 in colorectal carcinoma is more controversial; there are studies indicating that both the amount of IIA PLA2 content is increased [14, 15] and it is attenuated [18] in colorectal carcinomas. Furthermore, little data are available on the exact location of IIA PLA2 protein synthesis in colorectal tumours at mRNA level. In this study, we examined the distribution and sites of synthesis of IIA PLA2 in benign, premalignant and malignant human colorectal tumours as well as in peritumoural normal mucosa, with special emphasis on rectal carcinomas.

Materials and methods

Samples

Clinicopathological features of the study population are described in Table 1. The present series included two separate sets of series; the first consisted of paraffin-embedded tissue samples of seven hyperplastic polyps (five from the colon, two from the rectum), 14 colorectal adenomas (nine from the colon, four from the rectum, one localisation missing) and 11 carcinomas (eight from the colon, three from the rectum) collected between 1994 and 1999. The second set consisted of paraffin-embedded samples from 72 rectal carcinomas collected between 2000 and 2009. The biopsies and resection samples in both sets had been taken during colonoscopies or operations performed at Turku University Hospital. Representative samples were taken following the standard criteria of colorectal sampling to establish the histological diagnosis. For this study, the tissue samples were obtained from the files of the Department of Pathology, Turku University Hospital.

Among the 72 rectal carcinomas in the second set, none had distant metastases at the time of operation, and none of the patients had received any preoperative treatment prior to surgery. To make the study population as homogenous as possible, only tumours located in the medial or distal rectum were included. In addition, adenomas with different degrees of dysplasia were found in ten resection samples of carcinomas. These ten adenomas were included in the analyses of adenomas.

Immunohistochemistry for IIA PLA2 protein

IIA PLA2 protein distribution was analysed using immunohistochemical staining (IHC) in formalin-fixed, paraffin-embedded 5 μm-thick sections. The first set was stained using a G-protein purified in-house polyclonal rabbit IIA PLA2 IgG with a dilution of 1.04 μg/ml of IgG as described in detail earlier [24]. The cross-reactivity of the antibody has been tested against group IB, IIA, IID, IIE, IIF, III, V, X, XIIA and XIIB PLA2s. The antibody was shown to be specific for IIA PLA2 without significant cross-reactivity with other secretory small molecular weight PLA2s [25, 26]. For the larger second set (72 rectal carcinomas) Power Vision Kit (Immuno Vision Technologies, Co, USA) and LabVision Autostainer (Thermo Fisher Scientific, CA, USA) was used with the same IIA PLA2 antibody and dilution as mentioned above. For Autostainer the antigen was retrieved 2×7 min in pH 6.0 with DakoTarget Retrieval Solution (Dako, Glostrup, Denmark), and the slides were washed twice with Tris-buffered saline. In controls, the primary antibody was replaced by preimmune rabbit serum, with a dilution of 1:3,000. To further confirm the specifity of the in-house IIA PLA2 antibody, a commercial human monoclonal IIA PLA2 antibody (dilution of 1:3,000, Cayman Chemicals, Ann Arbor, Michigan, USA, catalog number 160500) was used for a group of ten rectal carcinomas with the Power Vision Kit and Lab Vision Autostainer methods as mentioned above.

Assessment of IHC

Assessment of IHC was performed by two authors (TA and JL) on light microscopy blinded to the clinicopathological data. The immunopositivity for IIA PLA2 in hyperplastic polyps, adenomas and carcinomas was determined by estimating the percentage of epithelial cells showing positive staining for IIA PLA2. For statistical purpose, the content of IIA PLA2 protein was determined to be zero when the percentage of immunopositive epithelial cells in the tumour was below 1%.

In carcinomas, IIA PLA2-immunopositive apoptotic cancer cells, necrotic areas (within the tumour), and cells in the invasive front were defined to be present or absent, respectively. The apoptotic cells were identified by their typical morphology (condensed, fragmented chromatin and a clear halo around the apoptotic cell). The invasive fronts were identified histologically by the presence of “tumour

Table 1 Clinicopathological features of the study population

Variable	Hyperplastic polyp $n=7$	Adenoma $n=24$	Carcinoma $n=83$
Sex			
Male	3 (43%)	14 (58%)	37 (45%)
Female	4 (57%)	10 (42%)	46 (55%)
Mean age (SD)	61.4 (±7.9)	73.3 (±8.8)	74.0 (±10.8)
Tumour localisation[a]			
Colon	5 (71%)	9 (39%)	8 (10%)
Rectum	2 (29%)	14 (61%)	75 (90%)
Postoperative tumour status[b]			
T1			5 (7%)
T2			27 (38%)
T3			37 (51%)
T4			3 (4%)
Postoperative nodal status[b]			
N0			45 (62%)
N1			15 (21%)
N2			12 (17%)
Postoperative stage (TNM)[b]			
Stage I			26 (36%)
Stage II			19 (26%)
Stage III			27 (38%)
Tumour grade			
Gr I		9 (38%)	16 (19%)
Gr II		14 (58%)	56 (68%)
Gr III		1 (4%)	11 (13%)

[a] Missing data of localisation of one adenoma

[b] Missing data of the T, N and stage of 11 carcinomas

budding" and an infiltrating growth pattern in the tumour–host interface.

The peritumoural mucosa was divided in the mucosa adjacent to carcinoma (proximal) and in the mucosa slightly further from carcinoma (distal). The presence or absence of IIA PLA2 protein in the peritumoural mucosa was determined, and the intensity was estimated and divided into four classes: 0 "no staining", 1 "weak staining", 2 "moderate staining" and 3 "intense staining". For statistical purpose, classes 0 and 1 as well as classes 2 and 3 were combined in the case of proximal epithelium. The staining intensities of distal epithelium were as well divided into two groups; "no staining" and "weak/moderate/intense staining".

In situ hybridisation for IIA PLA2 mRNA

Four hyperplastic polyps, 12 adenomas and nine carcinomas were evaluated for the expression of IIA PLA2 mRNA using the method described in detail earlier [27]. Briefly, in situ hybridisation (ISH) was performed on formalin-fixed, paraffin-embedded tissue sections by probing with human group II PLA2 anti-sense (test) and sense (control) single-stranded RNA riboprobes. A 0.45-kb cDNA sequence covering the protein coding area of human group II PLA2 in pUC18 plasmid [28] was inserted into the HindIII and BamHI sites of pGEM-3Z transcription vector (Promega, Madison, WI, USA). Digoxigenin-labelled anti-sense and sense RNA probes were synthesised by in vitro transcription with T7 and SP6 RNA polymerases, respectively, by using a DIG RNA Labelling Kit (Boehringer Mannheim, Mannheim, Germany), and the yields were estimated by using a DIG Nucleic Acid Detection Kit (Boehringer Mannheim). The probes were purified with Quick Spin 25 columns (Boehringer Mannheim). The digoxigenin label was detected with alkaline phosphatase-labelled anti-digoxigenin Fab fragments by using disodium-3-(4-metoxyspiro{1,2-dioxyetane-3,2′-(5′-chloro)tricyclo[3, 3, 1, 13, 7]decan}-4-yl) phenyl-phosphate (CSPD®, Boehringer Mannheim) as a substrate. The percentage of epithelial cells positive for IIA PLA2 ISH was estimated by a pathologist (JL) on light microscopy.

Statistical analysis

All statistical analyses were run using PASW Statistics® 18.01 for Windows (SPSS, Inc., Chicago, USA) software package. Frequency tables were analysed using the χ^2 test, with the likelihood ratio or Fisher's exact test for

categorical variables; 2×2 tables were used to calculate odds ratio (OR) and 95% confidence interval (CI) using the exact method. Non-parametric tests were used to compare the means of continuous variables because the mean IIA PLA2 -positivity in tumours was not normally distributed. The differences in the immunopositivity between tumours were analysed with Mann–Whitney or Kruskal–Wallis test for two- and multiple independent samples, respectively. In the ten cases with both adenoma and carcinoma present in the same specimen, the concordance of IIA PLA2-immunopositivity between adenomas and carcinomas was calculated using non-parametric paired-samples test (Wilcoxon-signed ranks test). Correlation between IIA PLA2 protein content in IHC and mRNA expression in ISH was calculated using bivariate correlation test (Spearman's rho) for non-parametric variables. All statistical tests were performed as two-sided and declared significant at p value <0.05.

Results

The results for IHC and ISH for IIA PLA2 are summarised in Tables 2 and 3, and the examples of the localisation of IIA PLA2 protein and mRNA in colorectal tumours and adjacent mucosa are presented in Figs. 1 and 2.

Protein content and mRNA expression of IIA PLA2 in hyperplastic polyps and adenomas

There was no immunoreactive IIA PLA2 protein in hyperplastic polyps. A total of 19 (79%) of 24 adenomas showed positive immunoreaction for IIA PLA2 protein in IHC (Fig. 1a–b). The percentage of epithelial cells positive for IIA PLA2 protein in 24 adenomas varied from 0% to 60% (mean 14.8%, 95% CI 6.9–23). There was no significant difference in the mean percentage of IIA PLA2-immunopositive epithelial cells between colonic and rectal adenomas (p=0.30). In the adenoma presented in Fig. 1, there was an old haemorrhage in the stroma containing hemosiderin-phagocyted macrophages. Hemosiderin is seen both in the IHC and ISH (Fig. 1a–d).

ISH was performed in four hyperplastic polyps and 12 adenomas. There were no IIA PLA2 mRNA expression in hyperplastic polyps whereas 67% of adenomas showed IIA PLA2 mRNA expression varying from 1% to 30% (mean 5.0%, Fig. 1c–d).

Protein content and mRNA expression of IIA PLA2 in carcinomas

A total of 57 (69%) of all carcinomas were totally devoid of immunoreactive IIA PLA2 protein (Fig. 2a). In the 26 carcinomas (31%) positive for IIA PLA2 protein, the percentage of immunopositive cancer cells varied from 1% to 20% (mean 0.8%, 95% CI 0.2–1.4). There was no difference in the mean percentage of IIA PLA2-immunopositive cells between colonic and rectal carcinomas (p=0.63).

ISH was performed in nine carcinomas and showed expression of IIA PLA2 mRNA in three of them. The percentage of positive malignant epithelial cells varied from 0% to 10% (mean 1.3%). The IIA PLA2 protein content in IHC and mRNA expression in ISH were intimately correlated (r=0.93, p<0.001) in hyperplastic polyps, adenomas and carcinomas.

Table 2 The immunoreactivity of group IIA PLA2 protein in colorectal tumours

Tumour type and localisation	Number of cases (%)	Number of IIA PLA2 -positive cases (%)	Mean IIA PLA2-positivity in percents (95% CI)[b]	Significance (p value)[c]
Hyperplastic polyp	7	0	0	=0.001 vs. adenoma
Colon	5 (71)			
Rectum	2 (29)			
Adenoma[a]	24	19 (79)	14.8 (6.9–23)	<0.001 vs. carcinoma
Colon	9 (39)	6 (67)	10.8 (0–24)	0.058 vs. colon carcinoma
				0.30 vs. rectum adenoma
Rectum	14 (61)	12 (86)	17.1 (5.1–29)	<0.001 vs. rectum carcinoma
Carcinoma	83	26 (31)	0.8 (0.2–1.4)	
Colon	8 (10)	2 (25)	0.3 (0–0.6)	0.63 vs. rectum carcinoma
Rectum	75 (90)	24 (32)	0.9 (0.2–1.5)	

[a] Localisation data of one adenoma missing

[b] Mean% of IIA PLA2 immunopositive epithelial cells in tumours. p value=0.018 for differences between groups (hyperplastic polyps, adenomas and carcinomas) in colonic tumours and <0.001 in rectal tumours as analysed with Kruskal–Wallis test

[c] Mann–Whitney U test

Table 3 The expression of group IIA PLA2 mRNA in colorectal tumours with ISH

Tumour type	Number of cases	Number of IIA PLA2 mRNA-positive cases (%)	Mean IIA PLA2 mRNA content in percents (min, max)
Hyperplastic polyp	4	0	0
Adenoma	12	8 (67)	5.0 (min 0%, max 30%)
Carcinoma	9	3 (33)	1.3 (min 0%, max 10%)

In the 72 rectal carcinomas of the second set, there was a tendency to an increase of IIA PLA2-immunopositivity with tumour grade, but the difference did not reach statistical significance (p=0.094). In five carcinomas with an excessive mucinotic component, there were significantly (p=0.025) more epithelial cells positive for IIA PLA2 protein (mean 5.4%, min 0, max 20, Fig. 2b) than in carcinomas with no excessive mucin production (n=67, mean 0.54%, min 0, max 10).

In the 15 rectal carcinomas (21%) with IIA PLA2-immunopositive apoptotic cells (Fig. 2c), there also were more immunoreactive vital malignant epithelial cells than in the carcinomas with no detectable IIA PLA2 immunopositive apoptotic cells (p<0.001). The same difference was seen in the 15 carcinomas (21%) with IIA PLA2-immunopositive necrotic areas (p=0.001, Fig. 2c). Apoptotic cells and necrotic areas showed concordant immunoreaction for IIA PLA2 in 58 cases (81%, OR=8.2, p=0.001) and discrepant reaction in 14 cases (19%).

Comparison of immunopositivity for IIA PLA2 protein between hyperplastic polyps, adenomas and carcinomas

The differences between the mean percentages of IIA PLA2 protein detected with IHC in hyperplastic polyps, adenomas and carcinomas were statistically significant both in the colon and rectum (p=0.018 and p<0.001 in Kruskal–Wallis test, respectively). Adenomas always showed the highest content of IIA PLA2 protein. When the IIA PLA2-immunopositivity in only adenomas and carcinomas was compared according to tumour location, the differences between the mean percentages of IIA PLA2 protein were highly significant in the rectum (p<0.001) but did not reach the statistical significance in the colon (p=0.058). In the ten cases with an adenoma present in the same specimen with carcinoma, adenoma always showed IIA PLA2 protein in IHC (mean 20.8%, 95% CI 4.9–37), whereas carcinoma showed immunopositivity for IIA PLA2 protein in three specimens only (mean 0.4%, min 0, max 2, p=0.001, see Fig. 2a).

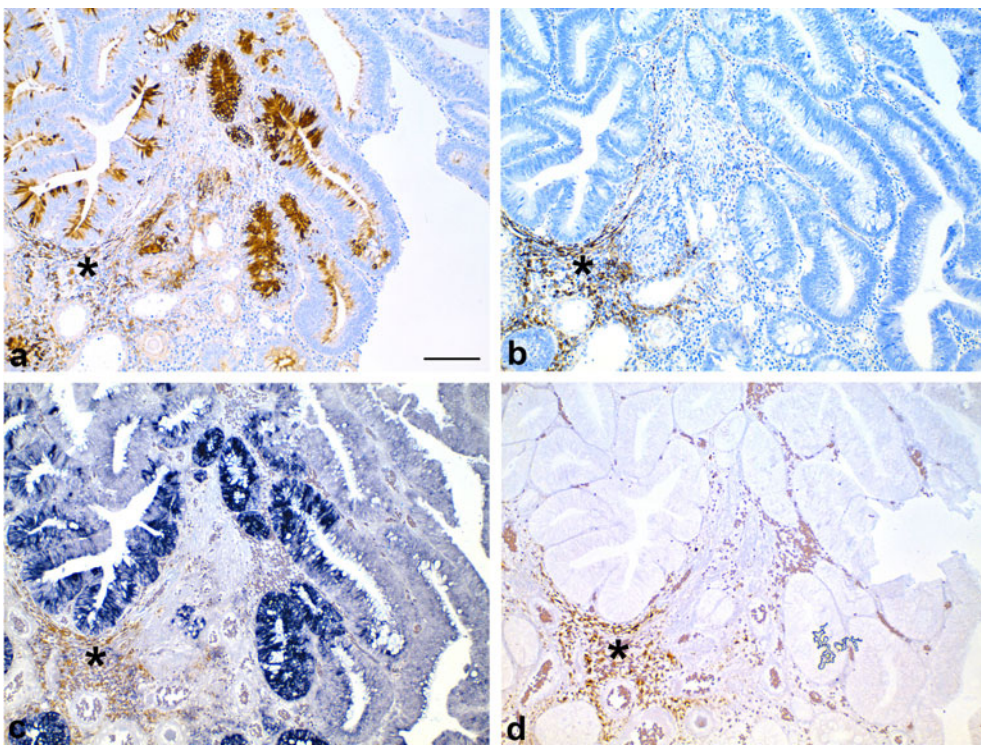

Fig. 1 Localisation of IIA PLA2 protein and mRNA in colonic adenoma. **a** Colonic adenoma showing IIA PLA2-immunopositive epithelial cells in IHC. The immunoreactive material was usually localised in the apical cytoplasm of epithelial cells. Occasional IIA PLA2-immunopositive metaplastic Paneth cells were seen. *Bar* 200 μm. **b** Same adenoma as in a stained with rabbit 0-serum (negative control for IHC). **c** Positive reaction with mRNA ISH in the same epithelial cells of the adenoma that showed positive immunoreaction for IIA PLA2 protein in **a**. Anti-sense (test) probe. **d** An adjacent section of the colonic adenoma shown in **c**. Sense (control) probe. An area of hemosiderin-containing macrophages is marked with an *asterisk*

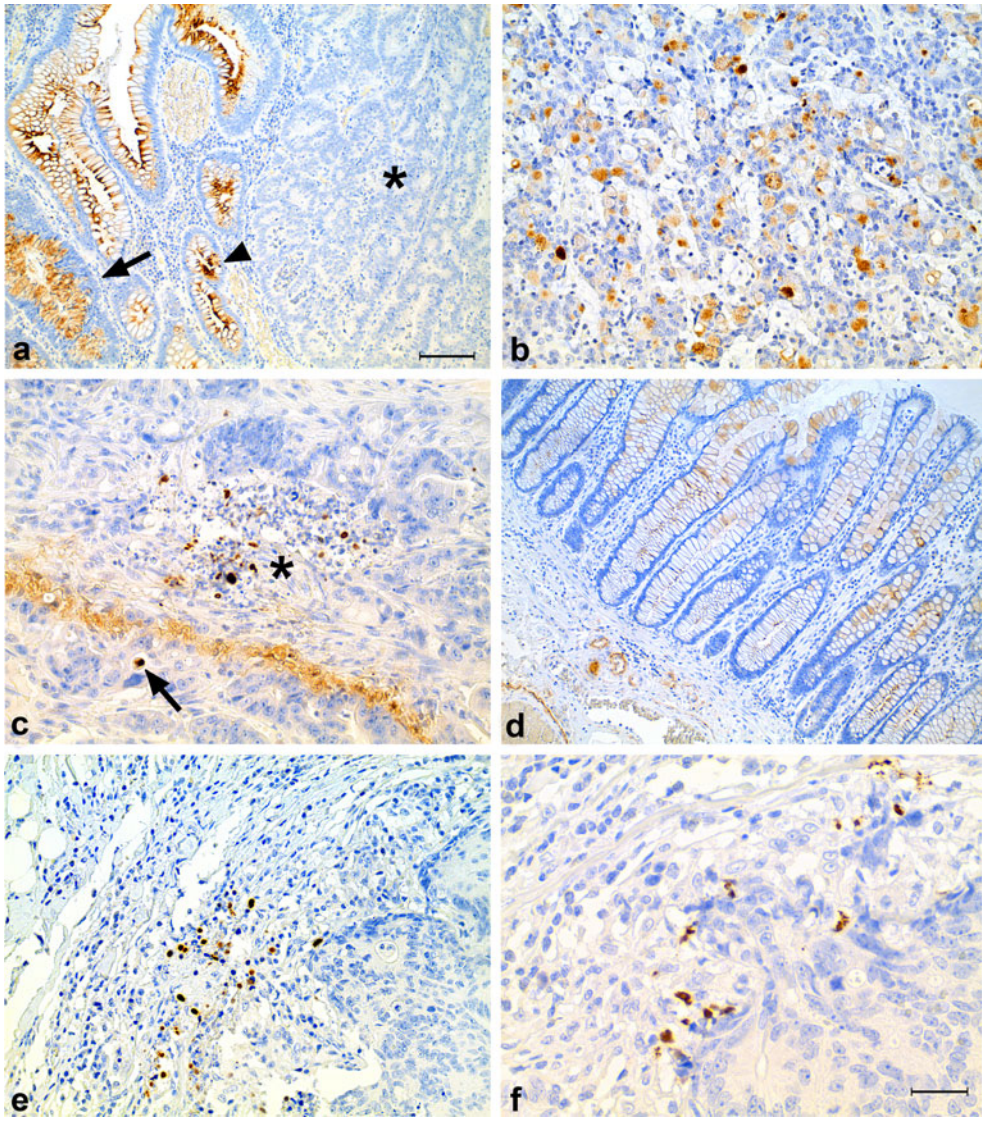

Fig. 2 Localisation of IIA PLA2 protein in colorectal tumours and peritumoural mucosa. **a** Rectal adenoma (*arrow*) and proximal peritumoural mucosa (*arrowhead*) showing IIA PLA2-immunopositive epithelial cells in IHC. Epithelial cells in carcinoma (*asterisk*) are completely devoid of IIA PLA2 protein. When present, the immunoreactive material was usually localised in the cytoplasm of epithelial cells either in apical or granular pattern. *Bar* 200 μm. **b** Carcinoma with an excessive mucinotic component showing IIA PLA2-immunopositive epithelial cells (compare to carcinoma in **a**). **c** Apoptotic cell (*arrow*) and necrotic area (*asterisk*) showing positive immunoreaction for IIA PLA2 protein. In eight cases (11%), there were both IIA PLA2 immunopositive apoptotic cells and necrotic areas in the same specimen, and in 50 cases (69%) both apoptotic cells and necrotic areas were devoid of IIA PLA2 immunoreaction. **d** Distal peritumoural mucosa showing a weak positive immunoreaction for IIA PLA2 protein (compare to proximal peritumoural mucosa in **a**). **e** Invasive front showing immunopositive cells in the tumour–host interface. Usually, it was impossible to determine whether immunoreactive cells were stroma cells or apoptotic or necrotic cancer cells, but the ISH showed positive reaction only in malignant epithelial cells. Outside the invasive front, there usually were some stroma cells positive for IIA PLA2 with IHC and ISH. Furthermore, immunopositivity for IIA PLA2 was present in the elastic lamina of blood vessel walls. **f** Higher magnification of another invasive front with numerous IIA PLA2-positive cells. *Bar* 100 μm

IIA PLA2 in the peritumoural normal mucosa and in the invasive front

The proximal peritumoural mucosa showed immunoreaction for IIA PLA2 protein in 96% of cases. The staining intensity in the proximal peritumoural mucosa (Fig. 2a; 67% showing moderate or intense staining) was considerably stronger than the staining intensity in the more distal mucosa (Fig. 2d; 16% showing moderate staining and none showing intense staining; $p=0.012$, OR 8.7). The peritumoural mucosa also showed the expression of IIA PLA2 with ISH.

In 32 out of 72 carcinomas (44%), IIA PLA2-positive cells were found in the invasive front (i.e. in the tumour–

host interface, Fig. 2e–f). These 32 carcinomas showed a tendency to have more often IIA PLA2 protein detected with IHC in their apoptotic and necrotic malignant cells when compared to carcinomas with no IIA PLA2 immunopositive cells in their invasive front ($p=0.08$ for apoptosis and $p<0.001$ for necrosis). It is important to note that hemosiderin pigment seen in the stromal macrophages (as in Fig. 1) was usually absent in the stroma of the invasive front and did not interfere in the interpretation of IIA PLA2 immunohistochemistry.

Discussion

Secretory phospholipase A2 group IIA is an enzyme involved in the mediation of inflammation [8, 9]. The expression of IIA PLA2 has been demonstrated to be increased in various human malignancies [1], including colorectal cancer [14, 15], and it has been suggested to play an important role in tumour development and progression [29–31]. In mice, the IIA PLA2 gene has been implicated as a candidate gene for Modifier of Min-1 locus [29, 32], which modifies tumour number in mice carrying a dominant germline mutation in their Apc-gene (the Min-mice) [33]. This raised the question of the human counterpart as a potential tumour suppressor gene. Although the gene for human IIA PLA2 (PLA2G2A) has been mapped to chromosome 1p35-36 [34], a region often lost in colorectal cancer [35], sequence analysis of the complete coding region has not revealed any somatic mutations of the PLA2G2A gene in colorectal cancer, suggesting that this gene is not likely to be a tumour-suppressor gene in humans [36].

In the present study, we examined the distribution and sites of synthesis of IIA PLA2 with IHC and ISH in hyperplastic polyps, adenomas and carcinomas, as well as in non-neoplastic peritumoural mucosa. None of the hyperplastic polyps showed IIA PLA2 protein or mRNA. Altogether 79% of adenomas contained IIA PLA2 protein, whereas only 31% of the colorectal carcinomas showed immunopositivity for IIA PLA2 protein. The expression of IIA PLA2 in adenomas and carcinomas was localised in epithelial cells with ISH, indicating that IIA PLA2 protein and mRNA are present in the same cells. Interestingly, in the ten cases with both adenoma and carcinoma adjacent to each other, epithelial cells of all adenomas were immunopositive for IIA PLA2 protein, whereas carcinoma showed IIA PLA2 protein in 33% of cases only. This may suggest that the malignant cells lose their ability to express IIA PLA2 when invasive carcinoma develops in the adenoma. Our results are in line with the findings of Kennedy et al. [19] who reported elevated gene and protein expression of IIA PLA2 in colorectal adenomas from FAP patients, and those of Edhemovic et al. [18] who found almost no IIA PLA2 activity in the colorectal carcinoma. In addition, Praml et al. [37] reported that lack of IIA PLA2 expression is very common among colorectal cancer cell lines in contrast to normal mucosa. In contrast, both the studies of Wendum et al. [14] and Buhmeida et al. [15] showed positive staining for IIA PLA2 in over 50% of the colorectal carcinomas. In the latter study, the patients with IIA PLA2-negative tumours had a better prognosis than the patients with positive tumours [15]. At least some of the discrepancies between these observations could be due to different methods, antibodies and their dilutions used in these different studies.

The ISH method we have used is based on RNAase-free conditions [27]. When IHC and ISH are positive in the same cells (i.e. epithelial cells), the interpretation is usually fairly easy, but in the context of apoptotic and necrotic cells, it may be difficult. In the present study, we found IIA PLA2 protein and mRNA usually in the same epithelial cells, and the presence of IIA PLA2 protein and mRNA in colonic epithelium correlated intimately in adenomas and carcinomas for individual samples. Moreover, the antibody used in this study has earlier been used in IHC and ISH in the samples from Chron's disease and colitis ulcerosa patients with good results (high signal, low background and concordance between IHC and ISH in Paneth cells of the small intestine and colon) [20, 21, 38].

We found five rectal carcinomas with excessive mucinotic component containing considerably more IIA PLA2-positive cancer cells than the non-mucinotic carcinomas. Increased content of IIA PLA2 in mucinotic carcinomas has been reported previously by Edhemovic et al. [18]. As mucinotic rectal carcinomas are commonly considered high-grade carcinomas, it is possible that poorly differentiated tumours express more IIA PLA2 than more differentiated tumours. In our series, we noticed a tendency to an increase of IIA PLA2 immunoreaction with tumour grade, but the difference did not reach statistical significance.

We also analysed IIA PLA2 immunopositivity in apoptotic and necrotic cells. Interestingly, there were more IIA PLA2-positive apoptotic and necrotic cells in carcinomas with more immunopositive vital cancer cells. In most cases, apoptotic cells and necrotic areas showed a concordant pattern in immunoreaction for IIA PLA2. These findings are noteworthy, as IIA PLA2 has been suggested to promote apoptosis of cancer cells [39]. One possible explanation is that the typically lost membrane asymmetry in cancer cells enables increased IIA PLA2 activity [39]. Furthermore, AA, the product of IIA PLA2's enzymatic activity, can stimulate an important apoptotic pathway via the activation of sphingomyelinases and the subsequent release of ceramide [40, 41]. In the light of our study, it seems unlikely that phospholipase itself would cause cell death because relatively few cancer cells expressed IIA

PLA2 protein. The more likely explanation is that the apoptotic or necrotic cancer cells are somehow engaged to express IIA PLA2, which could assist the host in removing apoptotic cells.

In the present series, the peritumoural non-neoplastic epithelium showed positive immunoreaction for IIA PLA2 in 96% of the cases. This is consonant with the findings of Edhemovic et al. [18] and Buhmeida et al. [15] who reported increased content of IIA PLA2 in normal mucosa adjacent to carcinoma. IIA PLA2 is inducible by pro-inflammatory cytokines, such as tumour necrosis factor α and interleukin 1β [42], both being abundantly present in the vicinity of carcinoma [43]. Thus, this increased IIA PLA2 protein content in normal mucosa adjacent to carcinoma may well result from an increased secretion of pro-inflammatory cytokines by the cancer cells as suggested earlier, too [18]. Our observation of the weak or absent intensity of immunoreaction in normal colonic mucosa more distally to cancer supports this view. In the studies where the normal colorectal epithelium has been reported to be devoid of IIA PLA2 protein [15, 16, 18], the specimens have been taken from the mucosa more distant to cancer site.

Frequently, the invasive front of rectal carcinomas showed immunopositive cells even in the absence of IIA PLA2 immunoreactivity in vital cancer cells in the same sample. This is an interesting finding because the cells in the invasive front are thought to represent a dynamic interface between pro- and anti-tumour factors [44]. The glands in the invasive front often showed disintegrated structures suggesting that these cells have possibly lost their symmetric membrane structure, which in turn may result in increased IIA PLA2 activity. In addition, abundant inflammatory cell infiltrate almost invariably present in the invasive front may also trigger IIA PLA2 production in some cells. Our observations could explain the previous results of Tribler et al. [45] who found that the peripheral areas of colon carcinoma contained significantly higher levels of IIA PLA2 protein than the samples taken from the central tumour regions. In our study, it was not always possible to determine in IHC whether immunoreactive cells in the invasive front were stromal cells or apoptotic or necrotic cancer cells. However, ISH showed IIA PLA2 mRNA only in malignant epithelial cells suggesting that at least the majority of IIA PLA2 protein present in the invasive front originates from the tumour cells rather than from the stromal cells.

We conclude that the majority of colorectal adenomas show IIA PLA2 expression, whereas the expression is disturbed and IIA PLA2 protein content is dramatically reduced in malignant colorectal tumours as compared to adenomas. In addition, peritumoural mucosa shows increased expression and content of IIA PLA2. It is possible that the down-regulation of IIA PLA2 has a role in colorectal carcinogenesis, but it remains to be established how and when the malignant cells lose their capability to produce IIA PLA2. In addition, the questions whether IIA PLA2 is needed in apoptotic cell death in colorectal carcinomas and whether radiation therapy affects IIA PLA2 expression via cancer cell death remain unanswered. Furthermore, our results confirm that IIA PLA2 in the invasive front is derived from the malignant epithelial cells.

Acknowledgments We are grateful to Sinikka Kollanus for her skilful and expeditious help in laboratory work, Jaakko Liippo for aid with the digital pictures and Prof. Timo Nevalainen for the polyclonal rabbit IIA PLA2 antibody used in the present study. This research work has been supported by the grants from The Special Government Funding (EVO) allocated to Turku University Hospital. The authors declare that they have no conflict of interest.

References

1. Laye JP, Gill JH (2003) Phospholipase A2 expression in tumours: a target for therapeutic intervention? Drug Discov Today 8:710–716
2. Tanaka T (2009) Colorectal carcinogenesis: review of human and experimental animal studies. J Carcinogen 8:5
3. Greenhough A, Smartt HJ, Moore AE, Roberts HR, Williams AC, Paraskeva C, Kaidi A (2009) The COX-2/PGE2 pathway: key roles in the hallmarks of cancer and adaptation to the tumour microenvironment. Carcinogenesis 30:377–386
4. Yuan CJ, Mandal AK, Zhang Z, Mukherjee AB (2000) Transcriptional regulation of cyclooxygenase-2 gene expression: novel effects of nonsteroidal anti-inflammatory drugs. Cancer Res 60:1084–1091
5. Wendum D, Comperat E, Boëlle PY, Parc R, Masliah J, Trugnan G, Fléjou JF (2005) Cytoplasmic phospholipase A2 alpha overexpression in stromal cells is correlated with angiogenesis in human colorectal cancer. Mod Pathol 18:212–220
6. Panel V, Boëlle PY, Ayala-Sanmartin J, Jouniaux AM, Hamelin R, Masliah J, Trugnan G, Fléjou JF, Wendum D (2006) Cytoplasmic phospholipase A2 expression in human colon adenocarcinoma is correlated with cyclooxygenase-2 expression and contributes to prostaglandin E2 production. Cancer Lett 243:255–263
7. Nevalainen TJ, Haapanen TJ (1993) Distribution of pancreatic (group I) and synovial-type (group II) phospholipases A2 in human tissues. Inflammation 17:453–464
8. Nevalainen TJ, Kortesuo PT, Rintala E, Märki F (1992) Immunochemical detection of group I and group II phospholipases A2 in human serum. Clin Chem 38:1824–1829
9. Rintala EM, Nevalainen TJ (1993) Group II phospholipase A2 in sera of febrile patients with microbiologically or clinically documented infections. Clin Infect Dis 17:864–870
10. Graff JR, Konicek BW, Deddens JA, Chedid M, Hurst BM, Colligan B, Neubauer BL, Carter HW, Carter JH (2001) Expression of group IIa secretory phospholipase A2 increases with prostate tumor grade. Clin Cancer Res 7:3857–3861
11. Jiang J, Neubauer BL, Graff JR, Chedid M, Thomas JE, Roehm NW, Zhang S, Eckert GJ, Koch MO, Eble JN, Cheng L (2002) Expression of group IIA secretory phospholipase A2 is elevated in

prostatic intraepithelial neoplasia and adenocarcinoma. Am J Pathol 160:667–671
12. Mirtti T, Laine VJ, Hiekkanen H, Hurme S, Rowe O, Nevalainen TJ, Kallajoki M, Alanen K (2009) Group IIA phospholipase A as a prognostic marker in prostate cancer: relevance to clinicopathological variables and disease-specific mortality. APMIS 117:151–161
13. Leung SY, Chen X, Chu KM, Yuen ST, Mathy J, Ji J, Chan AS, Li R, Law S, Troyanskaya OG, Tu IP, Wong J, So S, Bostein D, Brown PO (2002) Phospholipase A2 group IIA expression in gastric adenocarcinoma is associated with prolonged survival and less frequent metastasis. Proc Natl Acad Sci USA 99:16203–16208
14. Wendum D, Svreck M, Rigau V, Boëlle PY, Sebbagh N, Parc R, Masliah J, Trugnan G, Fléjou JF (2003) COX-2, inflammatory secreted PLA2, and cytoplasmic PLA2 protein expression in small bowel adenocarcinomas compared with colorectal adenocarcinomas. Mod Pathol 16:130–136
15. Buhmeida A, Bendardaf R, Hilska M, Laine J, Collan Y, Laato M, Syrjänen K, Pyrhönen S (2009) PLA2 (group IIA phospholipase A2) as a prognostic determinant in stage II colorectal carcinoma. Ann Oncol 20:1230–1235
16. Nevalainen TJ, Grönroos JM, Kallajoki M (1995) Expression of group II phospholipase A2 in the human gastrointestinal tract. Lab Invest 72:201–208
17. Hong KH, Bonventre JC, O'Leary E, Bonventre JV, Lander ES (2001) Deletion of cytosolic phospholipase A(2) suppresses Apc (Min)-induced tumorigenesis. Proc Natl Acad Sci USA 98:3935–3939
18. Edhemovic I, Snoj M, Kljun A, Golouh R (2001) Immunohistochemical localization of group II phospholipase A2 in the tumours and mucosa of the colon and rectum. Eur J Surg Oncol 27:545–548
19. Kennedy BP, Soravia C, Moffat J, Xia L, Hiruki T, Collins S (1998) Overexpression of the non-pancreatic secretory group II PLA2 messenger RNA and protein in colorectal adenomas from familial adenomatous polyposis patients. Cancer Res 58:500–503
20. Haapamäki MM, Grönroos JM, Nurmi H, Alanen K, Kallajoki M, Nevalainen TJ (1997) Gene expression of group II phospholipase A2 in intestine in ulcerative colitis. Gut 40:95–101
21. Haapamäki MM, Grönroos JM, Nurmi H, Alanen K, Nevalainen TJ (1999) Gene expression of group II phospholipase A2 in intestine in Crohn's disease. Am J Gastroenterol 94:713–720
22. Minami T, Tojo H, Shinomura Y, Matsuzawa Y, Okamoto M (1994) Increased group II phospholipase A2 in colonic mucosa of patients with Crohn's disease and ulcerative colitis. Gut 35:1593–1598
23. Minami T, Shinomura Y, Miyagawa J, Tojo H, Okamoto M, Matsuzawa Y (1997) Immunohistochemical localization of group II phospholipase A2 in colonic mucosa of patients with inflammatory bowel disease. Am J Gastroenterol 92:289–292
24. Nevalainen TJ, Märki F, Kortesuo PT, Grütter MG, Di Marco S, Schmitz A (1993) Synovial type (group II) phospholipase in cartilage. J Rheumatol 20:325–330
25. Grönroos JO, Laine VJO, Nevalainen TJ (2002) Bactericidal group IIA phospholipase A2 in serum of patients with bacterial infections. J Infect Dis 185:1767–1772
26. Nevalainen TJ, Eerola LI, Rintala E, Laine VJ, Lambeau G, Gelb MH (2005) Time-resolved fluoroimmunoassays of the complete set of secreted phospholipases A2 in human serum. Biochim Biophys Acta 1733:210–223
27. Laine VJ, Grass DS, Nevalainen TJ (1999) Protection by group II phospholipase A2 against *Staphylococcus aureus*. J Immunol 162:7402–7408
28. Di Marco S, Märki F, Hofstetter H, Schmitz A, van Oostrum J, Grütter MG (1992) Purification, analysis, and enzymatic activity of recombinant human synovial fluid phospholipase A2 and N-terminal variants. J Biochem 112:350–354
29. Cormier RT, Hong KH, Halberg RB, Hawkins TL, Richardson P, Mulherkar R, Dove WF, Lander ES (1997) Secretory phospholipase Pla2g2a confers resistance to intestinal tumorigenesis. Nat Genet 17:88–91
30. Cormier RT, Bilger A, Lillich AJ, Halberg RB, Hong KH, Gould KA, Borenstein N, Lander ES, Dove WF (2000) The Mom1AKR intestinal tumor resistance region consists of Pla2g2a and a locus distal to D4Mit64. Oncogene 19:3182–3192
31. Belinsky GS, Rajan TV, Saria EA, Giardina C, Rosenberg DW (2007) Expression of secretory phospholipase A2 in colon tumor cells potentiates tumor growth. Mol Carcinog 46:106–116
32. MacPhee M, Chepenik KP, Liddell RA, Nelson KK, Siracusa LD, Buchberg AM (1995) The secretory phospholipase A2 gene is a candidate for the Mom1 locus, a major modifier of ApcMin-induced intestinal neoplasia. Cell 81:957–966
33. Dietrich WF, Lander ES, Smith JS, Moser AR, Gould KA, Luongo C, Borenstein N, Dove W (1993) Genetic identification of Mom-1, a major modifier locus affecting Min-induced intestinal neoplasia in the mouse. Cell 75:631–639
34. Johnson LK, Frank S, Vades P, Pruzanski W, Lusis AJ, Seilhamer JJ (1990) Localization and evolution of two human phospholipase A2 genes and two related genetic elements. Adv Exp Med Biol 275:17–34
35. Leister I, Weith A, Brüderlein S, Ciepluch C, Kangwanpong D, Schlag P, Schwab M (1990) Human colorectal cancer: high frequency of deletions at chromosme 1p35. Cancer Res 50:7232–7235
36. Riggins GJ, Markowitz S, Wilson JK, Vogelstein B, Kinzler KW (1995) Absence of secretory phospholipase A2 gene alterations in human colorectal cancer. Cancer Res 55:5184–5186
37. Praml C, Amler LC, Dihlmann S, Finke LH, Schlag P, Schwab M (1998) Secretory type II phospholipase A2 (PLA2G2A) expression status in colorectal carcinoma derived cell lines and in normal colonic mucosa. Oncogene 17:2009–2012
38. Nevalainen TJ, Haapanen TJ, Rajala P, Ekfors T (1998) Expression of group IIA phospholipase A2 in Paneth cells of an adenoma of the rectum. A case report. APMIS 106:780–784
39. Fijneman RJ, Cormier RT (2008) The roles of sPLA2-IIA (Pla2g2a) in cancer of the small and large intestine. Front Biosci 13:4144–4174
40. Cao Y, Pearman AT, Zimmerman GA, McIntyre TM, Prescott SM (2000) Intracellular unesterified arachidonic acid signals apoptosis. Proc Natl Acad Sci USA 97:11280–11285
41. Ilsley JN, Nakanishi M, Flynn C, Belisnky GS, De Guise S, Adib JN, Dobrowsky RT, Bonventre JV, Rosenberg DW (2005) Cytoplasmic phospholipase A2 deletion enhances colon tumorigenesis. Cancer Res 65:2636–2643
42. Pruzanski W, Stefanski E, Vadas P, Kennedy BP, van den Bosch H (1998) Regulation of the cellular expression of secretory and cytosolic phospholipases A2, and cyclooxygenase-2 by peptide growth factors. Biochim Biophys Acta 1403:47–56
43. Szkaradkiewicz A, Marciniak R, Chudzicka-Strugala I, Wasilewska A, Drews M, Majewski P, Karpinski T, Zwozdziak B (2009) Proinflammatory cytokines and IL-10 in inflammatory bowel disease and colorectal cancer patients. Arch Immunol Ther Exp 57:291–294
44. Zlobec I, Lugli A (2009) Invasive front of colorectal cancer: dynamic interface of pro-/anti-tumor factors. World J Gastroenterol 15:5898–5906
45. Tribler L, Jensen LT, Jorgensen K, Brünner N, Gelb MH, Nielsen HJ, Jensen SS (2007) Increased expression of group IIA and X secretory phospholipase A2 in peritumoural versus central colon carcinoma tissue. Anticancer Res 27:3179–3185

Virchows Arch (2010) 457:669–676
DOI 10.1007/s00428-010-0960-2

ORIGINAL ARTICLE

Differential expressions and DNA methylation patterns of lysophosphatidic acid receptor genes in human colon cancer cells

Megumu Tsujino · Minako Fujii · Kyoko Okabe · Toshio Mori · Nobuyuki Fukushima · Toshifumi Tsujiuchi

Received: 16 May 2010 / Accepted: 31 July 2010 / Published online: 3 October 2010
© Springer-Verlag 2010

Abstract Lysophosphatidic acid (LPA), which is a bioactive phospholipid, interacts with specific G protein-coupled transmembrane receptors. Recently, alterations of LPA receptor genes have been reported in some tumor cells. In this study, we examined the expression profiles and DNA methylation status of LPA receptor 1–5 (LPA1–5) genes in human colon cancer cells and also looked for the mutations. Reverse transcription–polymerase chain reaction (PCR) and bisulfite sequencing analyses were carried out. While LPA1, LPA2, and LPA4 genes were expressed in DLD1, SW480, HCT116, CaCo-2, SW48, and LoVo cells, the expressions of LPA3 and LPA5 genes were various. These expression levels were correlated with DNA methylation status in the 5′ upstream regions of the LPA receptor genes. Mutation analysis was also performed using a PCR–single-strand conformation polymorphism method. Although no mutations in LPA1, LPA3 and LPA5 genes were found in all types of cells, LPA2 mutations in DLD1 and SW48 cells, and LPA4 mutation were found in DLD1 cells. On the basis of the present results, we demonstrate that these colon cancer cells will be available to understanding the molecular pathway through LPA receptors in the development of tumor cells, and that LPA receptors may be new molecular targets for therapeutic approaches and chemoprevention.

Keywords LPA · LPA receptor · DNA methylation · Colon cancer · Mutation

M. Tsujino · M. Fujii · K. Okabe · T. Tsujiuchi (✉)
Laboratory of Cancer Biology and Bioinformatics,
Department of Life Science, Faculty of Science and Engineering,
Kinki University,
3-4-1, Kowakae, Higashiosaka,
Osaka 577-8502, Japan
e-mail: ttujiuch@life.kindai.ac.jp

T. Mori
RI Center, Nara Medical University,
840 Shijo-cho, Kashihara,
Nara 634-8521, Japan

N. Fukushima
Laboratory of Molecular Neurobiology,
Department of Life Science, Faculty of Science and Technology,
Kinki University,
3-4-1, Kowakae, Higashiosaka,
Osaka 577-8502, Japan

Introduction

Lysophosphatidic acid (LPA) is a bioactive mediator which induces several cellular effects, including regulation of cell proliferation, differentiation, transcellular migration, morphogenesis, and protection from apoptosis [1–6]. In human ovarian cancer cells, LPA can induce not only cell proliferation, but also migration, invasion, and production of angiogenic factors, suggesting that LPA may play an important role in the pathogenesis of tumor cells [1–3, 6–9]. LPA interacts with at least five G protein-coupled transmembrane receptors, LPA receptor-1 (LPA1), LPA2, LPA3, LPA4, and LPA5 [8–12]. LPA1 is ubiquitously expressed in normal tissues, but the expressions of other LPA receptor subtypes are relatively restricted, suggesting these receptors may have different biological functions regarding LPA [1, 8, 9]. Previously, aberrant expressions of LPA receptors have been reported in human ovarian, colorectal, and thyroid tumors, indicating that alterations of the LPA receptor gene expression might be also involved in the malignant transformation of tumor cells as well as LPA per se [6, 7, 13–15]. In rodents, frequent mutations of the LPA1 gene

were also found in rat lung and liver tumors [16, 17]. These findings suggest that alterations of LPA receptor genes may be involved in the development of tumors in rats as well as human cases.

It is well-known that methylation of cytosine residues at CpG dinucleotides is a strong effector for the suppression of gene expression in mammalian genomes [18–20]. The cytosine methylation can reduce the binding affinity of transcription factors and influence chromatin structure [18–20]. It has been proposed that aberrant DNA methylation of gene promoter regions is one of the major mechanisms of gene silencing in several tumors [18–20]. Previously, we have reported that the loss of LPA1 expression is due to its aberrant DNA methylation in rat tumor cell lines [21].

In the present study, we measured the expression levels of LPA1, LPA2, LPA3, LPA4, and LPA5 genes and their DNA methylation status in human colon cancer cells, and also looked for mutations. Such information would be valuable for understanding molecular pathogenesis and clinical features of colon cancers associated with LPA receptors as well as for developing novel therapeutic agents.

Materials and methods

Cell culture

Six colon cancer cell lines used in this study were DLD1, SW480, HCT116, Caco-2, SW48, and LoVo. All cell lines were cultured in DMEM containing 10% fetal bovine serum in 5% CO_2 atm at 37°C.

Reverse transcription–polymerase chain reaction amplification for the LPA receptor gene expressions

Total RNA was extracted from each cell using ISOGEN (Nippon Gene, Inc., Toyama, Japan) and first-strand cDNA was synthesized from 0.5-μg samples with the Transcriptor First Strand cDNA synthesis kit (Roche Diagnostics Co. Ltd., Mannheim, Germany). To eliminate possible false positives caused by residual genomic DNA, all samples were treated with DNase.

Semi-quantitative reverse transcription–polymerase chain reaction (RT–PCR) analysis was performed as described

Table 1 The primer sequences used for the PCR–SSCP analysis

Genes		Forward	Reverse
LPA1	exon2-1	5′-GTACACAGCTTCTCCTAGCA-3′	5′-ACCTCTGCTAGTTGAAGCC-3′
	exon3-1	5′-GGACCTGTGCCTTCTTTTTC-3′	5′-AAGTAGGCCAACCCAGCAAA-3′
	exon3-2	5′-CGCCGCTTCCATTTTCCTAT-3′	5′-CTGGGTATAGCACCCATAAC-3′
	exon3-3	5′-TCCACACACGGATGAGCAAC-3′	5′-GGTTTATGTTAGTCACTGAGA-3′
	exon4-1	5′-TTTGCGACAATGGTGGCTTC-3′	5′-CAGAGGATCTGCCTAAAGGT-3′
	exon4-2	5′-CTGCCATGAACCCCATCATT-3′	5′-GGAGGCTGTTTATCCTCCAA-3′
LPA2	exon2-1	5′-TTCCAGGCCACCGTAGTCCT-3′	5′-AGGCGATGGCTGCTATGACC-3′
	exon2-2	5′-CATCATGGGCCAGTGCTACT-3′	5′-CAGCCCTCAAGTGAAAGTCG-3′
	exon2-3	5′-ACCAGCCCATCTACCTG-3′	5′-CCCACAATGAGCATGACCAC-3′
	exon2-4	5′-GATGGCCGTGCAGCTGCACA-3′	5′-AAGCAGGGTCCCTGTTGCCC-3′
	exon3-1	5′-AAACAAGCAGCTCTTGCACT-3′	5′-CGGAAGGTGCGGCGCATCTC-3′
	exon3-2	5′-AATGCTGCTGTGTACTCTTG-3′	5′-GTCAGTCCTGTTGGTTGGGT-3′
LPA3	exon1-1	5′-TTCTTTCTAGGATGTTCACT-3′	5′-AAACTGGGCCTGTGTTAAAC-3′
	exon1-2	5′-CGCTGGAATTGCCTATGTAT-3′	5′-CGTACACGTAGATCCGCAGG-3′
	exon1-3	5′-TGTCCAACCTCATGGCCTTCC-3′	5′-GGTACACCACAGATGCTCCGT-3′
	exon2-1	5′-GTTTGCCTTGCAGTTGTCAA-3′	5′-CTTCTTCATGGTGCCATACA-3′
	exon2-2	5′-AACTCCGTCGTGAACCCCAT-3′	5′-GGCATCCAGAGTTTAGGAAG-3′
LPA4	exon1-1	5′-CCTACCGGTCCATAGTGTCA-3′	5′-AGTGGCGGTTGAAGTTGTAA-3′
	exon1-2	5′-TGTCTTCTGTTTCCGCATGA-3′	5′-CCGCCACTGAGGACTAGGAT-3′
	exon1-3	5′-AGGAGGAATTCTGCCATTGT-3′	5′-AGCGCACCAGGGCATACAAG-3′
	exon1-4	5′-TGCTTTGTACCCTACAACTC-3′	5′-TATCTGGACCTGAACACATT-3′
LPA5	exon2-1	5′-CTGCCAGTGGAGCTAAACAT-3′	5′-CGGTGGGTAGGTCGGTAGTC-3′
	exon2-2	5′-AGCTCCTCAACCAACAGTTC-3′	5′-TGGTGCAGTGCGTAGTAGGA-3′
	exon2-3	5′-GTGAGCGTGTACATGTGTAAC-3′	5′-TCGTCGCTGAAGCTCTCGAA-3′
	exon2-4	5′-GGGCGCTCATCCTGGTGTTTG-3′	5′-CCGCCAGCGTGCTGTTGTAG-3′
	exon2-5	5′-ACCTCGTCATCTTCCTGCTGT-3′	5′-GACGGCGGACCTTTCGGATT-3′
	exon2-6	5′-GGTGTACTACTTTAGCGCCGA-3′	5′-AGCCCACCTTCTTGTGTGTA-3′

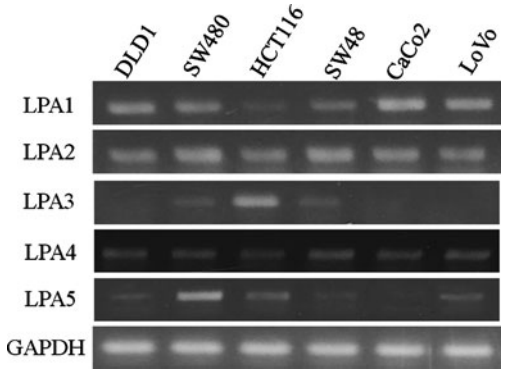

Fig. 1 Expressions of LPA receptor genes by semi-quantitative RT–PCR analysis

previously [21]. PCR amplification was carried out in a reaction volume of 10 μl containing 1 μM of each gene primer, 200 μM of each dNTP, 1×PCR buffer, 0.5 U of AmpliTaq Gold (Applied Biosystems Japan Ltd., Tokyo, Japan), and 0.5 μl of synthesized cDNA mixture. Primer pairs were as follows: for human LPA1 [National Center for Biotechnology Information (NCBI) accession number, NM_001401] forward (F), 5′-CGCCGCTTCCATTTTCC TAT-3′; reverse (R), 5′-CTGGGTATAGCACCCATAAC-3′ (annealing temperature, 59°C); for human LPA2 (NCBI accession number, NM_004720) F, 5′-AATGCTGCTGTG TACTCTTG-3′; R, 5′-GTCAGTCCTGTTGGTTGGGT-3′ (annealing temperature, 58°C); for human LPA3 (NCBI accession number, NM_012152) F, 5′-AACTCCGTCGT GAACCCCAT-3′; R, 5′-GGCATCCAGAGTTTAGGAAG-3′ (annealing temperature, 60°C); for human LPA4 (NCBI accession number, NM_005296) F, 5′-TGCTTTGTACCC TACAACTC-3′; R, 5′-TATCTGGACCTGAACACATT-3′ (annealing temperature, 57°C); and for human LPA5 (NCBI accession number, NM_020400) F, 5′-AGCTCCTCAAC CAACAGTTC-3′; R, 5′-TGGTGCAGTGCGTAGTAGGA-3′ (annealing temperature, 61°C). The human glyceraldehyde-

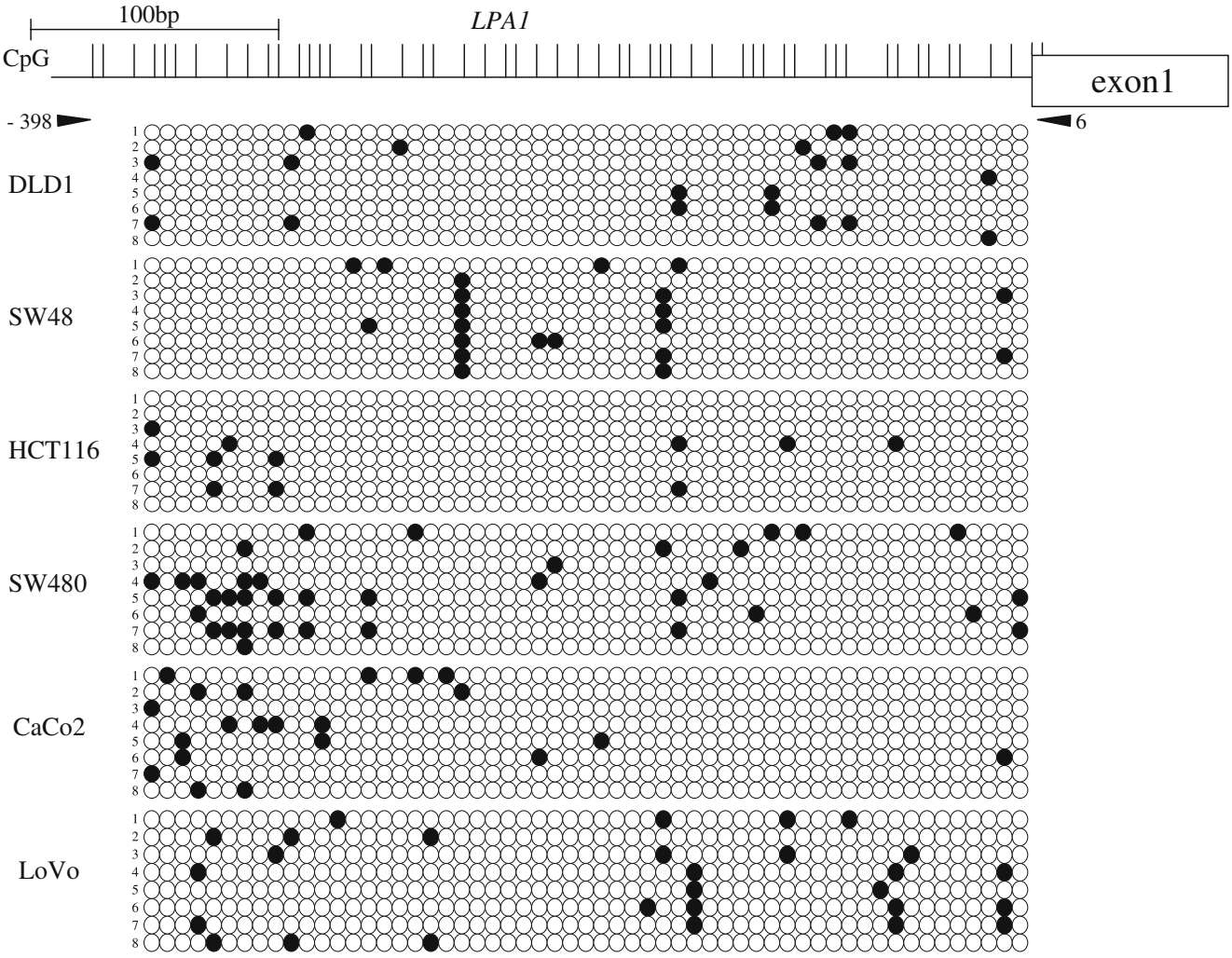

Fig. 2 Results of the methylation analysis of the 5′ upstream region of the human LPA1 gene evaluated by bisulfite sequencing. For each sample, eight clones were sequenced. The primer pair used for the bisulfite sequencing is indicated by *arrowheads*. Methylated CpG sites are shown by *closed circles* and unmethylated CpG sites are shown by *open circles*. The first base of exon1 was defined+1

3-phosphate dehydrogenase gene was used as an internal control to adjust the amounts of template. For each gene, multiple cycles of PCR amplification were tested. The cycle at which a sample having the highest expression reached an amplification plateau was determined, and a cycle number smaller than this was adopted for the analysis. The amplified products were then separated on 2% agarose gels containing 0.05 μg/ml of ethidium bromide.

Bisulfite sequencing

Genomic DNA was extracted with a DNeasy tissue kit (QIAGEN, Hilden, Germany) from each cell and was treated with an EpiTect Bisulfite kit (QIAGEN). For bisulfite sequencing, PCR was performed with the following primer sets: LPA1 (NCBI accession number, NM_057159.2) BS-F, 5′-TGGTGGTTGATGTTTTTTGAGTGG-3′; BS-R, 5′-ACAACAAAACAATATAAACCCAAC-3′; LPA2 (NCBI accession number, NM_004720.5) BS-F, 5′-GTGTGGATT TAAGATTATTTGGAG-3′; BS-R, 5′-ACCACCTAAAA AAACCCTACCCC-3′; LPA3 (NCBI accession number, NM_012152.2) BS-F, 5′-GGTGGTGGGTGTGGGTTGTA TTT-3′; BS-R, 5′-AAAACATCCCCAACCTACAAAACC-3′; and LPA5 (NCBI accession number, NM_020400.5) BS-F, 5′-GGGTTATTTGTTTTTGTGTTGTTTGG-3′; BS-R, 5′-CAAATAACTAACCCACCAACCTCTC-3′. PCR products were subcloned with a DynaExpress TA PCR cloning kit (BioDynamics Laboratory Inc., Tokyo, Japan) and sequenced with a BigDye terminator v3.0 cycle sequencing ready reaction kit (Applied Biosystems Japan Ltd.) and an ABI PRISM 310 genetic analyzer (Applied Biosystems Japan Ltd.). For each sample, eight clones were sequenced [21].

Polymerase chain reaction–single-strand conformation polymorphism analysis

The polymerase chain reaction–single-strand conformation polymorphism analysis (PCR–SSCP) analysis was conducted to look for mutations in the LPA receptor genes. The primers used in this study were designed to amplify ORF of the LPA1–5 genes with intron sequences flanking coding exons (Table 1). Briefly, PCR for SSCP analysis was performed in 10 μl of reaction mixture containing 1 μM of each primer, 200 μM of each dNTP, 1×PCR buffer, 2.5 U of AmpliTaq (Applied Biosystems Japan Ltd.), and 0.5 μl of genomic DNA extracted from each cell. PCR products were diluted with 10 μl of loading solution containing 90% formamide, 20 mM of EDTA, 0.05% xylene cyanol, and

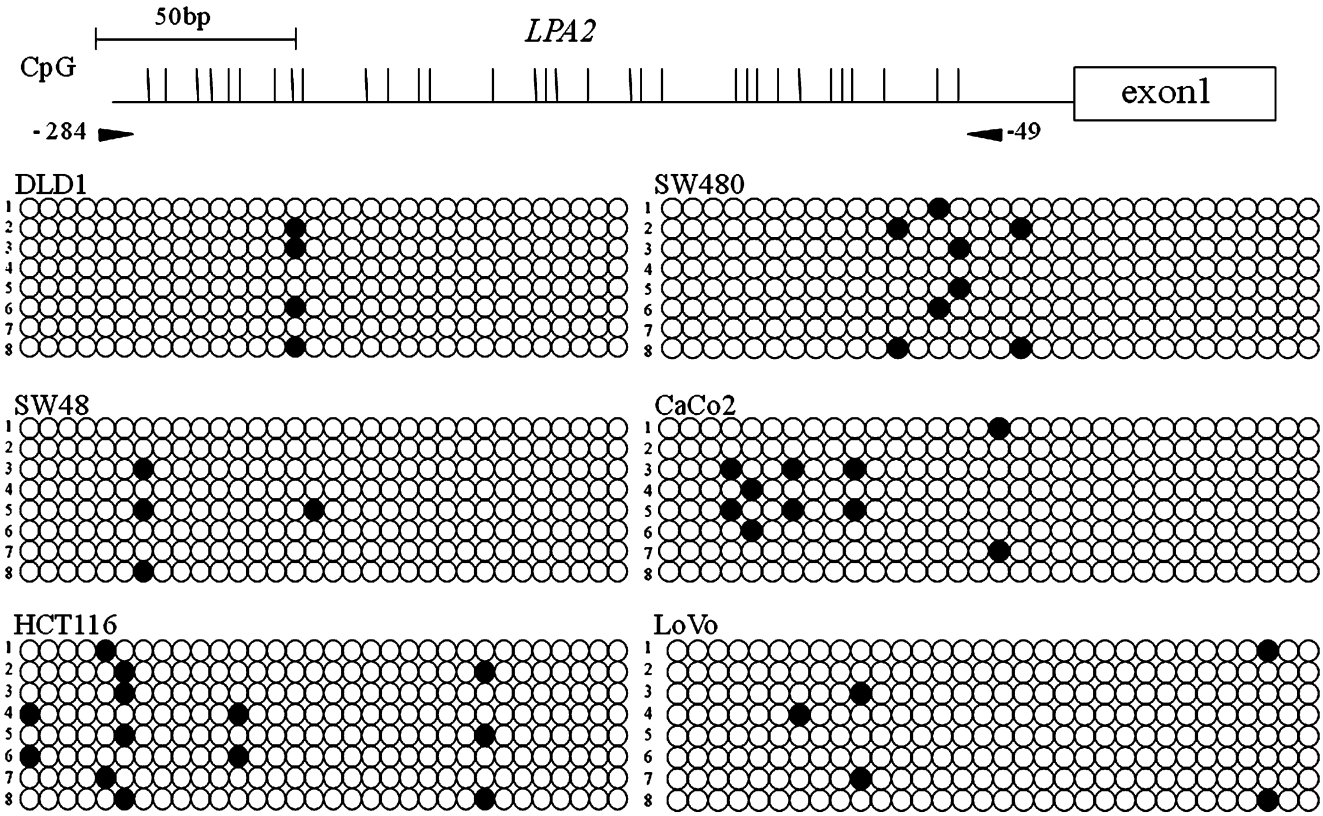

Fig. 3 Results of the methylation analysis of the 5′ upstream region of the human LPA2 gene evaluated by bisulfite sequencing. For each sample, eight clones were sequenced. The primer pair used for the bisulfite sequencing is indicated by *arrowheads*. Methylated CpG sites are shown by closed circles and unmethylated CpG sites are shown by *open circles*. The first base of exon1 was defined+1

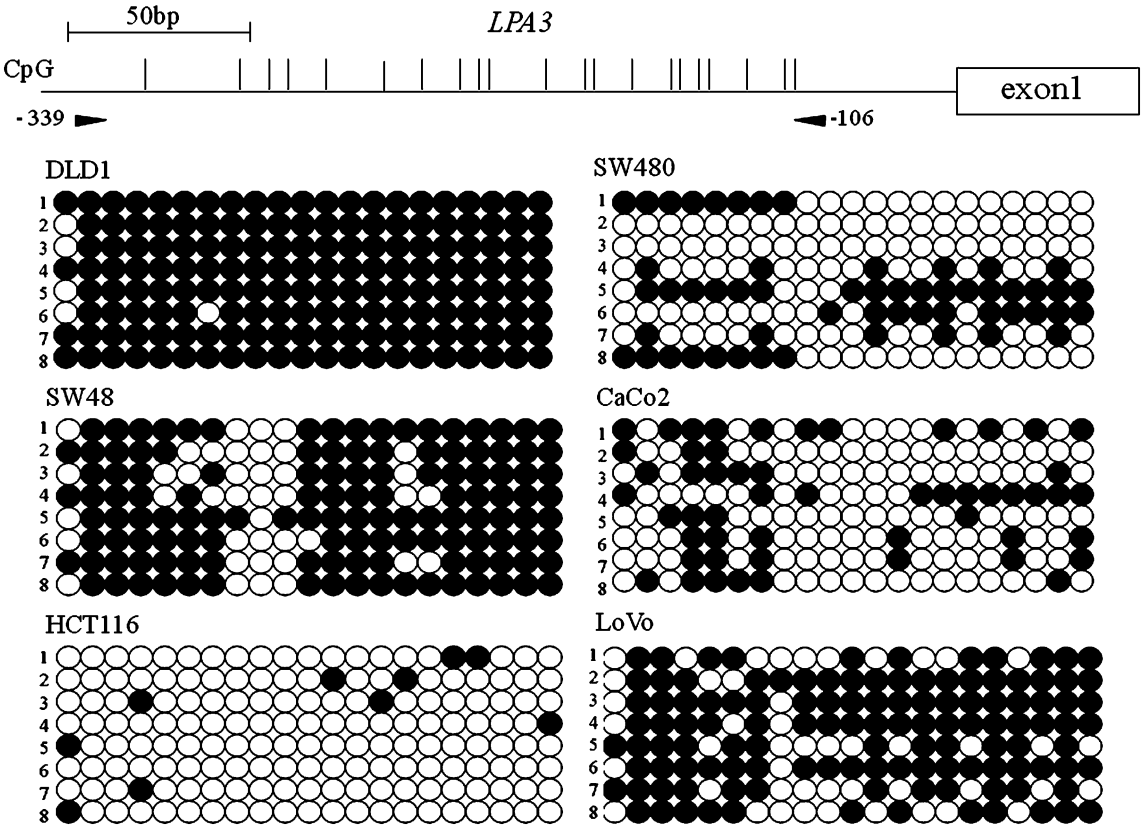

Fig. 4 Results of the methylation analysis of the 5′ upstream region of the human LPA3 gene evaluated by bisulfite sequencing. For each sample, eight clones were sequenced. The primer pair used for the bisulfite sequencing is indicated by *arrowheads*. Methylated CpG sites are shown by *closed circles* and unmethylated CpG sites are shown by *open circles*. The first base of exon1 was defined+1

Fig. 5 Results of the methylation analysis of the 5′ upstream region of the human LPA5 gene evaluated by bisulfite sequencing. For each sample, eight clones were sequenced. The primer pair used for the bisulfite sequencing is indicated by *arrowheads*. Methylated CpG sites are shown by *closed circles* and unmethylated CpG sites are shown by *open circles*. The first base of exon1 was defined+1

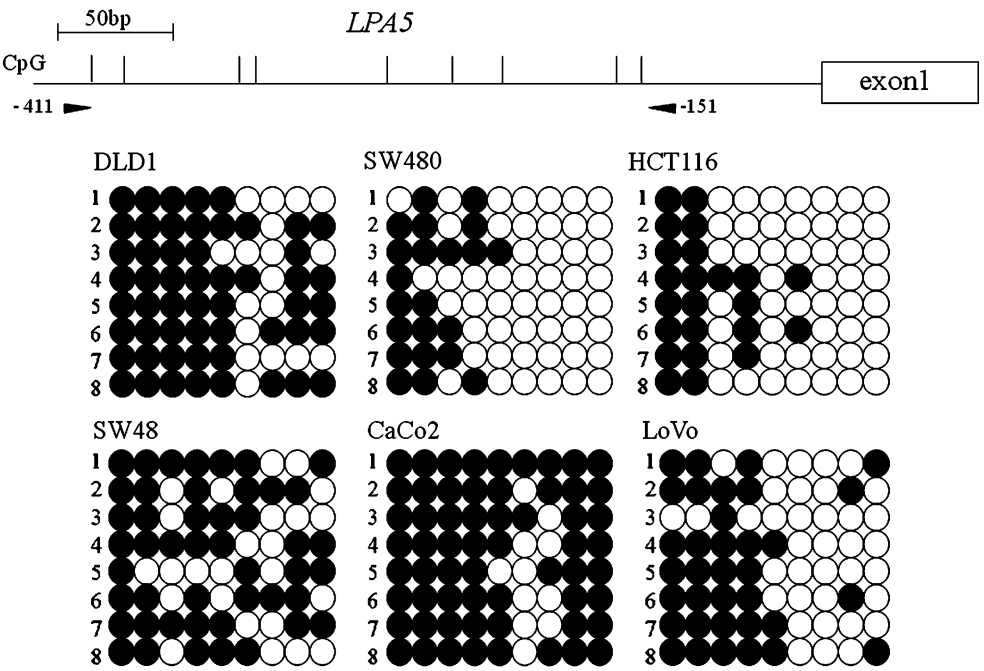

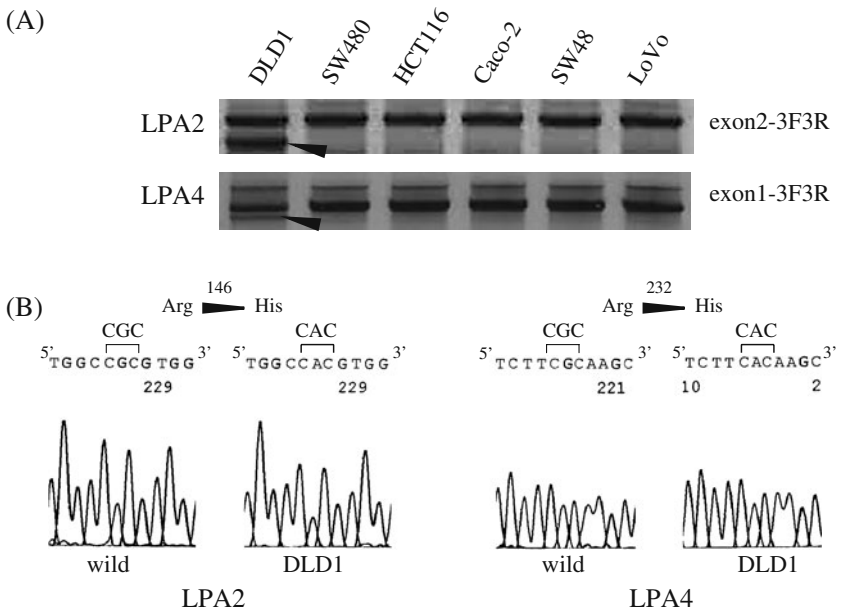

Fig. 6 Mutation of the LPA receptor genes in human colon cancer cells. **a** Representative results of PCR–SSCP analysis. The *arrowhead* indicates an abnormal band shift. **b** The mutation patterns of the LPA2 and LPA4 genes detected by the sequencing analysis

0.05% bromophenol blue. Aliquots containing 6 μl of diluted products were electrophoresed on polyacrylamide gels using a GeneGel Excel 12.5/24 kit (GE Healthcare UK, Ltd., Buckinghamshire, England) at 8°C, 15°C, 18°C, and 20°C for 90 min at 15 W, using a GenePhor Electrophoresis Unit (GE Healthcare UK Ltd.). After electrophoresis, the gels were stained with a DNA Silver Staining kit (GE Healthcare UK Ltd.).

Following the PCR–SSCP analysis, DNA fragments in abnormally shifted bands in the gel were extracted and re-amplified. The obtained PCR products were directly sequenced using a BigDye terminator v3.0 cycle sequencing ready reaction kit (Applied Biosystems Japan) and an ABI PRISM 310 genetic analyzer (Applied Biosystems Japan) [16, 17].

Results

A semi-quantitative RT–PCR analysis was performed to estimate expression levels of LPA receptor genes in colon cancer cells (Fig. 1). LPA1, LPA2, and LPA4 genes were expressed in all cell lines. By contrast, the LPA3 gene was highly expressed in HCT116 cells while no or weak expressions were found in other cell lines. The LPA5 gene was highly or moderately expressed in SW480 and HCT116 cells, but was not or was weakly expressed in other cells. These diverse expression levels of LPA receptor genes were confirmed by real-time RT–PCR analysis (data not shown).

Since there are few CpG sites in the 5′ upstream region of the LPA4 gene, we next performed a bisulfite sequence analysis to measure the methylation status of LPA1 (between nucleotide (nt.) −398 and 6; 57 CpG sites), LPA2 (between nt. −284 and −49; 32 CpG sites), LPA3 (between nt. −339 and −106; 21 CpG sites), and LPA5 (between nt. −411 and −151; 9 CpG sites) genes. The LPA1 and LPA2 genes were unmethylated in all cell lines (Figs. 2, 3). The LPA3 gene was highly methylated in DLD1, SW48, and LoVo cells and moderately methylated in SW480 and CaCo2 cells but unmethylated in HCT116 cell (Fig. 4). The LPA5 gene was weakly methylated in SW480 and HCT116 cells but highly methylated in other cells (Fig. 5).

Mutation analysis was performed using with PCR–SSCP method. Representative results are shown in Fig. 6. Although no mutations of LPA1, 3, and 5 genes were found in all cell lines, LPA2 mutations were detected in DLD1 and SW48, and LPA4 mutation in DLD1. Using with sequence analysis, LPA2 mutations were a GTG to GTA (Val to Val) transition at codon 136 and a CGC to CAC (Arg to His) transition at codon 146 in DLD1 and a GTG to GTA (Val to Val) transition at codon 136 and a CCC to CTC (Pro to Leu) transition at codon 230 in SW48. LPA4 mutations were a CGC to CAC (Arg to His) transition

Table 2 Mutations of LPA receptor genes in human colon cancer cells

Cells	LPA2	LPA4
DLD1	136 GTG to GTA (Val to Val)	232 CGC to CAC (Arg to His)
	146 CGC to CAC (Arg to His)	
SW48	230 CCC to CTC (Pro to Leu)	N.D.
	136 GTG to GTA (Val to Val)	

N.D. not detected

at codon 232 in DLD1. These results are summarized in Table 2.

Discussion

In the present study, the diverse expression levels of the LPA receptor genes due to DNA methylation were indicated in human colon cancer cells as well as LPA2 and LPA4 gene mutations, demonstrating that the alterations of the LPA receptor genes may play some roles in the pathogenesis in colon cancer cell.

Human cancer cell lines have been reported to show different expression patterns of the LPA receptor genes and different cellular responses to LPA. In ovarian cancer cells, the expression levels of the LPA1 gene were various while the expression levels of the LPA2 and LPA3 genes were markedly higher than those in normal ovarian epithelial cells [2, 6, 7]. The ovarian cancer cells with a high expression of LPA1 indicated a lower proliferative response to LPA [6]. Moreover, the increased LPA1 expressions induced cell death through apoptosis and anoikis in ovarian cancer cells, suggesting that LPA1 may act as a negative regulator for cell growth [2]. In colon cancer cells, although the expression levels of LPA1 also varied, LPA stimulated cell migration, proliferation, and adhesion in the LPA1 expressed cells [14]. These findings demonstrated that LPA1 could mediate both positive and negative regulation to cell growth dependent on the type of cancer cells and circumstances [14]. In contrast, LPA enhanced cell proliferation and secretion of angiogenic factors but not cell migration or adhesion in the exclusively LPA2-expressed colon cancer cells [14]. Therefore, it is suggested that the expression pattern of LPA receptors may be related to clinical characteristics of cancer cells through the different responses to LPA [14].

Some expression patterns of the LPA receptor genes detected in this study differ from those in the previous study using the Northern blot analysis [14]. For example, although the LPA1 gene was unexpressed in SW480 and LpVo cells in the previous study [14], we found these cells well expressed in these cells, correlating with DNA methylation status. It seems that this discrepancy may be due to the difference of analysis to measure the expression levels.

Recently, we have found that frequent mutations of the LPA1 gene occurred in rat hepatocellular carcinomas [17]. Moreover, LPA1 gene mutations were also detected in not only lung adenocarcinomas but also preneoplastic lesions in rats [16]. In contrast, no mutations of the LPA2, LPA3, LPA4, and LPA5 genes were found in rat lung adenocarcinomas [22]. These findings suggest that the LPA1 gene mutations may play an important role in the development of rat tumor cells as well as aberrant LPA receptor gene expressions but not LPA2, LPA3, LPA4, and LPA5 mutations. In contrast, to our knowledge no investigation of LPA receptor gene mutations in human tumor cells has been reported. In the present study, the LPA2 and LPA4 gene mutations were found in DLD1 and SW48 cells, and these five mutations were all G/C to A/T transition. In rat lung and liver tumors, G/C to A/T transitions in the LPA1 gene mutations were not frequent in rat lung and liver tumors. Only two out of seven lung adenocarcinomas and one out of 15 hepatocellular carcinomas indicated G/C to A/T transitions [16, 17]. Therefore, it seems that the difference of mutation patterns of LPA receptor genes may be dependent on the tumor cell types or species.

Three missense mutations out of five mutations detected in this study were observed in the putative intracellular domain [1]. Although it remains to be clarified whether these mutations could affect the signaling pathway on LPA stimulation or show distinct affinity of LPA binding, the different responses to LPA in these colon cancer cells may be due to not only the different expression levels of LPA receptor genes but also mutational alterations. In fact, our previous study demonstrated that an artificial mutated form of LPA1 that lacked the carboxyl terminal was constitutively active and oncogenic [23].

In conclusion, we demonstrate that colon cancer cells used in this study will be available to understanding the molecular pathway through the LPA receptors in the development of tumor cells, and that LPA receptors may be new molecular targets for therapeutic approaches and chemoprevention. Recently, the sixth LPA receptor, LPA6, has been identified [24, 25]. To better understand an involvement of LPA receptor genes in the pathogenesis of cancer cells, we are currently investigating the biological significance of mutated LPA receptors combined with analyses for LPA receptor gene expressions and mutations in other human tumor cells.

Acknowledgments This study was supported in part by the Foundation for Promotion of Cancer Research in Japan, and a grant-in-aid (20591765) for scientific research from the Ministry of Education, Culture, Sports, Science and Technology of Japan and by grants (RK17-027, RK-027) from the Faculty of Science and Engineering, Kinki University.

Conflicts of interest statement We declare that we have no conflict of interest.

References

1. Contos JJA, Ishii I, Chun J (2000) Lysophosphatidic acid receptors. Mol Pharmacol 58:1188–1196
2. Furui T, LaPushin R, Mao M, Khan H, Watt SR, Watt MAV (1999) Overexpression of Edg-2/vzg-1 induces apoptosis and anoikis in ovarian cancer cells in a lysophosphatidic acid-independent manner. Clin Cancer Res 5:4308–4318

3. Goetzl EJ, Dolezalova H, Kong Y, Hu YL, Jaffe RB, Kalli KR, Conover CA (1999) Distinctive expression and functions of the type 4 endothelial differentiation gene-encoded G protein-coupled receptor for lysophosphatidic acid in ovarian cancer. Cancer Res 59:5370–5375
4. Contos JJA, Fukushima N, Weiner JA, Kaushal D, Chun J (2000) Requirement for the lpA1 lysophosphatidic acid receptor gene in normal suckling behavior. Proc Natl Acad Sci USA 97:13383–13389
5. Contos JJA, Ishii I, Fukushima N, Kingsbury MA, Ye X, Kawamura S, Brown JH, Chun J (2002) Characterization of lpa (2) (Edg4) and lpa(1)/lpa(2) (Edg2/Edg4) lysophosphatidic acid receptor knockout mice: signaling deficits without obvious phenotypic abnormality attributable to lpa(2). Mol Cell Biol 22:6921–6929
6. Fang X, Schummer M, Mao M, Yu S, Tabassam FH, Swaby R, Hasegawa Y, Tanyi JL, LaPushin R, Eder A, Jaffe R, Erickson J, Mills GB (2002) Lysophosphatidic acid is a bioactive mediator in ovarian cancer. Biochim Biophys Acta 1582:257–264
7. Fujita T, Miyamoto S, Onoyama I, Sonoda K, Mekada E, Nakano H (2003) Expression of lysophosphatidic acid receptors and vascular endothelial growth factor mediating lysophosphatidic acid in the development of human ovarian cancer. Cancer Lett 192:161–169
8. An S, Bleu T, Halmark OG, Goetzl EJ (1998) Characterization of a novel subtype of human G protein-coupled receptor for lysophosphatidic acid. J Biol Chem 273:7906–7910
9. Bandoh K, Aoki J, Hosono H, Kobayashi S, Kobayashi T, Murakami-Murofushi K, Tsujimoto M, Arai H, Inoue K (1999) Molecular cloning and characterization of a novel human G-protein-coupled receptor, EDG7, for lysophosphatidic acid. J Biol Chem 274:27776–27785
10. Noguchi K, Ishii S, Shimizu T (2003) Identification of p2y9/GPR23 as a novel G protein-coupled receptor for lysophosphatidic acid, structurally distant from the Edg family. J Biol Chem 278:25600–25606
11. Lee CW, Rivera R, Gardell S, Dubin AE, Chun J (2006) GPR92 as a new G12/13 and Gq coupled lysophosphatidic acid receptor that increases cAMP: LPA5. J Biol Chem 281:23589–23597
12. Lin M-E, Herr DR, Chun J (2010) Lysophosphatidic acid (LPA) receptors: signaling properties and disease relevance. Prostaglandins Other Lipid Mediat 91:130–138
13. Schulte KM, Beyer A, Kohrer K, Oberhauser S, Roher HD (2001) (2001) Lysophosphatidic acid, a novel lipid growth factor for human thyroid cells: over-expression of the high-affinity receptor edg4 in differentiated thyroid cancer. Int J Cancer 92:249–256
14. Shida D, Kitayama J, Yanaguchi H, Okaji Y, Tsuno NH, Watanabe T, Takuwa Y, Nagawa H (2003) Lysophosphatidic acid (LPA) enhances the metastatic potential of human colon carcinoma DLD1 cells through LPA1. Cancer Res 63:1706–1711
15. Shida D, Watanabe T, Aoki J, Hama K, Kitayama J, Sonoda H, Kishi Y, Yamaguchi H, Sasaki S, Sako A, Konishi T, Arai H, Nagawa H (2004) Aberrant expression of lysophosphatidic acid (LPA) receptors in human colorectal cancer. Lab Invest 84:1352–1362
16. Yamada T, Furukawa M, Hotta M, Yamasaki A, Honoki K, Fukushima N, Tsujiuchi T (2009) Mutations of lysophosphatidic acid receptor-1 gene during progression of lung tumors in rats. Biochem Biophys Res Commun 378:424–427
17. Obo Y, Yamada T, Furukawa M, Hotta M, Honoki K, Fukushima N, Tsujiuchi T (2009) Frequent mutations of lysophosphatidic acid receptor-1 gene in rat liver tumors. Mutat Res 660:47–50
18. Zingg JM, Jones PA (1997) Genetic and epigenetic aspects of DNA methylation on genome expression, evolution, mutation and carcinogenesis. Carcinogenesis 18:869–882
19. Jones PA, Baylin SB (2002) The fundamental role of epigenetic events in cancer. Nat Rev Genet 3:415–428
20. Jones PA (2002) DNA methylation and cancer. Oncogene 21:5358–5360
21. Tsujiuchi T, Shimizu K, Onishi M, Sugata E, Fujii H, Mori T, Honoki K, Fukushima N (2006) Involvement of aberrant DNA methylation on reduced expression of lysophosphatidic acid receptor-1 gene in rat tumor cell lines. Biochem Biophys Res Commun 349:1151–1155
22. Wakabayashi N, Tsujino M, Tajiri M, Taki M, Koshino A, Ikeda H, Fukushima N, Tsujiuchi T (2010) No mutations of lysophosphatidic acid receptor genes in lung adenocarcinomas induced by N-nitrosobis(2-hydroxypropyl)amine in rats. J Toxicol Pathol 23:63–66
23. Shano S, Hatanaka K, Ninose S, Moriyama R, Tsujiuchi T, Fukushima N (2008) A lysophosphatidic acid receptor lacking the PDZ-binding domain is constitutively active and stimulates cell proliferation. Biochim Biophys Acta 1783:748–759
24. Shimomura Y, Wajid M, Ishii Y, Shapiro L, Petukhowa L, Gordon D, Christiano AM (2008) Disruption of P2RY5, an orphan G protein-coupled receptor, underlies autosomal recessive woolly hair. Nat Genet 40:335–339
25. Pasternack SM, von Kügelgen I, Aboud KAJ, Lee Y-A, Rüschendorf F, Voss K, AHillmer AM, Molderings GJ, Franz T, Ramirez A, Nürnberg P, Nöthen MM, Berz RC (2008) G protein-coupled receptor P2Y5 and its ligand LPA are involved in maintenance of human hair growth. Nat Genet 40:329–334

Virchows Arch (2010) 457:677–692
DOI 10.1007/s00428-010-0980-y

ORIGINAL ARTICLE

Stromal impact on tumor growth and lymphangiogenesis in human carcinoma xenografts

Elin Hadler-Olsen · Hilde Ljones Wetting · Oddveig Rikardsen · Sonja E. Steigen · Premasany Kanapathippillai · Reidar Grénman · Jan-Olof Winberg · Gunbjørg Svineng · Lars Uhlin-Hansen

Received: 17 June 2010 / Revised: 10 August 2010 / Accepted: 12 September 2010 / Published online: 3 October 2010
© The Author(s) 2010. This article is published with open access at Springerlink.com

Abstract Squamous cell carcinomas (SCCs) arising in the oral cavity are associated with poor survival, mainly due to metastatic disease. In contrast, skin SCCs rarely metastasize and are usually curable. To study influence of tongue and skin stroma on cancer growth and induction of lymphangiogenesis, xenograft tumors of human carcinoma cells were established either in tongue or skin of BALB/c nude mice. Two oral and two skin SCC cell lines were used, as well as an endometrial adenocarcinoma cell line. Tongue tumors established from all cell lines were larger than corresponding skin tumors. Peritumoral lymphatic vessel density was up to five times higher in tongue than in corresponding skin tumors, and mRNA level of the lymphangiogenic growth factor vascular endothelial growth factor (VEGF)-C was twice as high in tongue tumors compared with corresponding skin tumors. Contrary to lymphatic vessel density, blood vessel density was higher in skin tumors than in tongue tumors. In a cohort of patient samples, lymphatic vessel density was found to be higher in tongue SCCs compared with skin SCCs, supporting a clinical relevance of our findings. Our results show that the tumor stroma has a profound impact on cancer growth and induction of lymphangiogenesis and angiogenesis. The difference in lymphatic vessel density between tongue and skin tumors may be important in directing metastatic potential of tumors arising in these organs.

Keywords Mouse model · Orthotopic · Oral cancer · Skin cancer · Lymphangiogenesis · Angiogenesis

E. Hadler-Olsen (✉) · P. Kanapathippillai · J.-O. Winberg · G. Svineng · L. Uhlin-Hansen
Department of Medical Biology, Faculty of Health Sciences, University of Tromsø, 9037 Tromsø, Norway
e-mail: elin.hadler-olsen@uit.no

H. L. Wetting
Department of Pharmacy, Faculty of Health Sciences, University of Tromsø, Tromsø, Norway

O. Rikardsen
Ear, Nose and Throat Department, University Hospital North Norway, Tromsø, Norway

S. E. Steigen · L. Uhlin-Hansen
Department of Pathology, University Hospital North Norway, Tromsø, Norway

R. Grénman
Department of Otorhinolaryngology, Head and Neck Surgery, University of Turku and Turku University Hospital, Turku, Finland

Introduction

Squamous cell carcinomas (SCCs) can arise in various locations of the body, including skin, oral mucosa, esophagus, lungs and cervix, but the tumor aggressiveness is dependent on the "host" organ. Oral SCCs are characterized by an aggressive behavior and associated with a low 5-year survival rate, mainly because of metastatic disease [1, 2]. In contrast, skin SCCs seldom metastasizes, and most patients have a very good prognosis [3].

It is well recognized that cancer growth and progression are strongly influenced by the non-malignant part of the tumor, the tumor stroma, which is composed of an extracellular matrix (ECM) and various cells types such as fibroblasts, smooth muscle cells, endothelial cells and inflammatory cells [4]. Malignant cells communicate with and modify their microenvironment through the release of

various molecules, as well as by cell–cell and cell–matrix contacts. When stimulated, the stromal cells influence cancer progression by producing growth factors and proteases that modulate growth, apoptosis, angiogenesis, lymphangiogenesis, invasion and metastasis [5, 6].

The importance of angiogenesis in cancer progression is well documented [7]. Less focus has been on the role of lymphangiogenesis, although SCCs mainly metastasize via lymphatic vessels [8]. The lack of reliable markers of lymphatic endothelial cells has held back studies on lymphangiogenesis, but recently more specific markers have been identified which have given rise to increased knowledge of the role of the lymphatic system in cancer [9–11]. Many cancer types, such as melanomas, oral, cervical, and non-small cell lung cancers can induce lymphangiogenesis, and lymphatic vessel density is often correlated with metastases and poor survival [12–15].

A large number of cytokines and growth factors are reported to affect angiogenesis and lymphangiogenesis. Vascular endothelial growth factor (VEGF)-C and VEGF-D are important lymphangiogenic growth factors [16, 17], mediating proliferation, survival and increased migration of cultured human lymphatic endothelial cells [17]. VEGF-C knockout mice die in utero due to a complete lack of lymphatic vessels and subsequent accumulation of fluid in the tissues [16]. The VEGF-C deficient phenotype can be rescued by VEGF-D [16], indicating an overlapping function of these growth factors. Both factors are secreted from various cell types in an active form that can bind their principal receptor, VEGFR-3. In normal adult tissue, this receptor is restricted to lymphatic endothelial cells, but can also be expressed on tumor vascular endothelial cells [10, 18–20]. In the extracellular environment VEGF-C and VEGF-D can be processed by proteases to a mature form with higher affinity for VEGFR-3 [19, 21].

In order to investigate the role of the stroma for tumor growth and lymphangiogenesis, we established a xenograft model in which different human carcinoma cell lines were injected in the tongue or the skin of BALB/c nude mice. Cancer cells are reported to grow faster and be more aggressive in the orthotopic environment compared with a heterotopic environment [22, 23]. To control for this effect, we used cell lines established from skin and tongue SCCs, as well as an endometrial adenocarcinoma cell line. Independently of orthotopic or heterotopic growth of the tumor cells, we found that the tumor stroma had a strong impact on several aspects of tumor progression, including growth and lymphangiogenesis.

Materials and methods

Cell lines and culturing

The human cancer cell lines and culture media used are listed in Table 1. The HSC-4 cell line was a kind gift from Professor M. Yanagishita, Tokyo Medical and Dental University, Japan. The establishment of the UT-SCC-7 and UT-SCC-12A cell lines is done as described in Grénman et al. [24]. The SCC-25 cell line was purchased from ATCC (Manassas, VA), and the Ishikawa cells from Sigma-Aldrich (St. Louis, MO). All cell lines were incubated in a humidified atmosphere of 5% CO_2 at 37°C.

Animals and establishment of xenograft tumors

To determine a suitable number of cells to be injected, pilot studies were performed. A concentration of 300,000 cells in 25 μl 0.9% NaCl was chosen. Cultured cells were detached by trypsin treatment (0.25% in PBS with 0.05% Na_2EDTA), washed once in serum containing cell culture medium, once in 0.9% NaCl and thereafter resuspended in 0.9% NaCl at a concentration of 12 million cells/ml. Six- to 8-week-old BALB/c nude mice (Harlan Laboratories,

Table 1 Cell lines and culture media

Cell line	Origin	Medium
SCC-25	Tongue SCC	DMEM/HamF-12, 10% FBS, 0.5 mM L-glutamine, 50 U penicillin and 50 μg/ml streptomycin, 400 ng/ml hydrocortisone
HSC-4	Lymph node metastasis of tongue SCC	DMEM, 10% FBS, 0.5 mM L-glutamine, 50 U penicillin and 50 μg/ml streptomycin
UT-SCC-12A	Skin SCC, nose	DMEM, 10% FBS, 0.5 mM L-glutamine, 50 U penicillin and 50 μg/ml streptomycin, 0.1 mM non-essential amino acids
UT-SCC-7	Lymph node metastasis of skin SCC, regio temporalis	DMEM, 10% FBS, 0.5 mM L-glutamine, 50 U penicillin and 50 μg/ml streptomycin, 0.1 mM non-essential amino acids
Ishikawa	Endometrial adenocarcinoma	RPMI 1640, 10% FBS, 0.5 mM L-glutamine, 50 U penicillin and 50 μg/ml streptomycin

Indianapolis, IN) were anaesthetised with a mixture of 0.5 mg ketamine and 0.1 mg xylazine hydrochloride subcutaneously before 25 μl of cancer cell suspension was injected into the anterior part of the tongue or subcutaneously on the abdomen. For each cell line tongue tumors were established in 12 mice and skin tumors in 12 mice, except for the UT-SCC-7 cell line from which six tongue and six skin tumors were established. The mice were weighed every second day to ensure that they did not lose more than 10% of their body weight, and were sacrificed with CO_2 after 5–28 days. Tumors were either fixed in a Zn-based fixative (ZBF) (36.7 mM $ZnCl_2$, 27.3 mM $ZnAc_2 \times 2H_2O$ and 0.63 mM $CaAc_2$ in 0.1 mol/l Tris pH 7.4) or submerged in RNAlater (Sigma-Aldrich St. Louis, MO) immediately after the mice were sacrificed. Draining lymph nodes were fixed in ZBF, whereas liver and lungs were fixed in 4% neutral buffered formalin (NBF). Blood samples were collected, mixed with heparin (15 U/ml heparin blood) and centrifuged at 11,000×*g* for 5 min before plasma was isolated. The project was approved by the Norwegian Animal Research Authority.

Metastasis

ZBF-fixed lymph nodes were paraffin embedded, sectioned and H/E-stained to look for metastases. The presence of metastases was confirmed by immunohistochemical staining with a pan cytokeratin antibody (Zymed laboratories, purchased from Invitrogen, Carlsbad, CA). NBF-fixed livers and lungs were sliced and examined for metastases under a dissecting microscope. In addition, lymphatic permeation of cancer cells was assessed on sections of tongue and skin tumors of the various cell lines immunohistochemically stained with the lymphatic endothelial cell marker Lyve-1. The sections/samples were scored as positive if clusters of cancer cells were found within one or more lumens with Lyve-1-positive lining.

Tumor size

ZBF-fixed tongue and skin tumors were dehydrated, paraffin embedded (oriented in the same way) and serially sectioned to measure the size of the tumors. During sectioning, the area of the tumor was studied in a light microscope (Leica DM2000, Leica, Wetzlar, Germany). The sections with the largest tumors were H/E stained, and the tumor area was accurately measured using a Leica Application Suite Interactive measurement tool (Leica, Wetzlar, Germany). The mean area was calculated based on the five largest tumors in tongue and skin of each cell line, except for the HSC-4 cell line where only three detectable skin tumors were found at each time point. Tumor size was measured after 28 days of in vivo growth for all cell lines except the UT-SCC-12A cell line for which tumors were measured after 15 days of in vivo growth.

Immunohistochemistry

Four-micrometer thick sections of ZBF-fixed, paraffin-embedded tissue from the mouse xenograft model or of formalin-fixed human tongue or skin SCCs on Superfrost Plus slides were analyzed by immunohistochemistry. The antibodies, dilutions and incubation conditions are listed in Table 2. Horseradish peroxidase (HRP)-labeled secondary antibody and diaminobenzidine (DAB)-substrate (EnVision$^+$ system-HRP for rabbit primary antibodies, Dako, Glostrup, Denmark or Ventana XT Ultra View Universal DAB, Tucson, AZ) were used for visualization. Immunohistochemistry was performed as previously described [25]. The CD31 and CD68 antibodies were monoclonal rat anti-mouse antibodies, and immunohistochemical procedure for these antibodies included a linking rabbit anti-rat antibody (Dako 1:400). Sections where primary antibody was omitted and replaced by 1.5% normal goat serum were used as negative controls. Staining for

Table 2 Antibodies

Antibody	Dilution	Incubation
Rabbit anti-bovine cytokeratin(Pan) pab, Zymed Laboratories # 08-0059	Predilute	1 h RT
Rabbit anti-human PHH-3 pab, Millipore # 06-570	1:500	32 min., RT
Rabbit anti-human caspase-3 active pab, R&D systems # AF835	1:900	30 min., RT
Rat anti-mouse CD-31 mab, BD Pharmingen #550274	1:10	ON, 4°C
Rabbit anti-mouse Lyve-1 pab, AbCam # ab14917	1:1,000	30 min., RT
Mouse anti-human D2-40, Dako # M3619	1:25	32 min., RT
Rabbit anti-human VEGF-C pab, Zymed Laboratories # 182255	1:150	ON, 4°C
Rabbit anti-human VEGF-D pab, Santa Cruz # sc-13085	1:100	ON, 4°C
Rat anti-mouse CD-68 mab, AbCam # ab53444[a]	1:600	30 min., RT
Rabbit anti-rat immunoglobulins, Dako # E0468	1:400	30 min., RT

[a] Antigen retrieval 1.3 mg/ml Pepsin 30 min RT

Abbreviations: *RT* room temperature, *ON* over night

podoplanin (D2-40) and PHH-3 was performed using a Ventana (Tucson, AZ) automated immunohistochemical stainer according to the manufacturer's instructions. Unless otherwise specified, staining of xenograft tumors were performed on tumors after 28 days of in vivo growth for all cell lines except the UT-SCC-12A cell line from which tumors were analyzed after 15 days of in vivo growth.

Fraction of mitotic and apoptotic cells

To calculate the fraction of cells undergoing apoptosis and mitosis, immunohistochemical staining with the apoptotic marker active caspase-3, and the proliferation marker PHH3 were performed. Three apoptotic/mitotic hotspots were recognized at low power magnification (40×) in three parallel tongue and skin tumors of each cell line. The fraction of apoptotic and mitotic cells were determined by calculating the mean number of apoptotic or mitotic cells per total number of cells on photographs taken with a Leica DFC 420 camera on a Leica DM2000 microscope (Leica, Wetzlar, Germany) of the hotpots at high-power magnification (400×).

Determination of blood vessel density

Sections of normal tongue and skin tissue of BALB/c nude mice, as well as tongue and skin xenograft tumors of the various cell lines were stained with the vascular endothelial cell marker CD31. For each cell line mean vessel density (MVD) was calculated according to the method described by Weidner et al. [26]. Three vascular hotspots were recognized at low power magnification (40×) in three parallel tongue and skin tumors of each cell line. Lumens with CD31-positive lining were counted in each hotspot at 200× magnification to calculate the MVD. In addition, MVD was measured by counting lumens containing erythrocytes on H/E-stained sections. These calculations were performed the same way as the CD31 counting, except that five parallel tongue and skin tumors were evaluated for each cell line, and counting was performed at 400× magnification. Vessel density was calculated in the tumor and in the stromal tissue within a 0.5 mm radius from the outer border of a tumor island.

Determination of lymphatic vessel density

Sections of tongue and skin xenograft tumors of each cell line, as well as normal tongue and skin tissue of BALB/c nude mice, were stained with the lymphatic endothelial cell marker Lyve-1. Peritumoral lymphatic vessel density was calculated as the mean of three hotspots per section for at least three parallel tumors, as a modification of the method described by Weidner et al. [26]. Hotspots were recognized at low power magnification and counted at 200× magnification. Each hotspot had an area of 0.25 mm^2 and was located within a radius of 0.5 mm from the outer border of a tumor island. Only lymphatic vessels with an evident lumen were counted. Intratumoral lymphatic vessel density was calculated for tumors with intratumoral lymphatic vessels. Three visual fields containing hotspots were recognized per tumor and counted at 200× magnification. In addition, 21 skin and 21 tongue SCCs, randomly chosen from the archives of the Surgical Pathology Department at the University Hospital North Norway, were immunohistochemically stained with the lymphatic endothelial cell marker D2-40. For each tumor, three hotspots were recognized at 100× magnifications and counted at 200× magnification. The mean number of lymphatic vessels per visual field was calculated.

Immunohistochemical scoring of VEGF-C and VEGF-D

Immunohistochemical staining with antibodies against the lymphangiogenic growth factors VEGF-C and VEGF-D were scored according to Kobel et al. [27]. Staining intensity of the tumor cells was designated as non-existent (0), weak (1), moderate (2) or strong (3). The number of positive cells was scored as no cells stained (0), less than 10% (1), 10–50% (2), 51–80% (3) or more than 80% (4). The final score was calculated by multiplication of these two variables.

Quantification of VEGF-C and VEGF-D mRNA

Tumor samples were separated from stroma under a dissecting microscope and homogenized in a TissueLyzer homogenizer (Qiagen, Hilden, Germany) with 5-mm steal beads. Total RNA was extracted using RNeasy Fibrous Tissue Mini kit (Qiagen, Hilden, Germany) according to the manufacturer's instructions. On-column DNase treatment of the RNA samples was performed using Qiagen's RNase-Free DNase set according to the product manual. Quantity and purity of the extracted RNA was determined using the NanoDrop spectrophotometer (Thermo Fisher Scientific, Wilmington, DE), and RNA integrity was assessed using the Experion-automated electrophoresis system (Bio-Rad Laboratories, Hercules, CA). VEGF-C and VEGF-D mRNA expression levels were quantified by reverse transcription quantitative PCR (RT-qPCR) performed on a Stratagene Mx3000P instrument (Stratagene, La Jolla, CA). Primers for SYBR Green based assays were purchased from Qiagen (Hilden, Germany) (listed in Table 3). Primer specificities and absence of primer dimers were determined by SYBR Green melting curve analysis. Reverse transcription of

Table 3 QuantiTec primer assays from Qiagen

Gene symbol	Assay name	Cat.no	Amplicon length (bp)	RefSeq accession number
VEGF-C	Hs_VEGFC_1_SG	QT00061579	96	NM_005429
VEGF-D	Hs_FIGF_1_SG	QT00003997	138	NM_004469
ACT-B	Hs_ACTB_1_SG	QT00095431	146	NM_001101
TFRC	Hs_TFRC_1_SG	QT00094850	81	NM_001128148

total RNA was performed using Reverse Transcriptase Core Kit (Eurogentec, SA, Searing, Belgium) with random nonamer primers according to the manufacturer's recommendations, using 200 ng RNA per 10-μl cDNA reaction. cDNA corresponding to 20 ng RNA was amplified for 40 cycles in a 25-μl PCR mix (RT^2Real-Time™ SYBR Green/ROX PCR Master Mix (SA Biosciences, Frederick, MD)). Cycling conditions: 95°C for 10 min, 40 cycles at 95°C for 30 s and 60°C for 1 min. Duplicate reverse transcription reactions were performed for each RNA sample, and duplicate PCR analyses were performed on each cDNA sample. The absence of genomic DNA was confirmed by performing a no reverse transcription control, and absence of contaminations was assessed by including a no template control in every run. The delta–delta Ct method [28] was used to determine the relative amount of target gene in the tumor samples normalized against the average expression of the two reference genes *ACT-B* and *TFRC*.

Quantification of myeloid cells

CD68 staining was performed to evaluate proportion of macrophages, Langerhans cells and dendritic cells in the inflammatory infiltrate. The number of CD68-positive cells surrounding both tongue and skin tumors was very low, therefore no detailed scoring of this staining was performed. To evaluate number of mast cells in the inflammatory infiltrate, chemical staining with May–Grünwald–Giemsa was performed following standard procedures on three parallel tongue and skin tumors of each cell line. Three mast cell hotspots within a radius of 0.5 mm from the outer border of a tumor island were recognized in each section and counted at 400× magnification. Furthermore, an assessment of the inflammatory infiltrate was made on H/E-stained sections of tongue and skin tumors of the different cell lines. The extent of inflammatory reaction was assessed and scored as negligible (0), weak (1), moderate (2) or strong (3). The proportion of neutrophils in the inflammatory infiltrate was evaluated, based on morphological characteristics, and scored as <1% (0), 1–30% (1), 31–70% (2) or >70% (3). The number of neutrophils was then estimated by multiplication of these two variables.

Quantification of serum amyloid P in plasma

To measure the level of the major mouse acute phase protein serum amyloid P (SAP) in circulation, plasma from mice with tongue and skin tumors of the various cell lines were subjected to enzyme-linked immunoassay using a Mouse Serum Amyloid P ELISA kit (Kamiya Biomedical Company, Seattle, WA). Samples were diluted 1:10,000, and the assay was performed according to the product manual.

Statistics

Two-tailed *t* tests were used to evaluate differences between tongue and skin tumors for the different parameters analyzed. Data are presented as means±standard error of the mean (SEM). Independent replicates (*N*) for the different data are identified in tables and figure legends. *P* values <0.05 were accepted as statistically significant. Graphics and statistical analyses were performed using SPSS 15.0 for Windows.

Results

Tumors in tongue and skin of BALB/c nude mice were established by injecting 300,000 cancer cells at each site in separate animals. Five different human cell lines were used, two oral and two skin SCCs, as well as an endometrial adenocarcinoma cell line (Table 1). The mice were sacrificed 15 or 28 days after cancer cell injection, except for mice with tumors of the skin SCC cell line UT-SCC-12A. This cell line grew faster than the other cell lines in tongue, and therefore all mice with UT-SCC-12A tumors were sacrificed after 15 days.

All cell lines formed larger tumors in tongue than in skin

It is well known that tumor size is an important prognostic factor. To study how the microenvironment in the tongue and the skin affected tumor growth, we measured the size of the tumors as described in the "Materials and methods" section. This revealed that all cell lines formed larger tumors in the tongue than in the skin. The average area of the SCC-25, HSC-4 and UT-SCC-12A tongue tumors were seven to 17

times larger than the corresponding skin tumors, while the differences were smaller for tumors of the UT-SCC-7 and Ishikawa cell lines (Figs. 1 and 2). In addition to being smaller, the skin tumors of the UT-SCC-12A and HSC-4 cell lines often regressed spontaneously during the first 2 weeks. Although all mice had detectable tumors 1 week after injection, 14 out of 18 animals injected with UT-SCC-12A cells in the skin had detectable tumors after 14 days, and only nine out of 18 animals injected with HSC-4 cells in the skin had detectable tumors after 28 days. The number of cells injected in skin was raised to five million, but still the tumors often regressed during the first 2 weeks.

The fraction of mitotic and apoptotic cells was calculated for the skin and tongue tumors of the various cell lines, as a difference in one or both of these parameters would be expected based on the observed discrepancy in tumor size. For all cell lines a higher fraction of mitotic cells was seen in the tongue tumors compared with the skin tumors (Table 4), whereas the fraction of apoptotic cells showed only minor differences between the skin and tongue tumors for all cell lines (Table 5).

Lymph node metastases from tongue tumors were detected, but not from skin tumors

In general, oral SCCs are characterized by frequent lymph node metastases, while skin SCCs seldom metastasize. In tumors from our xenograft model, regional lymph node metastasis were detected in nine out of 18 of the tongue tumors of the skin SCC cell line UT-SCC-12A (Fig. 3a), and also from two out of 18 of the tongue tumors of the Ishikawa cell line. No metastases were detected from tongue tumors of the other cell lines or from any of the skin tumors. Lymphatic permeation of cancer cells was found in ten out of 31 evaluated tongue tumors (Fig. 3b) and in four out of 27 evaluated skin tumors stained with the lymphatic endothelial cell marker Lyve-1.

Blood vessel density was higher in skin tumors than in tongue tumors

Sections of the various tongue and skin tumors from our xenograft model were immunohistochemically stained with the vascular endothelial cell marker CD31 (Fig. 4a–d), and MVD determined in order to investigate if vascularisation was correlated to tumor size. Surprisingly, the skin tumors showed a higher MVD than the corresponding tongue tumors (data not shown). Within some tongue tumors there were endothelial cells that had lost CD31 positivity, evident as unstained tubular structures containing red blood cells (Fig. 4d). As this made the CD31-based calculations somewhat uncertain, MVD was also calculated by counting lumens containing erythrocytes on H/E-stained sections. These calculations confirmed the results obtained by counting CD31-positive tubular structures. The MVD for skin tumors of the UT-SCC-12A, UT-SCC-7 and Ishikawa cell lines were on average 2.3 times higher than for the corresponding tongue tumors, while smaller differences were seen between skin and tongue tumors of the SCC-25 and HSC-4 cell lines (Fig. 4e). MVD for tongue tumors of all cell lines pooled was significantly higher than MVD for skin tumors of all cell lines pooled (Fig. 4e). MVD was also calculated in normal tongue and skin, by counting CD31-positive tubular structures in hotspots in the anterior, free moving part of the tongue as well as in the

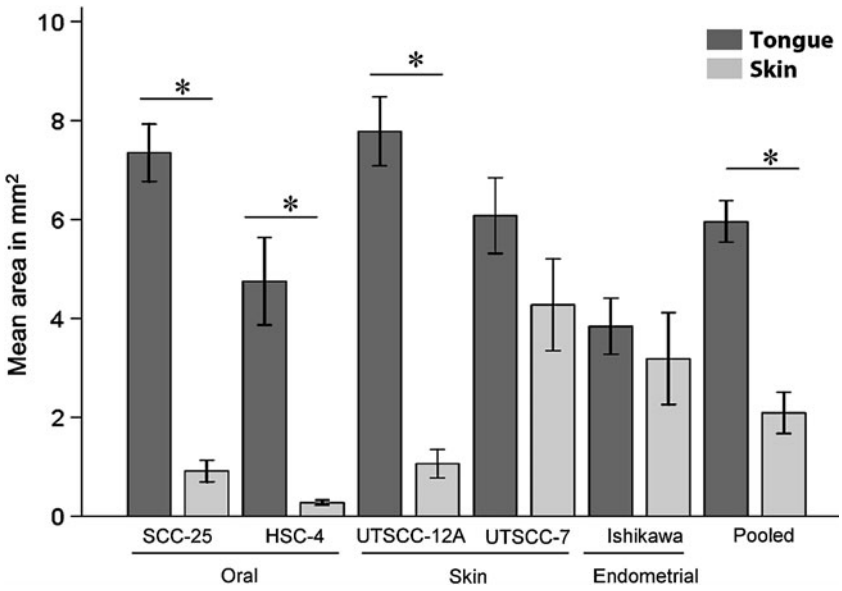

Fig. 1 Size of tongue and skin tumors. Graph shows mean area in mm^2 (±SEM) of tongue (*black bars*) and skin (*grey bars*) tumors of the various cell lines. $N=5$ for SCC-25, UT-SCC-12A, UT-SCC-7 and Ishikawa tumors. $N=3$ for skin tumors and $N=5$ for tongue tumors of the HSC-4 cell line. $N=25$ for pooled tongue tumors, and $N=23$ for pooled skin tumors of all cell lines. *$P<0.01$

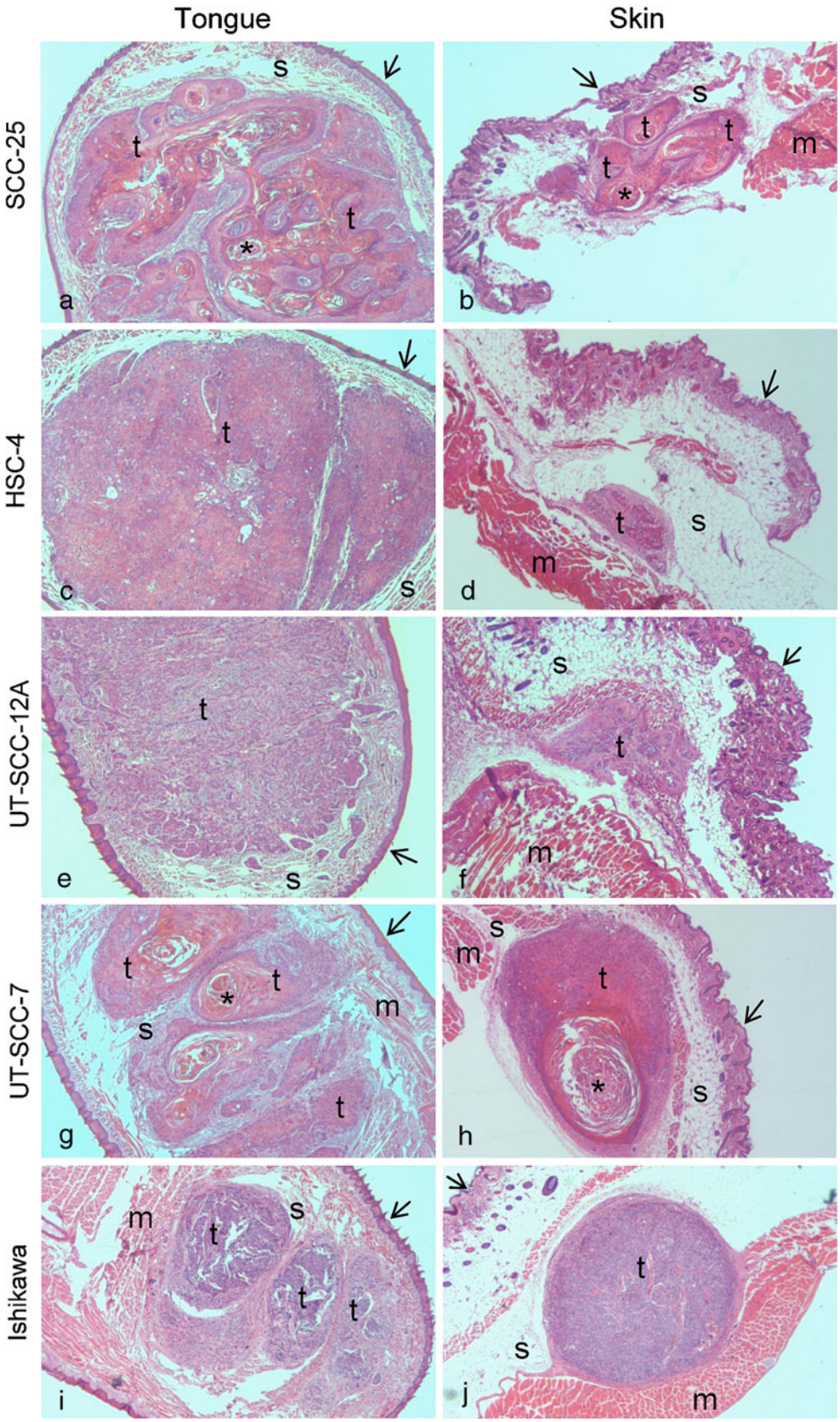

Fig. 2 H/E staining of tongue and skin tumors. H/E-stained sections of representative tongue tumors (**a**, **c**, **e**, **g** and **i**) and skin tumors (**b**, **d**, **f**, **h** and **j**) of the SCC-25 (**a** and **b**), HSC-4 (**c** and **d**), UT-SCC-12A (**e** and **f**), UT-SCC-7 (**g** and **h**) and Ishikawa (**i** and **j**) cell lines. Labeling indicates: *t* tumor, *s* stroma, *m* striated muscle, *asterisk* keratinous pearl; *arrow* surface epithelium. Original magnification, 100×

Table 4 Fraction of mitotic cells

Cell line	Mean±SEM		*P*
	Tongue	Skin	
SCC-25	46±10	30±4	0.341
HSC-4	26±13	14±1	0.455
UT-SCC-12A	58±4	15±4	0.001
UT-SCC-7	100±53	47±5	0.422
Ishikawa	66±9	51±8	0.257
Pooled	61±12	31±5	0.038

N=3 for all cell lines, except SCC-25 skin where *N*=2. *N*=15 for pooled tongue tumors and *N*=14 for pooled skin tumors

skin. This revealed that blood vessel density was similar in these two sites (data not shown).

Lymphatic vessel density was higher in tongue tumors than in skin tumors

Lymphatic vessel density is found to correlate with lymph node metastases in many cancers. We therefore investigated if lymphatic vessel density differed between tongue and skin tumors in our xenograft model. Tongue and skin tumors, as well as normal tongue and skin tissue of the mice, were immunohistochemically stained with the lymphatic endothelial cell marker Lyve-1 (Fig. 5a, b). Positive staining was seen in tubular structures. None of these contained red blood cells, supporting that these were lymphatic vessels. In the normal tongue and skin tissue of the mice, no difference in lymphatic vessel density was observed between the two different sites (results not shown). In the tumor tissue, lymphatic vessels were mainly seen in the stroma surrounding the tumor. In addition, intratumoral lymphatic vessels were seen in some tumors, primarily in the tongue. Peritumoral lymphatic vessel density was up to five times higher in tongue compared with skin tumors (Fig. 5c). Functional lymphatic vessels (containing a lumen) were almost completely absent surrounding the skin tumors of the oral SCC cell lines SCC-25 and HSC-4. The other cell lines seemed to be able to induce formation of new lymphatic vessels in association with the skin tumors, but to a much lesser extent than in the tongue. In the tongue, numerous lymphatic vessels surrounded the tumors. These vessels were often concentrated in hotspots towards the basis of the tongue. To study the time course of lymphangiogenesis, tongue tumors of the HSC-4 cell line were stained with Lyve-1 after 5, 10 and 15 days of tumor growth. Five days after cancer cell injection (Fig. 6a), the number of lymphatic vessels surrounding the tumors was about the same as in the normal tongue, while a marked increase was seen both within and surrounding the tumors from day 5 till days 10 and 15 after cancer cell injection (Fig. 6b, c).

In addition to staining of lymphatic vessels, some Lyve-1-positive single cells were seen in the tissue surrounding both tongue and skin tumors. Lyve-1 is reported to be expressed by tumor associated macrophages [29] and by high-endothelial venules of lymph nodes [30]. There is also evidence that lymphatic endothelial progenitor cells and multi-potent mesenchymal stem cells can contribute to formation of lymphatic vessels [31–34]. The Lyve-1-positive single cells may represent one or several of these cell types.

Table 5 Fraction of apoptotic cells

Cell line	Mean±SEM		*P*
	Tongue	Skin	
SCC-25	23±84	24±9	0.957
HSC-4	63±24	90±66	0.679
UT-SCC-12A	20±6	30±10	0.456
UT-SCC-7	18±5	13±5	0.555
Ishikawa	43±13	55±27	0.708
Pooled	35±7	40±12	0.689

N=2 for SCC-25 skin, HSC-4 skin and UT-SCC-7 tongue, *N*=3 for SCC-25 tongue, HSC-4 tongue, UT-SCC-12A tongue and skin, UT-SCC-7 skin and Ishikawa tongue and skin. *N*=14 for pooled tongue tumors and *N*=13 for pooled skin tumors

Increased expression of VEGF-C in tongue tumors

Three parallel tongue and skin tumors of each cell line were stained with antibodies against VEGF-C and VEGF-D to determine if different expression of these growth factors could explain the observed distinction in lymphatic vessel density between tongue and skin tumors from our xenograft model. Three parallel tongue and skin tumors of each cell line were stained with antibodies against VEGF-C and VEGF-D. In all tumors, staining for both growth factors was primarily seen in the cancer cells, but some stromal cells were also positive (Fig. 7). The staining varied between the parallels and no significant differences were observed between tongue and skin tumors of the various cell lines (data not shown).

To more precisely quantify the expression of VEGF-C and VEGF-D, the mRNA level of both growth factors was analyzed by RT-qPCR in five tongue tumors and four skin tumors of the Ishikawa cell line. The expression of VEGF-C mRNA was about twice as high in tongue tumors compared with skin tumors (2.1±0.37 (mean±SEM)), whereas no difference was found in the expression level of VEGF-D (data not shown).

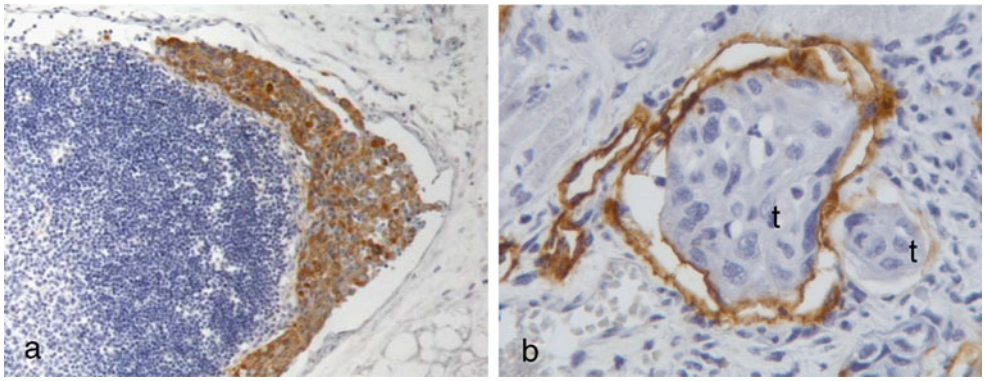

Fig. 3 Lymphatic metastases. **a** Lymph node metastases from a xenograft tongue tumor of the skin SCC cell line UT-SCC-12A immunohistochemically stained with cytokeratin. Cytokeratin staining is shown in *brown* and nuclei are stained *blue*. Original magnification, 100×. **b** Tongue lymphatic vessels immunohistochemically stained with Lyve-1 containing UT-SCC-12A tumor cells (labeled *t*). Lyve-1 staining is shown in *brown* and cell nuclei are stained *blue*. Original magnification, 400×

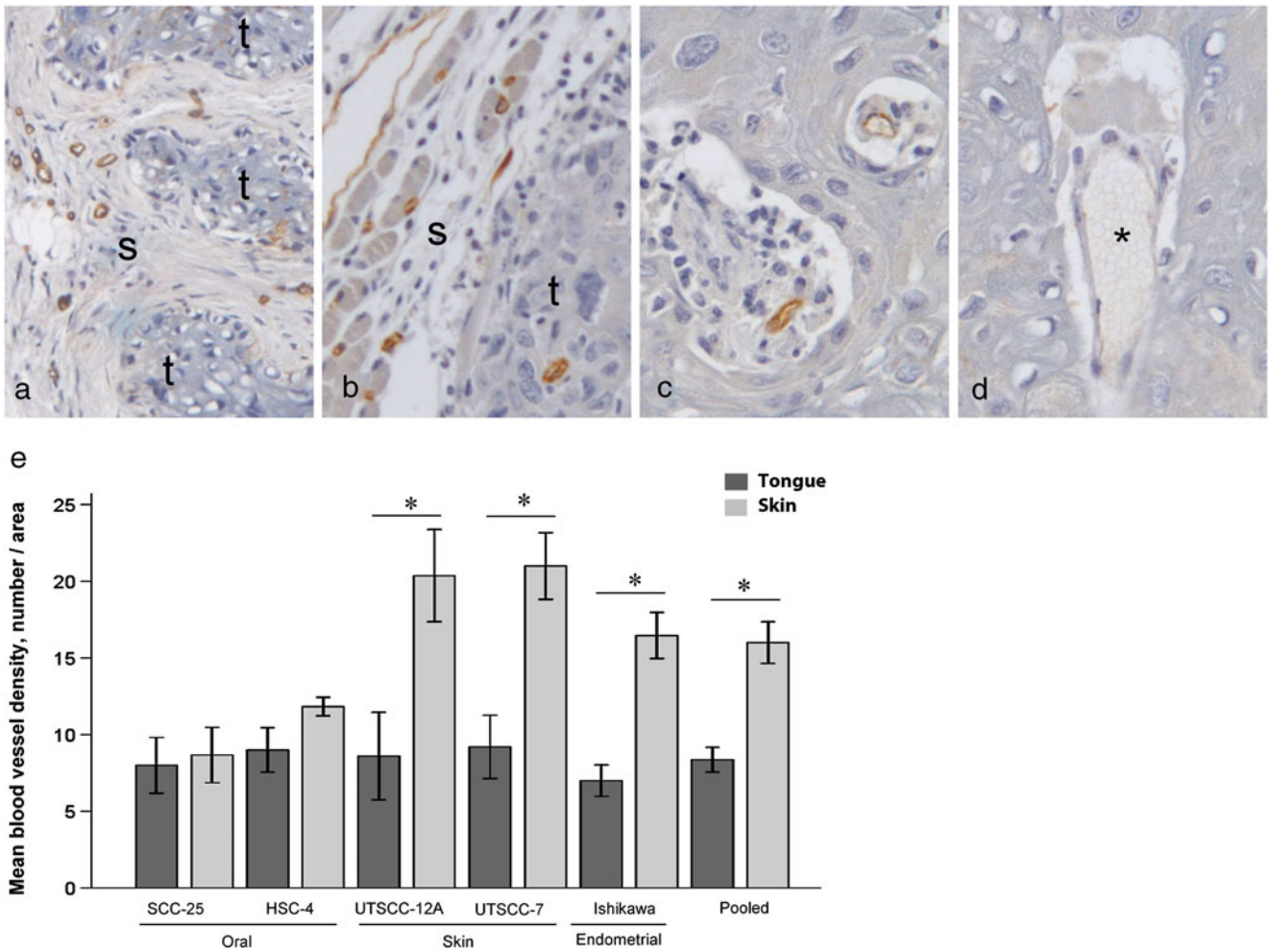

Fig. 4 Blood vessel density. *Pictures* show representative immunohistochemical CD31 staining of **a** skin tumor and **b** tongue tumor of the oral SCC cell line HSC-4. CD31 staining is shown in *brown* and cell nuclei are stained *blue*. Tumor and stromal areas are indicated with *t* and *s*, respectively. Original magnification, 100×. **c** CD31-positive blood vessels within intratumoral stromal tissue of a tongue tumor of the HSC-4 cell line. Original magnification, 400×. **d** CD31-negative blood vessel within the same tumor as in **c**). Blood vessel without CD31 staining is labeled with *asterisk*. Original magnification, 400×. **e** *Graph* shows mean blood vessel density (MVD; ±SEM) of tongue (*black bars*) and skin (*grey bars*) tumors of the different cell lines, calculated by counting lumens containing red blood cells. $N=5$ for SCC-25, UT-SCC-12A, UT-SCC-7 and Ishikawa tumors. $N=3$ for skin tumors and $N=5$ for tongue tumors of the HSC-4 cell line. $N=25$ for pooled tongue tumors, and $N=23$ for pooled skin tumors of all cell lines. *$P<0.05$

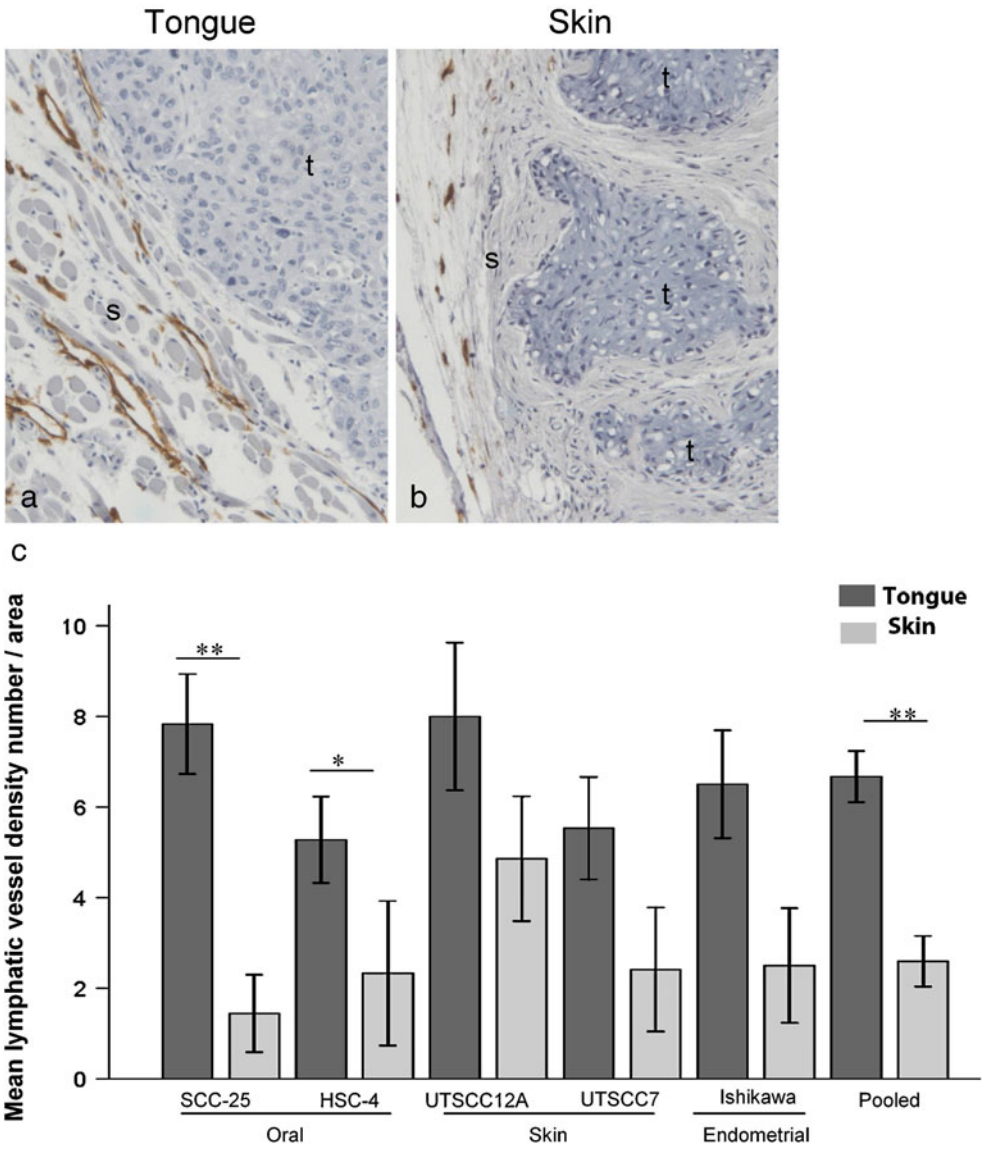

Fig. 5 Lymphatic vessel density. *Pictures* show representative immunohistochemical Lyve-1 staining of tumors of the HSC-4 cell line in **a** tongue and **b** skin. Lyve-1 staining is shown in brown and cell nuclei are stained blue. Tumor and stromal areas are indicated with *t* and *s*, respectively. Original magnification, 100×. **c** *Graph* shows peritumoral mean lymphatic vessel density (±SEM) of tongue (*black bars*) and skin (*grey bars*) tumors of the various cell lines as number of vessels per area. $N=6$ for SCC-25 and UT-SCC-12A tumors, $N=4$ for UT-SCC-7 and Ishikawa tumors. $N=6$ for HSC-4 tongue tumors, and $N=3$ for HSC-4 skin tumors. $N=26$ for pooled tongue tumors, and $N=24$ for pooled skin tumors of all cell lines. *$P<0.05$; **$P<0.005$

Human tongue SCCs have higher lymphatic vessel density than human skin SCCs

To investigate if the density of lymphatic vessels surrounding skin and tongue SCCs in humans showed the same pattern as in our mouse model, tumor tissue from patients with skin or tongue SCCs were immunohistochemically stained with the lymphatic endothelial cell marker podoplanin (D2–40) (Fig. 8). This revealed that lymphatic vessel density was significantly higher in tongue (17.9±1.8 (mean±SEM)) than in skin (10.7±1.1) tumors ($P=0.02$).

Increased number of inflammatory cells in tongue tumors compared with skin tumors in the xenograft model

It is well known that inflammatory mediators contribute significantly to tumor progression [35, 36]. We therefore studied the presence of different types of inflammatory cells in the tongue and skin tumors in our xenograft model. For all cell lines the inflammatory infiltrate was more pronounced in tongue tumors compared with the corresponding skin tumors. The number of neutrophils was determined by morphological evaluation of H/E-stained sections of skin and tongue tumors. The number of neutrophils was two to three times higher in tongue tumors compared with the corresponding skin tumors (Fig. 9a). The number of tumor associated mast cells, assessed by May–Grünwald–Giemsa staining, were also higher in tongue tumors compared with skin tumors for all cell lines, except the UT-SCC-7 cell line where the opposite was seen (Table 6). The number of macrophages, Langerhans and dendritic cells, assessed by CD68-positive cells, was low in both tongue and skin, and further quantification was therefore not performed.

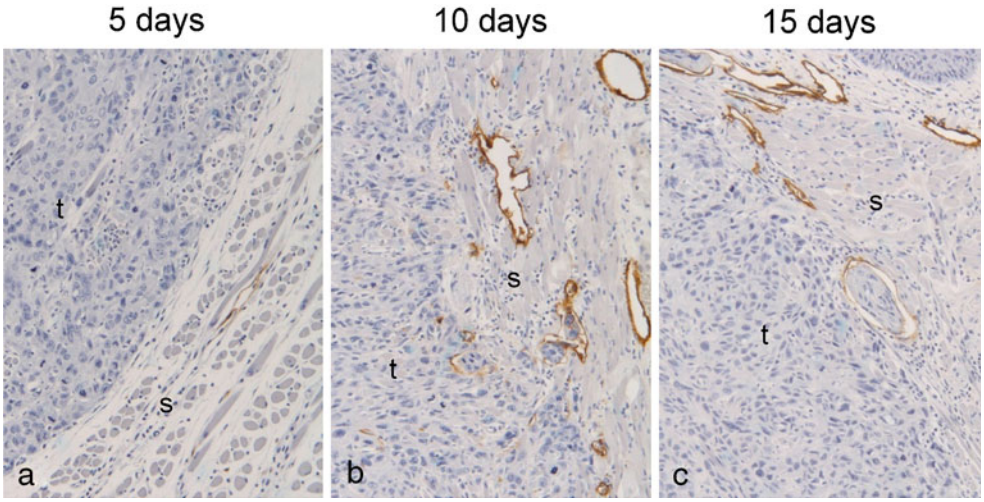

Fig. 6 Lymphangiogenesis. *Pictures* show representative immunohistochemical Lyve-1 staining of tongue tumors of the HSC-4 cell line after **a** 5 days, **b** 10 days and **c** 15 days. Lyve-1 staining is shown in *brown* and cell nuclei are stained *blue*. Tumor and stromal areas are indicated with *t* and *s*, respectively. Original magnification, 100×

SAP is a major acute phase protein in mice. To investigate if the intensity of the tumor associated inflammation was reflected in the level of this protein, ELISA was used to quantify SAP in plasma from the tumor bearing mice. This revealed that mice with tongue tumors of all cell lines had a slight but consistently higher plasma level of SAP than mice with corresponding skin tumors (Fig. 9b).

Discussion

Oral cancers mainly metastasize via lymphatic vessels to regional lymph nodes, and there is a well-established association between lymphatic vessel density, lymph node metastases and overall prognosis for oral cancers [13, 37]. It is known that the tumor stroma has a profound impact on

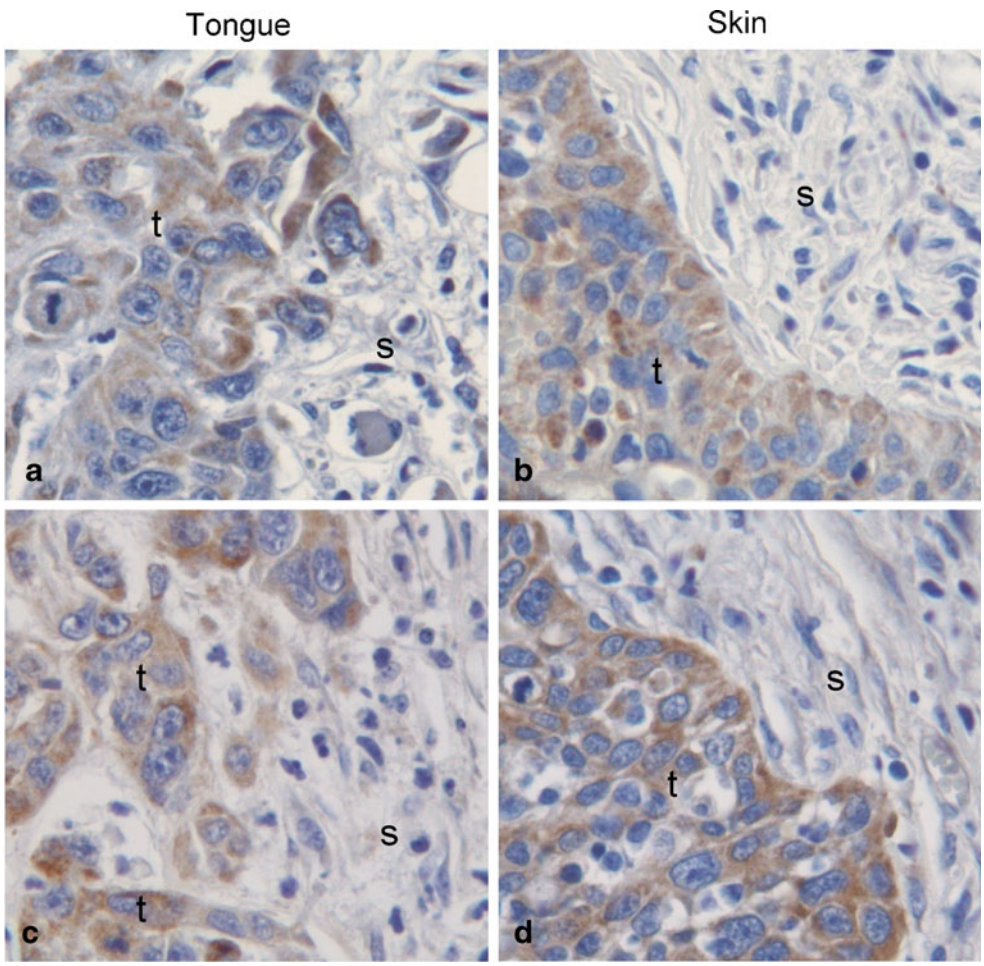

Fig. 7 Lymphatic endothelial growth factors. *Pictures* show representative immunohistohemical staining with antibodies against VEGF-C (**a** and **b**) and VEGF-D (**c** and **d**) of tumors of the UT-SCC-12A cell line in tongue (**a** and **c**) and skin (**b** and **d**). VEGF-C/-D staining is shown in *brown* and cell nuclei are stained *blue*. Tumor and stromal areas are indicated with t and s, respectively. Original magnification, 400×

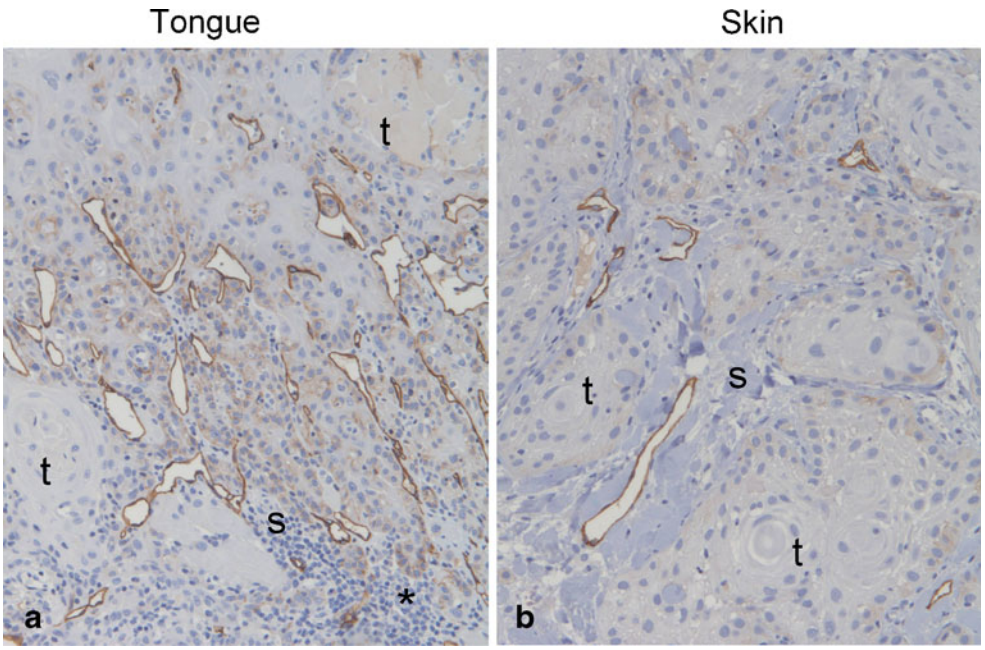

Fig. 8 Lymphatic vessels in human SCCs. *Pictures* show representative immunohistochemical staining with antibody against podoplanin (D2-40) of tumor tissue from patients with tongue SCC (**a**) and skin SCC (**b**). Podoplanin staining is shown in brown and cell nuclei are stained blue. Tumor and stromal areas are indicated with *t* and *s*, respectively, *asterisks* indicate area with prominent inflammatory infiltrate. Original magnification, 100×

many aspects of cancer development and progression. Lymphangiogenetic growth factors can be produced both by tumor cells and stromal cells, although little is known about the significance of tumor–stroma interactions for lymphangiogenesis. Our xenograft model is well suited for investigating stromal influence on this process. We found that the lymphatic vessel density was much higher in tongue tumors of all cell lines than in the corresponding skin tumors. In the skin, there was a remarkable lack of lymphatic vessels surrounding the majority of the tumors. Those that were seen were mostly located in the subepithelial connective tissue and probably represented preexisting vessels. In general, the tongue tumors were larger than the skin tumors, and this could possibly contribute to the stronger induction of lymphangiogenesis in tongue tumors compared with skin tumors. However, the size differences between tongue and skin tumors of the Ishikawa and the UT-SCC-7 cell lines were rather small, but still the tongue tumors induced much more lymphatic vessel formation than the skin tumors. Therefore, it does not appear to be any significant correlation between tumor size and lymphangiogenesis in our model.

Many aspects of the molecular mechanisms of lymphangiogenesis are obscure. The best established inducers of lymphangiogenesis are the growth factors VEGF-C and VEGF-D, which can be produced by both tumor and stromal cells. These growth factors mainly signal through the VEGFR-3 receptor found on lymphatic endothelial cells and induce proliferation and migration of these cells [17, 38, 39]. Blocking VEGFR-3 signaling has been shown in many studies to inhibit lymphangiogenesis, indicating that the VEGF-C/-D–VEGFR-3 signaling axis is essential for formation of new lymphatic vessels [40, 41]. In the present study, we found that the mRNA level of VEGF-C was twice as high in tongue tumors compared with the corresponding skin tumors. Immunohistochemical staining for VEGF-C and VEGF-D showed no significant difference in staining intensity between tongue and skin tumors. This discrepancy in results at mRNA and protein level may be due to the different sensitivities of the two methods.

VEGF-C and VEGF-D are secreted in an active form that can bind VEGFR-3. However, they can be further processed by proteases in the extracellular environment to a mature form with higher affinity for VEGFR-3 [21, 42]. There was a more prominent inflammatory reaction surrounding the tongue tumors compared with the skin tumors, where neutrophils and mast cells comprised a high proportion of the inflammatory cells. These cell types are known to produce a number of proteolytic enzymes, including MMP-2, MMP-9, MMP-25, tryptases and chymases [43–45]. Higher levels of such proteases in tongue tumors than in skin tumors may result in an increased proteolytic processing of VEGF-C and VEGF-D to the more active forms, and subsequent enhanced lymphangiogenetic signaling in the tongue. In a separate study using the same xenograft model, we have actually shown a significantly increased proteolytic activity in tongue tumors compared with skin tumors [46]. Proteolytic activity is also fundamental for cell migration and for the tissue remodeling required for formation of new vessels [47].

Our analysis of tumors from patients with oral and skin SCCs showed that lymphatic vessel density was significantly higher in tongue compared with skin SCCs (Fig. 8),

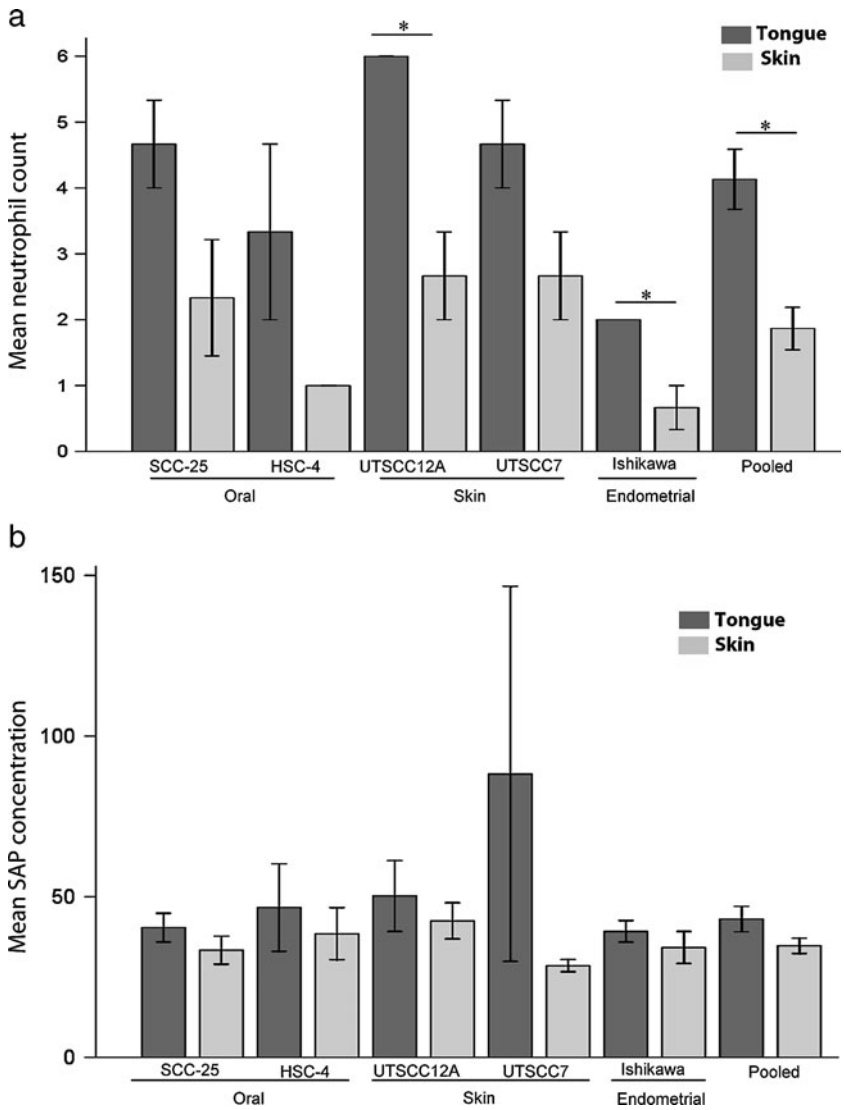

Fig. 9 Assessment of inflammation. **a** *Graph* shows mean neutrophil numbers (±SEM) of tongue (*black bars*) and skin (*grey bars*) tumors of the various cell lines. $N=3$ for all cell lines, and $N=15$ for pooled tongue and skin tumors. $^*P<0.05$. **b** The *graph* shows mean plasma level of SAP in ng/ml × 10^4 (±SEM) in mice with tongue (*black bars*) and skin (*grey bars*) tumors of the various cell lines. $N=3$ for all cell lines, except UT-SCC-7 where $N=2$, and $N=14$ for pooled tongue and skin tumors

suggesting that our xenograft model reflects clinically relevant aspects of lymphangiogenesis in oral and cutaneous SCCs. The increased lymphangiogenesis in tongue tumors may contribute to the different metastatic potential of tongue and skin SCCs. Patients with oral SCCs may therefore benefit from treatment targeting lymphangiogenesis.

Table 6 Mast cell number

Cell line	Mean±SEM		*P*
	Tongue	Skin	
SCC-25	6±1	3±0.5	0.140
HSC-4	13±2	4±1	0.014
UT-SCC-12A	3±1	2±1	0.711
UT-SCC-7	5±1	7±2	0.545
Ishikawa	5±2	3±1	0.489
Pooled	6±1	4±1	0.058

$N=3$ for all cell lines. $N=15$ for pooled tongue and skin tumors

There are many studies highlighting the importance of angiogenesis in cancer growth and progression [7]. The transition from small dormant tumors to actively growing, invasive and metastatic tumors is shown to be associated with the so-called angiogenic switch, which implies that cancer cells gain the ability to induce formation of new blood vessels [7, 48]. Blood vessel density is further found to correlate with invasiveness and metastasis of many cancers [49–52]. We therefore hypothesized that the differences in growth rate and invasiveness between the tongue and skin tumors in our experiments could be explained by a difference in vascularisation of the tumors in the two organs. To our surprise, we found that the skin tumors were more vascularised than the tongue tumors. Even the smallest and most encapsulated skin tumors had numerous

blood vessels surrounding them. A clear relationship between mean vessel density and prognosis for patients with oral SCCs is not established, as different studies report conflicting results [53–55]. Sparse vascularisation or rapidly growing tumors can result in areas with hypoxic conditions [56]. Hypoxia provokes adaptive systems in the cancer cells and induces production of substances that regulate metabolism, angiogenesis, pH, cell migration and cell survival [56]. Hypoxia is therefore generally accepted as a promoter of tumor growth, though it can also induce apoptosis [57]. The lower vessel density in the tongue tumors may induce hypoxia which further stimulates a more aggressive progression of the tongue cancers compared with the skin cancers. In accordance with this hypothesis, two recent studies showed that the use of antiangiogenic therapy resulted in increased local invasion and distant metastases in experimental mouse models [58, 59].

We found that tumors grew faster in the tongue than in the skin irrespective of the tumor cells' origin. Our results therefore challenge the established belief that cancer cells grow better in ortotopic than in heterotopic environments. To our knowledge there are few studies addressing heterotopic growth of cancer cells in organs associated with aggressive cancers. Our results indicate that the tongue offers a more favorable microenvironment for tumor growth than the skin, which is reflected in the clinical behavior of tongue and skin SCCs in humans. This may partly be related to different structural factors such as different composition of the ECM, resident immunity, temperature and exposure to light or trauma. This further highlights the important role of the stroma in directing growth and progression of cancers.

Acknowledgements This work was supported by grants from The Norwegian Cancer Society, The North Norwegian Regional Health Authorities and The Erna and Olav Aakre Foundation for Cancer Research. The authors are indebted to Professor M. Yanagishita, Tokyo Medical and Dental University, Japan for kindly providing the HSC-4 cell line. The authors thank Dr. P. McCourt for critical reading and linguistic revision of the manuscript.

Conflicts of interest The authors declare that they have no conflict of interest.

Open Access This article is distributed under the terms of the Creative Commons Attribution Noncommercial License which permits any noncommercial use, distribution, and reproduction in any medium, provided the original author(s) and source are credited.

References

1. Funk GF, Karnell LH, Robinson RA, Zhen WK, Trask DK, Hoffman HT (2002) Presentation, treatment, and outcome of oral cavity cancer: a National Cancer Data Base report. Head Neck 24:165–180
2. Kovacs AF, Stefenelli U, Seitz O, Middendorp M, Diener J, Sader R, Grunwald F (2009) Positive sentinel lymph nodes are a negative prognostic factor for survival in T1-2 oral/oropharyngeal cancer-a long-term study on 103 patients. Ann Surg Oncol 16:233–239
3. McGuire JF, Ge NN, Dyson S (2009) Nonmelanoma skin cancer of the head and neck I: histopathology and clinical behavior. Am J Otolaryngol 30:121–133
4. De WO, Mareel M (2003) Role of tissue stroma in cancer cell invasion. J Pathol 200:429–447
5. Pupa SM, Menard S, Forti S, Tagliabue E (2002) New insights into the role of extracellular matrix during tumor onset and progression. J Cell Physiol 192:259–267
6. Sund M, Kalluri R (2009) Tumor stroma derived biomarkers in cancer. Cancer Metastasis Rev 28:177–183
7. Hanahan D, Folkman J (1996) Patterns and emerging mechanisms of the angiogenic switch during tumorigenesis. Cell 86:353–364
8. Leong SP, Cady B, Jablons DM, Garcia-Aguilar J, Reintgen D, Jakub J, Pendas S, Duhaime L, Cassell R, Gardner M, Giuliano R, Archie V, Calvin D, Mensha L, Shivers S, Cox C, Werner JA, Kitagawa Y, Kitajima M (2006) Clinical patterns of metastasis. Cancer Metastasis Rev 25:221–232
9. Banerji S, Ni J, Wang SX, Clasper S, Su J, Tammi R, Jones M, Jackson DG (1999) LYVE-1, a new homologue of the CD44 glycoprotein, is a lymph-specific receptor for hyaluronan. J Cell Biol 144:789–801
10. Kaipainen A, Korhonen J, Mustonen T, van Hinsbergh VW, Fang GH, Dumont D, Breitman M, Alitalo K (1995) Expression of the fms-like tyrosine kinase 4 gene becomes restricted to lymphatic endothelium during development. Proc Natl Acad Sci U S A 92:3566–3570
11. Breiteneder-Geleff S, Soleiman A, Kowalski H, Horvat R, Amann G, Kriehuber E, Diem K, Weninger W, Tschachler E, Alitalo K, Kerjaschki D (1999) Angiosarcomas express mixed endothelial phenotypes of blood and lymphatic capillaries: podoplanin as a specific marker for lymphatic endothelium. Am J Pathol 154:385–394
12. Dadras SS, Lange-Asschenfeldt B, Velasco P, Nguyen L, Vora A, Muzikansky A, Jahnke K, Hauschild A, Hirakawa S, Mihm MC, Detmar M (2005) Tumor lymphangiogenesis predicts melanoma metastasis to sentinel lymph nodes. Mod Pathol 18:1232–1242
13. Zhao D, Pan J, Li XQ, Wang XY, Tang C, Xuan M (2008) Intratumoral lymphangiogenesis in oral squamous cell carcinoma and its clinicopathological significance. J Oral Pathol Med 37:616–625
14. Renyi-Vamos F, Tovari J, Fillinger J, Timar J, Paku S, Kenessey I, Ostoros G, Agocs L, Soltesz I, Dome B (2005) Lymphangiogenesis correlates with lymph node metastasis, prognosis, and angiogenic phenotype in human non-small cell lung cancer. Clin Cancer Res 11:7344–7353
15. Gombos Z, Xu X, Chu CS, Zhang PJ, Acs G (2005) Peritumoral lymphatic vessel density and vascular endothelial growth factor C expression in early-stage squamous cell carcinoma of the uterine cervix. Clin Cancer Res 11:8364–8371
16. Karkkainen MJ, Haiko P, Sainio K, Partanen J, Taipale J, Petrova TV, Jeltsch M, Jackson DG, Talikka M, Rauvala H, Betsholtz C, Alitalo K (2004) Vascular endothelial growth factor C is required for sprouting of the first lymphatic vessels from embryonic veins. Nat Immunol 5:74–80
17. Makinen T, Veikkola T, Mustjoki S, Karpanen T, Catimel B, Nice EC, Wise L, Mercer A, Kowalski H, Kerjaschki D, Stacker SA, Achen MG, Alitalo K (2001) Isolated lymphatic endothelial cells transduce growth, survival and migratory signals via the VEGF-C/D receptor VEGFR-3. EMBO J 20:4762–4773

18. Joukov V, Pajusola K, Kaipainen A, Chilov D, Lahtinen I, Kukk E, Saksela O, Kalkkinen N, Alitalo K (1996) A novel vascular endothelial growth factor, VEGF-C, is a ligand for the Flt4 (VEGFR-3) and KDR (VEGFR-2) receptor tyrosine kinases. EMBO J 15:290–298
19. Achen MG, Jeltsch M, Kukk E, Makinen T, Vitali A, Wilks AF, Alitalo K, Stacker SA (1998) Vascular endothelial growth factor D (VEGF-D) is a ligand for the tyrosine kinases VEGF receptor 2 (Flk1) and VEGF receptor 3 (Flt4). Proc Natl Acad Sci USA 95:548–553
20. Petrova TV, Bono P, Holnthoner W, Chesnes J, Pytowski B, Sihto H, Laakkonen P, Heikkila P, Joensuu H, Alitalo K (2008) VEGFR-3 expression is restricted to blood and lymphatic vessels in solid tumors. Cancer Cell 13:554–556
21. Joukov V, Sorsa T, Kumar V, Jeltsch M, Claesson-Welsh L, Cao Y, Saksela O, Kalkkinen N, Alitalo K (1997) Proteolytic processing regulates receptor specificity and activity of VEGF-C. EMBO J 16:3898–3911
22. Killion JJ, Radinsky R, Fidler IJ (1998) Orthotopic models are necessary to predict therapy of transplantable tumors in mice. Cancer Metastasis Rev 17:279–284
23. Myers JN, Holsinger FC, Jasser SA, Bekele BN, Fidler IJ (2002) An orthotopic nude mouse model of oral tongue squamous cell carcinoma. Clin Cancer Res 8:293–298
24. Grenman R, Pekkola-Heino K, Joensuu H, Aitasalo K, Klemi P, Lakkala T (1992) UT-MUC-1, a new mucoepidermoid carcinoma cell line, and its radiosensitivity. Arch Otolaryngol Head Neck Surg 118:542–547
25. Hadler-Olsen E, Kanapathippillai P, Berg E, Svineng G, Winberg JO, Uhlin-Hansen L (2010) Gelatin in situ zymography on fixed, paraffin-embedded tissue: zinc and ethanol fixation preserve enzyme activity. J Histochem Cytochem 58:29–39
26. Weidner N, Carroll PR, Flax J, Blumenfeld W, Folkman J (1993) Tumor angiogenesis correlates with metastasis in invasive prostate carcinoma. Am J Pathol 143:401–409
27. Kobel M, Weichert W, Cruwell K, Schmitt WD, Lautenschlager C, Hauptmann S (2004) Epithelial hyaluronic acid and CD44v6 are mutually involved in invasion of colorectal adenocarcinomas and linked to patient prognosis. Virchows Arch 445:456–464
28. Livak KJ, Schmittgen TD (2001) Analysis of relative gene expression data using real-time quantitative PCR and the 2(-Delta Delta C(T)) Method. Methods 25:402–408
29. Schledzewski K, Falkowski M, Moldenhauer G, Metharom P, Kzhyshkowska J, Ganss R, Demory A, Falkowska-Hansen B, Kurzen H, Ugurel S, Geginat G, Arnold B, Goerdt S (2006) Lymphatic endothelium-specific hyaluronan receptor LYVE-1 is expressed by stabilin-1+, F4/80+, CD11b+macrophages in malignant tumours and wound healing tissue in vivo and in bone marrow cultures in vitro: implications for the assessment of lymphangiogenesis. J Pathol 209:67–77
30. Wrobel T, Dziegiel P, Mazur G, Zabel M, Kuliczkowski K, Szuba A (2005) LYVE-1 expression on high endothelial venules (HEVs) of lymph nodes. Lymphology 38:107–110
31. Salven P, Mustjoki S, Alitalo R, Alitalo K, Rafii S (2003) VEGFR-3 and CD133 identify a population of CD34+ lymphatic/vascular endothelial precursor cells. Blood 101:168–172
32. Jiang S, Bailey AS, Goldman DC, Swain JR, Wong MH, Streeter PR, Fleming WH (2008) Hematopoietic stem cells contribute to lymphatic endothelium. PLoS ONE 3:e3812
33. Religa P, Cao R, Bjorndahl M, Zhou Z, Zhu Z, Cao Y (2005) Presence of bone marrow-derived circulating progenitor endothelial cells in the newly formed lymphatic vessels. Blood 106:4184–4190
34. Conrad C, Niess H, Huss R, Huber S, von Luettichau I, Nelson PJ, Ott HC, Jauch KW, Bruns CJ (2009) Multipotent mesenchymal stem cells acquire a lymphendothelial phenotype and enhance lymphatic regeneration in vivo. Circulation 119:281–289
35. Murdoch C, Muthana M, Coffelt SB, Lewis CE (2008) The role of myeloid cells in the promotion of tumour angiogenesis. Nat Rev Cancer 8:618–631
36. Kundu JK, Surh YJ (2008) Inflammation: gearing the journey to cancer. Mutat Res 659:15–30
37. Beasley NJ, Prevo R, Banerji S, Leek RD, Moore J, van Trappen TP, Cox G, Harris AL, Jackson DG (2002) Intratumoral lymphangiogenesis and lymph node metastasis in head and neck cancer. Cancer Res 62:1315–1320
38. Jeltsch M, Kaipainen A, Joukov V, Meng X, Lakso M, Rauvala H, Swartz M, Fukumura D, Jain RK, Alitalo K (1997) Hyperplasia of lymphatic vessels in VEGF-C transgenic mice. Science 276:1423–1425
39. Veikkola T, Jussila L, Makinen T, Karpanen T, Jeltsch M, Petrova TV, Kubo H, Thurston G, McDonald DM, Achen MG, Stacker SA, Alitalo K (2001) Signalling via vascular endothelial growth factor receptor-3 is sufficient for lymphangiogenesis in transgenic mice. EMBO J 20:1223–1231
40. Roberts N, Kloos B, Cassella M, Podgrabinska S, Persaud K, Wu Y, Pytowski B, Skobe M (2006) Inhibition of VEGFR-3 activation with the antagonistic antibody more potently suppresses lymph node and distant metastases than inactivation of VEGFR-2. Cancer Res 66:2650–2657
41. Burton JB, Priceman SJ, Sung JL, Brakenhielm E, An DS, Pytowski B, Alitalo K, Wu L (2008) Suppression of prostate cancer nodal and systemic metastasis by blockade of the lymphangiogenic axis. Cancer Res 68:7828–7837
42. Stacker SA, Stenvers K, Caesar C, Vitali A, Domagala T, Nice E, Roufail S, Simpson RJ, Moritz R, Karpanen T, Alitalo K, Achen MG (1999) Biosynthesis of vascular endothelial growth factor-D involves proteolytic processing which generates non-covalent homodimers. J Biol Chem 274:32127–32136
43. Borregaard N, Sorensen OE, Theilgaard-Monch K (2007) Neutrophil granules: a library of innate immunity proteins. Trends Immunol 28:340–345
44. Pejler G, Abrink M, Ringvall M, Wernersson S (2007) Mast cell proteases. Adv Immunol 95:167–255
45. Stevens RL, Adachi R (2007) Protease-proteoglycan complexes of mouse and human mast cells and importance of their beta-tryptase-heparin complexes in inflammation and innate immunity. Immunol Rev 217:155–167
46. Hadler-Olsen E et al. (2010) Organ specific regulation of tumour invasiveness and gelatinolytic activity at the invasive front. Eur J Cancer. doi:10.1016/j.ejca.2010.09.006
47. Deryugina EI, Quigley JP (2006) Matrix metalloproteinases and tumor metastasis. Cancer Metastasis Rev 25:9–34
48. Naumov GN, Akslen LA, Folkman J (2006) Role of angiogenesis in human tumor dormancy: animal models of the angiogenic switch. Cell Cycle 5:1779–1787
49. Depasquale I, Thompson WD (2005) Microvessel density for melanoma prognosis. Histopathology 47:186–194
50. Macchiarini P, Fontanini G, Hardin MJ, Squartini F, Angeletti CA (1992) Relation of neovascularisation to metastasis of non-small-cell lung cancer. Lancet 340:145–146
51. Salvesen HB, Gulluoglu MG, Stefansson I, Akslen LA (2003) Significance of CD 105 expression for tumour angiogenesis and prognosis in endometrial carcinomas. APMIS 111:1011–1018
52. Weidner N, Folkman J, Pozza F, Bevilacqua P, Allred EN, Moore DH, Meli S, Gasparini G (1992) Tumor angiogenesis: a new significant and independent prognostic indicator in early-stage breast carcinoma. J Natl Cancer Inst 84:1875–1887
53. Hannen EJ, Riediger D (2004) The quantification of angiogenesis in relation to metastasis in oral cancer: a review. Int J Oral Maxillofac Surg 33:2–7

54. Ranieri G, Labriola A, Achille G, Florio G, Zito AF, Grammatica L, Paradiso A (2002) Microvessel density, mast cell density and thymidine phosphorylase expression in oral squamous carcinoma. Int J Oncol 21:1317–1323
55. Tae K, El-Naggar AK, Yoo E, Feng L, Lee JJ, Hong WK, Hittelman WN, Shin DM (2000) Expression of vascular endothelial growth factor and microvessel density in head and neck tumorigenesis. Clin Cancer Res 6:2821–2828
56. Rademakers SE, Span PN, Kaanders JH, Sweep FC, van der Kogel AJ, Bussink J (2008) Molecular aspects of tumour hypoxia. Mol Oncol 2:41–53
57. Ruan K, Song G, Ouyang G (2009) Role of hypoxia in the hallmarks of human cancer. J Cell Biochem 107:1053–1062
58. Paez-Ribes M, Allen E, Hudock J, Takeda T, Okuyama H, Vinals F, Inoue M, Bergers G, Hanahan D, Casanovas O (2009) Antiangiogenic therapy elicits malignant progression of tumors to increased local invasion and distant metastasis. Cancer Cell 15:220–231
59. Ebos JM, Lee CR, Cruz-Munoz W, Bjarnason GA, Christensen JG, Kerbel RS (2009) Accelerated metastasis after short-term treatment with a potent inhibitor of tumor angiogenesis. Cancer Cell 15:232–239

Virchows Arch (2010) 457:693–703
DOI 10.1007/s00428-010-0981-x

ORIGINAL ARTICLE

Hemoglobin level predicts outcome for vulvar cancer patients independent of GLUT-1 and CA-IX expression in tumor tissue

Hedwig P. van de Nieuwenhof · Joanne A. de Hullu · Johannes H. A. M. Kaanders · Johan Bulten · Leon F. A. G. Massuger · Léon C. L. T. van Kempen

Received: 28 July 2010 / Revised: 1 September 2010 / Accepted: 12 September 2010 / Published online: 2 October 2010
© The Author(s) 2010. This article is published with open access at Springerlink.com

Abstract Intratumoral hypoxia has been associated with poor prognosis in several solid tumors. The aim of this study was to determine whether the hypoxia-associated markers glucose transporter (GLUT)-1 and carbonic anhydrase (CA)-IX expression and preoperative hemoglobin (Hb) levels correlate with presence of inguinofemoral or distant metastases, and disease-free survival (DSS) in vulvar squamous cell carcinoma (SCC) patients. Vulvar SCC (n=103) were reviewed for histopathological characteristics by an expert gynecopathologist and stained for GLUT-1 and CA-IX. Clinical data and preoperative Hb levels were obtained from medical records. No significant correlations were observed between GLUT-1 or CA-IX expression patterns and preoperative Hb levels, presence of inguinofemoral or distant metastases and DSS. However, anemic patients (Hb<11.2 g/dL) had significantly more inguinofemoral metastases and lower Hb level was an independent prognostic factor for a worse DSS (p<0.001). The number of comorbidic conditions was inversely correlated with preoperative Hb level. Preoperative Hb levels are associated with poor DSS for vulvar SCC patients, whereas tumor hypoxia reflected by GLUT-1 and CA-IX expression does not have a predictive value. Because preoperative Hb levels inversely correlated with the number of comorbidic conditions and not with GLUT-1 or CA-IX expression, it is most likely that preoperative Hb levels represent overall physical condition.

Keywords Vulvar squamous cell carcinoma · Prognosis · Hypoxia · Anemia · Comorbidity

H. P. van de Nieuwenhof (✉) · J. A. de Hullu · L. F. A. G. Massuger
Departments of Obstetrics and Gynecology,
Radboud University Nijmegen Medical Centre,
P.O. Box 9101, 6500 HBNijmegen, The Netherlands
e-mail: H.Nieuwenhof@obgyn.umcn.nl

J. H. A. M. Kaanders
Department of Radiation Oncology,
Radboud University Nijmegen Medical Centre,
Nijmegen, The Netherlands

J. Bulten · L. C. L. T. van Kempen
Department of Pathology,
Radboud University Nijmegen Medical Centre,
Nijmegen, The Netherlands

Introduction

Vulvar squamous cell carcinoma (SCC) accounts for 3–5% of all gynecological malignancies. Positive inguinofemoral lymph nodes have been found to be the most important prognostic factor for vulvar SCC [1–3]. Currently, the standard treatment for patients with early stage vulvar SCC is wide local excision with uni- or bilateral inguinofemoral lymphadenectomy via separate incisions that may lead to impressive morbidity such as lymphedema. There are no non-invasive diagnostic tests that are able to exclude inguinofemoral lymph node metastasis with a high enough certainty to safely omit a complete inguinofemoral lymphadenectomy [4]. Fortunately, the sentinel lymph node procedure is an upcoming promising staging technique [5].

Limited research has been performed on immunohistochemical markers to predict the presence of positive inguinofemoral lymph nodes and the prognosis of the individual patient with vulvar SCC. Fons et al. have analyzed 16 immunohistochemical markers with potentially prognostic value for patients with vulvar SCC. Lack of caspase three expression, a key effector of cellular death,

was associated with poor disease-specific survival (DSS) in a multivariate analysis [6]. In addition, increased epidermal growth factor receptor (EGFR) expression and increased angiogenic response have been found to be associated with decreased survival [7–11].

Hypoxia occurs in anemia [12], cancer, prolonged exercise, and long-term ischemia with durations of several hours or more [13]. Hypoxia may induce cell death, although tumor cells may adapt to the hypoxic microenvironment by inducing a hypoxia-inducible factor (HIF)-1 mediated angiogenic response, and/or by altering their metabolic activity [14]. The overall cellular consequences of hypoxia are a decreased proliferation rate, increased radio- and multidrug resistance, and increased invasive and metastatic potential [15]. These adaptive responses promote tumor progression and treatment resistance to both radio- and chemotherapy. Several studies have shown that tumor hypoxia is significantly related to poor patient prognosis in various malignancies such as head and neck cancer, and cervical cancer [16, 17].

Several immunohistochemical markers can assess hypoxia. HIF-1 is considered a master regulator of the cellular response to hypoxia. However, although HIF-1 indicates tumor aggressiveness, it is debatable whether it is also a reliable marker of tumor hypoxia as HIF1 induction is also dependent on other microenvironmental conditions [14]. Among others, HIF-1 regulates the expression of the surface transmembrane glucose transporters (GLUTs), especially GLUT-1 and carbonic anhydrases (CAs) which are both involved in energy metabolism [18–21]. Whereas GLUTs import glucose across the cell membrane in an energy independent manner to fuel anaerobic glycolysis [22], the subsequent intracellular acidification is antagonized by CAs [23]. This results in an acidic extracellular environment that may promote progression toward a more malignant phenotype [24]. Of all CAs, CA-IX has the greatest magnitude of induction under hypoxic conditions.

Oxygen delivery to tumors depends on tissue perfusion and the oxygen-carrying capacity of the blood. It has been suggested that a decrease in the oxygen-carrying capacity of the blood caused by anemia may be a major causative factor for the development of tissue hypoxia [25, 26]. In a rat model, Kelleher et al. indeed demonstrated that tumor-related anemia resulted in substantial worsening of tumor oxygenation [27]. Both high CA-IX, GLUT-1 and low preoperative hemoglobin (Hb) levels were found to be associated with a poor DSS in different tumor types, e.g., cervical, ovarian, and head and neck carcinomas [28–36].

Studies that have analyzed the correlation between hypoxia and prognosis in vulvar SCC are limited. In a small-scale study (20 patients), only preoperative anemia showed a correlation with nodal metastasis [37]. Therefore, the aim of this study is to determine whether GLUT-1 and CA-IX expression and preoperative hemoglobin levels correlate with presence of inguinofemoral or distant metastases and DSS in a large group of vulvar SCC patients.

Materials and methods

From January 1st 1988 until December 31st 2005, 167 consecutive patients with vulvar SCCs were treated with a curative intent in the Radboud University Nijmegen Medical Centre. Only patients whose treatment consisted of primary surgery were included. Tumors with a depth of invasion of 1 mm or more in the operation specimen were selected for this study. A total number of 103 paraffin-embedded primary vulvar SCCs that met the above-mentioned criterion with long-term follow-up were available for this study (last month of follow-up—August 2008). All slides were reviewed for histopathological characteristics by an expert gynecopathologist (JB). Clinical data were obtained from medical records and comorbidity was registered in accordance with the Comorbidity Index of Mary E. Charlson [38].

All patients were staged according to the surgicopathological staging system for vulvar carcinoma of the International Federation of Gynecology and Obstetrics (FIGO). When a recurrence was diagnosed, the localization of the recurrence was registered as local, skin bridge, groin, pelvic, or distant. For analytical purposes, skin bridge recurrences were considered to be groin recurrences and pelvic recurrences considered to be distant recurrences.

Immunohistochemistry

Formalin-fixed paraffin-embedded tissue sections (4 μm) were mounted onto Superfrost slides (Menzel-Gläser, Braunschweig, Germany) and dried overnight at 37°C. Tissues were dewaxed in xylene, rehydrated through graded alcohols, and rinsed three times in phosphate-buffered saline (PBS; pH 7.4) for 10 min. Following an antigen retrieval step [sodium citrate (0.01 M; pH 6.0), 95°C, 10 min], tissue sections were preincubated with 20% normal goat serum in PBS and subsequently incubated overnight at 4°C with a polyclonal rabbit-anti-GLUT-1 (Dako, Glostrup, Denmark; 1:200) or rabbit-anti-CA-IX (0.1 μg/mL, kindly provided by Dr. E. Oosterwijk, Dept. of Experimental Urology, Radboud University Nijmegen Medical Centre). Antibodies were diluted in PBS containing 1% bovine serum albumin (BSA). Slides were rinsed in PBS for 10 min and incubated with biotinylated anti-rabbit IgG (Vector, Burlingame, CA, USA) for 30 min at room temperature (RT). A biotin–avidin peroxidase (CA-IX) or alkaline phosphatase (GLUT-1) complex was generated

according to standard procedures (Vector). Peroxidase was visualized with 3-amino-9-ethylcarbazole (AEC, ScyTek, Logan, UT, USA) and briefly counterstained with Mayer's hematoxylin. Alkaline phosphatase was visualized with Fast Blue (20 mL Tris–HCl pH 8.2, 4 mg Naphtol AS-MX, 4.8 mg Levamisole, and 20 mg Fast Blue BB salt) and counterstained with Nuclear fast red (Vector). Slides were mounted with Imsol (Klinipath, Duiven, The Netherlands) and subsequently with Permount (Fisher Scientific, Fairlawn, NJ, USA). Negative controls (buffer only) were included in each analysis.

For GLUT-1/CD31 double staining, the sodium-citrate antigen retrieval step and preincubation with normal serum was followed by incubation with monoclonal mouse-anti CD31 (Dako, clone JC70A, 1:20) overnight at 4°C. After washing the slides with PBS for 10 min, tissue sections were incubated with biotinylated anti-mouse IgG (Vector), an avidin–peroxidase complex (Vector) generated and visualized with AEC. Subsequently, the GLUT-1 staining protocol (Fast Blue) was performed as described above.

Evaluation of staining

Slides were scored (HvdN, LvK) blinded to clinicopathological data and results of other stainings. Because GLUT-1 and CA-IX function as transmembrane proteins, only membranous staining was considered a positive result. The percentage of positive cells and localization of staining was determined and categorized in the following manner: negative, less than 5% of tumor cells stained, between 5% and 25%, between 25% and 75%, and over 75%. To avoid small numbers, for GLUT-1 staining, the only tumor with less than 5% cells stained was grouped together with 5–25% and for CA-IX staining, tumors with over 75% tumor cells stained (three tumors) were grouped together in a category ≥25% tumor cells stained.

Hemoglobin levels

Preoperative hemoglobin levels were recorded from the medical charts. All hemoglobin levels were taken within 1 week prior to surgery.

Statistical analysis

Data were entered in a computerized database and analyzed using SPSS software (version 16.0.1 for Windows, SPSS). Patient and tumor characteristics were compared using χ^2 and two-tailed Student's t tests. Survival analysis was performed by the Kaplan–Meier product limit method, and survival rates were compared using log-rank statistics. Cox regression analysis was used for confounder analysis. All time-dependent outcomes were calculated from time of pathological diagnosis. Patient data were censored when a disease event had not occurred at the last follow-up. For the endpoint "presence of inguinofemoral or distant metastases", an event was defined as occurrence of inguinofemoral metastases or metastasis in a distant organ. For DSS, only deaths due to vulvar SCC were analyzed as events. Patients who are still alive or died due to other causes than vulvar SCC were censored at the date of last follow-up. Values of $p < 0.05$ were considered significant.

Results

Primary treatment and staging

A total number of 30 patients underwent a wide local excision, 72 patients had a radical vulvectomy and for one patient an exenterative procedure was performed. Postoperative radiotherapy was given to 31 patients (30%); no patients were treated with adjuvant chemotherapy.

Median age of the patients was 72 years (range 31–92 years). Nine (8.7%) patients had a FIGO stage I tumor, 43 (41.7%) patients a stage II, 32 (31.1%) patients a stage III, and 19 patients (18.5%) a stage IV tumor.

Expression of GLUT-1 and CA-IX

To assess hypoxia in vulvar SCCs, we performed immunohistochemical analyses for the tissue hypoxia-associated markers GLUT-1 and CA-IX. The median area stained by GLUT-1 was 25% of the whole tumor. Often a diffuse staining of a large tumor area was observed, with a focally increased staining intensity (Fig. 1). Both cytoplasmic and membranous GLUT-1 staining was observed, but only membranous staining was considered positive staining. In several cases, GLUT-1 expression was observed directly adjacent to a blood vessel (Fig. 1e–f).

CA-IX staining was less pronounced than GLUT-1, with a median staining area of only 1% (Fig. 2). CA-IX staining was often observed at a distance from vessels.

Hemoglobin levels

With the aim to assess the role of anemia, preoperative hemoglobin levels were recorded from medical charts. Hemoglobin levels were available for 77 patients. Eight patients (7.8%) had a Hb value below 11.2 g/dL and were considered to be anemic. Eight patients had a Hb level between 11.2 and 12.6 g/dL, and 15 patients had a Hb level between 12.6 and 13.4 g/dL. Twenty patients had a Hb level between 13.4 and 14.2 g/dL, and 26 patients had a Hb level of 14.2 g/dL or higher.

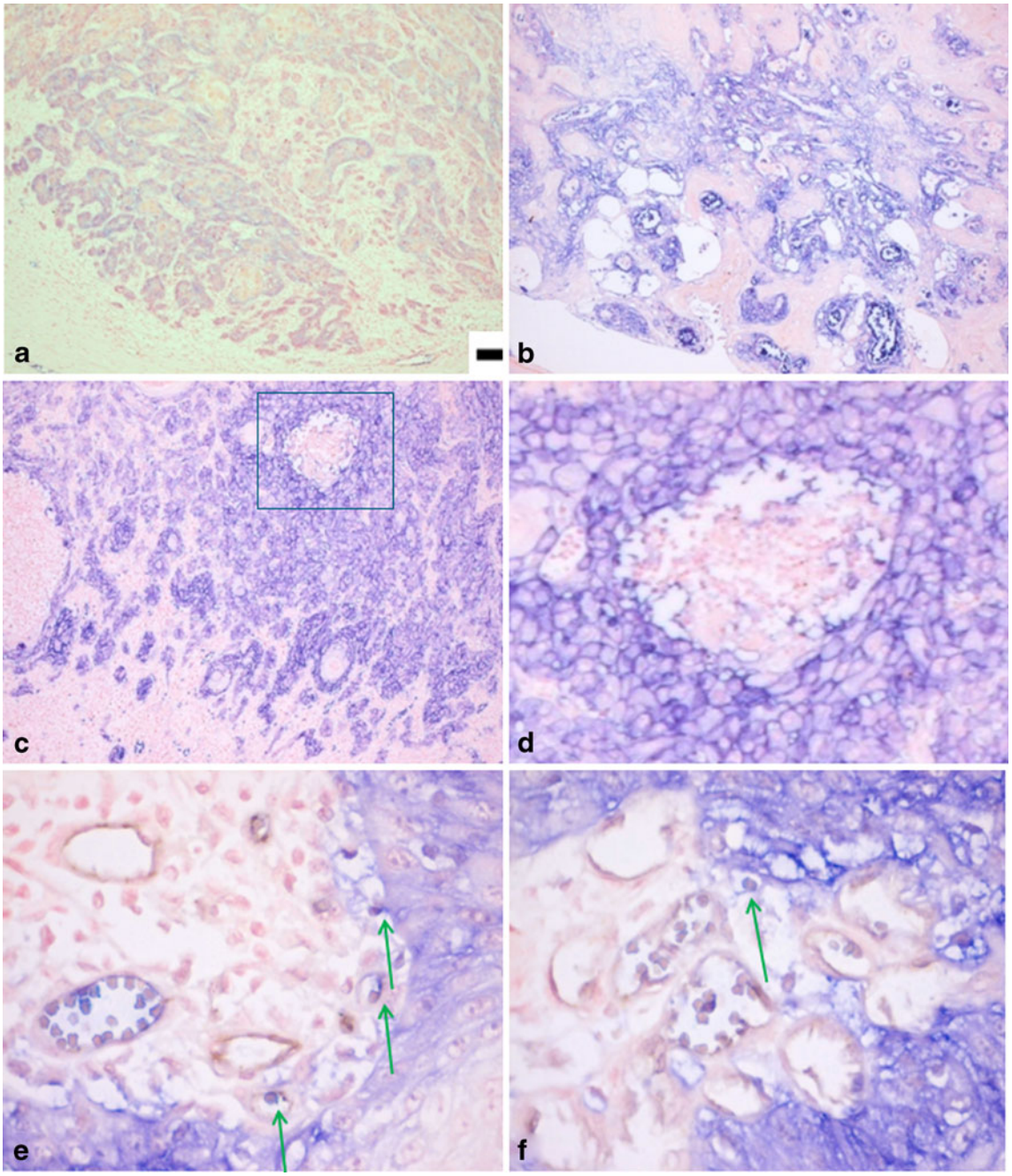

Fig. 1 GLUT-1 staining in vulvar squamous cell carcinomas. Representative image of a negative staining (**a**), 40% (**b**), and 90% positivity (**c**). High-power magnification (**d**) of indicated area in (**c**) demonstrates clear membranous localization. *Scale bars* (**a**)–(**c**): 50 μm, (**d**): 10 μm. Membranous GLUT-1 staining of tumor cells (*blue*) adjacent to erythrocyte-containing blood vessels (*red*) can be observed (**e** and **f**). Erythrocytes are GLUT-1 positive and serve as an internal control for positive staining. Microvessels, where diffusion can occur, are indicated (*arrows*)

GLUT-1, CA-IX, and preoperative Hb levels in relation to tumor characteristics

Tumor characteristics in relation to expression of GLUT-1 and CA-IX are summarized in Table 1. Less-differentiated tumors demonstrated lower GLUT-1 expression levels. There were no differences between tumor characteristics with respect to GLUT-1 and CA-IX expression at the invasive front of the tumors (data not shown).

Anemic patients (<11.2 g/dL) presented with tumors with a larger diameter than patients with Hb levels within the normal range (Table 2). Subsequently, the correlation between GLUT-1 or CA-IX expression and Hb levels was determined. GLUT-1 and CA-IX were inversely correlated

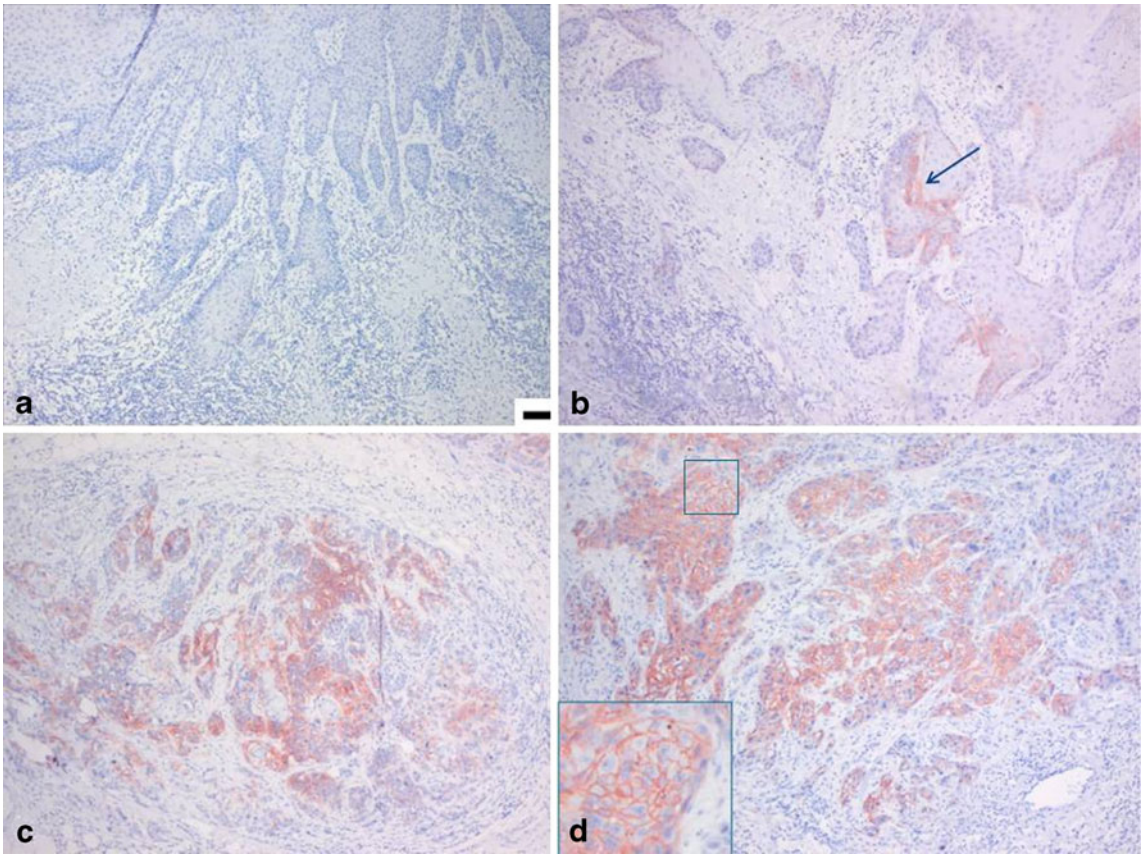

Fig. 2 CA-IX staining in vulvar squamous cell carcinomas. Representative image of a negative staining (**a**), 10% (**b**), 60% (**c**), and 90% positivity (**d**). High-power magnification of indicated area in (**d**) demonstrates clear membranous localization. *Scale bars* (**a**)–(**c**): 50 μm, (**d**): 10 μm

(p=0.003, 95% CI −0.479 to −0.104). No correlation was found between preoperative Hb levels and CA-IX or GLUT-1 expression.

GLUT-1, CA-IX, and preoperative Hb levels in relation to presence of inguinofemoral metastases

For GLUT-1 and CA-IX expression patterns, no differences were found for presence of inguinofemoral or distant metastases (Fig. 3a, b). An imbalance between oxygen supply and consumption is more likely to occur in large tumors (large diameter or great depth of invasion). Therefore, we performed a subanalysis for large tumors (diameter ≥38 mm or depth of invasion ≥8 mm, which are both the mean values). Expression of GLUT-1 and CA-IX did not differ between tumors smaller or greater than a diameter of 38 mm or between tumors with a depth of invasion smaller or greater than 8 mm. In addition, GLUT-1 and CA-IX expression were not associated with presence of inguinofemoral or distant metastases in this subgroup of large tumors (data not shown).

For preoperative Hb levels, significant differences were found for presence of inguinofemoral metastases or distant (log rank=0.001) when stratified as in Table 2, and log rank <0.001 (Fig. 3c) when stratified between anemic patients (Hb<11.2 g/dL) and patients with normal Hb levels (>11.2 g/dL).

GLUT-1, CA-IX, and preoperative Hb levels and disease-specific survival

Univariate Cox regression analysis showed that both GLUT-1 (HR 0.876, 95% CI 0.583–1.115) and CA-IX (HR 1.086, 95% CI 0.794–1.477) were not predictive for DSS, whereas preoperative Hb value was a prognostic factor (p<0.001, HR=0.146, 95% CI 0.059–0.358). In addition, the number of positive inguionofemoral lymph nodes and development of groin or distant recurrence correlated with a poor DSS (p< 0.001). When these variables were included in a multivariate Cox proportional hazards analysis, preoperative Hb level turned out to be an independent prognostic factor for poor DSS (p=0.021). These findings were confirmed in a linear regression analysis, demonstrating that groin, pelvic, or distant recurrences are independent of preoperative Hb level (p=0.262). The Kaplan–Meier survival curves with corresponding log-rank values for GLUT-1, CA-IX, and Hb

Table 1 Tumor characteristics of 103 vulvar SCCs in relation to GLUT-1 and CA-IX expression patterns

		GLUT-1					CA-IX				
		Negative	5–25%	25–75%	≥75%	*p* value[a]	Negative	<5%	5–25%	≥25%	*p* value
Local	Number	40	12	28	23		47	12	31	13	
Depth of invasion (mm)	Median	8	8	8.75	7	NS	6	10.5	8	9	NS
	Range	1.7–27	3–15	1–18	1–35		1–27	4–20	2–35	3–25	
Tumor diameter (mm)	Median	31.5	37.5	35	30	NS	30	49.5	30	50	NS
	Range	11–70	16–65	6–90	5–120		5–90	16–70	14–65	15–120	
Differentiation grade	Well	5%	8.3%	7.1%	43.5%	0.001	21.3%	8.3%	12.9%		NS
	Moderately	50%	66.7%	64.3%	30.4%		53.2%	58.3%	41.9%	61.5%	
	Poor	42.5%	16.7%	28.6%	17.4%		19.1%	25%	45.2%	38.5%	
	Unknown	2.5%	8.3%		8.7%		6.4%	8.3%			
Regional											NS
Number of positive nodes	Mean	0.95	1.92	1.21	0.74	NS	0.85	1.42	1.42	0.85	
	Range	0–5	0–8	0–4	0–4		0–7	0–8	0–5	0–3	
Capsular	No	17.5%	8.3%	39.3%	21.7%	NS	19.1%	8.3%	32.3%	30.8%	NS
Breakthrough	Yes	22.5%	33.3%	21.4%	13%		14.9%	33.3%	29%	15.4%	
	Not applicable	57.5%	58.3%	35.7%	65.2%		61.7%	58.3%	38.7%	53.8%	
	Missing	2.5%		3.6%			4.3%				
FIGO stage						NS					NS
	I	12.5%	8.3%		13%		12.8%		6.5%	7.7%	
	II	40%	50%	35.7%	47.8%		48.9%	58.3%	25.8%	38.5%	
	III	30%	16.7%	42.9%	26.1%		21.3%	25%	45.2%	38.5%	
	IV	17.5%	25%	21.4%	13%		17%	16.7%	22.6%	15.4%	
Recurrence						NS					NS
	No recurrence	72.5%	50%	57.1%	65.2%		66%	66.7%	64.5%	53.8%	
	Local	12.5%	8.3%	28.6%	26.1%		23.4%	8.3%	19.4%	15.4%	
	Groin	5%	16.7%	14.3%	4.3%		4.3%	16.7%	6.5%	23.1%	
	Distant	10%	2.5%		4.3%		6.4%	8.3	9.7%	7.7%	

GLUT glucose transporter, *CA* carbonic anhydrase, *FIGO* International Federation of Gynecology and Obstetrics, *NS* not significant

[a] *p* values are only given when significant

Table 2 Tumor characteristics of 77 vulvar SCCs in relation to preoperative Hb levels

		Hb (g/dL)					
		<11.2	11.2–12.6	12.6–13.4	13.4–14.2	≥14.2	*p* value[a]
Local	Number	8	8	15	20	26	
Depth of invasion	Median	9.5	10.5	9	9	7	NS
	Range	2–25	8–15	1.7–27	2–18	1–15	
Tumor diameter	Median	51.5	35	38	29	28	0.05
	Range	28–120	21–80	10–60	12–90	5–60	
Differentiation grade	Well	37.5%	12.5%	20%	25%	19.2%	NS
	Moderately	62.5%	37.5%	46.7%	60%	42.3%	
	Poor		50%	33.3%	15%	30.8%	
	Unknown					7.7%	
Regional							
Number of positive nodes	Mean	1.87	1.63	0.73	1.10	1.15	NS
	Range	0–3	0–5	0–3	0–3	0–8	
Capsular breakthrough	No	37.5%	37.5%	33.3%	25%	15.4%	NS
	Yes	50%	37.5%	6.7%	10%	26.9%	
	Not applicable	12.5%	25%	60%	65%	53.8%	
	Missing					3.8%	
FIGO stage							
	I			20%	10%	7.7%	NS
	II	12.5%	25%	33.3%	50%	46.2%	
	III	50%	75%	33.3%	20%	30.8%	
	IV	37.5%		13.3%	20%	15.4%	
Recurrence							
	No recurrence	25%	87.5%	66.7%	75%	61.5%	NS
	Local	25%	12.5%	20%	5%	23.1%	
	Groin	25%		13.3%	15%	3.8%	
	Distant	25%			5%	11.5%	

Hb hemoglobin, *FIGO* International Federation of Gynecology and Obstetrics, *NS* not significant

[a] *p* values are only given when significant; anemic patients were compared with non-anemic patients

level are shown in Fig. 4a–c. There was no difference in DSS between tumors with and without GLUT-1 and CA-IX expression at the invasive front (data not shown). This was also found in a subanalysis for patients treated with adjuvant radiotherapy (31 patients); preoperative Hb levels were predictive for DSS (p=0.041), but not GLUT 1 and CAIX expression in the tumor (log rank p=0.507 and 0.568, respectively).

Comorbidity

The lack of a correlation between Hb levels and expression of hypoxia-associated markers provided no evidence for a link between anemia and tissue hypoxia. The correlation between Hb levels and poor DSS has led us to analyze whether Hb levels reflect the physical condition of the patients. Twenty-eight patients had no comorbidic conditions according to Charlson et al. [38], whereas one to six comorbidic conditions were observed in 75 patients (Table 3). The number of comorbidic conditions and Hb value were inversely associated in a linear regression model (p=0.020, 95% CI −0.295 to −0.026).

Discussion

Our study of 103 patients with vulvar SCC did not reveal a prognostic value for the expression of the tissue hypoxia-associated markers GLUT-1 and CA-IX. Although anemia has been linked to tissue hypoxia [14], we did not find such a correlation. However, low Hb values were associated with multiple comorbidic factors and turned out to be an independent prognostic factor for a poor DSS. Literature about the relation between the expression of hypoxia-associated markers and lymph node metastasis or survival for vulvar SCCs patients is limited. A small-scale study

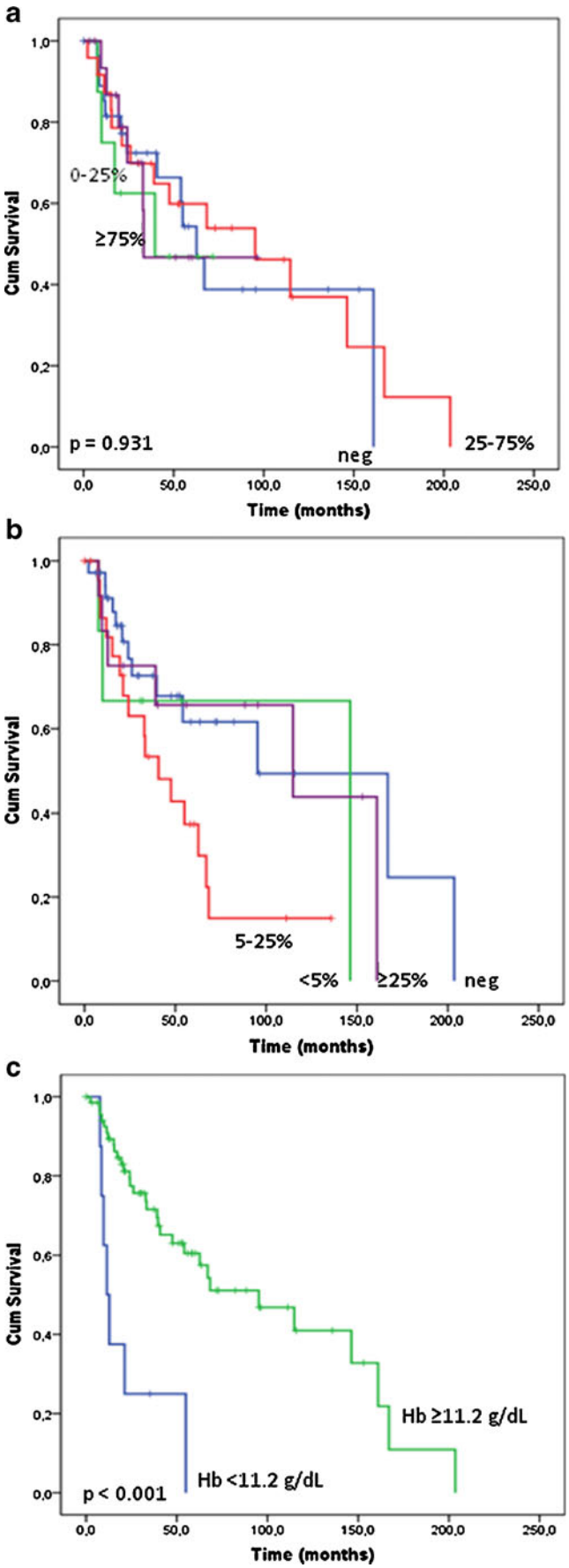

◀ **Fig. 3** Low preoperative Hb level correlates with increased risk of inguinofemoral or distant metastases. Presence of inguinofemoral or distant metastases curves for patients subdivided into different GLUT-1 expression patterns (**a**), CA-IX patterns (**b**), and preoperative Hb levels (**c**). Low preoperative Hb levels significantly correlate with increased risk of inguinofemoral or distant metastases

comprising 20 patients likewise failed to demonstrate a significant correlation between various measures of tumor oxygenation and nodal metastasis [37].

Patients' anemia may contribute to the establishment of intratumoral hypoxic conditions by reducing oxygen delivery to tumor tissues. In our study, no correlation between Hb levels and hypoxia-associated markers could be demonstrated. Similarly, no association between Hb levels in patients before surgery and expression of hypoxia-associated markers was observed in 45 head and neck cancer and 79 colorectal adenocarcinomas [39, 40]. It is generally known that anemia has a negative impact on survival for cancer and non-cancer patients [41, 42]. However, previous research has focused on its correlation with hypoxia, but not as a representative for physical condition. We demonstrated an increased number of comorbidic conditions in vulvar SCC patients with low Hb values (<11.2 g/dL), which in turn correlates with very poor prognosis (Fig. 4c). This is consistent with the study of Wu et al. who also found that the cohort of patients with anemia had the highest prevalences of several diseases [42], with even minimal deviations from an optimal range being associated with an increased risk of 30-day postoperative mortality [42]. A deterioration of prognosis with Hb levels below 11.2 g/dL was also observed for cervical cancer patients treated with radiotherapy [43]. The differential diagnosis of anemia is extensive with chronic illness as a frequent cause. Cardiac and vascular conditions were most often present in our study population and may both be causes of the observed anemia in those patients. Because bleeding from a vulvar tumor rarely occurs, this factor is not likely to explain the low Hb levels in patients with large tumors. Therefore, it is more likely that low preoperative Hb levels represent an impaired physical condition than tumor hypoxia.

In our study, increasing percentages of GLUT-1 and CA-IX expression were not associated with differences in primary tumor characteristics (Table 1), presence of inguinofemoral or distant metastases (Fig. 3), and DSS (Fig. 4). This may indicate that tumor hypoxia is not relevant for vulvar cancer or that the markers are of insufficient specificity. Tumor hypoxia can be induced by an inadequate function of the tumor vasculature independent of Hb levels. Furthermore, CA-IX and GLUT-1 do not necessarily behave in a coherent fashion [44] as we also observed in this study. The role of GLUT-1 as an endogenous marker for tumor hypoxia was found to be questionable [45]. Expression of GLUT-1 is induced by a

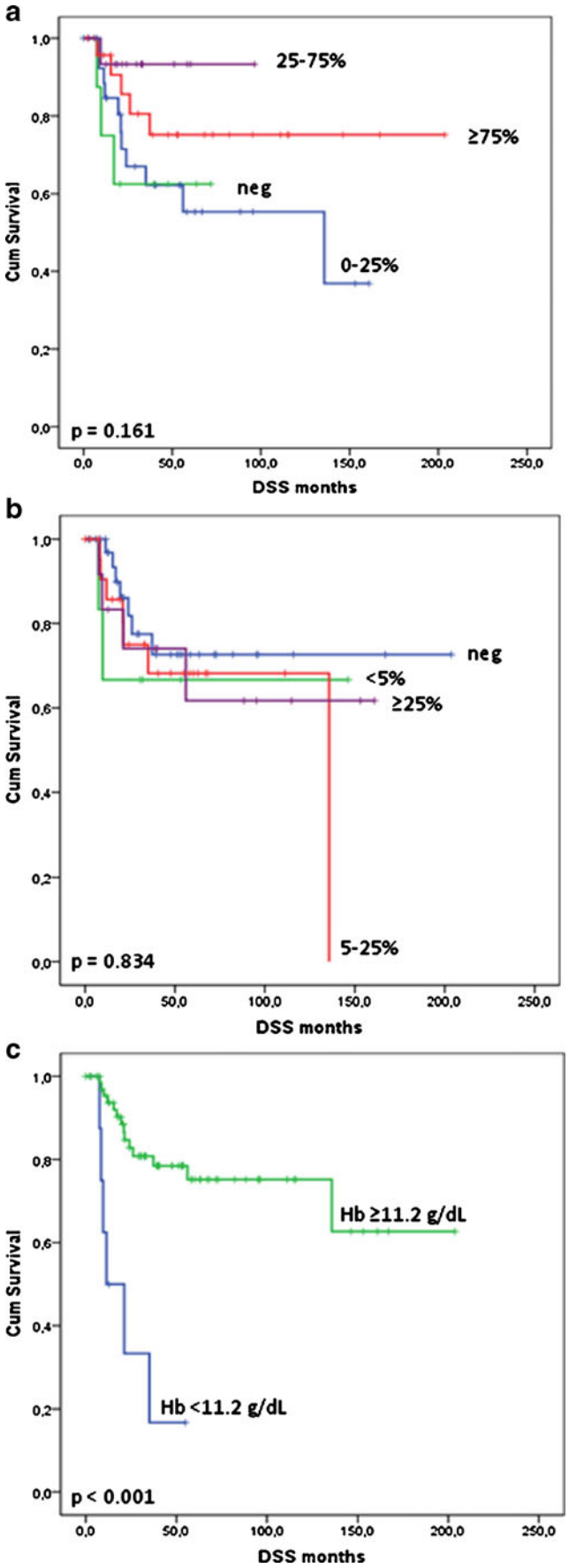

◀ **Fig. 4** Anemic vulvar SCC patients have a poor disease-free survival. Disease-free survival *curves* for patients subdivided into different GLUT-1 expression patterns (**a**), CA-IX patterns (**b**), and preoperative Hb levels (**c**). Low preoperative Hb levels significantly correlate with reduced DSS

variety of stimuli besides hypoxia, including glucose deprivation, oncogenic transformation, inhibition of oxidative phosphorylation, and osmotic stress [45]. Although GLUT expression has been demonstrated at a distance from vessels and adjacent to necrosis, the relationship with hypoxia has not been investigated [26]. Because we detected GLUT-1 expression directly adjacent to erythrocyte-containing blood vessel, we conclude that GLUT-1 is not a genuine hypoxia marker in vulvar SCC.

In prostate cancer, GLUT-1 mRNA expression correlates with loss of differentiation [46]. In contrast, we detected high GLUT-1 protein expression (i.e., >75%) more frequently in well-differentiated SCC than in moderate and poorly differentiated tumors (Table 1, $p=0.001$). The relevance for vulvar SCC biology is currently unknown. However, this correlation is not observed in all other cases in which GLUT-1 is expressed by less than 75% of the tumor cells. It has to be noted, however, that our semi-quantitative scoring of staining profiles is not as accurate as quantitative PCR. Small changes mRNA expression may have a prominent effect on tumor cell biology, but this altered gene expression may not be detected at the protein level in a semi-quantitative manner. CA-IX expression has been studied in a number of tumor types supporting the notion that CA-IX represents tumor aggressiveness. CA-IX is strongly induced by hypoxia in a broad range of tumor cells [47, 48] and considerable co-localization with pimonidazole staining was observed [16, 48]. High expression of CA-IX is associated with poor survival in breast cancer, small cell lung cancer, head and neck and cervical tumors

Table 3 Overview of patients' comorbidity

Patients	103
No comorbidic conditions	28
Myocardial	38
Vascular	54
Pulmonary	7
Neurological	6
Endocrine	26
Renal	1
Liver	1
Gastrointestinal	1
Cancer	11
Miscellaneous	7

The total number exceeds the total number of patients included (103) as some patients had multiple comorbidic conditions

[30, 33–35], but an inverse correlation has been demonstrated for renal clear cell and rectal carcinomas [49–51], indicating that the prognostic or predictive value for CA-IX expression depends on tumor type. Our study does not indicate prognostic value of CA-IX expression for vulvar SCC patients.

In conclusion, we found that high GLUT-1 and CA-IX protein expression levels do not predict DSS for vulvar SCC patients. Furthermore, their expression did not correlate with preoperative Hb levels. However, preoperative Hb levels could predict DSS independently of the development of a groin or distant recurrence, and also correlated with the number of comorbidic conditions. It is most likely that preoperative Hb levels represent overall physical condition more than it predicts tumor hypoxia.

Acknowledgment We thank Dr. J. Hendriks (Department of Epidemiology and Biostatistics, Radboud University Nijmegen Medical Centre) for his expert help regarding the statistical methods used in this study.

Disclosure/conflict of interest None

Open Access This article is distributed under the terms of the Creative Commons Attribution Noncommercial License which permits any noncommercial use, distribution, and reproduction in any medium, provided the original author(s) and source are credited.

References

1. Lataifeh I, Nascimento MC, Nicklin JL, Perrin LC, Crandon AJ, Obermair A (2004) Patterns of recurrence and disease-free survival in advanced squamous cell carcinoma of the vulva. Gynecol Oncol 95(3):701–705
2. Preti M, Ronco G, Ghiringhello B, Micheletti L (2000) Recurrent squamous cell carcinoma of the vulva: clinicopathologic determinants identifying low risk patients. Cancer 88(8):1869–1876
3. Raspagliesi F, Hanozet F, Ditto A, Solima E, Zanaboni F, Vecchione F et al (2006) Clinical and pathological prognostic factors in squamous cell carcinoma of the vulva. Gynecol Oncol 102(2):333–337
4. Oonk MH, Hollema H, de Hullu JA, van der Zee AG (2006) Prediction of lymph node metastases in vulvar cancer: a review. Int J Gynecol Cancer 16(3):963–971
5. van der Zee AG, Oonk MH, de Hullu JA, Ansink AC, Vergote I, Verheijen RH et al (2008) Sentinel node dissection is safe in the treatment of early-stage vulvar cancer. J Clin Oncol 26(6):884–889
6. Fons G, Burger MP, ten Kate FJ, van der Velden (2007) Identification of potential prognostic markers for vulvar cancer using immunohistochemical staining of tissue microarrays. Int J Gynecol Pathol 26(2):188–193
7. Growdon WB, Boisvert SL, Akhavanfard S, Oliva E, as-Santagata DC, Kojiro S et al (2008) Decreased survival in EGFR gene amplified vulvar carcinoma. Gynecol Oncol 111(2):289–297
8. Johnson GA, Mannel R, Khalifa M, Walker JL, Wren M, Min KW et al (1997) Epidermal growth factor receptor in vulvar malignancies and its relationship to metastasis and patient survival. Gynecol Oncol 65(3):425–429
9. Nayha VV, Stenback FG (2007) Increased angiogenesis is associated with poor prognosis of squamous cell carcinoma of the vulva. Acta Obstet Gynecol Scand 86(11):1392–1397
10. Obermair A, Kohlberger P, Bancher-Todesca D, Tempfer C, Sliutz G, Leodolter S et al (1996) Influence of microvessel density and vascular permeability factor/vascular endothelial growth factor expression on prognosis in vulvar cancer. Gynecol Oncol 63 (2):204–209
11. Oonk MH, de Bock GH, van der Veen T, Hoor KA, de Hullu JA, Hollema H et al (2007) EGFR expression is associated with groin node metastases in vulvar cancer, but does not improve their prediction. Gynecol Oncol 104(1):109–113
12. Varlotto J, Stevenson MA (2005) Anemia, tumour hypoxemia, and the cancer patient. Int J Radiat Oncol Biol Phys 63(1):25–36
13. Qutub AA, Popel AS (2007) Three autocrine feedback loops determine HIF1 alpha expression in chronic hypoxia. Biochim Biophys Acta 1773(10):1511–1525
14. Hoogsteen IJ, Marres HA, Bussink J, van der Kogel AJ, Kaanders JH (2007) Tumour microenvironment in head and neck squamous cell carcinomas: predictive value and clinical relevance of hypoxic markers. A review. Head Neck 29(6):591–604
15. Hockel M, Vorndran B, Schlenger K, Baussmann E, Knapstein PG (1993) Tumour oxygenation: a new predictive parameter in locally advanced cancer of the uterine cervix. Gynecol Oncol 51 (2):141–149
16. Kaanders JH, Wijffels KI, Marres HA, Ljungkvist AS, Pop LA, van den Hoogen FJ et al (2002) Pimonidazole binding and tumour vascularity predict for treatment outcome in head and neck cancer. Cancer Res 62(23):7066–7074
17. Sundfor K, Lyng H, Rofstad EK (1998) Tumour hypoxia and vascular density as predictors of metastasis in squamous cell carcinoma of the uterine cervix. Br J Cancer 78(6):822–827
18. Gnarra JR, Zhou S, Merrill MJ, Wagner JR, Krumm A, Papavassiliou E et al (1996) Post-transcriptional regulation of vascular endothelial growth factor mRNA by the product of the VHL tumour suppressor gene. Proc Natl Acad Sci USA 93 (20):10589–10594
19. Hanahan D, Folkman J (1996) Patterns and emerging mechanisms of the angiogenic switch during tumourigenesis. Cell 86(3):353–364
20. Ivanov SV, Kuzmin I, Wei MH, Pack S, Geil L, Johnson BE et al (1998) Down-regulation of transmembrane carbonic anhydrases in renal cell carcinoma cell lines by wild-type von Hippel–Lindau transgenes. Proc Natl Acad Sci USA 95(21):12596–12601
21. Maxwell PH, Wiesener MS, Chang GW, Clifford SC, Vaux EC, Cockman ME et al (1999) The tumour suppressor protein VHL targets hypoxia-inducible factors for oxygen-dependent proteolysis. Nature 399(6733):271–275
22. Macheda ML, Rogers S, Best JD (2005) Molecular and cellular regulation of glucose transporter (GLUT) proteins in cancer. J Cell Physiol 202(3):654–662
23. Sly WS, Hu PY (1995) Human carbonic anhydrases and carbonic anhydrase deficiencies. Annu Rev Biochem 64:375–401
24. Ivanov S, Liao SY, Ivanova A, Danilkovitch-Miagkova A, Tarasova N, Weirich G et al (2001) Expression of hypoxia-inducible cell-surface transmembrane carbonic anhydrases in human cancer. Am J Pathol 158(3):905–919
25. Vaupel P, Mayer A (2005) Hypoxia and anemia: effects on tumour biology and treatment resistance. Transfus Clin Biol 12(1):5–10
26. Hoogsteen IJ, Marres HA, van der Kogel AJ, Kaanders JH (2007) The hypoxic tumour microenvironment, patient selection and hypoxia-modifying treatments. Clin Oncol (R Coll Radiol) 19 (6):385–396
27. Kelleher DK, Mattheinsen U, Thews O, Vaupel P (1996) Blood flow, oxygenation, and bioenergetic status of tumours after erythropoietin treatment in normal and anemic rats. Cancer Res 56(20):4728–4734

28. Airley R, Loncaster J, Davidson S, Bromley M, Roberts S, Patterson A et al (2001) Glucose transporter glut-1 expression correlates with tumour hypoxia and predicts metastasis-free survival in advanced carcinoma of the cervix. Clin Cancer Res 7 (4):928–934
29. Cantuaria G, Fagotti A, Ferrandina G, Magalhaes A, Nadji M, Angioli R et al (2001) GLUT-1 expression in ovarian carcinoma: association with survival and response to chemotherapy. Cancer 92(5):1144–1150
30. Chia SK, Wykoff CC, Watson PH, Han C, Leek RD, Pastorek J et al (2001) Prognostic significance of a novel hypoxia-regulated marker, carbonic anhydrase IX, in invasive breast carcinoma. J Clin Oncol 19(16):3660–3668
31. Fortin A, Wang CS, Vigneault E (2008) Effect of pretreatment anemia on treatment outcome of concurrent radiochemotherapy in patients with head and neck cancer. Int J Radiat Oncol Biol Phys 72(1):255–260
32. Furudoi A, Tanaka S, Haruma K, Yoshihara M, Sumii K, Kajiyama G et al (2001) Clinical significance of human erythrocyte glucose transporter 1 expression at the deepest invasive site of advanced colorectal carcinoma. Oncology 60 (2):162–169
33. Giatromanolaki A, Koukourakis MI, Sivridis E, Turley H, Talks K, Pezzella F et al (2001) Relation of hypoxia inducible factor 1 alpha and 2 alpha in operable non-small cell lung cancer to angiogenic/molecular profile of tumours and survival. Br J Cancer 85(6):881–890
34. Koukourakis MI, Giatromanolaki A, Sivridis E, Simopoulos K, Pastorek J, Wykoff CC et al (2001) Hypoxia-regulated carbonic anhydrase-9 (CA9) relates to poor vascularization and resistance of squamous cell head and neck cancer to chemoradiotherapy. Clin Cancer Res 7(11):3399–3403
35. Loncaster JA, Harris AL, Davidson SE, Logue JP, Hunter RD, Wycoff CC et al (2001) Carbonic anhydrase (CA IX) expression, a potential new intrinsic marker of hypoxia: correlations with tumour oxygen measurements and prognosis in locally advanced carcinoma of the cervix. Cancer Res 61(17):6394–6399
36. Winter WE III, Maxwell GL, Tian C, Sobel E, Rose GS, Thomas G et al (2004) Association of hemoglobin level with survival in cervical carcinoma patients treated with concurrent cisplatin and radiotherapy: a Gynecologic Oncology Group Study. Gynecol Oncol 94(2):495–501
37. Stone JE, Parker R, Gilks CB, Stanbridge EJ, Liao SY, Quino-Parsons C (2005) Intratumoural oxygenation of invasive squamous cell carcinoma of the vulva is not correlated with regional lymph node metastasis. Eur J Gynaecol Oncol 26(1):31–35
38. Charlson ME, Pompei P, Ales KL, MacKenzie CR (1987) A new method of classifying prognostic comorbidity in longitudinal studies: development and validation. J Chronic Dis 40 (5):373–383
39. Koukourakis MI, Giatromanolaki A, Sivridis E, Pastorek J, Karapantzos I, Gatter KC et al (2004) Hypoxia-activated tumour pathways of angiogenesis and pH regulation independent of anemia in head-and-neck cancer. Int J Radiat Oncol Biol Phys 59(1):67–71
40. Koukourakis MI, Giatromanolaki A, Polychronidis A, Simopoulos C, Gatter KC, Harris AL et al (2006) Endogenous markers of hypoxia/anaerobic metabolism and anemia in primary colorectal cancer. Cancer Sci 97(7):582–588
41. Caro JJ, Salas M, Ward A, Goss G (2001) Anemia as an independent prognostic factor for survival in patients with cancer: a systemic, quantitative review. Cancer 91(12):2214–2221
42. Wu WC, Schifftner TL, Henderson WG, Eaton CB, Poses RM, Uttley G et al (2007) Preoperative hematocrit levels and postoperative outcomes in older patients undergoing noncardiac surgery. JAMA 297(22):2481–2488
43. Dunst J, Kuhnt T, Strauss HG, Krause U, Pelz T, Koelbl H et al (2003) Anemia in cervical cancers: impact on survival, patterns of relapse, and association with hypoxia and angiogenesis. Int J Radiat Oncol Biol Phys 56(3):778–787
44. Jonathan RA, Wijffels KI, Peeters W, de Wilde PC, Marres HA, Merkx MA et al (2006) The prognostic value of endogenous hypoxia-related markers for head and neck squamous cell carcinomas treated with ARCON. Radiother Oncol 79(3):288–297
45. Mayer A, Hockel M, Wree A, Vaupel P (2005) Microregional expression of glucose transporter-1 and oxygenation status: lack of correlation in locally advanced cervical cancers. Clin Cancer Res 11(7):2768–2773
46. Stewart GD, Gray K, Pennington CJ, Edwards DR, Riddick AC, Ross JA et al (2008) Analysis of hypoxia-associated gene expression in prostate cancer: lysyl oxidase and glucose transporter-1 expression correlate with Gleason score. Oncol Rep 20(6):1561–1567
47. Lal A, Peters H, St CB, Haroon ZA, Dewhirst MW, Strausberg RL et al (2001) Transcriptional response to hypoxia in human tumours. J Natl Cancer Inst 93(17):1337–1343
48. Wykoff CC, Beasley NJ, Watson PH, Turner KJ, Pastorek J, Sibtain A et al (2000) Hypoxia-inducible expression of tumour-associated carbonic anhydrases. Cancer Res 60(24):7075–7083
49. Bui MH, Seligson D, Han KR, Pantuck AJ, Dorey FJ, Huang Y et al (2003) Carbonic anhydrase IX is an independent predictor of survival in advanced renal clear cell carcinoma: implications for prognosis and therapy. Clin Cancer Res 9(2):802–811
50. Murakami Y, Kanda K, Tsuji M, Kanayama H, Kagawa S (1999) MN/CA9 gene expression as a potential biomarker in renal cell carcinoma. BJU Int 83(7):743–747
51. Rasheed S, Harris AL, Tekkis PP, Turley H, Silver A, McDonald PJ et al (2009) Assessment of microvessel density and carbonic anhydrase-9 (CA-9) expression in rectal cancer. Pathol Res Pract 205(1):1–9

Virchows Arch (2010) 457:705–713
DOI 10.1007/s00428-010-0986-5

ORIGINAL ARTICLE

Interaction of Snail and p38 mitogen-activated protein kinase results in shorter overall survival of ovarian cancer patients

Susanne Hipp · Daniela Berg · Bilge Ergin · Tibor Schuster · Alexander Hapfelmeier · Axel Walch · Stefanie Avril · Barbara Schmalfeldt · Heinz Höfler · Karl-Friedrich Becker

Received: 30 June 2010 / Revised: 8 September 2010 / Accepted: 24 September 2010 / Published online: 19 October 2010
© Springer-Verlag 2010

Abstract Epithelial ovarian cancer is a highly metastatic disease and the leading cause of death among cancer of the female genital tract. Abnormal epidermal growth factor receptor (EGFR) signalling has been shown to be involved in epithelial–mesenchymal transition (EMT), an early step during metastasis. Additionally, over-expression of the E-cadherin repressor Snail, a key regulator of EMT, has previously been found to be associated with unfavourable prognostic features. Thus, the aim of our study was to elucidate the role of EGFR-dependent signalling pathways for Snail expression in ovarian cancer. For this purpose, we analysed 25 formalin-fixed and paraffin-embedded (FFPE) primary tumours and their corresponding metastases for the expression of 25 signalling pathway molecules by reverse phase protein arrays. We found a significant correlation of Snail with EGFR$^{(Tyr1086)}$ and p38 MAPK$^{(Thr180/Tyr182)}$ in primary ovarian carcinoma and with EGFR$^{(Tyr1086)}$ in their corresponding metastasis. Additionally, we showed that high expression levels of Snail in primary tumours combined with high expression levels of the phosphorylated p38 MAPK$^{(Thr180/Tyr182)}$ in metastasis lead to an increased risk for death in ovarian carcinoma patients. Thus, for future combinatorial cancer therapy, drug combinations that best target the deregulated protein network in each individual patient should be selected.

Keywords Snail · p38 · Ovarian cancer · Reverse phase protein microarray (RPPA) · Formalin-fixed and paraffin-embedded tissues (FFPE)

Electronic supplementary material The online version of this article (doi:10.1007/s00428-010-0986-5) contains supplementary material, which is available to authorized users.

S. Hipp · D. Berg · B. Ergin · S. Avril · H. Höfler · K.-F. Becker (✉)
Institut für Pathologie, Technische Universität München,
Trogerstrasse 18,
81675 Munich, Germany
e-mail: kf.becker@lrz.tum.de

T. Schuster · A. Hapfelmeier
Institut für medizinische Statistik und Epidemiologie, Technische Universität München,
Munich, Germany

A. Walch · H. Höfler
Helmholtz Zentrum München, Deutsches Forschungszentrum für Gesundheit und Umwelt GmbH, Pathologie,
Neuherberg, Germany

B. Schmalfeldt
Frauenklinik und Poliklinik der Technischen Universität München,
Munich, Germany

Introduction

Ovarian cancer is a highly metastatic disease exhibiting one of the leading causes of cancer death among women in the developed world [1, 2]. Unfortunately, this disease is often not diagnosed until in advanced stages (FIGO stages III–IV) and not before metastatic setting of the tumour due to the lack of early-stage detection [3]. It is known that metastasis still represents the major cause of the failure of cancer treatment. Therefore, the identification of molecules or signalling pathways involved in metastasis has high impact for the development of an optimal therapy for cancers for which early-stage detection is still an obstacle. In addition to the clarification of the protein network within primary tumours, a critical question is to what extent signalling pathway changes do occur upon metastasis [4]. Immunohistochemistry (IHC) may not be suitable for the analysis of subtle quantitative changes in multiple classes of proteins taking place simultaneously within a tissue. Hence, for optimal patient selection and therapy, new

techniques being able to detect the entire spectrum of deregulated pathways in tumours before and during treatment are needed in addition to IHC. Reverse phase protein array (RPPA) is a very promising new technology that allows the simultaneous analysis of multiple parameters over time, before and after treatment, between disease and non-disease states and between responders and non-responders. Since formalin fixation and paraffin embedding is the standard method for tissue handling in almost all hospitals worldwide, we performed our profiling studies on formalin-fixed and paraffin-embedded (FFPE) ovarian cancer tissues. In fact, it became possible to successfully extract full-length, immunoreactive proteins from FFPE tissues only recently. Therefore, the extraction of full-length proteins from FFPE tissues [5], which then can be applied for RPPA [5–7], represents a powerful tool for the quantitative analysis of protein-based networks in cancer tissues.

Metastasis of ovarian cancer involves a series of cellular events including cell-to-cell and cell-to-matrix adhesion as well as proteolytic activities leading to shedding and dispersal of malignant cells [8, 9]. The differentiation of epithelial cells towards a mesenchymal state, called epithelial–mesenchymal transition (EMT), has been recognised as a key step during cancer metastasis and is known as vital for the physiology of ovarian surface epithelium as well as for the growth and dissemination of ovarian cancer [1, 10, 11]. Deregulated epidermal growth factor receptor (EGFR) triggers diverse signalling pathways in tumour cells such as the mitogen-activated protein (MAP) kinases [10, 12] and is considered as one of the major causes of tumour progression and metastasis [13]. The EGFR is often mutated or over-expressed in many epithelial cancers including ovarian cancer [14], and its over-expression is associated with more aggressive disease and poor clinical outcome. Recently, it was shown that EGFR activation induces matrix metalloprotease-9 production and promotes migration and invasion in ovarian cancer cells [15]. Additionally, EGFR regulates E-cadherin protein expression. For example, chronic treatment with EGF leads to loss of cell–cell adherence junctions and to the down-regulation of E-cadherin expression on the transcriptional level [16]. Reduction of E-cadherin expression is known to be a hallmark of EMT. Membranous E-cadherin expression can be modified by various mechanisms including gene mutations [17–19], promoter hyper-methylation [19–21], post-translational modifications [22] and transcriptional repression [23–25].

Snail is one of the most prominent transcriptional repressors of E-cadherin. It binds to the E-boxes of the E-cadherin promoter, which represses gene transcription [23, 24]. Snail is regulated on the transcriptional level as well as on the protein level. Glycogen synthase kinase-3β (GSK-3β) and p21-activated kinase (PAK1) control Snails' subcellular localisation and regulate Snail protein stability [26–28]. Previous studies showed that over-expression of Snail in endometrial carcinoma metastases correlates with higher tumour grade and abnormal E-cadherin expression [29]. Additionally, it is known that Snail over-expression is associated with lower overall survival of ovarian cancer patients [30] and that E-cadherin down-regulation is associated with Snail up-regulation in human ovarian cancer [31, 32].

Recently, it was shown that abnormal tyrosine kinase signalling plays a role in the regulation of EMT during development and in cell culture studies [33]. However, studies demonstrating a clear correlation between receptor tyrosine kinase signalling and Snail, a master regulator of EMT, in ovarian cancer is still missing. Given the association between EGFR over-expression and high metastatic potential, we hypothesised that the EGFR pathway may contribute to the regulation of Snail expression in ovarian carcinoma. Here, we show first a high correlation of EGFR-related signalling pathways with Snail protein expression in ovarian carcinoma and an increased risk for death in ovarian carcinoma patients having high expression levels of Snail in primary tumours and the phosphorylated p38 MAPK$^{(Thr180/Tyr182)}$ in metastasis.

Materials and methods

Tissue samples

FFPE tissue samples from a total of 25 patients who had undergone primary surgery for newly diagnosed advanced stage (FIGO IIIC and IV) ovarian carcinoma were included in this study. The clinicopathological characteristics of the patients are summarised in Table 1. The study was approved by the Ethics Committee of the Technical University of Munich, Germany. Only patients without chemotherapy or radiotherapy within 6 months prior to surgery were included in the study. Follow-up data were available for 24 patients, with a median follow-up time of 55 months. The median follow-up was calculated by the inverse Kaplan–Meier approach [34]. During follow-up time, 16 of 24 patients died. From one patient (no. 18), no follow-up data were available. Additionally, we omitted the two cases of serous carcinomas grade 1 (nos. 18 and 25) from all statistical analysis because these cancer types have a very indolent behaviour that is not comparable with the biology of conventional high grade ovarian carcinomas.

Reference haematoxylin/eosin-stained sections of the tissues were histological verified by an experienced pathologist (AW). Only tissues with at least 85% of tumour cells were included in the study. Different areas within each tumour were sampled. Adjacent unstained sections of the same paraffin blocks were used for protein extraction.

Table 1 Clinicopathological characteristics of the ovarian cancer patients used in this study

No.	Subtype	Tumour grade	T	N	M	Localisation metastasis	Figo	Status	Survival/last follow-up (months)	Age
1	Serous	3	3c	1	0	O	3c	Dead	19.7	52.8
2	Serous	3	3c	x	1	O	4	Dead	3.3	80.0
3	Serous	3	3b	1	0	O	3c	Alive	30.6	74.8
4	Serous	2	3c	x	0	O	3c	Dead	26.5	52.1
5	Serous	2	3c	0	0	P	3c	Dead	23.4	69.5
6	Endometrioid	3	3c	1	0	O	3c	Dead	32.4	47.1
7	Serous	3	3c	x	0	O	3c	Alive	0.1	80.2
8	Serous	3	3c	x	1	O	4	Alive	54.7	55.4
9	Serous	3	3c	1	1	L	4	Dead	0.8	49.3
10	Serous	3	3c	x	0	O	3c	Dead	17.9	80.2
11	Endometrioid	3	3c	x	1	O/P	4	Dead	16.2	55.4
12	Serous	3	3c	1	0	P	3c	Alive	56.8	73.6
13	Serous	2	3c	1	0	O	3c	Dead	55.7	29.5
14	Serous	3	3c	1	0	O	3c	Alive	47.7	64.2
15	Serous	3	3c	1	0	O	3c	Dead	14.0	65.3
16	Serous	3	3c	1	x	O	3c	Alive	30.7	68.8
17	Clear cell carcinoma	3	3c	1	0	O	3c	Dead	5.5	58.9
18	Serous	1	3c	x	x	x	3c	n.d.	n.d.	71.4
19	Serous	3	3c	x	1	P	4	Dead	6.4	71.6
20	Serous	2	3c	0	0	O	3c	Dead	50.0	36.9
21	Serous	3	3c	1	0	P	3c	Dead	31.2	41.2
22	Serous	3	3c	x	0	P	3c	Alive	49.2	61.1
23	Serous	3	3c	x	0	O	3c	Dead	17.7	78.2
24	Serous	3	3c	1	0	O	3c	Dead	48.8	48.3
25	Serous	1	3c	x	0	O	3c	Alive	55.0	76.8

Localisation of the metastasis: *L* lymph node metastasis, *O* omentum metastasis, *P* peritoneal metastasis

Protein extraction from formalin-fixed tissue samples

After standard deparaffination of tissue sections (10 μm), proteins were extracted as previously described [5], using the Qproteome FFPE Tissue Kit (Qiagen, Hilden, Germany).

Immunoblotting

Total protein extracts were subjected to sodium dodecyl sulphate-polyacrylamide gel electrophoresis, and blotting was performed on nitrocellulose membranes (Whatman/Schleicher and Schuell, Dassel, Germany). Blots were developed using the ECLPlus and ECLadvance Western Blot Detection Systems (Amersham/GE Healthcare Europe GmbH, Muenchen, Germany).

Reverse phase protein microarray

RPPA was generated using the BioOdyssey™ Calligrapher™ MiniArrayer (Biorad, Muenchen, Germany). For every lysate and every dilution (undiluted, 1:2, 1:4, buffer), three replicates were applied onto a nitrocellulose-coated glass slide (Fast™ Slide, Whatman/Schleicher and Schuell, Dassel, Germany). Lysate microarrays were developed using the ECLPlus and ECLadvance Western Blot Detection System. For estimation of total protein amounts, parallel arrays were stained with Sypro Ruby Protein Blot Stain (Molecular Probes, Eugene, OR, USA) according to the manufacturer's instructions and visualised on an Eagle Eye (Stratagene, La Jolla, CA, USA). Developed films were scanned individually on a scanner (Scanjet 3770, Hewlett-Packard, Hamburg, Germany) with 1,200 dpi and were saved as TIFF files. Density of protein spots was measured using Scion Image (Scion Corporation, Frederick, MA, USA). Relative expression levels of proteins were calculated by normalising to total protein.

Antibodies

Antibodies used for western blot and RPPA are listed in Supplementary Table 1. Before protein profiling, however, the specificities of all antibodies used in protein lysate microarray analysis were first confirmed, as previously

described. (Supplementary Fig. 1). Parts of this figure have been published recently [35].

Hierarchical clustering

Unsupervised hierarchical clustering was performed by using Cluster and Tree View software [36].

Statistical analysis

Correlation analysis

Bivariate relationships of quantitative data were assessed by the Spearman rank correlation coefficient (rho), using SPSS version 16.0 (SPSS, Inc, Chicago, IL, USA). To correct for multiple testing, Bonferroni adjustment was conducted in the multiple correlation analyses regarding Snail to warrant a global significance level of 5%.

Survival analysis

Statistical analyses on patient survival were carried out with the software package R Version 2.7.1.

As the main interest was on examining the influence of risk factors on survival, Cox proportional hazard models were fit to the data. Hazard ratios describing the factorial change of risk by a one-point increment on the scale of a risk factor were calculated and reported with 95% confidence intervals (CI). As the biological pathway suggested relations between several factors regarding survival, interaction terms were included in the model process. The introduction of interactions allows the observer to examine mutual effects of risk factors. To illustrate the examined influence on risk and therefore facilitate the interpretation of the model parameters, surface plots for the hazard ratio were created.

Statistical survival analyses were conducted at a 0.05 level of significance. Statistical analysis on prognosis is based on the data of primary tumours and metastasis.

Results

Reverse phase protein microarray technology

The RPPA represents a very promising new high-throughput technology for signalling pathway profiling over time, before and after treatment, between disease and non-disease states and between responders and non-responders. This method allows analysis of multiple samples for the expression of one protein under the same experimental conditions in parallel. Moreover, it is suited for signal transduction profiling of small numbers of cultured cells or cells isolated by laser capture microdissection from human biopsies. After protein extraction from FFPE tissues, each patient sample is arrayed in triplicates on nitrocellulose-coated slides in a miniature dilution curve. Thus, each analyte/antibody combination can be analysed in the linear dynamic range. Then, the density of protein spots is measured. In addition to applying the detection antibody, one or more slides spotted in parallel are stained with a total protein detection reagent (e.g. SYPRO® Ruby staining solution). This step is necessary for normalisation of the signals obtained by the antibodies to total protein (Fig. 1).

Profiling of signalling proteins of primary tumours and metastasis of ovarian cancer patients using RPPA

Cancer cells of epithelial origin, including ovarian cancer cells, undergo EMT as an early event during metastasis. EGFR over-expression and deregulated signalling pathways are considered to be linked to cancer invasion/metastasis. But the specific involvement of EGFR signalling in EMT of ovarian carcinoma remains elusive.

Therefore, we investigated whether EGFR activation is involved in Snail regulation in primary tumours and/or metastases of ovarian cancer. To this end, we performed RPPA analysis with protein extracts from 23 FFPE primary tumours and their corresponding metastases generating a tumour specific protein network portrait. Although patient-specific signalling is apparent, the protein expression can be divided each into two groups (Fig. 2a). In the primary tumours, the phosphorylated forms of HER2$^{(Tyr1248)}$, p38 MAPK$^{(Thr180/Tyr182)}$ and PAK1$^{(Thr212)}$ are located in one cluster together with the active form of EGFR$^{(Tyr1086)}$ and Snail, indicating that these molecules may be involved in the EGF-dependent regulation of Snail. In metastases, however, only the phosphorylated forms of STAT3$^{(Tyr705)}$ and HSP27$^{(Ser82)}$ seem to be involved in the EGFR-dependent regulation of Snail expression (Fig. 2b). Neither in primary tumours nor in metastasis was a statistically significant association between Snail expression and clinicopathological parameters found (Table 2).

To underpin the observations from our cluster analysis, we additionally performed Spearman correlation (Table 3). Again, we found Snail correlating with the active forms of EGFR$^{(Tyr1086)}$ and p38 MAPK$^{(Thr180/Tyr182)}$ in primary ovarian carcinoma and with phospho-EGFR$^{(Tyr1086)}$ in their corresponding metastasis.

In further Spearman correlation analysis, we evaluated signalling networks related to primary tumours and their corresponding metastasis and EMT. Again, we could detect differences between primary tumours and metastasis. Only the expression of 11 of the 25 proteins analysed correlated statistically significant in primary tumours and metastases (Table 4).

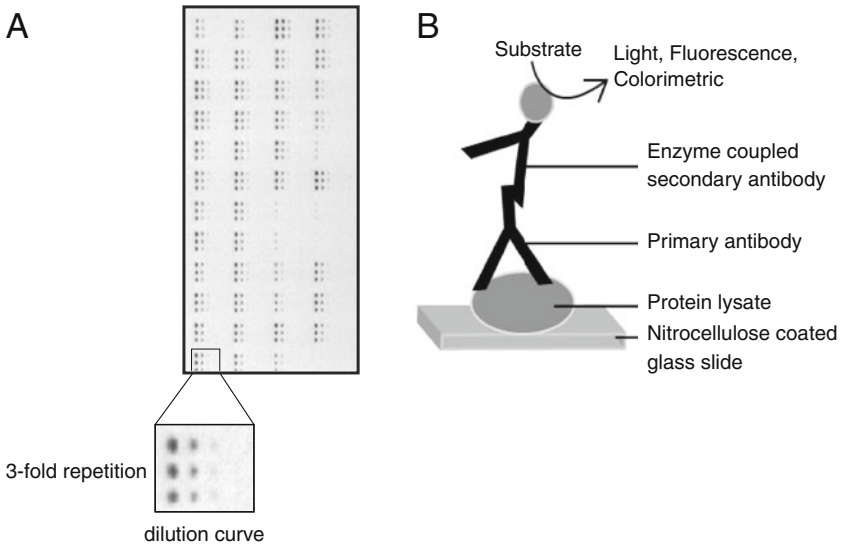

Fig. 1 Reverse phase protein microarray. **a** Protein lysates from FPPE cancer tissue samples were spotted on a nitrocellulose-coated glass slide, followed by incubation with the primary antibody. Per lysate, a 3-fold dilution curve in three replicates was spotted. For normalisation of the antibody signals to total protein, the slide was stained with Sypro Ruby reagent. **b** Patient samples are arrayed onto a nitrocellulose-coated glass slide and incubated with a primary antibody of interest. Detection is carried out by using an enzyme coupled secondary antibody together with its target substrate

Interaction of Snail and p38 mitogen-activated protein kinase leads to shorter overall survival of ovarian cancer patients

So far, we documented a strong correlation between Snail and the phosphorylated forms of EGFR$^{(Tyr1086)}$ and p38 MAPK$^{(Thr180/Tyr182)}$ in primary ovarian tumours. Now, we asked whether specific combinations of Snail and these proteins have a prognostic value. In Cox hazard regression analyses summarised in Table 5, patients with high expression levels of both Snail and the phosphorylated form of p38 MAPK showed a significantly higher risk of death.

The first two models show the results of the univariable analyses of Snail and E-cadherin in primary

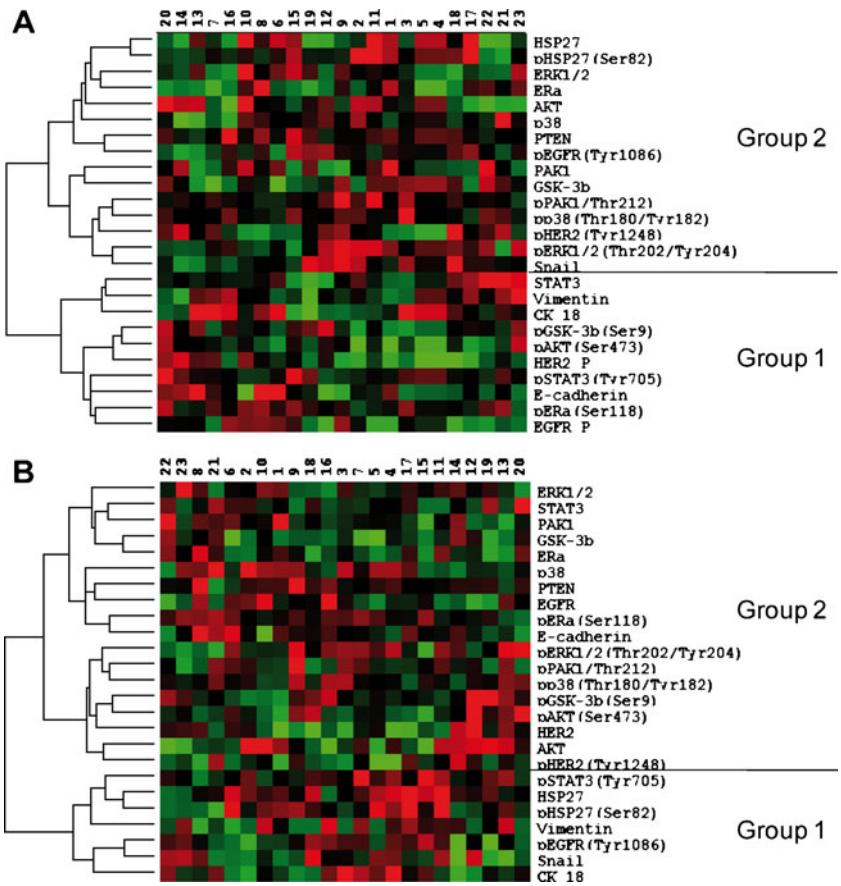

Fig. 2 Protein network portrait. Twenty-five proteins were used in the analysis of primary tumours (**a**) and metastases (**b**). The patients are numbered in the *horizontal axis*, and the protein expression is on the *vertical axis*. Higher protein expression levels are represented in *red*; lower levels, in *green*

Table 2 Median and interquartile range of Snail in quantitative clinicopathological parameters for primary tumours and metastasis

		Snail			
		N	Median	(range)/[IQR][a]	*p*
Primary tumours					
Grade	2	4	0.09	(0.08; 1.26)	0.218
	3	19	0.40	[0.23; 0.69]	
T	3b	1	0.79		–[b]
	3c	22	0.32	[0.12; 0.66]	
N	0	2	0.68	(0.09; 1.26)	–[b]
	1	12	0.29	[0.15; 0.77]	
	x	9	0.40	(0.08; 0.76)	
M	0	17	0.24	[0.10; 0.73]	0.164
	1	5	0.44	(0.33; 1.10)	
	x	1	0.42		
Figo	3c	18	0.26	[0.10; 0.71]	0.174
	4	5	0.44	(0.33; 1.10)	
Subtype	1	19	0.33	[0.10; 0.76]	–[b]
	2	2	0.31	(0.21; 0.40)	
	3	2	0.45	(0.30; 0.60)	
Age		23	Spearman's rho, +0.124		0.573
Metastasis					
Grade	2	4	0.27	(0.10; 0.39)	0.054
	3	19	0.47	[0.27; 0.64]	
T	3b	1	0.46		–[b]
	3c	22	0.42	[0.26; 0.63]	
N	0	2	0.27	(0.15; 0.39)	–[b]
	1	12	0.37	[0.24; 0.63]	
	x	9	0.47	(0.26; 0.96)	
M	0	17	0.38	[0.25; 0.55]	0.164
	1	5	0.58	(0.26; 0.81)	
	x	1	0.64		
Figo	3c	18	0.39	[0.25; 0.62]	0.199
	4	5	0.58	(0.26; 0.81)	
Subtype	1	19	0.44	[0.26; 0.63]	–[b]
	2	2	0.54	(0.26; 0.81)	
	3	2	0.38	(0.29; 0.47)	
Age		23	Spearman's rho, + 0.32		0.138

For continuous variables, Spearman correlation coefficient is given

[a] Interquartile range (*IQR*) instead of range was reported for group sample sizes ≥10

[b] No group comparisons were conducted because of insufficient group sample sizes

tumours, revealing that there is no evidence for a single significant impact of Snail (p value=0.790) and E-cadherin (p=0.156) on the risk of death. The 95% confidence intervals of the hazard ratio estimations show that the factorial risk increment (for a one-unit increase of Snail/E-cadherin) in the underlying population have to be expected in a range 0.22 to 3.22 (Snail) and 0.12 to 1.40 (E-cadherin) with a probability of 95%. If there was a statistically significant association of Snail or E-cadherin and survival, the critical value of one would not be included in these intervals.

As the biological pathway suggested relations between Snail of the primary tumour and the phosphorylated form of

Table 3 Spearman rank correlations (rho) relating Snail expression and expression of various proteins in primary tumours and their corresponding metastases

Protein	Rho	*p* value
Primary tumour		
pEGFR$^{(Tyr1086)}$	**0.874**	**<0.0001**
pHER2$^{(Tyr1248)}$	0.629	0.0324
pp38$^{(Thr180/Tyr182)}$	**0.708**	**0.0038**
pPAK1$^{(Thr212)}$	0.693	0.00625
Metastasis		
pEGFR$^{(Tyr1086)}$	**0.760**	**0.0006**
pHSP27$^{(Ser82)}$	0.148	>0.9999
pSTAT3$^{(Tyr705)}$	0.323	>0.9999

Significant at a Bonferroni-adjusted level of significance p<0.006

Table 4 Spearman rank correlation (rho): protein expression in primary tumour versus metastases

Protein	Rho	*p* value
pAKT$^{(Ser473)}$	**0.734**	**<0.001**
AKT	**0.746**	**<0.001**
Cytokeratin18	0.590	0.003
E-cadherin	0.480	0.020
pEGFR$^{(Tyr1086)}$	0.482	0.020
EGFR	**0.656**	**0.001**
pER$\alpha^{(Ser118)}$	0.527	0.010
ERα	**0.800**	**<0.001**
pERK1/2$^{(Thr202/Tyr204)}$	0.051	0.818
ERK1/2	**0.673**	**<0.001**
pGSK-3$\beta^{(Ser9)}$	**0.858**	**<0.001**
GSK-3β	**0.635**	**0.001**
pHER2$^{(Tyr1248)}$	0.615	0.002
HER2	**0.658**	**0.001**
pHSP27$^{(Ser82)}$	0.569	0.005
HSP27	0.556	0.006
pp38$^{(Thr180/Tyr182)}$	**0.785**	**<0.001**
p38	0.445	0.033
pPAK1$^{(Thr212)}$	**0.704**	**<0.001**
PAK1	0.542	0.008
PTEN	**0.735**	**<0.001**
pSTAT-3$^{(Tyr705)}$	0.468	0.024
STAT-3	**0.701**	**<0.001**
Snail	0.404	0.056
Vimentin	0.612	0.002

Statistical significant at a Bonferroni-adjusted level of significance of 0.0018

Table 5 Cox proportional hazard models for the factors Snail, E-cadherin, and interaction of Snail with pp38$^{(Thr180/Tyr182)}$ in primary tumours and metastasis

Model		Coefficient	Hazard ratio	95% CI		*p* value
				Hazard ratio		
				Lower	Upper	
1	Snail	−0.18	0.83	0.22	3.22	0.790
2	E-cadherin	−0.86	0.42	0.12	1.40	0.156
3	Snail	−4.80	0.0083	0.00014	0.4875	0.021
	pp38$^{(Thr180/Tyr182)}$	−0.702[a]	0.496	0.282	0.872	0.015
	Interaction	1.289[b]	3.630	1.318	9.995	0.012[c]

[a] Per an absolute increment of pp38$^{(Thr180/Tyr182)}$ of 0.10

[b] Per an absolute increment of [Snail×10×pp38$^{(Thr180/Tyr182}$)] of one

[c] Significant at a 5% significance level

p38 MAPK$^{(Thr180/Tyr182)}$ of the metastasis, an interaction term was included in the model which is displayed by model 3 (Table 5). In addition to each risk factor's contribution to the hazard ratio, this interaction term incorporates a change of risk by different parameter constellations. All coefficient *p* values are lower than the 5% significance level. Thus, there is a reasonable evidence that an individual's hazard can be explained by Snail, pp38 MAPK$^{(Thr180/Tyr182)}$, and their interaction. To assess the hazard ratio of an individual in comparison with a person with an expression of Snail=0 and pp38 MAPK$^{(Thr180/Tyr182)}$=0 (reference person), one has to solve the equation hazard ratio=exp(−4.80×Snail−7.00×pp38 MAPK$^{(Thr180/Tyr182)}$+12.81×Snail×pp38$^{(Thr180/Tyr182)}$). To facilitate the interpretation of this relationship, the hazard ratio is illustrated in (Fig. 3). The illustration reveals that high values of both Snail and pp38$^{(Thr180/Tyr182)}$ lead to a high risk for death. A low value in one factor combined with a high value in the other factor will produce a low likelihood ratio.

Discussion

Metastasis is still a major barrier of cancer therapy and represents furthermore one of the primary causes of mortality in many cancers, including ovarian carcinoma. Therefore, it is crucial to understand the biology of cancer cells with high metastatic potential to identify tumours that are likely to undergo metastasis. This would be inalienable to improve current cancer therapies. Additionally, it is known that tumours with deregulated EGFR pathways exhibit a high potential to undergo invasion and migration. However, the specific involvement of EGFR in EMT, an early event during metastasis, and tumour invasion remains elusive [16]. Thus, the current study was undertaken to elucidate whether EGFR-related signalling pathways may contribute to the regulation of the EMT key regulator Snail.

Until now, IHC is routinely used for protein analysis in FFPE cancer tissues. This technique combines anatomical, immunological, and biochemical methods for the identification of specific tissue components via antigen/antibody reaction. Additionally, IHC is an excellent detection technique and has the tremendous advantage of being able to show exactly where a given protein is located within the tissue. However, its major disadvantage is that unlike RPPA, precise protein quantification is difficult and

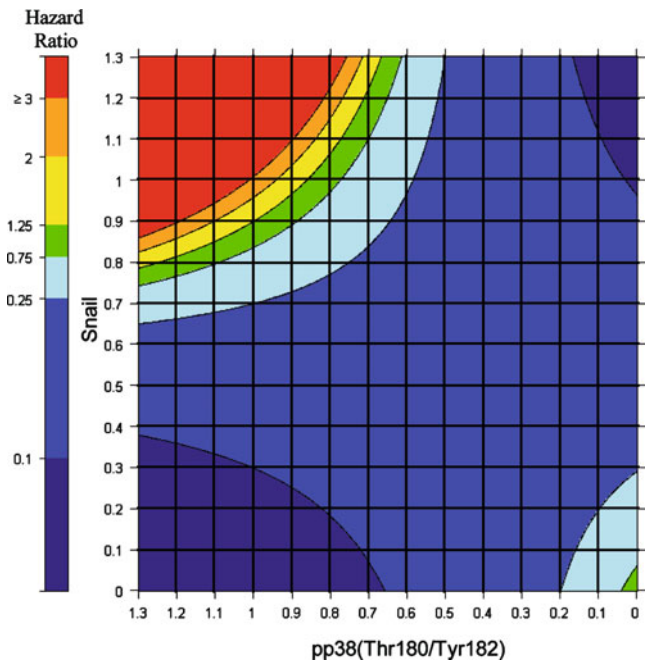

Fig. 3 Estimated hazard ratio in depending on the interaction of Snail and pp38 $^{(Thr180/Tyr182)}$. *Colours* indicate the magnitude of the hazard ratio, which is calculated in reference to the risk of death associated with a zero expression of both Snail and pp38$^{(Thr180/Tyr182)}$

depends in part on the observer. Thus, RPPA has some advantages over IHC. For example, RPPA allows fast analysis of many protein markers in parallel, and this technique is also compatible with low sample volume. Furthermore, in our group, we established a method to standardise and quantify protein expression in patients by the use of purified proteins allowing the determination of protein expression more precisely than it is possible by IHC [7]. Therefore, RPPA is expected to bear advantages for patient and therapy selection, although the correlation between protein abundance and histology is lost. Previous experiments showed that protein expression (e.g. HER2) correlated very well in the RPPA analysis when compared with the "gold standard" IHC, even in small tissue samples such as biopsies [5]. Thus, these results indicate that RPPA technology can reliably be used for biomarker assessment.

In this study, we generated a tumour-specific signalling network portrait of 23 FFPE primary ovarian carcinomas and their corresponding metastasis using RPPA. Consistent with previous results [4], we demonstrated clear differences in protein expression profiles of primary tumours and their metastases (Fig. 2a, b). However, in this context, the specific metastatic process of ovarian cancer should be considered. Both parallel and linear developments of ovarian and extra-ovarian manifestations are possible. Therefore, differences in protein expression observed in this study could be explained by these two cancer progression models. For example, cases that show clear differences in signalling pathways may be generated in parallel. Therefore, these findings indicate the need to additionally compare signalling pathway activity between primary tumours and metastases to understand signal transduction of the tumour within its metastatic microenvironment. Thus, for targeted therapy decisions and optimal patient selections, it is crucial to include patients' metastatic lesions also.

Here, we found Snail significantly correlating with the active forms of EGFR$^{(Tyr1086)}$ and p38 MAPK$^{(Thr180/Tyr182)}$ in primary ovarian carcinomas and with phosphor-EGFR$^{(Tyr1086)}$ in the metastasis. These results are in line with recent reports that described these molecules to play a role in the regulation of Snail. For example, p38 MAPK and ERK1/2 have been shown to act as mediators of Snail and Slug expression after UV exposure in keratinocytes [37]. PAK1 promotes Snail's nuclear accumulation and consequently its repressor activity in human breast cancer [27].

We also asked whether signalling pathways regulating Snail would be of prognostic value. Applying Cox proportional hazard models, we found a statistically significant association between the interaction of the phosphorylated form of p38 MAPK$^{(Thr180/Tyr182)}$ and Snail, and worse overall survival prognosis. This indicates that up-regulation of Snail via p38 MAPK leads to an adverse clinical outcome for ovarian cancer patients. Since the available sample size was rather small and therefore an overly optimistic fit in the survival analysis cannot be excluded, further studies with sufficient sample sizes should be performed to confirm our results. However, the ranges of the 95% confidence intervals of the Cox regression equation, which reflect the uncertainty by sample size, should be considered in the application of our proposed prediction model.

To conclude, our results showed an EGFR-dependent up-regulation of Snail expression in ovarian carcinoma. Additionally, we found for the first time that co-over-expression of phospho-p38 MAPK$^{(Thr180/Tyr182)}$ in metastatic lesions and Snail in primary tumours results in reduced overall survival in patients with ovarian cancer. Thus, for future combinatorial cancer therapy, drug combinations that best target the deregulated protein network in each individual patient should be selected.

Acknowledgements The authors wish to thank Christa Schott for excellent technical assistance. This study is supported by the German Federal Ministry of Education and Research (BMBF) grant no. 01GR0805 to KFB and the Deutsche Forschungsgemeinschaft [*DFG*, grant number BE1501/3-2] to KFB and HH.

Conflict of interest KFB is a named inventor of a patent related to protein extraction from formalin-fixed tissues. He had full access to all of the data in this study and takes complete responsibility for the integrity of the data and the accuracy of the data analysis. Qiagen GmbH, the owner of the patent, did not assert control over the authors' right to publish.

References

1. Ahmed N, Thompson EW, Quinn MA (2007) Epithelial–mesenchymal interconversions in normal ovarian surface epithelium and ovarian carcinomas: an exception to the norm. J Cell Physiol 213:581–588
2. Parkin DM, Bray F, Ferlay J, Pisani P (2005) Global cancer statistics, 2002. CA Cancer J Clin 55:74–108
3. Vergara D, Merlot B, Lucot JP, Collinet P, Vinatier D, Fournier I, Salzet M (2010) Epithelial–mesenchymal transition in ovarian cancer. Cancer Lett 291:59–66
4. Sheehan KM, Calvert VS, Kay EW, Lu FD, Espina V, Aquino J, Speer R, Araujo R, Mills GB, Liotta LA, Petricoin EF 3rd, Wulfkuhle JD (2005) Use of reverse phase protein microarrays and reference standard development for molecular network analysis of metastatic ovarian carcinoma. Mol Cell Proteomics 4:346–355
5. Becker KF, Schott C, Hipp S, Metzger V, Porschewski P, Beck R, Nahrig J, Becker I, Hofler H (2007) Quantitative protein analysis from formalin-fixed tissues: implications for translational clinical research and nanoscale molecular diagnosis. J Pathol 211:370–378
6. Paweletz CP, Charboneau L, Bichsel VE, Simone NL, Chen T, Gillespie JW, Emmert-Buck MR, Roth MJ, Petricoin IE, Liotta LA (2001) Reverse phase protein microarrays which capture disease progression show activation of pro-survival pathways at the cancer invasion front. Oncogene 20:1981–1989

7. Berg D, Hipp S, Malinowsky K, Bollner C, Becker KF (2010) Molecular profiling of signalling pathways in formalin-fixed and paraffin-embedded cancer tissues. Eur J Cancer 46:47–55
8. Geho DH, Bandle RW, Clair T, Liotta LA (2005) Physiological mechanisms of tumor-cell invasion and migration. Physiology (Bethesda) 20:194–200
9. Thompson EW, Newgreen DF, Tarin D (2005) Carcinoma invasion and metastasis: a role for epithelial–mesenchymal transition? Cancer Res 65:5991–5995, discussion 5995
10. Ahmed N, Maines-Bandiera S, Quinn MA, Unger WG, Dedhar S, Auersperg N (2006) Molecular pathways regulating EGF-induced epithelio-mesenchymal transition in human ovarian surface epithelium. Am J Physiol Cell Physiol 290:C1532–C1542
11. Bagnato A, Rosano L (2007) Epithelial–mesenchymal transition in ovarian cancer progression: a crucial role for the endothelin axis. Cells Tissues Organs 185:85–94
12. Yarden Y, Shilo BZ (2007) SnapShot: EGFR signaling pathway. Cell 131:1018
13. Lo HW, Hsu SC, Xia W, Cao X, Shih JY, Wei Y, Abbruzzese JL, Hortobagyi GN, Hung MC (2007) Epidermal growth factor receptor cooperates with signal transducer and activator of transcription 3 to induce epithelial–mesenchymal transition in cancer cells via up-regulation of TWIST gene expression. Cancer Res 67:9066–9076
14. Psyrri A, Kassar M, Yu Z, Bamias A, Weinberger PM, Markakis S, Kowalski D, Camp RL, Rimm DL, Dimopoulos MA (2005) Effect of epidermal growth factor receptor expression level on survival in patients with epithelial ovarian cancer. Clin Cancer Res 11:8637–8643
15. Cowden Dahl KD, Symowicz J, Ning Y, Gutierrez E, Fishman DA, Adley BP, Stack MS, Hudson LG (2008) Matrix metalloproteinase 9 is a mediator of epidermal growth factor-dependent e-cadherin loss in ovarian carcinoma cells. Cancer Res 68:4606–4613
16. Lu Z, Ghosh S, Wang Z, Hunter T (2003) Downregulation of caveolin-1 function by EGF leads to the loss of E-cadherin, increased transcriptional activity of beta-catenin, and enhanced tumor cell invasion. Cancer Cell 4:499–515
17. Becker KF, Atkinson MJ, Reich U, Becker I, Nekarda H, Siewert JR, Hofler H (1994) E-cadherin gene mutations provide clues to diffuse type gastric carcinomas. Cancer Res 54:3845–3852
18. Berx G, Becker KF, Hofler H, van Roy F (1998) Mutations of the human E-cadherin (CDH1) gene. Hum Mutat 12:226–237
19. Machado JC, Oliveira C, Carvalho R, Soares P, Berx G, Caldas C, Seruca R, Carneiro F, Sobrinho-Simoes M (2001) E-cadherin gene (CDH1) promoter methylation as the second hit in sporadic diffuse gastric carcinoma. Oncogene 20:1525–1528
20. Grady WM, Willis J, Guilford PJ, Dunbier AK, Toro TT, Lynch H, Wiesner G, Ferguson K, Eng C, Park JG, Kim SJ, Markowitz S (2000) Methylation of the CDH1 promoter as the second genetic hit in hereditary diffuse gastric cancer. Nat Genet 26:16–17
21. Liu FS (2007) Molecular carcinogenesis of endometrial cancer. Taiwan J Obstet Gynecol 46:26–32
22. Rashid MG, Sanda MG, Vallorosi CJ, Rios-Doria J, Rubin MA, Day ML (2001) Posttranslational truncation and inactivation of human E-cadherin distinguishes prostate cancer from matched normal prostate. Cancer Res 61:489–492
23. Batlle E, Sancho E, Franci C, Dominguez D, Monfar M, Baulida J, Garcia De Herreros A (2000) The transcription factor Snail is a repressor of E-cadherin gene expression in epithelial tumour cells. Nat Cell Biol 2:84–89
24. Cano A, Perez-Moreno MA, Rodrigo I, Locascio A, Blanco MJ, del Barrio MG, Portillo F, Nieto MA (2000) The transcription factor Snail controls epithelial–mesenchymal transitions by repressing E-cadherin expression. Nat Cell Biol 2:76–83
25. Hemavathy K, Ashraf SI, Ip YT (2000) Snail/slug family of repressors: slowly going into the fast lane of development and cancer. Gene 257:1–12
26. Schlessinger K, Hall A (2004) GSK-3beta sets Snail's pace. Nat Cell Biol 6:913–915
27. Yang Z, Rayala S, Nguyen D, Vadlamudi RK, Chen S, Kumar R (2005) Pak1 phosphorylation of Snail, a master regulator of epithelial-to-mesenchyme transition, modulates Snail's subcellular localization and functions. Cancer Res 65:3179–3184
28. Zhou BP, Deng J, Xia W, Xu J, Li YM, Gunduz M, Hung MC (2004) Dual regulation of Snail by GSK-3beta-mediated phosphorylation in control of epithelial–mesenchymal transition. Nat Cell Biol 6:931–940
29. Blechschmidt K, Kremmer E, Hollweck R, Mylonas I, Hofler H, Kremer M, Becker KF (2007) The E-cadherin repressor Snail plays a role in tumor progression of endometrioid adenocarcinomas. Diagn Mol Pathol 16:222–228
30. Blechschmidt K, Sassen S, Schmalfeldt B, Schuster T, Hofler H, Becker KF (2008) The E-cadherin repressor Snail is associated with lower overall survival of ovarian cancer patients. Br J Cancer 98:489–495
31. Elloul S, Silins I, Trope CG, Benshushan A, Davidson B, Reich R (2006) Expression of E-cadherin transcriptional regulators in ovarian carcinoma. Virchows Arch 449:520–528
32. Imai T, Horiuchi A, Wang C, Oka K, Ohira S, Nikaido T, Konishi I (2003) Hypoxia attenuates the expression of E-cadherin via up-regulation of SNAIL in ovarian carcinoma cells. Am J Pathol 163:1437–1447
33. Larue L, Bellacosa A (2005) Epithelial–mesenchymal transition in development and cancer: role of phosphatidylinositol 3' kinase/AKT pathways. Oncogene 24:7443–7454
34. Schemper M, Smith TL (1996) A note on quantifying follow-up in studies of failure time. Control Clin Trials 17:343–346
35. Hipp S, Walch A, Schuster T, Losko S, Laux H, Bolton T, Hofler H, Becker KF (2009) Activation of epidermal growth factor receptor results in Snail protein but not mRNA over-expression in endometrial cancer. J Cell Mol Med 13:3858–3867
36. Eisen MB, Spellman PT, Brown PO, Botstein D (1998) Cluster analysis and display of genome-wide expression patterns. Proc Natl Acad Sci USA 95:14863–14868
37. Hudson LG, Choi C, Newkirk KM, Parkhani J, Cooper KL, Lu P, Kusewitt DF (2007) Ultraviolet radiation stimulates expression of Snail family transcription factors in keratinocytes. Mol Carcinog 46:257–268

Virchows Arch (2010) 457:715–725
DOI 10.1007/s00428-010-0993-6

ORIGINAL ARTICLE

Can nuclear magnetic resonance (NMR) spectroscopy reveal different metabolic signatures for lung tumours?

Iola F. Duarte · Cláudia M. Rocha · António S. Barros · Ana M. Gil · Brian J. Goodfellow · Isabel M. Carreira · João Bernardo · Ana Gomes · Vitor Sousa · Lina Carvalho

Received: 11 June 2010 / Revised: 23 August 2010 / Accepted: 29 September 2010 / Published online: 13 October 2010
© Springer-Verlag 2010

Abstract This study aims to evaluate the potential of ^{1}H NMR spectroscopy, combined with multivariate statistics, for discriminating between tumour and non-involved (control) pulmonary parenchyma and for providing biochemical information on different histological types. Paired tissue samples from 24 primary lung tumours were directly analysed by high-resolution magic angle spinning (HRMAS) ^{1}H NMR spectroscopy (500 MHz), and their spectral profiles subjected to principal component analysis (PCA) and partial least squares regression discriminant analysis (PLS-DA). Tumour and adjacent control parenchyma were clearly discriminated in the PLS-DA model with a high level of sensitivity (95% of tumour samples correctly classified) and 100% specificity (no false positives). The metabolites giving rise to this separation were mainly lactate, glycerophosphocholine, phosphocholine, taurine, reduced glutathione and uridine di-phosphate (elevated in tumours) and glucose, phosphoethanolamine, acetate, lysine, methionine, glycine, *myo*- and *scyllo*-inositol (reduced in tumours compared to control tissues). Furthermore, PLS-DA of a subset of tumour samples allowed adenocarcinomas to be discriminated from carcinoid tumours and epidermoid carcinomas, highlighting differences in metabolite levels between these histological types, and therefore revealing valuable knowledge on the biochemistry of different types of bronchial-pulmonary carcinomas.

Keywords Lung tumour · NMR spectroscopy · HRMAS · Metabolic profile · Multivariate statistics

I. F. Duarte · C. M. Rocha · A. M. Gil · B. J. Goodfellow
CICECO, Department of Chemistry, University of Aveiro,
Campus Universitário de Santiago,
3810-193 Aveiro, Portugal

A. S. Barros
QOPNA, Department of Chemistry, University of Aveiro,
Campus Universitário de Santiago,
3810-193 Aveiro, Portugal

I. M. Carreira
Cytogenetics Laboratory and CNC, Faculty of Medicine,
University of Coimbra,
3000 Coimbra, Portugal

J. Bernardo · A. Gomes · V. Sousa · L. Carvalho
University Hospitals of Coimbra,
3000-075 Coimbra, Portugal

V. Sousa · L. Carvalho
Institute of Pathological Anatomy, Faculty of Medicine,
University of Coimbra,
3000 Coimbra, Portugal

I. F. Duarte (✉) · B. J. Goodfellow · I. M. Carreira · J. Bernardo · A. Gomes · V. Sousa · L. Carvalho
CIMAGO, Faculty of Medicine, University of Coimbra,
3000 Coimbra, Portugal
e-mail: ioladuarte@ua.pt

Introduction

The importance of altered metabolism in tumour physiology has long been recognised and debated, as there is cumulative evidence that neoplastic cells show distinct metabolic behaviour to face nutrient and oxygen availability and to meet high energy and biosynthetic demands for matrix-interaction and progression. Cancer metabolic phenotype is already being exploited in diagnosis, namely through the *in vivo* non-invasive quantitative assessment of glucose metabolism by FDG-PET imaging, and in chemoprevention by employing some antimetabolite drugs. Until recently, knowledge of tumour metabolic processes was largely inferred from genomic and proteomic studies, but

this approach has limitations, as it does not account for factors such as posttranslational modifications, allosteric regulation or metabolic compartmentalization. Recent technological developments employing advanced analytical techniques such as nuclear magnetic resonance (NMR) spectroscopy have enabled the direct assessment of the metabolic composition of biological tissues and fluids, thus providing unique and complementary insights into tumour biology. Indeed, this so called metabonomics (or metabolomics) approach has shown great potential for identifying cancer biomarker profiles with diagnostic and/or prognostic value and for monitoring the pharmacodynamic effects of chemotherapy [1–4].

The application of NMR metabonomics to lung cancer metabolic characterization is still in its infancy. A few studies involving NMR of tissue extracts have focused on the measurement of specific metabolite levels to determine differences between normal and tumour tissue and within tumours of different histological types [5], as well as to assess the prognostic value of some of these metabolites [6, 7], and to evaluate lung tumour responsiveness to erlotinib [8]. Another work, also using NMR of tissue extracts together with blood plasma analysis, demonstrated the value of ^{13}C stable-isotope-assisted metabolomics to elucidate metabolic perturbations in lung cancer [9]. Metabolic profiling of tissue extracts has, however, some important limitations as extraction methods may cause the loss or chemical modification of cellular components, and are selective for either lipophilic or hydrophilic compounds, thus limiting the information about the real metabolic events taking place *in vivo*.

The direct analysis of intact tissues has been enabled by high-resolution magic angle spinning (HRMAS) NMR, which allows the simultaneous detection of both lipids and small metabolites with a resolution comparable to that of liquid state NMR, and has been established as a valuable tool in cancer research [4]. In particular, it proved to be very powerful for corroborating and complementing non-invasive *in vivo* magnetic resonance spectroscopy studies by aiding assignment and quantification of the *in vivo* data, generally characterised by poor resolution and signal-to-noise at clinical magnetic field strengths [10–14]. Moreover, much research work has focused on the metabolic differentiation between tumour and healthy tissues, aiming to find possible biomarkers for the presence and/or grade of different cancers such as breast [15, 16], brain [17, 18], prostate [19–21], cervical [22–24], colorectal [25, 26], hepatic [27], renal [28, 29] and gastric cancer [30].

The first applications of HRMAS NMR to human lung tissue have recently been reported. In the work by Jordan *et al*. [31], paired tissue and serum samples from patients with squamous cell carcinoma and adenocarcinoma of the lung were analysed and the two cancer types differentiated. On the other hand, our group addressed the detailed characterization of lung tissue composition and the differentiation between tumour and non-involved adjacent tissue [32]. In that work, involving a relatively small number of cases, unsupervised multivariate methods applied to ^{1}H HRMAS spectra highlighted different metabolic profiles characterising lung tumour and control tissue. However, no correlation was found between metabolic profile and histological classification of the tumours.

In this work, paired tumour and adjacent non-involved (control) tissues from 24 primary pulmonary carcinomas have been analysed by ^{1}H HRMAS NMR. Both unsupervised and supervised multivariate methods were applied to the spectral data, and the predictive ability of the classification models for differentiating between lung tumours and control tissues was assessed. Moreover, metabolic discrimination of different histological types, namely adenocarcinomas, carcinoid tumours and epidermoid carcinomas was attempted.

Materials and methods

Lung tumours

In total, 24 cases of primary lung tumours (15 males and nine females, age range 32–79 years, mean age 62± 12 years) were included in this study. Final diagnosis and TNM staging were established by the histopathological study. The malignant epithelial tumours were characterised as 11 adenocarcinomas (10 mixed subtype, one acinar), four epidermoid carcinoma, three typical carcinoids, three sarcomatoid carcinomas (two pleomorphic, one giant cell) and two large cell carcinomas (one lymphoepithelioma-like, one neuroendocrine large cell carcinoma); an inflammatory myofibroblastic tumour, classified as a mesenchymal tumour according to the 2004 WHO Classification of Tumours [33] was also included (Table 1). In all cases, the surrounding parenchyma had two or more histological characteristics of "smoking lung", mainly emphysema and bronchiolitis.

Tissue handling

Lung tumour and non-involved adjacent parenchyma samples were retrieved from surgical specimens within a maximum of 30 min after surgery, immediately snap-frozen in liquid nitrogen and stored at −80°C until NMR analysis. Sampling for diagnosis was routinely performed and only redundant tissue was included in this study. Each sample stored for NMR had approximately 5 mm^3 and in cases where larger samples could be collected, two fragments were collected, in order to assess the influence of tissue

Table 1 Demographic and histological data

Case no.	Gender	Age (years)	Stage	Neoplastic cells in mirror sections (%)	Histological type
1	M	32	n.a.	n.a.	Inflammatory myofibroblastic tumour
2	M	66	n.a.	>50%	Carcinoid tumour (typical carcinoid)
3	F	57	IB	50%	Adenocarcinoma (mixed subtype)
4	F	75	IB	n.a.	Adenocarcinoma (mixed subtype)
5	M	71	IIB	50%	Adenocarcinoma (mixed subtype)
6	M	81	n.a.	>50%	Adenocarcinoma (mixed subtype)
7	F	58	IA	<50%	Sarcomatoid carcinoma (pleomorphic carcinoma)
8	M	79	n.a.	<50% (necrosis)	Large cell carcinoma (lymphoepithelioma-like carcinoma)
9	M	62	IIA	<<50% (inflammation, necrosis)	Epidermoid carcinoma
10	F	77	IIB	50%	Adenocarcinoma (mixed subtype)
11	F	55	IB	>50%	Adenocarcinoma (mixed subtype)
12	F	42	IA	>50% (inflammation)	Adenocarcinoma (acinar adenocarcinoma)
13	F	64	IB	<50%	Adenocarcinoma (mixed subtype)
14	M	66	IIB	100% (necrosis, fibrosis, inflammation)	Epidermoid carcinoma
15	M	68	n.a.	>50% (inflammation)	Sarcomatoid carcinoma (pleomorphic carcinoma)
16	M	49	IB	>50% (necrosis)	Adenocarcinoma (mixed subtype)
17	F	65	IB	<50%	Epidermoid carcinoma
18	M	58	IB	>50%	Epidermoid carcinoma
19	M	68	IIIA	<50% (inflammation)	Adenocarcinoma (mixed subtype)
20	M	46	IIB	100%	Sarcomatoid carcinoma (giant cell carcinoma)
21	M	64	n.a.	100%	Carcinoid tumour (typical carcinoid)
22	M	60	IIB	>50%	Large cell carcinoma (neuroendocrine carcinoma)
23	F	51	IIB	>50% (necrosis)	Adenocarcinoma (mixed subtype)
24	M	62	IIA	100%	Carcinoid tumour (typical carcinoid)

n.a. not available

heterogeneity on the spectral profiles. In total, 25 control tissues and 26 tumour samples were subjected to NMR analysis. Their mirror sections underwent histological observation and the percentage of neoplastic cells was determined to be higher or lower than 50% (Table 1).

Sample preparation

The frozen tissue samples were washed with a few drops of D_2O saline (0.9%) and about 40 mg of thawed cold tissue were packed into 50 μl HRMAS rotors with top inserts conferring the samples a cylindrical geometry. Ten microlitres of D_2O saline containing 0.25% 3-(trimethylsilyl) propionate sodium salt (TSP)-d_4 were also added to provide a signal for lock (D_2O) and for shimming (TSP), the process of resolution optimization carried out for each sample before starting spectral acquisition.

NMR measurements

NMR spectra were acquired on a Bruker Avance DRX-500 spectrometer operating at 500.13 MHz for ^{1}H observation, at 277 K, using a 4 mm HRMAS probe, in which the rotor containing the sample was spun at the magic angle (54.7° relative to the magnetic field) and a spinning rate of 4 kHz. For each sample, a standard 1D ^{1}H NMR spectrum with water suppression was acquired ("noesypr1d" in Bruker library, SW 6,510 Hz, TD 32 K data points, relaxation delay 4 s, 256 scans). All spectra were processed with a line broadening of 0.3 and a zero filling factor of 2, manually phased and baseline corrected. The chemical shifts were referenced internally to the alanine signal at δ 1.48.

Multivariate statistical analysis

A total of 51 spectra corresponding to 24 paired tissues (plus three additional fragments of samples T2, T5 and N5) have been considered for multivariate analysis. Data matrices, consisting of rows that represent observations (samples) and columns that represent variables (spectral intensity at each data point), have been built from standard 1D spectra, using three different spectral regions: (a) δ 0.5 to 8.75 (whole spectral range), excluding the suppressed water signal (δ 4.8–5.15), as well as contaminant ethanol (δ

1.18, 3.66) and polyethyleneglycol (PEG, δ 3.71) signals; (b) δ 0.5 to 4.8 sub-region, excluding ethanol, PEG and lactate (δ 1.33, 4.12) signals and (c) δ 5.70 to 8.75 sub-region. Normalisation was applied to each spectrum by adjusting the total area to unity. Then, after scaling the data to unit variance, principal component analysis (PCA) and partial least squares regression discriminant analysis (PLS-DA) were applied using the software Simca-P 11.5 (Umetrics, Sweden). PCA is an exploratory unsupervised method that allows intrinsic clustering of samples to be determined without a priori knowledge of sample class membership. PLS-DA, on the other hand, is a supervised approach useful for classification purposes, as it incorporates class membership information (as Y variables) in order to maximise class separation. In both methods, the output consists of a scores scatter plot, where each point represents an individual sample spectrum and similar samples will group together in clusters, and a loadings plot, which reveals the relative contribution of spectral variables (i.e. metabolites) to the positioning of samples on the scores scatter plot. The robustness and predictive ability of the PLS-DA model for discriminating tumours from control samples were tested by Monte Carlo cross-validation (MCCV) [34]. The principle of cross-validation consists of selecting part of the data for model development (calibration set) and then predicting class membership of left-out samples (validation set), for comparison with the actual values and determination of prediction errors. By using MCCV, this procedure was repeated 200 times (iterations), each time randomly changing the composition of the calibration set (comprising 60% of samples) and the validation set (comprising the remaining 40% of samples). Each iteration consisted of internal cross-validation of the calibration set using seven blocks, and prediction of class membership for samples in the validation set. For each of the 200 randomly generated classification models, the number of latent variables (LV), the Q^2 (expressing the cross-validated explained variability) and the classification rate (percentage of samples correctly classified) were recovered. The selection of model complexity was based on the most frequent list of model properties that maximises the classification rate (i.e. lower LV and higher Q^2). The sensitivity and the specificity of the PLS-DA model were then depicted from the confusion matrix resulting from the 200 MCCV iterations.

Results

Metabolic profiles of tumour vs. non-involved parenchyma

Figure 1 shows the average ^{1}H HRMAS spectra of lung tumours (n=26) and their adjacent non-involved (control) pulmonary parenchyma (n=25). According to previous assignment work [32], a range of amino acids (e.g. alanine, glycine, glutamine, valine), organic acids (e.g. lactate, acetate), choline metabolites, carbohydrates (e.g. glucose, *myo*- and *scyllo*-inositol), nucleosides (e.g. uridine, adenosine/inosine) and lipids were present, giving rise to complex overlapped profiles. Signals from ethanol (δ 1.18, 3.66) and polyethyleneglycol (PEG, δ 3.71), which were more intense in control tissue, probably arose from exogenous sources, and, as such, have been excluded from multivariate analysis, as mentioned in the Materials and methods. Ethanol contamination could have arisen from insufficient drying of ethanol-washed tools used for cutting the tissue samples, and PEG may have originated from the anaesthetic formulation administered to patients before surgery.

Visual comparison of tumour and control spectra showed several differences in the relative levels of some compounds. The tumour spectra had on average higher lipids, lactate, phosphocholine (PC) and glycerophosphocholine (GPC), creatine and taurine, whereas acetate, methionine, and glucose were higher in the spectra of most non-involved tissues. Moreover, in the low-field region, the majority of tumours were characterised by the higher relative intensity of broad signals, probably arising from small peptides such as glutathione.

In order to verify the significance of these observations and search for other sources of variability in the data that could be useful to differentiate the tumours from non-involved (control) tissues, PCA has been applied to the standard 1D spectra. When the whole spectral range (δ 0.5 to 8.75 ppm) was considered, the resulting scores scatter plot (Fig. 2a) showed most tumours to be located in negative PC1 and all control tissues to fall in positive PC1, together with four tumour samples, which were separated from controls along PC2. Thus, it was clear from this unsupervised analysis, with no input about sample identification (either as tumour or control), that the two tissue types were characterised by inherently different metabolic signatures. In fact, the NMR profiles could differentiate between non-involved and tumour tissues even in cases where the mirror sections of the tumour samples analysed had less than 50% of neoplastic cells (being less representative of the tumour). This differentiation could be further improved when the supervised method PLS-DA was applied, resulting in a scores map where all the tumour samples were located in negative LV1 and all the controls were in positive LV1 (Fig. 2b). The prediction ability of this model was estimated by MCCV, as described in Materials and methods. The average Q^2 for the 200 runs was 0.90 within a range from 0.76 to 1.0, meaning that a large fraction of the total variation could be predicted by cross-validation procedures. According to the resulting confusion matrix (Table 2), the PLS-DA model showed 95% sensitivity, with only 5% of tumour samples being

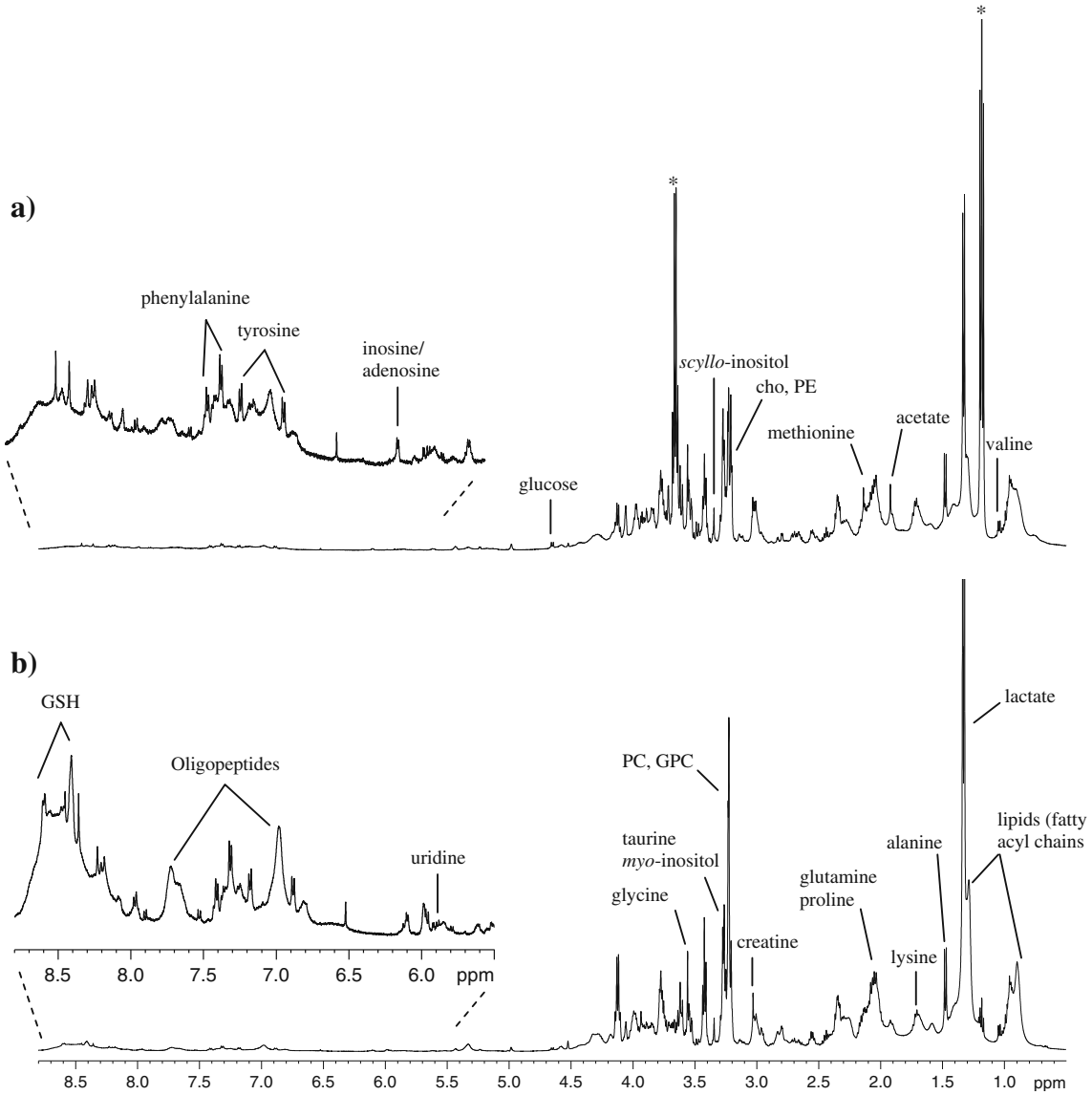

Fig. 1 Average standard 1D ^{1}H HRMAS NMR spectra (500 MHz, NS 256) of human lung tissue: **a** non-involved adjacent (control; n=25); **b** tumour (n=26), *asterisks* ethanol contamination

misclassified as control, and 100% specificity, i.e. all control tissues were correctly classified (no false positives). The classification rate (total number of samples correctly classified) was 97.5%.

Inspection of LV1 loadings (Fig. 2c) helps identifying the metabolites which contribute to the separation shown in the scores plot: signals with negative LV1 loadings correspond to metabolites with higher levels in tumour samples (negative LV1 scores), whereas signals with positive LV1 loadings arise from compounds which are likely to be elevated in controls (positive LV1 scores). Moreover, the loadings colouring as a function of variable importance in the projection (VIP) provides information on the magnitude of the variables (metabolites) importance for explaining the scores. Based on this analysis, the metabolites with higher importance for class discrimination, i.e. for distinguishing tumours from control tissues, have been identified and are listed in Table 3, where the ranking according to VIP value and the direction of variation (increased or decreased in tumour compared to control tissue) are also shown. Among these metabolites, lactate, GPC, PC, taurine, reduced glutathione (GSH) and uridine di-phosphate (UDP) were elevated in tumours, whereas glucose, phosphoethanolamine, acetate, lysine, methionine, glycine, *myo*- and *scyllo*-inositol were reduced. On the other hand, lipid and creatine signals, which, on average, were higher in tumours than in controls, showed low VIP values, suggesting that the difference in their levels was not significant or consistent enough to influence class separation.

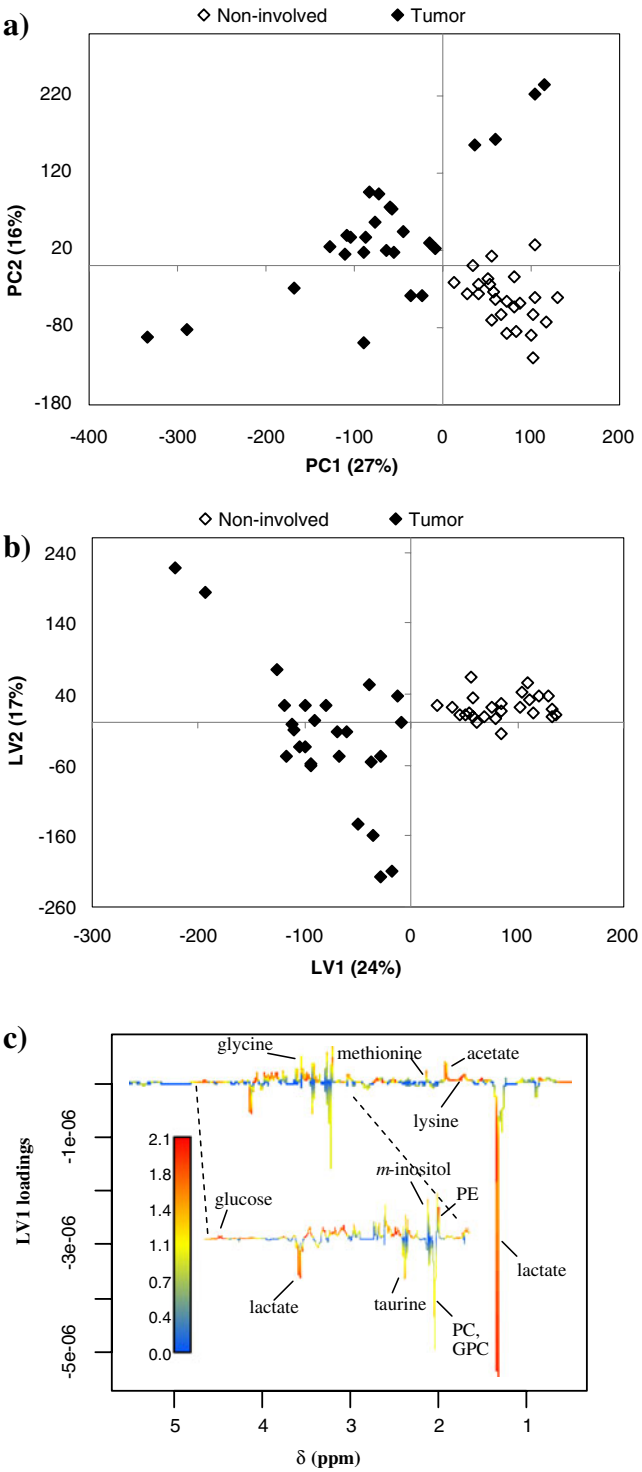

Fig. 2 Multivariate analysis of 1D ^{1}H HRMAS NMR spectra (δ 0.5–8.75, excluding suppressed water, ethanol and PEG signals) of control and tumour tissues (n=51): **a** PCA scores scatter plot; **b** PLS-DA scores scatter plot; **c** PLS-DA loadings LV1 (expansion of 0.5–5.5 region), coloured as a function of variable importance in the projection

Table 2 Confusion matrix calculated from PLS-DA of tumour (n=26) and control (n=25) tissue spectra with Monte Carlo cross-validation (200 runs)

True class	Predicted class	
	Tumour	Control
Tumour	0.95	0.05
Control	0	1

Values indicate the ratio between predicted samples and the total number of samples in each class (row)

Lactate significantly accounted for the differentiation between tumours and controls, but is a rather unspecific marker of metabolic derangement and may partially arise from hypoxia during tissue collection. Therefore, to remove its influence and assess the classification power of the other metabolites, lactate signals (δ 1.33 and 4.12) have been excluded and PLS-DA applied to the new matrix comprising the same 51 spectra in the sub-region δ 0.5–4.8. The resulting scores scatter plot (Fig. 3a) showed that separation between the tumour and control tissues was still observed, with LV1 loadings (Fig. 3b) pointing out the same variations noted before. Nevertheless, one sample (T1), corresponding to an inflammatory myofibroblastic tumour, was now grouped with the non-involved tissues. Indeed, the spectrum of this sample, apart from the higher lactate level, showed little difference compared to the profile of its paired control.

On the other hand, when the low-field region (δ 5.70 to 8.75) was considered, accounting only for the contribution of minor compounds, two groups were distinguished along LV1, one with positive scores comprising all non-involved tissues and three tumours (T5a, T9 and T22) and another group with negative scores which included the remaining tumours (Fig. 3c). The spectrum of sample T1 was particularly weak in the region considered, where hardly no signals were detected and, indeed, it has been classified as an outlier and excluded from this analysis. The LV1 loadings (Fig. 3d) indicated that the main features responsible for the separation revealed by the scores map arose from UDP, GSH and other broad signals at δ 6.98 and 7.72 (indicated with arrows and possibly assigned to oligopeptides), which were higher in most tumours (those with negative PC1 scores). Samples T5a, T9 and T22 were exceptions to this observation as confirmed by visual inspection of their respective spectra.

Metabolic profiles of different histological types

In order to investigate if different histological types show typical metabolic profiles, the spectra of adenocarcinomas (n=12) have been compared to those of carcinoids (n=4)

Table 3 List of metabolites with larger contribution for the discrimination between tumour and control tissue, identified by analysis of PLS-DA loadings and their respective VIP values

Metabolite	δ (ppm)[a]	Ranking[b]	Direction of variation[c]
Lactate	1.33, 4.12	1	↑
Glucose	4.65, 5.24	2	↓
Lysine	1.47, 1.73, 1.92, 3.03	3	↓
Phosphoethanolamine	3.20	4	↓
Methionine	2.14	5	↓
Acetate	1.92	6	↓
myo-inositol	3.28, 3.54, 3.62, 4.06	7	↓
Uridine di-phosphate (UDP)	5.97, 7.97	8	↑
Glycerophosphocholine (GPC)	3.23	9	↑
Taurine	3.26, 3.43	10	↑
Reduced glutathione (GSH)	8.41, 8.60	11	↑
scyllo-inositol	3.35	12	↓
Phosphocholine (PC)	3.22	13	↑
Glycine	3.56	14	↓

[a] Chemical shifts correspond to signals clearly distinguished in the loadings profile (not necessarily representing complete spin systems)

[b] Ranking according to VIP list produced by PLS-DA of whole spectral region (δ 0.5–8.75)

[c] Increased or decreased in tumour compared to control tissue

and epidermoid carcinomas (n=4) through multivariate statistics. The scores plot resulting from applying PLS-DA to the spectra of adenocarcinomas and carcinoids is shown in Fig. 4a. The two classes were clearly separated along LV1, with respective loadings (Fig. 4b) showing strong negative correlation for GPC, taurine, ascorbate and several broad signals (δ 0.94, 1.41, 1.69, 1.96, 2.30, 3.00, 4.32,), not yet assigned but possibly arising from oligopeptides, indicating higher levels of these features in carcinoids. On the other hand, these samples were characterised by reduced lipid content and relatively lower levels of valine, choline and glycine (highest VIP values for positive signals in LV1 loadings) compared to adenocarcinomas. It should also be noted that sample T19 was located further away from the remaining adenocarcinomas in the scores plot, mainly due to its richer lipid composition. The application of PLS-DA to adenocarcinomas and epidermoid tumours resulted in a reasonable separation between these two types along LV1 (Fig. 4c). However, sample T19 was again separated from the other adenocarcinomas and closer to epidermoid tumours in LV1, although slightly separated from them along LV2. LV1 loadings (Fig. 4d) suggested that, compared to adenocarcinomas, epidermoid tumours presented higher lipid, lactate, creatine and GSH and decreased taurine and PC.

Among the tumours compared, two of the 12 adenocarcinomas and two of the four epidermoid carcinomas had necrotic areas, as determined by histological observation of their mirror sections. In order to assess the possible influence of necrosis on the tissues' metabolic profile, the dataset has been modelled by PLS-DA taking the presence of necrosis as classifier. Although the spectra of partially necrotic samples showed a trend for higher lactate and lipid contents, in agreement with previous observations [27, 32], PLS-DA modelling resulted in poorer separation between necrotic and non-necrotic tissues (not shown), compared to the discrimination achieved for different histological types. Therefore, it maybe concluded that the presence of necrosis was not a dominating variability source in our dataset and that its influence on the tissue composition was less important than the histological type.

Discussion

Metabolic profiles of lung tumours and non-involved pulmonary parenchyma (control tissue), obtained by ^{1}H HRMAS NMR spectroscopy, have been compared and compositional features associated with malignancy highlighted by multivariate modelling of the data. Unsupervised principal component analysis showed good separation between tumour and control tissues, corroborating the results previously obtained for a smaller number of cases [32]. This result supported the hypothesis that the metabolic signatures of the two tissue types could be useful for discriminating tumour from "healthy" lung, and thus, supervised PLS-DA was applied to test this hypothesis and evaluate the classification power of the metabolic information. The PLS-DA model built using the whole spectral range (δ 0.5–8.75), and validated through MCCV, showed high sensitivity (95%) and 100% specificity, thus demonstrating that consistent biochemical differences do exist between lung tumour and control tissue and that HRMAS NMR spectroscopy combined with multivariate statistics is suitable for detecting them. These differences were confirmed by applying PLS-DA to spectral subregions, either comprising major constituents or minor components. Moreover, when the influence of lactate was discarded, the discrimination between tumour and control tissue was maintained, with the exception of one sample corresponding to an inflammatory myofibroblastic tumour which is a mesenchymal tumour macroscopically dense and exhibiting fusiform cells, histiocytes and endothelial cells as cellular constituents approaching those of normal pulmonary parenchyma, which may thus justify their similar metabolic profiles. It is also interesting to note the

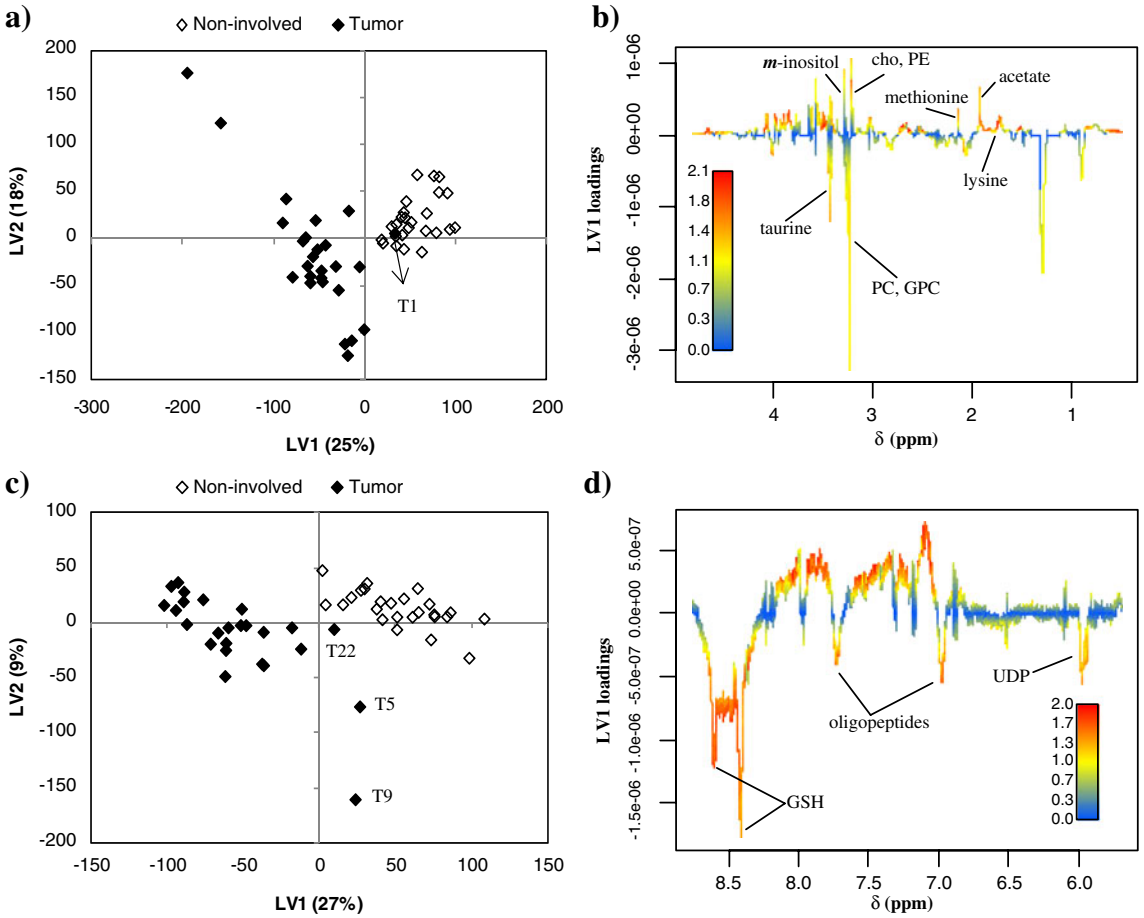

Fig. 3 Multivariate analysis of 1D ^{1}H HRMAS NMR spectra of control and tumour tissues: **a** scores scatter plot and **b** LV1 loadings resulting from PLS-DA of the δ 0.5–4.8 sub-region after exclusion of lactate signals (as well as PEG and ethanol signals), **c** scores scatter plot and **d** LV1 loadings resulting from PLS-DA of the δ 5.70–8.75 sub-region. Loadings are coloured as a function of variable importance in the projection

larger scattering within the tumour tissues, compared to the control samples, which were more closely grouped in the PCA and PLS-DA scores plots. Different factors may contribute for this larger variability within the tumours, such as the different histological types considered (discussed below), and the variable percentage of neoplastic cells in the tumour samples, estimated by histological observation of mirror sections. Still, regarding the latter, the results showed that NMR could detect consistent metabolic differences between paired control and tumour tissues even for tumours sampled with higher amounts of stroma.

Based on the PLS-DA loadings interpretation, a ranked list of metabolites with larger contribution for discriminating between tumour and control tissue has been presented. In agreement with previous work [32], alterations involving key metabolites in glucose and phospholipid metabolisms were found in all tumour samples relative to the non-involved pulmonary tissue. In particular, elevated lactate and reduced glucose levels were a typical feature of the tumours, confirming the glycolytic shift (Warburg effect) characterising many types of cancer tissues [25, 27], including lung [7]. GPC and PC were also among the most discriminating metabolites, being higher in tumours compared to control tissue, which, again, confirms our previous findings [32] and is a well-known metabolic event in tumours [15, 20, 24, 25, 27], related to accelerated cell proliferation and the role of choline-containing compounds as precursors of cell membrane phospholipids [35]. On the other hand, phosphoethanolamine was suggested to be reduced in tumours, while the variation in choline levels did not appear to be significant. Acetate, which may also be involved in glycerophospholipid metabolism, presented decreased levels. The metabolism of amino acids also seems to be considerable affected in lung tumours, as several of these compounds showed important variations between control and tumour tissue. Taurine was elevated in tumours, whereas lysine, methionine and glycine were lower than in control tissues. *Myo*- and *scyllo*-inositol were also reduced in tumours, possibly in relation with local changes in osmotic regulation. These osmolytes have also been found to be reduced in renal neoplasms [29] relatively to normal kidney cortex and medulla, whereas, on the other

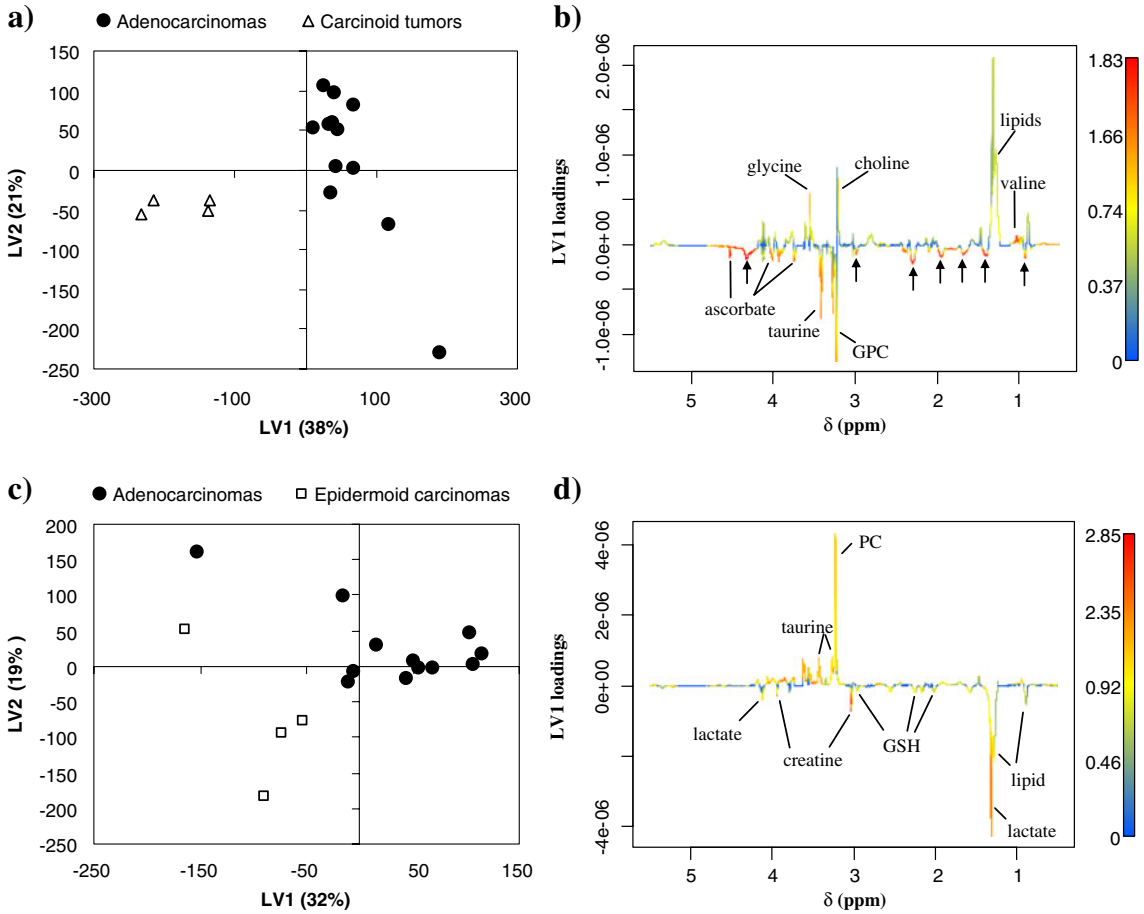

Fig. 4 PLS-DA of ^{1}H HRMAS NMR spectra (δ 0.5–8.75, excluding suppressed water, ethanol and PEG signals) of adenocarcinomas (n=12) and carcinoids (n=4): **a** scores scatter plot and **b** LV1 loadings, and of adenocarcinomas (n=12) and epidermoid carcinomas (n=4): **c** scores scatter plot and **d** LV1 loadings. Loadings are coloured as a function of variable importance in the projection

hand, *scyllo*-inositol was reported to be higher in colorectal cancer relatively to normal colon mucosae [25]. Other findings were increased UDP and GSH levels, the former being associated with nucleotide metabolism and the latter possibly reflecting the role of glutathione as a major intracellular antioxidant [36].

Regarding comparison of different histological types, PLS-DA of a sub-set of tumour samples allowed discriminating adenocarcinomas from carcinoid tumours and also from epidermoid carcinomas. The limited number of samples available for each type prevented, at this stage, proper validation of the results. Still, it is reasonable to state that the three histological types considered, with distinct microscopic morphology, also differ on the levels of particular metabolites. Thus, the NMR profile enables the metabolic characterisation of different types of lung tumours, and therefore, a better knowledge of their biochemistry.

In conclusion, ^{1}H HRMAS NMR was found to be suitable, in tandem with multivariate analysis, for characterising the tumours both in terms of malignancy biomarkers and in respect to different histological types. One of the main strengths of this methodology is the possibility of direct analysis of the intact tissue, retrieving biochemical information on altered cellular metabolism, which is not available through conventional histopathological analysis. This may provide additional criteria for improving clinical decisions. In subsequent studies, the potential of this approach to aid a more accurate staging of lung cancer disease will also be explored.

Acknowledgements Funding is acknowledged from the Foundation for Science and Technology (FCT), Portugal, and FEDER (research project FCT/PTDC/QUI/68017/2006; FCOMP-01-0124-FEDER-007439) and from CIMAGO, University of Coimbra (project 14/06). C.R. further acknowledges FCT for the doctoral grant SFRH/BD/63430/2009, and IFD acknowledges L'Oréal Portugal, FCT and the National UNESCO Committee for funding this work through the L'Oréal Medals of Honor for Women in Science 2007.

Conflict of interest statement We declare that we have no conflict of interest.

References

1. Griffin JL, Shockor JP (2004) Metabolic profiles of cancer cells. Nat Rev Cancer 4:551–561
2. Spratlin JL, Serkova NJ, Eckhardt SG (2009) Clinical applications of metabonomics in oncology: a review. Clin Cancer Res 15:431–440
3. Merz AL, Serkova NJ (2009) Use of nuclear magnetic resonance-based metabonomics in detecting drug resistance in cancer. Biomark Med 3:289–306
4. Sitter B, Bathen TF, Tessem M-B, Gribbestad IS (2009) High-resolution magic angle spinning (HR MAS) MR spectroscopy in metabolic characterization of human cancer. Prog Nucl Magn Reson Spectrosc 54:239–254
5. Hanaoka H, Yoshioka Y, Ito I, Niitu K, Yasuda N (1993) In vitro characterization of lung cancers by the use of ^{1}H nuclear magnetic resonance spectroscopy of tissue extracts and discriminant factor analysis. Magn Reson Med 29:436–440
6. Guo JF, Higashi K, Yokota H, Nagao Y, Ueda Y, Kodama Y, Oguchi M, Taki S, Tonami H, Yamamoto I (2004) In vitro proton magnetic resonance spectroscopic lactate and choline measurements, ^{18}F-FDG uptake, and prognosis in patients with lung adenocarcinoma. J Nucl Med 45:1334–1339
7. Yokota H, Guo J, Matoba M, Higashi K, Tonami H, Nagao Y (2007) Lactate, choline and creatine levels measured by vitro ^{1}H-MRS as prognostic parameters in patients with non-small-cell lung cancer. J Magn Reson Imaging 25:992–999
8. Fan TW-M, Lane AN, Higashi RM, Bousamra M, Kloecker G, Miller DM (2009) Metabolic profiling identifies lung tumour responsiveness to erlotinib. Exp Mol Pathol 87:83–86
9. Fan TW-M, Lane AN, Higashi RM, Farag MA, Gao H, Bousamra M, Miller DM (2009) Altered regulation of metabolic pathways in human lung cancer discerned by ^{13}C stable isotope-resolved metabolomics (SIRM). Mol Cancer 8:41
10. Swanson MG, Vigneron DB, Tabatabai ZL, Males RG, Schmitt L, Carroll PR, James JK, Hurd RE, Kurhanewicz J (2003) Proton HR-MAS spectroscopy and quantitative pathologic analysis of MRI/3D-MRSI-targeted postsurgical prostate tissues. Magn Reson Med 50:944–954
11. Tugnoli V, Schenetti L, Mucci A, Parenti F, Cagnoli R, Righi V, Trinchero A, Nocetti L, Toraci C, Mavilla L, Trentini G, Zunarelli E, Tosi MR (2006) Ex vivo HR-MAS MRS of human meningiomas: a comparison with in vivo ^{1}H MR spectra. Int J Mol Med 18:859–869
12. Mountford C, Lean C, Malycha P, Russell P (2006) Proton spectroscopy provides accurate pathology on biopsy and in vivo. J Magn Reson Imaging 24:459–477
13. Thomas MA, Lipnick S, Velan SS, Liu X, Banakar S, Binesh N, Ramadan S, Ambrosio A, Raylman RR, Sayre J, DeBruhl N, Bassett L (2009) Investigation of breast cancer using two-dimensional MRS. NMR Biomed 22:77–91
14. Wilson M, Davies NP, Grundyd RG, Peet AC (2009) A quantitative comparison of metabolite signals as detected by in vivo MRS with ex vivo ^{1}H HR-MAS for childhood brain tumours. NMR Biomed 22:213–219
15. Sitter B, Lundgren S, Bathen TF, Halgunset J, Fjosne HE, Gribbestad IS (2006) Comparison of HR MAS MR spectroscopic profiles of breast cancer tissue with clinical parameters. NMR Biomed 19:30–40
16. Bathen TF, Jensen LR, Sitter B, Fjosne HE, Halgunset J, Axelson DE, Gribbestad IS, Lundgren S (2007) MR-determined metabolic phenotype of breast cancer in prediction of lymphatic spread, grade, and hormone status. Breast Cancer Res Treat 104:181–189
17. Erb G, Elbayed K, Piotto M, Raya J, Neuville A, Mohr M, Maitrot D, Kehrli P, Namer IJ (2008) Toward improved grading of malignancy in oligodendrogliomas using metabolomics. Magn Reson Med 59:959–965
18. Monleon D, Morales JM, Gonzalez-Darder J, Talamantes F, Cortes O, Gil-Benso R, Lopez-Gines C, Cerda-Nicolas M, Celda B (2008) Benign and atypical meningioma metabolic signatures by high-resolution magic-angle spinning molecular profiling. J Proteome Res 7:2882–2888
19. Cheng LL, Burns MA, Taylor JL, He W, Halpern EF, McDougal WS, Wu C-L (2005) Metabolic characterization of human prostate cancer with tissue magnetic resonance spectroscopy. Cancer Res 65:3030–3034
20. Tessem M-B, Swanson MG, Keshari KR, Albers MJ, Joun D, Tabatabai ZL, Simko JP, Shinohara K, Nelson SJ, Vigneron DB, Gribbestad IS, Kurhanewicz J (2008) Evaluation of lactate and alanine as metabolic biomarkers of prostate cancer using ^{1}H HR-MAS spectroscopy of biopsy tissues. Magn Reson Med 60:510–516
21. van Asten JJA, Cuijpers V, Hulsbergen-van de Kaa C, Soede-Huijbregts C, Witjes JA, Verhofstad A, Heerschap A (2008) High resolution magic angle spinning NMR spectroscopy for metabolic assessment of cancer presence and Gleason score in human prostate needle biopsies. Magma 21:435–442
22. Sitter B, Bathen TF, Hagen B, Arentz C, Skjeldestad FE, Gribbestad IS (2004) Cervical cancer tissue characterized by high-resolution magic angle spinning MR spectroscopy. Magma 16:174–181
23. Mahon MM, deSouza NM, Dina R, Soutter WP, McIndoe GA, Williams AD, Co IJ (2004) Preinvasive and invasive cervical cancer: an ex vivo proton magic angle spinning magnetic resonance spectroscopy study. NMR Biomed 17:144–153
24. De Silva SS, Payne GS, Thomas V, Carter PG, Ind TEJ, deSouza NM (2009) Investigation of metabolite changes in the transition from pre-invasive to invasive cervical cancer measured using ^{1}H and ^{31}P magic angle spinning MRS of intact tissue. NMR Biomed 22:191–198
25. Chan ECY, Koh PK, Mal M, Cheah PY, Eu KW, Backshall A, Cavill R, Nicholson JK, Keun HC (2009) Metabolic profiling of human colorectal cancer using high-resolution magic angle spinning nuclear magnetic resonance (HR-MAS NMR) spectroscopy and gas chromatography mass spectrometry (GC/MS). J Proteome Res 8:352–361
26. Piotto M, Moussallieh F-M, Dillmann B, Imperiale A, Neuville A, Brigand C, Bellocq J-P, Elbayed K, Namer IJ (2009) Metabolic characterization of primary human colorectal cancers using high resolution magic angle spinning 1H magnetic resonance spectroscopy. Metabolomics 5:292–301
27. Yang Y, Li C, Nie X, Feng X, Chen W, Yue Y, Tang H, Deng F (2007) Metabonomic studies of human hepatocellular carcinoma using high-resolution magic-angle spinning ^{1}H NMR spectroscopy in conjunction with multivariate data analysis. J Proteome Res 6:2605–2614
28. Tate AR, Foxall PJD, Holmes E, Moka D, Spraul M, Nicholson JK, Lindon JC (2000) Distinction between normal and renal cell carcinoma kidney cortical biopsy samples using pattern recognition of ^{1}H magic angle spinning (MAS) NMR spectra. NMR Biomed 13:64–71
29. Righi V, Mucci A, Schenetti L, Tosi MR, Grigioni WF, Corti B, Bertaccini A, Franceschelli A, Sanguedolce F, Schiavina R, Martorana G, Tugnoli V (2007) Ex vivo HR-MAS magnetic resonance spectroscopy of normal and malignant human renal tissues. Anticancer Res 27:3195–3204
30. Tugnoli V, Mucci A, Schenetti L, Righi V, Calabrese C, Fabbri A, Di Febo G, Tosi MR (2006) Ex vivo HR-MAS magnetic resonance spectroscopy of human gastric adenocarcinomas: a comparison with healthy gastric mucosa. Oncol Rep 16:543–553

31. Jordan KW, Adkins CB, Su L, Halpern EF, Mark EJ, Christiani DC, Cheng LL (2009) Comparison of squamous cell carcinoma and adenocarcinoma of the lung by metabolomic analysis of tissue–serum pairs. Lung Cancer 68:44–50
32. Rocha CM, Barros AS, Gil AM, Goodfellow BJ, Humpfer E, Spraul M, Carreira IM, Melo JB, Bernardo J, Gomes A, Sousa V, Carvalho L, Duarte IF (2010) Metabolic profiling of human lung cancer tissue by ^{1}H high resolution magic angle spinning (HRMAS) NMR spectroscopy. J Proteome Res 9:319–332
33. Travis WD, Brambilla E, Müller-Hermelink HK, Harris C (2004) World Health Organization Classification of Tumours: tumours of the lung, pleura, thymus and heart. IARC Press, Lyon
34. Xu Q-S, Liang Y-Z (2001) Monte Carlo cross validation. Chemometr Intell Lab Syst 56:1–11
35. Glunde K, Ackerstaff E, Mori N, Jacobs MA, Bhujwalla ZM (2006) Choline phospholipid metabolism in cancer: consequences for molecular pharmaceutical interventions. Mol Pharm 3:496–506
36. Balendiran GK, Dabur R, Fraser D (2004) The role of glutathione in cancer. Cell Biochem Funct 22:343–352

Virchows Arch (2010) 457:727–734
DOI 10.1007/s00428-010-0984-7

ORIGINAL ARTICLE

Nasal seromucinous hamartoma (microglandular adenosis of the nose): a morphological and molecular study of five cases

Andrea Ambrosini-Spaltro · Luca Morandi · Dominic V. Spagnolo · Alberto Cavazza · Massimo Brisigotti · Stefania Damiani · Sanjiv Jain · Vincenzo Eusebi

Received: 26 August 2010 / Revised: 8 September 2010 / Accepted: 15 September 2010 / Published online: 5 October 2010
© Springer-Verlag 2010

Abstract Five cases of nasal seromucinous hamartoma were studied and their clinical, morphological, immunohistochemical and molecular data are reported. The patients, three females and two males, ranged in age from 49 to 66 years (mean 56 year, SD±7.91). All lesions were located in the nasal cavity. In four cases where follow-up was obtained, no recurrence was evident. In all cases, numerous small seromucinous tubules, embedded in a cellular stroma, were present in the lamina propria. Tubules were lined by one layer of cuboidal cells which displayed luminal phenotype positive for lysozyme and EMA in four, and S100 protein in all cases. Collagen IV and laminin positive basal lamina outlined the tubules which lacked basal cells. Stromal spindle cells present among tubules were immunoreactive for calponin in all cases and for alpha-smooth muscle actin in four cases. DNA mutation analysis of mitochondrial D-loop region was performed by direct sequencing in order to verify the mutation rate of these lesions. The tubules of the five seromucinous hamartomas showed a higher mutation rate especially in heteroplasmy (0.52% homoplasmy, 2.02% heteroplasmy) in comparison to normal seromucinous glands which exhibited a lower mutation frequency (0.83%). This is considered a sign of a low cellular proliferation rate consistent with a benign process. It is concluded that nasal seromucinous hamartomas are benign glandular proliferations that may resemble microglandular adenosis of the breast. Their distinction from benign and malignant mimics is discussed.

Keywords Seromucinous hamartoma · Nasal cavity · Microglandular adenosis

A. Ambrosini-Spaltro · L. Morandi · S. Damiani · V. Eusebi (✉)
Sezione di Anatomia Istologia e Citologia Patologica "Marcello Malpighi", Dipartimento di Oncologia ed Ematologia,
Università di Bologna, Ospedale Bellaria,
Bologna, Italy
e-mail: vincenzo.eusebi@ausl.bologna.it

D. V. Spagnolo
Department of Anatomical Pathology,
PathWest Laboratory Medicine WA,
Queen Elizabeth II Medical Centre,
Nedlands, Western Australia, Australia

A. Cavazza
Unità Operativa di Anatomia Patologica,
Arcispedale S. Maria Nuova,
Reggio Emilia, Italy

M. Brisigotti
Unità Operativa di Anatomia Patologica, Ospedale Infermi,
Rimini, Italy

S. Jain
Department of Anatomical Pathology, ACT Pathology,
The Canberra Hospital,
Canberra, Australia

Introduction

Seromucinous hamartoma (SH) is a rare benign glandular proliferation of the sinonasal tract and nasopharynx which was described by Baillie and Batsakis in 1974 [1]. These authors reported a polypoid mass of the nasopharynx, composed of a lobular arrangement of numerous small seromucinous tubules immersed in cellular connective tissue. Similar lesions were subsequently described as

Table 1 List of all antibodies used

Antigen	Source	Clone
Alpha-SMA	Cell marque	1A4
Calponin	Cell marque	CALP
Desmin	Ventana	DE-R-II
p63	Cell marque	4A4
CK14	Cell marque	LL002
Laminin	Thermo scientific	LMN02 (alias 4C7)
Collagen IV	Cell marque	CIV22
S100	Ventana	4C4.9
Ki67	Ventana	30-9
Lysozyme	Cell marque	Polyclonal
EMA	Cell marque	E29

SMA smooth muscle actin; *S100* protein S100; *EMA* epithelial membrane antigen; *CK14* cytokeratin 14

nasopharyngeal hamartoma [2] and hamartoma of the nose and nasopharynx [3]. Chuang and Lin reported a case in the paranasal sinuses, noticing a close similarity with microglandular adenosis (MGA) of the breast [4].

The aim of the present paper was to study five cases of nasal SH in order to further define the clinical, morphological, immunohistochemical and molecular features of this condition. For molecular analysis, the mitochondrial DNA (mtDNA) mutation rate was specifically studied, as situations of homoplasmy are indicative of malignant lesions, while lesions showing heteroplasmy are more frequently hyperplastic [5].

Materials and methods

Five cases of nasal polyps showing morphological features consistent with SH were collected. Two cases were retrieved from the files of the Section of Anatomic Pathology "Marcello Malpighi" of the University of Bologna. The other three cases were recruited from other institutions (AC, SJ, MB).

All cases were histologically reviewed by two of us (AAS, VE).

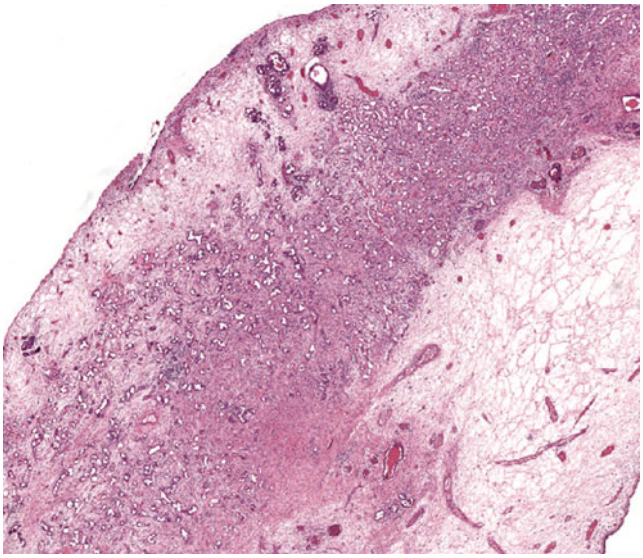

Fig. 1 *Case 3 (H&E).* The seromucinous glands proliferate parallel to the overlying mucosa; the lesional stroma is cellular, in contrast to the stroma of the rest of the polyp which is loosely oedematous. At low power, the lesion may mimic adenocarcinoma

For molecular comparison with SH, normal control nasal turbinate mucosa from five patients of the same age range was retrieved from the histology files. All cases had been fixed in 10% buffered formalin and embedded in paraffin as routine.

Immunohistochemical analysis

Five-micrometre sections of selected blocks from all cases were immunostained using an automated immunostainer (Ventana Medical Systems, Inc, Tucson, Arizona, USA). The antibodies used are listed in Table 1.

Molecular analysis

From each of the five lesional cases, cells from the proliferating seromucinous tubules in the lamina propria and from the overlying respiratory epithelium were selectively microdissected for comparison. Similarly, normal mucosa from the five control cases was also harvested.

Table 2 Clinical features

Case number	Sex	Age	Site	FU	Major axis (cm)
1	M	50	Nasal cavity	A&W, 8 years	3.5
2	F	66	Nasal cavity	A&W, 8 years	3
3	F	63	Nasal cavity	A&W, 7 years	1.5
4	M	49	Nasal cavity (arising from nasal septum)	A&W, 1 year	2.5
5	F	52	Nasal cavity	NA	1

FU follow-up, *A&W* alive and well, *NA* not available

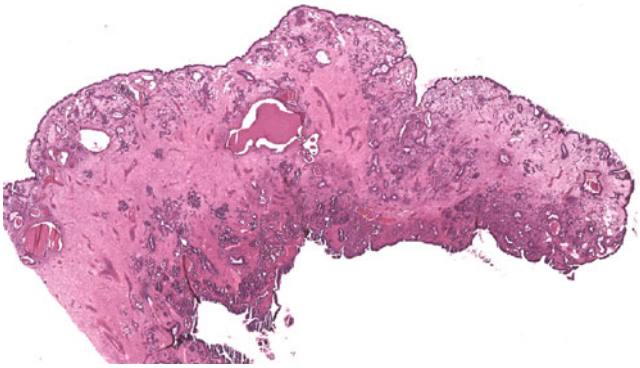

Fig. 2 *Case 4 (H&E).* The polypoid lesion exhibits seromucinous glands distributed along the major axis. Cystically dilated spaces intermixed with the proliferation are evident

Pertinent areas were microdissected using the laser assisted SL μcut Microtest (MMI GmbH Glattbrugg, Switzerland), as previously described [6, 7].

Mitochondrial DNA was extracted using the high pure PCR template kit (Roche, Manheim, Germany) following the manufacturer's instructions.

A negative control, to which no tissue was added, was processed in parallel with each sample to exclude any contamination. MtDNA D-loop sequence analysis was performed by amplifying four overlapping segments of about 300 bp, covering the entire region from position 16,056 to position 729 (see www.mitomap.org for revised Cambridge mtDNA reference sequence). The D-loop region was chosen as it contains hot spots for mtDNA mutation in cancer cells [5, 8–12]. Primers used have been previously described [6]. PCR products were directly sequenced using CEQ2000 XL instrument (Beckman Coulter, Inc., Fullerton, CA, USA) following the manufacturer's instructions. Multiple sequence alignment and mutation rate were calculated using MEGA 4.1 software (Molecular Evolutionary Genetics Analysis, MEGA, The Biodesign Institute, Tempe, AZ, USA).

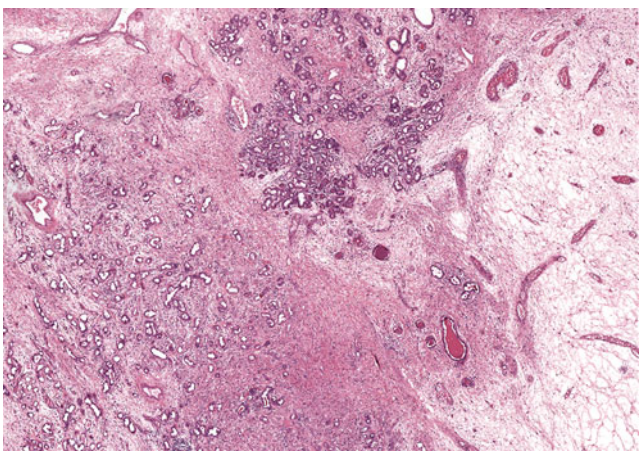

Fig. 3 *Case 3 (H&E).* The proliferating tubules (*left*) are easily distinguished from the normal residual seromucinous glands (*right*)

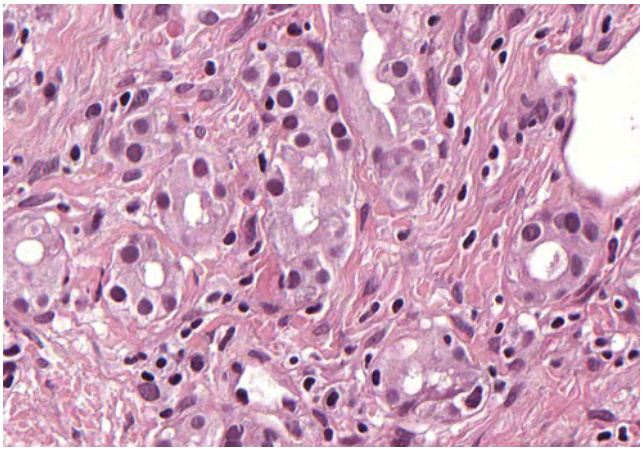

Fig. 4 *Case 1 (H&E).* The tubules are lined by a single layer of cuboidal epithelium, with amphophilic to eosinophilic cytoplasm and regular, monomorphic nuclei

Results

Clinical features

Clinical features are summarised in Table 2. There were three females and two males, with ages ranging from 49 to 66 years (mean 56 year, SD±7.91). All the lesions were polyps in the nasal cavity. In case 4, the lesion arose from the nasal septum.

Follow-up available in four of the five cases ranged from 1 to 8 years (mean 6 years, SD±3.4). All patients are alive and well, with no nasal symptoms.

Histological features

The histological features are similar in all cases and will be described together. All lesions were polypoid and consisted of a proliferation of small tubules of the same size as pre-existing normal acini located in the lamina propria. The

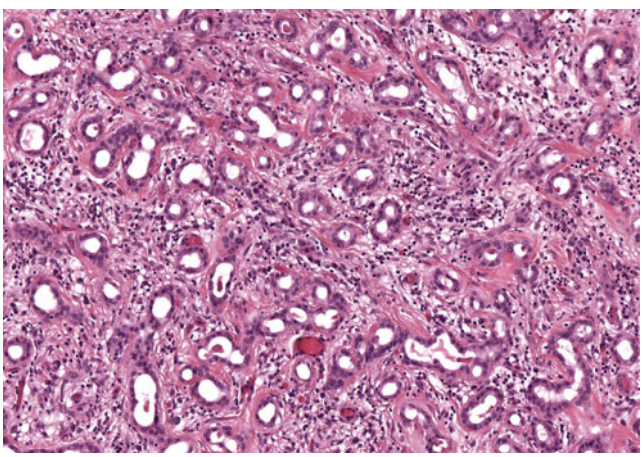

Fig. 5 *Case 3 (H&E).* The tubules are encircled by a thick basal lamina

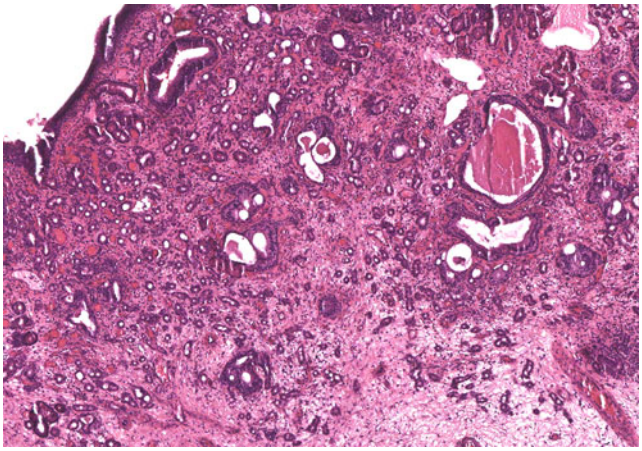

Fig. 6 *Case 4 (H&E).* Tubules are admixed with invaginations of superficial epithelium into the lamina propria, forming small cysts lined by respiratory epithelium

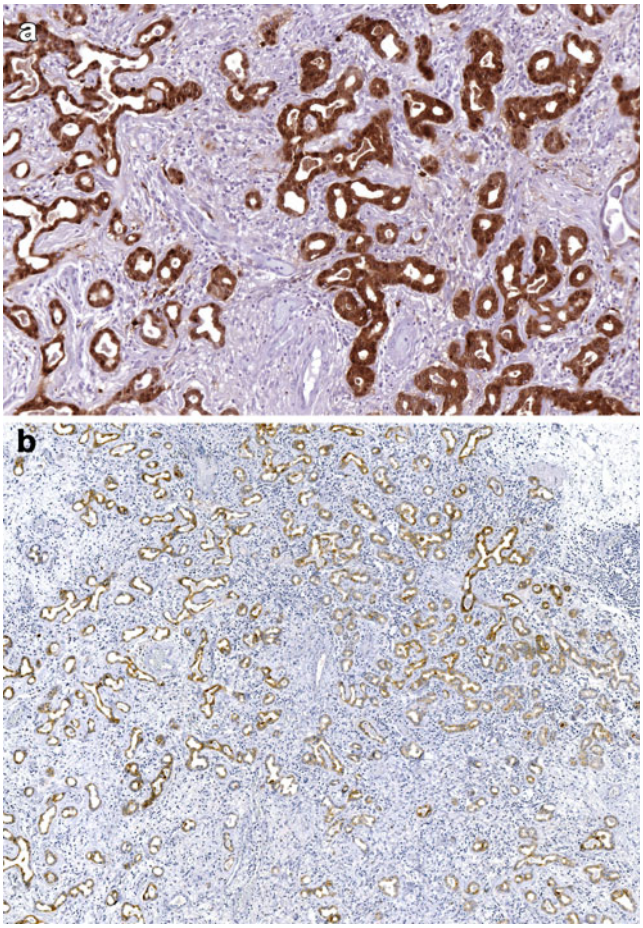

Fig. 7 The tubules are diffusely and strongly immunoreactive for protein S100 (**a**, case 3) and for EMA (**b**, case 3)

tubules proliferated mostly in a laminar fashion beneath and parallel to overlying respiratory epithelium (Figs. 1, 2). Tubules were intermingled with and of the same size of pre-existing acini (Fig. 3). The tubules were composed of a single layer of cuboidal epithelium exhibiting little variation in size and shape. The cytoplasm varied from amphophilic to eosinophilic; occasional mucinous goblet cells were observed. Nuclei were round to ovoid with little variation in size (Fig. 4). Mitoses were absent. Eosinophilic secretion was occasionally present within the lumina of the tubules. The tubules were encircled by thick eosinophilic basal lamina (Fig. 5). The stroma present among the tubules was composed of numerous spindle cells, contrasting with the oedematous loose stroma of the non-lesional part of the polyps and in addition contained mild chronic inflammatory infiltrate composed chiefly of small lymphocytes (Fig. 5).

In all cases, invaginations into the lamina propria by the superficial respiratory ciliated epithelium resulted in the formation of small cysts (Fig. 6). In case 2, the proliferation of the native respiratory epithelium was so exuberant as to mimic the features of a respiratory epithelial adenomatoid hamartoma (REAH), admixed with the tubular proliferation [13–17].

Table 3 Immunohistochemical features

Number	SMA (stroma)		Calponin (stroma)		Desmin (stroma)		p63		CK14		Laminin		Coll IV		S100		Ki67		Lysozyme		EMA	
	S	R	S	R	S	R	S	R	S	R	S	R	S	R	S	R	S	R	S	R	S	R
1	−	−	+	+	−	−	−	+	−	−	−	−	+	+	+	−	1%	2%	+	foc+	+	foc+
2	foc+	foc+	+	+	−	−	−	+	−	−	+	+	+	+	foc+	−	1%	2%	+	foc+	foc+	foc+
3	+	+	+	−	foc+	−	−	+	−	−	−	−	+	+	+	−	1%	1%	+	foc+	+	+
4	+	+	+	+	−	−	−	+	−	−	−	+	+	−	+	−	1%	2%	−	foc+	foc+	foc+
5	+	+	+	+	foc+	foc+	−	+	−	−	foc+	−	+	+	foc+	−	2%	5%	foc+	foc+	−	foc+

N case number; *SMA* smooth muscle actin; *CK14* cytokeratin 14; *Coll IV* collagen IV; *S100* S100 protein; *EMA* epithelial membrane antigen; + positive; − negative; *foc+* focally positive; *S* seromucinous component; *R* respiratory epithelium (superficial and invaginated)

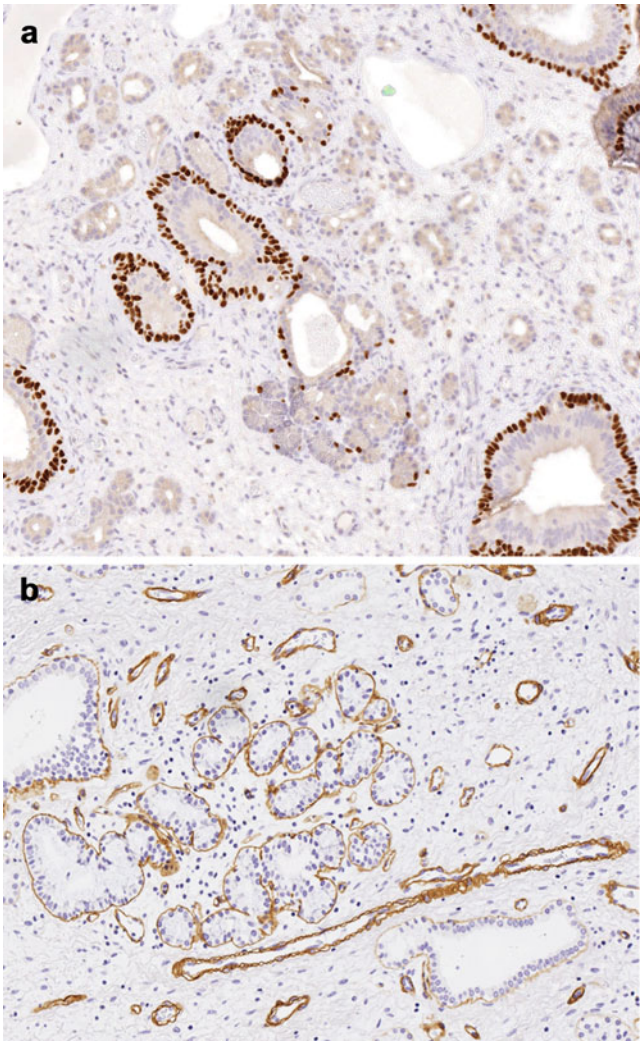

Fig. 8 Basal cells reactive for p63 are detected only around invaginated respiratory epithelium and are absent around proliferating seromucinous tubules (**a**, case 4), which are instead decorated by laminin positive basal lamina (**b**, case 2)

The five cases of normal turbinate mucosa selected for genetic analysis showed normal acinar glands regularly distributed in the lamina propria.

Immunohistochemical features

All immunohistochemical features are summarised in Table 3.

Tubules

The cytoplasm of the cuboidal cells lining the tubules was positive for S100 protein in all cases (Fig. 7a) and for lysozyme and EMA (Fig. 7b) in four. Virtually, all tubules were devoid of basal cells, as seen by the lack of p63 (Fig. 8a) and CK 14 positive elements and were outlined by basal lamina positive for laminin in two cases (cases 2 and 5; Fig. 8b) and for collagen IV in all cases.

The tubular epithelial cells had a proliferation index of 1–2% (Ki67).

Respiratory epithelium and residual acinar glands from both lesional and normal tissues

Respiratory epithelium was negative for S100 protein in all cases, while it exhibited positivity for EMA and focal immunoreactivity for lysozyme in all cases. Basal cells positive for p63 were consistently present in all cases (Fig. 8a), but CK14 immunoreactivity was not seen. Laminin positive basal lamina was observed in two cases

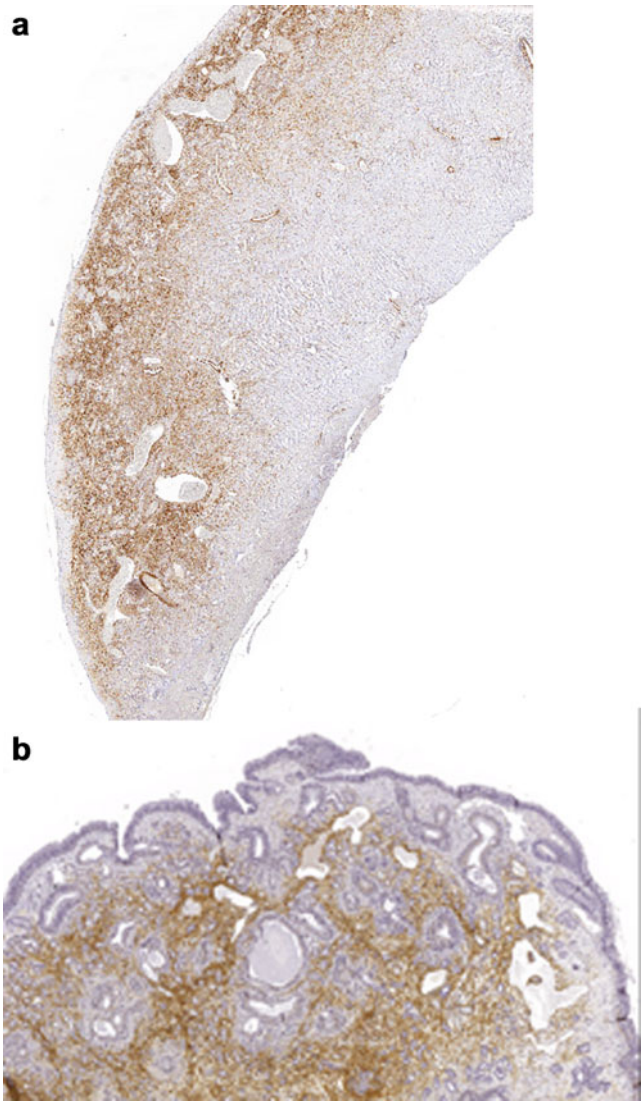

Fig. 9 The cellular stroma around the proliferating tubules is reactive for both calponin (**a**, case 1) and SMA (**b**, case 4)

Table 4 Molecular features

Number	Homoplasmy	Heteroplasmy	Total
Lesional cases			
1	0.87	3.42	4.30
2	0.26	1.39	1.65
3	0.69	2.00	2.69
4	0.77	1.93	2.7
5	0	1.34	1.34
Mean	0.52	2.02	2.50
Normal cases			
1	0	1.00	1.04
2	0	0.62	0.62
3	0.19	0.38	0.57
4	0.77	0.77	1.55
5	0.19	0.57	0.76
Mean	0.23	0.67	0.83

The percentages indicate mutation frequency in mitochondrial DNA, as detected by the comparison between seromucinous tubules, normal glands and superficial respiratory epithelium

(cases 2 and 4) and collagen IV immunoreactivity was found in four cases (cases 1, 2, 3 and 5).

The residual normal seromucinous glands, observed in four cases (cases 1–4), were encircled by basal cells expressing both p63 and CK14. In these four cases, the residual glands also showed the presence of a laminin- and collagen IV-positive basal lamina.

Stroma

The cellular stroma in which the tubules were embedded exhibited immunoreactivity for calponin in all cases (Fig. 9a), for smooth muscle actin (SMA) in four cases (Fig. 9b) and for desmin in two cases.

The stroma elsewhere in the polyps, and in the adjacent normal nasal tissues, was negative for calponin, SMA and desmin.

Table 6 Summary of the similarities and differences between seromucinous hamartoma of the nose and microglandular adenosis of the breast

	SH of the nose	MGA of the breast
Similarities		
Small proliferating tubules	Present	Present
Secretion in the lumina	Eosinophilic	Eosinophilic
S100 protein immunoreactivity of luminal cells	Positive	Positive
Basal (myoepithelial) cells	Absent	Absent
Basal lamina	Present	Present
Differences		
EMA immunoreactivity of luminal cells	Positive	Negative
Lesional stroma	Cellular	Fibrofatty

SH seromucinous hamartoma, *MGA* microglandular adenosis

Molecular features

The seromucinous glands of the five cases of normal nasal mucosa exhibited a mtDNA mutation rate of 0.83% (0.23% homoplasmy, 0.67% heteroplasmy).

The tubules of the five SH cases had a higher (2.50%) mtDNA mutation rate, especially in heteroplasmy (0.52% homoplasmy, 2.02% heteroplasmy, see Table 4 for details).

Table 5 Summary of the previously reported seromucinous hamartoma (microglandular adenosis) of the nose and paranasal sites

Authors, Ref.	Number of reported lesions	Original diagnosis	Sex	Age	Site	FU
Baillie et al. [1]	1	Glandular (seromucinous) hamartoma of the nasopharynx	M	26	Nasopharynx, attached to the posterior vomer	A&W, 2 1/2 years
Zarbo et al. [2]	1	Nasopharyngeal hamartoma	M	32	Nasopharynx	A&W, 2 years
Graeme-Cook et al. [3]	1	Hamartoma	F	57	Posterosuperior left nasal cavity	A&W, 1 year
	2	Hamartoma	F	67	Posterior left nasal cavity	A&W, 10 months
	3	Hamartoma	F	78	Nasopharyngeal mass	A&W, 4 months
Chuang et al. [4]	1	Microglandular adenosis	M	54	Paranasal sinus	A&W, 6 months
Weinreb et al. [18]	7[a]	Seromucinous hamartoma	4M, 3F	14–85	Nasal cavity	4 A&W, 1 rec, 6 months to 5 years

A&W alive and well, *rec* recurrence

[a] Cases are collectively described

Discussion

Seromucinous hamartoma is a rare lesion of the nasal cavity which may cause nasal obstruction and breathing difficulties. The polypoid lesion attached to the posterior vomer and expanding in the soft palate described by Baillie and Batsakis [1], that they named glandular (seromucinous) hamartoma, is very similar to the present cases. The lesions subsequently reported (with varying nomenclature) by Zarbo et al. [2], Graeme-Cook et al. [3], Chuang et al. [4] and Weinreb et al. [18] (Table 5) are also similar.

Our cases showed proliferating tubules closely simulating an invasive low-grade adenocarcinoma. Nevertheless, the organoid pattern of growth with parallel spread under and along the surface epithelium, the lack of cytologic atypia and mitoses, the presence of collagen IV and laminin positive basal lamina around the tubules together with lack of recurrences in the four cases where follow-up was available, are all features indicating a benign glandular proliferation. Chuang and Lin [4] suggested close similarity of their case to MGA of the breast, a rare benign lesion which may also simulate invasive carcinoma [19–22].

If our five cases are compared with previously reported MGA of the breast [23], both similarities and differences are evident. Both lesions are characterised by small proliferating tubules, presence of eosinophilic secretion in the lumina, S100 protein positivity of luminal cells, lack of basal (myoepithelial) cells and presence of basal lamina. In spite of these similarities, there are consistent differences. In MGA of the breast, the proliferating cells are EMA negative and are immersed in fibrofatty stroma [23]. By contrast, the cells of our SH cases were clearly EMA positive and were immersed in a cellular stroma (Table 6).

The present cases also differ from pure REAH [13–17, 24], composed of glands lined almost exclusively by ciliated respiratory epithelium, although cases of mixed REAH and seromucinous hamartomas were described by Weinreb et al., suggesting the existence of a possible spectrum between the two lesions [18, 25]. In the present cases, invaginated respiratory epithelium was identified in all cases (and particularly in case 2), thus confirming the possibility of overlapping features between the two hamartomatous proliferations.

Jo et al. reported an association with REAH in 6/29 cases of sinonasal adenocarcinomas, with a similar immunohistochemical profile, suggesting that REAHs may also be related to adenocarcinomas [26].

The genetic alterations here studied in SH documented an increased mtDNA mutation rate, especially heteroplasmic, in the seromucinous proliferation in contrast to the five normal cases. This favours the view that the number of divisions seen in these lesions was not enough to produce the homoplasmic condition, typical of malignant lesions [5, 27].

Most of the somatic mutations found in mtDNA cancer cells are homoplasmic (i.e. all mitochondria share the same mutation), while fewer cells have heteroplasmic mutations (i.e. a mixture of wild type and mutant mtDNA) [5, 10–12, 27]. Accordingly, mtDNA D-loop homoplasmic mutations were recently shown to be present in poorly differentiated hepatocellular carcinoma [8], in non-small cell lung cancer [9, 28], in colorectal cancer [10] and in breast cancer [11]. On the contrary, Park et al. evidenced an increased level of heteroplasmic mtDNA mutations in benign nasal polyps [12].

By computer simulation, Coller and co-workers showed that random drift alone, following the rules of population genetics, can explain how tumours can accumulate mtDNA variants that cannot be found in normal tissues of the patient, even if these variants are functionally neutral providing no advantage to cancer cells [5].

Taking into account the benign clinical behaviour, the absence of morphological features of malignancy and the presence of mtDNA mutations in heteroplasmy, it can be concluded that this uncommon nasal tubular proliferation has to be regarded a benign nasal lesion.

Conflict of interest statement We declare that we have no conflict of interest.

References

1. Baillie EE, Batsakis JG (1974) Glandular (seromucinous) hamartoma of the nasopharynx. Oral Surg Oral Med Oral Pathol 38:760–762
2. Zarbo RJ, McClatchey KD (1983) Nasopharyngeal hamartoma: report of a case and review of the literature. Laryngoscope 93:494–497
3. Graeme-Cook F, Pilch BZ (1992) Hamartomas of the nose and nasopharynx. Head Neck 14:321–327
4. Chuang SS, Lin CN (2000) Microglandular adenosis arising in chronic paranasal sinusitis. Histopathology 36:376–377
5. Coller HA, Khrapko K, Bodyak ND et al (2001) High frequency of homoplasmic mitochondrial DNA mutations in human tumors can be explained without selection. Nat Genet 28:147–150
6. Morandi L, Marucci G, Foschini MP et al (2006) Genetic similarities and differences between lobular in situ neoplasia (LN) and invasive lobular carcinoma of the breast. Virchows Arch 449:14–23
7. Morandi L, Asioli S, Cavazza A et al (2007) Genetic relationship among atypical adenomatous hyperplasia, bronchioloalveolar carcinoma and adenocarcinoma of the lung. Lung Cancer 56:35–42
8. Tamori A, Nishiguchi S, Nishikawa M et al (2004) Correlation between clinical characteristics and mitochondrial D-loop DNA mutations in hepatocellular carcinoma. J Gastroenterol 39:1063–1068
9. Matsuyama W, Nakagawa M, Wakimoto J et al (2003) Mitochondrial DNA mutation correlates with stage progression and prognosis in non-small cell lung cancer. Hum Mutat 21:441–443
10. Lievre A, Chapusot C, Bouvier AM et al (2005) Clinical value of mitochondrial mutations in colorectal cancer. J Clin Oncol 23:3517–3525

11. Tseng LM, Yin PH, Chi CW et al (2006) Mitochondrial DNA mutations and mitochondrial DNA depletion in breast cancer. Genes Chromosomes Cancer 45:629–638
12. Park SY, Shin MG, Kim HR et al (2009) Alteration of mitochondrial DNA sequence and copy number in nasal polyp tissue. Mitochondrion 9:318–325
13. Sangoi AR, Berry G (2007) Respiratory epithelial adenomatoid hamartoma: diagnostic pitfalls with emphasis on differential diagnosis. Adv Anat Pathol 14:11–16
14. Braun H, Beham A, Stammberger H (2003) Respiratory epitheloid adenomatoid hamartoma of the nasal cavity—case report and review of the literature. Laryngorhinootologie 82:416–420
15. Roffman E, Baredes S, Mirani N (2006) Respiratory epithelial adenomatoid hamartomas and chondroosseous respiratory epithelial hamartomas of the sinonasal tract: a case series and literature review. Am J Rhinol 20:586–590
16. Wenig BM, Heffner DK (1995) Respiratory epithelial adenomatoid hamartomas of the sinonasal tract and nasopharynx: a clinicopathologic study of 31 cases. Ann Otol Rhinol Laryngol 104:639–645
17. Mortuaire G, Pasquesoone X, Leroy X et al (2007) Respiratory epithelial adenomatoid hamartomas of the sinonasal tract. Eur Arch Otorhinolaryngol 264:451–453
18. Weinreb I, Gnepp DR, Laver NM et al (2009) Seromucinous hamartomas: a clinicopathological study of a sinonasal glandular lesion lacking myoepithelial cells. Histopathology 54:205–213
19. Clement PB, Azzopardi JG (1983) Microglandular adenosis of the breast—a lesion simulating tubular carcinoma. Histopathology 7:169–180
20. Tavassoli FA, Norris HJ (1983) Microglandular adenosis of the breast. A clinicopathologic study of 11 cases with ultrastructural observations. Am J Surg Pathol 7:731–737
21. Rosen PP (1983) Microglandular adenosis. A benign lesion simulating invasive mammary carcinoma. Am J Surg Pathol 7:137–144
22. Tavassoli FA, Eusebi V (2009) Benign lesions. In: Tavassoli FA, Eusebi V (eds) AFIP atlas of tumor pathology. Tumors of the mammary gland, Fourth Series. Fascicle 10. American Registry of Pathology, Washington DC, pp 21–51
23. Eusebi V, Foschini MP, Betts CM et al (1993) Microglandular adenosis, apocrine adenosis, and tubular carcinoma of the breast. An immunohistochemical comparison. Am J Surg Pathol 17:99–109
24. Ozolek JA, Hunt JL (2006) Tumor suppressor gene alterations in respiratory epithelial adenomatoid hamartoma (REAH): comparison to sinonasal adenocarcinoma and inflamed sinonasal mucosa. Am J Surg Pathol 30:1576–1580
25. Weinreb I (2010) Low grade glandular lesions of the sinonasal tract: a focused review. Head Neck Pathol 4:77–83
26. Jo VY, Mills SE, Cathro HP et al (2009) Low-grade sinonasal adenocarcinomas: the association with and distinction from respiratory epithelial adenomatoid hamartomas and other glandular lesions. Am J Surg Pathol 33:401–408
27. Gekeler J, Zsurka G, Kunz WS et al (2009) Clonal expansion of different mtDNA variants without selective advantage in solid tumors. Mutat Res 662:28–32
28. Suzuki M, Toyooka S, Miyajima K et al (2003) Alterations in the mitochondrial displacement loop in lung cancers. Clin Cancer Res 9:5636–5641

Virchows Arch (2010) 457:735–739
DOI 10.1007/s00428-010-0982-9

ORIGINAL ARTICLE

Warfarin embryopathy: fetal manifestations

Helen Wainwright · Peter Beighton

Received: 1 March 2010 / Revised: 1 September 2010 / Accepted: 20 September 2010 / Published online: 5 October 2010
© Springer-Verlag 2010

Abstract During the period 1991–2007, autopsy was undertaken in 13 fetuses with warfarin embryopathy. Pregnancy data and radiographic babygrams were available in each instance. Gestational age ranged from 17 to 37 weeks. Eleven of the fetuses had the characteristic nasal hypoplasia, but only three had radiological epiphyseal stippling. Cerebral hemorrhage was a major feature of autopsy in 8 of the fetuses, and it is evident that bleeding is a significant factor in the pathogenesis of warfarin embryopathy. A wide variety of additional visceral manifestations which were observed at autopsy have been tabulated. There was no obvious correlation between maternal or gestational age and the presence and severity of any specific embryopathic feature. No information was available concerning the dose and timing of warfarin administration in this series.

Keywords Embryopathy · Malformation · Warfarin

Introduction

Warfarin is an anticoagulant which is frequently prescribed for persons at risk of thrombosis or embolism. Specific indications include prior cardiac valve replacement, deep vein thrombosis, recurrent pulmonary emboli and atrial fibrillation.

In South Africa, acute rheumatic fever and cardiac valvular damage are common, and many affected persons receive prosthetic heart valve replacement [1]. A significant proportion of these individuals are young women, and prophylactic warfarin therapy is often utilized during pregnancy. In this setting, the risk of valvular thrombosis is balanced against the likelihood of fetal damage in the form of warfarin embryopathy [2].

Warfarin embryopathy has attracted considerable medical attention and the major manifestations of nasal hypoplasia and stippling of the epiphyses are well recognized. The potential for a wider range of manifestations is less well known. Since 1991, autopsy has been undertaken in 13 fetuses with warfarin embryopathy, and intracranial hemorrhage has emerged as a major pathogenic factor. In order to provide a perspective of the embryopathic potential of warfarin, our findings are documented and depicted in this article.

Materials and methods

Comprehensive autopsy reports concerning 13 fetuses with warfarin embryopathy are archived in the Division of Anatomical Pathology, University of Cape Town. Pregnancy details, including the indications for maternal warfarin therapy, were available and babygrams had been performed in all instances. Our analysis of these data forms the basis for this review. Three of these cases had significant epiphyseal stippling and were previously documented and discussed by the authors in an article devoted to this skeletal anomaly [3].

H. Wainwright
Division of Anatomical Pathology, Faculty of Health Sciences,
University of Cape Town,
Observatory 7925,
Cape Town, South Africa

P. Beighton (✉)
Division of Human Genetics, Faculty of Health Sciences,
University of Cape Town,
Observatory 7925,
Cape Town, South Africa
e-mail: Peter.Beighton@uct.ac.za

Results

The first of the autopsies was performed in 1991 and the last in 2007. Since the latter date, there have been no further referrals of fetuses with warfarin embryopathy. Gestational age ranged from 17 to 37 weeks. Eight mothers had mechanical heart valves and were aged 17–36 years. No data concerning the dose and timing of warfarin administration was provided in the referral documents.

On external examination, eleven fetuses had shortening and flattening of the nose; the remaining two had normal noses. The characteristic deep grooves of the nasal alar were present in only one case (Fig. 1).

Radiographs revealed widespread epiphyseal stippling in two fetuses (Fig. 2); a third had dot calcification in the talus. Three had 11 pairs of ribs, one had a short sternum, and one had delayed bone maturation. One fetus had dystrophic toes, while six had no radiologic abnormality of any kind.

A striking autopsy finding was cerebral hemorrhage in 8 of the 13 cases. Two of these had hemorrhage prior to 20 weeks gestation, four developed hemorrhage between 21 and 30 weeks, and two between 31 and 40 weeks. The hemorrhage was present in multiple sites within the brain in five of the eight fetuses.

Two fetuses had hydrocephalus, of which one was due to hematohydrocephalus (Fig. 3). In the latter, organized hemorrhage in the Sylvian aqueduct had impeded circulation of cerebral spinal fluid, resulting in proximal hydrocephaly. White matter necrosis was present in two cases, associated with dystrophic calcification in one instance.

Other malformations included obstruction at the pelviureteric junction in two fetuses. There were single instances of premature closure of the ductus arteriosus, optic nerve neuroma, macroglossia, anal agenesis, and Leydig cell hyperplasia in the testis. The premature closure of the ductus arteriosus was seen as a pinhole aperture at autopsy. Three of the fetuses with congenital malformations also had cerebral hemorrhage.

Case details and the autopsy findings in the 13 fetuses are presented in Table 1.

Fig. 2 Antero-posterior babygram. Widespread radio-opaque stippling is evident in the sacrum, carpus, tarsus and proximal regions of the femora and humeri

Fig. 1 The face of the affected fetus showing severe nasal hypoplasia and the characteristic grooves on the alar nasi

Fig. 3 Coronal section of the brain at autopsy. Intracranial hemorrhage has resulted in gross dilatation of the lateral ventricles and destruction of the septum pellucidum

Table 1 Autopsy observations and pregnancy factors in the 13 affected fetuses

Case no	Maternal indication for anticoagulants	Maternal age (year)	Gestationweeks	Sex	Fetal weight	Ultrasound	X-ray	Facies	Autopsy
1. 54/91	"Cardiac"	–	28	F	1,065 FSB	Hydrocephalus	Stippled spine, long bones, scapula. 11 ribs	Hydrocephalus, flat nasal bridge	Prem closure of ductus arterioisus, R subdural hemorrhage, Intraventricular hemorrhage, hydrocephaly, abnormal position of bile duct
2. 57/92	PVR, heparin for 1st trimester	–	35	M	2,272 MSB	Normal	Normal	Flat nose	Chorioamnionitis, focal villitis, small head circumference, liqified brain
3. 39/93	MVR, AVR	23	20	F	173 MSB	Hydrops	Normal	Normal nose	Short sternum, sclerosed placenta
4. 121/96	"Cardiac"	26	17	F	126 MSB	Intrauterine death, ventriculomegaly, echo-dense cerebellum	Normal	Short nose	Hemosiderin deposition, subarachnoid hemorrhage, asymmetric IUGR
5. 156/97	"Cardiac"	23	30	F	1,551 Intrauterine death	Breech	11 ribs, no stippling	Small flat nose	Subaponeurotic hemorrhage, subarachnoid hemorrhage, white matter necrosis, PUJ
6. 1/98	MVR	17	33	M	1,980 MSB	Normal	Normal	Normal nose	Asymmetrical IUGR, no placenta
7. 156/00	DVT	27	29	M	2,100 MSB	Polyhydramnios PUJ obstruction	Dot calcification of talus	Flat nose	Cerebellar maturation 32–33 weeks
8. 181/00	MVR, heparin for 1st trimester	–	37	M	3,930 MSB	–	Small distal femoral ossification centers	Short nose, Large for gestational age, Delayed skeletal and cerebellar maturation	Subarachnoid hemorrhage, intracerebral hemorrhage, astrocytosis
9. 56/02	AVR and MVR	36	30	M	1,990 MSB	–	Small distal femoral ossification centers	Flat nasal tip	L cerebral hemorrhage
10. 1/03	DVT, recurrent. Smoking and alcohol	40	20	M	510 MSB	–	11 pairs of ribs	Flat short nose, long philtrum	Bilateral intraventricular history, subarchnoid hemorrhage
11. 7/04	Thrombocytosis	30	18	F	180 FSB	Warfarin embryopathy, hypoplastic PUJ's	Stippled heels, tibia, humerii femora, sella	Nasal hypoplasia, macroglossia	Optic nerve neuroma, myocardial calcification (dystrophic)
12. 73/05	Recurrent pulmonary emboli	27	34	M	2,730 MSB	Intrauterine death	Normal	Hydrocephaly, flat nose, dystrophic toes	Bilateral IVH with rupture
13. 775/07	HIV positive, indication for warfarin unknown	30	22	M	600 FSB	Hydrocephaly and flat nose	Normal	Flat nose, hydrocephaly, absent anus	Previous hemorrhage causing obstructive hydrocephaly, Leydig cell hyperplasia

AVR Aortic valve replacement, *DVT* deep vein thrombosis, *FSB* fresh stillbirth, *IUGR* intrauterine growth restriction, *IVH* intraventricular hemorrhage, *MSB* macerated stillbirth, *MVR* mitral valve replacement, *PUJ* pelvi-ureteric junction abnormality, *PVR* pulmonary valve replacement

Discussion

Most published series of warfarin embryopathy include liveborn survivors and reflect the less severe spectrum of the embryopathy [4]. Approximately 15–20% of warfarin-exposed pregnancies end in spontaneous abortion or stillbirth and an equal proportion result in abnormal liveborn infants. In only 60% of at-risk pregnancies, there is a normal outcome [5].

The characteristic features of warfarin embryopathy in the neonate are nasal hypoplasia with deep nasal alar grooves and widespread epiphyseal stippling. Nasal hypoplasia was the most frequent external abnormality in our cases, but only one fetus had the alar grooves. In this context, it has been shown that prenatal septal growth is maximal at 6 to 9 weeks gestation and that the resultant facial profile is maintained until birth [6].

Stippling of the epiphyses is a descriptive term used to denote the radiographic appearance of multiple calcific foci in abnormal developing bone. The stippling is thought to be due to interference by warfarin with the formation of a vitamin K-dependent protein, matrix Gla protein, present in endochondral pre-ossification [7]. The differential diagnosis in the fetus and neonate includes the heterogeneous Conradi–Hunermann group of genetic conditions and, less frequently, skeletal dysplasias and chromosomal disorders. In South Africa, due to the high frequency of rheumatic valvular disease and prosthetic valve replacement, warfarin embryopathy is high on the list of differential diagnoses of epiphyseal stippling in any affected neonate [3]. It is surprising that only 2 of the 13 cases in our current series had widespread stippling, while another had minimal involvement of the talus. The two fetuses with stippling both had additional malformations; it is possible that a warfarin dosage effect was responsible, but no data were available concerning details of therapy during these pregnancies. Visceral manifestations included an anomalous bile duct, pelvi-ureteric junction obstruction, macroglossia, and anal agenesis.

In the South African context, it is of interest that in the period 1991–2007, approximately one fetus with a documented history of maternal warfarin therapy during pregnancy was referred for autopsy to HW's department in Cape Town each year. With increasing recognition of the danger to the fetus, the indications for maternal warfarin therapy became increasingly stringent toward the end of this period. The decline in the referral rate and the absence of any referrals since 2007 probably reflect this alteration in the therapeutic approach.

Fetal intracranial hemorrhage has been reported in an instance of warfarin embryopathy [8]. In this context, the recognition of cerebral bleeding in 8 of the 13 fetuses suggests that early fetal hemorrhage may be a major pathogenic factor in the development of structural malformations in warfarin embryopathy. This observation has relevance to maternal and pregnancy management. A review of neurologic sequelae in surviving neonates indicated two main teratogenic patterns: dorsal midline dysplasia with agenesis of the corpus callosum and the Dandy–Walker syndrome with midline cerebellar atrophy [7]. In the current series, the presence of extensive cerebral hemorrhage obscured any underlying intracranial malformations of this type.

In South Africa, a significant proportion of pregnant women are HIV-positive. The age-specific prevalence rates for females aged 25–29 years are over 30% [9]. In our series, only one instance of positive maternal HIV was recorded. The majority of maternal to offspring HIV transmissions occur during delivery, but fetal infection during pregnancy may also occur. With increasing awareness of maternal HIV status, it is likely that fetal warfarin embryopathy will be encountered more frequently in the offspring of HIV positive women. At present, however, the possible range of fetal damage from the combination of warfarin embryopathy, HIV infection, and maternal anti-HIV therapy can only be a matter for speculation.

The embryopathic potential of maternal warfarin therapy is well documented [10]. Nevertheless, despite the adverse effects on 30% of fetuses, it has been claimed that the use of warfarin throughout pregnancy offers the greatest protection from thrombosis to the mother with prosthetic heart valves [11, 12]. Neither low-molecular weight heparin nor unfractionated heparin crosses the placenta and therefore does not have a teratogenic effect. However, they carry a maternal mortality of 1–4% from valve thrombosis. Other complications include maternal thrombocytopenia and osteoporosis [13]. A South African randomized controlled trial of these two options was discontinued following two maternal deaths from valve thrombosis on low molecular weight heparin [14]. Recent guidelines of the American College of Cardiology/American Heart Association and European Society of Cardiology favor warfarin throughout pregnancy as well as dose-adjusted subcutaneous or intravenous unfractionated heparin between the 6th and 12th weeks [15]. Nevertheless, the optimal anticoagulation strategy remains unsettled [15]. Low-dose Warfarin has been advocated but there is evidence that fetal damage is not necessarily dose-dependent [16].

The wide range of malformations which were detected in these cases in this series emphasizes the importance of autopsy in fetuses and deceased neonates. The anatomical distribution of these abnormalities provides further insight into the mechanisms of Warfarin embryopathy. In the future, with improvement in health, the need for warfarin therapy during pregnancy will decrease. At this stage, accounts of fetal warfarin embryopathy may be relegated to the archaic literature.

Acknowledgments PB received research funding from the South African Medical Research Council and the National Research Foundation. Our thanks are offered to Professor P Commerford for his helpful and insightful comments during the preparation of the article.

Conflicts of interest None

References

1. Essop MR, Nkomo VT (2005) Rheumatic and nonrheumatic valvular heart disease: epidemiology, management and prevention in Africa. Circulation 112(23):3584–3591
2. Choi C, Midwall S, Chaille P, Conti CR (2007) Treatment of mechanical valve thrombosis during pregnancy. Clin Cardiol 30 (6):271–276
3. Wainwright H, Beighton P (2010) Lethal epiphyseal stippling in the foetus and neonate; pathological implications. Virchows Arch 456:301–308
4. Hall JG, Pauli RM, Wilson KM (1980) Maternal and fetal sequelae of anticoagulation during pregnancy. Am J Med 68(1):122–140
5. Blickstein D, Blickstein I (2003) The risk of fetal loss with warfarin anticoagulation. Int J Gynaecol Obstet 78:221–225
6. Howe AM, Hawkins JK, Webster WS (2004) The growth of the nasal septum in the 6–9 week period of foetal development — warfarin embryopathy offers a new insight into prenatal facial development. Aust Dent J 49(4):171–176
7. Raghav S, Reutens D (2007) Neurological sequelae of intrauterine warfarin exposure. J Clin Neurosci 1114(2):99–103
8. Masamoto H, Uehara H, Mekaru K, Uezato T, Sakumoto K, Aoki Y (2009) Warfarin-associated fetal intracranial hemorrhage in woman with mitral valve replacements: a case report. Am J Perinatol 26(8):597–600
9. Rehle T, Shisana O (2009) National population-based HIV surveys — the method of choice for measuring the HIV epidemic. S Afr Med J 99:633–636
10. Mehndiratta S, Suneja A, Gupta B, Bhatt S (2010) Fetotoxicity of warfarin anticoagulation. Arch Gynecol Obstet 282:335–337
11. Chan WS, Anand S, Ginsberg JS (2000) Anticoagnulation of pregnant women with mechanical heart valves. Arch Int Med 160:191–196
12. Van Kuilenburg JT, Verheugt FW, van Dijk AP (2007) Prosthetic heart valve thrombosis, anticoagulation and pregnancy: a case report and review of the literature. Neth Heart J 15(9):306–309
13. Ginsberg JS, Chan WS, Bates SM, Kaatz S (2003) Anticoagulation of pregnant women with mechanical heart valves. Arch Int Med 163:694–698
14. Pieper PG, Balci A, Van Dijk AP (2008) Pregnancy in women with prosthetic heart valves. Neth Heart J 16:406–411
15. Srivastava AR, Modi P, Sahi S, Niwariya Y, Singh H, Banerjee A (2007) Anticoagulation for pregnant patients with mechanical heart valves. Ann Card Anaesth 10(2):95–107
16. Khan AO (2007) Optic nerve dysfunction in a child following low-dose maternal warfarin exposure. Ophthalmic Genet 28 (3):183–184

Virchows Arch (2010) 457:741–747
DOI 10.1007/s00428-010-0998-1

ORIGINAL ARTICLE

Quality management and accreditation of research tissue banks: experience of the National Center for Tumor Diseases (NCT) Heidelberg

Esther Herpel · Christoph Röcken · Heike Manke · Peter Schirmacher · Christa Flechtenmacher

Received: 26 August 2010 / Revised: 6 October 2010 / Accepted: 8 October 2010 / Published online: 27 October 2010
© Springer-Verlag 2010

Abstract Tissue banks are key resource and technology platforms in biomedical research that address the molecular pathogenesis of diseases as well as disease prevention, diagnosis, and treatment. Due to the central role of tissue banks in standardized collection, storage, and distribution of human tissues and their derivatives, quality management and its external assessment is becoming increasingly relevant for the maintenance, acceptance, and funding of tissue banks. Little experience exists regarding formalized external evaluation of tissue banks, especially regarding certification and accreditation. Based on the accreditation of the National Center of Tumor Diseases (NCT) tissue bank in Heidelberg (Germany), criteria, requirements, processes, and implications were compiled and evaluated. Accreditation formally approved professional competence and performance of the tissue bank in all steps involved in tissue collection, storage, handling as well as macroscopic and histologic examination and final (exit) examination of the tissue and transfer supervised by board-certified competent histopathologists. Thereby, accreditation provides a comprehensive measure to evaluate and document the quality standard of tissue research banks and may play a significant role in the future assessment of tissue banks. Furthermore, accreditation may support harmonization and standardization of tissue banking for biomedical research purposes.

Keywords Tissue bank · Quality management · Accreditation · DIN/ISO 17020:2004

E. Herpel (✉) · P. Schirmacher · C. Flechtenmacher
Institute of Pathology, University Hospital,
INF 220, 69120 Heidelberg, Germany
e-mail: esther.herpel@med.uni-heidelberg.de

E. Herpel
Tissue Bank of the National Center for Tumor Diseases,
University Hospital Heidelberg,
Heidelberg, Germany

C. Röcken
Institute of Pathology, Christian-Albrechts-University,
Kiel, Germany

H. Manke
DAkkS, Deutsche Akkreditierungsstelle GmbH,
Berlin, Germany

Introduction

Tissue banks represent essential resources and platforms for biomedical research [1–4] serving basic, translational, and clinical research projects by providing human tissues and their respective derivatives as well as offering access to key technologies. Research tissue banks require reliable and sustainable solutions for several key issues to provide high-quality material based on optimized procedures for acquisition, storage, documentation of specimens, expert evaluation according to the specific project needs, and standardized material transfer procedures. Furthermore, some biobanks additionally offer project management as an essential component, including advice and support in project planning, support in the use of bioresources-associated technologies, and even project tracking and recall procedures [1]. Especially the expert evaluation of tissue specimens for research projects represents an essential tissue bank function and is a key element of good scientific practice in research projects based on human tissues [5]. The failure to provide expert evaluation of tissues is a frequent cause for incorrect data in biomedical research based on human tissues, causing considerable

damage to the respective projects, the scientific community, and also companies relying on these results.

To guarantee a consistent level of quality and good scientific practice, it is mandatory for research tissue banks to provide quality management systems that ensure correct performance. Furthermore, a defined and transparent quality management system within research tissue banks is increasingly expected by funding organizations and even researchers and cooperating industrial partners. Several attempts have recently been made to formulate the requirements for research tissue banks and to set standards for their procedures [6–8]. In contrast, specific quality management and its external evaluation have attracted far less attention and systematic consideration. Only recently authorized external assessments by a third party, i.e., certification and accreditation, have become accessible for tissue banks.

Based on the experiences of the Tissue Bank of the National Center of Tumor Diseases in Heidelberg (Germany), the accreditation process with respect to research tissue banks was critically evaluated.

Quality management components in tissue banks

Tissue banks have been established to provide high-quality samples of normal and diseased human tissues for the purpose of biomedical research. Thus, a tissue bank must provide optimized technical solutions for the acquisition, storage, documentation, and transfer of specimens that comply with national and international standards and legal requirements [6–11]. Additionally, expert evaluation of the tissue samples according to the specific needs of a given project is mandatory and standardized material transfer procedures should be established [5,12]. Expert evaluation includes an entry control, in which the type of tissue sample is examined and verified with regard to anatomical origin, tissue status (normal or diseased), and general tissue condition (vital, necrotic, or autolytic). It also includes an exit control, which confirms that tissue taken from the repository fulfills all of the requirements (e.g., histologic tumor type, tumor grade, percentage of tumor cells) requested by the recipient. Furthermore, a tissue bank should provide active project management including specific advice and support in project planning, support in the use of bioresource-associated technologies, and even project tracking and recall procedures. To guarantee good scientific practice and to meet the interests of all participants—especially cooperating scientists—in a transparent manner, it is mandatory for a tissue bank to establish a quality management system. The NCT tissue bank's quality management system represents a set of coordinated procedures and activities that guide and control the performance of all persons involved with regard to their specific responsibilities, positions, and interactions [13]. Therefore, the NCT tissue bank's quality management system has been implemented to address all of its structures and procedures (Table 1; Figs. 1 and 2).

Structural components of the NCT tissue bank include the rights, responsibilities, and obligations for members and partners of the tissue bank as well as for patients providing tissues and researchers using tissues and technologies provided by the tissue bank:

- Agreed upon "rules of procedures" that clearly define policy and aims, organizational structure, and regulations of the tissue bank.
- Guarantee of independence, impartiality, and integrity of the tissue bank and its personnel.
- Legal status of the tissue bank, including its affiliations and the specification of actions to be taken in case of a change in status or even termination of its activity and a financial disclosure of the tissue bank (e.g., non-profit organization, commercial institution).
- Sustainability of the tissue bank as guaranteed by a long-term financing plan based on full-cost estimates addressing all of its activities.
- Clearly defined interfaces to the clinical and diagnostic units, especially those regarding patient care and routine diagnostics.
- Internal (e.g., tissue bank advisory board) and/or external reviews of the tissue bank to evaluate its performance.

Procedural measures are those that directly affect the quality of the provided specimens as well as good scientific

Table 1 Most important standard operating procedures (SOPs) of the NCT tissue bank Heidelberg

Structural standard operating procedures
Responsibilities of leadership
Definition of politics
Definition of aims
Organizational structure
Description of functions
Training schedules
Training plan
Scientific/procedural standard operating procedures
Patient consent
Entry controls of fresh tissue and other materials
Asservation of fresh tissues
Storage of fresh frozen tissues
Processing of tissues/materials
Project coordination
Pathological and anatomical evaluation of tissues (exit control)
Tracking of projects

Fig. 1 Quality management components of NCT tissue bank

Quality Management System	
Structural components	**Procedural/scientific components**
1. Organizational structure	1. Project assessment
2. Regulations	2. Tissue evaluation and characterization (exit control)
3. Internal and external review system	3. Project tracking
4. Patient consent modalities	

practice in handling of tissues, project management, and even project tracking and recall procedures:

- Standard operating procedures (SOPs) for all technical procedures within the NCT tissue bank such as acquisition, storage as well as preparation, examination, and re-evaluation of tissues including reporting the results in the case of a request according to national and international standards and guidelines [6–10], including documentation.
- Standard regulations detailing how projects are handled starting from the application up to the material transfer and project tracking. This includes standardized application forms and definition of procedures for reviewing and decision making (Fig. 2).
- Professional evaluation by board-certified surgical pathologists of the tissues prior to material transfer to the respective research project (exit control) as the core element of tissue banking that significantly contributes to good scientific practice. It is protocolled and included into the standard Material Transfer Agreements.
- Project tracking and appropriate recall procedures, including sanctions in case of non-compliance. Results of project tracking are documented in order to improve handling and quality management.

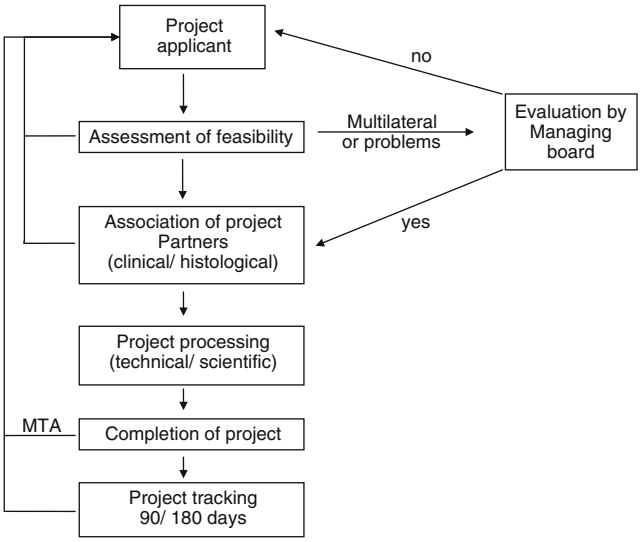

Fig. 2 Standard project management in NCT tissue bank. Every application for project support to the NCT tissue bank is assessed and specified together with the project leader (required number, type, and quality of materials) and for feasibility; bilateral projects (involving only material from one institution) are directly processed if there are in accordance with all regulations; multilateral projects or specific problems arising require approval by the managing board (rejections are communicated to the project leader). All projects mandatorily involve an expert scientific, clinical, and histopathologic project partners as nominated by the tissue bank. After completion of project, processing pseudonymized materials and data are handed over to the project leader together with a Material Transfer Agreement (MTA). Every project is tracked after 90 and 180 days regarding initiation of experiments and material quality and all project management data are documented

An effective quality management system requires the documentation of all of these parameters in a manner amenable to reviewing procedures. The results of these reviewing procedures and measures to improve deficiencies are protocolled and followed-up.

External reviewing and documentation of quality management: accreditation vs. certification

Evaluation of quality management performance is increasingly expected by funding organizations, researchers, and even cooperating industrial partners. Different measures such as internal reviews or reports to an advisory board are used (Table 2). Although they may meet all practical needs, these measures lack standardization and comparability. Thus, an objective evaluation of quality management systems has been increasingly considered and has recently entered realm of tissue banks.

External objective evaluation of the quality management system can be provided either by certification or by accreditation. Certification addresses adherence to designated standards or defined requirements for products, persons, or attendances. It does not include the validation of the examination procedures and the results regarding their correctness or the level of professional competence in accordance with the current state of the art for scientific and technical knowledge. In contrast, accreditation addresses result-oriented performance by authorized and adequately trained personnel providing the required professional

Table 2 Internal and external controls of the quality system

Measure	Characteristics		
	Control by	Control mechanism	Aims
Internal and external review	Internal/ external	Regular report of head of tissue bank	Information and internal control
Advisory board meeting	Internal	Regular report of head of tissue bank	Information of tissue bank partners
Certification	External	Internal and external audits; user trainings; quality management handbook	Confirmation of operational sequences with standards or requirements
Accreditation	External	Internal audits and external assessments; user trainings; quality management handbook	Confirmation of operational and technical sequences with an international standard; confirmation of professional competence and quality

competence. Thus, accreditation formally recognizes the competence to carry out all procedures in tissue banking including sampling, handling, storage, examination, evaluation, and reporting of results as well as transfer to third parties (individual researchers, institutions, or industrial partners).

Certification of tissue banks is undoubtedly possible. However, important key indicators for the quality of a tissue bank such as the evaluation of tissue specimens by competent histopathologists, the competent performance of entry and exit controls of tissues and the reporting of the results, which represent essential elements of good scientific practice, are not addressed by the certification process. In contrast, professional competence in tissue banking, especially in terms of tissue evaluation, is only assessed by accreditation. Therefore, the National Center of Tumor Diseases tissue bank in Heidelberg (Germany) had decided to use accreditation due to "ISO/IEC17020:2004 General criteria for the operation of various types of bodies performing inspection" as its measure for external and independent evaluation of its quality management [14].

Conditions for the accreditation of tissue banks

Since the NCT tissue bank was the first institution of its kind to aspire accreditation, the accreditation body had to verify whether the activities of a tissue bank were eligible for accreditation and which standards should be applied in the process. No respective international experiences or examples existed. Over the past 10 years, more than 70 institutions for pathology have been accredited in Germany according to the ISO/IEC 17020 standard. Therefore, the first step was to question whether this international standard was applicable for the accreditation of a tissue bank. Firstly, a sector committee (advisory expert panel for the accreditation body) already existed for the subject of pathology, which had developed subject-specific criteria for accreditation that could be applied to the work of pathologists for a tissue bank. Secondly, pathologists generally possess the professional experience and expertise in the sampling, storage, diagnostic evaluation, and distribution of human tissue samples. Thirdly, experts of the field (board-certified pathologists and neuropathologists) as well as an independent expert review board of pathologists within the sector committee were available for the assessment within the realm of the accreditation process for the tissue bank.

The ISO/IEC 17020 establishes the internationally standardized competence criteria for areas that perform expert evaluations (=diagnosis) based on examinations (=findings). These competence criteria had to be interpreted by the sector committee of the accreditation body with respect to the specialty at hand in order to be able to apply them for the accreditation, e.g., in the field of pathology. An accreditation according to these standards mandatorily requires that activities of a tissue bank include the evaluation of findings and consequent diagnoses. This would not be the case if a tissue bank would be solely involved in the sampling, storage, and distribution of tissue samples. This includes tissue banks that are run independently of institutions for pathology (e.g., by clinical institutions or some biotechnology companies). The certification of such tissue banks is possible as the result of a lack of standards and regulations; however, the accreditation according to the ISO/IEC 17020 is excluded under these circumstances.

The analysis of the activities, processes, and expertise in the NCT tissue bank showed that it compares to the activities and expertise of a department of surgical pathology. The sampling of tissues designated for the NCT tissue bank and the histological evaluation of the type, quality, and composition of the samples was performed by either a board-certified surgical pathologist or a trainee under the direct supervision of a board-certified pathologist. The selection and sampling of tissues for the NCT tissue bank were performed in accordance with the principles applied to patient material under clinical diagnostic conditions. The only difference was, e.g., for the production of a tissue microarray that the "sampling" in this case was taken from a pre-existing paraffin block instead of a sample taken from resection material. In both cases, the

specific expertise of a pathologist was applied. This process always culminated in the formulation of a diagnosis, which was communicated in the form of a report at the time of sample delivery (exit control), in this case for a researcher instead of a clinician. Clinical data, blood, and serum products as optional, additional, and project-specific components provided by the clinical cooperation partners were not included in the considerations of the accreditation process. Based on this assessment, the accreditation body decided that the NCT tissue bank performs a service that can be accredited according to the ISO/IEC 17020 standard because expert evaluations (=diagnosis) of tissues are based on examinations (=findings), which are communicated to a researcher (instead of a clinician) at the time of material delivery (tissue sample, TMA, etc.).

Accreditation of the National Center of Tumor Diseases Tissue Bank, Heidelberg

Accreditation requires a systematic approach and the stepwise implementation of a quality management system including several stages: preparation, the review process, and the post-reviewing period (Fig. 3).

Preparation Since the foundation of the NCT tissue bank in 2005, standard operating procedures for all relevant procedures have been defined (Table 1, Fig. 1) and were constantly improved and adapted to national and international regulations. In consequence, in 2006 the NCT tissue bank stratified all existing workflows regarding organizational structures, responsibilities, procedures, processes, and resources, including all activities that directly or indirectly contribute to quality, and tested them for weak points and practicability. For tissue bank processes not previously listed, new SOPs were implemented in the NCT tissue bank's quality management system. Interfaces to interacting institutions (e.g., German Cancer Research Center, hospital facilities) and especially the Institute of Pathology were reviewed, documented, and formalized. In 2007, the first quality management manual covering all working processes related to the NCT tissue bank (Table 1, Fig. 1) was finished and implemented in daily practice. From that time point on, regular internal audits were performed to evaluate the quality management system.

Accreditation process After formalization of the quality management system was completed, the NCT tissue bank applied for accreditation according to ISO/IEC 17020:2004. The quality management system was adapted to the standards [15,16] set forth by one of the predecessors of the national accreditation body DAkkS, and the application was filed in mid-2008 to the "Deutsches Akkreditierungs-

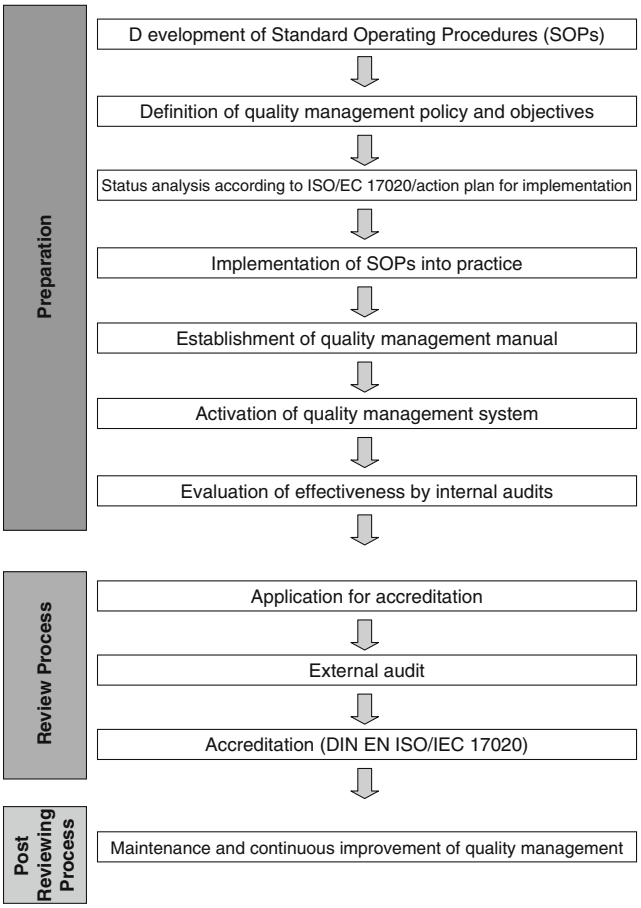

Fig. 3 Systematic approach to tissue bank accreditation

system Prüfwesen GmbH (DAP)" [now the national accreditation body "Deutsche Akkreditierungsstelle GmbH (DAkkS)"], which initiated the accreditation of the NCT tissue bank. At the end of 2008, the NCT tissue bank was subjected to a 3-day on-site review by an authorized and independent external assessor team of the DAP [lead assessor for the management system and a technical assessor (senior board-certified surgical pathologist with special training in accreditation)]. By this assessment of the NCT tissue bank, the following aspects were evaluated in accordance with the standards set forth by the ISO/IEC 17020:

- the quality management system including its documentation,
- the structure and the legal status,
- the procedures for sampling, storage, handling, examination, and evaluation of requested material including records and reports,
- the fulfillment of legal requirements including all ethical issues,
- the responsibilities of the top management of the tissue bank and the scientific advisory board,

- the competence of the head of the tissue bank and the laboratory as well as the medical experts involved and the procedures for the maintenance of competence of all personnel including the pathologists, and
- the performance of effective and target achievement of the NCT tissue bank's quality management system.

After the successful review, the NCT tissue bank was accredited In April 2009 according to ISO/IEC 17020 by the DAP as the first research tissue bank in Europe.

Post-reviewing process After successful accreditation in April 2009, the quality management system was further improved; internal audits and regular education and training programs were performed. In February 2010, the NCT tissue bank successfully completed the first external surveillance assessment by the DAkkS (former DAP).

Discussion and future developments

The National Center of Tumor Diseases tissue bank in Heidelberg, Germany, was the first tissue bank to subject its quality management system to external evaluation by an accreditation body. This process had revealed several aspects (Table 3) that should be considered prior to decision making.

With regard to staff members, accreditation (as well as certification) is an important tool for communication and to promote adherence to regulations by staff members because all procedures and working processes are defined in the quality management documentation. Instructions for all staff members are likely to be followed more strictly as they are controlled continuously by audits and reviews and are improved regularly if necessary. All staff members are necessarily and actively involved into the design of the quality management system and the review process so that there is continuous incentive for further education. Although initially an adverse attitude towards certification or accreditation may occur as it may be considered to be a form of supervision, this process holds significant potential to strengthen the identification of all participants with the tissue bank, to increase the feeling of responsibility, and to offer staff members greater visibility. Thus, over time the staff's attitude towards accreditation is likely to develop in a positive manner, especially when it becomes more and more familiar with the accreditation procedure.

Table 3 Aspects of tissue bank accreditation

Positive	To be considered
Induces comprehensive system analysis	High effort (personnel, time, costs)
Higher internal and external acceptance (confidence, "marketing")	Difficulty to acquire specific funding for accreditation
Relevant for industrial interactions ("label"; quality assurance)	
Integrates performance of all participants	
Transparent workflows for all participants; facilitates incorporation of new staff members	
Fixes tight link to expert histological analysis, i.e., pathology	
Relevant tool to justify and gain funding for tissue banks	

The increased work load—especially during the preparation and accreditation process and its specific documentation— as well as the resulting direct and indirect costs have to be seen as the main aspects to be considered. Only institutions that are able to provide these resources (personnel and finances) will be able to successfully complete the accreditation process; therefore, planning of the accreditation process should include a critical review of the available resources. The required specific effort depends on the pre-existing level of quality management, documentation, and experience in accreditation procedures.

With regard to external partners, positive aspects dominate; accreditation documents quality in an official and visible manner. This will increase confidence in the performance of the tissue bank, especially for cooperating scientists and funding institutions; it may even become an important argument for funding and sustainability of the tissue bank as well as unifying tissue banking efforts at a given location. Furthermore, since the performance of tissue evaluation within the tissue bank, especially the exit control, is linked to the specific qualification level, it closely links tissue banking with the professional expertise of board-certified surgical pathologists. Therefore, it is a good, indirect measure to eradicate "wild", uncontrolled tissue collections, which represent a major threat to good scientific practice. On a long-term basis, it may be discussed whether accreditation may be one of the means to guarantee tissue bank quality on a national or international level. This is an important aspect with regard to large cooperative projects or grant applications based on significant decentralized tissue resources. Due to the increasing impact of translational research and especially targeted therapy, the importance of developing specific and individual targets and predictive markers is rising. Investigating subgroup-specific targets implicates that tissue collectives may be too small in a local research unit. Since accreditation according to ISO/IEC 17020 represents an international standard, it may be helpful to harmonize national and international tissue banking and support the generation of large and comparable tissue collectives even of small

subgroups for translational research and targeted therapy [17]. Accreditation is likely to become increasingly relevant for cooperating projects involving industrial partners. Industrial research also depends on high-quality tissue resources for drug development and the identification of novel targets and biomarkers [18]. On the other hand, industrial partners will ask for objective confirmation of the tissue bank's high-quality performance. In light of all of these aspects, accreditation offers an attractive perspective to improve quality management, transparency, and external acceptance of competent tissue banks.

Conflict of interest statement We declare that we have no conflicts of interest.

References

1. Herpel E, Koleganova N, Schirmacher P (2008) Tissue bank of the National Centre for Tumour Disease. An innovative platform for translational tumour. Pathologe 29(Suppl 2):204–209
2. Riegman PH, Dinjens WN, Oosterhuis JW (2007) Biobanking for interdisciplinary clinical research. Pathobiology 74:239–244
3. Riegman PH, Morente MM, Betsou F, de Blasio P, Geary P (2008) Biobanking for better healthcare. Mol Oncol 2:213–222
4. Stege A, Hummel M (2008) Experience with establishment and operation of a biobank. Pathologe 29(Suppl 2):214–217
5. Bevilacqua G, Bosman F, Dassesse T, Hofler H, Janin A, Langer R, Larsimont D, Morente MM, Riegman P, Schirmacher P, Stanta G, Zatloukal K, Caboux E, Hainaut P (2010) The role of the pathologist in tissue banking: European Consensus Expert Group Report. Virchows Arch 456:449–454
6. Moore HM, Compton CC, Lim MD, Vaught J, Christiansen KN, Alper J (2009) Biospecimen research network symposium: advancing cancer research through biospecimen science. Cancer Res 69:6770–6772
7. National Cancer Institute NIoH, U.S. Department of Health and Human Services (2007) National Cancer Institute best practice for biospecimen resources. Available at http://biospecimens.cancer.gov/practices/default.asp. Accessed 3 January 2008
8. OECD (2007) Best practice guidelines for biological resource centers. Available at http://www.oecd.org/sti/biotechnology/brc. Accessed 5 April 2007
9. (ISBER) ISfBaER (2005) Best practices for repositories. I: collection, storage, and retrieval of human biological material research. Cell Preserv Technol 3:5–48
10. Deutscher Ethikrat (2010) Humanbiobanken für die Forschung. Available at http://www.ethikrat.org/publikationen/stellungnahmen/humanbiobanken. Accessed 16 June 2010
11. Morente MM, Alonso S (2005) Current challenges of human tumour banking. Hematol Oncol 23:54–56
12. Grizzle WE, Woodruff KH, Trainer TD (1996) The pathologist's role in the use of human tissues in research—legal, ethical, and other issues. Arch Pathol Lab Med 120:909–912
13. Kiehntopf M, Böer K (2008) Biomaterialbanken—Checkliste zur Qualitätssicherung. Medizinisch Wissenschaftliche Verlagsgesellschaft, Berlin
14. Manke H, Rocken C (2008) Accreditation in pathology. Pathologe 29:388–398
15. DAP Anforderungskatalog für Prüfmittel, Geräte und Zubehör in der Pathologie, DGA-TM-34. Available at www.dap.de/95doc/DGA-TM-34.pdf. Accessed 15 January 2008
16. DAP (2004) Leitfaden zur Interpretation der Anforderung der DIN EN ISO/IEC 17020:2004 und technischen Kriterien für deren Anwendung zur Akkreditierung in der Pathologie/Neuropathologie. Available at http://www.dap.de/95doc/DAP-TM-30.pdf. Accessed 15 January 2008
17. Zika E, Paci D, Braun A, Rijkers-Defrasne S, Deschenes M, Fortier I, Laage-Hellman J, Scerri CA, Ibarreta D (2010) A European survey on biobanks: trends and issues. Public Health Genomics (Epub ahead of print; PMID: 20395653)
18. Innovative Medicine Initiative (2008) The Innovative Medicines Initiative (IMI) research agenda. Available at http://imi.europa.eu/sra_en.html. Accessed 15 May 2010

Virchows Arch (2010) 457:749
DOI 10.1007/s00428-010-0991-8

REVIEW AND PERSPECTIVE

Book review

Jörg M. Nährig

Received: 17 September 2010 / Accepted: 23 September 2010 / Published online: 19 October 2010
© Springer-Verlag 2010

Keywords AFIP · Atlas of tumor pathology · 4th series · Breast

Fascicle 10 *Tumors of the Mammary Gland* is a recent book in the Armed Forces Institute of Pathology (AFIP) Atlas of Tumor Pathology, fourth series. Not unlike the authors of other volumes, fascicle 10 presents illustrious names within the international community of pathologists, Drs. Fattaneh A. Tavassoli and Vincenzo Eusebi. This recently available volume supersedes the third edition of this fascicle published 17 years before by Rosen and Oberman. Tavassoli and Eusebi's book is structured similarly to the other AFIP fascicles, and it covers the many aspects of breast disease *in detail*, from anatomy to recent molecular genetics findings. The major focus of this book is the daily use by pathologists for the diagnosis of both common and the rare breast diseases. In the 18 concise chapters that provide innumerable details, extensive discussions, and up-to-date references, the authors share their great expertise and experience. Most of the numerous microscopic photographs are high quality, and many chapters contain helpful tables with differential diagnoses. It would not be Dr. Tavassoli's book if it did not contain sections on the DIN and LIN classification systems. In fact, since the current classification is unsatisfying, this classification system has, at present, no convincing alternative.

This is a superb new book on breast pathology currently available on the market, and it should find its place on the desktop of many pathologists worldwide, from those just beginning a career in pathology to those ending a long career in pathology. This book is also highly recommended for those in any specialty dealing with breast diseases, particularly radiologists and clinicians ("Caesar," as Azzopardi used to say).

J. M. Nährig (✉)
Institut für Allgemeine Pathologie und Pathologische Anatomie,
Technische Universität München (TUM),
Trogerstrasse 18,
81675 Munich, Germany
e-mail: joerg.naehrig@lrz.tum.de